University of Alberta

Late Paleocene Mammals from near Red Deer, Alberta, and a Phylogenetic Analysis of the Earliest Lipotyphla (Mammalia, Insectivora)

by

Craig Smith Scott

A thesis submitted to the Faculty of Graduate Studies and Research
in partial fulfillment of the requirements for the degree of

Doctor of Philosophy

in

Systematics and Evolution

Department of Biological Sciences

Edmonton, Alberta
Spring 2008

Your file Votre référence
ISBN: 978-0-494-45595-1
Our file Notre référence
ISBN: 978-0-494-45595-1

Abstract

Current evidence points to the Paleocene as one of the most important intervals in the evolutionary history of mammals, with the fossil record recording a remarkable adaptive radiation of therians soon after the mass extinctions at the end of the Mesozoic. The taxonomic diversity and systematics of late Paleocene mammals from localities in fossiliferous strata of the Paskapoo Formation in the vicinity of Red Deer, south central Alberta was investigated, with emphasis on the phylogenetic relationships of early Tertiary lipotyphlan insectivorans. Mammals from these localities are more taxonomically diverse than previously understood, with 76 species (24 new) in 51 genera (11 new) recognized among 14 orders. The local faunas are dominated by mammals of small body size, with multituberculates, insectivorans, and plesiadapiforms constituting over 75 percent of the total number of specimens; large mammals are few, represented only by rare specimens of pantodonts and larger-bodied arctocyonid condylarths. Significant discoveries include new genera of a didelphimorphian marsupial, erinaceomorph and soricomorph insectivorans, a viverravid carnivoran, arctocyonid condylarths, titanoideid and cyriacotheriid pantodonts, and a eutherian of uncertain taxonomic position. Other discoveries include the oldest known lipotyphlan petromastoid and postcranium and the first evidence of a venom delivery system in an extinct mammal. New and previously reported material from the Alberta Basin and elsewhere permit the first comprehensive phylogenetic analysis of early Tertiary stem lipotyphlans. While a soricomorph-erinaceomorph dichotomy was recovered, a close association of Litolestes, Cedrocherus, and Oncocherus with extant erinaceids was not supported, nor was inclusion of "Leptacodon" munusculum or "Leptacodon" packi with

other species of Leptacodon. A new soricomorph genus from the Paleocene of Alberta may represent the first North American record of Amphidozotheriinae, and Limaconyssus, previously considered an aberrant nyctitheriid, is better considered a geolabidid. A preliminary correlation indicates strongest resemblance to the coeval Birchwood local fauna of central Alberta and Cedar Point Quarry local fauna of Wyoming, suggesting an early middle Tiffanian age. Diversity analyses using standardized samples and rank abundance curves suggest that the Tiffanian interval in Alberta fails to show a significant decline in mammalian species diversity as would be predicted by recent late Paleocene global cooling models.

This dissertation is dedicated to the memory of Mr. Dennis C. Wighton, Mrs. Alice (Betty) Speirs, and Dr. Bruce G. Naylor

Acknowledgments

Several people and institutions have provided assistance, advice, and constructive criticism during the course of my research. I reserve the highest levels of gratitude for my supervisor, Dr. R. C. Fox, for suggesting the Blindman River and Joffre Bridge fossil mammal faunas as a potential dissertation topic, and then allowing me the freedom to develop the project as appropriate. The specimens from the Blindman River and Joffre Bridge localities are among the finest in the UALVP collections, and I consider it a great privilege to have been permitted to use them in my research. I extend thanks to Dr. R. A. Stockey for agreeing to act in the role of co-supervisor, and to the supervisory, candidacy, and examining committees for their insight and guidance: Drs. B. S. Heming, P. R. Willoughby, M. W. Caldwell, P. Lemelin, and J. Meng.

I offer my thanks to the University of Alberta Laboratory for Vertebrate Paleontology (UALVP), the Department of Biological Sciences, and the University of Alberta for providing me with working space, access to research equipment, and financial support. I extend profound thanks to Yonqin Sun, UALVP, for her skilled preparation of even the most delicate of specimens. Yongqin's contributions to this dissertation cannot be overstated---without her speedy preparations, much of the Blindman River and Joffre Bridge material would have been unavailable for this study. I thank to Dr. M. Caldwell for generously allowing me unfettered access to his microscopy and digital photographic equipment. The final six months of my research were completed while I was employed at the Royal Tyrrell Museum of Palaeontology (RTMP), and I thank Dr. B. Naylor, A. Neuman, and Dr. D. Brinkman for providing me with the opportunity to complete the dissertation during working hours---without the support of the RTMP, the dissertation would still be a work in progress.

I am grateful to a number of institutions for allowing me access to specimens, by way of loan or visits, which proved invaluable for my research. I extend thanks to Dr. Jin Meng, I. Rutzky, and J. Galkin (American Museum of Natural History), Dr. K. Beard and A. Tabrum (Carnegie Museum of Natural History), Drs. T. and R. Smith (L'Institut royal des Sciences naturelles de Belgique), Dr. R. Cifelli and B. Davis (University of Oklahoma), Dr. F. Jenkins and C. Schaff (Museum of Comparative Zoology, Harvard),

Dr. J. Gardner and J. Wilke (Royal Tyrrell Museum of Palaeontology), Drs. W. Clemens and P. Holroyd (University of California Museum of Paleontology), Drs. P. Gingerich and G. Gunnell (University of Michigan Museum of Paleontology), Dr. R. Emry (Smithsonian Institution, National Museum of Natural History), Dr. J. Lillegraven and M. Cassiliano (University of Wyoming), Drs. J. Gauthier and W. Joyce, and D. Brinkman (Peabody Museum, Yale University), Dr. D. Krause and D. Boyer (Stony Brook University), and Dr. R. Fox (University of Alberta Laboratory for Vertebrate Paleontology).

I wish to extend special thanks to E. Stafford for his untiring assistance with formatting.

Many people have made significant contributions to collections from the Blindman River and Joffre Bridge localities over the years and clearly without the assistance of these individuals there would be no collections to work on. I thank (in no particular order) P. Johnston, S. Godfrey, M. Webb, M. Wilson, A. Murray, B. Naylor, K. Gao, R. Fox, D. Brinkman, D. Spivak, J. Perry, S. Ziemmer, G. Youzwyshyn, G. Stonley, T. MacDonald, Z. Johanson, A. Lindoe, K. Soehn, B. Rankin, M. Fox, D. Wighton, A. Speirs, G. Hoffman, W. Sloboda, T. Fremd, S. Rickabaugh, M. Johnston, S. Johnston, J. Cline, M. Dumont, J. Acorn, and G. Denomme.

Funding has been provided to me by University of Alberta Province of Alberta Graduate Fellowships, Andrew Stewart Memorial Prize (University of Alberta), Department of Biological Sciences Teaching Assistantships, and a University of Alberta Graduate Students Association Professional Development Grant.

I offer thanks to my fellow graduate students, past and present, in the UALVP and University of Alberta Paleobotany Group, for their friendship, advice, and patience. Special thanks to S. Little, A. Dutchak, L. Budney, S. Pierce, T. Bullard, S. Smith, R. Mindell, T. Konishi, B. Barr, L. MacKenzie, and T. Cook for putting up with me for so long.

Finally, I thank my parents, John and Cathie, for their support, patience, and good advice.

Table of Contents

List of Tables

List of Figures

List of Symbols, Nomenclature, and Abbreviations

Institutional Abbreviations

AMNH	American Museum of Natural History, New York, New York
CMNH	Carnegie Museum of Natural History, Pittsburgh, Pennsylvania
IRScNB	L'Institut royal des Sciences naturelles de Belgique, Brussels, Belgium
KUVP	University of Kansas Vertebrate Paleontology Collections, Lawrence, Kansas
LACM	Natural History Museum of Los Angeles County, Los Angeles, California
MCZ	Museum of Comparative Zoology, Harvard University, Cambridge, Massachusetts
MNHN	Muséum national d'Histoire naturelle, Paris, France
NMC	National Museum of Natural Sciences, Ottawa, Ontario
SMM	Science Museum of Minnesota, St. Paul, Minnesota
TMP	Tyrrell Museum of Palaeontology, Drumheller, Alberta
UALVP	Laboratory for Vertebrate Paleontology, University of Alberta, Edmonton, Alberta
UAMZ	University of Alberta Museum of Zoology, University of Alberta, Edmonton, Alberta
UCMP	University of California Museum of Paleontology, Berkeley, California
UM	The University of Michigan Museum of Paleontology, Ann Arbor, Michigan
USGS	United States Geological Survey, Denver, Colorado
USNM	United States National Museum of Natural History, Smithsonian Institution, Washington, D. C.
UW	University of Wyoming Geological Museum, Laramie, Wyoming
YPM	Peabody Museum of Natural History, Yale University, New Haven, Connecticut
YPM-PU	Princeton University Collections accessioned at the Peabody Museum of Natural History, Yale University, New Haven, Connecticut

Anatomical Abbreviations

a	acetabulum
ACu	astragalar cuboid facet
AEc	astragalar ectal facet
AFi	astragalar fibular facet
aiis	anterior inferior iliac spine
ana	astragalar navicular facet
apt	anterior plantar tubercle
ASu	astragalar sustentacular facet
ATim	astragalar tibial facet (medial)
brfo	brachialis fossa
C	upper canine
c	lower canine
CaCu	calcaneal cuboid facet
CaEc	calcaneal ectal facet
CaFi	calcaneal fibular facet
CaSu	calcaneal sustentacular facet
cc	cochlear canaliculus
cen	centrum
CuAs	astragalar facet of the cuboid
CuCa	calcaneal facet of the cuboid
CuEc	ectocuneiform facet of the cuboid
CuMtIV/V	facets for metatarsals IV and V of the cuboid
CuNa	navicular facet of the cuboid
D	deciduous upper tooth
d	deciduous lower tooth
dent	dentary
dft	distal flexor tubercle
EnMtI	hallucal facet of entocuneiform

EnNa	navicular facet of entocuneiform
fc	tympanic exposure of facial canal
fms	fossa for stapedius muscle
fo	fenestra ovalis
fort	transverse foramen
fr	fenestra rotundum
fsr	flexor sheath ridge
ftt	fossa for tensor tympani muscle
gtff	groove for tendon of flexor fibularis
h	astragalar head
I	upper incisor
i	lower incisor
iam	internal acoustic meatus
ips	sulcus for inferior petrosal sinus
is	ischium
isp	ischial spine
ist	ischial tuberosity
lam	lamina
lc	lateral condyle
LuMg	magnum facet of the lunate
LuRa	radial facet of the lunate
LuSc	scaphoid facet of the lunate
LuUn	unciform facet of the lunate
M	upper molar
m	lower molar
mc	broken medial condyle
MgII	facet for metacarpal II of the magnum
MgIII	facet for metacarpal III of the magnum
MgIV	facet for metacarpal IV of the magnum
MgLu	lunate facet of the magnum
MgSc	scaphoid facet of the magnum

MgTd	trapezoid facet of the magnum
MgUn	unciform facet of the magnum
mt	mastoid tubercle
MtVCu	cuboid facet of metatarsal V
MtVMtIV	facet for metatarsal IV of metatarsal V
mx	maxilla
n	astragalar neck
nc	neural canal
P	upper premolar
p	lower premolar
pat	patellar groove
pect	iliopectineal eminence
ped	pedicle
pft	proximal flexor tubercle
plg	groove for the tendon of peroneus longus
plp	plantar process
pmx	premaxilla
poz	postzygapophysis
pp	peroneal process
pro	promontorium
prz	prezygapophysis
RaLu	lunate facet of the radius
RaUlp	proximal ulnar facet of the radius
rbit	bicipital tuberosity
rce	radial capitular eminence
rfov	radial fovea for humeral capitulum
rp	rostral tympanic process
sa	sulcus astragali
saf	subarcuate fossa
sic	sulcus for internal carotid artery
smf	stylomastoid foramen

spa	sulcus for promontory artery, internal carotid plexus of nerves
spp	spinous process
sqs	medial wall of squamosal sinus
supc	supinator crest
sut	sustentaculum tali
tc	tuber calcanei
th	tympanohyal
tr	astragalar trochlea
trlc	lateral crest of astragalar trochlea
trmc	medial crest of astragalar trochlea
trof	trochanteric fossa
trp	transverse process
tt	third trochanter
ucop	ulnar coronoid process
uhd	ulnar head
UnIII	facet for metacarpal III of the unciform
UnIV	facet for metacarpal IV of the unciform
UnV	facet for metacarpal V of the unciform
UnCn	cuneiform facet of the unciform
UnLu	lunate facet of the unciform
UnMg	magnum facet of the unciform
unt	tubercle of the unciform
uolp	ulnar olecranon process
urad	ulnar radial notch
ustp	ulnar styloid process
utrn	ulnar trochlear notch
X	upper tooth unidentifiable to position
x	lower tooth unidentifiable to position

North American Land Mammal Ages

Cf	Clarkforkian
Pu	Puercan
Ti	Tiffanian
To	Torrejonian
Wa	Wasatchian

Measurements, Statistics, and Miscellaneous

cf	confer
CV	coefficient of variation
H	height
L	length
L1	length 1
M	mean
N	sample size
OR	observed range
P	parameter
SD	standard deviation
TaW	talonid width
TrW	trigonid width
W	width
*	estimated measurement

1 General Introduction, Geological Setting, Localities, and Conventions

1.1 Introduction and Objectives

THE CONTINENTAL Paleocene of North America (from approximately 65 to 55 million years ago) documents the densest and most nearly complete record of Early Cenozoic mammal evolution in the world (Lofgren et al., 2004; Rose, 2006). Fossil mammals in depositional centers from Canada to southern Texas have not only allowed unparalleled insight into mammalian evolution in the Western Interior of North America, but also form the basis for regional biostratigraphic correlation, crucial for placing terrestrial sediments into a global geochronologic context (Lofgren et al., 2004). Current evidence points to the Paleocene as one of the most important intervals in the evolutionary history of mammals: the fossil record documents a remarkable adaptive radiation of therians (marsupials and eutherians) soon after the mass extinctions at the end of the Mesozoic, with nearly all of the modern mammalian orders having appeared by the end of the Eocene (Alroy, 1999; Novacek, 1999; Archibald and Deutschman, 2001; Rose and Archibald, 2005). The fossil record of mammals during the Paleocene is of particular interest in light of recent incongruences between molecular- and morphological-based phylogenetic hypotheses: these competing hypotheses suggest that mammalian interordinal divergence times have their roots either much earlier in the Cretaceous (the so-called long- or short-fuse models as based on molecular evidence, e.g., Springer, 1997; Kumar and Hedges, 1998; Murphy et al. 2001; Arnason et al., 2002; Springer et al. 2003; Springer et al., 2007) or during a short period of time immediately following the Cretaceous-Tertiary extinction event (the so-called explosive model based on morphological evidence, e.g., Alroy, 1999; Foote et al., 1999; Meng et al., 2003; Wible et al., 2007). As fossils provide the only direct, material evidence of these past evolutionary events, a better knowledge of the early record of this post-Cretaceous adaptive radiation is essential, and in this regard the fossil record in western Canada has played, and will continue to play, a crucial role.

Although mammals of Paleocene age have long been known from Alberta (e.g., Brown, 1914; Matthew, 1914; Simpson, 1927), it was Loris Russell's pioneering work in

the Calgary and Foothills regions (e.g., Russell, 1926, 1929a, 1932a, 1948, 1958), followed by a concentrated research program initiated by Richard C. Fox and the University of Alberta Laboratory for Vertebrate Paleontology in 1966, that resulted in the discovery of numerous Late Mesozoic and Early Tertiary fossil mammal localities in the Alberta Basin (see summary in Fox, 1990a). The fossil mammals recovered at these localities document patterns of mammal evolution from Late Cretaceous through late Paleocene time, and have figured prominently in the understanding of local and regional geology, stratigraphy, and mammalian evolution and vertebrate paleofaunal composition (e.g., Fox, 1971a-b, 1984a-e, 1990b, 1991a, 1994, 2002, 2004, 2005; Krishtalka, 1973; Krause, 1978; Youzwyshyn, 1988; Stonley, 1988; Gao and Fox, 1996; Webb, 1996; Scott, 2003, 2006; Scott et al., 2002; Fox and Naylor, 2006). Of the more than 50 fossil mammal-bearing localities of Paleocene age known from the Alberta Basin, those in sediments of the Paskapoo Formation exposed in the south central part of the province in the vicinity of the City of Red Deer are among the most productive, collectively documenting mammalian evolution during the late part of the Paleocene epoch (Fox, 1990a). Fossil mammals were first discovered in this area by Barnum Brown and field parties from the American Museum of Natural History during a reconnaissance for dinosaur fossils along the Red Deer River; the specimens were subsequently described by Simpson (1927). Since that time, 10 additional localities have been discovered in the area (DW-1, DW-2, DW-3, Mel's Place, Burbank, Red Deer River "mammal track site", Joffre Bridge Roadcut upper and lower levels, Joffre Bridge Mammal Site No. 1, Joffre Bridge East, and Joffre Pipeline, see Fox, 1990a), most of them on cutbanks of the Blindman and Red Deer rivers north and east of Red Deer, and at a large roadcut east of Red Deer (Fox, 1990a). Exceptionally well-preserved fossil mammals from these localities form the basis for the current study, with the following three objectives:

1) Identification, description, and diagnosis (when warranted) of late Paleocene mammals from the Blindman River and Joffre Bridge localities (see locality information later in the text). Despite the relatively dense fossil record of mammals from the Paleocene of the Western Interior, investigation into their taxonomy and phylogenetic relationships have often been hindered by the incomplete nature of the evidence. Fossils from the Blindman

River and Joffre Bridge localities however, preserve parts of the anatomy that have until now remained unknown among early Tertiary mammals. Knowledge of these anatomies permits, for the first time, detailed comparisons with near-contemporaneous mammals from localities from the Western Interior of North America, and an opportunity to test current taxonomic hypotheses as regards early Tertiary mammals. Preliminary research on fossil mammals from the Blindman and Joffre Bridge localities has focused almost exclusively on primates (e.g., Fox, 1984a-d, 1990b, 1991a-b, 1994, 2002), with the bulk of the collections remaining undescribed; hence, the first objective of the current study proposes to address this situation with a full taxonomic treatment of the fossil mammals from the Blindman and Joffre Bridge localities, encompassing identification, detailed descriptions, and extensively figuring relevant specimens. The detailed taxonomy of the mammals from the study localities forms the foundation for achieving the remaining two objectives.

2) The second objective proposes to investigate the phylogenetic relationships among early lipotyphlan mammals from the Western Interior of North America. Lipotyphlans (shrews, hedgehogs, moles, solenodons, and until relatively recently the tenrecs and golden moles) are the third most taxonomically diverse group of living eutherian mammals, and although they can be abundantly represented in mid- to late Paleocene mammalian local faunas (e.g., Simpson, 1937; Van Valen, 1966, 1967; Rose, 1981a-b; Gingerich, 1983; Youzwyshyn, 1988; Krause and Maas, 1990), their remains are most often isolated teeth or, more rarely, incomplete jaws with teeth. Confident taxonomic identification of these specimens has proven difficult, and as a result, broader questions as regards their phylogenetic affinities remain unanswered. Comprehensive studies of early Tertiary insectivorans (e.g., McDowell, 1958; Novacek, 1976; Bown and Schankler, 1982) have dealt primarily with later Eocene and Oligocene groups, for which the fossil record is far more complete; of the few studies focusing on lipotyphlans of Paleocene age, only those of Krishtalka (1976a-b), Novacek (1985), and Novacek et al. (1985) have attempted to address broader taxonomic and evolutionary questions regarding the affinities of "stem lipotyphlans". The exceptional preservation of the Blindman River and Joffre Bridge specimens provides skull, gnathic, and dental data that have otherwise

not been available for phylogenetic investigation. In an attempt to better understand the evolutionary relationships of stem lipotyphlans, this part of the current study proposes to use cladistic methods to propose a phylogenetic hypothesis of the earliest lipotyphlans, incorporating osteological data from the study specimens, as well as those from other important localities from the Western Interior of North America.

3) The third objective is an examination of the taxonomic composition of the Blindman and Joffre Bridge localities, with the intent of biostratigraphic correlation and a more precise estimate of geochronologic age; these estimates, in combination with those from other local faunas in the Alberta Basin (Fox and Scott, in prep.), can in turn be used to test the validity of the current North American Mammal Age biostratigraphic framework beyond the Western Interior of the United States. In addition to assessing the relative age of the study local faunas, the taxonomic composition data will also be used in a preliminary analysis of mammalian faunal change during late parts of the early Paleocene and the early parts of the late Paleocene (i.e., from middle Torrejonian through the early middle Tiffanian; see later in the text) in the southern parts of the Alberta Basin. In his classic paleofaunal analyses on localities of early Paleocene through early Eocene age in Montana and Wyoming, Rose (1981a-b) suggested that mammalian taxonomic diversity was higher in the Torrejonian (early Paleocene) and Wasatchian (early Eocene) than during the intervening Tiffanian and Clarkforkian (late Paleocene) land mammal ages. Rose (1981a-b) related these differences to changes in paleotemperature (as inferred from the paleobotanical record), with the Torrejonian and Wasatchian representing periods of warmer and more equable conditions, while the Tiffanian and Clarkforkian represented periods of cooler temperatures and less stable environmental conditions. While the results of recent studies (e.g., Krause and Maas, 1990; Maas et al., 1995; Alroy et al., 2000; Secord, 2004) are consistent with those of Rose (1981a-b), none of these studies included data from the Canadian record, particularly the results of Youzwyshyn (1988) and Fox (1990a) that suggested the decrease in mammalian diversity during the earliest Tiffanian was not apparent in the record from Alberta. Data from two well-sampled Alberta localities, the middle Torrejonian (To3) Who Nose? locality (Scott, 2003) and the earliest Tiffanian (Ti1) Cochrane 2 locality (Youzwyshyn, 1988; Fox, 1990a; Scott et al.,

2002), as well as data from the Blindman River and Joffre Bridge local faunas, will be used to further test Rose's (1981a-b) hypotheses.

The main body of this study is organized into 11 chapters. Chapter 2 briefly summarizes the non-mammalian fauna and flora of the study localities, while Chapters 3-11 are descriptive and systematic accounts of the fossil mammals from the Blindman River and Joffre Bridge localities. Chapter 3 documents a diverse assemblage of multituberculates, including new species of the neoplagiaulacids Ectypodus and Neoplagiaulax, as well as a new species of the ptilodontid Prochetodon. Chapter 4 records the presence of three marsupial taxa at the study localities, including a new genus of an unusual didelphimorphian. Chapter 5 is devoted to the Insectivora: 10 putative lipotyphlan genera are described, four of which are new, and new species of the lipotyphlans Limaconyssus and Litolestes, the pentacodontid Bisonalveus, and the putative palaeoryctid Pararyctes, are described. Chapter 5 also includes the first cladistics-based phylogenetic analysis of stem lipotyphlans. Chapter 6 documents new viverravid carnivorans from the study localities, while Chapter 7 is devoted to plesiadapiforms (a group of primitive primates or near-primates), with special emphasis on the relationships of Picrodontidae. Chapter 8 discusses the systematic positions of Elpidophorus and Eudaemonema, two dermopteran-like eutherians. Chapter 9 documents a diverse assemblage of condylarths, including two new genera of arctocyonids, while Chapter 10 describes two new genera of pantodonts. Finally, chapter 11 describes a new, enigmatic genus of eutherian mammal, the ordinal affinities of which are uncertain. The study concludes (Chapter 12) with an assessment of the age of the Blindman and Joffre Bridge local faunas, and a preliminary analysis of mammalian faunal change during the earliest parts of the late Paleocene in Alberta.

1.2 Geological Setting

Regional geological setting.—Upper Mesozoic and lower Tertiary paralic and continental sediments of western Canada were deposited as a series of transgressive and regressive cycles associated with two depocentres: the Alberta Basin in the west and the

Williston Basin in the east, with the two being separated in southeastern Alberta by the Bow Island Arch (Dawson et al., 1994). The Alberta Basin is a segment of a large foreland basin extending from Alaska to New Mexico that was filled by clastic debris derived from erosion of the orogenic highlands to the west (Jerzykiewicz, 1997). The uppermost Cretaceous and Paleocene strata within the basin form eastward-thinning clastic wedges deposited during the final stages of the Laramide Orogeny and subsequent Tertiary tectonic quiescence (Dawson et al., 1994; Catuneanu and Sweet, 1998; Fig. 1); these rocks form the bedrock in the Interior Plains of southern Alberta and extend throughout the Foothills to the Front Ranges of the Rocky Mountains (Bally et al., 1966). Paleocene age rock in the study area consists of the upper parts of the Scollard Formation and the more geographically extensive and better exposed Paskapoo Formation (Allan and Sanderson, 1945; Lerbekmo and Coulter, 1985); the Cretaceous-Tertiary boundary has been unequivocally identified in the study area at the base of the Nevis (No. 13) coal seam on the basis of palynological extinctions and an iridium anomaly (Lerbekmo et al., 1979; Sweet and Hills, 1984; Lerbekmo and Coulter, 1985; Lerbekmo and St. Louis, 1986; Lerbekmo et al., 1987).

Geographic distribution of the Paskapoo Formation.—The name "Paskapoo Series" has been used for a series of discontinuous outcrops along the Blindman and Red Deer rivers (Paskapoo is the Cree term for "blind man") (Selwyn, 1874; Tyrrell, 1887; Carrigy, 1970). The type locality was not recorded; as such, the Paskapoo Formation is considered a composite (Carrigy, 1970). Strata of the Paskapoo Formation are extensive throughout the central Alberta Plains, comprising most of the surface bedrock (Demchuk and Hills, 1991; Fig. 1). The Paskapoo strata are preserved in an asymmetrical syncline or homocline (Carrigy, 1971:15), with steep dips to the west near the Foothills, and low, gradual dips eastwardly. The thickness varies from zero at the erosional edge of the plains, to 240m (787 ft) in the type area, to an excess of 1000m (3280 ft) westward (Carrigy, 1971; McLean, 1990). Tyrrell (1887) proposed the term "Paskapoo Series" for outcroppings in the central Alberta Plains region. He correlated this series with the "Porcupine Hills Series" of Dawson (1883), the "Willow Creek Series" and all but the lowest 200 m of the "St. Mary's River Series", and proposed that the contact between the "Paskapoo Series" and the underlying "Edmonton Series" represented the Cretaceous-

Tertiary boundary (Dawson et al., 1994). The concept of the "Paskapoo Series" was extended to the Foothills region by Russell (1932b), but he was unable to correlate the foothills outcrops directly with the type sections in the Red Deer River Valley. Indeed, Russell (1929a, 1932a-b, 1958) considered the outcrops in the foothills of southwestern Alberta a western extension of the "Paskapoo Series", an hypothesis apparently supported by Tozer's (1953, 1956) studies of uppermost Cretaceous and early Tertiary non-marine molluscan faunas. Allan and Sanderson (1945) formally recognized the Edmonton and Paskapoo series as separate formations. In extensive studies of the lithostratigraphy and petrography of the uppermost Cretaceous (Lancian) and Paleocene strata of the Alberta Plains, Carrigy (1970, 1971) delimited the Paskapoo Formation from the Porcupine Hills Formation based on petrographic differences, but never established a true boundary, laterally or vertically, between the two (Demchuk and Hills, 1991). Most recently, Demchuk and Hills (1991) subdivided the Paskapoo Formation into three members, but did not indicate lithostratigraphic differences between any of these units and the Porcupine Hills Formation. Uncertainties as regards regional stratigraphic nomenclature have recently prompted Jerzykiewicz (1997) to propose referral of the Paskapoo Formation to a second order sequence, the Entrance-Paskapoo Sequence. For consistency of nomenclature and brevity, all fossil mammal-bearing localities within Red Deer and area are generally referred to this sequence, with further referral to a specific unit within this sequence to be considered tentative. As presently understood, the Paskapoo Formation disconformably overlies the Maastrichtian and early Paleocene Scollard Formation (Allan and Sanderson, 1945; Lerbekmo et al., 1990; Lerbekmo et al., 1992; Lerbekmo and Sweet, 2000); in the Red Deer River Valley, the disconformable contact between the two formations occurs at the base of a 50 m thick buff-weathering, coarse-grained sandstone overlying mudrock and coal of the Scollard Formation above the Ardley (No. 14) Coal Seam (Lerbekmo et al., 1992). The temporal duration of the hiatus remains uncertain: in the Ardley area east of Red Deer, the disconformity is apparently minor and represents but a short interval of time, whereas farther south, in the area of Scollard Canyon, the disconformity may be more extensive (Lerbekmo et al., 1990); more recently, Lerbekmo et al. (1992) have suggested that the hiatus at the base of the Paskapoo Formation in the northern parts of the Red Deer Valley is even greater than

previously believed, representing in excess of 2 million years. The disconformity is recognized in the Hand Hills region near Drumheller (Lerbekmo et al., 1995), and in the Calgary and Cochrane regions in southwestern Alberta (Lerbekmo and Sweet, 2000). Upper Cretaceous and Paleocene sediments of the Central Plains were largely eroded by easterly flowing fluvial systems during the Eocene through Pleistocene (Leckie and Cheel, 1989; Edwards, 1994), with regional, post-Paleocene uplift and erosion resulting in the removal of nearly 1 km of post-Paleocene age sediments; topographically high erosional remnants of the Paskapoo Formation are disconformably overlain by these post-Paleocene age sediments, including those of Miocene through Pliocene age in Swan Hills region (Allan, 1919; L. Russell, 1967; Demchuk and Hills, 1991), and by a few meters of Miocene through Pleistocene age Hand Hills Formation in the Hand Hills northeast of Drumheller (Storer, 1976, 1978; Demchuk and Hills, 1991; Lerbekmo et al., 1995). In Canada, the Paskapoo Formation is laterally equivalent to the Coalspur Formation of the Foothills to the northwest, the Porcupine Hills Formation of the Foothills to the southwest, and the Ravenscrag Formation at the easternmost parts of the syncline and in the Williston Basin of southwestern Saskatchewan; in the northern parts of the Western Interior of the United States, the Paskapoo Formation is equivalent to the Lebo and Tongue River formations of southern Montana and North Dakota, and the Fort Union Formation of Wyoming (Fig. 2).

Descriptive lithology of the Paskapoo Formation.—Strata of the Paskapoo Formation consist primarily of massively-bedded or disturbed to cross-bedded, buff-weathering medium to coarse-grained sandstones; these strata are often cliff-forming and are best seen in outcrop along the Pembina River west of the City of Edmonton (Tozer, 1956), in the Red Deer River Valley in south-central Alberta (Tyrrell, 1887; Allan and Sanderson, 1945; Carrigy, 1970, 1971; Demchuk and Hills, 1991), and at various natural and man-made exposures in and around the City of Calgary and the town of Cochrane (Rutherford, 1927; Russell, 1929a-b; Youzwyshyn, 1988; Scott, 2003; Lerbekmo and Sweet, 2000). In addition to the coarse sandstones, the Paskapoo Formation further consists of subordinate interbedded hard to soft mudstone, siltstone and sandstone, chocolate brown to greenish-grey siltstone and mudstone, shale, with additional limestone, coal, pebble conglomerate and bentonite (McLean, 1990). Thin coal beds are

usually always present, but can reach economic thicknesses in certain parts of the formation (for example, the Obed-Marsh coal zone northeast of Hinton), and lenses of quartzite pebbles become common westwardly (Locker, 1973). Conglomerates are a minor constituent, and when present constitute only thin, lenticular cobble layers (a notable exception to this is the Entrance Conglomerate) (Demchuk and Hills, 1991). Primary sedimentary structures are generally absent, with the exception of minor trough cross-bedding and rare planar and ripple cross-lamination (Demchuk and Hills, 1991). Demchuk and Hills (1991) recently designated and diagnosed three members of the Paskapoo Formation on the basis of lithologic information retrieved from outcrops and core samples. These members (Haynes, Lacombe, and Dalehurst, in ascending superpositional order) are identifiable in outcrop and are useful in placing isolated outcrops in their proper stratigraphic context. The fossil mammal localities included in the present study are exposed at outcrops on the Blindman River and Red Deer River, and at a large roadcut at Joffre Bridge east of Red Deer (see later in the text), and have been referred to the Lacombe Member: the Lacombe Member is primarily argillaceous, and is characterized by an abundance of light grey to olive green, fine-grained siltstones, mudrocks, and shales, with buff-weathering, planar to wavy-bedded sandstones being less prominent than in the underlying Haynes Member (Demchuk and Hills, 1991). Hoffman and Stockey (1999) suggested that the lowermost levels of the Joffre Bridge Roadcut locality may straddle the boundary between the Haynes and Lacombe members.

1.3 Localities

The study localities are clustered in two distinct but geographically proximate areas. The first set, collectively referred to here as the Blindman River localities, occurs at successive cutbanks on the Blindman River southeast of the village of Blackfalds, Alberta, approximately 10 km north of the City of Red Deer, and at the confluence of the Blindman and Red Deer rivers approximately 1.5 km downstream of Mel's Place (see later in the text) (Fox, 1990a; Fig. 3). The Blindman River localities include Dennis Wighton (DW) localities DW-1, DW-2, and DW-3, as well as Mel's Place, and the Burbank locality. The second set of localities occurs near Joffre Bridge, approximately

12 km east of Red Deer; Joffre Bridge crosses the Red Deer River approximately 18 km downstream of its confluence with the Blindman River. The Joffre Bridge localities include the Joffre Bridge Roadcut localities, Joffre Bridge Mammal Site No. 1, and Erickson's Landing (Fox, 1990a; Fig. 3). The study localities are discussed in detail as follows.

Blindman River and Burbank localities.—The Blindman River localities occur in NE1/4, S13-14, T39, R27, W4, at an altitude of approximately 838m above sea level (Fox, 1990a; Figs. 3, 4). Dennis Wighton discovered sites DW-1 through 3 in 1977, and Melanie Fox discovered Mel's Place in 1981. DW-1, the first of the Blindman localities to be discovered, is now exhausted, likely having been a small lens of concentrated mammalian remains (Fox, 1990a). DW-2 has yielded the bulk of specimens from the Blindman localities, being quarried from 1978 to the present. Mel's Place and DW-3 have been sampled infrequently, as high river levels have often limited their access. The Burbank localities refer to series of outcrops at the confluence of the Blindman and Red Deer rivers in S13, T39, R27, W4, at an altitude of approximately 838m asl (Fox, 1990a). A. Speirs discovered the locality in 1977, and collected the first mammalian fossil, a well-preserved dentary of a primitive eutherian. Since their discovery, the Blindman River localities have produced an extraordinary number of vertebrate specimens, including extensively preserved multituberculate and "necrosaurid" skeletons, incomplete mammalian skulls, and complete and nearly complete jaws with teeth. The Blindman River localities are contained in sediments that, in part, comprise the composite stratotype section of the Paskapoo Formation (McLean, 1990). The strata consist primarily of olive green to grey, generally friable silty shales, montmorillonitic shale and claystone, and thin beds of freshwater limestone, clay pebble conglomerate, and lacustrine clays (Hickey and Peterson, 1978; Taylor and Stockey, 1984). A persistent lignite, possibly the same one noted by Tyrrell (1887), occurs at the top of the fossil mammal bearing layer and is a useful marker for visual correlation of the Blindman River localities.

The exposure at DW-2, the best sampled of the Blindman River localities, consists of an approximately 5 m vertical section that consists of:

a) Well-indurated grey-green argillaceous siltstones basally, containing well-preserved freshwater gastropods and bivalves, fragmentary plant fossils, rare insect fossils, and

isolated but often abundant fish scales; an incomplete but well-preserved amiid skull was also recovered from this layer (Grande et al., 2000);

b) A dark silty shale resting conformably on the basal layer; it contains abundant but badly broken freshwater molluscs and rare mammalian fossils;

c) A black, mollusc-rich shale resting conformably on the dark silty layer; this layer contains well-preserved fossil mammals and non-mammalian vertebrates (see later in the text), and abundant, badly broken freshwater molluscs;

d) A 2-10 cm lignite resting on top of the mammal layer;

e) A 3-30 cm layer of light to dark grey montmorillonitic shale and silty shale occurring above the lignite; these sediments contain well-preserved plant fossils (Taylor and Stockey, 1984); this layer is capped by approximately 1 m of montmorillonitic claystone and sandstone;

f) Glacial till occurring at the top of the sequence, just below prairie level.

The predominantly fine-grained, generally darkly coloured sediments at the Blindman River localities argue for deposition having been in oxygen-poor stagnant or slow moving fluvial systems in flood basins adjacent to active or abandoned stream channels (Hickey and Peterson, 1978; Taylor and Stockey, 1984; Reineck and Singh, 1980; Fox, 1990a), an hypothesis that is strengthened by the associated fossil mammals. Although most of the mammalian skeletal remains have been disarticulated, they bear little evidence of having been transported a significant distance; additionally, the majority of mammals preserved at the Blindman River localities are of small body size (as estimated from tooth dimensions), further suggesting a low-energy depositional system. The presence of moisture-tolerant fossil plants, particularly specimens of the sphenopsid Equisetum and the taxodiaceous conifer Glyptostrobus Endlicher (see, e.g., Henry and McIntyre, 1926), in addition to the prominent lignite bed indicates that the depositional environment was probably warm, humid, and probably heavily vegetated, and may have developed as backswamps or even large shallow lakes (R. Russell, 1967). Pockets of freshwater molluscs and vertebrate remains are characteristic of flood basin deposits, and these may be frequently exposed subaerially (Reineck and Singh, 1980); many of the mammalian fossils from the Blindman River localities bear evidence of such exposure (e.g., tooth marks from scavenging).

Joffre Bridge Roadcut.—The Joffre Bridge Roadcut is located approximately 12 km east of Red Deer; it was exposed in 1978 during a relocation project for Highway 11 (Fox, 1990a; Figs. 3, 5). The site is in NW1/4S13, T38, R26, W4, at an altitude of 818m asl (lower level) and 838m asl (upper level). The first mammal remains were discovered by D. Wighton in 1978 in what has been dubbed the "lower level"; since that time, many well-preserved specimens have been recovered by A. Speirs and field parties from the UALVP. The vertebrate fossils are preserved in unstratified grey clay, poorly lithified brown mudstones and siltstones, and in fissile black shales (Fox, 1990a). To date, well-preserved plant (see, e.g., Hoffman and Stockey, 1999), insect (see, e.g., Wilson, 1978), fish (see, e.g., Wilson, 1996), and mammal remains (see, e.g., Fox, 1990a) have been recovered, most notably a rich deposit of teleost fish and the skull and postcranium of two large titanoideid pantodonts. Comprehensive studies on the stratigraphy, sedimentology, and paleoenvironmental context of the Joffre Bridge Roadcut by Hoffman (1995) and Hoffman and Stockey (1999) render detailed descriptions here unnecessary; a brief overview of the entire section is provided here, with special attention given to the fossil mammal horizons.

Hoffman (1995) and Hoffman and Stockey (1999) identified seven distinct, vertically sequential stratigraphic units representing five stages of deposition:

a) A basal silty mudstone comprises Unit 1. The layer is characterized by root traces and sporadic, broken mollusc shells, but other identifiable fossils have yet to be discovered in this unit.

b) Unit 2 is equivalent to the Joffre Bridge Roadcut lower level of Fox (1990a). The layer consists of approximately 10 cm of grey clay overlain by a thin 1-2 cm coal seam and a thick, massively bedded coarse to medium grained sandstone. Fossil vertebrates are rare but well-preserved when present; many of the mammal jaws recovered in this unit were oriented subvertically. Macrofloral fossils are not present. Hoffman and Stockey (1999) interpreted units 1 and 2 as having been deposited in a floodplain environment, with the absence of plant fossils being the result of post-depositional bioturbation and pedogenesis; the near-vertical orientation of many of the vertebrate specimens may also have resulted from post-depositional pedogenesis.

c) Unit 3 consists of in excess of 10 m of fluvially deposited, grey to buff, fine- to medium-grained sandstone, with minor sideritic concretions and silty clasts. Vertebrate fossils are not present in Unit 3, but macrofloral fossils, mostly poorly preserved fruits of the magnoliopsid Joffrea Crane et Stockey, occur above the contact with the underlying Unit 2, but better-preserved fruits and leaves have been recovered from the silty clasts. Hoffman and Stockey (1999) indicated that the sequence becomes finer-grained upwards, grading into the overlying Unit 4, suggesting decreasing flow and the onset of channel abandonment.

d) Unit 4 consists primarily of green-grey siltstone with interbedded lenses of fine-grained sandstone, mudstone, and claystone that become more frequent towards the top of the unit; sedimentary structure is limited to parallel to slightly wavy bedding throughout the unit. Fossilized remains of leaves and reproductive structures are common, with in situ seedlings of Joffrea and the Joffre plane tree (a relative of modern Platanus Linnaeus, see Pigg and Stockey, 1991) present in the lower half of the unit (see Hoffman and Stockey, 1999, fig. 4). Faunal remains are restricted to mollusc shells, fish scales, and impressions of insect wings and larvae in the lower half of the unit (Wighton, 1982; Wighton and Wilson, 1986). Unit 4 apparently represents a continuation of channel abandonment that was initiated towards the top of Unit 3 (Hoffman, 1995; Hoffman and Stockey, 1999).

e) Unit 5 is equivalent to the Mollusc Layer of Taylor and Stockey (1984), and is characterized by well-cemented dark brown to black siltstones, carbonaceous mudstones, and lenses of coal (see Hoffman and Stockey, 1999, fig. 5). The layer is replete with the shells of small freshwater gastropods and bivalves, many of which are unbroken. Although fossilized remains of mammals and fish are rare in this unit, at least one skeleton of the osteoglossomorph Joffrichthys Li and Wilson has been recovered. Hoffman (1995) and Hoffman and Stockey (1999) have interpreted the dark, mollusc-rich sediments of Unit 5 as having been deposited in a poorly drained swamp environment.

f) Unit 6 is an approximately 1 m coarsening upward sequence of light brown to green mudstone and siltstone; Hoffman (1995) and Hoffman and Stockey (1999) divided Unit 6 into four subdivisions based on fossil content of which the lowermost, or Concretion Zone (6a), contains the fossilized remains of vertebrates. Zone 6a (equivalent to the

"upper level" of Fox, 1990a) consists of poorly consolidated buff to light grey mudstone and siltstone, with occasional calcitic concretions developed near the base of the unit. Plant remains are common and consist mostly of branches of the taxodiaceous conifers Glyptostrobus and Metasequoia Miki, as well as rarer leaves of the magnoliopsid Beringiaphyllum Manchester, Crane, et Golovneva (see Hoffman and Stockey, 1999, fig. 6). Zone 6a is significant for having produced two incomplete but well-preserved pantodont specimens, both of which include the skull and significant parts of the postcranium. Unit 6 is notable in its preservation of parts of free-floating aquatic plants (Stockey, Hoffman, and Rothwell, 1997; Hoffman and Stockey, 1999). The upper most parts of Unit 6, the Fish Layer (Zone 6d), are significant in preserving a mass-death assemblage of over 1700 articulated skeletons of three species of freshwater teleosts (Wilson, 1996), the majority of which are referable to the paracanthopterygian Massamorichthys Murray; 69 specimens are referable to the osmerid Speirsaenigma Wilson and Williams, and two specimens are referable to the osteoglossid Joffrichthys. g) Unit 7 caps the sequence: it consists of medium-grained sandstone with evidence of trough cross-bedding (see Hoffman and Stockey, 1999, fig. 7). Hoffman (1995) and Hoffman and Stockey (1999) have interpreted Units 6 and 7 as having been deposited as a crevasse splay, with the lower parts possibly representative of the distal margin of the splay.

Joffre Bridge Mammal Site No. 1.—Joffre Bridge Mammal Site No. 1 is located across the Red Deer River, north and somewhat east of the Joffre Bridge Roadcut localities, in SW1/4S24, T38, R26, W4, at about 830 m asl (Fox, 1990a; Figs. 3, 6). D. Krause discovered the first fossil mammals in 1974; since that time, field parties from the UALVP have quarried additional specimens, resulting in a small collection. The fossils are preserved in dark grey to brown siltstones and black fissile shales that are rich in broken mollusc shells, and a thin lignite lies directly on top of the fissile shale. The setting is similar to, although approximately 8 m lower, than that seen at the Blindman River localities (see earlier in the text); given the regional dip towards the east and the similarity in fossil content, it is likely that the fossiliferous layers at the Blindman River localities and the Joffre Bridge Mammal Site No. 1 are correlative. In addition to well-preserved mammal fossils, a number of amiid bones and scales, as well as bones of the

choristodere Champsosaurus Cope, have been recovered at this locality (Fox, 1990a). Hoffman (1995) and Hoffman and Stockey (1999) have indicated that lenses of unstratified grey clay, similar to that seen in Unit 2 of the Joffre Bridge Roadcut section, are sometimes present at the base of massively bedded sandstone cliffs on the north side of the river, but their stratigraphic position relative to the fossiliferous layers identified here is uncertain.

Erickson's Landing.—The fossils from the locality known as Erickson's Landing represent the first record of Paleocene mammals in Canada (Brown, 1914; Simpson, 1927; Fox, 1990a; Fig. 3). The sample was collected by Barnum Brown and field party from a slump block on the banks of the Red Deer River near Erickson's Landing, although the exact location of the original block and its origin have yet to be determined (Krause, 1978). Fox (1990a), citing personal communication from L. S. Russell, has indicated that the original slump block occurred at the base of the river bank that contains the Joffre Bridge Mammal Site No. 1, but that there was no way to determine from which of the two shell beds cropping out in the area the slump was derived. Stonley (1988) cited reference to the Erickson's Landing fauna by Allan and Sanderson (1945), who suggested that Brown collected the mammal specimens from a slumped block of sandstone at the Brookseley Bridge, the original pilings of which are located alongside those of the current Joffre Bridge. Although it is probable that the slump originally came from what is currently recognized as Joffre Bridge Mammal Site No. 1, the continued uncertainties regarding its provenance argue for treating Erickson's Landing as a separate locality. The faunule includes the holotypes of Elpidophorus elegans Simpson, 1927 and Propalaeosinopa albertensis Simpson, 1927.

Other localities of Paleocene age in the Alberta Basin are cited in this study, and in some cases specimens from these localities are included in the systematic paleontology as referred specimens or, more rarely, as type specimens (e.g., the type specimen of one of the new species of the insectivoran Limaconyssus described in this study is from the late middle Paleocene Gao Mine locality of south central Alberta). Information on the location and geology of these localities, as well as the relative age of the local faunas is presented in Fox (1988, 1990a), Stonley (1988), Youzwyshyn (1988), MacDonald (1996), Webb (1996), Scott et al. (2002), and Scott (2003, 2004, 2006).

1.4 Dental Terminology, Measurements, and Conventions

All measurements were made by the author using a Wild M3 Zoom binocular microscope with 10X oculars fitted with a micrometer calibrated against a millimetre scale. Measurements were estimated to the nearest tenth of a millimetre, the finest degree of accuracy that could be reproduced consistently. Anatomical terminology follows the Nomina Anatomica Veterinaria (1994) where possible, rather than anthropological conventions (e.g., the distolateral bone in the carpus is referred to as the unciform, rather than the hamate, and the proximal bone in the tarsus is referred to as the astragalus, rather than the talus). Anatomical direction with respect to teeth follows standard odontological conventions, with the terms anterior, posterior, labial, and lingual used for cheek teeth; anterior, posterior, lateral, and medial are used with respect to incisors. Anatomical direction with respect to skeletal elements follows standard zoological conventions. Descriptions of many of the mammals in this study require the use of specialized terminology or measurements, and these are described as follows.

Multituberculata.—Multituberculate dental nomenclature follows Krause (1977). Following the results of Hahn (1987), the enlarged, blade-like tooth in the lower dental row is considered to be the lower fourth premolar (p4) rather than the "molar blade" ("m_b") (Sloan, 1981, 1987). "Exodaenodont lobe" refers to the ventral projection of enamel on the labial side of the anterior root on the p4 of many multituberculates. Outline drawings of upper and lower fourth premolars were made with the aid of a camera lucida following the methodology of Jepsen (1940) and Krause (1977).

Cusp number and their expression in formulae follow the methods and rationale of Krause (1977). P4 formulae of the form (w)x:y:z designate cusps of the external (x), middle (y), and internal (z) rows, respectively. Cusps on the anterolabial lobe (w) are hypothesized neomorphs and are listed prior to cusps of the external row. Upper molar cusp formulae of the form x:y:z designate cusps of the external (x), middle (y), and internal (z) rows, respectively. Lower molar cusp formulae of the form x:y designate cusps of the external (labial) (x) and internal (lingual) (y) rows, respectively.

Baseline of standard measurement refers to a line that extends from the apex of the anterobasal concavity posteriorly to the point where the posterolabial shelf intersects the posterior margin of the crown (Krause, 1982). Height of crown of multituberculate p4 (H) is recorded as the perpendicular distance between [the first serration] and the baseline (Krause, 1987, p. 596). L1 is a measure of length of multituberculate p4 along the baseline between perpendicular lines drawn from the anterior crown margin and from the first true serration (Fig. 7). Length (L) is a straight-line measurement of the maximum anteroposterior length of crown. Width of p4 was not measured (Krause, 1977, following the rationale of Ramaekers, 1975).

Therians.—Therian dental nomenclature follows Van Valen (1966) and Szalay (1969) as modified in this study (Fig. 8). Therian incisor nomenclature follows Gingerich (1976). Therian dental measurements follow Clemens (1966). Outline drawings of upper and lower teeth were made with the aid of a camera lucida where applicable. Crown length is a straight-line measurement of the maximum anteroposterior length of crown. Trigonid (TrW) and talonid (TaW) widths represent maximum labiolingual measurements. Specialized, non-standard dental nomenclatures are required for marsupials and carnivorans, and these are briefly described as follows.

Marsupialia.—The naming of stylar cusps on marsupial upper molars follows Clemens (1966); the letter designation of the various stylar cusps (i.e., A-E) implies no homology with ancestral therian cusps (the exception is stylar cusp B, which is probably homologous with the stylocone, or ancestral cusp B, of other therians).

Carnivora.—Carnivoran dental nomenclature follows MacIntyre (1966) for P4 and M1; lower molar dental terminology follows Van Valen (1966) and Szalay (1969) as modified in this study. The carnivoran p4 is highly specialized when compared to that of most other therians: primitively, the crown usually bears an enlarged anterior cusp, a tall protoconid, and one or two large cusps developed on the posterior slope of the protoconid. The anterior cusp is here considered the paraconid, consistent with the opinions of MacIntyre (1966) and Gingerich and Winkler (1985). The homologies of the post-protoconid cusps remain uncertain: MacIntyre (1966) considered the anterior of these cusps as representing the hypoconid, while the second cusp represents a neomorph, the "post-hypoconid", and a small "hypoconulid" can be developed at the summit of the

posterior cingulid. Gingerich and Winkler (1985) agreed with these opinions, but suggested that the second, or more posterior, of the post-protoconid cusps represents the hypoconulid. Flynn and Galiano (1982) suggested that the homologies of these cusps are uncertain and designated the more anterior cusp the "first posterior accessory cusp" and more posterior cusp the "second posterior accessory cusp", and these opinions are followed here. Carnivoran dental measurements follow Gingerich and Winkler (1985).

1.5 Literature Cited

ALLAN, J. A. 1919. Geology of the Swan Hills in Lesser Slave Lake district, Alberta. Geological Survey of Canada Summary Report for 1918, C:7-13.

ALLAN, J. A., and J. O. G. SANDERSON. 1945. Geology of Red Deer and Rosebud sheets, Alberta. Research Council of Alberta, Report No. 13, 115 pp.

ALROY, J. 1999. The fossil record of North American mammals: Evidence for a Paleocene evolutionary radiation. Systematic Biology, 48:107-118.

ALROY, J., P. L. KOCH, and J. C. ZACHOS. 2000. Global climate change and North American mammalian evolution. Paleobiology, 26:259-288.

ARCHIBALD, J. D., and D. H. DEUTSCHMAN. 2001. Quantitative Analysis of the Timing of the Origin and Diversification of Extant Placental Orders. Journal of Mammalian Evolution, 8:107-124.

ARNASON, U., J. A. ADEGOKE, K. BODIN, E. W. BORN, Y. B. ESA, A. GULLBERG, M. NILSSON, R. V. SHORT, XU X., and A. JANKE. 2002. Mammalian mitogenomic relationships and the root of the eutherian tree. Proceedings of the National Academy of Sciences, 99:8151-8156.

BALLY, A. W., P. L. GORDY, and G. A. STEWART. 1966. Structure, seismic data, and orogenic evolution of southern Canadian Rocky Mountains. Bulletin of Canadian Petroleum Geology, 14:337-381.

BOWN, T. M., and M. J. KRAUS. 1979. Origin of the tribosphenic molar and metatherian and eutherian dental formulae, pp. 172-181. In J. A. LILLEGRAVEN, Z. KIELAN-JAWOROWSKA, and W. A. CLEMENS (eds.), Mesozoic Mammals: The First Two-Thirds of Mammalian History, University of California Press, Berkeley.

BOWN, T. M., and D. SCHANKLER. 1982. A review of the Proteutheria and Insectivora of the Willwood Formation (lower Eocene), Bighorn Basin, Wyoming. U. S. Geological Survey Bulletin, 1523:1-79.

BROWN, B. 1914. Cretaceous Eocene correlation in New Mexico, Wyoming, Montana, Alberta. Bulletin of the Geological Society of America, 25:355-380.

CARRIGY, M. A. 1970. Proposed revision of the boundaries of the Paskapoo Formation in the Alberta Plains. Bulletin of Canadian Petroleum Geology 18:156-165.

CARRIGY, M. A. 1971. Lithostratigraphy of the uppermost Cretaceous (Lance) and Paleocene strata of the Alberta Plains. Research Council of Alberta Bulletin 27:161 pp.

CATUNEANU, O., and A. R. SWEET. 1998. Maastrichtian-Paleocene foreland-basin stratigraphies, western Canada: a reciprocal sequence architecture. Canadian Journal of Earth Sciences, 36:685-703.

CLEMENS, W. A. 1966. Fossil mammals of the type Lance Formation, Wyoming. Part II. Marsupialia. University of California Publications in Geological Sciences, 62:1-122.

COOPER, M. 2000. Geological Highway Map of Alberta. Canadian Society of Petroleum Geologists. 1:1 500 000 map.

DAWSON, G. M. 1883. Preliminary report on the Geology of the Bow and Belly River Region, North West Territory, with Special Reference to the Coal Deposits. Geological Survey of Canada, Reports on Progress 1880-1882, Part B.

DAWSON, F. M., C. G. EVANS, R. MARSH, and R. RICHARDSON. 1994. Chapter 24. Uppermost Cretaceous and Tertiary Strata of the Western Canada Sedimentary Basin, pp. 387-406. In G. D. MOSSOP and I. SHETSEN (comps.), Geological Atlas of the Western Canada Sedimentary Basin. Canadian Society of Petroleum Geologists and Alberta Research Council, Calgary and Edmonton.

DEMCHUK, T. D., and L. V. HILLS. 1991. A re-examination of the Paskapoo Formation in the central Alberta Plains: the designation of three new members. Bulletin of Canadian Petroleum Geology 39:270-282.

EDWARDS, W. A. D. 1994. Geological History of Eocene to Pleistocene deposits, p. 397. In G. D. MOSSOP and I. SHETSEN (comps.), Geological Atlas of the Western

Canada Sedimentary Basin. Canadian Society of Petroleum Geologists and Alberta Research Council, Calgary and Edmonton.

FLYNN, J. J., and H. GALIANO. 1982. Phylogeny of early Tertiary Carnivora, with a description of a new species of Protictis from the middle Eocene of northwestern Wyoming. American Museum Novitates, 2725:1-64.

FOOTE, M., J. P. HUNTER, C. M. JANIS, and J. J. SEPKOSKI, JR. 1999. Evolutionary and preservational constraints on origins of biologic group: divergence times of eutherian mammals. Science, 283:1310-1314.

FOX, R. C. 1971a. Early Campanian multituberculates (Mammalia: Allotheria) from the Upper Milk River Formation, Alberta. Canadian Journal of Earth Sciences, 8:916-938.

FOX, R. C. 1971b. Marsupial mammals from the Early Campanian Milk River Formation, Alberta, Canada, pp. 145-164. In D. M. KERMACK and K. A. KERMACK (eds.), Early Mammals. Zoological Journal of the Linnean Society, 50, supplement to no. 1, London.

FOX, R. C. 1984a. First North American record of the Paleocene primate Saxonella. Journal of Paleontology, 58:892-894.

FOX, R. C. 1984b. The dentition and relationships of the Paleocene primate Micromomys Szalay, with description of a new species. Canadian Journal of Earth Sciences, 21:1262-1267.

FOX, R. C. 1984c. A new species of the Paleocene primate Elphidotarsius Gidley: Its stratigraphic position and evolutionary relationships. Canadian Journal of Earth Sciences, 21:1268-1277.

FOX, R. C. 1984d. Melaniella timosa, n. gen. and sp., an unusual mammal from the Paleocene of Alberta, Canada. Canadian Journal of Earth Sciences, 21:1335-1338.

FOX, R. C. 1984e. Paranyctoides maleficus (new species), an early eutherian mammal from the Cretaceous of Alberta, pp. 9-20. In R. M. MENGEL (ed.), Papers in Vertebrate Paleontology Honoring Robert Warren Wilson, Carnegie Museum of Natural History, Special Publication.

FOX, R. C. 1988. Late Cretaceous and Paleocene mammal localities of southern Alberta. Occasional Paper of the Tyrrell Museum of Palaeontology, 6:1-38.

FOX, R. C. 1990a. The succession of Paleocene mammals in western Canada, pp. 51-70. In T. M. BOWN and K. D. ROSE (eds.), Dawn of the Age of Mammals in the Northern Part of the Rocky Mountain Interior, North America, Geological Society of America Special Paper, 243.

FOX, R. C. 1990b. Pronothodectes gaoi n. sp., from the late Paleocene of Alberta, Canada, and the early evolution of the Plesiadapidae (Mammalia, Primates). Journal of Paleontology, 64:637-647.

FOX, R. C. 1991a. Saxonella (Plesiadapiformes: ?Primates) in North America: S. naylori, sp. nov., from the late Paleocene of Alberta, Canada. Journal of Vertebrate Paleontology, 11:334-349.

FOX, R. C. 1991b. Systematic Position of Pronothodectes gaoi Fox from the Paleocene of Alberta: Reply. Journal of Paleontology, 65:700-701.

FOX, R. C. 1994. The primitive dental formula of the Carpolestidae (Plesiadapiformes, Mammalia) and its phylogenetic implications. Journal of Vertebrate Paleontology, 13 (for 1993):516-524.

FOX, R. C. 2002. The dentition and relationships of Carpodaptes cygneus (Russell) (Carpolestidae, Plesiadapiformes, Mammalia), from the late Paleocene of Alberta, Canada. Journal of Paleontology, 76:864-881.

FOX, R. C. 2004. A new palaeoryctid (Insectivora: Mammalia) from the Late Paleocene of Alberta, Canada. Journal of Palaeontology, 78:612-616.

FOX, R. C. 2005. Microcosmodontid multituberculates (Allotheria, Mammalia) from the Paleocene and Late Cretaceous of western Canada. Palaeontographica Canadiana, 23:1-109.

FOX, R. C., and B. G. NAYLOR. 2006. Stagodontid marsupials from the Late Cretaceous of Canada and their systematic and functional implications. Acta Palaeontologica Polonica, 51:13-36.

GAO, K-Q., and R. C. FOX. 1996. Taxonomy and evolution of Late Cretaceous lizards (Reptilia: Squamata) from western Canada. Bulletin of the Carnegie Museum of Natural History, 33:1-107.

GINGERICH, P. D. 1976. Cranial anatomy and evolution of early Tertiary Plesiadapidae (Mammalia, Primates). Museum of Paleontology, The University of Michigan, Papers on Paleontology, 15:1-140.

GINGERICH, P. D. 1983. New Adapisoricidae, Pentacodontidae, and Hyopsodontidae (Mammalia, Insectivora and Condylarthra) from the late Paleocene of Wyoming and Colorado. Contributions from the Museum of Paleontology, The University of Michigan, 26:227-255.

GINGERICH, P. D., and D. A. WINKLER. 1985. Systematics of Paleocene Viverravidae (Mammalia, Carnivora) in the Bighorn Basin and Clark's Fork Basin, Wyoming. Contributions from the Museum of Paleontology, The University of Michigan, 27:87-128.

GRANDE, L., LI G.-Q., and M. V. H. WILSON. 2000. Amia cf. pattersoni from the Paleocene Paskapoo Formation of Alberta. Canadian Journal of Earth Sciences, 37: 31-37.

HAHN, G. 1987. Neue Beobachtungen zum Schädel- und Gebiss-Bau der Paulchoffatiidae (Multituberculata, Ober-Jura). Palaeovertebrata, 17:155-196.

HENRY, A., and M. MCINTYRE. 1926. The swamp cypresses, Glyptostrobus of China and Taxodium of America, with notes on allied genera. Proceedings of the Royal Irish Academy, 37(B):90-114.

HICKEY, L. J., and R. K. PETERSON. 1978. Zingiberopsis, a fossil genus of the ginger family from late Cretaceous to early Eocene sediments of western interior North America. Canadian Journal of Botany, 56:1136-1152.

HOFFMAN, G. L. 1995. Paleobotany and paleoecology of the Joffre Bridge Roadcut locality (Paleocene), Red Deer, Alberta. Unpublished M. Sc. thesis, University of Alberta, Edmonton, 208 pp.

HOFFMAN, G. L., and R. A. STOCKEY. 1999. Geological setting and paleobotany of the Joffre Bridge Roadcut fossil locality (late Paleocene), Red Deer Valley, Alberta. Canadian Journal of Earth Sciences, 36:2073-2084.

JEPSEN, G. L. 1940. Paleocene faunas of the Polecat Bench Formation, Wyoming. Proceedings of the American Philosophical Society, 83:217-340.

JERZYKIEWICZ, T. 1997. Stratigraphic framework of the uppermost Cretaceous to Paleocene strata of the Alberta Basin. Geological Survey of Canada Bulletin, 510:1-20.

KRAUSE, D. W. 1977. Paleocene multituberculates (Mammalia) of the Roche Percée local fauna, Ravenscrag Formation, Saskatchewan, Canada. Palaeontographica Abteilung A, 186:1-36.

KRAUSE, D. W. 1978. Paleocene primates from western Canada. Canadian Journal of Earth Sciences, 15:1250-1271.

KRAUSE, D. W. 1982. Evolutionary history and paleobiology of early Cenozoic Multituberculata (Mammalia), with emphasis on the family Ptilodontidae. Unpublished Ph. D. dissertation, The University of Michigan, Ann Arbor, 575 pp.

KRAUSE, D. W. 1987. Baiotomeus, a new ptilodontid multituberculate (Mammalia) from the middle Paleocene of western North America. Journal of Paleontology, 61:595-603.

KRAUSE, D. W., and M. C. MAAS. 1990. The biogeographic origins of late Paleocene-early Eocene mammalian immigrants to the Western Interior of North America, pp. 71-105. In: T. M. BOWN and K. D. ROSE (eds.), Dawn of the Age of Mammals in the Northern Part of the Rocky Mountain Interior, Geological Society of America, Special Paper, 243:71-105.

KRISHTALKA, L. 1973. Late Paleocene mammals from the Cypress Hills, Alberta. Special Publications of the Museum, Texas Tech University, 2:1-77.

KRISHTALKA, L. 1976a. Early Tertiary Adapisoricidae and Erinaceidae (Mammalia, Insectivora) of North America. Bulletin of Carnegie Museum of Natural History, 1:1-40.

KRISHTALKA, L. 1976b. North American Nyctitheriidae (Mammalia, Insectivora). Annals of Carnegie Museum, 46:7-28.

KUMAR S., and S. B. HEDGES. 1998. A molecular timescale for vertebrate evolution. Nature, 392:917-920.

LECKIE, D. A., and R. J. CHEEL. 1989. Sedimentology of the Cypress Hills Formation (U. Eocene to Miocene): a semi-arid braidplain deposit. Canadian Journal of Earth Sciences, 26:1918-1931.

LERBEKMO, J. F., and K. C. COULTER. 1985. Late Cretaceous to early Paleocene magnetostratigraphy of a continental sequence: Red Deer Valley, Alberta, Canada. Canadian Journal of Earth Sciences, 22:567-583.

LERBEKMO, J. F., and R. M. ST. LOUIS. 1986. The terminal Cretaceous iridium anomaly in the Red Deer River valley, Alberta, Canada. Canadian Journal of Earth Sciences, 23:120-124.

LERBEKMO, J. F., and A. R. SWEET. 2000. Magnetostratigraphy and biostratigraphy of the continental Paleocene in the Calgary area, southwestern Alberta. Bulletin of Canadian Petroleum Geology, 48:285-306.

LERBEKMO, J. F., M. E. EVANS, and G. S. HOYE. 1990. Magnetostratigraphic evidence bearing on the magnitude of the sub-Paskapoo disconformity in the Scollard Canyon-Ardley area of the Red Deer Valley, Alberta. Bulletin of Canadian Petroleum Geology, 38:197-202.

LERBEKMO, J. F., A. R. SWEET, and D. R. BRAMAN. 1995. Magnetobiostratigraphy of Late Maastrichtian to early Paleocene strata of the Hand Hills, south central Alberta, Canada. Bulletin of Canadian Petroleum Geology, 43:35-43.

LERBEKMO, J. F., A. R. SWEET, and R. M. ST. LOUIS. 1987. The relationship between the iridium anomaly and palynofloral events at three Cretaceous-Tertiary boundary localities in western Canada. Geological Society of America Bulletin, 99:325-330.

LERBEKMO, J. F., T. D. DEMCHUK, M. E. EVANS, and G. S. HOYE. 1992. Magnetostratigraphy and biostratigraphy of the continental Paleocene of the Red Deer Valley, Alberta, Canada. Bulletin of Canadian Petroleum Geology, 40:24-35.

LERBEKMO, J. F., C. SINGH, D. M. JARZAN, and D. A. RUSSELL. 1979. The Cretaceous-Tertiary boundary in south-central Alberta – a revision based on additional

dinosaurian and microfloral evidence, Canada. Journal of Earth Sciences, 16:1866-1968.

LOCKER, J. G. 1973. Petrographic and engineering properties of fine-grained rocks of Central Alberta. Bulletin of the Alberta Research Council, 30:1-144.

LOFGREN, D. L., J. A. LILLEGRAVEN, W. A. CLEMENS, P. D. GINGERICH, and T. E. WILLIAMSON. 2004. Paleocene biochronology: The Puercan through Clarkforkian Land Mammal Ages, pp. 43-105. In M. O. WOODBURNE (ed.), Cenozoic mammals of North America: geochronology and biostratigraphy. Columbia University Press, New York.

MACDONALD, T. E. 1996. Late Paleocene (Tiffanian) mammal-bearing localities in superposition, from near Drumheller, Alberta. Unpublished M.Sc. thesis, University of Alberta, Edmonton, 248 pp.

MACINTYRE, G. T. 1966. The Miacidae (Mammalia, Carnivora). Part I. The systematics of Ictidopappus and Protictis. Bulletin of the American Museum of Natural History, 131:115-210.

MAAS, M. C., M. R. L. ANTHONY, P. D. GINGERICH, G. F. GUNNELL, and D. W. KRAUSE. 1995. Mammalian generic diversity and turnover in the late Paleocene and early Eocene of the Bighorn and Crazy Mountains basins, Wyoming and Montana (USA). Palaeogeography, Palaeoclimatology, Palaeoecology, 115:181-207.

MATTHEW, W. D. 1914. Evidence of the Paleocene vertebrate fauna on the Cretaceous-Tertiary problem. Bulletin of the Geological Society of America, 25:381-402.

MCDOWELL, S. B. 1958. The Greater Antillean insectivores. Bulletin of the American Museum of Natural History, 115:113-214.

MCLEAN, J. R. 1990. Paskapoo Formation, pp. 480-481. In D. J. GLASS (ed.), Lexicon of Canadian Stratigraphy, volume 4, Western Canada, Canadian Society of Petroleum Geologists, Calgary.

MENG, J., Y. HU, and C. LI. 2003. The osteology of Rhombomylus (Mammalia, Glires): implications for phylogeny and evolution of Glires. Bulletin of the American Museum of Natural History 275:1-247.

MURPHY, W. J., E. EIZIRIK, S. J. O'BRIEN, O. MADSEN, M. SCALLY, C. J. DOUADY, E. TEELING, O. A. RYDER, M. J. STANHOPE, W. W. DE JONG, and M. J. SPRINGER.

2001. Resolution of the early placental mammal radiation using Bayesian phylogenetics. Science, 294: 2348-2351.

NOMINA ANATOMICA VETERINARIA, 4th edition. 1994. Adolf Holzhausen's Successors, Vienna.

NOVACEK, M. J. 1976. Insectivora and Proteutheria of the later Eocene (Uintan) of San Diego County, California. Natural History Museum of Los Angeles County, Contributions in Science, 283:1-52.

NOVACEK, M. J. 1985. The Sespedectinae, a new subfamily of hedgehog-like insectivores. American Museum Novitates, 2833:1-24.

NOVACEK, M. J. 1999. 100 million years of land vertebrate evolution: the Cretaceous-Early Tertiary Transition. Annals of the Missouri Botanical Garden, 86:230-258.

NOVACEK, M. J., T. M. BOWN, and D. SCHANKLER. 1985. On the classification of the early Tertiary Erinaceomorpha (Insectivora, Mammalia). American Museum Novitates, 2822:1-22.

PIGG, K. B. and R. A. STOCKEY. 1991. Platanaceous plants from the Paleocene of Alberta, Canada. Review of Palaeobotany and Palynology, 70:125-146.

RAMAEKERS, P. 1975. Using polar coordinates to measure variability in samples of Phenacolemur: a method of approach, pp. 106-135. In F. S. SZALAY (ed.), Approaches to primate paleobiology. Contributions to Primatology, 5.

REINECK, H. E., and I. B. SINGH. 1980. Depositional sedimentary environments with reference to terrigenous clastics. Springer-Verlag, Berlin.

ROSE, K. D. 1981a. The Clarkforkian Land Mammal Age and mammalian faunal composition across the Paleocene-Eocene boundary. University of Michigan Papers on Paleontology, 26:1-197.

ROSE, K. D. 1981b. Composition and species diversity in Paleocene and Eocene mammal assemblages: an empirical study. Journal of Vertebrate Paleontology, 1:367-388.

ROSE, K. D. 2006. The Beginning of the Age of Mammals. The Johns Hopkins University Press, Baltimore.

ROSE, K. D., and J. D. ARCHIBALD. 2005. The Rise of Placental Mammals. The Johns Hopkins University Press, Baltimore.

RUSSELL, L. S. 1926. A new species of the genus Catopsalis Cope from the Paskapoo Formation of Alberta. American Journal of Science, 12:230-234.

RUSSELL, L. S. 1928. A new fossil fish from the Paskapoo beds of Alberta. American Journal of Science, 15:103-107.

RUSSELL, L. S.1929a. Paleocene vertebrates from Alberta. American Journal of Science, 17:162-178.

RUSSELL, L. S.1929b. Upper Cretaceous and lower Tertiary gastropods from Alberta. Transactions of the Royal Society of Canada, 23:81-90.

RUSSELL, L. S.1932a. New data on the Paleocene mammals of Alberta, Canada. Journal of Mammalogy, 13:38-54.

RUSSELL, L. S.1932b. The Cretaceous-Tertiary transition of Alberta. Transactions of the Royal Society of Canada 26:121-156.

RUSSELL, L. S.1948. A Middle Paleocene mammal tooth from the Foothills of Alberta. American Journal of Science, 246:152-156.

RUSSELL, L. S.1958. Paleocene mammal teeth from Alberta. National Museum of Canada Bulletin, 147:96-103.

RUSSELL, L. S. 1967. Paleontology of the Swan Hills area, north-central Alberta. Contributions in Life Sciences from the Royal Ontario Museum, 71:1-31.

RUSSELL, R. J. 1967. River and delta morphology. Technical Report No. 52. Coastal Studies Institute, Louisiana State University, Baton Rouge, Louisiana:1-55.

RUTHERFORD, R. L. 1927. Geology along the Bow River between Cochrane and Kananaskis, Alberta. Scientific and Industrial Research Council of Alberta Report, 17:1-29.

SCOTT, C. S. 2003. Late Torrejonian (middle Paleocene) mammals from south central Alberta. Journal of Paleontology, 77:745-768.

SCOTT, C. S. 2004. A new species of the ptilodontid multituberculate Prochetodon (Mammalia, Allotheria) from the Paleocene Paskapoo Formation of Alberta, Canada. Canadian Journal of Earth Sciences, 41:237-246.

SCOTT, C. S. 2006. A new erinaceid (Mammalia, Insectivora) from the late Paleocene of western Canada. Canadian Journal of Earth Sciences 43:1695-1709.

SCOTT, C. S., R. C. FOX, and G. P. YOUZWYSHYN. 2002. New earliest Tiffanian (late Paleocene) mammals from Cochrane 2, southwestern Alberta, Canada. Acta Palaeontologica Polonica, 47:691-704.

SECORD, R. 2004. Late Paleocene biostratigraphy, isotope stratigraphy, and mammalian systematics of the northern Bighorn Basin, Wyoming. Unpublished Ph. D. dissertation, The University of Michigan, Ann Arbor, 532 pp.

SELWYN, A. R. C. 1874. Observations in the Northwest Territory from Fort Gary to Rocky Mountain House. Geological Survey of Canada, Report Program, 1874-1874:17-62.

SIMPSON, G. G. 1927. Mammalian fauna and correlation of the Paskapoo Formation of Alberta. American Museum Novitates, 268:1-10.

SIMPSON, G. G. 1937. The Fort Union of the Crazy Mountain Field, Montana and its mammalian faunas. Bulletin of the United States Museum, 169:1-287.

SLOAN, R. E. 1981. Systematics of Paleocene multituberculates from the San Juan Basin, New Mexico, pp. 127-160. In S. G. LUCAS, J. K. RIGBY, Jr., and B. KUES (eds.), Advances in San Juan Basin Paleontology. University of New Mexico Press, Albuquerque, New Mexico.

SLOAN, R. E. 1987. Paleocene and latest Cretaceous mammals, rates of sedimentation and evolution, pp. 165-200. In J. E. FASSETT and J. K. RIGBY, Jr. (eds.), The Cretaceous–Tertiary Boundary in the San Juan and Raton Basins, New Mexico and Colorado. Geological Society of America Special Paper, 209.

SPRINGER, M. S. 1997. Molecular clocks and the timing of the placental and marsupial radiations in relation to the Cretaceous-Tertiary boundary. Journal of Mammalian Evolution, 4:285-302.

SPRINGER, M. S., W. J. MURPHY, E. EIZIRIK, and S. J. O'BRIEN. 2003. Placental mammal diversification and the Cretaceous-Tertiary boundary. Proceedings of the National Academy of Sciences, U. S. A., 100:1056-1061.

SPRINGER, M. S., A. BURK-HERRICK, R. MEREDITH, E. EIZIRIK, E. TEELING, S. J. O'BRIEN, and W. J. MURPHY. 2007. The adequacy of morphology in reconstructing the early history of placental mammals. Systematic Biology, 56:673-684.

STOCKEY, R. A., G. L. HOFFMAN, and G. W. ROTHWELL. 1997. The fossil monocot Limnobiophyllum scutatum: resolving the phylogeny of Lemnaceae. American Journal of Botany, 84:355-368.

STONLEY, G. J. 1988. Late Paleocene Mammals of the Swan Hills Local Fauna (Paskapoo Formation), Alberta. Unpublished M. Sc. thesis, University of Alberta, Edmonton, 265 pp.

STORER, J. E. 1976. Mammals of the Hand Hills Formation, southern Alberta, pp. 186-209. In C. S. CHURCHER (ed.), Athlon: Essays on palaeontology in honour of Loris Shano Russell, Royal Ontario Museum, Life Sciences Miscellaneous Contributions.

STORER, J. E. 1978. Tertiary sands and gravels in Saskatchewan and Alberta: correlation of mammalian faunas, pp. 595-602. In C. R. STELCK and B. D. E. CHATTERTON (eds.), Western Arctic and Canadian Biostratigraphy, Geological Association of Canada Special Paper, 18.

SWEET, A. R., and L. V. HILLS. 1984. A palynological and sedimentological analysis of the Cretaceous-Tertiary boundary, Red Deer River valley, Alberta, Canada. Sixth International Palynological Conference:160A.

SZALAY, F. S. 1969. Mixodectidae, Microsyopidae, and the insectivore-primate transition. Bulletin of the American Museum of Natural History, 140:193-330.

TAYLOR, T. N., and R. A. STOCKEY. 1984. Field Guide, Second International Organization of Paleobotany Conference, Edmonton, Alberta, pp. 17-24.

TOZER, E. T. 1953. The Cretaceous-Tertiary transition in southwestern Alberta. Alberta Society of Petroleum Geologists Third Annual Field Conference and Symposium:23-31.

TOZER, E. T. 1956. Uppermost Cretaceous and Paleocene non-marine molluscan faunas of western Alberta. Geological Survey of Canada Memoir, 280:1-125.

TYRRELL, J. B. 1887. Report on a part of northern Alberta, and portions of adjacent districts of Assiniboia and Saskatchewan. Geological Survey of Canada, 1886 Summary Report, Part E.

VAN VALEN, L. 1966. Deltatheridia, a new order of mammals. Bulletin of the American Museum of Natural History, 132:1-126.

VAN VALEN, L. 1967. New Paleocene insectivores and insectivore classification. Bulletin of the American Museum of Natural History, 135:217-284.

WEBB, M. W. 1996. Late Paleocene mammals from near Drayton Valley, Alberta. Unpublished M. Sc. thesis, University of Alberta, Edmonton, 258 pp.

WIBLE, J. R., G. W. ROUGIER, M. J. NOVACEK, and R. J. ASHER. 2007. Cretaceous eutherians and Laurasian origin for placental mammals near the K/T boundary. Nature, 447:1003-1006.

WIGHTON, D. C. 1982. Middle Paleocene insect fossils from south-central Alberta, pp. 577-578. In Proceedings of the 3rd North American Paleontological Convention, 2.

WIGHTON, D. C., and M. V. H. WILSON. 1986. The Gomphaeschninae (Odonata: Aeschnidae): new fossil genus, reconstructed phylogeny, and geographical history. Systematic Entomology, 11:505-522.

WILSON, M. V. H. 1978. Paleocene insect faunas of western North America. Quaestiones Entomologicae, 14:13-34.

WILSON, M. V. H. 1996. Taphonomy and paleoecology of a mass-death layer of fishes in a fluvial sequence of the Paleocene Paskapoo Formation, Alberta. Canadian Journal of Earth Sciences, 33:1487-1498.

YOUZWYSHYN, G. P. 1988. Paleocene mammals from near Cochrane, Alberta. Unpublished M. Sc. thesis, University of Alberta, Edmonton, 484 pp.

Figure 1.1.—1. Generalized schematic cross section (southwest-northeast trending) of Front Ranges, Foothills, and Alberta Syncline, and associated strata. Vertical exaggeration approximately 20X. 1, Paskapoo Formation (Paleocene); 2, Scollard Formation (Maastrichtian/Paleocene); 3, Horseshoe Canyon Formation (Maastrichtian); 4, Bearpaw Formation (Late Campanian/Maastrichtian); 5, Belly River Group (Campanian); 6, Alberta Group (Cenomanian-Santonian). Adapted from Cooper (2000). 2. Geographic distribution of Paskapoo, Porcupine Hills, and Coalspur formations (raised light grey topography) in south central and southern Alberta.

1

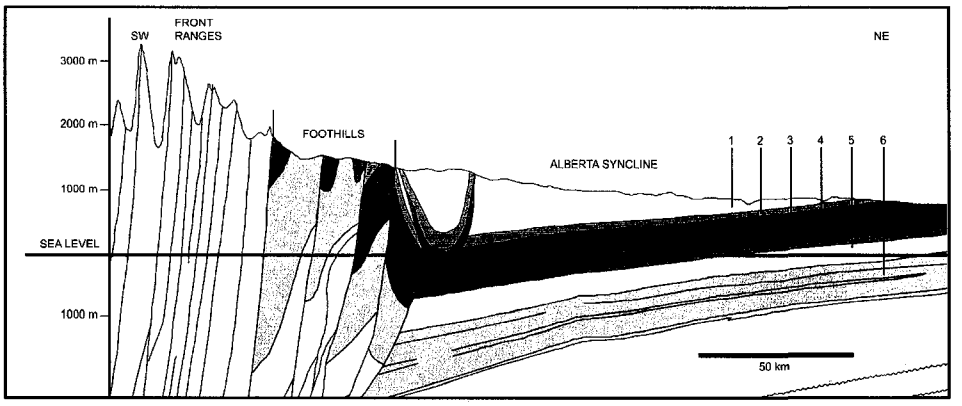
SW
FRONT RANGES
NE
3000 m
2000 m
1000 m
SEA LEVEL
1000 m
FOOTHILLS
ALBERTA SYNCLINE
1
2
3
4
5
6
50 km

2

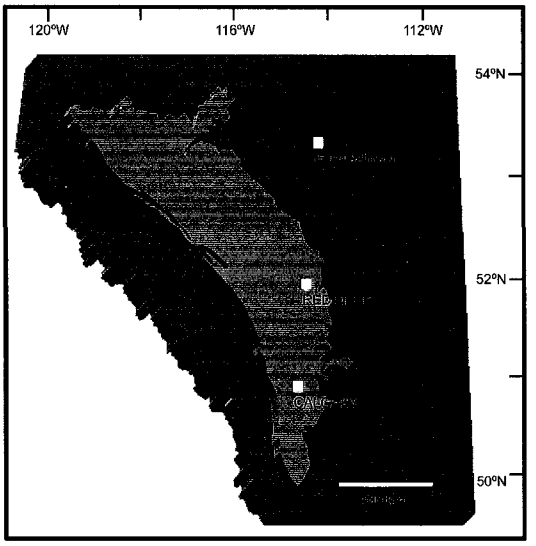
120°W
116°W
112°W
54°N
52°N
50°N

Figure 1.2.—Paskapoo Formation and its correlatives in the northern part of the Western Interior of North America.

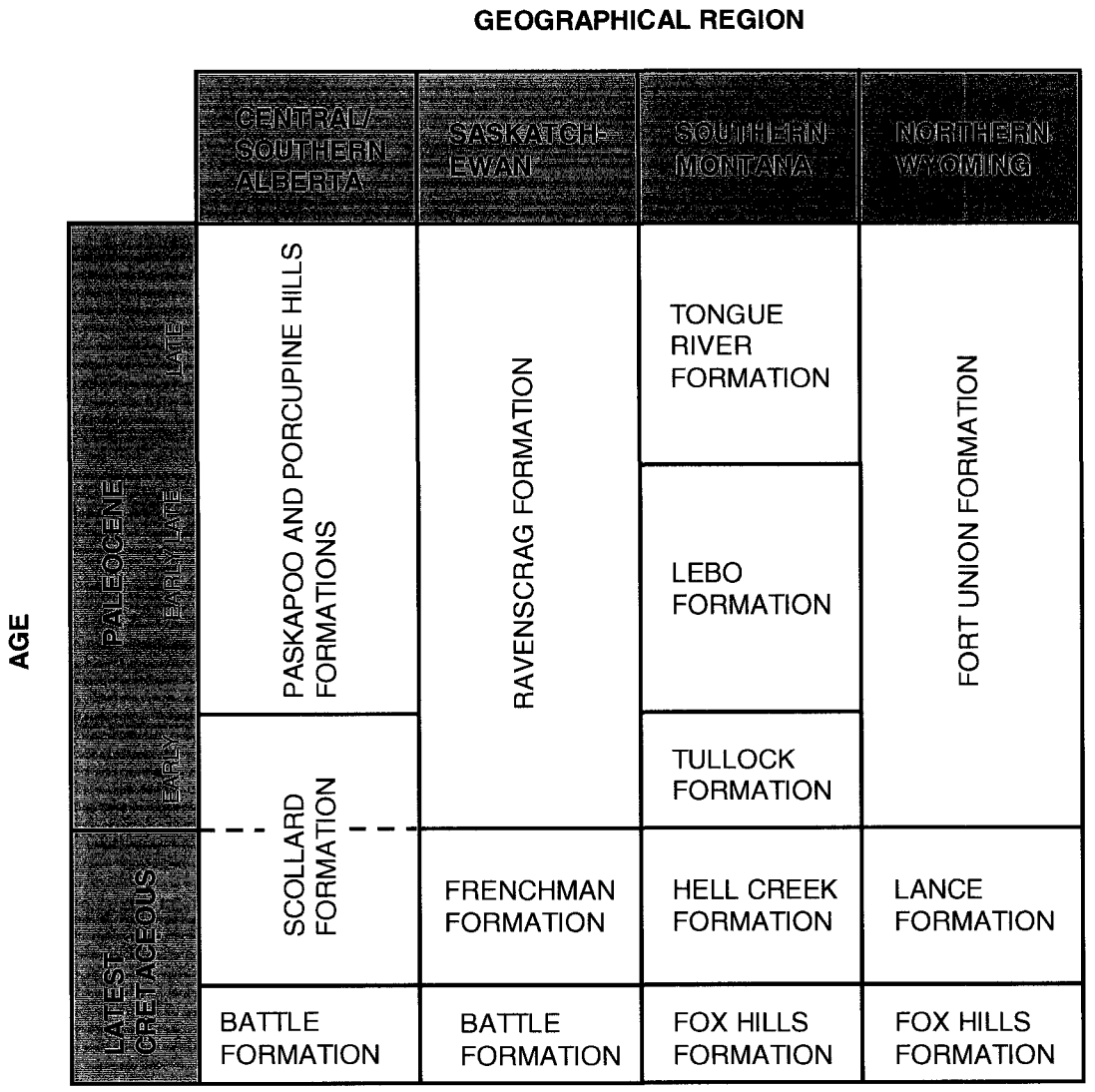
GEOGRAPHICAL REGION
CENTRAL/ SOUTHERN ALBERTA
SASKATCH-EWAN
SOUTHERN MONTANA
NORTHERN WYOMING
AGE
PALEOCENE
LATE
EARLY
LATE
LATEST CRETACEOUS
PASKAPOO AND PORCUPINE HILLS FORMATIONS
RAVENSCRAG FORMATION
TONGUE RIVER FORMATION
LEBO FORMATION
TULLOCK FORMATION
FORT UNION FORMATION
SCOLLARD FORMATION
FRENCHMAN FORMATION
HELL CREEK FORMATION
LANCE FORMATION
BATTLE FORMATION
BATTLE FORMATION
FOX HILLS FORMATION
FOX HILLS FORMATION

Figure 1.3.—Topographic (1) and simplified (2) maps of study areas in south central Alberta. 1, Blindman River localities (DW-1, DW-2, DW-3, Mel's Place; 52°21′N, 113°46′W, UTM coordinates Zone 12; 311 158, 5 804 257, datum=NAD27); 2, Burbank (52°21′N, 113°45′W, UTM coordinates Zone 12; 312 226, 5 804 082, datum=NAD27); 3, Joffre Bridge Roadcut (52°16′N, 113°36′W, UTM coordinates Zone 12; 322 367, 5 794 595, datum=NAD27); 4, Joffre Bridge Mammal Site No. 1 (52°16′N, 113°35′W, UTM coordinates Zone 12; 322 773, 5 795 112, datum=NAD27); 5, ?Erickson's Landing (52°15′N, 113°35′W, UTM coordinates Zone 12; 323 306, 5 793 744, datum=NAD27).

1

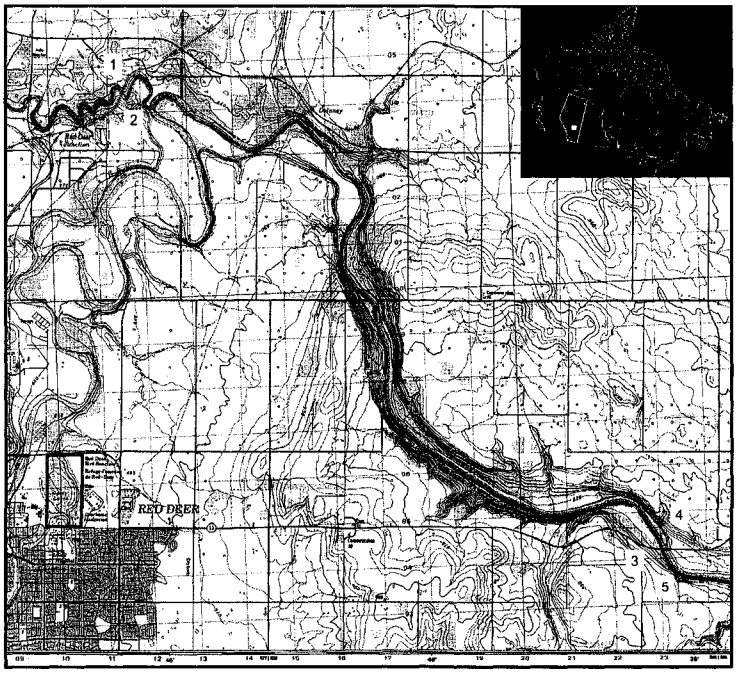

2

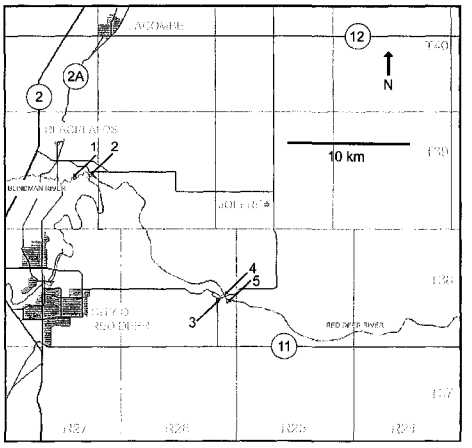

Figure 1.4.—1, 2. DW-2 locality as exposed on Blindman River north of Red Deer, Alberta. 1, view of DW-2 on north bank of Blindman River; 2, view of approximately 3 m of section at DW-2, showing montmorillonitic siltstone (basally), silty shale and mollusc-rich shale of mammal layer (arrow), and overlying montmorillonitic claystone.

1

2

Figure 1.5.—1, 2. Joffre Bridge Roadcut locality as exposed on Provincial Highway 11 14 km east of Red Deer, Alberta. 1, view of present day Joffre Bridge Roadcut on south side of Highway 11, showing approximate locations of lower (L) and upper (U) mammal-bearing layers; 2, Joffre Bridge Roadcut circa 1978 showing pantodont layer (P) (Unit 6a of Hoffman and Stockey, 1999) and Fish Layer (F) (Unit 6d of Hoffman and Stockey, 1999). Photograph courtesy of Mark Wilson.

1

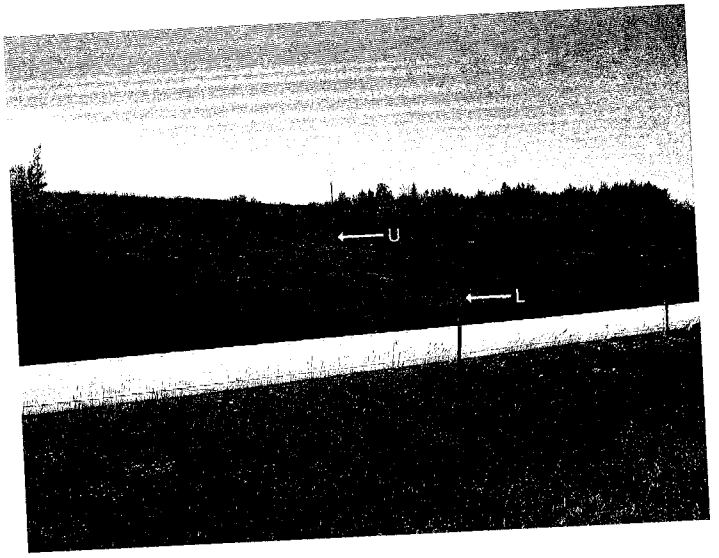

2

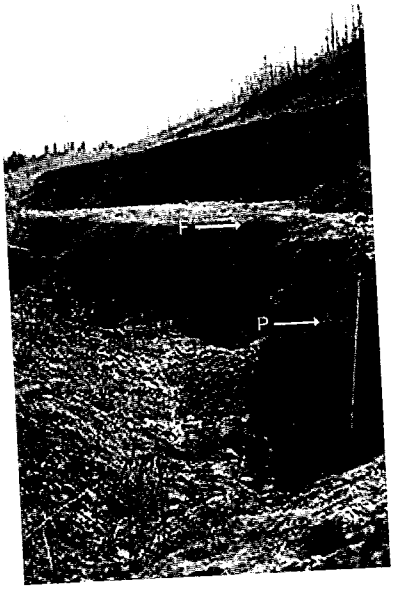

Figure 1.6.—1, 2. Joffre Bridge Mammal Site No. 1 on north bank of the Red Deer River as seen from Joffre Bridge Roadcut (1) and from Joffre Bridge (2). Arrow points to approximate position of dark, mollusc-rich mammal-bearing layer approximately 22 m above river level.

1

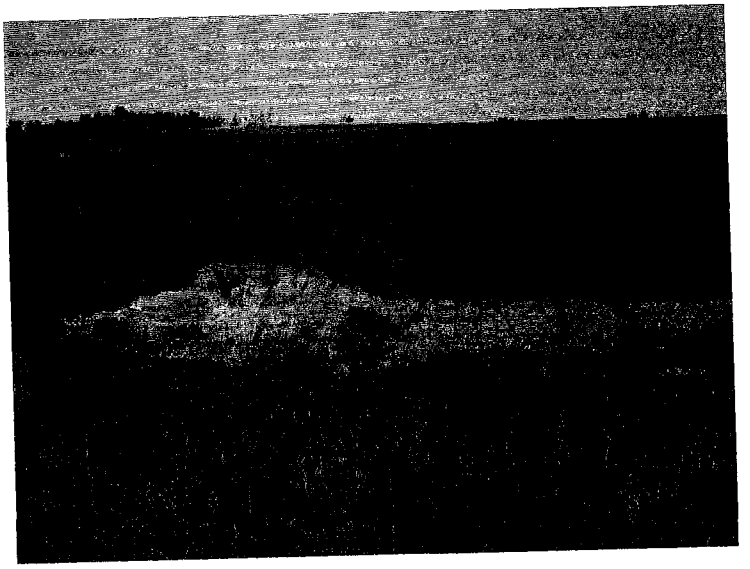

2

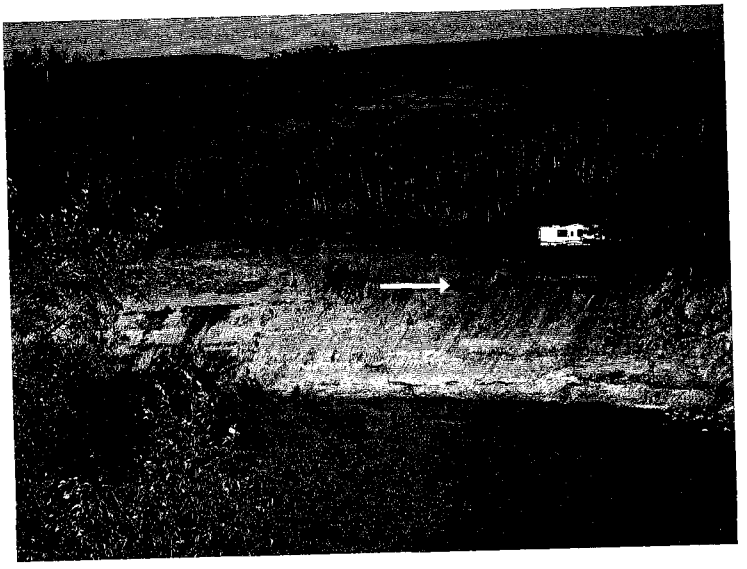

Figure 1.7.—Orientation for standard measurements of multituberculate p4s, labial view (anterior to left). Hatched line represents baseline. H = height, L = length, L1 = length 1. Asterisk points to first serration. Diagram adapted from Sloan (1981).

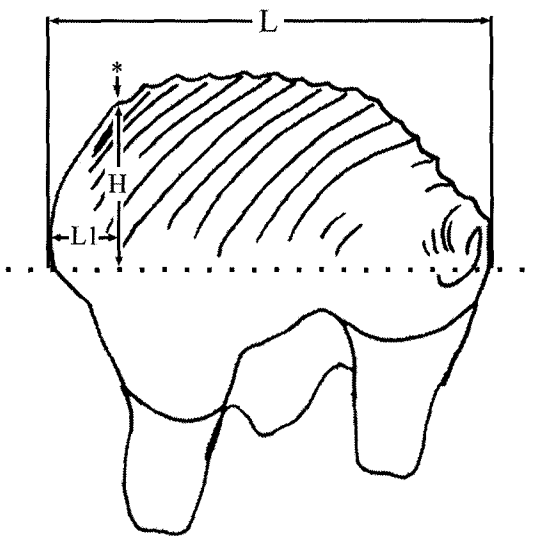
L
*
H
L1

Figure 1.8.—Diagrams of upper (1) and lower (2) therian molars illustrating dental nomenclature as used in this study. Diagram adapted from Bown and Kraus (1979).

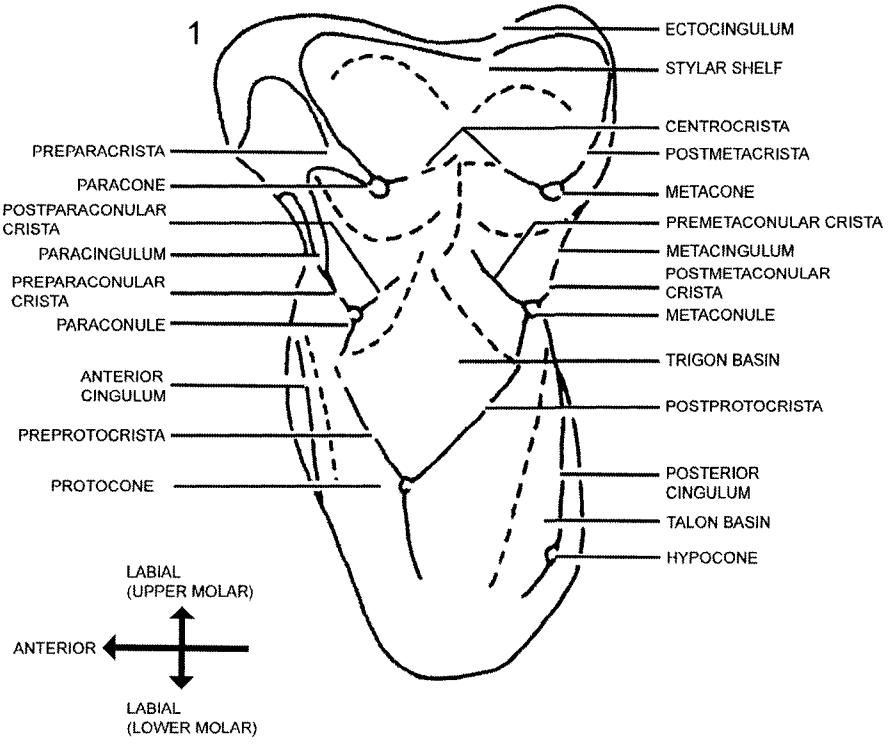
1
ECTOCINGULUM
STYLAR SHELF
CENTROCRISTA
POSTMETACRISTA
METACONE
PREMETACONULAR CRISTA
METACINGULUM
POSTMETACONULAR CRISTA
METACONULE
TRIGON BASIN
POSTPROTOCRISTA
POSTERIOR CINGULUM
TALON BASIN
HYPOCONE
PREPARACRISTA
PARACONE
POSTPARACONULAR CRISTA
PARACINGULUM
PREPARACONULAR CRISTA
PARACONULE
ANTERIOR CINGULUM
PREPROTOCRISTA
PROTOCONE
LABIAL (UPPER MOLAR)
ANTERIOR
LABIAL (LOWER MOLAR)

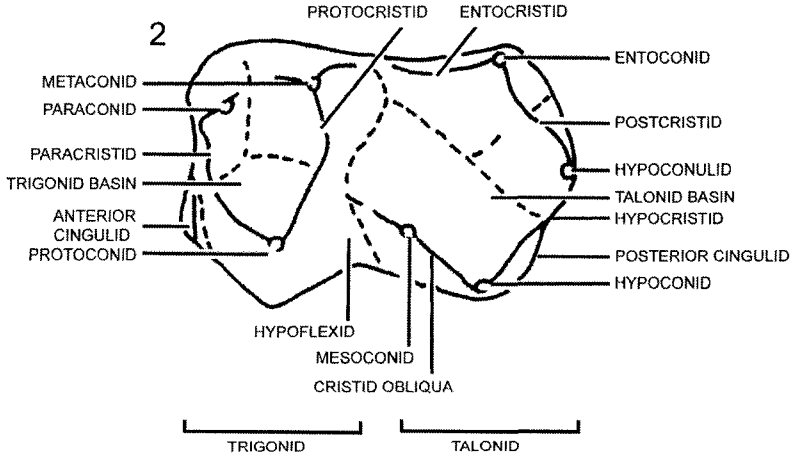
2
PROTOCRISTID
ENTOCRISTID
ENTOCONID
POSTCRISTID
HYPOCONULID
TALONID BASIN
HYPOCRISTID
POSTERIOR CINGULID
HYPOCONID
METACONID
PARACONID
PARACRISTID
TRIGONID BASIN
ANTERIOR CINGULID
PROTOCONID
HYPOFLEXID
MESOCONID
CRISTID OBLIQUA
TRIGONID
TALONID

2 Non-mammalian Fauna and Flora of the Study Localities

2.1 Introduction

WHILE MAMMALS undoubtedly represented a significant part of the fauna that existed during the Paleocene in south central Alberta, the non-mammalian component was equally important, although it is on the whole more poorly represented. Non-mammalian vertebrates and invertebrates have been documented in association with mammalian remains at each of the study localities, while important micro- and macrofloral fossils have been recovered from beds immediately above or below the mammal-bearing horizons. The invertebrates, non-mammalian vertebrates, and flora of the study localities are briefly reviewed below; a complete listing of taxa from the study localities is presented in Appendix 1.

2.2 Invertebrates

Molluscs.—The fossilized remains of molluscs from the Paskapoo Formation were first described from outcroppings in the areas of Calgary and Cochrane in a series of papers by L. Russell (1929, 1931). Although fossil molluscs have been documented at nearly every one of the study localities, either in association with the remains of small vertebrates, or in beds immediately above or below, virtually none have been studied in detail. Mollusc shells were first documented at outcrops on the Blindman River by Tozer (1956) at localities south of Bentley, approximately 10 km northwest of the Blindman River localities; Tozer's (1956) description of the sediments at these localities (grey argillaceous limestone) suggests that these are very likely equivalent to the lowest layers in the Blindman River section at DW-2. Tozer (1956) documented a diverse assemblage of bivalves and gastropods at the Bentley localities, including the bivalve Sphaerium Scopoli and the gastropod Viviparus Montfort. Tozer (1956) recognized a small assemblage of gastropods from the Blindman River at its union with the Red Deer River at what is probably the Burbank locality (as originally recorded by Whiteaves in 1885), and a diverse assemblage of both bivalves and gastropods has been documented in fissile

carbonaceous shales on the north bank of the Red Deer River at what is now recognized as Joffre Bridge Mammal Site No. 1.

Arthropods.—Wighton's interest in fossil insects led to the discovery of the Blindman River localities in 1977, and to the first publications on insects of Paleocene age from Alberta in 1978 (Wilson, 1978a-b) and 1979 (Mitchell and Wighton, 1979). The arthropod fossils that have been discovered at the DW-2, Burbank, and Joffre Bridge Roadcut localities are remarkably diverse, both in terms of taxonomy and life history stages; for example, several specimens preserve the larvae of coleopterans and trichopterans, while fossilized pupae are known for tipulid flies, and nymphal stages are known for odonatans and ephemeropterans (Mitchell and Wighton, 1979; Wighton and Wilson, 1986). The combined taxonomic diversity of the arthropod fauna is high: eight orders representing 18 families of insects have been documented so far, as well as a single order and family of acariform mite. Insect fossils found at the study localities include representatives of a diversity of dragonflies (Odonata), beetles (Coleoptera), flies (Diptera), and true bugs (Hemiptera), as well as rarer fossils of ants (Hymenoptera), mayflies (Ephemeroptera) and caddisflies (Trichoptera) (Wilson, 1978a-b; Wighton, 1980, 1982; Mitchell and Wighton, 1979; Kevan and Wighton, 1981; Wighton and Wilson, 1986). Although the most abundant insect fossils found at the study localities are isolated beetle elytra (Taylor and Stockey, 1984), exquisitely preserved specimens of click beetle (Elateridae) larvae are known, showing the detailed structure of the spiracles and setae, and specimens of adult clubtail dragonflies (Gomphidae) showing the delicate patterns of wing venation are not uncommon (Mitchell and Wighton, 1979; Wighton and Wilson, 1986). Many of the insect taxa discovered at DW-2 and the Joffre Bridge Roadcut have extant relatives that have larval and/or nymphal stages that are aquatic (e.g., odonatans, tipulids, trichopterans), or adults that are aquatic (e.g., belostomatids and dytiscids), consistent with the inferred depositional environment.

2.3 Vertebrates

Fish.—Disarticulated remains of a limited diversity of fish are present at all of the study localities, either in association with fossil tetrapods or in vertically adjacent strata,

although their abundance at each locality can differ significantly: for example, fish are poorly represented at the Blindman River localities, with their record consisting almost entirely of isolated scales, teeth, and occasional skull bones or vertebrae; in contrast, fish are more abundantly represented at the Joffre Bridge Roadcut (e.g., Wilson and Williams, 1991; Li, 1994; Murray, 1994, 1996; Li and Wilson, 1996a-b; Wilson, 1996), where a remarkable death assemblage of fossil fish has recently been documented and described from the so-called "Fish Layer" of Hoffman and Stockey (1999) (see Wilson and Williams, 1991; Li and Wilson, 1996a-b; Wilson, 1996; Wilson and Li, 1997). With the exception of the "Fish Layer" at Joffre Bridge and an incomplete but well-preserved skull of Amia from the DW-2 locality (Grande et al., 2000), the fish remains at the study localities consist primarily of the disarticulated bones, scales, and teeth of amiids and lepisosteids, although rarer specimens representing a diversity of bony fish are known from Erickson's Landing (=?Joffre Bridge Mammal Site No. 1) (Wilson, 1980, 1986). Comparisons with extant relatives of many of the fish that have been identified at the study localities suggest that these animals may have inhabited fluvial or fluvio-lacustrine environments with slow moving or near-stagnant water, a conclusion that is consistent with the depositional environment of the localities (Wilson, 1996); some of the fish (e.g., percopsids) probably fed on insects or crustaceans (Wilson, 1996), while others, such as Esox Linnaeus (pike) and Lepisosteus Linnaeus (gar), were almost certainly more active and predatory, and likely fed on other fish (Nelson, 1984).

Amphibians.—Considering that the inferred depositional environment for all of the study localities is semiaquatic to aquatic, the scarcity of amphibian fossils is surprising. Most of the study localities document the presence of amphibians, but the specimens are fragmentary and often unidentifiable. Fox (1984) reported the occurrence of an unidentified anuran, in addition to specimens of the caudatans Scapherpeton and Opisthotriton from the DW-2 locality. Rare specimens of the albanerpetontid Albanerpeton are known from DW-2 (Gardner, 2000a-b, 2001, 2002), but these have yet to be described.

Reptiles.—Reptiles are generally poorly known in the Paleocene of Alberta, although a number of well-preserved specimens have been recovered from the study localities. Reptiles are most often represented by disarticulated bones and teeth of the

choristodere Champsosaurus Cope; an incomplete but well-preserved skeleton of a large species of Champsosaurus, possibly C. gigas Erickson, is known from the DW-2 locality (pers. obs.). Isolated lacertilian scales, vertebrae, and teeth are known from the Blindman River localities and Joffre Bridge Roadcut, and a well-preserved "necrosaurid" skeleton, possibly referable to Palaeosaniwa Gilmore, is known from DW-2 (Fox, 1984); a number of well-preserved lacertilian lower jaws from DW-2 have recently been prepared, but these remain unidentified and undescribed. Turtles are generally rare: with the exception of a poorly preserved trionychid carapace from the DW-2 locality, turtle fossils are restricted to fragments of the carapace, plastron, and occasional phalanges or incomplete limb bones (pers. obs.). Crocodylians are known only from isolated teeth and occasional scutes. With the exception of the lacertilians, all of the known reptiles at the study localities are aquatic (e.g., trionychids) or semiaquatic (e.g., champsosaurs, crocodylians).

Birds.—A single specimen from DW-2, an avian coracoid, constitutes the known record of birds from the Paleocene of Alberta (pers. obs.).

2.4 Flora

Flora.—Studies on early Tertiary mega- and microflora of the Red Deer River Valley have a long and rich history, beginning with the early work of Penhallow (1902) and Bell (1949) on megafloral fossils found at localities on the Blindman and Red Deer rivers, particularly the Burbank locality (Taylor and Stockey, 1984). Exquisitely preserved plant fossils have been recovered from DW-2, Burbank, and, especially, the Joffre Bridge Roadcut (e.g., Hickey and Peterson, 1978; Stockey and Crane, 1983; Crane and Stockey, 1985, 1986; Pigg, and Stockey, 1991; Hoffman, 1995; Hoffman and Stockey, 1994, 1997, 1999). Megafloral fossils at these localities range from fragmentary specimens to near-complete leaves and reproductive structures, seedlings, and even whole plants (Hoffman and Stockey, 1999); two trees have been reconstructed based on the various specimens from the Joffre Bridge Roadcut alone (the Cercidiphyllum-like Joffrea speirsae Crane and Stockey, and the platanaceous Joffre plane tree; see Crane and Stockey, 1985; Pigg and Stockey, 1991). The megafloral remains are preserved as

compressions or impressions, and seedlings in growth position have been recovered from the Joffre Bridge Roadcut (Hoffman and Stockey, 1999). Hoffman (1995) and Hoffman and Stockey (1999) provided detailed interpretations of the Joffre Bridge flora, and indicated that the overall taxonomic diversity, while low (28 taxa), was consistent with that of coeval middle Tiffanian aged floras from other parts of the Western Interior of North America (e.g., Hickey, 1980; Gemmill and Johnson, 1997).

In addition to macrofloral fossils, a diversity of fossil pollen is known from the Blindman River, Burbank, and Joffre Bridge Roadcut localities, and these were instrumental in Demchuk's (1987, 1990) palynostratigraphic zonation of the Paskapoo Formation in south central Alberta. Representative pollen from the Juglandaceae (walnuts and relatives) and Tiliacaeae (lindens) commonly occur at the Blindman River and Joffre Bridge Roadcut localities.

2.5 Literature Cited

BELL, W. A. 1949. Uppermost Cretaceous and Paleocene flora of western Alberta. Geological Survey of Canada Bulletin, 13:1-231.

BENTON, M. J. 2004. Vertebrate Paleontology, 3rd edition. Blackwell Science Ltd, Oxford.

CRANE, P. R., and R. A. STOCKEY. 1985. Growth and reproductive biology of Joffrea speirsii gen. et sp. nov., a Cercidiphyllum-like plant from the Late Paleocene of Alberta, Canada. Canadian Journal of Botany, 63:340-364.

CRANE, P. R., and R. A. STOCKEY. 1986. Morphology and development of pistillate inflorescences in extant and fossil Cercidiphyllaceae. Annals of the Missouri Botanical Garden, 73:382-393.

DALY, H. V., J. T. DOYEN, and A. H. PURCELL III. 1998. Introduction to Insect Biology and Diversity, 2nd edition. Oxford University Press, Oxford.

DEMCHUK, T. D. 1987. Palynostratigraphy of Paleocene strata of the central Alberta Plains. Unpublished M. Sc. thesis, University of Alberta, Edmonton, 151 pp.

DEMCHUK, T. D. 1990. Palynostratigraphic zonation of Paleocene strata in the central and south-central Alberta Plains. Canadian Journal of Earth Sciences, 27:1263-1269.

EVANS, G.O. 1992. Principles of Acarology. CAB International, Cambridge.

FOX, R. C. 1984. First North American record of the Paleocene primate Saxonella. Journal of Paleontology, 58:892-894.

GARDNER, J. D. 2000a. Revised taxonomy of albanerpetontid amphibians. Acta Palaeontologica Polonica, 45:55-70.

GARDNER, J. D. 2000b. Systematics of albanerpetontids and other lissamphibians from the Late Cretaceous of western North America. Unpublished Ph. D. dissertation, University of Alberta, Edmonton, 577 pp.

GARDNER, J. D. 2001. Monophyly and the affinities of albanerpetontid amphibians (Temnospondyli; Lissamphibia). Zoological Journal of the Linnean Society, 131:309-352.

GARDNER, J. D. 2002. Monophyly and intra-generic relationships of Albanerpeton (Lissamphibia; Albanerpetontidae). Journal of Vertebrate Paleontology, 22:12-22.

GEMMILL, C. E. C., and K. R. JOHNSON. 1997. Paleontology of a late Paleocene (Tiffanian) megaflora from the northern Great Divide Basin, Wyoming. Palaios, 12:439-448.

GRANDE, L., LI G.-Q., and M. V. H. WILSON. 2000. Amia cf. pattersoni from the Paleocene Paskapoo Formation of Alberta. Canadian Journal of Earth Sciences, 37: 31-37.

HARTMAN, J. H., and B. ROTH. 1998. Late Paleocene and early Eocene nonmarine molluscan faunal change in the Bighorn Basin, northwestern Wyoming and south-central Montana, pp. 323-379. In M.-P. AUBRY, S. G. LUCAS, and W. A. BERGGREN (eds.), Late Paleocene-early Eocene climatic events in the marine and terrestrial records, Columbia University Press, New York.

HICKEY, L. J. 1980. Paleocene stratigraphy and flora of the Clark's Fork Basin, pp. 33-49. In P. D. GINGERICH (ed.), Early Cenozoic paleontology and stratigraphy of the Bighorn Basin, Wyoming, The University of Michigan Papers on Paleontology, 24.

HICKEY, L. J., and R. K. PETERSON. 1978. Zingiberopsis, a fossil genus of the ginger family from late Cretaceous to early Eocene sediments of western interior North America. Canadian Journal of Botany, 56:1136-1152.

HOFFMAN, G. L. 1995. Paleobotany and paleoecology of the Joffre Bridge Roadcut locality (Paleocene), Red Deer, Alberta. Unpublished M. Sc. thesis, University of Alberta, Edmonton, 208 pp.

HOFFMAN, G. L. and R. A. STOCKEY. 1994. Sporophytes, megaspores and massulae of Azolla stanleyi Jain & Hall from the Paleocene Joffre Bridge locality, Alberta. Canadian Journal of Botany, 72:301-308.

HOFFMAN, G. L. and R. A. STOCKEY. 1997. Morphology and paleoecology of Ricciopsis speirsae sp. nov. (Ricciaceae), a fossil liverwort from the Paleocene Joffre Bridge locality, Canada. Canadian Journal of Botany, 75:1375-1381.

HOFFMAN, G. L., and R. A. STOCKEY. 1999. Geological setting and paleobotany of the Joffre Bridge Roadcut fossil locality (late Paleocene), Red Deer Valley, Alberta. Canadian Journal of Earth Sciences, 36:2073-2084.

KEVAN, D. K. M., and D. C. WIGHTON. 1981. Paleocene orthopterids from south-central Alberta, Canada. Canadian Journal of Earth Sciences, 12:1824-1837.

LI G.-Q. 1994. New osteoglossomorphs (Teleostei) from the Upper Cretaceous and Lower Tertiary of North America and their phylogenetic significance. Unpublished Ph. D. thesis, University of Alberta, Edmonton, Alberta, 321 pp.

LI G.-Q., and M. V. H. WILSON. 1996a. Phylogeny of Osteoglossomorpha, pp. 163-174. In M. L. J. STAISSNY, L. PARENTI, and G. D. JOHNSON (eds.), Interrelationships of fishes revisited, Academic Press, New York.

LI G.-Q., and M. V. H. WILSON. 1996b. The discovery of Heterotidinae (Teleostei: Osteoglossidae) from the Paleocene Paskapoo Formation of Alberta, Canada. Journal of Vertebrate Paleontology, 16:198-209.

MITCHELL, P., and D. C. WIGHTON. 1979. Larval and adult insects from the Paleocene of Alberta. Canadian Entomologist, 111:777-782.

MURRAY, A. M. 1994. Description of two new species of basal paracanthopterygian fishes from the Palaeocene of Alberta, and a phylogenetic analysis of the

percopsiforms (Teleostei: Paracanthopterygii). Unpublished M. Sc. Thesis, University of Alberta, Edmonton, 198 pp.

MURRAY, A. M. 1996. A new Paleocene genus and species of percopsid, Massamorichthys wilsoni, (Paracanthopterygii) from Joffre Bridge, Alberta, Canada. Journal of Vertebrate Paleontology, 16:642-652.

NELSON, J. S. 1984. Fishes of the World, 2nd Edition. John Wiley and Sons, New York.

PENHALLOW, D. P. 1902. Notes on Cretaceous and Tertiary plants of Canada. Transactions of the Royal Society of Canada, 8:31-91.

PIGG, K. B. and R. A. STOCKEY. 1991. Platanaceous plants from the Paleocene of Alberta, Canada. Review of Palaeobotany and Palynology, 70:125-146.

RUSSELL, L. S.1929. Upper Cretaceous and lower Tertiary gastropods from Alberta. Transactions of the Royal Society of Canada, 23:81-90.

RUSSELL, L. S.1931. Mollusca from the Upper Cretaceous and lower Tertiary of Alberta. Transactions of the Royal Society of Canada, 25:9-19.

STOCKEY, R. A. and P. R. CRANE. 1983. In situ Cercidiphyllum-like seedlings from the Paleocene of Alberta, Canada. American Journal of Botany, 70:1564-1568.

TAYLOR, T. N., and R. A. STOCKEY. 1984. Field Guide, Second International Organization of Paleobotany Conference, Edmonton, Alberta, pp. 17-24.

TOZER, E. T. 1953. The Cretaceous-Tertiary transition in southwestern Alberta. Alberta Society of Petroleum Geologists Third Annual Field Conference and Symposium:23-31.

TOZER, E. T. 1956. Uppermost Cretaceous and Paleocene non-marine molluscan faunas of western Alberta. Geological Survey of Canada Memoir, 280:1-125.

WIGHTON, D. C. 1980. New species of Tipulidae from the Paleocene of central Alberta, Canada. Canadian Entomologist, 112:621-628.

WIGHTON, D. C. 1982. Middle Paleocene insect fossils from south-central Alberta, pp. 577-578. In Proceedings of the 3rd North American Paleontological Convention, 2.

WIGHTON, D. C., and M. V. H. WILSON. 1986. The Gomphaeschninae (Odonata: Aeschnidae): new fossil genus, reconstructed phylogeny, and geographical history. Systematic Entomology, 11:505-522.

WILSON, M. V. H. 1978a. Paleocene insect faunas of western North America. Quaestiones Entomologicae, 14:13-34.

WILSON, M. V. H. 1978b. Evolutionary significance of North American Paleogene insect faunas. Quaestiones Entomologicae, 14:35-42.

WILSON, M. V. H. 1980. Oldest known Esox (Pisces: Esocidae), part of a new Paleocene teleost fauna from western Canada. Canadian Journal of Earth Sciences, 17:307-312.

WILSON, M. V. H. 1986. Paleocene teleostean fishes of North America. American Society of Ichthyologists and Herpetologists, 66th Annual Meeting, Program with Abstracts.

WILSON, M. V. H. 1996. Taphonomy and paleoecology of a mass-death layer of fishes in a fluvial sequence of the Paleocene Paskapoo Formation, Alberta. Canadian Journal of Earth Sciences, 33:1487-1498.

WILSON, M. V. H. and LI G.-Q. 1997. Importance of new North American fossil osteoglossomorphs for phylogeny and biogeography of the group. Journal of Vertebrate Paleontology, 17, supplement to no. 3:85A.

WILSON, M. V. H. and R. R. G. WILLIAMS. 1991. New Paleocene genus and species of smelt (Teleostei: Osmeridae) from freshwater deposits of the Paskapoo Formation, Alberta, Canada, and comments on osmerid phylogeny. Journal of Vertebrate Paleontology, 11:434-451.

2.6 Appendix 1.—Non-mammalian Fauna and Flora of the Study Localities

Localities are abbreviated as follows: DW=Blindman River localities; Bu=Burbank locality; JBMS=Joffre Bridge Mammal Site No. 1; JBRC=Joffre Bridge Roadcut.

1. Molluscs (classification follows Hartman and Roth, 1998)

Phylum MOLLUSCA

Class BIVALVIA

Family PISIIDAE

Genus SPHAERIUM Scopoli

SPHAERIUM AEQUALE Russell [DW, JBMS]

Class GASTROPODA

Family VIVIPARIDAE

Genus VIVIPARUS Montfort

VIVIPARUS LEAI (Meek and Hayden) [JBMS]

VIVIPARUS RAYNOLDSANUS (Meek and Hayden) [DW]

Family PLEUROCERIDAE

Genus LIOPLACODES Meek

LIOPLACODES NEBRASCENSIS (Meek and Hayden) [DW, JBMS]

Family BITHNYIIDAE

Genus REESIDELLA Yen

REESIDELLA sp., cf. R. PROTEA [JBMS]

Family VALVATIDAE

Genus VALVATA Muller

VALVATA BICINCTA Whiteaves [DW, Bu, JBMS]

VALVATA sp., cf. V. SUBUMBILICATA [DW]

Family HYDROBIIDAE

Genus HYDROBIA Hartmann

HYDROBIA, species indeterminate [DW, Bu]

Family ELLOBIIDAE

Genus PLEUROLIMNAEA Meek

PLEUROLIMNAEA TENUICOSTA (Meek and Hayden) [DW, Bu, JBMS]

Family PHYSIDAE

Genus PHYSA Draparnaud

PHYSA CANADENSIS Whiteaves [DW]

Family ANCYLIDAE

Genus FERRISSIA Walker

FERRISSIA MINUTA (Meek and Hayden) [JBMS]

Genus PALAEANCYLUS Yen

PALAEANCYLUS RADIATULUS (Whiteaves) [DW, Bu]

Family uncertain

Genus PSEUDOCOLUMNA Wenz

PSEUDOCOLUMNA HAYDENIANA (Cockrell) [Bu]

2. Insects and mites (insect classification follows Daly et al., 1998; acariform classification follows Evans, 1992; specimens represent adults unless otherwise noted)

Phylum ARTHROPODA

Class INSECTA

Order EPHEMEROPTERA (nymph)

EPHEMEROPTERA, genus and species indeterminate [JBRC]

Order ODONATA

Family AESCHNIDAE

Genus ALLOAESCHNA Wighton and Wilson (nymph and adult)

ALLOAESCHNA PASKAPOOENSIS Wighton and Wilson [DW]

ALLOAESCHNA MARKLAE Wighton and Wilson [DW]

ALLOAESCHNA QUADRATA Wighton and Wilson [JBRC]

AESCHNIDAE, genus and species indeterminate [JBRC]

Order ORTHOPTERA

Family PROPHALANGOPSIDAE

Genus ALBERTOILUS Kevan and Wighton

ALBERTOILUS CERVIRUFI Kevan and Wighton [JBRC]

Family PHASMOMIMIDAE

Genus PHASMOMIMELLA Kevan and Wighton

PHASMOMIMELLA PASKIPOENSIS Kevan and Wighton [?JBMS]

Genus PHASMOMIMULA Kevan and Wighton

PHASMOMIMULA ENIGMA Kevan and Wighton [JBRC]

Family TETTIGONIIDAE

TETTIGONIIDAE, genus and species indeterminate [JBRC]

Family PROMASTACIDAE

Genus PROMASTACOIDES Kevan and Wighton

PROMASTACOIDES ALBERTAE Kevan and Wighton [JBRC]

Order HEMIPTERA

Family ?BELOSTOMATIDAE

?BELOSTOMATIDAE, genus and species indeterminate

Family ?PENTATOMIDAE

?PENTATOMIDAE, genus and species indeterminate

Family CERCOPIDAE

CERCOPIDAE, genus and species indeterminate

Family CIXIIDAE

CIXIIDAE, genus and species indeterminate

Order HYMENOPTERA

Family FORMICIDAE

FORMICIDAE, genus and species indeterminate

Order COLEOPTERA

Family ?ELATERIDAE (larva)

?ELATERIDAE, genus and species indeterminate

Family CURCULIONIDAE

CURCULIONIDAE, genus and species indeterminate

Family CHRYSOMELIDAE

Genus DONACIA Fabricius

DONACIA sp.

Family TENEBRIONIDAE

TENEBRIONIDAE, genus and species indeterminate

Family DYTISCIDAE

DYTISCIDAE, genus and species indeterminate

Family CARABIDAE

CARABIDAE, genus and species indeterminate

Order DIPTERA

Family TIPULIDAE

Genus PSEUDOLIMNOPHILA Wighton

PSEUDOLIMNOPHILA SPEIRSAE Wighton

Genus LIMNOPHILA Brown

LIMNOPHILA MARKLAE Wighton

Genus TIPULA Linnaeus

TIPULA TUBIFERA Wighton

TIPULIDAE, genus and species indeterminate

Order TRICHOPTERA (larva)

TRICHOPTERA, genus and species indeterminate

Class ARACHNIDA

Order ACARIFORMES

Family ORIBATIDAE

cf. HYDROZETES

3. Fish (classification follows Nelson, 1984)

Phylum CHORDATA

Class ACTINOPTERYGII

Family LEPISOSTEIDAE

Genus LEPISOSTEUS Linnaeus

LEPISOSTEUS sp. [all]

Family AMIIDAE

Genus AMIA Linnaeus

AMIA sp., cf. A. PATTERSONI [DW]

Genus CYCLURUS Agassiz

CYCLURUS "LACUS" [?JBMS]

CYCLURUS sp. [JBRC] (unpublished)

AMIIDAE, genus and species indeterminate [all?]

Family OSTEOGLOSSIDAE

Genus JOFFRICHTHYS Li and Wilson, 1996

JOFFRICHTHYS SYMMETROPTERUS Li and Wilson, 1996 [JB]

JOFFRICHTHYS sp. [JB, JBMS?]

Family ESOCIDAE

cf. ESOX TIEMANI [?JBMS]

Family HIODONTIDAE

HIODONTIDAE, genus and species indeterminate [?JB]

Family GONORHYNCHIDAE

cf. NOTOGONEUS sp. [?JBMS]

Family CATOSTOMIDAE

cf. AMYZON sp. [?JBMS]

Family OSMERIDAE

Genus SPEIRSAENIGMA Wilson and Williams, 1991

SPEIRSAENIGMA LINDOEI Wilson and Williams, 1991 [JB]

Family PERCOPSIDAE

Genus MASSAMORICHTHYS Murray, 1996

MASSAMORICHTHYS WILSONI Murray, 1996 [JB]

cf. AMPHIPLAGA sp. [?JBMS]

Family ASINEOPIDAE

cf. ASINEOPS sp. [?JBMS]

4. Amphibians (classification modified from Gardner, 2000b)

Subclass LISSAMPHIBIA

Order CAUDATA

Family BATRACHOSAUROIDIDAE

Genus OPISTHOTRITON Auffenberg

OPISTHOTRITON sp. [DW]

Family SCAPHERPETONTIDAE

Genus SCAPHERPETON Cope

SCAPHERPETON sp. [DW]

Order ANURA

ANURA, genus and species indeterminate [DW]

?LISSAMPHIBIA

Order ALLOCAUDATA

Family ALBANERPETONTIDAE

Genus ALBANERPETON Estes and Hoffstetter

ALBANERPETON new species [DW]

5. Reptiles (classification follows Benton, 2004)

Class SAUROPSIDA

Order TESTUDINES

Family TRIONYCHIDAE

Genus TRIONYX Saint-Hilaire

TRIONYX sp. [DW]

Family BAENIDAE

BAENIDAE, genus and species indeterminate [DW]

Order SQUAMATA

Suborder LACERTILIA

Family "NECROSAURIDAE"

Genus PALAEOSANIWA Gilmore

PALAEOSANIWA sp. [DW]

Family ANGUIDAE

Genus ODAXOSAURUS Gilmore

ODAXOSAURUS sp. [DW]

Order CROCODYLIA

CROCODYLIA, genus and species indeterminate [DW]

Order CHORISTODERA

Family CHAMPSOSAURIDAE

Genus CHAMPSOSAURUS Cope

CHAMPSOSAURUS sp., cf. C. GIGAS [DW, JBMS]

6. Megaflora (based on Taylor and Stockey, 1984; Hoffman and Stockey, 1999)

Class HEPATICOPSIDA

Family RICCIACEAE

Genus RICCIOPSIS Lundblad

RICCIOPSIS SPEIRSIAE Hoffman et Stockey [JBRC]

Class BRYOPSIDA

Family incertae sedis

Genus MUSCITES Brongniart

MUSCITES sp. [JBRC]

Class LYCOPSIDA

Family ISOETACEAE

Genus ISOETITES Münster

ISOETITES sp. [JBRC]

Class SPHENOPSIDA

Family EQUISETACEAE

Genus EQUISETUM Linnaeus

EQUISETUM ARCTICUM Heer [DW, Bu]

EQUISETUM sp. [JBRC]

Class POLYPODIOPSIDA

Family ONOCLEACEAE

Genus ONOCLEA Linnaeus

ONOCLEA HESPERIA Brown [DW]

Class FILICOPSIDA

Family OSMUNDACEAE

Genus OSMUNDA Linnaeus

OSMUNDA MACROPHYLLA Penhallow [JBRC, DW]

Family DENNSTAEDTIACEAE

Genus DENNSTAEDTIA (Michaux)

DENNSTAEDTIA BLOMSTRANDII (Heer) [JBRC, DW]

Family AZOLLACEAE

Genus AZOLLA Lamarck

AZOLLA STANLEYI Jain et Hall [JBRC]

Class GINKGOOPSIDA

Family GINKGOACEAE

Genus GINKGO Linnaeus

GINKGO sp. [JBRC]

Class CONIFEROPSIDA

Family TAXODIACEAE

Genus GLYPTOSTROBUS Endlicher

GLYPTOSTROBUS EUROPAEUS (Brongniart) [JBRC]

Genus METASEQUOIA Miki

METASEQUOIA OCCIDENTALIS (Newberry) [JBRC]

Class MAGNOLIOPSIDA

Family SABIACEAE

cf. MELIOSMA ROSTELLATA [JBRC]

Family CERCIDIPHYLLACEAE

Genus JOFFREA Crane and Stockey

JOFFREA SPEIRSII Crane et Stockey [JBRC]

Genus CERCIDIPHYLLUM Siebold et Zuccarini

CERCIDIPHYLLUM FLEXUOSUM Siebold et Zuccarini [DW]

Family JUGALANDACEAE

Genus CARYA Nuttall

CARYA ANTIQUORUM Newberry [DW]

Family CELASTRACEAE

Genus CELASTRINITES Saporta

"CELASTRINITES" INSIGNIS Heer [DW]

Family VITACEAE

Genus RHAMNITES Newberry

RHAMNITES OVATUS Newberry [DW]

Family LAURACEAE

"SASSAFRAS" THERMALE (Lesquereux) [DW]

Family PLATANACEAE

Genus PLATANUS Linnaeus

PLATANUS NOBILIS Newberry [JBRC]

PLATANUS REYNOLDSII Newberry [DW]

Genus MACGINICARPA Manchester

MACGINICARPA MANCHESTERI Pigg et Stockey [JBRC]

Genus PLATANANTHUS Manchester

PLATANANTHUS SPEIRSIAE Pigg et Stockey [JBRC]

Family ULMACEAE

Genus CHAETOPTELEA Liebmann

CHAETOPTELEA MICROPHYLLA (Newberry) [JBRC]

Family CORNACEAE

Genus BERINGIAPHYLLUM Manchester, Crane, et Golovneva

BERINGIAPHYLLUM CUPANIOIDES (Newberry) [JBRC, DW]

Genus AMERSINIA Manchester, Crane, et Golovneva

AMERSINIA OBTRULLATA Manchester, Crane, et Golovneva [JBRC]

Family SAPINDACEAE

Genus DEVIACER Manchester

DEVIACER sp. [JBRC]

cf. "ACER" ARCTICUM [JBRC]

Family OXALIDACEAE

Genus AVERRHOITES Hickey

AVERRHOITES AFFINIS (Newberry) [JBRC]

Family incertae sedis

Genus FORTUNA McIver et Bassinger

FORTUNA MARSILIOIDES (Bell) [JBRC]

Genus WARDIAPHYLLUM Hickey

WARDIAPHYLLUM DATURAEFOLIUM (Ward) [JBRC]

"POPULUS" PENHALLOWII [JBRC, DW]

Class LILIOPSIDA

Family ALISMATACEAE

Genus ALSIMAPHYLLITES Brown

ALSIMAPHYLLITES GRANDIFOLIUS (Penhallow) [JBRC, DW]

Family ARACEAE

Genus LIMNOBIOPHYLLUM Krassilov

LIMNOBIOPHYLLUM SCUTATUM (Dawson) [JBRC]

cf. LEMNOSPERMUM [DW]

Family ZINGIBERACEAE

Genus ZINGIBEROPSIS Hickey et Peterson

ZINGIBEROPSIS ATTENUATA Hickey et Peterson [JBRC]

Family incertae sedis

Specimens preserving elongate, parallel-veined leaves [JBRC]

7. Pollen (based on Demchuk, 1987, 1990)

Family JUGLANDACEAE

Genus MOMIPITES Wodehouse

MOMIPITES WYOMINGENSIS Nichols and Ott [JBRC, Bu]

MOMIPITES WALTMANENSIS Nichols and Ott [JBRC, DW, Bu]

MOMIPITES VENTIFLUMINIS Nichols and Ott [JBRC, Bu]

MOMIPITES ANNELLUS Nichols and Ott [DW, Bu]

MOMIPITES TRIORBICULARIS (Leffingwell) [JBRC, DW, Bu]

MOMIPITES ACTINUS Nichols and Ott [DW]

MOMIPITES LEFFINGWELLI Nichols and Ott [JBRC, Bu]

Genus CARYAPOLLENITES Raatz and Potonie

CARYAPOLLENITES PRODROMUS Nichols and Ott [JBRC, DW, Bu]

CARYAPOLLENITES IMPARALIS Nichols and Ott [JBRC, DW, Bu]

CARYAPOLLENITES WODEHOUSEI Nichols and Ott [Bu]

Family TILIACEAE

Genus TILLIAEPOLLENITES Potonie

TILLIAEPOLLENITES DANEI (Anderson) [JBRC, DW, Bu]

Family uncertain

Genus KURTZIPITES Anderson

KURTZIPITES ANNULATUS Norton [JBRC]

Genus AQUILAPOLLENITES Rouse

AQUILAPOLLENITES SPINULOSUS Funkhouser [DW, Bu]

3 Multituberculates (Mammalia, Allotheria) from the Paleocene of Alberta, Canada, with Descriptions of New Species of Ectypodus Matthew and Granger, Neoplagiaulax Lemoine, and Prochetodon Jepsen[1]

3.1 Introduction

MULTITUBERCULATES WERE a long-lived (Late Jurassic-late Eocene), primarily Laurasian group of mammals that saw their greatest numbers and diversity in the middle to late Paleocene, but declined quickly thereafter until their final occurrence in the late Eocene or earliest Oligocene (Krause, 1982a-c). Multituberculates were common members of early Tertiary terrestrial vertebrate communities, and at least some species may have been among the first mammals to enter into an exclusively herbivorous adaptive zone (Fox, 1971; Novacek and Clemens, 1977). The multituberculate record from the Western Interior of North America is the best known and densest stratigraphically in the world, with a temporal range extending from the Late Jurassic to the late Eocene, and geographically from southern Texas to Ellesmere Island (see summary in Weil, 1999). The Canadian record of multituberculates spans the late Santonian/early Campanian to the late Eocene, and has figured importantly in understanding local and regional biostratigraphy, and in assessing the pattern of mammalian evolution across the K/T boundary and on into the early Tertiary (e.g., Russell, 1958; Lillegraven, 1969; Fox, 1971, 1997, 2002; Sahni, 1972; Krause, 1977; Johnston and Fox, 1984; Storer, 1991; Scott, 2003a). In spite of these exceptional records, the systematics of Tertiary North American multituberculates remain frustratingly unclear: unlike the well-preserved djadochtatherioideans from the Upper Cretaceous of East Asia (e.g., Simpson, 1925; Kielan-Jaworowska, 1970; Kielan-Jaworowska and Hurum, 1997), the record of North American multituberculates has been limited more often than not to isolated teeth, or more rarely, incomplete cranial, gnathic, or postcranial remains (e.g., Krause, 1980, 1982a-c; Krause and Jenkins, 1983; Scott, 2003a; Fox, 2005; Scott and Krause, 2006).

[1] Parts of this chapter have been published. Scott, 2004. Canadian Journal of Earth Sciences, 41:237-246; Scott, 2005. Journal of Paleontology, 79:1189-1213.

Multituberculates from the Paskapoo Formation of Alberta were first discovered in the early part of the twentieth century (L. Russell, 1929, 1932, 1967; Fox, 1990). Since Russell's initial work, numerous new local faunas from the Alberta and Williston basins have been described, collectively documenting a dense record of middle and late Paleocene mammals, including taxonomically diverse multituberculates, with no less than 20 localities in south-central Alberta and southern Saskatchewan alone known to preserve multituberculate fossils (Krishtalka, 1973; Krause, 1977; Johnston and Fox, 1984; Youzwyhsyn, 1988; Fox, 1990; Fox, 2002; Scott, 2003a-b). Of these localities, those of early middle Tiffanian (Ti3) age along the Blindman River and northeast of the City of Red Deer are exceptional in both specimen quality and numbers, and document a diversity of ptilodontid, microcosmodontid, and, especially, neoplagiaulacid multituberculates [the Neoplagiaulacidae Ameghino, 1890 are a group of Late Cretaceous-late Eocene, primarily North American cimolodontan multituberculates characterized by ptilodontoidean plesiomorphies (e.g., microprismatic enamel, slender and procumbent i1, greatly enlarged and arcuate p4, increased number of molar cusps; see Simmons, 1993; Kielan-Jaworowska and Hurum, 2001].

This chapter reviews the multituberculates from the Blindman River localities, and reports on new species of the neoplagiaulacids Ectypodus and Neoplagiaulax, and the ptilodontid Prochetodon. Included among these specimens is the most dentally complete Cenozoic neoplagiaulacid discovered to date.

3.2 Systematic Paleontology

Class MAMMALIA Linnaeus, 1758

Subclass ALLOTHERIA Marsh, 1880

Order MULTITUBERCULATA Cope, 1884

Suborder CIMOLODONTA McKenna, 1975

Superfamily PTILODONTOIDEA (Sloan and Van Valen, 1965)

Family NEOPLAGIAULACIDAE Ameghino, 1890

Remarks.—Of the multituberculate taxa known from the early Tertiary of the Western Interior of North America, neoplagiaulacids are invariably the most numerous and diverse, but are often among the most poorly preserved, rendering taxonomic identification difficult. Despite recent phylogenetic analyses suggesting paraphyly of the family (e.g., Simmons, 1993; Rougier et al., 1997; Weil, 1999), the taxonomic core of Neoplagiaulacidae has remained relatively stable. The neoplagiaulacid genera recognized here include the North American Mesodma Jepsen, 1940, Parectypodus Jepsen, 1930, Mimetodon Jepsen, 1940, Xyronomys Rigby, 1980, Xanclomys Rigby, 1980, Fractinus Higgins, 2003, and Krauseia Vianey-Liaud, 1986; the Euramerican genera Ectypodus Matthew and Granger, 1921, Neoplagiaulax Lemoine, 1882, and Cernaysia Vianey-Liaud, 1986; and the Asian genus Mesodmops Tong and Wang, 1994. Neoplagiaulacidae are here recognized as a family of ptilodontoidean multituberculates, rather than a subfamily of the Ptilodontidae as per some recent classifications (e.g., McKenna and Bell, 1997).

Genus MESODMA Jepsen, 1940

Mesodma JEPSEN, 1940, p. 267.

Type species.—Mesodma ambigua Jepsen, 1940.

Other included species.—M. formosa (Clemens, 1964); M. primaeva (Clemens, 1964); M. thompsoni Clemens, 1964; M. hensleighi Lillegraven, 1969; M. senecta Fox, 1971; M. garfieldensis Archibald, 1982; M. pygmaea Sloan, 1987.

MESODMA PYGMAEA Sloan, 1987

Figures 3.1.1-3.1.16, Table 3.1

Mesodma pygmaea SLOAN, 1987, p. 188.

Holotype.—AMNH 35298, incomplete left dentary with p4-m2 (Sloan, 1987, p. 188, fig. 10). Gidley Quarry, Upper Lebo Beds, Fort Union Formation of Montana, early

Paleocene (middle Torrejonian, To2, Protoselene opisthacus/Mixodectes pungens Interval Zone of Lofgren et al., 2004).

Material examined.—From DW-2: UALVP 46227, incomplete right maxilla with P1-3, M1-2, and associated m1; UALVP 46228-33, P4 (total: 6); UALVP 46235-41, M1 (total: 7); UALVP 46242, incomplete left dentary with i1, p3-4, m1; UALVP 46243, incomplete left dentary with i1, p4 (fragment), m1-2; UALVP 46244-48, p4 (total: 5); UALVP 46249-51, m1 (total: 3); UALVP 46252-57, m2 (total: 6).

From Joffre Bridge Roadcut lower level: UALVP 46258, p4.

Age and occurrence.—Middle Torrejonian (Protoselene opisthacus/Mixodectes pungens Interval Zone, To2, early Paleocene) to late middle Tiffanian (Plesiadapis churchilli/P. simonsi Lineage Zone, Ti4, late Paleocene) of the Western Interior of North America (Lofgren et al., 2004).

Description.—Maxilla and zygomatic arch: UALVP 46227 preserves the right maxilla and anterior part of the zygomatic arch, the first discovered in Mesodma pygmaea. UALVP 46227 may be more extensively preserved than is suggested here, with postcranial bones in possible association with the skull fragment, but the discovery of an incomplete maxilla of the peradectine marsupial Peradectes Matthew and Granger, 1921 in the same block makes this association uncertain; for the present, only the skull fragment can be confidently referred to M. pygmaea.

The maxilla is damaged anteriorly and dorsally, but from the proportions of the parts preserved, the facial process appears to have been tall and broad, smaller but otherwise similar to that in the neoplagiaulacid Neoplagiaulax cimolodontoides (see later in this chapter) and probably forming most of the anterolateral cranial wall (Simpson, 1937a). The maxillary process of the zygomatic arch forms an obtuse angle with the snout, similar to that in Neoplagiaulax, and contrasting with that in taeniolabidids (see, e.g., Sloan and Van Valen, 1965) and Microcosmodon (see Fox, 2005) in which the maxillary process flares abruptly laterally. Neither the premaxilla-maxilla suture nor the infraorbital canal is preserved. Although P4 is missing and the maxilla has been broken and shifted slightly, the root of the maxillary process of the zygomatic arch originates dorsal to P4, but whether the posterior edge of the process is dorsal to the posterior margin of P4 as in Neoplagiaulax and Ptilodus Cope, 1881, further anterior as in some

plagiaulacidans, or further posterior as in taeniolabidids (see Rougier et al., 1997), cannot be determined. The maxillary process of the zygomatic arch is thin, with its lateral surface perforated by a pair of small foramina and its ventral surface flat; the process extends laterally and slightly dorsally. A short, faint zygomatic ridge is developed along the ventrolateral border of the process, but it is weakly developed and does not extend onto the lateral surface of the process like those in some djadochtatherioidean multituberculates [e.g., Chulsanbaatar Kielan-Jaworowska, 1974 and Nemegtbaatar Kielan-Jaworowska, 1974; see Gambaryan and Kielan-Jaworowska (1995)].

Upper dentition (Figs. 3.1.1-3.1.8): Upper premolars: P1-3: UALVP 46227 preserves P1-3 in articulation with the maxilla. P1 and P2 are virtually identical to those in UALVP 10792, an incomplete maxilla from the late Tiffanian (Ti4) Roche Percée locality, Ravenscrag Formation, Saskatchewan (Krause, 1977). Krause characterized the teeth in UALVP 10792 as premolar Type A (P1) and Type B (P2), and suggested that the incomplete maxilla pertained to either Mesodma pygmaea or Mimetodon silberlingi (Simpson, 1935); the M1 and M2 in UALVP 46227 are closer to those of M. pygmaea [see Krause (1977) and below] than to those of Mim. silberlingi, suggesting UALVP 10792 may be best referred to M. pygmaea. The crowns of P1 and P2 are both subcircular and contain three cusps: the labial cusp is lenticular and larger than the lingual cusps, and bears a short, anterior crest; the two lingual cusps are closely spaced and nearly triangular in cross section. P3 is virtually identical to Krause's (1977) Type C premolar from Roche Percée, the crown being subquadrate in outline and containing four cusps in two parallel rows; compared to P1 and P2, the crown of P3 is anteroposteriorly longer and lower, and the cusps are triangular in cross section.

P4: Cusp formula (0)2-3:5-6:0 [mode=(0)2:6:0; N=5]. P4 is short and low, with little elevation posteriorly. Owing to a weakly developed anterolabial lobe, the crown is only slightly wider anteriorly than posteriorly. The lobe supports two large conical cusps, the posterior of which is larger and taller; a small cuspule can occur more posteriorly on the lobe. The cusps of the middle row are approximately equal in size and height, except for the ultimate cusp, which is larger and taller. The anterior slope is straight to slightly convex, with the ultimate or penultimate cusp highest above the base of the crown. The posterior slope is short, shallow, and straight to slightly concave, and a

posterobasal cusp is absent. The P4s from the Blindman River localities are virtually identical to SMM P77.8.38, a P4 referred to Mesodma pygmaea from the middle Tiffanian (Ti3) of North Dakota [Brisbane locality (Holtzman, 1978)], differing from those of M. pygmaea from the late Tiffanian of Saskatchewan and Alberta [Roche Percée and the Police Point locality, Ravenscrag Formation, Alberta (Krishtalka, 1973)] in being slightly shorter and with one fewer cusp in the middle row.

Upper molars: M1-M2: M1 cusp formula 7-8:9:5 (mode=7:9:5; N=5); M2 cusp formula 4:3 (N=1). The M1 of Mesodma pygmaea from the Blindman River localities is virtually identical to that of M. pygmaea from the Roche Percée and Police Point localities (Krishtalka, 1973; Krause, 1977), differing only in having one fewer external cusp. The M2 is similar to that of M. pygmaea from other localities in western Canada described by Krishtalka (1973) and Krause (1977), differing only in having one additional cusp in the middle row.

Lower dentition (Figs. 3.1.9-3.1.16): Lower premolars: p3: The crown of p3 is short and peg-like, with no accessory cuspules.

p4: The profile of p4 is low and asymmetrical, with the anterior margin slightly convex, the dorsal crest smoothly arcuate, and the posterior slope virtually straight. Except for the well-developed posterolabial shelf, the labial side of the crown is flat, and the exodaenodont lobe is narrow and deep. The anterobasal concavity is shallow, and the anterior root bears a weak vertical sulcus. The anterior margin of the crown is broad and flat, especially dorsal to the anterobasal concavity, and the leading edge is steep up to the low first serration. The apogee of the dorsal crest occurs at the fourth serration, and the height of the first serration above the anterobasal concavity is approximately one-third the length of the crown. The cutting edge bears 10 or 11 serrations (mode=11; N=4), the first of which is set off anteriorly from the succeeding serrations; the apices of the remaining serrations are equidistant from one another, and their bases become larger and stouter posteriorly. The crown below the serrations bears well-developed labial and lingual ridges that extend anteroventrally in a gentle arc; the ridges are coarse anteriorly but become weaker posteriorly, and are absent at the penultimate and ultimate serrations.

Lower molars: m1-m2: m1 cusp formula 6-7:4 (mode=7:4; N=3); m2 cusp formula 3-4:2 (mode=4:2; N=6). The m1s resemble that of Mesodma pygmaea from

Roche Percée (Krause, 1977), differing only in having one fewer cusp in the external row; the referred m2s are likewise similar to those from Roche Percée, but differ in that the last two external cusps are only incipiently divided.

Discussion.—The specimens of Mesodma pygmaea from the Blindman River localities are consistent with Sloan's (1987) diagnosis of the species. The upper and lower fourth premolars closely resemble those of M. pygmaea from Roche Percée, Police Point, and the Brisbane localities, differing mainly in their slightly smaller size; the few differences outlined above are not considered taxonomically significant. M. pygmaea is a stratigraphically long-ranging taxon (late Torrejonian through late Tiffanian) that appears to be restricted to the northern part of the Rocky Mountain Interior (the single record of M. pygmaea from the Black Peaks Formation, Texas, has been challenged [see Schiebout, 1974; Krause, 1977]).

?MESODMA sp.

Figures 3.1.17, 3.1.18, Table 3.2

Material examined.—From DW-1: UALVP 46259, p4.

From DW-2: UALVP 46260, p4.

Description.—p4: The crown of UALVP 46259 and 46260 is low in profile, with a steeply rounded anterior edge and shallow posterior slope. The labial face is flat while the lingual surface is slightly convex, especially near the base of the crown. The exodaenodont lobe is narrow and pointed ventrally, much as in p4 of Mesodma pygmaea, and the posterolabial shelf is well developed, forming a near vertical protuberance near the posterior margin of the tooth. The anterobasal concavity is deep and the anterior root is grooved anteriorly. The cutting edge is more evenly symmetrical dorsally compared to p4s of M. pygmaea and bears nine serrations that become larger and more swollen posteriorly; the distance between the second and third serrations is greater than that between any other adjacent serrations. Coarse labial and lingual ridges are developed ventral to the serrations but become weaker posteriorly. The antepenultimate labial ridge trifurcates, with a single branch descending anteriorly, while the remaining two curves posteriorly. The crown ventral to the ultimate and penultimate serrations lacks ridges.

Discussion.—The referred p4s most resemble those of small neoplagiaulacids, particularly Mesodma and Xyronomys Rigby, 1980, and exhibit a mosaic of derived (e.g., high first serration, evenly arcuate profile) and primitive (e.g., low crown height) neoplagiaulacid features (Sloan, 1981; Johnston and Fox, 1984). UALVP 46259 and 46260 are smaller than p4s referred to Mesodma pygmaea from the Blindman River localities, but their lengths are close to those recorded for M. pygmaea from Roche Percée (Krause, 1977); they differ, however, in being slightly lower crowned, in having a higher first serration and a more nearly symmetrical cutting edge. UALVP 46259 and 46260 are also superficially similar to p4s of Xyronomys from the late Torrejonian Swain Quarry, Wyoming, and the early Puercan Rav W-1 locality, Saskatchewan (Rigby, 1980; Johnston and Fox, 1984), particularly in the crown being rather low. They differ, however, in being shorter with fewer serrations, and in having a much stronger exodaenodont lobe and more obliquely oriented ridges. A better assessment of the affinities of ?Mesodma sp. must await the discovery of additional specimens.

Genus MIMETODON Jepsen, 1940

Mimetodon JEPSEN, 1940, p. 314.

Type species.—Mimetodon churchilli Jepsen, 1940.

Other included species.—Mimetodon silberlingi (Simpson, 1935); Mim. krausei Sloan, 1981.

MIMETODON SILBERLINGI (Simpson, 1935)

Figures 3.1.19-3.1.24, Table 3.3

?Ectypodus silberlingi SIMPSON, 1935, p. 226.

Mesodma silberlingi SLOAN in VAN VALEN and SLOAN, 1966, p. 270.

Mimetodon silberlingi SCHIEBOUT, 1974, p. 12.

Mimetodon silberlingi KRAUSE, 1977, p. 24.

Holotype.—USNM 9798, incomplete left dentary with i1, p4-m2 (Simpson, 1935, p. 226). Gidley Quarry, upper Lebo Beds, Fort Union Formation of Montana, early Paleocene (middle Torrejonian, To2, Protoselene opisthacus/Mixodectes pungens Interval Zone of Lofgren et al., 2004).

Material examined.—From DW-1: UALVP 46261, incomplete left dentary with i1, p3-4.

From DW-2: UALVP 46262, 46263, P4; UALVP 46264, incomplete right dentary with i1, p3-4; UALVP 46265, incomplete left dentary with i1, p4; UALVP 46266-68, p4 (total: 3).

From Birchwood: UALVP 39122, p4.

Age and occurrence.—Middle Torrejonian (Protoselene opisthacus/Mixodectes pungens Interval Zone, To2, early Paleocene) to late Tiffanian (Plesiadapis simonsi/P. gingerichi Lineage Zone, Ti5, late Paleocene) of the Western Interior of North America (Lofgren et al., 2004).

Description.—Upper dentition (Figs. 3.1.19-3.1.21): P4: Cusp formula (0)1:8:0 [mode=(0)1:8:0; N=2]. The P4 of Mimetodon silberlingi is larger than P4 of Mesodma pygmaea. The anterior slope is faintly convex in profile, while the posterior slope is virtually straight; a posterobasal cusp is not present. The anterolabial lobe is well developed, forming a prominent bulge on the otherwise long and narrow crown; the lobe supports a small conical cusp, two fewer than the modal number on P4s of Mim. silberlingi from the Roche Percée locality (Krause, 1977), but equal to that in Mim. silberlingi from the late Torrejonian Who Nose? locality, Paskapoo Formation, Alberta (Scott, 2003a). The cusps of the middle row are smaller than in M. pygmaea and remain subequal in size along the length of the row; the middle row is virtually straight, without the curvature seen on P4 of some species of Neoplagiaulax [e.g., P4 of N. serrator (see later in the text)]. The ultimate cusp, or ultimate and penultimate cusps together, is highest above the base of enamel.

Dentary and lower dentition (Figs. 3.1.22-3.1.24): Three specimens of Mimetodon silberlingi from DW-2 (UALVP 46261, 46264, 46265) preserve parts of the dentary, although none include the condylar or coronoid processes, or teeth other than i1, p3, or p4 (Fig. 3.1.22-3.1.24). The dentary of Mim. silberlingi resembles that in other

neoplagiaulacids and ptilodontoid multituberculates generally (Simpson, 1937a; Jepsen, 1940), but differs in several ways. The anterior parts of the horizontal ramus are short, robust, and deep, especially beneath the posterior root of p4; the ramus in Mim. churchilli is developed in much the same manner (see Jepsen, 1940 and later in this chapter). The symphysis is relatively shorter than that in other neoplagiaulacids, and the articular surface is comma-shaped, with the tail of the comma directed posteriorly and ventrally; the articular surface is smooth and nearly flush with the surrounding bone, and its posterior margin is delimited by a prominent dorsoventrally directed flange. The alveolar process for i1 is short and deep, as it is in Neoplagiaulax hazeni and Mim. churchilli (see Jepsen, 1940); the diastema between the base of i1 and p3 is long. The dorsal margin of the incisor alveolar process is not raised into a keel as it is in dentaries of Neoplagiaulax hazeni and N. paskapooensis (e.g., Jepsen, 1940 and later in this chapter). Anteriorly the masseteric fossa extends almost to below the level of the anterior root of p4; a shallow, circular fovea masseterica (Gambaryan and Kielan-Jaworowska, 1995) occurs directly ventral to the anterior root of p4, somewhat more anteriorly than in Ectypodus elaphus (see later in this chapter) but of nearly equal size. A mental foramen opens anteriorly and laterally anteroventral to p3.

i1: The lower incisor is shorter and deeper than in most other neoplagiaulacids, comparable, although relatively smaller, to that in Mimetodon churchilli, Neoplagiaulax hazeni, and N. cimolodontoides (see Jepsen, 1940 and later in this chapter). The crown is anteroposteriorly short and laterally compressed, and is less procumbent (i.e., the apex is directed more nearly vertically than anteriorly) than in Mesodma and Ectypodus. When viewed in cross section, the lateral surface of i1 is markedly convex, whereas the medial surface is flat; a well-developed ventromedial crest originates apically and runs the length of the crown, while a shorter, fainter crest is developed along the dorsolateral margin. The root is short relative to the length of the crown, terminating below the midpoint of p4.

Lower premolars: p3: The crown of p3 is short and peg-like and inserts into the anterobasal concavity of p4.

p4: The lateral profile of p4 is long and low. The cutting edge is asymmetrically arcuate, with the anterior margin short and steep and the posterior slope long and straight.

Except for a well-developed posteroexternal shelf, the labial face of the crown is flat and bears a weakly developed exodaenodont lobe; the lobe is short, shallow, and smoothly rounded ventrally, rather than drawn out to an acute point. Lingually the crown is slightly convex. The cutting edge has 10-12 serrations (mode=10; N=4). The anterior margin is steep, slightly less so than in Mesodma pygmaea, and weakly convex; the first serration is low, and a single pseudoserration can be present. The cutting edge is low and shallowly convex, and the posterior slope descends from the apogee at the fifth serration to near the base of the crown. The first and second labial ridges are closely spaced and intersect near the anterior margin of the crown, whereas the remaining ridges become coarser and further apart posteriorly; ridges are not developed below the ultimate serration.

Discussion.—The specimens of Mimetodon silberlingi from the Blindman River localities closely resemble those of Mim. silberlingi from Roche Percée (Krause, 1977) and Who Nose? (Scott, 2003a). The few differences (e.g., slightly higher P4 crown and a weaker exodaenodont lobe on p4) are considered variation owing to geologic age, provenance, or both. Mim. silberlingi is a long-ranging taxon, both geographically (Alberta to Texas) and temporally (Torrejonian to Tiffanian).

MIMETODON CHURCHILLI Jepsen, 1940

Figures 3.2.1-3.2.5, Table 3.4

Mimetodon churchilli JEPSEN, 1940, p. 317.

Holotype.—PU 14525, incomplete left dentary with i1, p3-4, m1 (Jepsen, 1940, p. 317, fig. 20). Princeton Quarry, Silver Coulee Beds, Fort Union Formation of Wyoming, late Paleocene (late Tiffanian, Ti5, Plesiadapis churchilli/P. simonsi Lineage Zone of Lofgren et al., 2004).

Material examined.—From Joffre Bridge Roadcut upper level: TMP 2002.47.03, incomplete right dentary with i1, p3-4, m1-2.

From DW-2: UALVP 46269, 46270, p4.

Age and occurrence.—Early middle Tiffanian (Protoselene opisthacus/Mixodectes pungens Interval Zone, Ti3, late Paleocene) to late Tiffanian (Plesiadapis simonsi/P. gingerichi Lineage Zone, Ti5, late Paleocene) of the Western Interior of North America.

Description.—Dentary and lower dentition (Figs. 3.2.1-3.2.5): Only the anterior parts of the dentary in TMP 2002.47.03 are preserved. Although it is considerably larger, the horizontal ramus of Mimetodon churchilli closely resembles that of Mim. silberlingi. The ramus is robust, particularly below p4, and in the alveolar process is short, deep, and not drawn out dorsally as a sharp keel. A large mental foramen opens anterolaterally, ventral to the diastema between i1 and p3. The symphyseal surface is poorly preserved, but appears to have differed little from that in Mim. silberlingi. A deep masseteric fossa extends anteriorly to at least the level of the posterior root of m1, and the base of the coronoid process takes its origin lateral to the lower molars, extending anteriorly to the level of the posterior root of m1.

i1: As in Mim. silberlingi, the i1 in Mim. churchilli is short and deep, and bears an anteroposteriorly short and laterally compressed crown. The i1 in TMP 2002.47.03 is slightly damaged near its base, altering its original position in the jaw; nonetheless, the tooth appears to have been more procumbent than in Mim. silberlingi. The lateral surface of the crown is convex, whereas the medial surface is flat and bears a prominent ventral crest that runs from apex to base. A shorter crest is developed dorsolaterally.

Lower premolars: p3: The p3 of Mim. churchilli is small, peg-like, and inserts into the anterobasal concavity on p4.

p4: The crown of p4 is similar to that of Mim. silberlingi, albeit significantly larger (the p4 in Mim. churchilli is approximately 40 per cent longer than that in Mim. silberlingi). The profile is low and long, higher anteriorly than posteriorly, with an arcuate cutting edge (Figs. 3.2.1, 3.2.4). The exodaenodont lobe is deeper than in Mim. silberlingi, but is similarly short anteroposteriorly; the posterolabial shelf is well developed, forming a near-vertical ridge at the posterior margin of the crown. The anterior margin is slightly steeper than in Mim. silberlingi, and no pseudoserrations are developed. The cutting edge has 12 (N=1) or 13 (N=2) serrations that are larger and coarser posteriorly; the last two or three serrations are swollen and nearly circular in cross

section. The cutting edge is weakly convex posteriorly, descending gently from the fourth or fifth serration to the posterior margin of the crown. Labial and lingual ridges are developed below the serrations and are closely spaced anteriorly; the first and second, or first, second, and third labial ridges are delicate and meet anteroventrally, while the remaining labial ridges are coarser and more widely spaced. The lingual ridges run more obliquely posterodorsally-anteroventrally relative to the labial ridges and become coarser and further apart posteriorly; ridges are faint to absent below the last two or three serrations. The anterobasal concavity is deeply excavated, similar to that in Neoplagiaulax hazeni and N. cimolodontoides (e.g., Jepsen, 1940 and later in this chapter), and the anterior root bears a weak vertical groove.

Lower molars: m1 cusp formula 8:5; m2 cusp formula 6:4. Other than bearing two additional cusps in the external row, the m1 in TMP 2002.47.03 closely resembles that in the type specimen. The crown is subrectangular in occlusal aspect, with the two cusp rows slightly divergent posteriorly. The cusps of the external row are wide at their bases, subpyramidal anteriorly but more nearly crescentic posteriorly, and are subequal in height. The ultimate external cusp is weakly divided on its lingual wall, and is considerably longer than the preceding cusps. A narrow cingulid is developed labial to the external row. The cusps of the internal row are tall with flat internal and convex lingual walls; the first three cusps are subpyramidal, whereas the last two cusps are crescentic. The labial sides of the external and internal cusps are irregularly but strongly grooved, and weaker grooving is present on the lingual sides of the external cusps.

The m2 is subtrapezoidal in occlusal outline. The cusps of the external row are low, closely spaced, and strongly crescentic, whereas the four cusps of the internal row are larger but similarly crescentic. The last three cusps of the external row are poorly differentiated labially, but are clearly separate lingually. Deep grooves are developed on the labial side of the internal cusps, and shallow grooving is present on the labial and lingual sides of the external cusps.

Discussion.—Mim. churchilli is among the most poorly represented North American neoplagiaulacids, and until now was known only from the type specimen, a referred p4 (Jepsen, 1940), and a recently referred lower incisor (Secord, 2004), all from the late Tiffanian (Ti5) Princeton Quarry of Wyoming. The Albertan specimens differ

only in minor details from the Wyoming specimens: the i1 is somewhat less robust, and bears a more conspicuous ventromedial ridge; the p4 is slightly smaller, with more obliquely oriented lingual ridges; and m1 bears more cusps in the external row (eight as opposed to six in PU 14525). The Albertan specimens represent the first occurrence of this poorly known taxon outside of the type locality in Wyoming, and the first record of sympatric occurrences of species of Mimetodon.

Genus ECTYPODUS Matthew and Granger, 1921

Charlesmooria KÜHNE, 1969, p. 200.

Type species.—Ectypodus musculus Matthew and Granger, 1921.

Other included species.—E. tardus (Jepsen, 1930); E. powelli Jepsen, 1940; E. lovei (Sloan, 1966); E. childei (Kühne, 1969); E. szalayi Sloan, 1981; Ectypodus aphronorus Sloan, 1987; E. elaphus new species.

ECTYPODUS ELAPHUS new species

Figures 3.2.6-3.2.20, 3.3; Table 3.5

Ectypodus sp. 1 FOX, 1990, p. 61.
Ectypodus sp., cf. E. szalayi MACDONALD, 1996, p. 17.

Diagnosis.—Small species of Ectypodus (mean length p4, E. elaphus, 50 percent less than p4, E. musculus, 23 percent less than p4, E. powelli and E. aphronorus, the three largest species of the genus); differs further from E. musculus and E. aphronorus in p4 being much lower crowned relative to length. Most similar to E. szalayi, E. powelli, and E. tardus but differs from these in p4 being lower crowned and more asymmetrical in lateral profile; differs further in having p4 with a lower first serration, steeper anterior crown margin, and apogee of the serrated crest further anteriorly. Differs further from E. szalayi in lower molars having fewer cusps in both rows. Differs further from E. tardus

in retaining p3 and in P4 having a longer, straighter posterior slope. Differs from E. childei in retaining p3 and in having a better-developed exodaenodont lobe on p4.

Description.—Upper dentition (Figs. 3.2.6-3.2.11): Upper premolars: P4: Cusp formula (0)2:6:0 [mode=(0)2:6:0; N=5]. The anatomy of the referred P4s is in agreement with Sloan's (1981) characterization for that of Ectypodus: the crown is high relative to its length, with straight anterior and straight to slightly concave posterior margins, and a weakly developed posterobasal cusp (see Fig. 3.2.7). In occlusal aspect, the crown narrows at the posterior margin of the poorly developed anterolabial lobe, similar to P4 in both E. powelli and E. tardus (see Krause, 1980, 1982a; Krishtalka, 1984). The anterolabial lobe supports two prominent cusps, with one or two tiny cuspules variably developed anterior or posterior to the cusps of the external row. The middle cusp row is virtually straight, and the apogee occurs slightly anterior relative to P4 in other neoplagiaulacids, imparting a more trenchant profile to the crown. The anterior root is nearly circular in cross section, whereas the posterior root is laterally compressed. Neither an interradicular crest nor an accessory root is developed.

Upper molars: M1: Cusp formula 7:9:5 (N=1). The referred M1 is nearly identical to those described by Krause (1980) for E. powelli from the Bighorn Basin of Wyoming, differing only in its slightly smaller size (e.g., mean length, M1, E. elaphus=2.4, N=1 versus mean length, M1, E. powelli=2.5, N=7; Krause, 1980). The dimensions and overall morphology of UALVP 46225 are also near those of M1, Mesodma pygmaea, and their cusp formulae overlap; M1 of E. elaphus can, however, be distinguished from that of M. pygmaea in being slightly larger, in having a longer internal cusp row (the row begins at the third, rather than the fourth cusp of the middle row), and in having pyramidal rather than crescentic posterior cusps in the middle row.

Dentary and lower dentition (Figs. 3.2.12-3.2.20): The holotype of E. elaphus preserves significant parts of the dentary (Figs. 3.2.12-3.2.14). The horizontal ramus is slightly damaged ventral to the ascending ramus and posteroventral to the condylar process, and the ventral margin anterior to p4 is broken or otherwise missing, but despite the damage, the overall anatomy of the dentary is generally similar to that of other neoplagiaulacids (e.g., dentaries of Ectypodus and Neoplagiaulax as described by Jepsen, 1940 and Krishtalka, 1984). A single, large mental foramen occurs on the incisor

alveolar process, slightly anterior to p3, and opens laterally. Posterior to p4, the ventral margin of the horizontal ramus is concave at the level of the anterior root of m1, while the remaining parts are slightly convex. The posterior margin below the condylar process has been broken away, but probably differed little from that of E. tardus, being straight to slightly concave posteriorly (Sloan, 1979; Krishtalka, 1984). The masseteric fossa is well excavated posteriorly, and extends anteriorly to a shallow masseteric fovea below the posterior root of p4. The masseteric crest (Simpson, 1926) is wide at the level of the ascending ramus, but narrows posteriorly, becoming confluent with the horizontal ramus below and anterior to the level of the condylar process; the crest continues as a low ridge to the condyle. Although the medial side of the dentary is extensively damaged, the parts that remain indicate that the pterygoid fossa was very deep, with its anterior border extending to the posterior root of m2 and delimited by a distinct rim. The pterygoid crest is wide medially. The coronoid process is damaged dorsally and posteriorly, but from the dimensions of the parts that remain, it appears to have been tall, extending well above the apex of p4, and gracile in construction. The condyle is ovate in dorsal outline and mediolaterally broad, extending slightly further medially than laterally. The articulating surface slopes internally and is virtually flat mediolaterally, but faintly convex anteroposteriorly.

Lower premolars: p3: The crown of p3 is of typical neoplagiaulacid morphology, being peg-like and inserting into the anterobasal concavity of p4.

p4: As in other species of Ectypodus, the p4 in E. elaphus is high and arcuate (Figs. 3.2.12, 3.3), but slightly more asymmetrical in lateral profile. The labial face of the crown is virtually flat and bears a poorly developed posteroexternal shelf and a prominent exodaenodont lobe that is deeper than broad; in some specimens the lobe is peaked ventrally, whereas in others it may be slightly more circular and uniformly arcuate. The lingual side is shallowly convex, especially towards the base of the crown. The enamel-lined anterobasal concavity is deeply notched on all specimens, and the anterior root bears a shallow vertical groove. The anterior margin of the crown is steep and slightly convex, and progresses dorsally to the first serration; an incipient serration is developed on only one specimen. The dorsal crest is arcuate and bears 10 or 11 serrations (mode=11; N=13) that become larger and stouter posteriorly; the third or

fourth serration is highest above the baseline, further anterior than in other species of Ectypodus and more closely approximating p4 in some species of Mesodma. The posterior margin of the crown is virtually straight, descending from the apogee to the ultimate serration. Short anteroventrally directed ridges occur labially and lingually below the first serration, and join with the second labial and lingual ridges slightly anterior and ventral to the first serration. The second labial and lingual ridges are nearly straight and are oriented anteroventrally, with little ventral curvature. The remaining labial and lingual ridges extend anteroventrally in a smooth arc, becoming heavier posteriorly until the penultimate or antepenultimate serration where they are considerably weaker. Ridges are absent at the terminal serration.

Lower molars: m1: Cusp formula 8:4 (mode=8:4; N=5). The crown of m1 is subrectangular in occlusal outline, with the two cusp rows diverging posteriorly and the intercusp valley relatively deep. The cusps of the external row are significantly lower than those of the internal row, and are crescentic, especially posteriorly, whereas those of the internal row are quadrate to pyramidal. The first two cusps of the external row, as well as the last two cusps of the internal row, are often fused together, but are incipiently divided on their valley-facing surfaces; grooving is present on the labial surface of the internal row. The referred m1's are nearly identical to those referred to E. tardus from the Eocene Willwood Formation, Wyoming (Krishtalka, 1984), but also resemble those of Mesodma pygmaea; m1 of E. elaphus can be distinguished from that of M. pygmaea by its greater length (e.g., length m1, E. elaphus=1.78, N=1 versus mean length m1, M. pygmaea, Roche Percée locality=1.70, N=3; Krause, 1977) and having at least two additional cusps in the external row.

m2: Cusp formula 4:2 (N=1). The referred m2 is similar to that in both Ectypodus and Mesodma (e.g., Krause, 1977; Krishtalka, 1984). The m2 of E. elaphus can be distinguished from that of M. pygmaea only in its slightly greater width (e.g., mean width, m2, E. elaphus=0.90, N=1 versus mean width, m2, M. pygmaea, Roche Percée=0.8, N=1; Krause, 1977).

Etymology.—Elaphos, Greek, deer or stag, in reference to the City of Red Deer near where specimens of E. elaphus have been found.

Holotype.—UALVP 45994, incomplete left dentary with p3-4 and alveoli for i1, m1-2 (Figs. 3.2.12-3.2.14). DW-2 locality, Paskapoo Formation of Alberta, late Paleocene [early middle Tiffanian, Ti3 (Fox, 1990), Plesiadapis anceps/P. rex Lineage Zone of Lofgren et al., 2004].

Other material examined.—From Joffre Bridge Road Cut lower level: UALVP 46024, m1.

From DW-1: UALVP 45995, P4.

From DW-2: UALVP 45996, 45997, 45998, 45999, P4 (total: 4); UALVP 46225, M1; UALVP 46000, incomplete left dentary having p4; UALVP 46001, incomplete right dentary having p4; UALVP 46002, incomplete right dentary having p4; UALVP 46003, 46004, 46005, 46006, 46007, 46008, 46009, 46010, 46011, 46012, 46013, 46014, 46015, 46016, 46017, 46018, p4 (total: 16); UALVP 46019, 46020, 46021, 46022, 46023, m1 (total: 5); UALVP 46226, m2.

From Hand Hills West upper level: UALVP 34964, P4.

Age and occurrence.—Early middle Tiffanian (Plesiadapis anceps/P. rex Lineage Zone, Ti3, late Paleocene) of Alberta.

Discussion.—The high, arcuate profile of p4 and the straight anterior and posterior margins of P4 are consistent with Sloan's (1981) diagnosis of Ectypodus, and the referred specimens are here interpreted as representing a new species. The upper and lower teeth are only tentatively associated, particularly since P4 and M1 are infrequent in the sample; confidence in their correct association is increased when considering the length of the referred P4s (approximately 70 percent the length of p4, see Sloan, 1981). Among the known species of Ectypodus, the referred teeth most closely resemble those of E. powelli [including E. sp., cf. E. powelli from Roche Percée, Saskatchewan (Krause, 1977), and E. sp., cf. E. powelli from the Blindman River localities (Fox, 1990 and see later in this chapter)], an unnamed species of Ectypodus from the late Puercan (Pu3) Rav W-1 locality of Saskatchewan (Johnston and Fox, 1984), and, especially, E. szalayi from the middle Torrejonian (To2) Gidley Quarry of Montana (Sloan, 1981): the p4s of E. elaphus and E. szalayi are of similar size [mean length p4, E. elaphus=2.63, N=15; mean length p4, E. szalayi=2.8 (Sloan, 1987)] and p4 serration number [p4 modal serration number, E. elaphus=11; p4 modal serration number, E. szalayi=11 (Sloan, 1987)], and in

these respects the p4 of the two taxa cannot easily be distinguished. Subtle differences in coronal anatomy, however, separate the two taxa: relative to p4 of E. szalayi, that of E. elaphus is lower crowned and more asymmetrical (i.e., less evenly arcuate) in profile (Fig. 3.2.12, and compare with Sloan, 1981, text-fig. 6.10, Vianey-Liaud, 1986, text-fig. 49, and Gambaryan and Kielan-Jaworowska, 1995, fig. 4a); the anterior margin is steeper and more nearly vertical; the first serration is lower; and the apogee is further anterior on the crown.

Sloan (1981, 1987) regarded E. szalayi as the basal member of the Ectypodus lineage, forming a morphological link between Mesodma formosa (Marsh, 1889) and later species of Ectypodus. Although direct derivation of E. szalayi from M. formosa is debatable, the p4 coronal anatomy of E. szalayi is clearly primitive among species of Ectypodus. When p4 of E. szalayi and E. elaphus are compared, that of E. elaphus is the more primitive, a conclusion supported by comparisons with p4 of less derived neoplagiaulacids (e.g., Mesodma): the first serration is lower, the anterior margin is steeper and more nearly vertical, and the crown is lower and less symmetrically arcuate. Additionally, the m1 of E. elaphus has fewer cusps in both rows compared to that of E. szalayi but a greater number relative to that of any species of Mesodma (Sloan, 1987).

E. szalayi is known from the middle Torrejonian to earliest Tiffanian (To2-Ti1) of the Western Interior of North America, while E. elaphus is known only from the early middle Tiffanian (Ti3) of Alberta [in addition to its occurrence at the Blindman River localities, E. elaphus is also known from the early middle Tiffanian (Ti3) Hand Hills West upper level locality (Fox, 1990; MacDonald, 1996)]. Despite the contradictory stratigraphic occurrences of the younger and arguably more primitive E. elaphus and the older and more derived E. szalayi, the dentition of E. elaphus is structurally intermediate between those of Mesodma and E. szalayi, independent of geological time, and little change would be required to arrive at an E. szalayi-like morphology from that of E. elaphus. The records of both E. szalayi and E. elaphus are poor relative to coeval neoplagiaulacids; further sampling is needed to address the stratigraphic incongruence and clarify the relationship of E. szalayi to E. elaphus, and the relationships of both to other species of Ectypodus.

ECTYPODUS sp., cf. E. POWELLI

Figures 3.2.21-3.2.25, Table 3.6

Material examined.—From DW-1: UALVP 46271, incomplete left maxilla with P4, M1-2.

From DW-2: UALVP 46272-77, P4 (total: 6); UALVP 46278, M1; UALVP 46279, p4.

Description.—Upper dentition (Figs. 2.21-2.23): Upper premolars: P4: Cusp formula (0)3-5:6-8:0 [mode=(0)4:6:0; N=7]. The P4 of Ectypodus sp., cf. E. powelli is high, with the ultimate or ultimate and penultimate cusps highest above the base of enamel (Fig. 3.2.22). The anterolabial lobe is weakly developed, and the external row can bear three to five cusps that increase in size to the third or fourth cusp. A slight swelling bearing a small cuspule occurs on one specimen external to the anterolabial lobe. The cusps of the middle row increase in size and height posteriorly. The anterior slope can be straight to slightly convex, while the posterior slope is long and slightly concave; the apogee occurs slightly more anterior to that on P4 of other neoplagiaulacids. The referred P4s are nearly identical to that in UM 69868, an incomplete left maxilla from the Clarkforkian (latest Paleocene) of Wyoming, referred to E. powelli (Krause, 1980).

Upper molars: M1 cusp formula 8-9:10:4-5 (N=2); M2 cusp formula 3:3 (N=1). The molars of Ectypodus sp., cf. E. powelli are generally similar in both size and overall anatomy to those of E. powelli, E. tardus, and Mimetodon silberlingi; they are closest to molars E. powelli from the Clarkforkian of Wyoming described by Krause (1980), differing only in the internal cusp row of M1 originating at the fifth cusp of the middle row, rather than the third or fourth. The cusps of the middle row of M1 are subrectangular in horizontal section, differing from those of Mimetodon in which they become more nearly crescentic posteriorly.

Lower dentition (Figs. 3.2.24, 3.2.25): Lower premolars: p4: The p4 of Ectypodus sp., cf. E. powelli is high and semicircular in lateral profile (Fig. 3.2.24). The labial face of the crown is flat, while the lingual side is faintly convex. The exodaenodont lobe is anteroposteriorly narrow and pointed ventrally, and is more anterior than on p4 in

Mesodma or Mimetodon. The crown height at the exodaenodont lobe is 2.5 mm, about 87 percent of the standard length. A short, robust posterolabial shelf occupies the area immediately beneath the ultimate serration. The anterobasal concavity is shallow and the anterior root is grooved, but whether or not p3 was present in life cannot be determined. The cutting edge bears 12 serrations that become larger and more nearly conical posteriorly; the first serration is high on the long anterior margin of the crown, and the apogee occurs at the third and fourth serrations. Coarse, obliquely oriented ridges are developed labially and lingually, with the first and second labial ridges, and first through third lingual ridges, joining near the anterior margin of the crown. Labial and lingual ridges are not present beneath the last two serrations.

Discussion.—The coronal anatomy of teeth referred to Ectypodus sp., cf. E. powelli from Alberta is consistent with Sloan's (1981) generic diagnosis for Ectypodus: the crown of P4 is high, with the ultimate cusp in the principal row highest, and the anterior and posterior slopes are relatively straight. Additionally, p4 is higher and more arcuate than in more basal neoplagiaulacids, and the third or fourth serration is highest above the baseline of standard length. The referred teeth most closely resemble those of the late Tiffanian and early Clarkforkian E. powelli and Wasatchian E. tardus. Although Krishtalka (1984) suggested E. powelli and E. tardus were possibly synonymous, Krause (1982a), on the basis of better-preserved material of E. tardus, demonstrated the validity of both taxa, and that opinion is followed here. The specimens from the Blindman River localities closely resemble teeth of both E. powelli and E. tardus, but differ from those of the latter in being slightly larger, in P4 having a greater number of external cusps, and in p4 having a better-developed exodaenodont lobe and deeper anterobasal concavity. The specimens also differ from teeth of E. elaphus in being slightly larger (e.g., p4, Ectypodus sp., cf. E. powelli approximately 8 per cent longer than p4, E. elaphus), in p4 being higher and more nearly semicircular in profile, and in P4 having more cusps in the external row.

Several authors have noted the close similarity in the teeth of Ectypodus powelli and E. tardus (e.g., McKenna, 1960; Krause, 1982a; Krishtalka, 1984), with the presence or absence of p3 cited as a possible distinction between the two. In his description of E. powelli from the Polecat Bench Formation of Wyoming, Jepsen (1940) noted an absence

of p3 in the hypodigm jaws, a feature confirmed in larger samples from the Bighorn Basin (Krause, 1982a). Krishtalka (1984), following Sloan (1979, 1981), suggested the presence of p3 in E. powelli and E. tardus may be variable, citing a deep anterobasal concavity on some p4s of E. tardus as evidence of p3 having been present in life. The anterobasal concavity in UALVP 46279 is deep, suggesting at least the ephemeral presence of p3 (i.e., p3 having been present at some earlier stage in life and subsequently shed ontogenetically); ontogenetic loss of p3 has also been proposed for the microcosmodontid Microcosmodon conus Jepsen, 1930 from the Princeton locality (Jepsen, 1930; Fox, 2005). Given the apparent variability in the presence of p3 in E. powelli and E. tardus, its presence or absence is likely of little value in distinguishing the two taxa, an opinion previously stated by McKenna (1960).

Although UALVP 46279 is similar to YPM-PU 14425, a p4 from the Princeton Quarry included in Jepsen's (1940) hypodigm for E. powelli, these teeth together differ from p4s of E. powelli from the Clarkforkian of northwestern Wyoming (Krause, 1980): the profiles of UALVP 46279 and YPM-PU 14425 are more nearly semicircular (i.e., are less asymmetrical), the first serration is relatively lower, and the posterior slope of the crown is shorter. In light of these differences, and considering the paucity of specimens from the Blindman River localities, the teeth described above are conservatively referred to Ectypodus sp., cf. E. powelli.

Ectypodus powelli is a stratigraphically long-ranging taxon known from a number of localities in the Western Interior of North America; if confirmed by subsequent sampling, its occurrence at the Blindman River localities would be the oldest so far discovered in Canada.

Genus NEOPLAGIAULAX Lemoine, 1882

Plagiaulax: LEMOINE, 1880, p. 12.

Type species.—Neoplagiaulax eocaenus (Lemoine, 1880).

Other included species.—Neoplagiaulax copei Lemoine, 1885; N. grangeri (Simpson, 1935); N. hunteri (Simpson, 1936); N. hazeni (Jepsen, 1940); N. macrotomeus

(Wilson, 1956); N. nanophus Holtzman, 1978; N. macintyrei Sloan, 1981; N. burgessi Archibald, 1982; N. kremnus Johnston and Fox, 1984; N. annae Viany-Liaud, 1986; N. nicolai Viany-Liaud, 1986; N. sylvani Viany-Liaud, 1986; N. jepi Sloan, 1987; N. mckennai Sloan, 1987; N. "nelsoni" Sloan, 1987; N. donaldorum Scott and Krause, 2006; N. serrator new species; N. cimolodontoides new species; N. paskapooensis new species.

NEOPLAGIAULAX SERRATOR new species

Figures 3.4.1-3.4.6, 3.5.1-3.5.7, 3.6; Tables 3.7, 3.10

Neoplagiaulax hunteri: KRISHTALKA, 1973, p. 10 (in part).
Neoplagiaulax n. sp. 1: FOX, 1990, p. 61.
Neoplagiaulax sp., cf. N. hunteri WEBB, 1996, p. 23.
Neoplagiaulax sp. MACDONALD, 1996, p. 25.

Diagnosis.—Medium-sized species of Neoplagiaulax, larger than both N. macintyrei and N. nanophus (mean length p4 of N. serrator 25 percent longer than that in N. macintyrei and N. nanophus), but smaller than N. mckennai and N. grangeri (mean length p4 of N. serrator 25 percent smaller than that in N. mckennai and N. grangeri); differs from all other species of Neoplagiaulax in having a greater modal p4 serration count; most similar to N. hunteri, N. kremnus, and N. eocaenus, but differs from these in P4 and p4 being lower crowned relative to length, in p4 having a steeper anterior margin and a lower first serration; differs further from N. eocaenus in retaining p3.

Description.—Upper dentition (Figs. 3.4, 3.5.1): Upper premolars: P1: The crown of P1 approximates that of Type D P1s from the late middle Tiffanian (Ti4) Roche Percée local fauna of Saskatchewan (Krause, 1977) in having a posterolingual cusp and two closely approximated cusps arranged anterolingual-posterolabially (Figs. 3.4.3, 3.4.6). The crown differs, however, in being smaller and suboval rather than semicircular in outline, and the lingual side is more convex relative to that of P1 described by Krause (1977). The posterolingual cusp is nearly triangular in cross section, whereas the slightly taller external cusps are lenticular and joined for nearly half their height; the posterointernal margin of the crown is sometimes swollen and extended posteriorly.

P2: Except for their smaller size, the referred P2s are virtually identical to those described by Krause (1977) as Type E premolars from Roche Percée. The tooth is two-rooted, and the crown is circular in occlusal outline and dominated by a large, lenticular labial cusp. Two smaller, subequal lingual cusps are positioned directly lingual from the labial cusp and are triangular in cross section. The anterior ridge present in the Roche Percée teeth is only weakly developed or absent among the referred P2s, and a cuspule anterior to the labial cusp is sometimes present. As in P1, the posterointernal margin of the crown is sometimes swollen and elongate, but unlike P1, the anterior margin overhangs the anterior root.

P3: The referred P3s are low crowned relative to P1 and P2, with lower cusps and a more prominent posterior lobe, closely approximating Krause's (1977) Type F premolars from Roche Percée. The tooth is two-rooted and subrectangular in outline, and the crown bears four cusps arranged in two parallel rows. The posterolabial cusp is the largest and tallest, while the remaining three are of uniform size and height; the two cusps of the lingual row are usually joined for nearly half their height. A strong interdental facet is developed posteriorly.

P4: Cusp formula (0)1-2:9-11:0 [mode=(0)1:10:0; N=31]. In occlusal aspect, the crown is slightly convex labially and wider anteriorly than posteriorly. The anterolabial lobe is well developed and bears a single large cusp situated opposite the second or third cusp of the middle row; some specimens can bear a much smaller cusp anterior to this cusp. The crown is long relative to its height, with the anterior slope moderately convex in lateral profile, and the posterior slope gently sloping and straight to slightly concave (Figs. 3.4.2, 3.4.5). The cusps of the middle row are subequal in size, and increase in height posteriorly to the antepenultimate, penultimate, or penultimate and ultimate cusps together. The referred P4s are similar in most features to those of N. hunteri from Roche Percée and the early Tiffanian (Ti2) Scarritt Quarry of Montana (Simpson, 1936), but differ in being shorter and narrower, with shorter and shallower posterior slopes, and in being proportionately lower-crowned relative to their length.

Upper molars: M1: Cusp formula 7-8:10-12:5-8 (mode=7:12:6; N=11). The referred M1s are most similar to the single M1 of N. hunteri from Roche Percée (Krause, 1977), differing only in their slightly shorter length and fewer cusps. The cusps of the

external row are flat on their internal walls and rounded labially, while those of the middle row are four-sided anteriorly but become larger and more nearly crescentic posteriorly. The internal row is variable in length, originating at the third, fourth, fifth, or sixth cusp of the middle row; the cusps are large and conspicuous posteriorly, but become smaller anteriorly, eventually grading into a papillate ridge. As with M1 in N. hunteri, the valley-facing slopes of the cusps in N. serrator are deeply grooved.

M2: Cusp formula 3-4:4 (mode=3:4; N=16). As with M1, the M2 of N. serrator is similar to that of N. hunteri from Roche Percée (Krause, 1977), differing only in its smaller size and in having a weaker external crest.

Dentary and lower dentition (Fig. 3.5): The dentary of Neoplagiaulax serrator is similar to that of other species of Neoplagiaulax and ptilodontoid multituberculates generally (Simpson, 1937a; Jepsen, 1940; Krishtalka, 1984). The symphyseal surface is anteroposteriorly short and comma shaped, with the arm of the comma directed posteriorly and ventrally; the symphyseal bone is finished and not rough or rugose. The alveolar process for the incisor is long and shallow, with i1 projecting anteriorly and dorsally, much like mandibles in N. hunteri (Sloan, 1987), but different from that in N. hazeni in which the incisor alveolar process is short and deep and the enlarged i1 less procumbent (Figs. 3.5.5, 3.5.6). The dorsal margin of the incisor alveolar process between i1 and p4 is drawn out as a shallow keel, similar to that in Ectypodus powelli (see Jepsen, 1940). The horizontal ramus is robust and deep, especially below p4 and the molars, and is oriented obliquely relative to the incisor, similar to those of ptilodontoid multituberculates generally. The masseteric and pterygoid fossae are well excavated and extend anteriorly to beneath the posterior root of p4; the masseteric and pterygoid crests are strongly developed, much more so than those of Ectypodus (see earlier in this chapter). The pterygoid fossa terminates anteriorly in a large, subovate inferior dental foramen (Miao, 1988). The coronoid process is best preserved on the type specimen: the process is robust, with the bone thick and the lateral wall well excavated for insertion of the mandibular adductors. The long ascending process originates lateral to the midpoint of m1, and is anterodorsally curved; the posterior border is shorter and shallowly concave. Although the apex of the coronoid process is slightly damaged, it was clearly well above the apogee of the p4 crown and smoothly rounded dorsally. The dentary

narrows posterior to the coronoid process, and forms a short but robust condylar process that terminates in a large, broad condyle. The condyle is oriented parallel with the lower molars, with the articulating surface positioned above the level of the tooth row, and tilted slightly posteriorly. The articulating surface is subovate in dorsal outline, wider than long, and extends further medially than laterally relative to the long axis of the dentary; the surface is shallowly concave mediolaterally. The dentary is robust beneath the condyle, and the bone forming the posterior margin is thickened into a posteriorly convex ridge. All of the dentaries of N. serrator at hand bear at least two mental foramina, the larger positioned anteroventral to p3 on the alveolar process for i1, the smaller slightly ventral to p3.

i1: The i1 of N. serrator is long and slender, convex laterally and flat medially, with well developed dorsal, ventral, and medial ridges.

Lower premolars: p3: The crown of p3 is small, peg-like, and without accessory cuspules.

p4: In lateral view, the crown of p4 is long and low, with the cutting edge forming a smooth arc dorsally (Figs. 3.5.1, 3.5.2, 3.5.5, 3.6). The anterior margin of the crown is slightly convex and steep, whereas the posterior margin is shallowly arcuate and descends posteroventrally at an angle of about 45 degrees from horizontal. The distance between the base of the exodaenodont lobe and the dorsal margin is approximately three-quarters the anteroposterior length of the crown, and the height of the first serration is approximately one-third the anteroposterior length. The exodaenodont lobe varies in structure, but is most often shallow and pointed ventrally (Figs. 3.5.1, 3.5.2); the posteroexternal shelf is weakly developed. The labial and lingual faces of the crown are both flat and the cutting edge bears between 16 and 19 serrations (mode=17; N=33), highest among known neoplagiaulacids. The first serration is positioned low on the crown relative to other species of Neoplagiaulax, and the distance between it and the next serration is longer than that between subsequent serrations. When the dentary is held in a horizontal plane, the apogee of the cutting edge is at the sixth through tenth serrations, a feature that is considered characteristic of Neoplagiaulax (Sloan, 1981). The serrations are delicate anteriorly but become larger and coarser posteriorly, with the last four or five being stout and nearly conical. The pattern of ridges originating from below the first

serration varies among the specimens at hand, but usually consists of a single, short labial ridge that may or may not join with the second ridge; a median ridge directed anteriorly along the anterior face of the crown, where it may bifurcate or simply end abruptly; and a longer lingual ridge that joins either with the second or third lingual ridge. The second lingual ridge may traverse the lingual face of the crown directly, or it may join with the third ridge. The remaining labial and lingual ridges are roughly parallel to each other; the more posterior ridges are shorter and often coarser. The labial and lingual surfaces of the crown beneath the last three or four serrations do not bear ridges, and the posterolabial face of the crown frequently bears a large, circular wear facet. The enamel at the posteroexternal shelf is crenulated, and the anterobasal concavity is deep and notched for reception of p3.

Lower molars: m1: Cusp formula 9-10:4-5 (mode=10:5; N=15). The crown of m1 is subrectangular in occlusal aspect, with the two cusp rows diverging posteriorly. The cusps of the external row are wide at their bases, subpyramidal anteriorly, but become strongly crescentic posteriorly. Except for the first one or two, the cusps of the external row are approximately the same size, but increase in height posteriorly to the fifth or sixth cusp, after which they remain subequal. The ultimate external cusp can be larger than the preceding cusps. A short row bearing one or two small cuspules is developed labial to the external row on one specimen. The cusps of the internal row are tall with flat internal and convex lingual walls; as with the external cusps, the bases of the internal cusps are inflated. The first cusp of the internal row is small and short, but the remaining cusps are considerably larger and taller, with the ultimate internal cusp largest, sometimes nearly twice the length of the preceding cusp. The labial sides of the external and internal cusps are irregularly but strongly grooved, and weaker grooving is sometimes present on the lingual sides of the external cusps. The m1 is similar to that of N. hunteri from Roche Percée (Krause, 1977), but is smaller and has modally one fewer cusp in the external row.

m2: Cusp formula 4-6:2-3 (mode=5:2; N=22). The m2 of N. serrator is subtrapezoidal in occlusal outline, with the bases of the external and internal cusps wide. The cusps of the external row are strongly crescentic and subequal in size and height, while the two cusps of the internal row are larger, with the first crescentic and the second

subpyramidal in cross-section. The last two, and sometimes three, cusps of the external row are poorly differentiated externally, and an incipiently developed third cusp is sometimes present on the internal row. Unlike on m1, grooving on m2 is strongest on the lingual side of the internal cusp row.

Etymology.—Serrator, Latin, sawyer; in reference to the great number of serrations on p4.

Holotype.—UALVP 46025, incomplete skull having left P1-4, M1-2, right P1-4, M1?-2, and associated incomplete right dentary having i1, p3-4, m1-2 (Fig. 4.1). DW-2 locality, Paskapoo Formation of Alberta, late Paleocene [early middle Tiffanian, Ti3 (Fox, 1990), Plesiadapis anceps/P. rex Lineage Zone of Lofgren et al., 2004].

Other material examined.—From Joffre Bridge Roadcut lower level: UALVP 46134, 46135, p4.

From DW-2: UALVP 46026, incomplete right maxilla having P4, M1, and associated left dentary having i1, p4, m2, and associated right dentary having i1, p3-4, m1-2; UALVP 46027, incomplete left maxilla having P1-4, M1-2; UALVP 46028, incomplete left maxilla having P1-4, M1-2; UALVP 46029, incomplete right maxilla having P1-4; UALVP 46030, incomplete left maxilla having P1-2, P4, M1-2; UALVP 46031, incomplete right maxilla having P1-4, M2; UALVP 46032, incomplete left maxilla having P1-4, M1-2; UALVP 46033, incomplete left maxilla having M1-2; UALVP 46034, incomplete right maxilla having P1-3; UALVP 460, 46035-46061, P4 (total: 27); UALVP 46062-46068, M1 (total: 7); UALVP 46069-46079, M2 (total: 11); UALVP 46080, incomplete right dentary having i1, p3-4, m1-2; UALVP 46081, incomplete left dentary having i1, p3-4, m1-2; UALVP 46082, incomplete left dentary having i1, p3-4, m1-2; UALVP 46083, incomplete right dentary having p3-4, m1-2; UALVP 46084, incomplete right dentary having i1, p3-4, m1-2; UALVP 46085, incomplete left dentary having i1, p3-4, m1-2; UALVP 46086, incomplete right dentary having p4, fragmentary m1; UALVP 46087, incomplete left dentary having i1, p3-4, m1-2; UALVP 46088, incomplete right dentary having p4, fragmentary m1; UALVP 46089, incomplete right dentary having fragmentary p4; UALVP 46090, incomplete right dentary having p3-4, m1-2; UALVP 46091, incomplete left dentary having i1, p3-4, m1-2; UALVP 46092, incomplete left dentary having p4; UALVP 46093, incomplete right

dentary having p4, m1-2; UALVP 46094-46113, p4 (total: 20); UALVP 46114-46118, p4 fragments; UALVP 46119-46122, m1 (total: 4); UALVP 46123-46133, m2 (total:11).

From Hand Hills West upper level: UALVP 35238, 35239, M1; UALVP 34946, 34985, p4; UALVP 35241, 35242, 35244, m1 (total: 3); UALVP 34965, 34966, 34968, 34969, 46136, 46137, m2 (total: 6).

From Birchwood: UALVP 39126, 39128, 39129, 39134, p4 (total: 4).

From Police Point (UAR-1): UALVP 5657, 5658, 5660, 5661, P4 fragments.

Age and occurrence.—Early middle Tiffanian (Plesiadapis anceps/P. rex Lineage Zone, Ti3, late Paleocene) to late middle Tiffanian (Plesiadapis rex/P. churchilli Lineage Zone, Ti4, late Paleocene) of Alberta.

Discussion.—The major features of the dentition of N. serrator are consistent with Sloan's (1981) diagnosis for the genus, and identify these specimens as pertaining to Neoplagiaulax. Among the North American species of Neoplagiaulax, N. serrator most closely resembles N. hunteri (including N. cf. hunteri from the Blindman River localities, see Fox, 1990) and N. kremnus from the late Puercan (Pu3) Rav-W1 locality, Saskatchewan (Johnston and Fox, 1984) in corresponding parts of the dentition, but differs in a number of important features. The crown of P4 is lower relative to its length, narrower, and the anteroexternal cusps are more poorly developed than those of N. hunteri or N. kremnus. The lateral profiles of p4 differ appreciably (Fig. 3.6): that of N. serrator is comparatively lower relative to its length, and lacks the abruptly truncated posterior margin seen in p4 of N. hunteri; as a result, the crown of p4 of N. serrator is much less trapezoidal in profile compared to that of N. hunteri and, to a lesser degree, N. kremnus. The anterior margin of p4 is more steeply inclined in N. serrator than in either N. hunteri or N. kremnus, the first serration is slightly lower, and the modal serration number is greater. Additionally, the labial face of p4 is flat rather than convex (a convex labial face is considered diagnostic of N. hunteri, see Krause, 1977). In addition to the differences in crown structure, the coronal dimensions of N. serrator are beyond or slightly overlap the low end of the ranges given by Krause (1977) for N. hunteri from Roche Percée, and only slightly overlap those of N. hunteri from Scarritt Quarry (Simpson, 1936) and the late middle Tiffanian (Ti4) Judson locality of North Dakota (Holtzman, 1978; Kihm and Hartman, 2004); Student's t-test applied to mean lengths of

both P4 and p4 in the Blindman River and Roche Percée samples resulted in statistical significance ($p<0.01$) that N. serrator and N. hunteri are conspecific, consistent with the two samples having been drawn from separate species.

Among other species of Neoplagiaulax, N. serrator bears superficial resemblance to N. eocaenus from the Cernaysian (late Paleocene?-early Eocene) Cernay-lès-Reims and Mont de Berru faunas of France (D. Russell, 1964; Savage and Russell, 1983; Vianey-Liaud, 1986). Individuals of both taxa have p4 with similar lateral profiles (Figs. 3.5.1, 3.5.2, 3.5.5 and compare with D. Russell, 1964, fig. 8 and Vianey-Liaud, 1986, text-fig. 5) and P4 with similar cusp counts, yet they differ widely in many respects: the p4 of N. serrator is larger, with more serrations; the anterior margin is much steeper and less uniformly arcuate; the first serration is comparatively lower; and the exodaenodont lobe is narrower. Additionally, P4 of N. serrator is slightly larger relative to that of N. eocaenus, with a longer and shallower posterior slope, and a better-developed external cusp. One of the difficulties in assessing a possible relationship between N. serrator and N. eocaenus stems from the wide range of morphological variation present in the samples of N. eocaenus from Cernay and Berru. Vianey-Liaud's (1986) study of Cernaysian multituberculates included many new specimens from the Paris Basin that she referred to N. eocaenus; examination of the figured p4s and P4s (Vianey-Liaud, 1986, text-figs. 6, 10) however, reveals an unusually large range of variation, suggesting N. eocaenus may be a composite, encompassing multiple, perhaps closely related neoplagiaulacid taxa. Given the possible biogeographic implications of closely related species of Neoplagiaulax from North American and Europe, a taxonomic reassessment of N. eocaenus and clarification of relationships between the European and North American species of Neoplagiaulax is in order, but well outside the scope of the present chapter.

Although probably closely related to Neoplagiaulax hunteri and N. kremnus, N. serrator is not easily derivable from these or any other of the known and described species of Neoplagiaulax. The mosaic of low crown height of P4 and p4 and low first serration (plesiomorphic neoplagiaulacid features) and the large number of serrations (apomorphic neoplagiaulacid feature) (Johnston and Fox, 1984) is unique among species of Neoplagiaulax. N. burgessi Archibald, 1982, the earliest known species of the genus, seems too derived in p4 crown height, having an apical crest that is high relative to its

length, and the unusual angular anterior profile is clearly unlike that of N. serrator; likewise, N. "nelsoni" (hypothesized as ancestral to N. hunteri by Sloan, 1987) is also too derived in having comparatively high crowned upper and lower fourth premolars. Derivation of N. serrator from these or any other species of Neoplagiaulax possessing high-crowned fourth premolars would require reversal to a low-crowned state, a trend seen neither in any hypothesized Neoplagiaulax lineage, nor in neoplagiaulacids generally (Sloan, 1987). Among other species of Neoplagiaulax, N. nanophus may approximate the ancestry of N. serrator: the p4 of N. nanophus is much lower relative to its length, and the anterior margin is steep, character states much closer to those in N. serrator. N. nanophus is a poorly known taxon, occurring only at the Judson locality, North Dakota (Holtzman, 1978), and possibly at the Diss locality, Alberta (Fox, 1990); clarification of a possible relationship between N. serrator and N. nanophus must await better-preserved material of the latter.

N. serrator also occurs at the middle Tiffanian (Ti3) Hand Hills West upper level and Birchwood localities, and the late Tiffanian (Ti4) Police Point locality of Alberta (Krishtalka, 1973; Fox, 1990; MacDonald, 1996; Webb, 1996).

NEOPLAGIAULAX PASKAPOOENSIS new species

Figures 3.7.1-3.7.11, 3.8; Tables 3.8, 3.10

Neoplagiaulax hunteri: KRISHTALKA, 1973, p. 10 (part).
Neoplagiaulax n. sp. 2: FOX, 1990, p. 61.

Diagnosis.—Large-sized species of Neoplagiaulax, larger than both N. macintyrei and N. nanophus (mean length p4 of N. paskapooensis 35 percent longer than that of N. macintyrei and N. nanophus), but smaller than N. mckennai and N. grangeri (mean length p4 of N. paskapooensis 10 percent less than that of N. mckennai and N. grangeri). Differs from all other species of Neoplagiaulax in P4 having greater modal cusp number in the external row, and M1 having modally fewer cusps in all rows; differs further in having a longer and lower crowned p4 with a more posteriorly positioned first serration and broader exodaenodont lobe. Differs further from N. serrator in having a shallower

anterior margin on p4. Coronal morphology closest to that of N. hazeni and N. copei but differs from these in being smaller, in P4 and p4 being lower crowned relative to length, and in molars having fewer, but more robust cusps.

Description.—Upper dentition (Figs. 3.5.1, 3.5.2, 3.5.6-3.5.8): The holotype of Neoplagiaulax paskapooensis is the first discovered neoplagiaulacid specimen in which the entire replacement upper dentition is preserved, and the most nearly complete neoplagiaulacid specimen as regards total dentition (only the lower left m2 is missing). Upper incisors are virtually unknown for neoplagiaulacid multituberculates, with Krause's (1980, 1982a) descriptions of isolated teeth referred to Ectypodus powelli and E. tardus from the Bighorn Basin of Wyoming the most recent.

I2: The I2 is long and shallowly curved in lateral profile, convex dorsally and concave ventrally, with a tapering apex and laterally compressed root (see Fig. 3.7.2). The crown is short relative to the root, with the enamel constituting about one-third the total length of the tooth. The root of both I2s as preserved is oriented anterointernal-posteroexternal, such that the crowns appear to converge anteriorly; interdental facets on the dorsomedial surface of the crowns are absent, however, suggesting the left and right second incisors were probably held more or less subparallel to one another in life, with limited tooth-on-tooth contact, rather than being buttressed against each other at an acute angle as in microcosmodontids and djadochtatherioideans (Krause, 1977; Fox, 2005). Two well-developed ridges originating at the apex of the crown run posteromedially and posterolaterally, respectively, and divide the crown into superior and inferior surfaces: the superior surface is convex, and the enamel extends only a short distance posteriorly, while the inferior surface is virtually flat. A short median ridge, also originating at the apex, runs posteriorly along the inferior surface of the crown; the median ridge is weaker than the medial and lateral crests, but its development is enhanced by wear on the ventrolateral surface. The median ridge divides the inferior face of the crown into a wide and flat dorsomedial surface, and a narrower ventrolateral occlusal surface. In life, I2 was probably held in its alveolus rotated slightly laterally, bringing the ventrolateral surface of the crown into the occlusal plane; strong wear is present on this surface, evidence of its occlusion with i1. A posterobasal accessory cuspule is not developed.

The ventral surface of both roots is partially hidden by bone and matrix, but appears to be slightly convex, and as a result the root is nearly elliptical in cross section. In describing the dentition of UM 69868, an immature individual of Ectypodus powelli from the Bighorn Basin of Wyoming, Krause (1980) referred five isolated incisiform teeth to various tooth positions; teeth "B" and "C" (Krause, 1980, p. 1168, text-fig. 4) were considered I2s by Krause, while tooth "E" (Krause, 1980, p. 1168, text-fig. 4) was considered dI3; importantly, each of these teeth bears a root that is ∩-shaped rather than elliptical. Recently described specimens from the Paskapoo Formation of Alberta document the replacement of deciduous upper and lower incisors by their permanent successors in the microcosmodontid multituberculate Microcosmodon conus Jepsen, 1930; the roots of both dI2 and di1 are characterized by a long posteroventral (for dI2) or posterodorsal (for di1) hollow for reception of the anterosuperior (for I2) or anteroinferior (for i1) surface of the succeeding permanent tooth, giving the root a ∩-shape in cross section (and see later in the text); additionally, the roots of both dI2 and di1 in M. conus are short and taper rapidly to a small, circular terminus (Fox, 2005). Similar incisors referable to Mesodma or Cimexomys Sloan and Van Valen, 1965 are known from the Cretaceous Bug Creek Anthills (R. C. Fox, pers. comm., 2003), suggesting the mode of replacement of deciduous incisors may have been similar among microcosmodontid, ptilodontoid, and "Paracimexomys-grade" multituberculates. As described above, the root of I2 in N. paskapooensis is elliptical in cross section, with no indication of a hollowing on the posteroventral surface, confirming its identity as a permanent I2; in having ∩-shaped roots, it is reasonable to suggest that teeth "B", "C", and "E" of Krause (1980) might be deciduous, an assertion further bolstered by the short, tapering root of the figured "I2" (Krause, 1980, p. 1168, text-fig. 4). Similarly, the three isolated I2s (all with ∩-shaped roots) described and figured by Krause (1982a, p. 277-279, text-fig. 3) (UCMP 44908, UM 72596, and UM 74670) as pertaining to Ectypodus tardus are likely deciduous.

I3: The I3 of neoplagiaulacid multituberculates is known only for Ectypodus powelli and E. tardus, having been described by Krause (1980, 1982a), with at least one I3 of E. tardus in articulation with the premaxilla (YPM-PU 17674; Krause, 1982a, p. 277, text-fig. 3); thus, UALVP 46138 is the first discovered neoplagiaulacid specimen in

which both I3s of a single individual are preserved, and the only known neoplagiaulacid in which left and right I2 and I3 are preserved together in articulation with the cheek teeth. Postmortem distortion of UALVP 46138 has resulted in dorsoventral, as well as slight transverse compression of the rostrum; the roots and alveoli of both I3s are internal and posterior relative to those of I2, suggesting that these teeth occupied a more medial position relative to I2, a condition until now unknown in ptilodontoid multituberculates [a laterally positioned I3 in ptilodontoid multituberculates is known only for the ptilodontid Ptilodus montanus (Douglass, 1908) (from alveoli, see Simpson, 1937a, p. 742)]. A more precise estimate of the position of I3 on the palate cannot be made from the evidence at hand; the position of the roots and alveoli suggests the teeth were slightly inset medially from the margin of the palate, perhaps similar to that in the cimolomyid Meniscoessus Cope, 1882 (see Clemens and Kielan-Jaworowska, 1979; Archibald, 1982, fig. 27) or Microcosmodon conus (Fox, 2005), but unlike in djadochtatherioideans or the eucosmodontid Stygimys Sloan and Van Valen, 1965, in which I3 is inset far medially, with the crown directly posterior to that of I2.

The crown of I3 is shorter, stouter, and wider anteriorly compared to that of I2 (Fig. 3.8.2). The tooth is gently curved posteriorly, its root paralleling that of I2, and the posterior part of the crown is slightly swollen. Both I3s on UALVP 46138 have been shifted in their respective alveoli due to post-mortem distortion; the right I3, however, probably more closely approximates the natural orientation of the tooth, with the crown directed anteromedially, and the apical surface directed ventrally. The crown is heavily enameled anteriorly, and the apex is broad and smoothly rounded. Medial and lateral crests divide the crown into superior and inferior surfaces, although they are much shorter and weaker relative to those on I2; unlike I2, there does not appear to be a median crest dividing the inferior surface into dorsal and ventral parts. There is no posterior accessory cuspule. Wear facets were not observed on I3, suggesting the crown did not occlude with i1, but the biting surfaces as preserved could not be examined in their entirety; given the marginal position of I3 (similar to that in Microcosmodon conus and taeniolabidids, see Fox, 2005), the crown was topographically in a position in which occlusion with i1 could have been possible.

Upper premolars: P1-3: Aside from their slightly larger size, the anterior premolars of N. paskapooensis are virtually identical to those described for N. serrator, and to those of N. hunteri from Roche Percée as described by Krause (1977). P2 differs from those of N. serrator and N. hunteri only in having two cusps, rather than one, in the internal row.

P4: Cusp formula (0-1)2-4:7-10:0 [mode=(0)4:8:0; N=9]. P4 of N. paskapooensis is anatomically closest to that of N. hazeni from the late Tiffanian (Ti5) Princeton Quarry, Wyoming (see Jepsen, 1940) and N. cf. hazeni from Roche Percée (see Krause, 1977) but is smaller and relatively lower crowned. The anterior slope is long and straight to weakly convex, while the posterior slope is concave and more steeply inclined than that of N. hazeni. A posterobasal cusp is variably present, but strong when developed; a single specimen bears two posterobasal cusps. The anterolabial lobe is well developed on all specimens, and bears between two and four large, coarse cusps; an additional cuspule may be present external to the anterolabial lobe (Fig. 3.8.1, 3.8.8). Depending on their respective sizes, the cusps of the anterolabial lobe may be nearly transversely opposed to the cusps on the middle row or staggered slightly. The cusps of the external row are coarse, with the third cusp invariably the largest and tallest. The ultimate, or penultimate and ultimate cusps together are furthest from the base of the enamel, in contrast with P4 of N. hazeni in which the prepenultimate cusp is furthest from the base (Krause, 1977).

Upper molars: M1: Cusp formula 7-8:9-10:4-5 (mode=7:10:4; N=6). The occlusal surface of M1 is slightly concave dorsally. The cusps of the external row are flat internally and weakly grooved, subequal in size and height except the first, which is smaller and lower. The cusps of the middle row are large and coarse, smooth to weakly grooved labially and lingually, and four-sided anteriorly, but become slightly more crescentic posteriorly. The internal cusp row is short, terminating at the fifth or sixth cusp of the middle row, and the cusps are slightly convex labially. The internal cusps are bulbous and remain distinct throughout the row, rather than grading into a papillate ridge; the terminal cusp is sometimes barely discernable, appearing instead as a crest. Relative to that of N. hazeni and N. cf. hazeni, the M1 of N. paskapooensis is smaller, with fewer cusps in all rows, and lacks the strong grooving on the labial and lingual surfaces of the

middle row; additionally, the cusps of the middle row are stouter and less crescentic, and the internal row is shorter.

M2: Cusp formula 3:3 (N=5). The external row is developed as a thick crest joined to the apices of the first and last cusps of the middle row; the crest can bear irregular cuspules, but fully developed cusps are absent. The second and third cusps of the middle row are large and stout, subcrescentic in cross section, and are subequal in size and height. The first cusp of the middle row is smaller and lower than the second or third, and is sometimes difficult to distinguish from the external crest; the cusps of the internal row are both lower and smaller than those of the middle row, and decrease in size and height posteriorly. As on M1, the cusps of the internal row are slightly convex labially, giving them a swollen appearance. Apart from incipient grooving on the lingual surface of the internal row, the labial and lingual surfaces of the cusps are smooth. M2 most closely resembles that of N. hazeni and N. cf. hazeni, differing only in its smaller size, fewer but more robust cusps, and in having a better-developed external cusp row.

Dentary and lower dentition (Figs. 3.7.3-3.7.5, 3.7.9-3.7.11): The dentary of N. paskapooensis is similar to that in other species of Neoplagiaulax and neoplagiaulacids generally. In comparison with the dentary of N. serrator, that of N. paskapooensis differs in a number of ways. The horizontal ramus is proportionately longer, especially posterior to m2, and shallower. The incisor alveolar process is deep, housing a robust i1, and is oriented slightly more oblique to the cheek teeth; as a result, the dentary appears more labially "bowed" in occlusal aspect. The symphyseal surface is raised above the level of the adjacent parts of the dentary, but the bone is much thicker compared to that of N. serrator, especially dorsally, and the keel along the dorsal margin of the incisor alveolar process is better developed; the adductor fossae are deeper, especially the pterygoid fossa, and the masseteric and pterygoid crests better developed. The inferior dental foramen is considerably larger than that of N. serrator, and is circular, rather than suboval, in cross section. The condylar process is shorter, the anterior border is shallower, and the condyle is positioned slightly lower relative to the tooth row. The condyle differs appreciably from that of N. serrator: the articular surface is longer and greater in surface area, slightly more convex dorsally, and is oriented more posterodorsally; as in N. serrator, the condyle is oriented posterointernally-

anteroexternally, parallel with the cheek teeth. A large mental foramen occurs anteroventral to p3, slightly lower and more posterior than that in N. serrator; a much smaller foramen occurs ventral to p3.

i1: The lower incisor is larger and more robust than that of N. serrator, nearing the proportions of i1s of N. hazeni (see Jepsen, 1940). The long and slender crown is procumbent, and curves dorsally and slightly medially. The crown is convex laterally and flat medially, with a well-developed ventromedial crest that runs nearly the length of the crown; a weaker dorsolateral crest runs posteriorly from the apex a short distance before fading out. A well-developed medial crest originating at the crown apex runs posteriorly to about the same level as the dorsal crest, bisecting the medial face of the crown into wide inferior and narrower superior surfaces; wear from occlusion with the ventrolateral surface of I2 is heaviest along the superior surface.

Lower premolars: p3: The crown of p3 is small and peg-like, without accessory cuspules, and inserts into the anterobasal concavity of p4.

p4: 13-14 serrations (mode=14; N=6) are developed on the low, long crown (Figs. 3.8.1, 3.8.9, 3.9). In labial aspect, the crown is subtrapezoidal, with the anterior and posterior margins of the cutting edge descending at approximately 45 degrees from horizontal. The exodaenodont lobe is both broader and generally shallower relative to that in other species of Neoplagiaulax, and smoothly rounded ventrally. The posteroexternal shelf is weak, and the adjacent enamel is moderately crenulated. The anterior margin of the cutting edge is gently inclined and virtually straight, in contrast with the steep, slightly convex margin in N. serrator. The anterior margin progresses posterodorsally to the first serration, which is positioned high and relatively further posteriorly compared to other species of Neoplagiaulax (the height of the first serration is approximately one sixth the anteroposterior length of the crown). The apogee occurs at the fourth or fifth serrations; the distance between the first two serrations is slightly greater than between any two succeeding, and the serrations become progressively coarser and more bulbous posteriorly. The first serration bears four distinct ridges, two labially and two lingually: these ridges run in parallel anteroventrally, with the anteriormost pair delimiting the broad anterior face of the crown, and the second pair being shorter and terminating slightly anteroventral to the first serration, or joining with

the externalmost ridges of the first serration. The remaining labial and lingual ridges are long and arcuate, and become further from one another posteriorly; neither labial nor lingual ridges are developed below the last three serrations. The anterobasal concavity is well defined, low and broad, and squared dorsally.

Lower molars: m1: Cusp formula 7:4-5 (mode=7:4; N=8). The crown of m1 is subrectangular in occlusal view, with the two cusp rows converging only slightly at the anterior margin of the crown, and the valley between the two rows very narrow; on some specimens the crown narrows lingually between the second and third cusps of the internal row. The cusps of the external row are large and stout, the first three or four being four-sided in horizontal section, whereas the last two or three are slightly crescentic; the cusps increase in size and height through to the fourth or fifth cusp, after which they remain subequal. The cusps of the internal row are taller than those of the external row, but are similarly stout, particularly at their bases. The first cusp is consistently smaller and slightly lower than the succeeding cusps, which are all subequal in size and height; the cusps are flat labially and rounded lingually, and have grooving on the valley-facing surfaces. The m1 of N. paskapooensis most closely resembles homologous teeth of N. cf. hazeni and N. hazeni among species of Neoplagiaulax, differing in its smaller size, narrower crown, lower cusp count, and in having external cusps that are less crescentic posteriorly.

m2: Cusp formula 4:2 (N=2). The cusps of the external row are subequal in both size and height, and are more crescentic in horizontal section than the posterior cusps on the external row of m1. As with those on m1, the cusps on m2 are stout, particularly at their bases, but grooving is absent on the valley-facing slopes. The penultimate and ultimate cusps may be only incipiently divided externally, whereas a distinct separation is conspicuous internally. The two cusps on the internal row are tall and massive, and show little decrease in either size or height posteriorly; the valley-facing slopes are often moderately grooved, while the lingual surface is convex. The anterior of the two internal cusps is strongly crescentic in horizontal section, whereas the posterior is triangular. The referred m2s are most similar to those of N. cf. hazeni and N. hazeni, but as with m1, they are smaller, narrower, with lower cusp counts, and a much shorter external row.

Etymology.—Paskapoo, Cree, blind man; in reference to the Paskapoo Formation, the lithostratigraphic unit preserving the holotype locality.

Holotype.—UALVP 46138, incomplete skull having left I2-3, P1-4, M1-2, right I2-3, P1-4, M1-2, and associated incomplete left dentary having i1, p3-4, m1, and incomplete right dentary having i1, p3-4, m1-2 (Figs. 8.1-8.5). DW-2 locality, Paskapoo Formation of Alberta, late Paleocene [early late Tiffanian, Ti3 (Fox, 1990), Plesiadapis anceps/P. rex Lineage Zone of Lofgren et al., 2004].

Other material examined.—From DW-2: UALVP 46140, incomplete skull having right P1-4, M1-2, left P4, M2, associated incomplete left dentary having i1, p4, and associated right i1; UALVP 46141-46149, P4 (total: 9); UALVP 46150-46153, M1 (total: 4); UALVP 46154-46156, M2 (total: 3); UALVP 46157, incomplete left dentary having p3-4 and alveoli for i1, m1-2; UALVP 46158-46161, p4 (total: 4); UALVP 46162-46165, p4 fragments; UALVP 46166-46171, m1 (total: 6); UALVP 46172, m2.

From Hand Hills West upper level: UALVP 34992, 34993, 34994, 34996, P4 (total: 4); UALVP 35237, 35240, M1; UALVP 46173-46177, M2 (total: 5); UALVP 34988, 34991, p4; UALVP 35247, m1; UALVP 34967, 46178, m2.

From Birchwood: UALVP 39124, 39125, 39127, p4 (total: 3).

From Police Point (UAR-1): UALVP 5655, 5656, 5663, 5665, P4 (total: 4).

Age and occurrence.—Early middle Tiffanian (Plesiadapis anceps/P. rex Lineage Zone, Ti3, late Paleocene) to late middle Tiffanian (Plesiadapis rex/P. churchilli Lineage Zone, Ti4, late Paleocene) of Alberta.

Discussion.—The dentition of N. paskapooensis bears closest similarity to that of N. hazeni from the Western Interior of the United States [Princeton Quarry, Wyoming (Jepsen, 1940; Sloan, 1987)] and N. cf. hazeni from Western Canada [including N. cf. hazeni from the Roche Percée locality of Saskatchewan (Krause, 1977), and N. sp., cf. N. hazeni from the Blindman River localities (see later in this chapter)], but differs in a number of features. The teeth of N. paskapooensis are smaller, with measurements at or outside the lower extreme of the range (e.g., length P4, N. paskapooensis=3.3-3.7, mean=3.48, N=10 versus length P4, N. cf. hazeni, Roche Percée=3.7-4, 2, mean=3.91, N=29). The P4 is lower, with straighter anterior and steeper, less concave posterior margins, fewer cusps, and the occasional presence of a strong posterobasal cusp;

additionally, the ultimate or penultimate and ultimate cusps together are highest from the base of the enamel, contrasting with P4 of N. cf. hazeni and N. hazeni in which the prepenultimate cusp is usually highest (Krause, 1977). The p4 profile of N. paskapooensis (Fig. 3.9) superficially resembles that of N. hazeni (e.g., Jepsen, 1940, pl. IV, fig. 1 and Sloan, 1987, fig. 11) and less so that of N. cf. hazeni from Roche Percée (Krause, 1977, pl. 4, figs. 1-2 and see Fig. 3.7), but nonetheless differs significantly from both: the crown is long relative to its height and subtrapezoidal in outline, contrasting with the higher and more nearly arcuate profile of p4 in N. hazeni and N. cf. hazeni; the first serration is lower on the serrated crest, and the anterior margin is less steep, resulting in a more pronounced anterior "beak". The molar dentition is close to that of N. hazeni and N. cf. hazeni, but differs in certain subtle features: the upper molars bear fewer cusps in all rows, and the cusps are larger, coarser, and less crescentic posteriorly; the internal row of M1 is shorter, terminating more posteriorly; and the lower molars are narrower and bear fewer cusps in both rows. The p4 of N. paskapooensis also broadly resembles that of N. copei from the Cernaysian of France (Vianey-Liaud, 1986), but differs even more than compared to N. hazeni or N. cf. hazeni: p4 of N. paskapooensis is smaller (mean length p4, N. paskapooensis=4.85, N=6 versus mean length p4, N. copei=5.51, N=27), lower crowned relative to length, with fewer serrations, and a comparatively narrower and deeper exodaenodont lobe.

Despite the strong resemblance to N. hazeni in both P4 and molar morphology, N. paskapooensis differs markedly in p4 coronal features, a situation comparable to that between N. serrator and N. hunteri (see earlier in this chapter); without the benefit of nearly complete specimens preserving premolars and molars, as well as upper and lower parts of the dentition in association, the non-diagnostic teeth could have been reasonably referred to N. hazeni. This further demonstrates the uniformity in neoplagiaulacid molar and, to a lesser degree, upper premolar morphology, and the importance of lower fourth premolars in neoplagiaulacid systematics.

N. paskapooensis is also known from the middle Tiffanian (Ti3) Hand Hills West upper level and Birchwood localities, and from the late Tiffanian (Ti4) Police Point locality of Alberta (Krishtalka, 1973; Fox, 1990; MacDonald, 1996; Webb, 1996).

NEOPLAGIAULAX CIMOLODONTOIDES new species

Figures 3.9.1-3.9.15, 3.10; Tables 3.9, 3.10

Neoplagiaulax n. sp. 3: FOX, 1990, p. 61.

Diagnosis.—Differs from all other species of Neoplagiaulax in p4 being high and arched, with a long, broad anterior margin and a wider and broader exodaenodont lobe; differs further in P4 having a poorly developed anterolabial lobe, and in having prominent ridges developed on the labial and lingual surfaces of the upper premolars. Differs further in M1 being subquadrate in occlusal aspect, with the inner cusp row nearly complete.

Description.—Skull and upper dentition (Figs. 3.9.1-3.9.7): The external features of the skull of ptilodontoid multituberculates are known primarily from well-preserved specimens of Ptilodus montanus Douglass, 1908 (e.g., Simpson, 1937a; Krause, 1982c; Wall and Krause, 1992), with additional information from skull fragments of Prochetodon cavus Jepsen, 1940 (e.g., Krause, 1980, 1982a), Ectypodus tardus (e.g., Sloan, 1979), and Krauseia (=Parectypodus) clemensi (Sloan, 1981). The holotype (UALVP 46201), as well as UALVP 46179 and 46180, preserve parts of the maxilla, zygomatic arch, and palate of N. cimolodontoides; collectively, these specimens represent the first adequately known skull parts of Neoplagiaulax (UALVP 46201 is more extensively preserved than is described here, but the skull has been dorsoventrally crushed, and most of the dermal roofing bones are badly fractured). The maxilla is best preserved on UALVP 46180: despite dorsoventral compression, the facial process is seen to be moderately deep, tapering little anteroposteriorly, and is confluent with the contours of the zygomatic arch, not abruptly flaring outwards as in Stygimys and taeniolabidids (Kielan-Jaworowska, 1970; Rougier et al., 1997; Fox, 2005, and see Fig. 3.9.5). The anterior margin of the maxilla is marked by a surface of finished bone for articulation with the posterior part of the premaxilla; the posterior margin is damaged, but a posterodorsal surface of finished bone may represent part of the articulation with the frontal, or delimitation of the anterior rim of the orbit. The dorsal margin bends medially towards its articulation with the nasal and frontal. The maxillary process of the

zygomatic arch originates dorsal to P4 (i.e., the posterior edge of the process is positioned dorsal to the posterior margin of P4, see Wible and Rougier, 2000), and extends laterally and slightly dorsally. The more posterior parts of the zygomatic arch are not preserved, and the presence of zygomatic ridges (sensu Gambaryan and Kielan-Jaworowska, 1995) cannot be determined from the evidence at hand. The lateral wall of the infraorbital canal on UALVP 46180 has been broken away, revealing the medial wall; from the dimensions of the parts preserved, the infraorbital foramen probably opened dorsal to P4 at the base of the anterior root of the zygomatic arch, but an estimation of the length of the canal and position of the maxillary foramen must await better preserved specimens. A small, circular foramen penetrates the medial wall of the infraorbital canal just dorsal to the anterior margin of P4, and may have carried fibres of the maxillary branch of the trigeminal nerve towards the anterior and medial parts of the rostrum (Rougier et al., 1997; Wible and Rougier, 2000; Fox, 2005). A shallow, rounded excavation occurs anterior to the inferred opening for the infraorbital canal, in a position similar to one described by Fox (2005) for Microcosmodon conus; the excavation in the maxilla of N. cimolodontoides is much less conspicuous than that in M. conus, and appears to be restricted anteroposteriorly above P3, and not continuing anteriorly towards P1. A short, faint horizontal ridge occurs ventral to the depression and slightly anterior to the maxillary root of the zygoma. The function of the depression and ridge is not clear, although Gambaryan and Kielan-Jaworowska (1995) described a similar ridge in the djadochtatherioidean Nemegtbaatar gobiensis Kielan-Jaworowska, 1974, speculating it may have served as a site of origin for the buccinator musculature. Numerous tiny vascular foramina perforate the surface of the maxilla, especially anteriorly and dorsally.

The secondary palate is best seen in UALVP 46180: the palatal process of the maxilla extends anteriorly to points slightly beyond P1, posteriorly to the anterior alveolus of M2, and medially to the midline. A small fragment of the palatine is still in articulation with the posteromedial part of the maxilla at the embrasure between the alveoli for M1 and M2. The palate is broad, slightly concave ventrally, and encloses a palatal vacuity medial to P3 and P4, the first described for Neoplagiaulax (see Fig. 3.9.5); the bone that defines the medial and posteriormost borders of the vacuity is damaged, but the shape and proportion of the parts preserved suggest the vacuity was large, occupying

over half the space between P3/P4 and the midline. The vacuity most closely resembles that of Ptilodus montanus (e.g., Simpson, 1937a; Wall and Krause, 1992), differing from that of Ectypodus tardus (e.g., Sloan, 1979) in being significantly shorter and wider. The midline suture is well preserved and can be traced for most of its length; the smooth sutural edge is raised and thickened, with no evidence of an interdigitation between it and the opposing surface, suggesting the two halves of the palate simply abutted one another in life, rather than forming a synarthrosis. A thick alveolar process houses the cheek teeth at the lateral border of the palate; the process is especially robust below and medial to the molars where the bone is thicker, rugose, and perforated by a series of small foramina. A small, circular depression occurs on the palatal surface medial to P3 and continues a short distance anteriorly as a shallow and elongate trough; a cluster of seven or eight small foramina occur within the circular depression, and several irregularly spaced foramina mark the surface of the trough. A similar depression occurs on the palate immediately posterior to I3 in Microcosmodon conus (Fox, 2005); the function of this depression is unknown. The margin of the palate is damaged anterior to P1; a small area of rounded, smooth bone occurs medial and slightly anterior to P1, and probably marks the posteriormost rim of the incisive foramen. Damage to the maxilla has also revealed an unusual canal immediately in front of the anterior root of P1, running obliquely above the roof of the palate medially and posteriorly (Fig. 3.9.5, arrow). The canal is subcircular in section, its diameter nearly as great as that of the alveolus for the anterior root of P1, and its internal walls are smooth and intermittently perforated with tiny foramina. The palatal process of the maxilla forms the ventral wall of the canal; although its posterior limit cannot be seen, the trajectory of the canal seems to be directed posteriorly above the secondary palate, following the shallow trough described above. Simpson (1937a, p. 740-743) described unusual funnel-shaped pockets at the anterior margin of the palatal process of the maxilla in Ptilodus montanus, suggesting they may have housed chemosensory epithelium of the vomeronasal organ, and Fox (2005) recently speculated on the presence of a vomeronasal organ in Microcosmodon; the canal on UALVP 46180 may be homologous with the anterior pockets in P. montanus, suggesting a vomeronasal organ may also have been present in at least some neoplagiaulacid multituberculates.

Only a small fragment of the palatine is preserved on UALVP 46180, articulating with the posteromedial part of the palatal process of the maxilla. An edge of smooth, finished bone medial to the embrasure between M1 and M2 represents the anterolateral rim of the choana, indicating its position was similar to that in Ptilodus and Ectypodus (Simpson, 1937a; Sloan, 1979), and slightly anterior relative to that in Microcosmodon (Fox, 2005).

Upper premolars: P1-3: The anterior premolars are similar to those described for Neoplagiaulax hunteri from the Roche Percée locality of Saskatchewan (Krause, 1977) and N. serrator, but differ in a number of features. The crowns are slightly larger than those of either N. hunteri or N. serrator, and are readily distinguished by unusual dorsoventrally oriented ridges on the enamel, between which are vertical grooves that are particularly strong around the cusps, a condition seen in premolars of some cimolodontid and ptilodontid multituberculates (see, for example, Lillegraven, 1969, Fox, 1971, Krause, 1977, and Scott et al., 2002, and see Figs. 3.9.1-3.9.7). The cusps of P1 are more evenly spaced than those of N. serrator, with a single anterior cusp and two transversely oriented posterior cusps; together, the cusps form an equilateral triangle in occlusal view, and correspond most closely with Krause's (1977) premolar type A from Roche Percée. As in P1 of N. serrator, the anterior and labial cusps on P1 of N. cimolodontoides are compressed and triangular in cross section, while the lingual cusp is more nearly conical. Crests originate from the apices of each of the three cusps, with the strongest on the anterointernal face of the anterior cusp. The posterointernal margin of the crown is elongate posteriorly, underlying the anterointernal face of P2, and connected to the posterior cusps by strong grooves; a small accessory cuspule occurs on the posterolabial side of the posteroexternal cusp. P1 is two-rooted, with large, stout roots. P2 is similar in shape to P1, having a single anterior cusp, followed by two transversely opposed posterior cusps, and differing from P2 of N. serrator, in which a single labial and two closely approximated lingual cusps occur. As in P1, the anterior and posterolabial cusps are compressed, while the lingual cusp is conical, and the posterointernal margin of the crown is elongate and underlies the anterodorsal face of P3; crests, although present, are not developed to the same extent as in P1. The crown of P3 is slightly larger and more nearly quadrate in occlusal view than P3 of N. serrator, and is slightly lower than the

preceding teeth. The crown consists of four cusps arranged in two parallel rows; the cusps of the labial row are compressed laterally, while those of the lingual row are more nearly conical. As in P1-2, the posterointernal corner of the P3 crown is elongate and strongly abuts the anterodorsal margin of P4.

P4: Cusp formula (0)0-1:8-9:0 [mode=(0)0:8:0; N=11]. The P4 of N. cimolodontoides most closely resembles that of N. hunteri from Roche Percée (Krause, 1977) among species of Neoplagiaulax: the crown in both species is high relative to length, and the main cusp row is aligned virtually straight anteroposteriorly; in occlusal aspect, however, the P4 of N. cimolodontoides is much narrower than that of N. hunteri, and the anterolabial lobe more poorly developed (e.g., compare Figs. 3.9.3, 3.9.7 with Krause, 1977, pl. 5, fig. 5). The anterolabial lobe on P4 of N. cimolodontoides and N. hunteri can occasionally bear cusps; when present in N. cimolodontoides, they are very tiny, whereas the single cusp of N. hunteri is well developed. The cusps of the external row are subequal in size, and the row is slightly to moderately convex in lateral profile; the ultimate or ultimate and penultimate cusps are highest above the base of the enamel. The posterior slope is steep, and can be virtually straight to strongly concave; unlike that of N. hunteri, the posterior margin of N. cimolodontoides can bear one or two strongly developed basal cusps. The enamel of the labial and lingual surfaces of P4 exhibits extensive ridging and grooving: the labial and lingual faces of the crown at each cusp support a single median crest that descends from the apex towards the base of the crown, bisecting the labial and lingual face of each cusp into anterior and posterior halves, and giving each cusp four sides. The crests are strongest at the apex of each cusp, and become weaker as they bifurcate or trifurcate towards the base of the crown. The pattern of wear on the P4 of N. cimolodontoides is similar to that seen in N. hunteri (Krause, 1977): the crown in many specimens is worn flat from the ultimate to the fourth or fifth cusp, and the posterointernal face is often devoid of ridges, having been worn smooth.

Upper molars: M1: Cusp formula 7:12-13:8 (N=2). The crown of M1 is subrectangular in occlusal aspect, the anterior margin slightly concave, and the posterior margin convex. The internal row is virtually complete, the cusps originating close to the anterior margin of the crown, midway past the first cusp of the middle row (Figs. 3.9.3, 3.9.7). The cusps of the internal row increase in both size and height posteriorly, with the

penultimate and ultimate cusps subequal; the valley-facing sides are flat, whereas the lingual surfaces are strongly convex. The cusps of the middle row are crescentic, increase in size posteriorly, and are closely spaced from each other, sometimes joined nearly to the apices by crests. The cusps of the external row increase in size posteriorly, with the penultimate cusp largest on all specimens; the cusps are flat on their valley-facing surfaces, and are convex labially. The valley-facing slopes of each cusp row are marked by deep grooves similar to those on M1 of N. hunteri.

M2: Cusp formula 3:6 (N=1). The morphology of the referred M2 is most similar to M2 of N. hunteri as described by Krause (1977), differing only in being longer relative to width, in having more cusps on the internal row, and in having deeper grooves on the valley-facing slopes of each cusp row.

Dentary and lower dentition (Figs. 3.9.8-3.9.15): Several incomplete dentaries referable to N. cimolodontoides have been discovered at the Blindman River localities, together preserving most of the dentary anterior to the condyle. Relative to the dentaries of both N. serrator and N. paskapooensis, that of N. cimolodontoides differs in the horizontal ramus being both relatively and absolutely shorter and shallower, and the ventral margin is more convex. The incisor alveolar process is shorter and stouter, similar to dentaries described by Jepsen (1940) for both N. hazeni and Mimetodon churchilli; as a result, the fourth premolar is positioned more anteriorly (i.e., closer to the i1 alveolus, Figs. 3.9.14, 3.9.15), with the large mental foramen occurring midway between the anterior margin of p4 and the base of i1. The dorsal margin of the incisor alveolar process is not drawn out into a keel, as in dentaries of N. serrator and N. paskapooensis, and the i1 is less procumbent. The symphyseal surface is virtually identical to that of N. serrator, being both smooth and comma-shaped; the ridge dorsal to the raised symphyseal surface is not thickened like that in N. paskapooensis. The coronoid process is best preserved on UALVP 46195: the anterior extremity of the process originates labial to m1, slightly more anterior than that of N. serrator and N. paskapooensis, and the long anterior margin extends steeply towards the apex. The apex and posterior margin of the coronoid process are broken on UALVP 46195, but the dimensions of the parts preserved suggest the profile may have been similar to that of N. serrator, but less robust and with a proportionately shallower lateral excavation for the

mandibular adductors. The condylar process is not preserved among the specimens at hand. The adductor fossae are well excavated, and the masseteric and pterygoid shelves strongly developed. The pterygoid fossa terminates anteriorly in a large, suboval inferior mandibular foramen.

di1: In addition to evidence bearing on the eruption sequence of the upper dentition, the holotype of N. cimolodontoides provides the first direct evidence of lower incisor replacement in Neoplagiaulax. The referred di1 is broken, both at the tip and base, but enough of the tooth remains to confirm its identity as the left di1; a small part of the root is implanted in the anterior part of the associated incomplete left dentary, ventral and slightly labial to the tip of the erupting i1. The crown of di1 is smaller, narrower, and shallower than that of i1, and does not curve dorsally to nearly the same extent. The anterior part of the crown is laterally compressed, and the enamel is thin over the entire anterior surface (the tip of the crown has been broken, allowing examination of the distribution of the enamel); the enamel becomes thinner posteriorly, fading out completely at the level of the dorsal hollow (see later in this chapter). An indistinct ridge occurs on the medioventral part of the crown in a similar position to that of the replacement incisor. The tooth broadens posteriorly toward the root; a broad, shallow hollow occurs on the posterodorsal surface, occupying nearly half the crown length as preserved, and giving the root a ∩-shape in cross section; the hollow, similar to that on di1s of Ectypodus powelli (Krause, 1980, and see earlier in this chapter), received the anteroinferior surface of the erupting permanent lower incisor (Fox, 2005).

i1: The crown of i1 is long, slender, and tapers toward the apex. The crown is shorter than that of N. serrator, but deeper and more robust, approaching the proportions of i1 of N. paskapooensis.

Lower premolars: p3: The p3 is similar to that of other neoplagiaulacids, having a small, peg-like crown that abuts the anterobasal concavity of the succeeding p4.

p4: The profile of p4 is high, arched, and leans slightly posteriorly, and bears superficial resemblance to p4s of cimolodontid multituberculates such as Anconodon Jepsen, 1940 and Cimolodon Marsh, 1889 (Figs. 3.9.9, 3.9.11, 3.9.14, 3.10). The crown is trapezoidal in outline, with the anterior margin slightly convex and the dorsal and posterior margins virtually straight; the anterior, dorsal, and posterior margins are

oriented at approximately 45 degrees to one another. The posterior margin is abruptly truncated posterior to the fifth or sixth serration, paralleling the condition on p4, N. hunteri. When the dentary is held in the horizontal plane, the apogee of the serrated edge occurs at the fourth or fourth and fifth serrations; the cutting edge bears 12 or 13 (mode=13; N=15) serrations. The anterior part of the crown is robust, with a swollen exodaenodont lobe that is anteroposteriorly wide, deep, and broadly rounded ventrally. The labial side of the crown is flat, although the exodaenodont lobe occasionally juts labially, giving the labial face a sigmoidal appearance in end view; the lingual face is slightly convex. The anterior margin of the crown is broad and flat, especially the enamel overhanging the anterobasal concavity, and the crown is significantly wider anteriorly than posteriorly. Relative to that of other species of Neoplagiaulax, the posterolabial shelf in N. cimolodontoides is well developed and in some specimens forms a prominent posterodorsally-anteroventrally oriented ledge; the enamel adjacent to the posterolabial shelf is wrinkled. In labial view, the leading edge of the serrated crest progresses to the first serration gently, in contrast to the steep anterior margin of N. serrator. The leading edge is slightly convex, in contrast to the long, straight anterior margin of p4s of Anconodon and Liotomus Cope, 1884, and the first serration is relatively high compared to that in N. serrator and comparable to that in N. paskapooensis. The first serration is set off anteriorly from the remaining serrations, and the distance between successive serrations decreases posteriorly to the sixth serration; the serrations posterior to the sixth serration become larger, conical, and remain equidistant from one another. A short, well-developed labial ridge occurs ventral to the first serration, and extends anteroventrally towards the anterobasal concavity, and can join with ridges descending from the second or third serration. Occasionally the first labial ridge bifurcates near its origin below the first serration, sending a weak branch anteriorly and ventrally. A short, well-developed lingual ridge descends from the first serration, and can join the second, third, or both, lingual ridges. Labial and lingual ridges ventral to the second serration are generally short and can join with either the first or third ridges; the remaining labial ridges gently curve anteroventrally across the crown. Wrinkling of the enamel obscures the posterior two or three labial ridges. The lingual ridges are oriented more nearly horizontally relative to the labial ridges, and become further apart

posteriorly; the enamel beneath the last two or three lingual serrations lacks distinct ridges, similar to that on the labial side of the crown. The anterior root is large and stout, and a robust interradicular crest can be developed between the anterior and posterior roots.

Lower molars: m1: Cusp formula 9-11:4-5 (mode=10:4; N=5). The coronal structure of m1 approximates that of m1 of N. hunteri from Roche Percée (Krause, 1977), but with notable differences: the crowns of both are subrectangular in occlusal aspect, but that of N. cimolodontoides is wider relative to its length (i.e., m1 length:width ratio, N. cimolodontoides=2.00, N=7 versus m1 length:width ratio, N. hunteri, Roche Percée locality=2.35, N=6). The two cusp rows diverge only slightly along their anteroposterior extent; consequently, the crown remains approximately the same width throughout its length, contrasting with that of N. hunteri in which the anterior part of the crown is narrow, and the two cusp rows diverge posteriorly. The cusps of both rows are swollen, particularly their bases, and are wide relative to those of N. hunteri. The cusps of the internal row are lower relative to those of other species of Neoplagiaulax, with the two cusp rows being more nearly equal in height, and the angle of the valley between the two rows wider. As in N. hunteri, the cusps of the external row are small and pyramidal anteriorly, but become progressively larger and more crescentic posteriorly, reaching their largest size at the fifth or sixth cusp. The terminal external cusp may be only incipiently divided externally, although on all specimens the ultimate and penultimate cusps are well differentiated internally. Well-developed grooves occur on the labial surfaces of the external cusps; on some specimens, wear along the posterolabial margin of the crown results in the formation of a weak shelf along the bases of the last three or four cusps. The internal row bears four or five massive cusps, the first of which is somewhat smaller and shorter than the remaining three or four; the second, third, and fourth cusps are subequal in both size and height; when present, the fifth cusp is both smaller and shorter than the preceding cusps. The valley-facing slopes of the internal cusps are deeply grooved, whereas the labial slopes are smooth and rounded; the labial surfaces of the internal cusps on some specimens are flat, and bear conspicuous horizontal striations from wear by the opposing M1.

m2: Cusp formula 6:3 (mode=6:3; N=6). The m2 of N. cimolodontoides is virtually identical to that of N. hunteri from Roche Percée (Krause, 1977), differing only in being smaller, and in having a slightly longer internal row bearing an additional cusp. The division between the ultimate and penultimate cusps on the internal row is sometimes incipient externally, but in all specimens a strong groove separates the cusps internally. Grooving is strongest on the valley-facing slopes of the internal cusps; as on m1, the labial surface of the internal cusps can be planed obliquely flat by the opposing M2.

Etymology.—Cimolodon, genus of cimolodontid multituberculate and stem of the familial name Cimolodontidae Marsh, 1889; Greek, -eides, likeness; in reference to the parallel similarity in dental features with those of cimolodontid multituberculates.

Holotype.—UALVP 46201, crushed skull having RP1-4, LP1-4, M1-2, associated incomplete left dentary having erupting i1, p4, associated incomplete right dentary having p4, associated isolated left di1, left and right m1s (Figs. 9.6-9.10). DW-2 locality, Paskapoo Formation of Alberta, late Paleocene [early middle Tiffanian, Ti3 (Fox, 1990), Plesiadapis anceps/P. rex Lineage Zone of Lofgren et al., 2004].

Other material examined.—From DW-2: UALVP 46179, incomplete right maxilla having P2-4, M1-2; UALVP 46180, incomplete left maxilla having P1-4, alveoli for M1, and anterior alveolus of M2; UALVP 46181-46189, P4 (total: 9); UALVP 46190-46192, M1 (total: 3); UALVP 46193, incomplete right dentary having p4; UALVP 46194, incomplete left dentary having m1-2; UALVP 46195, incomplete left dentary having fragmentary p4, m1-2; UALVP 46196, incomplete left dentary having p4, m1-2; UALVP 46197, incomplete right dentary having i1, p4; UALVP 46198, incomplete right dentary having fragmentary p4, m1; UALVP 46199, incomplete right dentary having p4, m2; UALVP 46200, incomplete right dentary having i1, p4, m1; UALVP 46202-46211, p4 (total: 10); UALVP 46212-46217, p4 fragments; UALVP 46218, 46219, m1; UALVP 46220-46223, m2 (total: 4).

From Mel's Place: UALVP 46224, m2.

From Hand Hills West upper level: UALVP 34947, p4.

From Birchwood: UALVP 47824, p4.

Age and occurrence.—Early middle Tiffanian (Plesiadapis anceps/P. rex Lineage Zone, Ti3, late Paleocene) of Alberta.

Discussion.—Eruption pattern of the upper dentition: The holotype of Neoplagiaulax cimolodontoides (UALVP 46201) is of an immature individual and preserves evidence of the pattern and timing of tooth eruption in both the upper and lower dentition, the first such evidence for Neoplagiaulax. The complete left post-incisor dentition is present on UALVP 46201, as well as P1-4 from the right side; the specimen also contains incomplete dentaries. At the time of death, P1-3 were in various stages of eruption, P4 and M1 were both fully erupted, and M2 was nearly completely erupted (Fig. 3.9.6); wear on the posteroapical surface of P4 indicates that this tooth was fully functional for some time prior to eruption of the more anterior premolars, a conclusion consistent with that of Clemens (1964) for the Lancian cimolodontid Cimolodon nitidus Marsh, 1889 (and see Fox, 2005 for a similar conclusion for the microcosmodontid Microcosmodon conus). The anterior premolars on UALVP 46201 are interpreted as being replacement, rather than deciduous, from comparisons with fully erupted permanent premolars on other specimens of N. cimolodontoides from the Blindman River localities: the coronal morphology of P1-3 in UALVP 46201 is virtually identical to those of UALVP 46179 and UALVP 46180, both containing undoubted replacement teeth. The P1 is just beginning to erupt, the apices of the crown virtually flush with the alveolar rim; the presence of bone overlapping the anterior and lingual margin of the crown indicates that resorption of the maxilla at the site of eruption was apparently still in progress at the time of death. The anteroposterior axis of the crown of P1 is in line with the more posterior premolars. The orientation of the crown relative to the horizontal axis of the skull is oblique, with the posterior end of the crown more dorsal in position; as a result, the posterior part of the crown of P1 would abut the anterodorsal part of the crown of P2 on completion of eruption. The crown of P2 is nearly fully erupted, but had not yet made contact with P3 at the time of death; the orientation of the crown relative to the horizontal axis of the skull is virtually identical to that of P1, and the posterior margin of the crown would ultimately abut the anterodorsal side of P3. P3 is fully erupted, with contact between its posterior margin and the anterodorsal surface of P4; wear on the labial cusps suggests P3 was fully functional and involved in mastication prior to full

eruption of the more anterior premolars. Both P4 and M1 were apparently fully erupted at the time of death, but M2 was still erupting: its crown is oriented anterodorsal-posteroventral with the apices of the cusps well below the level of those on M1, suggesting the tooth was still in the process of moving into the occlusal plane when death occurred. Both M1 and M2 show virtually no wear. The evidence seen in UALVP 42601 indicates the sequence of permanent premolar eruption in N. cimolodontoides was P4-P3-P2-P1, consistent both with Jepsen's (1940) hypothesis for premolar replacement in Neoplagiaulax (="Ectypodus" of Jepsen) and with direct evidence from Microcosmodon conus (Fox, 2005), and precisely opposite to that of Greenwald (1988). Although the timing of molar eruption relative to that of the premolars cannot be unequivocally established, the evidence at hand suggests P4 erupted early, followed by sequential eruption of P3-P1 with near-synchronous eruption of M1 and M2.

Eruption pattern of the lower dentition: In addition to the crushed skull, UALVP 46201 also preserves incomplete left and right dentaries, the left of which shows the replacement i1 erupting from the crypt. The tip of i1 is exposed anteriorly by slight breakage of the bone at the alveolar rim (Figs. 3.9.9, 3.9.10); given the association of di1 (see earlier in this chapter) with the dentary, it is likely the deciduous tooth was still in place in life, and the permanent successor was just beginning to move anteriorly into position. The tip of i1 projects only slightly over the dorsal margin of the incisor alveolar process, and is completely covered in enamel. The p4 is fully erupted, although slightly lower in position on the dentary as compared to older individuals, and the crown is much more oblique to the longitudinal axis of the jaw relative to those of adults, almost identical in position to that of immature individuals of Ptilodus wyomingensis Jepsen, 1940 as described and illustrated by Szalay (1965, p. 4, fig. 1). The width of the dentary at the anterior root of p4 is much greater than that of adult individuals, suggesting that the anterior root of p4 was "pushed out" laterally to accommodate the i1 below (Szalay, 1965); the p4 then moved to its adult position after eruption of i1 (likely with concomitant calcification of the roots, see Szalay, 1965). The stage of dental eruption in UALVP 46201 is nearly identical to that of AMNH 83003 (Ptilodus wyomingensis figured by Szalay, 1965), but the p3 had not yet erupted, suggesting that this individual may have been at a slightly earlier ontogenetic stage at the time of death. The exact

sequence of mandibular dental eruption cannot be determined unequivocally from the evidence at hand; although UALVP 46201 preserves both left and right m1s, the timing of their eruption relative to p4 is unclear, and neither m2 is preserved. The p3 of the left dentary had yet to erupt, further evidence in support of Jepsen's (1940) suggestion that it erupts after, or synchronously with, p4 (the associated right dentary of UALVP 46201 is badly damaged and contains only p4 and the bone immediately ventral to the crown, and provides no information bearing on the timing of p3 eruption). From the evidence provided by UALVP 46201, it is reasonable to conclude that p4 and m1 erupted prior to both p3 and i1, and that i1 may have erupted before p3. Little can be said regarding the timing of m2 eruption; Krause (1980) examined specimens of an immature individual of Ectypodus powelli from the Bighorn Basin of Wyoming, and inferred the mandibular eruption sequence as being di1-p4-m1-i1-m2, apparently consistent with evidence from immature individuals of Meniscoessus robustus Marsh, 1889 and Prionessus lucifer Matthew and Granger, 1925. The timing of m2 eruption in N. cimolodontoides probably differed from that in E. powelli: given that the crushed skull of UALVP 46201 contains a nearly completely erupted M2, it is probable that m2 had already erupted, or was similarly nearing completion of eruption, in order to provide an opposing occlusal surface for M2; this sequence of eruption is not unlike that documented by Krause (1980) for the djadochtatheriid Kryptobaatar parvus Kielan-Jaworowska, 1970. Given the evidence in UALVP 46201, the likeliest sequence of mandibular tooth eruption in N. cimolodontoides is di1-p4-m1-m2-i1-p3, although the timing of molar eruption relative to that of i1 is uncertain; more conclusive statements regarding mandibular tooth eruption and replacement must await discovery of better-preserved specimens.

The coronal anatomy of the P4 and p4 of N. cimolodontoides is consistent with Sloan's (1981) characterization of the genus (for example, height of crown at exodaenodont lobe less than standard length; p4:m1 ratio=1.90). The dentition of N. cimolodontoides is highly autapomorphic relative to other species of Neoplagiaulax, leaving little doubt of its status as a new species. The highly arched p4 profile and swollen exodaenodont lobe of N. cimolodontoides bears superficial resemblance to those of cimolodontid multituberculates, particularly Anconodon (e.g., L. Russell, 1929; Jepsen, 1940; Krause and Gingerich, 1983; Youzwyshyn, 1988; Scott and Krause, 2006).

Despite these resemblances, N. cimolodontoides clearly is not referable to the Cimolodontidae: relative to p4 of Anconodon cochranensis (L. Russell, 1929) from the earliest Tiffanian (Ti1) Cochrane 2 locality, Paskapoo Formation, Alberta (Youzwyshyn, 1988; Fox, 1990; Scott et al., 2002) and Douglass Quarry, Lebo Formation, Montana (Krause and Gingerich, 1983; Scott and Krause, 2006), that of N. cimolodontoides differs in profile, with the dorsal margin of the serrated crest lower and not nearly as arched, the posterior margin truncated, and the crown leans less posteriorly (Fig. 3.10); the exodaenodont lobe is less swollen; and the anterior margin of the crown is weakly convex and shorter. The P4 of N. cimolodontoides differs from that of Anconodon in being higher crowned, in having a weaker anterolabial lobe, and in having well-developed labial and lingual ridges; additionally, the molars of N. cimolodontoides are both shorter and wider than those of Anconodon, and the cusps appear more inflated (e.g., compare with L. Russell, 1932, fig. 1).

Among the known species of Neoplagiaulax, the dentition of N. cimolodontoides bears closest similarity to homologous teeth of N. hunteri from Roche Percée (Krause, 1977) and N. mckennai from the middle Tiffanian Love Quarry, Wyoming. The serrated crest on p4 in each is truncated posteriorly, and the crown of P4 is wide relative to length, with an anterolabial lobe that bears few cusps. N. cimolodontoides, however, differs from both N. hunteri and N. mckennai in the following: the lateral profile of p4 is more highly arched and posteriorly leaning (Fig. 3.10, and compare with Sloan, 1987, fig. 11); the anterior margin of p4 is only weakly convex and rises gently to the dorsal crest, in contrast with p4 of N. hunteri, in which the anterior margin is more strongly convex and rises sharply; p4 is lower crowned and the first serration is lower than on p4, N. mckennai; P4 is smaller and less transverse; and the premolars bear strongly developed, dorsoventrally oriented ridges, a feature previously unknown for any species of Neoplagiaulax.

Sloan (1987) hypothesized derivation of N. mckennai from N. hunteri; N. cimolodontoides, although very likely related to these two species, is almost certainly too derived to be near the ancestry of either. The suite of unusual dental specializations suggests N. cimolodontoides is outside the N. hunteri-N. mckennai lineage, with features paralleling those seen in cimolodontid multituberculates.

N. cimolodontoides is also known from the middle Tiffanian (Ti3) Hand Hills West upper level locality of Alberta (Fox, 1990; MacDonald, 1996).

NEOPLAGIAULAX sp., cf. N. HUNTERI

Figures 3.11.1-3.11.3

Material examined.—From DW-2: UALVP 46280, incomplete left dentary with p4, m1-2.

Description.—p4 (L=4.1; L1=1.1; H=1.8): The p4 of Neoplagiaulax sp., cf. N. hunteri is most similar to those of N. hunteri from the Judson and Brisbane localities of North Dakota (Holtzman, 1978), the early Tiffanian X-X locality of North Dakota (Hunter, 1999), and to a lesser degree that of N. hunteri from the Roche Percée locality of Saskatchewan (Krause, 1977). The crown is subtrapezoidal in profile, although the anterior and dorsal margins are slightly more arcuate compared to p4 of N. hunteri, and the labial face is flat, not convex [as on p4 of N. hunteri from Roche Percée (Krause 1977)]. The exodaenodont lobe is broad and rounded ventrally, and is swollen in appearance; the posterolabial shelf is weakly developed. The leading edge of the serrated crest is posteriorly reclined, and bears a low incipient serration. The first serration is comparatively higher than in N. hunteri, and the cutting edge supports 12 serrations, fewer than on p4 of N. hunteri from Judson, Brisbane, and the Roche Percée localities (p4 serrations, Neoplagiaulax sp., cf. N. hunteri, Blindman River localities=12 versus p4 serrations, N. hunteri, Judson and Brisbane localities=15-17 and p4 serrations, N. hunteri, Roche Percée locality=15; Krause, 1977; Holtzman, 1978). The posterior slope descends at approximately 65 degrees from horizontal and is virtually straight. The ridges on the crown below the serrations are coarse; those on the labial face are oriented slightly more oblique relative to the anterior margin, whereas those on the lingual face are more nearly parallel to the anterior margin.

Lower molars: m1 (L=2.3; W=1.0; cusp formula 7:5); m2 (L=1.5; W=1.1; cusp formula 5:2). The lower molars of UALVP 46280 are similar to those of Neoplagiaulax hunteri but with notable differences. The crown of m1 is slightly shorter than in N. hunteri from Roche Percée and bears seven cusps in the external row, four fewer than the

modal number as reported by Krause (1977), although both Simpson (1936) and Sloan (1987) reported cusp numbers as low as eight for m1 of N. hunteri from the type locality. The external cusps on m1 in UALVP 46280 are larger and less nearly crescentic than those on m1 of N. hunteri, and their labial surface lacks irregular grooving (compare with Krause, 1977, pl. 5, fig. 3). The crown of m2 is similar to that of N. hunteri, but as with m1, the cusps of the external row are fewer in number and less crescentic.

Discussion.—The teeth in UALVP 46280 suggest affinities with Neoplagiaulax hunteri, and the specimen may represent a fourth species of Neoplagiaulax from the Blindman River localities. In comparing the p4 of UALVP 46280 with that in other species of Neoplagiaulax known from the Blindman River localities, p4 of UALVP 46280 is smaller and significantly different in coronal structure than in N. paskapooensis and N. cimolodontoides, but is superficially similar to that in N. serrator: the p4 crowns of both taxa are similarly proportioned, with comparable crown height and well-developed, ventrally rounded exodaenodont lobes. Closer inspection, however, reveals a number of differences: the p4 of UALVP 46280 is slightly shorter (length p4, Neoplagiaulax sp., cf. N. hunteri=4.1 mm versus mean length p4, N. serrator=4.49 mm); the cutting edge bears fewer serrations, and the labial and lingual faces bear fewer ridges; the exodaenodont lobe is more swollen; and the posterior margin is more abruptly truncated. Additionally, the molars in UALVP 46280 differ significantly from those of N. serrator: the crown of m1, Neoplagiaulax sp., cf. N. hunteri, bears fewer cusps in the external row, and the external cusps on both m1 and m2 are larger and less crescentic than those on m1 and m2 of N. serrator.

The p4 of UALVP 46280 is closest to that of Neoplagiaulax hunteri from the Judson and Brisbane localities and the X-X locality of North Dakota (Holtzman 1978; Hunter 1999); collectively these teeth differ not only from p4 of N. hunteri in the Roche Percée sample, but also from topotypic p4s (Simpson, 1936; Sloan, 1987; pers. obs.). The p4 crown in UALVP 46280 and those from North Dakota are shorter and lower than in N. hunteri (sensu Krause, 1977), and the anterior margin is steeper; the exodaenodont lobe is narrower and shallower; and the posterior slope descends more gently to the posterior margin of the crown, in contrast with the abrupt posterior truncation on p4 of N. hunteri from Roche Percée and to a lesser degree from Scarritt Quarry. The differences

in coronal anatomy between specimens of Neoplagiaulax sp., cf. N. hunteri and N. hunteri from Alberta and North Dakota on one hand, and those of N. hunteri from Saskatchewan and Montana on the other, are of uncertain taxonomic significance; until larger samples from the Blindman River and North Dakota localities become available, UALVP 46280 is best referred only tentatively to N. hunteri.

NEOPLAGIAULAX sp., cf. N. HAZENI

Figures 3.11.4-3.11.12; Table 3.10

Material examined.—From DW-2: UALVP 46281, incomplete left maxilla with P1-4, M1-2; UALVP 46282, 46283, M1; UALVP 46284, M2; UALVP 46285, p4; UALVP 46286, m2.

From DW-3: UALVP 46287, p4.

Description.—Upper dentition (Figs. 3.11.4-3.11.12): Upper premolars: P1-3: The anterior upper premolars of Neoplagiaulax sp., cf. N. hazeni are preserved in articulation with the remaining cheek teeth in UALVP 46281 (Figs. 3.11.4-3.11.6). P1-3 are similar to premolar types D, E, and F, respectively, from the Roche Percée locality, Saskatchewan, referred to Neoplagiaulax sp., cf. N. hazeni by Krause (1977), and aside from their slightly larger size, resemble those of N. serrator. The crown of P1 bears three cusps, one posterolabial, and the other two connate and oriented anterolingually-posterolabially. The crown of P2 supports a single labial and two smaller lingual cusps; a small cuspule is present anterior to the labial cusp. The crown of P3 bears four equidistantly spaced cusps and an expanded posterior lobe.

P4: Cusp formula (0)3:9:0. Although wear has reduced the height of the crown, P4 appears to have been low relative to that of Neoplagiaulax serrator and N. cimolodontoides, approaching the proportions of P4 in N. paskapooensis and, especially, N. hazeni. The crown is only slightly wider anteriorly than posteriorly, owing to a poorly developed anterolabial lobe. The anterior slope is long and faintly convex, while the posterior slope is shorter, steeper, and strongly concave. The external row bears three cusps that increase in size and height posteriorly. The cusps of the middle row are worn posteriorly but appear to have increased in size posteriorly, with the ultimate cusp largest;

the penultimate or ultimate cusp is estimated to have been highest above the base of the crown. As in N. hazeni, the enamel overhangs the anterior root labially and anteriorly (Krause, 1977).

Upper molars: M1 cusp formula 7-8:11:7 (N=3); M2 cusp formula 4:5 (N=2). The cusps in the external row of M1 are flattened and bear deep grooves lingually; the cusps become larger and longer posteriorly. The cusps of the middle row are four-sided anteriorly but become increasingly crescentic posteriorly; the cusps bear deep vertical grooves on their lingual surface and posteriorly on their labial surface. The cusps of the internal row are swollen at their bases, four-sided, and increase in size and height posteriorly; the row continues to near the anterior margin of the crown as a low crest, and the labial surface bears deep vertical grooves.

The external row of M2 is developed as a low crest with poorly differentiated cusps (Figs. 3.11.6, 3.11.7). The crescentic cusps of the middle row are deeply worn, with prominent vertical grooves on both the labial and lingual surfaces. The cusps of the internal row are smaller than those of the middle row and are subcrescentic in cross section.

Lower dentition (Figs. 3.11.8-3.11.12): Lower premolars: p4: UALVP 46285 and 46287 are high and semicircular in profile, in contrast with the low and elongate p4 of Neoplagiaulax serrator and N. paskapooensis. The labial and lingual faces are flat. Although the anterobasal concavity is slightly damaged in both specimens, it appears to have been deeply notched for reception of p3; the posterolabial shelf is poorly developed. The exodaenodont lobe is deep and pointed ventrally, and the anterior margin of the lobe is confluent with the anterior margin of the crown, not forming the pronounced anterior "beak" seen on p4 of some other species of Neoplagiaulax (e.g., p4 of Neoplagiaulax sp., cf. N. hunteri, above, and p4 of N. donaldorum (Scott and Krause, 2006)]. The anterior margin is more posteriorly reclined than in p4 of N. hazeni from Princeton Quarry and Neoplagiaulax sp., cf. N. hazeni from Roche Percée (Jepsen, 1940; Krause, 1977), and extends posterodorsally to a relatively higher first serration. The height of the first serration above the anterobasal concavity is approximately 40 per cent of the standard length, as in p4 of Neoplagiaulax sp., cf. N. hazeni from Roche Percée (Krause, 1977). The dorsal margin of the cutting edge is smoothly arcuate and bears 14 serrations (N=2),

while the posterior slope descends in a gentle arc to the base of the crown. The serrations are closely approximated anteriorly but become further spaced, slightly larger, and more swollen posteriorly. Labial and lingual ridges extend anteroventrally from below the serrations, with the first two ridges of the labial, and first three ridges of the lingual surface joining each other anteriorly. The ridges become coarser posteriorly. Beneath the last three serrations no ridges are developed.

Lower molars: m2: The crown of UALVP 46286 is subtrapezoidal in occlusal view and slightly longer than wide (Fig. 3.11.7). The cusps of the external row are subequal in size and height, and are strongly crescentic. The cusps of the internal row are both taller and larger than those on the external row and decrease in height posteriorly. The internal cusps are crescentic anteriorly but become more nearly quadrate posteriorly. Deep vertical grooves are developed on the valley-facing surfaces of the internal and external cusps, and on the lingual surface of the internal cusps.

Discussion.—Jepsen (1940) originally described Neoplagiaulax hazeni (as Ectypodus hazeni) from the late Tiffanian Princeton locality, Wyoming; in his study of late middle Tiffanian multituberculates from Saskatchewan, Krause (1977) tentatively referred a large number of teeth to N. hazeni, but cited what he believed to be significant differences in P4 coronal anatomy between the Wyoming and Saskatchewan samples. The teeth of Neoplagiaulax sp., cf. N. hazeni from the Blindman River localities are closest to those of N. hazeni from the Princeton Quarry, and to a lesser extent, those of Neoplagiaulax sp., cf. N. hazeni from the Roche Percée locality, and are clearly separable from the four other species of Neoplagiaulax present in the Blindman River sample (see earlier in this chapter). Although the premolars and molars of Neoplagiaulax sp., cf. N. hazeni from Alberta are similar to those of N. hazeni and Neoplagiaulax sp., cf. N. hazeni (sensu Krause, 1977), they are slightly smaller, falling outside of the lower extremes of measurements recorded by Jepsen and Krause. The p4 of Neoplagiaulax sp., cf. N. hazeni from Alberta is lower crowned and the anterior margin is much shallower than that of Neoplagiaulax sp., cf. N. hazeni (sensu Krause, 1977) (e.g., compare Fig. 3.11.8 with Krause, 1977, pl. 4, fig. 1); in this regard, the p4 of Neoplagiaulax sp., cf. N. hazeni from Alberta more closely resembles that of N. hazeni (see Jepsen, 1940, pl. 4, fig. 1). Interestingly, the P4 crown of Neoplagiaulax sp., cf. N. hazeni is lower than in N. hazeni,

and the posterior margin shorter and slightly more concave, more similar in these regards to P4 of Neoplagiaulax sp., cf. N. hazeni (sensu Krause, 1977) from Roche Percée.

Although the specimens described above resemble corresponding elements of N. hazeni, the differences preclude referral either to that species, or to Neoplagiaulax sp., cf. N. hazeni (sensu Krause, 1977). Assessment of the taxonomic significance of these differences must await further sampling from the Blindman River localities.

NEOPLAGIAULACIDAE genus and species indeterminate

Figures 3.11.13, 3.11.14

Material examined.—From DW-2: UALVP 46288, p4.

Description.—p4 (L=5.3): The crown of UALVP 46288 is long, low, and asymmetrical in profile. The exodaenodont lobe is swollen and despite damage to its ventral margin, was probably broadly rounded ventrally. The posterolabial shelf is short and poorly developed, the anterobasal concavity is broad and shallowly notched for reception of p3, and a weak interradicular crest is present. The short and steep leading edge of the crown extends dorsally to a single low incipient serration; the dorsal margin is long and arcuate, and bears 13 serrations that are delicate anteriorly, but become larger and coarser posteriorly. The first serration is low (relative height=0.3), similar to p4 of Mesodma (see Sloan, 1981), and the apogee occurs at the fifth serration; the first three serrations are widely spaced, while the remaining serrations are much closer to one another. Both sides of the crown bear ridges that are close to each other anteriorly but become further apart posteriorly; the ridges on the lingual side are coarser and less oblique than those on the labial side; no ridges are developed beneath the last two serrations.

Discussion.—The lateral profile of UALVP 46288 resembles that of other neoplagiaulacid p4s, including that of Mesodma, Mimetodon, and especially Xyronomys (see Rigby, 1980; Johnston and Fox, 1984; Scott, 2003; Middleton and Dewar, 2004), but differs in being significantly larger (e.g., length p4, Neoplagiaulacidae genus and species indeterminate, Blindman River localities=5.3 versus length, p4, Xyronomys swainae Rigby, 1980, Swain Quarry=2.9), in having a stronger exodaenodont lobe, and in the

labial and lingual ridges being oriented less horizontally (p4 of the recently described Xyronomys robinsoni Middleton and Dewar, 2004 from the Puercan Littleton fauna, Colorado, although slightly larger than p4 in X. swainae, is of otherwise similar morphology and differs from UALVP 46288 in much the same way as does p4, X. swainae). The significance of these differences is uncertain given the small sample from the Blindman River localities, and UALVP 46288 is referred only to the Neoplagiaulacidae.

Family PTILODONTIDAE Cope, 1887

Genus PTILODUS Cope, 1881

Ptilodus COPE, 1881, p. 921.
Chirox COPE, 1884, p. 321.

Type species.—Ptilodus mediaevus Cope, 1881.

Other included species.—Ptilodus mediaevus Cope, 1881; P. montanus Douglass, 1908; P. wyomingensis Jepsen, 1940; P. fractus (Dorr, 1952); P. kummae Krause, 1977; P. tsosiensis Sloan, 1981; P. gnomus Scott, Fox, and Youzwyshyn, 2002.

PTILODUS "CEDRUS"

Figures 3.11.16-3.11.18, 3.12.1-3.12.6, 3.14; Table 3.11

Remarks.—In his study of ptilodontid multituberculates, Krause (1982b) referred teeth from the Cedar Point Quarry locality of northwestern Wyoming to a new species of Ptilodus, P. "cedrus". Although the material has yet to be published, this new species of Ptilodus has appeared repeatedly in print as Ptilodus sp. "C" or Ptilodus "cedrus", despite these being nomina nuda (e.g., Gunnell, 1994; Secord, 1997; Scott et al., 2002; Higgins, 2003). Ptilodus "cedrus" is used here to avoid confusion and the unnecessary use of yet another informal designation for this species while awaiting validation of the name by Krause.

Material examined.—From DW-1: UALVP 40455, P4; UALVP 46289, M1; UALVP 40464, p4 fragment.

From DW-2: UALVP 46290, incomplete skull with left P3-4, M1-2, right P1-4, M1-2, incomplete left dentary with i1, p3-4, m1-2, incomplete right dentary with i1, p3-4, m1-2; UALVP 46291, incomplete right premaxilla and maxilla with I2-3, P1-4, M1-2, with associated P1 and P2, humerus, and proximal ulna; UALVP 46292, incomplete maxilla with P2-3; UALVP 46293-95, P1 (total: 3); UALVP 46296-99, P2 (total: 4); UALVP 46302-06, P3 (total: 5); UALVP 40462, 46307-10, P4 (total: 5); UALVP 46311-15, M1 (total: 5); UALVP 46316, 46317, M2 (total: 2); UALVP 40454, incomplete left dentary with i1, p3-4; UALVP 40465, incomplete right dentary with i1, p3-4, m1-2; UALVP 46344, incomplete left dentary with p3-4; UALVP 46318, incomplete right dentary with p4, m1; UALVP 46319-21, i1 (total: 3); UALVP 40461, 46322-24, p4 (total: 4); UALVP 40457, 40458, 40460, 46325-35, incomplete p4s; UALVP 46336-38, m1 (total: 3); UALVP 46339, 46340, m2.

From Mel's Place: UALVP 40459, P4; UALVP 46341, 46342, incomplete p4s.

Age and occurrence.—Earliest Tiffanian (Plesiadapis praecursor/P. anceps Lineage Zone, Ti1, late Paleocene) to late middle Tiffanian (Plesiadapis churchilli/P. simonsi Lineage Zone, Ti4, late Paleocene) of the Western Interior of North America.

Description.—Upper dentition (Figs. 3.11.15-3.11.18, 3.12.1-3.12.4): Collectively, the specimens of Ptilodus "cedrus" from the Blindman River localities preserve parts of the skull and postcranium, including I3 in association with the cheek teeth, the first discovered for a ptilodontid multituberculate. Additional specimens preserve a nearly complete zygomatic arch and glenoid fossa, as well as both petrosals; these will be described elsewhere. As the cranial and post-cranial anatomy of Ptilodus is arguably the best known for any North American multituberculate (see, e.g., Simpson, 1937a; Krause and Jenkins, 1983), special attention is given here to the upper incisors, the teeth most poorly known in ptilodontids.

Upper incisors: UALVP 46291 preserves the first discovered ptilodontid I3, and the first specimen of a ptilodontid in which both I2 and I3 are preserved in association with the upper post-incisor dentition. The I2 of Ptilodus "cedrus" differs little from that of P. montanus, the only other ptilodontid in which I2 is known (see Simpson, 1937a-b;

Krause 1982c): although the apex has been appreciably worn, the crown appears to have been long, slender, and slightly curved, with the anterior surface convex and the posterior surface virtually flat (Fig. 3.11.15). The enamel extends only a short distance posterodorsally, in contrast with that on i1 (see later in this chapter). Short, well-defined crests occur medial and lateral to the large occlusal facet; while wear has obscured their original dimensions, the crests likely originated at the apex and ran posterodorsally, dividing the crown into anterior and posterior surfaces, as in I2 of P. montanus (Simpson 1937b) and Neoplagiaulax paskapooensis (see earlier in this chapter). A poorly developed posteromedial crest, also probably originating at the apex in unworn teeth, runs a short distance posterodorsally, giving the occlusal surface a subtriangular appearance in cross section. Accessory cusps are not developed.

The I3 of Ptilodus "cedrus" is similar to that in the neoplagiaulacid Neoplagiaulax paskapooensis, although the crown and root in Ptilodus "cedrus" are both longer and stouter, with the enamel extending only a short distance basally from the apex. The crown is anteroposteriorly compressed, but becomes slightly wider and more bulbous towards the base, and an accessory cuspule is not present (Fig. 3.11.15). The apex has been worn perpendicular to the dorsoventral axis of the tooth, and is virtually flat, exposing the underlying dentine. The enamel is thick, especially anteriorly, but thins posterodorsally. As on I2, lateral and medial crests are developed; these crests probably extended to the apex, similar to those on I2, and divide the crown into anterior and posterior surfaces. A weaker posteromedial crest further divides the posterior surface into medial and lateral sides and, like that on I2, gives the occlusal surface a subtriangular appearance.

Upper premolars: P1-3: The anterior premolars of Ptilodus "cedrus" do not differ significantly from those of other species of Ptilodus (e.g., anterior premolars described in detail by Krause, 1977 for P. kummae), being closest in size to those of P. montanus and P. wyomingensis. The P1 has three cusps arranged in an equilateral triangle on the crown; the anterior cusp is both smaller and lower than the two posterior cusps. The crown of P2 can be subrectangular, square, or even subcircular in outline. The crown bears four equidistant main cusps arranged in two parallel rows, and accessory cusps can occasionally occur anterolabially. The posterolingual margin of the crown is often

slightly extended posteriorly. The P3 generally has six main cusps arranged in two longitudinal rows on a subovate or subrectangular crown. One or two accessory cusps can occur anteriorly or anterolabially, supplementing the main cusps; the accessory cusps can be quite small or nearly as large as the main cusps. The enamel of the anterior premolars is smooth on the valley-facing surface of the cusps, whereas labially it is coarsely wrinkled.

P4: Cusp formula (0-1)6-8:10-11:0 [mode=(0)7:10:0; N=9]. The P4 of Ptilodus "cedrus" is similar to that in other ptilodontids, with the cutting edge straight to slightly concave in lateral view and with virtually no increase in cusp height anteroposteriorly (Fig. 3.11.18). The crown is long and narrow, with two subparallel rows of cusps and a weakly developed anterolabial lobe bearing one or two cuspules. The external row curves labially in a shallow arc, with the cusps somewhat irregularly spaced from one another. The cusps of the external row are subconical, especially posteriorly, but become more nearly pyramidal anteriorly; short, low crests can connect the first two, three, or four cusps to one another anteriorly and posteriorly. The cusps of the external row are flat laterally, while their medial faces are convex; the second or third cusp in the external row is usually largest on the crown. The external row extends posteriorly to the prepenultimate cusp of the middle row in all specimens at hand. The cusps of the middle row are subequal in size and height, and are connected to one another by high crests. The enamel is heavily wrinkled and forms prominent ridges and grooves on the labial and lingual surfaces of cusps of the middle row; weaker wrinkling of the enamel can also occur on the labial surface of the external cusps and anterolabial bulge. Strong apical and lingual wear occurs posteriorly on the cusps of the external and middle rows of some specimens.

Upper molars: M1: Cusp formula 8-9:9-10:5-6 (mode=8:9:5; N=7). The crowns of the upper molars are virtually identical to those of Ptilodus kummae (see Krause, 1977) and P. gnomus (see Scott et al., 2002), differing only in their larger size. The external and middle cusp rows of M1 are parallel and bend anterolabially; the cusps of the external and middle rows are directly opposed to one another anteriorly but become staggered posteriorly. The cusps of the external row are subconical anteriorly, but become more nearly pyramidal posteriorly. The cusps of the middle row are crescentic

posteriorly and bear grooves on their medial and lateral sides; the ultimate cusp in the middle row is the tallest on the crown, whereas the penultimate cusp is usually the largest. Although the cusps of the internal row terminate at the fourth, fifth, or sixth cusp of the middle row, a low, papillate ridge can continue to the anterior edge of the crown.

M2: Cusp formula 3:3-4 (mode=3:4; N=3). The external cusp row of M2 is low and ridge-like, convex labially, and with poorly differentiated cusps. The enamel at the base of the external row and in the anterior "pocket" formed between the external and middle rows is coarsely wrinkled. The first cusp of the middle row is large and pyramidal; the remaining two cusps are subequal in height, subcrescentic, and their apices bend anteriorly. The second cusp on the middle row is the largest and tallest on the crown. The cusps of the internal row are lower than those of the middle row and are pyramidal. High crests join the first two or three cusps on the internal row; the third or fourth cusp is lower than the first three and set off posteriorly. Deep, vertical grooves are present on the valley-facing sides of the middle and external rows.

Dentary and lower dentition (Figs. 3.12.2-3.12.6): The dentary of Ptilodus has been described in detail (see, e.g., Simpson, 1937a; Wall and Krause, 1992), and the specimens of Ptilodus "cedrus" from the Blindman River localities provide little in the way of additional information. Both the horizontal ramus and alveolar process are deeper than those in Neoplagiaulax (see earlier in this chapter), and the symphyseal surface is longer and deeper. The masseteric and pterygoid fossae are well excavated, and the masseteric fovea is similar to that in Ectypodus, occurring as a shallow, ovoid indentation confluent with the anterior part of the masseteric fossa (Gambaryan and Kielan-Jaworowska, 1995).

i1: The crown of i1 is long and slender, as in most other ptilodontoids (Jepsen, 1940; Kielan-Jaworowska and Hurum, 2001). In cross section, the crown is convex laterally and flat medially; the enamel is thick ventrally but thins dorsally. The medioventral longitudinal ridge is well developed and becomes stronger posteriorly; weaker dorsal and medial crests run a short distance posteriorly from the apex of the crown. A wear facet is often developed along the dorsal surface of the crown, beginning at the apex and progressing further posteriorly with increased wear; as discussed above, this facet is probably developed initially through occlusion with the opposing I2, but its

occurrence more posterodorsally on the crown is likely caused by food-tooth contact (Fox, 2005).

Lower premolars: p3: The crown of p3 is bulbous and peg-like, and can have an anteriorly positioned apical cuspule, much like in the ptilodontid Prochetodon speirsae (see later in this chapter).

p4: The coronal anatomy of p4 resembles that in other species of Ptilodus: the crown is high and nearly oval in lateral outline with a symmetrically arcuate cutting edge, and the labial surface is virtually flat and the lingual surface more convex, especially near the base of the crown (Fig. 3.12.5). The anterobasal concavity is deeply notched and dorsally peaked, as in P. gnomus (Scott et al., 2002). The exodaenodont lobe is long and deep, and can be rounded or sharply pointed ventrally; the lobe has an inflated appearance and juts laterally. The posterolabial shelf is only weakly developed and is often erased by wear. The anterior margin of the crown is convex in profile; it is slightly reclined relative to p4 of P. kummae and P. gnomus, and closer to p4 of P. montanus and P. wyomingensis. Above the anterobasal concavity, the crown protrudes anteriorly as a prominent "beak" [Fig. 12.5 and contrast with p4, P. kummae (Krause 1977, pl. 1, figs 1-2)]. The anterior margin curves gently to the high first serration and the cutting edge bears between 15 and 16 serrations (mode=15; N=8). The serrations are nearly equidistant anteriorly but become increasingly closer together and coarser posteriorly. Prominent ridges occur on the labial and lingual surfaces below the serrations, and become increasingly coarser and further apart posteriorly; the terminal three serrations lack both labial and lingual ridges.

Lower molars: m1 cusp formula 6-7:5-6 (N=5); m2 cusp formula 3-4:2 (mode=3:2; N=4). Except for their slightly larger size and greater cusp number, the molars of Ptilodus "cedrus" are virtually identical to those of P. kummae (Krause, 1977) and P. gnomus (Scott et al., 2002). The cusps of the external row on m1 are pyramidal anteriorly but become subcrescentic posteriorly; the ultimate and penultimate cusps in some specimens are fused. Vertical grooves occur on the valley-facing sides of the external cusps, becoming deeper posteriorly. The cusps of the internal row are pyramidal, and the third is the largest and tallest on the crown; the terminal two cusps are sometimes fused. Small cuspules can occur lingually near the anterior or posterior ends

of the internal row. As with the external row, vertical grooves occur on the valley-facing surface of the internal row.

The cusps of the external row on m2 are crescentic, with the first two or three cusps being subequal in size and height. The ultimate cusp on the external row is longer than the first two or three and can be joined with the preceding cusp. The two internal cusps are massive and swollen at their bases, with the more anterior of the two the larger and taller; both cusps are crescentic in cross section.

Discussion.—Incisor function in Ptilodus "cedrus": The function of the incisors was only a minor subject in the classic studies of the masticatory cycle in Ptilodus (Krause, 1982c; Wall and Krause, 1992), owing largely to the paucity of specimens. The long and slender incisors in Ptilodus "cedrus" likely functioned analogously to similar teeth of extant mammals (e.g., Bettongia Gray, Burramys Broom), being associated with food procurement, stabilization, and ingestion (Wall and Krause, 1992). Although the I2 and I3 of UALVP 46291 are not in direct articulation with the cheek teeth (and therefore not lending themselves to an analysis of function sensu Krause, 1982c or Wall and Krause, 1992), the wear surfaces do provide some evidence of the direction of jaw movement during the initial phase of the chewing cycle.

The occlusal surface of I2 is worn to a broad flat surface that slopes dorsomedially-ventrolaterally (Fig. 3.15A). The crown has been sufficiently worn such that the presence of an interdental facet cannot be determined, although Simpson (1926, 1937a-b) and Krause (1982c) suggested the opposing I2s of Ptilodus were probably held at an angle in the premaxilla such that their crowns converged, and possibly contacted each other medially (and see earlier in this chapter for similar conclusions for the neoplagiaulacid Neoplagiaulax paskapooensis). Simpson (1926) and Krause (1982c) suggested the crowns of I2 and i1 in Ptilodus could not come into contact with one another, a conclusion based on an analysis of specimens of P. montanus from the Fort Union of Montana; in contrast, Gambaryan and Kielan-Jaworowska (1995) believed this conclusion erroneous, citing preservational factors affecting the quality of the specimens then available for study. The occlusal surface of I2 on UALVP 46291 shows parallel, anteroposteriorly-directed striae, the first reported for upper incisors of Ptilodus, possibly indicative of tooth-tooth contact, suggesting i1 might have occluded with I2. The striae

are much weaker than those developed on the associated P4 and upper molars, but the function of the incisors was probably not one of grinding or gnawing [as it apparently was in the microcosmodontid Microcosmodon (e.g., Fox, 2005) or djadochtatherioideans (e.g., Kielan-Jaworowska, 1974)], and the striae probably reflect periodic episodes of grasping or piercing (Clemens, 1964; Krause, 1982c). The striae on I2 are oriented parasagittally, consistent with the apical surface of i1 having been drawn over the occlusal surface of I2. In addition to the broad wear facet on I2, the apical surface of I3 also shows evidence of strong wear. Nearly half the crown height of I3 has been worn away, with the apex worn to a flat surface; faint, shallow striae are developed along the length of the surface.

In an extensive analysis of Microcosmodontidae, Fox (2005) discussed the function of the incisors in Microcosmodon conus and suggested I3 occluded precisely with i1, a conclusion consistent with evidence of a bifid wear facet on the crown of I3. Fox further concluded that the long, dorsal facet on i1 could not have been made by contact with I2 without significant dislocation of the temporomandibular joint, instead suggesting abrasive food as a possible cause. Despite obvious differences in incisor function (i.e., grasping and piercing in Ptilodus "cedrus" vs. gnawing in M. conus), evidence from the occlusal surfaces of I2, I3, and i1 of Ptilodus "cedrus" suggests the occlusal relationships between these teeth appear to be generally similar to those of Microcosmodon conus. The striae on I2 indicate occlusion between I2 and i1 was possible, and probably occurred with some precision, although perhaps not to the same degree as in Microcosmodon. The function of I3 is less clear: although striae are developed, they are much weaker than those on I2 (and contrast with the strongly developed wear striae on I3 of M. conus, see Fox, 2005), and the wear facet is virtually flat, perpendicular to the dorsoventral axis of the crown. Given the position of I3 relative to I2 (I3 is somewhat posterolabial to I2, see Krause, 1982c), it seems unlikely that the crowns of I3 and i1 could occlude, either in a preliminary cropping or nipping phase, or during the palinal power stroke (Krause, 1982c; Wall and Krause, 1992). The striae on the crown of I3 may have been caused by contact with abrasive food items, similar to that on the anterodorsal surface of i1.

The specimens of Ptilodus "cedrus" from the Blindman River localities are similar to homologous teeth of Ptilodus "cedrus" from the middle Tiffanian Cedar Point Quarry locality, Wyoming (Krause 1982b), differing only in p4 being slightly larger and in having a shallower, rather than steep, anterior margin. Ptilodus "cedrus" is one of the most commonly occurring multituberculates in middle Tiffanian local faunas of the Western Interior of North America (e.g., Krause 1982b). As Krause (1982b) noted, upper and lower fourth premolars of Ptilodus "cedrus" are highly variable, and this appears to be true of the Blindman River sample (Fig. 14).

PTILODUS "TITANUS"

Figures 3.13, 3.14; Table 3.12

Remarks.—The specimens described below are referable to what has been informally dubbed Ptilodus sp. "T" or P. "titanus", a new species of Ptilodus from the Douglass Quarry locality of south central Montana that was described by Krause (1982b). As with Ptilodus "cedrus", the specific name "titanus" is placed in quotations to indicate its status as a nomen nudum.

Material examined.—From Joffre Bridge Mammal Site #1: UALVP 40467, incomplete skull with left P2-4, M1-2, right P1 (incomplete), P2-4, M1-2.

From Joffre Bridge Roadcut, lower level: UALVP 46345, P4.

From DW-2: UALVP 40456, 46300-01, P2 (total: 3).

From Cochrane 2: UALVP 18621, incomplete right maxilla with M1-2; UALVP 46350, M1; UALVP 18631, 46348-49, M2 (total: 3); UALVP 18620, incomplete right dentary with p3-4; UALVP 46351, 46352, p4; UALVP 46353, m1; 18638-40, 18805, 46354, incomplete m1s; UALVP 18629-30, 18633, m2 (total: 3).

Age and occurrence.—Earliest Tiffanian (Plesiadapis praecursor/P. anceps Lineage Zone, Ti1, late Paleocene) to early middle Tiffanian (Plesiadapis rex/P. churchilli Lineage Zone, Ti3, late Paleocene) of the Western Interior of North America (Lofgren et al., 2004).

Description.—Skull and upper dentition (Fig. 3.13): UALVP 40467 preserves left and right post-incisor skull fragments from a single individual (Fig. 3.13.1). Included

among these fragments are well-preserved left and right zygomata, the anterior part of the left palatine, and parts of the choanae; collectively, these fragments document the first known skull material for Ptilodus "titanus". The maxillary process of the zygomatic arch is stout, with the root slightly wider than the more posterior part of the process. The base of the maxillary process (as marked by its posterior margin, see Rougier et al., 1997) arises at the level of P4, slightly more posterior than that in P. montanus (Simpson 1937a), and extends laterally at an angle of about 135 degrees from the anteroposterior axis of the skull. The adductor chamber is relatively much wider than in P. montanus, and by inference Ptilodus "titanus" had considerably better-developed jaw adductors. Neither arch preserves the maxillary-squamosal suture, nor is there evidence on the parts preserved of a medially positioned jugal (Hopson et al., 1989). The anterior zygomatic ridge (Gambaryan and Kielan-Jaworowska, 1995) occurs low on the maxillary process, and is weakly developed compared to those in djadochtatherioideans; the ridge is restricted to the inferior surface of the process, and is not present laterally. The presence of intermediate and posterior zygomatic ridges, if these were present in life, cannot be determined. Little can be said of the palatine process of the maxillary, or of the palatine proper, as these bones have been damaged and distorted in preservation; the dimensions of the parts preserved, however, suggest a palatal morphology similar to that in P. montanus (see Simpson, 1937a) and Neoplagiaulax cimolodontoides (see earlier in this chapter). The lateral margin of the left palatal vacuity occurs medial to P3, P4, and the anterior part of M1, suggesting that it was a long and conspicuous opening. The left choana is damaged, but the anterior rim apparently occurs medial to the posterior part of the first molar, and the roof of the primary palate is shallowly concave. Broken bone lying adjacent to the damaged left choana may represent the remnants of the presphenoid and vomer.

Upper premolars: P2-3: The anterior premolars are virtually identical to those described for Ptilodus "cedrus", differing mainly in their larger size. The crown of P2 has four main cusps, but these can be supplemented by additional, smaller accessory cuspules on the anteroexternal margin. The crown of P3 supports six main cusps, but these too can be supplemented anteroexternally and posteroexternally by additional cuspules.

P4: Cusp formula (1-2)7-9:10-11:0 [mode=(2)8:10:0; N=4]. The P4 of Ptilodus "titanus" is of characteristic ptilodontid morphology, and is most similar to homologous teeth of Ptilodus "cedrus". The P4 of Ptilodus "titanus" and Ptilodus "cedrus" can be difficult to separate, as length, width, and cusp formulae overlap (Fig. 3.14, ,Tables 3.12, 3.13); they can be distinguished, however, in that of Ptilodus "titanus" being slightly wider (mean width P4, Ptilodus "cedrus"=2.49, N=9 versus mean width P4, Ptilodus "titanus"=2.83, N=3), and having a better-developed anterolabial lobe that usually bears at least two large, well-developed cusps labial to the external cusp row (contrast with P4 of Ptilodus "cedrus" in which the anterolabial lobe is more poorly developed and usually lacks cusps).

Upper molars: M1 cusp formula 8-9:10-11:5 (N=3); M2 cusp formula 3:3-4 (mode=3:4; N=4). As with the referred upper premolars, the upper molars of Ptilodus "titanus" are virtually indistinguishable from those of Ptilodus "cedrus" except for their larger size and greater number of cusps.

Lower dentition (Fig. 3.13): Lower premolars: p3: As in other species of Ptilodus, p3 of Ptilodus "titanus" is a small, peg-like tooth, with a bulbous crown; unlike that of Ptilodus "cedrus", the crown of p3 of Ptilodus "titanus" lacks accessory cuspules.

p4: The p4 of Ptilodus "titanus" resembles that of other species of Ptilodus: the blade is high, and in profile the cutting edge forms a symmetrical arc (Figs. 3.13.2, 3.14). The labial face is virtually flat, whereas the lingual side is slightly convex, and the anterobasal concavity is deeply notched, with a slight dorsal inflection of the enamel. The exodaenodont lobe is shallow, long, and smoothly rounded ventrally, differing from that of Ptilodus "cedrus" and P. montanus, in which the lobe is deeper and often pointed ventrally. Although its original proportions have been obscured by wear, the posterolabial shelf appears to have been only weakly developed. The anterior margin of the crown is long and convex, and grades smoothly with the anterior margin of the exodaenodont lobe (i.e., does not form a pronounced "beak"). The leading edge is steeper than that in Ptilodus "cedrus" and the first serration is comparatively higher. The cutting edge supports 13 or 14 serrations (N=2) that become larger, closer together, and more bulbous posteriorly. The crown beneath the first serration bears three ridges, one labial, one lingual, and one on the anterior margin; the ridges extend anteroventrally, with

the labial and lingual ridges joining with the second labial and lingual ridges, respectively, near the anterior margin of the crown. Succeeding ridges become shorter and weaker posteriorly, nearly disappearing at the level of the penultimate cusp on the labial and lingual sides. The enamel below the penultimate and ultimate serrations is irregularly wrinkled on the labial surface, but is smooth lingually. As in other species of Ptilodus, a distinct, circular wear facet occurs on the posterolabial face of p4.

Lower molars: m1 cusp formula 7:6 (N=1); m2 cusp formula 4:2 (N=2). As with M1-2, the lower molars of Ptilodus "titanus" are nearly identical to those of other species of Ptilodus, differing only in their larger size and greater cusp number.

Discussion.—Youzwyshyn (1988) referred a number of specimens from the Cochrane 2 locality to Ptilodus "titanus", and these specimens are included here. Although the teeth of Ptilodus "titanus" can be distinguished from those of Ptilodus "cedrus" in their generally larger size and greater modal number of cusps and serrations (Krause 1982b), correct referral of isolated teeth to either taxon to the exclusion of the other can be difficult. As noted earlier, the teeth of Ptilodus "cedrus" are highly variable (and see Krause, 1982b), and the largest specimens of Ptilodus "cedrus" can overlap the smaller ones of Ptilodus "titanus" (Fig. 14), with few consistent morphological characters separating the two. In addition to P4 of Ptilodus "titanus" being larger than that of Ptilodus "cedrus", the anterolabial lobe is generally better developed, and usually bears at least two well-developed cusps. The crown of p4 of Ptilodus "titanus" is larger and relatively higher, and the anterior margin is steeper and the exodaenodont lobe is weaker.

Ptilodus "titanus" is known primarily from the earliest Tiffanian of the Western Interior of North America (Krause, 1982b; Krause, 1987a; Krause and Maas, 1990); its presence at the Blindman River localities extends its stratigraphic range into the early middle Tiffanian. Ptilodus "titanus" is sympatric with two other ptilodontids in the Blindman River local fauna, Ptilodus "cedrus" and Prochetodon speirsae (see later in this chapter), documenting another locality of Paleocene age from Western Canada in which multiple ptilodontid taxa are known to co-occur (Fox, 1990; Scott et al., 2002).

Genus PROCHETODON Jepsen, 1940

Prochetodon JEPSEN, 1940, p. 310.

Type species.—Prochetodon cavus Jepsen, 1940.

Other included species.—Prochetodon taxus Krause, 1987b; Pro. foxi Krause, 1987b; Pro. speirsae new species.

PROCHETODON SPEIRSAE new species

Figures 3.15.1-3.15.10, 3.16; Table 3.13

Diagnosis.—Largest species of Prochetodon (p4 approximately 25 percent longer than that of Pro. foxi and Pro. taxus, and approximately 30 percent longer than that of Pro. cavus). Differs further from all other species of Prochetodon in p4 crown leaning less posteriorly, in having a less smoothly rounded anterior margin, and in having a deeper and better-defined exodaenodont lobe. Differs further from all other species of Prochetodon in m1 being larger and in having more cusps in the lingual row.

Description.—Dentary and lower dentition (Figs. 3.15.1-3.15.10): Several incomplete dentaries referable to Pro. speirsae have been recovered from Birchwood and Cochrane 2, collectively preserving most of the dentary anterior to the condyle (Figs. 3.15.4, 3.15.7). The horizontal ramus is bowed labially; the incisor alveolus is offset medially as in other ptilodontoid multituberculates, and the post-incisor teeth are oblique to the incisor, but parasagittal to the anteroposterior axis of the jaw. As noted by Jepsen (1940) for Pro. cavus, the ramus between i1 and p3 is robust and deep, much more so than in Ptilodus, and the diastema is proportionately shorter. The anterior alveolus is wide basally, housing the large i1, and the ventral border of the horizontal ramus is only moderately convex, suggesting the posterior part of the incisor root was narrow, and did not extend appreciably posteriorly past the level of p4. The symphysis is preserved only on UALVP 45689 (Fig. 3.15.5): the symphyseal surface is broken anteriorly, while the posterior part consists only of a small, oval-shaped area of bone that is slightly concave medially; this area of bone is bounded anteriorly and ventrally by a ridge of raised bone, separating it from the more anterior articulating surface of the symphysis. From the parts preserved, there is no observable evidence of the dentaries having been fused in life: the

bone of the symphyseal surface is smooth, lacking any sculpture or rugosities that would indicate an interfingering mechanism between the two articulating surfaces (Clemens, 1964; Fox, 2005). The anterior part of the masseteric fossa, preserved on UALVP 45689, was apparently deep and well excavated, especially posteriorly. The anterior extent of the masseteric fossa is not marked by a prominent crest: rather, the fossa continues anteriorly as a shallow masseteric fovea (Gambaryan and Kielan-Jaworowska, 1995) beneath the molar row, terminating ventral to the exodaenodont lobe of p4. A wide masseteric crest borders the ventral margin of the masseteric fossa, suggesting the presence in life of extensively developed mandibular adductor muscles (Simpson, 1926; Turnbull, 1970; Krause, 1982b; Fox, 2005). The ascending ramus of the coronoid process begins labial to m1 as in most other ptilodontoids, but is positioned relatively further anteriorly, similar to that of the microcosmodontid multituberculate Microcosmodon (see Fox, 2005). The lateral surface of the dentary is comparable to that of other ptilodontids and post-plagiaulacoid grade multituberculates generally in having a single mental foramen positioned ventral to p3 (Kielan-Jaworowska and Hurum, 1997); a second, larger foramen occurs about halfway between p3 and the base of i1.

i1: UALVP 45689 from the Birchwood locality preserves the lower incisor. Although broken at the tip, i1 appears to have been long and slender, narrowing apically from a relatively wide base, and procumbent, agreeing with Jepsen's (1940) description of i1, Pro. cavus, from the Fort Union Formation of Wyoming. The crown is larger, deeper, and more robust than that of similarly-sized ptilodontids (e.g., that of Ptilodus "titanus", see earlier in this chapter), and subovate in cross section, with the enamel becoming thinner dorsally, in contrast with that of, e.g., Neoliotomus Jepsen, 1940, in which the crown is robust, laterally compressed, and the enamel restricted to the ventrolateral surface (Krause, 1982c). The medioventral ridge appears to have been prominent.

Lower premolars: p3: As in other ptilodontoids, the peg-like p3 of Pro. speirsae is considerably smaller than p4. The crown is dorsoventrally elongate, slightly concave anteriorly, and swollen at its base; a single, tiny apical cuspule occurs on the anteriormost part of the crown, just slightly anterior to the enamel overhanging the anterobasal concavity of p4.

p4: p4 of Pro. speirsae has an anteroposteriorly elongate, low crown bearing 15 to 17 serrations. In lateral profile, the crown superficially resembles that of the eucosmodontid Neoliotomus and Ptilodus; the tooth differs from that of the former in being slightly higher crowned and having a better-developed exodaenodont lobe, and from the latter in having a longer, lower, and less symmetrically ovoid crown. The crown is slightly (e.g., UALVP 45682, Cochrane 2, Fig. 3.15.1) to moderately (e.g., UALVP 45690, Aaron's locality, Fig. 3.15.9) posteriorly leaning, although not to the same extent as in other species of Prochetodon (Krause 1987b). The labial face of the crown is virtually flat, whereas the lingual side is strongly convex. In contrast to the smoothly rounded anterior margin on p4 of other species of Prochetodon, that in Pro. speirsae bears a pronounced "beak", similar to p4 of some species of Ptilodus and Pro. cavus; as a result, the exodaenodont lobe is more distinct and set off from the crown, rather than grading into the anterior margin. The exodaenodont lobe is anteroposteriorly wider and reduced in depth relative to that of most species of Ptilodus, but more distinct than that of Pro. foxi and Pro. taxus. The anterobasal concavity is deep, the apex being distinctly and deeply notched for reception of the peaked crown of p3, and the posteroexternal shelf is more strongly developed relative to other species of Prochetodon, although wear has obscured this area, making inferences about the original dimensions of the shelf difficult. The leading edge of the serrated crest is long and posteriorly reclined in profile, unlike the steep, arcuate anterior margin of Ptilodus (Fig. 3.16), and ends in a low first serration. The anterior margin is broad and flat, approaching that of other species of Prochetodon, and the cutting edge bears 15 to 17 serrations that are relatively far apart from each other anteriorly, but become much closer together and stouter posteriorly; the posteriormost serrations become more nearly conical, differing from the finer, labiolingually compressed anterior serrations. The apogee occurs between the sixth and ninth serrations; posterior to the apogee, the serrated crest descends posteroventrally in a gentle arc. The labial and lingual ridges are oblique to the long axis of the tooth, especially those on the lingual face; the ridges are close to one another anteriorly, but become further apart posteriorly. The labial ridges descend from each of the serrations, save the last four or five where they are less distinct and obscured by wear. The first serration bears three short ridges, one labial, one lingual, and one anterior. The first six or seven

ridges are nearly straight and terminate near the anterior margin, while the remaining labial ridges tend to be oriented at a steeper angle relative to horizontal, and gently curve ventrally. The ridges on the lingual side are similar to those on the labial side, descending the lingual face of the crown anteroventrally, but are less distinct posterior to the 12th serration, where the enamel is strongly convex and smooth. The enamel on the posteroexternal face of the crown is strongly crenulated and often heavily worn. The anterior root is large, nearly twice the size of the posterior, and both point anteroventrally.

Lower molars: The molars are similar to those of other ptilodontids, having labial and lingual rows with large, massive cusps. The m1 has a cusp formula of 6-7:6, and is quadrate in occlusal aspect, with an unusually transverse anterior margin. The cusp rows remain relatively far apart from one another anteriorly, contrasting with those of Ptilodus and other species of Prochetodon in which the cusp rows tend to converge anteriorly. The anterolabial face is slightly swollen, and a slight narrowing of the crown occurs at approximately mid-length, further enhancing the transverse dimension of the anterior part of the crown. The cusp rows are subequal in height, contrasting those of other ptilodontoids in which the internal row is markedly taller than the external row. The cusps of the external row are subquadrate anteriorly, but become more crescentic posteriorly; the cusps of the internal row are uniformly quadrate. The last two cusps of the internal row can be fused along the lingual margin, but are incipiently divided along their valley-facing surfaces. Shallow vertical grooves are present on unworn teeth on the valley-facing surfaces of the lingual cusps; similar grooving on the external cusps apparently occurs only after extended wear. Incipiently developed vertical grooves are present on the labial face of the external row, a feature considered diagnostic of Prochetodon (Krause, 1987b). The single referred m2 has a cusp formula of 4:2, and is virtually identical to those of Ptilodus, save for its larger size. The cusps of the labial row are crescentic, whereas those of the lingual row are nearly quadrate; as in m1, the cusp rows are subequal in height.

Etymology.—Named in honour of the late Elizabeth (Betty) Speirs for her contributions to paleontological collections in Alberta.

Holotype.—UALVP 45682, incomplete left dentary having p4, m1-2 (Figs. 15.1-15.3). Cochrane 2 locality, Paskapoo Formation of Alberta, late Paleocene [earliest Tiffanian, Ti1 (Youzwyshyn, 1988; Fox, 1990; Scott et al., 2002), Plesiadapis praecursor/P. anceps Lineage Zone of Lofgren et al., 2004].

Other material examined.—From Joffre Bridge Mammal Site No. 1: UALVP 45695, p4; UALVP 45696, incomplete left dentary having p3-4.

From Birchwood: UALVP 45689, incomplete left dentary having i1, p3-p4, m1; UALVP 45703, incomplete left dentary having p3-4; UALVP 39137, p4 (fragment).

From Cochrane 2: UALVP 45697, incomplete right dentary having p3-4; UALVP 45683, 45684, 45688, p4s; UALVP 18641, 45685, p4 fragments; UALVP 45686, 45687, m1s.

From Aaron's locality: UALVP 45690, p4; UALVP 43352, 43307, 45691, 45692, 45693, 45694, p4 fragments.

Age and occurrence.—Earliest Tiffanian (Plesiadapis praecursor/P. anceps Lineage Zone, Ti1, late Paleocene) to early middle Tiffanian (Plesiadapis rex/P. churchilli Lineage Zone, Ti3, late Paleocene) of the Alberta.

Discussion.—The low, posteriorly leaning profile, and reduced exodaenodont lobe of p4 identify these specimens as belonging to Prochetodon (Krause, 1987b), although these features are not developed to the same extent as those of other species of the genus. Although significantly larger, the teeth of Pro. speirsae most closely approximate those of Pro. foxi: the p4 profiles are similarly long and low, the anterior margin of the serrated crest is flat, and the molars have weak grooves on the labial surface. In contrast, the p4 crown of Pro. speirsae is higher and more symmetrically arcuate, leans less posteriorly, and has a deeper and better-developed exodaenodont lobe, features shared with p4 of most species of Ptilodus (Krause, 1982a, 1987b). Krause (1987b) hypothesized derivation of Prochetodon from a Torrejonian or early Tiffanian species of Ptilodus, but suggested that suitable structural antecedents were not yet discovered. In possessing features characteristic of both Prochetodon and Ptilodus, Pro. speirsae may occupy this morphological "gap". The discovery of Pro. speirsae from the earliest Tiffanian gives some support to Krause's (1987b) suspicions concerning the

approximate age of the ancestry of Prochetodon, but a more precise estimate of this ancestry must await the discovery of better-preserved material.

Specimens of Prochetodon have been found only at localities north of the Wind River Basin, south central Wyoming (Krause 1987b); given this limited distribution and the apparent north-south provincialism seen in Late Cretaceous and Paleocene terrestrial faunas (see Weil, 1999 and Clemens, 2001 for summaries), it seems reasonable to infer that Prochetodon had a northern origin and may have been restricted to the more northern province. Prochetodon joins a growing, documented number of "progressive" mammalian taxa first appearing at northern latitudes prior to their first appearances in the more southern latitudes of the United States. Prior to this study, the earliest ostensible occurrence of Prochetodon was from late middle Tiffanian (Ti4) sediments in North Dakota (Judson locality; Holtzman, 1978; Krause, 1987b); the discovery of Pro. speirsae from the earliest Tiffanian of Alberta predates this occurrence by roughly one million years (Lofgren et al., 2004). Other examples of abruptly appearing, progressive mammals include the multituberculates Parectypodus Jepsen, 1930 (see Storer, 1991), Catopsalis Cope, 1882 (see Johnston and Fox, 1984; Fox, 1989), and Microcosmodontidae (Holtzman and Wolberg, 1977) (see Fox, 1989, 2005), the condylarths Baioconodon Gazin, 1941 and Mimatuta Van Valen, 1978 (see Johnston and Fox, 1984; Fox, 1989), and the recently reported stylinodontid taeniodont Schowalteria Fox and Naylor, 2003, all traditionally considered of "Paleocene-aspect", but occurring in the Late Cretaceous of Alberta and Saskatchewan. Importantly, these progressive elements appear abruptly, with no recognizable antecedents, suggesting immigration from as yet unsampled habitats (Fox, 2005). As discussed by Fox (2005) and Weil (1999a-b), the poorly sampled Cordilleran region may be a source area for many of these progressive immigrant taxa, possibly comprising higher altitude and/or basin margin faunas (Gunnell and Bartels, 2001) currently not yet known from the sedimentary record.

Suborder uncertain

Family MICROCOSMODONTIDAE (Holtzman and Wolberg, 1977)

Genus ALLOCOSMODON Fox, 2005

Microcosmodon: HOLTZMAN and WOLBERG, 1977, p. 6 (in part).
Allocosmodon FOX, 2005, p. 55.

Type and only species.—Allocosmodon woodi (Holtzman and Wolberg, 1977).

ALLOCOSMODON WOODI (Holtzman and Wolberg, 1977)
Figures 3.15.11-3.15.19, Table 3.14

Microcosmodon woodi HOLTZMAN and WOLBERG, 1977, p.6.
Allocosmodon woodi Fox, 2005, p. 56.

Holotype.—MCZ 19963, isolated right p4 (Holtzman and Wolberg, 1977, p. 6, figs 2.1-2.8). New Anthill locality (anthill 'L'), Shotgun Member, Fort Union Formation of Wyoming, late Paleocene (earliest Tiffanian, Ti1, Plesiadapis praecursor/P. anceps Interval Zone (Ti1) of Lofgren et al., 2004).

Material examined.—From Joffre Bridge Road Cut lower level: UALVP 46363, M1.

From DW-2: UALVP 46355-58, M1 (total: 4); UALVP 46359, p4; UALVP 46360-62, m1 (total: 3).

Age and occurrence.—Earliest Tiffanian (Plesiadapis praecursor/P. anceps Lineage Zone, Ti1, late Paleocene) to early middle Tiffanian (Plesiadapis rex/P. churchilli Lineage Zone, Ti3, late Paleocene) of the Western Interior of North America.

Description.—Upper dentition: Upper molars: M1: Cusp formula 6-7:7-8:5-7 (mode=7:8:5; N=5). The referred M1s add to the material described by Fox (2005) [only two M1s were referred to Allocosmodon woodi by Fox (2005)]. The crown of M1 is teardrop-shaped in occlusal aspect, with a transversely truncated anterior and broadly rounded posterior margin (Fig. 3.15.13). The tooth is more transverse relative to its length compared to homologous teeth of ptilodontoids, and proportionately shorter with stouter cusps. A large interdental facet occurs on the anterior rim of the crown, marking the position where the anterior part of the tooth met the posterior margin of P4. The

crown is slightly concave ventrally and bears three parallel rows of cusps separated from one another by wide intercusp valleys; the external and middle cusp rows may converge slightly at the anterior margin of the crown, or they may remain parallel. Deep, horizontal wear striae occur in the intercusp valleys. The cusps of the external row are well developed, and can be connected to each other by high crests; the ultimate external cusp is lower and more poorly developed, and is often reduced by wear to a ridge or crest connected to the base of the ultimate cusp in the middle row. The external cusps are conical, especially anteriorly, and their external sides are convex, while their internal sides are virtually flat. Deep vertical grooves are present on the valley-facing surfaces of the external cusps. The cusps of the middle row increase in size posteriorly, although their apices remain subequal in height (the differences in height owe more to the concavity of the crown, such that anterior and posterior cusps are generally higher than those occurring in the middle of the row). The cusps are subcrescentic and their apices bend anteriorly in unworn specimens, but are more nearly erect after extended wear. Vertical grooves can be present on the internal and external sides of the cusps. The internal cusp row is convex lingually and ends abruptly at the third or fourth cusp of the middle row; the cusps are labiolingually compressed and are often reduced by wear to a low ridge. UALVP 46355 preserves three accessory roots between the anterior and posterior roots, similar to descriptions of M1 of A. woodi (="Microcosmodon" woodi) by Holtzman and Wolberg (1977) from the early middle Tiffanian Brisbane locality of North Dakota.

Lower dentition (Figs. 3.15.14-3.15.19): Lower premolars: p4: The crown of p4 is long and low, slopes lingually, and bears six robust serrations connected to one another by a sharp keel (Figs. 3.15.14-3.15.16). The labial side of the crown is virtually flat, whereas the lingual side is swollen and convex. The exodaenodont lobe is long, shallow, and poorly differentiated ventrally; the posterolabial shelf is well developed and deeply pitted. A broad facet on the posterolabial margin of the crown marks the area of contact between p4 and m1. The leading edge of the serrated crest extends steeply posterodorsally from the top of the deeply notched anterobasal concavity to the first serration; the leading edge bends at its midpoint, becoming weakly concave dorsally. The apogee occurs at the second serration. The first serration (anterior serration of Fox,

2005) occurs midway between the dorsal peak of the anterobasal concavity and the second serration, and is set off slightly lingually from the anteroposterior axis of the crown. The labial surface of the first serration is flat, while its lingual surface is concave and the serration appears swollen in occlusal aspect. The first serration bears two strong ridges, the more anterior of which descends the anterior face of the crown to a point above the dorsal peak of the anterobasal concavity, forming a sharp keel. The second ridge extends ventrally a short distance down the lingual face of the crown, and marks the anterior limit of a deep pocket between the first and second serrations; a ridge descending from below the second serration delimits the posterior margin of the pocket. The remaining serrations are well developed and coarse, and increase in absolute height (i.e., from base to apex) to the ultimate serration, which is both smaller and lower. Weak, anteroventrally oriented labial ridges are developed below the second through fifth serrations; coarser lingual ridges are developed below the second through fourth serrations. The anterior root is both broader and shorter than the posterior root, and a small lingual accessory root is present.

Lower molars: m1: Cusp formula 8:5 (N=3). The crown of m1 is subrectangular in occlusal aspect, and bears two parallel rows of cusps that converge anteriorly (Fig. 15.19). A broad interdental facet occurs on the anterior face, marking the point of contact with p4; the posterior margin is truncated posterolabially-anterolingually. The crown is slightly convex dorsally, although not to the same degree as on m1 of Microcosmodon (Fox, 2005). The bases of the cusps are closely approximated, and the intercusp valley is narrow. The cusps of the external row lean posteriorly and increase in both height and width to the fourth cusp, while the remaining cusps are more nearly equal in height. The bases of the cusps posterior to the fourth cusp remain subequal in width, but become anteroposteriorly narrower; a well-developed ridge originating from the apex of the ultimate external cusp descends lingually to the base of the ultimate lingual cusp, forming the posterolabial margin of the crown. The first, or first and second external cusp is conical, while the remaining cusps are subpyramidal to subcrescentic. Shallow vertical grooves can occur on the labial side of the posterior labial cusps. The internal cusps are taller than those of the labial row, lean posteriorly, and have deep vertical grooves on their valley-facing sides. The first internal cusp is small and subconical, and its apex is

confluent with a short crest that extends anterolabially to the intercusp valley; the remaining cusps are subcrescentic and increase in height to the third cusp where they remain subequal in height. The ultimate lingual cusp is the largest in the row, and the sigmoid notch (Krause, 1977; Weil, 1998; Fox, 2005) is well developed and can bear small cuspules. Well-developed horizontal wear striae occur on the valley-facing surface of both cusp rows.

Discussion.—The few specimens described here document additional dental variation in A. woodi, but otherwise adds little in the way of new information (see Fox, 2005, for a thorough analysis of Allocosmodon and the Microcosmodontidae). DW-2 is currently the only locality at which Allocosmodon and Microcosmodon occur sympatrically, and one of only a handful of localities at which more than one microcosmodontid taxon has been documented.

3.3 Conclusions

Multituberculate Diversity in the Paleocene of Alberta

Multituberculates constitute nearly one third of the taxa in the Blindman River local fauna and are second only to "insectivorans" in number of specimens. The multituberculates are taxonomically rich, with fifteen species distributed among eight genera, an unusually high number for middle Tiffanian local faunas (e.g., compare with Holtzman, 1978; Wolberg, 1979; Rose, 1981a-b; Gunnell, 1994). Neoplagiaulacids are the most common multituberculates in terms of number of species and specimens, with Neoplagiaulax serrator representing 28 percent of the minimum number of individuals. Ptilodontids are generally uncommon, the exception being Ptilodus "cedrus", representing 14 percent of the minimum number of individuals. Many multituberculate species in the Blindman River local fauna are long-ranging, both temporally and geographically (e.g., Mesodma pygmaea), whereas others have been documented at only a handful of other localities (e.g., Mimetodon churchilli).

Neoplagiaulacid multituberculates are well represented in latest Torrejonian and earliest Tiffanian local faunas from Western Canada (Krause, 1977; Youzwyshyn, 1988;

Fox, 1990; Scott, 2003a-b), and from near-contemporaneous assemblages in the Western Interior of the United States (Rose, 1981a-b; Krause and Maas, 1990), but in many cases are known only from isolated teeth or incomplete gnathic remains. The articulated and associated specimens from the Blindman River localities demonstrate that neoplagiaulacid teeth, especially the molars and to a lesser extent P4, are morphologically conservative among taxa, differing only in very minor details across species and even genera: for example, the upper molars of N. serrator are virtually identical to those of N. hunteri from Roche Percée (Krause, 1977), differing only in their slightly smaller size on average; to confound matters further, the upper molars of N. serrator closely approximate the size, occlusal outline, and cusp count of upper molars of Ectypodus sp., cf. E. powelli, another neoplagiaulacid taxon known from the Blindman River faunas. Molars of N. serrator found without the benefit of articulated fourth premolars could have been reasonably referred to any of these taxa. Neoplagiaulacid molar morphology is so similar within and among taxa that even recent techniques used either to discriminate multituberculate taxa by molar morphology alone, or include molar characters in phylogenetic analyses have proven ineffective (e.g., Goto and Weil, 1997; Weil, 1998; Weil, 1999a): for example, the number of cusps per millimeter of the internal row of M1 (Weil, 1998) of N. serrator and N. cimolodontoides would necessarily be scored the same (as would that of the microcosmodontid Allocosmodon woodi, see Fox, 2005 for a critique of this character), despite there being notable differences in other features of the crown. Although difficulties such as these have been well documented (Clemens, 1964; Lillegraven, 1969; Novacek and Clemens, 1977; and Goto and Weil, 1997 for difficulties distinguishing molars of Lancian species of Mesodma; Krause, 1982a for similar difficulties in distinguishing molars of Ectypodus tardus from those of Parectypodus lunatus Krause, 1982a), the Blindman River specimens provide an additional troubling caution in that P4, long considered a diagnostic tooth for many neoplagiaulacids (see e.g., Sloan, 1981), may be difficult to refer to taxa without associated p4's. For example, P4 of N. paskapooensis is similar to that of N. hazeni (as are the molars), yet the two taxa differ widely with respect to p4 morphology. These results are both illuminating and cautionary, especially since many neoplagiaulacid samples consist almost entirely of

isolated teeth, and further emphasize the importance of p4 in multituberculate systematics (Novacek and Clemens, 1977; Kielan-Jaworowska and Hurum, 2001).

The three new species of Neoplagiaulax documented in this chapter are difficult to separate solely on the basis of quantitative characters (the dentitions of all three approximate one another in linear dimensions and meristic attributes, with significant overlap in both, see Figs. 3.17, 3.18), yet they can be distinguished, both from each other and from other congeners, on qualitative differences in coronal structure, particularly that of p4 (Fig. 3.18). The p4s of N. serrator, N. paskapooensis, and N. cimolodontoides differ from one another in profile, position of the first serration, crown height, and shape of the exodaenodont lobe; even more importantly, the interspecific differences in the coronal structure of p4 are also reflected in the morphology of teeth at other loci, both in upper and lower jaws, and in the mandibular anatomy (see Table 3.15 for summary), differences not expected in allopatric populations of a single species. The new species of Neoplagiaulax are of further interest in that the Blindman River localities document the presence of three, and possibly five species of the genus (N. serrator, N. paskapooensis, N. cimolodontoides, N. sp., cf. N. hazeni, N. sp., cf. N. hunteri), a large number from a single locality. Occurrences of syntopic species are well known in both extant (e.g., Rickart and Heany, 2001) and extinct (e.g., Clemens, 1966) faunas; among Paleocene local faunas, closely related syntopic multituberculate species have been recorded at a number of localities (e.g., Holtzman, 1978; Vianey-Liaud, 1986; Krause and Maas, 1990), with perhaps the most exceptional being the Cochrane 2 locality of Alberta: four species of the ptilodontid Ptilodus, along with species of Baiotomeus and Prochetodon have been documented, the greatest ptilodontid diversity known from a single locality (Youzwyshyn, 1988; Scott et al., 2002). Multituberculates have been likened to small rodents in habitus (Simpson, 1937b; Krause, 1986), and it is possible that they partitioned microhabitats and resources in much the same way as their extant analogues; in light of the great diversity seen among living rodents, the presence of multiple species of multituberculates in a more or less restricted geographical area seems less anomalous (and see Simpson, 1937b). The three new species of Neoplagiaulax are also known from the Hand Hills west upper level and Birchwood localities, and two (N. serrator and N. paskapooensis) from the Police Point locality of southeastern Alberta, indicating the

distribution of these taxa was widespread in central and southern Alberta during the latter part of the Tiffanian.

Despite the recognition of the new species of Neoplagiaulax from northern North America, none appears to be more closely related to European congeners than does any other North American form. Although the p4 of N. serrator and N. paskapooensis bears superficial similarity in structure to that of N. eocaenus (although see earlier in this chapter for discussion of the possible composite status of N. eocaenus) and N. copei, respectively (as does that of N. hunteri and N. hazeni), the differences in coronal structure between them are greater than that between N. serrator, N. paskapooensis, and other North American species of Neoplagiaulax (i.e., the new species of Neoplagiaulax appear to be more closely related to North American species of Neoplagiaulax, and do not share a more recent common ancestor with European Neoplagiaulax); for the present it seems reasonable to conclude that the similarities between the North American and European species of Neoplagiaulax are the result of high levels of parallelism within endemically evolving lineages, as Vianey-Liaud (1986) had suggested. It should be noted, however, that both Neoplagiaulax and Neoplagiaulacidae were found paraphyletic in recent phylogenetic studies (Simmons, 1993; Rougier et al., 1997; Weil, 1999a), and comparisons of the North American species of Neoplagiaulax with those from Western Europe suggest that the genus may represent a heterogeneous grouping of unrelated neoplagiaulacids (see Scott and Krause, 2006). Given the significance of neoplagiaulacid multituberculates in biogeographic and paleoecological reconstructions, a detailed systematic revision of the group would undoubtedly clarify many of these issues.

3.4 Literature Cited

AMEGHINO, F. 1890. Los plagiaulacideos argentinos y sus relaciones zoológicas, geológicas, y geográficas. Boletín des Instituto geográfico argentino, 11:143-201.

ANTHONY, M. R. L. and M. C. MAAS. 1990. Biogeographic provinciality in North American Paleocene mammalian faunas. Journal of Vertebrate Paleontology, 10 supplement to no.3:21A.

ARCHIBALD, J. D. 1982. A study of Mammalia and geology across the Cretaceous-Tertiary boundary in Garfield County, Montana. University of California Publications in Geological Science, 122:11-286.

CLEMENS, W. A., JR. 1964. Fossil mammals of the type Lance Formation, Wyoming: Part I. Introduction and Multituberculata. University of California Publications in Geological Sciences, 48:1-105. [dated 1963]

CLEMENS, W. A., JR. 1966. Fossil mammals of the type Lance Formation, Wyoming: Part II. Marsupialia. University of California Publications in Geological Sciences, 66:1-122.

CLEMENS, W. A. 2001. Patterns of mammalian evolution across the Cretaceous-Tertiary boundary. Mitteilungen des Museums für Naturkunde Berlin, Zoologische Reihe, 77:175-191.

CLEMENS, W. A., and Z. KIELAN-JAWOROWSKA. 1979. Multituberculata, pp. 99-149. In J. A. LILLEGRAVEN, Z. KIELAN-JAWOROWSKA, and W. A. CLEMENS (eds.), Mesozoic mammals: the first two-thirds of mammalian history. University of California Press, Berkeley, California.

COPE, E. D. 1881. Eocene Plagiaulacidae. American Naturalist, 15:921-922.

COPE, E. D. 1882. Mammalia in the Laramie Formation. American Naturalist, 16:830-831.

COPE, E. D. 1884. The Tertiary Marsupialia. American Naturalist, 18:686-697.

COPE, E. D. 1887. The marsupial genus Chirox. American Naturalist, 21:566-567.

DORR, J. A., JR. 1952. Early Cenozoic stratigraphy and vertebrate paleontology of the Hoback Basin, Wyoming. Bulletin of the Geological Society of America, 63:59-94.

DOUGLASS, E. 1908. Vertebrate fossils from the Fort Union beds. Annals of Carnegie Museum, 5:11-26.

FOX, R. C. 1971. Early Campanian multituberculates (Mammalia: Allotheria) from the Upper Milk River Formation, Alberta. Canadian Journal of Earth Sciences, 8:916-938.

FOX, R. C. 1989. The Wounded Knee local fauna and mammalian evolution near the Cretaceous-Tertiary boundary, Saskatchewan, Canada. Palaeontographica Abteilung A, 208:11-59.

FOX, R. C. 1990. The succession of Paleocene mammals in western Canada, pp. 51-70. In T. M. BOWN and K. D. ROSE (eds.), Dawn of the Age of Mammals in the Northern Part of the Rocky Mountain Interior, North America. Geological Society of America Special Paper, 243.

FOX, R. C. 1997. Late Cretaceous and Paleocene mammals, Cypress Hills Region, Saskatchewan, and mammalian evolution across the Cretaceous-Tertiary boundary, pp. 70-85. In L. M. MCANALLY (ed.), Upper Cretaceous and Tertiary Stratigraphy and Paleontology of southern Saskatchewan. Canadian Paleontology Field Conference, Field Trip Guidebook 6, Geological Association of Canada, St. John's, Newfoundland.

FOX, R. C. 2002. The oldest Cenozoic mammal? Journal of Vertebrate Paleontology, 22:456-459.

FOX, R. C. 2005. Microcosmodontid multituberculates (Allotheria, Mammalia) from the Paleocene and Late Cretaceous of western Canada. Palaeontographica Canadiana, 23:1-109.

FOX, R. C., and B. G. NAYLOR. 2003. A taeniodont from the Late Cretaceous of Alberta, Canada. Neues Jahrbuch für Geologie und Paläontologie-Abhandlungen, 229:393-420.

GAMBARYAN, P. P., and Z. KIELAN-JAWOROWSKA. 1995. Masticatory musculature of Asian taeniolabidoid multituberculate mammals. Acta Palaeontologica Polonica, 40:45-108.

GAZIN, C. L. 1941. Paleocene mammals from the Denver Basin, Colorado. Washington Academy of Sciences Journal, 31:289-295.

GOTO, S., and A. WEIL. 1997. No species differentiation in Lance Mesodma (Multituberculata, Mammalia) using variation in molar morphology. Journal of Vertebrate Paleontology, 17, supplement to no. 3:50A.

GREENWALD, N. S. 1988. Patterns of tooth eruption and replacement in multituberculate mammals. Journal of Vertebrate Paleontology, 8:265-277.

GUNNELL, G. F. 1994. Paleocene mammals and faunal analysis of the Chappo Type locality (Tiffanian), Green River Basin, Wyoming. Journal of Vertebrate Paleontology, 14:81-104.

GUNNELL, G. F., and W. S. BARTELS. 2001. Basin margins, biodiversity, evolutionary innovation, and the origin of new taxa, pp. 404-432. In G. F. GUNNELL (ed.), Eocene Biodiversity: Unusual Occurrences and Rarely Sampled Habitats. Kluwer Academic/Plenum Publishers, New York.

HIGGINS, P. 2003. A new species of Paleocene multituberculate (Mammalia: Allotheria) from the Hanna Basin, south-central Wyoming. Journal of Vertebrate Paleontology, 23:468-470.

HOLTZMAN, R. C. 1978. Late Paleocene mammals of the Tongue River Formation, western North Dakota. Report of Investigation, North Dakota Geological Survey, 65:1-88.

HOLTZMAN, R. C. and D. L. WOLBERG. 1977. The Microcosmodontinae and Microcosmodon woodi, new multituberculate taxa (Mammalia) from the Late Paleocene of North America. Scientific Publications of the Science Museum of Minnesota, New Series, 4:1-13.

HOPSON, J. A., Z. KIELAN-JAWOROWSKA, and E. F. ALLIN. 1989. The cryptic jugal of multituberculates. Journal of Vertebrate Paleontology, 9:201-209.

HUNTER, J. P. 1999. The radiation of Paleocene mammals with the demise of the dinosaurs: evidence from southwestern North Dakota. Proceedings of the North Dakota Academy of Science, 53:141-144.

JEPSEN, G. L. 1930. New vertebrate fossils from the lower Eocene of the Bighorn Basin, Wyoming. Proceedings of the American Philosophical Society, 69:117-131.

JEPSEN, G. L. 1940. Paleocene faunas of the Polecat Bench Formation, Wyoming. Proceedings of the American Philosophical Society, 83:217-340.

JOHNSTON, P. A., and R. C. FOX. 1984. Paleocene and Late Cretaceous mammals from Saskatchewan, Canada. Palaeontographica (A), 186:163-222.

KIELAN-JAWOROWSKA, Z. 1970. Results of the Polish-Mongolian palaeontological expeditions—Part II. New Upper Cretaceous multituberculate genera from Bayn Dzak, Gobi Desert. Palaeontologia Polonica, 21:35-49. [dated 1969]

KIELAN-JAWOROWSKA, Z. 1974. Results of the Polish-Mongolian Palaeontological Expeditions—Part V. Multituberculate succession in the Late Cretaceous of the Gobi Desert (Mongolia). Palaeontologia Polonica, 30:23-44.

KIELAN-JAWOROWSKA, Z., and J. H. HURUM. 1997. Djadochtatheria—a new suborder of multituberculate mammals. Acta Palaeontologica Polonica, 42:201-242.

KIELAN-JAWOROWSKA, Z., and J. H. HURUM. 2001. Phylogeny and systematics of multituberculate mammals. Palaeontology, 44:389-429.

KIHM, A. J., and J. H. HARTMAN. 2004. A reevaluation of the Brisbane and Judson local faunas (late Paleocene) of North Dakota, pp. 97-108. In M. R. DAWSON and J. A. LILLEGRAVEN (eds.), Fanfare for an uncommon paleontologist: papers in honor of Malcolm C. McKenna. Bulletin of Carnegie Museum of Natural History, 34.

KRAUSE, D. W. 1977. Paleocene multituberculates (Mammalia) of the Roche Percée local fauna, Ravenscrag Formation, Saskatchewan, Canada. Palaeontographica Abteilung A, 186:1-36.

KRAUSE, D. W. 1980. Multituberculates from the Clarkforkian Land-Mammal Age, late Paleocene-early Eocene, of western North America. Journal of Paleontology, 54:1163-1183.

KRAUSE, D. W. 1982a. Multituberculates from the Wasatchian Land-Mammal Age, early Eocene, of western North America. Journal of Paleontology, 56: 271-294.

KRAUSE, D. W. 1982b. Evolutionary history and paleobiology of early Cenozoic Multituberculata (Mammalia), with emphasis on the family Ptilodontidae. Unpublished Ph. D. dissertation, The University of Michigan, Ann Arbor, 575 pp.

KRAUSE, D. W. 1982c. Jaw movement, dental function, and diet in the Paleocene multituberculate Ptilodus. Paleobiology, 8:265-281.

KRAUSE, D. W. 1986. Competitive exclusion and taxonomic displacement in the fossil record; the case of rodents and multituberculates in North America. University of Wyoming Contributions to Geology Special Paper, 3:95-117.

KRAUSE, D. W. 1987a. Baiotomeus, a new ptilodontid multituberculate (Mammalia) from the middle Paleocene of western North America. Journal of Paleontology, 61:595-603.

KRAUSE, D. W. 1987b. Systematic revision of the genus Prochetodon (Ptilodontidae, Multituberculata) from the late Paleocene and early Eocene of western North America. Contributions from the Museum of Paleontology, The University of Michigan, 27:221-236.

KRAUSE, D. W., and P. D. GINGERICH. 1983. Mammalian fauna from Douglass Quarry, earliest Tiffanian (late Paleocene) of the eastern Crazy Mountain Basin, Montana. Contributions from the Museum of Paleontology, The University of Michigan, 26:157-196.

KRAUSE, D. W., and F. A. JENKINS, JR. 1983. The postcranial skeleton of North American multituberculates. Bulletin of the Museum of Comparative Zoology, 150: 199-246.

KRAUSE, D. W., and M. C. MAAS. 1990. The biogeographic origins of late Paleocene-early Eocene mammalian immigrants to the Western Interior of North America, pp.71-105. In T. M. BOWN and K. D. ROSE (eds.), Dawn of the Age of Mammals in the Northern Part of the Rocky Mountain Interior, North America. Geological Society of America Special Paper, 243.

KRISHTALKA, L. 1973. Late Paleocene mammals from the Cypress Hills, Alberta. Special Publications of the Museum, Texas Tech University, 2:1-77.

KRISHTALKA, L. 1984. Early Eocene multituberculates (Mammalia: Allotheria) from the Bighorn Basin, Wyoming. Carnegie Museum of Natural History Special Publications, 9:21-27.

KÜHNE, W. G. 1969. A multituberculate from the Eocene of the London Basin. Proceedings of the Geological Society of London, 1658:199-202.

LEMOINE, V. 1880. Communication sur les Ossements fossiles des terrains tertiaires inférieurs. Association Française pour l'Avancement des Sciences, Reims:3-40.

LEMOINE, V. 1882. Sur deux Plagiaulax tertiaires, recueillis aux environs de Reims. Comptes Rendus de l'Academie des Sciences, Paris, 95:1009-1011.

LEMOINE, V. 1885. Étude sur quelques Mammifères de petite taille de la faune cernaysienne des environs de Reims. Bulletin de la Société Géologique de France, 3e série, 13:203-217.

LILLEGRAVEN, J. A. 1969. Latest Cretaceous mammals of upper part of the Edmonton Formation of Alberta, Canada, and a review of marsupial-placental dichotomy in mammalian evolution. The University of Kansas Paleontological Contributions, 50 (Vertebrata 12):1-122.

LINNAEUS, C. 1758. Systema naturae per regna tria naturae, secundum classes, ordines, genera, species cum characteribus, differentiis, synonymis, locis. Tomus I: Regnum animale. Editio decima, reformata. Laurentii Salvii, Stockholm [Facsimile reprinted in 1956 by the British Museum of Natural History].

LOFGREN, D. L., J. A. LILLEGRAVEN, W. A. CLEMENS, P. D. GINGERICH, and T. E. WILLIAMSON. 2004. Paleocene biochronology: The Puercan through Clarkforkian Land Mammal Ages, pp. 43-105. In M. O. WOODBURNE (ed.), Cenozoic Mammals of North America: Geochronology and Biostratigraphy, Columbia University Press, New York.

MACDONALD, T. E. 1996. Late Paleocene (Tiffanian) mammal-bearing localities in superposition, from near Drumheller, Alberta. Unpublished M.Sc. thesis, University of Alberta, Edmonton, 248 pp.

MARSH, O. C. 1880. Notice of Jurassic mammals representing two new orders. American Journal of Science, 11:425-428.

MARSH, O. C. 1889. Discovery of Cretaceous Mammalia. American Journal of Science, 38:81-92.

MATTHEW, W. D., and W. GRANGER. 1921. New genera of Paleocene mammals. American Museum Novitates, 13:1-7.

MATTHEW, W. D., and W. GRANGER. 1925. Fauna and correlation of the Gashato Formation of Mongolia. American Museum Novitates, 189:1-12.

MCKENNA, M. C. 1960. Fossil Mammalia from the early Wasatchian Four Mile fauna Eocene of northwest Colorado. University of California Publications in Geological Sciences, 37:1-130.

MCKENNA, M. C. 1975. Toward a phylogenetic classification of the Mammalia, pp. 21-46. In W. P. LUCKETT and F. S. SZALAY (eds.), Phylogeny of the Primates. Plenum Press, New York.

McKENNA, M. C., and S. K. BELL. 1997. Classification of Mammals Above the Species Level. Columbia University Press, New York.

MIAO, D. 1988. Skull morphology of Lambdopsalis bulla (Mammalia, Multituberculata) and its implications to mammalian evolution. Contributions to Geology, University of Wyoming Special Paper, 4:1-104.

MIDDLETON, M. D., and E. W. DEWAR. 2004. New mammals from the early Paleocene Littleton fauna (Denver Formation, Colorado), pp. 59-80. In S. G. LUCAS, K. E. ZEIGLER, and P. E. KONDRASHOV (eds.), Paleogene Mammals. Bulletin of the New Mexico Museum of Natural History and Science, 26.

NOVACEK, M., and W. A. CLEMENS. 1977. Aspects of intrageneric variation and evolution of Mesodma (Multituberculata, Mammalia). Journal of Paleontology, 51:701-717.

RICKART, E. A., and L. R. HEANY. 2001. Shrews of the La Sal Mountains, southeastern Utah. Western North American Naturalist, 61:103-108.

RIGBY, J. K., JR. 1980. Swain Quarry of the Fort Union Formation, middle Paleocene (Torrejonian), Carbon County, Wyoming: geologic setting and mammalian fauna. Evolutionary Monographs, 3:1-179.

ROSE, K. D. 1981a. The Clarkforkian Land Mammal Age and mammalian faunal composition across the Paleocene-Eocene boundary. The University of Michigan Papers on Paleontology, 26:1-197.

ROSE, K. D. 1981b. Composition and species diversity in Paleocene and Eocene mammal assemblages; an empirical study. Journal of Vertebrate Paleontology, 1:367-388.

ROUGIER, G. W., M. J. NOVACEK, and D. DASHZEVEG. 1997. A new multituberculate from the Late Cretaceous locality Ukhaa Tolgod, Mongolia. Considerations on multituberculate interrelationships. American Museum Novitates, 3191:1-26.

RUSSELL, D. E. 1964. Les Mammifères paléocènes d'Europe. Mémoirs du Museum National d'Histoire Naturelle (France), Nouvelle Série, Série C, 13:1-321.

RUSSELL, L. S. 1929. Paleocene vertebrates from Alberta. American Journal of Science, 17:162-178.

RUSSELL, L. S. 1932. New data on the Paleocene mammals from Alberta, Canada. Journal of Mammalogy, 13:38-54.

RUSSELL, L. S. 1958. Paleocene mammal teeth from Alberta. Bulletin of the National Museum of Canada, 147:96-103.

RUSSELL, L. S. 1967. Paleontology of the Swan Hills area, north-central Alberta. Royal Ontario Museum Life Sciences Contributions, 71:1-31.

SAHNI, A. 1972. The vertebrate fauna of the Judith River Formation, Montana. Bulletin of the American Museum of Natural History, 147:321-412.

SAVAGE, D.E., and D. E. RUSSELL. 1983. Mammalian Paleofaunas of the World. Addison-Wesley Publishing Company, London, 432 pp.

SCHIEBOUT, J. A. 1974. Vertebrate paleontology and paleoecology of Paleocene Black Hills Formation, Big Bend National Park, Texas. Bulletin of the Texas Memorial Museum, 24:1-88.

SCOTT, C. S. 2003a. Late Torrejonian (middle Paleocene) mammals from south central Alberta, Canada. Journal of Paleontology, 77:745-768.

SCOTT, C. S. 2003b. Multituberculate mammals from Western Canada. Proceedings of the 13th Annual Canadian Paleontology Conference, 1:37-38.

SCOTT, C. S., and R. C. FOX. 2005. Windows on the evolution of Picrodus (Plesiadapiformes, Primates): morphology and relationships of a species complex from the Paleocene of Alberta. Journal of Paleontology, 79:635-657.

SCOTT, C. S., and D. W. KRAUSE. 2006. Multituberculates (Mammalia, Allotheria) from the earliest Tiffanian (Late Paleocene) Douglass Quarry, Eastern Crazy Mountains Basin, Montana. Contributions from the Museum of Paleontology, The University of Michigan, 31:211-243.

SCOTT, C. S., R. C. FOX, and G. P. YOUZWYSHYN. 2002. New earliest Tiffanian (late Paleocene) mammals from Cochrane 2, southwestern Alberta, Canada. Acta Palaeontologica Polonica, 47:691-704.

SECORD, R. 1997. Paleocene mammalian biostratigraphy of the Carbon Basin, southeastern Wyoming, and age constraints on local phases of tectonism. Rocky Mountain Geology, 33:119-154.

SECORD, R. 2004. Late Paleocene biostratigraphy, isotope stratigraphy, and mammalian systematics of the northern Bighorn Basin, Wyoming. Unpublished Ph. D. dissertation, The University of Michigan, Ann Arbor, 532 pp.

SIMMONS, N. B. 1993. Phylogeny of Multituberculata, pp.146-164. In F. S. SZALAY, M. J. NOVACEK, and M. C. MCKENNA (eds.), Mammal Phylogeny: Mesozoic Differentiation, Multituberculates, Monotremes, Early Therians and Marsupials. Springer-Verlag, New York.

SIMPSON, G. G. 1925. A Mesozoic mammal skull from Mongolia. American Museum Novitates, 201:1-11.

SIMPSON, G. G. 1926. Mesozoic Mammalia: IV. The multituberculates as living animals. American Journal of Science, 11:228-250.

SIMPSON, G. G. 1935. New Paleocene mammals from the Fort Union of Montana. Proceedings of the United States National Museum, 83:221-244.

SIMPSON, G. G. 1936. A new fauna from the Fort Union of Montana. American Museum Novitates, 873:1-27.

SIMPSON, G. G. 1937a. Skull structure of the Multituberculata. Bulletin of the American Museum of Natural History, 73:727-763.

SIMPSON, G. G. 1937b. The Fort Union of the Crazy Mountain Field, Montana and its mammalian faunas. Bulletin of the United States Museum, 169:1-287.

SLOAN, R. E. 1966. Paleontology and geology of the Badwater Creek area, central Wyoming, part 2. The Badwater Multituberculata. Annals of Carnegie Museum, 38:309-315.

SLOAN, R. E. 1979. Multituberculata, pp. 492-498. In R. W. FAIRBRIDGE and D. JABLONSKI (eds.), The Encyclopedia of Paleontology. Dowden, Hutchinson, and Ross, Inc., Stroudsburg, Pennsylvania.

SLOAN, R. E. 1981. Systematics of Paleocene multituberculates from the San Juan Basin, New Mexico, pp. 127-160. In S. G. LUCAS, J. K. RIGBY, JR., and B. KUES (eds.), Advances in San Juan Basin Paleontology. University of New Mexico Press, Albuquerque, New Mexico.

SLOAN, R. E. 1987. Paleocene and latest Cretaceous mammals, rates of sedimentation and evolution, pp. 165-200. In J. E. FASSETT and J. K. RIGBY, JR. (eds.), The Cretaceous-Tertiary Boundary in the San Juan and Raton Basins, New Mexico and Colorado. Geological Society of America Special Paper, 209.

SLOAN, R. E., and L. VAN VALEN. 1965. Cretaceous mammals from Montana. Science, 148:220-227.

STORER, J. E. 1991. The mammals of the Gryde local fauna, Frenchman Formation (Maastrichtian: Lancian), Saskatchewan. Journal of Vertebrate Paleontology, 11:350-369.

SZALAY, F. S. 1965. First evidence of tooth replacement in the Subclass Allotheria (Mammalia). American Museum Novitates, 2226:1-12.

TONG, Y., and J. WANG. 1994. A new neoplagiaulacid multituberculate (Mammalia) from the lower Eocene of Wutu Basin, Shandong. Vertebrata PalAsiatica, 32:275-284 (In Chinese, English summary).

TURNBULL, W. D. 1970. Mammalian masticatory apparatus. Fieldiana: Geology, 18:147-356.

VAN VALEN, L. 1978. The beginning of the Age of Mammals. Evolutionary Theory, 4:45-80.

VAN VALEN, L. and R. E. SLOAN. 1966. The extinction of the multituberculates. Systematic Zoology, 15:261-278.

VIANEY-LIAUD, M. 1986. Les Multituberculés Thanetians de France, et leurs repports avec les Multituberculés Nord-Americains. Palaeontographica (A), 191:85-171.

WALL, C. E., and D. W. KRAUSE. 1992. A biomechanical analysis of the masticatory apparatus of Ptilodus (Multituberculata). Journal of Vertebrate Paleontology, 12:172-187.

WEBB, M. W. 1996. Late Paleocene mammals from near Drayton Valley, Alberta. Unpublished M.Sc. thesis, University of Alberta, Edmonton, 258 pp.

WEIL, A. 1998. A new species of Microcosmodon (Mammalia: Multituberculata) from the Paleocene Tullock Formation of Montana, and an argument for the Microcosmodontinae. PaleoBios, 18:1-15.

WEIL, A. 1999a. Multituberculate phylogeny and mammalian biogeography in the Late Cretaceous and earliest Paleocene Western Interior of North America. Unpublished Ph.D. dissertation, University of California, Berkeley, 243 pp.

WEIL, A. 1999b. Biogeographic provinciality of mammalian faunas in the Late Cretaceous and Early Paleocene Western Interior of North America. Geological Society of America, Abstracts with Programs, 31:472A.

WIBLE, J. R., and G. W. ROUGIER. 2000. Cranial anatomy of Kryptobaatar dashzevegi (Mammalia, Multituberculata), and its bearing on the evolution of mammalian characters. Bulletin of the American Museum of Natural History, 247:1-124.

WILSON, R. W. 1956. A new multituberculate from the Paleocene Torrejon fauna of New Mexico. Transactions of the Kansas Academy of Science, 59:76-84.

WOLBERG, D. L. 1979. Late Paleocene (Tiffanian) mammalian fauna of two localities in eastern Montana. Northwest Geology, 8:83-93.

YOUZWYSHYN, G. P. 1988. Paleocene mammals from near Cochrane, Alberta. Unpublished M.Sc. thesis, University of Alberta, Edmonton, 484 pp.

Table 3.1.—Combined measurements and descriptive statistics for the dentition of Mesodma pygmaea Sloan from the early middle Tiffanian (Ti3) Joffre Bridge Roadcut lower level and DW-2 localities, Paskapoo Formation, Alberta.

Element	P	N	OR	M	SD	CV
P1	L	1	0.7	—	—	—
	W	1	0.5	—	—	—
P2	L	1	0.7	—	—	—
	W	1	0.6	—	—	—
P3	L	1	0.7	—	—	—
	W	1	0.5	—	—	—
P4	L	5	1.7-1.9	1.80	0.10	5.55
	W	5	0.7-0.8	0.72	0.04	5.55
M1	L	6	2.1-2.2	2.18	0.04	1.83
	W	6	1.0-1.1	1.02	0.04	3.92
M2	L	1	0.9	—	—	—
	W	1	1.1	—	—	—
p4	L	4	2.5-2.7	2.60	0.08	3.08
	L1	3	0.3-0.4	0.33	0.06	18.18
	H	3	0·7-0·9	0.80	0.10	12.5
m1	L	3	1.7	1.70	0	0
	W	3	0.7	0.70	0	0
m2	L	6	0.9-1.0	0.95	0.05	5.24
	W	6	0.8-0.9	0.85	0.05	5.88

Table 3.2.—Combined measurements and descriptive statistics for the dentition of ?Mesodma sp. from the early middle Tiffanian (Ti3) DW-1 and DW-2 localities, Paskapoo Formation, Alberta.

Element	P	N	OR	M	SD	CV
p4	L	2	2.5	2.50	0	0
	L1	2	0.3	0.30	0	0
	H	2	0.7	0.70	0	0

Table 3.3.—Measurements and descriptive statistics for the dentition of Mimetodon silberlingi (Simpson) from the early middle Tiffanian (Ti3) DW-1 and DW-2 localities, Paskapoo Formation, Alberta.

Element	P	N	OR	M	SD	CV
P4	L	2	2.3-2·5	2.40	0.14	5.83
	W	2	0.8	0.80	0	0
p4	L	4	2.9-3.4	3.10	0.24	7.74
	L1	4	0.3-0.5	0.43	0.10	23.25
	H	4	1.0-1.1	1.05	0.06	5.71

Table 3.4.—Combined measurements and descriptive statistics for the dentition of Mimetodon churchilli Jepsen from the early middle Tiffanian (Ti3) Joffre Bridge Roadcut upper level and DW-2 localities, Paskapoo Formation, Alberta.

Element	P	N	OR	M	SD	CV
p4	L	3	4.2-4.3	4.27	0.06	1.35
	L1	3	0.5-0.6	0.53	0.06	10.83
	H	3	1.4-1.6	1.53	0.11	7.53
m1	L	1	3.0	—	—	—
	W	1	1.2	—	—	—
m2	L	1	2.1	—	—	—
	W	1	1.1	—	—	—

Table 3.5.—Combined measurements and descriptive statistics for the dentition of Ectypodus elaphus new species from the early middle Tiffanian (Ti3) Joffre Bridge Roadcut lower level, DW-1, and DW-2 localities, Paskapoo Formation, Alberta.

Element	P	N	OR	M	SD	CV
P4	L	5	1.9-2.1	1.98	0.08	4.04
	W	5	0.6-0.7	0.68	0.04	5.88
M1	L	1	2.4	2.40	—	—
	W	1	1.0	1.00	—	—
p4	L	15	2.5-2.8	2.63	0.09	3.42
	L1	13	0.2-0.4	0.28	0.07	25.00
	H	13	0.8-1.1	0.96	0.10	10.42
m1	L	5	1.7-1.9	1.78	0.08	4.49
	W	5	0.70-0.80	0.74	0.05	6.76
m2	L	1	1.0	1.0	—	—
	W	1	0.90	0.90	—	—

Table 3.6.—Combined measurements and descriptive statistics for the dentition of Ectypodus sp., cf. E. powelli from the early middle Tiffanian (Ti3) DW-1 and DW-2 localities, Paskapoo Formation, Alberta.

Element	P	N	OR	M	SD	CV
P4	L	7	2.5-3.1	2.71	0.23	8.49
	W	7	0.9-1.3	1.04	0.15	14.42
M1	L	2	3.2-3.4	3.30	0.14	4.24
	W	2	1.3	1.30	0	0
M2	L	1	1.2	1.20	—	—
	W	1	1.4	1.40	—	—
p4	L	1	2.8	2.80	—	—
	L1	1	0.4	0.40	—	—
	H	1	1.0	1.00	—	—

Table 3.7.—Combined measurements and descriptive statistics for the dentition of Neoplagiaulax serrator new species from the early middle Tiffanian (Ti3) Joffre Bridge Roadcut lower level, DW-2, Hand Hills West upper level, and Birchwood localities, Paskapoo Formation, Alberta, and the late middle Tiffanian (Ti4) Police Point locality, Ravenscrag Formation, Alberta.

Element	P	N	OR	M	SD	CV
P1	L	5	1.2-1.4	1.32	0.09	6.82
	W	5	0.90-1.0	0.96	0.05	5.21
P2	L	6	1.1-1.3	1.23	0.08	6.50
	W	6	1.0-1.1	1.04	0.04	3.85
P3	L	7	1.1-1.3	1.23	0.09	7.32
	W	7	0.80-1.0	0.91	0.09	9.89
P4	L	31	2.8-3.4	3.10	0.14	4.52
	W	31	1.0-1.3	1.17	0.09	7.69
M1	L	11	2.8-3.1	2.91	0.10	3.44
	W	11	1.2-1.4	1.31	0.04	3.05
M2	L	16	1.2-1.5	1.36	0.10	7.35
	W	16	1.1-1.5	1.31	0.10	7.63
p4	L	35	4.1-4.7	4.49	0.16	3.56
	L1	33	0.50-0.80	0.66	0.08	12.12
	H	33	1.4-1.6	1.52	0.08	5.26
m1	L	15	2.2-2.6	2.37	0.10	4.22
	W	15	0.90-1.2	1.03	0.08	7.77
m2	L	22	1.1-1.5	1.35	0.09	6.67
	W	22	1.0-1.3	1.10	0.06	5.45

Table 3.8.—Combined measurements and descriptive statistics for the dentition of Neoplagiaulax paskapooensis new species from the early middle Tiffanian (Ti3) DW-2, Hand Hills West upper level, and Birchwood localities, Paskapoo Formation, Alberta, and the late middle Tiffanian (Ti4) Police Point locality, Ravenscrag Formation, Alberta.

Element	P	N	OR	M	SD	CV
P1	L	2	1.2-1.3	1.25	0.07	5.60
	W	2	1.0	1.00	0	0
P2	L	3	1.2-1.4	1.30	0.12	9.23
	W	3	1.1	1.10	0	0
P3	L	2	1.3-1.4	1.35	0.07	5.19
	W	2	0.9-1.0	0.95	0.07	7.37
P4	L	10	3.3-3.7	3.48	0.13	3.74
	W	10	1.2-1.5	1.35	0.10	7.41
M1	L	6	3.2-3.4	3.33	0.10	3.00
	W	6	1.4-1.7	1.52	0.13	8.55
M2	L	5	1.3-1.6	1.46	0.13	8.90
	W	5	1.3-1.6	1.48	0.13	8.78
p4	L	6	4.7-4.9	4.85	0.08	1.65
	L1	6	0.6-0.9	0.83	0.12	14.46
	H	6	1.7-1.8	1.73	0.05	2.89
m1	L	8	2.4-2.8	2.59	0.15	5.79
	W	8	1.1-1.3	1.15	0.08	6.96
m2	L	2	1.4	0	0	0
	W	2	1.3	0	0	0

Table 3.9.—Combined measurements and descriptive statistics for the dentition of Neoplagiaulax cimolodontoides new species from the early middle Tiffanian (Ti3) DW-2, Mel's Place, and Hand Hills West upper level, Paskapoo Formation, Alberta.

Element	P	N	OR	M	SD	CV
P1	L	3	1.3-1.4	1.38	0.06	4.35
	W	3	0.9-1.0	0.93	0.06	6.45
P2	L	4	1.3-1.4	1.33	0.06	4.51
	W	4	0.8-1.0	0.90	0.08	8.89
P3	L	4	1.2-1.4	1.3	0.08	6.15
	W	4	0.8	0.80	0	0
P4	L	11	2.9-3.5	3.20	0.17	5.31
	W	11	1.1-1.4	1.25	0.09	7.20
M1	L	3	2.5-2.9	2.73	0.21	7.69
	W	3	1.3-1.4	1.33	0.06	4.51
M2	L	1	1.5	1.50	—	—
	W	1	1.3	1.30	—	—
p4	L	15	4.1-4.5	4.27	0.14	3.28
	L1	15	0.80-1.2	1.00	0.10	10.00
	H	15	1.6-1.9	1.79	0.08	4.50
m1	L	7	2.1-2.4	2.24	0.10	4.46
	W	7	1.1	1.10	0	0
m2	L	7	1.2-1.4	1.36	0.08	5.88
	W	7	1.1-1.2	1.14	0.05	4.39

Table 3.10.—Combined measurements and descriptive statistics for the dentition of Neoplagiaulax sp., cf. N. hazeni from the early middle Tiffanian (Ti3) DW-2 and DW-3, Paskapoo Formation, Alberta.

Element	P	N	OR	M	SD	CV
P1	L	1	1.4	—	—	—
	W	1	1.1	—	—	—
P2	L	1	1.4	—	—	—
	W	1	1.1	—	—	—
P3	L	1	1.4	—	—	—
	W	1	0.9	—	—	—
P4	L	1	3.2	—	—	—
	W	1	1.3	—	—	—
M1	L	3	3.5-3.6	3.57	0.06	1.68
	W	3	1.6	1.60	0	0
M2	L	2	1.7-1.8	1.75	0.07	4.00
	W	2	1.5-1.6	1.55	0.07	4.52
p4	L	2	4.8-5.1	4.95	0.21	4.24
	L1	2	0.9-1.2	1.05	0.21	2.00
	H	2	2.1	2.10	0	0
m2	L	1	2.1	—	—	—
	W	1	1.6	—	—	—

Table 3.11.—Combined measurements and descriptive statistics for the dentition of Ptilodus "cedrus" from the early middle Tiffanian (Ti3) DW-1, DW-2, Mel's Place, and Stonley Mammal Site localities, Paskapoo Formation, Alberta.

Element	P	N	OR	M	SD	CV
P1	L	4	2.6-2.9	2.78	0.15	5.40
	W	4	2.0-2.4	2.18	0.17	7.80
P2	L	5	2.5-2.9	2.66	0.15	5.64
	W	5	1.9-2.5	2.16	0.24	11.11
P3	L	9	2.7-3.3	2.97	0.22	7.41
	W	8	1.9-2.3	2.11	0.14	6.64
P4	L	9	5.1-6.2	5.72	0.33	5.77
	W	9	2.1-2.9	2.49	0.24	9.64
M1	L	7	5.1-5.8	5.36	0.30	5.60
	W	7	2.3-2.7	2.46	0.15	6.10
M2	L	3	2.4-2.7	2.50	0.17	6.80
	W	3	2.4-2.7	2.57	0.15	5.84
p4	L	8	7.8-8.9	8.53	0.47	5.51
	L1	8	1.5-2.1	1.83	0.21	11.48
	H	8	2.6-3.0	2.90	0.19	6.55
m1	L	5	3.8-4.1	4.00	0.12	3.00
	W	5	1.6-1.9	1.82	0.13	7.14
m2	L	4	2.6-3.0	2.65	0.25	9.43
	W	4	2.1-2.3	2.15	0.10	4.65

Table 3.12.—Combined measurements and descriptive statistics for the dentition of Ptilodus "titanus" from the earliest Tiffanian (Ti1) Cochrane 2 locality, and the early middle Tiffanian (Ti3) Joffre Bridge Mammal Site #1, Joffre Bridge Roadcut, lower level, and DW-2 localities, Paskapoo Formation, Alberta.

Element	P	N	OR	M	SD	CV
P2	L	3	3.2-3.4	3.32	0.08	2.41
	W	3	2.5-3.2	2.90	0.26	8.97
P3	L	2	3.7-3.9	3.80	0.14	3.68
	W	2	2.9	2.90	0	0
P4	L	3	6.0-6.3	6.17	0.15	2.43
	W	3	2.6-3.0	2.83	0.21	7.42
M1	L	3	6.2-6.8	6.50	0.03	0.46
	W	3	2.7-2.9	2.77	0.12	4.33
M2	L	6	2.6-3.3	3.02	0.27	8.94
	W	6	2.9-3.2	3.03	0.14	4.62
p4	L	2	10.2-11.0	10.60	0.57	5.38
	L1	2	2.6-3.2	2.90	0.42	14.48
	H	2	3.8-3.9	3.85	0.07	1.82
m1	L	1	4.4	—	—	—
	W	1	2.0	—	—	—
m2	L	3	2.8-3.4	3.20	0.35	10.93
	W	3	2.5-2.6	2.57	0.06	2.33

Table 3.13.—Combined measurements and descriptive statistics for the dentition of Prochetodon speirsae new species from the earliest Tiffanian (Ti1) Cochrane 2 and Aaron's localities, and the early middle Tiffanian (Ti3) Joffre Bridge Mammal Site #1 and Birchwood localities, Paskapoo Formation, Alberta.

Element	P	N	OR	M	SD	CV
p4	L	8	9.0-11.0	10.19	0.42	4.12
	L1	8	2.1-2.9	2.44	0.30	12.30
	H	6	3.0-3.5	3.21	0.20	6.23
m1	L	4	4.5-4.6	4.55	0.05	1.10
	W	4	2.1-2.4	2.22	0.12	5.41
m2	L	1	2.9	—	—	—
	W	1	2.8	—	—	—

Table 3.14.—Combined measurements and descriptive statistics for the dentition of Allocosmodon woodi (Holtzman and Wolberg) from the early middle Tiffanian (Ti3) Joffre Bridge Roadcut lower level and DW-2 localities, Paskapoo Formation, Alberta.

Element	P	N	OR	M	SD	CV
M1	L	5	2.5-2.8	2.64	0.11	4.17
	W	5	1.4-1.7	1.46	0.13	8.90
p4	L	1	3.2	—	—	—
	L1	1	0.7	—	—	—
	H	1	0.9	—	—	—
m1	L	3	2.3-2.5	2.43	0.12	4.94
	W	3	1.1	1.1	0	0

Table 3.15.—Character summary for the new species of Neoplagiaulax from the middle Tiffanian (Ti3-4) of Alberta, Canada.

	Character	N. serrator	N. paskapooensis	N. cimolodontoides
P1-3	•P1 labial cusps	Closely approximated	Closely approximated	Equidistant
	•P2 cusps	3	4	3
P4	•P4 modal formula	(0)1:10:0	(0)4:8:0	(0)0:8:0
	•Anterolabial lobe	Well developed	Well developed	Poorly developed
	•Posterior slope	Shallow, concave	Steep, concave	Steep, straight to concave
	•Highest cusp	Prepenultimate, penultimate, or penultimate+ultimate	Ultimate or penultimate+ ultimate	Ultimate or penultimate+ ultimate
M1-2	•M1 modal formula	7:12:6	7:10:4	7:12-13:8
	•M1 internal row	Short	Short	Long
	•M1 middle row cusps	Deeply grooved, crescentic posteriorly	Weakly grooved, weakly crescentic posteriorly	Deeply grooved, crescentic posteriorly
	•M2 modal formula	3:4	3:3	3:6
Dentary	•Ramus	Deep	Narrow	Narrow
	•Condyle	Short, broad	Long, broad	Unknown
	•Diastema	Long	Short	Short
i1	•Crown	Long, slender	Long, deep	Short, deep
p4	•Modal serrations	17	14	13
	•Length vs. height	Long relative to height	Long relative to height	Short relative to height
	•Anterior margin	Steep	Shallow	Shallow
	•Posterior margin	Arcuate	Arcuate	Truncated, straight
	•Exodaenodont lobe	Narrow, deep	Broad, shallow	Broad, shallow, swollen
m1-2	•m1 modal formula	10:5	7:4	10:4
	•m1 external cusps	Crescentic posteriorly, grooved lingually	Pyramidal to weakly crescentic posteriorly, weakly grooved lingually	Crescentic posteriorly, grooved lingually
	•m2 modal formula	5:2	4:2	6:3

Figure 3.1.—1-16. Mesodma pygmaea Sloan from the early middle Tiffanian (Ti3) DW-2 locality, Paskapoo Formation, Alberta. UALVP 46227, incomplete left maxilla with P1-3, M1-2 in 1, labial and 2, occlusal view; 3-5, UALVP 46228, right P4 in 3, labial, 4, lingual, and 5, occlusal view; 6-8, UALVP 46235, right M1 in 6, labial, 7, lingual, and 8, occlusal view; UALVP 46258, left p4 in 9, labial and 10, lingual view; 11-13, UALVP 46249, left m1 in 11, labial, 12, lingual, and 13, occlusal view; 14-16, UALVP 46252, right m2 in 14, labial, 15, lingual, and 16, occlusal view.

17, 18. ?Mesodma sp. from the early middle Tiffanian (Ti3) DW-2 locality, Alberta. UALVP 46260, right p4 in 17, labial and 18, lingual view.

19-24. Mimetodon silberlingi (Simpson) from the early middle Tiffanian (Ti3) DW-1 (DW1) and DW-2 (DW2) localities, Paskapoo Formation, Alberta. 19-21, UALVP 46262 (DW2), right P4 in 19, labial, 20, lingual, and 21, occlusal view; 22-24, UALVP 46261 (DW1), incomplete left dentary with i1, p3-4 in 22, labial, 23, lingual, and 24, occlusal view.

Scale bars = 2 mm.


1
2
3
4
5
6
7
8
9
10
11
12
13
14
15
16
17
18
19
20
21
22
23
24

Figure 3.2.—1-5. Mimetodon churchilli Jepsen from the early middle Tiffanian (Ti3) DW-2 (DW2) and Joffre Bridge Roadcut lower level (JBUL) localities, Paskapoo Formation, Alberta. 1-3, TMP 2002.47.03 (JBUL), incomplete right dentary with i1, p3-4, m1-2 in 1, labial, 2, lingual, and 3, occlusal view; UALVP 46269 (DW2), right p4 in 4, labial and 5, lingual view.

6-20. Ectypodus elaphus new species from the early middle Tiffanian (Ti3) DW-2 locality, Paskapoo Formation, Alberta. 6-8, UALVP 45996, right P4 in 6, labial, 7, lingual, and 8, occlusal view; 9-11, UALVP 46225, right M1 in 9, labial, 10, lingual, and 11, occlusal view; 12-14, UALVP 45994 (holotype), incomplete left dentary with p3-4 and alveoli for i1, m1-2 in 12, labial, 13, lingual, and 14, occlusal view; 15-17, UALVP 46019, left m1 in 15, labial, 16, lingual, and 17, occlusal view; 18-20, UALVP 46226, right m2 in 18, labial, 19, lingual, and 20, occlusal view.

21-25. Ectypodus sp., cf. E. powelli from the early middle Tiffanian (Ti3) DW-1 (DW1) and DW-2 (DW2) localities, Paskapoo Formation, Alberta. 21-23, UALVP 46271 (DW1), incomplete left maxilla with P4, M1-2 in 21, labial, 22, lingual, and 23, occlusal view; UALVP 46279 (DW2), right p4 in 24, labial and 25, lingual view.

Scale bars = 2 mm.

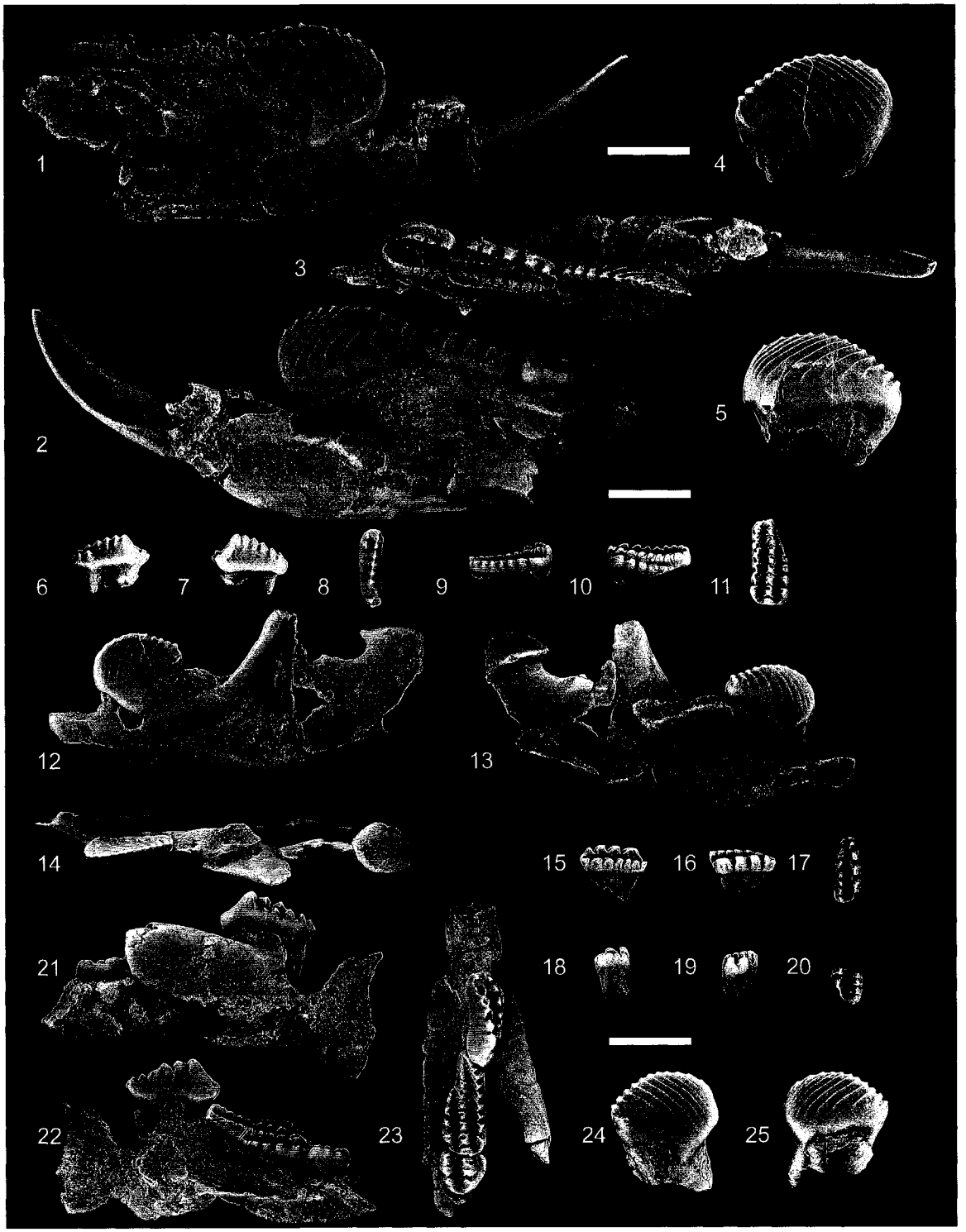
1
2
3
4
5
6
7
8
9
10
11
12
13
14
15
16
17
18
19
20
21
22
23
24
25

Figure 3.3.—Lateral profiles of p4 of 1, Ectypodus elaphus new species and 2, Ectypodus sp., cf. E. powelli from the Blindman River localities, middle Tiffanian (Ti3), Paskapoo Formation, Alberta. Outlines made with the aid of a camera lucida. The p4s are oriented along a line passing through the peak of the anterobasal concavity and the base of the posteroexternal ledge, and registered at a point midway along the baseline (see Krause, 1982b). Scale bar = 2 mm.

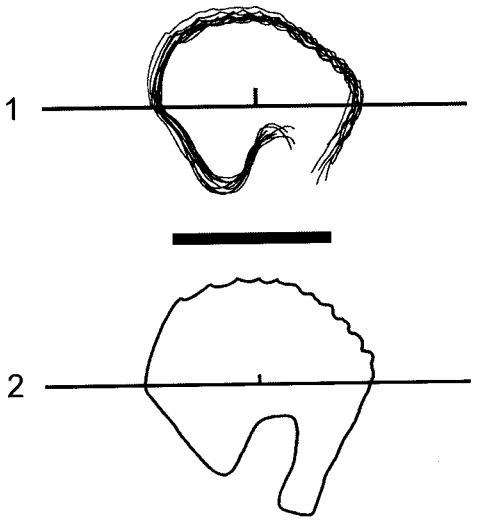
1
2

Figure 3.4.—1-6. Neoplagiaulax serrator new species from the early middle Tiffanian (Ti3) DW-2 locality, Paskapoo Formation, Alberta. 1-3, UALVP 46027, incomplete left maxilla with P1-4, M1-2 in 1, labial, 2, lingual, and 3, occlusal view; 4-6, UALVP 46028, incomplete left maxilla having P1-4, M1-2 in 4, labial, 5, lingual, and 6, occlusal view. Scale bars = 2 mm.

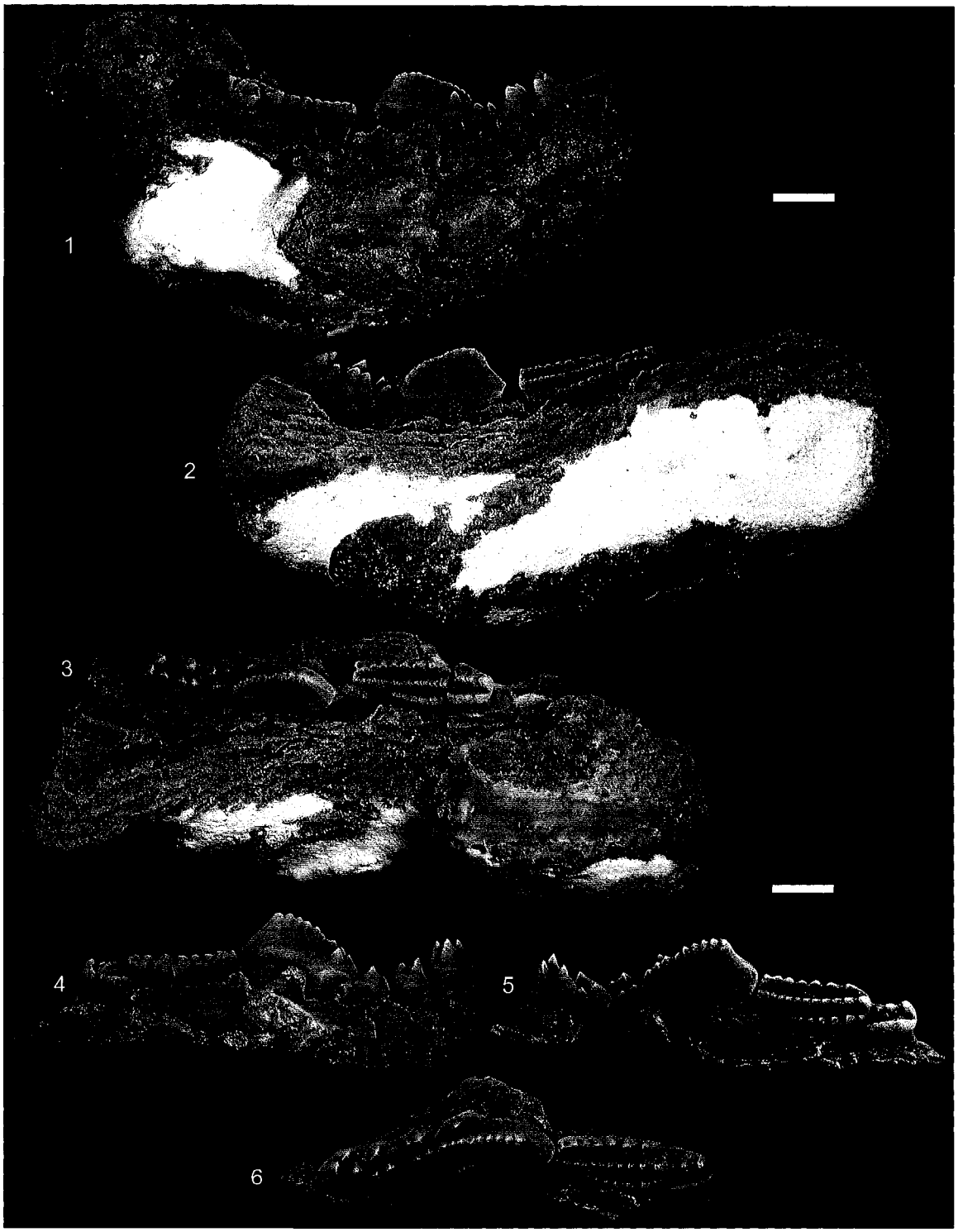
1
2
3
4
5
6

Figure 3.5.—1-7. Neoplagiaulax serrator new species from the early middle Tiffanian (Ti3) DW-2 locality, Paskapoo Formation, Alberta. 1, UALVP 46025 (holotype), incomplete skull with left P1-4, M1-2, RP1-4, M1?-2, and associated incomplete right dentary with i1, p3-4, m1-2; 2-4, UALVP 46080, incomplete right dentary with i1, p3-4, m1-2 in 2, labial, 3, lingual, and 4, occlusal view; 5-7, UALVP 46087, incomplete left dentary with i1, p3-4, m1-2 in 5, labial, 6, lingual, and 7, occlusal view. Scale bars = 2 mm.


1
2
3
4
5
6
7

Figure 3.6.—Lateral profiles of p4 of 1, Neoplagiaulax serrator new species from the early middle Tiffanian (Ti3), Paskapoo Formation, Alberta, and 2, Neoplagiaulax hunteri (Simpson) from the Roche Percée locality, late Tiffanian (Ti4), Ravenscrag Formation, Saskatchewan. Outlines made with the aid of a camera lucida. The p4s are oriented along a line passing through the peak of the anterobasal concavity and the base of the posteroexternal ledge, and registered at a point midway along the baseline (see Krause, 1982b). Scale bar = 2 mm.

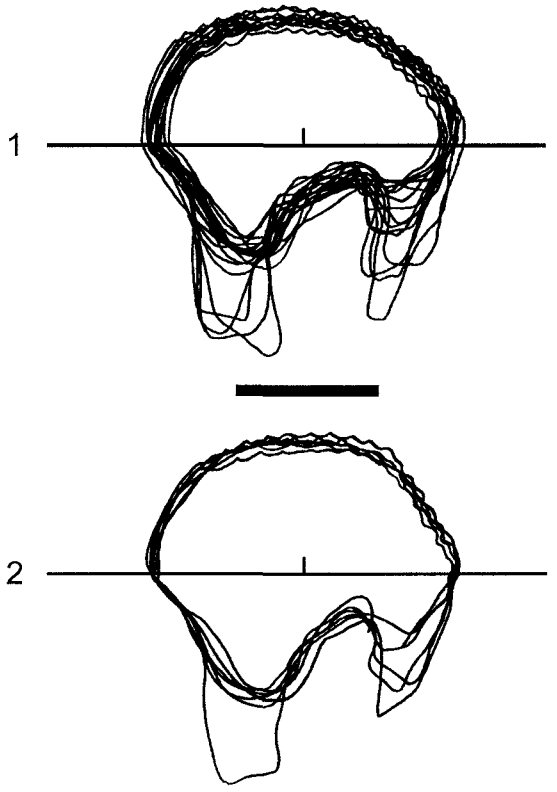
1
2

Figure 3.7.—1-11. Neoplagiaulax paskapooensis new species from the early middle Tiffanian (Ti3) DW-2 locality, Paskapoo Formation, Alberta. 1-5, UALVP 46138 (holotype), incomplete skull with left I2-3, P1-4, M1-2, right I2-3, P1-4, M1-2, and associated incomplete left dentary with i1, p3-4, m1, and incomplete right dentary with i1, p3-4, m1-2 in 1, labial (left p4, m1), lingual (left P1-4, M1-2), and occlusal (right P1-4, M1-2) view, 2, labial (left P1-4, M1-2), lingual (left p3-4, m1), and dorsal (left I2-3, right I2-3) view (inset shows the position of left and right I2 and I3), and right i1, p3-4, m1-2 in 3, labial, 4, lingual, and 5, occlusal view; 6-8, UALVP 46141, right P4 in 6, labial, 7, lingual, and 8, occlusal view; 9-11, UALVP 46157, incomplete left dentary with p3-4 and alveoli for i1, m1-2 in 9, labial, 10, lingual, and 11, occlusal view. Scale bars = 2 mm.

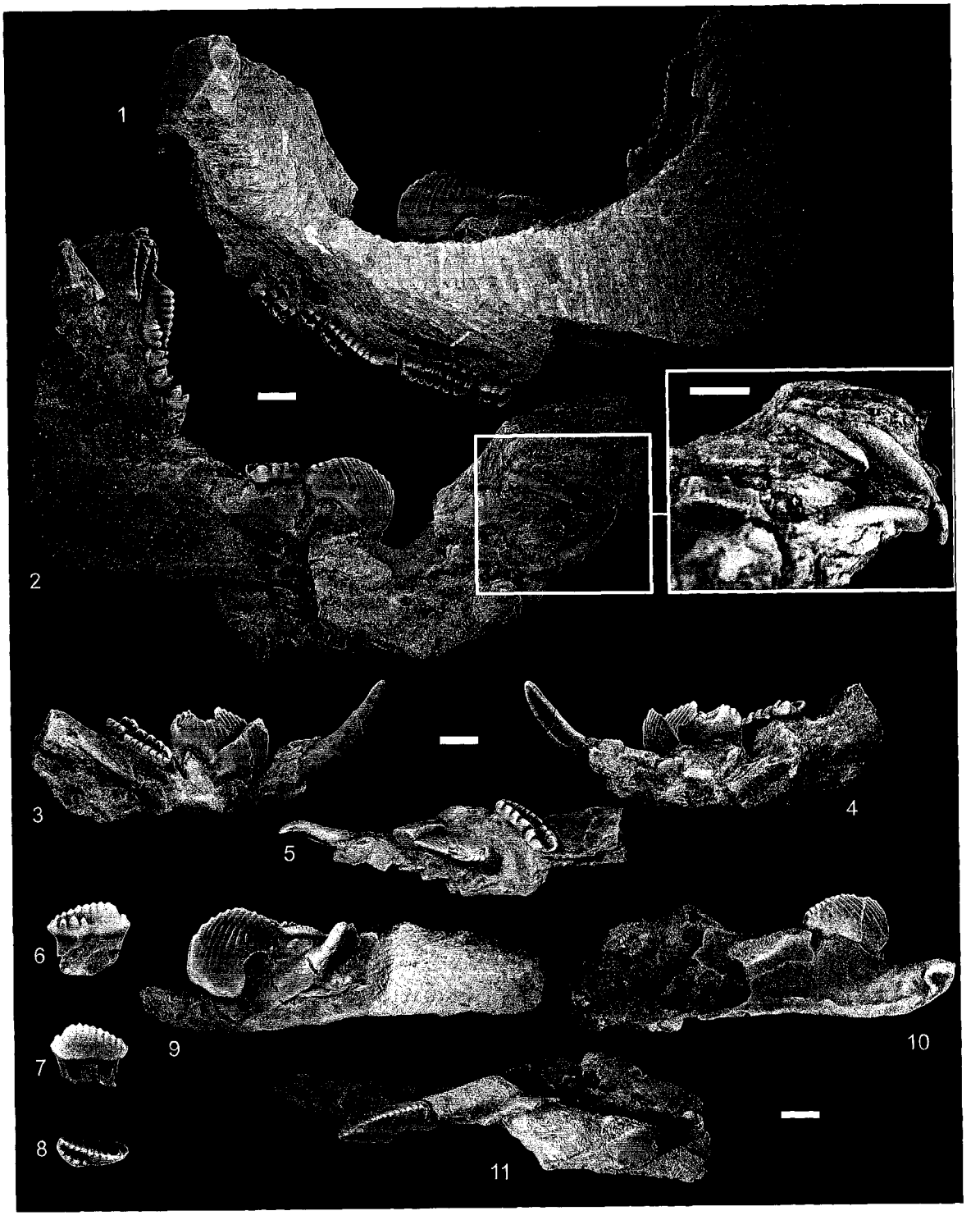
1
2
3
4
5
6
7
8
9
10
11

Figure 3.8.—Lateral profiles of p4s of 1, Neoplagiaulax paskapooensis new species from the early middle Tiffanian (Ti3), Paskapoo Formation, Alberta, and 2, Neoplagiaulax sp., cf. N. hazeni from the Roche Percée locality, late middle Tiffanian (Ti4), Ravenscrag Formation, Saskatchewan. Outlines made with the aid of a camera lucida. The p4s are oriented along a line passing through the peak of the anterobasal concavity and the base of the posteroexternal ledge, and registered at a point midway along the baseline (see Krause, 1982b). Scale bar = 2 mm.

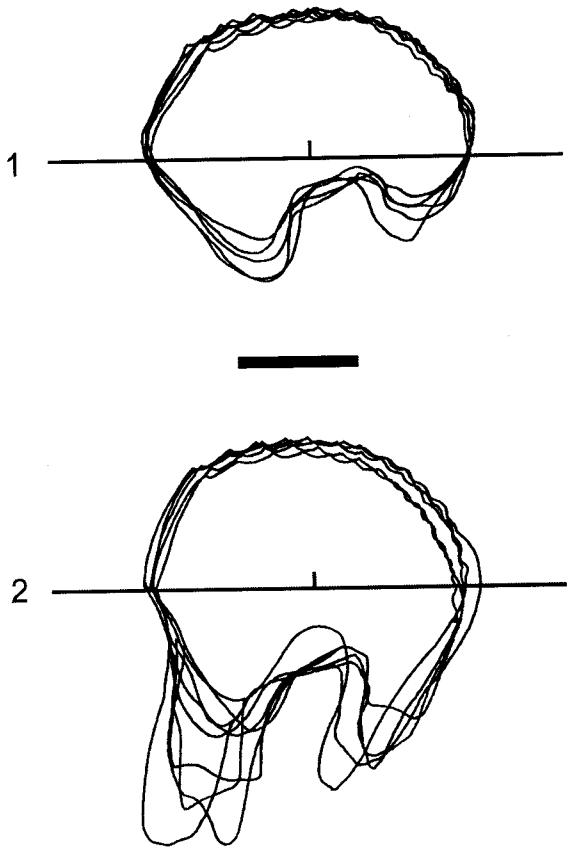
1
2

Figure 3.9.—1-15. Neoplagiaulax cimolodontoides new species from the early middle Tiffanian (Ti3) DW-2 locality, Paskapoo Formation, Alberta. 1-3, UALVP 46179, incomplete right maxilla with P2-4, M1-2 in 1, labial, 2, lingual, and 3, occlusal view; 4, 5, UALVP 46180, incomplete left maxilla with P1-4, alveoli for M1, and anterior alveolus of M2 in 4, labial and 5, occlusal view (arrow points to the canal anterior to P1, see text for discussion); UALVP 46201 (holotype, in part), crushed skull with left P1-4, M1-2 in 6, labial and 7, occlusal view; UALVP 46201 (holotype, in part), left di1 in 8, labial view; UALVP 46201 (holotype, in part), incomplete left dentary with erupting i1, p4 in 9, labial and 10, lingual view; 11-13, UALVP 46196, incomplete left dentary with p4, m1-2 in 11, labial, 12, lingual, and 13, occlusal view; UALVP 46197, incomplete right dentary with i1, p4 in 14, labial and 15, lingual view. Scale bars = 2 mm.

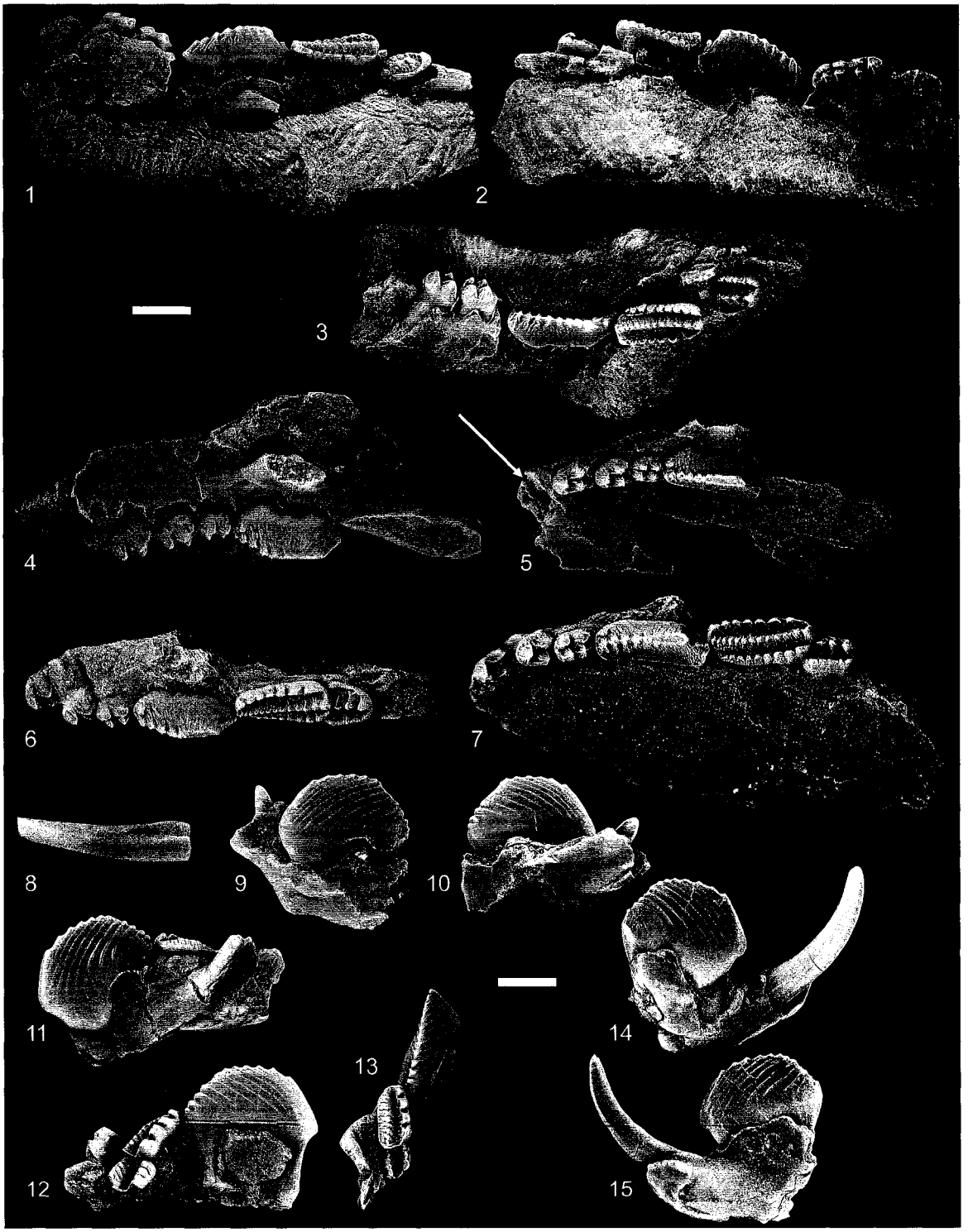
1
2
3
4
5
6
7
8
9
10
11
12
13
14
15

Figure 3.10.—Lateral profiles of p4s of 1, Neoplagiaulax cimolodontoides new species from the early middle Tiffanian (Ti3), Paskapoo Formation, Alberta, and 2, Anconodon cochranensis (Russell) from the Cochrane 2 locality, earliest Tiffanian (Ti1), Paskapoo Formation, Alberta. Outlines made with the aid of a camera lucida. The p4s are oriented along a line passing through the peak of the anterobasal concavity and the base of the posteroexternal ledge, and registered at a point midway along the baseline (see Krause, 1982b). Scale bar = 2 mm.

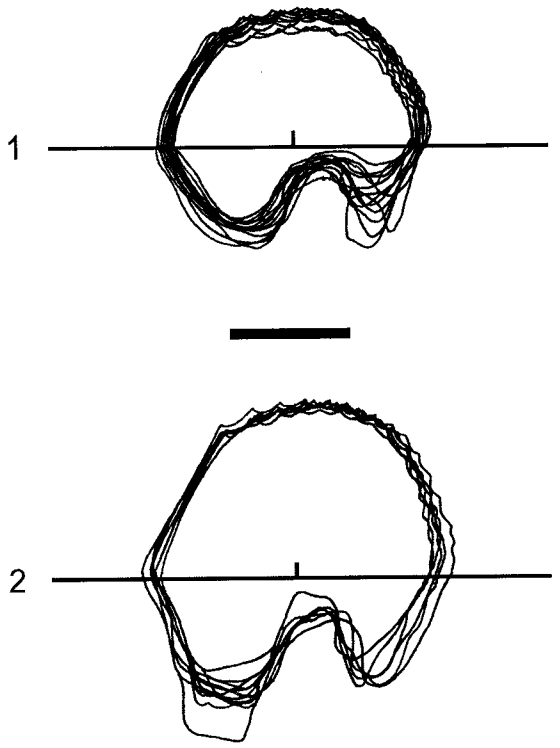
1
2

Figure 3.11.—1-3. Neoplagiaulax sp., cf. N. hunteri from the early middle Tiffanian (Ti3) DW-2 locality, Paskapoo Formation, Alberta. 1-3, UALVP 46280, incomplete left dentary with p4, m1-2 in 1, labial, 2, lingual, and 3, occlusal view.

4-12. Neoplagiaulax sp., cf. N. hazeni from the early middle Tiffanian (Ti3) DW-2 (DW2) and DW-3 (DW3) localities, Paskapoo Formation, Alberta. 4-6, UALVP 46281 (DW2), incomplete left maxilla with P1-4, M1-2 in 4, labial, 5, lingual, and 6, occlusal view; UALVP 46284 (DW2), left M2 in 7, occlusal view; UALVP 46287 (DW3), left p4 in 8, labial and 9, lingual view; 10-12, UALVP 46286 (DW2), left m2 in 10, labial, 11, lingual, and 12, occlusal view.

13, 14. Neoplagiaulacidae genus and species indeterminate from the early middle Tiffanian (Ti3) DW-2 locality, Paskapoo Formation, Alberta. UALVP 46288, right p4 in 13, labial and 14, lingual view.

15-18. Ptilodus "cedrus" from the early middle Tiffanian (Ti3) DW-2 locality, Paskapoo Formation, Alberta. 15-18, UALVP 46291, incomplete right premaxilla with I2 and I3, and associated and incomplete right maxilla with P1-4, M1-2; I2 and I3 shown 15, as preserved (15A, magnified occlusal view of I2; 15B, magnified occlusal view of I3), maxilla shown in 16, labial, 17, lingual, and 18, occlusal views.

Scale bars = 2 mm.

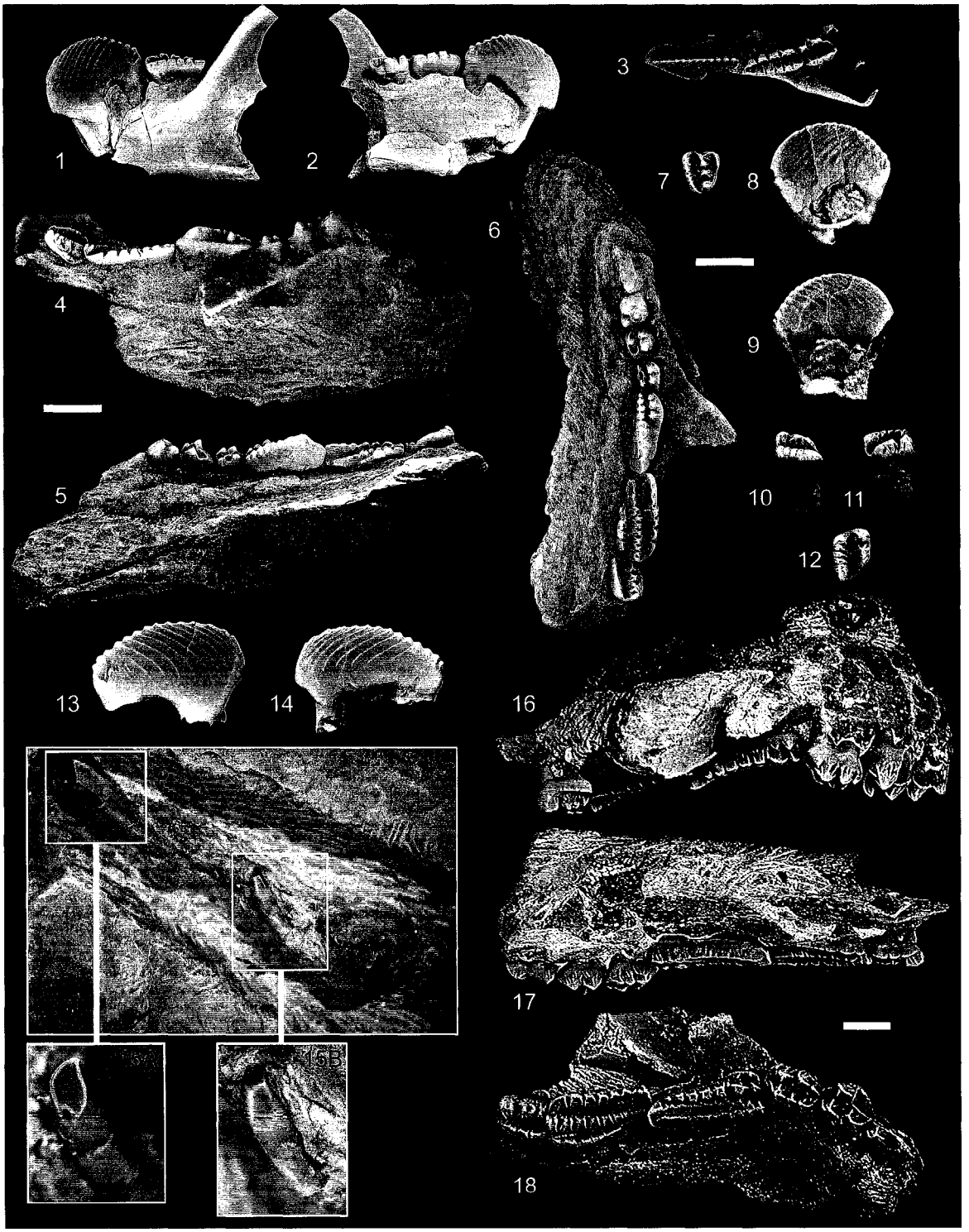
1
2
3
4
5
6
7
8
9
10
11
12
13
14
15A
15B
16
17
18

Figure 3.12.—1-6. Ptilodus "cedrus" from the early middle Tiffanian (Ti3) DW-2 locality, Paskapoo Formation, Alberta. 1-4, UALVP 46290, incomplete skull with left P3-4, M1-2 and right P1-4, M1-2, associated incomplete left dentary with i1, p3-4, m1-2, and associated incomplete right dentary with i1, p3-4, m1-2; incomplete right maxilla with P1-4, M1-2 in 1, occlusal view; incomplete right dentary with i1, p3-4, m1-2 in 2, lingual view; incomplete left maxilla with P3-4, M1-2 and incomplete left dentary with i1, p3-4, m1-2 in 3, occlusal (maxilla) and lingual (dentary), and 4, occlusal (dentary) view; UALVP 40465, incomplete right dentary with i1, p3-4, m1-2 in 5, labial and 6, occlusal views. Scale bars = 2 mm.


1
2
3
4
5
6

Figure 3.13.—1-9. Ptilodus "titanus" from the earliest Tiffanian (Ti1) Cochrane 2 (C2) locality, and the early middle Tiffanian (Ti3) Joffre Bridge Mammal Site No. 1 (JBMS) locality, Paskapoo Formation, Alberta. 1, UALVP 40467 (JBMS), incomplete skull with left P2-4, M1-2, right P1 (incomplete), right P2-4, M1-2 in occlusal view; UALVP 18620 (C2), incomplete right dentary with p3-4 in 2, labial and 3, lingual views; 4-6, UALVP 18638 (C2), right m1 in 4, labial, 5, lingual, and 6, occlusal views; 7-9, UALVP 18629 (C2), right m2 in 7, labial, 8, lingual, and 9, occlusal views. Scale bars = 5 mm.

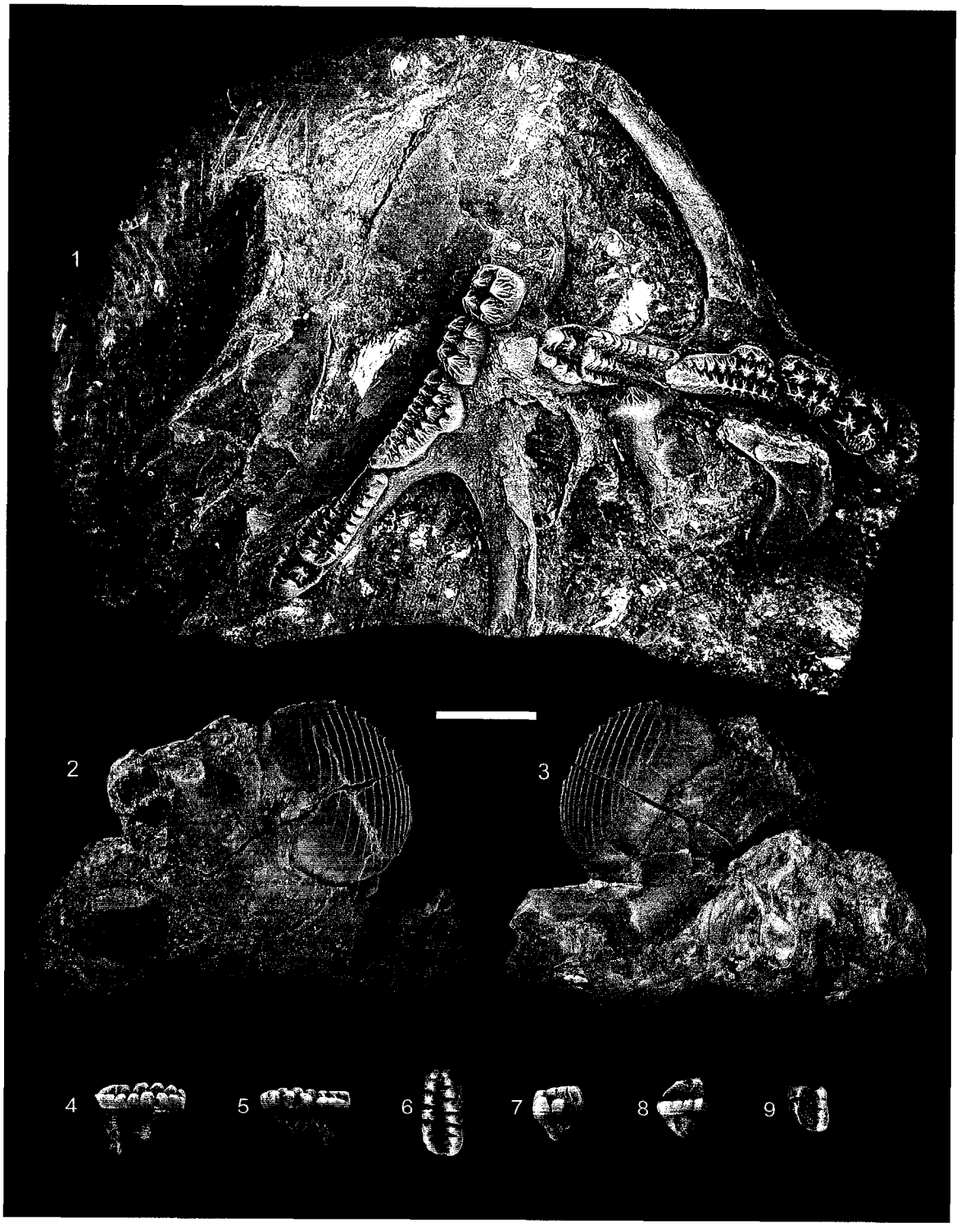
1
2
3
4
5
6
7
8
9

Figure 3.14.—Occlusal profiles of P4 and lateral profiles of p4 of Ptilodus "cedrus" and Ptilodus "titanus" from the earliest (Ti1) and early middle (Ti3) Tiffanian, Paskapoo Formation, Alberta. 1, occlusal profiles of P4 of Ptilodus "cedrus" (inner cluster, N=9) and Ptilodus "titanus" (outer cluster, N=4). 2, lateral profiles of p4 of Ptilodus "cedrus" (inner cluster, N=6) and Ptilodus "titanus" (outer profile, N=1). Outlines made with the aid of a camera lucida. P4s were oriented along the lingual and anterior surfaces of the crown; p4s are oriented along a line passing through the peak of the anterobasal concavity and the base of the posteroexternal ledge, and registered at a point midway along the baseline (see Krause, 1982b). Scale bars = 2 mm.

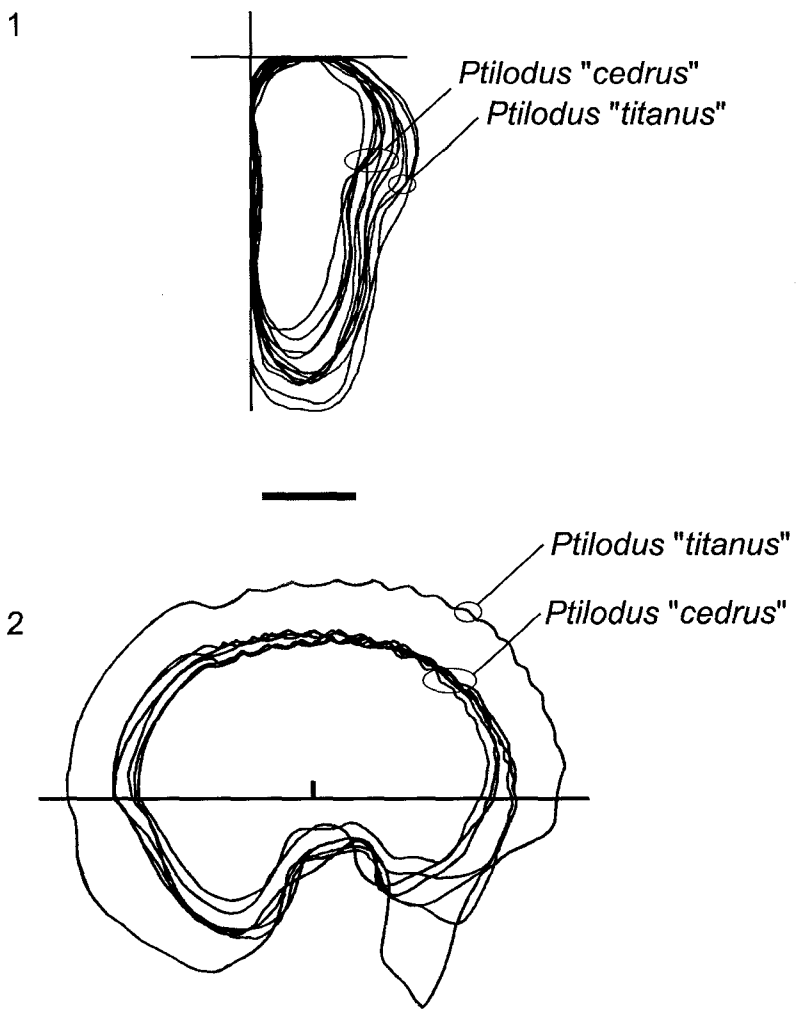
1
Ptilodus "cedrus"
Ptilodus "titanus"
Ptilodus "titanus"
2
Ptilodus "cedrus"

Figure 3.15.—1-10. Prochetodon speirsae new species from the earliest Tiffanian (Ti1) Cochrane 2 (C2) and Aaron's (AR) localities, and the early middle Tiffanian (Ti3) Birchwood (BW) locality, Paskapoo Formation, Alberta. 1-3, UALVP 45682 (holotype, C2), incomplete left dentary with p4, m1-2 in 1, labial, 2, lingual, and 3, occlusal view; 4-6, UALVP 45689 (BW), incomplete left dentary with p3-4, m1 in 4, labial, 5, lingual, and 6, occlusal view; UALVP 45703 (BW), incomplete left dentary with p3-4 in 7, labial and 8, lingual views; UALVP 45690 (AR), left p4 in 9, labial and 10, lingual views.

11-19. Allocosmodon woodi (Holtzman and Wolberg) from the early middle Tiffanian (Ti3) DW-2 locality, Paskapoo Formation, Alberta. 11-13, UALVP 46355, left M1 in 11, labial, 12, lingual, and 13, occlusal views; 14-16, UALVP 46359, right p4 in 14, labial, 15, lingual, and 16, occlusal views; 17-19, UALVP 46360, right m1 in 17, labial, 18, lingual, and 19, occlusal views.

Scale bars = 2 mm.

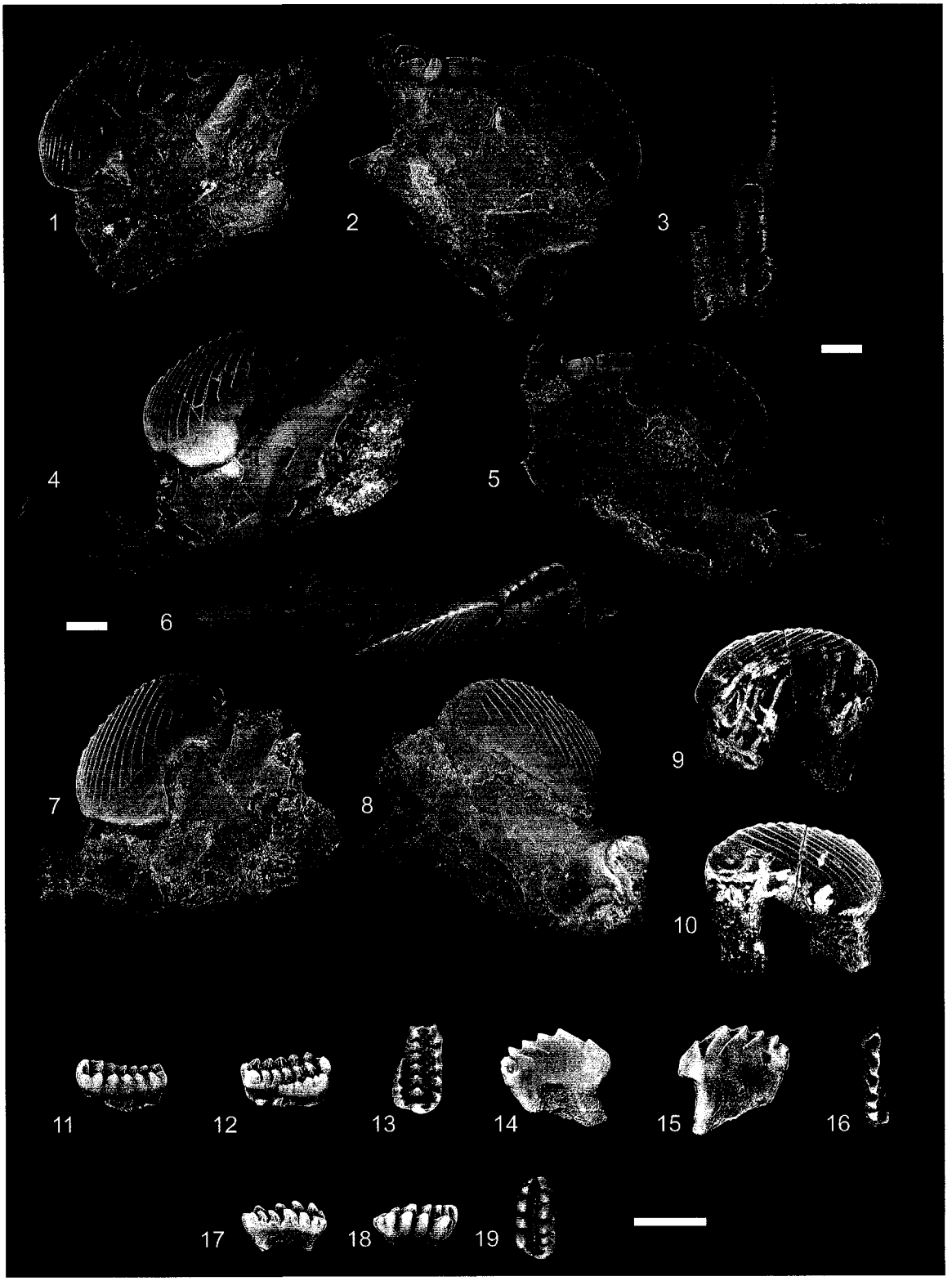
1
2
3
4
5
6
7
8
9
10
11
12
13
14
15
16
17
18
19

Figure 3.16.—Lateral profiles of p4 of Prochetodon sp., cf. Pro. foxi (inner outline, N=1) from the late middle Tiffanian (Ti4) Gao Mine locality, Paskapoo Formation, Alberta, Prochetodon speirsae new species (middle cluster, N=5) from the early middle Tiffanian (Ti3), Paskapoo Formation, Alberta, and Ptilodus "titanus" (outer outline, N=1) from the earliest Tiffanian (Ti1), Paskapoo Formation, Alberta. Outlines made with the aid of a camera lucida. The p4s are oriented along a line passing through the peak of the anterobasal concavity and the base of the posteroexternal ledge, and registered at a point midway along the baseline (see Krause, 1982b). Scale bar = 2 mm.

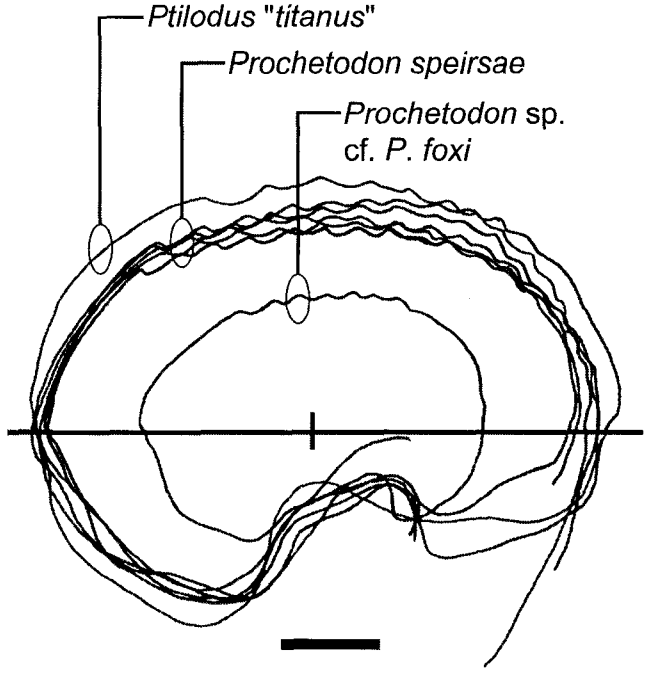
Ptilodus "titanus"
Prochetodon speirsae
Prochetodon sp.
cf. P. foxi

Figure 3.17.—1-6. Histograms showing log-normal distributions of P4 and p4 lengths in 1, 2, Neoplagiaulax serrator new species, 3, 4, Neoplagiaulax paskapooensis new species, and 5, 6, Neoplagiaulax cimolodontoides new species, from the early middle Tiffanian (Ti3), Paskapoo Formation, Alberta.

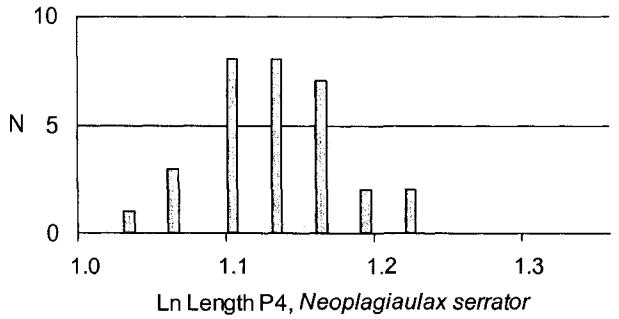

Ln Length P4, *Neoplagiaulax serrator*

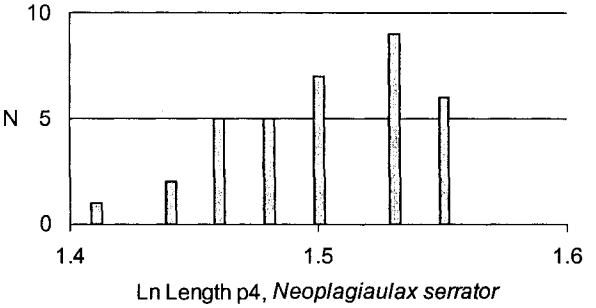

Ln Length p4, *Neoplagiaulax serrator*

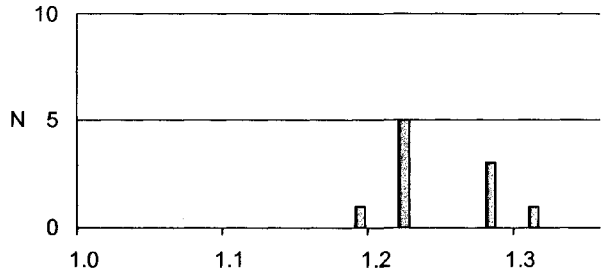

Ln Length P4, *Neoplagiaulax paskapooensis*

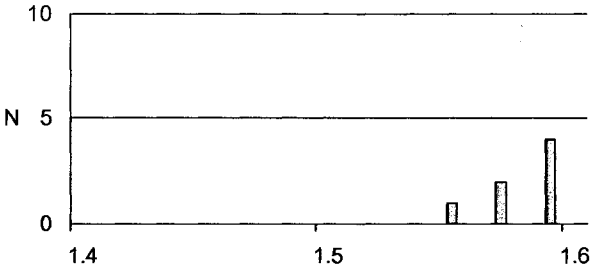

Ln Length p4, *Neoplagiaulax paskapooensis*

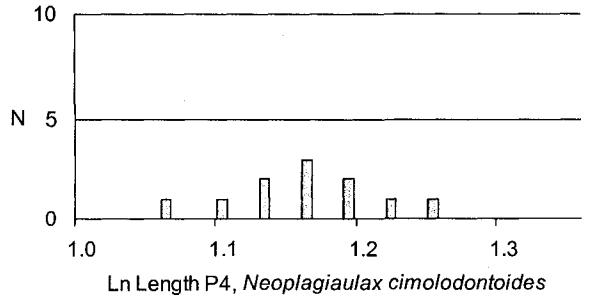

Ln Length P4, *Neoplagiaulax cimolodontoides*

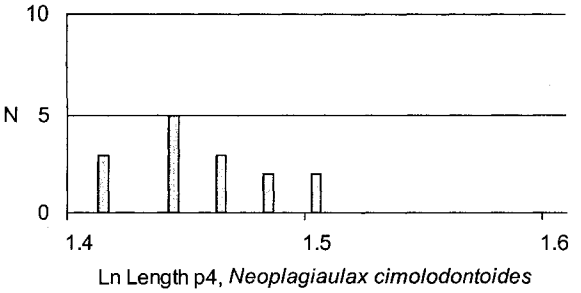

Ln Length p4, *Neoplagiaulax cimolodontoides*

Figure 3.18.—Lateral profiles of p4 of 1, Neoplagiaulax serrator new species, 2, Neoplagiaulax paskapooensis new species, and 3, Neoplagiaulax cimolodontoides new species from the early middle Tiffanian (Ti3), Paskapoo Formation, Alberta. Outlines made with the aid of a camera lucida. The p4s are oriented along a line passing through the peak of the anterobasal concavity and the base of the posteroexternal ledge, and registered at a point midway along the baseline (see Krause, 1982b). Scale bars = 2 mm.

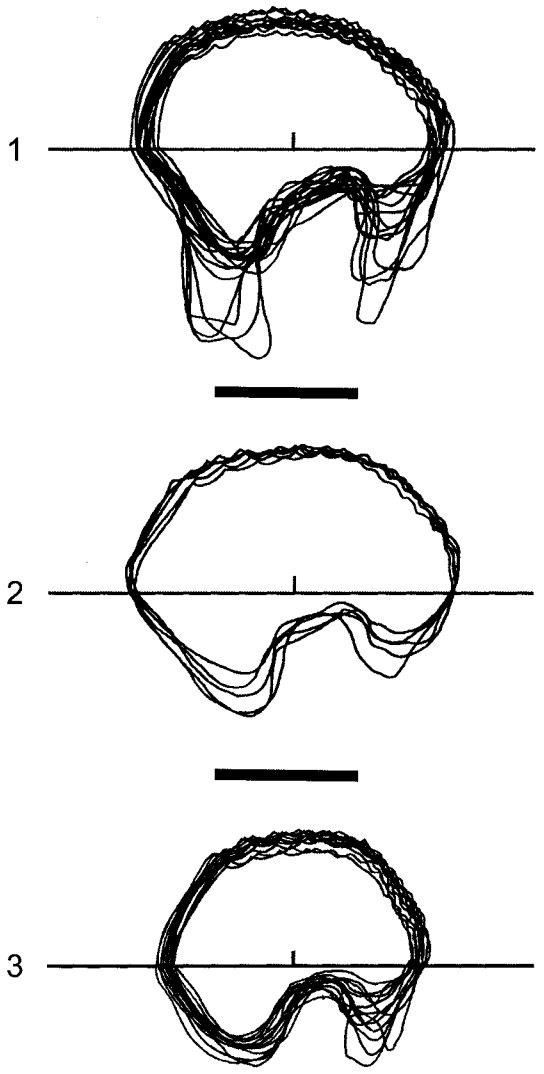
1
2
3

4 Didelphimorphians (Mammalia, Marsupialia) from the Late Paleocene of Alberta, Canada

4.1 Introduction

ALTHOUGH MARSUPIALS were among the most abundantly represented and taxonomically diverse mammals in the Late Cretaceous of North America, their numbers and diversity underwent a dramatic decline near the Cretaceous-Tertiary boundary, and remained low throughout the earliest parts of the Tertiary (see, e.g., Clemens, 1966; Lillegraven, 1969; Van Valen, 1978; Clemens, 1979; Johnston, 1980; Archibald, 1982, 1996; Johnston and Fox, 1984; Fox, 1987, 1997; Szalay, 1994; Lofgren, 1995; Lillegraven and Eberle, 1999; Wilson, 2005). In stark contrast to the explosive radiation of marsupials during the Paleocene in South America and their spectacular fossil record (see, e.g., Simpson, 1967; Paula Couto, 1970; Marshall, 1987; Case and Woodburne, 1986; Marshall and Muizon, 1988; Crochet and Sigé, 1993; Marshall et al., 1995; Muizon et al., 1997; Goin et al., 1998; Muizon, 1998; Muizon and Cifelli, 2001; Sigé et al., 2004; Case et al., 2004), early Tertiary marsupials in North America are poorly known, being both taxonomically depauperate and represented most often by isolated teeth or, more rarely, fragmentary jaws with teeth (Matthew and Granger, 1921; Simpson, 1935; Fox, 1983; Krishtalka and Stucky, 1983a; Johanson, 1996a; but see Bloch, 2001 for description of unusually large collections of the peradectid Peradectes protinnominatus McKenna, 1960 from Clarkforkian and Wasatchian limestone localities from the Clark's Fork and Bighorn basins of Wyoming). Although their fossil record improves towards the end of the Paleocene and into the Eocene (e.g., McKenna, 1960; Bown and Rose, 1979; Krishtalka and Stucky, 1983b; Korth, 1990), marsupials generally remain inconspicuous members of most early Tertiary mammalian local faunas; as a consequence, little is known of the dentition of most North American early Tertiary marsupials, and their evolutionary history remains poorly understood.

The Paleocene record of marsupials in North America is particularly sparse, with only two genera having been so far discovered. Although a small number of specimens from the late Torrejonian of Wyoming have been referred to the herpetotheriine

Swaindelphys Johanson, 1996b, the overwhelming majority of marsupial specimens of Paleocene age have been referred to the genus Peradectes Matthew and Granger, 1921 (including Thylacodon Matthew and Granger, 1921; see Clemens, 2006), a dentally conservative didelphimorphian (so-called "opossum-like" marsupials) that historically has been considered having had its ancestry with or near the Late Cretaceous alphadontid Alphadon Simpson, 1927 (e.g., Clemens, 1966, 1968, 1979; Crochet, 1979; Fox, 1983; but see Krishtalka and Stucky, 1983a, Montellano, 1988, Eaton, 1993, and Johanson, 1996a-b for different opinions). Peradectes is stratigraphically long-ranging, spanning the earliest Paleocene (Puercan) (Matthew and Granger, 1921; Archibald, 1982; Eberle and Lillegraven, 1998) to at least the Orellan (Oligocene) (Setoguchi, 1978; Storer, 1996) and geographically widespread, ranging from western California to southwestern Saskatchewan and central Alberta (e.g., Gazin, 1956; Holtzman, 1978; Youzwyshyn, 1988; Fox, 1990; Lofgren et al., 1999). Fragmentary or otherwise poorly preserved peradectid specimens from the Late Cretaceous or Paleocene of South America (Sigé, 1971, 1972; Marshall and Muizon, 1988; Muizon, 1992) and the Eocene of Europe (Crochet, 1977a-b, 1979, 1980; Koenigswald and Storch, 1998) have been tentatively referred to Peradectes, suggesting that the genus may have been geographically even more widely distributed than previously thought.

Despite their relatively poor fossil record, Peradectes and other peradectids can be recognized by their possession of a suite of dental specializations that set them apart from other contemporaneous didelphimorphians (Krishtalka and Stucky, 1983a; Fox, 1983; Johanson, 1996a-b). The upper molar crowns are somewhat transverse relative to their length, and are non-dilambdodont (i.e., the centrocrista is not deflected labially and appears straight, rather than V-shaped, in occlusal view), the conules generally are reduced in size, and the protocone is moderately compressed anteroposteriorly. The lower molar crowns bear relatively tall trigonids, anteroposteriorly short talonids (but see Johanson, 1996a-b for discussion on this character state), a cristid obliqua that joins the postvallid wall labial to the level of the protocristid notch, and an entoconid that is posterolabial, but subequal in size and height, to the hypoconulid. Postvallum-prevallid shear in near-vertical planes was important in the chewing cycle in peradectids (Fox, 1983), with horizontal grinding being relatively insignificant.

This chapter describes new dental and gnathic material of two species of Peradectes from the late Paleocene of Alberta, Canada, including the first specimen known to document the complete lower replacement dentition of a peradectid marsupial. Additionally, a new genus and species of uncertain familial status is described. The specimens provide new information on the dental anatomy of Peradectes, including important aspects of intraspecific variation, and documents for the first time the presence of three marsupial species from a single locality in the Paleocene of North America.

4.2 Systematic Paleontology

Class MAMMALIA Linnaeus, 1758

Subclass THERIA Parker and Haswell, 1897

Infraclass METATHERIA Huxley, 1880

Cohort MARSUPIALIA Illiger, 1811

Superorder AMERIDELPHIA Szalay, 1982 (sensu Kielan-Jaworowska et al., 2004))

Order DIDELPHIMORPHIA Gill, 1872

Family PERADECTIDAE Crochet, 1979

Comments on marsupial classification.—Few groups of Cretaceous and Early Tertiary therians have suffered as muddled a taxonomic history as the Marsupialia (see, e.g., Simpson, 1945; Clemens, 1979; Crochet, 1979; Szalay, 1982; Aplin and Archer, 1987; Reig et al., 1987; Marshall et al., 1990; Szalay, 1994; Johanson, 1996a; McKenna and Bell, 1997; Kielan-Jaworowska et al., 2004; Case et al., 2004), with more recent studies (e.g., Rougier et al., 1998; Luo et al., 2003; Asher et al., 2004) limiting the name to the crown group (and, therefore, in a much more exclusive sense than its traditional usage) within a broader Metatheria. Crown group definitions pose acute problems for marsupial systematics: many of the so-called "stem" or "basal" metatherians are undoubtedly more closely related to marsupials (and hence more closely related to the crown group) than they are to Deltatheroidea, the purported marsupial sister group within Metatheria (Rougier et al., 1998; Luo et al., 2003; see Cifelli, 2004; Kielan-Jaworowska et al., 2004); moreover, some of these basal metatherians may themselves be members of

the crown group (Aplin and Archer, 1987; Cifelli et al., 1996). Cogent arguments opposing the use of crown group concepts generally have been made (see, e.g., Lucas, 1990; Miao, 1991; Cifelli, 2004; Kielan-Jaworowska et al., 2004; Fox and Naylor, 2006), and convincing arguments in favour of a more traditional, stem-based classification that would have Late Cretaceous and Early Tertiary stem taxa included within Marsupialia (see, e.g., Cifelli, 2004; Kielan-Jaworowska et al., 2004; Fox and Naylor, 2006) have been proposed; these opinions are followed here. The recent classification of Kielan-Jaworowska et al. (2004) adopts a stem-based concept of Marsupialia, and the suprageneric taxonomy presented in that work is followed here.

Genus PERADECTES Matthew and Granger, 1921

Peradectes MATTHEW and GRANGER, 1921, p. 2.

Type species.—Peradectes elegans Matthew and Granger, 1921.

Other included species.—Peradectes pusillus Matthew and Granger, 1921; P. californicus (Stock, 1936); P. chesteri Gazin, 1952; P. pauli Gazin, 1956; P. protinnominatus McKenna, 1960; ?P. austrinum (Sigé, 1971); P. minor Clemens, 2006.

PERADECTES ELEGANS Matthew and Granger, 1921

Figures 4.1, 4.2.1-4.2.3; Table 4.1

Peradectes elegans MATTHEW and GRANGER, 1921, p. 2.

Holotype.—AMNH 17376, paired dentaries with Rp1, p3, m1-4 and Lp2-3, m1-4 (Matthew and Granger, 1921, p.2). Mason Pocket, Animas Formation of Colorado, late Paleocene (late middle Tiffanian, Ti4, Plesiadapis churchilli/P. simonsi Lineage Zone of Lofgren et al., 2004).

Paratype.—AMNH 17369, incomplete left maxilla having M1-4.

Material examined.—From DW-1: UALVP 46392, incomplete left dentary having m3-4; UALVP 46393, m2 or m3.

From DW-2: UALVP 46394, incomplete left maxilla with P3, M1-3; UALVP 16270, incomplete right dentary with i1-2, 4, c, p1-3, m1-4, and alveoli for i3, m4; UALVP 46395, incomplete right dentary with p3, m1-4, and alveoli for c, p1-2; UALVP 46396, incomplete left dentary with p3, m1-4; UALVP 46397, incomplete left dentary with m1-4; UALVP 46398, incomplete right dentary with p3, m2-3, and alveoli for c, p1-2; UALVP 46399, incomplete right dentary with m2-4 and alveoli for m1; UALVP 46400, incomplete left dentary with m2-3 and alveoli for c, p1-3, m1, m4; UALVP 46401, incomplete left dentary with p3, m2 (trigonid only), and alveoli for m1; UALVP 46402, m2 or m3; UALVP 46403, associated m2 and m3; UALVP 46404, 46405, m2 or m3.

Age and occurrence.—Earliest Tiffanian (Plesiadapis praecursor/P. anceps Lineage Zone, Ti1, late Paleocene) to late Tiffanian (Plesiadapis simonsi/P. gingerichi Lineage Zone, Ti5, late Paleocene) of the Western Interior of North America (Lofgren et al., 2004).

Description.—Upper dentition (Figs. 4.1.1-4.1.3): Upper premolars: Upper premolars of peradectid marsupials are poorly known, with Simpson's (1935) brief description of P2-3 the most recent for Peradectes elegans. The P3 in UALVP 46394 (L=1.2, W=0.6) is double-rooted, with the two roots faintly diverging dorsally. Although the anterior root has been broken away, the shape and dimensions of the parts that remain indicate it was nearly circular in cross section, in contrast with the posterior root, which is more anteroposteriorly elongate and bilaterally compressed. The crown is elongate and subovate in occlusal aspect, similar to P3 of Alphadon marshi Simpson, 1927 (see Lillegraven, 1969), and is dominated by a large and trenchant paracone. The crown is encircled by a robust cingulum: the ectocingulum is especially well developed at the posterolabial margin of the crown, where it supports a weak, labially positioned cuspule; the ectocingulum and lingual cingulum extend anteriorly from the cuspule, becoming weaker towards the midpoint of the crown, and then becoming stronger again towards the anterior margin. Unlike P3 on AMNH 17383, a distinct anterior cuspule is not developed on UALVP 46394 (see Simpson, 1935). In contrast to P3 of A. marshi, that of P. elegans is not strongly exodaenodont at the posterior root. The paracone is large, somewhat compressed labiolingually, and slightly recurved. A well-developed crest originating at

the apex of the paracone extends posteriorly and slightly lingually, and joins the basal cingulum at the posterolingual margin of the crown.

Upper molars (M1: L=1.6, W=1.4; M2: L=1.6, W=1.7; M3: L=1.4, W=1.8): The upper molars are consistent with those of Peradectes elegans (see descriptions in Simpson, 1935; Krishtalka and Stucky, 1983a; Johanson, 1996a), differing from upper molars of Alphadon Simpson, 1927 and Protalphadon Cifelli, 1990 in being smaller, with weaker conules, stylar cusps, and ectoflexi, and in having a less anteroposteriorly compressed protocone (Krishtalka and Stucky, 1983a; Johanson, 1996a). The crown of M1 forms a near-equilateral triangle in occlusal aspect, while those of M2-3 are more nearly isosceles in outline; the crowns of M1-3 are anteroposteriorly longer and less transverse relative to those of other species of Peradectes [including those of P. pusillus (Matthew and Granger, 1921), see Krishtalka and Stucky, 1983a; Eberle and Lillegraven, 1998]. The stylar shelves are narrower than those of Alphadon, and the anterior part of the shelf is greatly reduced on M1. Stylar cusp B is well developed on all molars at hand, followed in decreasing order of size and height by stylar cusps D and A. Cusp C is absent on M1 of UALVP 46394 and is poorly developed on the remaining teeth; the cusp occurs slightly anterior to the ectoflexus on M2-3, and can be fully cuspate, or labiolingually compressed and crest-like. The preparacrista and postmetacrista are well developed, particularly on M2-3, with the postmetacrista extending more posterolabially relative to the molars of other species of Peradectes. The paracone is smaller and lower than the metacone on all of the upper molars, and the two cusps are fully separated at their bases. The paraconule and metaconule are conspicuous, and their associated crests are well developed, with the postparaconular crista and premetaconular crista extending to the base of the paracone and metacone, respectively. The paracingulum is continuous to stylar cusp A. The protocone is anteroposteriorly long on all upper molars at hand, a diagnostic feature of P. elegans (Krishtalka and Stucky, 1983a); the protoconal cristae are short but strongly developed, and the postprotocrista extends posteriorly and labially, especially on M1 and M2, further lengthening the lingual parts of the crown.

Lower dentition (Figs. 4.1.4-4.1.9, 4.2.1-4.2.3): The lower dentition of Peradectes elegans is among the best known for Early Tertiary marsupials, and has been thoroughly described by Simpson (1935), Krishtalka and Stucky (1983a), Fox (1983), and Johanson

(1992, 1996a). UALVP 16270 was described in detail by Fox (1983); further preparation of this specimen has more fully exposed the lower incisors, and Fox's (1983) identification of these teeth as i1-2, 4 is confirmed. Although i1 has shifted during post-mortem disturbance such that the crown now occupies a position labial and posterior to that of i2, its alveolus can be clearly seen anterior to i2; the crown of i1 is smaller than that of i2, as Fox (1983) had originally reported. The crowns of the incisors are spatulate, and those of i1-2 have a weakly developed posterobasal heel.

Lower canine: The canine is large and robust, differing little from that of Didelphis virginiana Kerr, 1792, the extant Virginia opossum. The crown is tall, recurved, and lacks a posterobasal cuspule.

Lower premolars: A large, trenchant protoconid and a conspicuous heel dominate the crowns of the premolars. The crown of p1 is considerably smaller than those of p2-3, and leans anteriorly, nearly abutting the posterobasal parts of the lower canine. A small, anterolingually positioned paraconid occurs halfway up the crown of p2-3, and the anterior and posterior edges of the protoconid form raised crests. The crown of p3 is slightly taller than that of p2, and both are subequal or slightly taller than that of m1, a feature of Peradectes elegans that distinguishes it from P. protinnominatus (see Krishtalka and Stucky, 1983a). The heel on p3 is better developed than on p2, and the single talonid cusp (?hypoconid) is positioned slightly (p2) or far (p3) labial to the level of the protoconid. A short crest can sometimes occur on the lingual margin of the heel on p2-3, and a shallow basin is formed between it and the much better developed cristid obliqua. The crowns of p2-3 are weakly exodaenodont posteriorly.

Lower molars: The lower molars are similar to those of other peradectids, with moderately tall trigonids and notably lower talonids; the crowns increase in height and width from m1 to m3, while m4 is slightly shorter and narrower than m3. The trigonid cusps are virtually equidistant from one another, with the protoconid the tallest trigonid cusp, followed in order of decreasing height by the metaconid and paraconid. Although the paraconid+paracristid on m1 is low and leans anteriorly, it becomes increasingly higher, more nearly vertical, and more lingual in position from m2-4. The metaconid can be lingually opposite the protoconid, or slightly more posterior such that the protocristid is oriented anterolabially-posterolingually. The talonid increases in width from m1 to

m3, and is anteroposteriorly long (in keeping with the enlarged upper molar protocone) relative to those of other species of Peradectes (e.g., P. pauli, and see later in this chapter), but are considerably shorter than those of P. pusillus and Alphadon (Clemens, 1966; Archibald, 1982; Johanson, 1996a). As with other species of Peradectes, the cristid obliqua joins the postvallid wall low on the protoconid, and labial to the level of the trigonid notch (Krishtalka and Stuckey, 1983a). The entoconid and hypoconulid are subequal in size and height, whereas the hypoconid is slightly smaller and lower; the entoconid and hypoconulid are closely approximated (twinned) and are separated from each other by a weak notch. The talonid of m4 is shorter and slightly narrower than that on m1-3, and the entoconid and hypoconulid can be distinctly separate, or connate throughout most of their height. The anterior cingulid is well developed on m1-4, while the posterior cingulid is weak to absent on m1-3, and completely absent on m4.

Discussion.—The referred specimens differ little from homologous teeth of Peradectes elegans as described by Matthew and Granger (1921), Simpson (1935) and Krishtalka and Stucky (1983a). The dentition of P. elegans differs most notably from that of other species of Peradectes in the upper molars being less transverse relative to their length, in the molar protocone being uncompressed anteroposteriorly, and in m1 being more nearly equal in size to m2 (Krishtalka and Stucky, 1983a). P. elegans is also known from the earliest Tiffanian (Ti1) Cochrane 2 locality (Youzwyshyn, 1988) in addition to its occurrence in the early middle Tiffanian of Alberta.

PERADECTES PAULI Gazin, 1956

Figures 4.2.4-4.2.20, 4.3; Tables 4.2, 4.3

Peradectes pauli GAZIN, 1956, p. 14.

Revised diagnosis.—Differs from Peradectes pusillus in being significantly smaller and in having weaker stylar cusps. Differs from P. elegans in having upper molars that are more transverse relative to length, weaker stylar cusps, a smaller p2-3, and m1 slightly smaller than m2. Differs further from P. elegans in having a smaller, slightly procumbent, and more nearly premolariform lower canine with a well-developed

posterior cusp, a narrower talonid on m4, and a broader molar talonid notch. Differs from all other species of Peradectes except P. elegans and P. minor in having m4 with a longer talonid than trigonid, in having a less anteroposteriorly compressed molar protocone, and in having relatively better developed stylar cusps. Differs from P. minor in having weaker stylar cusps and conules.

Holotype.—USNM 20879, incomplete left dentary with m3-4 (Gazin, 1956, p. 14, pl. 2, figs. 4-5). Saddle locality; Fort Union Formation of Wyoming, late Paleocene (early Tiffanian, Ti2, Plesiadapis anceps/P. rex Lineage Zone of Lofgren et al., 2004).

Paratype.—USNM 20880, incomplete left dentary with m1 and part of m2.

Material examined.—From Joffre Bridge Roadcut lower level: UALVP 46408, incomplete right maxilla with M2.

From Joffre Bridge Mammal Site No. 1: UALVP 46411, incomplete left dentary with c, p1-3, supernumerary p3, m1-4, and associated and incomplete right dentary with i1-4, c, p1-3 (p2 broken), m1-4; UALVP 46412, m1;

From DW-2: UALVP 46406, incomplete right maxilla with P3, and associated incomplete right maxilla with M1-2; UALVP 46410, incomplete left maxilla with M2-3; UALVP 46409, incomplete right maxilla with M2-3; UALVP 46407, incomplete right maxilla with M2; UALVP 46413, M1; UALVP 46414, M3; UALVP 46415, M2 or M3; UALVP 46416, incomplete left dentary with p2-3, m1-4, and alveoli for c, p1; UALVP 46417, incomplete left dentary with p2, m1, and alveoli for i1-4, c, p1, p3, m2-3.

From Hand Hills West upper level: UALVP 34904-5, M1; UALVP 34905, M3; UALVP 34901, m2.

Age and occurrence.—Earliest Tiffanian (Plesiadapis praecursor/Plesiadapis anceps Lineage Zone, Ti1, late Paleocene) to late middle Tiffanian (Plesiadapis churchilli/P. simonsi Lineage Zone, Ti4, late Paleocene) of the Western Interior of North America (Lofgren et al., 2004).

Description.—Upper dentition (Figs. 4.2.4-4.2.20): Upper premolars: P3: The P3 of Peradectes pauli is known only from UALVP 46406 (Figs. 4.2.4-4.2.6). It differs from that of P. elegans in being slightly longer and more labiolingually compressed, and in having a weaker lingual cingulum.

Upper molars: M1: The crown of M1 is transverse relative to its length, and its three sides form a scalene triangle in occlusal aspect, with the posterior margin forming the long arm of the triangle. The trigon cusps are tall and sharp, with the metacone slightly higher than the subequal paracone and protocone. The anterior parts of the stylar shelf are reduced, although not to the same degree as on M1 of Peradectes elegans, and stylar cusp B is slightly more labially positioned, rather than abutting the labial base of the paracone. The metastylar lobe is well developed, flaring labially and posteriorly; a shallow ectoflexus is present. The stylar cusps are smaller than those on M1 of P. elegans, with cusp B being the largest, followed by a smaller cusp D; cusps A, C, and E are only weakly developed. The paracone and metacone are separate throughout their height, although they are more closely approximated than are the paracone and metacone on M1 of P. elegans; the bases of the paracone and metacone extend lingually to the same degree, and their lingual sides are convex, while their labial faces are virtually flat. The preparacrista and postmetacrista are both well developed, and the centrocrista is deeply notched and straight (i.e., not deflected towards the ectocingulum). The conules and their associated conular cristae are weakly developed relative to those on M1 of P. elegans, and the conules are slightly more lingual. The paracingulum is continuous to the parastylar corner of the crown, whereas the metacingulum is undeveloped. The protocone is anteroposteriorly compressed, similar to that on M1 of geologically younger species of Peradectes, and the trigon basin is shallow.

M2: The crown of M2 is wider than that of M1, and forms an isosceles triangle in occlusal outline, with the apex at the lingual margin. As with M1, the principal cusps on M2 are tall and sharp, with the metacone being the largest and tallest cusp, followed by a smaller and lower paracone and protocone. A shallow ectoflexus divides the labial margin of the crown into moderately developed parastylar and well-developed metastylar lobes; the ectoflexus is deeper than that on M2 of Peradectes elegans, and the stylar shelf is broader. The stylar cusps on M2 are better developed than those on M1, with a robust cusp B, and a smaller and lower cusp D. Cusp A is positioned anterior and slightly lingual to cusp B; its apex is lower, and a broad, V-shaped notch separates the two cusps. Cusp C is positioned just lingual to the deepest part of the ectoflexus, and while it is present on all M2's at hand, it is variably developed: the cusp can be robust, its

dimensions approaching those of cusp D (e.g., UALVP 46408, Figs. 4.2.13-4.2.15), or can be barely evident (e.g., UALVP 46406, Figs. 4.2.7-4.2.9). Cusp E is not developed. As with M1, the paracone and metacone on M2 are connected by a deeply notched centrocrista, and the preparacrista and postmetacrista are well developed; the labial side of the paracone and metacone are flat to slightly concave. The conules and conular cristae are better developed than those on M1, and are positioned further lingually. The paracingulum is continuous to the parastylar lobe, whereas the metacingulum is undeveloped. Although the protocone is slightly longer than on M1, it is nonetheless compressed relative to that on M2 of P. elegans.

M3: The M3 of Peradectes pauli is slightly more transverse relative to that in P. elegans. The occlusal outline of M3 is similar in most respects to that of M2, but the crown is anteroposteriorly shorter, and the ectoflexus is deeper, dividing the labial margin into better defined and more nearly symmetrical parastylar and metastylar lobes. The metacone is the largest and tallest of the trigon cusps, followed by a lower paracone and markedly anteroposteriorly compressed protocone. Cusp B is the largest and tallest stylar cusp, but it is positioned further labially than it is on M2; a long, high preparacrista extending anterolabially from the paraconal apex can join stylar cusp B, or terminate slightly anterior and lingual to that cusp. Cusp B is followed in decreasing order of size and height by cusps C, D, and A; cusp E is not developed. Although they are present on all M3s at hand, stylar cusps C and D can be either well developed or inconspicuous, and cusp C is consistently positioned at the deepest part of the ectoflexus. The paracone and metacone are more closely approximated than those on M3 of P. elegans, and are connected by a deeply notched centrocrista. In contrast with M2, the preparacrista and postmetacrista on M3 are subequal in length, reflecting the more nearly symmetrical shape of the parastylar and metastylar lobes. The conules are more lingual than those in P. elegans; the paracingulum extends uninterrupted to stylar cusp A, and the metacingulum is not present. The anteroposterior compression of the protocone is greater than that on M2, and the trigon basin is shallower.

Dentary and lower dentition (Fig. 4.3): UALVP 46411 is one of the best-preserved specimens of any known marsupial from the early Tertiary of North America, documenting the complete lower right dentition and all of the left post-incisor teeth from

a single individual. The dentary is similar to those in other primitive didelphimorphians [e.g., Protalphadon lulli (Clemens, 1966) and Alphadon marshi (see Clemens, 1966; Clemens, 1979)]: the horizontal ramus is shallow and smoothly convex ventrally, and the ascending ramus of the coronoid process is steep. Although the angular process is not preserved on any of the specimens at hand, the posterior parts of the mandible clearly indicate that it was medially inflected. The condyle in Peradectes pauli is unknown. The symphysis is long and shallow, extending posteroventrally to the level of p2; a conspicuous ridge delimits the articular surface dorsally, and a small foramen penetrates the symphyseal surface at about its anteroposterior midpoint. A small mandibular foramen opens posteromedially in the weakly excavated pterygoid fossa; the mandibular fossa is strongly excavated, but terminates well above the ventralmost parts of the ramus; thick crests delimit the fossa anteriorly and ventrally. Two subequal mental foramina penetrate the lateral surface of the dentary: the more anterior foramen occurs ventral to p1 and opens anterolaterally and slightly dorsally, while the posterior foramen occurs ventral to m1 and opens dorsolaterally; a tiny third foramen opens below p3 in one specimen (UALVP 46416, Figs. 4.3.1-4.3.3).

Lower incisors: The four lower incisors are in articulation in the right dentary in UALVP 46411, although i3-4 have been somewhat displaced by post-mortem disturbance. The incisors are aligned more or less anteroposteriorly, and their crowns are crowded together with no evidence of a diastema, either between adjacent incisors or between i4 and the canine. The crowns of i1 and i2 are procumbent and are similar, although less nearly horizontal, to those of the herpetotheriine Herpetotherium fugax Cope, 1873 (see Fox, 1983), but are slightly more procumbent than are those in Peradectes elegans (see Fox, 1983 and earlier in this chapter); i3-4 are more nearly vertical than are i1-2. The root of i2 (=i3 of Hershkovitz, 1982) is not appreciably "staggered" in its position relative to i1 or i3, and although the bone is damaged labial to the lower incisors, there is no evidence from the parts that remain of the thick buttressing that apparently characterizes the dentary of many didelphimorphians (Hershkovitz, 1982, 1995). The crowns of i1 and i2 are nearly twice the size of those of i3 and i4, and all the incisors are anteroposteriorly compressed and broadly spatulate towards their apices. A weak ridge extends posteriorly from the apex of each incisor, dividing the crown into

broad medial and narrower lateral parts. Faint posterobasal swellings are evident on each of i1 and i2, similar to those on incisors of P. elegans; the i3 of P. pauli has a conspicuous heel.

Lower canine: The lower canine of Peradectes pauli is a single rooted, bilaterally compressed tooth with a weakly recurved crown bearing a sharply pointed apex. The tooth is the largest and tallest in the row, but is considerably smaller and lower (relatively and absolutely) than that in P. elegans, and the crown is somewhat procumbent, rather than vertical. The canine differs further from that of P. elegans in having a well-developed posterobasal cuspule.

Lower premolars: p1: The p1 in Peradectes pauli is similar, albeit smaller, to that of P. elegans in anatomy and orientation. The tooth is two-rooted with an elongate, laterally compressed protoconid and a simple, unicuspid heel. The crown of p1 is strongly procumbent, projecting forward such that the anterior margin of the crown abuts the posterior part of the canine. The anterior root is smaller than the posterior root, and both are directed ventrally and somewhat posteriorly. A well-developed crest extends posteriorly from the apex of the protoconid to the heel; a shorter crest, also originating at the apex, extends a short distance anteriorly. As in P. elegans, a short diastema is developed between p1 and p2.

p2: The p2 is nearly twice the height of p1, and the crown is more nearly erect, rather than procumbent. A high, trenchant protoconid and a low but conspicuous heel dominate the crown. The protoconid is labiolingually compressed and keeled anteriorly and posteriorly by sharp crests. The paraconid is virtually undeveloped, being incorporated into the sharp paracristid. The talonid is low, approximately one-fourth the height of the protoconid, and is connected to the postvallid wall by a short, high crest. A talonid basin is not developed.

p3: The crown of p3 is much like that of p2, differing only in being anteroposteriorly shorter, the protoconid being slightly taller and more nearly vertical, and in having a more robust heel. The paraconid resembles that on p2, being almost wholly incorporated into the paracristid and terminating low on the anterolingual side of the protoconid. The talonid is taller and wider than that on p2, and its single cusp occurs slightly labial to the level of the apex of the protoconid, rather than being directly

posterior. The p3 on the left dentary of UALVP 46411 is of teratological interest: two teeth are developed at this locus, occurring side by side, and both within their own respective alveoli. The dentary bulges labially and lingually to accommodate the two teeth, and both have been shifted from the midline such that the longitudinal axis of the jaw passes between them. The more lingual of the two teeth is most similar to p3 in the right dentary of UALVP 46411, while the more labial is significantly different: the crown is wider and lower, more bulbous, and the heel is greatly reduced; a well-developed paraconid occurs anterolingual to the protoconid, a robust anterolabial cingulid is developed, and the posterior labial and lingual cingulids are reduced. Despite the differences in coronal anatomy between the labial and lingual p3s, the labial tooth is unlikely a retained dp3: the crown is premolariform, rather than molariform [where known, dp3 of primitive didelphimorphian marsupials is molariform, with a complete complement of well-developed trigonid and talonid cusps (e.g., dp3 of Protalphadon lulli and Alphadon marshi from the Lance Formation of Wyoming, see Clemens, 1966)].

Lower molars: The lower molars of Peradectes pauli are similar to those of P. elegans and most other peradectines in coronal anatomy: the trigonids are taller than the talonids, and support tall, sharp cusps; the talonids are anteroposteriorly short; the cristids obliquae join the trigonid walls labial to the level of the protocristid notch; and the entoconids and hypoconulids are subequal and closely appressed (Krishtalka and Stucky, 1983a). Unlike those in P. pusillus and P. elegans, the molar trigonids in P. pauli do not become increasingly taller, nor do the talonids become perceptibly broader from m1 to m3; rather, the trigonids are virtually equal in height, and the talonids remain as wide as, or slightly narrower than, the trigonids.

m1: The crown of m1 is subequal or slightly taller than that of p2 or p3; it is slightly smaller than either m2 or m3, and the talonid is shorter. The protoconid is the largest and tallest trigonid cusp, followed by the metaconid and low paraconid. The paraconid is subcircular in cross section, and is lower and less anterolingually projecting relative to that in Peradectes elegans. The metaconid is much lower than the protoconid, more anterior compared to that in P. elegans, and the protocristid is perpendicular, rather than oblique to the long axis; a corollary of the position of the metaconid is that the entoconid is less closely appressed to the postvallid wall, resulting in a talonid notch that

is broader than on molars of P. elegans. The entoconid and hypoconulid are closely appressed, sharing a common wall within the talonid basin (Krishtalka and Stucky, 1983a), and are separated from one another by a shallow notch.

m2-3: The crown of m2 and m3 is similar to that of m1, differing mainly in the trigonid being more anteroposteriorly compressed (the trigonid of m3 is slightly more compressed compared to that of m2), and the paraconid being more lingual, rather than anterolingual. The talonid on m2 can be somewhat broader than that on m1, but is never markedly wider than the trigonid, and the entoconid and hypoconulid are more closely appressed on m2-3 than they are on m1. The entoconid and hypoconid are subequal in height, and both are taller than the hypoconulid. Unlike that in Peradectes elegans, the hypoconulid on m2 and m3 in P. pauli is more erect and projects less posteriorly.

m4: The m4 trigonid in Peradectes pauli is more anteroposteriorly compressed than on m2 or m3. The metaconid is often positioned further anterior relative to that on m2 or m3, and the trigonid can appear somewhat skewed anterolingually. The talonid is labiolingually narrow, similar to m4 in other peradectids, and the talonid cusps are reduced in size and height; proportionately, the talonid on m4 of P. pauli is narrower than that in P. pusillus or P. elegans, and the cusps are considerably weaker. The entoconid and hypoconulid are closely appressed, and the hypoconid is more poorly developed relative to that in P. elegans; the entocristid is long, in accordance with the more anterior position of the metaconid.

Both anterior and posterior cingulids are present on m1-4, but neither continues appreciably labially. The anterior cingulid is well developed, whereas the posterior cingulid is more variable: the cingulid can be weak (e.g., UALVP 46417), similar to that in Peradectes elegans, or more robust (e.g., UALVP 46416, Figs. 4.3.1-4.3.3).

Discussion.—Peradectes pauli was based on two poorly preserved dentaries from the early Tiffanian (Ti2) Saddle Locality of Wyoming (Gazin, 1956). In his review of the late Paleocene mammals from the Judson and Brisbane localities of North Dakota, Holtzman (1978) suggested USNM 20879 and 20880 were likely individual variants of P. elegans, also known to occur at Saddle Locality. Although Krishtalka and Stucky (1983a) recognized P. pauli as a valid peradectid in their review of North American Paleogene marsupials (they were apparently either unaware of Holtzman's earlier

synonymization of P. pauli with P. elegans, or chose not to recognize it), most authors have nonetheless followed Holtzman's (1978) opinion (e.g., Rose, 1981). The more numerous and better-preserved specimens from DW-2 and Joffre Bridge, however, demonstrate that P. pauli is separable from P. elegans, and document a second occurrence of the two species at a single locality.

Although the teeth of Peradectes pauli and P. elegans, and to a lesser degree those of P. minor, exhibit similar linear dimensions, the three taxa are separable by subtle but consistent characters. The upper molars of P. elegans are less transverse relative to their length, appearing more nearly equilaterally triangular in occlusal outline, and generally exhibit stronger stylar cusps and conules than do those of P. pauli; the upper molars of P. minor, although transverse like those of P. pauli, differ in having stronger stylar cusps and conules. The crown of the lower canine of P. pauli is particularly interesting: it is smaller than that in P. elegans, more procumbent than vertical, and bears a conspicuous posterobasal accessory cusp. Given the strong similarities in the postcanine dentitions of P. pauli and P. elegans, the differences in canine coronal anatomy were initially thought to be attributable to sexual dimorphism, but such a phenomenon has not been recorded for any extinct peradectid (or extinct didelphimorphian), and dimorphism, when present, is most often expressed as differences in overall size or in other aspects of the osteology in Recent didelphimorphians (Ventura et al., 1998; Tague, 2003).

In addition to its occurrence at DW-2 and Joffre Bridge, P. pauli is also known from the earliest Tiffanian (Ti1) Cochrane 2 locality of Alberta (Youzwyshyn, 1988), as well as from the late middle Tiffanian (Ti4) Gao Mine locality (pers. obs.).

Family uncertain

Genus TYPHLODELPHYS new genus

Type and only known species.—Typhlodelphys gordi new species.

Diagnosis.—As for the type and only species.

Etymology.—Typhlos, Greek, blind, in reference to the Blindman River; delphys, Greek, womb, a common suffix for marsupial genus nomina.

TYPHLODELPHYS GORDI new species

Figure 4.4

Diagnosis.—Differs from all other didelphimorphian marsupials in having P2 and P3 with an incipient metacone. Differs further from other didelphimorphians except some Stagodontidae in having a single-rooted P1. Differs from Peradectes in having upper molars that are more transverse, with deeper ectoflexi, vestigial or absent stylar cusp C, with a strong parastylar-metastylar interlock, and a single-rooted P1. Differs from Nanodelphys McGrew, 1937 in being larger, in having better developed stylar cusps A, D, and E, in having a weaker stylar cusp B, and in having stronger conules. Differs from Didelphidae in upper molar centrocrista being straight and not labially deflected. Differs from Alphadontidae in having much weaker stylar cusps and a relatively more anteroposteriorly compressed protocone. Differs from Stagodontidae in being smaller, in having an uninflated P3, and in having a relatively larger molar paracone and a more compressed protocone.

Description.—Maxilla: Although the maxilla in UALVP 43007 is poorly preserved and distorted, a number of important features can be discerned. The infraorbital foramen is mostly crushed, but appears to have opened dorsal to the posterior root of P2 and the anterior root of P3. The maxillary root of the zygomatic arch is relatively small, although it spans the distance between the anterior root of M4 and the anterior root of M2, and the lateral surface of the maxilla presents a long jugal facet that runs anterodorsally-posteroventrally above the level of the molars. Judging by the extent of the facet on the maxilla, the jugal must have been a large element in Typhlodelphys, and had a broad exposure on the side of the skull, not unlike that in skulls of Didelphis virginiana. The palatal process of the maxilla is well preserved at the level of the upper canine and premolars, but becomes increasingly poorly preserved posteriorly. A short ridge of smoothly finished bone medial and slightly posterior to M4 may represent the lateral margin of a palatal vacuity.

Upper canine: The upper canine is known only from its alveolus. Although the alveolus is incomplete, the dimensions of the parts preserved indicate that the upper canine was greatly enlarged, much more so than that in Peradectes elegans (see Simpson,

1935, fig. 3), elongate, and bilaterally compressed. The walls of the alveolus do not bear evidence of the canine root having been subdivided (incipiently or otherwise), and the orientation and trajectory of the alveolus suggest that the upper canine was not procumbent, nor did it splay laterally.

Upper premolars: P1: As with the upper canine, the P1 of Typhlodelphys is known only from its alveolus. Diastemata are not developed, either between P1 and the upper canine or between P1 and P2. In contrast to most other didelphimorphian marsupials, P1 in Typhlodelphys was single rooted, a feature otherwise known only in advanced stagodontids (Lofgren, 1992; Fox and Naylor, 1986; Fox and Naylor, 2006); the alveolar walls bear no crests that might indicate that the P1 root was incipiently divided. The alveolus is circular in outline and vertically set in the maxilla, implying that P1 was not procumbent.

P2: The P2 of Typhlodelphys is two-rooted and the crown is undoubtedly larger than that of P1; in contrast to that in Peradectes elegans, P2 is notably smaller than P3 in Typhlodelphys (P2 and P3 are subequal in P. elegans; Simpson, 1935). The crown is extremely compressed labiolingually, bladelike in labial or lingual view, and is but half the width of P3. The crown is dominated by a tall, trenchant paracone, the apex of which is positioned slightly anterior to the midpoint of the crown. A short, weak ridge extends anteriorly from the paraconal apex to the base of the crown, but an anterior basal cuspule is not developed there. A longer and more robust ridge is present posteriorly, and a distinct swelling suggestive of an incipient metacone is developed just posterior to the paraconal apex; a posterobasal cusp is not present. A weak cingulum wraps around the posterolabial and posterolingual parts of the crown, but both fade away anteriorly.

P3: The P3 of Typhlodelphys is significantly larger and higher crowned than P2, and although the parts of the maxilla housing the canine and premolars have been twisted relative to those housing the molars, the P3 was clearly the tallest postcanine tooth. The crown is long and subovate in occlusal view, and bears a tall, trenchant paracone. Neither an anterior ridge nor an anterobasal cuspule is developed. A robust posterior ridge extends from the paraconal apex to the posterior margin of the crown where it unites with the basal cingulum; as on P2, an incipient metacone is present on the posterior ridge, but it is relatively larger and better differentiated than on P2, with shallow sulci

developed between the paracone and metacone labially and lingually. Prominent cingula are developed anteriorly and posteriorly, and although they weaken slightly towards the mid-length of the crown, they are continuous labially and lingually.

Upper molars: The upper molars in UALVP 43007 are well preserved, but are deeply worn, especially the protocones, which are completely erased on M1-3. The crown of M1 is nearly equilaterally triangular in occlusal outline, being only slightly wider transversely than long anteroposteriorly, and with prominent parastylar and metastylar lobes separated by a sharply defined ectoflexus. The metastylar lobe flares much farther labially than does the parastylar lobe. Cusp B is the largest and tallest of the stylar cusps, followed in order of decreasing size and height by cusps A and D; stylar cusps C and E are undeveloped. Stylar cusp A is set off on an anteriorly projecting parastylar spur, and arises from a level slightly lower than that of cusp B; a notch separates cusps A and B, and a trough-like wear facet has been scoured into the deepest part of the notch. Cusp B is labial of the paracone; a low preparacrista extends anterolabially from the paraconal apex, but terminates before reaching cusp B. Cusp D arises from the ectocingulum labial of the metacone. The metacone is larger and taller than the paracone, but the disparity in size and height between these cusps is not as pronounced as it is in M1 of P. elegans. The centrocrista is deeply notched and straight in occlusal view, and shows no deflection towards the labial margin of the crown; the postmetacrista is extremely long and sweeping. A robust paracingulum extends from the level of the paraconule to stylar cusp A, whereas the metacingulum is undeveloped. The conules, conular cristae, protocone, and protoconal cristae have been completely erased by wear, leaving a nearly horizontal facet in their place.

M2: The crown of M2 is more transverse than that of M1, and forms a near isosceles triangle in occlusal outline. The parastylar and metastylar lobes are more pronounced and more nearly equal than on M1, both in terms of size and their labial extent, and the ectoflexus is considerably deeper. As on M1, cusp B is the largest and tallest of the stylar cusps on M2, with cusps A and D smaller and lower; cusps C and E are undeveloped. Cusp A is set off on an anterior parastylar spur that abuts the labial part of the metastylar corner of M1. The paracingulum is weaker than that on M1, and the metacingulum is not present. A deep, trough-like wear facet is developed between cusps

A and B. Although the protocone and conules have been worn flat, the dimensions of the protoconal base indicate it was probably at least the same size as that on M1.

M3: The M3 of Typhlodelphys closely resembles M2, but is larger and more transverse, and the parastylar and metastylar lobes are even more pronounced and separated by a deeper ectoflexus; the parastylar lobe curls around the metastylar lobe of M2. In contrast with M1 and M2, stylar cusps A and B on M3 are subequal, with cusp A arising from a relatively higher position; cusp D is small, and cusps C and E are undeveloped. The protocone is notably less worn than on M2: it was probably subequal to the paracone in height, and was more anteroposteriorly compressed than on M1 or M2. Little can be said of the conules and their associated conular cristae. The paracingulum extends to cusp A, while the metacingulum is undeveloped.

M4: The crown of M4 is smaller than that of M2 or M3, but not greatly so, and is characteristically asymmetrically triangular in occlusal outline, with an elongate parastylar lobe and greatly reduced metastylar area. Although the stylar shelf is slightly damaged labial of the paracone, a shallow ectoflexus can be discerned labial to the deepest part of the centrocrista notch, and the parastylar lobe curls around the metastylar lobe of M3. Stylar cusps A and B are subequal in size and height, and both are more poorly developed than on the other upper molars; a long preparacrista extends from the paraconal apex to cusp B. Stylar cusps C, D, and E are undeveloped. The metacone is considerably smaller than the paracone, although the disparity is accentuated by heavier wear on the metacone. The protocone is anteroposteriorly compressed and approximately the same height as the paracone, but both of these cusps are lower than those on the other upper molars (as inferred by the dimensions of the bases of the worn molar protocones). Strip-like wear facets occur on the protoconal cristae, with a basin-like facet on the preprotoconal crista probably representing the remnants of the paraconule; a metaconule likely was not developed.

Etymology.—Gordi, in reference to Gordon P. Youzwyshyn and in recognition of his contributions to mammalian paleontology and to the UALVP collections.

Holotype.—UALVP 43007, incomplete left maxilla with P2-3, M1-4, and alveoli for C, P1 (Fig. 4). DW-2 locality, Paskapoo Formation of Alberta, late Paleocene [early

middle Tiffanian, Ti3 (Fox, 1990), Plesiadapis anceps/P. rex Lineage Zone of Lofgren et al., 2004].

Age and occurrence.—Type locality only.

Discussion.—The teeth of Typhlodelphys exhibit a curious mixture of primitive and derived didelphimorphian characters, and are unlike those of any of North American Early Tertiary marsupial so far discovered. The crowns are very transverse relative to their lengths, and the deep ectoflexus and flaring parastylar and metastylar lobes are more like upper molars of Late Cretaceous marsupials, particularly those of the late Santonian alphadontid Albertatherium Fox, 1971, and the Late Cretaceous stagodontids, particularly Eodelphis Matthew, 1916 and Didelphodon Marsh, 1889, than those of any peradectid. In contrast, the greatly reduced stylar cusps, in combination with the enlarged paracone, seem derived compared to those features in Late Cretaceous taxa, and are more consistent with early Tertiary peradectids. The unusual coronal anatomy of Typhlodelphys is so divergent from that of contemporaneous marsupials that classification in a separate family may be warranted, but such action is not taken presently; a better understanding of the phylogenetic position of Typhlodelphys must await recovery of additional specimens.

4.3 Conclusions

Peradectid Diversity in the Paleocene of North America

The relationships of early Tertiary North American marsupials, both to each other and to possible Late Cretaceous relatives, have not been systematically explored since Krishtalka and Stucky's (1983a) review, and although an analysis of this sort is well beyond the scope of the present chapter, a few comments on current views of peradectid relationships are warranted in light of the new information from the present sample. Krishtalka and Stucky (1983a) suggested that the coronal anatomy of Peradectes elegans characterized the primitive peradectid (an opinion supported by Johanson, 1996a-b), with P. pauli being derived in having wider upper molars with a more highly compressed protocone. Although P. pauli is almost certainly derived in its lower canine morphology, being more nearly premolariform rather than caniniform [compare, e.g., with lower

canines of the alphadontid Protalphadon lulli (Clemens, 1966)], the polarity of upper molar width and protocone compression is debatable. As Johanson (1996a) correctly noted, the putative dental plesiomorphies recognized by Krishtalka and Stucky (1983a) for P. elegans were based on a broadly construed Alphadon, a genus that has since been significantly revised (Cifelli, 1990; Johanson, 1996a), with Protalphadon Cifelli, 1990 now being considered among the most basal alphadontids (Johanson, 1996a; Kielan-Jaworowska et al., 2005). Under this new paradigm, the molars of P. elegans would be considered derived, being narrower relative to their length, and in having anteroposteriorly expanded protocones [although Johanson (1996a) recognized this dilemma, she chose to accept P. elegans as the primitive peradectid nonetheless, based on other criteria]. The new information from the Blindman River sample further complicates matters: the upper molars of P. pauli, although having somewhat smaller stylar cusps and a more compressed protocone relative to those in P. elegans (derived, fide Krishtalka and Stucky, 1983a), show a lower disparity in L/W ratio from M1 to M3 (primitive; a greater disparity in L/W ratio from M1 to M3 is supposedly derived, and is exhibited by one of the putatively most derived peradectids, P. chesteri (Gazin, 1952)). Acceptance of Krishtalka and Stucky's (1983a) phylogeny implies a wholesale reversal in the L/W ratios of M1 through M3 from P. elegans (Krishtalka and Stucky, 1983a, fig. 6, node 3; L/W ratios decrease from M1 through M3), to P. pauli (Krishtalka and Stucky, 1983a, fig. 6, node 5; L/W ratios are nearly equal from M1 through M3), to other geologically younger species of Peradectes (Krishtalka and Stucky, 1983a, fig. 6, node 6; L/W ratios decrease from M1 through M3), a scenario for which there is no supporting evidence. In addition to the L/W proportions of the upper molars of P. pauli being closer to those of basal alphadontids, they compare favourably with those of stratigraphically older species of Peradectes as well, including P. pusillus and the recently described P. minor. It is noted here that although the formal treatment of P. minor by Clemens (2006) includes a diagnosis (and the name is therefore available by the standards of the International Commission on Zoological Nomenclature), the diagnosis, although sufficient in differentiating P. minor from near-contemporaneous species of Peradectes, including P. pusillus and P. sp., cf. P. pusillus, does not adequately differentiate P. minor from other species of Peradectes. For example, the teeth of P. minor, although clearly

smaller than those of P. pusillus or P. sp., cf. P. pusillus, are of nearly identical size to those of P. elegans (see measurements in Matthew and Granger, 1921; Simpson, 1935; Krishtalka and Stucky, 1983a; Fox, 1983; this chapter) and P. pauli (see measurements in Gazin, 1956; this chapter); while P. minor may be separated from congeners on the basis of characters other than size, these differences are not explicit in the diagnosis, suggesting, although not conclusively, that short, wide upper molars may in fact be primitive for didelphimorphian marsupials. As is evident from this brief examination of upper molar structure, the evolution of North American peradectids is more complex than has been appreciated, and a revision of peradectid systematics is badly needed (an opinion shared by Clemens, 2006).

The North American record of early Tertiary didelphimorphian marsupials has been historically depicted as one of low taxonomic diversity and relatively few numbers of specimens. In the 23 years since Krishtalka and Stucky's (1983a) analysis of Paleocene and Eocene North American didelphimorphians and the resulting phylogeny, the only new evidence that can potentially be brought to bear on early Tertiary North American marsupial systematics consists of a new genus and species of herpetotheriine, Swaindelphys cifellii Johanson, 1996b, from the Torrejonian of Wyoming, and a new species of Peradectes, P. minor, from the Puercan of Montana. Although the published record plainly supports the notion that marsupials are poorly represented in the Early Tertiary compared to contemporaneous multituberculates and eutherians, the unpublished record, often cited in papers dealing with faunal analyses over the past 25 years, contains tantalizing evidence of a much greater marsupial diversity. Of particular importance are the studies of Standhardt (1980), Taylor (1984), and Buckley (1994) that report the occurrence of marsupials of Puercan age from the San Juan Basin of New Mexico and the Crazy Mountains Basin of south central Montana (see summaries in Williamson, 1996), and the discovery of a new species of Swaindelphys from the Torrejonian of New Mexico (T. E. Williamson, pers. comm., 2007). Clearly, a better understanding of the taxonomic diversity and geographic distribution of early Tertiary marsupials in North America must await publication of these results. The results of this study indicate that by early middle Tiffanian time, three species of didelphimorphian marsupials in two genera were present in Alberta, and that two of these (Peradectes elegans, P. pauli) range as far back as the

earliest parts of the Tiffanian (Youzwyshyn, 1988). The herpetotheriine Swaindelphys is presently known only from one locality, Swain Quarry, from the late Torrejonian of Wyoming, and the enigmatic Typhlodelphys from but one locality in the early middle Tiffanian of Alberta; clearly, a much longer evolutionary history of these taxa is implied, but documentation of this record remains elusive. The picture painted by these studies, however, is one of greater marsupial diversity during the earliest parts of the Tertiary in North America than is currently acknowledged, and that the dramatic decline in marsupial diversity and numbers through the K/T boundary may be less severe than previously appreciated.

4.4 Literature Cited

APLIN, K. P., and M. ARCHER. 1987. Recent advances in marsupial systematics with a syncretic classification. In M. ARCHER (ed.), Possums and Opossums: Studies in Evolution, Volume 1, xv–lxxii. Surrey Beatty and Sons Pty Limited, Chipping Norton, New South Wales.

ARCHIBALD, J. D. 1982. A study of Mammalia and geology across the Cretaceous-Tertiary boundary in Garfield County, Montana. University of California Publications in Geological Science, 122:11-286.

ARCHIBALD, J. D. 1996. Testing extinction theories at the Cretaceous-Tertiary boundary using the vertebrate fossil record, pp. 373-398. In N. MACLEOD and G. KELLER (eds.), The Cretaceous-Tertiary Mass Extinction: Biotic and Environmental Changes. W. W. Norton & Co., New York.

ASHER, R. J., I. HOROVITZ, and M. R. SÁNCHEZ-VILLAGRA. 2004. First combined cladistic analysis of marsupial mammal interrelationships. Molecular Phylogenetics and Evolution, 33:240-250.

BLOCH, J. I. 2001. Mammalian paleontology of freshwater limestones from the Paleocene-Eocene of the Clarks Fork Basin, Wyoming. Unpublished Ph. D. dissertation, The University of Michigan, Ann Arbor, 358 pp.

BOWN, T. M., and K. D. ROSE. 1979. Mimoperadectes, a new marsupial, and Worlandia, a new dermopteran, from the lower part of the Willwood Formation (early

Eocene), Bighorn Basin, Wyoming. Contributions from the Museum of Paleontology, The University of Michigan, 25: 89-104.

BUCKLEY, G. A. 1994. Paleontology, geology, and chronostratigraphy of the Simpson Quarry (early Paleocene), Bear Formation, Crazy Mountains Basin, south-central Montana. Unpublished Ph. D. dissertation, Rutgers University, 430 pp.

CASE, J. A., and M. O. WOODBURNE. 1986. South American marsupials: a successful crossing of the Cretaceous-Tertiary boundary. Palaios, 1:413-416.

CASE, J. A., F. J. GOIN, and M. O. WOODBURNE. 2004. "South American" marsupials from the Late Cretaceous of North America and the origin of marsupial cohorts. Journal of Mammalian Evolution, 11:223-255.

CIFELLI, R. L. 1990. Cretaceous mammals of southern Utah. I. Marsupials from the Kaiparowits Formation (Judithian). Journal of Vertebrate Paleontology, 10:295-319.

CIFELLI, R. L. 2004. Marsupial mammals from the Albian-Cenomanian (Early-Late Cretaceous) boundary, Utah. Bulletin of the American Museum of Natural History, 285:62-79.

CIFELLI, R. L., T. B. ROWE, W. P. LUCKETT, J. BANTA, R. REYES, and R. I. HOWES. 1996. Origin of marsupial pattern of tooth replacement: fossil evidence revealed by high resolution X-ray CT. Nature, 379:715-718.

CLEMENS, W. A. 1966. Fossil mammals of the type Lance Formation, Wyoming. Part II. Marsupialia. University of California Publications in Geological Sciences, 62:1-122.

CLEMENS, W. A. 1968. Origin and early evolution of marsupials. Evolution, 22:1-18.

CLEMENS, W. A. 1979. Marsupialia, pp. 192-220. In J. A. LILLEGRAVEN, Z. KIELAN-JAWOROWSKA, and W. A. CLEMENS (eds.), Mesozoic Mammals: The First Two-Thirds of Mammalian History. University of California Press, Berkeley, California.

CLEMENS, W. A. 2006. Early Paleocene (Puercan) peradectid marsupials from northeastern Montana, North American Western Interior. Palaeontographica Abteilung A, 277:19-31.

COPE, E. D. 1873. Third notice of the extinct Vertebrata from the Tertiary of the Plains. Palaeontological Bulletin, 16:1-8.

CROCHET, J.-Y. 1977a. Les Didelphidae (Marsupicarnivora, Marsupialia) holarctiques tertiares. Comptes rendus hebdomadaires des séances de l'Académie des sciences, Série D, 284:357-360.

CROCHET, J.-Y. 1977b. Les didelphidés paléocènes holartiques: historique et tendances évolutives. Géobios, mémoire special, 1:124-134.

CROCHET, J.-Y. 1979. Diversité systématique des Didelphidae (Marsupialia) Européens Tertiares. Géobios, 12:365-378.

CROCHET, J.-Y. 1980. Les marsupiaux du Tertiaire d'Europe. Éditions de la Fondation Singer-Polignac, Paris, 279 pp.

CROCHET, J.-Y. and B. SIGÉ. 1993. Les mammifères de Chulpas (Formation Umayo) transition Crétacé-Tertiare, Pérou: donnes préliminaries. Documents d'Laboratoire de Géologie Lyon, 125:97-107.

EATON, J. G. 1993. Therian mammals from the Cenomanian (Upper Cretaceous) Dakota Formation, southwestern Utah. Journal of Vertebrate Paleontology, 13:105-124.

EBERLE, J. J., and J. A. LILLEGRAVEN. 1998. A new important record of earliest Cenozoic mammalian history: geologic setting, Multituberculata, and Peradectia. Rocky Mountain Geology, 33:3-47.

FOX, R. C. 1971. Marsupial mammals from the early Campanian Milk River Formation, Alberta, Canada, pp. 145-164. In D. M. KERMACK and K. A. KERMACK (eds.), Early Mammals. Zoological Journal of the Linnean Society, 50, supplement to no. 1, London.

FOX, R. C. 1983. Notes on the North American Tertiary marsupials Herpetotherium and Peradectes. Canadian Journal of Earth Sciences, 20:1565-1578.

FOX, R. C. 1987. Palaeontology and the early evolution of marsupials, pp. 161-169. In M. ARCHER (ed.), Possums and Opossums: Studies in Evolution, Volume 1. Surrey Beatty and Sons Pty Limited, Chipping Norton, New South Wales.

FOX, R. C. 1990. The succession of Paleocene mammals in western Canada, pp. 51-70. In T. M. BOWN and K. D. ROSE (eds.), Dawn of the Age of Mammals in the

Northern Part of the Rocky Mountain Interior, North America. Geological Society of America Special Paper 243.

FOX, R. C. 1997. Late Cretaceous and Paleocene mammals, Cypress Hills region, Saskatchewan, and mammalian evolution across the Cretaceous-Tertiary boundary, pp. 70-85. In L. MCKENZIE-MCANALLY (ed.), Upper Cretaceous and Tertiary Stratigraphy and Paleontology of Southern Saskatchewan. St. John's, Newfoundland, Canadian Paleontology Conference, Field Trip Guidebook No. 6, Geological Association of Canada (Paleontology Division).

FOX, R. C., and B. G. NAYLOR. 1986. A new species of Didelphodon Marsh (Marsupialia) from the Upper Cretaceous of Alberta, Canada: Paleobiology and phylogeny. Neues Jahrbuch für Geologie und Paläontologie-Abhandlungen, 172:357-380.

FOX, R. C., and B. G. NAYLOR. 2006. Stagodontid marsupials from the Late Cretaceous of Canada and their systematic and functional implications. Acta Palaeontologica Polonica, 51:13-36.

GAZIN, C. L. 1952. The Lower Eocene Knight Formation of western Wyoming and its mammalian faunas. Smithsonian Miscellaneous Collections, 117:1-82.

GAZIN, C. L. 1956. Paleocene mammalian faunas of the Bison Basin in south-central Wyoming. Smithsonian Miscellaneous Collections, 131:1-57.

GILL, T. 1872. Arrangement of the families of mammals with analytical tables. Smithsonian Miscellaneous Collections, 11:1-98.

GOIN, F. J., E. V. OLIVEIRA, and A. M. CANDELA. 1998. Carolocoutoia ferigoloi, n. gen. et sp. (Protodidelphidae), a new Paleocene "opossum-like" marsupial from Brazil. Palaeovertebrata, 27:145-154.

HERSHKOVTIZ, P. 1982. The staggered marsupial lower third incisor (I_3), pp. 191-200. In E. BUFFETAUT, P. JANVIER, J.-C. RAGE, and P. TASSY (eds.), Phylogénie et Paléobiogéographie. Livre Jubillaire en l'honneur de Robert Hoffstetter. Géobios Mémiore Spécial, 6.

HERSHKOVTIZ, P. 1995. The staggered marsupial third lower incisor: hallmark of cohort Didelphimorphia, and a description of a new genus and species with staggered i3

from the Albian (Lower Cretaceous) of Texas. Bonner Zoologische Beiträge, 45:153-169.

HOLTZMAN, R. C. 1978. Late Paleocene mammals of the Tongue River Formation, western North Dakota. Report of Investigation, North Dakota Geological Survey, 65:1-88.

HUXLEY, T. H. 1880. On the application of the laws of evolution to the arrangement of the Vertebrata, and more particularly of the Mammalia. Proceedings of the Zoological Society of London, 43:649-662.

ILLIGER, C. 1811. Prodromus systematis mammalium et avium additis terminis zoographicus utriusque classis. 301 pp. C. Salfeld, Berlin.

JOHANSON, Z. 1992. Revision of Late Cretaceous Alphadon. M. Sc. thesis, University of Alberta, Edmonton, 340 pp.

JOHANSON, Z. 1996a. Revision of the Late Cretaceous North American marsupial genus Alphadon. Palaeontographica Abteilung A, 242:127-184.

JOHANSON, Z. 1996b. New marsupial from the Fort Union Formation, Swain Quarry, Wyoming. Journal of Paleontology, 70:1023-1031.

JOHNSTON, P. A. 1980. First record of Mesozoic mammals from Saskatchewan. Canadian Journal of Earth Sciences, 17:512-519.

JOHNSTON, P. A., and R. C. FOX. 1984. Paleocene and Late Cretaceous mammals from Saskatchewan, Canada. Palaeontographica Abteilung A, 186:163-222.

KERR, R. 1792. The Animal Kingdom, or Zoological system, of the Celebrated Sir Charles Linnaeus. Class I. Mammalia: Containing a complete systematic description, arrangement, and nomenclature, of all the known species and varieties of the Mammalia, or animals which give suck to their young; being a translation of that part of the Systema Naturae, as lately published, with great improvements, by Professor Gmelin of Goettingen. Together with numerous additions from more recent zoological writers, and illustrated with copperplates. A. Strahan and T. Cadell, London, and W. Creech, Edinburgh.

KIELAN-JAWOROWSKA, Z., R. L. CIFELLI, AND Z.-X. LUO. 2004. Mammals from the Age of Dinosaurs. Columbia University Press, New York, 630 pp.

KOENIGSWALD, W. VON, and G. STORCH. 1998. Messel, ein Pompeji der Paläontologie. Thorbecke Species Band 2.

KORTH, W. W. 1990. Middle Tertiary marsupials (Mammalia) from North America Journal of Paleontology, 68:376-397.

KRISHTALKA, L. and R. K. STUCKY. 1983a. Paleocene and Eocene marsupials of North America. Annals of Carnegie Museum, 52:229-263.

KRISHTALKA, L. and R. K. STUCKY. 1983b. Revision of the Wind River faunas, early Eocene of central Wyoming. Part 3. Marsupialia. Annals of Carnegie Museum, 52:205-227.

LILLEGRAVEN, J. A. 1969. Latest Cretaceous mammals of upper part of the Edmonton Formation of Alberta, Canada, and a review of marsupial-placental dichotomy in mammalian evolution. The University of Kansas Paleontological Contributions, 50 (Vertebrata 12):1-122.

LILLEGRAVEN, J. A., and J. J. EBERLE. 1999. Vertebrate faunal changes through Lancian and Puercan time in southern Wyoming. Journal of Paleontology, 73:691-710.

LINNAEUS, C. 1758. Systema naturae per regna tria naturae, secundum classes, ordines, genera, species cum characteribus, differentiis, synonymis, locis. Editio decima, reformata. Laurenti Salvii, Stockholm.

LOFGREN, D. L. 1992. Upper premolar configuration of Didelphodon vorax (Mammalia, Marsupialia, Stagodontidae). Journal of Paleontology, 66:162-164.

LOFGREN, D. L. 1995. The Bug Creek problem and the Cretaceous-Tertiary transition at McGuire Creek, Montana. University of California Publications in Geological Sciences, 140:1-185.

LOFGREN, D. L., M. C. MCKENNA, and S. L. WALSH. 1999. New records of Torrejonian-Tiffanian mammals from the Paleocene-Eocene Goler Formation, California. Journal of Vertebrate Paleontology, 19, supplement to no. 3:60A.

LOFGREN, D. L., J. A. LILLEGRAVEN, W. A. CLEMENS, P. D. GINGERICH, and T. E. WILLIAMSON. 2004. Paleocene biochronology: The Puercan through Clarkforkian Land Mammal Ages, pp. 43-105. In M. O. WOODBURNE (ed.), Cenozoic Mammals of North America: Geochronology and Biostratigraphy, Columbia University Press, New York.

LUCAS, S.G. 1990. The extinction criterion and the definition of the class Mammalia. Journal of Vertebrate Paleontology, 10, supplement to no. 3: 33A.

LUO, Z.-X., Q. JI, J. R. WIBLE, and C.-X. YUAN. 2003. An Early Cretaceous tribosphenic mammal and metatherian evolution. Science, 302:1934-1940.

MARSH, O. C. 1889. Discovery of Cretaceous Mammalia. American Journal of Science, 38:81-92.

MARSHALL, L. G. 1987. Systematics of Itaboraian (middle Paleocene) age "opossum-like" marsupials from the limestone quarry at Sao Jose de Itaborai, Brazil, pp. 91-160. In M. ARCHER (ed.), Possums and Opossums: Studies in Evolution. Royal Zoological Society of New South Wales, Surrey Beatty and Sons Pty Limited, Chipping Norton, New South Wales.

MARSHALL, L. G., and C. DE MUIZON. 1988. The dawn of the age of mammals in South America. National Geographic Research, 4:23-55.

MARSHALL, L. G., J. A. CASE, and M. O. WOODBURNE. 1990. Phylogenetic relationships of the families of marsupials. Current Mammalogy, 2: 433-502.

MARSHALL, L. G., C. DE MUIZON, and D. SIGOGNEAU-RUSSELL. 1995. Pucadelphys andinus (Marsupialia, Mammalia) from the early Paleocene of Bolivia. Mémoires du Muséum national d'Histoire naturelle, 165:7-164.

MATTHEW, W. D. 1916. A marsupial of the Belly River Cretaceous. Bulletin of the American Museum of Natural History, 35:477-500.

MATTHEW, W. D. and W. GRANGER. 1921. New genera of Paleocene mammals. American Museum Novitates, 13:1-13.

MCGREW, P. O. 1937. New marsupials from the Tertiary of Nebraska. Journal of Geology, 45:448-455.

MCKENNA, M. C. 1960. Fossil Mammalia from the early Wasatchian Four Mile fauna Eocene of northwest Colorado. University of California Publications in Geological Sciences, 37:1-130.

MCKENNA, M. C., and S. K. BELL. 1997. Classification of Mammals Above the Species Level. Columbia University Press, New York.

MIAO, D. 1991. On the origins of mammals, pp. 579-597. In H.-P. SCHULTZE and L. TRUEB (eds.), Origins of the Higher Groups of Tetrapods. Cornell University Press, Ithaca.

MONTELLANO, M. 1988. Alphadon halleyi (Didelphidae, Marsupialia) from the Two Medicine Formation (Late Cretaceous, Judithian) of Montana. Journal of Vertebrate Paleontology, 8: 378-382.

MUIZON, C. DE. 1992. La fauna de mamiferos de Tiupampa (Paleoceno Inferior, Formacion Santa Lucia), Bolivia, pp. 575-624. In R. SUAREZ-SORUCO (ed.), Fossils y facies de Bolivia, Vol. L Vertebrados. Revista de YPFB, Santa Cruz.

MUIZON, C. DE. 1998. Mayulestes ferox, a borhyaenoid (Metatheria, Mammalia) from the early Palaeocene of Bolivia. Phylogenetic and palaeobiologic implications. Geodiversitas, 20:19-142.

MUIZON, C. DE, and R. L. CIFELLI. 2001. A new basal "didelphoid" (Marsupialia, Mammalia) from the early Paleocene of Tiupampa (Bolivia). Journal of Vertebrate Paleontology, 21:87-97.

MUIZON, C. DE, R. L. CIFELLI, and R. CÉSPEDES PAZ. 1997. The origin of the dog-like borhyaenoid marsupials of South America. Nature, 389:486-489.

PARKER, T. J., and HASWELL, W. A. 1897. A Text-book of Zoology. Volume 2. Macmillan Press, London, 301 pp.

PAULA COUTO, C. DE. 1970. News on the fossil marsupials from the Riochican of Brazil. Anales de la Acadamia Brasiliera de Ciencias, 42:19-34.

REIG, O. A., J. A.W. KIRSCH, and L. G. MARSHALL. 1987. Systematic relationships of the living and neocenozoic American "opossum-like" marsupials (suborder Didelphimorphia), with comments on the classification of these and of the Cretaceous and Paleogene New World and European metatherians, pp. 1-89. In M. ARCHER (ed.), Possums and Opossums: Studies in Evolution, Volume 1. Surrey Beatty and Sons Pty Limited, Chipping Norton, New South Wales.

ROSE, K. D. 1981. The Clarkforkian Land Mammal Age and mammalian faunal composition across the Paleocene-Eocene boundary. University of Michigan Papers on Paleontology, 26:1-197.

ROUGIER, G. W., J. R. WIBLE, and M. J. NOVACEK. 1998. Implications of Deltatheridium specimens for early marsupial history. Nature, 396:459-463.

SETOGUCHI, T. 1978. Paleontology and geology of the Badwater Creek area, central Wyoming. Part 16. The Cedar Ridge local fauna (late Oligocene). Bulletin of Carnegie Museum of Natural History, 9:1-61.

SIGÉ, B. 1971. Les Didelphoidea de Laguna Umayo (Formation Vilquechico, Crétacé Supérieur, Pérou), et le peuplement marsupial d'Amérique du Sud. Comptes rendus hebdomadaires des séances de l'Académie des sciences, Série 2, 273:2479-2481.

SIGÉ, B. 1972. La faunule de mammifères du Crétacé Supérieur de Laguna Umayo (Andes péruviennes). Bulletin du Muséum national d'Histoire naturelle de Paris, 99, Sciences de la Terre, 19:375-409.

SIGÉ, B., T. SEMPERE, R. F. BUTLER, L. G. MARSHALL, and J.-Y. CROCHET. 2004. Age and stratigraphic reassessment of the fossil-bearing Laguna Umayo red mudstone unit, SE Peru, from regional stratigraphy, fossil record, and paleomagnetism Géobios, 37:771-794.

SIMPSON, G. G. 1927. Mesozoic Mammalia. VIII. Genera of Lance mammals other than multituberculates. American Journal of Science, Series 5, 14:121-130.

SIMPSON, G. G. 1935. The Tiffany fauna, upper Paleocene. I. Multituberculata, Marsupialia, Insectivora, and ?Chiroptera. American Museum Novitates, 795:1-19.

SIMPSON, G. G. 1945. The principles of classification and a classification of mammals. Bulletin of the American Museum of Natural History, 85: 14-350.

SIMPSON, G.G. 1967. The beginning of the age of mammals in South America. Part II. Bulletin of the American Museum of Natural History, 137:1-260.

STANDHARDT, B. R. 1980. Early Paleocene mammals of the Black Toe local fauna, Nacimiento Formation, New Mexico. Unpublished M. Sc. thesis, University of Arizona, Tucson, 109 pp.

STOCK, C. 1936. Sespé Eocene didelphids. Proceedings of the National Academy of Science, 22:122-124.

STORER, J. E. 1996. Eocene-Oligocene Faunas of the Cypress Hills Formation, Saskatchewan, pp. 240-261. In D. R. PROTHERO and R. J. EMRY (eds.), The Terrestrial Eocene-Oligocene Transition in North America, Cambridge University Press, Cambridge, Massachusetts.

SZALAY, F. S. 1982. A new appraisal of marsupial phylogeny and classification, pp. 621-640. In M. ARCHER (ed.), Carnivorous Marsupials. Royal Zoological Society of New South Wales, Sydney.

SZALAY, F. S. 1994. Evolutionary history of the marsupials and an analysis of osteological characters. Cambridge University Press, 481 pp.

TAGUE, R. G. 2003. Pelvic sexual dimorphism in a metatherian, Didelphis virginiana: implications for eutherians. Journal of Mammalogy, 84:1464-1473.

TAYLOR, L. H. 1984. Review of Torrejonian mammals from the San Juan Basin, New Mexico. Unpublished Ph. D. dissertation, University of Arizona, Tucson, 553 pp.

VAN VALEN, L. 1978. The beginning of the Age of Mammals. Evolutionary Theory, 4:45-80.

VENTURA, J., R. PEREZ-HERNANDEZ, and M. J. LOPEZ-FUSTER. 1998. Morphometric assessment of the Monodelphis brevicaudata group (Didelphimorphia: Didelphidae) in Venezuela. Journal of Mammalogy, 79:104-117.

WILLIAMSON, T. E. 1996. The beginning of the Age of Mammals in the San Juan Basin, New Mexico: biostratigraphy and evolution of Paleocene mammals of the Nacimiento Formation. Bulletin of the New Mexico Museum of Natural History, 8:1-141.

WILSON, G. P. 2005. Mammalian faunal dynamics during the last 1.8 million years of the Cretaceous in Garfield County, Montana. Journal of Mammalian Evolution, 12:53-76.

YOUZWYSHYN, G. P. 1988. Paleocene mammals from near Cochrane, Alberta. Unpublished M. Sc. thesis, University of Alberta, Edmonton, 484 pp.

Table 4.1.—Measurements and descriptive statistics for the lower dentition of Peradectes elegans Matthew and Granger from the early middle Tiffanian (Ti3) DW-2 locality, Paskapoo Formation, Alberta.

Element	P	N	OR	M	SD	CV
p1	L	1	0.9	—	—	—
	W	1	0.4	—	—	—
p2	L	1	1.3	—	—	—
	W	1	0.6	—	—	—
p3	L	4	1.2-1.4	1.30	0.08	6.28
	W	4	0.6	0.60	0	0
m1	L	4	1.5-1.6	1.55	0.06	3.72
	TrW	3	0.8	0.80	0	0
	TaW	4	0.8	0.80	0	0
m2	L	7	1.4-1.5	1.47	0.05	3.32
	TrW	6	0.9-1.0	0.92	0.04	4.45
	TaW	6	0.9-1.0	0.92	0.04	4.45
m3	L	6	1.4-1.7	1.57	0.10	6.59
	TrW	6	0.9-1.1	0.95	0.08	8.81
	TaW	6	0.9-1.2	1.00	0.13	12.65
m4	L	4	1.4-1.6	1.50	0.08	5.44
	TrW	4	0.9-1.0	0.93	0.05	5.41
	TaW	4	0.6-0.7	0.65	0.06	8.88

Table 4.2.—Combined measurements and descriptive statistics for the upper dentition of Peradectes pauli Gazin from the early middle Tiffanian (Ti3) DW-2, Joffre Bridge Roadcut lower level, and Joffre Bridge Mammal Site No. 1 localities, Paskapoo Formation, Alberta.

Element	P	N	OR	M	SD	CV
P3	L	1	1.4	—	—	—
	W	1	0.7	—	—	—
M1	L	1	1.4	—	—	—
	W	1	1.6	—	—	—
M2	L	6	1.4-1.6	1.48	0.10	6.63
	W	6	1.7-1.9	1.80	0.06	3.51
M3	L	3	1.3-1.5	1.40	0.10	7.14
	W	3	1.9	1.90	0	0

Table 4.3.—Combined measurements and descriptive statistics for the lower dentition of Peradectes pauli Gazin from the early middle Tiffanian (Ti3) DW-2 and Joffre Bridge Roadcut lower level localities, Paskapoo Formation, Alberta.

Element	P	N	OR	M	SD	CV
p1	L	2	0.8	0.80	0	0
	W	2	0.4	0.40	0	0
p2	L	2	1.1-1.2	1.15	0.07	6.15
	W	2	0.6	0.60	0	0
p3	L	3	1.1-1.2	1.13	0.06	5.09
	W	3	0.5-0.6	0.53	0.06	10.83
m1	L	4	1.4	1.40	0	0
	TrW	4	0.6-0.7	0.68	0.05	7.41
	TaW	4	0.7-0.8	0.75	0.06	7.70
m2	L	3	1.4-1.5	1.43	0.06	4.03
	TrW	3	0.8	0.80	0	0
	TaW	3	0.8-0.9	0.83	0.06	6.93
m3	L	3	1.3-1.4	1.37	0.06	4.22
	TrW	3	0.8	0.80	0	0
	TaW	3	0.7	0.70	0	0
m4	L	3	1.3-1.4	1.37	0.06	4.22
	TrW	3	0.8	0.80	0	0
	TaW	3	0.5-0.6	0.57	0.06	10.19

Figure 4.1.—1-9. Peradectes elegans Matthew and Granger from the early middle Tiffanian (Ti3) DW-2 locality, Paskapoo Formation, Alberta. 1-3, UALVP 46394, incomplete left maxilla with P3, M1-3 in 1, labial, 2, oblique lingual, and 3, occlusal view; 4-6, UALVP 16270, incomplete right dentary with i1-2, i4, p1-3, m1-3 in 4, labial, 5, lingual, and 6, occlusal view; 7-9, UALVP 46396, incomplete left dentary with p3, m1-4 in 7, labial, 8, lingual, and 9, occlusal view. Scale bars = 2 mm.

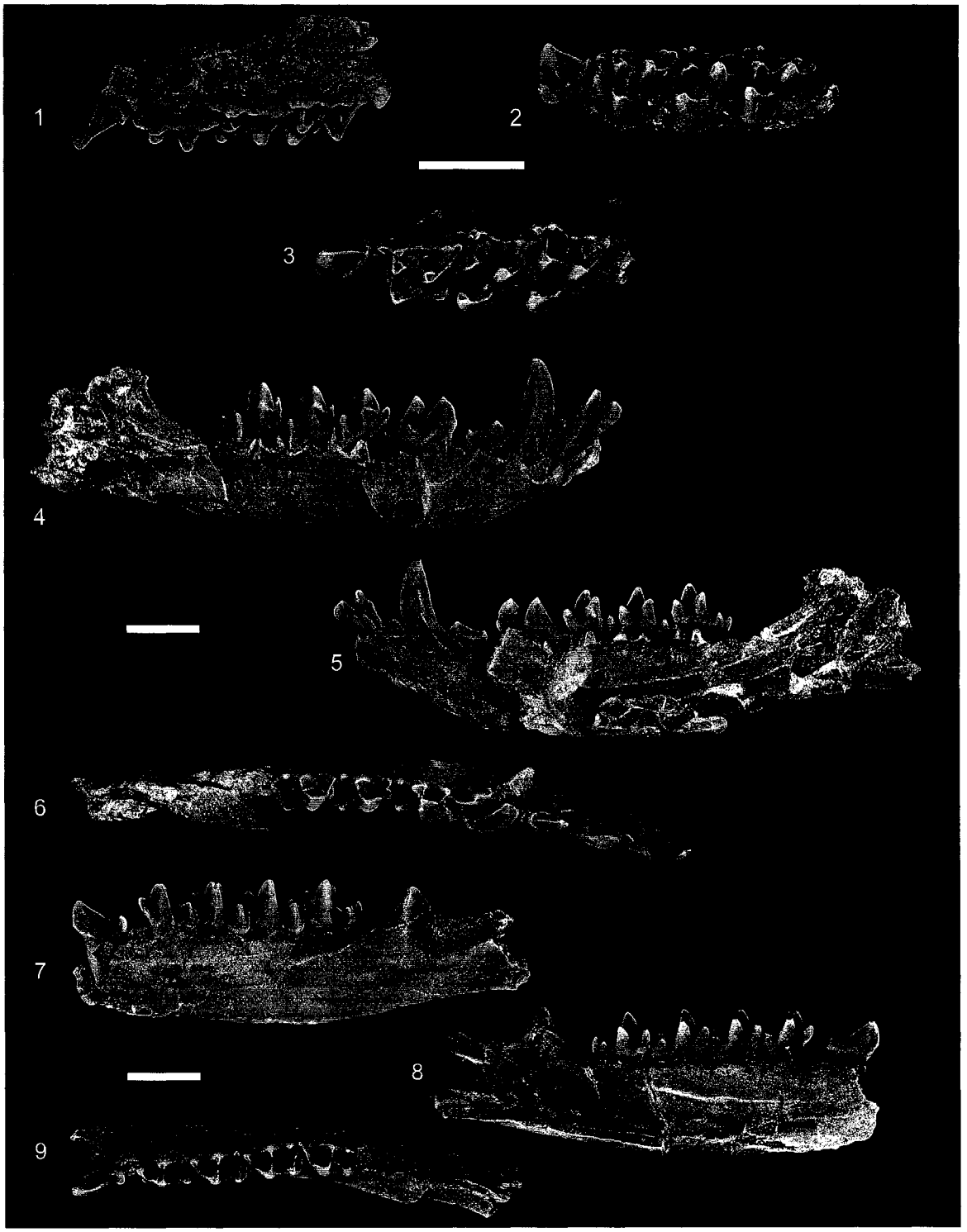
1
2
3
4
5
6
7
8
9

Figure 4.2.—1-3. Peradectes elegans Matthew and Granger from the early middle Tiffanian (Ti3) DW-2 locality, Paskapoo Formation, Alberta. 1-3, UALVP 46395, incomplete right dentary with p3, m1-4, and alveoli for c, p1-2 in 1, labial, 2, lingual, and 3, occlusal view.

4-20. Peradectes pauli Gazin from the early middle Tiffanian (Ti3) DW-2 (DW2) and Joffre Bridge Roadcut lower level (JBLL) localities, Paskapoo Formation, Alberta. 4-9, UALVP 46406 (DW2), incomplete right maxilla with P3 in 4, labial, 5, lingual, and 6, occlusal view, and associated incomplete right maxilla with M1-2 in 7, labial, 8, oblique lingual, and 9, occlusal view; 10-12, UALVP 46407 (DW2), incomplete right maxilla with M2 in 10, labial, 11, oblique lingual, and 12, occlusal view; 13-15, UALVP 46408 (JBLL), incomplete right maxilla with M2 in 13, labial, 14, oblique lingual, and 15, occlusal view; 16-17, UALVP 46409 (DW2), incomplete right maxilla with M2-3 in 16, labial and 17, occlusal view; 18-20, UALVP 46410 (DW2), incomplete left maxilla with M2-3 in 18, labial, 19, lingual, and 20, occlusal view.

Scale bars = 2 mm.

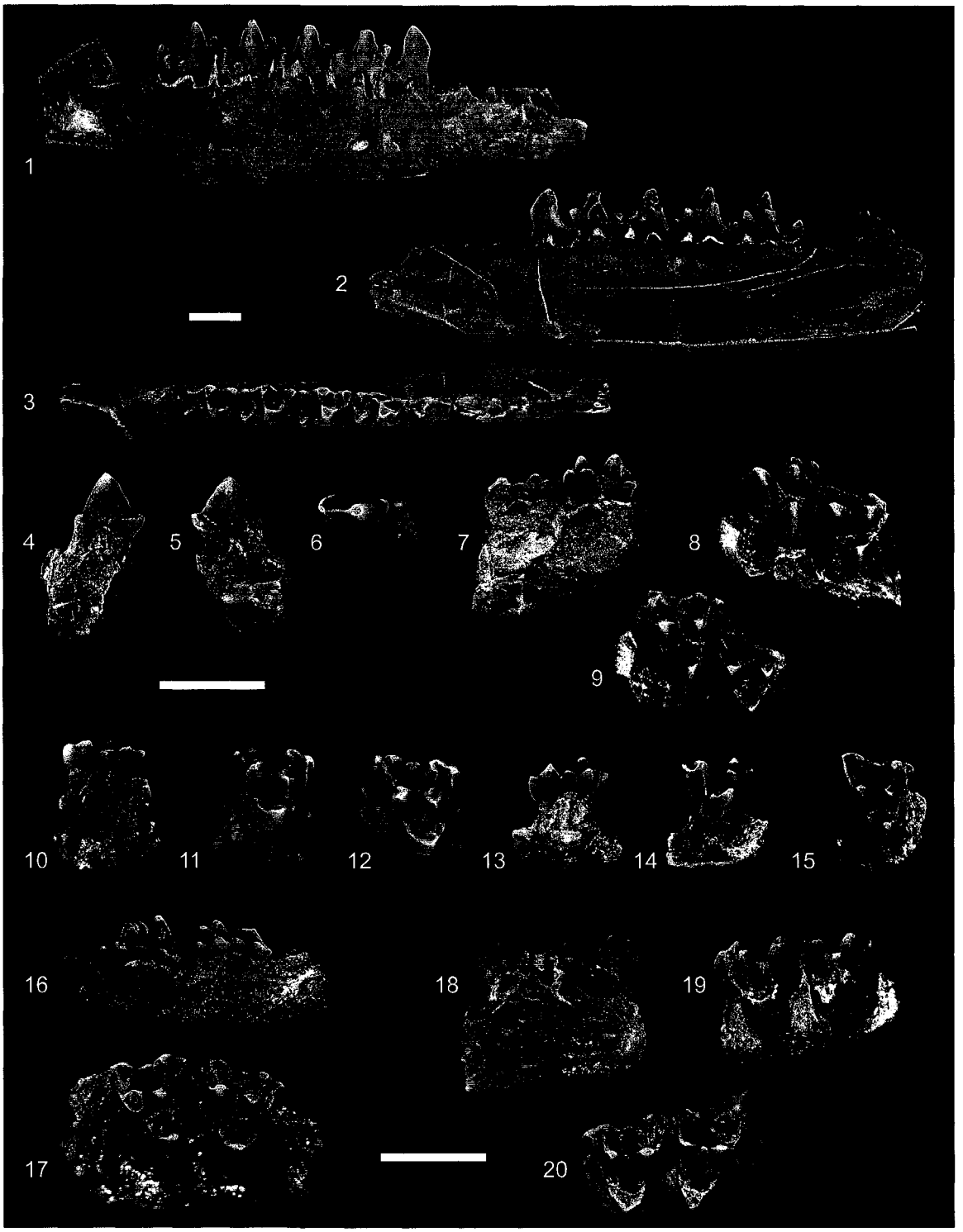
1
2
3
4
5
6
7
8
9
10
11
12
13
14
15
16
17
18
19
20

Figure 4.3.—1-9. Peradectes pauli Gazin from the early middle Tiffanian (Ti3) DW-2 (DW2) and Joffre Bridge Mammal Site No. 1 (JBMS) localities, Paskapoo Formation, Alberta. 1-3, UALVP 46416 (DW2), incomplete left dentary with p2-3, m1-4, and alveoli for c and p1 in 1, labial, 2, lingual, and 3, occlusal view; 4-9, UALVP 46411 (JBMS), incomplete right dentary with i1-4, c, p1-3 (p2 talonid only), m1-4 in 4, labial, 5, lingual, and 6, occlusal view, and associated incomplete left dentary with p1-3 (with labially positioned supernumerary p3), m1-4 in 7, labial, 8, lingual, and 9, occlusal view. Scale bars = 2 mm.

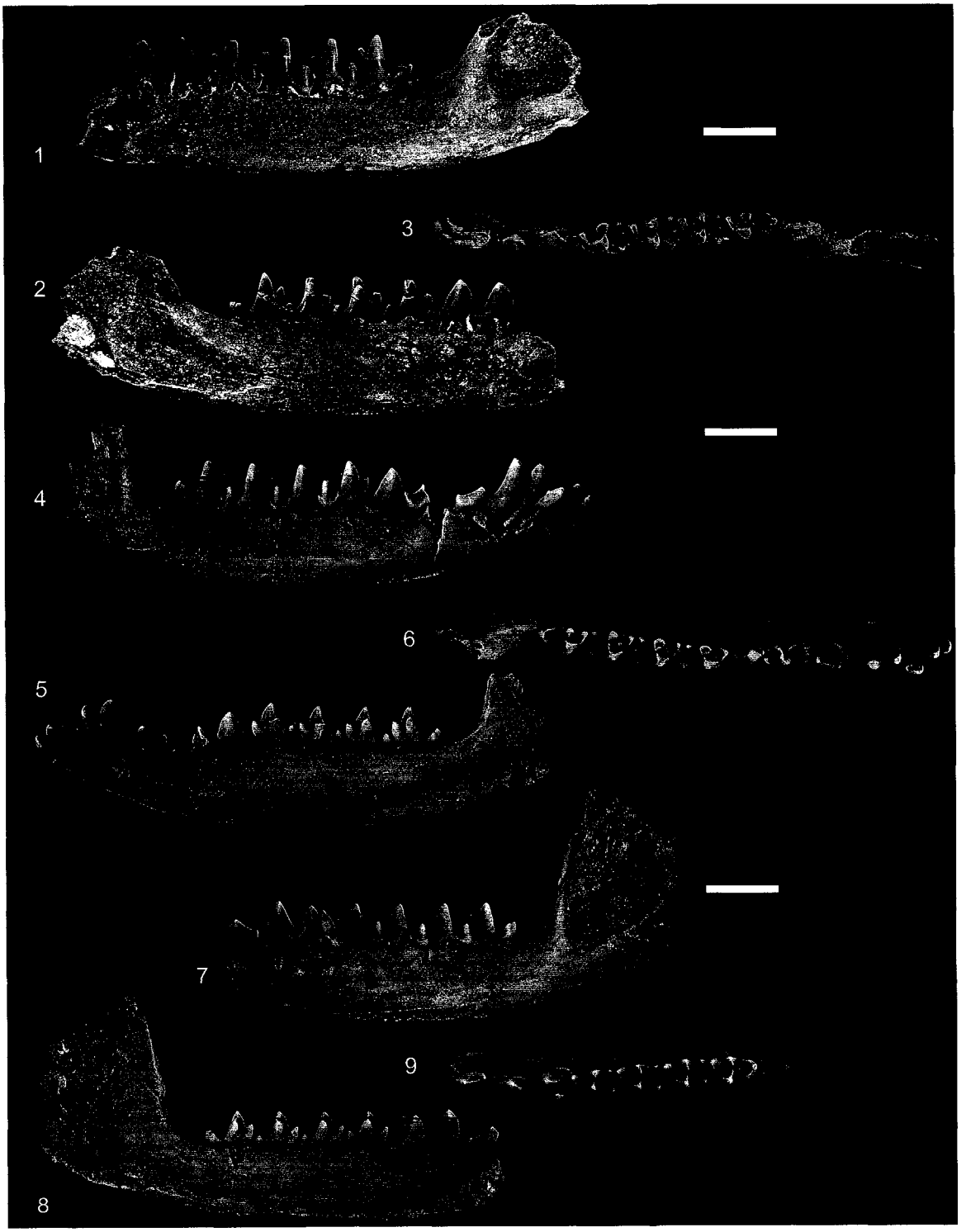
1
3
2
4
6
5
7
9
8

Figure 4.4.—1-3. Typhlodelphys gordi new genus and species from the early middle Tiffanian (Ti3) DW-2 locality, early middle Tiffanian (Ti3), Paskapoo Formation, Alberta. 1-3, UALVP 43007 (holotype), incomplete left maxilla with P3-4, M1-4, and alveoli for C and P1 in 1, labial, 2, occlusal (premolars), and 3, occlusal (molars) view. Scale bar = 2 mm.

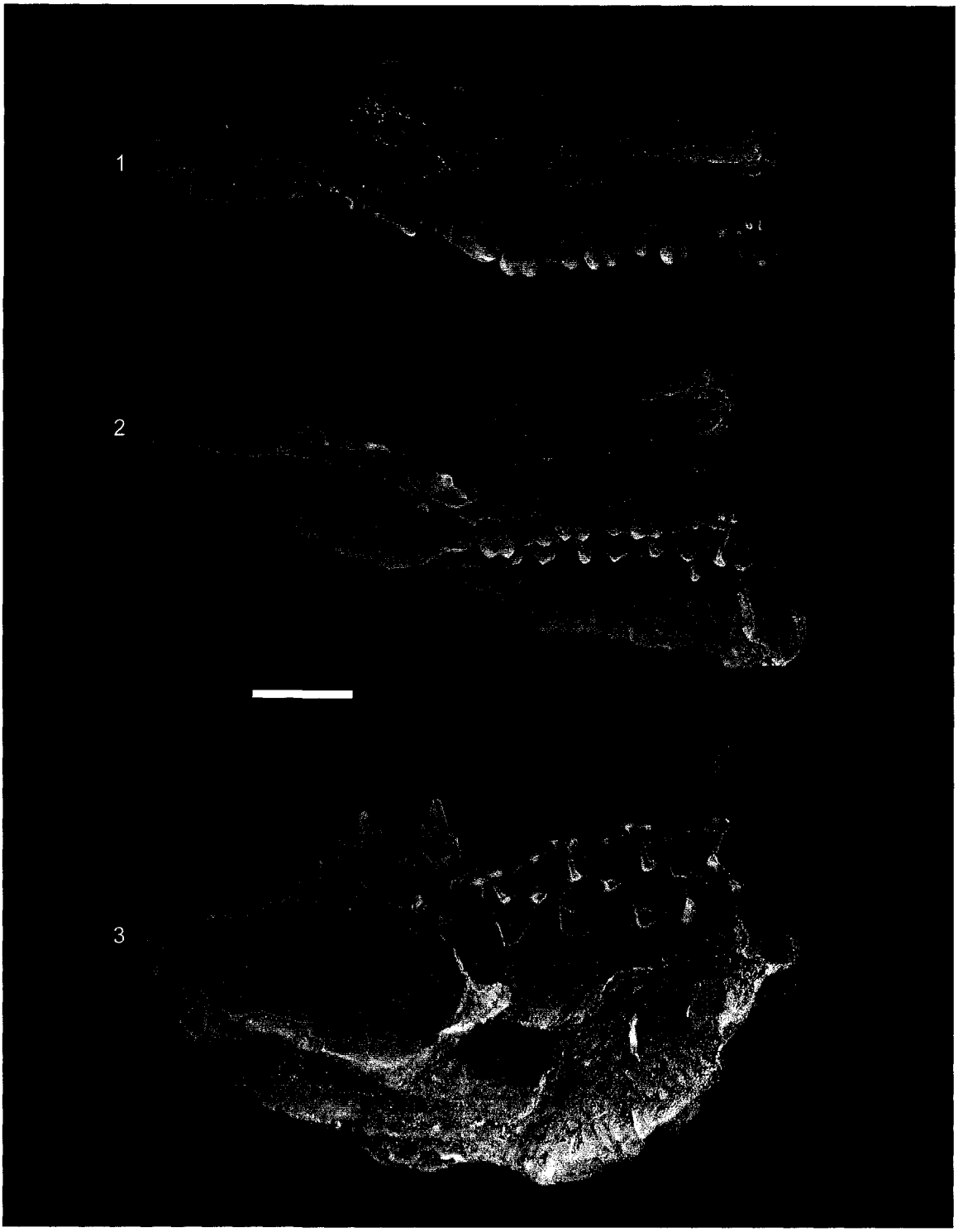
1
2
3

5 Insectivorans from the Late Paleocene of Alberta, Canada, and a Phylogenetic Analysis of the Earliest Lipotyphla[2]

5.1 Introduction

ALTHOUGH THE INSECTIVORA have long been a group of great interest to mammalogists, both neontologists and paleontologists alike, the advent of molecule-based phylogenetics in recent years has resulted in a remarkable increase in the number of publications, and controversies, regarding the systematics of this enigmatic group (see summary in Symonds, 2005). Extant insectivorans, represented only by the lipotyphlans [shrews, hedgehogs, moles, solenodons, and until relatively recently the tenrecs and golden moles; the nomen "Lipotyphla" is used here rather than the more recently proposed "Eulipotyphla" (e.g., Waddell et al., 1999) following the rationale of Archibald (2003)], are the third most taxonomically diverse group of living eutherian mammals, containing over 420 species in 60 genera (Nowak, 1999; Lopatin, 2005). As impressive as these figures are, however, the taxonomic bulk of Insectivora is extinct, with more than 250 genera so far discovered, and with a fossil record that extends back to the Paleocene, and very likely into the latest Cretaceous or earlier (McKenna and Bell, 1997). Despite nearly 250 years of research on extant and extinct insectivorans (see comprehensive summaries in Butler, 1972; Lopatin, 2005; Symonds, 2005), their phylogenetic relationships, and classifications derived from an understanding of these relationships, remain uncertain and often highly contentious, so much so that the title of Butler's (1972) summary of the state of affairs to date, "The problem of insectivore classification," seems as germane now as it did nearly 35 years ago.

Insectivora as currently construed (e.g., Lopatin, 2005) is a probably paraphyletic and/or polyphyletic group of small, shrew- or hedgehog-like mammals that were at one time considered to be of central importance in the evolution of Eutheria (see, e.g., Huxley 1880; Matthew 1909; Simpson 1945). As then conceived by Matthew (1909) and Simpson (1937a, 1945), Insectivora contained what are now recognized as lipotyphlans, as well as several Late Cretaceous and early Tertiary mammals that, while probably not

[2] Parts of this chapter have been published. Fox and Scott, 2005. Nature, 435:1091-1093.

ancestral to later insectivorans, share specializations that suggest a closer affinity to lipotyphlans (Insectivora, sensu stricto, see Butler, 1972, 1988) than to other eutherians (e.g., Zalambdalestes Gregory and Simpson, 1926, Pantolestidae, Leptictidae, Palaeoryctidae). The suite of primitive characters possessed by insectivorans prompted Matthew (1909) to designate the group as the "central stock" from which other placental mammals might have ultimately evolved, and while Simpson (1937a, 1945) endorsed this opinion, he noted the possible artificiality of the Insectivora, particularly when fossil groups are considered. Attempts have been made at solving the problem of insectivoran classification, including placing many of the constituent groups into an acknowledged "wastebasket" insectivoran taxon, the "Proteutheria" (see, e.g., Romer, 1966; Van Valen, 1967; Butler, 1972), to a complete abandonment of Insectivora in favour of dispersing the constituent groups among other higher-level taxa (e.g., McKenna and Bell, 1997). Many authors, however, continue to use the name Insectivora (sensu Novacek 1986) to acknowledge the lack of phylogenetic resolution among insectivoran mammals, but recognizing a central Lipotyphla and a number of extinct mammals whose phylogenetic positions may be closer to Lipotyphla than to other eutherians (e.g., Bloch, Secord, and Gingerich, 2004; Fox, 2004; Asher, 2005; Lopatin, 2005). Depending on one's point of view, recent molecular studies have either helped to clarify or further muddle some of the higher-level relationships of extant insectivorans; the results, while unexpected, are often well-supported (e.g., Stanhope et al., 1998; Murphy, Eizirik, Johnson et al., 2001; Murphy, Eizirik, O'Brien et al., 2001; Madsen et al., 2001; Douady et al., 2002; Asher et al., 2003). Under this new paradigm, Lipotyphla as traditionally understood is polyphyletic, with the endemic African tenrecoids (the tenrecids and chrysochlorids) forming a clade with other African mammalian groups (the Afrotheria of Stanhope et al., 1998), and the remaining lipotyphlans (including the Caribbean Solenodon Brandt) forming a clade of closely related Holarctic taxa. Although these groupings are unexpected when considering morphology alone, they have been consistently supported in molecular studies, as well as in so-called "total evidence" analyses that have combined morphological (from both extant and extinct taxa) and molecular data sets (see, e.g., Asher et al., 2003).

Although the taxonomic core of Insectivora consists of Lipotyphla and their fossil relatives [Lipotyphla is here used sensu Asher (2005), explicitly excluding the tenrecoids (the so-called zalambdodont lipotyphlans, but including Solenodon)], other extinct, enigmatic groups such as the Pantolesta, Palaeoryctidae, Apatotheria, and Didymoconida have also been included in Insectivora at one time or another (e.g., Simpson, 1945; McDowell, 1958; Van Valen, 1967; Butler, 1972, 1988; Lopatin, 2005; Bloch, Secord, and Gingerich, 2004); most of these groups have been more recently referred to other, higher level taxa, with many being classified in the Cimolesta, a purported clade of disparate (anatomically and probably phylogenetically) eutherians that are believed to be more closely related to the didelphodontine Cimolestes Marsh, 1889 than to other eutherians (McKenna, 1975; McKenna and Bell, 1997). As discussed by Rose (2006), however, evidence for the monophyly of this group is weak, as is evidence for monophyly of Cimolestes itself (e.g., Fox and Youzwyshyn, 1994). Given these uncertainties, three of the major groups included in Cimolesta, the Pantolesta, Apatotheria, and Palaeoryctidae, are included in this chapter; their affinities with other insectivorans are unclear, however, and they are referred here to Insectivora incertae sedis.

Evidence to date points to the Paleocene as having been an important episode in the early evolutionary history of the Insectivora (see summary in Rose, 2006): the interval saw the emergence of a number of early putative lipotyphlan taxa, including the possible establishment of at least one of the living lipotyphlan families, the Erinaceidae (Krishtalka, 1976a; Novacek, 1985; Novacek et al., 1985), as well as a diversification of insectivoran groups that were previously poorly represented (e.g., pantolestids, pentacodontids, leptictids, apatemyids). Insectivorans are often among the best represented mammals in local faunas of late Paleocene age (e.g., Jepsen, 1930; Rose, 1981a-b; Youzwyshyn, 1988; Gunnell, 1989; Fox, 1990; Krause and Maas, 1990; Webb, 1996; Bloch, 2001; Scott, 2003; Secord, 2004), although their small size and generally fragile skeletons often result in specimens being recovered that are extremely fragmentary or otherwise unidentifiable. Exquisite fossils from the Blindman River and Joffre Bridge localities are exceptions to this general rule: these specimens represent some of the best preserved and most nearly complete insectivoran fossils known from the

early Tertiary, and document parts of the craniodental, gnathic, and even postcranial anatomy of these small mammals. The objectives of this chapter are two-fold:
1) Document and describe the insectivoran fauna from the Blindman River and Joffre Bridge localities. Many of these taxa are new at the specific and generic levels, while a number of previously but poorly known taxa (e.g., "Leptacodon" munusculum Simpson, 1935a) are well-represented at these localities.
2) Investigate the phylogenetic relationships of the earliest lipotyphlans. Lipotyphlans are among the best represented of the insectivorans at the Blindman River and Joffre Bridge localities, and their exceptional preservation allows the incorporation of data that have otherwise not been available for phylogenetic investigation. In an attempt to understand better the evolutionary relationships of stem lipotyphlans, cladistic methodology is used to establish a phylogenetic hypothesis, incorporating osteological data from the study specimens, as well as those from other important localities from the Western Interior of North America.

5.2 Systematic Paleontology

Class MAMMALIA Linnaeus, 1758
Subclass THERIA Parker and Haswell, 1897
Infraclass EUTHERIA Gill, 1872
Superorder INSECTIVORA Bowdich, 1821 (sensu Novacek, 1986)
Order LIPOTYPHLA Haeckel, 1866
Suborder uncertain
Family GEOLABIDIDAE McKenna, 1960

Genus LIMACONYSSUS Gingerich, 1987

Limaconyssus GINGERICH, 1987, p. 304.

Type species.—Limaconyssus habrus Gingerich, 1987.

Other included species.—Limaconyssus incomperta new species; Limaconyssus subnuba new species.

Revised diagnosis.—Differs from Batodon Marsh, 1892 in having a much better developed p4 paraconid, in having relatively lower molar trigonids with anteroposteriorly compressed, blade-like paraconids, and in having a relatively smaller m3. Differs from Centetodon Marsh, 1872 in having a single-rooted p1, in having a lower and less blade-like p3, in p4 having a stronger paraconid and longer talonid, and in having slightly lower molar paraconids. Differs from Batodonoides Novacek, 1976 in being significantly larger, in having a larger p4 paraconid and better developed, multicuspate talonid, and in having better developed molar paraconids. Differs from all nyctitheriids in having p4 with a narrower talonid basin, relatively taller and more nearly vertical molar trigonids, and lower molar paraconids.

LIMACONYSSUS INCOMPERTA new species

Figure 5.1; Table 5.1

Limaconyssus sp.: YOUZWYSHYN, 1988, p. 108.
Limaconyssus sp. 1: STONLEY, 1988, p. 112.
Limaconyssus sp.: FOX, 1990, p. 59.
"Leptacodon" munusculum SIMPSON, 1935: SCOTT, 2003, p. 753 (in part).

Diagnosis.—Differs from Limaconyssus habrus in being smaller (mean length m1, L. incomperta approximately 21 percent shorter than length m1, L. habrus), and in having a relatively lower molar metaconid. Differs from L. subnuba (see later in the text) in being smaller (mean length m1, L. incomperta approximately 40 percent shorter than mean length m1, L. subnuba); differs further from L. subnuba in having a more prominent p3 paraconid and a relatively longer p4 talonid.

Description.—Dentary and lower dentition (Figs. 5.1.1-5.1.18): The dentary of Limaconyssus incomperta is known in several specimens, with UALVP 47279 and 47283 preserving most of the horizontal ramus, and UALVP 47279 preserving parts of the

coronoid process; the condylar and angular processes, as well as the condyle, are unknown. The long and slender horizontal ramus is extremely gracile, and achieves maximum depth at the level of p4 or m1. Two mental foramina are developed labially: the larger and more anterior of the foramina is ventral to the level of p2, while the smaller and more posterior foramen occurs ventral to the posterior root of p3; both foramina open laterally and anteriorly. The symphysis is poorly defined, being limited dorsally by only a feeble ridge of bone; the articular surface extends posteriorly to the level of the p1 alveolus, and consists of a small area of smooth bone. Taken together, the features of the symphysis suggest the two mandibular rami were only loosely connected in life, and that a considerable range of independent motion between the two was probably possible. Parts of the coronoid process are preserved in UALVP 47279: the process arises from the horizontal ramus at an angle of approximately 115 degrees from the horizontal, and it is weakly excavated laterally and medially.

Lower incisors: Although none of the lower incisor crowns of Limaconyssus incomperta is preserved in the present sample, alveoli for three lower incisors are present in UALVP 47279. The alveoli are striking in that they are considerably enlarged relative to the rest of the dentition (e.g., the dimensions of the i2 alveolus are nearly equivalent to those of p1). The alveolus for the medial incisor is mediolaterally compressed, and the aperture is oriented parallel to the symphyseal surface, opening almost directly anteriorly. The i2 alveolus is considerably larger than that for i1, more nearly circular in outline, and opens anterodorsally. The alveolus for the lateral incisor is slightly smaller than that for i2, is similarly circular in outline, but opens more dorsally than anteriorly. The dimensions and positions of the alveoli indicate that the lower incisors were procumbent and imbricated, with the anterior parts of the each successive tooth probably overhanging the posterior parts of the more anterior tooth.

Lower canine: The lower canine is represented only by its alveolus in UALVP 47279. The alveolus is larger than that for i3, slightly compressed mediolaterally, and separated from the i3 alveolus by a short diastema. The size and orientation of the lower canine alveolus suggest that the tooth was enlarged, probably slightly procumbent, and with its anterior parts overhanging the posterior part of i3.

Lower premolars: p1: The p1 alveolus of Limaconyssus incomperta is separated from the canine alveolus by a diastema that is slightly longer than that separating i3 from the lower canine. Other than its slightly smaller dimensions, the p1 alveolus closely resembles that for the lower canine.

p2: The two-rooted p2 is preserved only in UALVP 47279. The elongate crown is strongly compressed anteriorly, broadening only slightly posteriorly, and is dominated by a trenchant protoconid and a low heel. While a small paraconid was probably present originally, it has since been broken off; a metaconid is not developed. A poorly defined crest extends posteriorly from the protoconid apex to the low, unicuspid heel, and a conspicuous lingual cingulid extends a short distance anteriorly from the heel cusp.

p3: The p3 of Limaconyssus incomperta is only slightly larger than p2, but is otherwise similarly compressed. As with p2, the crown of p3 is dominated by a tall, sharp protoconid and a low talonid. A low but prominent, conical paraconid is developed well anterior of the protoconid at the summit of a robust cingulid; the paraconid is connected to the apex of the protoconid by a sharp, deeply notched paracristid. The anterior cingulid is short and relatively weak labially, but is much better developed lingually, running posteriorly along the base of the protoconid to the talonid where it defines the lingual margin of a shallow basin. The talonid is unicuspid, consisting only of a low hypoconid that is set off slightly labial to the anteroposterior midline; a prominent cristid obliqua extends from the hypoconid to the postvallid wall, and then continues dorsally to the protoconid apex. Exodaenodonty can be developed at the posterior root.

p4: The p4 of Limaconyssus incomperta is nearly twice the size of p3, but is similarly labiolingually compressed. As in other species of Limaconyssus, the p4 trigonid of L. incomperta bears tall, sharp cusps, and the talonid is very narrow and somewhat skewed labially. The protoconid is strongly compressed anteroposteriorly and is the tallest of the trigonid cusps: its basin-facing wall is virtually flat, its apex is recurved, and it is connected to the paraconid by a sharp paracristid. A conical metaconid arises from low on the posterolingual face of the protoconid: although the two cusps are connate for approximately half of their respective heights, the apices are well separated from one another, and a sulcus extending from the deep protocristid notch into

the trigonid basin further defines the two cusps. The metaconid is smaller and lower than the protoconid, and its apex projects dorsally and lingually. The paraconid is slightly larger than the metaconid: it arises from low on the anterior side of the protoconid, and although a sharp and deeply notched paracristid connects the two cusps, the paraconid is distinctly set off anteriorly from the protoconid. A low, sharp crest runs posterolingually from the paraconid to the base of the metaconid, defining the lingual margin of a low trigonid basin. The talonid is long, with the narrow basin defined by the straight to slightly lingually convex entocristid and cristid obliqua. The talonid supports three cusps: the hypoconid is the largest and tallest talonid cusp, followed by a smaller and lower entoconid; the hypoconulid is usually weakly developed. The hypoconid is strongly compressed anteroposteriorly, whereas the entoconid and hypoconulid are more nearly conical; the entoconid and hypoconulid are displaced slightly labially from the lingual margin of the talonid, skewing the talonid labially. The cristid obliqua contacts the postvallid wall lingual to the level of the protocristid notch, forming a deep hypoflexid. The crown is strongly exodaenodont at the posteriorly root.

Lower molars: m1: The lower molars of Limaconyssus incomperta resemble those of L. habrus in leaning lingually, in having nearly vertical (rather than anteriorly leaning) trigonids, and in having tall trigonids and talonids bearing sharp cusps. As on p4, the lower molar entoconid is positioned slightly labial of the lingual margin of the crowns, and the talonid appears somewhat labially skewed.

The trigonid of m1 bears a tall, anteroposteriorly compressed protoconid, lower metaconid, and a low blade-like paraconid that together form a near-isosceles triangle in occlusal outline. A sharp paracristid extends from the protoconid apex to the lingual margin of the crown; the paraconid is fully incorporated into the paracristid, without even a swelling to suggest its presence. The paraconid/paracristid complex is low and blade-like, and leans somewhat anteriorly. The metaconid is subconical and leans lingually and posteriorly, widening the sharp protocristid notch. The talonid consists of three well-defined cusps that together enclose a deep basin. As on p4, the hypoconid on m1 is the largest and tallest talonid cusp, being strongly anteroposteriorly compressed; it is connected to the hypoconulid by a high, sharp hypocristid. The hypoconulid and entoconid are low and stubby, and are more nearly conical than the hypoconid; the two

cusps are connected by a low postcristid. The cristid obliqua contacts the postvallid wall lingual to the level of the protocristid notch, and can bear a faint mesoconid swelling. The entocristid is deeply notched. The anterior and posterior cingulids are prominent, although discontinuous labially; the posterior cingulid extends labially from the apex of the hypoconulid, forming a narrow shelf that often bears evidence of heavy wear. The crown is exodaenodont at the posterior root.

m2: The m2 of Limaconyssus incomperta is slightly smaller and lower crowned than m1, but the coronal morphology is otherwise similar. The m2 trigonid is more compressed anteroposteriorly than on m1, with the paraconid/paracristid complex more closely appressed to the protoconid, and the entoconid is displaced further labially, giving the talonid a more pronounced labial skew.

m3: The m3 is poorly preserved in UALVP 47279 and 47282. The crown is smaller and lower crowned than that of m1 or m2, and the talonid is narrower. The trigonid and talonid cusps are broken off in both specimens, but the parts that remain indicate that the trigonid on m3 was compressed to nearly the same degree as on m2, and that the protoconid and hypoconid were the largest trigonid and talonid cusps, respectively.

Etymology.—Incomperta, Latin, of which one has no information, unknown, in reference to the poorly understood early evolutionary history of Limaconyssus specifically, and the Geolabididae generally.

Holotype.—UALVP 47278, incomplete left dentary with p4, m1. DW-2 locality, Paskapoo Formation of Alberta, Canada, late Paleocene [early middle Tiffanian, Ti3 (Fox, 1990), Plesiadapis anceps/P. rex Lineage Zone of Lofgren et al., 2004].

Other material examined.—From DW-2: UALVP 47279, incomplete left dentary with p2-4, m1-2, and alveoli for i1-3, c, p1, m3; UALVP 47282, incomplete right dentary with p4, m1 (broken), m2-3; UALVP 47283, incomplete right dentary with m1-2 and alveoli for c, p1-4, m3; UALVP 47284, incomplete right dentary with p3-4 and alveoli for p1-2, m1; UALVP 47285, incomplete left dentary with p4 and alveoli for p1-3; UALVP 47286, incomplete left dentary with p4.

From Swan Hills Site 1: UALVP 22520, incomplete right dentary with m1 and alveoli for p4, m2.

From Cochrane 2: UALVP 47287, M1 or M2; UALVP 28523, 28524, p4; UALVP 28522, m1; UALVP 28521, m2.

LIMACONYSSUS SUBNUBA new species

Figure 5.1; Table 5.2

Limaconyssus sp. 2: STONLEY, 1988, p. 116.

Diagnosis.—Differs from Limaconyssus incomperta in being significantly larger (mean length m1, L. subnuba approximately 40 percent longer than mean length m1, L. incomperta). Differs from L. habrus in being slightly larger (mean length m1, L. subnuba approximately 12 percent longer than length m1, L. habrus); differs further from L. habrus in having slightly lower cusps, a p4 metaconid that is lower and more poorly differentiated from the protoconid, and molar talonids that are longer relative to their width.

Description.—The referred specimens are virtually identical to comparable teeth of Limaconyssus incomperta, but differing in being approximately 40 percent larger, in having generally more robust proportions, and in having a weaker lower premolar and molar paraconid. Better preserved and more nearly complete specimens of L. subnuba are known from the Gao Mine locality of Alberta and will be described elsewhere.

Etymology.—Subnuba, Latin, rival, in reference to the co-occurrence of two species of Limaconyssus at the Cochrane 2, DW-2, and Swan Hills localities.

Holotype.—UALVP 47813, incomplete right dentary with p3-4, m1-3 (m3 talonid only). Gao Mine locality, Paskapoo Formation of Alberta, Canada, late Paleocene [late middle Tiffanian, Ti4 (Fox, 1990), Plesiadapis anceps/P. rex Lineage Zone of Lofgren et al., 2004].

Other material examined.—From DW-2: UALVP 47288, incomplete left dentary with m2-3.

From Hand Hills West upper level: UALVP 35080, p4.

From Swan Hills Site 1: UALVP 23922, incomplete right dentary with m1-2.

From Cochrane 2: UALVP 28525, p4; UALVP 28526, m2.

Discussion.—Specimens pertaining to Limaconyssus incomperta were first described by Youzwyshyn (1988) in his comprehensive study on the earliest Tiffanian Cochrane 2 locality of Alberta; Youzwyshyn (1988) referred the specimens to an unnamed new species of Limaconyssus, and indicated that they represented the earliest record of the genus (which was known only from the type specimen of L. habrus from the Clarkforkian of Wyoming; see Gingerich, 1987). Stonley (1988), in his study of fossil mammals from the late middle Tiffanian Swan Hills locality of northern Alberta, identified two species of Limaconyssus in the local fauna; the first of these (Limaconyssus species 1) is referred here to L. incomperta, while the second (Limaconyssus species 2) is referred to L. subnuba. L. incomperta is also known from the middle Torrejonian (To2) Who Nose? locality of southern Alberta (Scott, 2003, erroneously referred to "Leptacodon" munusculum in that paper). The teeth of both new species of Limaconyssus are remarkably similar to comparable teeth of L. habrus, differing mainly in their smaller (L. incomperta) or larger (L. subnuba) size, and in having lower cusps and a slightly weaker p4 metaconid. Although Gingerich (1987) referred Limaconyssus to the Nyctitheriidae, the better preserved specimens of L. incomperta and L. subnuba from Alberta suggest that Limaconyssus is more appropriately referred to the Geolabididae (and see later in the text). In contrast to nyctitheriids, the lower molars of Limaconyssus bear tall trigonids and much lower talonids (the trigonids of nyctitheriids are much lower than are those of geolabidids), and the trigonids are nearly vertical, rather than anteriorly leaning. The p4 talonid is long and narrow, similar to that in Centetodon (see Lillegraven et al., 1981; Asher et al., 2005), and the p4 metaconid is tall and well-differentiated from the protoconid. In contrast to those of nyctitheriids, the molar paraconid is low, with the anteroposteriorly compressed and blade-like paraconid/paracristid well below the level of the metaconid (again, similar to that of Centetodon). Additional specimens from Gao Mine (to be described elsewhere) show the lower premolars of L. subnuba to be "askew" in the dentary (see Bloch et al., 1998), with the crowns of p2-4 oriented anterolingually-posterolabially, similar to those in a number of species of Centetodon (e.g., Centetodon marginalis Cope, 1873) and unlike those of any nyctitheriid.

With the new records of Limaconyssus from Alberta, the stratigraphic range of the genus now extends from middle Torrejonian (To2) to late Clarkforkian (Cf3), a span of nearly seven million years (Berggren et al., 1995; Cande and Kent, 1995). Should referral of Limaconyssus to the Geolabididae prove correct, the extensive stratigraphic "gap" between the ostensibly earliest geolabidid Batodon (Late Cretaceous; see Lillegraven et al., 1981) and the earliest undoubted geolabidid Centetodon (late Clarkforkian/earliest Wasatchian; Lofgren et al., 2004) would be significantly narrowed.

Suborder ERINACEOMORPHA Gregory, 1910

Family uncertain

Genus XYNOLESTES new genus

Type and only known species.—Xynolestes denommei new species.

Diagnosis.—As for the type and only species.

Etymology.—Xynos, Greek, common; lestes, Greek, thief. In reference to the abundance of specimens of Xynolestes in the UALVP Paleocene collections.

XYNOLESTES DENOMMEI new species

Figures 5.2-5.4; Tables 5.3, 5.4

Diagnosis.—Differs from most other erinaceomorphs in having a combination of cusps that are sharp, rather than lower and inflated, a better developed P4 metacone, a molar paraconid that arises from a relatively lower position on the trigonid, an angular cristid obliqua, and in lacking a molar postcristid. Differs further from Dartonius Novacek, Bown, and Schankler, 1985 in having a two-rooted p2, a larger p4 with a better developed talonid, and higher, more blade-like molar paraconids. Differs further from Scenopaginae, Sespedectinae, and Amphilemuridae in having the anterior upper and lower premolars being unreduced in size and root number and in having much weaker molar hypocones. Differs further from Diacocherus Gingerich, 1983 (including Adunator Russell, 1964 and Mckennatherium Van Valen, 1965) in having a weaker P4 protocone, a

more elongate and blade-like postmetacrista on P4 and upper molar, a narrower p4 talonid, lower molar trigonids, and in having a more blade-like molar paraconid/paracristid. Differs further from litocherines, litolestines, and adapisoricines in having less inflated cusps and weaker molar hypocones.

Description.—Maxilla and upper dentition (Fig. 5.1): Although parts of the maxilla are present in UALVP 40512, 40514, and 40516, each of the specimens is damaged and preserves little in the way of informative anatomy. The small, circular infraorbital foramen opens dorsal to P3, and is directed anteriorly and slightly laterally. The maxillary foramen, marking the opening of the infraorbital canal on the medial side of the maxilla, is not visible on any of the specimens at hand; hence, the length of the canal cannot be accurately determined. The relatively anterior position of the infraorbital foramen, however, suggests that the canal was long (compare with the position of the infraorbital foramen in, e.g., Leptictis Leidy, 1968 in which it opens dorsal to M1, or in Echinosorex Raffles, in which it is positioned dorsal to P4, both with an infraorbital canal that is considered short, see Novacek, 1986), a primitive eutherian feature (Muller, 1934; Butler, 1956; Novacek, 1986). The zygomatic process of the maxilla originates dorsal to the posterior parts of M2. A slightly bevelled facet on the dorsolateral surface of the zygomatic process represents the point of articulation with the jugal, suggesting that this bone in Xynolestes may have contributed to the anterior parts of the zygomatic arch, rather than being reduced or otherwise limited to the more posterior parts of the zygoma (MacPhee and Novacek, 1993).

Upper premolars: P2: The P2 of Xynolestes is two-rooted and consists of a tall and trenchant paracone connected to a small posterior cuspule by a sharp postparacrista; a small accessory cuspule is developed anteriorly.

P3: The P3 of Xynolestes is three-rooted and triangular in occlusal outline. The crown consists of a large, conical paracone that is swollen, especially at its base; the paraconal apex leans posteriorly. A sharp postparacrista extends from the paraconal apex to the posterolabial corner of the crown, where it joins the posterior cingulum and ectocingulum; a preparacrista is not present, although a small parastylar cusp can be developed at the junction of the ectocingulum and anterior cingulum. The metacone is variably developed: a prominent swelling on the postparacrista in UALVP 40512 marks

the position of the metacone, with a short but sharp indentation intervening between the paracone and metacone labially, and the metaconal apex is clearly separate from that of the paracone; on UALVP 46917, however, the metacone is virtually undeveloped, with barely any swelling on the postparacrista. The protocone is small and conical, nearly vertical, and is positioned directly lingual to the paracone. The protoconal cristae are strongly developed and continue labially past the paracone to the para- and metastylar corners of the crown. Protoconal cingula are not developed, and neither hypocone nor pericone is present.

P4: The P4 of Xynolestes is significantly larger than P3, and is subequal or slightly larger than M1. The crown is triangular in outline, with the labial margin oriented slightly obliquely to a line drawn through the apices of the paracone and metacone, and is somewhat "twisted" at the longitudinal midline, such that the paracone leans posteriorly and the protocone leans anteriorly. A large, conical paracone and a smaller and shorter protocone dominate the crown. A low but prominent parastylar cusp is developed on a spur-like parastylar lobe that is set off anteriorly from the paracone: the parastylar cusp is conical, swollen at its base, and is more nearly vertical than the paracone. A short crest extends posteriorly from the parastylar cusp towards the base of the paracone, but a preparacrista is not developed, and the sulcus between the parastylar cusp and paracone usually bears evidence of strong wear. The paracone is massive, occupying nearly two-thirds the width of the crown. A metacone is developed on the posterior shoulder of the paracone, and the two cusps are connate for nearly their entire height, with their apices connected by a shallowly notched centrocrista. As on P3, the metacone on P4 varies in size and distinctiveness: on most specimens it is relatively large, and a deep sulcus intervenes between it and the paracone labially, while on other specimens the metacone is smaller and more poorly defined (e.g., UALVP 46918), with only a shallow labial groove separating the two cusps. Irrespective of their sizes, the paracone and metacone are undivided lingually, and a groove or sulcus does not intervene between the two cusps. The postmetacrista is long and blade-like, and sweeps posterolabially to join the posterior cingulum and ectocingulum. A short, sharp protocone occupies the lingual third of the crown, and it bears well-developed cristae: the preprotoconal crista is high and sharp, and runs anterolabially to meet the parastylar cusp;

as in most other erinaceomorphs, the postprotoconal crista is much shorter than the preprotoconal crista, is vertical, and extends directly to the base of the protocone where it fades away before reaching the posterior cingulum. A third crest, considerably weaker than the protoconal cristae, extends labially from the protoconal apex to the lingual base of the paracone. Whereas the posterior cingulum is prominent, extending as a robust ridge from low on the posterior side of the protocone to the metastylar corner of the crown, the anterior cingulum is only weakly developed. Neither a hypocone nor pericone is present.

Upper molars: M1: The M1 is wide labially but narrows abruptly at the level of the conules, and the crown is subtrapezoidal in occlusal outline. A subconical paracone, metacone, and anteriorly leaning protocone dominate the crown; the trigon cusps enclose a deep, gulley-like trigon basin. The stylar shelf is narrow, although it widens somewhat posteriorly, and the ectoflexus is shallow. A low but robust ectocingulum meets the paracingulum anteriorly to form a prominent, anteriorly projecting parastylar spur. The paracone and metacone are both tall and sharp, although the paracone is the larger and more lingually extending cusp. A low preparacrista runs anterolabially from the paraconal apex, joining the ectocingulum and paracingulum; in contrast, the postmetacrista is higher than the preparacrista, and runs directly labially from the metaconal apex as a prominent blade. The centrocrista is sharp and deeply notched. The paraconule, metaconule, and conular cristae are well developed: the paraconule is more lingual than the metaconule, and its apex leans anteriorly, paralleling the protocone, whereas the metaconule is more nearly vertical. The paraconular cristae are higher than the metaconular cristae, and the preparaconular crista continues anterolabially as a sharp paracingulum, joining the ectocingulum+preparacarista; in contrast, the postmetaconular crista continues labially past the metacone as the metacingulum, but terminates well dorsal of the postmetacrista and does not join the ectocingulum (i.e., double-rank shear is achieved posteriorly, see Fox, 1975). The internal conular cristae are short but well-defined. The protocone is subequal in size with the paracone, but is lower, and its apex leans anteriorly and slightly labially. The protoconal cristae are high and sharp, with the postprotoconal crista forming a shallow notch just lingual of its union with the metaconule. The M1 bears strongly developed protoconal cingula: the low anterior

cingulum arises on the crown at the level of the paraconule and terminates just anterior to the protocone where a discrete pericone can be developed (e.g., UALVP 40516). The posterior cingulum forms a short but lingually bulging hypoconal salient that usually bears a small, bulbous hypocone (e.g., UALVP 40516).

M2: The M2 of Xynolestes is smaller than M1, although the difference in size is not as great as that between M1 and M2 of erinaceids (Novacek, 1985; Novacek et al., 1985). The crown of M2 resembles that of M1, but differs in being wider relative to its length, in having a deeper ectoflexus that divides the labial margin of the crown into nearly symmetrical halves, in having a more labially, rather than anteriorly, projecting parastylar spur, and in having weaker protoconal cingula, especially the anterior cingulum.

M3: The M3 of Xynolestes is considerably smaller than M1 and M2, and is smaller relative to M2 than M2 is to M1. The crown is asymmetrically triangular in outline, with the parastylar lobe projecting anterolabially and the metastylar lobe undeveloped. The ectocingulum is robust near the parastylar lobe but weakens as it approaches the metacone. The paracone is larger than the metacone, and a weak and widely notched centrocrista connects the apices of the two cusps; as with M1 and M2, the paraconule of M3 is slightly more lingual than the metaconule. The protoconal cingula are robust, but terminate more labially than those on M1 or M2.

Dentary and lower dentition (Figs. 5.3, 5.4): The dentary of Xynolestes is long and shallow, with little change in depth along the horizontal ramus until about the level of p4, where it narrows slightly. A pair of small, subovate mental foramina is usually developed: the more anterior foramen is positioned ventral to p2 in a deep recess, and opens anterolaterally and slightly dorsally; the more posterior foramen is ventral to the posterior root of p3 or anterior root of p4, is dorsoventrally compressed, and opens laterally. The symphysis is anteroposteriorly short, extending posteriorly from the anterior parts of the ramus and narrowing towards the level of p1 where it fades away. The articular surface consists of dorsal and ventral ridges of bone, with a smooth, shallowly concave surface between the two; there is no bony rugosities evident on the articular surface, and the opposing rami were clearly not synostosed in life. The posterior parts of the dentary are poorly preserved in the present sample, and very little can be said

of the coronoid, condylar, or angular processes. The coronoid process is best seen on UALVP 46953 and 46929, where it forms a nearly 90-degree angle with the horizontal ramus just posterior to m3; a faint ridge of bone marking the ventral extent of the temporalis fossa extends posteriorly from below m3 medially. The masseteric fossa is deeply excavated.

Lower incisors: Xynolestes possessed three lower incisors, as evidenced by several specimens preserving their alveoli (e.g., UALVP 46886); one specimen (UALVP 46923) preserves i2-3 associated with other parts of the lower dentition, and another (UALVP 46903) preserves i2-3 in articulation with the dentary. Although i1 is unknown, its alveolus in UALVP 46886 suggests that its root was at least equivalent in size to that of i2. The incisors are procumbent and are oriented parasagittally and slightly oblique to the rest of the tooth row, and the crowns appear imbricated in lateral view, with the more posterior tooth overlapping the more anterior tooth; the lower canine and p1 are also imbricated, although these teeth are in-line with the other premolars and molars (see later in this chapter). When the jaw is held in its presumed in-life position, with the articular surface of the symphysis oriented vertically, the concave occlusal surfaces of the lower incisor crowns face dorsally and somewhat medially. The i2 and i3 of Xynolestes closely resemble one another in being single-rooted, with anteroposteriorly elongate, mediolaterally compressed crowns. The crown of i2 and i3 consists of a single enlarged cusp with a blunt apex, and a small posterior cusp separated from the main cusp by a deep, U-shaped notch. Crests extend anteriorly and posteriorly from the main cusp: the more anterior crest turns abruptly mediad and posteriorly, forming a prominent medial cingulid, whereas the posterior crest runs a short distance towards the U-shaped notch before fading away. A short crest runs posteromedially from the accessory cusp, eventually joining the medial cingulid. The i3 differs from i2 only in its smaller size, in being relatively wider, and in being more shallowly rooted.

Lower canine: The single-rooted lower canine is procumbent and considerably larger than the lateral incisor, and the anterior part of the crown overlaps the posterior part of i3. The crown is elongate and somewhat rectangular in lateral view, with long and parallel dorsal and ventral slopes, and considerably shorter anterior and posterior margins. The crown consists of an enlarged principal cusp and small posterior cuspule;

the crown is mediolaterally compressed anteriorly, but broadens posteriorly. Two sharp crests originate at the canine apex: the more anterior of these crests extends anteroventrally for a short distance before fading away, while the posterior crest is longer and sharper, and connects the canine apex to the small posterior cuspule. A weak crest curves anteromedially from the heel, forming a short, low shelf.

Lower premolars (Figs. 5.3, 5.4.1-5.4.12): p1: The p1 of Xynolestes is single-rooted, procumbent, and virtually identical to the lower canine, differing only in its slightly smaller size and in having a better developed posteromedial shelf. As with the lower incisors and canine, p1 is procumbent, with its crown overlapping that of the lower canine.

p2: The two-rooted p2 closely resembles p1, but the crown is both larger and broader. The p2 varies considerably in crown height and lateral outline: in some specimens (e.g., UALVP 46886) the crown is as tall as that of the much larger p3, and is subrectangular in lateral view, whereas in others (e.g., UALVP 40511) it is lower, with a shorter posterior slope, and appears more nearly triangular in lateral view. Irrespective of its height, the p2 crown is procumbent and overlaps the posterior part of p1. The p2 crown differs from that of p1 principally in its larger size, in being slightly wider, and in having a relatively better developed, unicuspid heel; a weak anterior cuspule can be present. As with p1, a short shelf is developed posteromedially, and a weak interradicular crest is present on some specimens (e.g., UALVP 46958).

p3: The p3 of Xynolestes is elongate and labiolingually compressed, although in some specimens (e.g., UALVP 40511) the crown can broaden to a greater or lesser degree posteriorly, giving the tooth a weak teardrop-shaped occlusal outline. The crown bears a well-developed protoconid, a low paraconid, and a tiny, unicuspid heel. The crown leans anteriorly, lengthening the posterior slope, but the procumbency that characterizes the more anterior teeth is not developed to nearly the same degree on p3. The protoconid is tall and sharp, and its apex is connected to the much smaller and lower paraconid by a sharp crest; a stronger crest extends posteriorly from the protoconid apex, joining the low and slightly labially offset heel. There is no trace of a metaconid. Weak anterolabial and anterolingual cingulids can be developed. A short but conspicuous crest curves anterolingually from the heel cusp, defining a small, shallow basin that appears

somewhat labially "twisted" in occlusal view. The hypoflexid is shallow. Exodaenodonty is variably developed: it is usually present at the posterior root in most specimens, although it may be weaker (e.g., UALVP 46943), stronger (e.g., UALVP 46886), or undeveloped (e.g., UALVP 34928); it is usually very weak or absent at the anterior root. As on p2, a weak interradicular crest is developed on some specimens.

p4: The p4 of Xynolestes is about the same height as the m1, but is significantly narrower. The crown consists of a dominant protoconid, a lower but equally prominent paraconid, a smaller metaconid, and a basined talonid with a variable number of tiny cusps. In contrast to the more anteriorly leaning anterior premolars, the p4 crown is more nearly vertical. The protoconid is tall and sharp, moderately compressed bilaterally, and has a vertically directed apex (i.e., not recurved). A weakly developed, conical metaconid originates approximately half way up the lingual side of the protoconid, with its apex directed dorsally and slightly lingually; the metaconid varies slightly in size, being stronger on some specimens (e.g., UALVP 40511), weaker on others (e.g., UALVP 46886), and the metaconid quickly diminishes in size and height with even the slightest wear. A shallowly notched protocristid connects the protoconid and metaconid. A sharp paracristid extends anterolingually from the protoconid apex and forms an acute notch just prior to its union with the conical paraconid. As with the metaconid, the paraconid varies slightly in size and position: on most specimens it is larger than the metaconid, anteriorly offset from the protoconid, and projects anteriorly and dorsally (e.g., UALVP 46886), while on other specimens it can be lower and more nearly vertical (e.g., UALVP 46959), or somewhat taller and sharper (e.g., UALVP 40511). Irrespective of these minor variations, the paraconid consistently arises from relatively low on the protoconid and is anterior in position, leaving the trigonid broadly open lingually. A low crest extends posterolingually from the paraconid, forming a low lingual shelf. The talonid is about one-third to one-half the width of the trigonid and is shallowly basined. Two or three small cusps are developed: of 26 p4s where the talonid cusps could be enumerated, 20 have three cusps (77 percent) whereas only six (23 percent) have two cusps. The entoconid is invariably the largest talonid cusp, and is positioned at or slightly labial to the lingual margin of the crown; the entoconid is well separated from the hypoconulid, and there is no postcristid developed between them. The hypoconid is slightly smaller

and lower than the entoconid, and has been reduced to a flat, labially sloping surface in many specimens. In specimens with a three-cusped talonid, the hypoconid and hypoconulid are subequal and connate for most of their height, and their apices are joined by a weak hypocristid. A sharp cristid obliqua runs from the hypoconid to the postvallid wall, joining the trigonid lingual to the level of the protocristid notch and well lingual of the anteroposterior midline of the crown; on unworn specimens (e.g., UALVP 46886) the cristid obliqua ascends the posterior wall of the metaconid, fading away as it nears the apex. An anterior cingulid is invariably present, although it can be stronger or weaker. The hypoflexid is considerably deeper than on p3, and strong exodaenodonty is usually developed at the posterior root.

Lower molars: m1: The lower molars of Xynolestes lean lingually and progressively decrease in size and height from m1 to m3, although as with the upper molars, the reduction in size is not as pronounced as in lower molars of erinaceids. The m1 is nearly rectangular in occlusal outline, with the trigonid and talonid subequal, or with the talonid slightly wider; the trigonid is steeply inclined. The trigonid consists of a tall, swollen protoconid, a slightly lower metaconid, and a low, crestiform paraconid that together form a nearly equilateral triangle in occlusal view. The protoconid is subconical, with its lingual wall slightly convex. A sharp paracristid descends anteriorly and lingually from the protoconid apex, then turns abruptly lingually to join the strongly compressed paraconid; a notch is developed in the deepest part of the paracristid. The paraconid is low, anteriorly projecting, and almost entirely incorporated into the paracristid; in some specimens a vestigial paraconid is suggested by a weak swelling at the lingualmost part of the paracristid. A short, weak crest is sometimes developed between the bases of the paraconid and metaconid. The metaconid is higher than the paraconid but lower than the protoconid, and its apex is positioned slightly posterolingual to that of the protoconid; a sharp, deeply notched protocristid connects the two cusps. The talonid is well-developed on m1 of Xynolestes, with tall, sharp cusps enclosing a deep basin. The hypoconid and entoconid are subequal in size, but the entoconid is the taller cusp, and their opposing walls converge to form a deep, angular basin. A sharp, deeply notched entocristid connects the entoconid to the postvallid wall, and the hypoconid becomes flattened dorsolingually-ventrolabially with extended wear. The

hypoconulid is slightly lower than the hypoconid, and is positioned just lingual of the mid-longitudinal axis of the crown; its basin-facing wall is flat, and its apex projects dorsally and slightly posteriorly. The hypoconid and hypoconulid are connected by a sharp hypocristid, whereas the entoconid and hypoconulid are separated by a deep sulcus (the so-called nyctalodont condition of Menu and Sigé, 1971). The cristid obliqua is unusual: it is nearly vertical as it descends from the apex of the hypoconid, but becomes horizontal as it runs anterolingually towards the postvallid wall, then abruptly angles dorsally as it scales the trigonid below or slightly lingual of the protocristid notch; it fades away as it nears the level of the notch, although a shallow groove can continue towards the metaconid apex on more heavily worn specimens. Although the anterior cingulid is robust on all specimens at hand, the posterior cingulid is generally weak. An ectocingulid is not present. The hypoflexid is deep, and a robust hypoflexid shelf is developed. Weak exodaenodonty can be developed at the posterior root.

m2: The m2 of Xynolestes resembles m1, but is smaller and lower crowned, and the trigonid is lower relative to the talonid. The trigonid is more anteroposteriorly compressed than on m1, resembling an isosceles, rather than equilateral triangle in occlusal outline; the paraconid is anteroposteriorly compressed, being fully incorporated into the paracristid. In contrast to m1, the metaconid on m2 is the largest and tallest trigonid cusp, and the protocristid notch is deeper. The talonid on m2 closely resembles that on m1: the hypoconid and entoconid are tall and sharp, while the hypoconulid is lower and posterodorsally projecting. The hypoconid and hypoconulid are connected by a short but well-defined hypocristid, while the entoconid is separated from the hypoconulid by a deep sulcus. The entocristid is sharp and V-shaped, and the cristid obliqua resembles that on m1, joining the postvallid wall slightly lingual of the protocristid notch. As on m1, the labial cingulid on m2 is robust anteriorly but weakens posteriorly, and the posterior cingulid is weak. The hypoflexid is deep, and is floored by a prominent shelf. Exodaenodonty is not developed.

m3: The m3 is smaller than m2, and smaller relative to m2 than m2 is to m1; the trigonid and talonid are more nearly equal in height than on m2. The trigonid is more anteroposteriorly compressed on m3 than on either m1 or m2, with the paracristid/paraconid proportionately more transverse and shelf-like. As on m2, the

metaconid on m3 is the largest trigonid cusp, and is slightly taller than the protoconid. The talonid is narrower than the trigonid, but is otherwise similar to that on m1 and m2: the hypoconid and entoconid are tall, the hypoconid and hypoconulid are joined by a hypocristid, and the entoconid and hypoconulid are closely appressed but remain unconnected. The hypoconulid is relatively better developed than on m1 or m2, more closely approximating the entoconid in size and height. The anterior cingulid is well-developed, and the hypoflexid is floored by a robust shelf.

Etymology.—Named in honour of Gerald Denomme and his contributions to the UALVP fossil mammal collections; his skillful field techniques resulted in discovery of many small, delicate specimens, many of which are referable to Xynolestes.

Holotype.—UALVP 46886, incomplete right dentary with p1-4, m1-3, and alveoli for i2-3, c. DW-2 locality, Paskapoo Formation of Alberta, late Paleocene [early middle Tiffanian, Ti3 (Fox, 1990), Plesiadapis anceps/P. rex Lineage Zone of Lofgren et al., 2004].

Other material examined.—From Cochrane 2: UALVP 24756, P4; UALVP 46887, M1; UALVP 28487, incomplete left dentary with i2-3 (roots only), c, and p1; UALVP 24703, incomplete left dentary with p2-4; UALVP 46888, incomplete right dentary with p2-4; UALVP 24699, incomplete left dentary with p4, m1, and alveoli for p3; UALVP 24704, incomplete left dentary with m1-2; UALVP 24695, incomplete left dentary with m1-2 and alveoli for m3; UALVP 46889, incomplete right dentary with p4, m1 roots; UALVP 24701, incomplete left dentary with p4, m2 and alveoli for p3, m1; UALVP 46890, incomplete right dentary with p4 and alveoli for p3; UALVP 24715, 46891-46897, p4 (total: 8); UALVP 24764, 46898-46902, m1 (total: 6); UALVP 24696-24698, 24752, 28476, m2 (total: 5).

From Aaron's Locality: UALVP 43435, incomplete right dentary with p4, m1-2, and alveoli for c, p1-3, m3.

From Joffre Bridge Mammal Site No. 1: UALVP 46903, incomplete right dentary with i2-3, c, p2-3, and alveolus for i1, p1.

From Joffre Bridge Road Cut lower level: UALVP 40511, incomplete right dentary with p2-4, m1-3; UALVP 46904, incomplete left dentary with m1-3; UALVP 46905, incomplete right dentary with p4, m1, and alveoli for p3; UALVP 40522,

incomplete left dentary with p4, m1-2 (trigonid only); UALVP 46906, incomplete right dentary with m1-3 (broken); UALVP 46907, incomplete right dentary with p4, m1; UALVP 40505, incomplete right dentary with p2, p4, and alveoli for c, p1, p3; UALVP 46908, incomplete left dentary with m3 and alveoli for m1-2; UALVP 46909, associated p4 and m1.

From DW-1: UALVP 46910, incomplete left dentary with p4, m1-2, and alveoli for m3; UALVP 46911, incomplete right dentary with m1 (broken), m2-3; UALVP 46912, m2.

From DW-2: UALVP 40512, incomplete left maxilla with P2-4, M1-2, and alveoli for M3; UALVP 40514, incomplete left maxilla with P2, DP3, P3, P4, M1-2; UALVP 40516, incomplete left maxilla with P4, M1-3; UALVP 46913, incomplete right maxilla with P4, M1-3; UALVP 46914, incomplete right maxilla with M1-2 and alveoli for P3-4; UALVP 46915, incomplete left maxilla with M2-3; UALVP 46916, incomplete left maxilla with M1-2; UALVP 46917, incomplete right maxilla with P3 and alveoli for P2; UALVP 46918, P4; UALVP 46919, M1; UALVP 46920, 46922, M2 (total: 3); UALVP 46923, incomplete right dentary with ?i2-3, p1, p3-4, m1-3; UALVP 46925, incomplete left dentary with p2-4, m1-3, and alveolus for p1; UALVP 40509, incomplete left dentary with p2-4, m1-3; UALVP 46926, incomplete left dentary with p2, p4, m1-3, and alveoli for i1-3, c, p1, p3; UALVP 46927, incomplete left dentary with p1, p4, m1-3, and alveoli for i3, c, p2-3; UALVP 46928, incomplete right dentary with p3-4, m1-3, and alveoli for p1-2; UALVP 40507, incomplete right dentary with p3-4, m1-3, and alveoli for p2; UALVP 46929, incomplete left dentary with p4, m1-3, and alveoli for p2-3; UALVP 46930, 46931, incomplete left dentary with p4, m1-3; UALVP 46932-46934, incomplete right dentary with p4, m1-3; UALVP 46935, incomplete left dentary with p3-4, m1, and alveoli for p1-2, m2; UALVP 46936, incomplete left dentary with m1-3 and alveoli for c, p1-4; UALVP 46937, incomplete right dentary with m1-3; UALVP 46938, incomplete left dentary with p3 (broken), p4, m1-2, m3 (broken); UALVP 46939, incomplete left dentary with p2-4, m1; UALVP 46940, incomplete left dentary with p2 (posterior root only), p4, m1, m2 (broken); UALVP 46941, incomplete right dentary with p3-4, m1-2; UALVP 46942, incomplete left dentary with p3-4, m1-2 (trigonid only); UALVP 46943, incomplete right dentary with p3-4, m1-2, and alveoli for p2, m3;

UALVP 46944, incomplete left dentary with p3 (broken), p4, m1-3 (m3 broken); UALVP 46945, incomplete left dentary with p4, m1-2, and alveoli for c, p1-3; UALVP 46946, incomplete left dentary with p4, m1-2, m3 (talonid only), and alveoli for p1-3; UALVP 46947, incomplete right dentary with p4, m1, m2 trigonid; UALVP 46948, incomplete right dentary with p3, erupting p4, m1, and alveoli for c, p1-2; UALVP 46949, incomplete right dentary with m1-2 (talonid only) and alveoli for m3; UALVP 46950, 46951, 40521, incomplete right dentary with m1-3; UALVP 46952, incomplete left dentary with m1-3; UALVP 46953, incomplete left dentary with m1-2 and erupting m3; UALVP 46954, incomplete left dentary with m1, m2-3 (both broken); UALVP 46955, incomplete right dentary with i2 root, p2-3, p4 roots, m1, and alveoli for i1, i3, c, p1; UALVP 46956, incomplete right dentary with p4, m1, m3, and alveoli for p1-3, m2; UALVP 46957, incomplete right dentary with p4 (talonid only), m1, and alveoli for p2-3; UALVP 46958, incomplete left dentary with p2-4 and alveoli for c, p1; UALVP 46959, incomplete left dentary with p4, m1, and alveoli for c, p1-3, m2; UALVP 46960, incomplete left dentary with p4, m1, and alveoli for p2-3; UALVP 46961, incomplete left dentary with p4, m1; UALVP 46962, incomplete left dentary with m1-2 and alveoli for p3-4; UALVP 46963, incomplete right dentary with m1-2 and alveoli for m3; UALVP 46964-46966, incomplete right dentary with m2-3 (total: 3); UALVP 46967, incomplete left dentary with m2-3; UALVP 46968, incomplete left dentary with m1 talonid, m2, and alveoli for m3; UALVP 46969, incomplete right dentary with m2 and alveoli for p2-4, m1, m3; UALVP 46970, incomplete left dentary with m2 and alveoli for m1, m3; UALVP 46971, incomplete right dentary with m2 and alveoli for m1, m3; UALVP 46972, incomplete right dentary with m2 and alveoli for m3; UALVP 46973, incomplete right dentary with p2-3 and alveoli for p1, p4; UALVP 46974, incomplete left dentary with p3 and alveoli for ?i2-3, c, p1-2; UALVP 46975, incomplete right dentary with p4 and alveoli for c, p1-3; UALVP 46976, incomplete left dentary with p4 and alveoli for p2-3, m1-2; UALVP 46977, incomplete left dentary with p4 and alveoli for p2-3; UALVP 46978, incomplete right dentary with p4 and alveoli for p2-3; UALVP 46979, incomplete left dentary with p4 and alveoli for p3; UALVP 46980, incomplete left dentary with p2 and alveoli for c, p1, p3-4; UALVP 46981, incomplete left dentary with m1 (talonid only) and m2; UALVP 46982, incomplete right dentary with m1 and alveoli

for c, p1-4, m2; UALVP 46983, p3; UALVP 46984-46990, p4 (total: 7); UALVP 46991, m1; UALVP 46992, 46993, m2; UALVP 46994, m1 or m2;

From Mel's Place: UALVP 46995, incomplete right dentary with m1-3.

From Birchwood: UALVP 39480, incomplete right dentary with m1-3.

From Hand Hills West upper level: UALVP 35147, M2; UALVP 39427, incomplete right dentary with p4, m1-2, and alveoli for i3, c, p1-3; UALVP 34928, incomplete right dentary with p3-4, m1-3; UALVP 35138, incomplete left dentary with p3-4 and alveoli for c, p1-2, m1; UALVP 34929, incomplete right dentary with p2-4, m1, and alveoli for c, p1; UALVP 39431, incomplete right dentary with m2-3; UALVP 35140, incomplete left dentary with p4 and alveoli for p3; UALVP 35142, incomplete left dentary with p4 and alveoli for p3; UALVP 34937, incomplete left dentary with m2 and alveoli for m3; UALVP 35139, 35144, p4; UALVP 34924, m1.

Discussion.—The upper and lower dentition of Xynolestes were associated on the basis of a similar decrease in molar size from M1/m1-M3/m3, and by a tight fit when upper and lower teeth were manually brought into occlusion. The teeth of Xynolestes bear resemblance to those of primitive nyctitheriids (e.g., Leptacodon) and erinaceomorphs (e.g., Dartonius): the crowns support sharp cusps, the p4 bears a well-developed paraconid and metaconid, and the molar paraconids are blade-like, and in these regards the coronal anatomy of Xynolestes probably does not depart significantly from that of primitive lipotyphlans generally. The teeth of Xynolestes have, however, a suite of characters that strongly suggest phylogenetic affinity with erinaceomorphs, rather than with soricomorphs (and see later in this chapter). For example, the P4 of Xynolestes, although possessing an elongate, blade-like postmetacrista (also seen in stem soricomorphs such as "Leptacodon" munusculum Simpson, 1935a), bears a short postprotocrista that drops steeply to the base of the protocone; this character is known only among erinaceomorphs (as well as the enigmatic genus Pontifactor West, 1974, considered a soricomorph by some authors (e.g., Krishtalka, 1976b; West, 1974; McKenna and Bell, 1997), but a lipotyphlan of uncertain higher level status by others (e.g., Butler, 1988; this study)]. Additionally, the metacone on P4 is relatively more poorly developed compared to that of most nyctitheriids, and is closer to that seen in many primitive erinaceomorphs, including Litolestes Jepsen, 1930 and Litocherus

Gingerich, 1983. The M1-2 of Xynolestes bears a low and slightly bulbous hypocone, and a small pericone, features that are more often seen in erinaceomorphs than in soricomorphs. As with the upper dentition, the lower dentition of Xynolestes bears a number of erinaceomorph-like features. For example, the lower premolars are procumbent, rather than vertical; procumbent lower premolars are known in a number of stem erinaceomorphs (e.g., Dartonius, Scenopagus McKenna and Simpson, 1959, some species of Diacocherus) and may have characterized the earliest erinaceomorphs; the p4 of Xynolestes bears a relatively weak metaconid, in contrast to most nyctitheriids which have a strongly developed metaconid on p4 (Krishtalka, 1976b; Lopatin, 2005). The lower molars of Xynolestes decrease in size from m1-3 and bear tall molar entoconids; although these features are not unique to erinaceomorphs among lipotyphlans, their distribution outside of Erinaceomorpha is patchy, being independently developed in but a few soricomorphs (e.g., Leptacodon tener Matthew and Granger, 1921; Plagioctenodon Bown, 1979).

Although Xynolestes is most likely an erinaceomorph, its position within the suborder is uncertain. The teeth of Xynolestes bear closest resemblance to those of the early Eocene genera Auroralestes Holroyd, Bown, and Schankler, 2004, Talpavoides Bown and Schankler, 1982, and, especially, Dartonius: Xynolestes and Dartonius both have procumbent lower premolars, relatively sharp, rather than blunt and inflated cusps, p4 with a short and narrow talonid, and lower molars that decrease in size from m1-3. Xynolestes differs from Dartonius in having a two-rooted, rather than single-rooted p2, a relatively larger p4 with a lower paraconid and a better-developed talonid (the talonid of Xynolestes usually bears three cusps, while that of Dartonius bears but a single cusp), and in having the molar paraconid arising from a relatively lower position on the trigonid. The taxonomic history of Dartonius is remarkably convoluted (see McKenna, 1960; Delson, 1971; Russell et al., 1975; Bown and Schankler, 1982; Novacek et al., 1985), but recent classifications suggest that the genus may represent an erinaceid (Novacek et al., 1985) or a near-erinaceid (McKenna and Bell, 1997). The results of the phylogenetic analysis presented in this study (see later in the text) suggest that Xynolestes and Dartonius possibly represent stem members of a clade that contains taxa that have been

previously referred to the Erinaceidae (e.g., Litolestes, Cedrocherus Gingerich, 1983) and the Adapisoricinae (e.g., Adapisorex Lemoine, 1883) (and see later in the text).

The earliest record of Xynolestes is from the earliest Tiffanian (Ti1) Cochrane 2 and Aaron's localities of Alberta, where it constitutes only 1 percent of the total number of specimens and minimum individuals; by middle late Tiffanian (Ti3) time, however, Xynolestes was much more abundantly represented, constituting nearly six percent of the total number of specimens, and about eight percent of the minimum number of individuals at the Blindman River and Joffre Bridge localities.

Family LITOLESTIDAE new family

Type genus.—Litolestes Jepsen, 1930

Included subfamilies.—Adapisoricinae Schlosser, 1887; Litocherinae Gingerich, 1983; Litolestinae new subfamily.

Diagnosis.—Differ from all other erinaceomorphs in having a combination of lower and more inflated cusps, in the crowns of p2-3 being larger (not peg-like) and nearly vertical (rather than procumbent), in having very low molar trigonids, in the valley-facing sides of trigonid cusps being swollen and markedly convex, especially the metaconid, and in the m1 paracristid being strongly flexed (i.e., the paraconid and protoconid arms of the paracristid form a 90 degree angle at their union). Differs further from other erinaceomorphs except Diacocherus and Xynolestes in P4 usually bearing a metacone and in M1-2 bearing a pericone.

Subfamily LITOLESTINAE new subfamily

Included genera.—Litolestes Jepsen, 1930; Cedrocherus Gingerich, 1983; Oncocherus Scott, 2006.

Diagnosis.—Differ from litocherines in molars significantly decreasing in size from m1-m3, in having more nearly square upper molars, a narrower p4 talonid, a strongly flexed molar paracristid on m2-3, and in having V-shaped molar talonid basins. Differ from adapisoricines in having a smaller metacone on P4, a weaker hypocone on

M1-2, in having steeper molar trigonids, and in the m3 hypoconulid not being appressed to the entoconid. Differ from erinaceids in having an undeveloped hypocone on P4, in having much weaker molar hypocones, in having a poorly developed paraconid on p4, and in lacking an enlarged, blade-like paraconid/paracristid on m1. Differ from other erinaceomorphs where known in having multilobate lower incisors.

Genus LITOLESTES Jepsen, 1930

Litolestes JEPSEN, 1930, p. 513.

Type species.—Litolestes ignotus Jepsen, 1930.

Other included species.—Litolestes avitodelphus new species.

LITOLESTES AVITODELPHUS new species

Figure 5.5; Table 5.5

Diagnosis.—Differs from Litolestes ignotus in being smaller (L m1, L. avitodelphus approximately 30 percent shorter than L m1, L. ignotus), and in having a relatively longer p4 with a more anteriorly positioned paraconid. Differs further from L. ignotus in having molars with less swollen cusps and weaker ectocingulids.

Description.—Dentary and lower dentition (Fig. 5.5): The dentary of Litolestes avitodelphus resembles those of other small insectivores in being anteroposteriorly elongate, slender, and slightly convex ventrally. The horizontal ramus reaches its greatest depth below m1. The symphysis extends from the anterior tip of the jaw posteriorly to a point below the level of p1; the articular surface consists of a pair of arms of raised bone, one dorsal and the other ventral, and an area of faintly concave and slightly rugose bone between them. As with the symphysis of Xynolestes, the two mandibular rami of L. avitodelphus were probably only loosely connected in life. Two small mental foramina are developed labially: the more anterior foramen occurs in a shallow recess below the level of the anterior root of p2, its subovate aperture opening anteriorly, laterally, and slightly dorsally; the more posterior foramen is smaller than the

anterior foramen, more nearly circular in outline, and opens anterolaterally below the level of the anterior root of p3.

The condylar and angular processes are well-preserved in UALVP 40528, but the coronoid process is mostly missing, although its impression remains in the rock accompanying the specimen (see Fig. 5.5.11). The angular process is drawn out posteriorly as an elongate, hook-like spine, with its axis slightly oblique to the tooth row. When the ramus is held with the ventral surface in a horizontal position, the dorsal surface of the angular process is level with the bases of the tooth crowns, and although its tip has been broken away, the angular process likely extended posteriorly to at least the level of the condyle. The lateral side of the angular process is flat, while the medial surface bears a prominent, shelf-like ridge ventrally; the ridge extends anteriorly onto the horizontal ramus, terminating below the small mandibular foramen. The horizontal ramus is excavated anterior of the mandibular foramen to below the level of m3, with its depth being somewhat exaggerated from mediolateral crushing of the ramus; the depression may have received an anterior slip of the internal pterygoid musculature in life. The horizontal ramus narrows posteriorly as a short but robust condylar process; the ramus is deeply excavated between the condylar process dorsally and the angular process ventrally, with a deep, C-shaped notch developed between the two. The condyle is positioned slightly above the level of the tooth row when the ramus is held horizontally. The condyle is somewhat cylindrical, transversely wide and oriented somewhat posterolaterally-anteromedially, and slopes medially, with its medial side approximately 35 degrees lower from horizontal than its lateral side. Laterally, the articular surface of the condyle faces mostly dorsally, but this surface continues progressively farther posteriorly and ventrally around the curvature of the condyle towards the medial side, and reaches the ventralmost parts of the condyle at the medial extremity; the majority of the articular facet faces posteriorly when the ramus is horizontal. The medial side of the condylar process is rugose and represents the area of distal attachment for the external pterygoid musculature.

The majority of the coronoid process has been broken away in UALVP 40528, but its impression remains in the rock associated with the specimen. The coronoid process was tall, towering well above the level of the tooth row, and forms an angle of

approximately 110 degrees with the mandibular ramus. Medially, a smoothly rounded ridge extends posteriorly from below the level of m3 to the mandibular foramen, separating the temporalis fossa dorsally from the pterygoideus fossa ventrally. The masseteric fossa is deeply excavated.

Lower dentition: Nothing of the upper dentition of Litolestes avitodelphus is known. The lower dentition is represented by p3-4 and the molars, although the hypodigm collectively documents loci for three lower incisors, a lower canine, and four premolars. Alveoli for three lower incisors are preserved in UALVP 40523, with the i1 root still in place. The i1 and i2 roots were subequal in size and mediolaterally compressed, while the i3 was smaller and squeezed between i2 and the lower canine. The spacing and orientation of the i1 root and the i2-3 alveoli suggest the crowns were probably procumbent and closely appressed to one another, similar to those seen in L. ignotus (see Schwartz and Krishtalka, 1976). Part of the lower canine crown is preserved on UALVP 40523. The tooth is single rooted and the crown appears to have leaned anteriorly, similar to that in L. ignotus (see Schwartz and Krishtalka, 1976); judging by the size of the root, the lower canine was not substantially enlarged relative to the cheek teeth.

Lower premolars: The p1 and p2 of L. avitodelphus are represented by their alveoli in UALVP 40523. The p1 alveolus is subovate and larger than that for the lower canine, whereas the p2 alveoli are smaller, but occupy the same amount of space as that for p1. No diastemata intervene between any of the anterior teeth.

p3: The crown of p3 is short and squat, and although it is narrow at its anterior end, it widens significantly posteriorly, resulting in a teardrop-shaped occlusal outline. A bulbous and low protoconid dominates the crown. Weak crests extend anteriorly and posteriorly from the protoconid apex, with the paracristid terminating at a small, anteriorly positioned paraconid. The posterior crest is longer and more sharply defined, and terminates at a small cuspid at the apex of a prominent transverse crest. The transverse crest can extend around the posterolingual margin of the crown, forming a short shelf.

p4: The p4 of Litolestes avitodelphus is about the same size as the m1, and is considerably larger than p3. The crown consists of a large and swollen protoconid, a low

but prominent paraconid, a small metaconid, and a narrowly basined talonid. The conical protoconid is tall, with a blunt, posterodorsally directed apex. A small but well-defined, conical metaconid occurs approximately half way up the lingual side of the protoconid, with its apex at approximately the same level as that of the paraconid. The metaconid varies in size, being larger on some specimens (e.g., UALVP 47275) and smaller on others (e.g., UALVP 40528), although it should be noted that the metaconid diminishes in size and height with even the slightest wear (see, e.g., UALVP 47276). A shallowly notched protocristid connects the protoconid and metaconid. The paracristid is ill-defined near the protoconid apex, but becomes stronger and more blade-like as it nears the paraconid. Although the paraconid varies slightly in size, it is always a robust cusp, arising from relatively high on the anterolingual face of the protoconid and projecting anterodorsally, thus leaving the trigonid broadly open lingually. A low crest extends posterolingually from the paraconid, forming a short lingual cingulid. As in L. ignotus, the p4 talonid basin of L. avitodelphus is lingual in position and narrow, occupying only a quarter the width of the trigonid, and is flanked by one or two diminutive cusps. The hypoconid is invariably the largest talonid cusp (or sole talonid cusp in specimens in which only one cusp is developed), while the entoconid is either absent or only weakly differentiated from the entocristid. The entocristid and cristid obliqua are subparallel, running posterolabially-anterolingually, imparting a slight labial twist to the talonid. The cristid obliqua can ascend the postvallid wall towards the apex of the metaconid. An anterior cingulid is invariably present. Owing to the extreme lingual position of the talonid basin, the hypoflexid is correspondingly deep. Although exodaenodonty is weak anteriorly, it is consistently strong at the posterior root.

Lower molars: m1: The lower molars of Litolestes avitodelphus progressively decrease in size and height from m1 to m3, similar to those in L. ignotus and Oncocherus Scott, 2006; the reduction in size is much more pronounced than in molars of other erinaceomorphs (e.g., Leipsanolestes Simpson, 1928, Xynolestes), and is closer to that seen in erinaceids. The m1 is nearly rectangular in occlusal outline, with the talonid slightly wider than the trigonid. In labial view, the trigonid leans anteriorly and is only slightly taller than the talonid. The trigonid consists of a tall, swollen protoconid, a slightly lower metaconid, and a low, crest-like paraconid/paracristid. The protoconid and

metaconid are conical, with their opposing walls swollen and convex. The paracristid is poorly defined near the protoconid apex, but strengthens as it descends the anterior face of the protoconid before turning abruptly lingually to join the paraconid; a wide notch is developed in the deepest part of the paracristid. The paracone is low, anteriorly projecting, and almost entirely incorporated into the paracristid, although its presence is sometimes suggested by a strong swelling at the lingual most part of the paracristid. The metaconid is lower than the protoconid and its apex leans slightly lingually; a sharp, deeply notched protocristid connects the protoconid and metaconid. The talonid supports tall, sharp cusps enclosing a deep basin. The hypoconid and entoconid are subequal in size, but the entoconid is the taller cusp. The basin-facing walls of the entoconid and hypoconid are flat and unite to form a deep, V-shaped basin. As in other erinaceomorphs, the hypoconid becomes flattened with extended wear. The hypoconulid is slightly shorter than the hypoconid, and is positioned centrally or just lingual of the longitudinal midline, closer to the entoconid; its basin-facing wall is flat, and its apex projects dorsally and slightly posteriorly. A low postcristid connects the entoconid and hypoconulid, while a slightly better defined hypocristid connects the hypoconulid and hypoconid. The cristid obliqua contacts the postvallid wall low and ventral to the level of the protocristid notch. The anterior cingulid is consistently robust, but the posterior cingulid is weaker, and in some specimens (e.g., UALVP 47275) it is virtually undeveloped. An ectocingulid is not present. The hypoflexid is anteroposteriorly short and deep, and a robust hypoflexid shelf is present. Exodaenodonty is strong at both roots.

m2: The m2 of Litolestes avitodelphus is both smaller and lower crowned than m1. The trigonid is anteroposteriorly compressed compared to that on m1, and the paracristid is longer and more transverse towards the lingual side of the crown. In contrast to m1, the metaconid on m2 is the largest and tallest trigonid cusp, and the protocristid notch is deeper. The talonid on m2 closely resembles that on m1: the hypoconid and entoconid are tall and sharp, with their opposing walls forming a deep, V-shaped basin, and the hypoconulid low and posterodorsally projecting. The entocristid is sharp and V-shaped, and the cristid obliqua resembles that on m1, joining the postvallid wall low and ventral to the level of the protocristid notch. The ectocingulid on m2 is robust anteriorly but weakens posteriorly, and the posterior cingulid is variably

developed. The hypoflexid is deep, and is floored by a prominent shelf. Exodaenodonty is developed at both roots.

m3: The m3 is smaller than m2, and smaller relative to m2 than m2 is to m1; the trigonid and talonid are more nearly equal in height than on m2. The paracristid/paraconid is relatively more transverse and shelf-like on m3 than it is on either m1 or m2, and the paraconid is slightly more labial in position. As on m2, the metaconid on m3 is the largest trigonid cusp, and is slightly taller than the protoconid. Although the talonid is narrower than the trigonid, it is otherwise similar to that on m1 and m2, with the hypoconid and entoconid being tall, and with their opposing walls forming a V-shaped basin. The hypoconulid is relatively better developed than on m1 or m2, more closely approximating the entoconid in size and height. The anterior cingulid is well-developed, and the hypoflexid is floored by a robust shelf.

Etymology.—Avitus, Latin, ancient or old; adelphus, Latin, brother, in reference to the earlier stratigraphic occurrence of Litolestes avitodelphus relative to Litolestes ignotus.

Holotype.—UALVP 40528, incomplete left dentary with p4, m1-3, and alveoli for p3. DW-2 locality, Paskapoo Formation of Alberta, late Paleocene, late Paleocene [early middle Tiffanian, Ti3 (Fox, 1990), Plesiadapis anceps/P. rex Lineage Zone of Lofgren et al., 2004].

Other material examined.—From Joffre Bridge Road Cut lower level: UALVP 40523, incomplete left dentary with i1 (root only), c (crown broken), p3-4, and alveoli for i2-3, p1-2; UALVP 47274, incomplete right dentary with m1-2 and alveoli for m3.

From DW-2: UALVP 47275, 47276, incomplete left dentary with p3-4, m1-2; UALVP 40504, incomplete right dentary with m1-3 and alveoli for p2-4; UALVP 47277, incomplete left dentary with m2-3.

Discussion.—While the referred teeth are low crowned and support inflated cusps and heavy crests, the p4 is enlarged relative to m1, and the lower molars decrease in size from m1-3, features that identify these specimens as pertaining to Litolestes, they differ from those of the only known species of Litolestes, L. ignotus, in a number of ways. For example, the referred teeth are nearly 30 percent smaller than those of L. igontus, and bear cusps that are less turgid; additionally, the paraconid on m2-3 is more cuspate and

less shelf-like, and the decrease in size from m1-3 is not as exaggerated as in L. ignotus. These differences are of a magnitude similar to that distinguishing species of other lipotyphlans, and the teeth in the present sample are referred to a new species of Litolestes, L. avitodelphus. While Litolestes can be locally abundant in late Paleocene sediments (e.g., Princeton Quarry, see Rose, 1981a-b; Secord, 2004), the genus is generally not well known, and is undocumented prior to Ti4 (Plesiadapis churchilli/P. simonsi Lineage Zone, see Lofgren et al., 2004); as such, L. avitodelphus represents the oldest known species of Litolestes.

Subfamily LITOCHERINAE Gingerich, 1983

Type genus.—Litocherus Gingerich, 1983.

Other genera.—Nayloria new genus.

Revised diagnosis.—Differ from other erinaceomorphs in having a prominent anterior cingulum on P4. Differ further from litolestines in molars decreasing less severely in size from M1/m1to M3/m3, in having upper molars that are more transverse relative to length, a wider p4 talonid, and in having deeply concave molar talonid basins. Differ further from litolestines in having better developed metacone on P4. Differ from adapisoricines in M2/m2 being smaller than m1, in having steeper molar trigonids, in having a relatively larger p3, and in having a more poorly developed p4 metaconid. Differ from erinaceids in molars decreasing less severely in size from M1/m1 to M3/m3, in P4 and upper molars lacking an enlarged hypocone, in having deeply concave molar talonid basins, and in having better developed molar hypoconulids.

Genus LITOCHERUS Gingerich, 1983

Litolestes JEPSEN, 1930, p. 513 (in part).
Litocherus GINGERICH, 1983, p. 232.

Type species.—Litocherus zygeus Gingerich, 1983.

Other included species.—Litocherus notissimus (Simpson, 1936); Litocherus lacunatus (Gazin, 1956).

LITOCHERUS NOTISSIMUS (Simpson, 1936)

Figures 5.6-5.15; Tables 5.6, 5.7

Litolestes notissimus SIMPSON, 1936, p. 23.

Holotype.—AMNH 33831, incomplete left dentary with p2-4, m1-3, incomplete right maxilla with P1-4, M1-3, and incomplete left maxilla with C, P1-3. Scarritt Quarry, Fort Union Formation of Montana, late Paleocene (early Tiffanian, Ti2, Plesiadapis anceps/P. rex Lineage Zone of Lofgren et al., 2004).

Paratype.—AMNH 33830, incomplete right dentary with p2-4, m1-3.

Material examined.—From Joffre Bridge Mammal Site No. 1: UALVP 40671, incomplete left dentary with c, p2-4, m1-3, and alveolus for p1; UALVP 40678, incomplete right dentary with m1-3 and alveoli for i1-3, c, p1-4; UALVP 40527, incomplete right dentary with p2-4, m1-3, and alveoli for c, p1; UALVP 40510, incomplete left dentary with posterior root of p2, p3-4, m1.

From Joffre Bridge Road Cut lower level: UALVP 47248, incomplete right maxilla with C, P1-4 (P3 and P4 broken), and M1 (broken); UALVP 47249, incomplete right maxilla with M2-3; UALVP 47250, P3; UALVP 47251, P4; UALVP 47252-47254 (total: 3), M1; UALVP 47255-47257 (total: 3), M2; UALVP 40668, incomplete left dentary with c, p2 (talonid only), p3-4, m1-2, and alveoli for i2-3, p1, m3; UALVP 40515, incomplete left dentary with c, p3-4, m1-2, and alveoli for p1-2, m3; UALVP 47258, incomplete right dentary with c, p2-4, alveolus for p1, and associated ?i3; UALVP 47259, incomplete right dentary with p2-3; UALVP 40503, incomplete right dentary with p3, m1-3, and alveoli for p4; UALVP 40513, incomplete right dentary with m1-2 and alveoli for p4, m3; UALVP 47260, incomplete right dentary with p2-4, m1 (broken), and alveoli for c, p1, m2-3; UALVP 40669, incomplete right dentary with m2-3; UALVP 47261, incomplete left dentary with m2 (talonid only) and m3; UALVP 47262, incomplete left dentary with p3-4 and alveoli for c, p1-2; UALVP 40677,

incomplete left dentary with p4 (talonid only) and m1; UALVP 47263, incomplete left dentary with p3 and alveoli for p1-2, p4; UALVP 47264, p4; UALVP 47265, 47266, m1; UALVP 47267, 47268, m2; UALVP 47269, 47270, m3.

From DW-1: UALVP 47271, m1.

From DW-2: UALVP 46379, incomplete left dentary with p2-4, m1-3, and alveoli for c, p1, and associated left and right petromastoids, right innominate (ischium, complete acetabulum, incomplete iliac blade), left innominate (ischium and incomplete acetabulum), left femoral diaphysis and distal epiphysis, left calcaneum, left cuboid, left entocuneiform, left metatarsal V, left proximal and intermediate phalanges; UALVP 46378, incomplete right maxilla with P2-3, associated incomplete left dentary with p3-4 and alveoli for p1-2, m1-3, and associated left and right innominates (both with incomplete ischium and acetabulum), and right astragalus, and incomplete phalanges; UALVP 33863, incomplete right maxilla with P4, M1-3, and associated incomplete left dentary with p1-4, m1-3; UALVP 47272, incomplete left and right maxillae with left P2-4, M1, right P3-4, M1-3, and alveoli for P2, and associated incomplete right dentary with p2, p4 (trigonid only), and alveoli for p1, p3; UALVP 33864, incomplete left maxilla with P2-4, M1-3, and alveoli for C, P1; UALVP 47273, incomplete right maxilla with C, P2-4 (labial half of P4 only), M1 (paracone missing); UALVP 47274, incomplete left maxilla with P3-4, M1-3, and alveoli for P2, and associated incomplete right maxilla with P4, M1; UALVP 40663, incomplete right maxilla with P4, M1-3; UALVP 47275, incomplete left maxilla with P4, M1-3, and alveoli for P3; UALVP 40519, incomplete left maxilla with P3, M1-3; UALVP 47276, incomplete right maxilla with P4, M1-2; UALVP 47277, incomplete right maxilla with P3-4, M1-2; UALVP 47278, incomplete right maxilla with M1-3; UALVP 47279, incomplete right maxilla with M1-2; UALVP 47280, incomplete right maxilla with M2-3; UALVP 47281, incomplete left maxilla with M2-3; UALVP 47282, incomplete left maxilla with P2-4; UALVP 47283, incomplete left maxilla with P3-4; UALVP 47284, incomplete right maxilla with P4; UALVP 47285, P3; UALVP 47286-47296 (total: 11), P4; UALVP 47298-47306 (total: 9), M1; UALVP 47307-47312 (total: 6), M2; UALVP 47313, M3; UALVP 47314, incomplete left dentary with c, p1-4, m1-2; UALVP 47315, incomplete right dentary with c, p1-2, m1-3, and alveoli for p3-4; UALVP 47316, incomplete right dentary with c, p3, and alveoli for p1-

2; UALVP 47317, incomplete left dentary with c, p1, and alveoli for p2-3; UALVP 47318, incomplete right dentary with p2-4, m1-2, alveoli for p1, m3, and associated lower canine; UALVP 47319, incomplete right dentary with c, p2-4, m1, and alveolus for p1; UALVP 47320, incomplete left dentary with p2 roots, p3-4, m1-3, and alveolus for p1; UALVP 47321, incomplete right dentary with p3-4, m1-3, and alveoli for p2; UALVP 40672, incomplete left dentary with p3-4, m1-3; UALVP 47322, incomplete left dentary with p3-4, m1-3 and alveoli for p1-2; UALVP 47323, incomplete right dentary with p4, m1-3; UALVP 47324, incomplete right dentary with erupting p3-4, m2-3, and alveoli for p1-2, m1; UALVP 47325, incomplete right dentary with erupting p4, m1-3, and alveoli for p2-3; UALVP 47326, incomplete left dentary with p2-4, m1, and alveoli for c, p1; UALVP 47327, incomplete right dentary with c, p3-4, and alveoli for p1-2; UALVP 47328, incomplete left dentary with p3, m1, m3, and alveoli for c, p1-2, m2; UALVP 47329, incomplete right dentary with p4, m1-3, and alveoli for p3; UALVP 47330, incomplete left dentary with p4, m1, m3, and alveoli for m2; UALVP 47331, incomplete left dentary with p4, m1-3; UALVP 40524, incomplete right dentary with p4 (talonid only), m1-3, and alveoli for p3; UALVP 40526, incomplete right dentary with m1-3 and alveoli for p4; UALVP 47332, 47333, incomplete left dentary with m1-3; UALVP 47334, incomplete right dentary with m1-3; UALVP 47335, incomplete right dentary with m2-3 and alveoli for m1; UALVP 47336, incomplete left dentary with m1-2; UALVP 47337, incomplete right dentary with m2-3; UALVP 47338-47340 (total: 3), incomplete left dentary with m2-3; UALVP 47341, incomplete left dentary with p3-4 and alveoli for p1-2, m1-2; UALVP 47342, incomplete right dentary with p4 and m1; UALVP 47343, incomplete left dentary with p4 and alveoli for p2-3; UALVP 47344, incomplete left dentary with m2 and alveoli for m1; UALVP 47345, incomplete right dentary with p1, p3, and alveoli for c, p4; UALVP 47346, incomplete right dentary with p4 and alveoli for p3; UALVP 47347, incomplete right dentary with p2 and alveoli for c, p1, and p3; UALVP 47348, 47349, p3; UALVP 47350-47354 (total: 5), p4; UALVP 47355-47362 (total: 8), m1; UALVP 47363-47367 (total: 5), m2; UALVP 47368, m1 or m2; UALVP 47369-47376 (total: 8), m3.

From Mel's Place: UALVP 47377, M1

From Birchwood: UALVP 47378, P4; UALVP 47379, incomplete left dentary with m2-3; UALVP 39461, incomplete left dentary with m1 (talonid only), m2, and alveoli for p2-4.

Age and occurrence.—Earliest Tiffanian (Plesiadapis praecursor/Plesiadapis anceps Lineage Zone, Ti1, late Paleocene) to late middle Tiffanian (Plesiadapis churchilli/P. simonsi Lineage Zone, Ti4, late Paleocene) of the Western Interior of North America (Lofgren et al., 2004).

Description.—Maxilla and upper dentition (Figs. 5.6, 5.7): Maxilla: Parts of the maxilla of Litocherus notissimus are known from a number of specimens in the present sample; UALVP 33864 is the most informative of these, and documents the facial process, infraorbital foramen, and anterior root the zygomatic arch. The premaxilla-maxilla suture is best seen on UALVP 47273, where it extends posterodorsally from just anterior to the upper canine in a smooth arc; the articulating surface is smooth, not digitate, and is slightly recessed from the surrounding bone, suggesting that the facial process of the premaxilla overlaid the anteriormost parts of the maxilla. The articulating surface continues dorsally and posteriorly past the level of the upper canine alveolus, where it fades away; the length of the suture suggests the facial process of the premaxilla may have been deep. The facial process of the maxilla bears a large, circular infraorbital foramen that opens dorsal to P3; the medial opening of the infraorbital canal, the maxillary foramen, is not preserved on any of the specimens at hand, although the relatively anterior position of the infraorbital foramen suggests the canal was likely long (see Xynolestes, earlier in this chapter). The bulk of the anterior root of the zygomatic arch originates dorsal to the posterior root of M2; the process is short, differing from the much larger and posteriorly extending maxillary root in erinaceids (Rich, 1981; Frost et al., 1991). A well-excavated fossa occurs just anterior to the anterior root of the zygoma, similar in both position and depth to that described for the Oligocene leptictid Leptictis (Novacek, 1986); the fossa is bounded ventrally by a short but well-defined shelf, and its deepest parts are perforated by tiny foramina. Novacek (1986) suggested that the presence of a deep antorbital fossa, as well as the enlarged infraorbital foramen in Leptictis, is evidence of well-developed snout musculature, and this seems no less reasonable for Litocherus as well. The more posterior parts of the facial process arise

from just above the anterior root of the zygoma, and the maxilla achieves its greatest depth at the level of P4. A conspicuous trough-like articular surface is developed along the posterodorsal part of the facial process just above the anterior root of the zygoma, and extends anteriorly to the level of M1; this surface almost certainly represents the point of articulation for the jugal; a similar trough is developed on UM 89741 and 89742, incomplete maxillae of L. notissimus from the early Tiffanian (Ti2) Scarritt Quarry of Montana (pers. obs.), demonstrating that this feature in UALVP 33864 is neither an artifact of preservation, nor an individual variant, but rather an important part of the articulation between the maxilla and jugal. A similar trough-like surface can be seen on the maxilla in the extant opossum, Didelphis virginiana: in D. virginiana, the ventromedial edge of the jugal articulates with the trough-like, anterodorsal surface of the maxilla in a tongue-in-groove fashion, with the tongue of the jugal fitting snugly into the groove or trough of the maxilla, and with the broad facial process of the jugal lapping onto the lateral aspect of the maxilla. In Litocherus, the trough is anteroposteriorly longer than in D. virginiana, suggesting that the jugal possibly had a relatively broader exposure on the side of the face, similar to that in the erinaceomorphs Macrocranion and Pholidocercus (Maier, 1979; Koenigswald and Storch, 1983; Storch, 1993), and contrasting with that in erinaceids in which the jugal is greatly reduced and limited to the middle part of the zygomatic arch (Butler, 1988; MacPhee and Novacek, 1993; Asher, 2005). The articular surface thins to a feather edge anteriorly and dorsally, possibly for articulation with the frontal; a separate facet for articulation with the lacrimal cannot be discerned. The palatal surface of the maxilla is poorly preserved among the specimens at hand, and the relative contribution of the maxilla to the orbital mosaic cannot be assessed.

Upper canine: The upper canine of Litocherus notissimus was described by Simpson (1936), although the tooth was not figured. Two canine morphs have been identified in the present sample, the first of which corresponds to that described by Simpson (1936). The crown of the first morph is elongate, caniniform and laniary, and faintly recurved; the root is large and mediolaterally compressed, and its lateral side is marked by a shallow, dorsoventrally directed groove. The second canine morph is smaller than the first, elongate, and with the apex narrowing to a sharp point. The crown is more obviously recurved than that of the first morph, and a weak but conspicuous

posterior heel is developed. As with the larger canine morph, the smaller morph is single-rooted, with the lateral and medial sides both indented by a shallow groove. The contrasting anatomies of the two canines are tentatively interpreted as owing to sexual dimorphism, rather than indicating the presence of two species; although sexual dimorphism is virtually unknown in extant lipotyphlans, it has recently been documented in the Antillean subfossil Nesophontes Anthony (Whidden and Wood, 2000).

Upper premolars: P1: P1 of Litocherus notissimus follows closely behind the canine, with no diastema intervening between the two teeth. The P1 is two-rooted, with the posterior root larger than the anterior root, and more nearly circular in cross section. The crown consists of a trenchant paracone that is faintly recurved; accessory cusps are not developed.

P2: The two-rooted P2 follows closely behind P1, with no diastema developed between the two teeth. The crown of P2 is longer, wider, and substantially taller than that of P1, but is nonetheless similar in its coronal anatomy, being dominated by a large, recurved paracone. Unlike P1, however, a small posterior heel is present on P2, and a poorly developed postparacrista can be developed, connecting the paraconal apex to the heel.

P3: A short diastema intervenes between P2 and P3. The crown of P3 is triangular in outline and is dominated by a swollen and faintly recurved paracone. A weakly developed parastylar lobe projects anteriorly, and can bear a low parastylar cusp; a preparacrista is not developed. The metacone is variably developed: on some specimens (e.g., UALVP 47273, Fig. 5.6.3) it is a small swelling on the postparacrista, while on others (e.g., UALVP 33864, Fig. 5.7.3), it is larger, more discrete, and separated from the paracone by a notch in the centrocrista. Still other specimens show an intermediate condition in which the metacone is smaller but clearly cusp-like, and one specimen (UALVP 47272) preserving associated left and right skull fragments shows P3 with a well-developed metacone on one side, while the contralateral P3 has a poorly developed metacone. A short postmetacrista curves posterolabially from the metaconal apex and can join with a poorly developed ectocingulum, or simply grade into the posterolabial corner of the crown; a metastylar cusp is not developed on any specimen at hand. The crown of P3 narrows considerably lingual to the paracone, and neither the

paraconule nor the metaconule is developed. The protocone is low, conical, and is supported by a separate lingual root. Low cristae extend from the protoconal apex: the preprotocrista runs a short distance labially, but weakens as it nears the parastylar corner of the crown; the postprotocrista is stronger than the preprotocrista, and extends posterolabially to join the postmetacrista and ectocingulum at the metastylar corner of the crown. A hypocone is not present.

P4: The P4 of Litocherus notissimus is somewhat hourglass-shaped in occlusal view, and the crown is dominated by a large, inflated paracone and a smaller protocone. The labial edge of the crown is straight to slightly oblique to the long axis of the crown, and the metastylar corner sometimes projects farther labial than the parastylar corner. The paracone is circular in cross section, massive, and posteriorly leaning; its apex is often truncated by heavy apical wear. A large, conical parastylar cusp is developed immediately anterior to the paracone, and although a preparacrista is not present, a short crest sometimes occurs low on the posterior side of the parastylar cusp, connecting it to the base of the paracone. A low but conspicuous postparacrista extends posteriorly from the apex of the paracone, turning abruptly labially. A swelling representing a metacone or metastylar cusp is usually present low on the postparacrista, but a distinct cusp is never formed; the swelling can be notably inflated (e.g., UALVP 47296), poorly developed (e.g., UALVP 47295), or wholly absent (e.g., UALVP 33864). While wear is usually present on the postparacrista and posterior side of the paracone, it is never heavy, even in specimens where the upper molars display deep wear. Although the cingula are robust anteriorly and posteriorly, the ectocingulum in most specimens is discontinuous or, at best, weakly continuous. The enamel is exodaenodont at the anterior root. The inflated, conical protocone is smaller and shorter than the paracone, and its apex leans anteriorly rather than posteriorly. A strong preprotocrista runs anteriorly and labially from the protoconal apex, joining the parastylar cusp at the anterolabial margin of the crown; the preprotocrista can unite with the anterior cingulum near the anterolingual side of the paracone, or remain separate to the parastyle. In contrast, the postprotocrista runs posteriorly from the protoconal apex, joining the posterior cingulum well lingual to the paracone and continuing on to the posterolabial corner of the crown. Neither paraconule nor metaconule is developed. Although the protoconal cingula are both robust, they are

discontinuous; the posterior cingulum is often wide and shelf-like (e.g., UALVP 47272), but a hypocone is never developed. The enamel on the lingual side of the protocone is weakly exodaenodont.

Upper molars: M1: The crown of M1 is subquadrate in outline. The three principal cusps are inflated at their bases, but narrow towards their apices, and together enclose a deep trigon basin. A shallow ectoflexus divides the labial side of the crown into an anteriorly projecting parastylar area, and a posterolabially projecting metastylar corner; the ectocingulum is low, but heavy and continuous. The paracone is slightly larger than the metacone, with its base extending farther labially and lingually; it is circular in cross section, although its basin-facing wall is often flattened from wear. The metacone is connected to the paracone by a low, widely notched centrocrista, and whereas the paracone is nearly vertical, the metacone leans somewhat posteriorly. A short preparacrista connects the paracone to the ectocingulum, while the postmetacrista is longer, forming a short, blade-like crest that curves posterolabially to join the ectocingulum. The conules and conular cristae are well developed, with the paraconule slightly more lingual than the metaconule: the preparaconular crista and postmetaconular crista extend labially as the paracingulum and metacingulum to the parastylar and metastylar corners, respectively, and remain separate from the protoconal cingula; the internal conular cristae terminate low on the lingual side of the paracone and metacone. The protocone is the largest of the principal cusps, and is only slightly shorter than the paracone. The labial side of the protocone is flat or faintly convex, while its long, sloping lingual side is convex; a shallow enamel lobe is sometimes developed at the lingual root. Low protoconal cristae connect the protoconal apex to the conules, and the preprotoconal crista is distinctly notched prior to its union with the paraconule. The protoconal cingula are low and discontinuous lingually. The anterior cingulum usually supports a low, bulbous pericone that appears either as a discrete cusp (e.g., UALVP 47272, Fig. 5.7.6) or as a swelling of the anterior cingulum (e.g., UALVP 47248, Fig. 5.6.6). The posterior cingulum widens towards the lingual margin of the crown, and supports a large, conical hypocone; in most specimens (e.g., UALVP 47248, Fig. 5.6.5) the hypocone is significantly inflated, and forms a conspicuous lobe adjacent to the protocone, while in other specimens (e.g., UALVP 47307) it is smaller and more closely

appressed to the protocone. A shallow lobe of enamel overhangs the lingual side of the hypocone on some specimens.

M2: The crown of M2 is smaller overall than that of M1, being subequally wide or slightly more transverse, but significantly shorter anteroposteriorly. M2 further differs from M1 in having a deeper ectoflexus, a more smoothly rounded and less anteriorly projecting parastylar lobe, and a weaker hypocone and pericone. As on M1, the preparaconular crista and postmetaconular crista on M2 extend to the labial corners of the crown as the paracingulum and metacingulum, respectively, and do not join the protoconal cingula. The protocone and hypocone bear shallow enamel lobes lingually.

M3: The crown of M3 is asymmetrically triangular in outline, with the parastylar corner well developed and anterolabially projecting, and the metastylar corner greatly reduced. The crown is smaller overall than that of M1 or M2, although its transverse width approaches that of M1 in some specimens. The preparacrista extends from the paraconal apex to the parastylar spur, joining the heavy ectocingulum; the ectocingulum weakens considerably posteriorly, and is undeveloped at the level of the metacone. The metacone is subequal or only slightly smaller than the paracone in some specimens, whereas in others it is more reduced. The conules on M3 are well-developed, and their associated crests are sharply defined; the paraconule is subequal or slightly larger than the metaconule, and is more lingual. As on M1 and M2, the internal conular cristae terminate near the bases of the paracone and metacone; the preparaconular crista extends to the parastylar spur as the paracingulum, but the postmetaconular crista is short, fading away as it nears the level of the metacone. The protocone is subequal in size and height to the paracone, anteriorly leaning, and bears a long lingual slope. Low cristae extend labially from the apex of the protocone to the conules. The protoconal cingula are well-defined, but are discontinuous lingually; neither a hypocone nor a pericone is developed.

Dentary and lower dentition (Figs. 5.8-5.10): Although the horizontal ramus is preserved in a number of specimens in the present sample, only UALVP 40515 and 46379 preserve significant parts of the coronoid, condylar, and angular processes. The horizontal ramus is long, shallow, and gently convex ventrally, with its deepest parts occurring ventral to p4 and m1; the ramus becomes increasingly shallow anteriorly. Although each of the dentaries of Litocherus notissimus at hand is incompletely

preserved, two specimens (UALVP 40515, 40668, Figs. 5.8.4, 5.8.7) preserving the lower canine in place suggest that the depth of the ramus may vary according to sex: on the dentary bearing a large canine (presumed male), the ramus is deep, whereas on the dentary bearing a smaller canine (presumed female), the ramus is notably shallower; this dimorphism is also seen in UM 89802 (male) and UM 89801 (female), topotypic specimens of L. notissimus from the early Tiffanian Scarritt Quarry of Montana (Figs. 5.9.10-5.9.15). The medial and lateral surfaces of the mandibular ramus are faintly convex in anterior view, and meet ventrally at a sharply defined ridge that may represent the area of distal insertion of the digastric musculature; the ridge continues anteriorly towards the symphysis, and posteriorly towards the level of m2 before grading into the ventral margin of the jaw. Two mental foramina are developed labially: the smaller and more posterior foramen is ventral to the level of p3, with its ovate aperture opening laterally and slightly dorsally; the larger foramen occurs ventral to the level of p2, and its circular aperture opens laterally and anteriorly. The articular surface of the symphysis is long, shallow, and bounded dorsally by a heavy ridge of bone that is flat medially from contact with the opposing lower jaw. The area of bone ventral to the ridge is smooth and concave, with no rugosities or interdigitations that would indicate that the two mandibular rami were synostosed in life. The anterior margin of the coronoid process ascends steeply from the posterodorsal margin of the mandibular ramus, and terminates at a broadly rounded apex that is positioned well above the level of the tooth row. The posterior edge of the coronoid process is short and concave, and terminates at a stout condylar process. The masseteric fossa is deep and areally extensive, occupying nearly the full height of the coronoid process and extending to near the ventral border of the horizontal ramus; although the anterior extent of the fossa is largely limited to parts of the ramus posterior to m3 by a raised ridge, a conspicuous muscle scar is sometimes developed on the anterior parts of the ridge (best seen in UALVP 40515, Figs. 5.8.4-5.8.6), suggesting that slips of the temporalis musculature may have inserted anterior to the masseteric fossa. The temporalis fossa is more shallowly excavated than the masseteric fossa, and does not extend as far ventrally: narrow crests limit the extent of the fossa anteriorly, while a low ridge extending posteriorly along the base of the coronoid process from the level of the tooth row defines its ventral border; a large, circular

mandibular foramen opens beneath this ridge directly above the proximal parts of the angular process. The horizontal ramus narrows posteriorly to a short but stout condylar process, and although the condyle is not well preserved, the position of the condylar process suggests that its articulating surface was well dorsal to the level of the tooth row. The angular process is preserved only in UALVP 46379: the process is dorsoventrally shallow, but wide and shelf-like in ventral view, and extends posteroventrally at an angle of about 20 degrees from the long axis of the horizontal ramus. The process bends weakly mediad along its length, and terminates at a dorsally hooked apex.

Lower incisors: Other than Simpson's (1936) brief description of an i2 in association with AMNH 33940, nothing about the number or morphology of the lower incisors of Litocherus notissimus has been previously documented. A topotypic specimen of L. notissimus (UM 89810) preserves alveoli for three small incisors: the dimensions of the alveoli indicate that i2 was the largest lower incisor, and that the teeth were procumbent, projecting anteriorly and dorsally at about a 45 degree angle from horizontal. UALVP 47258 preserves a small lower incisor, possibly i3, in association with an incomplete dentary housing the lower canine and p2-4. The incisor crown is wedge-shaped in occlusal outline, with the apex of the wedge anterior and the crown mediolaterally expanded posteriorly. The crown bears two cusps: a large, bilaterally compressed main cusp and a smaller, subconical accessory cusp positioned posterolabial to the main cusp. A moderately developed crest connects the apex of the main cusp with the accessory cusp, and a broad notch is formed in its deepest part, imparting a somewhat bilobate appearance to the crown.

Lower canine: As with the upper canines, two distinct lower canine anatomies are documented in the present sample, and these different morphs are tentatively interpreted here as owing to sexual dimorphism (similar morphs of the upper and lower canines are also present in the topotypic sample from Montana, pers. obs.). Seven specimens represent the smaller, and presumably female morph: the crown is premolariform and slightly anteriorly leaning, with a large main cusp and small but well-defined heel. The tooth is single rooted and positioned somewhat oblique to the longitudinal axis of the dentary such that the crown is oriented anterolaterally-posteromedially. The main cusp is weakly recurved and bears a sharply pointed apex. A well-developed crest runs a short

distance anteriorly from the apex of the main cusp before bending sharply medially and posteriorly, forming a low medial cingulid; a longer crest extends posteriorly from the main cusp to the low but conspicuous heel. The larger and presumably male morph is represented by four specimens: the crown is caniniform and recurved, with the apex is positioned well above the level of the tooth row and projecting posterodorsally and slightly medially. In contrast to that of the smaller morph, the crown of the larger morph is held nearly vertically in the jaw, rather than being procumbent. Although accessory crests are not present on the larger canines, a faint swelling suggestive of a weakly developed heel can be developed posterobasally.

Lower premolars: p1: Three specimens, UALVP 47314, 47315, and 47317, preserve the p1 of Litocherus notissimus, and a number of other specimens preserve the alveolus. The p1 bears a single stout root that is circular in cross section. The crown is smaller than that for either the canine (male or female morph) or p2, and is premolariform, with a dominant protoconid and a small, weakly cuspate heel. The tooth is slightly procumbent, with the anterior parts of the crown overlapping the posterior parts of the lower canine; diastemata are not developed, either between the canine and p1, or between p1 and p2.

p2: The two-rooted p2 bears a tall, slightly recurved protoconid and a low and weakly cuspate heel. A low paracristid extends anteriorly and medially from the protoconid apex, but a paraconid is not developed. The postvallid can support a weak crest connecting the protoconid to the heel, or the crest can be entirely undeveloped.

p3: The p3 of Litocherus notissimus is two-rooted and premolariform, with the crown being dominated by a large protoconid and a low heel. The crown is short relative to its width, and more or less teardrop shaped in occlusal outline, being narrow anteriorly and wide posteriorly. The protoconid is variably developed: in some specimens (e.g., UALVP 40515, Figs. 5.8.4-5.8.6) it is tall and vertical, with the apex nearly as high as that of p4, while in other specimens (e.g., UALVP 40668, Figs. 5.8.7-5.8.9) it is lower, more inflated, and slightly recurved. A weak paracristid is sometimes developed, extending anteriorly from the protoconid apex to a low anterior cingulid; a paraconid is present in some specimens (e.g., UALVP 40668, Figs. 5.8.7-5.8.9), whereas in others it is absent (e.g., UALVP 47314, Figs. 5.8.10-5.8.12). A metaconid is not present in any of

the specimens at hand. As with the protoconid, the p3 heel is variable in its development: on some specimens (e.g., UALVP 47314, Figs. 5.8.10-5.8.12) the posterior cingulid is drawn out dorsally as a small cuspid, whereas in other specimens (e.g., UALVP 40515, Figs. 5.8.4-5.8.6) the cuspid is not present, and the heel consists only of a transversely oriented crest. A sharply defined cristid obliqua runs posteriorly and slightly lingually from the protoconid apex to the heel, and the hypoflexid is deep; a low entocristid is developed on one specimen, and a small, shallow basin is formed between it and the cristid obliqua. Although exodaenodonty is developed at the posterior root on all specimens at hand, the lobe can be relatively shallow (e.g., UALVP 47314) or deeper and more pronounced (e.g., UALVP 40515).

p4: The p4 of Litocherus notissimus is considerably enlarged relative to p3 and m1. The crown is semimolariform and dominated by an inflated, slightly recurved protoconid and a small but well-developed talonid. As with that of p3, the crown of p4 widens considerably posteriorly and is roughly teardrop-shaped in occlusal outline. Although the paracristid is weakly developed near the protoconid apex, it becomes heavier and more conspicuous as it progresses anteriorly and slightly lingually to the anterior cingulid. The paraconid is anterior, or anterior and slightly lingual in position, and is variably developed: in most specimens (14/22, 64%, e.g., UALVP 47314, Figs. 5.8.10-5.8.12), it is a small conical cusp developed on the anterior cingulid as it wraps around the anterior side of the protoconid; although the paraconid in these specimens projects anteriorly, it is nonetheless closely appressed to the base of the protoconid. In other specimens (4/22, 18%, e.g., UALVP 40515), the paraconid resembles the more common morph, but is larger, while in others (2/22, 9%) it is virtually undeveloped, with only the cingulid present. In two specimens (9%, e.g., UALVP 40510, Figs. 5.8.1-5.8.3), the paraconid is substantially enlarged and set off anteriorly from the protoconid, with the two cusps being separated by a deeply notched paracristid; the paraconid in these specimens is not formed as a cingulid cusp, but rather arises from low on the anterior side of the protoconid. The metaconid arises from low on the posterolingual side of the protoconid, and although it is present on each of the p4s at hand, it varies considerably in its development. On most specimens (9/23, 39%, e.g., UALVP 40527, Figs. 5.9.1-5.9.3) it is small, conical, and well-differentiated from the protoconid; in these specimens, the

metaconid is closely appressed to the protoconid and the protocristid is virtually undeveloped. In other specimens (7/23, 30%, e.g., UALVP 40510, Figs. 5.8.1-5.8.3), the metaconid is weakly developed, appearing only as a poorly defined swelling on the posterolingual side of the protoconid, whereas in other specimens (7/23, 30%, e.g., UALVP 46379, Figs. 5.10.2-5.10.4), it is enlarged, conical, and separated from the protoconid by a deep, slit-like notch; on these specimens, the protocristid is well-developed. Although the talonid basin is short and narrow, extending no farther labially than about half the width of the protoconid, the hypoflexid is very deep and slopes lingually. The talonid can bear two (8/17, 47%) or three (9/17, 53%) cusps that enclose a shallow basin. In specimens having two talonid cusps (the entoconid and hypoconid), both are usually subequal in size and height, and are connected to each other by a low postcristid; on those specimens bearing three talonid cusps, the hypoconulid is usually the smallest, and all three cusps are closely appressed, with little development of a postcristid. The cristid obliqua contacts the postvallid wall low and slightly lingual to the longitudinal midline of the crown, and on some specimens can continue further dorsally towards the apex of the metaconid. A low entocristid is developed on all specimens at hand. Exodaenodonty is present at the posterior root, with the lobe usually extending considerably farther ventrally than the anterior lobe.

Lower molars: m1: The lower molars of Litocherus notissimus decrease in size and height posteriorly: the decrease in size and height is comparable to that in Xynolestes (see earlier in this chapter), but is not to the same degree as in the lower molars of erinaceids. The m1 is subrectangular in outline, with the trigonid slightly narrower than the talonid, and the postvallid wall oriented somewhat obliquely anterolabially-posterolingually. The trigonid cusps are subconical, with rounded apices and swollen internal walls, and are nearly equidistant from each other, forming a near-equilateral triangle in occlusal view. The protoconid and metaconid are subequal in height, although the metaconid is more swollen, and their apices lean slightly posteriorly. The paraconid is smaller and lower than the metaconid or protoconid, and appears as a swelling at the terminus of the robust paracristid; it is slightly labial to the level of the metaconid, and projects anteriorly. The paracristid is well defined, extending anteriorly from the protoconid apex, and then bending sharply lingually as it continues to the paraconid. The

protocristid is deeply notched. The talonid of m1 is wider than long and moderately deep; the flat and internally sloping walls of the tall hypoconid and entoconid meet as a smoothly rounded basin, contrasting with that in erinaceids (e.g., Litolestes) in which the basin is more nearly V-shaped. The hypoconid is the largest talonid cusp, but is slightly lower than the entoconid. A low cristid obliqua connects the hypoconid apex to the postvallid wall below or slightly lingual to the protocristid notch, while an equally low hypocristid extends from the hypoconid apex to the hypoconulid; a mesoconid is not developed. The inflated hypoconulid is smaller and lower than the other talonid cusps, anteroposteriorly compressed, and is closer to the entoconid than to the hypoconid; a slit-like notch interrupts the hypocristid between the hypoconid and hypoconulid, and the postcristid is weakly developed, connecting the apices of the entoconid and hypoconulid. The entoconid is tall, with a sharp apex, and a deeply notched entocristid connects the entoconid to the postvallid wall; an entoconulid is not present, although a swelling on the entocristid immediately anterior to the entoconid apex suggests its incipient development. An anterior cingulid is invariably developed on m1, originating from just ventral to the paraconid and wrapping around the labial side of the protoconid; the anterior cingulid terminates almost immediately after reaching the labial side of the protoconid in most m1s, but in some specimens it can continue farther posteriorly, and on three specimens it continues as a low, weak ridge to the hypoflexid. The posterior cingulid is more variably developed than the anterior cingulid: on some specimens, it is poorly developed or absent, whereas in others it forms a conspicuous shelf that extends labially from the hypoconulid, although never wrapping around to the labial side of the hypoconid. The hypoflexid is deep, and a prominent hypoflexid shelf is present posterior to the protoconid. Exodaenodonty is sometimes developed at the anterior and posterior roots.

m2: The m2 of Litocherus notissimus is smaller than m1, and the crown is lower, with the apices of the trigonid cusps barely taller than those of the m1 talonid. The trigonid is anteroposteriorly compressed, and the postvallid wall is more nearly perpendicular to the long axis of the jaw (rather than obliquely oriented, as in m1), and the trigonid angle is more acute. The metaconid is the largest trigonid cusp, being taller and more inflated than the protoconid, although both cusps have markedly swollen basin-facing walls. The paraconid and paracristid vary considerably in their development and

position. On a majority of specimens (27/38, 71%, e.g., UALVP 40515, Figs. 5.8.4-5.8.6) the paraconid is non-cuspate, being fully incorporated into the low, shelf-like paracristid; within this grouping, the paracristid can be medial in position (9/27, 33%), or located more lingually (18/27, 67%). The paraconid develops as a discrete swelling at the terminus of the paracristid on a minority of specimens (11/38, 29%, e.g., UALVP 40668, Figs. 5.8.7-5.8.9), and is lingually positioned. Irrespective of its degree of development, the paraconid/paracristid complex is always closely appressed to the metaconid, and the trigonid angle is much more acute than on m1. The protocristid is sharply defined and deeply notched. Although the crown of m2 is smaller than that of m1, the talonid of m2 is nearly as broad and long as that on m1, and its overall morphology is similar: the internal walls of the hypoconid and entoconid form a moderately deep, cup-shaped basin; the hypoconid is the largest cusp and is slightly lower than the tall entoconid; the hypoconulid is closer to the entoconid than the hypoconid; and the postcristid weakly developed. As with m1, a mesoconid is not developed, although a faint swelling occurs on the entocristid just anterior to the entoconid, suggesting an incipiently developed entoconulid. The anterior cingulid is well developed on m2, and most often terminates after wrapping around to the labial side of the protoconid, although in some specimens it can continue as a weak ridge to the hypoflexid. The development of the posterior cingulid on m2 varies in ways similar to that on m1. The hypoflexid is deep, with a prominent hypoflexid shelf developed posterior to the protoconid, and exodaenodonty can occur at the anterior and posterior roots.

m3: The crown of m3 is smaller and lower than that of m2. The trigonid is anteroposteriorly compressed to nearly the same degree as on m2, and the postvallid surface is oriented perpendicular to the long axis of the jaw. The paraconid is less distinct than on m2, being further incorporated into the paracristid, and the paraconid/paracristid complex is more shelf-like, leaning more anteriorly and being less closely appressed to the metaconid. The metaconid is relatively larger than the protoconid compared to those cusps on m2, although their basin-facing walls are similarly swollen; both protoconid and metaconid are smaller and lower than those on m2, with their apices barely above the talonid cusps on m2. The protocristid is sharply

defined and the protocristid notch is deep. The m3 talonid is longer but narrower than in m1 and m2, and the internal walls of the hypoconid and entoconid on m3 are flat, but become increasingly rounded ventrally, forming a cup-shaped basin; while the hypoconid is the largest talonid cusp, it is lower than the entoconid and hypoconulid. The swollen entoconid and hypoconulid are large and subconical, with the hypoconulid closer to the entoconid than to the hypoconid. The cristid obliqua is low, joining the postvallid wall ventral to the protocristid notch. The anterior cingulid is similar to that on m1 and m2, and can terminate anterolabially, or continue as a weak ectocingulid to the hypoflexid; the posterior cingulid can be short and shelf-like, or wholly undeveloped.

Petromastoid (Figs. 5.10-5.12): UALVP 46379 preserves the left and right petromastoid, the first known for any species of Litocherus and the oldest so far discovered for any lipotyphlan; although both are slightly damaged and incomplete, together they document much of the anatomy of the petrosal and mastoid, and permit a limited reconstruction of the carotid circulation within the middle ear cavity. The petromastoid is an endochondral ossification of the basicranium that houses the organs of hearing (cochlea) and equilibrium (semicircular canals and vestibular apparatus) within an extensive bony labyrinth, serves as an important passageway for a number of cranial nerves, arteries, and veins, and provides areas for the attachment of muscles and ligaments associated with the middle ear ossicles (Novacek, 1986; Wible, 1990; Wible et al., 2001). The petromastoid is divided into two anatomical parts: the more anterior pars cochlearis, consisting primarily of the promontorium enclosing the cochlea, and a posterodorsal pars canalicularis housing the semicircular canals; the vestibule containing the utriculus and sacculus is positioned roughly in the central part of the osseous labyrinth, and is in communication with the cochlear canal anteriorly and the semicircular canals posteriorly. The disposition of the petromastoids in skulls of extant mammals varies considerably, and orienting isolated and incomplete petromastoids of fossil mammals to their presumed "in life" positions can be difficult (see, e.g., MacIntyre, 1972; Wible et al., 2001). Regardless of its precise orientation in the skull, however, the petromastoid presents four main surfaces (the tetrahedral model of MacIntyre, 1972): a cerebellar surface (dorsal, or endocranial of other authors, see Wible et al., 2001; Ekdale et al., 2004) facing the brain and visible intracranially; a tympanic surface, facing the

middle ear cavity; a squamosal surface, overlain by the squamosal bone; and a mastoid surface, exposed on the posterior and lateral parts of the skull (MacIntyre, 1972, Wible, 1990). Each of these surfaces is preserved in varying levels of completeness in the two petromastoids in UALVP 46379.

The petromastoid in UALVP 46379 is represented by left and right elements: the tympanic part of the left petromastoid preserves the promontorium almost in its entirety, while the right promontorium is badly crushed, and neither element preserves the tegmen tympani, epitympanic recess, or the rostral-most parts of the promontorium. The promontorium is somewhat inflated and smoothly rounded on its tympanic surface; the broken rostral edge and surrounding bone of the promontorium are suggestive of there having been a rostral tympanic process originally, but confirmation of this must await the discovery of better preserved specimens. The medial and posteromedial margins of the promontorium are rounded: there is no evidence of articular surfaces on these margins for the basioccipital or basisphenoid, nor is there evidence for the presence of an entotympanic; a medial process or anterior extension of a caudal tympanic process is not present. The dorsomedial side of the promontorium is excavated by a shallow but conspicuous groove for the inferior petrosal sinus; in life, the sinus carried a vein that connected the cavernous sinus with the internal jugular vein. At the posterior end of this groove, where the sinus would have united with the jugular bulb, the bone is perforated by the foramen of the cochlear canaliculus. The posterior parts of the promontorium are penetrated by two conspicuous openings, the fenestra rotundum posteromedially, and the fenestra ovalis posterolaterally; the fenestra ovalis accommodated the footplate of the stapes in life. The boundary between the fenestra rotundum and fenestra ovalis is not marked by a sharp ridge (crista interfenestralis) anywhere along its length, and the fenestra rotundum is partly "shielded" posteriorly by weak caudal tympanic process; this ridge appears to be mostly complete, and probably would not have formed the base of a more pronounced caudal tympanic process. The promontorium is marked posteriorly by a shallow groove for the internal carotid artery; based on the position of the groove, the artery would have entered the middle ear from a medial position. The groove continues laterally and dorsally, becoming more deeply invaginated as it approaches the ventral border of the fenestra ovalis, where the internal carotid artery probably bifurcated in life,

sending a stapedial branch laterally through the stapedial foramen, and a promontorial branch anterolaterally across the promontorium (MacIntyre, 1972; MacPhee, 1981; Wible, 1990 Bloch and Silcox, 2001). The promontorium bears two sulci medial to its ventral apex. The more laterally-coursing sulcus is shallow and broad, with poorly defined margins, and it continues anterolaterally, becoming slightly deeper and better marked towards the periphery of the promontorium before abruptly ending. The more distal parts of the sulcus probably represent the site of proximal attachment of the tensor tympani, a muscle involved mediating the tension of the tympanic membrane and hence in sound dampening (MacPhee, 1981); the anatomical significance of the more proximal parts of the sulcus on the promontorium is unclear. The second and more medially positioned sulcus is much narrower than the lateral sulcus, has sharply defined, raised margins, and remains on the lateral aspect of the promontorium for its entire preserved length: it is likely to have held the internal carotid nerve plexus (and presumably the deep petrosal nerve) and the promontorial ramus of the internal carotid artery (MacIntyre, 1972; MacPhee, 1981). An incompletely preserved foramen occurs dorsal and slightly lateral to the fenestra ovalis on the left petromastoid: the foramen leads into the squamosal sinus and may represent part of the course of the dorsal ramus of the stapedial artery. The walls of the facial canal are badly damaged on the left petromastoid (these parts are missing altogether from the right side), but it appears that the canal was probably open and the nerve in contact with the middle ear as it approached the stylomastoid foramen. The stylomastoid foramen is well preserved on the right petromastoid: it is rimmed ventrolaterally by a medially projecting, fused tympanohyal element, and ventromedially by a process projecting from the dorsal margin of the weakly developed caudal tympanic process. A shallow fossa for the stapedius muscle occurs posterior and slightly dorsal to the level of the bone intervening between the fenestra rotundum and ovalis; in life the stapedius muscle functions in controlling the amplitude of sound waves by restricting movement of the stapes.

Two conspicuous openings are developed on the cerebellar surface, the internal acoustic meatus anteriorly, in life transmitting the petrous parts of the facial (VII) and vestibulocochlear (VIII) cranial nerves, and the subarcuate fossa posteriorly, in life housing the paraflocculus of the cerebellum; post-mortem damage to both petromastoids

in UALVP 46379 has distorted the shapes of these openings to a greater or lesser degree. The internal acoustic meatus is best preserved on the left petromastoid in UALVP 46379: it is subovate in outline, with the foramen acusticum inferius and foramen acusticum superius slightly recessed below the cerebellar surface and separated from one another by a low, transverse septum. The deeper parts of the internal acoustic meatus are damaged or otherwise obscured by hard, compacted sediment. The bone anterior and medial to the internal acoustic meatus is flat or faintly convex, but becomes strongly convex further medially, forming an inflated surface that narrows anteriorly to a more sharply defined ridge. This edge represents the upper lip bounding the sulcus for the inferior petrosal sinus. The bone anterior and lateral to the internal acoustic meatus is damaged in both petromastoids; as a result, the dimensions of the prefacial commissure and anterior tympanic wing cannot be determined. The subarcuate fossa is mediolaterally narrow, but very deep, and its lateral border forms the medial edge of a deeply excavated, dish-like area; this region likely housed a large squamosal sinus in life (Novacek, 1986). The mastoid is neither enlarged nor pneumatized.

Appendicular skeleton: Innominate (Figs. 5.10, 5.13.1-5.13.6): Right and left fragmentary innominates are preserved in two specimens (UALVP 46379 and 46378), and collectively document the caudal parts of the ilium, the acetabulum, parts of the superior ramus of the pubis, and most of the ischium; the bulk of the pubis and pubic symphysis, and the cranial parts of the ilium and auricular facets are missing. Judging by the dimensions of the broken ilium and the length of the ischium, the ilium would have been slightly longer than the ischium. Although partly crushed and broken, the proportions of the body of the ilium suggest that the iliac blade would not have been equal in dorsoventral and mediolateral dimensions: instead, the dorsolateral surface was slightly expanded relative to the ventrolateral surface, indicative of well-developed superficial and weaker lesser gluteal musculature. The acetabulum has a prominent lip that rims the acetabular fossa posteriorly and dorsally, and the acetabular fossa is nearly circular in outline, deep, and ventrally facing; these features suggest that the femur had capacity for strong flexion and extension at the hip, but a lower capacity for abduction and rotation. The posterior bony buttress of the acetabular fossa indicates the bulk of the body mass would be borne posteriorly, and that the stance was probably pronograde

(Scott and Boyer, in prep.). A robust anterior inferior iliac spine is developed anterior to the acetabulum, and a somewhat expanded area of bone is developed at the ventral most part of the body of the ilium: this expansion represents the iliopectineal eminence, and a ventrally directed crest, the iliopectineal crest, extends anteriorly and inferiorly to the superior ramus of the pubis; the eminence and crest represent areas of proximal attachment of the pectineus and adductor musculature. The ischium is mediolaterally narrow and dorsoventrally deep, and the ischial tuberosity, the site of proximal attachment of the hamstring musculature, is somewhat expanded dorsoventrally. The ischial spine projects prominently dorsally and is located close to the cranial end of the ischial ramus, slightly posterior to the posterior margin of the acetabulum.

Femur (Figs. 5.13.7-5.13.11): An incomplete left femur preserving the shaft and distal epiphysis is preserved in UALVP 46379. The diaphysis is relatively short proximodistally; it is mediolaterally narrow and anteroposteriorly deep. The proximal epiphysis is not preserved, and nothing can be said of the femoral head or greater and lesser trochanters. A prominent third trochanter with a distinct apex occurs about one-third of the way distally along the length of the shaft as preserved: the trochanter is positioned mediolaterally on the shaft of the femur, and flares conspicuously medially. The relative size and medial flaring of the third trochanter suggests that the superficial gluteal musculature was well developed in Litocherus notissimus, and the capacity for powerful extension of the leg at the hip was increased (Sargis, 2002). A well-developed trochanteric fossa is present proximally and posteriorly, although the inter-trochanteric crest is not well-developed. The distal diaphysis and distal epiphysis are both incompletely preserved, and the two parts cannot be seamlessly joined. The patellar groove is shallow and relatively narrow, with distinct medial and lateral ridges; these features, in combination with the deep femoral shaft, probably provided the tendon for the quadriceps musculature with a greater mechanical advantage during extension of the knee, with the crest-like margins of the patellar groove preventing significant excursion of the patella and quadriceps tendon during fast running. The medial and lateral condyles are roughly equal in mediolateral width, and distinct fossae for the medial and lateral collateral ligaments mark each of the epicondyles; a distinct pyriform groove for the

attachment of the popliteus muscle occurs on the distolateral margin of the lateral epicondyle.

Astragalus (Figs. 5.14.1-5.14.6): The astragalus is preserved in UALVP 46378 in association with an incomplete maxilla and dentary, incomplete left and right innominates, and incomplete phalanges. The body is subquadrate in dorsal view, with the trochlea angled somewhat distolaterally; the neck is long and its axis is angled medially relative to that of the trochlea. The body is significantly deeper dorsoventrally than either the head or the neck. The trochlea bears a deeply grooved astragalotibial facet, with the lateral margin being more sharply crested and distinctly elevated than the medial margin. The radius of curvature of the lateral margin of the body increases distally, and the lateral side of the body appears dorsally "peaked"; in contrast, the medial margin of the trochlea has an more nearly even radius of curvature along its proximodistal length. The groove for the tendon of the flexor fibularis musculature is developed on the posterior and proximal margins of the body: it is shallow and faces posteriorly and somewhat proximally. The fibular facet is roughly rectangular in outline, slightly convex, and faces laterally; its proximodorsal margin is marked by a small fossa representing the area of attachment of the astragalofibular ligament. The medial side of the astragalar body is shallower than the lateral side, and a cotylar fossa (representing the area of contact on the astragalus by a laterally hooked medial malleolus of the tibia) is not developed. The ventral surface of the astragalar body and neck bears conspicuous ectal and sustentacular facets for articulation with the calcaneum. The ectal facet is areally small, with its long axis oblique to, but about the same length as the flexor fibularis groove; the ectal facet is peaked dorsally, rather than being evenly concave, and faces more laterally than ventrally. A prominent, transverse ridge is developed at the proximal margin of the ectal facet. The sustentacular facet is oval in outline, is slightly convex ventrally, and lacks an accessory tail extending proximomedially towards the flexor fibularis groove; in contrast to the ectal facet, the sustentacular facet faces ventrally and medially, and is well separated from the ectal and navicular facets. The gap between the sustentacular facet and the flexor fibularis groove (sulcus astragali) is deeply invaginated, but an inferior astragalar foramen is not developed there. The medial margin of the astragalar neck is sharply ridged while the lateral margin is more rounded; the neck widens distally, joining

the mediolaterally broad head. The head is dorsoventrally compressed and ovoid in distal outline, with its major axis oriented dorsolaterally-ventromedially, and its dorsal surface marked by a faint depression of uncertain significance. The distal surface of the head bears the astragalar navicular facet: the facet is strongly convex and mainly covers the distal and lateral margin of the head, and distal portion of the neck. A small cuboid facet is present ventrolaterally.

Calcaneum (Figs. 5.14.7-5.14.12): The calcaneum is preserved in UALVP 46379, in association with incomplete lower jaw, left and right innominates, femur, cuboid, entocuneiform, metatarsal V, and proximal and distal phalanges. The calcaneum is relatively short proximodistally, with the tuber (that part of the calcaneum proximal to the calcaneal ectal facet) being about as long proximodistally as it is dorsoventrally deep; the body of the calcaneum is slightly longer than the tuber. The tuber is oriented at a slight medial angle to the axis of the body, and the shaft of the calcaneum has a slight lateral convexity. The proximal end of the tuber faces proximolaterally and is not appreciably expanded mediolaterally; the tuber is grooved for attachment of the calcaneal tendon. The dorsal surface of the calcaneum bears conspicuous ectal and sustentacular facets for articulation with the opposing astragalar facets. The ectal facet is proximodistally elongate and slightly mediolaterally compressed; the facet is concavoconvex, being significantly convex distally, but becoming flat to slightly concave proximally. The proximal margin of the ectal facet is marked by a transverse groove into which the ridge formed at the proximal margin of the astragalar ectal facet would have fit. Lateral to, and confluent with the ectal facet is a conspicuous fibular facet: the facet is convex, proximodistally elongate, dorsoplantarly narrow, and faces laterally. The sustentacular facet is set off from the body of the calcaneum on the ledge-like, slightly proximodistally sloping sustentaculum tali; the facet is shallowly concave and oval in dorsal outline, and it is broadly separated from the ectal facet and the distal sustentacular facet for the astragalar head. A shallow groove is developed on the ventrolateral margin of the sustentaculum tali, marking the position of the tendon of the flexor fibularis muscle. The peroneal tuberosity is developed near the distolateral margin of the calcaneal body: it is slightly distal to the level of the sustentaculum tali, and the process extends comparatively less far laterally than the sustentaculum does medially. The peroneal

tuberosity is large, occupying roughly a fifth the proximodistal length of the calcaneum, and is inset from the distal margin of the calcaneal body (i.e., it is not positioned at the extreme distal end of the bone); it projects proximally and dorsally, and it is elevated above the level of the sustentacular facet. The lateral surface of the peroneal tuberosity lacks a groove for the peroneus brevis tendon. The distal end of the calcaneum bears a large, flat cuboid facet: the facet is flat, nearly circular in distal outline, and faces distomedially; a distinct plantar pit is not developed. There is no obvious navicular facet on the calcaneal body, but a distal sustentacular facet for the astragalar head occurs just medial to the cuboid facet on the dorsomedial aspect of the calcaneal body; this facet was confluent with the astragalar facet on the cuboid. The ventral surface of the calcaneum supports a robust, medially-projecting plantar process distally.

Cuboid (Figs. 5.15.1-5.15.6): The cuboid is proximodistally long, mediolaterally narrow, and dorsoventrally deep. The proximal surface supports facets for four different bones, the largest and most lateral of which is for the calcaneum. The calcaneal facet is flat and faces proximally, dorsally, and laterally; the facet is subcircular in proximal outline, in agreement with the cuboid facet on the calcaneum. Medially adjacent to the calcaneal facet is the astragalar facet: it is mediolaterally narrow, faces mediodorsally, and is slightly concave. The astragalar facet extends to the medial margin of the cuboid where it contacts navicular facet. The navicular facet is proximodistally narrow but dorsoventrally deep, and is confluent with the ectocuneiform facet, the fourth proximal facet of the cuboid. The ectocuneiform facet is about the same size as that for the navicular, and terminates near the proximodistal midpoint of the cuboid. Distal to the ectocuneiform facet is a non-articular area that persists to the distal margin of the bone. The distal end of the cuboid supports a well-developed facet for metatarsals IV-V: the facet faces distally and slightly medially, and is shallowly concave and roughly equal in dorsoventral and mediolateral dimensions. The plantar surface of the cuboid is marked by a deep, transversely oriented groove for the tendon of the peroneus longus muscle, and a rugose peroneal tuberosity occurs at the proximal margin of the groove; the peroneal tuberosity bears a central pit for a robust short plantar ligament.

Entocuneiform (Figs. 5.15.7-5.15.11): The entocuneiform is slightly damaged, with the proximal margin missing. The bone is long and wedge-like in medial or lateral

view, being narrow mediolaterally and deep dorsoplantarly. The dorsal surface is drawn out as a sharp ridge, while the plantar surface is more rounded. There are no discernable facets on the medial surface for either the mesocuneiform or second metatarsal. The distal facet for the hallucal metatarsal is mediolaterally narrow and concave, and the joint between the entocuneiform and hallucal metatarsal would be saddle-shaped; the dorsal half of the facet is somewhat expanded mediolaterally. The plantar surface of the entocuneiform supports a prominent plantarodistal process for the distal attachment of the tendon of the tibialis posterior muscle.

Metatarsal V (Figs. 5.15.12-5.15.15): Metatarsal V is about twice the length of the proximal phalanx (see later in the text). The diaphysis is subovate in cross section, being slightly wider mediolaterally than anteroposteriorly deep; the shaft is nearly straight in the dorsoplantar plane, but is gently curved mediolaterally. The tuberosity for the tendon of the peroneus brevis muscle has been broken off, but the dimensions of the base indicate that it was robust and directed proximolaterally. The facet for the cuboid is virtually flat, while that for metatarsal IV is slightly convex; a robust plantar tuberosity is developed proximally. The distal trochlea is nearly cylindrical, rather than spherical, and bears a prominent median ridge.

Phalanges (Figs. 5.15.16-5.15.23): One complete and one proximal fragment of a proximal phalanx are preserved in UALVP 46379, as well as the proximal part of an intermediate phalanx; the phalanges are interpreted here as being part of the pes, given their association with other hind limb elements in UALVP 46379. The shaft of the proximal phalanx is virtually straight, with the widest and deepest parts located at the proximal end, and the narrowest dimensions at midshaft. The proximal facet for articulation with the metatarsal is concave, nearly semicircular in proximal outline, and oriented proximodorsally. The ventral margin of the proximal end is marked by a pair of prominent tuberosities, and ridges that may have supported the annular ligaments of the flexor tendon sheaths extend distally from the tuberosities. The middle part of the shaft is nearly circular in cross-section, but becomes slightly wider mediolaterally towards the distal end. A pair of tuberosities is developed near the distal end of the shaft; like the more proximal pair, the distal tuberosities probably secured the annular ligaments of flexor tendon sheaths. The distal end of the shaft supports a large, subcylindrical trochlea

for articulation with the intermediate phalanx; the trochlea is mediolaterally wide, but shorter proximodistally and dorsoplantarly, and faces distoventrally. The intermediate phalanx is smaller than the proximal phalanx, and its proportions suggest that it was likely much shorter. The proximal facet is strongly concave, and the shaft is straight and circular in cross-section. Ridges or tuberosities related to annular ligaments of flexor sheaths are not developed.

Discussion.—A comprehensive description and phylogenetic analysis of Litocherus notissimus based on specimens from the type locality, as well as specimens outlined in this chapter, are currently in preparation (Scott and Boyer, in prep.). Specimens that would ultimately be referred to the genotype Litocherus notissimus were first described by Simpson (1936) as "Litolestes" notissimus; Simpson (1936) noted a number of features of "L." notissimus that suggested phylogenetic affinities to certain hyopsodontid condylarths (e.g., low, inflated cusps, low molar paraconid/paracristid that often terminated near the transverse midline on the anterior side of the crown). Van Valen (1967) transferred Litolestes (including "L." notissimus) to the Adapisoricidae; although Van Valen (1967) did not provide a rationale for his decision, or make apparent what his concept of Adapisoricidae might be, Russell et al. (1975) apparently agreed with his decision and retained Litolestes as an adapisoricid. Russell et al. (1975) diagnosed Adapisoricidae, and suggested two distinct subfamilies could be recognized: the Adapisoricinae, containing but one genus, Adapisorex, and the Dormaaliinae, containing all other adapisoricids; Russell et al. (1975) further suggested that Litolestes, as well as other Litolestes-like adapisoricids, might be better referred to a separate subfamily within the Adapisoricidae. Krishtalka (1976a), in his classic study on North American adapisoricids and erinaceids, apparently disagreed, and instead referred Litolestes to the Erinaceidae, a decision that was based primarily on Litolestes ignotus having lower molars that decrease in size from m1-3, a blade-like paraconid on m1, and a low, shelf-like paraconid on m2 and m3. In his review of Paleocene age lipotyphlans from the late Paleocene of Wyoming and Colorado, Gingerich (1983) named Litocherus to receive specimens of a new adapisoricid from the early middle Tiffanian (Ti3) Cedar Point Quarry of Wyoming. Gingerich (1983) designated "Litolestes" notissimus, at that time known almost exclusively from the type locality in Montana, as the type species, and

included Gazin's (1956) "Litolestes" lacunatus from the late Paleocene of Wyoming; Gingerich (1983) followed Russell et al. (1975) in recognizing the Adapisoricidae, and designated Litocherus the genotype of the subfamily Litocherinae; he was either unaware of Krishtalka's (1976a) earlier referral of Litolestes to the Erinaceidae, or chose not to accept it, but either way, Litocherus was once again considered an adapisoricid. Novacek et al. (1985) clarified the ongoing issues of adapisoricid taxonomy, with the end result being the abandonment of Adapisoricidae, and the referral of Litocherus to Erinaceomorpha, incertae sedis. McKenna and Bell (1997) revived Gingerich's (1983) Litocherinae as a monotypic subfamily containing Litocherus.

While Litocherus has suffered a muddled taxonomic history, a consensus appears to have been reached that suggests that 1) Litocherus is not a hyopsodontid and 2) the genus is likely related to primitive erinaceomorphs; the specimens from Alberta represent the largest sample of L. notissimus outside of the topotypic collection from Scarritt Quarry, and appear to corroborate these assertions. As Gingerich (1983) noted, the teeth of Litocherus are unlike those of any hyopsodontid in having a well-developed preparacrista and, especially, postmetacrista on the upper molars, a weak or undeveloped ectocingulid on the lower molars, a more distinct molar paraconid, and a decrease in size between m1 and m2; in contrast, the upper molars of hyopsodontids (and apheliscids, see Zack, Penkrot, Krause, and Maas, 2005) bear only a weak preparacrista and postmetacrista, the ectocingulid on the lower molars is strong, the molar paraconid is almost always undeveloped, with the paracristid forming a low shelf, and the m2 is most often the largest lower molar. While litocherines can be distinguished from hyopsodontids on the basis of dental characters alone, new information from the petromastoid and postcranium further distinguish Litocherus from hyopsodontids, while supporting its inclusion in the Lipotyphla. For example, the promontorium of Litocherus bears some evidence of having had a rostral tympanic process and possibly a weak caudal tympanic process, and the ventral surface of the promontorium bears a groove for the promontorial branch of the internal carotid artery; these features are all absent from the petrosal of Hyopsodus Leidy, 1870, the only hyopsodontid for which basicranial information is well-known (Cifelli, 1982). A rostral and caudal tympanic process, as well as grooves for the stapedial and promontorial branches of the internal carotid artery are

characteristic of erinaceomorphs (MacPhee, 1981; Novacek et al., 1983; MacPhee et al., 1988; Frost et al., 1991), but admittedly these characters may be primitive for eutherians generally (Cartmill and MacPhee, 1980; Novacek, 1986; Wible, 1986). There is little evidence from either petrosal in UALVP 43099 that Litocherus had an ossified bulla [e.g., there is no evidence of sutural or articular surfaces for any midline bones (basioccipital or basisphenoid) on the surfaces of the rostral and caudal processes], a condition that was likely true of other stem erinaceomorphs (e.g., Diacodon, see Novacek et al., 1983; MacPhee et al., 1988), but one that is probably also primitive for eutherians.

The postcranium of Litocherus is suggestive of lipotyphlan, rather than hyopsodontid affinities. For example, the astragalus lacks a cotylar fossa, the long axis of the astragalar head is mediolaterally oriented, and the medial border of the tibial facet is dorsoventrally deep; in contrast, the astragalus of Apheliscus and Hyopsodus displays the opposite conditions of each of these characters (i.e., a cotylar fossa is present, an obliquely oriented long axis to the astragalar head, and a tibial facet with a medial border that is proximodistally deep; see Zack Penkrot, Bloch, and Rose, 2005, fig. 2). Furthermore, the tuber of the calcaneum is laterally convex, the peroneal tuberosity is large and proximally positioned, and the fibular facet is large and laterally facing, features that, in combination, are seen in many lipotyphlan calcanei, but not in those of any hyopsodontid (Scott and Boyer, 2006; Scott and Boyer, in prep.). Although the postcranium of Litocherus will be analyzed in greater detail elsewhere (Scott and Boyer, in prep.), a few preliminary points can be made regarding a possible mode of locomotion. Many of the osteological features of the postcranium of Litocherus are consistent with powerful flexion and extension of the leg at the hip; for example, the acetabulum is relatively deep, limiting movements at the hip to flexion and extension, while the robust third trochanter of the femur is consistent with having well-developed superficial gluteal musculature, essential for powerful extension at the hip (Sargis, 2002). The astragalus bears evidence of restricted movement at the upper ankle (talocrural) joint (e.g., deeply grooved tibial facet), while movement between the astragalus and calcaneum (astragalocalcaneal joint) was restricted to parasagittal, rather than rotatory motions (e.g., sustentacular facet well-separated from the navicular facet, peaked, rather than concave or helical ectal facet, see Heinrich and Rose, 1997). The obliquely oriented cuboid facet

of the calcaneum prevents inversion and eversion of the foot at the transverse tarsal joint, further limiting motion to the parasagittal plane (Szalay and Drawhorn, 1980; Heinrich and Rose, 1997). There is no evidence from the entocuneiform, metatarsal, or phalanges that would indicate that the pes of Litocherus had a capacity for grasping (Boyer, pers. comm., 2006). In all, the postcranial features of Litocherus are suggestive of an ambulatory or scansorial mode of locomotion, similar to those seen in extant tupaiids (e.g., Tupaia Raffles) and some ground squirrels (e.g., Sciurus Linnaeus).

The new basicranial and postcranial material, while useful in distinguishing Litocherus from non-erinaceomorph eutherians, is of limited use in detecting possible relationships within Erinaceomorpha, a regrettable situation that is primarily owing to the lack of comparative material for virtually all stem lipotyphlans. What little is known of the basicranium of stem erinaceomorphs comes from a few well-preserved, but essentially two-dimensional specimens of Macrocranion and Pholidocercus from the Eocene Messel oil shales of Germany, and a single specimen of the North American genus Diacodon (see MacPhee et al., 1988). The petromastoid of Litocherus resembles that of the three aforementioned genera in a general way (e.g., relatively flat promontorium, weak rostral and caudal tympanic processes, unenclosed internal carotid system of arteries, well-developed sulcus for the proximal parts of the stapedial artery), but as pointed out by MacPhee et al. (1988), these features are probably primitive; Litocherus may be more primitive than Diacodon and Macrocranion in having a larger promontorial branch of the internal carotid artery, but given the uncertainties regarding the accuracy to which osteological markers reflect the calibre of blood vessels and nerves (see, e.g., Conroy and Wible, 1978; Cartmill and MacPhee, 1980), inferences based on single specimens should be made with due caution. The phylogenetic position of Litocherus within Erinaceomorpha as reconstructed in this study is as the sister taxon to a new genus and species of litocherine, with both taxa forming a clade that is sister to the adapisoricines (see later in the text).

LITOCHERUS sp., cf. L. ZYGEUS

Figures 5.16, 5.17; Table 5.8

Material examined.—From Joffre Bridge Roadcut lower level: UALVP 40670, incomplete left dentary with p2-3, incomplete p4, m1-2, and alveolus for p1.

From DW-2: UALVP 47814, P4; UALVP 47248, M2; UALVP 47249, 47251 incomplete right dentary with p4, m1-2, and alveoli for p3, m3; UALVP 47250, incomplete right dentary with p2-4, m1-3, and alveolus for p1; UALVP 47252, incomplete left dentary with p4, m1, and alveoli for m2-3; UALVP 47253, incomplete left dentary with p4, m1-3, and alveoli for p1-3; UALVP 47254, incomplete right dentary with p4, m1-2, and alveoli for p1-3, m3.

From Birchwood: UALVP 39287, P4; UALVP 39477, incomplete right dentary with p4, m1-2, and alveoli for p2-3, m3; UALVP 47255, incomplete dentary with m1-2.

From Hand Hills West upper level: UALVP 35114, incomplete left dentary with p4, m1-2; UALVP 35095, incomplete left dentary with p3 (talonid only), p4, m2, and alveoli for p2, m1, m3; UALVP 35097, incomplete right dentary with m1-2; UALVP 35133, incomplete left dentary with p4 (talonid only), m1; UALVP 35090-91, 35093, 47256, 47257, p4; UALVP 35099, 35100-02, 35104-05, 35125-27, 35132, m1; UALVP 35129, 35131, 35135, m2; UALVP 35096, 35150-52, m3.

Description and discussion.—The referred specimens differ from those of Litocherus notissimus mainly in their greater size and in the cusps being more inflated. The P4 of L. sp., cf. L. zygeus is more transverse relative to its length than is that of L. notissimus, and the metacone is weaker. The p4 of L. sp., cf. L. zygeus is slightly larger than that of L. notissimus, and the p4 paraconid is generally much smaller, the molars are slightly wider, and the m2 paraconid/paracristid is more closely appressed to the metaconid. The dimensions of teeth of L. sp., cf. L. zygeus are generally greater than those of homologous teeth of L. notissimus from Alberta (see Tables 5.6-5.8), but there is a significant overlap between the two; similarly, the upper end of the ranges of measurements for the teeth of L. sp., cf. L. zygeus overlaps the lower end for comparable teeth of L. zygeus (see Gingerich, 1983). Gingerich (1983) distinguished L. zygeus from L. notissimus primarily on the basis of size (L. zygeus is approximately 22 percent larger in dental dimensions than L. notissimus); the specimens in the present sample appear to bridge the size gap between the two taxa, and the differences in size between L. notissimus and L. zygeus may be much less than previously believed. The qualitative

differences described earlier seem to better distinguish the two taxa than does size, but even in these there is substantial overlap. Resolution of this problem must await discovery of larger samples of L. sp., cf. L. zygeus and L. zygeus.

Genus NAYLORIA new genus

Type and only known species.—Nayloria albertensis.

Diagnosis.—As for the type and only species.

Etymology.—Named in honour of the late Bruce G. Naylor for his contributions to Alberta paleontology.

NAYLORIA ALBERTENSIS new species

Figure 5.18; Table 5.9

Diagnosis.—Differs from Litocherus in being smaller (L m1, Nayloria is approximately 28 percent shorter than m1, L. notissimus), in having a stronger metacone on P3, a smaller and less swollen protocone on P4, and in M2 being smaller relative to M1. Differs further from Litocherus in p2-3 being relatively shorter and more inflated, in having a generally larger paraconid and shorter hypoflexid on p4, in having more cuspate molar paraconids and less inflated molar paracristids. Differs further from Litocherus in having sharply developed accessory trigonid crests.

Description.—Maxilla and upper dentition (Figs. 5.18.1-5.18.3): The maxilla and upper dentition of Nayloria are known from a one specimen, UALVP 47258, preserving P3-4, M1-2. Although the maxilla is damaged and incomplete, it preserves a number of informative features. The infraorbital foramen opens dorsal to P3, and while its bony circumference is broken and incomplete, the parts that remain indicate that the aperture was large, deeper than mediolaterally wide, and faced mostly anteriorly and only slightly laterally. The infraorbital canal is virtually undamaged in UALVP 47258: it extends posteromedially through the maxilla to the level of M1 where it terminates at the maxillary foramen. The short, stubby maxillary root of the zygomatic arch originates at the level of the anterior root of M2; as on the maxilla of Litocherus and Xynolestes (see

earlier in this chapter), the posterodorsal edge of the maxilla of Nayloria bears a trough-like articular facet, and the lateral surface of the anterior root of the zygoma is deeply excavated; both of these landmarks likely represent areas of articulation for the jugal, and this bone clearly contributed significantly to the anterior parts of the zygomatic arch.

Upper premolars: P3 (W=1.3): The P3 of Nayloria is three-rooted and subtriangular in outline, with a large paracone and smaller metacone and protocone constituting the crown. The crown is damaged anterolabially, and the parastylar corner is broken off. The paracone is large and swollen, conical, and connected to a low but distinct metacone by a short centrocrista. A weak ectocingulum and posterior cingulum meet at the posterolabial corner of the crown, where a small metastylar cusp is developed. The protocone is about half the size and height of the paracone, conical, and its apex leans slightly anteriorly. The protoconal cristae are strong, and a hypocone is not developed.

P4 (L=1.6; W=1.8): Most of the labial side of the crown of P4 has been damaged or broken away, with little remaining of the coronal topology. The crown is larger than that of M1, and subtriangular in outline, with the parastylar lobe projecting anteriorly as a prominent spur supporting a low cusp. The protocone is the only undamaged cusp on the crown: it is relatively tall, with an acute apex, and leans anteriorly. Sharp cristae extend from the protoconal apex: the preprotoconal crista is high and runs anterolabially towards the base of the paracone where it fades away; the postprotoconal crista sweeps vertically and slightly posterolabially to the base of the protocone. A third, short protoconal crista runs directly labially from the protoconal apex, fading away as it approaches the paracone. Low but otherwise well-developed protoconal cingula extend towards the lingual margin of the protocone, but remain incomplete lingually. Weak exodaenodonty is developed at the lingual root.

Upper molars (M1: L=1.5, W=1.7; M2: L=1.3, W=1.5): The upper molars of Nayloria closely resemble those of other erinaceomorphs, particularly those of Litocherus (see earlier in this chapter): the crowns are subrectangular in outline, the cusps are low and somewhat inflated at their bases, and a small but distinct hypocone and pericone is developed. The shallow ectoflexus is developed on both molars, dividing the labial margin of the crown into nearly symmetrical lobes: the parastylar lobe on M1 is

anteriorly projecting, while on M2 it is smaller and more smoothly rounded. The ectocingulum is low but robust and labially complete on both molars. The paracone is larger and more labial in position than the metacone on both molars, and both paraconule and metaconule and their associated conular cristae are robust. The anteriorly leaning protocone is nearly as tall as the paracone. The hypocone is bulbous, conical, and closely appressed to the protocone. The pericone is smaller and lower than the hypocone; it is lingual in position on M1, but is more labial on M2. The protoconal cingula are well-defined, but extend only as far labially as the level of the conules; the cingula are incomplete lingually. As in P4, exodaenodonty is developed at the lingual root of the upper molars, forming weak but distinct lobes.

Dentary and lower dentition (Figs. 5.18.4-5.18.18): The horizontal ramus differs little from that in other erinaceomorphs, being long, shallow, and slightly convex ventrally. The symphyseal surface consists of two arms of raised bone that converge posteriorly, fading away at the level of p1. An excavated area of smooth bone intervenes between the two arms; as with Xynolestes and Litocherus, the articular surface in Nayloria shows no evidence of osseous interdigitations, suggesting the two mandibular rami were only loosely connected in life. The lateral surface of the dentary bears three mental foramina, the most anterior of which is very small and opening ventral to the lower canine; the next most posterior foramen is recessed into a shallow pit below p2, and its subovate aperture opens anterolaterally and dorsally. The posteriormost foramen is slightly smaller than the middle foramen, and its dorsoventrally compressed aperture opens below the posterior root of p3. The masseteric fossa is deeply excavated anteriorly, and a heavy temporalis crest separates the deep temporalis and shallower pterygoid fossa medially. The coronoid, condylar, and angular processes, as well as the condyle, are not preserved on any of the specimens at hand.

Lower incisors: Two of the three lower incisors of Nayloria are preserved in UALVP 40525. The crowns of i1 and i2 are spatulate, with a wide, anteroposteriorly compressed primary cusp, a small heel, and a faintly concave occlusal surface; in these regards, the lower incisors of Nayloria closely resemble those of Xynolestes. The incisors in UALVP 40525 have shifted slightly from post-mortem disturbance, but their original orientation appears to have been parasagittal, and it is likely that their crowns

were imbricated in lateral view, with the more posterior tooth overlapping the more anterior tooth. As in Xynolestes, when the jaw of Nayloria is held in its presumed in-life position, with the symphysis oriented nearly vertically, the concave occlusal surfaces of the incisor crowns face dorsally and somewhat medially. Apart from their being larger, the lower incisors of Nayloria differ little in coronal morphology from those of Xynolestes. Although the i3 of Nayloria is unknown, its alveolus is smaller than that for i1 or i2, essentially squeezed between the i2 and much larger lower canine.

Lower canine: The enlarged lower canine of Nayloria differs significantly from the smaller, more nearly premolariform canine of Xynolestes. The crown is tall and recurved, and is oriented obliquely anterolabially-posterolingually compared to the more posterior teeth; as such, its apex faces dorsally, posteriorly, and somewhat lingually. In contrast to the strongly procumbent lower canine in Xynolestes, this tooth in Nayloria is nearly vertical. The crown is dominated by a trenchant, moderately mediolaterally compressed protoconid. A weak crest runs down the anterolabial side of the protoconid, becoming stronger as it nears the base of the crown. The posterobasal part of the crown is somewhat swollen, but a posterior accessory cusp is not developed.

Lower premolars: p1: The crown of p1 is labiolingually compressed and procumbent. The crown is elongate and subrectangular in lateral outline, with long and parallel dorsal and ventral slopes, and considerably shorter anterior and posterior margins. The crown consists of an enlarged principal cusp that broadens posteriorly and basally, and supports a small posterior cuspule. A weak crest curves anteromedially from the heel, forming a short low shelf.

p2: The p2 of Nayloria is two-rooted. The crown is mediolaterally compressed, although not to the same degree as in p1, and bears a trenchant protoconid and a short, unicuspid heel. The crown is not procumbent, and its anterior parts do not overlap the posterior parts of p1. A weak crest extends anteriorly from the protoconid apex, but becomes more prominent as it nears the base of the crown; the crest then turns lingually and posteriorly, continuing a short distance as a shelf-like lingual cingulid. Neither a paraconid nor a metaconid is developed. The protoconid is connected to the low heel by a sharp crest. A short posterolingual cingulid is present on some specimens.

p3: A short diastema can intervene between p2 and p3 (e.g., UALVP 47273), or the two teeth can abut one another (e.g., UALVP 47266). The crown resembles that of p2, but differs in being taller and considerably wider, especially posteriorly, resulting in a more teardrop-shaped occlusal outline. The protoconid is low relative to crown length, and is considerably inflated, particularly near its base; a moderately deep exodaenodont lobe is developed at the posterior root, and a variably developed anterior lobe is sometimes present. A low, sharp paraconid is present, although the paracristid is poorly developed or altogether absent. A high, robust cingulid extends around the anterior margin of the crown: the labial cingulid usually terminates abruptly as it reaches the labial side of the protoconid, but the lingual cingulid can continue for a short distance posteriorly. The heel is short, about one-fourth to one-third the length of the protoconid, and consists only of a heavy raised crest that extends transversely across the posterior side of the protoconid at its base; on most specimens the crest is elevated at its lingual extremity as a small cuspid. A short crest can extend anterolingually from the heel cuspid, defining the lingual margin of a shallow basin.

p4: The p4 of Nayloria is the largest and tallest post-canine tooth, and its crown is significantly more massive and taller than that of p3. The crown is low and wide, with the trigonid forming the majority of its length, and the talonid restricted to a short, narrow basin at the posterolingual extremity. The protoconid is large and swollen, and leans posteriorly; a sharp paracristid extends anteriorly from the protoconid apex, joining a tall, conical, and faintly anterior-leaning paraconid at the anterior margin of the crown. The paraconid is massive, arising from a relatively high point on the protoconid, and is separated from it by a high but deeply notched paracristid. A bulbous, conical metaconid arises from relatively high on the posterolingual shoulder of the protoconid, and apices of the two cusps are connected by a strongly notched protocristid; the metaconid is subequal or slightly larger than the paraconid, and is positioned higher on the protoconid than is the paraconid. The talonid basin is short and narrow, occupying the extreme posterolingual part of the crown; the long labial slope of the talonid bulges labially past the level of the trigonid, but the basin itself occupies only one quarter the width of the trigonid. A well-developed entoconid and hypoconid are usually present on the talonid, and the two cusps are separated by a deep fissure, although on some specimens the

entoconid may be more poorly developed, and the fissure can be less apparent, especially on worn specimens. A sharp cristid obliqua contacts the postvallid wall below or slightly lingual of the level of the protocristid notch, but in either case the contact is far lingual of the mid-longitudinal axis of the crown; the cristid obliqua can continue towards the apex of the metaconid, and the hypoflexid is very deep. The entocristid is low and weak. A robust, shelf-like cingulid is present anteriorly, and the crown is exodaenodont, with deep, labially bulging lobes often being developed at both roots.

Lower molars: m1: The crown of m1 is shorter and less massive than that of p4, but larger than that of m2. The crown is subrectangular in occlusal outline, with no apparent constriction near the trigonid-talonid junction. A large protoconid and a lower but more swollen metaconid dominate the crown. A weak paracristid extends anteriorly from the protoconid, then abruptly bends lingually and runs to the paraconid as a high crest. Although the paracristid is considerably compressed, the paraconid itself can be somewhat conical and swollen, especially near its base, and usually is not fully incorporated into the paracristid. The protoconid and metaconid are transversely opposed, and are connected to one another by a sharp and deeply notched protocristid. The opposing walls of the protoconid and metaconid are swollen, but are unusual in their being drawn out as sharp crests that unite in the deepest parts of the trigonid basin; the central crests essentially form a second protocristid, anterior to the protocristid proper, with a deep, V-shaped pocket developed between the two sets of crests. The talonid is significantly swollen basally, bulging farther labially than the trigonid, although the basin itself is subequally wide or slightly narrower. The talonid bears a subequally tall entoconid and hypoconid, and a smaller, central or slightly lingually positioned hypoconulid; the talonid cusps are connected by a high, sharp postcristid. The opposing walls of the entoconid and hypoconid are moderately swollen and convex, and although they slope inwards, the basin floor is more rounded than V-shaped. The cristid obliqua contacts the postvallid wall lingual to the level of the protocristid notch, forming a deep hypoflexid; a mesoconid swelling can be developed on the cristid obliqua, but a distinct cusp is not formed. The entocristid is sharply defined, and forms a deep notch prior to joining the postvallid wall. The incomplete ectocingulid is heavy and robust anteriorly,

but short and poorly defined posteriorly. The crown is exodaenodont, with a shallow lobe present anteriorly, and a much deeper lobe developed posteriorly.

m2: The m2 of Nayloria is smaller and considerably lower crowned than m1. The crown closely resembles that of m1, but with a few notable differences. The trigonid cusps are less inflated than those on m1, although the paracristid is similarly compressed; the paraconid on m2 is more fully incorporated into the paracristid, and the paraconid/paracristid complex is lower and more shelf-like. The central crests on the m2 trigonid are much better developed than those on m1, with the crest extending from the metaconid being especially strong. The central crests form a sharp, second protocristid anterior to the protocristid proper, and the space between the protocristid and central crests is deep and pocket-like, while the sulcus between the central crests and the paracristid is trough-like. The talonid, although more nearly equal in height to the trigonid, closely resembles that on m1, with a tall and sharp entoconid and hypoconid, and a small and central or slightly lingually positioned hypoconulid. The talonid basin extends farther labially than on m1, and the basin floor is more nearly V-shaped. The crown is marked exodaenodont posteriorly.

m3: As in other erinaceomorphs, the m3 of Nayloria is significantly reduced in both size and height relative to m2. The crown resembles that of m2, but differs in that the paraconid is fully incorporated into the paracristid, and the paraconid/paracristid complex is lower, more anteriorly leaning, and more shelf-like. As on m1 and m2, the central trigonid crests are sharply defined on m3, particularly the crest arising from the metaconid; the crests unite anterior to the protocristid. The talonid on m3 is closer in height to the trigonid, and the hypoconulid is taller and more dorsally projecting. Unlike on m1 and m2, exodaenodonty is weak or absent on m3.

Etymology.—Albertensis, named for the province from which all of the specimens of Nayloria were collected.

Holotype.—UALVP 40525, incomplete left dentary with i1-2, c, p1, p4, m1-3, and alveoli for i3, p2-3. DW-2 locality, Paskapoo Formation of Alberta, late Paleocene, [early middle Tiffanian, Ti3 (Fox, 1990), Plesiadapis anceps/P. rex Lineage Zone (Ti3) of Lofgren et al., 2004].

Other material examined.—From Joffre Bridge Mammal Site No. 1: UALVP 47273, incomplete right dentary with p2-4, m1-3, and alveoli for c, p1; UALVP 47272, incomplete right dentary with p4, m1, and alveoli for m2-3.

From DW-2: UALVP 47258, incomplete left maxilla with P3-4 (P4 broken), M1-2, and alveoli for M3; UALVP 47259, incomplete right dentary with p2-4, m1-2, and alveoli for m3; UALVP 47260, incomplete left dentary with c, p1-2, and alveoli for p3-4, m1; UALVP 40502, incomplete right dentary with m1-3; UALVP 47261, 40528, incomplete left dentary with m1-3; UALVP 47262, incomplete right dentary with p3-4 and alveoli for c, p1-2; UALVP 47263, incomplete left dentary with p4 (talonid only), m1-3; UALVP 47264, 47265, m1.

From Birchwood: UALVP 47266, incomplete left dentary with p2-4 and alveolus for p1; UALVP 47267, incomplete right dentary with p2-4; UALVP 39499, incomplete right dentary with m2-3.

From Hand Hills West upper level: UALVP 47268, incomplete left dentary with p4 and alveoli for p2-3, m1; UALVP 47269-47271, p4 (total: 3).

Discussion.—The low swollen cusps, steep postprotocrista on P4, narrow p4 talonid basin, and molars that decrease size from m1 to 3 identify these specimens as pertaining to the Erinaceomorpha. The dentition of Nayloria is closest to that of Litocherus among known erinaceomorphs, with the two sharing a number of derived characters. For example, the P4 of Nayloria and Litocherus have a strongly developed anterior cingulum, a feature identified in this study as autapomorphic for litocherines (although it is homoplasious at higher levels in Lipotyphla, occurring in a number of nyctitheriids; see later in the text). Additionally, the molars of Litocherus and Nayloria decrease in size from m1 to m3, and the metaconid on p4 is weakly developed. Although the teeth of both taxa are similar, those of Nayloria differ in a number of important ways. For example, the protocone on P4 of Nayloria is not nearly as inflated as it is in Litocherus, and a prominent third protocone crest is developed, running labiad from the protoconal apex; furthermore, the upper molars of Nayloria are relatively more transverse than those of Litocherus, and the hypocone is taller and less bulbous. The p1 of Nayloria is much more procumbent than that of Litocherus, and while the cusps on the lower molars of Nayloria are turgid, similar to those in Litocherus, the molar crests are

relatively uninflated and sharp. Nayloria is unusual in having well-developed accessory trigonid crests: while the basin-facing walls of the trigonid in a number of erinaceomorphs are inflated (e.g., "Adapisorella"), none are drawn out into sharp crests as they are in Nayloria. While undoubtedly closely related to Litocherus, Nayloria displays a combination of characters that is comparable to that separating other erinaceomorph genera; as such, the specimens in the present sample are interpreted as representing a new genus and species.

Nayloria is known only from early middle Tiffanian sediments in Alberta; as such, it may prove useful in biostratigraphic correlation.

Subfamily ADAPISORICINAE Schlosser, 1887

Genus ADELOXENUS new genus

Type and only known species.—Adeloxenus adapisoricoides.

Diagnosis.—As for the type and only species.

Etymology.—Adelos, Greek, unseen or unknown; xenos, Greek, stranger, guest, in reference to the poorly known evolutionary history of Adeloxenus, and to the fact that specimens of Adeloxenus are unknown in Alberta prior to the early middle Tiffanian.

ADELOXENUS ADAPISORICOIDES new species

Figures 5.19.1-5.19.9; Table 5.10

Diagnosis.—Differs from adapisoricines in the following combination of characters: a p4 that is subequal to, rather than smaller than m1; a less inflated molar metaconid; the m1 metaconid being positioned lingually opposite the protoconid; the molar talonid basin being deeper and more concave; and the m1 talonid being subequal, rather than notably wider than the trigonid.

Description.—Dentary and lower dentition (Figs. 5.19.1-5.19.9): Although the dentary is preserved in UALVP 46997 (holotype), it is more nearly complete in UALVP 46998 (referred specimen), missing only the condyle and tip of the angular process. The

ramus is long and boat-shaped in later al view, with a faintly curved ventral margin. The ramus is shallow relative to its length, achieving its greatest depth ventral to the alveoli for m2 and m3. A pair of mental foramina is developed laterally: the more anterior of the two is positioned below the interalveolar space between p1 and p2; its aperture is subovate and opens anteriorly, laterally, and slightly dorsally. The more posterior foramen opens below the level of the posterior root of p3; it is smaller than the anterior foramen, its aperture is more nearly circular, and it opens dorsolaterally. The horizontal ramus becomes increasingly shallow anteriorly, but mediolaterally wider at the posterior parts of the symphysis. The symphysis itself is incompletely preserved, having been broken anterior to the i3 alveolus: the articular surface is concave medially and consists of an area of smooth bone that is delimited dorsally by a thick osseous ridge; the ventral limit of the articular surface is bounded by an arm of weakly raised bone. The articular surface of the symphysis extends posteriorly to below the level of the anterior root of p2 where it fades away. The coronoid process is preserved in its entirety in UALVP 46998: the long anterior margin forms an angle of approximately 120 degrees at its union with the horizontal ramus, and continues dorsally to a smoothly rounded apex that bears a weak, posteroventrally directed hook. The posterior margin of the coronoid process is strongly concave between the apical "hook" and the level of the condyle. The masseteric fossa is bounded by crests dorsally and anteriorly, and becomes increasingly deep anteroventrally; the fossa is areally extensive, nearly reaching the ventralmost parts of the ramus. In contrast with the deeply excavated masseteric fossa, the temporalis fossa is virtually flat and is nearly confluent with the pterygoid fossa, with only the mandibular foramen intervening between the two. The large foramen is positioned far posteriorly on the ramus, and its subovate opens posteriorly. Although the angular process is incomplete distally, the dimensions of its base suggest it may have continued posteroventrally to at least the level of the condyle; its labial surface is flat, while its lingual surface bears the proximal parts of a shelf-like ventral ridge that presumably separated the area of distal attachment for the superficial masseter below from that of the internal pterygoids above (Turnbull, 1970).

Lower incisors: The three lower incisors of Adeloxenus are represented only by their alveoli in UALVP 46998. The alveoli are mediolaterally compressed are oriented at

an angle of approximately 45 degrees to the horizontal, suggesting the crowns were somewhat procumbent. The alveolar walls of i1 are more damaged than are those of i2-3, but judging by the parts that are preserved, the i1 was probably the smallest of the three lower incisors as inferred from root diameter; the alveolar diameter of i2 and i3 are subequal and nearly double that of i1.

Lower canine: The dimensions of the lower canine alveolus of Adeloxenus indicate that the tooth was the largest in the lower dentition, with its anteroposterior length being nearly equal to that of the two alveoli of p2 or p3. The aperture is subovate in outline, oriented anterolaterally-posteromedially, and opens dorsally and slightly anteriorly. The canine alveolus abuts that for i3, but is separated from that for p1 by a short diastema.

Lower premolars: p1: The alveolus for p1 is slightly smaller than that for the lower canine, but is similarly oriented in the horizontal ramus (i.e., anterolaterally-posteromedially). The aperture is subovate and opens dorsally.

p2: The crown of the two-rooted p2 is dominated by a short, labiolingually compressed and slightly procumbent protoconid. A weak paracristid extends anteriorly from the protoconid apex to a high but small and poorly differentiated paraconid, forming a blade-like wing; the posterior slope of the protoconid is longer than the anterior slope. A metaconid is not developed. The p2 as preserved in UALVP 46997 is displaced somewhat posterodorsally, abutting p3 and damaging the p2 talonid and otherwise obscuring the posterior parts of the crown. A large cavitational wear facet has flattened the apex of the protoconid.

p3: In contrast to the slightly procumbent crown of p2, that of p3 is nearly vertical, with a tall, sharp protoconid, low paraconid, and well-developed talonid. The paracristid on p3 is short, like that on p2, but it does not project anteriorly, nor does it form a conspicuous blade-like structure. A metaconid is not developed. The crown widens towards the talonid, and a sharp cristid obliqua extends posteriorly from the protoconid apex to an enlarged, tall hypoconid. Although the posterolingual part of the talonid is damaged on p3, it appears that there was at least one other talonid cusp, possibly the entoconid; the second cusp is lower than the hypoconid, and the shallow

basin formed between these cusps and the postvallid wall slopes lingually. A moderately deep hypoflexid is present, and shallow exodaenodonty is developed at the posterior root.

p4: The p4 crown is almost fully molariform, with a robust paraconid and metaconid, and well-differentiated talonid cusps. Although the apex of the protoconid is missing in UALVP 46997, the dimensions of the parts that remain indicate that the protoconid was clearly the largest and tallest of the trigonid cusps. A conspicuous metaconid is developed off the lingual shoulder of the protoconid; its apex is lower than that of the protoconid, and the two cusps are connected by a short, shallowly notched protocristid. The conical paraconid arises from a relatively high point on the trigonid (the base of the paraconid joins the metaconid well above the level of the p3 talonid), with its apex directed anterodorsally; the paraconid is lingually, rather than anteriorly positioned, and the paracristid is sharply notched. The talonid is high, with the apices of the talonid cusp being nearly half the height of the trigonid cusps; in contrast to the reduced talonid on p4 of other erinaceomorphs (e.g., Litolestes, see Krishtalka, 1976a), that of Adeloxenus is expanded, both labially and posteriorly, such that the deep basin is nearly as long and as wide as the trigonid. The talonid is dominated by a tall hypoconid and a slightly smaller and lower entoconid and hypoconulid. A low cristid obliqua extends anterolingually from the hypoconid, joining the postvallid wall labial of the level of the protocristid notch and forming a deep but anteroposteriorly short hypoflexid. The hypoconulid is low but conspicuous, somewhat anteroposteriorly compressed, and projects posterodorsally; it is positioned on the anteroposterior midline of the crown. The entocristid is undeveloped, leaving the anterolingually sloping talonid basin open lingually. A shelf-like cingulid is developed anteriorly, but neither a posterior cingulid nor ectocingulid is present.

Lower molars: m1: The crown of m1 is subquadrate in occlusal outline, with the trigonid and talonid of nearly equal width. The trigonid consists of a subequal protoconid and metaconid, and an anteroposteriorly compressed paraconid. The protoconid and metaconid are inflated at their bases, but narrow to acute apices that are connected by a deeply notched protocristid; the protoconid is slightly higher than the metaconid and leans somewhat posteriorly. The paracristid extends anteriorly from the apex of the protoconid, becoming more robust as it nears the base, and then abruptly bends towards

the lingual margin of the crown; the angle formed at the union of the protoconid and paraconid arms of the paracristid is approximately 90 degrees. Like that on p4, the paraconid on m1 arises from a relatively high position on the trigonid, with its posterior parts joining the metaconid well dorsal to the base of the crown; the paraconid is almost wholly incorporated into the paracristid, and the entire complex is anteroposteriorly compressed and leans anteriorly. The talonid basin is about as long as it is wide, and each of the cusps is well-differentiated. The basin is deep and cuplike, contrasting with the V-shaped basins on molars of many erinaceids (Novacek et al., 1985); the deepest part of the basin is situated lingual to the anteroposterior midline, and the basin-facing walls of the talonid cusps are flat to concave. The entoconid is the tallest talonid cusp, and it is only marginally less massive than the hypoconid; the entoconid is situated somewhat posterolingually, but is not displaced to the far posterolingual corner of the crown (as it is in, e.g., Diacocherus). A sharply notched entocristid connects the entoconid to the postvallid wall. The hypoconulid is low, inflated, and situated on or slightly lingual to the anteroposterior midline of the crown; it is separated from the entoconid by a notched postcristid. The hypoconid is low but massive, and it is connected to the hypoconulid by a low, sharp hypocristid, and to the postvallid wall by a sharp cristid obliqua. The cristid obliqua joins the postvallid wall below the protocristid notch, and the hypoflexid is deep and not floored by a distinct shelf. The anterior cingulid is strong and shelf-like, whereas the posterior cingulid is undeveloped.

m2: The m2 of Adeloxenus is known only in the holotype. The crown closely resembles that of m1, but differs in a number of features. The tooth is slightly shorter and lower crowned than m1, but the trigonid and talonid are of about the same width. Although the metaconid and protoconid are nearly equal in height on m2, the metaconid is the more massive cusp, and the protoconid leans farther posteriorly than it does on m1. The paraconid is more fully incorporated into the paracristid on m2, the lingual extremity of the paraconid/paracristid is even farther lingual, and the entire complex is closely appressed to the metaconid (but not nearly to the same degree as that on m2 of Diacocherus or Mckennatherium; see Krishtalka, 1976a; Gingerich, 1983). The lingual parts of the talonid are damaged in UALVP 46997, leaving only the hypoconid and some of the basin, but other than the hypoconid being slightly lower, these parts differ little

from comparable parts on m1. The anterior cingulid is strongly developed and the hypoflexid, although deep, is anteroposteriorly short.

m3: The m3 of Adeloxenus is significantly smaller than m1 or m2. The trigonid is relatively more transverse than that on m1 or m2, and the paracristid/paraconid complex closely resembles that on m1 in being anteroposteriorly compressed and slightly anteriorly leaning. Although the protoconid is damaged, the dimensions of its base suggest it was probably larger than the metaconid. The talonid is about the same width as the trigonid, but is long relative to that on m1 or m2. The hypoconid and hypoconulid are subequal in size and height, and although both cusps are heavily worn, the hypoconulid does not appear to have been finger-like or posterodorsally projecting. The entoconid is reduced in size and is closely appressed to the hypoconulid, with the two cusps being partly merged and forming a weak lobe; the entoconid is connected to the postvallid wall by a long, sharp entocristid. The cristid obliqua joins the postvallid wall below the protocristid notch. As on m1 and m2, the anterior cingulid is robust, the posterior cingulid is undeveloped, and a deep hypoflexid is present.

Etymology.—Adapisoricoides, in reference to the similarities in the teeth of Adeloxenus with those of adapisoricines.

Holotype.—UALVP 46997, incomplete right dentary with p2-4, m1-3. DW-2 locality, Paskapoo Formation of Alberta, late Paleocene [early middle Tiffanian, Ti3 (Fox, 1990), Plesiadapis anceps/P. rex Lineage Zone of Lofgren et al., 2004].

Other material examined.—From DW-2: UALVP 46998, incomplete right dentary with m1 and alveoli for i1-3, c, p1-4, m2-3; UALVP 46999, 47247, m1.

Discussion.—Although Adeloxenus is poorly represented in the present sample, the specimens are sufficient to document the presence of an unusual adapisoricine from the late Paleocene of North America, one that is interpreted here as representing a new genus and species. As in other adapisoricines, the p3 of Adeloxenus is reduced relative to p4, the p4 bears a well-developed metaconid and talonid, and the lower molars are low-crowned, with shallowly inclined trigonids, and the characteristic, weakly lobate m3 hypoconulid and entoconid. The teeth of Adeloxenus differ from those of other adapisoricines in having a less inflated molar metaconid (the molar metaconid is turgid in other adapisoricines), a lower molar entoconid (the molar entoconid is tall in other

adapisoricines), and in having deeper molar talonid basins (the talonid basins are high and platform-like in other adapisoricines). The phylogenetic analysis presented in this study (see later in the text) suggests that Adeloxenus occupies a position in the Adapisoricinae, but outside the clade containing Adapisorex and "Adapisorella"; given the small sample size, little more can be inferred about the relationships of Adeloxenus, and a test of the phylogenetic position of the genus must await the discovery of better preserved specimens.

Specimens referable to Adeloxenus are also known from the early middle Tiffanian Cedar Point Quarry of Wyoming (Secord, 2004 and pers. obs., YPM-PU collections).

Genus "ADAPISORELLA"

"ADAPISORELLA" sp.

Figures 5.19.10-5.19.15

Material examined.—From DW-1: UALVP 46996, m2.

From Hand Hills West upper level: UALVP 35098, m2

Description.—m2 (L=1.90, SD=0.14, CV=7.44; TrW=1.55, SD=0.07, CV=4.56; TaW=1.70, SD=0.14, CV=8.32; N=2): The trigonid of m2 bears a massive, turgid protoconid and metaconid. The opposing walls of the protoconid and metaconid are strongly convex, and the protocristid connecting their apices is deeply notched. The weak paracristid descends the anterior face of the protoconid, becoming better defined and more blade-like as it nears the base; it then swings lingually, forming an open, L-shaped arc as it joins the low, swollen paraconid just shy of the lingual margin of the crown. A thick anterior cingulid is developed, extending around the labial base of the protoconid to the robust hypoflexid shelf. The talonid is wider than the trigonid, and the opposing walls of the hypoconid and entoconid form a relatively shallow, V-shaped basin. The hypoconid is the largest talonid cusp, occupying nearly half the width of the talonid; a low cristid obliqua connects the hypoconid to the postvallid wall below the level of the protocristid notch, and a weak mesoconid swelling is developed on the cristid

obliqua of one specimen. The entoconid is the tallest talonid cusp: it is turgid, with a sharp apex, and is connected to the postvallid wall by a sharply notched entocristid. The low hypoconulid is essentially wedged between the much larger hypoconid and entoconid just slightly lingual of the anteroposterior midline; it is inflated and slightly compressed anteroposteriorly.

Discussion.—The two referred specimens represent the earliest occurrence of a new genus from the late middle Tiffanian (Ti4) Gao Mine locality of Alberta (Fox and Scott, in prep.). The markedly inflated cusps, particularly the metaconid, and the shallow talonid basin closely resemble features of the lower molars of the adapisoricine Adapisorex Lemoine, 1883, known primarily from the Paleocene of France and Germany (Russell, 1964), but more recently discovered in the late middle Tiffanian of Alberta (Fox and Scott, in prep.).

Family uncertain

Genus DIACOCHERUS Gingerich, 1983

Diacodon COPE, 1875: JEPSEN, 1930, p. 511 (in part).
Diacocherus GINGERICH, 1983, p. 238

DIACOCHERUS sp., cf. D. MEIZON
Figure 5.20; Table 5.11

Material examined.—From DW-2: UALVP 47351, 47352, M1; UALVP 47353, incomplete right dentary with dp4, m1, and alveoli for p3; UALVP 47354, incomplete right dentary with m1-2; UALVP 47356, m1.

From Hand Hills West upper level: UALVP 47357, P4; UALVP 35119, m1; UALVP 35117, 35120, 35134, 47358, m2.

Description.—Upper dentition (Figs. 5.20.1-5.20.6): P4: The crown of P4 is transverse relative to its width, and is T-shaped in occlusal outline. The crown bears a large paracone, a smaller and lower metacone, and a robust protocone; the trigon basin is

open posteriorly. The labial margin of the crown is virtually straight, paralleling a line drawn anteroposteriorly through the apices of the paracone and metacone. The ectocingulum is low and weak. The paracone is sharp, narrowing apically to a sharp apex. A prominent parastylar spur occurs immediately anterior of the paracone, and while a parastylar cusp was likely present on the spur originally, it is now missing, having been worn flat. A preparacrista is not present. The metacone is developed off the posterior shoulder of the paracone: its apex is well separated from that of the paracone, and although a strong sulcus is developed between the two cusps labially, but the two cusps remain connate for most of their height. The postmetacrista is poorly developed, extending to the posterolabial corner of the crown as a low crest; this contrasts with the postmetacrista of other lipotyphlans in which it is higher and more blade-like. Conules are not developed. The protocone is slightly lower than the paracone, and its apex leans slightly anteriorly; the postprotocrista resembles that of many erinaceomorphs in extending posteriorly from the protoconal apex to join the posterior cingulum. The anterior cingulum is undeveloped, and a hypocone is not present.

M1: The two referred M1s closely resemble that of Diacocherus minutus from the late Paleocene Princeton Quarry of Wyoming (Jepsen, 1930), but are slightly larger and are closer in size to those expected for the larger D. meizon from Cedar Point Quarry (the upper dentition of D. meizon has yet to be discovered; Gingerich, 1983). The M1 crown is transverse relative to its length and is dominated by a subequally tall paracone and metacone, and a lower but more massive protocone. The stylar shelf is greatly reduced, with the continuous ectocingulum abutting the labial base of the paracone and metacone. The parastylar and metastylar corners of the crown are drawn out as weak anteriorly and posteriorly projecting spurs, with the metastylar spur projecting slightly more labially. The paracone and metacone are sharp and conical; the paracone leans slightly anteriorly, whereas the metacone is more nearly vertical. The preparacrista is only weakly developed, and the postmetacrista, although stronger than the preparacrista, is much weaker than in many other lipotyphlans (i.e., it does not form a long, sweeping blade-like crest that projects labially). Both conules are well-developed, with the paraconule slightly the larger and more lingual of the two. The conular cristae are prominent, with the internal wings joining the lingual bases of the paracone and metacone, and the

external wings continuing labially as an uninterrupted paracingulum and metacingulum; the posterior cingulum joins the postmetacrista, rather than remaining separate. The protocone is lingually opposite the deepest part of the centrocrista notch, and its labial wall is virtually flat, whereas its lingual wall is convex and forms a long, shallow slope. Short cristae extend labially from the protoconal apex to the conules. The posterior cingulum is well developed, extending lingually from the level of the metaconule towards the protocone, and becoming more conspicuous lingually. A hypocone is not developed. The anterior cingulum originates higher on the crown than does the posterior cingulum, but it is significantly shorter, and the cingula are discontinuous lingually.

Lower dentition (Figs. 5.20.7-5.20.18): Lower premolars: dp4: UALVP 47353 preserves an incomplete dentary with dp4 and m1 in place, and documents for the first time the anatomy of dp4 in Diacocherus. The crown of dp4 is long relative to its width, and the trigonid is dominated by a massive, anterodorsally projecting paraconid; the crown widens posteriorly to a deeply basined talonid. The conical and fully cuspate paraconid is positioned far anteriorly on the trigonid, and its apex is connected to the protoconid by a deeply notched and heavily worn paracristid; although the paraconid arises low on the trigonid, it is tall, with its apex just slightly lower than that of the metaconid. Despite the protoconid apex having been broken away, the dimensions of its base indicate it was both larger and taller than the metaconid. The metaconid is positioned slightly posterior to the level of the protoconid, and the two cusps are connate for about half the height of the metaconid; the protocristid is sharp and deeply notched. The talonid is wider than the trigonid, with its labial and lingual margins bulging beyond those of the trigonid. The deep talonid basin is bounded labially by a massive hypoconid, and posteriorly and posterolingually by a smaller and lower hypoconulid and entoconid, respectively. The hypoconulid is lingual of the longitudinal midline, nearly abutting the entoconid, and the anterolingually projecting paraconid of the succeeding m1 is nestled in the embrasure formed by their posterior sides. The hypoconid and hypoconulid are connected by a strong hypocristid, whereas the hypoconid and entoconid are not joined. The low cristid obliqua joins the postvallid wall just labial of the level of the protocristid notch, while the entocristid is undeveloped, leaving the talonid open lingually. The anterior cingulid is robust, forming a low shelf; the posterior cingulid is undeveloped.

Lower molars: The lower molars resemble those of Diacocherus meizon and D. minutus as described by Gingerich (1983). The m1 is slightly smaller than m2, and its talonid is notably wider than the trigonid, whereas the two are more nearly equal in m2. The paraconid on m1 is differentiated from the paracristid and projects anteriorly and lingually; the paraconid on m2 is reduced and more nearly incorporated into the paracristid, and the complex is higher and more closely appressed to the anterior side of the metaconid. The talonid basin on m1 and m2 is deep and cup-like, and is bounded by a subequally tall entoconid and hypoconid, and a smaller and slightly lingually positioned hypoconulid. The entoconid is positioned near the posterolingual extremity of the crown. The cristid obliqua joins the postvallid wall below or slightly labial to the level of the protocristid notch, while the entocristid is weakly developed, forming a broadly U-shaped notch and leaving the lingual side of the talonid open.

Discussion.—The sample of Diacocherus from the early middle Tiffanian of Alberta is significantly smaller than that from coeval localities in the Bighorn Basin of Wyoming (compare with samples from Cedar Point Quarry; Rose, 1981a-b; Secord, 2004). The specimens described here from Alberta are referred only to Diacocherus sp., cf. Diacocherus meizon: although the teeth broadly resemble those of D. meizon [e.g., the paracristid is relatively high on m2 and m3 (Gingerich, 1983), and the m2 is larger than m1 (Secord, 2004)], they differ in a number of ways. For example, the m1 of D. sp., cf. D. meizon bears sharper cusps, and a paraconid that is slightly lower and less closely appressed to the metaconid, and the m2 paraconid is more fully incorporated into the paracristid and less cuspate. The upper dentition of D. meizon is unknown; the referred P4 and M1 differ from comparable teeth in D. minutus in being slightly larger, in the P4 being more transverse relative to its length, and in M1 having a much narrower stylar shelf, weaker preparacrista, and shorter postmetacrista. D. meizon and D. minutus are most clearly differentiated on the basis of lower premolar characters (Secord, 2004); as these data are unavailable in the present sample, the teeth are here referred only to D. sp., cf. D. meizon.

Suborder SORICOMORPHA Gregory, 1910

Family uncertain

"LEPTACODON" MUNUSCULUM Simpson, 1935a

Figures 5.21, 5.22; Tables 5.12, 5.13

Leptacodon munusculum SIMPSON, 1935a, p. 228.

Revised diagnosis.—Differs from Leptacodon (s. s.) in having a smaller protocone on P4 and upper molars, in having a weakly developed posterior cingulum on P4 and upper molars, and in molar hypocone being very small or undeveloped. Differs further from Leptacodon in having a much narrower p4, with a short and narrow basin and a relatively better developed, anterodorsally projecting paraconid; differs further in having lower molars with a transverse, rather than angular ("flexed") paracristid, and in m3 hypoconulid being reduced in size and height. Differs from "Leptacodon" packi Jepsen, 1930 in being smaller, in having a better developed metacone on P3, a weaker metaconid on p4, and narrower molar talonids. Differs from Pontifactor West, 1974 in P4 having a metacone and postprotocrista that extends towards the metacone, and in molar centrocrista being straight, rather than deflected labially. Differs from Nyctitherium Marsh, 1872 in being smaller, in having a comparatively undeveloped P4 and molar posterior cingulum, in having a larger p4 paraconid, and in having lower molar hypoconulid in a less lingual position.

Holotype.—USNM 9819, incomplete left dentary with m1 and m3 (Simpson, 1935a, p. 228). Gidley Quarry, Fort Union Formation of Montana, early Paleocene (middle Torrejonian, To2, Protoselene opisthacus/Mixodectes pungens Interval Zone of Lofgren et al., 2004).

Material examined.—From Joffre Bridge Road Cut lower level: UALVP 47289, M1; UALVP 47290, incomplete left dentary with p2-4, m1-3, and alveoli for c, p1.

From DW-2: UALVP 33862, incomplete right maxilla with P3-4, M1-3, and alveoli for P2; UALVP 47291, associated M2 and M3; UALVP 47292-47294 (total: 3), P4; UALVP 47295, incomplete left dentary with p1-4, m1 (talonid only), m2-3, and alveolus for c; UALVP 47296, incomplete left dentary with p2-4, m1-3, and alveoli for c, p1; UALVP 47297, incomplete right dentary with p2-4, m1-3; UALVP 47298,

incomplete left dentary with p3-4, m1-3, and alveoli for p2; UALVP 47299, incomplete left dentary with p3-4, m1-3; UALVP 47300, incomplete left dentary with p2-4, m1-2, and alveolus for p1; UALVP 47301, incomplete right dentary with p3-4, m1-3; UALVP 47302, incomplete left dentary with p3-4, m1-2; UALVP 47303, incomplete right dentary with p4, m1-3, and alveoli for p3; UALVP 47304, incomplete left dentary with p4, m1-3; UALVP 40520, incomplete left dentary with m1-3; UALVP 47305, incomplete left dentary with p4, m1-2; UALVP 47306, incomplete right dentary with p4, m1-2; UALVP 47307, incomplete right dentary with canine root, p2, p4, and alveoli for p1, p3; UALVP 47308, incomplete left dentary with p4, m1, and alveoli for p1-3; UALVP 47309, incomplete left dentary with m1-2 and alveoli for p4, m3; UALVP 47310, incomplete right dentary with m1-2 and alveoli for m3; UALVP 47311, incomplete right dentary with m1-2; UALVP 47312, incomplete right dentary with m2-3 and alveoli for m1; UALVP 47313, incomplete left dentary with m2-3; UALVP 47314, incomplete left dentary with m2 and alveoli for m3; UALVP 47315, associated left m1, m2 and right m1; UALVP 47316, p4; UALVP 47317, 47318, m2; UALVP 47319, m3.

From Birchwood: UALVP 39481, incomplete right dentary with m2-3 and alveoli for m1.

Age and occurrence.—Middle Torrejonian (Protoselene opisthacus/Mixodectes pungens Interval Zone, To2, early Paleocene) to late middle Tiffanian (Plesiadapis churchilli/P. simonsi Lineage Zone, Ti4, late Paleocene) of the Western Interior of North America (Lofgren et al., 2004).

Description.—Maxilla and upper dentition (Figs. 5.21.1-5.21.12): Although the maxilla in UALVP 33862 is damaged and incomplete, it preserves two important features. The maxillary root of the zygomatic arch takes origin dorsal to the level of M2, and the infraorbital foramen is large and opens dorsal to the posterior root of P3.

Upper premolars: P2: The upper dentition of "Leptacodon" munusculum was previously unknown. None of the specimens in the present sample preserve the premaxilla or parts of the maxilla anterior to P2, and nothing can be said of the upper incisors or P1. The crown of P2 is missing on the maxilla in UALVP 33862, but its two alveoli are preserved, indicating that the tooth was two rooted and supported an elongate, mediolaterally compressed crown that lacked a separate lingual root.

P3: The P3 of "Leptacodon" munusculum is three-rooted, with a stout lingual root supporting a well-developed protocone. The crown is roughly T-shaped in outline and is dominated by a tall, conical, and slightly posteriorly leaning paracone. A weakly differentiated metacone is developed on the posterior shoulder of the paracone, and the two cusps are connected by a weak centrocrista. The postmetacrista continues posteriorly from the metaconal apex to a low, weak metastylar cusp. A prominent parastylar cusp occurs directly anterior to the paracone, but a preparacrista is not developed. The ectocingulum is strong at the level of the metastylar cusp, but is otherwise undeveloped. The crown narrows conspicuously lingual to the paracone. The protocone is short but otherwise well developed, and its apex leans anteriorly. Protoconal cristae extend labially from the protoconal apex, and continue as the paracingulum and metacingulum to the parastylar and metastylar corners of the crown. Conules, protoconal cingula, and a hypocone are not present.

P4: The crown of P4 is triangular in outline, and bears a tall, conical paracone, a well-differentiated metacone, and a short protocone. The labial margin of the crown is set at an oblique angle to a line drawn anteroposteriorly through the apices of the paracone and metacone, and the stylar shelf is weak posteriorly and virtually undeveloped anteriorly. The ectocingulum is low but robust, and continuous across the length of the crown; small, irregular cuspules can be developed on the ectocingulum, particularly at the level of the paracone. The metacone is larger and better differentiated than that on P3, and although the metacone is connate with the paracone for most of its height, the two cusps are well separated apically, and can be incipiently divided basally by labial and lingual sulci that run from the centrocrista notch to the base of the two cusps, or by a labial sulcus only (similar to P4 of Xynolestes). As on P3, a strong parastylar cusp occurs anterior to the paracone on a prominent spur-like parastylar lobe, with a deep notch separating the two cusps; the preparacrista is weak or undeveloped. The postmetacrista is high and blade-like, curving posterolabially to join the ectocingulum. A metastylar cusp is not developed. The protocone is somewhat skewed anteriorly, with the apex situated lingually opposite the paracone; the protocone is anteroposteriorly compressed and its apex is acute. The conules and their associated conular cristae are undeveloped. Sharp cristae run labially from the protoconal apex: the

preprotoconal crista joins the parastylar cusp, whereas the postprotoconal crista is low and terminates well dorsal of the postmetacrista. A third crest runs directly labially from the protoconal apex to the base of the paracone, dividing the labial side of the protocone and trigon basin into anterior and posterior halves. The protoconal cingula are low and conspicuous, but discontinuous with one another lingually. A hypocone is not present.

Upper molars: The M1 of "Leptacodon" munusculum is subtriangular in occlusal outline, and the crown supports tall, sharp principal cusps that surround a deep trigon basin. A weak ectoflexus is developed, dividing the labial side of the crown into weak lobes: the parastylar lobe is hook-like and projects anteriorly as a prominent spur, while the metastylar lobe projects farther labially. The ectocingulum is heavy and complete labially. The paracone and metacone are subequal in size, although the paracone is the slightly taller cusp; the two cusps are connected by a sharp, deeply notched centrocrista that is straight, rather than V-shaped (i.e., the centrocrista is not deflected towards the labial margin of the crown). The preparacrista runs anteriorly and slightly labially from the paraconal apex, joining the ectocingulum+paracingulum, while the postmetacrista is high, blade-like, and remains separate from the metacingulum. The conules and their associated cristae are strongly developed, with the paraconule slightly anterior to the level of the paracone, and farther lingual than the metaconule. The protocone is the lowest trigon cusp: its apex is anteriorly leaning and is connected to the conules by well-developed protoconal cristae. The protoconal cingula are low and discontinuous lingually; the posterior cingulum is only slightly expanded posteriorly and can support a tiny conical hypocone.

M2: The M2 is subequal or slightly larger than M1, and the crown is more transverse relative to its length. The M2 closely resembles M1 in the major features of the crown, differing mainly in the parastylar lobe being even more hook-like and projecting farther labially than anteriorly, in the preparacrista running labially, rather than anteriorly, and in the protoconal cingula being more prominent, particularly the posterior cingulum, which can be slightly expanded posteriorly and lingually.

M3: The M3 is only slightly smaller than the M2. The crown is asymmetrically triangular in occlusal outline, with a strongly projecting, hook-like parastylar lobe and an undeveloped metastylar lobe. The ectocingulum is heavy anteriorly, but fades away

posteriorly towards the metacone. The preparacrista extends anterolabially as a raised blade-like structure to the parastylar spur, and joins the ectocingulum+paracingulum at the anterolabial corner of the crown. The metacone is unreduced, and the conules and conular cristae are strongly developed. The protocone leans anteriorly and is connected to the conules by sharp protoconal cristae. The anterior cingulum is prominent, but the posterior cingulum is only weakly developed.

Dentary and lower dentition (Figs. 5.21.13-5.21.18, 5.22): The dentary of "Leptacodon" munusculum resembles those of other small insectivorans, but is deeper and generally more robust than that in Xynolestes and Litolestes, reaching its greatest depth below m1 or m2. None of the specimens of "L." munusculum in the present sample preserves parts of the dentary anterior to the lower canine, and all that can be said of the symphysis is that it extended posteriorly to the level of p1. Two mental foramina are developed labially: the more anterior and larger of the two foramina is deeply recessed and occurs below the level of the anterior root of p2, and its subovate aperture opens anteriorly, laterally, and slightly dorsally. The more posterior foramen is smaller, more nearly circular in outline, and opens anterolaterally below the level of the posterior root of p3, or between the posterior root of p3 and the anterior root of p4. The coronoid and condylar processes are not preserved on any of the specimens at hand. The angular process is preserved in two specimens (UALVP 47313, 47301), and it closely resembles that in Litolestes avitodelphus (see earlier in this chapter), differing primarily in its more robust proportions and in the medial shelf being relatively wider. The medial shelf of the angular process continues anteriorly onto the horizontal ramus as a short ridge that terminates below the mandibular foramen, itself being both larger more nearly circular compared to that in Lit. avitodelphus. Judging by the dimensions of its anterior margin in UALVP 47296, the coronoid process was likely very tall, and forms an angle of approximately 115 degrees with the horizontal ramus. The temporalis fossa is separated from the pterygoid fossa by a weakly developed ridge running posteriorly from the level of m3. The masseteric fossa is deeply excavated anteriorly, and a tiny foramen can occur in its deepest part.

Lower dentition: The lower incisors and canine of "Leptacodon" munusculum are unknown, although the canine alveolus and part of its root are preserved in UALVP

47307. As evidenced by its alveolus, the lower canine of "L." munusculum is slightly larger than p1 and bears but a single root. The orientation of the alveolus indicates the crown was most likely procumbent. A short diastema intervenes between the lower canine and p1.

Lower premolars: p1: The single-rooted p1 of "Leptacodon" munusculum closely resembles that in the erinaceomorph Xynolestes, differing mainly in its larger size and more robust proportions. The crown is elongate and subrectangular in lateral outline, with long and parallel dorsal and ventral slopes, and shorter anterior and posterior margins. The crown consists of an enlarged protoconid and small posterior cuspule; the crown is labiolingually compressed anteriorly, but broadens posteriorly and basally. Two sharp crests originate at the apex of the protoconid: the first extends anteriorly for a short distance before fading away, whereas the more posterior crest is longer and more conspicuous, and connects the protoconid to the small heel. A weak crest curves anteromedially from the heel, forming a short, low shelf. A short diastema intervenes between p1 and p2.

p2: In contrast to the anterior-leaning p2 of Xynolestes, the p2 of "Leptacodon" munusculum is nearly vertical (i.e., the anterior parts of the crown do not project anterior to the anterior root), and the crown does not overlap the posterior parts of p1. The crown bears a tall and labiolingually compressed protoconid and an elongate and slightly broader heel. A small, low cuspule is developed anterior to the protoconid, and can be connected to the protoconid apex by a weak paracristid. A metaconid is not developed. The heel consists of but a single, low median cuspule that can be connected to the protoconid by a low crest; a weak ridge is developed lingual of the cuspule, forming a short, low shelf. A short diastema occurs between p2 and p3.

p3: The crown of p3 is slightly larger than that of p2. The crown is elongate and labiolingually compressed, but broadens posteriorly, giving the tooth a weakly teardrop-shaped occlusal outline. The crown bears a tall protoconid, a low, anterodorsally projecting paraconid, and a tiny, unicuspid heel; a metaconid is not present. The protoconid is sharp, and its apex is connected to the much smaller and lower paraconid by a weakly developed paracristid; a stronger crest extends posteriorly from the protoconid apex, joining the low and slightly labially displaced heel. A short but conspicuous crest

curves anterolingually from the heel cusp, enclosing a small shallow basin. Neither an anterior nor a posterior cingulid is developed. Exodaenodonty is weakly developed at the posterior root.

p4: Although the p4 of "Leptacodon" munusculum is about the same height as m1, the crown is significantly narrower. The crown supports a dominant protoconid, a low but prominent paraconid, a small metaconid, and a basined talonid. The protoconid is tall and sharp, moderately compressed labiolingually, and has a vertical to weakly recurved apex. A small, conical metaconid is developed high on the lingual side of the protoconid, with its apex directed posterodorsally, and the two cusps being connected by a weakly notched protocristid; an anterobasal sulcus, like that on p4 of Limaconyssus (see earlier in this chapter), is not developed in "L." munusculum, and the protoconid and metaconid are separate only at their apices. A sharp paracristid extends anterolingually from the protoconid apex and forms a sharp notch just prior to its union with the paraconid. Although the paraconid can vary slightly in size, it is consistently larger than the metaconid on each of the p4s at hand, anterodorsally projecting, and anteriorly offset from the protoconid, leaving the trigonid broadly open lingually. The talonid is about one-half the width of the trigonid and is deeply basined. Three small cusps are developed on all of the p4s at hand, of which the entoconid and hypoconid are nearly equal in size and height. The entoconid is positioned at the posterolingual margin of the crown and is connected to the postvallid wall by a weak and low entocristid. The hypoconulid is smaller and lower than the entoconid, and is usually positioned midway between the hypoconid and entoconid, although in some specimens it can occur closer to the hypoconid. A postcristid is not developed. The hypoconid is labially opposite the entoconid, and is connected to the hypoconulid by a sharp hypocristid. A prominent cristid obliqua runs from the hypoconid to the postvallid wall, joining the trigonid lingual to the level of the protocristid notch and well lingual to the anteroposterior midline of the crown; the cristid obliqua can ascend the posterior wall of the metaconid, but fades away as it nears the deepest part of the protocristid notch. The anterior cingulid is robust and shelf-like, whereas the posterior cingulid is weak or undeveloped. The hypoflexid is considerably deeper than on p3, and exodaenodonty is developed at the posterior root.

Lower molars: The lower molars of "Leptacodon" munusculum have been described in detail by Simpson (1935), Krishtalka (1976b), Krause and Gingerich (1983), and Scott (2003), and the present sample provides no more significant information than is already known. The lower molars of "L." munusculum are short relative to their height, and bear sharp cusps and crests. The paraconid arises from a low point on the trigonid (i.e., the paraconid and metaconid are nearly fully separate to their bases), and is anteroposteriorly compressed and nearly incorporated into the paracristid, forming a high, anteriorly leaning blade. The paracristid notch is high, especially on m2 where it is almost at the same level as the protocristid notch, and the metaconid is well-developed. The talonid is about as wide as the trigonid, and the entoconid is low; the talonid on m3 is anteroposteriorly short.

Discussion.—As with many of the lipotyphlan taxa included in this study, upper and lower teeth of "Leptacodon" munusculum were not discovered in articulation or association; upper and lower teeth were associated on the basis of size, in their generally similar molar proportions (the molars of "L." munusculum are nearly equal in size, in contrast to those of other lipotyphlans in the present sample in which M3/m3 or M2/m2 and M3/m3 together are smaller than M1/m1), and in comparison with associations made by Youzwyshyn (1988) for "L." munusculum from the earliest Tiffanian Cochrane 2 locality of Alberta. The teeth of "L." munusculum differ from those of Leptacodon (s. s.) in a number of features, including having a smaller and more anteroposteriorly compressed protocone on P4 and the upper molars; in having weak P4 and upper molar protoconal cingula (a hypocone on the upper molars may or may not be developed); in the molars being nearly equal in size (as opposed to decreasing slightly from m1-3 as in L. tener and L. dormaalensis); in having a narrower and shorter p4 talonid basin; and in having taller and more transverse molar paraconids/paracristids. The phylogenetic relationships of "Leptacodon" munusculum are discussed in detail later in the chapter (see Phylogenetic Analysis: Results).

Family NYCTITHERIIDAE Simpson, 1928

Subfamily AMPHIDOZOTHERIINAE Sigé, 1976

Genus PSYDRONYCTIA new genus

Type and only known species.—Psydronyctia smithorum new species.

Diagnosis.—As for the type and only species.

Etymology.—Psydros, Greek, false; nykteris, Greek, bat, in reference to the superficial similarities in the teeth of Psydronyctia and many microchiropterans.

PSYDRONYCTIA SMITHORUM new species

Figures 5.23, 5.24; Tables 5.14, 5.15

Diagnosis.—Differs from all other amphidozotheriines in having a combination of the following character states: upper molar centrocrista only weakly deflected labially (i.e., incipient dilambdodonty); p4 cristid obliqua contacting the postvallid wall at the level of the protocristid notch, and not continuing towards the apex of the metaconid; lower molar posterior cingulid undeveloped; m3 moderately smaller than m2; and in having relatively wider m3 talonid. Differs further from Amphidozotherium Filhol, 1877 in having a larger, two-rooted p2-3 and taller molar paraconids/paracristids. Differs further from Euronyctia Sigé, 1997 in having well-developed lingual cingulids on p2-3, in having a relatively smaller p2, and a relatively larger p4. Differs from Nyctitheriinae in lacking a strongly developed anterior cingulum on P4 and upper molars, and in having a more obliquely oriented labial margin on P4. Differs further from Nyctitherium in having a paraconule and longer postcrista on P4, in having the molar protocone positioned farther anteriorly, a smaller and more premolariform lower canine, a taller and more anteroposteriorly compressed molar hypoconid, and in having a relatively smaller m2. Differs further from Saturninia Stehlin, 1940 in having an anteriorly projecting, rather than hook-like parastylar lobe on M1; in having weak upper molar dilambdodonty and stronger conules; a relatively smaller p2 and larger p3; in having the molar cristid obliqua join the postvallid wall lingual of the level of the protocristid notch; in having a taller molar entoconid; and in having a relatively smaller m3.

Description.—Upper dentition (Figs. 5.23.1-5.23.10): Upper premolars: P3: None of the teeth anterior to P3 are preserved on any of the specimens at hand. The P3 of

Psydronyctia is a small, three-rooted tooth. The crown is triangular in outline, longer than wide, and is dominated by a large paracone. A tiny cusp is developed anterior to the paracone at the union of the ectocingulum and paracingulum, but a distinct parastylar spur is not present. A small metacone is developed off the posterior shoulder of the paracone, and although its apex is clearly separate from that of the paracone, the two cusps remain connate for nearly all of their heights; weak sulci are developed labially and lingually between the paracone and metacone, suggesting their incipient separation. A short, sweeping postmetacrista extends from the metacone to the posterolabial corner of the crown, where a small metastylar cusp is developed; heavy wear is present on the postmetacrista. A low, conical protocone constitutes the lingual half of the crown. Low protoconal cristae extend labially from the protoconal apex, continuing as the para- and metacingulum to the anterolabial and posterolabial corners of the crown. The conules and hypocone are not developed.

P4: The protocone and paraconule on P4 are positioned at or slightly anterior to the level of the paracone, while the prominent hypoconal salient projects posteriorly; the combination of these unusual features results in the crown having a more or less reverse-crescent occlusal outline, with the posterior margin deeply concave, and the anterior margin bulging anteriorly. The labial margin of the crown is oriented obliquely anterolingually-posterolabially to a line drawn anteroposteriorly through the apices of the paracone and metacone; the stylar shelf is absent anteriorly and only weakly developed posteriorly. The paracone and metacone lean labially and are connate for approximately half their heights, above which the respective apices are well separated and curve somewhat posteriorly; both cusps are moderately compressed anteroposteriorly, and are subcrescentic in cross-section. The paracone is larger and more swollen than the metacone, and the two cusps are connected by a narrowly notched centrocrista. A low but prominent parastylar spur supporting a weak parastylar cusp is developed directly anterior to the paracone; a low preparacrista extends posteriorly from the parastylar cusp, joining the paracone near its base. A high, sweeping postmetacrista curves posterolabially from the metaconal apex, joining the low but robust ectocingulum and metacingulum at the posterolabial corner of the crown. A vague swelling is sometimes present on the postmetacrista near the posterolabial corner of the crown, but a separate

metastylar cusp is not developed. The postmetacrista is often heavily worn. The protocone is considerably shorter than either the paracone or metacone, and its apex is directed dorsally and anteriorly; the principal trigon cusps together enclose a narrow, posteriorly sloping basin. The protoconal cristae are both well developed: the preprotoconal crista is high and short, extending labially to a large paraconule, and then to the anterolabial margin of the crown as a robust paracingulum; the postprotoconal crista runs posterolabially towards the base of the metacone, but a metaconule is not developed here, and postprotocrista continues uninterrupted to the metastylar corner of the crown. A third crest extends directly labially from the protoconal apex, fading away as it approaches the base of the paracone. The posterior cingulum is strongly expanded, forming a broad, lobe-like talon that slopes posteriorly and labially; the talon supports a short, sharp hypocone posterior and slightly lingual to the protocone; a weak crest connects the hypoconal apex to the base of the protocone. The posterior cingulum can continue a short distance anteriorly from the hypocone towards the lingual side of the protocone, but it does not join the poorly developed anterior cingulum lingually. The centrocrista, and especially the preprotocrista+paraconule+paracingulum, is usually heavily worn.

Upper molars: M1: The coronal outline of M1 is somewhat crescent-shaped, resembling in this regard the outline of P4, but the anterior skewing of the protocone and paraconule on M1 is even more extreme, with the paraconule being well anterior to the level of the paracone, and the metaconule positioned only slightly posterior to the level of the centrocrista. The labial margin of the M1 crown is somewhat oblique to the anteroposterior axis of the crown, and the stylar shelf is weak posteriorly and undeveloped anteriorly. Although the paracone and metacone are subequal in height, the paracone is larger, more compressed anteroposteriorly, and leans somewhat anterolabially; both cusps are concave labially and are subcrescentic in cross-section. A conspicuous parastylar spur occurs directly anterior to the paracone, supporting a low parastylar cusp formed at the junction of the ectocingulum and paracingulum; although a low preparacrista connects the parastyle to the base of the paracone, a deep sulcus separates the two cusps, and its depth is often enhanced by heavy wear from the protocristid and protoconid of the opposing lower molar. The preparacrista is worn even

in the best-preserved specimens, and a stylocone, should one have been present originally, cannot be discerned. The centrocrista is weakly deflected labially, imparting a broad V-shape to the crest in occlusal view; the labial deflection of the centrocrista becomes more evident in later stages of wear. A mesostyle is not present, although the ectocingulum can bear a weak, localized thickening of the enamel directly labial of the centrocrista notch. As on P4, the postmetacrista on M1 is high and sweeps posterolabially to the metastylar corner of the crown, but this crest is much longer than that on P4, and is more blade-like; the postmetacrista terminates dorsal of both the ectocingulum and the metacingulum. The conules are conical and skewed anteriorly, and although both are prominently developed, the paraconule is hypertrophied, being significantly larger and taller than the metaconule, and jutting anteriorly. The preparaconular crista is high and blade-like, running directly labially from the paraconular apex to the parastylar corner of the crown, while the postparaconular crista is shorter but no less robust, and terminates near the base of the paracone. The metaconular cristae are lower than the paraconular cristae, with the postmetaconular crista extending posterolabially as a heavy metacingulum and the premetaconular crista fading away towards the trigon basin. The conules and their respective conular cristae enclose small, pocket-like basins. The protocone is shorter and smaller than either the paracone or metacone, and its sharp apex leans anteriorly in the same plane as the paracone. The principal cusps together enclose a deep basin that slopes posteriorly. The preprotoconal crista is virtually undeveloped as the enlarged paraconule abuts the protocone; the low postprotoconal crista extends a short distance to the metaconule. The posterior cingulum begins to expand posteriorly and labially at the level of the metaconule, forming a broad, posterolabially sloping talon; the posterior margin of the crown is deeply concave. The talon supports a low but sharp hypocone with its apex is positioned posterior and slightly lingual to that of the protocone. A weak crest can connect the hypocone to the base of the protocone, and the posterior cingulum continues anteriorly for a short distance before fading away. The anterior cingulum is virtually undeveloped.

M2: The M2 of Psydronyctia is slightly smaller than M1, being shorter relative to width and the crown is less anteriorly skewed, although the paraconule still juts anteriorly past the level of the paracone, and the principal cusps together enclose a deep basin that

slopes posteriorly. Although the stylar shelf is wide anteriorly and posteriorly, it is excavated by a deep ectoflexus that divides the labial margin of the crown into prominent anterolabially and posterolabially projecting lobes. A low parastylar cusp is developed at the union of the preparacrista and paracingulum, while the postmetacrista is high, blade-like, and swings posterolabially, but remains separate from the low metacingulum. In contrast to M1, the preparacrista on M2 is longer, higher, and directed labially, rather than anteriorly. The ectocingulum is low but robust, continuous, and can bear a weak thickening labial to the centrocrista notch. The paracone is larger and taller than the metacone, and both cusps are anteroposteriorly compressed, with the paracone leaning somewhat anterolabially and the metacone more nearly vertical; both cusps are concave labially and subcrescentic in cross-section. As on M1, the centrocrista on M2 is weakly deflected labially; the centrocrista, preparacrista, and postmetacrista together form a weak, W-shaped ectoloph. The conules are conical and skewed anteriorly, although not to the same degree as on M1 (the metaconule on M2, for example, is lingual of the metacone, rather than nearly lingually opposite the centrocrista notch). The paraconule is larger, higher, and more lingual in position than the metaconule, and the conular cristae are similar to those on M1, with the preparaconular crista usually heavily worn. The conules and their respective cristae enclose small, pocket-like basins. The protocone and protoconal cristae are virtually identical to those on M1, and the posterior cingulum is similarly expanded posterolabially. The hypocone is weaker than that on M1, and the anterior cingulum is weakly developed.

M3: The M3 is significantly smaller than M1 or M2. The crown is triangular in outline, with a strongly projecting parastylar and undeveloped metastylar lobe. The crown is dominated by a large, anteroposteriorly compressed paracone that is connected to a low parastylar cusp by a prominent preparacrista. As on M1 and M2, the centrocrista on M3 is weakly deflected labially. The ectocingulum is low and robust, especially anteriorly, but fades away towards the metacone. Both M3s in the present sample are heavily worn, erasing much of the topology of the conules, but the parts that remain suggest that the paraconule and paraconular cristae were well-developed, whereas the metaconule was probably weak or undeveloped. The protocone on M3 is low,

anteroposteriorly compressed, and leans anteriorly. The posterior cingulum is short but prominent, whereas the anterior cingulum is virtually undeveloped.

Dentary and lower dentition (Figs. 5.23.11-5.23.19, 5.24): The dentary of Psydronyctia is poorly represented among the specimens at hand, with only the horizontal ramus being well preserved. The ramus is long, weakly convex ventrally, and shallow, achieving its greatest depth ventral to m2 and narrowing anteriorly towards the symphysis. The symphysis is long and shallow, with the articular surface extending posteriorly to the level of p1; the articular surface consists of dorsal and ventral arms of smoothly finished, weakly raised bone surrounding a shallow, pocket-like depression that is perforated by tiny nutritive foramina. Two mental foramina are developed: the smaller and more posterior foramen occurs below the level of the anterior root of p4, while the larger and more deeply inset foramen opens anterolaterally below the level of p1; a tiny, third foramen is developed below the level of the canine in one specimen (UALVP 47337). When the dentary is held horizontally, the teeth lean lingually, with the canting becoming especially prominent posteriorly; when the ramus is held with the symphyseal surface in a near-vertical position (more nearly approximating an "in life" position), however, the jaw splays labially and the crowns are more nearly vertical.

Lower incisors: The number of lower incisors in Psydronyctia is uncertain. Two specimens (UALVP 47327, 40508) preserve two alveoli immediately anterior to the enlarged canine alveolus, but none of the specimens is complete enough anteriorly to rule out the possibility of there being a third incisor alveolus. The incisor alveoli in UALVP 47327 and 40508 are oriented slightly oblique to the rest of the tooth row, and differ in size, with the more posterior alveolus being slightly the larger; the orientation of the alveoli in the dentary indicate that the incisors were probably procumbent.

Lower canine: The lower canine of Psydronyctia is known only from its alveolus. A short diastema separates the canine alveolus from that of i2. The alveolar rim of the lower canine is anteroposteriorly elongate and somewhat compressed mediolaterally, and the shallow, posteroventral orientation of the alveolus suggests that the canine was likely procumbent, projecting anteriorly and probably overlapping the posterior parts of the lateral incisor. A diastema intervenes between the canine alveolus and that for smaller p1.

Lower premolars: p1: The p1 of Psydronyctia is known from one specimen, UALVP 47337. The tooth is small and single-rooted, with an anteriorly leaning crown that extends anteriorly over the diastema between it and the lower canine, and likely overlapped the posterior parts of the lower canine. The crown consists of a single enlarged cusp with a sharp apex, and a small but well-defined posterior cusp. Crests extend anteriorly and posteriorly from the protoconid: the more anterior crest runs a short distance anteriorly before fading away, while the more posterior crest is longer and sharper, and extends to the heel. The heel is conical and sharp, with its apex directed vertically. A short diastema can intervene between p1 and p2.

p2: The p2 of Psydronyctia is two rooted. The crown is mediolaterally compressed and blade-like, with a long, trenchant protoconid and a small heel. A short, sharp paracristid extends anteriorly from the protoconid apex, joining a low paraconid just lingual of the anteroposterior midline; a longer but otherwise similar crest runs posteriorly from the protoconid to the low heel. A short lingual cingulid can be developed posteriorly.

p3: The two-rooted p3 is considerably taller and longer than p2, but is similarly compressed, with a blade-like trigonid and a narrow talonid. The crown is dominated by a trenchant protoconid, the apex of which is sharp and somewhat recurved. The low paraconid is positioned immediately anterior to, and well separated from, the protoconid, and the two cusps are connected by a weak paracristid. A pair of robust cingulids arises from the paraconid apex and extends a short distance posteriorly; although the lingual cingulid is less prominent than the labial cingulid, it is longer, and can often extend as a low, weak ridge along the lingual side of the protoconid. The metaconid is variably developed: in some specimens (e.g., UALVP 47333), it is a small but distinct cusp, occurring high on the posterior side of the protoconid; in other specimens (e.g., UALVP 40508), it is represented only by a slight bulge in the enamel; and in still other specimens (e.g., UALVP 47337) it is undeveloped. The postvallid wall is long and sloping. The talonid consists of but a single cusp, the hypoconid, and an elongate, narrow basin bounded labially and lingually by the parallel entocristid and cristid obliqua. The prominent entocristid curves anterolingually from the hypoconid, and then continues along the lingual side of the crown as a weak cingulid that sometimes joins the

anterolingual cingulid. An equally prominent cristid obliqua runs anteriorly from the hypoconid, paralleling the entocristid, and contacts the postvallid wall on the anteroposterior midline; the cristid obliqua continues up the postvallid wall as a raised, sharp crest to the summit of the metaconid, or fades away as it approaches the apex of the protoconid on specimens where the metaconid is undeveloped. The hypoflexid is long and relatively shallow, and a short posterior cingulid continues anteriorly below the hypoflexid as a low shelf.

p4: As with p3, the trigonid of p4 is elongate and blade-like, with a trenchant protoconid and sharp paraconid. The paraconid is robust, set off far anteriorly from the remainder of the trigonid, and is connected to the protoconid by a sharp, deeply notched paracristid. The anterolabial and anterolingual cingulids are stronger than those on p3, with the lingual cingulid being especially prominent: it is high, sharp, and a deep pocket is formed between it and the lingual wall of the protoconid. A robust metaconid is developed off the posterolingual shoulder of the protoconid on each of the p4s at hand: it is slightly smaller and lower than the protoconid, and is connected to the latter by a deeply notched protocristid. In contrast to the sloping postvallid wall of p2 and p3, that of p4 is more nearly vertical. The talonid is slightly narrower than the trigonid, and the tall, sharp talonid cusps enclose a deep basin. The hypoconid is the largest and tallest talonid cusp: it is anteroposteriorly compressed, and positioned almost as far posteriorly as the hypoconulid, and is connected to the postvallid wall by way of a low, angular cristid obliqua. The cristid obliqua contacts the postvallid wall below the protocristid notch. The hypoconulid and entoconid are low and stubby, with the hypoconulid slightly closer to the entoconid than to the hypoconid. A deeply notched entocristid connects the entoconid to the postvallid wall, and a low postcristid connects the talonid cusps to one another. The hypoflexid is long and relatively deep, and although a posterior cingulid is not present, a low shelf is usually developed ventral to the hypoflexid. Exodaenodonty is strongly developed posteriorly.

Lower molars: m1: The crown of m1 is oriented slightly oblique to the long axis of the jaw. The trigonid and talonid are both anteroposteriorly compressed and transversely wide, and although the trigonid is taller than the talonid, the latter is wider; the well-developed paracristid, protocristid, cristid obliqua, and hypocristid together form

a moderate ectolophid. The trigonid is dominated by a tall, anteroposteriorly compressed protoconid, a slightly lower but more massive metaconid, and a low paraconid; the cusps together enclose a deep basin that is open lingually. The metaconid is lingually opposite the protoconid, and is connected to the latter cusp by a sharp, deeply notched protocristid. The posterior wall of the metaconid is unusual: it is deeply creased by a long, gutter-like sulcus that extends towards the apex of the metaconid from the point of contact between the cristid obliqua and postvallid wall. The paraconid is lingually positioned and somewhat cuspate (i.e., it is not fully incorporated into the paracristid), and leans anteriorly; the paracristid is long, forming a wide, L-shaped notch between the protoconid and paraconid. The paracristid and trigonid basin in some specimens is worn from occlusion with the P4 posterior cingulum and hypocone. The anterior cingulid is robust, forming a shelf-like structure that curves around the labial side of the protoconid, but does not continue to the hypoflexid. The talonid of m1 consists primarily of a tall, anteroposteriorly compressed and sharp hypoconid, and a low, stubby entoconid and hypoconulid that together enclose a deep, anterolingually sloping basin. The hypoconulid is positioned lingual of the midline and nearly abuts the entoconid; the two cusps are connected by a low, weakly developed postcristid. The cristid obliqua is low, angular (similar to that in Xynolestes; see earlier in the text), and contacts the postvallid wall below the postcristid notch; the entocristid is deeply notched. The hypoflexid is deep and is floored by a prominent shelf. The posterior cingulid is at best weakly developed, and on some specimens it is wholly undeveloped. The protocristid, paracristid, and hypocristid are often heavily worn, with trough-like facets scoured into their dorsal surfaces.

m2: The m2 of Psydronyctia differs from m1 primarily in being oriented slightly more oblique to the long axis of the jaw, in being slightly smaller, and in having a more anteroposteriorly compressed trigonid. In contrast to m1, the protocristid on m2 is widely, rather than narrowly notched, and the metaconid leans lingually. The postvallid crease on the metaconid is strongly developed, with the sulcus extending to the point of contact between the cristid obliqua and postvallid. The talonid on m2 differs little from that on m1: the cusps are sharp, the hypoconid is taller than either the entoconid or hypoconulid, the hypoconulid is lingual of the midline, and the hypocristid is better

developed than the postcristid. The anterior cingulid is even more robust than on m1, forming a broad platform that continues around the protoconid but terminates prior to reaching the hypoflexid. The hypoflexid is deep and is floored by a prominent shelf.

m3: The m3 is significantly smaller than either m1 or m2, with a much narrower talonid. The metaconid leans even more lingually than that on m2, lengthening the protocristid and widening the protocristid notch. The trigonid cusps are smaller and lower but are otherwise identical to those on m2, and their apices define an isosceles triangle in occlusal view. The metaconid sulcus is more poorly developed than that on m2. The hypoconid is the largest and tallest talonid cusp, followed in order of decreasing size and height by the hypoconulid and entoconid. The cristid obliqua and entocristid are both sharp, and the talonid basin is deep and anterolingually sloping. As on m1 and m2, the anterior cingulid is robust and platform-like, the hypoflexid is deep and bounded ventrally by a strong shelf, and the posterior cingulid is weakly developed.

Etymology.—Named in honour of Richard and Thierry Smith, Department de Paleontologie, Institut Royal des Sciences Naturelles de Belgique, Bruxelles, for their generosity in molding, casting, and lending important insectivoran specimens from the Eocene and Oligocene of Belgium for this study.

Holotype.—UALVP 43100, incomplete right dentary with p3-4, m1-3, and alveoli for ?i2-3, c, p1-2. DW-2 locality, Paskapoo Formation of Alberta, Canada, late Paleocene, late Paleocene [early middle Tiffanian, Ti3 (Fox, 1990), Plesiadapis anceps/P. rex Lineage Zone of Lofgren et al., 2004].

Other material examined.—From Joffre Bridge Road Cut lower level: UALVP 40501, incomplete left dentary with p4, m1-2 (m2 trigonid only).

From DW-1: UALVP 40508, incomplete right dentary with p3-4, m1-3, and alveoli for c, p1-2.

From DW-2: UALVP 47326, incomplete right maxilla with RP3-4 (broken), M1-3; UALVP 47327, incomplete right maxilla with P4, M1-2; UALVP 47328, associated M1 and M2; UALVP 47329, M1; UALVP 47330, M2; UALVP 47331, incomplete right dentary with p3-4, m1-3, and alveoli for c, p1-2; UALVP 47332, incomplete right dentary with p2, p4, m1-3, and alveoli for p1 and p3; UALVP 47333, incomplete left dentary with p3-4, m2-3, and alveoli for c, p1-2, and m1; UALVP 47334, incomplete left

dentary with p2-3 and alveoli for c, p1; UALVP 47335, incomplete right dentary with p2-3; UALVP 47336, incomplete right dentary with p3-4; UALVP 47337, incomplete right dentary with p1-3 and alveoli for ?i2-3, c; UALVP 47338, incomplete left dentary with p2, p4, m1, and alveoli for p3, m2; UALVP 47339, 47340, incomplete right dentary with p4, m1-2, and alveoli for m3; UALVP 47341, incomplete left dentary with m1-2 and alveoli for p1-4, m3; UALVP 47342, incomplete left dentary with m1-2; UALVP 47343, 47344, incomplete right dentary with m2-3; UALVP 47345, incomplete left dentary with m1-2; UALVP 47346, 47347, incomplete left dentary with m2-3; UALVP 47348, incomplete left dentary with m2 and alveoli for m3; UALVP 47349, incomplete right dentary with m2; UALVP 47350, p4.

From Hand Hills West upper level: UALVP 34939, incomplete right dentary with p2-3 and alveoli for c, p1, p4; UALVP 34934, incomplete right dentary with m2 (talonid only) and m3; UALVP 34933, incomplete left dentary with m3.

From Cochrane 2: UALVP 28519, P3; UALVP 28520, M1; UALVP 28518, m1.

Discussion.—The teeth of Psydronyctia most closely resemble those of derived nyctitheriids, including the North American genus Nyctitherium and the European Saturninia, and even more closely those of the amphidozotheriines Euronyctia and Amphidozotherium. While all of these taxa possess a P4 bearing a small, conical hypocone, and a characteristically expanded and lobe-like posterior cingulum on P4 and M1-2, the teeth of Psydronyctia differ from those of Nyctitherium and Saturninia in a number of subtle but consistent ways. Psydronyctia more closely resembles the amphidozotheriines in having a well-developed and anteriorly displaced paraconule on P4 and the upper molars, in having incipiently developed upper molar dilambdodonty, and in having the molar cristid obliqua contacting the postvallid wall lingual of the level of the protocristid notch, and extending towards the summit of the metaconid, with a deep sulcus formed in the postvallid wall, paralleling the cristid obliqua. Additionally, the P4 and upper molars of Psydronyctia do not support a heavy, pocket-like anterior cingulum like those on homologous teeth of nyctitheriines, and the m3 is relatively smaller. In all, the coronal anatomy of Psydronyctia is more consistent with that seen in the amphidozotheriines; the phylogenetic relationships of Psydronyctia are discussed further later in the chapter (see Phylogenetic Analysis: Results).

The discovery of an amphidozotheriine in the Paleocene of North America is completely unexpected. Prior to this study, the subfamily was known exclusively from Eocene and Oligocene deposits in England and continental western Europe (Crochet, 1974; Sigé, 1976, 1997; Hooker and Weidmann, 2000; Smith, 2003, 2004). The much earlier stratigraphic occurrence Psydronyctia, combined with the results of the phylogenetic analysis presented later in this chapter (Psydronyctia is considered the sister taxon to a clade containing the more derived Amphidozotherium and Euronyctia) suggests that the Amphidozotheriinae may have had their origins in North America, rather than in Europe.

LIPOTYPHLA, genus and species indeterminate

Figure 5.25; Tables 5.16, 5.17

Material examined.—From DW-1: UALVP 47320, associated P3 and P4.

From DW-2: UALVP 47321, incomplete left maxilla with M1-2 and associated incomplete right dentary with p1, p4, m1-3, and alveoli for c, p2-3; UALVP 47322, associated right P4, M1-3, fragmentary left P3-4, and incomplete left maxilla with M2-3; UALVP 47323, incomplete right maxilla with P3-4, M1, and alveoli for P2; UALVP 47324, incomplete left maxilla with M1 and alveoli for M2-3; UALVP 47325, incomplete left dentary with m1-3.

From Hand Hills West upper level: UALVP 35149, incomplete right maxilla with broken M1 and M2; UALVP 34925, m1.

From Birchwood: UALVP 39479, incomplete right dentary with m1-3.

Description.—Maxilla and upper dentition (Figs. 5.25.1-5.25.25): Although the maxilla is poorly represented in the present sample, one specimen, UALVP 47323, preserves the small, circular infraorbital foramen. The aperture opens dorsal to the level of the posterior root of P3, and while the canal is not preserved, the relatively anterior position of the foramen implies that it was probably long.

The incisors, canine, and anterior premolars are not known among the specimens at hand, although evidence from UALVP 47323 indicates P2 had two roots and was anteroposteriorly elongate.

Upper premolars: P3: The P3 bears three roots and the crown is triangular in occlusal outline. A tall, conical paracone dominates the crown: the cusp is considerably swollen at its base, but its apex is sharply pointed and leans somewhat posteriorly. The parastyle is low but conspicuous, being set off anteriorly from the paracone on a small, anteriorly jutting lobe; a preparacrista is not developed. A metacone is not present on either P3 in the present sample, and the postparacrista runs uninterrupted from the paraconal apex to the posterolabial margin of the crown where it joins a weak metastylar cusp at the junction of the ectocingulum and metacingulum. The ectocingulum is poorly developed and discontinuous labially. The subconical protocone is low but well developed and is supported by a separate lingual root. Robust protoconal cristae extend labially from the protoconal apex to the antero- and posterolabial corners of the crown. The conules and their associated crests, as well as the protoconal cingula, are undeveloped.

P4: The P4 is subtriangular in outline. The labial and posterior margins are significantly longer than the lingual and anterior margins, and the protocone is somewhat anteriorly skewed such that its apex is nearly at the level of the parastyle; the posterior margin of the crown is concave. The labial margin of the crown is oblique to the long axis, and the ectocingulum is heavy and continuous labially. The paracone is taller and more massive than that on P3, but it leans posteriorly in much the same manner; it is conical, with an inflated base that narrows to an acutely pointed apex. A prominent parastylar cusp occurs on the anteriorly jutting parastylar lobe, and a low, weak preparacrista connects it to the base of the paracone. The metacone is slightly lower and is not fully differentiated from the paracone, although deep labial and lingual sulci extending dorsally from the deepest parts of the centrocrista notch hint at their incipient separation. The metacone is more labiolingually compressed than the paracone, and the two cusps are connected to one another by a sharp but shallowly notched centrocrista. The postmetacrista is high and blade-like, sweeping posterolabially and terminating well above the ectocingulum and posterior cingulum; a shallow sulcus is developed between the metacone and the metastylar blade. The protocone is low, about one third the height of the paracone, conical, and leans anteriorly. A high preprotoconal crista curves anteriorly and lingually from the protoconal apex, and runs uninterrupted to the parastyle;

in contrast, the postprotocrista extends dorsally from the protoconal apex to the base of the protocone. Conules and conular cristae are not present. The posterior cingulum is low, heavy, and platform-like, and runs towards the metastylar corner of the crown where it fades away; it is somewhat posterolingually expanded at the level of the protocone, forming a weak hypoconal salient, although a hypocone is not developed, and can terminate low on the posterior side of the protocone, or can continue around the lingual side of the protocone to join the short, weak anterior cingulum.

Upper molars: M1: The upper molars decrease in size posteriorly from M1 to M3, with M2 being slightly smaller than M1, and M3 considerably smaller than M2. The crown of M1 is narrow relative to its length, and tall, sharp cusps. A shallow ectoflexus divides the labial side of the crown into an anteriorly projecting parastylar lobe and a prominent labially projecting metastylar blade. The parastylar lobe is not as spur-like as it is in many nyctitheriids, and instead more closely resembles that in the erinaceomorphs Litolestes and Litocherus; a parastylar cusp is not developed. The paracone and metacone are tall and subconical, and are joined by a widely notched centrocrista. The postmetacrista is elongate, curving towards the posterolabial corner of the crown as a high blade. Both conules and their respective conular cristae are prominent, with the paraconule slightly offset anteriorly and more lingual than the metaconule. The protocone is lower but more massive than the paracone or metacone, and heavy protoconal cristae extend labially to the conules. The protoconal cingula begin at the level of the conules and widen significantly towards the protocone; the cingula are remarkably heavy and can be continuous lingually. The anterior cingulum can support a tiny pericone, while the wider posterior cingulum supports a low, conical hypocone that can be connected to the protocone by a low crest.

M2: The crown of M2 is smaller overall compared to that of M1, being anteroposteriorly shorter, but usually more transverse. The crown closely resembles that of M1, differing mainly in having a more labially projecting parastylar lobe and shorter postmetacrista. The protoconal cingula are similar to those on M1 in being heavy and continuous lingually; the posterior cingulum on M2 is relatively narrower, but the hypocone is larger and more swollen, and is similarly connected to the protocone by a

low crest. Additional cuspules are developed on the anterior and posterior cingulum in one specimen.

M3: The M3 is smaller relative to M2 than M2 is to M1, and the crown is triangular in occlusal outline, with a prominent parastylar and reduced metastylar lobe. The preparacrista is high and blade-like, and extends from the paracone to the anterolabially projecting parastylar spur. The metacone is only slightly smaller than the paracone, and the two cusps are connected by a widely notched centrocrista. Both conules and conular cristae are well developed, the protocone is lower than the paracone and metacone, and the protoconal cingula are heavy, but discontinuous lingually.

Dentary and lower dentition (Figs. 5.25.26-5.25.31): The dentary is represented only by the horizontal ramus, which is robust, shallow, and slightly convex ventrally. Two mental foramina are developed: the more anterior foramen is small and circular in outline, and its posterior margin is partially shielded by a buttress of bone; the aperture is below the level of the anterior root of p2 and opens dorsolaterally and somewhat anteriorly. The second foramen is about the same size as the more anterior foramen, and opens laterally below the posterior root of p3. The mandibular foramen is preserved in UALVP 47325: it is large and subcircular in outline, opens posteriorly and medially, and is positioned slightly higher than the tooth row when the ramus is held horizontally.

Lower canine: The lower canine is known only from its alveolus in UALVP 47325. Although the alveolus is mediolaterally crushed, it clearly is about the same size as the p1 alveolus, and the lower canine was probably procumbent in much the same way as p1.

Lower premolars: p1: The single-rooted, procumbent p1 is greatly enlarged, with its apex at about the same height as the cusps of the lower molars. The crown is anteroposteriorly elongate, and its anterior parts would undoubtedly overlap the posterior parts of the lower canine. In lateral view, the crown is elongate and blade-like, subrectangular in outline, with long and parallel dorsal and ventral slopes, and considerably shorter anterior and posterior margins. The crown consists of an anteriorly positioned and hook-like protoconid and small heel cuspule; the crown is labiolingually compressed anteriorly, but broadens somewhat posteriorly. Two sharp crests originate at the apex of the protoconid: the paracristid extends anteriorly for a short distance before

turning lingually and forming a low shelf; the more posterior crest is longer and more conspicuous, and connects the protoconid apex to the small heel. A short but well-defined crest curves anteromedially from the heel, forming a short low shelf.

p4: The trigonid of p4 consists of a large protoconid, a low but well-developed paraconid, and a weakly developed metaconid. The protoconid is tall, subtriangular in cross section, and narrows to an acute, somewhat recurved apex. A small, conical metaconid is developed off the posterolingual shoulder of the protoconid about midway between the base and apex; the metaconid projects dorsally and is connected to the protoconid by a short protocristid that is further incised by a slit-like notch at its deepest part. The conical paraconid is a large, robust cusp that originates low on the protoconid, and projects anterodorsally; it is connected to the protoconid by a sharp paracristid that bears a narrow notch at its deepest part, and a second crest originating at the paraconid apex extends a short distance posterolingually, forming a low but wide shelf. The talonid is damaged in UALVP 47325, but it appears to have been at least as wide as the trigonid, although the basin itself is only slightly wider than half the width of the trigonid. The talonid supports three cusps that together enclose a shallow basin: the entoconid is short but well-developed, while the hypoconulid is small and knob-like, and closely abuts the much larger hypoconid; a low postcristid connects the entoconid and hypoconulid. The hypoconid is missing in UALVP 47325, but the dimensions of its base clearly indicate it was the largest of the talonid cusps. A sharp cristid obliqua connects the hypoconid to the postvallid wall lingual of the level of the protocristid notch, and then continues towards the summit of the metaconid, forming a deep hypoflexid. The anterior cingulid is heavy and shelf-like, and exodaenodonty is developed at the anterior and posterior roots.

Lower molars: m1: The lower molars decrease in size and height from m1 to m3, reflecting the same trend in the upper molars; the cusps are inflated at their bases but become much sharper towards their apices. The trigonid of m1 supports a well-developed paraconid, protoconid, and metaconid that together form a near-equilateral triangle in occlusal outline. The protoconid and metaconid are tall and faintly recurved, and their opposing walls are flat; a deeply notched protocristid connects the two cusps. The paraconid is nearly incorporated into the paracristid, but an ill-defined swelling at the

lingual extremity of the paracristid marks its presence; the paracristid is deeply notched. The talonid is transversely wide relative to its length, and juts labially past the margin of the trigonid. The basin is deeply concave. The hypoconid is the largest talonid cusp, but it is lower than the entoconid; it is somewhat compressed anteroposteriorly, and is connected to the postvallid wall by an angular cristid obliqua. The cristid obliqua contacts the postvallid wall well lingual of the level of the protocristid notch, and ascends the posterior wall of the metaconid towards the summit. The entoconid is tall (at least half the height of the metaconid) and conical. The hypoconulid is short and finger-like, and is positioned slightly closer to the entoconid than to the hypoconid. The anterior and posterior cingulids are heavy and shelf-like.

m2: Other than being smaller, the m2 closely resembles m1. The trigonid and talonid of m2 are closer to one another in height, and the trigonid is more compressed anteroposteriorly.

m3: The m3 is smaller than m2, but not disproportionately so (i.e., the m3 is smaller than m2 to the same degree as m2 is to m1). The trigonid is compressed to about the same degree as that of m2 and the cristid obliqua similarly joins the postvallid wall well lingual of the protocristid notch. The hypoconulid is much better developed on m3 than it is on m1 or m2: it is about as large as the entoconid, finger-like, and projects strongly dorsally and posteriorly.

Discussion.—Although upper and lower teeth were found in association in UALVP 47321, their referral to the same taxon is tentative. The teeth of this indeterminate taxon present an unusual combination of soricomorph and erinaceomorph characters: for example, the P3 is small, with a greatly inflated paracone and undeveloped metacone, similar to that in most erinaceomorphs (compare, e.g., with P3 of Litolestes ignotus, see Secord, 2004); similarly, the P4 bears a strongly developed, steep postprotocrista that is virtually identical to that seen in Litocherus, "Adapisorella," and other taxa identified in this study as erinaceomorphs. In contrast, the P4 supports a well-developed metacone, a feature that, while known in some erinaceomorphs (e.g., Adapisorex), is more typical of soricomorphs. Furthermore, the upper molars bear thick, shelf-like protoconal cingula that in some specimens can be complete across the lingual side of the protocone; a small, conical hypocone is developed on the posterior cingulum,

similar to that seen in the nyctitheriid Leptacodon tener, and a short hypocone crest can be present. Similar, seemingly contradictory character states are seen in the lower dentition: for example, the molars decrease in size from m1-3, similar to those in Xynolestes (and of other stem erinaceomorphs), and the entoconid is very tall, particularly on m2, but the molar cristid obliqua contacts the postvallid wall far lingual of the protocristid notch, continuing towards the summit of the metaconid and grooving the posterior wall of the trigonid, just as it does in many soricomorphs (e.g., Psydronyctia). A particularly unusual feature of this indeterminate taxon is the p1: in most stem lipotyphlans this tooth is slightly smaller than the lower canine and p2 (e.g., Xynolestes), but the p1 in the indeterminate genus and species is comparatively enormous, with the crown nearly as large as that of the p4.

The teeth of this indeterminate taxon broadly resemble those of Leptacodon tener and L. dormaalensis, but are larger and more robust overall, with stronger molar cingula and weaker hypocones, more inflated protoconid and hypoconid, stronger cingulids (especially anteriorly and below the hypoflexid), and a higher and more blade-like paracristid and protocristid. Although the lower molar talonids of the indeterminate taxon and L. tener are wider than the trigonids, those of L. tener are less compressed anteroposteriorly, and the cristid obliqua is lower and joins the postvallid wall below the protoconid notch, and does not ascend the posterior wall of the metaconid. A closer resemblance is seen with Xynolestes:

1) The P4 is broadly similar, although the cusps in that of Xynolestes are less swollen and the crown is longer relative to its width;

2) The upper molars are similar in occlusal outline, and the cingula are similarly developed; the molar hypocone in Xynolestes is slightly more swollen;

3) The molars decrease in size in both taxa, although the decrease in size is more pronounced in Xynolestes;

4) The p4 talonid in both taxa is anteroposteriorly short and narrow;

5) The lower molars of the indeterminate taxon resemble those of Xynolestes, but differ in having a more posteriorly leaning, rather than vertical metaconid, and in having lower, anteriorly leaning paraconids/paracristids.

While the close resemblance with Xynolestes is suggestive of erinaceomorph affinities, there are a number of crossing characters that contradict such a referral. As such, these unusual specimens are referred here only to the Lipotyphla.

Order PANTOLESTA McKenna, 1975

Family PANTOLESTIDAE Cope, 1884

Genus BESSOECETOR Simpson, 1936

Palaeictops MATTHEW, 1899 (in part); VAN VALEN 1967, p. 232.
Palaeosinopa MATTHEW, 1901 (in part); SIMPSON 1935a, p. 230.
Thylacodon MATTHEW and GRANGER, 1921 (in part); RUSSELL in RUTHERFORD, 1927, p. 41.
Propalaeosinopa SIMPSON, 1927a, p. 2.
Bessoecetor SIMPSON, 1936, p. 9.

Type species.—Bessoecetor thomsoni Simpson, 1936.
Other included species.—Bessoecetor septentrionalis (Russell, 1929).

Remarks.—Propalaeosinopa was based on specimens from the early middle Tiffanian (Ti3) Erickson's Landing locality; Scott et al. (2002) argued that AMNH 15543B, the type specimen for P. albertensis Simpson, 1927a (the type species of Propalaeosinopa), is too poorly preserved for assessment, and that Propalaeosinopa should be regarded as a nomen nudum. Furthermore, Scott et al. (2002) synonymized P. thomsoni and P. diluculi with Russell's (1929) Diacodon septentrionalis, and referred this species to Bessoecetor, designating B. septentrionalis as the type species; in accordance with Article 67 of the International Code of Zoological Nomenclature (1999), however, the type species of Bessoecetor is B. thomsoni, not B. septentrionalis as Scott et al. (2002) had so designated.

BESSOECETOR THOMSONI Simpson, 1936

Figures 5.26, 5.27; Tables 5.18, 5.19

Bessoecetor thomsoni SIMPSON, 1936, p. 9.

Propalaeosinopa thomsoni (SIMPSON, 1936); ROSE 1981a, p. 150.

Propalaeosinopa septentrionalis; FOX, 1990, p. 58 (in part).

Bessoecetor septentrionalis (RUSSELL, 1929); SCOTT, FOX, and YOUZWYSHYN 2002, p. 700 (in part).

Revised diagnosis.—Differs from Bessoecetor septentrionalis in having a proportionately larger lower canine, smaller p4, m2-3, and m3, and with m1-2 entoconid and hypoconulid more closely appressed. Differs further from B. septentrionalis in having weaker molar conules and hypocone, greater exodaenodonty at the posterior root of p4, and in having a shallower mandibular ramus.

Holotype.—AMNH 33810, incomplete left dentary with p2-4, m1-3, and alveoli for c, p1. Scarritt Quarry, Fort Union Formation of Montana, late Paleocene (early Tiffanian, Ti2, Plesiadapis anceps/P. rex Lineage Zone of Lofgren et al., 2004).

Paratypes.—AMNH 33812, incomplete right maxilla with P2-4, M1-3; AMNH 33820, fragmentary skull with ?left upper canine, LP1-4, M1-3, RP1, P3-4, M1-3, and associated incomplete left dentary with p4, m1-3.

Material examined.—From Joffre Bridge Roadcut lower level: UALVP 47359, incomplete dentary with m1-2; UALVP 47360, m1; UALVP 47361, m2.

From DW-2: UALVP 47362, incomplete maxilla with P4, M1-3, and associated incomplete dentary with p2-4, m1-2; UALVP 47363, incomplete left maxilla with P4, M1-3, and alveoli for P2-3; UALVP 47364, incomplete maxilla with P4, M1-3; UALVP 47365, incomplete right maxilla with M1-2; UALVP 47366, incomplete maxilla with P4, M1-2 (broken); UALVP 47367, incomplete maxilla with P4 and alveoli for P3; UALVP 47368, incomplete right maxilla with P3-4; UALVP 47369-47371 (total: 3), P4; UALVP 47372-47377 (total: 6), M1; UALVP 47378-47380 (total: 3), M2; UALVP 47381, incomplete left dentary with p4 and alveoli for m1-2, and associated incomplete right dentary with p4 and alveoli for p3, m1; UALVP 47382, incomplete right dentary with p2-4, m1-3, and alveoli for c, p1; UALVP 47383, incomplete right dentary with p2-3, m1-3,

and alveoli for c, p1, p4; UALVP 47384, incomplete right dentary with c, p4, m1-3, and alveoli for p1-3; UALVP 47385, incomplete dentary with m1-3 and alveoli for p2-4; UALVP 47386, 47387, incomplete left dentary with p4, m1-3; UALVP 47388, incomplete dentary with p4 (talonid only), m1-3; UALVP 47389, incomplete dentary with p4, m1-2; UALVP 47390, incomplete left dentary with p2 (talonid only), p3-4, m2-3, and alveoli for c, p1, m1; UALVP 47391, incomplete dentary with p3-4, m1, and alveoli for c, p1-2; UALVP 47392, incomplete left dentary with m1-3; UALVP 47393, incomplete dentary with p4, m1, and alveoli for c, p1-3; UALVP 47394, incomplete dentary with m1-2 and alveoli for p3-4; UALVP 47395, 47396, incomplete right dentary with m1-2; UALVP 47397, incomplete dentary with m2-3 and alveoli for p2-4, m1; UALVP 47398-47401 (total: 4), incomplete dentary with m2-3; UALVP 47402, incomplete dentary with m1 and alveoli for p4; UALVP 47403, incomplete dentary with p3-4; UALVP 47404, incomplete dentary with p3 and alveoli for p2; UALVP 47405, incomplete dentary with c, ?p2; UALVP 47406, incomplete dentary with m2; UALVP 47407, incomplete dentary with m3; UALVP 47408, incomplete right dentary with dp4, erupting p2-3, erupting m3, and alveoli for p1, m1-2; UALVP 47409, p3; UALVP 47417, p4; UALVP 47410-47412 (total: 3), m1; UALVP 47413, m2; UALVP 47414, 47415, m3.

From Burbank: UALVP 47416, incomplete dentary with p2 (talonid only), p3-4, m2-3, and alveoli for m1.

From Birchwood: UALVP 39459, incomplete dentary with m2-3 and alveoli for m1; UALVP 39473, incomplete dentary with m3 and alveoli for m2; UALVP 39457, p4; UALVP 39458, m1; UALVP 39466, 39474, m2.

Age and occurrence.—Early Tiffanian (Plesiadapis anceps/P. rex Lineage Zone, Ti2, late Paleocene) to early middle Tiffanian (Plesiadapis rex/P. churchilli Lineage Zone, Ti3, late Paleocene) of the Western Interior of North America.

Description.—Maxilla and upper dentition (Figs. 5.26.1-5.26.17): Simpson (1936) described the dentition of Bessoecetor thomsoni in detail; although the specimens from Alberta closely resemble those from Scarritt Quarry, they document aspects of intraspecific variation, as well as previously unknown anatomical features of the skull and mandible. Although two specimens (UALVP 47362, 47363) document the anterior root of the zygomatic arch, neither specimen preserves the process particularly well, and

the extent of its contact with the jugal cannot be determined from the evidence at hand. The process originates at the level of M3 and appears to have been relatively stout at its root, but quickly narrows posteriorly. The infraorbital foramen has been mediolaterally compressed and somewhat distorted from postmortem disturbance in UALVP 47362, but it is well preserved on UALVP 47363: the large, subcircular aperture is positioned above P4 and M1, and opens anteriorly and slightly laterally.

The upper premolars of Bessoecetor thomsoni from Alberta closely resemble those in the paratypes from Montana, differing only in minor features. The paracone of P3 is slightly less swollen and more labiolingually compressed, and a weak parastylar cusp can be present; the P4 is smaller, with the metacone varying in size from no more than a slight thickening on the postparacrista, to a more conspicuous swelling; a distinct metaconal apex is not developed. A small hypocone is present on some specimens (e.g., UALVP 47369), and an ill-defined swelling on the preprotoconal crista may represent the paraconule. The upper molars of B. thomsoni from Alberta differ little from those described by Simpson (1936): the ectoflexus on M1 is often shallower than that in B. thomsoni from Montana, and the hypocones and conules are generally larger and more swollen.

Dentary and lower dentition (Figs. 5.26.18-5.26.23): Simpson (1936) briefly described the dentary of Bessoecetor thomsoni; specimens from DW-2 preserve significant parts of the horizontal ramus, as well as the coronoid and angular processes, and the condyle, all previously unknown for Bessoecetor. The horizontal ramus is long and shallow, faintly convex ventrally, and narrows anteriorly towards the symphysis. A pair of mental foramina perforates the labial side of the horizontal ramus: the more anterior foramen is positioned ventral to p2, and its small, subcircular aperture opens laterally and anteriorly; the more posterior and larger foramen occurs below m1, and its subovate aperture opens laterally. The coronoid process has a long, steep anterior margin, a smoothly rounded and slightly recurved apex, and a short but deeply embayed posterior border. The ramus narrows posterior to the coronoid process and adductor fossa to form a robust, posterodorsally projecting condylar process that supports a large condyle (although the condyle is imperfectly preserved, UALVP 47384 and 47386 collectively document the condyle in its entirety, its medial side on UALVP 47386, and

its lateral side on UALVP 47384). The condyle is medially sloping and transversely broad, extending well past the margins of the coronoid process, but further laterally than medially; it is subcylindrical, and the articular surface, while nearly flat mediolaterally, is faintly convex anteroposteriorly, wrapping around the posteromedial border of the condyle towards the neck of the condylar process. The masseteric fossa is deeply excavated, with its anterior border defined by a thick crest that fades away before reaching the ventral margin of the ramus; in contrast, the temporalis fossa is virtually flat, and a conspicuous bony protuberance is developed on the horizontal ramus posteromedial to m3; the protuberance probably represents the point of insertion for the anterior tendinous parts of the deep temporalis musculature (Turnbull, 1970). The mandibular foramen, preserved only in UALVP 47386, is positioned anteroventral to the condylar process, and its circular aperture opens posteriorly and medially. The angular process is preserved in UALVP 47386 and 47401: it is short and hook-like, with its apex pointing posterodorsally, and its ventromedial margin bounded by a thick crest.

The lower dentition of Bessoecetor thomsoni was described by Simpson (1936). The teeth from Alberta closely resemble those in AMNH 33810, differing only in minor details: the p2 and p3 of B. thomsoni from Alberta can bear a small but conspicuous anterior cuspule; the p4 is slightly smaller and wider, but is otherwise identical to that on AMNH 33810; and the molar paraconids are slightly more lingual. Two specimens, UALVP 47384 and 47405, preserve the lower canine, the first reported for Bessoecetor. The lower canine of B. thomsoni is single-rooted, and the crown is premolariform, consisting of a large, slightly recurved protoconid and a small but well-defined heel. Although p1 is not preserved among any of the specimens at hand, the diameter of its alveolus is less than that of the canine root, indicating the canine was the larger and taller of the two teeth. A conspicuous paracristid curves anteromedially from the apex of the canine, and forms part of the ventromedial border of the crown; a paraconid is not developed. A sharp crest extends posteriorly from the canine apex, joining the low heel. Occlusion with the opposing upper canine has scoured a deep, strip-like facet into the posteromedial surface of the crown.

Discussion.—Pantolesta are an extinct order of insectivorous to semicarnivorous mammals known primarily from the Paleogene of North America and Europe (Rose,

2006). Although pantolestids of Eocene and Oligocene age are represented by incomplete skulls and postcranial remains [see e.g., Pantolestes Cope, 1872 (see Matthew, 1909); Buxolestes Jaeger, 1970 (see Koenigswald et al., 2005a; Rose and Koenigswald, 2005); Palaeosinopa Matthew, 1901 (see Dorr, 1977)], pantolestids of Paleocene age are known almost exclusively from dentitions and, more rarely, skull and postcranial remains [an important example of the latter is the late Paleocene pentacodontid Aphronorus Simpson, 1935a (see Gingerich et al., 1983; Boyer and Bloch, 2003)]. Pantolestans are characterized by their sectorial premolars, with the fourth premolar often enlarged and modified either for shearing or crushing, and comparatively primitive molars, with the upper molars usually bearing well-developed cingula and hypocones (Simpson, 1937a); the teeth of at least some Eocene and Oligocene pantolestids are massive, low-crowned, and bear large, inflated cusps that were well-suited for processing more resistant food items (Dorr, 1977). Features of the skull and postcranium indicate many pantolestids may have had a filled a semiaquatic, otter-like niche, feeding on fish or mollusks (Matthew, 1909; Dorr, 1977; Koenigswald et al., 2005a; Rose and Koenigswald, 2005).

Cope (1884) erected the monogeneric family Pantolestidae for the North American species of Pantolestes, believing them closely related to, but distinct from the artiodactyl families Anoplotheriidae and Dichobunidae. In uniting within Pantolestidae a number of disparately classified genera, Matthew (1909) was the first to explicitly recognize the insectivorous features of the pantolestid dentition; he later (Matthew, 1918) referred the family to the Insectivora [sensu Simpson (1937a), and roughly equivalent to Proteutheria of Romer (1966) and Insectivora of Novacek (1986)], an opinion subsequently followed by most authors (see e.g., Matthew, 1918; Simpson, 1936, 1937a; Gazin, 1956; Van Valen, 1967; Gingerich et al., 1983). In his review of Pantolestes, Matthew (1909) also considered, albeit tentatively, that pantolestids (s. s., known principally from Palaeosinopa and Pantolestes) and the early Paleocene Pentacodon Scott, 1892 were closely related, an opinion accepted and expanded upon by Simpson (1937a, 1945) by his recognition of two distinct pantolestid subfamilies, the Pantolestinae, to which he referred Bessoecetor, "Propalaeosinopa," Palaeosinopa, and Pantolestes, and the Pentacodontinae, to which he referred Pentacodon and Aphronorus.

Simpson's (1937a, 1945) classification of the Pantolestidae has since endured (e.g., Van Valen, 1967); McKenna and Bell's (1997) recent classification recognizes Simpson's two subfamilial divisions of Pantolestidae, as well as an additional Eurasian subfamily, the Dyspterninae. Since Simpson's (1937a, 1945) review and classification of the family, the record of pantolestids has improved significantly, with important specimens having been recovered from localities in North America, Europe, Mongolia, and more recently, central Asia (e.g., Jaeger, 1970; Koenigswald, 1980, 1983; Dashzeveg and Russell, 1992; Smith, 1997, 2001; Lucas and Emry, 2000; Eberle and McKenna, 2002; Rose and Koenigswald, 2005; Lopatin, 2005); pantolestids are particularly well represented in the Eocene of Wyoming and Germany, where exceptionally well-preserved, nearly complete skeletons have been recovered from the Green River and Messel shales (see e.g., Koenigswald, 1980; Koenigswald et al., 2005a; Rose and Koenigswald, 2005). Although these specimens provide anatomical information that will undoubtedly bear importantly on the affinities and paleoecology of these stratigraphically younger pantolestids, the record of the earliest members of the group remains poor.

Simpson (1936) erected the genus Bessoecetor for a well-preserved dentary from the early Tiffanian Scarritt Quarry of Montana, designating B. thomsoni the type species; Simpson (1937a) distinguished B. thomsoni from the closely related B. "diluculi" by its relatively smaller p4, m2-3, and in having a less inflated paracone on P4. Van Valen (1967) and Dorr (1977) considered the two species of Bessoecetor subjective junior synonyms of "Propalaeosinopa albertensis", named by Simpson (1927a) for a poorly preserved, fragmentary mandible discovered in talus of the Paleocene Paskapoo Formation on the Red Deer River of central Alberta. Van Valen (1967) considered the differences noted by Simpson (1936, 1937a) between B. thomsoni, B. "diluculi", and "P. albertensis" as owing to geographical or temporal variation, particularly since no new specimens that could be definitively referred to B. thomsoni had since been discovered. With the exception of Holtzman (1978), few authors have subsequently accepted Van Valen's (1967) opinion, with most considering the type of "P. albertensis" too poorly preserved for assessment (see e.g., Rose, 1981a; Krause and Gingerich, 1983; Scott et al., 2002; but see Secord, 2004 for a different opinion). In considering the poor condition of AMNH 15543B and in the absence of clearly diagnostic characters, Scott et al. (2002)

considered Simpson's (1927a) "Propalaeosinopa" a nomen nudum, synonymizing B. thomsoni and B. "diluculi" with B. septentrionalis, a species originally and erroneously referred to the lipotyphlan genus Diacodon by Russell (1929). Newly prepared specimens from the Blindman River localities, as well as recently collected specimens from the Birchwood locality, indicate that B. thomsoni is in fact a valid species, with the differences noted by Simpson (1936) being taxonomic, rather than being simply geographic or temporal variants. With the additional and more nearly complete specimens from Alberta, further differences between B. thomsoni and B. septentrionalis are apparent: the mandibular ramus of B. thomsoni is notably shallower than that of B. septentrionalis; the lower canine of B. thomsoni is relatively larger than that of B. septentrionalis; moderate exodaenodonty is developed at the posterior root of p4 of B. thomsoni; and the m3 talonid of B. thomsoni is narrower than that of B. septentrionalis, and the hypoconulid is more closely appressed to the entoconid.

Mandibular dental eruption in Bessoecetor thomsoni: The timing of eruption of parts of the lower dentition can be estimated from UALVP 47408, an incomplete dentary of an immature individual preserving parts of the replacement dentition in different stages of eruption. UALVP 47408 preserves the deciduous p4 in place, erupting p2, p3, and m3, as well as the alveoli for m1-2; although the dentary anterior to p2 is not preserved, the condylar process, medial half of the condyle, and mandibular foramen are all preserved. The horizontal ramus on UALVP 47408 is considerably narrower, but only slightly shallower than those of adult individuals (e.g., UALVP 47382, Figs. 26.18-26.20), preserving the full complement of post-p1 replacement teeth). The medial half of the condyle bears a weakly convex articular surface that slopes medially. The mandibular foramen is positioned near the base of the condylar process and is nearly level with the alveolar rims; its small, circular aperture opens posterolaterally.

UALVP 47408 preserves the deciduous fourth premolar, although the apices of the cusps are heavily worn, erasing much of the original topology of the crown. The dp4 is fully molariform, with a well-developed trigonid and talonid. The protoconid and metaconid are large and closely appressed, and connate for at least one third of their height; although the paraconid is all but worn away, it was clearly set off anteriorly from the protoconid and connected to an accessory, anterolingually positioned cusp, similar to

the dp4 of Paleotomus junior Scott, Fox, and Youzwyshyn, 2002; the paraconid, accessory cusp, and anterior sides of the protoconid and metaconid enclose a deep trigonid basin. The talonid is wider than the trigonid, and its cusps are worn flat; the dimensions of their bases indicate that the hypoconid and entoconid were of similar size, followed by the smaller hypoconulid. The talonid basin is deeply concave.

The p2 and m3 are partially erupted, with the cusp apices slightly above the level of the alveolar rim; in contrast, the p3 is only slightly emergent, with the protoconid apex flush with the alveolar rim. The m1 and m2 are not present, having fully erupted and subsequently been lost prior to burial. From the stage of eruption on UALVP 47408, it can be inferred that both m1 and m2 erupted before p2 or p3, with m1 probably the earlier as evidenced by heavier wear relative to m2 on other specimens preserving these teeth (e.g., UALVP 47382). The p2 and m3 began erupting at nearly the same time, and both preceded p3; p4 was apparently the final post-p1 tooth to erupt. Little can be said of the timing of eruption of p1 in B. thomsoni, although evidence from extant eutherians indicates p1 erupts around the same time or earlier than m1 (Ziegler, 1971; Slaughter et al., 1974; Luckett, 1993); part of the posterior alveolar wall of p1 is preserved on UALVP 47408, suggesting the tooth may have been present and lost prior to burial, but more conclusive evidence must await the discovery of better-preserved specimens. The hypothesized mandibular eruption sequence for B. thomsoni is (p1/?dp1)-m1-m2-m3/p2-p3-p4, a sequence that has also been documented in the Late Cretaceous eutherians Asioryctes Kielan-Jaworowska, 1975 and Kennalestes Kielan-Jaworowska, 1969, as well as in the extant tenrecid Setifer Gray [and see discussions in Luckett (1993); Bloch et al. (1998)]. Although the eruption sequence of (p1/?dp1)-m1-m2-m3/p2-p3-p4 is believed to be primitive for therians (Ziegler, 1971; Bloch et al., 1998), the evidence is far from conclusive. For example, a recent reevaluation of the dentition of the basal tribosphenidan Slaughteria eruptens Butler, 1978 from the Albian of Texas suggests that the primitive therian postcanine replacement pattern may be (?dp3)-dp4-m1/p3-p2-p4 (Kobayashi et al., 2002), suggesting the long-held perception that an anteroposterior tooth replacement sequence is primitive for Theria may itself be a modification from a still more primitive condition.

The discovery of B. thomsoni at DW-2 extends the stratigraphic range of the taxon into the early middle Tiffanian, and documents the presence of two closely related species of Bessoecetor from a single locality (see later in this chapter).

BESSOECETOR SEPTENTRIONALIS (Russell, 1929)

Figures 5.28, 5.29; Tables 5.20, 5.21

Thylacodon sp. nov.; RUSSELL in RUTHERFORD, 1927, p. 41.

Diacodon septentrionalis RUSSELL, 1929, p. 173.

Palaeosinopa diluculi SIMPSON, 1935a, p. 230.

Bessoecetor diluculi SIMPSON, 1937a, p. 122.

Propalaeosinopa albertensis SIMPSON, 1927a; VAN VALEN 1967, p. 226.

Propalaeosinopa diluculi (SIMPSON, 1935a); ROSE 1981a, p. 150.

Propalaeosinopa septentrionalis; FOX, 1990, p. 58.

Bessoecetor septentrionalis (RUSSELL, 1929); SCOTT, FOX, and YOUZWYSHYN 2002, p. 700.

Revised diagnosis.—Differs from Bessoecetor thomsoni in having a relatively smaller lower canine, larger p4, m2-3, and m3 with talonid cusps equidistant from one another. Differs further from B. thomsoni in having larger and more bulbous molar conules and hypocone, weaker exodaenodonty at the posterior root of p4, and in having a more robust mandibular ramus.

Holotype.—UALVP 126, incomplete left dentary with m3. Cochrane 1 locality, Paskapoo Formation of Alberta, late Paleocene [earliest Tiffanian, Ti1 (Fox, 1990), Plesiadapis praecursor/P. anceps Lineage Zone of Lofgren et al., 2004].

Material examined.—From Joffre Bridge Roadcut lower level: UALVP 47418, incomplete dentary with m1 (talonid only), m2-3; UALVP 47419, incomplete dentary with m1, m2 (fragment), m3.

From DW-2: UALVP 47815, incomplete right maxilla with P3-4, M1-2; UALVP 47420, 47421, incomplete right maxilla with P4, M1-3; UALVP 47422, 47423, incomplete maxilla with M1-3; UALVP 47424, incomplete maxilla with M2-3; UALVP

47425, incomplete maxilla with M2; UALVP 47426, P4; UALVP 47427-47431 (total: 5), M1; UALVP 47432-47435 (total: 4), M2; UALVP 47816, incomplete right dentary with ?i2, p2 (talonid only), and alveoli for i3, c, p1, and anterior root of p2; UALVP 47436, incomplete left dentary with p3, m2-3, and alveoli for p2, p4, m1, and associated and incomplete right dentary with p2-4, m1-3, and alveoli for c, p1; UALVP 47437, incomplete left dentary with m1-3, and associated and incomplete right dentary with p3 (talonid only), p4, m1-3, and alveoli for p2; UALVP 47438, incomplete left dentary with p4, m1-3; UALVP 47439, incomplete dentary with p4, m1, m3, and alveoli for p2-3; UALVP 47440, incomplete dentary with p2-4, m1; UALVP 47441, incomplete right dentary with p3-4, m1, and alveoli for c, p1-2; UALVP 47442, incomplete dentary with p2-4; UALVP 47443, incomplete right dentary with p3-4 and alveoli for c, p1-2; UALVP 47444, incomplete left dentary with p3-4 and alveoli for c, p1-2; UALVP 47445, incomplete dentary with m1-2 and alveoli for m3; UALVP 47446, incomplete dentary with m1-2; UALVP 47447, incomplete dentary m1 (talonid only), m2-3; UALVP 47448, incomplete dentary with m2-3 and alveoli for m1; UALVP 47449-47452 (total: 4), incomplete dentary with m2-3; UALVP 47453, incomplete dentary with m2; UALVP 47454, incomplete dentary with m3; UALVP 47455, p4; UALVP 47456, m1; UALVP 47457, m3.

From Burbank: UALVP 40517, incomplete dentary with p4, m1-3.

From Birchwood: UALVP 39454, P4.

Age and occurrence.—Middle Torrejonian (Mixodectes pungens/ Plesiadapis praecursor Interval Zone, To2, early Paleocene) to late middle Tiffanian (Plesiadapis rex/P. churchilli Lineage Zone, Ti4, late Paleocene) of the Western Interior of North America.

Description.—Bessoecetor septentrionalis is well represented in Paleocene faunas from the Western Interior of North America; since most of the dentition of B. septentrionalis has been described in detail [e.g., Simpson, 1935a (described as "Palaeosinopa diluculi"); Simpson, 1937a (briefly described and figured as B. "diluculi"); Holtzman, 1978 (described as "Propalaeosinopa albertensis" and Palaeosinopa sp., cf. P. "simpsoni"); Rigby, 1980 (described as "Propalaeosinopa diluculi"); Scott et al., 2002], the objective here will be to focus on the cranial, dental, and gnathic parts that are poorly

known or previously undiscovered, and to contrast further this anatomy with comparable parts of B. thomsoni.

Maxilla and upper dentition (Figs. 5.28.1-5.28.14): Two specimens of Bessoecetor septentrionalis preserve parts of the maxilla (UALVP 47815, 47420), including the infraorbital foramen and maxillary process of the zygomatic arch. The infraorbital foramen is positioned above the posterior root of P4 and most of M1, similar to that of B. thomsoni, but its aperture is relatively larger. A small foramen that may have transmitted superior alveolar branches of the infraorbital nerve (of V_2) perforates the medial wall of the infraorbital canal. Preparation of UALVP 47420 has exposed the medial side of the maxilla, revealing parts of the infraorbital canal; although the bone forming the dorsal parts of the canal and rim of the maxillary foramen (the entrance to the infraorbital canal) has been broken away, the parts that remain indicate the canal was short, terminating no further posterior than the anterior root of M2, and was considerably expanded posteriorly. A deeply excavated, obliquely oriented groove is developed on the internal surface of the maxilla anterior to the infraorbital canal, running anteroventrally from the level of P4 to the level of the posterior root of P3 (Fig. 5.28.7); the groove is incomplete in UALVP 47420 as the maxilla is broken anteriorly and posteriorly, but almost certainly represents parts of the nasolacrimal duct, similar to that on the maxilla of the leptictid Leptictis (see Novacek, 1986, fig. 7). The maxillary process of the zygomatic arch takes origin at the level of M3, identical to that in B. thomsoni.

Upper premolars: P3: The P3 of Bessoecetor septentrionalis has not been described in detail previously. The crown is subtriangular in occlusal view and is supported by two roots, the posterior of which is larger and wider than the anterior. An enlarged and somewhat inflated paracone dominates the P3 crown; a heavy crest extends posteriorly from the paraconal apex to the metastylar corner, but neither a metacone nor a metastyle is developed. A low, ledge-like cingulum is present anteriorly, wrapping around the anterior side of the paracone and extending a short distance posteriorly; a similarly developed posterior cingulum is also present, but the cingula are discontinuous labially. A notable swelling occurs posterolingually, but a distinct protocone is not developed.

P4: Simpson (1936, 1937a) distinguished the P4 of Bessoecetor septentrionalis from that of B. thomsoni by its smaller size and more compressed protocone, and the present sample supports these observations: a comparison of the P4s of B. thomsoni and B. septentrionalis from DW-2 reveals a difference in size, with the P4 of B. septentrionalis averaging 15 percent larger than that of B. thomsoni), and the paracone and protocone of B. septentrionalis are considerably more inflated than those of B. thomsoni.

Dentary and lower dentition (Figs. 5.28.15-5.28.26, 5.29.1-5.29.15): The dentary of Bessoecetor septentrionalis closely resembles that of B. thomsoni, differing primarily in its larger size and more robust construction. UALVP 47816 preserves the anterior parts of the horizontal ramus, including the symphyseal surface and one of the lower incisors, the first discovered for Bessoecetor. The mandibular symphyseal surface consists of an elongate patch of smooth bone that is raised above the surrounding surface of the ramus; the patch narrows posteroventrally, all but disappearing by the level of p2. A thick crest delimits the dorsal extent of the symphyseal surface anteriorly, but quickly fades away posteriorly, while the more ventral parts are deeply excavated and perforated by a large nutritive foramen. The condyle is well preserved on UALVP 47449, with only its medial extremity being slightly damaged. The condyle is broader than long and medially sloping, similar to that of B. thomsoni; the articular surface is faintly convex anteroposteriorly, and wraps around the posteromedial side of the condyle towards the neck of the condylar process, providing a more extensive contact with the glenoid fossa medially. The masseteric fossa is deeply excavated and limited anteriorly by a robust crest. The posteroventral parts of the mandible are drawn out as a long angular process that bears a thick, shelf-like crest ventromedially, providing a broad area of attachment for the internal pterygoid musculature. A short flange occurs on the medial side of the condyle for insertion of the external pterygoid musculature (see Turnbull, 1970; Novacek, 1986).

The lower dentition of Bessoecetor septentrionalis closely resembles that of B. thomsoni, differing mainly in the relative size of c, p4, m2, and m3. UALVP 47816 preserves one of the lower incisors in articulation with the dentary, and is tentatively identified as i2: a patch of finished bone representing the walls of a small, shallow

alveolus occurs posterolateral to the incisor, indicating that a small tooth intervened between the preserved incisor and canine in life. Alternatively, the preserved incisor could represent i1, with the small lateral alveolus representing that for i2, with i3 having been lost; damage to the ramus medial to the preserved incisor makes a choice between these alternatives impossible. The incisor in B. septentrionalis is small and somewhat anteroposteriorly compressed, with a short, spatulate crown. The tooth is slightly procumbent, with the strongly concave occlusal surface facing dorsally and faintly medially. The crown consists of a single cusp that is narrow basally but significantly broadens apically; sharp crests border the occlusal surface, and a thick midline ridge extends from the apex to the base, dividing the occlusal surface into roughly equal medial and lateral halves. Wear is evident along the apical margin of the crown, and a deeply gouged facet is developed laterally, approximately midway between the base and apex.

Lower canine: Although the lower canine in B. septentrionalis is represented only by its alveolus, the dimensions of the aperture indicate that it was relatively smaller than that for B. thomsoni.

Lower premolars: The lower premolars in Bessoecetor septentrionalis are similar to those in B. thomsoni, differing primarily in their larger size. The talonid on p3 invariably consists of a single cusp and a short lingual crest that together circumscribe a shallow basin. The crown of p4 bears a tall protoconid, a low paraconid, and a well-developed talonid that usually bears two conspicuous cusps and a weak basin; some specimens have but a single talonid cusp (e.g., UALVP 47438), while others have three (e.g., UALVP 47443). The p4 of B. septentrionalis differs importantly from that of B. thomsoni in its larger size, taller and more sectorial protoconid, and weaker exodaenodonty at the posterior root.

Discussion.—The taxonomic history of B. septentrionalis was outlined in detail by Scott et al. (2002). The specimens from central Alberta are virtually identical to those from the earliest Tiffanian (Ti1) Cochrane 2 locality, and the middle Torrejonian (To2) Who Nose? locality (Scott, 2003), both from south central Alberta. As discussed previously, the synonymy of B. thomsoni with B. septentrionalis is considered invalid here; as such, two species of Bessoecetor are known from the Blindman River, Joffre Bridge, and Birchwood localities.

?BESSOECETOR sp.

Figures 5.29.16-5.29.18

Material examined.—From DW-2: UALVP 47817, m1.

Description and discussion.—The coronal morphology of UALVP 47817 (L=1.6; TrW=1.2; TaW=1.3) closely resembles that of m1, Bessoecetor thomsoni and B. septentrionalis, but with dimensions outside the lower end of the recorded ranges for each (L m1, ?Bessoecetor sp. approximately 50 percent shorter than L m1, B. thomsoni and B. septentrionalis). UALVP 47817 may represent a new species of Bessoecetor with teeth significantly smaller than those of either B. thomsoni or B. septentrionalis; similar teeth are known from the late middle Tiffanian (Ti4) Roche Percée locality of southeastern Saskatchewan (pers. obs.).

Family PENTACODONTIDAE Simpson, 1937a

Genus BISONALVEUS Gazin, 1956

Bisonalveus GAZIN, 1956, p. 17.

Type species.—Bisonalveus browni Gazin, 1956.

Other included species.—Bisonalveus holtzmani Gingerich, 1983; B. toxidens new species.

BISONALVEUS TOXIDENS new species

Figures 5.30-5.33, 5.34.1-5.34.6; Tables 5.22, 5.23

Bisonalveus n. sp.: FOX, 1990, p. 61.

Bisonalveus browni: FOX and SCOTT, 2005, p. 1091.

Diagnosis.—Differs from Bisonalveus browni in having a relatively smaller and single-rooted p2, a smaller m3, and lower molars with shorter and deeper talonids, deeper hypoflexids, and deeper exodaenodont lobes. Differs further from B. browni in upper molars having better-developed paracones and conules; stronger and cuspidate posterior cingula, and deeper exodaenodont lobes. Differs from B. holtzmani in being smaller (L m1, B. toxidens approximately 30 percent shorter than L m1, B. holtzmani), in having lower molars with taller and less inflated cusps, shorter and deeper talonids, and stronger anterior cingulids.

Description.—Skull and upper dentition (Figs. 5.30, 5.31): The skull and upper antemolar dentition is virtually unknown in Bisonalveus, with only the holotype of B. toxidens known to preserve teeth anterior to M1; Fox and Scott (2005) figured the maxilla and anterior teeth in UALVP 43114 (identified in that paper as pertaining to B. browni) but did not describe them in detail. Recently prepared specimens referable to B. toxidens from Alberta preserve significant parts of the maxilla and zygomatic arch, providing the first information regarding the proportions of the snout and the orientation of the more anterior teeth. The most informative specimen in the present sample is UALVP 47462 (Figs. 5.31.9-5.31.11), an incomplete maxilla preserving the facial process, infraorbital foramen, and maxillary root of the zygomatic arch. The facial process of the maxilla is tall and bears a thick, near-vertical articular surface anteriorly for the premaxilla; judging from the length of the suture, the premaxilla also bore a tall facial process. The lateral surface of the maxilla contains the large, circular foramen of the infraorbital canal; it is positioned dorsal to the interdental space between P3 and P4 and opens anteriorly and laterally. UALVP 47463 and 47461 preserve the medial aspect of the maxilla, exposing the length of the infraorbital canal: the canal runs obliquely medially and posteriorly from the infraorbital foramen to the level of the anterior margin of M1, where a large, circular maxillary foramen is developed; the infraorbital canal transmitted the maxillary branch of the trigeminal nerve (V_2) and associated vasculature in life, and the comparatively short canal is considered a derived feature among eutherians (Butler, 1956; Novacek, 1986). The anterior root of the zygomatic arch is preserved in four specimens: it is both mediolaterally narrow and dorsoventrally shallow, projecting more or less posteriorly from its origin labial or slightly posterolabial to M2,

similar to that in many other eutherians [e.g., Leptictis and Diacodon (see Butler, 1956; Novacek, 1986)], including other pentacodontines [e.g., Aphronorus orieli Gazin, 1969 (see Gingerich et al., 1983)]. The ventrolateral surface of the zygomatic process is marked by a heavy ridge that becomes more conspicuous anteriorly towards the root, where it then swings anterodorsally towards the anteroventral margin of the orbit; a shallow depression is formed posterior and dorsal to the ridge. The depression probably represents the scar formed by the jugal as it lapped onto the side of the maxilla, with the ridge marking its anteriormost extent; a ventral depression is not developed, suggesting that the jugal of B. toxidens was not furcated. A smaller, shallower depression occurs anterior to the jugal scar, possibly representing the origin of extrinsic snout muscles (Novacek, 1986). In palatal view, the molars and last two premolars in UALVP 47462 form a smooth and shallow arc; anterior to P3, however, the maxilla turns sharply anteriorly and broadens towards the canine. The alveoli for the upper canine and first two premolars are closely crowded, with those for the premolars small and housing teeth that are reduced in size, indicating the snout of B. toxidens was robust and probably foreshortened.

Upper incisors: The upper incisors of Bisonalveus toxidens are known from the type specimen where they are associated with the rest of the upper dentition, and from an isolated I3 (UALVP 47820). The I3 in UALVP 43114 is preserved adjacent to the upper canine, but the position of this tooth is an artefact of post-mortem disturbance: the I3 crown is twisted away from an "in life" position, and it is closely appressed to the upper canine; evidence from UALVP 47820, an incomplete maxilla that preserves bone anterior to the canine alveolus, indicates that a large diastema intervenes between I3 and the upper canine in B. toxidens, allowing the lower canine to pass between the two teeth during occlusion. The tooth interpreted here as I2 rests very close to I3 as preserved, but it has probably been displaced prior to burial as well. The I1 is located farther from the other incisors, having obviously been moved a significant distance prior to burial; it is interpreted here as the first incisor, rather than P1, on the basis of its much smaller root.

The crown of I1 is worn almost to the base, erasing nearly all of its topological features; what can be seen of the base of the crown indicates it was longer than broad, and the posterior margin was drawn out as a raised, sharp carina, similar to that on the

upper canine (Fox and Scott, 2005). The crowns of I2 and I3 are similar, with that of I3 being slightly larger; both are virtually flat medially, but faintly convex laterally. The crowns resemble that of the canine in being long and rapier-like, with sharp apices; in anterior view the crowns are seen to curve faintly lingually, while in lateral view they are virtually straight. The posterior surface of the I2 and I3 crown narrows to a sharp, well-defined carina that extends from apex to base. The anterior surface of the I2 crown is heavily worn in UALVP 43114, but a sharp crest is clearly developed, running the length of the crown to its base; wear is strongest anteriorly and medially from occlusion with the opposing i2. The anterior surface of I3 is peculiarly modified, closely resembling that of the upper canine: it is subdivided by a wide, deep groove, relatively equivalent in its dorsoventral and mediolateral dimensions to those on the upper canine, but with the groove being slightly shallower. The enamel-lined groove runs the length of the crown, narrowing to acutely V-shaped contours apically and expanding to widely C-shaped contours towards the base. Wear is heaviest along the posterior and lateral parts of the crown, presumably from contact with the lower canine, an interpretation supported by the presence of strong wear facets on the anterior crest of the lower canine (see later in this chapter). A smaller, strip-like facet occurs along the anteromedial border of the groove, consistent with contact from the opposing i3.

Upper canine: The upper canine of Bisonalveus toxidens was described in detail by Fox and Scott (2005); although no additional specimens have been recovered since that publication, a recently prepared maxilla (UALVP 47462) preserves the canine alveolus, providing additional information regarding the orientation of the upper canine in the maxilla. As preserved, the canine alveolus in UALVP 47462 is kidney bean-shaped in outline, with the bone on the lateral side of the alveolar aperture having buckled mediad and forming the concave margin of the kidney bean. Although the concave labial margin of the aperture at first seems to correspond with the groove of the upper canine (similar to that developed on the maxilla of certain cercopithecoid primates, e.g., the macaques), close examination indicates that this correspondence is owing to a coincidental result of post-mortem distortion, and the alveolus clearly could not accommodate the upper canine crown if the groove and the internally buckled bone of the maxilla are lined up. The aperture is longer than broad (corresponding closely to the

dimensions of the upper canine), and is oriented somewhat posterolateral-anteromedial, oblique to the long axis of the maxilla; when articulated in the maxilla, the upper canine would be in line with P3 through M3, with its grooved surface facing anteriorly, but somewhat more medially than was described by Fox and Scott (2005). The bone of the palatal process just anterior to the canine alveolus in UALVP 47462 becomes increasingly concave dorsally, ending at an edge of finished bone and forming the margins of what superficially resembles the rim of an alveolus near the maxillary-premaxillary suture; the edge of finished bone probably represents the fossa for reception of the lower canine when the teeth reached full occlusion, similar to that developed in the maxilla and premaxilla of the didelphid marsupial Didelphis virginiana.

Upper premolars: P1: P1 of Bisonalveus toxidens is known only from its alveolus in UALVP 47462. The aperture is closely appressed to that for the upper canine, but is slightly inset from the labial margin of the maxilla, and is circular in outline.

P2: The P2 is known only from the type specimen, and from its alveoli in UALVP 47462. The tooth is two-rooted, with the posterior root slightly larger than the anterior, and the two roots are oriented faintly obliquely to the long axis of the maxillary palatal process, but in a direction opposite to that of the canine (i.e., posterolingual-anterolabial). The crown is premolariform, consisting of a tall and faintly recurved paracone and tiny metastylar cuspule. The paracone is subcircular in cross section, and supports well-developed anterior and posterior crests that originate at its apex: the anterior crest extends anteriorly and terminates at the base of the crown, while the posterior crest runs posteriorly and slightly labially to the metastylar cusp. A weak cingulum is present posterolingually.

P3: P3 was previously unknown for any species of Bisonalveus. Although the P3 of B. toxidens is variably developed, it is consistently larger and much more fully molarized than P2. The crown is asymmetrically triangular in outline, with the metastylar lobe projecting farther labially than the reduced parastylar lobe; a stylar shelf is not developed. The crown consists of a greatly enlarged and faintly recurved paracone, tiny metacone, and moderately developed protocone supported by a separate lingual root. The paracone is circular in cross section and is considerably inflated, particularly at the base. The preparacrista and parastylar lobe are virtually undeveloped, the latter

represented by little more than the thickened anterolabial extremity of the paracingulum; a small parastylar cusp can be present. The metacone is developed on the posterior flank of the paracone, and is considerably smaller and lower than the latter. A shallow labial sulcus hints of an incipient separation of the paracone and metacone, but only the apices of the two cusps are clearly separate, and these are connected to one another by a short and shallowly notched centrocrista. The postmetacrista is variably developed: it can be short and straight (e.g., UALVP 47463), extending posteriorly to the metastylar corner of the crown, or it can be longer, bending posterolabially to join the posterior cingulum and ectocingulum (e.g., UALVP 43114). As with the postmetacrista, the conules on P3 of B. toxidens are variably developed: a metaconule is present on UALVP 43115 and 47470, while the paraconule is developed only on UALVP 47462; the conules are undeveloped on UALVP 47463. When present, the paraconule is small but distinct, and closely appressed to the protocone, whereas the metaconule is poorly differentiated from the postprotocrista; conular cristae are not developed. The protocone can be robustly or only moderately developed, but in either case it is lower and slightly anterior to the level of the paracone, with its apex being slightly recurved. The protoconal cristae and cingula are well-developed, and a hypocone is not present.

P4: The crown of P4 is considerably larger and more fully molariform than that of P3, with a better-developed metacone, protocone, and conules. The paracone closely resembles that on P3: it is tall and conical, slightly recurved, and joined for most of its height with the metacone. In contrast with P3, the metacone on P4 is significantly larger, and although the two cusps are connate for most of their height, their separation is much more pronounced, with deep sulci developed labially and lingually, and with the apices connected by a wider and more deeply notched centrocrista. The stylar shelf is narrow, especially labial of the paracone. The ectocingulum is better developed than on P3, and one or two parastylar cuspules can occur at the union of the ectocingulum and paracingulum; the enamel at the anterior root forms a shallow exodaenodont lobe. The preparacrista is weak or absent, whereas the postmetacrista is conspicuous, curving posterolabially to join the ectocingulum and metacingulum; the postmetacrista can support one or two small cuspules. Both paraconule and metaconule are well developed, although the paraconule is invariably the larger and more inflated. The paraconule is

closely appressed to the base of the paracone, with its apex directed dorsally, anteriorly, and somewhat lingually, widening the V-shaped embrasure between it and the paracone. The low preparaconular crista joins the anterior cingulum and continues to the parastylar corner of the crown; the postparaconular crista is undeveloped. The metaconule is smaller and shorter than the paraconule, more lingually positioned, and is doubled in some specimens, with the two conules coalescing after extended wear; the postmetaconular crista joins the posterior cingulum before extending to the metastylar corner of the crown. The protocone, protoconal cristae, and protoconal cingula are much better developed than those on P3.

Upper molars: M1: The crown of M1 resembles that of P4, but differs in being more nearly quadrate in outline, in having larger and more fully separated paracone and metacone, and in having a significantly better developed protocone; the principal trigon cusps enclose a deep and narrow, posteriorly sloping basin. The paracone is tall, conical, and significantly inflated towards its base, and is connected to the metacone by a deeply notched centrocrista. The metacone is lower and less swollen than the paracone, and although the two cusps are better separated than on P4, they remain partly connate at their bases. A shallow ectoflexus superficially divides the labial margin of the crown into roughly symmetrical, rounded lobes. The ectocingulum is heavy, especially anteriorly where it becomes much more robust and can support a prominent parastylar cuspule. The enamel labial of the paracone forms a deep exodaenodont lobe overhanging the anterior root. The bulbous paraconule juts anteriorly, and a strong preparaconular crista runs anterolabially to join the anterior cingulum; the preparaconular crista occasionally bears a small cuspule. The metaconule is small and slightly more labial in position than the paraconule, and the postparaconular and metaconular cristae are undeveloped. Although the protocone is lower than the paracone, it is much more massive at its base, especially lingually, where can form a prominent, lobe-like bulge; its apex leans anteriorly, paralleling that of the paracone. Well-developed protoconal cristae extend to the conules from the protoconal apex: the preprotocrista is short and deeply notched near the base of the paraconule, and often bears one or two additional cuspules; the postprotocrista is longer and lower, bending abruptly labiad posterior to the protocone before continuing to the apex of the metaconule. The anterior and posterior cingula are extremely robust and

platform-like, with the posterior cingulum being wider and running uninterrupted to the metastylar corner. The anterior cingulum can support a small pericone at its lingual extremity, while a hypoconal swelling is usually developed on the posterior cingulum immediately posterior of the protocone.

M2: The M2 of Bisonalveus toxidens differs significantly from M1 and M3 in its substantially larger size and greatly hypertrophied paracone. The M2 superficially resembles the M1 of many viverravid carnivorans in occlusal outline: the crown is asymmetrically triangular or quadrangular, with a prominent parastylar area and greatly reduced metastylar corner; unlike M1 of viverravids, however, the parastylar lobe on M2 of B. toxidens is undeveloped, the area instead being occupied solely by the massive, conical paracone. The base of the paracone is especially swollen, and the labial side of the crown is oriented anterolabially-posterolingually, with the paraconal apex far labial of the level of the M1 metacone; as a result, the inflated base of the paracone is the most labial point in the tooth row, and the preparaconular crista and anterior cingulum are significantly lengthened, increasing the potential for prevallum shear (a condition analogous to that in M1s of viverravid carnivorans, although achieved in entirely different ways). The stylar shelf is wholly undeveloped, with only the robust ectocingulum occupying this area; the enamel dips at the base of the paracone, forming a deep exodaenodont lobe that is considerably larger than that on M1 or M3. The metacone is much smaller than the paracone, and its labial wall is virtually flat, while its lingual side is convex. Unlike that on M1 or M3, the metacone on M2 is directed posteriorly and lingually, bringing the elongated premetacrista into closer contact with the hypocristid of the corresponding m2 during occlusion, similar to that on M1 of primitive carnivorans (Fox and Youzwyshyn, 1994). The preparacrista is virtually undeveloped, while the postmetacrista is low, sweeping posterolabially to join the ectocingulum at the metastylar corner of the crown. As with M1, the anterior parts of the crown are raised above the more posterior parts, and the trigon basin slopes posteriorly. The conules resemble those on M1: the conical paraconule is much larger and more inflated than the metaconule, with the high, sharp preparaconular crista extending anterolabially to meet the robust anterior cingulum; a large cuspule is often developed on the preparaconular crista. The tiny metaconule is barely more than a swelling on the

postprotocrista, and the postparaconular and metaconular cristae are undeveloped. The protocone is only slightly better developed than that on M1 and leans similarly anteriorly. A high and deeply notched preprotocrista extends to the paraconule, while the postprotocrista is low, unnotched, and curves gently to the apex of the metaconule. The conspicuous, platform-like cingula are heavier than those on M1, and although a prominent hypoconal bulge is usually present, a distinct hypocone is never developed.

M3: The crown of M3 is asymmetrically triangular in outline, but proportionately much shorter anteroposteriorly than M1 or M2, with a labially protruding parastylar and greatly reduced metastylar lobes. As with M1 and M2, the conical paracone is larger than the metacone (although not to nearly the same degree as that on M2), and their apices are connected by a widely notched centrocrista. The ectocingulum is well developed, especially anteriorly where a parastylar cusp can be formed at the junction of the ectocingulum and paracingulum; the ectocingulum gradually fades posteriorly and is undeveloped at the metacone. A shallow exodaenodont lobe occurs at the anterior root. Although the paraconule is small, its associated crests are well developed, particularly the preparaconular crista, which extends anterolabially to the parastylar corner of the crown; the metaconule and its associated crests are weak or absent. The protocone leans anteriorly, and the protoconal cristae are both high and sharp. The anterior and posterior cingula are wide and platform-like, the former extending to the parastylar corner of the crown, the latter ending near the lingual base of the metacone; a hypoconal lobe is not developed.

Dentary and lower dentition (Figs. 5.32, 5.33, 5.34.1-5.34.6): The dentary of Bisonalveus toxidens is well represented in the UALVP collections, with more than 100 specimens collectively documenting the mandibular anatomy in its entirety, including the lower incisors; a number of specimens representing immature individuals provide information regarding the ontogeny of the mandible and pattern of tooth eruption. The dentary closely approximates that of the leptictid Leptictis in general proportions (Novacek, 1986): it is boat-shaped in lateral view, with a long and shallow horizontal ramus, tall coronoid process, and small condyle. The horizontal ramus is deepest at the level of m3 in adults (e.g., UALVP 40560, Figs. 5.32.11-5.32.13), and then narrows considerably towards the symphysis; the ventral margin of the ramus is gently convex.

When viewed from occlusal aspect, the ramus is seen to curve faintly laterally until the level of p3, where it then bends sharply, becoming more or less anteroposterior in its orientation, in keeping with the similarly directed rostrum (see earlier in this chapter). The ramus is considerably smaller and, especially, shallower in immature individuals (see e.g., UALVP 40535, 47525, Figs. 5.34.1-5.34.6), achieving its greatest depth at the symphysis.

The symphyseal surface is long and shallow, terminating at the level of the anterior root of p3. A sharp ridge delimits the articular surface of the symphysis dorsally: the ridge runs anteroposteriorly to the canine alveolus, and then descends at a gentle angle to the ventral margin of the ramus below p3. A second ridge marks the ventral limit of the symphysis, running from the i3 alveolus posteriorly to the level of p3 where it joins the dorsal ridge, then continues posteriorly as a well-defined crest that probably represents the distal attachment of the mylohyoid or anterior digastric musculature (Turnbull, 1970). The articular surface is nearly smooth, with few irregularities or rugosities developed in the bone, suggesting that the two rami were only loosely sutured in life, permitting substantial movement between the two jaws during mastication. One, or sometimes two, small nutritive foramina are developed in the symphyseal bone. The orientation of the symphysis bears importantly on the inferred position of the mandible: when the jaw is held with the symphysis in the vertical plane (an assumed "in life" position), the jaw is rotated laterally, bringing the occlusal surfaces of the lingually-leaning p4 and molars into the horizontal plane, and splaying the canine and first three premolars strongly laterally (see Fig. 32.1); as a further consequence of the rotation of the jaw, the incisors, represented by their alveoli on most specimens, become nearly vertical in their orientation. The unusual orientation of the jaw has important consequences as regards dental function, particularly with respect to the venom-delivery system (VDS) (see later in this chapter). Two variably developed mental foramina are usually present: the first is positioned ventral to the posterior root of p3 or anterior root of p4, its subovate or circular aperture opening dorsolaterally; the second foramen occurs ventral to p2, and can be larger or smaller than the more posterior foramen; its subovate aperture opens anterolaterally.

The coronoid process in Bisonalveus toxidens is enormous relative to the size of the ramus, with its apex towering well above the level of the molar row (e.g., UALVP 47514, Figs. 5.33.1-5.33.3). The coronoid process begins its ascent slightly posterior to m3 in adults (e.g., UALVP 47514), slightly farther posterior than in immature individuals (e.g., UALVP 40535), and at an angle of approximately 125 degrees; its apex is smoothly rounded and slightly hooked posteriorly, and its posterior margin is concave. The masseteric fossa is deeply excavated, with its anterior margin delimited by a robust crest. A faint crest originating at the lateral side of the condylar process runs anteroventrally, defining the lower border of the temporalis part of the mandibular fossa and separating it from the area of distal attachment for the superficial masseter. The temporalis fossa is weakly excavated, and is separated from the pterygoid fossa by a strong ridge. A conspicuous mandibular foramen is developed in the pterygoid fossa ventral to the condylar process, its aperture opening posteriorly and faintly medially.

The short, stout, and posteriorly directed condylar process supports a small condyle that is positioned well above the tooth row. The cylindrical condyle extends farther medially than laterally, and its articulating surface is broadly convex and directed posteriorly and dorsally. Although the condyle slopes slightly laterally when the ramus is held vertically, the more likely "in-life" position (as dictated by the orientation of the symphyseal surface, see previously) would have the dentary rotated further labially, bringing the occlusal surfaces of the lingually leaning molars into the horizontal plane, while the condyle slopes even farther laterally; the unusual configuration of the condyle suggests that the articulating surface of the glenoid fossa would face somewhat ventromedially.

The angular process in Bisonalveus toxidens is a short, thin flange in immature individuals (e.g., UALVP 40535), with its posterior extremity smoothly rounded or slightly hooked dorsally. The lateral surface is shallowly excavated for insertion of the superficial masseter, while its medial surface bears a conspicuous crest that separates the area for distal attachment of the superficial masseter below from the internal pterygoid above. In more mature individuals, the angular process is further drawn out posteriorly, and the apical hook is more prominent; in presumed adults (e.g., UALVP 47511), the angular process is considerably longer and more robust than in immature individuals, and

the pterygoid crest is significantly more robust, forming a shelf-like prominence ventromedially.

Lower dentition: Lower incisors: The three lower incisors of Bisonalveus toxidens are known only from the holotype. The teeth are small and closely crowded, with elongate and slightly curved roots. The incisor crowns are badly damaged in UALVP 43114, with only that of i3 well enough preserved for description; although the crowns of i1-2 are missing, the dimensions of their bases indicate they were subequal in size and slightly smaller than i3. The crown of i3 is anteroposteriorly compressed and chisel-like; a strip-like wear facet is developed along the apex of the crown, widening towards the lateral margin. Although the lower incisors of B. toxidens are known only in UALVP 43114, their alveoli are represented in several specimens, providing information on their orientation in the jaw. The alveoli are best seen in UALVP 47510 (Figs. 5.32.17-5.32.19): the anteroposteriorly compressed apertures are closely appressed to one another, with no development of diastemata, and are arranged in a gentle arc originating at the mandibular symphysis; the i3 alveolus is closely appressed to the much larger canine alveolus. When the horizontal ramus is held vertically, the alveolar apertures face almost medially, but when the jaw is rotated laterally to better approximate an "in-life" position, the incisor alveoli open dorsally, and the incisors were probably subvertical, rather than procumbent.

Lower canine: The highly modified lower canine of Bisonalveus toxidens was briefly described by Fox and Scott (2005). The crown differs significantly from the large, subconical canines of more primitive therians: it is short, barely taller than the succeeding teeth (the canines in UALVP 43114 and 47503 have been partially extruded from the alveolus and hence appear taller than they actually are; see UALVP 47502 for a closer approximation of canine height), wider than long, and faintly procumbent. The crown is premolariform, closely resembling that of p1 and p2, and consists solely of a short and stout protoconid. The crown curves anteroposteriorly, with the apex pointing faintly posteriorly, but also labiolingually, with the apex projecting prominently lingually; as such, the protoconid is curved in two distinct planes, anteroposteriorly and labiolingually, imparting a "twisted" appearance to the crown, with the protoconid apex facing posterolingually. The enamel on the posterior side of the crown extends

considerably farther ventrally than it does on the anterior side. Two well-developed crests descend from the protoconid apex, dividing the crown into convex labial and lingual sides: the anterior crest runs anteriorly and lingually, then curves posteriorly, continuing as a robust cingulid along the swollen lingual base of the protoconid; the second crest runs posteriorly and labially, fading away as it approaches the base of the crown. As discussed in Fox and Scott (2005), although the lower canine of B. toxidens retains primitive occlusal relationships with the opposing upper canine (i.e., the posterior side of the lower canine occludes against the anterior surface of the upper canine), the crown is highly modified as part of the VDS (see later in this chapter). A large, subovate facet is developed along the posterior side of the crown, evidence of extensive contact with the upper canine; the facet widens significantly basally, flattening the posterior surface of the crown, and in the most heavily worn specimens extends past the base of the crown, incising the root. Parallel, obliquely directed striations are developed within the body of the facet, and are particularly strong ventrally. A second facet is developed on the anterior side of the crown along the edge of the anterior crest from occlusion with the posterolateral margin of I3.

Lower premolars: p1: The faintly procumbent, single-rooted p1 of Bisonalveus toxidens broadly resembles the lower canine: a trenchant protoconid dominates the crown, its labial side being strongly convex and its lingual face virtually flat, except posterolingually, where the base is swollen. In contrast to the lower canine, the protoconid on p1 is vertical, rather than recurved. Sharp crests originating at the protoconid apex divide the crown into labial and lingual halves: the anterior crest curves gently anterolingually, then bends posteriorly as a lingual cingulid; the more posterior crest runs posteriorly to the base of the crown, where it can join a weakly developed heel before continuing anteriorly, completing the lingual cingulid. There is no evidence of a paraconid, metaconid, or distinct talonid cusps.

Although the single-rooted p2 of Bisonalveus toxidens closely resembles p1, its size varies considerably, from being just slightly smaller than p1 (e.g., UALVP 47503) to wholly absent, with a diastema developed between p1 and p3 (e.g., UALVP 43114), with a range of sizes in between these extremes (represented by teeth or its alveolus); in any

case, p2 is consistently smaller than p1 in all specimens preserving these teeth. The p2 can differ further from p1 in having less well-developed crests and a weaker heel.

p3: The p3 of Bisonalveus toxidens is premolariform, two-rooted, and supports a well-developed protoconid and weakly basined talonid. The crown is variably developed, although not to the same degree as that of p2: it is most often nearly as wide as it is long, with a considerably swollen exodaenodont lobe developed at the posterior root; in contrast, the crown can be narrower posteriorly, and the exodaenodont lobe shallower and less labially protruding. The protoconid is tall and swollen at its base; a thick crest extends from the protoconid apex towards the anterior margin of the crown, curving lingually and then posteriorly as a robust lingual cingulid. Although the paraconid is not developed, a small cuspule arising from the lingual cingulid occurs in some specimens (e.g., UALVP 47510); a metaconid is not present on any specimen at hand. The talonid consistently bears a large hypoconid that is connected to the postvallid wall by a sharp cristid obliqua; additional talonid cusps are not present, although vague swellings on the postcristid hints at their incipient development. The postcristid extends from the hypoconid apex lingually then anteriorly, becoming indistinguishable from the lingual cingulid and forming the posterior and lingual margins of a shallow basin. The hypoflexid is narrow and deep, and the ectocingulid can be strongly developed (e.g., UALVP 47521) or nearly absent (e.g., UALVP 47503).

dp3: The deciduous p3 of Bisonalveus toxidens is preserved in two specimens (UALVP 40535 and 47525); the identity of this tooth was confirmed by partial dissection of the medial side of the mandible on UALVP 47525, revealing the succeeding permanent p3 (see Fig. 5.34.5). The crown of dp3 is much less molariform than that of dp4 (see later in this chapter), and more closely resembles its permanent successor. The crown of dp3 consists primarily of a tall protoconid and bicuspid talonid; a weak crest descends anteriorly from the paraconid apex to a small cuspule formed at the union of the weak anterior and lingual cingulids. A sharp crest extends posteriorly from the protoconid apex, meeting a short cristid obliqua running anterolingually from the apex of the large hypoconid; a tiny entoconid is developed lingual to the hypoconid, and the two cusps are connected by a low postcristid. A low crest extends a short distance anteriorly

from the entoconid, defining the lingual border of the shallow talonid basin. The hypoflexid is deep, and a posterior cingulid is not present.

p4: The p4 of Bisonalveus toxidens is fully molariform, with a well-defined protoconid, metaconid, and talonid. The crown bears two deep exodaenodont lobes, one at each of the roots; the crown is somewhat constricted between the two lobes, giving the tooth a weakly hourglass shape in occlusal view. A massive, inflated protoconid dominates the trigonid: its labial and lingual walls are broadly convex and its apex projects somewhat posteriorly. A prominent paracristid extends anterolingually from the protoconid apex, curving posteriorly to continue as the lingual cingulid. The paraconid is most often incorporated into the low, shelf-like paracristid, although a small cuspule can be occasionally developed at the union of the paracristid and lingual cingulid. The metaconid is variably developed: it is rudimentary in some specimens, arising low on the posterolingual shoulder of the protoconid, and connected to it by a short protocristid; in other specimens it is larger, arising from higher and more anterior on the lingual wall of the protoconid and connected to it by a sharply notched protocristid. The short and deeply basined talonid is slightly wider than the trigonid, with the swollen exodaenodont lobe jutting farther labially. The talonid consists of a well-developed hypoconid, smaller entoconid, and a variably developed hypoconulid. The hypoconid is tall and sharp, its apex nearly the same height as that of the metaconid in some specimens, and is connected to the postvallid wall by a short cristid obliqua; the entoconid is lower than the hypoconid, but similarly sharp, and is connected to it by a sharp postcristid. The talonid basin slopes lingually. A hypoconulid can intervene between the hypoconid and entoconid, but when present it is poorly developed. A weak protostylid crest runs down the posterolabial side of the protoconid, disappearing as it nears the base of the crown. The ectocingulid is robust anteriorly, but is otherwise inconspicuous.

dp4: The deciduous p4 of Bisonalveus toxidens resembles p4, but is more fully molariform, with a strongly developed paraconid and distinct talonid cusps. Exodaenodonty is developed anteriorly and posteriorly as on p4, but the lobes are shallower and less swollen. The trigonid is triangular in outline, with an anteriorly positioned paraconid, recurved protoconid, and posterolingual metaconid. The protoconid and metaconid are subequal and somewhat labiolingually compressed, and are

connected to one another by a deeply notched protocristid; the cuspidate paraconid is much better developed than on p4, slightly anteroposteriorly compressed, and connected to the protoconid by a low, sweeping paracristid. The talonid is relatively wider than that on p4, and protrudes farther labially than the trigonid; it consists of a tall hypoconid, smaller entoconid, and poorly developed hypoconulid that together enclose a deep basin. A small mesoconid can be developed on the low cristid obliqua. The anterior cingulid is conspicuous, but quickly disappears as it rounds the protoconid; a posterior cingulid is not present.

Lower molars: m1: The crown of m1 is weakly hourglass-shaped in occlusal outline, with the trigonid leaning posteriorly and set off from the talonid by weak labial and lingual indentations. Exodaenodonty is developed at both roots, but the anterior lobe is deeper and more swollen. The trigonid is dominated by a massive and turgid protoconid, a smaller but slightly taller metaconid, and conspicuous, conical paraconid; the cusps form a near-equilateral triangle in occlusal outline and together enclose a shallow basin. As on p4, the protoconid on m1 is considerably swollen towards its base, strongly convex labially and lingually, and its apex points somewhat posteriorly. A low paracristid runs anteriorly from the protoconid apex before bending abruptly lingually towards the vertical to slightly anterior leaning paraconid. The posteriorly leaning metaconid is larger and better differentiated from the protoconid compared to that on p4, and is positioned immediately lingual, or slightly posterolingual to the protoconid; a deeply V-shaped protocristid connects the apices of the protoconid and metaconid. Accessory crests similar to those on the molar trigonids of many arctocyonid condylarths are usually developed on m1 of Bisonalveus toxidens, extending basinward from the apices of the protoconid and metaconid (e.g., UALVP 47415, Figs. 5.33.1-5.33.3). The talonid is marginally narrower than the trigonid, but nearly as tall, owing to the latter leaning posteriorly; a prominent hypoconid, entoconid, and poorly developed hypoconulid enclose a deep and anteroposteriorly short basin. The hypoconid and entoconid are both sharp, with the hypoconid the taller and more swollen of the two. The hypoconulid is weakly developed, appearing only as an ill-defined single, or sometimes doubled swelling on the postcristid. The cristid obliqua joins the postvallid just ventral to the protocristid notch, and can bear a small mesoconid; the entocristid is low and can bear

a conical entoconulid. The ectocingulid is robust anteriorly, but quickly fades away as it approaches the swollen labial side of the protoconid; the posterior cingulid is undeveloped.

m2: The m2 of Bisonalveus toxidens closely resembles m1, differing mainly in its larger size, wider talonid, and considerably more massive protoconid. The crown is hourglass shaped in occlusal outline, with a strong constriction developed between the trigonid and talonid. The trigonid is more transverse than on m1, and leans strongly posteriorly, bringing the trigonid and talonid to nearly equal heights; exodaenodonty is stronger compared to m1, with the anterior lobe deeper and jutting farther labially. The trigonid cusps are swollen, especially the massive protoconid; the paracristid is low, running a short distance anteriorly before bending lingually at a near 90 degree angle towards the paraconid, and then ascending the anterolingual side of the cusp to its apex. The paraconid is erect and slightly anteroposteriorly compressed, whereas the metaconid is more swollen, posteriorly leaning, and connected to the protoconid by a widely V-shaped protocristid. As on m1, accessory crests are developed on the trigonid of m2, extending basinward from the apices of the cusps; small cuspules are often present on the accessory crests, and a larger, well-defined cusp is usually developed on the paracristid and metaconid arm of the protocristid. The talonid on m2 is narrower than the trigonid, consisting of a tall, swollen hypoconid, lower entoconid, and a much reduced hypoconulid that together enclose a deep basin. Short accessory crests extend basinward from the apices of the hypoconid and entoconid, similar to those on the trigonid; the hypoconulid appears most often as a vague single or doubled swelling on the postcristid. Because the apex of the hypoconid is well above the level of the deepest part of the protocristid, the cristid obliqua descends, rather than ascends to the postvallid wall, joining it just ventral to the protocristid notch; a large mesoconid is usually developed on the cristid obliqua, and a deep, slit-like notch is incised into the crest prior to its union with the postvallid wall. The entocristid is short, acutely notched, and bears a small entoconulid. The anterior cingulid is robust, but does not continue around the labial side of the protoconid, although a weakly papillated ridge can be present; the hypoflexid shelf is conspicuous, often supporting a number of tiny cuspules.

m3: The m3 of Bisonalveus toxidens is considerably smaller than either m1 or m2, but is nonetheless similar in most features: the trigonid leans posteriorly, bringing it and the talonid into nearly the same occlusal plane; the protoconid is the largest trigonid cusp, followed by a less swollen but taller metaconid, and reduced, conical paraconid; a deep exodaenodont lobe is present anteriorly; accessory crests are developed on the basin-facing walls of the trigonid cusps; and the protocristid is widely V-shaped, but sharply notched at its ventral apex. The talonid is significantly narrower than that on m1 or m2, and is broadly lobate posteriorly, superficially resembling the m3 of many plesiadapiform primates. The inflated hypoconid is the tallest talonid cusp, and is connected to the postvallid wall by a short cristid obliqua that usually bears a swollen mesoconid. The entoconid is proportionately much smaller than on m2, and the notch in the entocristid is wider. The hypoconulid is unusually constructed, consisting of two distinct cusps and a smaller postcristid cuspule arranged in a gentle arc posteriorly; the cusps together form a broad lobe that constitutes the posterior margin of a long talonid basin. The anterior cingulid is better developed than that on m1 or m2, continuing around the protoconid and past the level of the hypoflexid, where it then terminates; a posterior cingulid is not developed.

Etymology.—Toxicum, Latin, poison; dens, Latin, tooth, in reference to the venom-conducting upper canine.

Holotype.—UALVP 43114, incomplete skull with left I1-3, C, P2-4, M1-3, and associated dentaries with left c, p1-4, m1-3 and right i1-3, c, p1, p3-4, m1-3. DW-2 locality, Paskapoo Formation of Alberta, late Paleocene [early middle Tiffanian, Ti3 (Fox, 1990), Plesiadapis anceps/P. rex Lineage Zone of Lofgren et al., 2004].

Other material examined.—From Joffre Bridge Roadcut upper level: TMP 2001.25.02, incomplete maxilla with fragmentary M1-3; UALVP 40666, M3; UALVP 47458, p4.

From DW-1: UALVP 47459, M1; UALVP 47460, M2; UALVP 40549, incomplete dentary with m1-3.

From DW-2: UALVP 47461, incomplete left maxilla with P4, M1-3, and associated incomplete right dentary with p3-4, m1, and alveoli for c, p1-2; UALVP 47462, incomplete right maxilla with P3-4, M1-3, and alveoli for C, P1-2; UALVP

47463, incomplete left maxilla with P3-4, M1-3; UALVP 47464, ?I3; UALVP 40559, incomplete maxilla with P4, M1; UALVP 47466, incomplete maxilla with P4, M1-2; UALVP 47467, incomplete left maxilla with M1-3; UALVP 47821, incomplete maxilla with M1-3; UALVP 47468, incomplete maxilla with incomplete M1-3; UALVP 40542, incomplete maxilla with M1-2; UALVP 40561, incomplete maxilla with M1-2; UALVP 47469, incomplete maxilla with M1-2; UALVP 47822, associated M2-3; UALVP 47820, I3; UALVP 43115, 47470-47472 (total: 3), upper canine; UALVP 47473, 40538, DP4; UALVP 40553, 40556, 47474-47478 (total: 7), P4; UALVP 47479-47483, 40555, 40557 (total: 7), M1; UALVP 47484-47495, 40546 (total: 13), M2; UALVP 47496, 47497, M3; UALVP 47498, fragmentary M1; UALVP 47499, associated incomplete left and right dentaries with left p3-4, m1-3, and right c, p1, p3-4, m1-3; UALVP 47500, associated incomplete left and right dentaries with left p3-4, m1-3, and alveoli for i1-3, c, p1-2, and right p4, m1-3; UALVP 47501, associated incomplete left and right dentaries with left m2-3, and right m2-3; UALVP 47502, 47503, incomplete right dentary with c, p1-4, m1-3, and alveoli for i1-3; UALVP 47504, incomplete dentary with c, p1, p3-4, m1-3, and alveolus for p2; UALVP 40562, incomplete dentary with p1-4, m1-2 (m2 incomplete), and alveoli for m3; UALVP 47505, incomplete dentary with p2-4, m1-2, and alveoli for i3, c, p1, and m3; UALVP 40560, incomplete left dentary with p3-4, m1-3, and alveoli for c, p1-2; UALVP 47506, incomplete left dentary with p3-4, m1-3, and alveoli for p1-2; UALVP 47507, incomplete dentary with c, p3-4, m1, and alveoli for i1-3, p1-2; UALVP 40551, incomplete dentary with p3-4, m1-3; UALVP 40552, incomplete dentary with p3-4, m1-3, and alveoli for c, p1-2; UALVP 47508, incomplete dentary with p3-4, m1-3, and alveoli for c, p1-2; UALVP 47509, incomplete dentary with p3-4, m1-2, and alveoli for i1-3, c, p1-2, and m3; UALVP 47510, incomplete left dentary with p3-4, m1, and alveoli for c, p1-2; UALVP 40535, incomplete left dentary with dp3-4, m1-2, erupting m3, and alveoli for c, p1-2; UALVP 47511, incomplete left dentary with p4, m1-3, and alveoli for p1-3; UALVP 47512, incomplete dentary with p4, m1-3, and alveoli for p3; UALVP 47513, incomplete dentary with p4, m1-3, and alveoli for c, p1-3; UALVP 47514, incomplete right dentary with p4, m1-3; UALVP 47515, incomplete dentary with p4, m1-3; UALVP 47516, incomplete dentary with p4, m1-2, and alveoli for c, p1-3, and m3; UALVP 47517, incomplete dentary with p4, m1-2, and alveoli for c, p1-3, and m3;

UALVP 47518, incomplete dentary with p3-4, m1, and alveoli for c, p1-2; UALVP 40540, incomplete dentary with p3-4, m1, and alveoli for c, p1-2; UALVP 47519, incomplete dentary with p3-4, m1, and alveoli for i1-3, c, p1-2; UALVP 47520, incomplete dentary with p4, m1-2; UALVP 40558, incomplete dentary with p2, p4, m1, p3 roots, and alveoli for c, p1, and m2; UALVP 47521, incomplete left dentary with p2-4, and alveoli for i1-3, p1; UALVP 47522, incomplete dentary with p3-4, and alveoli for c, p1-2; UALVP 40548, incomplete dentary with p4, m1-2, and alveoli for c, p1-3, and m3; UALVP 47523, incomplete dentary with p3, m1-2, and alveoli for c, p1-2; UALVP 40544, incomplete dentary with p4 and m2; UALVP 47524, incomplete dentary with p4, m1 (trigonid), p3 roots, and alveoli for i1-3; UALVP 47525, incomplete left dentary with dp3, erupting p4, m1, and alveoli for c, p1-2, m2-3; UALVP 47526, incomplete dentary with m1-2, and alveoli for p4; UALVP 47527, incomplete dentary with m1-3; UALVP 47528, incomplete dentary with m1-3, and alveoli for p4; UALVP 47529, incomplete dentary with m1-3; UALVP 47530, incomplete dentary with m1-3; UALVP 47531, incomplete dentary with m1-3; UALVP 47532, incomplete dentary with p4, m1-3, and alveoli for p3; UALVP 47533, incomplete dentary with m1-2, trigonid of m3, and alveoli for p4; UALVP 47534, incomplete dentary with m1-2; UALVP 47535, incomplete dentary with m2-3, and alveoli for m1; UALVP 47536, 47537, incomplete right dentary with m2-3; UALVP 40534, incomplete dentary with m2-3; UALVP 47538, incomplete right dentary with m2-3; UALVP 47539, incomplete dentary with m2-3; UALVP 47540, incomplete dentary m2-3; UALVP 40550, incomplete dentary with m2-3; UALVP 47541, incomplete dentary with m2-3; UALVP 40532, incomplete dentary with m2-3; UALVP 47542, incomplete dentary with p4, m1, and alveoli for c, p1-3, and m2; UALVP 47543, incomplete dentary with p3-4, and alveoli for i1-3, c, p1-2; UALVP 47544, incomplete dentary with m1-2 (m2 trigonid only), and alveoli for p2-4; UALVP 47545, incomplete dentary with m1-2 (m1 trigonid only); UALVP 47547, incomplete dentary with m1; UALVP 47548, incomplete dentary with m3, and alveoli for m2; UALVP 47549, incomplete dentary with m2, and alveoli for m3; UALVP 40545, incomplete dentary with m3; UALVP 47550, incomplete dentary with m3; UALVP 47551, incomplete dentary with m3; UALVP 40539, incomplete dentary with m2 (trigonid only), and alveoli for p3-4, m1; UALVP 47552, dp4; UALVP 40536, 47553-

47556 (total: 5), p4; UALVP 40537, 40541, 47557-47666 (total: 12), m1; UALVP 47667 (trigonid only)-47671 (trigonid only) (total: 5), m2; UALVP 40530, 40531, 40547, 47672-47676 (total: 8), m3.

From DW-3: UALVP 47546, incomplete dentary with m1, and alveoli for m2-3.

From Birchwood: UALVP 47677, 47678, upper canine; UALVP 47679, P4; UALVP 47680, 47681, M1; UALVP 39420, 39421, 39422, 39423, 39424, 47682, 47683 (total: 7), M2; UALVP 39425, M3; UALVP 39432, incomplete dentary with p3-4, m1-3, and alveoli for ?i1-3, c, p1-2; UALVP 47684, incomplete dentary with p3-4, m1-3; UALVP 39434, incomplete dentary with p4, m1-3, p3 roots, and alveoli for p1-2; UALVP 39431, incomplete dentary with p4, m1-2, and alveoli for p1-3; UALVP 39428, incomplete dentary with p4, m1-2; UALVP 39429, incomplete dentary with m1-3, and alveoli for p4; UALVP 39430, incomplete dentary with m1-3, and posterior root of p4; UALVP 39439, incomplete dentary with m1-3, and posterior root of p4; UALVP 39426, incomplete dentary with m1-3; UALVP 39433, incomplete dentary with p3-4, and alveoli for c, p1-2; UALVP 39427, incomplete dentary with p4, m1, and alveoli for p1-3; UALVP 39435, incomplete dentary with p4, m1, and alveoli for p3; UALVP 39436, incomplete dentary with p4, m1-2, and alveoli for p3 and m3; UALVP 47685, incomplete dentary with p4, m1-2, and alveoli for p2-3; UALVP 39437, incomplete dentary with m1-2, and roots of p4; UALVP 47686, incomplete dentary with m1-2; UALVP 47687, incomplete dentary with m1-2, and alveoli for m3; UALVP 39440, incomplete dentary with m2-3, and alveoli for p4, m1; UALVP 47688, incomplete dentary with m2-3; UALVP 39441, incomplete dentary with m2-3; UALVP 39442, incomplete dentary with m2-3 (m2 talonid only); UALVP 39453, incomplete dentary with m2-3 (m2 talonid only); UALVP 39438, incomplete dentary with m1-2 (m1 talonid only), and alveoli for m3; UALVP 47689, incomplete dentary with p4, m1, and alveoli for p3; UALVP 47690, incomplete dentary with p4, m1 roots, and m2; UALVP 39448, incomplete dentary with m1, and alveoli for p4; UALVP 47691, incomplete dentary with m1, and alveoli for m2-3; UALVP 39444, incomplete dentary with m1; UALVP 39449, incomplete dentary with m2, and alveoli for m1 and m3; UALVP 39446, incomplete dentary with m1; UALVP 39443, p3; UALVP 39447, 39452, 39475, m1; UALVP 39445, 39450, 39451,39476, m2.

Age and occurrence.—Late Paleocene (Tiffanian) of western Canada.

Discussion.—Mandibular dental eruption in Bisonalveus toxidens: The timing of eruption of parts of the lower replacement dentition of B. toxidens can be estimated from UALVP 40535 and 47525, incomplete dentaries of immature individuals that preserve parts of the replacement dentition in different stages of eruption. UALVP 47525 preserves dp3, erupting permanent p4, m1, and the alveoli for c, p1-2, and m2-3; UALVP 40535 preserves dp3-4, m1-2, erupting m3, and alveoli for c, p1, and p2. With m1 and m2 having already erupted, and with dp3 and dp4 still in the jaw, the m3 on UALVP 40535 is just beginning to erupt, with the apices of the trigonid cusps flush with the alveolar rim; collectively, this evidence suggests the molars of B. toxidens were probably all fully erupted before dp3-4 were replaced. This inferred replacement pattern is further supported by the distribution and intensity of wear on teeth of adult individuals (e.g., UALVP 47503, Figs. 5.32.5-5.32.7): wear is heaviest on m1, followed in decreasing order of intensity by m2, m3, p4, and finally p3. Wear on dp3 on UALVP 40535 is heavier than on dp4, indicating it erupted earlier, yet it was clearly replaced later than dp4: the permanent p4 on UALVP 47525 is just beginning to emerge from the crypt, while the heavily worn dp3 remains in the tooth row, and the permanent p3 remaining deep in the crypt (see Fig. 5.34.5). Little can be said of the timing of eruption of p1 or p2: a broken root occupies the p2 alveolus in UALVP 47525, but whether it pertains to the deciduous or replacement tooth is uncertain; wear on the permanent p2 is highly variable, but apical wear on the protoconid is generally heavier than on p3, suggesting an earlier eruption of p2.

The hypothesized mandibular eruption sequence for B. toxidens is (?dp2)-dp3-dp4-m1-m2-m3/(?p2)-p4-p3. As discussed earlier, the primitive mandibular eruption pattern among therians is equivocal, with (p1/?dp1)-dp2-dp3-dp4-m1-m2-m3/p2-p3-p4 or (?dp2-dp3)-dp4-m1-(?m2-?m3)/p3-p2-p4 considered primitive (see Ziegler, 1971; Bloch et al., 1998; Kobayashi et al., 2002). It is important to note that p3 is replaced earlier than p4 in both alternatives, and in this regard the replacement pattern in B. toxidens is clearly different and probably derived: a similar replacement pattern (i.e., dp4 being replaced earlier than dp3) has been documented in various lipotyphlans (see Ziegler, 1971), and is considered one of the earliest modifications of the primitive anteroposterior

replacement pattern that may be related to molarization of the posterior premolars (Slaughter et al., 1974).

Dental function in Bisonalveus toxidens: Clearly the most unusual and surprising discovery as regards the dentition of B. toxidens is its possession of a venom-conducting system, expressed principally in the modified upper and lower canines. Fox and Scott (2005) briefly discussed the function of the canines in transmitting venom to prey items; the new specimens of B. toxidens provide additional information regarding the function of the venom-delivery apparatus, as well as other parts of the dentition.

The single-rooted upper canine of B. toxidens is long and dagger-like, differing from those of more primitive eutherians in which the canine is curved posteriorly. The posterior surface of the crown is raised as a sharp keel or carina that extends the length of the crown, terminating near the base at a low heel. The anterior surface of the tooth bears a deep and narrow groove, extending from the base of the crown to its tip: the enamel-lined groove has C-shaped contours towards the base, but narrows apically, becoming more nearly V-shaped in cross section; the channel is unobstructed throughout its length; Fox and Scott (2005) interpreted the deep groove in the upper canine as part of a highly modified venom-conducting apparatus wherein venom, possibly produced by a modified salivary gland, flowed freely down the length of the canine during the initial phases of prey-capture and ingestion, functionally analogous to the grooved lower caniniform teeth in the Caribbean Solenodon Brandt (see McDowell, 1958; Rabb, 1959; Dufton, 1992) and the fangs of certain opisthoglyphic colubroid snakes (Lake and Trevor-Jones, 1996; Jackson, 2003). As discussed previously, the lower canine of B. toxidens retains primitive occlusal relationships, with its posterior side occluding against the anterior surface of the upper canine. When the mandible was elevated and the teeth brought into occlusion, the stout lower canine moved obliquely dorsomedially, its flat posterior surface contacting the grooved anterior surface of the upper canine. Crests, ridges, or other raised coronal topologies that might fit into the groove on the upper canine are not developed, and it appears that the lower canine had no additional specialized function in mastication during canine occlusion. The long, dagger-like crown of the upper canine could readily be cleared from the much shorter lower canine when the mandible was depressed, enhancing the action of the upper canine in stabbing prey. The unusual

configuration of the dentary further enhances the efficiency of the VDS: when the jaw is held with the symphysis in the vertical plane (an "in-life" position), the jaw is rotated slightly laterally, bringing the occlusal surfaces of the lingually-leaning p4 and molars into the horizontal plane, and splaying the canine and first three premolars strongly laterally (see Fig. 5.32.1); furthermore, because the jaw is rotated laterally, the incisors, represented by their alveoli on most specimens, become nearly vertical in their orientation. As a consequence of the strong lateral splaying, the lower canines are functionally reduced in height, allowing the long upper canines to be more easily cleared when the mandible is depressed. As with the canine, the anterior surface of I3 in B. toxidens is deeply grooved, suggesting the venom-conducting apparatus was not restricted solely to the canine locus, but may have extended to at least the lateral incisor as well; I1 and I2 on UALVP 43114 are too worn to determine whether or not these teeth also had an anterior groove. The distribution of wear facets on I3 indicates the tooth probably functioned in a similar manner to that of the canine: wear is heaviest posteriorly, laterally, and basally from occlusion with the anterior surface of the enlarged lower canine; wear is also developed anteriorly from occlusion with the corresponding i3, but like that on the canine, is apparently restricted to the more basal parts of the crown, indicating the groove remained unobstructed through most of its extent.

Although the postcanine dentition of Bisonalveus toxidens (and other species of Bisonalveus generally) broadly resembles that of other pentacodontines, it is atypical in a number of ways. Whereas the upper and lower fourth premolars of Pentacodon and Aphronorus are relatively enormous, those in Bisonalveus are not appreciably enlarged, and the P4 in Bisonalveus is more fully molariform, with well-developed conules and weaker cingula; the molars of Pentacodon and Aphronorus decrease in size from M1/m1 to M3/m3, while the M2/m2 in Bisonalveus is the largest postcanine tooth; the lower molar protoconids in Bisonalveus are considerably inflated, and the crowns are exodaenodont, especially on m2, whereas those structures in Pentacodon and Aphronorus are comparatively unmodified; and the cusps and crests are sharper in Bisonalveus, while those in Pentacodon and Aphronorus are lower and bunodont. Fox and Scott (2005) considered the dentition of B. toxidens consistent with that of a small predator, with the posterior premolars and molars furnishing suitable platforms, basins, cusps, and crests for

rendering the bodies of small invertebrates that had first been immobilized by salivary venom introduced by the modified upper canines; this hypothesis is further corroborated by the unusual structure of the M2. As discussed earlier in the text, the occlusal outline of the M2 of B. toxidens broadly resembles that of the M1 of many viverravid carnivorans (and see Chapter 6) in being asymmetrically triangular, with a strongly projecting parastylar area (the parastylar lobe is anterolabially projecting in viverravids, while the greatly enlarged paracone projects in Bisonalveus); the M1 parastylar lobe of viverravids forms part of the specialized P4/m1/M1 shearing apparatus that has long been considered diagnostic of carnivorans (e.g., Gingerich and Winkler, 1985; Fox and Youzwyshyn, 1994). In addition to the hypertrophied parastylar lobe, the M2 of B. toxidens and the M1 of viverravids share a number of other features that are clearly adapted to shearing against the postvallid wall of the m1. For example, the paraconule is greatly enlarged in both taxa, being raised well above the occlusal plane of the reduced metaconule, and a high, sharp preparaconular crista extends to the parastylar corner of the crown in each, providing double rank shear anteriorly (Fox, 1975); furthermore, a deep carnassial notch is incised into the preprotocrista just lingual of the paraconule in the M2 of B. toxidens and the M1 of viverravids. Additionally, the metacone on M2 of B. toxidens leans slightly posteriorly, bringing the elongated premetacrista into closer contact with the hypocristid of the corresponding m2 during occlusion, similar to, but less well developed than that on M1 of primitive carnivorans (Fox and Youzwyshyn, 1994). The m2 of B. toxidens also displays evidence of adaptations towards carnivory: for example, the trigonid is significantly expanded labiolingually, lengthening the postvallid surface available for shear by the M2, and the opposing carnassial notches on the preprotocrista and cristid obliqua would have functioned in concert during centric occlusion. Furthermore, the accessory crests and additional cusps (e.g., the mesoconid) would likely have provided additional shearing surfaces during occlusion. Although the relatively inflated teeth of B. toxidens are at first glance suggestive of a crushing function, the peculiar adaptations towards carnivory as manifested in the structure of M2 and m2 indicate that B. toxidens was probably even more predatory than previously believed.

The specimens that are referred here to Bisonalveus toxidens were first identified in a faunal listing by Fox (1990) as representing a new species of Bisonalveus, a hypothesis that was corroborated by Webb (1996) in his study on the early middle Tiffanian fossil mammal fauna from Birchwood. Fox and Scott's (2005) referral of UALVP 43114 to B. browni was overly conservative: B. toxidens is distinguished from B. browni principally in having a reduced, single-rooted p2, a smaller m3, and lower molars with shorter and deeper talonids, deeper hypoflexids, and deeper exodaenodont lobes. B. toxidens is the most abundantly represented taxon in the DW-2 local fauna, well-documenting the differences from B. browni as discussed earlier in the text.

FAMILY INCERTAE SEDIS

Genus PALEOTOMUS Van Valen, 1967

Palaeosinopa MATTHEW, 1901, p. 22 (in part).
Niphredil VAN VALEN, 1978, p. 66.

Type species.—Palaeosinopa senior Simpson, 1937b, p. 4.

Other included species.—Paleotomus radagasti (Van Valen, 1978); Paleotomus milleri Rigby, 1980; Paleotomus carbonensis Secord, 1998; Paleotomus junior Scott, Fox, and Youzwyshyn, 2002.

PALEOTOMUS SENIOR (Simpson, 1937b)

Figures 5.34.7-5.34.12

Palaeosinopa senior SIMPSON, 1937b, p. 4.
Palaeosinopa simpsoni VAN VALEN, 1967, p. 222.
Paleotomus senior VAN VALEN, 1967, p. 250.

Holotype.—AMNH 33990, right m3 (Simpson, 1937b, p. 4, fig. 1). Scarritt locality, Fort Union Formation of Montana, late Paleocene (early Tiffanian, Ti2, Plesiadapis anceps/P. rex Lineage Zone of Lofgren et al., 2004).

Material examined.—From DW-2: UALVP 47692, P4; UALVP 47693, m2.

Age and occurrence.—Middle Torrejonian (Protoselene opisthacus/Mixodectes pungens Interval Zone, To2, early Paleocene) to early middle Tiffanian (Plesiadapis rex/P. churchilli Lineage Zone, Ti3, late Paleocene) of the Western Interior of North America.

Description.—Upper dentition (Figs. 5.34.7-5.34.9): P4 (L=4.1; W=4.0): The P4 of Paleotomus senior was previously unknown. The crown is semimolariform, T-shaped in occlusal outline, and consists primarily of a tall and slightly recurved paracone and lower protocone. The labial roots are considerably compressed labiolingually, while the lingual root is stouter and faintly compressed anteroposteriorly. The parastylar corner of the crown bears a large, conical cusp that is connected to the paraconal apex by a heavy preparacrista. The stylar shelf and ectocingulum are weak anteriorly, but become better developed posteriorly. A blade-like postparacrista extends posteriorly from the apex of the conical paracone, joining a significantly smaller crest arising from the apex of a low metastylar cusp; the two crests form a sharp, V-shaped notch at their union. The metacone is only weakly developed: it appears as a poorly defined swelling on the posterior shoulder of the paracone, with only its apex distinctly separate. Conules are not developed. The crown narrows considerably lingual to the paracone, with a strong, deeply concave embayment developed between the anterior sides of the paracone and protocone. The protocone is sharp and nearly vertical, and the protoconal cristae extend labially to the parastylar and metastylar corners of the crown, respectively; a tall, blade-like accessory crest extends a short distance labially from the apex of the protocone. The anterior and posterior cingula are short and discontinuous lingually.

Lower dentition (Figs. 5.34.10-5.34.12): m2 (L=4.2; TrW=3.8; TaW=3.7): UALVP 47693 closely resembles the m2 of Paleotomus senior, described in detail by Krause and Gingerich (1983): the trigonid is considerably taller than the talonid, and is dominated by a large protoconid, slightly lower metaconid, and high, blade-like paraconid/paracristid. Weak carnassial notches incise the paracristid and protocristid.

The talonid consists of a massive and conical hypoconid, smaller hypoconulid, and low entoconid enclosing a shallow, lingually sloping basin. The ectocingulid is undeveloped, save the short, thick anterior cingulid.

Discussion.—Although Paleotomus senior is poorly represented at DW-2, the two specimens are sufficient to document the first occurrence of this rare taxon in the early middle Tiffanian of Alberta. Paleotomus senior at DW-2 may represent the youngest occurrence of the taxon. Two teeth from the coeval Brisbane locality of North Dakota (see Holtzman, 1978; Kihm and Hartman, 2004) were referred to "Palaeosinopa sp., cf. P. simpsoni" (synonymized with P. senior, see Gingerich, 1980a; Scott et al., 2002) by Holtzman (1978), but were not figured. The North Dakota specimens are closer in dimensions to homologous teeth of Paleotomus junior Scott, Fox, and Youzwyshyn, 2002 (also at DW-2, see later in this chapter) than to those of P. senior, but a more precise referral must await direct comparison of the Alberta and North Dakota specimens.

PALEOTOMUS JUNIOR Scott, Fox, and Youzwyshyn, 2002

Figures 5.34.13-5.34.21; Table 5.24

Paleotomus junior SCOTT, FOX, and YOUZWYSHYN, 2002, p. 701.

Holotype.—UALVP 28556, left m3 (Scott, Fox, and Youzwyshyn, 2002, p. 701). Cochrane 2 locality, Paskapoo Formation of Alberta, late Paleocene [earliest Tiffanian, Ti1 (Youzwyshyn, 1988; Fox, 1990), Plesiadapis praecursor/P. anceps Lineage Zone of Lofgren et al., 2004].

Material examined.—From DW-2: UALVP 47694, P4; UALVP 47695, incomplete right dentary with p3-4, m1-2, and alveoli for ?i3, c, p1-2, m3; UALVP 47696, incomplete right dentary with p2-4 and alveoli for c, p1; UALVP 47697, 47698, m1.

Age and occurrence.—Middle Torrejonian (Protoselene opisthacus/Mixodectes pungens Interval Zone, To2, early Paleocene) to early middle Tiffanian (Plesiadapis rex/P. churchilli Lineage Zone, Ti3, late Paleocene) of the Western Interior of North America.

Description.—The dentition of Paleotomus junior was described by Scott et al. (2002) and Scott (2003). Included among the specimens from DW-2 are P4 and a well-preserved, nearly complete dentary preserving alveoli for the lateral incisor, canine, and anterior premolars, all previously unknown for P. junior.

Upper dentition (Figs. 5.34.13-5.34.15): P4: The P4 of Paleotomus junior closely resembles that of P. senior described previously, differing mainly in its significantly smaller size: the crown is semimolariform, T-shaped in occlusal outline, and consists primarily of a tall and slightly recurved paracone and lower protocone. Although the parastylar corner of the crown is broken in UALVP 47694, it likely bore a small cusp, similar to P4 of P. senior. The metacone of P. junior is more poorly developed than in P. senior, and the protocone is proportionately smaller. An accessory crest is developed on the lingual side of the protocone, similar to that in P. senior.

Dentary and lower dentition (Figs. 5.34.16-5.34.21): UALVP 47695 preserves most of the horizontal ramus and anterior parts of the masseteric fossa. The ramus is long, shallow, and weakly concave ventrally, differing from the more robust mandible of Paleotomus senior (see Krause and Gingerich, 1983). The articular surface of the symphysis consists of an area of raised, finished bone that is delimited dorsally by a heavy crest that fades posteriorly towards the canine alveolus, and a weaker ventral crest that extends a short distance posteriorly along the ventral margin of the horizontal ramus. The bone intervening between the dorsal and ventral crests is rugose and perforated by numerous foramina. As with those of many other small Paleocene mammals, the symphysis in P. junior bears no evidence of having been co-ossified or even tightly sutured in life, and substantial movement between the two mandibular rami was likely possible. Two mental foramina are developed: the first is small, subovate in outline, and positioned ventral to the alveolus for p1, its aperture opening anterolaterally; the second is larger, dorsoventrally compressed, and positioned ventral to the roots of m1, its aperture opening laterally. A prominent crest marks the anterior extremity of the deep masseteric fossa.

UALVP 47695 preserves the alveolus for the lateral incisor, identified tentatively here as that for i3. The shallow alveolus is circular in cross section and leans anteriorly, suggesting that the i3 was small and slightly procumbent. Two specimens preserve the

alveoli for the lower canine and p1 (UALVP 47695, 47696). The large canine alveolus is somewhat labiolingually compressed, and its subovate aperture opens dorsally and laterally, suggesting the lower canine probably splayed laterally. The single alveolus for p1 is smaller than that for the lower canine, but substantially larger than that for the anterior root of p2; although its circular aperture opens dorsally, the orientation of the alveolus in the mandible is posteriorly and ventrally, suggesting p1 may have been procumbent and closely appressed to the posterior margin of the canine.

p2: The p2 of Paleotomus junior has not been described previously. The p2 resembles that of p3 (see Scott et al., 2002): the crown consists of a large sectorial protoconid and small, unicuspid heel. A sharp crest descends anterolingually from the apex of the protoconid, fading away as it nears the base of the crown; a paraconid is not developed. A second crest runs posteriorly from the protoconid apex, meeting a short, anteriorly directed crest from the apex of the heel; a deep notch is developed at their union. As with p3, a short crest originating at the apex of the heel cusp runs a short distance anterolingually, forming a shallow talonid basin.

Discussion.—Although Paleotomus is here considered a pantolestan of uncertain affinities, the systematic position of the genus continues to be problematic: it has at various times been considered a deltatheridian (sensu Van Valen, 1967), a pantolestid (Gingerich, 1980a-b; Krause and Gingerich, 1983), a didelphodontan cimolestan (McKenna and Bell, 1997), or a eutherian of uncertain affinities (Scott et al., 2002; Scott, 2003) (and see Scott et al., 2002 for a review of the taxonomic history of the genus). The mosaic of didelphodontan characters on the one hand [e.g., closely appressed molar paraconid/paracristid and metaconid (see Van Valen, 1967)], and pantolestid characters on the other [e.g., protoconid increases in size from m1-3, molar hypocone (see Gingerich, 1980a-b; Krause and Gingerich, 1983)] renders a more precise taxonomic referral of Paleotomus difficult, although the well-developed anterior and posterior premolar crests and blade-like premolar talonids are clearly reminiscent of those structures in the pantolestine Bessoecetor (see earlier in this chapter).

Paleotomus junior was first reported from the earliest Tiffanian Cochrane 2 locality (Scott et al., 2002), and subsequently from the late Torrejonian Who Nose? locality (Scott, 2003), both from the Paskapoo Formation of Alberta. The presence of P.

junior at DW-2 extends its stratigraphic range into the early middle Tiffanian, coeval with P. senior.

Order APATOTHERIA Scott and Jepsen, 1936
Family APATEMYIDAE Matthew, 1909
Subfamily UNUCHINIINAE Van Valen, 1966

Genus UNUCHINIA Simpson, 1937c

Apator SIMPSON, 1936, p. 16.
Unuchinia SIMPSON, 1937c, p. 78.

Type species.—Unuchinia asaphes Simpson, 1936.

Other included species.—Unuchinia dysmathes Holtzman, 1978; Unuchinia diaphanes Gunnell, 1988.

Revised diagnosis.—Primitive apatemyid differing from all other apatemyids in having two lower incisors, a two-rooted P2, a well-developed P3, and lower molars with tall, sharp cusps. Differs further from all other apatemyids except Jepsenella in having upper molars that are markedly transverse relative to their length. Differs further from Jepsenella in having upper molars that support a larger protocone and better-developed stylar lobes.

UNUCHINIA DYSMATHES Holtzman, 1978
Figures 5.35-5.37; Tables 5.25, 5.26

Unuchinia dysmathes HOLTZMAN, 1978, p. 39.

Holotype.—SMM P77.6.31, incomplete right dentary with m1-3 and alveoli for i1-2, p2-4 (Holtzman, 1978, p.39). Judson locality, Fort Union Formation of North Dakota, late Paleocene [early middle Tiffanian, Ti3 (Kihm and Hartman, 2005), Plesiadapis anceps/P. rex Lineage Zone of Lofgren et al., 2004].

Material examined.—From Joffre Bridge Roadcut lower level: UALVP 47699, M2; UALVP 47700, M3.

From DW-1: UALVP 47701, M3; UALVP 47702, i1;

From DW-2: UALVP 47818, incomplete right premaxilla with I1 and alveolus for I2, associated incomplete right maxilla with P3-4, M1-3, and alveoli for P2, and associated incomplete left maxilla with P2-3; UALVP 47703, incomplete right maxilla with M2-3 and associated P2; UALVP 47704, incomplete right maxilla with M1-3 and associated left M1 or M2; UALVP 47705, associated I1 and I2; UALVP 47706-47711 (total: 6), I1; UALVP 47712-47715 (total: 4), I2; UALVP 47716, P2; UALVP 47717, P4; UALVP 47718, M1; UALVP 47719, M3; UALVP 47819, incomplete left dentary with p2, p4, m1, and alveoli for i1-2, p3, m2-3; UALVP 47720, incomplete right dentary with p4 (talonid only), m1-3, and alveoli for p2-3; UALVP 47721, incomplete right dentary with p4, m1-2, and associated i1-2, m3; UALVP 47722, incomplete left dentary with i1-2; UALVP 47723-47725 (total: 3), i1; UALVP 47726, i2; UALVP 47727, p2; UALVP 47728, dp4; UALVP 47729-47731 (total: 3), m1; UALVP 47732, 47733, m2.

From Birchwood: UALVP 47734, 39494, I1; UALVP 39467, M1; UALVP 39495, p2.

Age and occurrence.—Early middle Tiffanian (Plesiadapis rex/P. churchilli Lineage Zone, Ti3, late Paleocene) to late middle Tiffanian (Plesiadapis churchilli/P. simonsi Lineage Zone, Ti4, late Paleocene) of the Western Interior of North America.

Description.—Skull and upper dentition (Fig. 5.35): Premaxilla: The upper dentition of Unuchinia was previously unknown; UALVP 43112 preserves most of the upper teeth in place in the premaxilla and maxilla, and although these bones were not found in articulation, they were recovered from the same block in association. A single large, semi-procumbent tooth and a large subovate alveolus are developed wholly within the premaxilla in UALVP 43112, confirming the identities of the first two enlarged teeth as incisors, rather than a single incisor and canine. The premaxilla is damaged but is essentially complete: it preserves I1 in place, as well as the large alveolus for I2; the presence of an alveolus for I3 cannot be determined from the evidence at hand, but should one have been present originally, it would have been much smaller than I1 or I2. The lateral surface of the premaxilla has largely eroded away, exposing the long root of

I1; numerous small nutritive foramina perforate what remains of the lateral side of the premaxilla, and these become more densely distributed towards the alveolar rim, suggestive of U. dysmathes having had a highly vascularized and possibly mobile muzzle in life (Radinsky and Ting, 1984). The facial process is damaged dorsally; whether or not the premaxilla made contact with the frontal, as in other apatemyids (Jepsen, 1934), must await the discovery of better preserved specimens than are presently available. The medial side of the premaxilla is essentially smooth, excepting a large anteroventral bony buttress where the contralateral premaxilla articulated. The palatal process is transversely narrow; a semicircular notch medial to the I1 alveolus represents part of the large incisive foramen, and a rugose ridge of bone medial to the I2 alveolus may represent the point of articulation with the palatal process of the maxilla. As in other apatemyids, the upper incisors of Unuchinia are considerably enlarged relative to the cheek teeth, and their coronal anatomy resembles that in upper incisors of Labidolemur Matthew and Granger, 1921 and Apatemys Marsh, 1872.

I1: The I1 of Unuchinia dysmathes is slightly procumbent, projecting anteriorly and ventrally at an angle of about 50 degrees from horizontal when the palatal surface of the premaxilla is held horizontally (approximating an "in-life" position). The crown of I1 resembles that in other apatemyids [e.g., I1 of Labidolemur (see Gingerich, 1982b) and Apatemys (Gingerich, 1982b; Gingerich and Rose, 1982)] in being robust, mediolaterally compressed, and hook-shaped in lateral view; the crown is relatively larger, and the apical hook more prominent when compared with I1 in Labidolemur and Apatemys. When the I1 is viewed in situ from palatal aspect, the crown is seen to arc medially, converging towards the contralateral I1; when viewed from anterior aspect, however, the tip splays faintly laterally, and the two I1s may not have abutted one another, an inference supported in part by the absence of a medial interdental facet. The root is elongate and strongly mediolaterally compressed. A stout, sharply bent anterocone and a small posterocone dominate the biting surface of the crown; additional cuspules are not developed. A tall, narrow crest connects the apices of the anterocone and posterocone along the lateral edge of the crown, and in some specimens appears to form a faintly serrated surface. The lateral side of the crown is virtually flat, whereas the medial side is convex and somewhat swollen, and the enamel extends farther posteriorly on the lateral

surface than on the medial surface. A short, well-defined crest extends posterodorsally from the apex of the anterocone along the medial surface of the crown, forming a flattened ledge; the enamel adjacent to this crest on the anterior surface of the crown on some specimens (e.g., UALVP 47706) is cleft, forming a short but deep longitudinal groove. When left and right I1s are held in their "in-life" positions, the apex of each splays laterally, while the anterior clefts face anteriorly; the embrasure between the two I1s forms an angle of approximately 90 degrees, with the sharp medial crests defining the apex. The enamel on I1 is thicker, and extends further dorsally, on the lateral surface than on the medial surface.

I2: UALVP 47818 preserves the alveolus for I2 directly posterior to I1; although it is slightly damaged along the posterior margin, the aperture was clearly subovate in outline and separated from I1 by a short diastema; the orientation of the alveolus in the premaxilla suggests the crown of I2 was slightly procumbent. The coronal anatomy of I2 closely resembles that of Labidolemur (see, e.g., Gingerich, 1982b) and, to a lesser degree, that of Apatemys and Heterohyus Gervais, 1848 (see, e.g., Koenigswald et al., 2005a-b). The short root is stout and subovate near the crown, but becomes increasingly mediolaterally compressed posteriorly. The crown of I2 is peculiar: a large anterocone dominates the biting surface, bending ventrally at the crown-root junction, and appearing strongly hook-like in lateral view. A posterocone, considerably smaller than that on I1, is developed posteriorly and slightly mediad of the anterocone; its apex is connected to that of the anterocone by a short, sharp crest. As with I1, the enamel on I2 is thicker, and extends further dorsally, on the lateral surface than on the medial surface; the lateral face is virtually flat, while the medial face is slightly concave. The anterior surface of the I2 crown is unusual: its outline is that of a dorsoventrally elongate scalene triangle, the boundaries of which are formed by sharp crests. The two long arms of the triangle are comprised of medial and lateral crests arising from the apex of the anterocone: the medial crest is the shorter of the two, running dorsally to a small and slightly compressed medial accessory cusp, while the lateral crest is longer, and extends dorsally and anteriorly to a conspicuous lateral accessory cusp. A faintly cuspate crest extends between the two accessory cusps, forming the third and shortest arm of the triangle. The anterior surface of the crown defined by the crests is shallowly depressed and basin-like, and the enamel

is conspicuously thinner in the basin than on the medial or lateral surface of the crown. The orientation of I2 in the premaxilla is of some interest, particularly as regards incisor function: extrapolating the orientation of I2 from its alveolus suggests the tooth was moderately procumbent, with its anterior parts projecting over the short diastema intervening between I1 and I2. The anterocone is more strongly "hooked" than that of I1 and faces more ventrally, with the apices of the I1 and I2 anterocone probably in the same occlusal plane; when aligned in the premaxilla, the anterocone, posterocone, and lateral crest of I1 are in-line with the lateral accessory cusp, anterocone, posterocone, and lateral crests of I2, essentially forming a near-continuous lateral blade. Incisor function is elaborated further below.

Upper premolars: Nothing can be said of the morphology of the teeth intervening between I2 and P2 in Unuchinia dysmathes, should any have been present. The upper antemolar dentition of Paleocene apatemyids remains poorly known (see e.g., West, 1973), with well-preserved comparative material extremely limited and, where known, restricted to derived forms, most notably the North American Sinclairella Jepsen, 1934 and Apatemys, and the European Heterohyus (e.g., Jepsen, 1934; West, 1973; Bown and Schankler, 1982; Gingerich, 1982b; Gingerich and Rose, 1982; Koenigswald, 1987, 1990; Kalthoff et al., 2004; Koenigswald et al, 2005a-b). UALVP 47818 documents one of the most nearly complete upper dentitions of any Paleocene apatemyid so far discovered; from the evidence at hand, it appears the likeliest dental formula for the upper dentition of U. dysmathes is I1-2, P2-4, M1-3.

P2: The P2 of Unuchinia dysmathes is documented in articulation with the left maxilla, and by its alveoli in the right maxilla in UALVP 4781, and by two isolated teeth, one of which was in association with M1-3. The tooth resembles that in the apatemyine Labidolemur kayi Simpson, 1929 (see Gingerich and Rose, 1982) in being enlarged relative to P3, blade-like, and faintly recurved. The two roots of P2 are significantly curved, extending posteriorly and dorsally into the maxilla; both roots are subovate in cross section, with the posterior root slightly larger than the anterior root. The crown is simply constructed, consisting of a tall, labiolingually compressed paracone and a small, variably developed metastylar cuspule. The paracone is slightly recurved and lingually leaning, broadly resembling the "hooked" anterocone on I1 and I2 in lateral profile; its

anterior surface is strikingly similar to that of I2, with a slightly depressed triangular face bordered by faintly elevated crests; although distinct accessory cuspules are not present on the anterior face of the crown, vague swellings of the enamel suggest their incipient development. A thick crest extends posteriorly from the apex of the paracone to the base of the crown, where a small metastylar cuspule can sometimes be present. The posterior alveolus of P2 is separated from the succeeding P3 by a short diastema in the right maxilla in UALVP 47818, but the tooth is closely appressed to P3 on the associated maxillary fragment from the left side.

P3: The P3 of Unuchinia dysmathes is two-rooted and premolariform, with a well-developed paracone, small parastylar and metastylar cuspules, and a weak protoconal swelling. The posterior root is transversely wide, nearly twice the width of the anterior root, and shallowly fissured on its posterior surface. The paracone is tall, somewhat labiolingually compressed, and nearly vertical, in contrast to the posteriorly leaning P2. An ill-defined crest extends anteriorly from the paraconal apex to a low parastylar cusp; a better-developed crest sweeps posterolingually to the metastylar corner of the crown, where it can join a low metastylar cuspule. An ectocingulum is not present. The lingual margin of the crown is marked by a weak swelling developed over the posterior root at the confluence of the short anterior and posterior cingula.

P4: P4 is significantly larger than P3, and the crown bears a well-developed protocone that is supported by a lingual root. The crown is triangular in occlusal outline, and consists primarily of a tall paracone and a lower protocone. A weak preparacrista connects the paracone to a small parastylar cuspule, while the high, labially concave postparacrista sweeps posterolingually to the metastylar corner, joining with one or two tiny metastylar cuspules; a metacone is not present, nor is there any swelling on the postparacrista that would suggest its incipient development. The ectocingulum is conspicuous posteriorly, arising from the small metastylar cuspules, but weakens considerably towards the parastylar corner; a small cuspule can occur on the ectocingulum near mid-crown length. Conules and their associated crests are undeveloped, and the anterior and posterior cingula run uninterrupted to the parastylar and metastylar corners of the crown, respectively. The protocone is broad at its base, but

quickly narrows towards the anteriorly positioned apex; the anterior and posterior cingula extend to the protoconal apex. A hypocone is not present.

Upper molars: M1: The M1 crown of Unuchinia dysmathes is subtriangular in occlusal outline, with a well-developed paracone, metacone, and protocone enclosing a deep trigon basin. The lingual half of the crown is twisted such that the protocone leans strongly anteriorly, resembling M1s of some pantolestine pantolestids (e.g., Bessoecetor), leptictids (e.g., Prodiacodon Matthew, 1929), and palaeoryctids (e.g., Palaeoryctes Matthew, 1913). The paracone is the tallest cusp, with its apex just slightly higher than that of the protocone and metacone; both paracone and metacone are conical, with sharp apices, and the two are connected by a deep and sharply notched centrocrista. The preparacrista is short but high, running as a raised blade to the ectocingulum and anteriorly projecting parastylar lobe; a deep, transversely oriented facet is often developed in the embrasure between the parastyle and paracone from occlusion with the corresponding lower molar protoconid. The postmetacrista is significantly longer than the preparacrista, sweeping posterolabially to the prominent, labially projecting metastylar lobe. An ectoflexus is not developed. The ectocingulum is conspicuous anteriorly but quickly disappears towards the metastylar lobe, and may bear numerous tiny cuspules. The crown narrows considerably lingual to the paracone and metacone; conules and their associated crests are wholly undeveloped, and the anterior and posterior margins of the trigon basin are defined solely by the protoconal cristae. The protocone is tall and sharp, and leans anteriorly such that its apex is lingually opposite the paracone. The protoconal cristae extend labially from the apex, with the preprotoconal crista running uninterrupted to the parastylar lobe, while the lower postprotoconal crista fades away as it nears the base of the metacone. The low, conical hypocone is developed on the posteriorly bulging posterior cingulum; the cusp is nearly vertical in its orientation. A weak anterior cingulum is present low on the anterior side of the protocone.

M2: The crown of M2 resembles that of M1, but is considerably more transverse. The parastylar and metastylar lobes are both strongly developed, extending far labially and forming a deep ectoflexus between them: the parastylar lobe is long and finger-like, projecting farther labially than the metastylar lobe on M1, although its apex does not "hook" over the metastylar lobe on M1; the metastylar lobe on M2 is narrower than the

parastylar lobe, but is anteroposteriorly longer and more smoothly rounded. The faintly cuspidate ectocingulum is strong anteriorly, but weakens considerably posteriorly, becoming increasingly diffuse as it nears the metastylar corner. The anteriorly leaning paracone is taller, more nearly conical, and is positioned further labially than the metacone; a deeply notched centrocrista connects the paraconal apex with that of the more labiolingually-compressed metacone. The preparacrista is long and elevated, crossing the stylar shelf obliquely towards the apex of the parastylar lobe, where it can join with a small cuspule; the postmetacrista resembles that on M1, sweeping posterolabially to the metastylar corner of the crown. As with M1, conules and their associated crests are not developed on M2, although a faint swelling of the enamel on the postprotoconal crista near the base of the metacone may represent an incipient metaconule. The protocone is similar to that on M1: it is tall, with an acute apex, and leans anteriorly; the protoconal cristae resemble those on M1, with the preprotoconal crista running labially to the parastyle and the postprotoconal crista fading away near the metacone. The hypoconal shelf on M2 is larger and bulges further lingually than on M1, and the hypocone is relatively taller; the anterior and posterior cingula are discontinuous lingually.

M3: Although the crown of M3 of Unuchinia dysmathes is anteroposteriorly short, it is nearly as wide as that of M2. The crown is asymmetrically triangular in occlusal outline, with straight anterior and weakly concave posterior margins. The most notable coronal feature of M3 is the long, finger-like parastylar lobe that projects anteriorly and labially, its apex sometimes extending even farther labially than the metastylar lobe of M2; by contrast, the metastylar lobe is wholly undeveloped. As on M1 and M2, the ectocingulum on M3 is faintly cuspidate and strong anteriorly, but disappears completely posterior to the paracone. The paracone is large and anteriorly leaning, and a well-developed, blade-like preparacrista extends from its apex to the parastylar corner, joining the ectocingulum and anterior cingulum. The metacone is stout, conical, and projects slightly posteriorly, and its apex is connected to that of the paracone by a short centrocrista. The conules are absent. The lingual half of the crown is twisted like that on M1 and M2, but the protocone leans much more strongly anteriorly.

The hypocone is not developed, instead being replaced by a shelf-like posterior cingulum; the anterior cingulum is weak or absent.

Dentary and lower dentition (Figs. 5.36, 5.37): The dentary of Unuchinia dysmathes is poorly preserved among the specimens at hand, with only UALVP 47819 preserving significant parts of the horizontal ramus and coronoid process; the condyle and angular process are not preserved in the Alberta sample, although these structures are known from the type specimen from North Dakota (Holtzman, 1978). The jaw is unusually deep relative to the size of the teeth, a feature that has been previously noted for jaws of Unuchinia (see Simpson, 1936; Holtzman, 1978). The anteroventral part of the mandibular fossa extends slightly posterior to the level of m3, and a large mental foramen opens anterolaterally below the anterior root of p4; the foramen is not recessed in a labial fossa like that on jaws of Labidolemur and Apatemys (see McKenna, 1963; Gingerich, 1982b; Gingerich and Rose, 1982).

Lower incisors: The lower incisors of Unuchinia dysmathes are known from a number of isolated specimens, as well as from an anterior jaw fragment containing the i1-2 in articulation, the first discovered for Unuchinia. The lower incisors are significantly enlarged relative to the cheek teeth, a characteristic of apatemyids generally (McKenna, 1963); Unuchinia is more primitive than the apatemyines in retaining the second lower incisor. The two incisors are procumbent and closely appressed to one another, with the crown of i2 fitting snugly into a slight depression on the posterolateral side of i1; the procumbent and blade-like p2 would likely be appressed to the lateral surface of i2 in life, and the three anterior teeth are arranged en echelon.

i1: The i1, previously unknown for Unuchinia, resembles that in other apatemyids: the tooth is long, with a dorsally recurved crown and straight, bilaterally compressed root. The root is faintly convex laterally, but is flat medially. A long, shallow fossa extends along the medial side of the root, narrowing as it approaches the crown; the fossa divides the enamel into dorsal and ventral parts before fading away farther anteriorly. The occlusal surface is strongly concave, with the tip bending dorsally at about midcrown length. The lateral extremity of the biting surface is delimited by a heavy crest that runs the length of the crown, and although the crest is weakly ridged, distinct serrations like those on i1 of Jepsenella Simpson, 1940 and Labidolemur are not

developed (McKenna, 1963; West, 1973). The lateral crest fades away as it follows the contours of the crown posteriorly to a raised area of enamel, but a margoconid is not developed there. The medial surface of the crown bears a long, flat interdental facet that begins at the base and extends anteriorly for approximately two-thirds of its length, at which point the crown curves gently laterally, diverging slightly from the midsagittal plane and forming an embrasure between the opposing i1s. The medial extent of the biting surface is delimited by a short but conspicuous crest that extends from the apex of the crown posteriorly to the point where the crown begins to splay laterally. Enamel is not present posterolaterally where the crown of i2 abutted that of i1. The enamel is significantly thicker on the ventral and lateral surfaces of the crown.

i2: The i2 of Unuchinia was known previously only for Unuchinia diaphanes. The i2 broadly resembles i1: the tooth is long and mediolaterally compressed, with a hook-like, dorsally concave crown and transversely narrow root. UALVP 47722 and 47721 demonstrate that the crown of i2 is closely appressed to i1 in life, with the flat medial side abutting the posterolateral surface of i1. A weakly excavated fossa resembling that on i1 runs the length of the medial side of the root on i2, and continues a short distance onto the crown before becoming weaker and eventually fading out towards the anterior parts of the interdental facet; the fossa divides the enamel on the medial side of the crown into shallow dorsal and ventral strips that eventually coalesce and form of the anteriormost parts of the interdental facet. The concave occlusal surface of the crown is bounded laterally by a raised crest that extends from base to apex; a prominent cusp is developed on this crest slightly anterior of the base of the crown. As with i1, the tip of i2 diverges laterally at the level of the interdental facet, but the lateral splay is even more severely developed than on i1; a short crest runs posteromedially from the tip of the crown to the level of the interdental facet. The enamel on the lateral side of i2 is even more restricted in its distribution than on i1, extending only a short distance posterior to the level of the lateral cusp.

Lower premolars: p2: The p2 of Unuchinia dysmathes was previously unknown; it is represented in the present sample by four teeth, one of which is in articulation with the dentary. The p2 bears a short and faintly compressed root that is stout and moderately bulbous towards the crown, but tapers quickly towards its base, and numerous

longitudinal furrows are developed just below the base of the crown. The crown of p2 is large and blade-like, bilaterally compressed and strongly procumbent, with the more anterior parts of the crown resting on the dentary. The enamel on p2 is unevenly distributed on the crown, extending significantly farther ventrally on the labial side. The tall, sharp protoconid is positioned far anteriorly and slightly lingual to the midline; a sharp, steep paracristid curves anterolingually from the protoconid apex to the base of the crown, and joins with a poorly differentiated lingual cingulid. A robust cusp occurs low on the posterolingual margin of the crown; a long, high crest originating at the apex of the cusp runs up the posterolabial side of the protoconid, forming a sharp edge.

p3: Although the single-rooted p3 of Unuchinia dysmathes has yet to be discovered, it is represented by its alveolus in two specimens in the present sample (UALVP 47720 and 47819). The alveolus is considerably smaller than that for p2, and it is shifted labially, as if being "squeezed" labiad between the enlarged p2 and p4. The ovate aperture is oriented obliquely anterolabially-posteromedially across the dentary; the alveolus projects only a short distance posteroventrally and labially into the dentary, and the crown of p3 probably leaned labially.

p4: The p4 of Unuchinia dysmathes is two-rooted, differing from the more derived, single-rooted p4 in U. asaphes. The crown is premolariform and consists of a tall, sharp protoconid and a well-developed, basined heel. The labial side of the protoconid is virtually flat, while its lingual side is convex. A sharp paracristid descends steeply from the protoconid apex to the anterolingual margin of the crown where it joins a short but conspicuous lingual cingulid; a low shelf is developed at the junction of the paracristid and lingual cingulid. The talonid consists of an enlarged hypoconid and a poorly differentiated entoconid; a low postcristid connects the two talonid cusps, and a weak entocristid extends from the entoconid to the postvallid wall, enclosing a shallow talonid basin. The cristid obliqua joins a sharp crest that extends posteriorly from the protoconid apex, and a shallow notch is formed at their union. The p4 crown leans lingually at an angle of approximately 20 degrees from vertical.

Lower molars (Figs. 5.36.19-5.36.21, 5.37): m1: The lower molar crowns of Unuchinia dysmathes lean lingually, the trigonids are elevated relative to the talonids, the paraconids are blade-like and project anteriorly, and the talonid basins are shallow and

slope lingually. The m1 trigonid is equilaterally triangular in occlusal outline, with the metaconid slightly posterior to the level of the protoconid, and the paraconid leaning anteriorly; the cusps enclose a shallow basin. The metaconid is the largest trigonid cusp on m1, although its apex is slightly lower than that of the protoconid. The protoconid and metaconid are inflated at their bases, but become sharper apically; the two cusps are connected to one another by a deeply notched protocristid. The paraconid is weakly cuspate and not fully incorporated into the robust paracristid, and is more labial than that on m2 and m3; the paracristid extends steeply anteriorly from the protoconid apex before bending sharply lingually to join the paraconid. A weak crest running posteriorly from the paraconid towards the base of the metaconid occurs on some specimens. Heavy wear can be developed on the paracristid, prevallid surface of the protoconid, and especially on the metaconid arm of the protocristid, where a long, strip-like facet is usually present, extending from the metaconid apex obliquely ventrolabially to the hypoflexid. The hypoconid is the largest and tallest talonid cusp, followed by a much smaller hypoconulid and entoconid. The hypoconulid is shifted slightly labial of the anteroposterior midline, imparting a "twisted" appearance to the talonid that is reminiscent of, but not as exaggerated as that in palaeoryctids. The postcristid, hypocristid, and entocristid are all low but sharply defined, and together enclose a wide and shallow basin; the low cristid obliqua joins the postvallid wall below or slightly labial to the level of the protocristid notch, and a weak mesoconid is present in some specimens. The anterior cingulid is robust and shelf-like, but neither an ectocingulid nor posterior cingulid is developed.

m2: The m2 closely resembles m1, differing mainly in its larger size and in having a more anteroposteriorly compressed trigonid (the occlusal outline of the trigonid forms an isosceles, rather than equilateral triangle). The paraconid is blade-like and projects even more strongly anteriorly than on m1, and the paracristid is lower and longer. The talonid is broad, with a large hypoconid and much weaker hypoconulid and entoconid; a weak mesoconid is sometimes developed on the short cristid obliqua.

m3: The m3 is the largest tooth in the molar series, with the crown longer and the trigonid slightly wider than that of m2. The trigonid is even more anteroposteriorly compressed than on m2, and the paraconid is slightly more erect and labially positioned. A low and widely notched paracristid sweeps gently from the protoconid apex

anterolingually to the cuspate paraconid; although the metaconid is the largest trigonid cusp, the protoconid is taller and more massive than on m2. The talonid of m3 is long and narrow and, like those of m1 and m2, is skewed slightly labially. The long hypoconulid is the largest and tallest talonid cusp, projecting posterodorsally in a finger-like manner; the hypoconid is lower and more nearly conical, whereas the entoconid is barely developed. A long postcristid+entocristid connects the hypoconulid with the postvallid wall. The cristid obliqua is low, joining the postvallid wall medial of the protocristid notch, and can bear a conspicuous mesoconid. As with m1 and m2, the hypoflexid is deep and usually heavily worn; additional wear is developed on the pre- and postvallid surfaces, and in the embrasure between the hypoconid and hypoconulid.

Discussion.—Apatotherians are an unusual group of extinct, probably insectivorous mammals known primarily from the late Paleocene through Oligocene of North America and Europe (see, e.g., Gervais, 1859; Marsh, 1872; Filhol, 1890; Matthew, 1921; Matthew and Granger, 1921; Jepsen, 1934; Simpson, 1940; Szalay, 1968; West, 1973; Sigé, 1975; Russell et al., 1979; Gingerich, 1982b; Gingerich and Rose, 1982; Koenigswald, 1987, 1990; Koenigswald et al., 2005a-b, and see McKenna, 1963 for a thorough historical review). Apatemyids are characterized primarily by their enlarged upper and lower incisors, their peculiar hatchet-shaped lower second premolars, and, where known, postcranial adaptations indicative of arboreality, including greatly elongate digits that are believed to have been used in extracting wood-boring insect larvae from trees (see, e.g., Koenigswald, 1987, 1990; Koenigswald and Schierning, 1987; Bloch, 2001; Bloch and Boyer, 2001). Although the first described North American apatemyids were classified as a kind of insectivoran (sensu lato) (Marsh, 1872), Matthew's (1909) provisional classification of Apatemys with the now-recognized microsyopid Uintasorex Matthew, 1909 and the omomyid Trogolemur Matthew, 1909 in the Apatemyidae (although still in the Insectivora) began what is now generally considered an erroneous association of apatemyids (and other small, primate-like mammals with enlarged, procumbent incisors) with primate or near-primate taxa.

Among the different primate groups at one time considered closely related to the Apatemyidae, the Plesiadapiformes, a group of archaic primates characterized by, among other features, their enlarged and complex incisors, figured prominently in Matthew's

classifications (see, e.g., Matthew, 1915, 1918; Matthew and Granger, 1921; Simpson, 1929; Jepsen, 1930). Despite Jepsen (1934) having distinguished the Apatemyidae from the Plesiadapidae in his comprehensive review of the two groups, and having provisionally returned the apatemyids to the Insectivora, most authors subsequently followed Simpson's (1940) opinion in considering the group a kind of primate of uncertain affinity (e.g., Scott and Jepsen, 1936; Romer, 1945; Camp et al., 1949). McKenna (1963) reviewed the Paleocene apatemyids and referred the family Apatemyidae to the Insectivora, while Szalay (1968) thought them most closely related to the Palaeoryctidae. Although the most recent comprehensive classification of mammals place Apatemyidae in the Cimolesta, a heterogeneous assemblage of eutherians believed to be related to carnivorans and creodonts (McKenna and Bell, 1997), a consensus on the affinities of apatemyids has yet to be achieved (see, e.g., Bloch, 2001; Bloch and Boyer, 2001; Koenigswald et al., 2005a-b).

While the higher-level affinities of apatemyids remain doubtful, the interrelationships of the various apatemyid genera seem more certain. Apatotheria as currently conceived contains the monotypic family Apatemyidae that contains two subfamilies, the Apatemyinae and the Unuchiniinae. Apatemyinae include the best known and most advanced of the apatemyids: the North American genera Jepsenella, Labidolemur, and Sinclairella; the European Heterohyus and Eochiromys Teilhard de Chardin, 1927; and the Euramerican genus Apatemys. In contrast, the Unuchiniinae are poorly known, being represented by a single genus, Unuchinia, from the Paleocene of North America (the holotype of Unuchinia asaphes, AMNH 33894, was described by Simpson in 1936 as "Apator" asaphes; the generic name was later found to be preoccupied and was emended in Simpson, 1937c); Simpson (1936, 1937c) did not suspect the apatemyid affinities of Unuchinia, and he referred the genus to the Insectivora with question. In his review of the Paleocene Apatemyidae, McKenna (1963) tentatively considered Unuchinia a kind of apatemyid, an opinion echoed by Van Valen (1967), Holtzman (1978), Gingerich (1982b), and Gunnell (1988). The discovery of U. dysmathes and U. diaphanes provided corroborating evidence for the apatemyid affinities of Unuchinia, but until the present study, no upper teeth referable to any species of

Unuchinia were known. The new specimens from Alberta confirm McKenna's (1963) suspicions of the apatemyid affinities of Unuchinia.

The present sample will be discussed at greater length elsewhere (Scott, in prep.); as such, only a brief discussion is provided here. The peculiar coronal anatomy of the I1 and I2 of Unuchinia is known only among apatemyids: these teeth closely resemble those of Labidolemur (see, e.g., Gingerich and Rose, 1982), Apatemys (see, e.g., Koenigswald et al., 2005b), and Heterohyus (see, e.g., Koenigswald and Schierning, 1987), differing mainly in being considerably larger relative to the cheek teeth, particularly I1, which in Unuchinia is longer and shallower. The cheek teeth of U. dysmathes are clearly more primitive than those of Labidolemur and Apatemys among North American apatemyids differing from teeth of these taxa as follows:

1) The P2 of Unuchinia is enlarged relative to the other premolars, as in other apatemyids where these teeth are known; the tooth differs from that of Labidolemur and Apatemys in being double-rooted [the P2 in other apatemyids bears a single, stout root, although grooves are developed, at least labially (e.g., Apatemys, see Koenigswald et al., 2005b, pl. 3B), suggesting a fusion of two previously separate roots]. Additionally, the P2 of Unuchinia more closely resembles the I2 in coronal morphology than does the P2 in Labidolemur and Apatemys;

2) The P3 is well-developed in Unuchinia, whereas this tooth is absent in other apatemyids;

3) The upper molars of Unuchinia are considerably more transverse relative to their length, giving the crowns a more nearly rectangular, rather than square, outline;

4) The upper molar stylar lobes are better developed in Unuchinia, particularly the parastylar lobe of M2, which is greatly elongate and finger-like;

5) As discussed in Holtzman (1978) and Gunnell (1988), Unuchinia differs from other apatemyids in possessing two lower incisors; the i1 of Unuchinia resembles that in other apatemyids (see, e.g., West, 1973; Gingerich and Rose, 1982; Koenigswald et al., 2005b) in being long, mediolaterally compressed, and bearing a hook-like apex, but differs in being relatively shorter and stouter; the i1 of many apatemyids often develop a series of serrations or incipient lobes, similar to extant soricids (e.g., Jepsen, 1934; McKenna, 1963; West, 1973), but these are not developed on the i1 of Unuchinia;

6) The enlarged, blade-like p2 of Unuchinia is less procumbent than that in Labidolemur or Apatemys, and the crown does not strongly overlap the posterior side of i2; in these regards, the p2 of Unuchinia resembles that of Jepsenella (see West, 1973);
7) Although p3 is yet to be discovered in Unuchinia, its alveolus indicates that the tooth was smaller than either p2 or p4 (but still a large tooth when compared to the vestigial p3 of Labidolemur kayi Matthew and Granger, 1921 and L. serus Gingerich, 1982b), and displaced towards the labial margin of the jaw; most post-Labidolemur apatemyids lack p3
8) While the p4 of Unuchinia can be two-rooted (U. dysmathes and U. diaphanes) or single-rooted (U. asaphes), it is always a large tooth, differing from the reduced and single-rooted p4 in other apatemyids (excluding Jepsenella);
9) As discussed by Simpson (1936) and Holtzman (1978), the lower molars of Unuchinia differ significantly from those of other apatemyids; the present sample offers little in the way of additional information to that presented in those studies.
Three nominal species of Unuchinia are known, spanning the late Torrejonian (To3) through the late Tiffanian (Ti5) (see Lofgren et al., 2004). Unuchinia dysmathes differs from U. diaphanes in being considerably larger, but the difference in size between U. dysmathes and U. asaphes is slight (mean length m1, U. dysmathes from Alberta=2.45 versus length m1, U. asaphes from Montana=2.3; mean length m2, U. dysmathes from Alberta=2.48 versus length m2, U. asaphes from Montana=2.5). Although the p4 of U. asaphes bears a single root [a point of difference with U. dysmathes discussed by Holtzman (1978) in his description of the topotypic material from the early middle Paleocene Judson and Brisbane localities of North Dakota], the significance of this is weakened by the small samples for both species. The teeth of U. asaphes and U. dysmathes are nearly identical in size and coronal anatomy, suggesting the possibility that U. asaphes and U. dysmathes may be synonymous, with the p4 root number being intraspecifically variable; more definitive conclusions in these regards must clearly await the discovery of better preserved specimens than are currently available.

The earliest undoubted record of Unuchinia is the late Torrejonian (To3) Rock Bench Quarry of Wyoming (Gunnell, 1988), but isolated upper first incisors that,

although much smaller, closely resemble the I1 of U. dysmathes are known from the middle Torrejonian Who Nose? locality of southern Alberta (Scott, 2003; pers. obs.).

Family PALAEORYCTIDAE Winge, 1917

Subfamily DIDELPHODONTINAE Matthew, in Matthew and Granger, 1918

Genus GELASTOPS Simpson, 1935a

Gelastops SIMPSON, 1935, p. 227.

Type species.—Gelastops parcus Simpson, 1935.

Other included species.—Gelastops joni Rigby, 1980.

GELASTOPS sp., cf. G. PARCUS

Figures 5.38.1-5.38.3

Material examined.—From DW-2: UALVP 47800, M1.

Description.—M1 (L=2.6; W=3.2): The crown of M1 is triangular in occlusal outline, with the labial margin much longer than the lingual margin. The crown supports a large, anteriorly leaning paracone, a smaller and lower metacone, and an anteroposteriorly compressed, anteriorly leaning protocone. A weak ectoflexus occurs midway along the length of the length of the labial margin of the crown, and the parastylar and metastylar lobes are well differentiated, with the metastylar lobe projecting slightly farther labially. The parastylar lobe is drawn out as a hook-like process and supports a tiny parastylar cusp. The paracone is somewhat labiolingually compressed, and a weak preparacrista runs anterolabially from its apex to a weak stylocone; the stylocone is slightly smaller than the parastylar cusp, and separated from it by a notch. The metacone is joined with the paracone for about one half its height, but the apices of the two cusps are widely separated above this level; the cusps are connected to each other by a sharp, blade-like centrocrista that is deeply notched. The postmetacrista is somewhat elevated and blade-like as it crosses the stylar shelf towards the posterolabial

corner of the crown. The ectocingulum is low but robust, and it supports a number of small cuspules. Both a paraconule and a metaconule are present on M1, but they are weakly developed and closely appressed to the protocone; the paraconule is larger and slightly more labial than the metaconule, and both conules lack internal wings. The protocone is anteroposteriorly compressed, sharp, and leans anteriorly. The protoconal cristae extend labially to the conules: the preparaconular crista joins the preparaconular crista, and then continues as a robust paracingulum to the parastylar lobe; similarly, the postprotoconal crista runs to the metaconule, joins the postmetaconular crista, and then continues as the metacingulum, but fades away as it approaches the metastylar blade. A weakly developed anterior cingulum is present, but the posterior cingulum is undeveloped.

Discussion.—UALVP 47800 most closely resembles M1 of various didelphodontine palaeoryctids, but particularly that of Gelastops. Like that of Gelastops, the M1 crown in UALVP 47800 supports a paracone and metacone that are connate for about half of their height, an anteroposteriorly compressed and sharp protocone, and weakly developed conules, features that are also known in a number of other didelphodontine taxa and primitive eutherians generally (Archibald and Averianov, 2006). The upper dentition of Gelastops is not well known, but the referred M1 is smaller than USNM 9554 (M2), the only upper molar known for G. parcus Simpson, 1935a, and is closer in size to UALVP 44193, an isolated M2 from the middle Torrejonian (To2) Who Nose? locality of southern Alberta (Scott, 2003). Scott (2003) referred UALVP 44193 with question to the Cimolestidae (=Didelphodontinae of this study), but noted a number of similarities between that specimen and USNM 9554. Other specimens of a Gelastops-like didelphodontine are known from the ?late Torrejonian (To3) Nordic Ski and earliest Tiffanian (Ti1) Cochrane 2 localities of southern Alberta (Youzwyshyn 1988, and pers. obs.). A decision as to whether or not these teeth can be referred to Gelastops or some other didelphodontine taxon must await discovery of more nearly complete specimens, including those of the genotype G. parcus.

?PALAEORYCTIDAE

Genus PARARYCTES Van Valen, 1966

Pararyctes VAN VALEN, 1966, p. 57.

Type species.—Pararyctes pattersoni Van Valen, 1966.

Other included species.—Pararyctes rutherfordi Scott, Fox, and Youzwyshyn, 2002; Pararyctes colossa new species.

PARARYCTES PATTERSONI Van Valen, 1966

Figures 5.38.4-5.38.8, 5.39, 5.40, 5.41.1-5.41.6; Tables 5.27, 5.28

Pararyctes pattersoni VAN VALEN, 1966, p. 57.

Holotype.—UW 2002, upper left M1. Saddle locality, Fort Union Formation of Wyoming, late Paleocene (early Tiffanian, Ti2, Plesiadapis anceps/P. rex Lineage Zone of Lofgren et al., 2004).

Material examined.—From Joffre Bridge Road Cut lower level: UALVP 47735, M1; UALVP 47736, incomplete right dentary with m1-2 and alveoli for p4; UALVP 47737, m1 or m2.

From DW-1: UALVP 47738, m1 or m2;

From DW-2: UALVP 40952, incomplete skull having right lateral incisor, C, P1-4, M1-3, left P1, P3-4, M1-3, and alveoli for left medial and lateral incisors, C, P2, with associated incomplete left dentary with medial incisor root, lateral incisor (base of crown), c, p1-4, m1-3, and associated postcranial bones; UALVP 47739, incomplete associated left and right maxillae with right P4, M1-3, left P4, M1-2, and associated incomplete right dentary with c, p4, m1-3, and alveoli for lateral incisor, p1-3; UALVP 47740, incomplete left maxilla with P3-4, M1-3, and associated incomplete right dentary with p4, m2-3, and alveoli for m1, and associated isolated lower lateral incisor; UALVP 47741, incomplete left maxilla with posterior root of upper canine, P1, P3-4, M1-3, and alveoli for anterior root of upper canine, P2; UALVP 47742, incomplete left maxilla with P3-4, M1-3; UALVP 40564, incomplete right maxilla with P3-4, M1-2 (M2 damaged);

UALVP 47743, incomplete left maxilla with P4, M1-2; UALVP 47744, incomplete right maxilla with P3-4, M1, and alveoli for P1-2, M3; UALVP 47745, incomplete left maxilla with M1-3; UALVP 47746, 47747, incomplete left maxilla with M1-2; UALVP 47748, incomplete right maxilla with M2-3; UALVP 47749, incomplete right maxilla with P4, M1; UALVP 47749-47751 (total: 3), M1; UALVP 47750, M2; UALVP 47751, incomplete M2; UALVP 47752, 47753, M1 or M2 UALVP 47754, M3; UALVP 47755, incomplete right dentary with lower medial and lateral incisors (roots), c, p1-4, m1-3; UALVP 47756, incomplete right dentary with lower lateral incisor, c, p1-4, m1 (talonid only), m2-3, and associated lower medial incisor; UALVP 47757, incomplete right dentary with lower medial incisor (damaged), lower lateral incisor, c, p1-3, m1-3, and alveoli for p4; UALVP 47758, incomplete left dentary with c, p1, p4, m1, m2-3 (both damaged), and alveoli for p2-3; UALVP 47759, incomplete right dentary with lower lateral incisor, c, p4, m1-3, and alveoli for lower medial incisor, p1-3; UALVP 47760, incomplete right dentary with c, p4, m1-3, and alveoli for medial and lateral incisors, p1-3; UALVP 47761, incomplete right dentary with p3-4, m1-3, and alveoli for p1-2; UALVP 47762, 47763, incomplete left dentary with p4, m1-3, and alveoli for c, p1-3; UALVP 47764, incomplete left dentary with p4, m1-3, and alveoli for lateral incisor, c, p1-3; UALVP 47765, incomplete left dentary with p4, m1-3, and alveoli for p2-3; UALVP 47766, 47767, 47768, incomplete right dentary with p4, m1-3; UALVP 47769, incomplete right dentary with dp3-4, m1, and alveoli for m2-3; UALVP 47770, incomplete right dentary with m1-3 and alveoli for p3-4; UALVP 47771, incomplete left dentary with c, p4, m1, and alveoli for p1-3, m2-3; UALVP 47772, incomplete right dentary with p4, m1-2, and alveoli for m3; UALVP 47773, incomplete left dentary with m1-3 and alveoli for c, p1-4; UALVP 47774, incomplete right dentary with m1 talonid, m2-3; UALVP 47775, 47776, incomplete left dentary with m2-3; UALVP 47777, incomplete right dentary with m2-3 and alveoli for p4, m1; UALVP 47778, incomplete left dentary with c, p2, p4, and alveoli for p1, p3; UALVP 47779, incomplete right dentary with p3-4; UALVP 47780, incomplete left dentary with p3-4; UALVP 47781, incomplete right dentary with m1, m3, and alveoli for p4, m2; UALVP 47782, incomplete left dentary with p4 and alveoli for p2-3, m1-3; UALVP 47783, incomplete right dentary with m2; UALVP 47784, incomplete left dentary with m2; UALVP 47785,

incomplete left dentary with m3; UALVP 47786, incomplete right dentary with m3; UALVP 47787, incomplete right dentary with m2 talonid and m3; UALVP 47788, p3; UALVP 47789, p4; UALVP 47790, associated isolated p2, m1, and m2; UALVP 47791, 47792, m1; UALVP 47793-47796 (total: 4), m2 UALVP 47797, 47798, m1 or m2; UALVP 47799, m3.

From Mel's Place: UALVP 40563, incomplete right maxilla with P2-4 and alveolus for P1.

From Birchwood: UALVP 39472, incomplete right dentary with m1 (talonid only), m2-3, and alveoli for lateral incisor, c, p1-4; UALVP 39471, incomplete right dentary with p4, m1, and alveoli for c, p1-3, m2-3;

From Hand Hills West upper level: UALVP 35155, M1; UALVP 35076, incomplete right dentary with p4, m1-3, and alveoli for medial and lateral incisors, c, p1-3; UALVP 39469, incomplete left dentary with m2 and alveoli for medial and lateral incisors, c, p1-4, m1, m3; UALVP 39468, incomplete right dentary with p4, m1-3, and alveoli for p2-3; UALVP 39468, incomplete left dentary with p4, m1-3, and alveoli for p2-3; UALVP 35079, incomplete left dentary with m1-2; UALVP 35078, 35082, 35084, m1; UALVP 35081, 35083, m2.

Age and occurrence.—Early Tiffanian (Plesiadapis anceps/P. rex Lineage Zone, Ti2, late Paleocene) to late middle Tiffanian (Plesiadapis churchilli/P. simonsi Lineage Zone, Ti4, late Paleocene) of the Western Interior of North America (Lofgren et al., 2004).

Description.—Skull and upper dentition (Figs. 5.38.4-5.38.8, 5.39.1-5.39.8): UALVP 40952 preserves the skull, lower jaws, and parts of the postcranium; only the dentition is described here, with the remainder to be described elsewhere (Scott, in prep.).

Upper incisors: The number of upper incisors in Pararyctes pattersoni is likely two, although this remains uncertain: the anterior parts of the snout are damaged in UM 80855 and UALVP 40952 (the only specimens known in which these teeth are in articulation with the premaxilla), and the premaxilla-maxilla suture is completely obliterated in both specimens. Although UALVP 40592 and UM 80855 preserve evidence of two teeth anterior to the double-rooted upper canine, the possibility of there having been a small incisor directly medial to the large blade-like anterior tooth (as there

is, e.g., in the palaeoryctid Ottoryctes Bloch, Secord, and Gingerich, 2004) cannot be ruled out. Asher et al. (2002) and Boyer (in prep.) scored Pararyctes as having two upper incisors based on their observations of UM 80855; this number is tentatively accepted here, although the homologies of these teeth are uncertain and they are referred to here as "anterior upper incisor" and "posterior upper incisor" respectively.

Anterior upper incisor: The anteriormost upper incisor in UALVP 40592 is broken away, leaving only part of the root. The tooth is large and single-rooted, somewhat mediolaterally compressed and subtriangular in cross section. The homologous tooth in UM 80855 is caniniform and blade-like, and virtually straight in lateral view. A moderate diastema intervenes between the anterior upper incisor and the next tooth.

Posterior upper incisor: The posterior upper incisor bears a single stout, bilaterally compressed root that is faintly grooved medially and laterally, suggesting an incipient division or, contrarily, a fusion of two formerly separate roots. The crown is considerably smaller and lower than that of the anterior incisor in UM 80855, and is more nearly premolariform, bearing but a single, somewhat inflated paracone and a weak posterior crest. Heavy wear is developed anteriorly, forming an elongate, flat strip that extends from near the base of the crown to the apex. A second facet is developed apically, flattening the apex; the anterior and apical facets form an angle of approximately 110 degrees at their junction. A third facet is developed posteriorly, running from the apex to near the base of the crown, but this facet is considerably weaker than the anterior or apical facets. A short diastema is developed between the posterior upper incisor and the upper canine.

Upper canine: The upper canine in Pararyctes pattersoni is virtually identical to the posterior upper incisor, differing only in having two well-developed roots and in having a longer and more conspicuous posterior crest.

Upper premolars: P1: The single-rooted, peg-like P1 is greatly reduced in size and is essentially squeezed between the much larger upper canine and P2. The low and bulbous crown is featureless, lacking any development of additional cusps or crests.

P2: The P2 of Pararyctes pattersoni closely resembles the posterior upper incisor and upper canine: the tooth bears a single, mediolaterally compressed root that supports a

large paracone that is somewhat compressed apically, but becomes more inflated towards the base. A weak crest runs from the paracone apex posteriorly, but neither a metacone nor a metastylar cusp is developed. As in the upper posterior incisor, the root of P2 is faintly grooved labially and lingually.

P3: The P3 is slightly larger than P2, and is two-rooted. The crown bulges posterolingually, forming an incipient protoconal salient that is weakly exodaenodont lingually. The crown resembles that of P2 in bearing a large and inflated paracone, but differs in having a short preparacrista that curves anterolingually to form a shelf-like cingulum; a low parastylar cusp can be developed at the anterior extremity of the preparacrista. A low but well-defined metastylar cusp occurs at union of the postparacrista and conspicuous metacingulum. The cingulum can be discontinuous (e.g., UALVP 44741) or continuous (e.g., UALVP 40564) lingually.

P4: The P4 of Pararyctes pattersoni is larger than P3, three-rooted, and somewhat T-shaped in occlusal outline, with a strong anterior emargination between the parastylar cusp and protocone. The crown is dominated by a tall, posteriorly leaning paracone and lower protocone. The paracone is subconical and is inflated, especially near its base; the cusp narrows to a sharply pointed apex that is posteriorly recurved. A conspicuous parastylar spur is developed anterior of the paracone, supporting a low but prominent parastylar cusp; a preparacrista is not developed, and the paracone and parastylar cusp are separated by a wide notch. A sharp postparacrista runs steeply posterolabially from the paraconal apex to a well-developed metastylar cusp; on some specimens a weak carnassial notch separates the paracone and metastylar cusp. A small, nipple-like metacone can be developed on the posterior shoulder of the paracone, although it is usually obliterated by heavy wear on the postparacrista. The ectocingulum is strong posteriorly but is absent anteriorly. The protocone is nearly as massive as the paracone, but it is substantially lower and more nearly vertical, with its apex only slightly posteriorly recurved. Well-developed cristae extend labially from the protoconal apex, fading away as they near the parastylar and metastylar cusps, respectively. The conules and their associated cristae are not present. Although an anterior cingulum is not present, a short posterior cingulum is developed low on the crown; the cingulum becomes more robust lingually and can support a tiny hypocone (e.g., UALVP 47749). Wear is

concentrated on the postparacrista (or postmetacrista), and especially on the posterior side of the protocone, where a wide, strip-like facet is often gouged into the cusp from near the protoconal apex towards the base of the crown, widening basally and extending onto the posterior cingulum.

Upper molars: M1: The crown of M1 is considerably transverse relative to its length, and consists principally of a nearly fully connate paracone and metacone and a tall, sharp protocone that together enclose a shallow trigon basin. The crown is weakly invaginated by an ectoflexus that superficially divides the labial margin into an anteriorly projecting parastylar spur and a more labially projecting metastylar lobe. The stylar shelf is narrow anteriorly but widens considerably at the level of the metacone, and although the ectocingulum is robust anteriorly, it weakens towards the ectoflexus and fades away completely at the level of the metacone. The paracone and metacone are connate for the majority of their heights, with only their respective apices being separated by a shallow notch; weak labial and lingual sulci are developed just below the centrocrista notch, but these fade away almost immediately and do not approach the bases of the paracone and metacone. The paracone is tall, conical, and nearly vertical, whereas the metacone is somewhat compressed labiolingually and is directed posteroventrally. The parastylar spur is prominent, jutting anteriorly past the level of the protocone; the spur supports a prominent conical cusp at the union of the ectocingulum and paracingulum. A low, weak preparacrista connects the paracone and parastylar cusp, with the two cusps being separated from one another by a deep trough that nearly always exhibits strong wear from the m1 protoconid; a stylocone is not developed [Holtzman (1978) reported a "weak stylocone" on M1 of Pararyctes pattersoni from the early middle Tiffanian Judson and Brisbane localities of North Dakota]. The long postmetacrista sweeps posterolabially to the metastylar lobe. The sharp protocone is nearly as tall as the paracone, and is extremely compressed anteroposteriorly, so much so that its posterior side appears concave in lingual view; the protocone leans somewhat anteriorly. Narrow cristae run labially from the protoconal apex: the preprotoconal crista extends to the level of the paracone, and then continues on to the parastylar spur as a paracingulum; the postprotoconal crista extends towards the metastylar corner of the crown as a low metacingulum, but terminates at the base of the metacone. The conules are virtually

undeveloped or absent: when present, they appear as faint swellings or slight inflections of the protoconal cristae, with the paraconule being the larger and slightly more lingual of the two. The anterior cingulum is low and shelf-like, whereas the posterior cingulum is higher, wider, and supports a low, finger-like hypocone; the cingula are discontinuous lingually.

M2: M2 closely resembles M1, but differs in the following ways: the crown is wider; the ectoflexus is deeper; the parastylar lobe is more smoothly rounded and less spur-like; the preparacrista is better developed; and the posterior cingulum is wider.

M3: The crown of M3 is asymmetrically triangular in occlusal outline, with a projecting, hook-like parastylar lobe and undeveloped metastylar area. The preparacrista is high and sharp, and extends labially from the paraconal apex to a small parastylar cusp. The protocone is anteroposteriorly compressed, and the preprotoconal crista is high and blade-like, extending labially to join the parastylar cusp. The protoconal cingula are both well developed, and a hypocone is not developed.

Dentary and lower dentition (Figs. 5.38.4-5.38.8, 5.39.9-5.39.14, 5.40, 5.41.1-5.41.6): The dentary of Pararyctes pattersoni is preserved in several specimens in the present sample that collectively document almost the entire bony anatomy of the lower jaw and dentition. The dentary is anteroposteriorly shorter and more robust compared to those of many of the insectivorans from the present sample (compare, e.g., with the dentary of Litolestes avitodelphus), more closely approaching the overall proportions of dentaries of pantolestids than those of stem lipotyphlans. The mandible is virtually straight ventrally, with almost no convexity, and is uniformly deep from the level of p2 through that of m3. The jaw widens transversely below the level of p2 to accommodate the roots of the enlarged p2, the lower canine, and the lower incisors. The symphysis extends from the anterior tip of the jaw posteriorly to a point below the level of p2. The symphyseal surface is raised above the surrounding bone, and the articular surface and is deeply pitted and rugose; there is no evidence that would suggest the mandibular rami were co-ossified, but the rugosities clearly indicate the dentaries were held together tightly in life. Two mental foramina are present: the more anterior foramen opens below p2, its circular aperture opening anterolaterally; the more posterior foramen is ovate in outline, and opens laterally below the level of the anterior root of m1.

The angular process is damaged among all the specimens at hand, but it is most nearly complete on UALVP 47759 (Figs. 5.40.10-5.40.13). The short process is drawn out posteroventrally, with its axis slightly oblique to the tooth row and its posterior margin extending posteriorly to the level of the condyle. When the ramus is held with its ventral surface in a horizontal position, the dorsal surface of the angular process is well below the level of the bases of the tooth crowns. The lateral surface is excavated proximally, and a large, flat tubercle is developed distally, providing an extensive area of insertion for the superficial masseter. The medial surface is shallowly concave and bears a prominent, shelf-like ridge ventrally; the ridge extends anteriorly onto the ramus, terminating below the small mandibular foramen. The large, mediolaterally expanded condyle is supported by a robust condylar process; the condyle is low, positioned at the level of the apices of the tooth crowns when the ramus is held horizontally. The articular surface of the condyle is oriented virtually perpendicular to the long axis of the jaw, and forms an anteroposteriorly compressed oval in outline; the condyle slopes medially, with its medial side approximately 35-45 degrees lower from horizontal than its lateral side. Laterally, the articular surface is restricted more or less to the dorsal parts of the condyle, but the facet continues progressively farther ventrally towards the medial side, eventually reaching the ventralmost parts of the condyle near the transverse midpoint of the condyle; the majority of the articular facet faces posteriorly when the ramus is horizontal. The medial side of the condylar neck is excavated by a deep fossa for the distal attachment of the external pterygoids.

The coronoid process is well preserved in several specimens (e.g., UALVP 47760, 47759). The anterior margin takes origin posterior to m3, farther posteriorly than on dentaries of soricids and Apternodus (Asher et al., 2002). In contrast with those of many of the insectivorans in the present sample, the coronoid process in Pararyctes is relatively low, anteroposteriorly short, and nearly vertical (i.e., not posteriorly reclined), with the anterior margin forming an angle of approximately 90-100 degrees at its union with the mandibular ramus. The coronoid process is drawn out dorsally as a narrow spine, while the posterior margin is vertical or weakly concave. Medially, the limits of the poorly excavated temporalis fossa are marked by smoothly rounded crests, with a weak ventral crest separating it from the pterygoideus fossa ventrally; a prominent

tubercle is developed at the anteroventral limit of the temporalis fossa medially, possibly the site of distal attachment for a slip of the deep temporalis muscle. A compound craniomandibular joint is not developed in Pararyctes, nor is there evidence of a deep, pocket-like medial fossa (as there are in, e.g., soricids and the zalambdodont lipotyphlan Apternodus, see Asher et al., 2005). The masseteric fossa is deeply excavated and extends close to the ventral margin of the mandibular ramus.

Lower incisors: As with the upper incisors, the number of lower incisors in Pararyctes appears to be two, although the homologies of these teeth are uncertain; as such, they are designated "anterior" and "posterior", respectively. Of the two lower incisors, only the posterior is known from articulated specimens in the Blindman River sample; the anterior lower incisor is known from an isolated but associated tooth (UALVP 47756), and by three specimens preserving its alveolus, each containing part of the root. The two lower incisors of Pararyctes are closely similar, and differ mainly in size, proportion, and position. The incisors are considerably enlarged compared to the cheek teeth, and are procumbent (the posterior incisor forms an angle of approximately 135 degrees at the alveolar rim; the orientation of the anterior incisor alveolus indicates it was similarly procumbent) and bear elongate, lanceolate crowns that are slightly concave dorsally. The roots are somewhat mediolaterally compressed (less so on the anterior incisor, considerably so on the posterior incisor) and are oriented anterolaterally-posteromedially, with the crowns splaying slightly laterally (the unusual orientation of the lower incisors accounts for the lateral "bulge" in the dentary described earlier). The incisor crowns are mediolaterally compressed and bear a single, acutely pointed principal cusp. A sharp crest extends posteriorly from the apex of the principal cusp, delimiting the lateral extent of the occlusal surface; the crest swings medially at the base of the crown, where it forms a slightly elevated shelf that can support a small margoconid. The medial surface of both lower incisors is unusual: it is deeply excavated by a long sulcus that runs from near the apex to the base of the crown; the dorsal and ventral rims of the sulcus are drawn out as sharp crests. The biting surface of both lower incisors appears to have been primarily on the posteromedial surface, where a long, strap-like facet is developed from occlusion with the anterior surface of the corresponding upper incisor; a

second facet is present near the base of the crown posterolaterally. Wear is not developed in the medial sulcus.

Lower canine: The lower canine of Pararyctes pattersoni is single-rooted and incisiform, and although it is considerably smaller and lower crowned than the posterior incisor, it resembles that tooth in its coronal anatomy. The crown is procumbent and lanceolate, with its anterior parts closely appressed to the base of the posterior incisor; the crown bears a relatively low but sharply pointed principal cusp and a long posterior crest that terminates posteriorly as a short, transverse shelf that can support a low but conspicuous cuspule. The crown is narrow anteriorly but becomes increasingly wide posteriorly, and the medial side and base are swollen. As with the lower incisors, the biting surface of the lower canine faces dorsally and somewhat medially.

Lower premolars: p1: The single-rooted p1 of Pararyctes pattersoni is the smallest tooth in the lower jaw, having been reduced to a squat, bulbous peg that is essentially squeezed between the preceding and succeeding teeth. The tooth is set off labially from the lower canine and p2 and is oriented obliquely anterolabially-posterolingually; as a result, the anterolingual part of the crown abuts the posterolabial side of the lower canine. Despite its peculiar orientation and small size, the crown of p1 most closely resembles that of the lower canine: it is procumbent and bears a low, bulbous protoconid, a blunt posterior crest, and a short transverse posterior shelf. As with the lower canine, the base of the p1 crown is considerably swollen.

p2: The single-rooted p2 of Pararyctes pattersoni is slightly smaller than the lower canine, but considerably larger than p1 and p3. The crown is procumbent, although not to the same degree as the lower canine or p1, but it is similarly swollen at its base. The crown is dominated by a tall protoconid that is connected to a low heel by a sharp posterior crest; a sharp paracristid is developed anteriorly, but neither a paraconid nor a metaconid is present. Weak lingual cingulids are developed anteriorly and posteriorly, but remain discontinuous.

p3: Other than its smaller size and lower and more nearly vertical crown, the p3 of Pararyctes closely resembles p2: it is single-rooted, the crown is swollen and somewhat wedge-shaped in occlusal view, the heel is low and can support a small cuspule, and

weak lingual cingulids are developed anteriorly and posteriorly. Weak exodaenodonty is present posteriorly.

dp3: The dp3 of Pararyctes pattersoni is preserved in one specimen, UALVP 47769. Although the crown of dp3 is larger, taller, and more nearly vertical than the replacement p3, it is similarly single-rooted. The crown bears a tall, slightly labiolingually compressed protoconid and a weakly developed heel. A sharp paracristid extends directly anteriorly from the protoconid apex, and terminates near the base of that cusp; neither a paraconid nor metaconid is developed. A similarly sharp crest extends posteriorly from the protoconid apex to a low heel; the heel is tightly recessed below the trigonid of the dp4 in UALVP 47769, but it appears that a distinct talonid cusp was not present on dp3.

p4: The double-rooted p4 is slightly more variable in its coronal anatomy than any of the other premolars. The crown consists principally of a tall, sharp and somewhat recurved protoconid and a variably developed talonid. A small, conical paraconid arises from a low position on the anterolingual side of the protoconid; the paraconid projects anterodorsally and is not connected to the protoconid apex by a paracristid. A metaconid is not present. The protoconid varies in height: on some specimens (e.g., UALVP 47760) the apex can extend above that of m1, while in others (e.g., UALVP 47761) it can be distinctly lower, although it should be noted that the protoconid apex is often heavily worn, and even slight wear can radically alter the height of the cusp. A sharp, deeply notched crest connects the protoconid apex to the hypoconid; the notch is narrow and acute in unworn specimens, but becomes increasingly wide with wear. The hypoconid is tall and conical, and its apex is positioned in line with that of the protoconid. A sharp crest extends lingually from the hypoconid apex, and then bends anteriorly at the posterolingual margin of the crown; the crest continues anteriorly where it joins the postvallid wall and defines the lingual margin of a deep talonid basin. Neither an entoconid nor a hypoconulid are developed, although the lingual talonid crest can bear small cuspules. A hypoflexid and posterior exodaenodonty are developed on p4, but both are highly variable: in UALVP 47755, for example, the exodaenodont lobe is deep, and the hypoflexid is anteroposteriorly short and transversely deep, whereas in UALVP

47756, the exodaenodont lobe is weaker and the hypoflexid is shallower and less anteroposteriorly constricted.

dp4: The crown of dp4 is molariform, with well-developed protoconid, metaconid, and paraconid, and a short but well-defined talonid. The protoconid and metaconid are nearly equal in size and height and are connected to one another by a deeply notched protocristid. A sharp paracristid extends anteriorly from the protoconid apex to the conical paraconid; the paracristid is shallowly notched. The paraconid arises from a relatively low position on the metaconid, and leans somewhat anteriorly. The talonid is short and low, being overhung by the paraconid of m1; a small entoconid and hypoconid are present, but a hypoconulid is not developed. The short cristid obliqua contacts the postvallid wall labial of the level of the protocristid notch, forming a relatively shallow hypoflexid. The talonid basin is shallow. A heavy, shelf-like cingulid is developed anteriorly, but a posterior cingulid is not present. Exodaenodonty is strong at the posterior root, forming a deep lobe that extends far ventrally.

Lower molars: m1: The lower molars of Pararyctes pattersoni are dominated by an elevated trigonid and talonid, with the difference in their respective heights being considerably less than that seen in palaeoryctids. The teeth are oriented slightly oblique to the long axis of the jaw such that the crowns face more or less anterolabially-posterolingually, and the obliquity increases from m1 to m3. The trigonid of m1 is slightly wider than the talonid and bears a well-developed paraconid, metaconid, and protoconid. The paraconid is positioned midway or slightly lingual of the longitudinal midline of the crown, and is elevated well above the apex of the p4 hypoconid; it is somewhat anteroposteriorly compressed and anteriorly projecting. A sharp and widely notched paracristid connects the paraconid to the protoconid apex; a carnassial notch is not developed at the deepest part of the paracristid notch. The metaconid and protoconid are subequal in size and height, and are pyramidal, with flat basin-facing walls; a sharp, deeply notched protocristid connects the two cusps, and a carnassial notch is not developed at the deepest part of the notch. The talonid is both shorter and narrower than the trigonid, and bears three well-developed cusps that together enclose a relatively shallow basin that slopes posterolabially-anterolingually. The hypoconid is the tallest and largest talonid cusp, followed in decreasing order of size by the entoconid and

hypoconulid. Although the hypoconulid is closely appressed to the hypoconid (and would be considered labial in position), the unusual orientation of the molars in the jaw results in the hypoconulid being positioned on the midlongitudinal axis of the horizontal ramus; a short hypocristid connects the hypoconulid and hypoconid, and a notch is not developed between the two cusps. The entoconid is positioned at the posterolingual corner of the crown, and is connected to the hypoconulid by a long, faintly notched postcristid; a low entocristid closes off the lingual side of the talonid basin. A short cristid obliqua joins the postvallid wall below the protocristid notch, forming a deep but anteroposteriorly long hypoflexid. A low, shelf-like cingulid is present anteriorly, whereas the posterior cingulum is undeveloped. Exodaenodonty is developed to varying degrees posteriorly: on some specimens (e.g., UALVP 47760) it is pronounced, forming a conspicuous lobe, whereas in other specimens (e.g., UALVP 40952) it is weaker, and in a few specimens it is virtually undeveloped.

m2: The m2 of Pararyctes pattersoni closely resembles m1, differing mainly in being slightly larger, with a wider trigonid supporting a larger protoconid and metaconid, a longer paracristid, and a slightly narrower talonid. Exodaenodonty is developed in much the same manner as on m1, and exhibiting the same range of variation.

m3: Although the crown of m3 resembles that on m2, it differs in a number of features, particularly in the structure of the talonid. The crown is slightly larger than that on m2, and the trigonid is wider and the talonid narrower; additionally, the paracristid is longer, and the paracristid notch is wider. The talonid on m3 is moderately flexed dorsally, elevating the apex of the hypoconulid and bringing it closer to the postvallid wall. The talonid basin is much more elongate and narrower than that on m1 or m2, and the hypoconulid is enlarged, finger-like, and dorsally projecting. As on m1 and m2, the hypoconulid is closer to the hypoconid than to the entoconid. The anterior cingulid is strongly developed, whereas the posterior cingulum is absent. Exodaenodonty is not present.

Discussion.—While Pararyctes pattersoni was not formally described until 1967, the first known specimen that would eventually be referred to that taxon was collected by Russell (1932) from the Cochrane 2 locality of Alberta (Van Valen, 1966). Russell (1932) referred the specimen (UALVP 428) with question to "Diacodon" septentrionalis.

Van Valen (1966) referred the Alberta specimen, as well as six teeth from the early Tiffanian (Ti2) Saddle locality of Wyoming to P. pattersoni, and distinguished the genus from a number of palaeoryctids, most notably Palaeoryctes puercensis Matthew, 1913. The present sample represents one of the largest single samples of P. pattersoni now known. The teeth of P. pattersoni from Alberta differ from those in the hypodigm in a few notable features: for example, the crowns of the referred M1s are narrower than that in UW 2002, and the protoconal cingula are slightly wider, although the posterior cingulum in UW 2002 is damaged posterolingually. An important point of difference concerns the P4: Van Valen (1966) referred an incomplete maxilla containing P4 and the labial half of M1 (UW 2005) to P. pattersoni, and distinguished the P4 from that of a few palaeoryctids. The crown of P4 in UW 2005 differs significantly from that in the present sample: for example, the protocone in UW 2005 is considerably compressed anteroposteriorly, giving the crown a T-shaped occlusal outline; in contrast, the P4 of P. pattersoni from Alberta has a longer and more inflated paracone and protocone, and a well-developed posterior cingulum is present, and in some specimens supports a low hypocone. UW 2005 was not examined firsthand during this study, but the morphology of the P4 in this specimen is more consistent with that of many palaeoryctines, including Palaeoryctes and Ottoryctes; should the identity of UW 2005 be confirmed as pertaining to P. pattersoni by additional collections from the type locality, however, then the specimens from Alberta may in fact represent a new species of Pararyctes.

The large sample from the Blindman River and Joffre Bridge localities provides important information that bears on the hypothesized eruption sequence of the replacement teeth in Pararyctes as proposed by Fox (1983), most notably a clarification of tooth identities. Comparisons of nearly complete upper and lower dentitions of P. pattersoni with the teeth in UALVP 16268 (representing a new species of Pararyctes) has revealed the following:

1) The teeth identified as dP1-2 in UALVP 16268 are probably the two-rooted upper canine and single-rooted P1 (P1 being a small peg, as in P. pattersoni);

2) The tooth identified as dC1 in UALVP 16268 may in fact be the replacement posterior upper incisor; if so, it is in keeping with the replacement of the posterior lower incisor (see later in the text);

3) The evidence for replacement of dP4 by two teeth in UALVP 16268 is somewhat ambiguous—the anterior parts of the maxilla in UALVP 16268 have been broken at the level of P4 and rotated ventrally such that the P3 has been drawn closer to the erupting P4 (compare the plane of the apices of the molar cusps in Fox, 1983, fig. 1 with that of the protocone and upper canine apex);

4) The two alveoli between P1 and P3 may have held a two-rooted P2; although this tooth is single-rooted in P. pattersoni, the root is grooved labially and lingually, suggesting fusion of two formally separate roots; conversely, the more anterior of these alveoli may have held the posterior root of P3 (as noted previously, that part of the maxilla housing P3 has been broken and moved prior to burial);

5) The permanent antemolar teeth in P. pattersoni (see, e.g., Figs. 5.40.4-5.40.6) are identical to teeth in UALVP 16268 identified by Fox (1983) as ?dp1-3; these teeth in UALVP 16268 more likely represent the lower canine and p1-2 (a possibility that was entertained by Fox, 1983); the small p3 is emerging from the crypt in UALVP 16268, with its deciduous predecessor likely having been shed before death (a deciduous p3 of P. pattersoni is preserved in UALVP 47769, see Figs. 5.41.4-5.41.6);

6) The enlarged caniniform tooth is probably the posterior lower incisor, while the tooth immediately anterior (identified as i3 by Fox, 1983) is possibly the anterior lower incisor; while there is no evidence of a third lower incisor on any specimen of P. pattersoni preserving the appropriate parts in the present sample, perhaps there was one in this species of Pararyctes [Fox, 1983 identified an empty alveolus adjacent to the tooth identified as i3 (=anterior lower incisor here), suggesting the presence of an additional tooth];

7) The posterior lower incisor is apparently in the process of being replaced at the same time as p4 in UALVP 16268.

Even with the new information provided by the large sample of P. pattersoni, the relatively poor preservation of the anteriormost parts of the lower jaw in UALVP 16268, the uncertainty as to the number of lower incisors in both P. pattersoni and UALVP 16268, and a near-complete lack of information on incisor replacement timing and patterns in fossil and extant mammals continue to make interpretation of UALVP 16268 difficult. The close similarities in the coronal anatomy and number of teeth in P.

pattersoni and UALVP 16268 suggest at the very least that Pararyctes probably had four, rather than five premolars, with the enlarged anterior teeth representing the two lower incisors. The eruption sequence of the permanent dentition may have been similar to that in many other insectivorans and primitive eutherians generally, with p2 having erupted prior to p3, which erupted prior to p4 (e.g., Ziegler, 1971; Slaughter et al., 1974; Bloch et al., 1998) although the possibility of P3/p3 and P4/p4 having erupted simultaneously cannot be discounted on the current evidence.

The phylogenetic relationships of Pararyctes have historically been difficult to address given the limited evidence in the published record: other than Van Valen's (1966) formal description of the hypodigm specimens, the only other material referred to Pararyctes has been a few teeth from the late Paleocene of Alberta (Krishtalka, 1973) and North Dakota (Holtzman, 1978), the aforementioned specimen (UALVP 16268) from the Diss locality of Alberta (Fox, 1983), and specimens from the early Tiffanian (Ti2) Scarritt Quarry of Montana (Krause and Maas, 1990). A consensus on the relationships of Pararyctes has yet to be reached: despite its unusual features (e.g., protoconal cingula, high molar talonid), Van Valen (1966) referred Pararyctes to the Palaeoryctinae, an opinion repeated in Van Valen (1967); although this opinion has been followed by most subsequent authors (e.g., Gingerich, 1982a; Asher et al., 2002; Bloch et al., 2004), there are a number of detractors that suggest the differences between Pararyctes on the one hand, and palaeoryctids on the other, are too great for these taxa to be considered as representing a natural group (e.g., Kellner and McKenna, 1996 and McKenna and Bell, 1997). While a detailed investigation of the phylogenetic affinities of Pararyctes is beyond the scope of the present study, it is noted here that a meaningful comparison between Pararyctes and the palaeoryctids is complicated by the heterogeneity (and possible non-monophyly) of the Palaeoryctidae as currently construed. For example, although the dentitions of Palaeoryctes puercensis and Eoryctes melanus Thewissen and Gingerich, 1989 are very similar, their basicranial anatomies differ significantly, with the promontorium of Eoryctes providing bony tubes that enclosed the stapedial and promontorial branches of the internal carotid artery (Thewissen and Gingerich, 1989; Bloch et al., 2004); in contrast, the promontorium of Palaeoryctes puercensis, as well as that of Pararyctes (known from UM 80855) is smooth, and bears no bony tubes (Gunnell,

1989); other differences in basicranial anatomy among the taxa presently considered palaeoryctids are cited in Fox (2004). The promontorial anatomy of Pararyctes is most similar to that of Pal. puercensis, but most, if not all of these similarities, are probable primitive for eutherians generally (e.g., lacking bony enclosures for the stapedial and promontorial rami of the internal carotid artery; MacPhee, 1981). Until a comprehensive review of Palaeoryctidae is undertaken to clarify these issues, the phylogenetic position of Pararyctes and other palaeoryctid-like eutherians will continue to be uncertain. Pararyctes is tentatively referred here to the Palaeoryctidae, following the recent opinions of Asher et al. (2002) and Bloch et al. (2004).

PARARYCTES COLOSSA new species

Figures 5.41.7-5.41.9

Diagnosis.—Differs from other species of Pararyctes in being much larger (L m1, P. colossa approximately 65 percent longer than m1, P. pattersoni; L m1, P. colossa approximately 15 percent longer than m1 P. rutherfordi).

Description and discussion.—Other than its much larger size (L m1=3.1, TrW=2.1, TaW=1.9; L m2=3.4, TrW=2.5, TaW=2.3; L m3=3.5, TrW=2.4, TaW=1.9), little distinguishes the dentition of Pararyctes colossa from that of other species of Pararyctes. The m3 talonid is relatively (and absolutely) larger in P. colossa, and the molar crowns are more posteriorly leaning. As in P. pattersoni, a large mental foramen is developed below m1.

Etymology.—Colossus, Latin, large; in reference to the large size of P. colossa relative to other species of Pararyctes.

Holotype.—UALVP 47800, incomplete right dentary with m1-3. DW-2 locality, Paskapoo Formation of Alberta, Canada, late Paleocene, late Paleocene [early middle Tiffanian, Ti3 (Fox, 1990), Plesiadapis anceps/P. rex Lineage Zone of Lofgren et al., 2004].

5.3 A Phylogenetic Analysis of the Earliest Lipotyphlans

5.3.1 Introduction and Objectives

The phylogenetic relationships of extant lipotyphlans have received a great deal of attention in the years since Butler's (1988) and MacPhee and Novacek's (1993) reviews of the morphological evidence for monophyly of the order. Molecular-based methods of phylogeny reconstruction have corroborated some of the morphology-based hypotheses of lipotyphlan in-group relationships (e.g., Asher, 1999), and have refuted others (e.g., Stanhope et al., 1998); perhaps the most surprising of these results, however, is the nearly consistent conclusion that Lipotyphla represent an assemblage of disparately related insectivorous eutherians (e.g., Stanhope et al., 1998; Emerson et al., 1999; Mouchaty et al., 2000a-b; Madsen et al., 2001; Murphy, Eizirik, Johnson et al., 2001; Murphy, Eizirik, O'Brien et al., 2001; Arnason et al., 2002; Asher et al., 2003; Douady et al., 2004; Asher, 2005). Under this new paradigm, Lipotyphla as traditionally understood are polyphyletic, with the endemic African tenrecoids (the tenrecids and chrysochlorids) forming a clade with other African mammalian groups (the Afrotheria of Stanhope et al. 1998), and the remaining lipotyphlans (including the Caribbean Solenodon) forming a clade of closely related Holarctic taxa.

With the exception of a few studies (e.g., Asher et al., 2002; Lopatin, 2005; Asher et al., 2005), the interrelationships of the earliest lipotyphlans has not been the subject of recent investigation; questions pertaining to the early evolutionary history of the order have more often than not focused on the better-known lipotyphlan families from the Eocene and Oligocene, and have been directed at resolving their phylogenetic relationships with extant lipotyphlans (e.g., Novacek, 1985; Rich, 1981) or, even more broadly, with other eutherians (e.g., Asher, 1999; Asher et al., 2005). While the Eocene and Oligocene undoubtedly represented intervals of great diversification of lipotyphlans, evidence to date points to the Paleocene as having been an important episode in the early evolutionary history of the Lipotyphla (McDowell, 1958; Russell, 1964; Butler, 1972; Krishtalka, 1976a-b; Bown and Schankler, 1982; Butler, 1988; MacPhee and Novacek, 1993; Asher, 2005; Rose, 2006). The interval saw the emergence of a number of early

families, the Erinaceidae (Novacek, 1985; Novacek et al., 1985). The fossil record of the earliest lipotyphlans is on the whole poor: although stem lipotyphlans can be abundantly represented in local faunas (e.g., Rose, 1981a-b; Gingerich, 1983; Youzwyshyn, 1988; Krause and Maas, 1990; Secord, 2004), their fossils are fragmentary and consist almost entirely of isolated teeth, incomplete lower jaws with teeth, and rare skull fragments; with the exception of Litocherus notissimus (see earlier in this chapter), the anatomy of the skull and postcranium of Paleocene age lipotyphlans from North America and elsewhere is not known. Obviously, the paucity of non-dental fossils limits the diversity of data that can potentially be brought to bear on lipotyphlan systematics; indeed, the traditionally-recognized diagnostic characters of Lipotyphla are all non-dental (MacPhee and Novacek, 1993; Asher, 2005; but see McDowell, 1958 and Butler, 1988), and the referral of Paleocene age stem lipotyphlans to the Lipotyphla rests on dental resemblances alone. Nonetheless, these records represent the only direct evidence of the earliest lipotyphlans, and a better understanding of the early evolutionary history of the order can only come from analysis of these fragmentary specimens.

The objectives of this analysis are to examine the phylogenetic relationships among stem lipotyphlans from the Paleocene of North America, particularly those represented in Alberta, and to explore the broader relationships of these taxa to some of the better-known lipotyphlans from the Eocene of North America and Europe. "Stem lipotyphlans" here refers to an assemblage of generally poorly known or otherwise poorly understood eutherians that have historically been allied with the living groups of lipotyphlans, but for most cannot be readily referred to any of the extant families. Indeed, many of the stem lipotyphlans included in this study have convoluted taxonomic histories and have been repeatedly shuffled among higher level taxa in classifications (see, e.g., Simpson, 1945; Van Valen, 1967; Russell et al., 1975; Krishtalka, 1976a-b; Novacek, 1985; McKenna and Bell, 1997; Lopatin, 2005), reflecting their generally primitive dental anatomy and the often fragmentary nature of the evidence. In spite of these uncertainties, most studies on the earliest lipotyphlans have followed Butler's (1956) two-fold division of the order into two taxonomically broad, higher level assemblages, the suborders Erinaceomorpha (hedge-hog like lipotyphlans) and Soricomorpha (shrew-like lipotyphlans) [Butler, 1956; McKenna and Bell, 1997); a more

recent classification of lipotyphlans (Wilson and Reeder, 2005) elevates Erinaceomorpha and Soricomorpha to ordinal level. Previous comprehensive analyses of stem lipotyphlans are few (e.g., Butler, 1972, 1988), and many of the more recent studies have focused on particular stem lipotyphlan families or subfamilies (e.g., Lillegraven et al., 1981; Novacek, 1985; Missiaen and Smith, 2005), or examined more broadly the relationships among select erinaceomorph or soricomorph taxa (e.g., Krishtalka, 1976a-b; Novacek, 1982, 1985; Novacek et al., 1985); as such, this analysis represents a first attempt at examining specifically the interrelationships of the earliest lipotyphlans in a cladistic framework, and the first to comprehensively examine Late Cretaceous and Paleocene age soricomorphs and erinaceomorphs in the same analysis. Given that prior phylogenetic analyses of early lipotyphlans are few (Novacek, 1982, 1985, and Missiaen and Smith, 2005 are exceptions), the current study necessarily relies on a novel dataset, and the results of the phylogenetic analysis should be viewed as preliminary. Some of the relevant questions that will be addressed in this analysis include:

1) Is the Erinaceomorpha/Soricomorpha dichotomy established by Paleocene, or even Late Cretaceous time?

2) Can any of the newly identified putative erinaceomorphs or soricomorphs from Alberta be classified with any of the presently recognized stem lipotyphlan families or subfamilies?

3) What are the relationships of the Paleocene North American lipotyphlans to those from Europe? What are the biogeographic implications of these relationships?

4) Is Litolestes an erinaceid?

5) Is Leptacodon monophyletic?

6) Is Paranyctoides a soricomorph?

7) Is Limaconyssus a nyctitheriid?

8) Is Diacocherus (=Adunator, Mckennatherium) the most primitive erinaceomorph?

5.3.2 Methods

Character Analysis and Descriptions

This analysis uses 96 parsimony-informative characters based on observations of specimens and descriptions in the literature. The data matrix is presented in Appendix 2 and the main references and specimens examined are listed in Appendix 1. The characters used in this analysis are almost exclusively dental, reflecting the strong preservational bias towards teeth in the earliest lipotyphlans. Characters were selected based primarily on three criteria: (1) use in studies on closely related taxa by previous authors, (2) ability to be categorized into discrete states; and (3) a non-autapomorphic distribution (Asher, 1999; Meng et al., 2003). The second criterion met with mixed success, as some of the features used to distinguish stem lipotyphlan genera are subtle; where necessary, diagrams are used to clarify some of the coding decisions. There are few cladistics-based analyses of early lipotyphlans, and many of the characters and their states used in this study are new; where applicable, characters that have been used in previous analyses were identified and referenced appropriately. The homologies of soricid antemolar teeth are uncertain and continue to be a matter of debate (summarized in Asher et al., 2002); Asher et al. (2002) are followed in recognizing I1-3, C, P3-4, M1-3 in the upper dentition of Crocidura, while only i1, p4, and m1-3 are reasonably certain for the lower teeth; characters pertaining to teeth between i1 and p4 are scored as missing. The following characters are numbered consecutively and correspond to the matrix presented in Appendix 3.

Maxilla

1. Anterior root of zygomatic arch: M2 (0); M3 (1); M1 (2)

Follows Asher et al. (2002). The maxillary root of the zygomatic arch can originate at a relatively anterior position, at the level of M2 (state 0), farther posterior, at the level of M3 (state 1), or farther anterior (state 2). In taxa possessing a long anterior root, the anteriormost part of the root was used to code this character.

2. Position of the infraorbital foramen: P3 (0); P4 (1)

The position of the infraorbital foramen has often been used as a proxy for infraorbital canal length (e.g., Butler, 1956; McDowell, 1958; Butler, 1972). Most of the putative erinaceomorphs for which this feature is preserved have a relatively anteriorly positioned

foramen, usually at the level of P3, while most putative soricomorphs have the foramen positioned farther posterior, usually at the level of P4. The position of the foramen in Kennalestes (at the level of P3), as well as in other primitive placental mammals (e.g., Maelestes Wible, Rougier, Novacek, and Asher, 2007; Kulbeckia, Nessov, 1993; Zhelestes Nessov, 1985), as well as in metatherians (e.g., Didelphis virginiana) suggests that a more anteriorly positioned foramen is probably primitive for therians.

3. Extent of jugal on maxilla: extensive (0); reduced (1)

This character describes the relationship between the jugal and the side wall of maxilla. A reduced jugal has often been cited as a synapomorphy of lipotyphlans (e.g., Butler, 1972, 1988); MacPhee and Novacek (1993), Asher (2005), and Asher et al. (2003) have argued against the validity of this character, suggesting that the continuity of the zygomatic arch, rather than its bony constituents, is the more useful character. An enlarged jugal is clearly present in many stem lipotyphlans (state 0): for example, specimens of Macrocranion and Pholidocercus preserve a jugal that laps extensively onto the side of the face (Koenigswald and Storch, 1983), and a conspicuous facet for the jugal is present on maxillae of Litocherus, Nayloria, and a number of other taxa. In contrast, the jugal appears to be at the very least reduced in some taxa (e.g., Centetodon), with the maxilla alone forming the anterior root of the zygoma [the jugal may be limited to the middle of the arch, absent, or reduced and seamlessly fused to the zygomatic process of the maxilla (e.g., MacPhee and Novacek, 1993; Asher et al., 2003) in these taxa, but in each case it clearly does not make an extensive contact with the maxilla on the side of the face.] A broad contact between the jugal and maxilla is present in Kennalestes and the marsupial Didelphis, suggesting that state 0 is primitive for therians.

Teeth generally

4. Principal cusps: cusps tall and sharp (0); cusps lower and inflated (at least at bases) (1); cusps bunodont (2)

Based on Hooker (2001). Many stem lipotyphlans have teeth that support tall, sharp principal cusps (e.g., Psydronyctia), while others have teeth with cusps that are lower and

inflated at their bases (e.g., "Adapisorella"). The tooth crowns of sespedectids and some amphilemurids are bunodont, with low, turgid cusps with rounded apices. Ordered.

Upper canine

5. Upper canine roots: 1(0); 2(1)

Based on Asher et al. (2002).

6. Upper canine morphology: caniniform (0); premolariform (1)

Caniniform canines are enlarged and laniary (e.g., Macrocranion), whereas premolariform canines are smaller and more closely resemble the upper premolars (e.g., Diacocherus).

Upper premolars

7. P2 roots: 2(0); 1(1); P2 absent (2)

Based on Bloch, Secord, and Gingerich (2004).

8. P3 metacone: present (0); absent (1); P3 absent (2)

Based on Bloch, Secord, and Gingerich (2004).

9. P3 protocone: present (0); absent (1)

Based on Bloch, Secord, and Gingerich (2004).

10. P4 labial margin: virtually parasagittal, not oblique to long axis (0); slightly oblique to long axis (1); very oblique (2)

Based on Hooker and Weidmann (2000). This character refers to the angle formed by the labial margin of the crown and an imaginary line drawn anteroposteriorly through the paracone and metacone (or paralleling the long axis of the skull should the metacone not be developed); it is possibly correlated with character 13 (length and morphology of the "postcrista"). In some taxa the labial margin of P4 is parasagittal (e.g., Prodiacodon, state 0; Fig. 5.42.1), while in others it is slightly oblique, with the labial margin and imaginary line forming an angle of about 25-30 degrees, and the parastyle is nearly

directly anterior of the paracone (e.g., Litolestes, state 1; Fig. 5.42.2). In still other taxa the labial margin of P4 is very oblique, with an angle of about 45 degrees formed, and the parastyle is anterolingual of paracone (e.g., Amphidozotherium, state 2; Fig. 5.42.3). Ordered.

11. P4 parastylar lobe: lobe strongly developed and anteriorly projecting (0); lobe weakly developed (1); lobe undeveloped (2)

Based on Asher et al. (2002). The parastylar lobe on P4 is strongly developed in primitive eutherians (e.g., Kennalestes), and projects anteriorly from anterior of the paracone (state 0); the lobe usually supports a prominent parastyle, and the embrasure between the parastyle and paracone is often scoured by the p4 protoconid. In contrast, the parastylar lobe of some erinaceomorphs is notably reduced and not anteriorly projecting (e.g., Litocherus, state 1); in these taxa, the parastyle is less prominent, lower, and usually appressed to the anterior face of the paracone. Some lipotyphlans (e.g., Echinosorex, Adapisorex) lack a parastylar lobe on P4 (state 2).

12. P4 metacone: undeveloped (0); weakly developed within postparacrista, apex barely separate, labial sulcus (1); moderately developed, apex separate, labial and lingual sulci (2); well-developed, fully separate from paracone (3)

Based on Novacek (1982), Butler (1988), Bloch et al. (1998), Archibald and Averianov (2006). The development of the P4 metacone has figured importantly in the systematics of Lipotyphla (e.g., Novacek, 1982; Butler, 1988). Archibald and Averianov (2006, and contra Archibald et al., 2001) suggest that a metacone (represented by a swelling) is probably primitive for Eutheria, as it is present in basal eutherians such as the asioryctitheres Daulestes, Ukhaatherium, and Kennalestes (inexplicably, this character was not included in their cladistic analysis of Asioryctitheria). In contrast, Ji et al. (2002) indicated that the stratigraphically older Eomaia lacks a metaconal swelling, and a metacone is absent in the asioryctithere Uchkudukodon (Archibald and Averianov, 2006). Clearly the polarity of this character remains uncertain (a point made previously by Novacek, 1982), and the decision was made here to leave character 12 unordered. The outgroups used in this analysis collectively exhibit states 0, 1, and 3: with respect to

Kennalestes, the opinion of Archibald and Averianov (2006) is followed here, and a metacone is coded as weakly present, while a metacone can be undeveloped or weakly developed in Cimolestes (Lillegraven, 1969; Clemens, 1973); the P4 metacone in Prodiacodon is fully separated from the paracone (Fig. 5.43.4, state 3). With respect to stem lipotyphlans, the P4 metacone can be wholly undeveloped, with the metaconal apex undifferentiated from the postcrista, and with no swelling to indicate its vestigial (or incipient) presence (e.g., Litolestes, state 0; Fig. 5.43.1), weakly developed, with only the metaconal apex clearly differentiated (the remainder of the metacone is connate with the paracone, with a conspicuous sulcus developed labially but not lingually, e.g., Xynolestes, state 1; Fig. 5.43.2), or moderately developed, with the metaconal apex clearly differentiated and farther separated from the paraconal apex (the centrocrista notch is deep, and the metacone is more fully separated from the paracone, with sulci developed labially and lingually, e.g., Leptacodon rosei, state 2; Fig. 5.43.3).

13. P4 postcrista: short and blade-like (0); long and blade-like (1); weak, blade very low or undeveloped (2)

With the exception of Diacocherus and Pholidocercus, all of the ingroup taxa have a P4 with a blade-like crest extending posterolabially from the either the paracone or metacone. When a metacone is developed on P4, the identity of this crest is certain (i.e., the postmetacrista), but when the metacone is absent the crest could represent the postparacrista or combined postparacrista and metacrista (i.e., the pre- and postmetacrista). Butler (1988) has suggested the term "metacrista" be used for this crest, implying that the metacone has been lost in taxa with P4 having only a paracone and protocone, but there is little justification for this given the uncertainty regarding the polarity of the P4 metacone (see character 12); as such, the term "postcrista" is used here for this crest, with no implication of its homology. The state of the "postcrista" is based on that part of the crest that is actually involved in direct shear with the paracristid—that is, the crest extending from the apex of the paracone in those taxa that lack a metacone, or from the apex of the metacone in those that have one. As the centrocrista has a functional relationship with the hypoconid of the lower p4, it is by definition not directly involved with shear against the paracristid.

The postcrista is considered short and blade-like when it is elevated as a high blade and extends but a short distance labially, and does not protrude far past the labial margin of the crown (e.g., "Adapisorella", state 0; Fig. 5.44.1). In contrast, a long postcrista is elevated as a high blade and sweeps posterolabially, jutting well past the labial margin of the crown (e.g., Euronyctia, state 1; Fig. 5.44.2); as noted earlier, this state often occurs in taxa with an extremely oblique labial margin on P4 (e.g., Leptacodon munusculum). A low or undeveloped postcrista extends posterolabially to the ectocingulum, but is low and not raised as a high blade (e.g., Diacocherus, state 2; Fig. 5.44.3).

14. P4 hypocone: undeveloped (0); small and conical (1); enlarged and bulbous (2)
Based on Butler (1988), Frost et al. (1991), Gould (1995), Missiaen and Smith (2005). A hypocone is primitively absent on P4 (e.g., Cimolestes, state 0). A low, conical hypocone is present on P4 of some nyctitheriids, most notably in amphidozotheriines (Sigé, 1976; Hooker and Weidmann, 2000, state 1). An enlarged, bulbous P4 hypocone is known only in the erinaceids and Scenopagus in the present sample (state 2). Ordered.

15. P4 posterior cingulum: weak or undeveloped (0); conspicuous, narrow and ridge-like, or expanded towards lingual margin of crown and shelf-like, extending lingually past level of protoconal apex (1); greatly expanded and lobe-like, projecting posteriorly and labially (2); confluent with postprotocrista (3)
With the exception of Cimolestes and Batodon (state 1; Fig. 5.45.1), all of the taxa in this analysis have a posterior cingulum on P4. In most, the cingulum is low and ridge-like, and expands only slightly towards the lingual margin of the crown (e.g., "Leptacodon" munusculum, state 1; Fig. 5.45.2). In soricids and a number of putative soricomorph taxa (e.g., Amphidozotherium), the cingulum is widely expanded posteriorly and labially, forming an enlarged talon that slopes labially and dorsally (state 2; Fig. 5.45.3). A potentially ambiguous condition occurs in a number of taxa that have P4 bearing a strong crest that comes off of the apex of the protocone, then plunges vertically down the posterior side of the protocone where it then bends labially and continues to the metastylar corner of the crown as a low cingulum (e.g., Macrocranion, state 3; Fig.

5.45.4); a hypocone can be developed at the union of the vertical crest and posterior cingulum. This condition closely resembles the nannopithex fold in many primates, in which the posterior cingulum alone ascends the posterior wall of the protocone (Szalay and Delson, 1979; Silcox, 2001), making the identity of this similar structure in the ingroup sample difficult. The crest originating at the protoconal apex is interpreted here as a postprotocrista, rather than an extended posterior cingulum for the following reason: in some taxa (e.g., Litolestes), the postprotocrista drops vertically, similar to that in Macrocranion, but does not join the posterior cingulum; rather, the postprotocrista terminates just ventral of the posterior cingulum, while the posterior cingulum continues on towards the lingual margin of the crown, and does not ascend the protocone. Echinosorex is coded as state 1 for character 15: although the P4 of Echinosorex superficially resembles that of soricids and amphidozotheriines, the area of the posterior cingulum in Echinosorex (and most erinaceids) is occupied by an enlarged and swollen hypocone (and see character 14), rather than by a posterolabially expanded posterior cingulum.

16. P4 anterior cingulum: very weak or undeveloped (0); prominent (1)

17. P4 paraconule: slightly anterolingual of level of paracone (0); enlarged and anteriorly displaced (1); paraconule undeveloped (2)

Most of the ingroup taxa lack conules on P4. When present, the P4 paraconule is most often lingually opposite or only slightly anterolingual of the level of the paracone (e.g., Xynolestes, state 0). In many nyctitheriids (e.g., Euronyctia) the paraconule is enlarged and considerably anteriorly displaced from the level of the paracone, and juts far anteriorly (state 1). Whether or not conules are primitive for Lipotyphla generally is complicated by the most basal putative soricomorphs (e.g., Leptacodon) lacking conules, but the most basal putative erinaceomorph (e.g., Diacocherus) having them; the absence of conules on P4 may be primitive for eutherians generally (Archibald and Averianov, 2006).

18. P4 metaconule: well developed (0); weakly developed (1); undeveloped (2)

19. P4 postprotocrista: undeveloped (0); steep, extending dorsally towards the base of protocone (1); extending labially (2)

Nearly every ingroup taxon in this analysis that has been previously identified as a soricomorph (e.g., Leptacodon, Amphidozotherium, Centetodon) has a P4 postprotocrista that extends labially towards the metacone (or paracone, should a metacone not be developed, e.g., Centetodon), while the posterior cingulum extends towards the lingual margin of the crown, but separate from the postprotocrista (state 2). In contrast, the P4 postprotocrista of putative erinaceomorphs (e.g., Diacocherus, Litocherus, Adapisorex) extends towards the base of the crown from its origin at the protoconal apex and approaches the posterior cingulum (state 1), and in some taxa (e.g., Macrocranion) the two structures can be confluent. In some taxa (e.g., Asionyctia) the postprotocrista is undeveloped. The P4 postprotocrista in each of the outgroup taxa extends labially from the protoconal apex, suggesting that this is the primitive state.

Upper molars

20. Anterior stylar shelf on M1-2: wide on both (0); narrow on M1, wider on M2 (1); narrow on both (2)

The stylar shelf (that part of the crown intervening between the base of the paracone and metacone and the ectocingulum) is primitively wide anteriorly (i.e., between the paracone and the ectocingulum) on M1 and M2 (e.g., Kennalestes, state 0). Most of the ingroup taxa are derived in having a significantly reduced stylar shelf labial to the paracone on M1 (e.g., "Leptacodon" munusculum, state 1). Erinaceids and a few putative erinaceomorphs (e.g., Adapisorex, Pholidocercus) have an undeveloped stylar shelf on M1 and M2 (state 2).

21. Ectoflexus on M1-2: deep in both (0); shallow in both (1); undeveloped on M1 (labial border virtually straight and obliquely oriented), shallow on M2 (2); undeveloped on both (3)

Based on Bloch et al. (1998), Hooker (2001), Asher et al. (2002). Eutherian upper molars primitively bear a deep ectoflexus that divides the labial margin of the crown into well-

defined parastylar and metastylar lobes (Kielan-Jaworowska et al., 1979; Fox, 1984; Luo et al., 2002; Ji et al., 2002; Archibald and Averianov, 2006) (e.g., Kennalestes, state 0). Most of the ingroup taxa in this study have M1 and M2 with a relatively shallower ectoflexus (e.g., Litocherus, state 1), where the parastylar and metastylar lobes, although defined, are not separated by a deep notch. Crocidura and the amphidozotheriines are unusual in having an undeveloped ectoflexus on M1 (state 2), with the labial margin of the crown straight and oriented oblique to the long axis of the crown. Erinaceids and a few putative erinaceomorphs lack an ectoflexus on M1 and M2 (state 3).

22. Parastylar lobe on M1: strongly anterolabially projecting, not spur-like (0); weakly projecting (1); anteriorly projecting and spur-like (2); anterior margin of the crown flush (3)

Based on Novacek (1985), Hooker (2001), Asher et al. (2002). The M1 parastylar lobe is primitively enlarged, anterolabially projecting, and usually hooked, and the protoconid of the opposing lower molar occludes in the notch between the parastylar cusp and paracone (e.g., Kennalestes, state 0) (Fox, 1984; Archibald and Averianov, 2006); many of the stem lipotyphlans included in this analysis display this character state (e.g., "Leptacodon" munusculum; Fig. 5.46.1). Weaker projecting parastylar lobes (e.g. Litocherus, "Adapisorella", state 1; Fig. 5.46.2) have the parastylar corner of the crown drawn out somewhat, but it does not strongly project past the anterior margin of the crown; in many cases the parastylar "lobe" is no more than a prominent ectocingulum+paracingulum. A parastylar lobe that is flush with the anterior margin of the crown is characteristic of erinaceids and a number of putative erinaceomorphs (e.g., Adapisorex, state 3; Fig. 5.46.4). The M1 of amphidozotheriines and Wyonycteris is unusual in having a strongly anteriorly projecting parastylar lobe, with the labial margin of the crown virtually straight (state 2; Fig. 5.46.3).

23. Molar stylocone: present (0); absent (1)

24. Postmetacrista on M1-2: low crest, not raised and blade-like (0); short and blade-like (1); elongate and blade-like (2); markedly elongate on M1, shorter on M2 (3)

The M1 and M2 postmetacrista in nearly every ingroup taxon is high and blade-like to some degree. As with P4, the postmetacrista is considered short and blade-like when it is elevated as a high blade and extends a short distance labially (e.g., Nayloria, state 1; Fig. 5.47.2); in contrast, an elongate postmetacrista is elevated as a high blade and sweeps posterolabially, jutting well past the labial extent of the parastylar lobe (e.g., "Leptacodon" munusculum, state 2; Fig. 5.47.3). A low or undeveloped postcrista extends posterolabially to the ectocingulum, but is low and not raised as a high blade (e.g., Diacocherus, state 0; Fig. 5.47.1). Soricids and a few putative soricomorphs have the M1 postmetacrista considerably elongated, extending far labially and posteriorly, while the M2 postmetacrista is shorter (e.g., Euronyctia, state 3; Fig. 5.47.4). The M1-2 postmetacrista in erinaceids has traditionally been equated with the condition seen in most soricids (i.e., state 3, markedly elongate on M1, shorter on M2) (Butler, 1988), and although this is true of many derived erinaceids (e.g., Erinaceus), the M1-2 postmetacrista of more basal erinaceids (e.g., Podogymnura, Hylomys, Echinosorex; see Frost et al., 1991) is much shorter and is here scored as state 1.

25. Molar centrocrista: straight (0); incipiently deflected labially (1); fully deflected labially, reaching the ectocingulum (2)

Based on Hooker (2001). The molar centrocrista can be straight in occlusal aspect, with no suggestion of a labial deflection (e.g., Adapisorex, state 0, Fig. 5.48.1), slightly deflected towards the labial margin of the crown and widely V-shaped in occlusal (e.g., Psydronyctia, state 1, Fig. 5.48.2), or fully deflected and narrowly V-shaped in occlusal view (i.e., completely dilambdodont, e.g., Wyonycteris, state 2, Fig. 5.48.3). The 0 state of this character occurs in a majority of the ingroup taxa and all three of the outgroup taxa. Ordered.

26. Molar mesostyle: absent (0); present (1)

Multiple, non-homologous structures have been considered "mesostyles", and these are discussed in more detail in Chapter 8. This character is strictly defined here as a distinct cusp developed on the ectocingulum labial of the centrocrista notch; the mesostyle may (e.g., Euronyctia) or may not (e.g., Pholidocercus) be associated with a labially deflected centrocrista.

27. Size of paracone on M1-2: subequal in size with metacone (0); inflated relative to metacone (1)

The paracone on M1 and M2 of Adapisorex and "Adapisorella" is markedly inflated relative to the metacone.

28. Shape of molar paracone and metacone: subcircular in cross section (0); subcrescentic in cross section (1); fully crescentic (2)

Based on Munthe and West (1980), Gould (2001). The paracone and metacone are primitively circular or subcircular in cross section (state 0). In contrast, the paracone and metacone can be compressed anteroposteriorly, imparting a somewhat crescentic shape to the cross section of the cusps (i.e., the labial side of the cusps is concave) (e.g., Euronyctia, state 1). Fully crescentic cusps are characteristic of soricids (e.g., Crocidura, state 2): in addition to being anteroposteriorly compressed, the labial sides of the paracone and metacone are strongly concave. Ordered.

29. Separateness of molar paracone and metacone: partially connate at base (0); fully separate (1)

Based on Bloch et al. (1998). The paracone and metacone in many primitive eutherians are often connate for about the lower third of their height (e.g., Kennalestes, state 0; see Archibald and Averianov, 2006); with the exception of Batodon, Saturninia, and Amphidozotherium, all of the ingroup taxa display state 1.

30. Position of molar protocone: lingual to centrocrista notch (0); slightly anterior to the level of the centrocrista notch (1); anteriorly displaced to the level of the paracone (2)

Based on Rich (1981), Gould (2001). The protocone can be lingually opposite the centrocrista notch (e.g., Kennalestes, state 0), or slightly anterior to the level of the centrocrista notch (e.g., Leptacodon munusculum, state 1). Most taxa in this analysis have state 0 or state 1. The amphidozotheriines and a few putative soricomorphs differ in having the protocone displaced far anteriorly, such that the protoconal apex is in nearly line with that of the paracone (e.g., Psydronyctia, state 2). Ordered.

31. Size of molar protocone: not enlarged (less than half the labiolingual width of crown), lower than paracone (0); enlarged (half, or greater than half the labiolingual width of crown), subequal or taller than paracone (1)

Based on Hooker (2001). The molar protocone is primitively small and low, occupying less than half of the transverse width of the crown (see Fox, 1984; Paranyctoides, state 0); in contrast, the protocone is much larger and taller in most of the stem lipotyphlans included in this analysis, occupying greater than half of the labiolingual width of the crown (e.g., Litocherus, state 1).

32. Molar anterior cingulum: weak or undeveloped (0); ridge-like (1); flaring anteriorly (2)

Based on Missiaen and Smith (2005). Nearly all of the ingroup taxa have a moderately developed anterior cingulum and exhibit state 1 (e.g., Leptacodon munusculum). In a few taxa (e.g., Nyctitherium) the anterior cingulum is much better developed and flares anteriorly. Although a weak or undeveloped anterior cingulum is probably primitive for Eutheria (Kielan-Jaworowska et al, 1979; Fox, 1984; Ji et al., 2002; Archibald and Averianov, 2006), two of the three outgroup taxa included here (Kennalestes, Prodiacodon) display state 1.

33. Molar pericone: absent (0); present (1)

34. Posterior cingulum on M1-2: undeveloped (0); ridge-like or weakly expanded lingually (1); conspicuously expanded lingually, not lobate (2); greatly expanded and lobate (3)

Based on Bloch et al. (1998), Missiaen and Smith (2005). Most of the ingroup taxa exhibit state 2 and have a posterior cingulum that widens conspicuously posteriorly towards the lingual margin of the crown (e.g., Litocherus, state 2; Fig. 5.49.3); the posterior cingulum may (e.g., Wyonycteris) or may not (e.g., Leptacodon tener) support a hypocone. Taxa having an enlarged hypocone were coded as having a conspicuously widened but non-lobate posterior cingulum (e.g., Scenopagus). Soricids, amphidozotheriines, and a few other nyctitheriids (e.g., Nyctitherium) have a posterior cingulum that is greatly expanded posteriorly and labially, forming a lobe-like talon (state 3; Fig. 5.49.4). A number of taxa included in the ingroup have a ridge-like posterior cingulum that does not widen lingually (e.g., "Leptacodon" munusculum, state 1, Fig. 5.49.2). The upper molars of Cimolestes lack a posterior cingulum (state 0; Fig. 5.49.1). Ordered.

35. Hypocone on M1-2: undeveloped (0); small and uninflated (1); swollen (2); extremely swollen (3)

Based on Gould (2001), Asher et al. (2002). In most of the ingroup taxa the hypocone is small and subconical, uninflated, and does not bulge lingually (e.g., Leptacodon rosei, state 1). Taxa with a markedly expanded talon (e.g., Amphidozotherium, Crocidura) are also coded as state 1, as the hypocone is only weakly developed [this contrasts the coding decision of Asher et al. (2002), who considered the enlarged posterior cingulum of soricids as an equivalent of the hypocone proper]. In contrast, many of the putative erinaceomorphs (e.g., Litocherus) have a hypocone that is swollen, and as a result appears more closely appressed to the protocone; the lingual side of the hypocone in these taxa bulges slightly, and the hypocone and protocone are incipiently separated as distinct lobes (state 2). The hypocone in some taxa (e.g., Adapisorex, Echinosorex) is markedly swollen and enlarged such that it nears the dimensions of the protocone (state 3), and bulges lingually, forming a distinct hypoconal lobe. Ordered.

36. Molar hypocone crest: absent (0); present (even incipiently) (1)

Based on Butler (1948), Rich (1981), Novacek (1985), Storch and Qui (1991), Gould (1995, 2001). The hypocone crest extends from the hypocone to the posterior wall of the

protocone, connecting the two cusps. The hypocone crest is best seen in Echinosorex in which it is high and sharp. Novacek (1985) coded all of the non-galericine, brachyericine, and erinaceine erinaceomorphs as lacking the hypocone crest [the hypoconid (sic!) crest of Novacek, 1985], but a weak crest is sometimes developed in specimens of Scenopagus and Macrocranion. The crest is apparently not restricted to erinaceomorphs, as it occurs in specimens of Leptacodon tener (see McKenna, 1968) and Pontifactor (West, 1974; Krishtalka, 1976b); it is also developed in the indeterminate genus and species from DW-2 (see earlier in the text).

37. Conules on M1-2: paraconule slightly anterolingual of level of paracone (0); paraconule offset anteriorly (1); paraconule absent (2); both conules absent (3)

The paraconule is most often only slightly lingual of the level of the paracone, and it is not conspicuously enlarged (e.g., Nayloria, state 0). In contrast, the paraconule can be notably offset anteriorly such that it is well past the level of the paracone, and is enlarged relative to the metaconule (e.g., Psydronyctia, state 2). The paraconule in Sespedectes and Echinosorex is undeveloped (state 2), while both conules are absent (state 3) in Crocidura and at least some specimens of the nyctitheriid Saturninia.

38. Conular cristae on M1-2: internal and external conular wings conspicuous on both conules (0); internal conular wings weak or absent on both conules (1); metaconular cristae present only (2); paraconular and metaconular cristae absent (3)

Based on Missiaen and Smith (2005). Conular cristae (i.e., external and internal conular "wings") are present on M1 and M2 primitively (Fox, 1984; Archibald and Averianov, 2006), although they are generally poorly developed, especially the internal wings; shallow, concave conular basins are formed between the external and internal wings (state 0). Most of the ingroup taxa have conspicuous internal and external conular wings (e.g., "Leptacodon" munusculum), although in some taxa (e.g., Saturninia) the internal wings are undeveloped (state 1), or with internal and external wings being undeveloped (e.g., Sespedectes). Saturninia is unusual in sometimes having external conular wings, but lacking the conules themselves.

39. Parastylar lobe on M3: projecting (0); reduced (1)

Based on Novacek (1985), Gould (1995, 2001). The parastylar lobe on M3 is well-developed relative to the metastylar lobe, and projects anteriorly and labially in most of the ingroup taxa (e.g., "Leptacodon" munusculum, state 0). In contrast, the parastylar lobe is greatly reduced in some taxa (e.g., Adapisorex), and projects no farther labially than does the metastylar lobe.

Dentary

40. Number of mental foramina: one (0); two (1); greater than two (2)

41. Angular process size and shape: short, spike-like (0); elongate, hook-like (1); expanded posterodorsally, broadly rounded (2)

The angular process is poorly known for most of the ingroup taxa, but where known it is surprisingly diverse in size and shape, implying differences in both the relative development and insertion of the adductor musculature; these differences in turn suggest functional differences with respect to mastication. Most of the ingroup taxa exhibit state 1; Pholidocercus is apparently unique in having an angular process that is enlarged and rounded (state 2), similar to that in many ungulates (Radinsky, 1985).

42. Condyle shape: spherical (0); transverse (1)

Based on McDowell (1958), Butler (1988), Asher et al. (2002). The mandibular condyle has figured importantly in the systematics of soricids and their putative extinct relatives, as well as in the systematics of zalambdodonts (see Asher et al., 2002). The condyle is more or less spherical in a number of taxa (e.g., Diacocherus, state 0); although this is probably the primitive condition for eutherians generally (e.g., a spherical condyle is known for the asioryctithere Uchkudukodon, see Archibald and Averianov, 2006), it is unknown for each of the outgroup taxa used in this analysis. In contrast, many of the ingroup taxa have a condyle that is transverse relative to its length (e.g., Litolestes, state 1). The condyle in many soricids, as well the geolabidid Centetodon, is functionally bifid, with the articular facets being incipiently (e.g., Centetodon) or almost fully (e.g.,

Crocidura) divided into upper and lower parts (McDowell, 1958; Repenning, 1967; Lillegraven et al., 1981; Asher et al., 2002); the basic structure of the condyle in either of these instances is, however, transverse, rather than ball-shaped, and the condyle in Centetodon and Crocidura is coded here as state 1.

Lower incisors

43. Crown of i1: peg-like, crown not expanded apically (0); subspatulate, crown expanded apically (1); concavoconvex main cusp and small heel separated by deep fissure (2); elongate concavoconvex crown with multiple lobes (>2), each separated by a deep fissure (3); enlarged and elongate, blade-like (4)

Most of the stem lipotyphlans where such information is known have state 1, 2, or 3. The coronal anatomy of i2 was not included as a separate character because all taxa in which i1-2 are known show the same state for both teeth, although in those with multilobate incisors, the number of lobes may differ between the two teeth, usually with i2 having a greater number of lobes. Amphilemurids, Diacocherus, and galericines have simple, unmodified lower incisors that are subspatulate, with the crown mediolaterally expanded towards the apex. Taxa exhibiting state 2 have i1 with a mitten-shaped crown, with a somewhat elongate main cusp that is convex anterolaterally and concave posteromedially, and a heel developed posterior to the main cusp and is separated from it by a deep fissure (e.g., Leptacodon munusculum, Xynolestes); the heel can be taller, as it is in Centetodon (see Lillegraven et al., 1981, fig. 12), and the crown appears somewhat bilobed. In other taxa (e.g., Ceutholestes, Amphidozotherium), the crowns of i1-2 are multilobate, with the number of lobes being variably developed, but always greater than two (state 3); the occurrence of state 3 in the putative erinaceomorph Litolestes suggests that multilobate incisors have evolved independently. Soricids are the only lipotyphlans examined here with lower incisors that exhibit state 4; a multilobate i1 has evolved independently in a number of extant and extinct soricids (e.g., Sylvisorex, see Repenning, 1967), but basal soricids (e.g., Domnina, Crocidura) have an elongate, blade-like crown with no lobes or serrations.

44. Size of i2: subequal to i1 (0); larger than i1 (1); smaller than i1 (2)

Based on Bloch, Secord, and Gingerich (2004).

45. Size of i3: subequal to i2 (0); much smaller than i1 and i2 (1); larger than i2 (2)

Lower canine

46. Lower canine: enlarged, caniniform (0); small (subequal or slightly larger than p1 or next posterior tooth), procumbent, premolariform (1)

Many taxa have a lower canine that is enlarged and caniniform, having a tall, laniary or slightly mediolaterally compressed principal cusp that is recurved (e.g., Nayloria, state 0); in contrast, some taxa have a lower canine that is smaller, procumbent, and with a crown that more closely resembles the p1 or p2 (e.g., Leptacodon rosei, state 1). In many cases the size of the lower canine had to be estimated from the dimensions of its alveolus: a lower canine with an alveolus that is significantly larger than that for p1 or the combined alveoli for p2 (should p1 be absent) was scored as state 0. The size and anatomy of the lower canine had to be scored separately from those of the upper canine because of the situation in Macrocranion, where the upper canine is caniniform, while the lower canine is premolariform (see Novacek et al., 1985).

Lower premolars

47. Premolar lingual cingulids: absent (0); present (1)

Lingual cingulids are defined here as shelf-like crests that continue posteriorly from the lingual side of the paraconid. Lingual cingulids are best seen in Limaconyssus and Psydronyctia.

48. Dimensions of p1-3: long relative to width (0); short relative to width (1)

Putative soricomorphs (e.g., "Leptacodon" munusculum) have anterior lower premolars crowns that are long relative to their width, and appear more or less blade-like (state 0); conversely, the anterior lower premolars of most putative erinaceomorphs (e.g., Litolestes) are short relative to their width, with a widely expanded posterior margin; the crowns in these taxa appear wedge-like in occlusal aspect.

49. p2-3 crowns: nearly vertical (0); procumbent (1)

In most of the ingroup taxa the anterior lower premolars are nearly vertical, with the anterior margin of the crown erect and not strongly overhanging the posterior parts of the preceding tooth (e.g., Leptacodon, Centetodon, state 0; Fig. 5.50.1). The anterior lower premolar crowns in some taxa, however, are procumbent, being anteriorly extended, with the anterior margins strongly overlapping the posterior parts of the preceding tooth (e.g., Xynolestes, Scenopagus, state 1; Fig. 5.50.2); the crowns are subrectangular in labial outline (i.e. they appear as rectangles that are oriented anterodorsally, with long, parallel posterodorsal and posteroventral slopes, and shorter anterior and posterior slopes, see Schwartz and Krishtalka, 1976).

50. Size of p2: subequal or slightly smaller (>half the size) than p3 (0); larger than p3 (1); much smaller (half the size or less) than p3 (2)

The p2 can be subequal or only slightly smaller than p3 (e.g., "Leptacodon" munusculum, state 0) or larger than p3 (e.g., Leptacodon rosei, state 2). In some taxa (e.g., Amphidozotherium) the p2 is greatly reduced compared to p3 (state 3).

51. Size of p3: subequal or slightly smaller (>half the size) than p4 (0); approximately half the size of p4 (1); smaller (<half the size) than p4, crown not peg-like (2); smaller (<half the size) than p4, crown peg-like (3)

Most of the ingroup taxa have p3 that is only slightly smaller than p4 (e.g., Leptacodon munusculum, Sespedectes, state 0) or about half the size of p4 (e.g., Litocherus, Dartonius). The amphilemurids and the amphidozotheriine Amphidozotherium are unusual in their p1-3 being small and peg-like (state 3).

52. Paraconid on p3: weak (0); well-developed (1); paraconid absent (or paracristid only) (2)

The p3 paraconid is weak or absent in a majority of ingroup taxa (e.g., Euronyctia, state 0; Sespedectes, state 2). In some taxa the p3 paraconid is much better developed, being both larger and projecting well above the base of the crown (e.g., Psydronyctia, state 1).

53. Talonid on p3: unicuspid, no basin (0); unicuspid, weakly basined (1); bicuspid, basined (2)

The p3 talonid is primitively unicuspid and unbasined (e.g., Kennalestes, state 0); in some taxa (e.g., Leptacodon rosei) a weak basin may be present (state 1) [a basin here refers to a depression formed between a labial cristid obliqua and a lingual crest (?entocristid)]. A bicuspid, basined talonid on p3 is autapomorphic for Ceutholestes (state 2).

54. Size of p4: subequal to m1 (0); larger than m1 (1); smaller (about half the size) than m1 (2)

55. Origin of p4 paraconid: low (0); high (1); paraconid absent (2)

When present, the paraconid on p4 can originate relatively low on the trigonid (e.g., "Leptacodon" munusculum, state 0; Fig. 5.51.1) or relatively high (e.g., Litolestes, state 1; Fig. 5.51.2). Most of the taxa that have been regarded as soricomorphs have a low paraconid, while those that have been considered erinaceomorphs have a higher paraconid. The p4 paraconid was considered "high" in this analysis when the posterior side of the paraconid joins the protoconid at a relatively high position; in taxa with a "low" paraconid, the paraconid and protoconid are separated from each other nearly to the base of the trigonid. The absolute size of the paraconid is decoupled from its origin on the trigonid (i.e., although the paraconid can originate at a relatively low position on the trigonid, it can be strongly developed, with its apex nearly at the same level as that on a paraconid that arises from a relatively high position on the trigonid).

56. Development of p4 paraconid: weak (0); moderately developed (1); strongly developed (2)

Based on Butler (1948), Rich (1981), Gould (1995, 2001). Character 56 describes the overall size of the paraconid on p4, irrespective of where it originates on the protoconid. In some taxa (e.g., Batodon), the p4 paraconid is poorly developed and barely projects above the base of the trigonid (state 0); in contrast, many of the other ingroup taxa have a p4 paraconid that is significantly better developed. A moderately developed p4

paraconid is approximately one fourth to one third the height of the protoconid as measured from base to apex of each cusp [e.g., Litocherus notissimus and Adeloxenus; state 1]; in contrast, a strongly developed paraconid is large and nearly half the height of the protoconid [e.g., "Leptacodon" munusculum, Limaconyssus; state 2].

57. Position of p4 paraconid: anterior and separated from protoconid (0); anterolingual and appressed to protoconid (1); lingual (2); offset obliquely anterolingually (3)

Based on Gould (1995, 2001), Bloch et al. (1998). The p4 paraconid is distinctly separate and anteriorly positioned in a majority of ingroup taxa (e.g., Psydronyctia, state 0; Fig. 5.52.1); in these taxa, the p4 paraconid is on, or only slightly lingual, to an imaginary line drawn parasagittally through the protoconid apex. In contrast, the paraconid in taxa with a more fully molariform p4 (e.g., Leptacodon rosei, state 2; Fig. 5.52.3) is positioned significantly lingual to an imaginary line drawn parasagittally through the protoconid apex. In a few taxa (e.g., Litocherus) the p4 paraconid is anterolingually positioned, but closely appressed to the base of the protoconid (state 1; Fig. 5.52.2). Galericines are unique in having the p4 paraconid displaced obliquely anterolingually, lengthening the paracristid blade (state 3; Fig. 5.52.4).

58. Metaconid on p4: absent (0); small, weakly differentiated from protoconid (1); well-developed, clearly differentiated from protoconid and separated by a deep protocristid notch (2); fully separate from protoconid (3)

Based on Bloch et al. (1998), Archibald and Averianov (2006). In contrast to the more ambiguous polarity of the P4 metacone, the p4 metaconid is likely primitively absent in eutherians (Ji et al., 2002; Archibald and Averianov, 2006), and this cusp is not present in Kennalestes or Cimolestes (state 0; Fig. 5.53.1). Most of the ingroup taxa have p4 with a metaconid. The metaconid is considered weakly developed if only the apex is clearly differentiated from the lingual shoulder of the protoconid (e.g., Litocherus, state 1; Fig. 5.53.2). A well-developed metaconid is further differentiated from the protoconid: the two cusps are separated by a deeply notched protocristid, and a deep sulcus is developed between the two cusps anteriorly (e.g., Limaconyssus, state 2; Fig. 5.53.3). A fully

separated metaconid is seen in taxa that have a fully molariform p4 (e.g., Ceutholestes, Prodiacodon, state 3; Fig. 5.53.4). Ordered.

59. Position of p4 metaconid: lingual to protoconid (0); posterolingual to protoconid (1); anterolingual to protoconid (2)

Based on Butler (1988).

60. Width of p4 talonid basin: basin wide (>half the width of trigonid) (0); basin moderately wide (approximately half the width of trigonid) (1); narrow (approximately one third the width of trigonid) (2); basin absent, single cusp or postcristid only (3); basin wider than trigonid (4)

Basin width was measured as a standard maximum labiolingual distance from the hypoconid to the lingual margin of the talonid; this distance was then compared to the maximum labiolingual width of the trigonid. The distance of the basin was measured from the hypoconid, rather than from the cristid obliqua, because the cristid obliqua can vary in its position as it extends from the hypoconid to the postvallid wall. If the hypoconid is absent on p4, then the maximum distance between the labial and lingual crests of the talonid basin was used. Most of the ingroup taxa that have been previously considered soricomorphs have a wide (e.g., Leptacodon rosei, state 0) or moderately wide (e.g., "Leptacodon" munusculum, state 1) talonid basin; in contrast, most of the putative erinaceomorphs have a narrow talonid basin (e.g., Litolestes, state 2). Ceutholestes is autapomorphic in having a talonid basin that is wider than the trigonid (state 4).

61. Length of p4 talonid basin: short (less than or equal to half the length of trigonid) (0); long (greater than half the length of trigonid) (1)

Basin length was measured from the postvallid wall to either the anterior margin of the hypoconulid (this reduces overestimating the basin length because of posteriorly leaning hypoconulids), or to the postcristid if a hypoconulid is not present; this distance was then compared to the maximum anteroposterior length of the trigonid. Although it seems intuitive that basin length and width might be correlated, there are a number of taxa where the talonid can be long, but notably narrow (e.g. Limaconyssus).

62. Position of p4 entoconid: absent (0); lingual (1); posterolingual (2); offset labially (3)

A lingually positioned entoconid is developed lingually opposite or slightly anterior of the level of the hypoconid (e.g., "Leptacodon" munusculum, state 1). A posterolingual entoconid occurs near the posterolingual margin of the talonid, and the entoconid, hypoconid, and hypoconulid (when present) are nearly transversely in-line across the posterior margin of the talonid (e.g., Diacocherus, state 2). In some taxa (e.g., Limaconyssus), the p4 entoconid is labially offset from the lingual margin of the crown, and the talonid appears somewhat "twisted" or labially skewed (state 3).

63. Size of p4 hypoconid: largest (or sole) talonid cusp (0); subequal or smaller than entoconid (1); hypoconid undeveloped (2)

64. Size of p4 hypoconulid: poorly differentiated or absent (0); conspicuous (1)

65. Posterior exodaenodonty on p4: undeveloped (0); shallow (1); deep (2)

Although this character is somewhat intragenerically variable, there are notable differences in this character among the ingroup taxa. Degree of exodaenodonty was measured by comparing the ventral extent of the posterior lobe (where developed) on p4 with the base of the enamel at the anterior root of p4. If the p4 lobe was equal or extended only a short distance below the base of the enamel at the anterior root, the lobe was considered shallow (e.g., Oncocherus, state 1); in contrast, if the lobe extended well below the base of the enamel at the anterior root of p4, the lobe was considered deep (e.g., Xynolestes, Litolestes, state 2). Ordered.

66. Contact of p4 cristid obliqua and postvallid wall: absent (0); at or slightly labial to the level of the protocristid notch (1); lingual to notch (2); lingual and continuing towards metaconid summit (3)

Lower molars

67. Height of molar trigonid: much taller than talonid (0); lower, trigonid and talonid closer in height (1); trigonid very low, talonid and trigonid nearly equal in height (2)

Based on Rich (1981), Bloch, Secord, and Gingerich (2004). Trigonid height was assessed by comparing the height of the tallest talonid cusp (from base of the enamel to apex) to that of the tallest trigonid cusp (from base of the enamel to apex). If the height of the tallest trigonid cusp was greater than half the height of the tallest talonid cusp, the trigonid was considered to be much taller (e.g., Cimolestes, state 0; Fig. 5.54.1); if the height of the tallest talonid cusp was approximately half that of the tallest trigonid cusp, the trigonid was considered lower (e.g., "Leptacodon" munusculum, state 1; Fig. 5.54.2); and if the tallest talonid cusp was over half the height of the tallest trigonid cusp, the trigonid was considered very low (e.g., Adapisorex, state 2; Fig. 5.54.3). Nearly all of the ingroup taxa have molar trigonids that are relatively low, with most of the putative erinaceomorphs having very low trigonids. Ordered.

68. Inclination of molar trigonid: subvertical (0); steeply inclined (1); shallowly inclined (2)

The inclination of the trigonid was measured by drawing an imaginary line longitudinally along the lingual side of the crown, and one drawn paralleling the postvallid wall; the intersection of these two lines forms an angle that represents the inclination of the trigonid. The angle of trigonid inclination in some taxa is nearly 90 degrees, or subvertical (e.g., Cimolestes, state 0; Fig. 5.54.1), while in others the angle is closer to 100 or 110 degrees (e.g., Leptacodon munusculum, state 1; Fig. 5.54.2); in some taxa the angle of inclination is extremely large, approaching 120 degrees or more (e.g., Adapisorex, state 2; Fig. 5.54.3). Ordered.

69. Valley facing sides of trigonid cusps: flat or slightly concave (0); somewhat swollen (1); markedly convex (2)

Ordered.

70. Molar metaconid height: metaconid subequal in height to protoconid on m1, subequal or becoming slightly taller than protoconid on m2-3 (0); metaconid taller than protoconid on m1, becoming much taller than protoconid on m2-3 (1)
Based (in part) on Bloch et al. (1998).

71. Molar metaconid size: not appreciably inflated relative to protoconid (0); inflated relative to protoconid (1)

72. Molar paraconid origin: low (0); high (1)
The origin of the molar paraconid on the trigonid was determined by examining the level of the notch between the paraconid and its union with the metaconid in lingual view: in those taxa with a high paraconid (e.g., Diacocherus, state 1; Fig. 5.55.2), this notch is usually at or slightly higher than the level of the preceding talonid (hypoconulid or postcristid), whereas in those with the low state (e.g., "Leptacodon" munusculum, state 0; Fig. 5.55.1), the paraconid occurs below this level, and the metaconid and paraconid are separated almost to their bases. This method proved more effective at determining the position of the paraconid on the trigonid than that based on the position of the paracristid notch: in many taxa (e.g., Limaconyssus) the paracristid notch can be high, but the paraconid itself originates at a relatively low position on the trigonid, and is fully separate from the metaconid.

73. Form of the m1 paraconid/paracristid: anteroposteriorly compressed (0); ridge- or shelf-like (1); strongly blade-like (2)
Based on Krishtalka (1976a-b), Novacek et al. (1985), Butler (1988). Nearly all of the taxa examined in this analysis have an anteroposteriorly compressed m1 paraconid and paracristid (e.g., "Leptacodon" munusculum, state 0). A distinction has sometimes been made between a paraconid/paracristid that is "crestiform" and one that is "lophiform" (see, e.g., Krishtalka, 1976a-b; Novacek et al., 1985), but the difference seems to be one related only to the overall degree of cusp swelling (i.e., those taxa that have swollen cusps also tend to have "lophiform" paraconid/paracristids); the basic anatomy of the paraconid/paracristid in either case is anteroposterior compression. Taxa that have been

previously considered "dormaaliids" (see Novacek, 1985; Novacek et al., 1985) have an m1 paraconid/paracristid that is reduced to a low ridge or shelf (e.g., Scenopagus, state 1); this has presumably been independently acquired in the nyctitheriid Ceutholestes (see Gingerich and Rose, 1982). Galericines and soricids have m1 with a hypertrophied, blade-like paraconid/paracristid (state 3). The form of the m1 paraconid/paracristid does not covary with that in m2-3; as such, they are coded separately.

74. Shape of m1 paracristid: nearly transverse (0); flexed (1); greatly elongate, displaced obliquely anteriorly (2)

Based on Novacek (1985), Butler (1988), Gould (1995). In the transverse state (0), the paracristid extends nearly directly lingually from its origin on the protoconid, with the two arms of the paracristid (paraconid and protoconid) forming an obtuse angle that can approach 180 degrees in some taxa, and the trigonid is somewhat anteroposteriorly compressed. State 0 is seen most clearly in "Leptacodon" munusculum and Limaconyssus (Fig. 5.56.1), and in the erinaceomorphs Scenopagus and Macrocranion (where the paraconid and paracristid form a long ridge that is appressed to the metaconid). A strongly flexed paracristid (state 1) has the protoconid arm and paraconid arm of the paracristid uniting to form an angle of approximately 90 degrees (i.e., the paracristid is directed anteriorly from its origin on the protoconid, then abruptly bends lingually), and the trigonid has a more nearly quadrate occlusal outline. The flexed state is seen most clearly in the adapisoricines Adapisorex (Fig. 5.56.2) and "Adapisorella", and in some soricomorphs (e.g. Leptacodon rosei). In soricids, galericines, and Entomolestes (Fig. 5.56.3), the paracristid blade is greatly elongate and runs obliquely anterolingually, increasing the area of the prevallid surface for shear. As with the previous character, the shape of the m1 paracristid does not covary with that in m2-3, and they are coded separately.

75. Position of m1 metaconid: lingual of protoconid (0); anterolingual to protoconid (1); posterolingual to protoconid (2)

Nearly all of the ingroup taxa exhibit state 0 or state 2. State 1 is characteristic of Echinosorex and Crocidura, but also Entomolestes; Butler (1988) has suggested that, on

the basis of characters 74 and 75, the Tupaiodontinae (including Entomolestes) may be closely related to galericines.

76. Form of the m2-3 paraconid/paracristid: anteroposteriorly compressed (0); ridge- or shelf-like (1)

77. m2-3 paracristid/paraconid shape: nearly transverse (0); flexed (1); greatly elongate, displaced obliquely anteriorly (2)

78. Talonid dimensions on m1-2: about as long as wide (0); short relative to width (1)

The talonid on m1-2 can be nearly as wide as it is long (e.g., Adapisorex, state 0), or conspicuously wider relative to length (e.g., Scenopagus, Xynolestes, state 1).

79. Molar talonid basin: deeply rounded, concave (0); deep and angular (1); high and platform-like (2)

Based on Krishtalka (1976a-b), Gingerich (1983), Novacek et al. (1985). The majority of ingroup taxa have molar talonids that are deeply concave (e.g., "Leptacodon" munusculum, state 0). Krishtalka (1976a) noted that the molar talonids of erinaceids (to which he referred Litolestes ignotus, Leipsanolestes, and Entomolestes) were characterized by deeply V-shaped basins formed by the flat internal walls of the hypoconid and entoconid (state 1); Novacek et al. (1985) agreed, and referred a number of poorly known lipotyphlans from the Eocene of North America to the Erinaceidae, as well as Adapisorex and Neomatronella from the Paleocene of France. Novacek et al.'s (1985) opinion regarding Adapisorex is not followed here: the molar talonid basin of Adapisorex, as well as that in "Adapisorella", is not deeply excavated, but rather is extremely shallow, and the occlusal surface is nearly horizontal and platform-like; this is particularly evident on the molars of Adapisorex (state 2).

80. Talonid width on m1-2: subequal or only slightly wider than trigonid (0); notably wider than trigonid (1); notably wider on m1, subequal or narrower on m2 (2)

81. Cristid obliqua position: joins postvallid wall below protocristid notch (0); joins postvallid wall labial to protocristid notch (1); joins postvallid wall lingual to protocristid notch (2); joins postvallid wall lingual to protocristid notch, extending a short distance dorsally; deep sulcus formed on the posterior wall of metaconid (3)
Based on Bloch et al. (1998). The cristid obliqua can join the postvallid wall just ventral the protocristid notch (e.g., Leptacodon dormaalensis, state 0), ventral and slightly labial to the level of the notch (e.g., Scenopagus, state 1), or ventral and lingual to the notch (e.g., Nayloria, state 2). An unusual condition is seen in a number of putative soricomorphs (e.g., Wyonycteris, Euronyctia) in which the cristid obliqua contacts the postvallid wall ventrolingual to the protocristid notch, but then continues dorsally towards the summit of the metaconid; a deep fold in the enamel on the posterior wall of the metaconid is formed, creating a long, dorsolingually-ventrolabially sloping gutter that parallels the cristid obliqua (state 3).

82. Molar cristid obliqua shape: arcuate (0); angular (1)
The cristid obliqua in most of the ingroup taxa is concave dorsally and appears smoothly arcuate in labial view (e.g., Litocherus, state 0). A few taxa, however, have an unusual cristid obliqua: it is nearly vertical as it descends from the apex of the hypoconid, but becomes horizontal as it runs anterolingually towards the postvallid wall, then abruptly angles dorsally as it scales the trigonid lingual of the protocristid notch (e.g., Xynolestes, state 1).

83. Molar ectocingulid: absent (0); present (1)
The ectocingulid is scored as present only if it is continuous labially (i.e., extends posteriorly past the hypoflexid and joins the posterior cingulid).

84. Molar entocristid notch: virtually undeveloped, talonid fully open lingually (0); well-developed, talonid notch acute and sharply V-shaped (1); high, talonid basin closed lingually (2)

85. Molar postcristid: present (0); absent (1)

The postcristid connects the entoconid and hypoconulid, and can be well developed (e.g., Prodiacodon) or more weakly developed (e.g., Leptacodon rosei); both are coded as present (state 0). In contrast, a number of ingroup taxa lack a postcristid, and the entoconid and hypoconulid are separated by a notch or fissure (e.g., Xynolestes, state 1); an undeveloped postcristid is equivalent to the nyctalodont condition of Menu and Sigé (1976).

86. Molar entoconid height: much lower than tallest trigonid cusp (0); about half the height of the tallest trigonid cusp (1); taller than half the height of tallest trigonid cusp, vertical (2); tall, slightly lower than tallest trigonid cusp, leaning lingually (3)

Based on Krishtalka (1976a-b), Bown and Schankler (1982), Novacek (1985), Novacek et al. (1985), Hooker (2001). The height of the entoconid has figured importantly in the systematics of early lipotyphlans, with a tall entoconid usually being considered characteristic of erinaceomorphs, while a shorter entoconid being more typical of soricomorphs. A closer inspection of the distribution of this character state, however, suggests that a tall entoconid is more taxonomically widespread, with the putative soricomorph Leptacodon tener, and even soricids having a relatively tall entoconid. In most of the putative soricomorphs, the entoconid is about half the height of the tallest trigonid cusp (e.g., Leptacodon munusculum, state 1), whereas in most of the putative erinaceomorphs it is taller than half the height of the tallest trigonid cusp (e.g., Litocherus, state 2); in some erinaceomorphs (e.g., Macrocranion) the entoconid is both tall and lingually leaning (state 3; assessed by examining the entoconid and protoconid apices: a lingually leaning entoconid has its apex displaced lingually such that, when viewed in occlusal aspect, the crown appears slightly constricted between the trigonid and talonid on the lingual side of the crown). The entoconid is short (state 0) in the

outgroup taxa, and this state is also present in Asionyctia, geolabidids (e.g., Centetodon), and a number of nyctitheriids (e.g., Amphidozotherium).

87. Entoconid position on m1 and m2: lingual, nearly transversely opposite the hypoconid (0); posterolingual, nearly directly lingual to hypoconulid (1); slightly labial to the lingual margin of the crown

Based on Butler (1972), Krishtalka (1976a). The talonid cusps are primitively equidistant from one another (Kielan-Jaworowska et al., 1979; Fox, 1984), as they are in each of the outgroup taxa (e.g., Kennalestes), with the entoconid opposite the hypoconid (i.e., in a relatively lingual position, state 0). The entoconid can be offset posteriorly such that the three talonid cusps form a near straight line at the posterior margin of the talonid (e.g., Diacocherus, Scenopagus, state 1), with the entoconid slightly posterior to an imaginary line drawn labiolingually through the hypoconid. In some specimens of Saturninia gracilis, the entoconid is offset slightly labially, and the talonid appears somewhat "twisted", similar to that in palaeoryctids.

88. Molar hypoconid height: subequal or lower than entoconid (0); tallest talonid cusp (1)

89. Anteroposterior compression of molar hypoconid and protoconid: not compressed (0); compressed (1)

The protoconid and hypoconid are strongly compressed anteroposteriorly in a number of the ingroup taxa (e.g., Amphidozotherium, Psydronyctia, state 1), and appear as near-vertical pillars in labial or lingual view.

90. Hypoconulid size and height on m1-2: tall and finger-like (0); low, inflated and somewhat anteroposteriorly compressed (1); small, nearly incorporated into hypocristid (2); hypoconulid absent (3)

91. Hypoconulid position on m1-2: central (0); slightly lingual (1); well lingual, close to or abutting entoconid (2)

The molar hypoconulid is primitively equidistant from the entoconid and hypoconid (Fox, 1984) (e.g., Centetodon, state 0), but it is lingually displaced to various degrees in most of stem lipotyphlans examined here. The hypoconulid can be slightly lingual of the midlongitudinal axis of the crown (e.g., Leptacodon munusculum, state 1), or much farther lingual and nearly abutting the entoconid (e.g., Psydronyctia, Wyonycteris, state 2). Ordered.

92. Molar anterior cingulid: well-developed (0); weak or absent (1)

93. Molar posterior cingulid: absent or weak (0); prominent and shelf-like (1)
Most of the stem lipotyphlans in this analysis lack a well-developed posterior cingulid (e.g., Xynolestes, state 0). Taxa coded as state 1 for this character exhibit a well-developed, shelf-like posterior cingulid that usually show signs of heavy wear; state 1 is best seen in the galericines (e.g., Echinosorex, state 1).

94. Size of m2: subequal or slightly larger than m1 [$\ln(Lm1 \times Wm1)/(Lm2/Wm2) \leq 0$] (0); smaller than m1 [$0 < \ln(Lm1 \times Wm1)/(Lm2/Wm2) \leq 1$] (1); greatly reduced relative to m1 [$\ln(Lm1 \times Wm1)/(Lm2/Wm2) > 1$] (2)
States for this character were assessed using the formula in Scott (2006). Ordered.

95. Size of m3: subequal or slightly smaller than m2 [$\ln(Lm2 \times Wm2)/(Lm3/Wm3) \leq 0.1$] (0); smaller than m2 [$0.2 < \ln(Lm2 \times Wm2)/(Lm3/Wm3) \leq 0.35$] (1); greatly reduced relative to m2 [$\ln(Lm2 \times Wm2)/(Lm3/Wm3) > 0.4$] (2)
States for this character were assessed using the formula in Scott (2006). Ordered.

96. Width of m3 talonid: subequal or slightly narrower than trigonid (0); much narrower (1)

97. Position of m3 hypoconulid: central or slightly lingual of centre (0); well lingual of centre, appressed to entoconid (1); hypoconulid undeveloped (2)

98. Size and form of m3 hypoconulid: enlarged, finger-like, posteriorly projecting (0); subequal to other talonid cusps, not projecting (1); small and partly merged with entoconid, forming a weak lobe (2)

Based on Bloch, Secord, and Gingerich (2004). The hypoconulid on m3 is large and finger-like in primitive eutherians, projecting strongly dorsally and posteriorly (Fox, 1984); many of the stem lipotyphlans in this analysis exhibit this character state (e.g., Diacocherus; Fig. 5.57.1). In contrast, the m3 hypoconulid can be significantly reduced in size, and not project posterodorsally (e.g., Oncocherus, state 1; Fig. 5.57.2). Adapisorex, "Adapisorella", and Adeloxenus are unusual in having an m3 hypoconulid that is small and appressed to the entoconid, and the two cusps partly coalesce into a weak, posteriorly projecting lobe (state 2; Fig. 5.57.3).

5.3.3 Taxon Sample

General comments.—This analysis focuses on the interrelationships of stem lipotyphlans, particularly those taxa of Paleocene age from North America. Two starting assumptions are made: Lipotyphla are considered a monophyletic clade following the opinions of Novacek (1986) and McKenna and Bell (1997). This assumption may or may not be valid, but the testing of lipotyphlan monophyly would entail including a number of additional, non-lipotyphlan taxa in this analysis; this would be a mammoth undertaking, and is clearly beyond the scope of this study. Because of the large numbers of characters and taxa in this analysis, it was necessary to run it at the genus level (Leptacodon was an exception to this, see later in the text), and the second assumption here is that the genera included as terminals are monophyletic. Most of the taxa included here are either monotypic (e.g., Ceutholestes) or contain but a few species (e.g., Litolestes), and the assumption of monophyly is probably valid; more speciose taxa (e.g., Saturninia, Centetodon), however, are problematic, and this assumption may not hold. Genera that contain more than one species were coded for what is considered to be the most basal species; in many cases the decision was based on previous work (e.g., Macrocranion, see Smith et al., 2002; Centetodon, see Lillegraven et al., 1981; Asher et

al., 2005), while in others (e.g., Limaconyssus, Diacocherus) the decision was made after examining the relevant material. In some cases the availability of material, or the relative completeness of the fossils, dictated which species were used; for example, Litolestes avitodelphus is likely the most primitive species of Litolestes (see earlier in the text), but the upper dentition is unknown, and consequently Litolestes ignotus (where both upper and lower teeth are known) was also used. In cases where multiple species are used, any character conflicts among those species were coded as polymorphisms (e.g., Adapisorex from North America and Europe).

5.3.4 Outgroup Taxa

Although the most appropriate outgroups for examining the interrelationships among lipotyphlans would be basal lipotyphlans, these taxa are themselves the subject of interest in this analysis; consequently the outgroup taxa must be chosen from outside Lipotyphla. The sister group of Lipotyphla continues to be a subject of great debate (e.g., McDowell, 1958; Van Valen, 1967; Novacek, 1986; MacPhee and Novacek, 1993; Stanhope et al., 1998; Asher, 1999; Douady et al., 2002; Waddell and Shelley, 2003; Asher et al., 2005). The results of recent molecular analyses of eutherian relationships have varied wildly with respect to the position of Lipotyphla [e.g., sister group to Carnivora+Pholidota+Perissodactyla+Cetartiodactyla+Chiroptera (Douady et al., 2002; Waddell and Shelley, 2003; Murphy et al., 2004), sister group to Chiroptera (Malia et al., 2002), sister group to Euarchontoglires (Archonta+Glires) (Asher et al., 2005); sister group to Artiodactyla+Cetacea (Amrine-Madsen et al., 2003); Erinaceomorpha sister group to Rodentia+Primates+Cetferungulata+"African mammals"+Soricomorpha+Chiroptera, Soricomorpha sister group to Cetferungulata+Chiroptera (Arnason et al., 2002); sister group to Cetartiodactyla+Pegasoferae (Nishihara et al., 2006)], and the differing opinions presented here are far from exhaustive; clearly a consensus on this issue is yet to be reached. The Leptictidae, a family of Late Cretaceous to Oligocene insectivorans, has historically been considered either lipotyphlan (e.g., Leidy, 1868; Gregory, 1910; Butler, 1956) or a close lipotyphlan relative (e.g., Novacek, 1986; MacPhee and Novacek, 1993);

the results of recent morphological (e.g., Shoshani and McKenna, 1998; Asher, 1999) and combined morphological and molecular analyses (e.g., Asher et al., 2005) have found leptictids to be the sister taxon to Lipotyphla, or nested within a clade that is sister to Lipotyphla (but see Asher et al., 2003). Given these results, Leptictidae, represented by the Paleocene-Eocene taxon Prodiacodon Matthew, 1929, is included as an outgroup in this analysis. Prodiacodon was chosen instead of the putatively more primitive Gypsonictops Simpson, 1927b from the Late Cretaceous of North America because it is generally better known and could be scored for more of the characters; because Prodiacodon (and leptictids generally) is a relatively derived eutherian (e.g., strong protoconal cingula, molar hypocone, molariform P4/p4), it was necessary to include other, more basal outgroup taxa, represented in this analysis by the asioryctithere Kennalestes Kielan-Jaworowska, 1969, and the palaeoryctoid Cimolestes Marsh, 1889. Archibald and Averianov's (2006) review of Asioryctitheria is the most recent and comprehensive for the group; their results suggest that Kennalestes may be the basalmost taxon in the Asioryctidae, a clade also containing Asioryctes and Ukhaatherium; the results of Archibald and Averianov's (2006) cladistic analysis place a number of other taxa basal to Asioryctidae, including Daulestes, Bulaklestes, and Uchkudukodon, but these taxa are not as well known as Kennalestes and Asioryctes. Kennalestes is among the most nearly completely represented of the asioryctitheres, and is in many ways less derived than Asioryctes (Archibald and Averianov, 2006); as such, Kennalestes was deemed the most appropriate of the asioryctitheres for use in this analysis. Palaeoryctids (including palaeoryctines and didelphodontines) have long been considered close relatives of the Lipotyphla (e.g., Matthew, 1913; Saban, 1954; Vandebroek, 1961; Van Valen, 1967; Lillegraven et al., 1981; McKenna et al., 1984; Novacek, 1986; Thewissen and Gingerich, 1989; MacPhee and Novacek, 1993; Bloch, Secord, and Gingerich, 2004; but see McKenna, 1975; McKenna and Bell, 1997), with the Didelphodontinae (=Cimolestidae of McKenna and Bell, 1997) generally, and Cimolestes specifically likely being among the most primitive. The Late Cretaceous species Cimolestes cerberoides Lillegraven, 1969 is likely among the most primitive of the species referred to Cimolestes (compare the dentitions of, e.g., C. cerberoides with that of C. magnus Clemens and Russell, 1965, and C. propalaeoryctes Lillegraven, 1969), although the probable non-

monophyly of the genus is problematic (Fox and Youzwyshyn, 1994); nonetheless, C. cerberoides clearly is among the most dentally "generalized" palaeoryctids, and is included in this analysis.

5.3.5 Ingroup Taxa

The ingroup consists of 39 terminals representing taxa that are known primarily from the Paleogene of North America and Europe (see Appendix 1), an extant erinaceid (Echinosorex Raffles) and an extant soricid (Crocidura Wagler). Of the 39 terminal taxa included here, 16 are known exclusively from the Paleocene of North America (Leipsanolestes, "Adapisorella", Adeloxenus, Litocherus, Nayloria, Oncocherus, Cedrocherus Gingerich, 1983, Litolestes, Xynolestes, Leptacodon tener Matthew and Granger, 1921, "L." munusculum, "L." packi, L. rosei Gingerich, 1987, Psydronyctia, Ceutholestes Rose and Gingerich, 1987, and Limaconyssus), while Wyonycteris Gingerich, 1987, Adapisorex, and Diacocherus are known from the Paleocene of North America and Europe. Since one of the goals of this analysis is to determine whether or not any of the new lipotyphlan taxa identified in this study (see earlier in the text) might be referred to the better-known stem lipotyphlan families from the Paleogene of North America or Europe, a broad sampling of some of these stem lipotyphlans is included (see Appendix 1). Two Late Cretaceous taxa (Batodon Marsh, 1892 and Paranyctoides Fox, 1979) are included: Batodon is often considered the earliest geolabidid (see Novacek, 1976; McKenna and Bell, 1997; but see Wible et al., 2007), while Paranyctoides is thought to represent the earliest nyctitheriid (Fox, 1979, 1984, but see Archibald et al., 2001; Archibald and Averianov, 2001; Wible et al., 2007). Asionyctia may represent the oldest nyctitheriid in Asia (Missiaen and Smith, 2005), and it is included here. The erinaceid Echinosorex and the soricid Crocidura are included as representatives of so-called crown Lipotyphla. Two of the ingroup taxa are particularly problematic and are discussed further.

Leptacodon.—The lone exception to using genera as terminals is the Euramerican genus Leptacodon: the monophyly of this taxon has been repeatedly questioned (e.g., Krishtalka, 1976b; Bown and Schankler, 1982; Youzwyshyn, 1988; Scott, 2003), with

some authors considering "L." munusculum and "L." packi to be more closely related to the Eocene nyctitheriids Pontifactor and Nyctitherium, respectively. One of the goals of this analysis is to test the monophyly of Leptacodon, particularly now that the previously poorly known species L. munusculum is much better represented (see earlier in the text); as such, the better-known species of Leptacodon (L. tener, L. munusculum, L. packi, L. rosei, and L. dormaalensis) are included as terminals.

Diacocherus.—The taxonomic status of Diacocherus, Adunator Russell, 1964, and Mckennatherium Van Valen, 1965 remains unclear. Krishtalka (1976a) examined all of the relevant specimens and concluded that "Diacodon" minutus (=Diacocherus minutus) and the European genus Adunator are synonymous, while recognizing Mckennatherium as a valid North American genus; in contrast, Bown and Schankler (1982) revisited the issue and concluded that Adunator, Mckennatherium, and "Diacodon" minutus were inseparable on the basis of dental morphology. Later, and on the basis of new specimens collected from the early middle Tiffanian (Ti3) Cedar Point Quarry, Gingerich (1983) named a new genus, Diacocherus, with Diacodon minutus as its type species; Gingerich recognized Mckennatherium as a valid genus, but explicitly rejected a close relationship between Adunator (viewed as a valid European genus by Gingerich) and North American litocherines (including Diacocherus and Mckennatherium). More recently, Secord (2004), in an unpublished doctoral dissertation, considered Diacocherus a subjective junior synonym of Adunator, but recognized Mckennatherium as a valid taxon. Although newly collected specimens of Diacocherus from the late middle Tiffanian (Ti4) Gao Mine locality of Alberta have shed some light on the problem [at least one of the specimens from Gao Mine preserves the upper and lower dentition in articulation, and confirms Gingerich's (1983) associations of the upper and lower dentitions of D. minutus; Fox, in prep.], the taxonomic uncertainties of Diacocherus, Mckennatherium, and Adunator will persist until all of the relevant material can be examined; clearly this is an issue of alpha taxonomy that is beyond the scope of the current analysis. Diacocherus, Mckennatherium, and Adunator are unquestionably closely related, and for the purposes of this study are treated as synonymous. Character states for Diacocherus are coded for the middle Tiffanian species D. meizon: D. meizon is well-represented in collections from Gao Mine and Cedar Point Quarry, and is likely

the more primitive of the two species of Diacocherus (R. C. Fox, pers. comm., 2006; D. minutus is derived in having a more fully molariform p4).

Taxa not included in this analysis.—With the exception of those stem lipotyphlan families that are included in the ingroup, most of the post-Paleocene age lipotyphlans are not considered here: the immediate goal of this analysis is evaluating the relationships among the geologically earliest lipotyphlans, and clearly the more derived lipotyphlan families (e.g. brachyericines, plesiosoricids) are not relevant to this goal. A number of taxa have at various times been considered lipotyphlans, but are not included in this analysis. These include, among others, the adapisoriculids (see, e.g., Gheerbrant, 1988, 1991; Gheerbrant and Russell, 1989, 1991; Gheerbrant et al., 1998), didymoconids (e.g., Meng, 1990; Meng et al., 1994; Lopatin, 2001, 2003), micropternodontids (e.g., Szalay and McKenna, 1971; McKenna et al., 1984), palaeoryctids (e.g., McKenna et al., 1984), and Creotarsus (e.g., Van Valen, 1967). Some of these taxa (e.g., adapisoriculids) are very poorly known, while the lipotyphlan affinities of others (e.g., didymoconids, micropternodontids, palaeoryctids) have been questioned (e.g., Butler, 1988; Meng, 1990; MacPhee and Novacek, 1993). A number of generally poorly known insectivorans from the Paleocene and Eocene of east Asia have been at various times considered members of the Nyctitheriidae (see, e.g., Russell and Dashzeveg, 1986; Averianov, 1995; McKenna and Bell, 1997; Kondrashov et al., 2004; Lopatin, 2005); of these taxa, only Asionyctia Missiaen and Smith, 2005 is considered in this analysis.

5.3.6 Analytical Protocol

This analysis relies on 98 characters scored for three outgroup taxa and 39 ingroup taxa. The data were analyzed using PAUP*4.0 (Swofford, 2000); in addition to searches, PAUP was used to compute consensus trees, generate tree statistics and decay indices, and to map the distribution of character states. The large amount of data precluded exact tree searching methods, and the analysis was run as an heuristic search using TBR branch swapping, with the rooting option imposing a monophyletic ingroup and a paraphyletic outgroup. The analysis was run with characters 4, 10, 14, 25, 28, 30, 34, 35, 58, 65, 67, 68, 91, 94, and 95 as ordered (Wagner parsimony; Farris, 1970;

Swofford and Maddison, 1987). Character ordering continues to be a hotly debated topic in parsimony analysis (e.g., Hauser and Presch, 1991; Lipscomb, 1992; Wilkinson, 1992; Silcox et al., 2001), with many authors unwilling to impose a priori hypotheses of character change in an analysis; in such cases, for example, a character state change from 0 to 1 is as likely, and requires the same number of "steps", as a change from 0 to 2 or from 0 to 3. Although mechanisms such as heterochrony have been cited as reasons against a priori assumptions of character state ordering (e.g., Hauser and Presch, 1991; Silcox, 2001), it is less often appreciated that ignoring a potential morphocline (e.g., the development of the metaconid on p4, see character 58) can result in significant information loss (Page et al., 1992; Wilkinson, 1992; Slowinski, 1993). The simple morphoclines proposed here are consistent with Lipscomb's (1992) similarity criterion for hypothesizing character state order, and many are well-entrenched in the evolutionary history of eutherians, and usually express further modifications of a previously modified anatomy (e.g., the relative development of a labially flexed centrocrista in dilambdodont lipotyphlans, the anterior inclination of the molar trigonid). While heterochrony could conceivably result in, e.g., an undeflected molar centrocrista changing to a fully dilambdodont centrocrista in one "evolutionary step" (i.e., without having to pass through a transitional, or incipiently, dilambdodont state, see character 25), the available evidence from both fossil and extant mammals suggests this not to be the case, and that an assumption of morphocline is warranted. Character ordering in this analysis was used where determined to be defensibly realistic, counter-evidence lacking (e.g., character 10, the obliquity of the labial margin of P4 changes from virtually straight, to slightly oblique, to extremely oblique; this set of character states was considered naturally ordinated sensu Livezey and Zusi, 2006). With the exception of ordering, all characters were considered unweighted, and no character was considered irreversible (i.e., Camin-Sokal parsimony was not invoked; Camin and Sokal, 1965). Character polarity was determined a posteriori by rooting phylogenetic trees (Farris, 1982; Nixon and Carpenter, 1993; Bryant, 2001). Character states were optimized using both ACCTRAN and DELTRAN options; these optimizations do not alter the topology of the tree, only the position at which a given character state is placed when alternative arrangements are equally parsimonious: ACCTRAN favours reversals over convergences when both

interpretations are equally probable, whereas DELTRAN favours convergences over reversals (Swofford, 2000). Clade support was assessed using decay values: decay values assess clade support by using the original data matrix to search for trees successively longer than the shortest tree(s) until all clades collapse (Bremer, 1988, 1994); the number of extra steps needed to collapse a given clade is termed the decay or Bremer index. Decay indices were calculated here using the heuristic search option. Bootstrap analysis (Felsenstein, 1985) was not performed following the rationale of Sanderson (1989), Kluge and Wolf (1993), Bremer (1994), Carpenter (1996), and Geisler (2001).

*5.3.7 **Results***

The heuristic search yielded 20 equally parsimonious trees of 785 steps (CI=0.456; RI=0.528; RC=0.241); the strict and majority rule consensus trees are presented in Figures 5.58 and 5.59. As indicated by the low consistency and decay indices, the data set described here produced topologies with a great deal of homoplasy, a result that is common when large datasets with many taxa are examined (Sanderson and Donoghue, 1989, 1996; Asher, 1999; Asher et al., 2005); support for many of the clades in this analysis is poor, although it should be noted that decay indices can be seriously affected by missing data and the number of most parsimonious trees (Wilkinson, 2003), and should be interpreted with these caveats in mind. In spite of the low clade support, conflict between each of the optimal trees is minor, and each of the shortest trees recovered the same basic topology, with the major sources of variation being the inferred relationships of "Leptacodon" munusculum, "Leptacodon" packi, and the lower-level relationships among some of the erinaceomorphs. Two major clades were recovered in each of the optimal trees, consistent with previous hypotheses of a fundamental lipotyphlan dichotomy into so-called soricomorphs, or "shrew-like" taxa, and erinaceomorphs, or so-called "hedgehog-like" taxa (Butler, 1972, 1988). The first clade consists of taxa that have previously been regarded as soricomorphs, including the extant shrew Crocidura plus the nyctitheriines and amphidozotheriines; this clade is poorly supported, with a decay index of 1. The second clade consists of taxa that have been previously regarded as erinaceomorphs, including the extant gymnure Echinosorex plus

taxa that have traditionally been referred to as "dormaaliids" and "adapisoricids" (see Novacek et al., 1985); this clade is better supported than the soricomorph clade, and collapses with two additional steps. The soricomorph and erinaceomorph clades are in an unresolved polychotomy with two species of Leptacodon ("L." munusculum and "L." packi) in the strict consensus tree, but are resolved as sister groups in the majority rule tree. A third clade consisting of Pontifactor and Paranyctoides is resolved as sister to the soricomorph+erinaceomorph clade, while a fourth clade containing the geolabidid Centetodon and the nyctitheriid Limaconyssus is sister to ((soricomorphs+erinaceomorphs)(Pontifactor+Paranyctoides)); the third and fourth major clades fall outside of the soricomorph+erinaceomorph clade in each of the shortest trees. Batodon is recovered as basal to all other ingroup taxa. Many of the Paleocene taxa included in this analysis are poorly resolved in the strict consensus tree; because the major goal of this study was to determine the relationships of these stem lipotyphlans, both to each another, as well as to stratigraphically younger lipotyphlans, the better resolved majority rule tree is preferred. Of the 20 optimal trees recovered in this analysis, one (tree 10, see Fig. 5.60) was chosen for further discussion: tree 10 is nearly identical to the majority rule tree, differing only in having resolved the positions of Xynolestes, Dartonius, and the trichotomy of (Adapisorex+"Adapisorella"+Adeloxenus+Leipsanolestes) (Litocherus+Nayloria)(Oncocherus+Cedrocherus+Litolestes). Each of the internal nodes is identified in Figure 5.60, and character changes at each node are listed in Appendix 4; putative synapomorphies for a number of the more important clades are discussed below. In the following discussion, the term "unequivocal" refers to character change that is consistent regardless of optimization criteria (i.e., character state changes that occur under both ACCTRAN and DELTRAN optimizations); in contrast, the term "equivocal" refers to character change that occurs under one optimization criterion, but not the other. Most of the synapomorphies supporting the various clades in this analysis are ambiguous in that they show homoplasy in different parts of the optimal trees, but are nonetheless optimized as local synapomorphies for the clades discussed below.

5.3.8 Discussion

One of the most interesting discoveries of this analysis is the remarkable level of homoplasy in the dataset: only a few of the synapomorphies proposed here are uniquely derived, and although branch lengths for many of the clades identified in this analysis are well supported by numbers of potential synapomorphies (e.g., Node 12), most of these are homoplasious in different parts of the tree. A number of the lipotyphlans included in this analysis are known only from upper or lower dentitions (e.g., Pontifactor, Ceutholestes), and the missing data are clearly problematic for unequivocal character optimizations. In spite of the relatively poor support, a number of major clades were recovered in all optimal trees, including two major divisions within the Lipotyphla, the Erinaceomorpha and Soricomorpha, consistent with previous opinions (e.g., Saban, 1954; Butler, 1956, 1972, 1988; MacPhee and Novacek, 1993; McKenna and Bell, 1997; Lopatin, 2005). The major clades relevant to the objectives of this analysis are discussed in detail below.

Node 3, Lipotyphla.—As with many of the higher level clades in this analysis, the clade uniting the ingroup taxa (Lipotyphla) is poorly supported, with a decay value of only one. Five unequivocal synapomorphies support the clade: 13 (1), P4 postcrista long and blade-like; 18(2), P4 metaconule undeveloped; 24(2), postmetacrista on M1-2 elongate and blade-like; 30(1), molar protocone slightly anterior of the level of the centrocrista notch; and 31(1), molar protocone enlarged. In addition to the unequivocal synapomorphies, ACCTRAN identified four additional synapomorphies [6(1), upper canine premolariform, 38(0), conular cristae robust, 43(2), i1 main cusp separated from heel by fissure, and 65(2), posterior exodaenodonty on p4 strong]; of these synapomorphies, only character 43 (conular cristae) may be reliable: only seven of the ingroup taxa could be scored for upper canine morphology, while only 13 taxa could be scored for i1 morphology, and posterior exodaenodonty on p4 is one of the most homoplasious characters in the analysis. DELTRAN suggests an additional four synapomorphies in support of Lipotyphla [17(2), P4 paraconule undeveloped; 20(1), anterior stylar shelf narrow on M1; 60(2), width of p4 talonid basin narrow; and 65(1), posterior exodaenodonty on p4 weak]. Characters 17 and 60 may be reasonable

synapomorphies, although neither can be scored for all of the ingroup taxa: an undeveloped P4 paraconule [17(2)] is characteristic of nearly all of the ingroup taxa where this character could be scored; DELTRAN suggests independent acquisition of a P4 paraconule in Cryptotopos and the amphidozotheriines (see later in the text). A narrow talonid on p4 characterizes most of the erinaceomorphs in this analysis, and if this character state is accepted as a lipotyphlan synapomorphy, then its presence in erinaceomorphs is a retained lipotyphlan plesiomorphy. Although most of the synapomorphies posited here are uniquely derived for Lipotyphla relative to the outgroup taxa, they clearly must be viewed with caution, as many of the ingroup taxa are known only from either upper or lower dentitions and could not be adequately scored for all of these characters. Each of the putative synapomorphies listed here is further modified at less inclusive nodes.

Node 5, Geolabididae.—Limaconyssus is reconstructed in this analysis as the sister taxon to Centetodon, and both are included in the Geolabididae; as such, Limaconyssus represents the first known Paleocene geolabidid (see further discussion later in the text). The Geolabididae receive moderate clade support (decay value of 2) and are supported by three unequivocal synapomorphies in this analysis: 82(1), molar cristid obliqua shape angular; 89(1), molar hypoconid and protoconid anteroposteriorly compressed and pillar-like; 95(1), m3 smaller than m2. Each of these characters can be scored for Centetodon and Limaconyssus, but the derived states are only local synapomorphies for this clade; they are convergently acquired in a number of soricomorph clades or terminal taxa, depending on optimization criteria. ACCTRAN suggests five additional synapomorphies [1(2), anterior root of zygomatic arch at level of M1; 3(1), extent of jugal on maxilla reduced; 5(1), upper canine roots two; 24(3), postmetacrista on M1 greatly elongate; 47(1), premolar lingual cingulids present], four of which [1(2), 3(1), 5(1), 24(3)] pertain to characters that could not be scored for Limaconyssus and are viewed here as unreliable; the fifth synapomorphy [47(1)] is probably reliable, having been acquired independently in Psydronyctia and the extant shrew Crocidura. DELTRAN suggests a single equivocal synapomorphy [65(2), p4 posterior exodaenodonty strong]; as discussed earlier in the text, p4 exodaenodonty is extremely homoplasious in this analysis and is not viewed as reliably supporting node 5.

Two issues regarding the Geolabididae, position of the alleged geolabidid Batodon, and the position of the family relative to Soricomorpha, warrant further comment.

Marsh (1892) originally allocated Batodon to the Cimolestidae (a family that Marsh thought to have affinities with extant opossums), but noted similarities with the teeth of many insectivorans; the genus was transferred to the Palaeoryctidae by Van Valen (1967), Lillegraven (1969), and Clemens (1973). McKenna (in Novacek, 1976) suggested that Batodon may represent the earliest geolabidid, an opinion that was formalized in McKenna and Bell (1997) and accepted by Bloch et al. (1998) and Lopatin (2005). Butler (1988) was not persuaded by McKenna's (in Novacek, 1976) opinion, and continued to regard Batodon as a "palaeoryctoid". Wible et al. (2007) consider Batodon as the sister taxon of the recently described "cimolestan" Maelestes Wible, Rougier, Novacek, and Asher, 2007. Clearly the phylogenetic position of Batodon continues to be as problematic as ever, a consequence that is due in large part to a lack of well-preserved specimens [virtually nothing of Batodon is known from specimens other than those described by Marsh (1892), Lillegraven (1969), Clemens (1973), and Wood and Clemens (2001)]. The results of this analysis place Batodon at the root of Lipotyphla (i.e., sister taxon to all of the other lipotyphlans included in the analysis), and do not support a close relationship between Batodon and the Geolabididae; support for this placement is weak, however (decay value of one step, one unequivocal synapomorphy). More importantly, this analysis did not include palaeoryctids as members of the ingroup; as such, the possibility that Batodon may be more closely related to the palaeoryctids was not examined here.

The taxonomic history of the Geolabididae is remarkably tortuous (see Lillegraven et al., 1981 for summary), but more recent classifications have placed the family as a member of the Soricomorpha (see Butler, 1972; Krishtalka, 1975, 1976b; Lillegraven et al., 1981; McKenna and Bell, 1997; but see Asher et al., 2002; Asher et al., 2005); the results of this analysis do not support inclusion of the Geolabididae within the soricomorph clade, but rather reconstructs the family as the sister group to (Paranyctoides+Pontifactor(Soricomorpha+Erinaceomorpha)). The results of recent analyses by Asher (1999), Asher et al. (2002), and Asher et al. (2005) suggest that Centetodon (and presumably geolabidids generally) may be the sister to, or part of, a

clade of zalambdodont lipotyphlans (=afrosoricids+Solenodon+Nesophontes+apternodontids), or in an unresolved polychotomy with other "eulipotyphlans" (soricomorphs+erinaceomorphs+Solenodon); where so reconstructed, the Centetodon+zalambdodont clade is either sister group to other lipotyphlans (Soricomorpha+Erinaceomorpha), or sister group to the Soricomorpha. The results of this analysis are congruent with at least some of the most parsimonious trees recovered by Asher (1999) (see, e.g., Asher, 1999, fig. 2, sets 1-2) in having Centetodon (and presumably other geolabidids) falling outside the (Soricomorpha+Erinaceomorpha) clade.

More definitive statements regarding the affinities of Batodon and the Geolabididae must await a subsequent analysis that includes a sampling of palaeoryctids and zalambdodont lipotyphlans; for the present, the Geolabididae, although weakly supported, are interpreted as falling outside the (Soricomorpha+Erinaceomorpha) clade.

Node 9, unnamed.—Asionyctia + Erinaceomorpha receive low clade support (decay value of 1), and are supported by only three unequivocal synapomorphies: 34(2), posterior cingulum on M1-2 expanded lingually but non-lobate; 49(1), p2-3 crowns procumbent; and 72(1), molar paraconid origin high; each of these is optimized as a local synapomorphy, having been convergently acquired in other, non-erinaceomorph taxa. For example, a lingually expanded posterior cingulum on M1 and M2 has been cited previously as a potential synapomorphy of Erinaceomorpha (Novacek et al., 1985), and although it is present in all erinaceomorphs in this analysis where the character can be scored, it is also convergently acquired in a number of nyctitheriids. In addition to their being present in a number of erinaceomorph taxa, procumbent crowns on p2 and p3 are present in Plagioctenodon and Amphidozotherium; this character state may be correlated with an anterior dentition that is reduced in size. A high molar paraconid [72(1)] is a local synapomorphy of Erinaceomorpha, having been independently acquired in Plagioctenodon and Ceutholestes. In addition to the unequivocal synapomorphies, ACCTRAN postulates two additional, equivocal synapomorphies: 52(2), p3 paraconid undeveloped, and 86(0), molar entoconid height much lower than metaconid.

The position of Asionyctia as the sister taxon to Erinaceomorpha was unexpected. Missiaen and Smith (2005) considered Asionyctia to be part of an endemic clade of East

Asian nyctitheriids, the Asionyctiinae. Other than Asionyctia, this analysis did not include any of the taxa identified by Missiaen and Smith (2005) as asionyctiines (e.g., Bumbanius Russell and Dashzeveg, 1986, Voltaia Nessov, 1987), so the monophyly of this subfamily was not investigated; nevertheless, Missiaen and Smith (2005) suggested that the Asionyctiinae are the sister group to all other nyctitheriids (Missiaen and Smith, 2005, fig. 3), an hypothesis that is not supported by this analysis. While the teeth of Asionyctia resemble those of other nyctitheriids generally, most of these characters are probably plesiomorphic (e.g., transverse upper molars, spur-like upper molar parastyle, low molar entoconid). In contrast, a number of characters are decidedly more erinaceomorph-like [e.g., P4 metacone undeveloped, P4 postprotocrista undeveloped (seen in derived erinaceomorphs), p3 procumbent rather than vertical, p4 and molar paraconid arising from a relatively high position, weak or undeveloped p4 metaconid]; two of these characters (p3 procumbent and molar paraconid origin high) were identified in this analysis as potential synapomorphies uniting Asionyctia with Erinaceomorpha, and a case could be made for inclusion of the former with the latter (i.e., Node 9 could be named Erinaceomorpha). Such action is not taken presently, however, until a more extensive sample of putative asionyctiines can be included in the analysis.

Node 10, Erinaceomorpha.—Node 10 corresponds most closely to Erinaceomorpha as traditionally recognized (Krishtalka, 1976a; Novacek, 1982, 1985; Novacek et al., 1985; McKenna and Bell, 1997). Clade support is moderate (decay value of 2), and three unequivocal synapomorphies are identified: 10(1), labial margin of P4 slightly oblique to long axis of crown; 35(2), molar hypocone swollen; and 86(2), molar entoconid height taller than half the height of tallest trigonid cusp; two of these characters [35(2) and 86(2)] have been previously cited as erinaceomorph synapomorphies (Krishtalka, 1976b; Novacek, 1982, 1986; Novacek et al., 1985). A swollen hypocone on M1 and M2 is uniquely derived (=unambiguous) in this analysis, being further modified at less inclusive erinaceomorph clades, and while 10(1) and 86(2) are not uniquely derived (tall entoconids are also present in, e.g., Leptacodon tener), they are nonetheless reconstructed as local synapomorphies for this clade. Five additional equivocal synapomorphies are postulated for Node 5: ACCTRAN suggests 24(0), postmetacrista on M1-2 low and not blade-like; 56(2), p4 paraconid strongly developed; and 57(1), p4

paraconid anterolingual and appressed to protoconid, while DELTRAN suggests 19(1), P4 postprotocrista extending towards base of protocone; and 59(1), p4 metaconid posterior to level of protoconid. Of these potential synapomorphies, character 19 is of particular importance: its optimization at node 10 is preferred (with independent acquisition in Pontifactor); the alternative arrangement as posited by ACCTRAN optimizes character 19 at node 6 and requires subsequent reversal on the stem leading to Soricomorpha. A steep postprotocrista on P4 is characteristic of every erinaceomorph included in this analysis. Acceptance of the ACCTRAN optimization for character 24 necessitates a re-development of a blade-like postmetacrista on M1 and M2 at node 16; the DELTRAN optimization of character 24(0) at node 11 is preferred, with a low and poorly developed postmetacrista on M1 and M2 being characteristic of most of the taxa in the unnamed clade stemming from node 11; this clade includes many erinaceomorphs that have traditionally been called "dormaaliids" or "adapisoricids". The remaining equivocal synapomorphies are probably reliable, but their alternative, equally parsimonious arrangements on the tree are no less biologically reasonable. The various erinaceomorph clades are broadly similar to those proposed by Novacek (1985) and Novacek et al. (1985), but differ in detail; these clades are briefly discussed below.

Node 11, unnamed.—The unnamed clade stemming from Node 11 contains a number of taxa that have been traditionally and variously referred to as "dormaaliids," "adapisoricids," or "creotarsines" (Van Valen, 1967; Russell et al., 1975; Krishtalka, 1976a; Novacek, 1985; Novacek et al., 1985), as well as the enigmatic erinaceomorph Diacocherus, and the extant galericine Echinosorex. Although branch support is weak (one step), seven unequivocal synapomorphies support the clade: 4(1), principal cusps low and inflated; 10(0), labial margin of P4 straight; 20(2), anterior stylar shelf on M1-2 narrow; 43(1), i1 crown subspatulate; 51(0), p3 subequal or slightly smaller than p4; 76(1), paracristid on m2-3 ridge- or shelf-like; and 87(1), entoconid on m1-2 posterolingual; of these synapomorphies, only character 51 may be unreliable as characters pertaining to i1 could not be scored for Scenopagus. ACCTRAN posits four additional equivocal synapomorphies: 11(1), P4 parastylar lobe weak; 13(2), P4 postcrista low or undeveloped; 71(1), molar metaconid inflated; and 84(0), molar entocristid notch virtually undeveloped. Of these, only 11(1) may be reliable; the more

conservative, and probably correct DELTRAN optimization for characters 13, 71, and 84 is preferred, with the derived state of each being acquired in Diacocherus alone; the alternative ACCTRAN optimization requires multiple, independent reversals at less inclusive nodes within unnamed clade 11. DELTRAN suggests only one potential synapomorphy: 24(0), M1-2 postmetacrista low and not blade-like. As discussed previously under node 10, the DELTRAN optimization for character 24(0) at node 11 is preferred, with independent development of a blade-like postmetacrista on M1 and M2 in both Sespedectes and Echinosorex.

Although the interrelationships of Eocene and younger lipotyphlans is not a primary objective of this investigation, a few comments on the phylogenetic positions of some of these taxa contained in unnamed clade 11 are warranted. The arrangement of taxa in this clade differs somewhat from that proposed in previous hypotheses of early lipotyphlan relationships, but broadly resembles the classifications as suggested by Krishtalka (1976a) (within the Adapisoricidae) and Novacek et al. (1985) (within the Dormaaliidae+Amphilemuridae). In contrast with these studies, the results of this analysis suggest a close relationship between the amphilemurid Pholidocercus and Macrocranion (Node 13). Although the phylogenetic position of Macrocranion has long been a subject of debate (see, e.g., Heller, 1935; Tobien, 1962; Van Valen, 1967; Krishtalka, 1976a; Koenigswald and Storch, 1983; Novacek et al., 1985; MacPhee et al., 1988; McKenna and Bell, 1997), it has almost always been hypothesized to have a close relationship with either the amphilemurids or the "dormaaliids" (but see Butler, 1988; Penkrot et al., 2004). The association of Pholidocercus and Macrocranion in this analysis receives moderate branch support (decay index of 2 steps), and a number of unequivocal and equivocal synapomorphies are suggested (Node 13, see Appendix 3). Perhaps one of the most unexpected findings of this analysis is the close association of the scenopagine Scenopagus and the sespedectine Sespedectes with the erinaceids, represented by the extant moonrat Echinosorex (Node 14). Ever since Krishtalka's (1975, 1976a) classic studies on early Tertiary adapisoricids and erinaceids, most authors have subsequently followed his opinions and have regarded Scenopagus and Sespedectes as "adapisoricids" (or "dormaaliids" of Novacek et al., 1985), while the Paleocene erinaceomorph Litolestes is thought to represent the earliest erinaceid (e.g., Bown and Schankler, 1982; Novacek,

1985; Novacek et al., 1985; McKenna and Bell, 1997; Lopatin, 2005; Scott, 2006). A notable dissenter to this near-consensus was Butler (1988), who almost 20 years ago suggested that Scenopagus, and its Oligocene descendant Ankylodon, may be among the early Tertiary lipotyphlans that are most closely related to extant erinaceids; Butler (1988) further suggested that Litolestes and other putative erinaceids recognized by Krishtalka (1976a) and Novacek et al. (1985) are probably not closely related to Erinaceidae. This subject is further discussed later in the text (see Node 19).

Node 16, unnamed.—Node 16 unites Xynolestes, Dartonius, and a number of erinaceomorphs that have previously been considered erinaceids. The clade is supported by moderate decay index (2 steps) and five unequivocal, although not uniquely derived synapomorphies: 33(1), molar pericone present; 79(1), molar talonid basin deep and angular; 94(1), m2 size smaller than m1; 95(1), m3 size smaller than m2; and 98(1), m3 hypoconulid subequal to other talonid cusps, not projecting. Of these, only character 33 is problematic, because upper teeth are as yet unknown for Adeloxenus, Leipsanolestes, Cedrocherus, and Dartonius. ACCTRAN postulates four additional potential synapomorphies at Node 16 [24(1), postmetacrista on M1-2 short and blade-like; 52(0), p3 paraconid weak; 53(1), p3 talonid unicuspid and weakly basined; and 65(2), p4 posterior exodaenodonty strong], while DELTRAN posits one other [24(1), postmetacrista on M1-2 short and blade-like]. A state change in character 24 (postmetacrista on M1-2) to a short, blade-like condition is optimized at node 16 as a reversal (ACCTRAN) from an undeveloped state, or as a modification of the presumably primitive condition in which the postmetacrista was longer (DELTRAN); as discussed previously (Node 11), the DELTRAN optimization is accepted here as more probable. Xynolestes, one of the new lipotyphlan taxa documented at the Blindman River and Joffre Bridge localities, nests as the most basal taxon in this clade.

Node 18, Litolestidae.—Node 18 unites what are here identified as litolestines (Node 19), litocherines (Node 22), and adapisoricines (Node 24). The clade is recovered in all optimal trees, and has good branch support (3 steps). 4(1), cusps lower and inflated; 49(0), p2-3 crowns vertical; 67(2), molar trigonid very low; 69(2), valley-facing sides of trigonid cusps markedly convex; 74(1), m1 paracristid flexed, all unequivocally support the clade. ACCTRAN postulates an additional two equivocal synapomorphies

[56(1), p4 paraconid moderately developed; and 77(1), m2-3 paracristid flexed], while DELTRAN suggests four others [13(0), P4 postcrista short and blade-like; 22(1), M1 parastylar lobe weakly projecting; 44(1), i2 size larger than i1; and 53(1), p3 talonid unicuspid and weakly basined]. Characters relating to the upper dentition as posited by DELTRAN are equivocal at nodes 17 or 18 because the upper dentition of Dartonius is unknown, while 44(1) is probably unreliable given that lower incisor characters can only be scored for Nayloria, Litocherus, Litolestes, and Adeloxenus among the taxa that are united at node 18. The ACCTRAN optimization for character 77(1) is probably incorrect, requiring independent reversals of the flexed m2-3 paracristid in Nayloria and Leipsanolestes; the DELTRAN optimization is preferred (Node 19), with a flexed paracristid on m2-3 developing independently in adapisoricines (Node 24). The taxa included at Node 18 have, at one time or another, been referred to the Adapisoricidae (see, e.g., Van Valen, 1967; Russell et al., 1975; Gingerich, 1983); Adapisoricidae could be retained as a valid family that would include taxa stemming from Node 18, but the introduction of yet another new concept for this family, in addition to its convoluted taxonomic history and numerous, often contradictory usages of the name, makes this alternative undesirable, and the new nomen Litolestidae is preferred. Although the Litolestidae cannot be diagnosed on the basis of uniquely derived synapomorphies (e.g., a flexed m1 paracristid is also present in Macrocranion, Pholidocercus, and a few nyctitheriids), the combination of characters is known only in litolestids among the lipotyphlans examined here.

Node 19, Litolestinae.—Litolestinae contain three genera (Litolestes, Oncocherus, Cedrocherus) that have previously been linked with extant erinaceids (Krishtalka, 1976a; Novacek, 1982, 1985; Novacek et al., 1985; McKenna and Bell, 1997; Scott, 2006). The clade is not recovered in the strict consensus tree, but was recovered in the 50% majority rule tree, occurring in 80% of the optimal trees. Two unequivocal synapomorphies support the clade: 94(2), m2 much smaller than m1; and 95(2), m3 much smaller than m2; both of these characters are identified in this analysis as homoplasies convergent with Echinosorex. ACCTRAN suggests an additional two synapomorphies [43(3), i1 crown multilobate; and 52(2), p3 paraconid undeveloped], neither of which can be viewed as reliable: lower incisor characters could not be scored for Oncocherus or

Cedrocherus, and the p3 paraconid is polymorphic in each of Oncocherus, Litolestes, and Cedrocherus. DELTRAN suggests one equivocal synapomorphy [77(1), m2-3 paracristid flexed]; as discussed previously (Node 18), this optimization is accepted here.

The position of Litolestinae as reconstructed in this analysis [sister taxon to (Litocherinae(Leipsanolestes(Adapisoricinae)))] contrasts strongly with the opinions of Krishtalka (1975, 1976a), Novacek (1982, 1985), Novacek et al. (1985), and McKenna and Bell (1997), which suggest an alternative arrangement in which these taxa are more closely related to the erinaceids. Novacek et al. (1985), citing Krishtalka (1976a, 1977), suggested a suite of dental characters that putatively unite Litolestes, Cedrocherus, Leipsanolestes, and a number of other taxa with erinaceids. While some of these characters are known in extant erinaceids, the results of this analysis suggest that they probably evolved independently in both groups; additional characters posited by Krishtalka (1976a), Novacek (1985), and Novacek et al. (1985) that putatively link litolestines and erinaceids do not actually characterize litolestines at all. These characters are briefly reviewed as follows:

1) V-shaped molar talonid basin. This character was originally cited by Krishtalka (1976a) as a synapomorphy uniting erinaceids and Litolestes, Leipsanolestes, and possibly Entomolestes. A V-shaped molar talonid basin unites Litolestes, Cedrocherus, and Oncocherus in this analysis, but is optimized as a homoplasy, originating once on the stem leading to Node 16 and once in Echinosorex and Entomolestes. If Entomolestes is accepted as a near-soricid (as reconstructed in this analysis), then a V-shaped talonid basin evolved convergently in erinaceomorphs and soricomorphs.

2) Marked reduction in size from m1-3. This character complex is often cited as a key synapomorphy for erinaceids (Krishtalka, 1976a; Novacek, 1982, 1985; Novacek et al., 1985), but its distribution is taxonomically more broad, both among lipotyphlans [e.g., derived geolabidids such as Batodonoides Novacek, 1976, the plesiosoricid Butselia Quinet and Misonne, 1965, numerous soricids (Repenning, 1967)] and insectivorans more generally (e.g., the pentacodontid Aphronorus). A greatly reduced m2 [94(2)] is optimized as a local synapomorphy for the Litolestinae in this analysis, and is convergent with Echinosorex, while a greatly reduced m3 [95(2)] occurs in the adapisoricine

Adapisorex, as well as the amphidozotheriines Amphidozotherium and Euronyctia and extant shrews.

3) m1 paraconid salient and anteriorly projecting. While a hypertrophied, blade-like, and anterolingually displaced paraconid/paracristid is an important erinaceid character (it forms part of the specialized P4-m1 shearing complex that is characteristic of the Erinaceidae; Butler, 1948; Rich, 1981), it is not developed in any of the taxa identified as stem erinaceids by Krishtalka (1976a), Novacek (1985), or Novacek et al. (1985). As Butler (1988) discussed, the paraconid/paracristid in litocherines (litolestines of this study, in part) is relatively low and blade-like (as it is in lipotyphlans primitively), not hypertrophied, and rather than being anterolingually displaced like that in Echinosorex, the paracristid is sharply flexed, and the trigonid is nearly square, rather than triangular, in occlusal outline. A sharply flexed m1 paracristid is plesiomorphous (optimized at Node 18, see earlier in the text), and homoplasious, having also evolved independently in the amphilemurids (Node 13) and a few soricomorphs.

4) m1-2 hypoconulids markedly reduced in size. Although the hypoconulid on m1 and m2 is low in the taxa identified here as litolestines (i.e., it does not project in a finger-like manner), the cusp is not greatly reduced (or absent) like that in the erinaceids; rather, the hypoconulid in litolestines is swollen and somewhat anteroposteriorly compressed.

5) Hypocones on M1-2 better developed than are those in Dormaaliidae. Novacek et al. (1985) suggested that this character potentially unites erinaceids with Litolestes (with the exception of the adapisoricines Adapisorex and Neomatronella, the upper dentition of all of the other stem erinaceids included by Novacek et al., 1985, and Novacek, 1985 was, and remains, unknown). Clearly this characterization is incorrect: the hypocone on M1-2 of Litolestes (and all other litolestines included in this analysis) is considerably smaller than that of any "dormaaliid", including, e.g., Scenopagus, Pholidocercus, and Macrocranion.

6) Hypocone crest. The hypocone crest joins the hypocone to either the protocone or the metaconule (Butler, 1948; Rich, 1981; Frost, 1991; Gould, 1995). The hypocone crest was considered by Novacek et al. (1985) as being present in most erinaceids, but no such crest has been documented in Litolestes or any of the other litolestines identified in

this study. A hypocone crest is known in the adapisoricine "Adapisorella" (see this study), but is also present in some specimens of the "dormaaliids" Scenopagus (see Butler, 1988; pers. obs.) and Macrocranion (see Russell et al., 1975, pl. II, figs. 1-2), as well as the putative nyctitheriids Pontifactor and Leptacodon tener.

Novacek (1985) further cited the presence of a strong labial cingulid on m1-2 as uniting Litolestes, Cedrocherus, and erinaceids, but the cingulids in Litolestes and Oncocherus (cingulids in Cedrocherus are not known), while weakly complete in some specimens, are never developed to the same degree as those in even the most primitive erinaceids. All of the litolestines identified in this analysis differ further from erinaceids (sensu stricto) in P4 lacking a hypocone [the hypocone on P4 is well-developed in Erinaceidae (Rich, 1981; Novacek, 1985; Frost, 1991)] and p4 having a comparatively weak, non-blade-like paraconid [a blade-like paraconid is characteristic of many erinaceids (Rich, 1981), and, importantly, characterizes the most primitive erinaceids, including Galerix Pomel and Eochenus Wang and Li].

Butler (1988) discussed much of this in some detail, and his main conclusion regarding Litolestes and other taxa that are included here in the Litolestinae, Litocherinae, and Adapisoricinae (i.e., that they are not erinaceids) is supported by this analysis; Butler (1988) chose to classify Litolestes, Cedrocherus, Litocherus, and Auroralestes Holroyd, Bown, and Schankler, 2004 (=Eolestes Bown and Schankler, 1982) in the Litocherinae (sensu Gingerich, 1983) as a subfamily of the Dormaaliidae; a close phylogenetic relationship of these taxa (excluding Auroralestes, which was not included in this analysis) is supported by this analysis, although the higher-level classification of Butler (1988) is not followed here.

Node 22, Litocherinae.—As with Node 19, the clade uniting Litocherus and Nayloria was not recovered in the strict consensus tree; it was recovered in the 50% majority rule tree, but occurred in only 65% of the optimal trees. Branch support is poor (one step). Three unequivocal synapomorphies support the clade: 54(1), p4 larger than m1; 55(0), p4 paraconid origin low; and 71(1), molar metaconid inflated relative to protoconid. ACCTRAN posits two additional synapomorphies [16(1), P4 anterior cingulum prominent; 56(2), p4 paraconid strongly developed], while DELTRAN posits one [79(0), molar talonid basin concave]. The ACCTRAN optimization of 16(1) is

probably correct, and a prominent anterior cingulum on P4 is present only in Litocherus and Nayloria among the erinaceomorphs.

Gingerich (1983) named Litocherinae to receive Litocherus, Diacocherus, Leipsanolestes, Cedrocherus, and Mckennatherium, citing a number of characters that apparently distinguished them from other adapisoricids; Gingerich's concept of Adapisoricidae was not made clear, but presumably he followed the usage of Russell et al. (1975). Novacek et al. (1985), while agreeing with Krishtalka's (1976a) and Gingerich's (1983) recognition of Litocherus as a genus distinct from Litolestes, were not convinced of the validity of the Litocherinae, and chose instead to regard Litocherus and Diacocherus (including Mckennatherium) as erinaceomorphs of uncertain affinity; Litolestes and Leipsanolestes were referred to the Erinaceidae. McKenna and Bell (1997) considered Litocherinae to be monotypic and included only Litocherus. The Litocherinae as recognized here contain Litocherus and Nayloria, and are distinguished from litolestines in having an enlarged p4 (convergent with Litolestes), a low p4 paraconid, an inflated molar metaconid (convergent with some adapisoricines, "dormaaliids", and Diacocherus), and a prominent anterior cingulum on P4 (uniquely derived among the erinaceomorphs).

Node 24, Adapisoricinae.—The clade uniting Adeloxenus, "Adapisorella", and Adapisorex is one of the more robustly supported clades in this analysis, and is roughly equivalent to the restricted Adapisoricidae as used by McKenna and Bell (1997). The clade was recovered in all optimal trees, and has a decay index of 2 steps. Five unequivocal synapomorphies support the clade: 64(1), p4 hypoconulid conspicuous; 68(2), molar trigonids shallowly inclined; 94(0), size of m2 subequal or slightly smaller than m1; 97(1), m3 hypoconulid appressed to entoconid; and 98(2), m3 hypoconulid and entoconid form a weak lobe. Character 98(2) is a uniquely derived synapomorphy, while the remaining four unequivocal synapomorphies are local only, being homoplasious in other parts of the tree. One equivocal synapomorphy is posited by ACCTRAN [58(2), p4 metaconid strongly differentiated from protoconid] and DELTRAN [77(1), m2-3 paracristid flexed]. The ACCTRAN optimization demands a reversal of character 58(2) to a weakly differentiated metaconid on p4 of Adapisorex (Node 25), whereas the more conservative, and probably correct, DELTRAN optimization suggests that this character

was independently derived in "Adapisorella" and Adeloxenus. As discussed previously (Node 18), the DELTRAN optimization for character 77(1) at Node 19 is accepted here as being more likely, with independent acquisition of a flexed paracristid on m2-3 in the adapisoricids.

Adapisoricinae as used here is equivalent to Adapisoricinae as used by Russell et al. (1975), and Adapisoricidae as used by McKenna and Bell (1997): Adapisoricinae as conceived by Russell et al. (1975) contained but one genus, Adapisorex, while McKenna and Bell (1997) added the early Sparnacian genus Neomatronella to the subfamily. Adapisoricinae as recognized here contains Adeloxenus, "Adapisorella", and Adapisorex; although Neomatronella was not included in this analysis, the teeth are clearly similar to those of other adapisoricines as recognized here (and see Russell et al., 1975, pl. I), but differ in m3 not having the entoconid and hypoconulid closely approximated and weakly lobate; Neomatronella may be best united with Leipsanolestes at the more inclusive, unnamed Node 23. Russell et al. (1975) distinguished Adapisoricinae from the Dormaaliinae, the other adapisoricid subfamily (sensu Russell et al., 1975), mainly on the structure of p4 (the p4 of adapisoricines has a considerably wider talonid than does any dormaaliine, with well-differentiated cusps). The enlarged p4 talonid of adapisoricines is identified as a plesiomorphy in this analysis, being optimized at Node 23, while a well-developed p4 hypoconulid is identified as a local synapomorphy at Node 24. Leipsanolestes, previously considered a near-erinaceid (Krishtalka, 1976a; Novacek et al., 1985), is reconstructed as the sister taxon to Adapisoricinae, although its position here is tenuous: of the nine potential synapomorphies supporting Node 23, six of these cannot be scored for Leipsanolestes as the upper dentition is unknown.

Adapisorex and "Adapisorella" are distinguished from Adeloxenus by a suite of unequivocal synapomorphies at Node 25: 54(2), p4 smaller than m1; 71(1), molar metaconid inflated relative to protoconid; 75(2), m1 metaconid posterolingual of protoconid; 79(2), molar talonid basin high and platform-like; and 80(2), m1 talonid wider than trigonid, m2 talonid subequal to trigonid. A high and platform-like talonid basin is uniquely derived at Node 25, occurring only in Adapisorex and "Adapisorella". Because the upper dentition of Leipsanolestes and Adeloxenus is unknown, characters relating to the upper teeth are equivocal and can be optimized at either Node 23

(ACCTRAN) or Node 25 (DELTRAN); although both optimizations are reasonable given the lack of data, DELTRAN is preferred, with an enlarged molar paracone [27(1)] being uniquely derived in Adapisorex and "Adapisorella".

Node 26, Soricomorpha.—The taxa united at Node 26 have been traditionally identified as soricomorphs (Butler, 1972, 1988; McKenna and Bell, 1997). Clade support is slightly lower than that for Erinaceomorpha (decay value of 1 step). Soricomorpha are supported by four unequivocal synapomorphies in this analysis: 12(1), P4 metacone weakly developed in postparacrista; 51(0), p3 subequal or slightly smaller than m1; 62(1), p4 entoconid lingually positioned; and 63(1), p4 hypoconid subequal or smaller than entoconid. None of these synapomorphies is uniquely derived. ACCTRAN posits two additional synapomorphies [19(2), P4 postprotocrista extending labially; and 60(0), p4 talonid basin wide], while DELTRAN suggests one additional synapomorphy [86(1), molar entoconid about half the height of the tallest trigonid cusp]. Character 19(2) is probably best viewed as plesiomorphic (a labially extending P4 postprotocrista is present in each of the outgroup taxa), while the DELTRAN optimization of 60(0) at Node 27 is preferred (the ACCTRAN alternative demands reversal of this character back to a narrow p4 talonid basin in "Leptacodon" munusculum). The DELTRAN optimization for 86(1) at Node 26 is probably correct, with a moderately tall molar entoconid having been independently acquired in Paranyctoides.

The positions of Pontifactor, Asionyctia, and Geolabididae render Soricomorpha as recognized by McKenna and Bell (1997) polyphyletic in this analysis (and see previously in the text). As zalambdodonts (including the apternodontids and parapternodontids), palaeoryctids, micropternodontids, nesophontids, or solenodontids (taxa that have at one time or another been considered closely related to extant shrews; e.g., Simpson, 1931; Saban, 1954; McDowell, 1958; Lillegraven et al., 1981; Asher et al., 2002) were not included in this analysis, the nesting of the extant shrew Crocidura within what has traditionally been recognized as Nyctitheriidae is not completely unexpected; given this lack of opportunity for alternative placements, little weight should be given to its position as a derived nyctitheriid as reconstructed here. Two taxa, "Leptacodon" munusculum and "L." packi, are reconstructed as stem soricomorphs (discussed further at Node 29).

Node 28, Nyctitheriidae.—Although branch support is weak (decay value of one step), three synapomorphies are unequivocally optimized at Node 28: 12(2), P4 metacone well-developed; 34(2), posterior cingulum on M1-2 expanded lingually (non-lobate); and 61(1), p4 talonid greater than half the length of trigonid. ACCTRAN posits two additional equivocal synapomorphies [2(1), infraorbital foramen at level of P4; 40(0), one mental foramen], while DELTRAN suggests two others [43(3), i1 crown elongate and multilobate; 44(1), i2 larger than i1]. Of the equivocal synapomorphies, only 40(0) may be reliable as characters 2, 43, and 44 could not be scored for most of the taxa stemming from Node 28. Nyctitheriidae as recognized here is consistent with recent opinions (e.g., McKenna and Bell; Lopatin, 2005), although support for the clade is weak. Nyctitheriids are distinguished from the non-nyctitheriid soricomorphs in the ingroup in having a better-developed metacone on P4 (convergent with "L." munusculum, although the character is polymorphic in this taxon), in having a strongly expanded posterior cingulum on M1-2, and in having a longer and wider talonid on p4.

As with the Geolabididae, the taxonomic history of Nyctitheriidae is extensive and often confusing. Simpson's (1928) original concept of the family (including Nyctitherium, Entomacodon Marsh, 1872, Centetodon, Myolestes Matthew, 1909, and Protentomodon Simpson, 1928) differs significantly from subsequent opinions (e.g., Van Valen, 1967; Sigé, 1976; Krishtalka, 1976b; Butler, 1988; McKenna and Bell, 1997; Lopatin, 2005), but a more or less stable taxonomic core of Leptacodon, Nyctitherium, and Saturninia, and the amphidozotheriines has emerged in more recent classifications. Although an argument could be made for restricting Nyctitheriidae to the taxa stemming from Node 31 (i.e., to include only Nyctitherium, Saturninia and the amphidozotheriines), as three uniquely derived synapomorphies unambiguously support the clade, such action is not taken presently. As with many of the other higher-level clades, branch support at Node 31 is weak (one step), and removal of Leptacodon (s. s.) from Nyctitheriidae based on current evidence does little to promote taxonomic stability; as such, Leptacodon (s. s.) is retained in the Nyctitheriidae as a stem taxon.

The results of a recent study on isolated tarsal bones referred to the European nyctitheriid Cryptotopos suggest that, contrary to all previous opinions, Cryptotopos and other nyctitheriids may be more closely related to primates and tree shrews than to

lipotyphlans (Hooker, 2001). Lopatin (2005) justifiably questioned the results of this study, suggesting that referral of the isolated tarsals to Cryptotopos was not warranted in the absence of dentally associated specimens. It is further noted here that one of the putative synapomorphies uniting the Nyctitheriidae with Archonta (minus bats) in Hooker's (2001) preferred cladogram (Hooker, 2001, fig. 31), a dorsoplantarly deep astragalar fibular facet, is more widely distributed among eutherians than is suggested in that study (Novacek, 1980), and characterizes not only archontans, but also carnivorans, some condylarths, tenrecoids, leptictids, and sciurid rodents (Scott and Boyer, in prep.). An additional synapomorphy uniting nyctitheriids with archontans as posited by Hooker (2001), a reversal from a strongly dilambdodont condition on the upper molars to one in which the centrocrista is straight (i.e., not deflected labially), is viewed here as biologically very unlikely. Although the results of Hooker's (2001) study are both interesting and provocative, a better assessment of his conclusions must await the discovery of more nearly complete specimens of nyctitheriids.

Node 29, Leptacodon (sensu stricto).—Two unequivocal synapomorphies unite three species of Leptacodon (L. rosei, L. tener, L. dormaalensis) to the exclusion of "L." packi and "L." munusculum: 74(1), m1 paracristid flexed; and 77(1), m2-3 paracristid flexed. Three additional equivocal synapomorphies are posited by ACCTRAN [9(1), P3 protocone absent; 42(0), condyle circular in shape; and 98(0), m3 hypoconulid enlarged and finger-like]. Of the equivocal synapomorphies, only 98(0) is reliable, as neither character 9 or 42 can be scored for L. rosei or L. dormaalensis.

The taxonomic history of Leptacodon and the many species referred to it at one time or another is remarkably confusing; as Krishtalka (1976b) noted, much of the confusion regarding the affinities of Leptacodon has stemmed from an inclusion of a number of unrelated species in the genus (e.g., "L." ladae Simpson, 1935a, "L." jepseni, McKenna, 1960). Although the genotype L. tener was originally referred to the Leptictidae (Matthew and Granger, 1921), the species was eventually referred to the Nyctitheriidae (McKenna, 1968; Robinson, 1968); McKenna (1968) and Robinson (1968) clearly restricted the concept of Leptacodon to the genotype only (Krishtalka, 1976b). A number of authors have expressed doubts as to the monophyly of Leptacodon, focusing particularly on two enigmatic taxa, "L." munusculum and "L." packi. For

example, McKenna (1960), while incorrectly referring "L." jepseni to Leptacodon, considered "L." packi to be a leptictid, and that "L." munusculum and L. tener were generically distinct, an opinion that Van Valen (1967) apparently agreed with (Van Valen, 1967 further suggested that "L." ladae and "L." jepseni were also separable at the generic level, opinions that were accepted and formalized years later; see Krishtalka, 1976b; Novacek et al., 1985). Krishtalka (1976b) further suggested that the affinities of "L." munusculum were with the Eocene genus Nyctitherium, while those of "L." packi might be with the poorly known Eocene genus Pontifactor; Bown and Schankler (1982), while agreeing that "L." munusculum and "L." packi were atypical of Leptacodon (s. s.), were not persuaded by Krishtalka's (1976b) opinions regarding the affinities of these taxa, suggesting instead that "L." munusculum and "L." packi may themselves be closely related, but separable from L. tener. Much of the confusion with respect to the affinities of "L." packi and "L." munusculum has stemmed from a lack of information about the upper dentition of each, a situation that has improved recently (Gingerich et al., 1983; Youzwyshyn, 1988; Secord, 2004; this study). While the taxonomic content of Leptacodon continues to be a source of discord and confusion, a relatively stable core of L. tener, L. rosei, and L. dormaalensis seems to be currently accepted (see Smith, 1996); other putative species of Leptacodon are poorly known (e.g., L. proserpinae Van Valen, 1978; L. nascimentoi Estravis, Godinot, and Gingerich, 1996).

Leptacodon is paraphyletic in this analysis, with the positions of "L." packi and "L." munusculum being unstable: in a majority of optimal trees (65 percent) the two taxa form successively more distant outgroups to Node 28, while the remaining nine optimal trees have "L." packi and "L." munusculum as successive outgroups to Node 9 (Asionyctia+Erinaceomorpha). Interestingly, in no optimal tree was "L." packi and "L." munusculum found to be more closely related to Leptacodon (s. s.) to the exclusion of other soricomorphs, nor was "L." packi found to have a special relationship with Nyctitherium (as suggested by Krishtalka, 1976b) or "L." munusculum to Pontifactor (also suggested by Krishtalka, 1976b). Support for the positions of "L." packi and "L." munusculum in the majority rule tree is, however, weak (one step at Node 26 and Node 27). The results of this analysis, although weakly supported, suggest that "L." packi and "L." munusculum are probably not species of Leptacodon (s. s.), but rather represent

either stem nyctitheriids or stem soricomorphs. The latter alternative is tentatively accepted here: the Nyctitheriidae are supported by three unequivocal synapomorphies at Node 28 [12(2), P4 metacone well-developed; 34(2), posterior cingulum on M1-2 expanded lingually (non-lobate); and 61(1), p4 talonid greater than half the length of trigonid], while Leptacodon (s. s.) is distinguished from "L." packi and "L." munusculum by two unequivocal synapomorphies (see earlier in the text). "L." packi and "L." munusculum are further distinguished from Leptacodon (s. s.) by a number of more subtle characters (ones that could not be unambiguously scored in this analysis), including having slightly higher and sharper cusps, a smaller and more anteroposteriorly compressed molar protocone, and better developed molar conules and conular cristae, particularly the postparaconular and premetaconular cristae. Where known, the lower incisors of Leptacodon (s. s.) are multilobate, while those of "L." munusculum more closely resemble those of Xynolestes and Nayloria.

Node 31, unnamed.—Node 31 links two taxa that have been traditionally recognized as nyctitheriines (Saturninia and Nyctitherium) with the amphidozotheriines and extant shrews. Although the clade is recovered in all optimal trees, branch support is poor, collapsing after one additional step. Four unequivocal synapomorphies support the clade: 14(1), P4 hypocone small and conical; 15(2), P4 posterior cingulum greatly expanded and lobe-like; 34(3), M1-2 posterior cingulum greatly expanded and lobe-like; and 51(1), p3 approximately half the size of p4; of these synapomorphies, 14(1), 15(2), and 34(3) are uniquely derived and unambiguously support the clade. ACCTRAN posits one additional synapomorphy [82(1), molar cristid obliqua angular], while DELTRAN posits two others [40(0), mental foramina number one; and 98(1), m3 hypoconulid subequal with other talonid cusps and not projecting]. An arcuate molar cristid obliqua is convergently acquired in geolabidids (see Node 5); its optimization at Node 31 (ACCTRAN) or Node 33 (DELTRAN) is equally likely, requiring reversals in Saturninia (ACCTRAN) or at Node 40 (DELTRAN). Optimization of 98(1) at Node 31 is more conservative: a reduced m3 hypoconulid is characteristic of all taxa stemming from Node 31, and demands an independent acquisition in "L." packi; the alternative requires numerous reversals. Either optimization for character 40(0) seems likely.

Node 32, Nyctitheriinae.—The nyctitheriines Saturninia and Nyctitherium are united at Node 32; a close relationship between these two genera has been hypothesized previously (e.g., Robinson, 1968; Sigé, 1976; Krishtalka, 1976; Bown and Schankler, 1982; Missiaen and Smith, 2005; Lopatin, 2005). 16(1), P4 anterior cingulum prominent; 63(0), p4 hypoconid largest talonid cusp; 86(0), molar entoconid low and nub-like; and 93(1), posterior cingulid prominent and shelf-like all unequivocally support the clade. ACCTRAN posits two additional equivocal synapomorphies [10(1), labial margin of P4 slightly oblique to long axis of crown; and 65(2), posterior exodaenodonty on p4 strong]. None of the unequivocal synapomorphies is uniquely derived. The DELTRAN optimization of 10(1) as an independent acquisition in Nyctitherium is probably correct, rather than the ACCTRAN optimization suggested at Node 32, but the polymorphism of this character in Saturninia makes a choice between the two alternatives equivocal.

Node 37, Amphidozotheriinae.—The Amphidozotheriinae are supported by three unequivocal synapomorphies: 30(2), molar protocone anteriorly displaced to the level of the paracone; 51(0), p3 subequal or slightly smaller than p4; and 75(2), m1 metaconid posterolingual of level of protoconid. ACCTRAN suggests an additional two synapomorphies [65(2), posterior exodaenodonty on p4 strong; and 88(1), molar hypoconid tallest talonid cusp], while DELTRAN posits three others [17(1), P4 paraconule enlarged and anteriorly displaced; 32(0), molar anterior cingulum weak or undeveloped; and 37(1), molar paraconule offset anteriorly]. None of the unequivocal synapomorphies is uniquely derived. A tall molar hypoconid [88(1)] is optimized either as a local synapomorphy of Amphidozotheriinae that is subsequently reversed in Euronyctia (ACCTRAN), or as independent acquisitions in Psydronyctia and Amphidozotherium (DELTRAN). The DELTRAN optimizations for 17(1) and 37(1) are probably correct, with an enlarged P4 paraconule and an anteriorly offset paraconule on M1-2 being local synapomorphies at Node 37 (both convergently acquired in Cryptotopos); the alternative ACCTRAN optimizations at Node 33 are unreliable given that the upper dentition in Plagioctenodon and Ceutholestes is unknown and could not be scored for these characters. The position of character 32(0) at either Node 34 or Node 36 is complicated, again, by the inability for this character to be scored for Plagioctenodon and Ceutholestes.

The Amphidozotheriinae were named by Sigé (1976) to include Amphidozotherium and the poorly known Paradoxonycteris Revilliod, 1922; Euronyctia was subsequently referred to the subfamily by Hooker and Weidmann (2000). Amphidozotheriines are characterized by a suite of unusual characters: for example, the P4 and upper molars of amphidozotheriines bear greatly expanded hypoconal lobes (although the hypocone itself is usually only weakly developed), and the P4 and upper molars tend to develop a labially deflected centrocrista; this is particularly well developed in Euronyctia. The lower teeth are characterized by a reduced m3, an angular molar cristid obliqua, and anteroposteriorly compressed, pillar-like molar protoconid and hypoconid; in advanced amphidozotheriines the antemolar dentition is reduced in size, and in some taxa (e.g., Amphidozotherium), the lower premolars are but single-rooted pegs. As pointed out by Sigé (1976), Hooker and Weidmann (2000), and as confirmed by this analysis, many of these are independently acquired in other nyctitheriids: for example, a lobate hypoconal salient on P4 and the upper molars is present in the nyctitheriines (Node 32), and an angular molar protoconid and hypoconid also occur in the geolabidids. Amphidozotheriines can be distinguished from nyctitheriines (excluding Cryptotopos), however, in the P4 and upper molar protocone being anteriorly displaced to the level of the paracone, and in the anterior cingulum on P4 and the upper molars being weak or undeveloped (and see Node 32).

Amphidozotheriinae as recognized here contain Psydronyctia as a stem member, as well as Amphidozotherium and Euronyctia; the latter two taxa are derived relative to Psydronyctia (see Node 38) in having the p4 cristid obliqua contacting the postvallid wall lingual of the level of the protocristid notch, and continuing towards the apex of the metaconid [66(3)], in having a strongly developed posterior cingulid on the lower molars [93(1)], in having a smaller m3 [95(2)], and in having an extremely narrow m3 talonid [96(1)]. Recognition of Psydronyctia as a primitive amphidozotheriine in this analysis is particularly interesting: prior to this analysis, the subfamily was known only from the late Eocene and Oligocene of Europe, and as such, Psydronyctia represents not only the oldest amphidozotheriine, but also the first known from outside of Europe. Should the phylogenetic position of Psydronyctia prove correct, the origins of the Amphidozotheriinae may well have been in North America.

Amphidozotheriinae are recovered as the sister group to an unusual clade containing Wyonycteris, Entomolestes, and the extant soricid Crocidura. The position of Wyonycteris is peculiar and may be the result of missing data (25 percent of the characters could not be scored for the genus, including seven of the potential synapomorphies suggested for Node 39). Gingerich (1987) originally suggested that Wyonycteris represents the earliest member of Chiroptera, citing a number of dental characters that resembled those of archaeonycterid (e.g., Icaronycteris Jepsen, 1966) and palaeochiropterygid (e.g., Palaeochiropteryx Revilliod, 1917) bats, but this assertion was subsequently challenged (e.g., Hand et al., 1994; Smith, 1995), and Wyonycteris is now considered a nyctitheriid of uncertain affinity in recent classifications (e.g., McKenna and Bell, 1997; but see Smith, 1995). The position of Entomolestes as sister to extant shrews may also be owing to missing data (only 56 percent of the characters could be scored, and more than half of the potential synapomorphies at Node 39 pertain to characters that could not be scored for Entomolestes). Although Entomolestes is currently believed to be closely related to erinaceids (Novacek et al., 1985; Butler, 1988; McKenna and Bell, 1997; Lopatin, 2005), a number of authors have previously entertained the possibility that the genus may be closely related to shrews (e.g., Patterson and McGrew, 1937; McKenna, 1960; Robinson, 1966a): for example, the antemolar dentition of Entomolestes, like that of soricids, is reduced in size, the p4 talonid is virtually undeveloped, and the molar paraconid/paracristid projects strongly anterolingually, lengthening the prevallid wall and presumably enhancing the capacity for shear. As Robinson (1966a) noted, however, many erinaceids also reduce the antemolar dentition, and the molar paraconid/paracristid, at least on m1, is developed in much the same manner in soricids and erinaceids (Butler, 1988). A resolution to this problem must await the discovery of upper teeth that can be confidently referred to Entomolestes.

5.4 Conclusions

This analysis represents the first attempt at comprehensively analyzing the phylogenetic relationships of so-called stem lipotyphlans (including both soricomorphs and erinaceomorphs) using cladistic-based methods. Although weakly supported on the

whole, some of the results are consistent with those arrived at in studies using more traditional methods, while others are not. A number of questions that were posed prior to this analysis (see earlier in the text) are returned to here.

1) Is the Erinaceomorpha/Soricomorpha dichotomy established by Paleocene, or even Late Cretaceous time?

The results of this analysis suggest that a division of stem lipotyphlans into so-called "shrew-like" and "hedgehog-like" taxa was present by at least middle Torrejonian (To2) time, where two taxa, the stem soricomorph "Leptacodon" munusculum and the erinaceomorph Diacocherus, are known in North America (Simpson, 1935a; Van Valen, 1965; Rose, 1981-b); the putative geolabidid Limaconyssus is also known from the middle Torrejonian of Alberta (pers. obs.). The occurrence of these stem lipotyphlans in the early Paleocene obviously implies a still longer evolutionary history, but documentation of that history remains elusive. "L." munusculum, Diacocherus, and Limaconyssus represent definitive occurrences of the Lipotyphla in the early Paleocene; fragmentary specimens from the late Puercan (Pu3) Purgatory Hill local fauna have been referred to Leptacodon proserpinae (see Van Valen, 1978), but these specimens are badly preserved, and whether they are appropriately referred to Leptacodon, or even to the Lipotyphla, are legitimate questions. Clearly more conclusive answers to these issues can only come with a better knowledge of fossil mammals from the earlier parts of the Paleocene and Late Cretaceous. The necessity of an improved record of fossil mammals of this age, particularly that of stem lipotyphlans, is even more important in light of new, morphology based estimates of placental mammal divergence times (e.g., Wible et al., 2007) that suggest an explosive diversification of crown clade eutherians (=Placentalia), including lipotyphlans, at or near the Cretaceous-Tertiary boundary.

2) Can any of the newly identified putative erinaceomorphs or soricomorphs from Alberta be classified with any of the presently recognized stem lipotyphlan families or subfamilies?

All but one of the newly identified stem lipotyphlans from Alberta can be reasonably classified within existing families or subfamilies; support for these groupings varies from

weak (decay value of one step) to moderate (decay value of three steps). Limaconyssus (represented by two new species in the present sample), previously considered a nyctitheriid (Gingerich, 1987), is here considered a geolabidid. Litolestes (represented by a new species in the present sample) is considered a member of the Litolestinae, while Nayloria is sister to Litocherus in the Litocherinae. Although not formally treated in this study, "Adapisorella" is identified here as sister to Adapisorex within a monophyletic Adapisoricinae. The new genus Adeloxenus is reconstructed as a stem adapisoricine, sister to (Adapisorex+"Adapisorella"). A new genus, Psydronyctia, possibly represents the earliest amphidozotheriine, and the first known from North America. The results of this analysis suggest that Xynolestes is probably among "the most primitive erinaceomorphs; it is reconstructed as a stem member of a clade containing the litolestines, litocherines, and adapisoricines.

3) What are the relationships of the Paleocene North American lipotyphlans to those from Europe? What are the biogeographic implications of these relationships?
A close relationship between Nyctitherium and Saturninia has long been suspected (e.g., Robinson, 1968; Krishtalka, 1976b; Bown and Schankler, 1982; McKenna and Bell, 1997; Missiaen and Smith, 2005), and the results of this analysis support these opinions. A second North American nyctitheriid, Psydronyctia, is hypothesized to be the earliest amphidozotheriine, and the first known from outside of Europe. The late Paleocene nyctitheriids Ceutholestes and Plagioctenodon are contained in a more inclusive clade with the European taxon Cryptotopos and the amphidozotheriines, but a lack of information on the upper dentitions of Ceutholestes and Plagioctenodon make these associations tenuous. The late Paleocene record of Psydronyctia significantly predates the earliest record of other amphidozotheriines (late Eocene of Spain; Sigé, 1997), suggesting that the origins of Amphidozotheriinae may have been in North America, and that a significant part of the evolutionary history of the subfamily remains unknown. A second unexpected discovery in this analysis was the identification of specimens referable to the Adapisoricinae from North America. Like the Amphidozotheriinae, the Adapisoricinae (sensu McKenna and Bell, 1997) were previously known only from Paleocene age deposits in continental Europe (see Russell, 1964; Herman and Sigé, 1975;

López-Martínez and Peláez-Campomanes, 1998). Adapisoricines are first known in Europe from the Walbeck fissure fillings of Germany (Russell, 1964); an earliest Tiffanian (Ti1) age has been argued for the local fauna (Savage and Russell, 1983), but this is equivocal, being based mainly on the stage of evolution of some of the included taxa. The earliest record of Adapisoricinae in North America is middle late Tiffanian (Ti3, Adeloxenus and "Adapisorella"); a North American origin for the family is possible (the putatively basalmost adapisoricine, Adeloxenus, is North American), but the issue will remain uncertain until the age of the Walbeck localities can be better established, and the phylogenetic relationships of the various species of Adapisorex are investigated. The discovery of Psydronyctia and Adapisorex in North America, as well as the occurrences of Neoplagiaulax, Arctocyon Blainville, Leptacodon, Wyonycteris, Diacocherus (=Adunator), Saxonella Russell, Plesiadapis Gervais, Chiromyoides Stehlin, Dissacus Cope, and possibly Peradectes, Palaeosinopa, and viverravid carnivorans on both continents in the Paleocene (see Savage and Russell, 1983) further suggests that intercontinental dispersals between North America and Europe during the Paleocene may have been more frequent than previously suspected (e.g., Savage and Russell, 1983; Woodburne and Swisher, 1995).

4) Is Litolestes an erinaceid?

As discussed previously (see Node 19), the results of this analysis suggest that Litolestes and other litolestines are more closely related to the litocherines and adapisoricines than to erinaceids. If the phylogenetic position of Litolestinae proves correct, a corollary of this discovery is that, contrary to previous opinions (e.g., Krishtalka, 1976a; Novacek, 1985; Novacek et al., 1985; McKenna and Bell, 1997), erinaceids are probably not present in the late Paleocene of North America (and see Butler, 1988). The earliest undoubted erinaceids are East Asian, known from the early Eocene of Kyrgyzstan and middle Eocene of China (Lopatin, 2005), while the earliest undoubted North American erinaceids are Oligocene in age (McKenna and Bell, 1997).

5) Is Leptacodon monophyletic?

The results of this analysis suggest that Leptacodon is probably not monophyletic if "L." munusculum and "L." packi are included, a result that is consistent with other that of other studies (e.g., Krishtalka, 1976b; Bown and Schankler, 1982). Leptacodon (s. s.) was recovered in all optimal trees in this analysis, and is best restricted to include only the genotype L. tener, as well as L. rosei and L. dormaalensis. "L." munusculum and "L." packi are reconstructed in this analysis as stem soricomorphs broadly, or more narrowly as stem nyctitheriids.

6) Is Paranyctoides a soricomorph?

Paranyctoides falls outside of the clade containing soricomorphs and erinaceomorphs in this analysis, although its association with the Eocene putative nyctitheriid Pontifactor is bizarre and almost certainly erroneous, and can probably be attributed to missing data: Pontifactor could be scored for only 36 percent of the characters, while Paranyctoides could be scored for only 64 percent, two of the lowest percentages among the ingroup taxa. Paranyctoides was originally thought to be closely related to the Nyctitheriidae (Fox, 1979), and although this hypothesis may still be reasonable, even in light of the unusual association with Pontifactor, Paranyctoides nonetheless lack a number of potential apomorphies identified in this analysis as uniting soricomorphs and erinaceomorphs [e.g., unequivocal synapomorphies at Node 8: 23(1), stylocone absent; 56(1), p4 paraconid well developed; 68(1), molar trigonid steeply inclined; 91(1), m1-2 hypoconulid slightly lingual of the anteroposterior midline]. Given the results of this analysis and the fact that Paranyctoides remains poorly known, the genus is here considered a lipotyphlan of uncertain affinity, consistent with Fox's (1979, 1984) original suggestions. Recent studies on early eutherian mammal relationships (e.g., Archibald et al., 2001; Wible et al., 2007) have identified Paranyctoides as being closely related to the "zhelestids," a probably paraphyletic group of ungulate-like eutherians known primarily from the Late Cretaceous of Middle Asia; clearly the results of these studies attest to the almost wholly primitive nature of Paranyctoides.

7) Is Limaconyssus a nyctitheriid?

As discussed earlier in the chapter, Limaconyssus is considered the first geolabidid of Paleocene age.

8) Is Diacocherus (=Adunator, Mckennatherium) the most primitive erinaceomorph? A number of authors (e.g., Krishtalka, 1976a; Novacek, 1982, 1985; Novacek et al., 1985; Butler, 1988) have suggested that Diacocherus may be the most primitive erinaceomorph. While the genus clearly retains a number of eutherian plesiomorphies (e.g., tall molar trigonids, relatively transverse upper molars, unmodified lower incisors), it is derived in many ways: for example, the cusps are lower and more bulbous than are those in Xynolestes and primitive soricomorphs; the postcrista on P4 and the upper molars is weakly developed; and the P4 metacone is well differentiated from the paracone. Some of these characters are shared with scenopagines, as Krishtalka (1976a) noted, but others are probably specializations developed within the evolutionary history of Diacocherus itself (e.g., unusually swollen metaconid on m2, high, shelf-like paraconid/paracristid on m2-3). The results of this analysis are inconclusive as to whether or not Diacocherus represents the most primitive erinaceomorph: Xynolestes and Diacocherus both occupy basal positions in their respective clades, and each has a suite of primitive and derived characters. Diacocherus is derived relative to Xynolestes in all of those features optimized at Node 11 (e.g., lower and more inflated cusps, shelf-like paraconid/paracristid on m2-3) as well as in a number of autapomorphies (e.g., inflated m2 metaconid, position of the p4 entoconid), but is clearly more primitive in having taller molar trigonids and a subequal m1 and m2. As alluded to earlier in the chapter, a better understanding of the evolutionary relationships of Diacocherus is hindered by the composite nature of the genus: a number of similar, but probably distinct taxa have been included in Diacocherus (compare, e.g., specimens of "Mckennatherium" ladae with those of Diacocherus minutus; Krishtalka, 1976a, figs. 2A-B, 3); clearly a revision the alpha taxonomy of the North American and European forms referred previously to Diacocherus, Adunator, and Mckennatherium is essential. While Novacek (1985) and Novacek et al. (1985) conservatively suggested that the Diacocherus radicle be placed in the Erinaceomorpha incerate sedis, Krishtalka (1976a) indicated that Mckennatherium might be ancestral, or at least closely related to Scenopagus; the results of this analysis

suggest that Diacocherus occupies a basal position in a clade containing scenopagines, sespedectines, and amphilemurids, consistent with Krishtalka's (1976a) views.

5.5 Concluding Remarks

While the results of this analysis are consistent with a number of previous contentions regarding the phylogenetic relationships of stem lipotyphlans, the results are, admittedly, poorly supported by conventional indicators of clade support, and the resulting classifications should be viewed as provisional. Nonetheless, the analysis provides a novel morphological dataset and a suitable starting point for future investigations, and when new evidence becomes available it can be used to test and assess the relationships proposed here. The prospects for obtaining new information that can be brought to bear on stem lipotyphlan relationships is promising: new and exceptionally well-preserved fossils of insectivorans have recently been discovered in freshwater limestone deposits from the late Paleocene and early Eocene of Montana and Wyoming (e.g., Bloch, 2001; Bloch and Boyer, 2001; Bloch, Secord, and Gingerich, 2004; Bloch, Boyer et al., 2004; Silcox et al., in press); many of these specimens preserve detailed anatomy of the basicranium and postcranium, data that are unknown for virtually all stem lipotyphlans and early insectivorans generally, and consequently were not included in this analysis. Newly collected specimens from the Blindman River localities, and especially those from the late middle Paleocene Gao Mine locality of Alberta, also document parts of the cranium and postcranium of stem lipotyphlans and other insectivorans (e.g., Fox, 2004; Scott and Boyer, 2006). While these specimens are generally more poorly preserved than the limestone specimens from the United States, they are perhaps even more crucial in understanding the phylogenetic relationships of early lipotyphlans as they represent taxa that are significantly older, and in many cases more primitive, than those taxa that are known from the Clarkforkian and Wasatchian of Montana and Wyoming. As useful as these new discoveries will undoubtedly be, the evidence to date suggests that the Lipotyphla probably originated in the Late Cretaceous or earliest parts of the Paleocene; as such, geologically older fossils are necessary to provide insight into the earliest parts of their history.

5.6 Literature Cited

AMRINE-MADSEN, H, K. P. KOEPFLI, R. K. WAYNE, and M. S. SPRINGER. 2003. A new phylogenetic marker, apolipoprotein B, provides compelling evidence for eutherian relationships. Molecular Phylogenetics and Evolution, 28:225-40.

ARCHIBALD, J. D. 2003. Timing and biogeography of the eutherian radiation: fossils and molecules compared. Molecular Phylogenetics and Evolution, 28:350-359.

ARCHIBALD, J. D. and A. O. AVERIANOV. 2001. Paranyctoides and allies from the Late Cretaceous of North America and Asia. Acta Palaeontologica Polonica, 46:533-551.

ARCHIBALD, J. D. and A. O. AVERIANOV. 2006. Late Cretaceous asioryctitherian eutherian mammals from Uzbekistan and phylogenetic analysis of Asioryctitheria. Acta Palaeontologica Polonica, 51:351-376.

ARCHIBALD, J. D., A. O. AVERIANOV, and E. G. EKDALE. 2001. Late Cretaceous relatives of rabbits, rodents, and other extant eutherian mammals. Nature, 414:62-65.

ARNASON, U., J. A. ADEGOKE, K. BODIN, E. W. BORN, Y. B. ESA, A. GULLBERG, M. NILSSON, R. V. SHORT, XU X., and A. JANKE. 2002. Mammalian mitogenomic relationships and the root of the eutherian tree. Proceedings of the National Academy of Sciences, 99:8151-8156.

ASHER, R. J. 2005. Insectivoran-Grade Placental mammals: Character Evolution and Fossil History, pp. 50-70. In K. D. ROSE and J. D. ARCHIBALD (eds.), The Rise of Placental Mammals: Origin and Relationships of the Major Clades, The Johns Hopkins University Press, Baltimore.

ASHER, R. J., M. C. MCKENNA, R. J. EMRY, A. R. TABRUM, D. G. KRON. 2002. Morphology and relationships of Apternodus and other extinct, zalambdodont, placental mammals. Bulletin of the American Museum of Natural History, 273:1–117.

ASHER, R. J., M. J. NOVACEK, and J. H. GEISLER. 2003. Relationships of endemic African mammals and their fossil relatives based on morphological and molecular evidence. Journal of Mammalian Evolution, 10:131-194.

ASHER, R. J., R. J. EMRY, and M. C. MCKENNA. 2005. New material of Centetodon (Mammalia, Lipotyphla) and the importance of (missing) DNA sequences in systematic paleontology. Journal of Vertebrate Paleontology 25:911–923.

AVERIANOV, A. O. 1995. Nyctitheriid insectivores from the Upper Paleocene of Southern Kazakhstan (Mammalia: Lipotyphla). Senckenbergiana Lethaea, 75:215–219.

BERGGREN, W. A., D. V. KENT, C. C. SWISHER, III, AND M.-P. AUBRY. 1995. A revised Cenozoic geochronology and chronostratigraphy, pp. 129-212. In W. A. BERGGREN, D. V. KENT, M.-P. AUBRY, and J. HARDENBOL (eds.), Geochronology, time scales and global stratigraphic correlation, SEPM Special Publication, 54.

BLAINVILLE, H. M. D. de. 1838. Recherches sur l'ancienneté des Mammifères insectivores à la surface de la terre; précédées de l'histoire de la science à ce sujet, des principes de leur classification et de leur distribution géographique actuelle. Comptes Rendus Hebdomadaires de Seances de l'Academie des Sciences, 6:738-744.

BLOCH, J. I. 2001. Mammalian paleontology of freshwater limestones from the Paleocene-Eocene of the Clarks Fork Basin, Wyoming. Unpublished Ph.D. dissertation, The University of Michigan, Ann Arbor, 358 pp.

BLOCH, J. I., and D. M. BOYER. 2001. Taphonomy of small mammals in freshwater limestones from the Paleocene of the Clarks Fork Basin, pp. 185-198. In P. D. GINGERICH (ed.), Paleocene-Eocene stratigraphy and biotic change in the Bighorn and Clarks Fork basins, Wyoming, The University of Michigan Museum of Paleontology Papers on Paleontology, 33.

BLOCH, J. I., and M. T. SILCOX. 2001. New basicrania of Paleocene-Eocene Ignacius: Re-evaluation of the plesiadapiform-dermopteran link. American Journal of Physical Anthropology, 116:184-198.

BLOCH, J. I., K. D. ROSE, and P. D. GINGERICH. 1998. New species of Batodonoides (Lipotyphla, Geolabididae) from the early Eocene of Wyoming: smallest mammal known? Journal of Mammalogy, 79:804-827.

BLOCH, J. I., R. SECORD, and P. D. GINGERICH. 2004. Systematics and phylogeny of late Paleocene and early Eocene Palaeoryctinae (Mammalia, Insectivora) from the

Clarks Fork and Bighorn basins, Wyoming. Contributions from the Museum of Paleontology, The University of Michigan, 31:119-154.

BLOCH, J. I., D. M. BOYER, P. HOUDE, and M. T. SILCOX. 2004. New skeletons of Paleocene-Eocene Labidolemur kayi (Mammalia, Apatemyidae): ecomorphology and relationship of apatemyids to primates and other mammals. Journal of Vertebrate Paleontology, 24, supplement to no. 3:40A.

BOWDICH, T. E. 1821. An analysis of the natural classifications of Mammalia for the use of students and travelers. Paris, J. Smith. 115+[31] pp.

BOWN, T. M. 1979. Geology and mammalian paleontology of the Sand Creek facies, lower Willwood Formation (lower Eocene), Washakie County, Wyoming. Geological Survey of Wyoming, Memoir, 2:1-151.

BOWN, T. M., and D. SCHANKLER. 1982. A review of the Proteutheria and Insectivora of the Willwood Formation (lower Eocene), Bighorn Basin, Wyoming. U. S. Geological Survey Bulletin, 1523:1-79.

BOYER, D. M., and J. I. BLOCH. 2003. Comparative anatomy of the pentacodontid Aphronorus orieli (Mammalia, Pantolesta) from the Paleocene of the western Crazy Mountains Basin, Montana. Journal of Vertebrate Paleontology 23, supplement to no. 3:36A.

BREMER, K. 1988. The limits of amino acid sequence data in angiosperm phylogenetic reconstruction. Evolution, 42: 795-803.

BREMER, K. 1994. Branch support and tree stability. Cladistics, 10: 295-304.

BRYANT, H. N. 2001. Character polarity and the rooting of cladograms, pp. 321-340. In G. P. WAGNER (ed.), The Character Concept in Evolutionary Biology, Academic Press, San Diego.

BUTLER, P. M. 1948. On the evolution of the skull and teeth in the Erinaceidae, with special reference to fossil material in the British Museum. Proceedings of the Zoological Society of London, 118:446-500.

BUTLER, P. M. 1956. The skull of Ictops and the classification of the Insectivora. Proceedings of the Zoological Society, London, 126:453-481.

BUTLER, P. M. 1972. The problem of insectivore classification, pp. 253-265. In K. A. JOYSEY and T. S. KEMP (eds.), Studies in Vertebrate Evolution, Oliver and Boyd, Edinburgh.

BUTLER, P. M. 1978. A new interpretation of the mammalian teeth of tribosphenic pattern from the Albian of Texas. Breviora, 78:1-27.

BUTLER, P. M. 1988. Phylogeny of the insectivores, pp. 253-265. In M. J. BENTON (ed.), The Phylogeny and Classification of the Tetrapods Vol. 2. Mammals. Systematics Association Special Volume 35B, Clarendon Press, Oxford.

BUTLER, P. M., R. S. THORPE, and M. GREENWOOD. 1989. Interspecific relations of African crocidurine shrews (Mammalia: Soricidae) based on multivariate analysis of mandibular data. Zoological Journal of the Linnean Society, 96: 373-412.

CAMP, C. L., S. P. WELLES, and M. GREEN. 1949. Bibliography of fossil vertebrates 1939-1943. Memoire of the Geological Society of America, 37:1-371.

CAMIN, J. H., and R. R. SOKAL. 1965. A method for deducing branching sequences in phylogeny. Evolution, 19: 311-326.

CANDE, S. C., and D. V. KENT. 1995. Revised calibration of the geomagnetic polarity timescale for the Late Cretaceous and Cenozoic. Journal of Geophysical Research, 100:6093-6095.

CARPENTER, J. M. 1996. Uninformative bootstrapping. Cladistics, 12:177-181.

CARTMILL, M., and R. D. E. MACPHEE. 1980. Tupaiid affinities: the evidence of the carotid arteries and cranial skeleton, pp. 95-132. In W. P. LUCKETT (ed.), Comparative biology and evolutionary relationships of the tree shrews, Plenum Press, New York and London.

CIFELLI, R. L. 1982. The petrosal structure of Hyopsodus with respect to that of some other ungulates, and its phylogenetic implications. Journal of Paleontology, 56:795-805.

CLEMENS, W.A. 1973. Fossil mammals of the type Lance Formation, Wyoming. Part III. Eutheria and summary. University of California Publications in Geological Sciences, 94: 1-102.

CLEMENS, W. A., and L. S. RUSSELL. 1965. Mammalian fossils from the upper Edmonton Formation. University of Alberta Geology Bulletin, 2:32-40.

CONROY, G. C., and J. R. WIBLE. 1978. Middle ear morphology of Lemur variegatus: some implications for primate paleontology. Folia Primatologica, 29:81-85.

COPE, E. D. 1872. Second account of new Vertebrata from the Bridger Eocene. Proceedings of the American Philosophical Society, 12 (separata Paleontological Bulletin no. 2):466-468. [dated August 3]

COPE, E. D. 1873. Synopsis of new Vertebrata from the Tertiary of Colorado, obtained during the summer of 1873. Washington, D. C., U. S. Government Printing Office, 19 pp.

COPE, E. D. 1875. Systematic catalogue of Vertebrata of the Eocene of New Mexico, collected in 1874. Report to the Engineer Department, U.S. Army, in charge of Lieut. Geo. M. Wheeler, April 17 1875, Washington, D. C., p. 5-37.

COPE, E. D. 1884. Second addition to the knowledge of the fauna of Puerco epoch. Proceedings of the American Philosophical Society, 21:309-324.

CROCHET, J.-Y. 1974. Les Insectivores des phosphorites du Quercy. Palaeovertebrata, 6:109-159.

CROMPTON, A. W. and Z. KIELAN-JAWOROWSKA. 1978. Molar structure and occlusion in Cretaceous mammals, pp. 249-287. In P. M. BUTLER and K. A. JOYSEY (eds.), Development, Function and Evolution of Teeth, Academic Press, New York.

DASHZEVEG, D., and D. E. RUSSELL. 1992. Extension of dyspternine Pantolestidae (Mammalia, Cimolesta) in the Early Oligocene of Mongolia. Geobios, 25:647-650.

DELSON, E. 1971. Fossil mammals of the early Wasatchian Powder River local fauna, Eocene of northwest Wyoming. Bulletin of the American Museum of Natural History, 146:309-364.

DORR, J. A. 1977. Partial skull of Paleosinopa simpsoni (Mammalia, Insectivora), latest Paleocene Hoback Formation, central western Wyoming, with some general remarks on the family Pantolestidae. Contributions from the Museum of Paleontology, The University of Michigan, 24: 281-307.

DOUADY, C. J., P. I. CHATELIER, O. MADSEN, W. W. DE JONG, F. CATZEFLIES, M .S. SPRINGER, and M. J. STANHOPE. 2002. Molecular phylogenetic evidence

confirming the Eulipotyphla concept and in support of hedgehogs as the sister group to shrews. Molecular Phylogenetics and Evolution, 25:200-209.

DOUADY C. J., M. SCALLY, M. S. SPRINGER, and M. J. STANHOPE. 2004. "Lipotyphlan" phylogeny based on the growth hormone receptor gene: a reanalysis. Molecular Phylogenetics and Evolution, 30:778-788.

DUFTON, M. J. 1992. Venomous mammals. Pharmacology and Therapeutics, 53:199-215.

EBERLE, J. J., and M. C. MCKENNA. 2002. Early Eocene Leptictida, Pantolesta, Creodonta, Carnivora, and Mesonychidae (Mammalia) from the Eureka Sound Group, Ellesmere Island, Nunavut. Canadian Journal of Earth Sciences, 39:899-910.

EKDALE E. G., J. D. ARCHIBALD, and A. O. AVERIANOV. 2004. Petrosal bones of placental mammals from the Late Cretaceous of Uzbekistan. Acta Palaeontologica Polonica, 49:161-176.

EMERSON, G. L., C. W. KILPATRICK, B. E. MCNIFF, J. OTTENWALDER, and M. W. ALLARD. 1999. Phylogenetic relationships of the order Insectivora based on complete 12S rRNA sequences from mitochondria. Cladistics, 15:221-230.

ESTRAVIS, C., M. GODINOT, and P. D. GINGERICH. 1996. Leptacodon nascimentoi n. sp., un nouveau Nyctitheriidae (Mammalia, Lipotyphla) de l'Éocène inférieur de Silveirinha (Baisxo Mondego, Portugal). Palaeovertebrata, 25:279-286.

FARRIS, J. S. 1970. Methods for computing Wagner trees. Systematic Zoology,19:83-92.

FARRIS, J. S. 1982. Outgroups and parsimony. Systematic Zoology, 31:328-334.

FELSENSTEIN, J. 1985. Confidence limits on phylogenies: An approach using the bootstrap. Evolution, 39:783-791.

FILHOL, H. 1877. Recherches sur les phosphorites du Quercy. Étude des fossiles qu'on y rencontre et spécialement des Mammifères. 561 pp. Masson, Paris.

FILHOL, H. 1890. Description d'un nouveau genre d'insectivore provenantdes dépots de phosphate de chaux du Quercy. Bulletin de la Societé philomatique de Paris, serie II, 8:176–177.

FOX, R. C. 1975. Molar structure and function in the Early Cretaceous mammal Pappotherium: Evolutionary implications for Mesozoic Theria. Canadian Journal of Earth Sciences, 12:412-442.

FOX, R. C. 1979. Mammals from the Upper Cretaceous Oldman Formation, Alberta. III. Eutheria. Canadian Journal of Earth Sciences, 16:114-125.

FOX, R. C. 1983. Evolutionary implications of tooth replacement in the late Paleocene mammal Pararyctes. Canadian Journal of Earth Sciences, 20:19-22.

FOX, R. C. 1984. Paranyctoides maleficus (new species), an early eutherian mammal from the Cretaceous of Alberta. Special Publication of the Carnegie Museum of Natural History, 9:9-20.

FOX, R. C. 1990. The succession of Paleocene mammals in western Canada, p. 51-70. In T. M. BOWN and K. D. ROSE (eds.), Dawn of the Age of Mammals in the northern part of the Rocky Mountain Interior. Geological Society of America Special Paper, 243.

FOX, R. C. 1994. Composition of the holotype of the North American Late Cretaceous mammal Cimolestes cerberoides Lillegraven, 1969. Journal of Paleontology, 68: 910-911.

FOX, R. C. 2004. A new palaeoryctid (Insectivora: Mammalia) from the late Paleocene of Alberta, Canada. Journal of Paleontology, 78:612–616.

FOX, R. C., and G. P. YOUZWYSHYN. 1994. New primitive carnivorans (Mammalia) from the Paleocene of western Canada, and their bearing on relationships of the order. Journal of Vertebrate Paleontology, 14:382-404.

FOX, R. C., and C. S. SCOTT. 2005. First evidence of a venom delivery apparatus in extinct mammals. Nature, 435:1091-1093.

FROST, D. R., WOZENCRAFT, W. C., and HOFFMANN, R. S. 1991. Phylogenetic relationships of hedgehogs and gymnures (Mammalia: Insectivora: Erinaceidae). Smithsonian Contributions to Geology, 518:2-69.

GAZIN, C. L. 1956. Paleocene mammalian faunas of the Bison Basin in south-central Wyoming. Smithsonian Miscellaneous Collections, 131:1-57.

GAZIN, C. L. 1969. A new occurrence of Paleocene mammals in the Evanston Formation, southwestern Wyoming. Smithsonian Contributions to Paleobiology, 2:1-16.

GEISLER, J. H. 2001. New morphological evidence for the phylogeny of Artiodactyla, Cetacea, and Mesonychidae. American Museum Novitates, 3344:1-53.

GERVAIS, P. 1848-1852. Zoologie et paléontologie Françaises. Paris, Arthus Bertrand, text, 2 vols.; atlas, 80 pls.

GERVAIS, P. 1859. Zoologie et paléontologie Françaises. Deuxieme edition. Paris, text, pp. i-viii, 1-544, figs. 1-51, atlas, pp. i-xii, pls. 1-84.

GHEERBRANT, E. 1988. Afrodon chleuhi nov. gen., nov. sp., "insectivore" (Mammalia, Eutheria) lipotyphlé (?) du Paléocène marocain: données préliminaires. Comptes Rendus de l'Académie des Sciences de Paris, II, 307:1303-1309.

GHEERBRANT, E. 1991. Bustylus (Eutheria, Adapisoriculidae) and the absence of ascertained marsupials in the Paleocene of Europe. Terra Nova, 3:586-592.

GHEERBRANT, E., and D. E. RUSSELL. 1989. Presence of the genus Afrodon (Eutheria, Lipotyphla (?), Adapisoriculidae) in Europe; new data for the problem of trans-Tethyan relations between Africa and Europe around the K/T boundary. Palaeogeography, Palaeoclimatology, Palaeoecology, 76:1-15.

GHEERBRANT, E., and D. E. RUSSELL. 1991. Bustylus cernaysi, nouvel adapisoriculidé (Mammalia, Eutheria) paléocène d'Europe. Geobios, 24:467-481.

GHEERBRANT, E., J. SUDRE, S. SEN, C. ABRIAL, B. MARANDAT, B. SIGÉ, and M. VIANEY-LIAUD. 1998. Nouvelles données sur les mammifères du Thanétien et de l'Yprésien du bassin d'Ouarzazate (Maroc) et leur contexte stratigraphique. Palaeovertebrata, 27:155-202.

GILL, T. 1872. Arrangement of the families of mammals with analytical tables. Smithsonian Miscellaneous Collections, 11:1-98.

GINGERICH, P. D. 1980a. A new species of Palaeosinopa (Insectivora: Pantolestidae) from the late Paleocene of western North America. Journal of Mammalogy, 61:449-454.

GINGERICH, P. D. 1980b. Tytthaena parrisi, oldest known oxyaenid (Mammalia, Creodonta) from the late Paleocene of western North America. Journal of Paleontology, 54: 570-576.

GINGERICH, P. D. 1982a. Aaptoryctes (Palaeoryctidae) and Thelysia (Palaeoryctidae?): new insectivorous mammals from the late Paleocene and early Eocene of western North America. Contributions from the Museum of Paleontology, The University of Michigan, 26:37-47.

GINGERICH, P. D. 1982b. Studies on Paleocene and early Eocene Apatemyidae (Mammalia, Insectivora): Part II. Labidolemur and Apatemys from the early Wasatchian of the Clark's Fork Basin, Wyoming. Contributions from the Museum of Paleontology, The University of Michigan, 26: 57-69.

GINGERICH, P. D. 1983. New Adapisoricidae, Pentacodontidae, and Hyopsodontidae (Mammalia, Insectivora and Condylarthra) from the late Paleocene of Wyoming and Colorado. Contributions from the Museum of Paleontology, The University of Michigan, 26:227-255.

GINGERICH, P. D. 1987. Early Eocene bats (Mammalia, Chiroptera) and other vertebrates in freshwater limestones of the Willwood Formation, Clarks Fork Basin, Wyoming. Contributions from the Museum of Paleontology, University of Michigan, 27:275-320.

GINGERICH, P. D., and K. D. ROSE. 1982. Studies on Paleocene and early Eocene Apatemyidae (Mammalia, Insectivora): Part I. Dentition of Clarkforkian Labidolemur kayi. Contributions from the Museum of Paleontology, The University of Michigan, 26:49-55.

GINGERICH, P. D., and D. A. WINKLER. 1985. Systematics of Paleocene Viverravidae (Mammalia, Carnivora) in the Bighorn Basin and Clark's Fork Basin, Wyoming. Contributions from the Museum of Paleontology, The University of Michigan, 27:87-128.

GINGERICH, P. D., P. HOUDE, and D. W. KRAUSE. 1983. A new earliest Tiffanian (late Paleocene) mammalian fauna from the Bangtail Plateau, western Crazy Mountain Basin, Montana. Journal of Paleontology, 57:957-970.

GOULD, G. C. 1995. Hedgehog phylogeny (Mammalia, Erinaceidae)—the reciprocal illumination of the quick and the dead. American Museum Novitates, 3131:1-45.

GOULD, G. C. 2001. The phylogenetic resolving power of discrete dental morphology among extant hedgehogs and the implications for their fossil record. American Museum Novitates, 3340:1-52.

GREGORY, W. K. 1910. The orders of mammals. Bulletin of the American Museum of Natural History, 27:1-254.

GREGORY, W. K., and G. G. SIMPSON. 1926. Cretaceous mammal skulls from Mongolia. American Museum Novitates, 225:1-20.

GRENYER, R., and A. PURVIS. 2003. A composite species-level phylogeny of the "Insectivora" (Mammalia: Order Lipotyphla Haeckel, 1866). Journal of Zoology, 260:245-257.

GUNNELL, G. F. 1988. New species of Unuchinia (Mammalia: Insectivora) from the middle Paleocene of North America. Journal of Paleontology, 62:139-141.

GUNNELL, G. F. 1989. Evolutionary history of Microsyopoidea (Mammalia, ?Primates) and the relationship between Plesiadapiformes and Primates. The University of Michigan, Papers on Paleontology, 27:1-157.

GUNNELL, G. F. 1994. Paleocene mammals and faunal analysis of the Chappo Type Locality (Tiffanian), Green River Basin, Wyoming. Journal of Vertebrate Paleontology, 14:81-104.

HAECKEL, E. 1866. Generelle Morphologie der Organismen, vol. 2: Systematische Einteilung in die allgemeine Entwickelungsgeschichte. Georg Reimer, Berlin.

HAND, S. J., M. J. NOVACEK, H. GODHELP, and M. ARCHER. 1994. First Eocene bat from Australia. Journal of Vertebrate Paleontology, 14:375-381.

HAUSER, D. L., and W. PRESCH. 1991. The effect of ordered characters on phylogenetic reconstruction. Cladistics, 7:243-266.

HEINRICH, R. E., and K. D. ROSE. 1997. Postcranial morphology and locomotor behaviour of two early Eocene miacoid carnivorans, Vulpavus and Didymictis. Palaeontology, 40:279-305.

HELLER, F. 1935. Amphilemur eocaenicus n. g. et n. sp., ein primitiver Primate aus dem Mitteleozän des Geiseltales bei Halle a. S. Nova Acta Leopoldina, N. F., 2:293-300.

HERMAN, J., and B. SIGÉ. 1975. Présence du genre Paléocène Adapisorex (Lipotyphla, Mammalia) dans les Sables d'Orp-le-Grand (Heersien) a Maret en Brabant (Belgique). Géobios, 8:231-239.

HOLROYD, P. A., T. M. BOWN, and D. M. SCHANKLER. 2004. Auroralestes, gen. nov., a replacement name for Eolestes Bown and Schankler, 1982, a preoccupied name. Journal of Vertebrate Paleontology, 24:979.

HOLTZMAN, R. C. 1978. Late Paleocene mammals of the Tongue River Formation, western North Dakota. Report of Investigation, North Dakota Geological Survey, 65:1-88.

HOOKER, J. J. 2001. Tarsals of the extinct insectivoran family Nyctitheriidae (Mammalia): evidence for archontan relationships. Zoological Journal of the Linnean Society, 132:501-529.

HOOKER, J. J., and M. WEIDMANN. 2000. The Eocene mammal faunas of Mormont, Switzerland. Systematic revision and resolution of dating problems. Schweizerische Palaeontologische Abhandlungen, 120:1-141.

HUTTERER, R. 2005. Insectivora, pp. 212-311. In D. E. WILSON and D. M. REEDER (eds.), Mammal Species of the World, 3rd edition, Johns Hopkins University Press, Baltimore.

HUXLEY, T. H. 1880. On the application of the laws of evolution to the arrangement of the Vertebrata, and more particularly of the Mammalia. Proceedings of the Royal Society, London, 43:649-662.

INTERNATIONAL CODE OF ZOOLOGICAL NOMENCLATURE: FOURTH EDITION. INTERNATIONAL COMMISSION ON ZOOLOGICAL NOMENCLATURE. 1999. International Trust for Zoological Nomenclature, London. ISBN 0 85301 006 4. xxix+306 pp.

JACKSON, K. 2003. The evolution of venom-delivery systems in snakes. Zoological Journal of the Linnean Society, 137:337-354.

JAEGER, J. J. 1970. Pantolestidae nouveaux (Mammalia, Insectivora) de l'Éocène moyen de Bouxwiller (Alsace): Palaeovertebrata, 3:63-82.

JEPSEN, G. L. 1930. Stratigraphy and paleontology of the Paleocene of northeastern Park County, Wyoming. Proceedings of the American Philosophical Society, 69:463-528.

JEPSEN, G. L. 1934. A revision of the American Apatemyidae and the description of a new genus, Sinclairella, from the White River Oligocene of South Dakota. Proceedings of the American Philosophical Society, 74:287-305.

JEPSEN, G. L. 1966. Early Eocene bat from Wyoming. Science, 154:1333-1339.

JI Q., LUO Z.-X., YUAN C.-X., J. R. WIBLE, ZHANG J. P., and J. A. GEORG. 2002. The earliest known eutherian mammal. Nature, 416:816-822.

KALTHOFF, D. C., W. v. KOENIGSWALD, and C. KURZ. 2004. A new specimen of Heterohyus nanus (Apatemyidae, Mammalia) from the Eocene of Messel (Germany) with unusual soft part preservation. Courier Forschungsinstitut Senckenberg, 252:1-12.

KELLNER, A. W., and M. C. MCKENNA. 1996. A leptictid mammal from the Hsanda Gol Formation (Oligocene), central Mongolia, with comments on some Palaeoryctidae. American Museum Novitates, 3168:1-13.

KIELAN-JAWOROWSKA, Z. 1969. Preliminary data on the Upper Cretaceous eutherian mammals from Bayn Dzak, Gobi Desert, pp. 171-191. In Z. KIELAN-JAWOROWSKA (ed.), Results of the Polish-Mongolian Palaeontological Expeditions, pt. I. Palaeontologia Polonica, 19.

KIELAN-JAWOROWSKA, Z. 1975. Preliminary description of two new eutherian genera from the Late Cretaceous of Mongolia, pp. 5-16. In Z. KIELAN-JAWOROWSKA (ed.), Results of the Polish-Mongolian Palaeontological Expeditions, pt. VI. Palaeontologia Polonica, 33.

KIELAN-JAWOROWSKA, Z. 1981. Evolution of the therian mammals in the Late Cretaceous of Asia. Part IV. Skull structure in Kennalestes and Asioryctes. Palaeontologia Polonica, 42:25-78.

KIELAN-JAWOROWSKA, Z., T. M. BOWN, and J. A. LILLEGRAVEN. 1979. Eutheria, pp. 222-258. In J. A. LILLEGRAVEN, Z. KIELAN-JAWOROWSKA, and W. A. CLEMENS (eds.), Mesozoic Mammals: the first two-thirds of mammalian history. University of California Press, Berkeley.

KIHM, A. J., and J. H. HARTMAN. 2004. A reevaluation of the biochronology of the Brisbane and Judson Local Faunas (late Paleocene) of North Dakota. Bulletin of the Carnegie Museum of Natural History, 36:97-107.

KLUGE, A. G. and A. J. WOLF. 1993. Cladistics: what's in a word? Cladistics, 9:183-199.

KOBAYASHI, Y., D. A. WINKLER, and L. L. JACOBS. 2002. Origin of tooth-replacement pattern in therian mammals: evidence from a 110 Myr old fossil. Proceedings of the Royal Society B, 269:369-373.

KOENIGSWALD, W. v. 1980. Das Skelett eines Pantolestiden (Proteutheria, Mammalia) aus dem mittleren Eozän von Messel bei Darmstadt. Paläontologische. Zeitschrift, 54:267-287.

KOENIGSWALD, W. v. 1983. Der erste Pantolestide (Proteutheria, Mammalia) aus dem Eozän des Geiseltals bei Halle. Zeitschrift für geologische Wissenschaften Berlin, 11: 787-793.

KOENIGSWALD, W. v. 1987. Apatemyiden-Skelette aus dem Mitteleozän von Messel und ihre paläobiologische Aussage. Carolinea, 45:31-35.

KOENIGSWALD, W. v. 1990. Die Paläobiologie der Apatemyiden (Insectivora s. l.) und die Ausdeutung der Skelettfunde von Heterohyus nanus aus dem Mitteleozän von Messel bei Darmstadt. Palaeontographica Abteilung A, 210:41-77.

KOENIGSWALD, W., and G. STORCH. 1983. Pholidocercus hassiacus, ein Amphilemuride aus dem Eozän der "Grube Messel" bei Darmstadt (Mammalia, Lipotyphla). Senckenbergiana Lethaea, 64:403-445.

KOENIGSWALD, W. v., and H.-P. SCHIERNING. 1987. The ecological niche of an extinct group of mammals, the early Tertiary apatemyids. Nature, 326:595-597.

KOENIGSWALD, W. v., K. D. ROSE, L. GRANDE, and R. D. MARTIN. 2005a. Die Lebensweise eozäner Säugetiere (Pantolestidae und Apatemyidae) aus Messel (Europa) im Vergleich zu neuen Skelettfunden aus dem Fossil Butte Member von Wyoming. Geologisches Jahrbuch Hessen, 132:43-52.

KOENIGSWALD, W. v., K. D. ROSE, L. GRANDE, and R. D. MARTIN. 2005b. First apatemyid skeleton from the lower Eocene Fossil Butte Member, Wyoming, compared to the European apatemyid from Messel, Germany. Palaeontographica Abteilung A, 272:149-169.

KONDRASHOV, P. E., A. V. LOPATIN, and S. G. LUCAS. 2004. Late Paleocene (Gashatan) Nyctitheriidae (Mammalia, Lipotyphla) from Mongolia. New Mexico Museum of Natural History and Science Bulletin, 26: 185-193.

KRAUSE, D. W., and P. D. GINGERICH. 1983. Mammalian fauna from Douglass Quarry, earliest Tiffanian (late Paleocene) of the eastern Crazy Mountain Basin, Montana. Contributions from the Museum of Paleontology, The University of Michigan, 26:157-196.

KRAUSE, D. W., and M. C. MAAS. 1990. The biogeographic origins of late Paleocene-early Eocene mammalian immigrants to the Western Interior of North America, pp. 71-105. In: T. M. BOWN and K. D. ROSE (eds.), Dawn of the Age of Mammals in the Northern Part of the Rocky Mountain Interior, Geological Society of America, Special Paper, 243:71-105.

KRISHTALKA, L. 1973. Late Paleocene mammals from the Cypress Hills, Alberta. Special Publications of the Museum, Texas Tech University, 2:1-77.

KRISHTALKA, L. 1975. Systematics and relationships of early Tertiary Lipotyphla (Mammalia, Insectivora) of North America. Unpublished Ph. D. dissertation, Texas Tech University, 168 pp.

KRISHTALKA, L. 1976a. Early Tertiary Adapisoricidae and Erinaceidae (Mammalia, Insectivora) of North America. Bulletin of Carnegie Museum of Natural History, 1:1-40.

KRISHTALKA, L. 1976b. North American Nyctitheriidae (Mammalia, Insectivora). Annals of Carnegie Museum, 46:7-28.

KRISHTALKA, L. 1977. Early Eocene Euramerican Insectivora, pp. 135-139. In Les Faunes de Mammifères du Paléogène d'Eurasie, Geobios 10, supplement 1.

KRISHTALKA, L., and R. M. WEST. 1977. Paleontology and geology of the Bridger Formation, southern Green River Basin, southwestern Wyoming. Part 2. The Bridgerian insectivore Entomolestes grangeri. Milwaukee Public Museum Contributions in Biology and Geology 14:1-11.

KRISHTALKA, L., and R. M. WEST. 1979. Paleontology and geology of the Bridger Formation, southern Green River Basin, southwestern Wyoming. Part 4. The Geolabididae (Mammalia, Insectivora). Milwaukee Public Museum Contributions in Biology and Geology, 27:1-10.

LAKE, A. R. and T. R. TREVOR-JONES. 1996. The venom apparatus of the boomslang or tree snake, Dispholidus typus. South African Journal of Science, 92:167-169.

LEIDY, J. 1868. Notice of some remains of extinct Insectivora from Dakota. Proceedings of the Academy of Natural Sciences, Philadelphia, 1868:315-316.

LEIDY, J. 1870. Remarks on a collection of fossils from the western Territories. Proceedings of the Academy of Natural Sciences, Philadelphia, 22:109-110.

LEMOINE, V. 1883. Etude sur le Neoplagiaulax de la faune éocène inférieure des environs de Reims. Bulletin de la Société Géologique de France, 3e série, 11:249-271.

LILLEGRAVEN, J. A. 1969. Latest Cretaceous mammals of upper part of the Edmonton Formation of Alberta, Canada, and review of marsupial-placental dichotomy in mammalian evolution. The University of Kansas Paleontological Contributions, 50 (Vertebrata 12):1-122.

LILLEGRAVEN, J. A., M. C. MCKENNA, and L. KRISHTALKA. 1981. Evolutionary relationships of Middle Eocene and younger species of Centetodon (Mammalia, Insectivora, Geolabididae) with a description of the dentition of Ankylodon. University of Wyoming Publications, 45:1-97.

LINNAEUS, C. 1758. Systema naturae per regna tria naturae, secundum classes, ordines, genera, species cum characteribus, differentiis, synonymis, locis (editio decima, reformata). Laurenti Salvii, Stockholm.

LIPSCOMB, D. L. 1992. Parsimony, homology and the analysis of multistate characters. Cladistics, 8: 45-65.

LIVEZEY, B. C., and R. L. ZUSI. 2006. Higher-order phylogeny of modern birds (Theropoda, Aves: Neornithes) based on comparative anatomy: I. Methods and characters. Bulletin of Carnegie Museum of Natural History, 37:1-544.

LOFGREN, D. L., J. A. LILLEGRAVEN, W. A. CLEMENS, P. D. GINGERICH, and T. E. WILLIAMSON. 2004. Paleocene biochronology: The Puercan through Clarkforkian Land Mammal Ages, pp. 43-105. In M. O. WOODBURNE (ed.), Late Cretaceous and Cenozoic Mammals of North America: Geochronology and Biostratigraphy. Columbia University Press, New York.

LOPATIN, A. V. 2001. The skull structure of Archaeoryctes eurysalis sp. nov. (Didymoconidae, Mammalia) from the Paleocene of Mongolia and the taxonomic position of the family. Paleontological Journal, 35:97-107.

LOPATIN, A. V. 2003. A new species of Ardynictis (Didymoconidae, Mammalia) from the middle Eocene of Mongolia. Paleontological Journal, 37:303-311.

LOPATIN, A. V. 2005. Early Paleogene insectivore mammals from Asia and establishment of the major groups of Insectivora. Paleontological Journal, 40, supplement to no. 3:205-405.

LÓPEZ MARTÍNEZ, N., and P. PELÁEZ-CAMPOMANES. 1998. Late Paleocene Mammals from the Tremp Formation (Southern Pyrenees, Lleida, Spain). Strata, serie 1, 9:79-82.

LUCAS, S. G., and R. J. EMRY. 2000. Eocene pantolestids from the Zaysan Basin, Kazakhstan. Journal of Vertebrate Paleontology, 20, supplement to no. 3:54A-55A.

LUCKETT, W. P. 1993. An ontogenetic assessment of dental homologies in therian mammals, pp.182-204. In F. S. SZALAY, M. J. NOVACEK, and M. C. MCKENNA (eds.), Mammal Phylogeny: Mesozoic Differentiation, Multituberculates, Monotremes, Early Therians, and Marsupials. Springer-Verlag, New York.

LUO Z.-X., JI Q., WIBLE, J. R., and YUAN C.-X. 2002. An Early Cretaceous tribosphenic mammal and metatherian evolution. Science, 302:1934-1940.

MACINTYRE G.T. 1972. The trisulcate petrosal pattern of mammals, pp. 275-303. In T. DOBZHANSKY, M. K. HECHT, and W. C. STEERE (eds.), Evolutionary Biology 6, Plenum Press, New York.

MACPHEE, R. D. E. 1981. Auditory regions of primates and eutherian insectivores. Contributions to Primatology, 18. Karger, Zurich.

MACPHEE, R. D. E., and M. J. NOVACEK. 1993. Definition and relationships of Lipotyphla, pp. 21-31. In F. S. SZALAY, M. J. NOVACEK, and M. C. MCKENNA (eds.), Mammal Phylogeny: Placentals, Springer-Verlag, New York.

MACPHEE, R. D. E., M. J. NOVACEK, and G. STORCH. 1988. Basicranial morphology of early Tertiary erinaceomorphs and the origin of primates. American Museum Novitates, 2921:1-42.

MADSEN, O., M. SCALLY, C. J. DOUADY, D. J. KAO, R. W. DEBRY, R. ADKINS, H. M. AMRINE, M. J. STANHOPE, W. W. DE JONG, and M. J. SPRINGER. 2001. Parallel adaptive radiations in two major clades of placental mammals. Nature, 409:610-614.

MAIER, W. 1979. Macrocranion tupaiodon, an adapisoricid (?) Insectivore from the Eocene of "Grube Messel" (Western Germany). Palaeontologische Zeitschrift, 53:38-62.

MALIA, M. J., R. M. ADKINS, and M. W. ALLARD. 2002. Molecular support for Afrotheria and the polyphyly of Lipotyphla based on analyses of the growth hormone receptor gene. Molecular Phylogenetics and Evolution, 24:91-101.

MARSH, O. C. 1872. Preliminary description of new Tertiary Mammals. Parts I-IV. American Journal of Science, 4:122-128, 202-224.

MARSH, O. C. 1889. Discovery of Cretaceous Mammalia. Part II. American Journal of Science, 38:177-180.

MARSH, O. C. 1892. Discovery of Cretaceous Mammalia. Part III. American Journal of Science, 43:249-262.

MATTHEW, W. D. 1899. A provisional classification of the freshwater Tertiary of the West. Bulletin of the American Museum of Natural History, 12:19-77.

MATTHEW, W. D., 1901. Additional observations on the Creodonta. Bulletin of the American Museum of Natural History, 14: 1-38.

MATTHEW, W. D. 1909. The Carnivora and Insectivora of the Bridger Basin, Middle Eocene. Memoir of the American Museum of Natural History, 9:291-567.

MATTHEW, W. D. 1913. A zalambdodont insectivore from the basal Eocene. Bulletin of the American Museum of Natural History, 32:307-314.

MATTHEW, W. D. 1915. Part I: Order Ferae (Carnivora). Suborder Creodonta, pp. 4-103. In W. D. MATTHEW and W. GRANGER (auths.), A revision of the lower Eocene Wasatch and Wind River faunas, Bulletin of the American Museum of Natural History, 34.

MATTHEW, W. D. 1918. Insectivora (cont.), Glires, Edentata, pp. 565-657. In W. D. MATTHEW and W. GRANGER (auths.), A revision of the Lower Eocene Wasatch and Wind River faunas, Bulletin of the American Museum of Natural History, 38.

MATTHEW, W. D. 1921. Stehlinius, a new Eocene insectivore. American Museum Novitates, 14:1-5.

MATTHEW, W. D. 1929. Preoccupied names. Journal of Mammalogy, 10: 171.

MATTHEW, W. D., and W. GRANGER. 1921. New genera of Paleocene mammals. American Museum Novitates, 13:1-7.

MCDOWELL, S. B. 1958. The Greater Antillean insectivores. Bulletin of the American Museum of Natural History, 115:113-214.

McGREW, P. O. 1959. The geology and paleontology of the Elk Mountain and Tabernacle Butte area, Wyoming. Bulletin of the American Museum of Natural History, 117:117-176.

McKENNA, M. C. 1960. Fossil Mammalia from the early Wasatchian Four Mile fauna Eocene of northwest Colorado. University of California Publications in Geological Sciences, 37:1-130.

McKENNA, M. C. 1963. Primitive Paleocene and Eocene Apatemyidae (Mammalia, Insectivora) and the primate-insectivore boundary. American Museum Novitates, 2160:1-39.

McKENNA, M. C. 1968. Leptacodon, an American Paleocene nyctithere (Mammalia, Insectivora). American Museum Novitates, 2317:1-12.

McKENNA, M. C. 1975. Toward a phylogenetic classification of the Mammalia, pp. 21-46. In W. P. LUCKETT and F. S. SZALAY (eds.), Phylogeny of the Primates, Plenum Publishing Corporation, New York.

McKENNA, M. C., and S. K. BELL. 1997. Classification of Mammals Above the Species Level. Columbia University Press, New York, xii + 631 pp.

McKENNA, M. C., and G. G. SIMPSON. 1959. A new insectivore from the middle Eocene of Tabernacle Butte, Wyoming. American Museum Novitates, 1952:1-12.

McKENNA, M. C., Z. KIELAN-JAWOROWSKA, and J. MENG. 2000. Earliest eutherian mammal skull, from the Late Cretaceous (Coniacian) of Uzbekistan. Acta Palaeontologica Polonica, 45:1-54.

McKENNA, M. C., X. XUE, and M. ZHOU. 1984. Prosarcodon lonanensis, a new Paleocene micropternodontid palaeoryctoid insectivore from Asia. American Museum Novitates, 2780:1-17.

MENG, J. 1990. A new species of Didymoconidae and comments on related locality and stratigraphy. Vertebrata PalAsiatica, 28:206-217.

MENG, J., S.-Y. TING, and J. A. SCHIEBOUT. 1994. The cranial morphology of an early Eocene didymoconid (Mammalia, Insectivora). Journal of Vertebrate Paleontology, 14:534-551.

MENG, J., Y. HU, and C. LI. 2003. The osteology of Rhombomylus (Mammalia, Glires): implications for phylogeny and evolution of Glires. Bulletin of the American Museum of Natural History 275:1-247.

MENU, H., and B. SIGÉ. 1975. Nyctalodontie et myotodontie, importants caracteres de grades évolutifs ches les chiropteres entomophages. Comptes rendus de l'Académie des sciences Paris. Série D: Sciences Naturelles, 272:1735-1738.

MISSIAEN, P., and T. SMITH. 2005. A new Paleocene nyctitheriid insectivore from Inner Mongolia (China) and the origin of Asian nyctitheriids. Acta Palaeontologica Polonica, 50:513-522.

MOUCHATY, S. K., A. GULLBERG, A. JANKE, and U. ARNASON. 2000b. Phylogenetic position of the tenrecs (Mammalia: Tenrecidae) of Madagascar based on analysis of the complete mitochondrial genome sequences of Echinops telfairi. Zoologica Scripta, 29:307-317.

MOUCHATY, S. K., A. GULLBERG, A. JANKE, and U. ARNASON. 2000a. The phylogenetic position of the Talpidae within Eutheria based on analysis of complete mitochondrial sequences. Molecular Biology and Evolution, 17:60-67.

MULLER, J. 1934. The orbitotemporal region of the skull of the Mammalia. Archives Néerlandaises de Zoologie, 1:118-259.

MUNTHE, J., and R. M. WEST. 1980. Insectivora of the Miocene Daud Khel local fauna, Mianwali district, Pakistan. Milwaukee Public Museum Contributions in Biology and Geology, 38:1-17.

MURPHY, W. J., E. EIZIRIK, W. E. JOHNSON, Y.-P. ZHANG, O. A. RYDER, and S. J. O'BRIEN. 2001. Molecular phylogenetics and the origins of placental mammals. Nature 409, 614-618.

MURPHY, W. J., E. EIZIRIK, S. J. O'BRIEN, O. MADSEN, M. SCALLY, C. J. DOUADY, E. TEELING, O. A. RYDER, M. J. STANHOPE, W. W. DE JONG, and M. J. SPRINGER. 2001. Resolution of the early placental mammal radiation using Bayesian phylogenetics. Science, 294: 2348-2351.

MURPHY, W. J., P. PEVZNER, and S. J. O'BRIEN. 2004. Mammalian phylogenomics comes of age. Trends in Genetics, 20:631-639.[

NESSOV, L. A. [Nesov, L. A.] 1985. New mammals from Cretaceous of the Kizylkum Desert. Vestnik Leningradskogo Universiteta, Seriâ 7, 17:8-18. [In Russian with English summary]

NESSOV, L.A. [Nesov, L. A.] 1987. Results of search and study of Cretaceous and early Paleogene mammals on the territory of the USSR. E egodnik Vsesoûznogo Paleontologičeskogo Obŝestva, 30:199-218. [In Russian]

NESSOV, L. A. [Nesov, L. A.] 1993. New Mesozoic mammals of middle Asia and Kazakhstan and comments about evolution of theriofaunas of Cretaceous coastal plains of Asia. Trud Zoologichyeskogo Instituta, Rossiiskaya Akadyemiya Nauk, 249:105-133. [In Russian with English summary]

NISHIHARA, H., M. HASEGAWA, and N. OKADA. 2006. Pegasoferae, an unexpected mammalian clade revealed by tracking ancient retroposon insertions. Proceedings of the National Academy of Sciences, 103:9929-9934.

NIXON, K. C., and J. M. CARPENTER. 1993. On outgroups. Cladistics, 9:413-426.

NOVACEK, M. J. 1976. Insectivora and Proteutheria of the later Eocene (Uintan) of San Diego County, California. Natural History Museum of Los Angeles County, Contributions in Science, 283:1-52.

NOVACEK, M. J. 1977. A review of Paleocene and Eocene Leptictidae (Proteutheria: Mammalia) from North America. PaleoBios, 24:1-42.

NOVACEK, M. J. 1980. Cranioskeletal features in tupaiids and selected Eutheria as phylogenetic evidence, pp. 35-93. In W. P. LUCKETT (ed.), Comparative Biology and Evolutionary Relationships of Tree Shrews, Plenum Press, New York.

NOVACEK, M. J. 1982. Diacodon alticuspis, an erinaceomorph insectivoran from the early Eocene of northern New Mexico. University of Wyoming Contributions to Geology, 20:135-139.

NOVACEK, M. J. 1985. The Sespedectinae, a new subfamily of hedgehog-like insectivores. American Museum Novitates, 2833:1-24.

NOVACEK, M. J. 1986. The skull of leptictid insectivores and the higher-level classification of the eutherian mammals. Bulletin of the American Museum of Natural History, 183:1-111.

NOVACEK, M. J., T. M. BOWN, and D. SCHANKLER. 1985. On the classification of the early Tertiary Erinaceomorpha (Insectivora, Mammalia). American Museum Novitates, 2822:1-22.

NOVACEK, M. J., M. C. MCKENNA, N. A. NEFF, and R. L. CIFELLI. 1983. Evidence from the earliest known erinaceomorph basicranium that insectivorans and primates are not closely related. Nature, 306:683-684.

NOWAK, R. M. 1999. Walker's Mammals of the World. The Johns Hopkins University Press, Baltimore.

PAGE, L. M., P. A. CEAS, D. L. SWOFFORD, and D. G. BUTH. 1992. Evolutionary relationships within the Etheostoma squamiceps complex (Percidae; subgenus Catonotus) with descriptions of five new species. Copeia, 1992:615-646.

PARKER, T. J., and W. A. HASWELL. 1897. A Text-book of Zoology. Vol. 2. Macmillan Press, London, 301 pp.

PATTERSON, B., and P. O. MCGREW. 1937. A soricid and two erinaceids from the White River Oligocene. Publications of the Field Museum of Natural History, Geology Series, 6:245-272.

PENKROT, T., S. ZACK, and S. STRAIT. 2004. New postcrania of Macrocranion (Eutheria: Amphilemuridae) from the early Eocene, Bighorn Basin, Wyoming. Journal of Vertebrate Paleontology, 24:101A.

QUINET, G. E. 1964. Morphologie dentaire des mammifères éocènes de Dormaal. Bulletin du groupement international de recherche en stomatologie, 7:272-294.

QUINET, G. E., and X. MISONNE. 1965. Les insectivores zalambdodontes de l'Oligocène inferieur belge. Bulletin de l'Institut Royal des Sciences Naturelles de Belgique, 41:1-14.

RABB, G. B. 1959. Toxic salivary glands in the primitive insectivore Solenodon. Natural History Miscellanea, 190:1-3.

RADINSKY, L. 1985. Patterns in the evolution of ungulate jaw shape. American Zoologist, 25:303-314.

RADINSKY, L., and S.-Y. TING. 1984. The skull of Ernanodon, an unusual fossil mammal. Journal of Mammalogy, 65:155-158.

REPENNING, C. A. 1967. Subfamilies and genera of the Soricidae. Geological Survey Professional Paper, 565:1-74.

REVILLIOD, P. 1917. Revilliod, P. 1917: Fledermäuse aus der Braunkohle von Messel bei Darmstadt. Abhandlungen der Grossherzoglich-hessischen Geologischen-Landesanstalt zu Darmstadt, 7:157-201.

REVILLIOD, P. 1922. Contribution à l'étude des Chiroptères des terrains tertiares. 3. Mémoires de la Société de Paléontologie de Suisse, 45:133-195.

RICH, T. H. V. 1981. Origin and history of the Erinaceinae and Brachyericinae (Mammalia, Insectivora) in North America. Bulletin of the American Museum of Natural History, 171:1-116.

RIGBY, J. K., Jr. 1980. Swain Quarry of the Fort Union Formation, Middle Paleocene (Torrejonian), Carbon County, Wyoming: Geologic setting and mammalian fauna. Evolutionary Monographs 3:1-179.

ROBINSON, P. 1966a. Talpavus and Entomolestes (Insectivora, Adapisoricidae). American Museum Novitates, 2339:1-7.

ROBINSON, P. 1966b. Fossil Mammalia of the Huerfano Formation, Eocene, of Colorado. Bulletin of the Peabody Museum of Natural History, 21:1-85.

ROBINSON, P. 1968. Nyctitheriidae (Mammalia, Insectivora) from the Bridger Formation of Wyoming. University of Wyoming Contributions to Geology, 7:129-138.

ROMER, A. S. 1945. Vertebrate Paleontology (2nd ed.). The University of Chicago Press, 687 pp.

ROMER, A. S. 1966. Vertebrate Paleontology (3rd ed.). The University of Chicago Press, Chicago, viii+468 pp.

ROSE, K. D. 1981a. The Clarkforkian Land Mammal Age and mammalian faunal composition across the Paleocene-Eocene boundary. The University of Michigan Papers on Paleontology, 26: 1-197.

ROSE, K. D. 1981b. Composition and species diversity in Paleocene and Eocene mammal assemblages: an empirical study. Journal of Vertebrate Paleontology, 1:367-388.

ROSE, K. D. 2006. The Beginning of the Age of Mammals. The Johns Hopkins University Press, 640 pp.

ROSE, K. D., and P. D. GINGERICH. 1987. A new insectivore from the Clarkforkian (earliest Eocene) of Wyoming. Journal of Mammalogy, 68:17-27.

ROSE, K. D., and W. v. KOENIGSWALD. 2005. An exceptionally complete skeleton of Palaeosinopa (Mammalia, Cimolesta, Pantolestidae) from the Green River Formation, and other postcranial elements of the Pantolestidae from the Eocene of Wyoming. Palaeontographica Abteilung A, 273:55-96.

RUSSELL, D. E. 1964. Les Mammifères paléocènes d'Europe. Mémoirs du Museum national d'Histoire naturelle (France), nouvelle série, série C, 13:1-321.

RUSSELL, D. E., P. LOUIS, and D. E. SAVAGE. 1975. Les Adapisoricidae de l'Éocène inférieur de France. Réévaluation des formes considérées affines. Bulletin du Muséum national d'Histoire naturelle, 3^{e} série, 327:129-193.

RUSSELL, D. E., M. GODINOT, P. LOUIS, and D. E. SAVAGE. 1979. Apatotheria (Mammalia) de l'Éocène inférieur de France et de Belgique. Bulletin du Muséum national d'Histoire naturelle, 4^{e} série, 1:203-243.

RUSSELL, D. E., and D. DASHZEVEG. 1986. Early Eocene insectivores (Mammalia) from the People's Republic of Mongolia. Palaeontology, 29:269-291.

RUSSELL, L. S. 1929. Paleocene vertebrates from Alberta. American Journal of Science, 17:162-178.

RUSSELL, L. S. 1932. New data on the Paleocene mammals of Alberta, Canada. Journal of Mammalogy, 13:48-54.

RUTHERFORD, R. L. 1927. Geology along the Bow River between Cochrane and Kananaskis, Alberta. Scientific and Industrial Research Council of Alberta Report 17: 1-29.

SABAN, R. 1954. Phylogenie des Insectivores. Bulletin du Muséum national d'Histoire naturelle, 2^{e} série, 26:419-433.

SANDERSON, M. J. 1989. Confidence limits on phylogenies: The bootstrap revisited. Cladistics, 5: 113-129.

SANDERSON, M. J., and M. J. DONOGHUE. 1989. Patterns of variation in levels of homoplasy. Evolution, 43:1781-1795.

SANDERSON, M. J., and M. J. DONOGHUE. 1996. The relationship between homoplasy and confidence in a phylogenetic tree, pp. 67-89. In M. J. SANDERSON and L.

HUFFORD (eds.), Homoplasy and the Evolutionary Process, Academic Press, San Diego.

SARGIS, E. J. 2002. The postcranial morphology of Ptilocercus lowii (Scandentia, Tupaiidae): an analysis of primatomorphan and volitantian characters. Journal of Mammalian Evolution, 9:137-160.

SAVAGE, D. E., and D. E. RUSSELL. 1983: Mammalian Paleofaunas of the World. Addison-Wesley Publishing Company, New York.

SCHLOSSER, M. 1887. Die Affen, Lemuren, Chiropteren, Insektivoren, Marsupialier, Creodontier und Carnivoren des Europäischen Tertiärs und deren Beziehungen zu ihren lebenden und fossilen außereuropäischen Verwandten: Part 1. Beitrage zur Palaontologie und Geologie, Osterreich-Ungarns und des Orients, 6:1-224.

SCHWARTZ, J., and L. KRISHTALKA. 1976. The lower antemolar dentition of Litolestes ignotus, a late Paleocene erinaceid (Mammalia, Insectivora). Annals of Carnegie Museum, 46:1-6.

SCOTT, C. S. 2003. Late Torrejonian (middle Palaeocene) mammals from south central Alberta, Canada. Journal of Paleontology, 77:745–768.

SCOTT, C. S. 2006. A new erinaceid (Mammalia, Insectivora) from the Late Paleocene of western Canada. Canadian Journal of Earth Sciences, 43:1695-1709.

SCOTT, C. S., and D. M. BOYER. 2006. First skeletal material of Litocherus notissimus (Simpson) (Mammalia, Erinaceomorpha) from the late Paleocene of south central Alberta, Canada. Journal of Vertebrate Paleontology 26, supplement to number 3:123A.

SCOTT, C. S., R. C. FOX, and G. P. YOUZWYSHYN. 2002. New earliest Tiffanian (late Paleocene) mammals from Cochrane 2, southwestern Alberta, Canada. Acta Palaeontologica Polonica, 47:691-704.

SCOTT, W. B. 1892. A revision of the North American Creodonta, with notes on some genera which have been referred to that group. Proceedings of the Academy of Natural Sciences of Philadelphia, 44:291-323.

SCOTT, W. B., and G. L. JEPSEN. 1936. The mammalian fauna of the White River Oligocene. Part I, Insectivora and Carnivora. Transactions of the American Philosophical Society, 28 (new series):1-153.

SECORD, R. 1998. Paleocene mammalian biostratigraphy of the Carbon Basin, southeastern Wyoming, and age constraints on local phases of tectonism. Rocky Mountain Geology, 33:119-154.

SECORD, R. 2004. Late Paleocene biostratigraphy, isotope stratigraphy, and mammalian systematics of the northern Bighorn Basin, Wyoming. Unpublished Ph. D. dissertation, The University of Michigan, Ann Arbor, 532 pp.

SHOSHANI, J., and M. C. MCKENNA. 1998. Higher taxonomic relationships among extant mammals based on morphology, with selected comparisons of results from molecular data. Molecular Phylogenetics and Evolution, 9:572-584.

SIGÉ, B. 1974. Pseudorhynchocyon cayluxi Filhol, 1892, insectivore géant des phosphorites du Quercy. Palaeovertebrata, 6:33-46.

SIGÉ, B. 1975. Insectivores primitifs de l'Éocène supérieur et Oligocène inférieur d'Europe occidentale. Apatemyidés et Leptictidés. Collections internationales C. N. R. S., 218:653-673.

SIGÉ, B. 1976. Insectivores primitifs de l'Éocène supérieur et Oligocène inférieur d'Europe occidentale. Nyctitheriides. Mémoires du Muséum national d'Histoire naturelle, série C, Sciences de la terre, 34:1-140.

SIGÉ, B. 1997. Les mammifères insectivores des nouvelles collections de Sossis et sites associés (Éocène supérieur, Espagne). Géobios, 30:91-113.

SIGÉ, B. and G. STORCH. 2001. Un nouveau Saturninia (Nyctitheriidae, Lipotyphla, Mammalia) de l'assise OK (Oberkohle, MP14) du bassin lignifère du Geiseltal (Eocène moyen supérieur d'Allemagne). Senckenbergiana lethaea 81:343-346.

SILCOX, M. T. 2001. A phylogenetic analysis of Plesiadapiformes and their relationship to Euprimates and other archontans. Unpublished Ph. D. dissertation, The Johns Hopkins University, Baltimore, Maryland, 728 pp.

SILCOX M. T., D. W. KRAUSE, M. C. MAAS, and R. C. FOX. 2001. New specimens of Elphidotarsius russelli (Mammalia, ?Primates, Carpolestidae) and a revision of plesiadapoid relationships. Journal of Vertebrate Paleontology, 21:132-152.

SILCOX M. T., J. I. BLOCH, D. M. BOYER, and P. HOUDE. In press. Cranial anatomy of Labidolemur kayi and the relationships of the Apatemyidae. Journal of Vertebrate Paleontology.

SIMPSON, G. G. 1927a. Mammalian fauna and correlation of the Paskapoo Formation of Alberta. American Museum Novitates, 268:1-10.

SIMPSON, G. G. 1927b. Mammalian fauna of the Hell Creek Formation of Montana, American Museum Novitates, 267:1-7.

SIMPSON, G. G. 1928. A new mammalian fauna from the Fort Union of southern Montana. American Museum Novitates, 297:1-15.

SIMPSON, G. G. 1929. A collection of Paleocene mammals from Bear Creek, Montana. Annals of Carnegie Museum of Natural History, 19:115-122.

SIMPSON, G. G. 1931. A new classification of. mammals. Bulletin of the American Museum of Natural History, 59:259-293.

SIMPSON, G. G. 1935a. New Paleocene mammals from the Fort Union of Montana. Proceedings of the United States National Museum, 83:221-224.

SIMPSON, G. G. 1935b. The Tiffany fauna, upper Paleocene. I. — Multituberculata, Marsupialia, Insectivora, and ?Chiroptera. American Museum Novitates, 795:1-19.

SIMPSON, G. G. 1936. A new fauna from the Fort Union of Montana. American Museum Novitates, 873:1-27.

SIMPSON, G. G. 1937a. The Fort Union of the Crazy Mountain Field, Montana and its mammalian faunas. Bulletin of the U. S. National Museum, 169:1-287.

SIMPSON, G. G. 1937b. Additions to Upper Paleocene fauna of the Crazy Mountain field. American Museum Novitates, 940:1-15.

SIMPSON, G. G. 1937c. Unuchinia, a new name for Apator Simpson, not Semenow. Journal of Paleontology, 11:78.

SIMPSON, G. G. 1940. Studies on the earliest primates. Bulletin of the American Museum of Natural History, 77:185-212.

SIMPSON, G. G. 1945. The principles of classification and a classification of mammals. Bulletin of the American Museum of Natural History, 85:1-350.

SLAUGHTER, B. H., R. H. PINE, and N. E. PINE. 1974. Eruption of cheek teeth in Insectivora and Carnivora. Journal of Mammalogy, 55:115-125.

SLOWINSKI, J. B. 1993. "Unordered" versus "ordered" characters. Systematic Biology, 42:155-165.

SMITH, R. 1997. Palaeosinopa russelli (Mammalia, Pantolesta), une espèce nouvelle du Membre de Dormaal, proche de le limite Paléocène-Éocène. Bulletin de l'Institut royal des Sciences naturelles de Belgique: Sciences de la terre, 67:153-159.

SMITH, R. 2001. Les pantolestidés (Mammalia, Pantolesta) de l'Éocène inférieur de Prémontré (Aisne, France). Palaeovertebrata, 30:11-35.

SMITH, R. 2003. Les vertébrés terrestres de l'Oligocène inférieur de Belgique (Formation de Borgloon, MP 21): inventaire et interprétation des données actuelles. Coloquios de Paleontologia. Volumen Extraordinario, 1: 647-657.

SMITH, R. 2004. Insectivores (Mammalia) from the earliest Oligocene (MP 21) of Belgium. Netherlands Journal of Geosciences, 83: 187-192.

SMITH, T. 1995. Presence du genre Wyonycteris (Mammalia, Lipotyphla) a la limite Paléocène-Éocène en Europe. Comptes Rendus de l'Académie des Sciences de Paris, 321:923-930.

SMITH, T. 1995. Leptacodon dormaalensis (Mammalia, Lipotyphla), un nyctithere primitif de la transition Paléocène-Éocène de Belgique. Belgian Journal of Zoology, 126:153-167.

SMITH, T. and R. SMITH. 1995. Le genre Dormaalius Quinet, 1964 de l'Eocène inférieur de Belgique, synonyme du genre Macrocranion Weitzel, 1949 (Mammalia, Lipotyphla). Service géologique de Belgique, Professional Paper 274:119-131.

SMITH, T., J. I. BLOCH, S. G. STRAIT, and P. D. GINGERICH. 2002. New species of Macrocranion (Mammalia, Lipotyphla) from the earliest Eocene of North America and its biogeographic implications. Contributions from the Museum of Paleontology, The University of Michigan, 30:373-384.

STANHOPE, M. J., V. G. WADDELL, O. MADSEN, W. W. de JONG, S. B. HEDGES, G. C. CLEVEN, D. J. KAO, and M. S. SPRINGER. 1998. Molecular evidence for multiple origins of the Insectivora and for a new order of endemic African mammals. Proceedings of the National Academy of Sciences USA, 95:9967-9972.

STEHLIN, H. G. 1940. Zur Stammesgeschichte der Soriciden. Eclogae geologicae Helvetiae 33: 298-306.

STOCK, C. 1935. Insectivora from the Sespe uppermost Eocene, California. Proceedings of the National Academy of Sciences, 21:214-219.

STONLEY, G. J. 1988. Late Paleocene mammals of the Swan Hills Local Fauna (Paskapoo Formation), Alberta. M. Sc. thesis, University of Alberta, Edmonton, 265 pp.

STORCH, G. 1993. Morphologie und Paläobiologie von Macrocranion tenereum, einem Erinaceomorphen aus dem Mittel-Eozän von Messel bei Darmstadt. Senckenbergiana Lethaea, Frankfurt, 73:61-81.

STORCH, G. 1996. Paleobiology of Messel erinaceomorphs, pp. 215-224. In M. GODINOT and P. D. GINGERICH (eds.), Paléobiologie et Evolution des Mammifères Paléogènes: Volume Jubilaire en Hommage à Donald E. Russell. Palaeovertebrata, 25:215-224.

STORCH, G., and Z. QIU. 1991. Insectivores (Mammalia: Erinaceidae, Soricidae, Talpidae) from the Lufeng hominoid locality, Late Miocene of China. Geobios, 24:601-621.

SWOFFORD, D. L. 2000. Phylogenetic Analysis Using Parsimony (PAUP) version 4.0 β4, program. Sinauer Associates, Inc., Sunderland, Massachusetts.

SWOFFORD, D. L., and W. P. MADDISON. 1987. Reconstructing ancestral character states under Wagner parsimony. Mathematical Biosciences, 87:199-229.

SYMONDS, M. R. E. 2005. Phylogeny and life histories of the "Insectivora": controversies and consequences. Biological Reviews, 80:93-128.

SZALAY, F. S. 1968. Origins of the Apatemyidae (Mammalia, Insectivora). American Museum Novitates, 2352:1-11.

SZALAY, F.S., and E. DELSON. 1979. Evolutionary History of the Primates. Academic Press, New. York.

SZALAY, F. S., and G. DRAWHORN. 1980. Evolution and diversification of the Archonta in an arboreal milieu, pp. 133-169. In W. P. LUCKETT (ed.), Comparative biology and evolutionary relationships of the tree shrews, Plenum Press, New York and London.

SZALAY, F. S., and M. C. MCKENNA. 1971. Beginning of the age of mammals in Asia: the late Paleocene Gashato fauna, Mongolia. Bulletin of the American Museum of Natural History, 144: 269-317.

TEILHARD DE CHARDIN, P. 1927. Les mammifères de l'Éocène inférieur de la Belgique. Mémoires du Musée royal d'Histoire naturelle de Belgique, 36:1-33.

THEWISSEN, J. G. M. and P. D. GINGERICH. 1989. Skull and endocranial cast of Eoryctes melanus, a new palaeoryctid (Mammalia: Insectivora) from the early Eocene of western North America. Journal of Vertebrate Paleontology, 9:459-470.

TOBIEN, H. 1962. Insectivoren (Mamm.) aus dem Mitteleozän (Lutetium) von Messel bei Darmstadt. Notizblatt des Hessischen Landesamtes für Bodenforschung zu Weisbaden, 90:7-47.

TURNBULL, W. D. 1970. Mammalian masticatory apparatus. Fieldiana: Geology, 18:147-356.

VANDEBROEK, G. 1961. The comparative anatomy of the teeth of lower and nonspecialized mammals, pp. 215-313. In International Colloquium on the Evolution of Lower and Nonspecialized Mammals. Brussels: Koninklijke Vlaamse Academie voor Wetenschappen.

VAN VALEN, L. 1965. A middle Palaeocene primate. Nature, 207:435-436.

VAN VALEN, L. 1966. Deltatheridia, a new order of mammals. Bulletin of the American Museum of Natural History, 132:1-126.

VAN VALEN, L. 1967. New Paleocene insectivores and insectivore classification. Bulletin of the American Museum of Natural History, 132:1-126.

VAN VALEN, L. 1978. The beginning of the Age of Mammals. Evolutionary Theory, 4:45-80.

WADDELL, P. J., N. OKADA, and N. HASEGAWA. 1999. Towards resolving the interordinal relationships of placental mammals. Systematic Biology, 48:1-5.

WADDELL, P. J., and S. SHELLEY. 2003. Evaluating placental inter-ordinal phylogenies with novel sequences including RAG1, -fibrinogen, ND6, and mt-tRNA, plus MCMC-driven nucleotide, amino acid, and codon models. Molecular Phylogenetics and Evolution, 28:197-224.

WALSH, S. L. 1998. Notes on the anterior dentition and skull of Proterixoides (Mammalia: Insectivora: Dormaaliidae), and a new dormaaliid genus from the early Uintan (middle Eocene) of Southern California. Proceedings of the San Diego Society of Natural History, 34:1-26.

WEBB, M. W. 1996. Late Paleocene mammals from near Drayton Valley, Alberta. M. Sc. thesis, University of Alberta, Edmonton, 258 pp.

WEITZEL, K. 1949. Neue Wirbeltiere (Rodentia, Insectivora, Testudinata) aus dem Mitteleozän von Messel bei Darmstadt. Abhandlung der Senckenbergischen Naturforschenden Gesellschaft, 480: 1-24.

WEST, R. M. 1973. Antemolar dentitions of the Paleocene apatemyid insectivorans Jepsenella and Labidolemur. Journal of Mammalogy, 54:33-40.

WEST, R. M. 1974. New North American middle Eocene nyctithere (Mammalia, Insectivora). Journal of Paleontology, 48:983-987.

WHIDDEN, H. P., and C. B. WOOD 2000. Assessment of sexual dimorphism in the Antillean insectivoran Nesophontes. American Zoologist, 40:1257A.

WIBLE, J. R. 1986. Transformations in the extracranial course of the internal carotid artery in mammalian phylogeny. Journal of Vertebrate Paleontology, 6:313-325.

WIBLE, J. R. 1990. Late Cretaceous marsupial petrosal bones from North America and a cladistic analysis of the petrosal in therian mammals. Journal of Vertebrate Paleontology, 10:183-205.

WIBLE, J. R., G. W. ROUGIER, M. C. MCKENNA, and M. J. NOVACEK. 2001. Earliest eutherian ear region: a petrosal referred to Prokennalestes from the Early Cretaceous of Mongolia. American Museum Novitates, 3322:1-44.

WIBLE, J. R., G. W. ROUGIER, M. J. NOVACEK, and R. J. ASHER. 2007. Cretaceous eutherians and Laurasian origin for placental mammals near the K/T boundary. Nature, 447:1003-1006.

WILKINSON, M. 1992. Ordered versus unordered characters. Cladistics, 8:375-385.

WILKINSON, M. 2003. Missing data and multiple trees: stability and support. Journal of Vertebrate Paleontology, 23:311-323.

WILSON, D. E., and D. M. REEDER (eds.). 2005. Mammal Species of the World: A Taxonomic and Geographic Reference. The Johns Hopkins University Press, Baltimore, Maryland.

WINGE, H. 1917. Udsigt over Insektaedernes indbyrdes Slaegtskab. Videnskabelige Meddelelser fra Dansk Naturhistorisk Forening Copenhagen, 68:83-203. [In Danish]

WOOD, C. B., and W.A. CLEMENS. 2001. A new specimen and a functional re-association of the molar dentition of Batodon tenuis (Placentalia, incertae sedis), Latest

Cretaceous (Lancian), North America. Bulletin, Museum of Comparative Zoology, 156: 99-118.

WOODBURNE, M. O., and C. C. SWISHER. 1995. Land mammal high–resolution geochronology, intercontinental overland dispersals, sea level, climate, and vicariance, pp. 335-364. In W. A. BERGGREN, D. V. KENT, M.-P. AUBRY, and J. HARDENBOL (eds.), Geochronology, Time Scales, and Global Stratigraphic Correlation, Society for Sedimentary Geology, (SEPM) Special Publication, 54.

YOUZWYSHYN, G. P. 1988. Paleocene mammals from near Cochrane, Alberta. Unpublished M. Sc. thesis, University of Alberta, Edmonton, 484 pp.

ZACK, S. P., T. A. PENKROT, D. W. KRAUSE, and M. C. MAAS. 2005. A new apheliscine "condylarth" mammal from the late Paleocene of Montana and Alberta and the phylogeny of "hyopsodontids". Acta Palaeontologica Polonica, 50:809-830.

ZACK, S. P., T. A. PENKROT, J. I. BLOCH, and K. D. ROSE. 2005. Affinities of "hyopsodontids" to elephant shrews and a Holarctic origin of Afrotheria. Nature, 434:497-501.

ZIEGLER, A. C. 1971. A theory of the evolution of therian dental formulas and replacement patterns. Quarterly Review of Biology, 46:226-249.

Table 5.1.—Combined measurements and descriptive statistics for the dentition of Limaconyssus incomperta new species from the earliest Tiffanian (Ti1) Cochrane 2 locality, the early middle Tiffanian (Ti3) DW-2 locality, and the late middle Tiffanian (Ti4) Swan Hills locality, Paskapoo Formation, Alberta.

Element	P	N	OR	M	SD	CV
p2	L	1	0.7	—	—	—
	W	1	0.3	—	—	—
p3	L	2	0.7-0.8	0.75	0.07	9.43
	W	2	0.3-0.4	0.35	0.07	20.20
p4	L	8	0.9-1.1	1.01	0.06	6.33
	W	8	0.5-0.6	0.54	0.05	9.63
m1	L	4	1.0-1.1	1.03	0.05	4.88
	TrW	4	0.6-0.7	0.63	0.05	8.00
	TaW	5	0.5-0.7	0.60	0.07	11.79
m2	L	5	0.9-1.0	0.97	0.05	5.34
	TrW	5	0.7-0.8	0.72	0.04	5.70
	TaW	5	0.6-0.7	0.65	0.05	8.43
m3	L	1	0.8	—	—	—
	TrW	1	0.6	—	—	—
	TaW	1	0.4	—	—	—

Table 5.2.—Combined measurements and descriptive statistics for the dentition of Limaconyssus subnuba new species from the earliest Tiffanian (Ti1) Cochrane 2 locality, the early middle Tiffanian (Ti3) DW-2 and Hand Hills West upper level localities, and the late middle Tiffanian (Ti4) Swan Hills and Gao Mine localities, Paskapoo Formation, Alberta.

Element	P	N	OR	M	SD	CV
p3	L	1	1.1	—	—	—
	W	1	0.6	—	—	—
p4	L	2	1.3	1.30	0	0
	W	2	0.9	0.90	0	0
m1	L	2	1.4-1.5	1.45	0.07	4.88
	TrW	2	1.0	1.00	0	0
	TaW	2	0.9-1.0	0.95	0.07	7.44
m2	L	4	1.3-1.4	1.33	0.05	3.77
	TrW	4	1.0-1.1	1.03	0.05	4.88
	TaW	4	0.8-1.0	0.90	0.08	9.07
m3	L	1	1.0	—	—	—
	TrW	2	0.8-0.9	0.85	0.07	8.32
	TaW	1	0.6	—	—	—

Table 5.3.—Combined measurements and descriptive statistics for the upper dentition of Xynolestes denommei new genus and species from the earliest Tiffanian (Ti1) Cochrane 2 locality, and the early middle Tiffanian (Ti3) DW-2 and Hand Hills West upper level localities, Paskapoo Formation, Alberta.

Element	P	N	OR	M	SD	CV
P2	L	2	0.8-1.0	0.90	0.14	15.71
	W	2	0.5-0.6	0.55	0.07	12.86
P3	L	3	1.4-1.5	1.43	0.06	4.03
	W	3	0.6	0.83	0.06	6.93
P4	L	7	1.4-1.5	1.44	0.05	3.70
	W	7	1.3-1.4	1.37	0.08	5.51
M1	L	8	1.3-1.4	1.35	0.05	3.96
	W	8	1.5-1.6	1.55	0.05	3.45
M2	L	12	1.0-1.2	1.13	0.08	6.70
	W	12	1.3-1.4	1.36	0.05	3.79
M3	L	3	0.9-1.0	0.93	0.06	6.19
	W	3	1.1	1.10	0	0

Table 5.4.—Combined measurements and descriptive statistics for the lower dentition of Xynolestes denommei new genus and species from the earliest Tiffanian (Ti1) Cochrane 2 and Aaron's localities, and the early middle Tiffanian (Ti3) DW-1, DW-2, Mel's Place, Joffre Bridge Mammal Site No. 1, Joffre Bridge Roadcut lower level, Birchwood, and Hand Hills West upper level localities, Paskapoo Formation, Alberta.

Element	P	N	OR	M	SD	CV
c	L	1	1.0	—	—	—
	W	1	0.4	—	—	—
p1	L	4	0.9-1.0	0.95	0.06	6.08
	W	4	0.4	0.40	0	0
p2	L	15	0.8-1.0	0.95	0.07	7.85
	W	15	0.4-0.5	0.45	0.05	11.56
p3	L	25	0.8-1.1	0.98	0.08	8.51
	W	25	0.4-0.6	0.52	0.05	9.98
p4	L	68	1.0-1.4	1.20	0.11	9.29
	W	68	0.6-0.9	0.73	0.07	10.07
m1	L	67	0.9-1.0	1.31	0.09	6.19
	TrW	67	0.8-1.2	0.96	0.08	8.41
	TaW	67	0.8-1.1	0.94	0.09	9.63
m2	L	61	1.0-1.2	1.08	0.06	6.04
	TrW	60	0.8-1.0	0.88	0.09	9.94
	TaW	60	0.7-1.0	0.87	0.09	9.86
m3	L	27	0.9-1.1	0.96	0.06	5.97
	TrW	27	0.6-0.9	0.74	0.08	10.76
	TaW	27	0.5-0.8	0.69	0.10	14.14

Table 5.5.—Combined measurements and descriptive statistics for the lower dentition of Litolestes avitodelphus new species from the early middle Tiffanian (Ti3) DW-2 and Joffre Bridge Roadcut lower level localities, Paskapoo Formation, Alberta.

Element	P	N	OR	M	SD	CV
p3	L	2	0.8-0.9	0.85	0.07	8.32
	W	2	0.4-0.5	0.45	0.07	15.71
p4	L	3	1.4-1.5	1.47	0.06	3.94
	W	3	0.8-0.9	0.83	0.06	6.93
m1	L	5	1.1-1.3	1.18	0.08	7.09
	TrW	5	0.9-1.0	0.96	0.05	5.71
	TaW	5	1.0-1.2	1.08	0.08	7.75
m2	L	6	0.9-1.0	0.97	0.05	5.34
	TrW	6	0.7-0.8	0.75	0.05	7.30
	TaW	6	0.6-0.7	0.65	0.05	8.43
m3	L	3	0.8-0.9	0.87	0.06	6.66
	TrW	3	0.5-0.6	0.57	0.06	10.19
	TaW	3	0.5	0.50	0	0

Table 5.6.—Combined measurements and descriptive statistics for the upper dentition of Litocherus notissimus (Simpson) from the early middle Tiffanian (Ti3) DW-2, Mel's Place, Joffre Bridge Roadcut lower level, and Birchwood localities, Paskapoo Formation, Alberta.

Element	P	N	OR	M	SD	CV
C (♀)	L	1	1.3	—	—	—
	W	1	0.8	—	—	—
C (♂)	L	1	1.5	—	—	—
	W	1	1.0	—	—	—
P1	L	1	0.8	—	—	—
	W	1	0.4	—	—	—
P2	L	6	1.1-1.3	1.20	0.09	7.45
	W	6	0.6-0.7	0.67	0.05	7.75
P3	L	12	1.8-1.9	1.87	0.05	2.64
	W	12	1.4-1.7	1.55	0.08	5.15
P4	L	26	2.0-2.4	2.18	0.12	5.41
	W	25	2.4-2.7	2.53	0.09	3.73
M1	L	23	1.7-2.1	1.95	0.09	4.61
	W	23	2.5-2.9	2.72	0.11	4.14
M2	L	23	1.5-2.0	1.73	0.13	7.50
	W	23	2.5-2.9	2.73	0.11	4.02
M3	L	12	1.3-1.6	1.44	0.09	6.25
	W	12	1.9-2.3	2.11	0.11	5.14

Table 5.7.—Combined measurements and descriptive statistics for the lower dentition of Litocherus notissimus (Simpson) from the early middle Tiffanian (Ti3) DW-1, DW-2, Joffre Bridge Mammal Site No. 1, Joffre Bridge Roadcut lower level, and Birchwood localities, Paskapoo Formation, Alberta.

Element	P	N	OR	M	SD	CV
c (♀)	L	7	1.0-1.2	1.09	0.07	6.36
	W	7	0.6-0.7	0.64	0.05	8.31
c (♂)	L	4	1.1-1.3	1.23	0.10	7.82
	W	4	0.9-1.1	1.00	0.08	8.16
p1	L	3	0.9-1.0	0.97	0.06	5.97
	W	3	0.5-0.6	0.53	0.06	10.83
p2	L	1	1.2-1.6	1.34	0.11	8.11
	W	1	0.7-0.9	0.73	0.06	8.39
p3	L	29	1.5-1.9	1.70	0.10	6.09
	W	28	0.7-1.1	0.94	0.10	10.18
p4	L	35	2.0-2.4	2.25	0.12	5.21
	W	34	1.1-1.4	1.31	0.10	7.53
m1	L	43	1.9-2.2	2.07	0.08	4.08
	TrW	41	1.3-1.7	1.44	0.10	6.76
	TaW	40	1.3-1.7	1.49	0.09	6.33
m2	L	42	1.6-1.9	1.78	0.08	4.62
	TrW	41	1.2-1.6	1.40	0.09	6.09
	TaW	41	1.3-1.6	1.41	0.10	6.75
m3	L	40	1.5-2.0	1.70	0.11	6.47
	TrW	39	1.0-1.4	1.16	0.13	10.93
	TaW	39	0.8-1.3	1.05	0.10	9.48

Table 5.8.—Combined measurements and descriptive statistics for the dentition of Litocherus sp., cf. L. zygeus from the early middle Tiffanian (Ti3) DW-2, Joffre Bridge Roadcut lower level, Birchwood, and Hand Hills West upper level localities, Paskapoo Formation, Alberta.

Element	P	N	OR	M	SD	CV
P4	L	2	2.4	2.40	—	—
	W	2	2.7-2.8	2.75	0.07	2.57
M2	L	1	2.0	—	—	—
	W	1	2.9	—	—	—
p2	L	2	1.4-1.5	1.45	0.07	4.88
	W	2	0.7	0.70	0	0
p3	L	2	1.8-1.9	1.85	0.07	3.82
	W	2	1.2	1.20	0	0
p4	L	13	2.4-2.7	2.52	0.11	4.33
	W	13	1.4-1.7	1.58	0.09	5.67
m1	L	21	2.2-2.4	2.30	0.08	3.49
	TrW	21	1.5-1.7	1.64	0.07	4.08
	TaW	21	1.6-1.8	1.69	0.07	4.31
m2	L	13	1.8-2.0	1.87	0.09	5.07
	TrW	13	1.5-1.7	1.62	0.07	4.26
	TaW	13	1.5-1.7	1.60	0.07	4.42
m3	L	6	1.7-1.8	1.73	0.05	2.98
	TrW	6	1.1-1.3	1.22	0.10	8.08
	TaW	6	1.1-1.3	1.18	0.08	6.36

Table 5.9.—Combined measurements and descriptive statistics for the lower dentition of Nayloria albertensis new genus and species from the early middle Tiffanian (Ti3) DW-2, Joffre Bridge Mammal Site No. 1, Joffre Bridge Roadcut lower level locality, Birchwood, and Hand Hills West upper level localities, Paskapoo Formation, Alberta.

Element	P	N	OR	M	SD	CV
c	L	1	0.9	—	—	—
	W	1	0.7	—	—	—
p1	L	1	0.8	—	—	—
	W	1	0.4	—	—	—
p2	L	5	1.0-1.1	1.06	0.05	5.17
	W	5	0.7-0.8	0.72	0.04	6.21
p3	L	5	1.3-1.4	1.38	0.04	3.24
	W	5	0.5-0.7	0.60	0.07	11.79
p4	L	11	1.6-1.9	1.77	0.10	5.69
	W	11	0.9-1.1	0.97	0.08	8.08
m1	L	9	1.4-1.6	1.50	0.09	5.77
	TrW	9	0.9-1.1	0.98	0.07	6.82
	TaW	9	1.0-1.2	1.08	0.07	6.19
m2	L	7	1.2-1.3	1.24	0.05	4.30
	TrW	7	0.8-1.0	0.91	0.07	7.55
	TaW	7	0.8-1.0	0.94	0.08	8.34
m3	L	6	1.0-1.2	1.10	0.09	8.13
	TrW	6	0.7-0.8	0.73	0.05	7.04
	TaW	6	0.7-0.8	0.75	0.05	7.30

Table 5.10.—Measurements and descriptive statistics for the dentition of Adeloxenus adapisoricoides new genus and species from the early middle Tiffanian (Ti3) DW-2 locality, Paskapoo Formation, Alberta.

Element	P	N	OR	M	SD	CV
p2	L	1	1.0	—	—	—
	W	1	0.4	—	—	—
p3	L	1	1.2	—	—	—
	W	1	1.0	—	—	—
p4	L	1	1.6	—	—	—
	W	1	1.2	—	—	—
m1	L	4	1.9-2.1	2.00	0.08	4.08
	TrW	4	1.4-1.5	1.43	0.05	3.51
	TaW	4	1.3-1.4	1.38	0.05	3.64
m2	L	1	1.8	—	—	—
	TrW	1	1.6	—	—	—
	TaW	1	1.6	—	—	—
m3	L	1	1.8	—	—	—
	TrW	1	1.2	—	—	—
	TaW	1	1.1	—	—	—

Table 5.11.—Combined measurements and descriptive statistics for the dentition of Diacocherus sp., cf. D. meizon from the early Tiffanian (Ti3) DW-2 and Hand Hills West upper level localities, Paskapoo Formation, Alberta.

Element	P	N	OR	M	SD	CV
P4	L	1	1.7	—	—	—
	W	1	2.0	—	—	—
M1	L	2	1.7	1.70	0	0
	W	2	1.9-2.0	1.95	0.07	3.63
dp4	L	1	2.0	—	—	—
	TrW	1	0.9	—	—	—
	TaW	1	1.1	—	—	—
m1	L	4	1.8-2.0	1.93	0.10	4.97
	TrW	4	1.0-1.1	1.05	0.06	5.50
	TaW	4	1.2-1.3	1.25	0.06	4.62
m2	L	5	1.9-2.1	2.02	0.08	4.14
	TrW	5	1.2-1.3	1.26	0.05	4.35
	TaW	5	1.4-1.5	1.44	0.05	3.80

Table 5.12.—Combined measurements and descriptive statistics for the upper dentition of "Leptacodon" munusculum Simpson from the early middle Tiffanian (Ti3) DW-2, Joffre Bridge Roadcut lower level, and Birchwood localities, Paskapoo Formation, Alberta.

Element	P	N	OR	M	SD	CV
P3	L	1	1.2	—	—	—
	W	1	1.0	—	—	—
P4	L	4	1.2-1.3	1.25	0.06	4.62
	W	4	1.4-1.5	1.45	0.06	3.98
M1	L	2	1.2	1.20	0	0
	W	2	1.6	1.60	0	0
M2	L	2	1.2	1.20	0	0
	W	2	1.7	1.70	0	0
M3	L	2	0.9-1.0	0.95	0.07	7.44
	W	2	1.4	1.40	0	0

Table 5.13.—Combined measurements and descriptive statistics for the lower dentition of "Leptacodon" munusculum Simpson from the early middle Tiffanian (Ti3) DW-2, Joffre Bridge Roadcut lower level, and Birchwood localities, Paskapoo Formation, Alberta.

Element	P	N	OR	M	SD	CV
p1	L	1	0.8	—	—	—
	W	1	0.3	—	—	—
p2	L	6	0.9-1.1	0.98	0.08	7.66
	W	6	0.3-0.4	0.38	0.04	10.65
p3	L	9	1.0-1.1	1.06	0.05	4.99
	W	9	0.5-0.6	0.53	0.05	9.37
p4	L	16	1.2-1.3	1.23	0.06	4.89
	W	16	0.5-0.7	0.66	0.06	9.59
m1	L	18	1.1-1.3	1.17	0.06	4.90
	TrW	18	0.8-1.0	0.86	0.07	8.10
	TaW	19	0.8-1.0	0.86	0.06	7.08
m2	L	24	1.2-1.4	1.26	0.06	5.12
	TrW	24	0.8-1.0	0.87	0.06	7.35
	TaW	24	0.8-1.0	0.86	0.06	7.50
m3	L	14	1.1-1.3	1.19	0.06	5.16
	TrW	14	0.7-1.0	0.79	0.08	9.80
	TaW	14	0.7-0.8	0.75	0.07	8.67

Table 5.14.—Combined measurements and descriptive statistics for the upper dentition of Psydronyctia smithorum new genus and species from the earliest Tiffanian (Ti1) Cochrane 2 locality, and early middle Tiffanian (Ti3) DW-1, DW-2, Joffre Bridge Roadcut lower level, and Hand Hills West upper level localities, Paskapoo Formation, Alberta.

Element	P	N	OR	M	SD	CV
P3	L	2	1.0-1.1	1.05	0.07	6.73
	W	2	0.8-0.9	0.85	0.07	8.32
P4	L	2	1.3-1.4	1.35	0.07	5.24
	W	2	1.4	1.40	0	0
M1	L	4	1.3-1.4	1.35	0.06	4.28
	W	4	1.6-1.7	1.65	0.06	3.50
M2	L	4	1.2-1.3	1.23	0.05	4.08
	W	4	1.5-1.6	1.58	0.05	3.17
M3	L	1	1.0	1.17	—	—
	W	1	1.2	0.86	—	—

Table 5.15.—Combined measurements and descriptive statistics for the lower dentition of Psydronyctia smithorum new genus and species from the earliest Tiffanian (Ti1) Cochrane 2 locality, and early middle Tiffanian (Ti3) DW-1, DW-2, Joffre Bridge Roadcut lower level, and Hand Hills West upper level localities, Paskapoo Formation, Alberta.

Element	P	N	OR	M	SD	CV
p1	L	1	0.8	—	—	—
	W	1	0.3	—	—	—
p2	L	6	0.6-0.7	0.67	0.05	7.75
	W	6	0.3	0.30	0	0
p3	L	9	1.2-1.3	1.23	0.05	4.05
	W	9	0.4-0.5	0.42	0.04	10.44
p4	L	10	1.3-1.4	1.35	0.05	3.90
	W	10	0.5-0.6	0.56	0.05	9.22
m1	L	11	1.1-1.3	1.22	0.06	4.95
	TrW	11	0.7-0.8	0.76	0.05	6.61
	TaW	11	0.7-0.9	0.80	0.06	7.91
m2	L	15	1.1-1.2	1.17	0.05	4.18
	TrW	16	0.7-0.8	0.75	0.05	6.89
	TaW	16	0.7-0.8	0.76	0.05	6.56
m3	L	10	1.0-1.1	1.05	0.05	5.02
	TrW	10	0.6-0.7	0.62	0.04	6.80
	TaW	10	0.4-0.5	0.48	0.04	8.78

Table 5.16.—Combined measurements and descriptive statistics for the upper dentition of Lipotyphla, genus and species indeterminate from the early middle Tiffanian (Ti3) DW-1, DW-2, and Hand Hills West upper level localities, Paskapoo Formation, Alberta.

Element	P	N	OR	M	SD	CV
P3	L	3	1.0-1.1	1.03	0.06	5.59
	W	2	1.2-1.3	1.25	0.07	5.66
P4	L	3	1.5-1.6	1.53	0.06	3.77
	W	4	1.6-1.7	1.63	0.05	3.08
M1	L	4	1.6-1.7	1.68	0.05	2.99
	W	4	1.8-1.9	1.83	0.05	2.74
M2	L	3	1.4-1.5	1.47	0.06	3.94
	W	3	1.8-1.9	1.83	0.06	3.15
M3	L	2	1.4	1.40	0	0
	W	2	1.6-1.7	1.65	0.07	4.29

Table 5.17.—Combined measurements and descriptive statistics for the lower dentition of Lipotyphla, genus and species indeterminate from the early middle Tiffanian (Ti3) DW-2, Birchwood, and Hand Hills West upper level localities, Paskapoo Formation, Alberta.

Element	P	N	OR	M	SD	CV
p1	L	1	1.4	—	—	—
	W	1	0.6	—	—	—
p4	L	1	1.4	—	—	—
	W	1	0.8	—	—	—
m1	L	4	1.5-1.6	1.58	0.05	3.17
	TrW	4	1.0-1.1	1.08	0.05	4.65
	TaW	4	1.2	1.20	0	0
m2	L	3	1.3-1.4	1.37	0.06	4.22
	TrW	3	1.0-1.1	1.03	0.06	5.59
	TaW	3	1.1	1.10	0	0
m3	L	3	1.3	1.30	0	0
	TrW	3	0.9-1.0	0.97	0.06	5.97
	TaW	3	0.9-1.0	0.93	0.06	6.19

Table 5.18.—Measurements and descriptive statistics for the upper dentition of Bessoecetor thomsoni Simpson from the early Tiffanian (Ti3) DW-2 locality, Paskapoo Formation, Alberta.

Element	P	N	OR	M	SD	CV
P3	L	1	2.1	—	—	—
	W	1	0.4	—	—	—
P4	L	8	2.1-2.2	2.15	0.05	2.49
	W	8	1.8-2.0	1.88	0.07	3.77
M1	L	10	2.2-2.4	2.38	0.08	3.31
	W	10	3.0-3.2	3.06	0.07	2.28
M2	L	7	2.4-2.5	2.44	0.05	2.19
	W	7	3.4-3.6	3.53	0.08	2.14
M3	L	3	2.1-2.2	2.17	0.06	2.66
	W	3	3.3-3.4	3.33	0.06	1.73

Table 5.19.—Combined measurements and descriptive statistics for the lower dentition of Bessoecetor thomsoni Simpson from the early Tiffanian (Ti3) DW-2, Burbank, Joffre Bridge Roadcut lower level, and Birchwood localities, Paskapoo Formation, Alberta.

Element	P	N	OR	M	SD	CV
c	L	2	1.2	1.20	0	0
	W	2	0.7-0.9	0.8	0.14	17.68
p2	L	4	1.5-1.6	1.58	0.05	3.17
	W	4	0.6-0.7	0.63	0.05	8.00
p3	L	10	1.6-1.8	1.73	0.07	3.90
	W	10	0.6-0.8	0.73	0.07	9.25
p4	L	16	2.4-2.6	2.51	0.07	2.71
	W	16	1.0-1.2	1.11	0.07	6.15
m1	L	23	2.4-2.5	2.45	0.05	2.08
	TrW	23	1.6-1.8	1.67	0.05	3.23
	TaW	23	1.5-.1.8	1.65	0.07	4.04
m2	L	28	2.2-2.6	2.38	0.08	3.50
	TrW	28	1.6-2.0	1.73	0.09	5.19
	TaW	28	1.5-1.9	1.68	0.09	5.62
m3	L	21	2.4-2.7	2.54	0.08	3.17
	TrW	21	1.5-1.8	1.71	0.09	5.52
	TaW	21	1.4-1.6	1.47	0.06	3.94

Table 5.20.—Measurements and descriptive statistics for the upper dentition of Bessoecetor septentrionalis (Russell) from the early Tiffanian (Ti3) DW-2 and Birchwood localities, Paskapoo Formation, Alberta.

Element	P	N	OR	M	SD	CV
P3	L	2	2.3-2.4	2.35	0.07	3.01
	W	2	0.7	0.70	0	0
P4	L	5	2.4-2.5	2.46	0.05	2.23
	W	5	2.2-2.4	2.34	0.09	3.82
M1	L	10	2.3-2.5	2.42	0.08	3.26
	W	10	3.0-3.1	3.05	0.05	1.73
M2	L	11	2.4-2.6	2.52	0.08	2.98
	W	11	3.6-3.7	3.65	0.05	1.43
M3	L	2	2.4	2.40	0	0
	W	2	3.5	3.50	0	0

Table 5.21.—Combined measurements and descriptive statistics for the lower dentition of Bessoecetor septentrionalis (Russell) from the early Tiffanian (Ti3) DW-2, Burbank, Joffre Bridge Roadcut lower level, and Birchwood localities, Paskapoo Formation, Alberta.

Element	P	N	OR	M	SD	CV
p2	L	2	1.8-2.0	1.90	0.10	5.26
	W	2	0.7-0.8	0.77	0.06	7.53
p3	L	7	2.1-2.3	2.17	0.08	3.48
	W	7	0.8-0.9	0.84	0.05	6.34
p4	L	11	2.7-3.0	2.85	0.10	3.64
	W	11	1.2-1.4	1.27	0.06	5.08
m1	L	12	2.3-2.6	2.44	0.08	3.25
	TrW	12	1.6-1.8	1.73	0.06	3.60
	TaW	14	1.6-1.8	1.69	0.06	3.64
m2	L	16	2.4-2.6	2.51	0.08	3.08
	TrW	16	1.7-1.9	1.78	0.07	3.68
	TaW	16	1.7-1.8	1.75	0.05	2.95
m3	L	17	2.7-3.0	2.89	0.10	3.56
	TrW	17	2.0-2.2	2.06	0.06	3.00
	TaW	17	1.6-1.8	1.71	0.06	3.51

Table 5.22.—Combined measurements and descriptive statistics for the upper dentition of Bisonalveus toxidens new species from the early Tiffanian (Ti3) DW-1, DW-2, Joffre Bridge Roadcut lower level, and Birchwood localities, Paskapoo Formation, Alberta.

Element	P	N	OR	M	SD	CV
C	L	6	2.0-2.2	2.05	0.08	4.08
	W	6	1.0-1.1	1.07	0.05	4.84
P3	L	2	1.7-1.8	1.75	0.07	4.04
	W	2	1.2-1.5	1.35	0.21	15.71
P4	L	14	2.0-2.2	2.06	0.09	4.14
	W	14	2.1-2.5	2.36	0.09	3.98
M1	L	23	2.1-2.4	2.26	0.07	3.19
	W	23	2.5-2.8	2.68	0.10	3.73
M2	L	31	2.3-2.6	2.42	0.07	2.96
	W	32	3.3-3.7	3.55	0.10	2.86
M3	L	11	1.5-1.8	1.67	0.12	7.12
	W	11	2.6-2.8	2.71	0.08	3.07

Table 5.23.—Combined measurements and descriptive statistics for the lower dentition of Bisonalveus toxidens new species from the early middle Tiffanian (Ti3) DW-1, DW-2, Joffre Bridge Roadcut lower level, and Hand Hills West upper level localities, Paskapoo Formation, Alberta.

Element	P	N	OR	M	SD	CV
c	L	6	1.0-1.3	1.15	0.10	9.12
	W	6	1.0-1.2	1.07	0.08	7.65
p1	L	6	0.7-0.9	0.80	0.08	9.41
	W	6	0.5-0.6	0.50	0.05	10.33
p2	L	7	0.6-0.7	0.64	0.05	8.31
	W	7	0.5-0.6	0.53	0.05	9.23
p3	L	30	1.6-1.8	1.66	0.06	3.34
	W	30	1.2-1.4	1.31	0.05	3.86
p4	L	57	1.9-2.3	2.15	0.08	3.64
	W	57	1.4-1.8	1.55	0.10	6.36
m1	L	86	2.1-2.4	2.22	0.08	3.74
	TrW	84	1.5-1.9	1.72	0.07	4.09
	TaW	85	1.5-1.9	1.69	0.07	4.33
m2	L	82	2.3-2.7	2.47	0.09	3.47
	TrW	78	1.6-2.2	2.01	0.10	5.08
	TaW	77	1.5-2.0	1.79	0.08	4.75
m3	L	62	2.2-2.6	2.39	0.08	3.52
	TrW	61	1.4-1.9	1.59	0.07	4.71
	TaW	61	1.1-1.6	1.39	0.08	5.59

Table 5.24.—Measurements and descriptive statistics for the dentition of Paleotomus junior Scott, Fox, and Youzwyshyn from the early middle Tiffanian (Ti3) DW-2 locality, Paskapoo Formation, Alberta.

Element	P	N	OR	M	SD	CV
P4	L	1	3.3	—	—	—
	W	1	3.1	—	—	—
p2	L	1	2.2	—	—	—
	W	1	1.3	—	—	—
p3	L	2	3.2-3.3	3.25	0.07	2.18
	W	2	1.1-1.2	1.15	0.07	6.15
p4	L	2	3.9-4.1	4.00	0.14	3.54
	W	2	1.6-1.7	1.65	0.07	4.29
m1	L	3	3.2-3.3	3.23	0.06	1.79
	TrW	3	2.0-2.2	2.10	0.10	4.76
	TaW	3	1.8-2.1	1.97	0.15	7.77
m2	L	1	3.5	—	—	—
	TrW	1	2.4	—	—	—
	TaW	1	2.1	—	—	—

Table 5.25.—Combined measurements and descriptive statistics for the upper dentition of Unuchinia dysmathes Holtzman from the early Tiffanian (Ti3) DW-1, DW-2, Joffre Bridge Roadcut lower level, and Birchwood localities, Paskapoo Formation, Alberta.

Element	P	N	OR	M	SD	CV
I1	D	10	3.0-3.3	3.12	0.12	3.94
	W	10	1.7-1.8	1.75	0.05	3.01
I2	D	5	3.3-3.5	3.42	0.08	2.45
	W	5	1.6-1.7	1.66	0.05	3.30
P2	L	3	2.3-2.4	2.33	0.06	2.47
	W	3	1.2-1.3	1.27	0.06	4.56
P3	L	2	1.9	1.90	0	0
	W	2	1.2-1.3	1.25	0.07	5.66
P4	L	2	2.3	2.30	0	0
	W	2	2.3-2.4	2.35	0.07	3.01
M1	L	4	2.3-2.4	2.38	0.05	2.11
	W	4	3.4-3.5	3.45	0.06	1.67
M2	L	4	2.2-2.3	2.28	0.05	2.20
	W	4	4.4-4.5	4.45	0.06	1.30
M3	L	5	1.8-1.9	1.82	0.04	2.46
	W	5	3.8-4.0	3.86	0.09	2.32

Table 5.26.—Combined measurements and descriptive statistics for the lower dentition of Unuchinia dysmathes Holtzman from the early Tiffanian (Ti3) DW-1, DW-2, Joffre Bridge Roadcut lower level, and Birchwood localities, Paskapoo Formation, Alberta.

Element	P	N	OR	M	SD	CV
i1	D	6	3.2-3.3	3.27	0.05	1.58
	W	6	1.9-2.0	1.95	0.05	2.81
i2	D	4	2.6-2.7	2.63	0.05	1.90
	W	4	1.6-1.7	1.68	0.05	2.99
p2	L	3	2.8-2.9	2.87	0.06	2.01
	W	3	1.3	1.30	0	0
p4	L	2	2.2-2.3	2.25	0.07	3.14
	W	2	1.1	1.10	0	0
m1	L	6	2.4-2.5	2.45	0.05	2.24
	TrW	6	1.6-1.8	1.73	0.08	4.71
	TaW	6	1.6-1.7	1.63	0.05	3.16
m2	L	4	2.4-2.5	2.48	0.05	2.02
	TrW	4	1.8-1.9	1.88	0.05	2.67
	TaW	4	1.7-1.8	1.75	0.06	3.30
m3	L	2	3.0-3.1	3.05	0.07	2.32
	TrW	2	1.9-2.0	1.95	0.07	3.63
	TaW	2	1.6	1.60	0	0

Table 5.27.—Combined measurements and descriptive statistics for the upper dentition of Pararyctes pattersoni Van Valen from the early Tiffanian (Ti3) DW-2, Mel's Place, Joffre Bridge Roadcut lower level, and Hand Hills West upper level localities, Paskapoo Formation, Alberta.

Element	P	N	OR	M	SD	CV
I (lateral)	L	1	1.1	—	—	—
	W	1	0.7	—	—	—
C	L	1	1.1	—	—	—
	W	1	0.9	—	—	—
P1	L	3	0.3	0.30	0	0
	W	3	0.3	0.30	0	0
P2	L	2	0.6	0.60	0	0
	W	2	0.5	0.50	0	0
P3	L	7	0.7-0.8	0.74	0.05	7.20
	W	7	0.5-0.6	0.56	0.05	9.59
P4	L	12	1.6-1.9	1.78	0.09	4.88
	W	12	1.9-2.2	2.03	0.09	4.28
M1	L	18	1.8-2.0	1.87	0.08	4.11
	W	18	2.2-2.5	2.33	0.08	3.29
M2	L	13	1.6-1.7	1.65	0.05	3.14
	W	13	2.8-3.0	2.90	0.09	2.99
M3	L	9	1.4-1.5	1.44	0.05	3.65
	W	9	2.8-3.0	2.90	0.09	2.99

Table 5.28.—Combined measurements and descriptive statistics for the lower dentition of Pararyctes pattersoni Van Valen from the early Tiffanian (Ti3) DW-1, DW-2, Joffre Bridge Roadcut lower level, Birchwood, and Hand Hills West upper level localities, Paskapoo Formation, Alberta.

Element	P	N	OR	M	SD	CV
i (medial)	D	1	1.3	—	—	—
	W	1	1.0	—	—	—
i (lateral)	D	3	1.1-1.2	1.17	0.06	4.95
	W	3	1.0-1.1	1.03	0.06	5.59
c	L	10	1.2-1.3	1.24	0.05	4.16
	W	10	0.7-0.9	0.80	0.07	8.33
p1	L	5	0.7-0.8	0.76	0.05	7.21
	W	5	0.5-0.6	0.56	0.05	9.78
p2	L	6	1.2-1.4	1.30	0.06	4.87
	W	6	1.0-1.1	1.03	0.05	5.00
p3	L	8	1.0-1.1	1.05	0.05	5.09
	W	8	0.7-0.9	0.79	0.06	8.14
p4	L	27	1.7-2.1	1.94	0.10	5.20
	W	27	0.7-1.1	1.01	0.10	9.51
m1	L	33	1.8-2.0	1.90	0.08	4.05
	TrW	33	1.3-1.5	1.43	0.06	4.09
	TaW	34	0.9-1.1	1.02	0.06	6.28
m2	L	39	1.7-2.2	1.98	0.12	6.30
	TrW	39	1.4-1.7	1.51	0.08	5.29
	TaW	39	1.0-1.3	1.16	0.08	6.52
m3	L	30	1.9-2.1	2.01	0.07	3.29
	TrW	30	1.3-1.6	1.43	0.08	5.60
	TaW	30	0.7-1.0	0.91	0.08	8.97

Figure 5.1.—1-18. Limaconyssus incomperta new species from the earliest Tiffanian (Ti1) Cochrane 2 (C2) locality, the early middle Tiffanian (Ti3) DW-2 (DW2) locality, and the late middle Paleocene (Ti4) Swan Hills (SH) locality, Paskapoo Formation, Alberta. 1-3, UALVP 47278 (holotype, DW2), incomplete left dentary with p4, m1 in 1, labial, 2, lingual, and 3, occlusal views; 4-6, UALVP 28523 (C2), right p4 in 4, labial, 5, lingual, and 6, occlusal views; 7-9, UALVP 47279 (DW2), incomplete left dentary with p2-4, m1-2, and alveoli for i1-3, c, p1, m3 in 7, labial, 8, lingual, and 9, occlusal views; 10-12, UALVP 47284 (DW2), incomplete right dentary with p3-4 and alveoli for p1-2, m1 in 10, labial, 11, lingual, and 12, occlusal views; 13-15, UALVP 22520 (SH), incomplete right dentary with m1 and alveoli for p4, m2 in 13, labial, 14, lingual, and 15, occlusal views; 16-18, UALVP 47282 (DW2), incomplete right dentary with p4, m1 (broken), m2-3 in 16, labial, 17, lingual, and 18, occlusal views.

19-24. Limaconyssus subnuba new species from the early middle Tiffanian (Ti3) DW-2 (DW2) locality, and the late middle Paleocene (Ti4) Gao Mine (GM) locality, Paskapoo Formation, Alberta. 19-21, UALVP 47813 (holotype, GM), incomplete right dentary with p3-4, m1-3 (m3 broken), m2-3 in 19, labial ,20, lingual, and 21, occlusal views; 22-24, UALVP 47288 (DW2), incomplete left dentary with m2-3 in 19, labial, 20, lingual, and 21, occlusal views.

Scale bars = 2 mm.

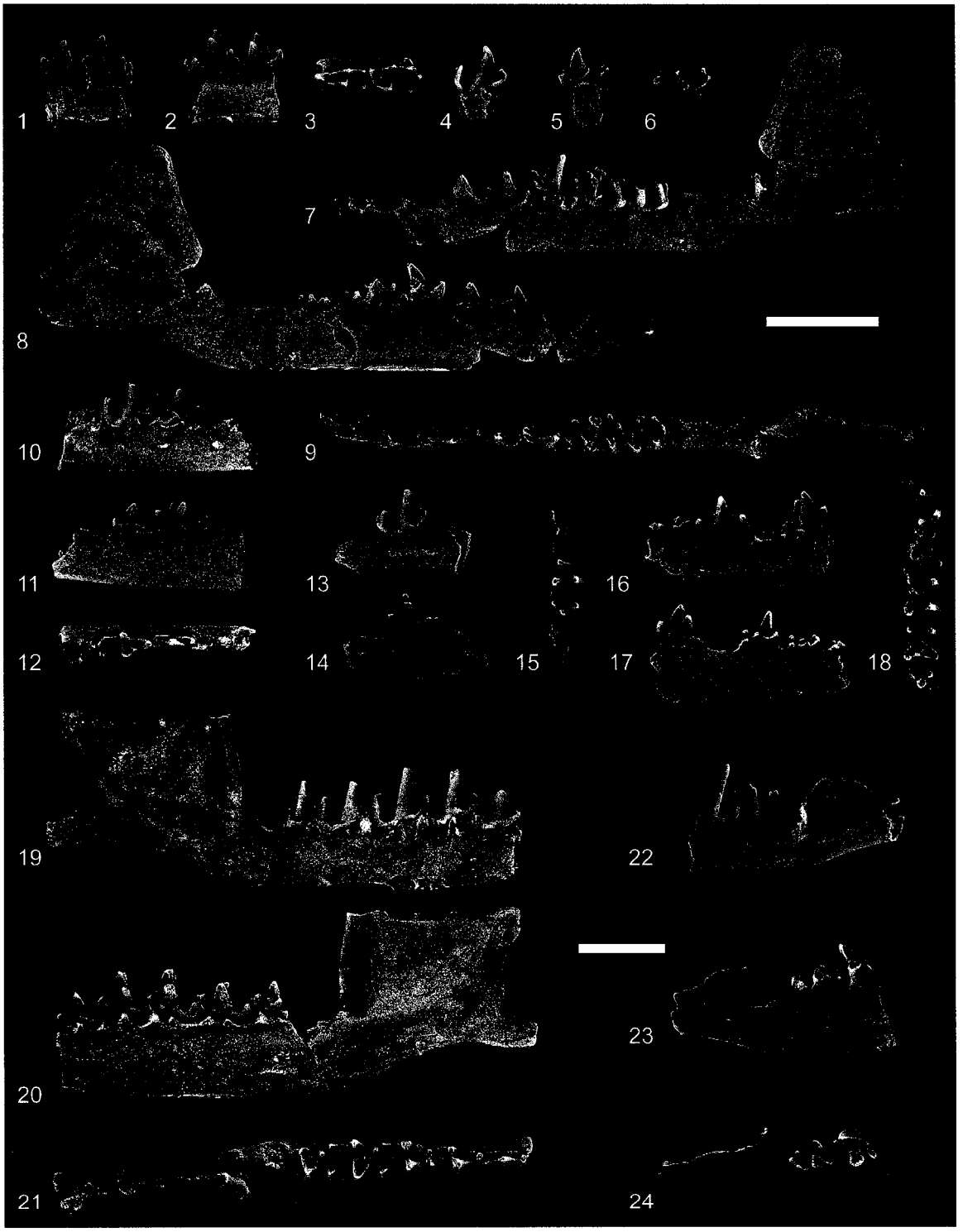
1
2
3
4
5
6
7
8
10
9
11
13
16
12
14
15
17
18
19
22
20
23
21
24

Figure 5.2.—1-15. Xynolestes denommei new genus and species from the early middle Tiffanian (Ti3) DW-2 locality, Paskapoo Formation, Alberta. 1-6, UALVP 40514, associated left maxillary fragments with P2, DP3, P3, P4, M1-2; 1-3, left maxillary fragment with P2, DP3, and erupting P3 in 1, labial, 2, occlusal (P2), and 3, occlusal (DP3) views; 4-6, left maxillary fragment with P4, M1-2 in 4, labial, 5, oblique lingual, and 6, occlusal views; 7-9, UALVP 46917, incomplete right maxilla with P3 and alveoli for P2 in 7, labial, 8, oblique lingual, and 9, occlusal views; 10-12, UALVP 40512, incomplete left maxilla with P2-4, M1-2, and alveoli for M3 in 10, labial, 11, oblique lingual, and 12, occlusal views; 13-15, UALVP 40516, incomplete left maxilla with P4, M1-3 in 13, labial, 14, oblique lingual, and 15, occlusal views. Scale bars = 1 mm.

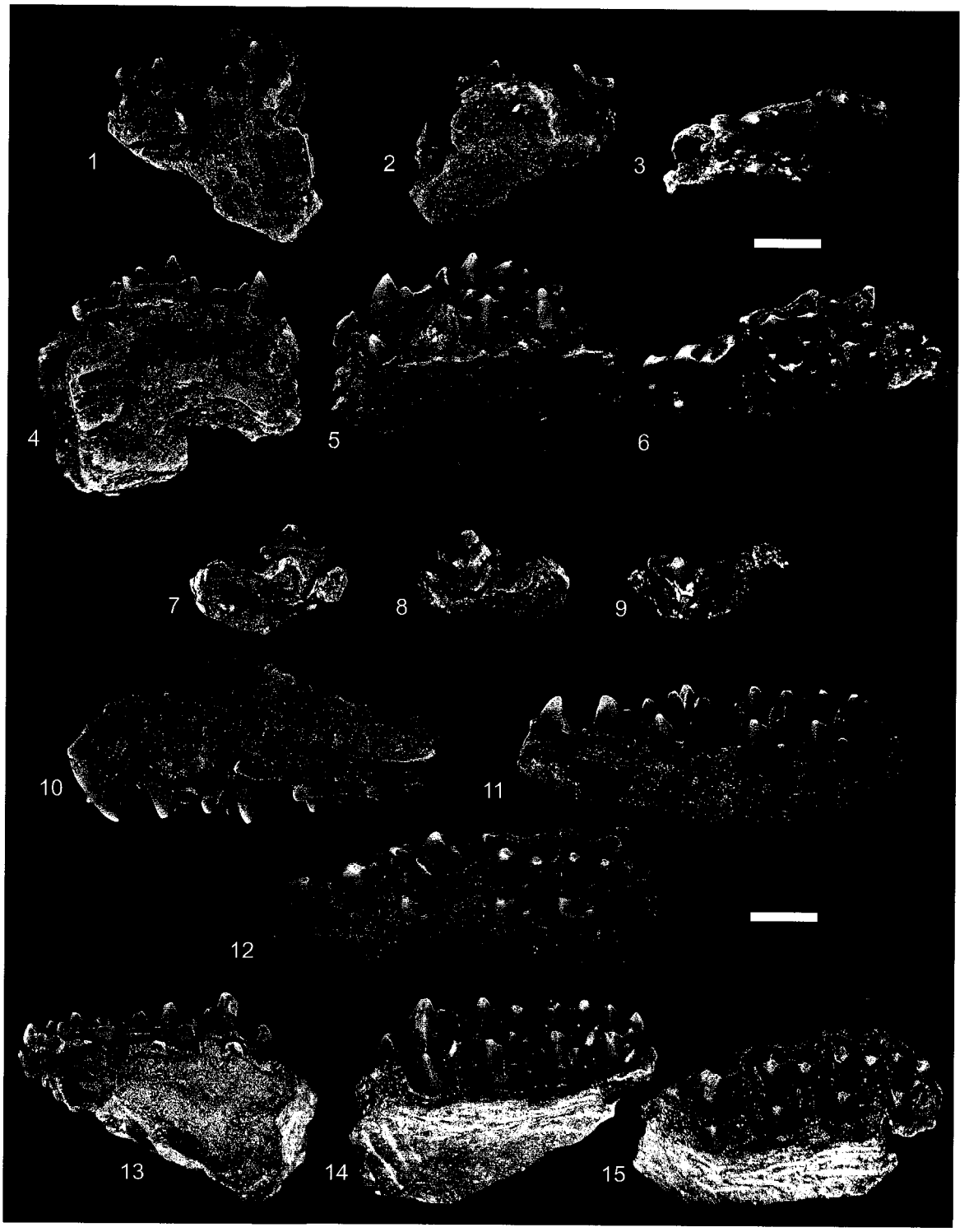
1
2
3
4
5
6
7
8
9
10
11
12
13
14
15

Figure 5.3.—1-12. Xynolestes denommei new genus and species from the early middle Tiffanian (Ti3) DW-2, Joffre Bridge Mammal Site No. 1 (JBM1), and Joffre Bridge Roadcut lower level (JBLL) localities, Paskapoo Formation, Alberta. 1-3, UALVP 46924 (holotype, DW2), incomplete right dentary with p1-4, m1-3 in 1, labial, 2, lingual, and 3, occlusal views; 4-6, UALVP 46903 (JBM1), incomplete right dentary with i2-3, c, p2-3, and alveolus for i1, p1 in 4, labial, 5, lingual, and 6, occlusal views; 7-9, UALVP 46927, incomplete left dentary with p1, p4, m1-3, and alveoli for i3, c, p2-3 in 7, labial, 8, lingual, and 9, occlusal views; 10-12, UALVP 40511 (JBLL), incomplete right dentary with p2-4, m1-3 in 10, labial, 11, lingual, and 12, occlusal views. Scale bars = 1 mm.

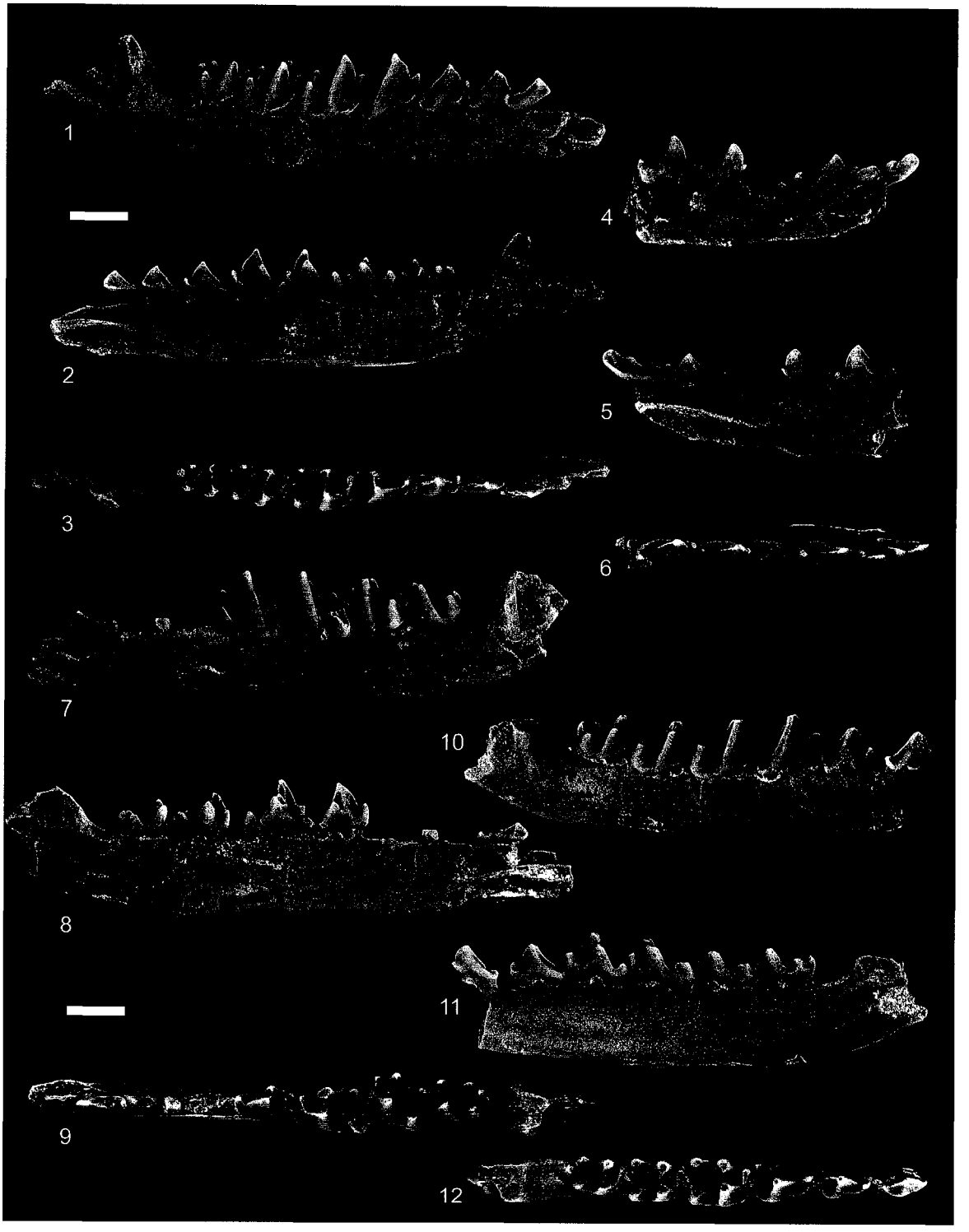
1
4
2
5
3
6
7
10
8
11
9
12

Figure 5.4.—1-15. Xynolestes denommei new genus and species from the early middle Tiffanian (Ti3) DW-2 (DW2) and Hand Hills West upper level (HHW) localities, Paskapoo Formation, Alberta. 1-3, UALVP 46959 (DW2), incomplete left dentary with p4, m1, and alveoli for c, p1-3, m2 in 1, labial, 2, lingual, and 3, occlusal views; 4-6, UALVP 46929 (DW2), incomplete left dentary with p4, m1-3, and alveoli for p2-3 in 4, labial, 5, lingual, and 6, occlusal views; 7-9, UALVP 46943 (DW2), incomplete right dentary with p3-4, m1-2, and alveoli for p2, m3 in 7, labial, 8, lingual, and 9, occlusal views; 10-12, UALVP 34928 (HHW), incomplete right dentary with p3-4, m1-3 in 10, labial, 11, lingual, and 12, occlusal views; 13-15, UALVP 46953 (DW2), incomplete left dentary with m1-2 and erupting m3 in 13, labial, 14, lingual, and 15, occlusal views. Scale bars = 1 mm.

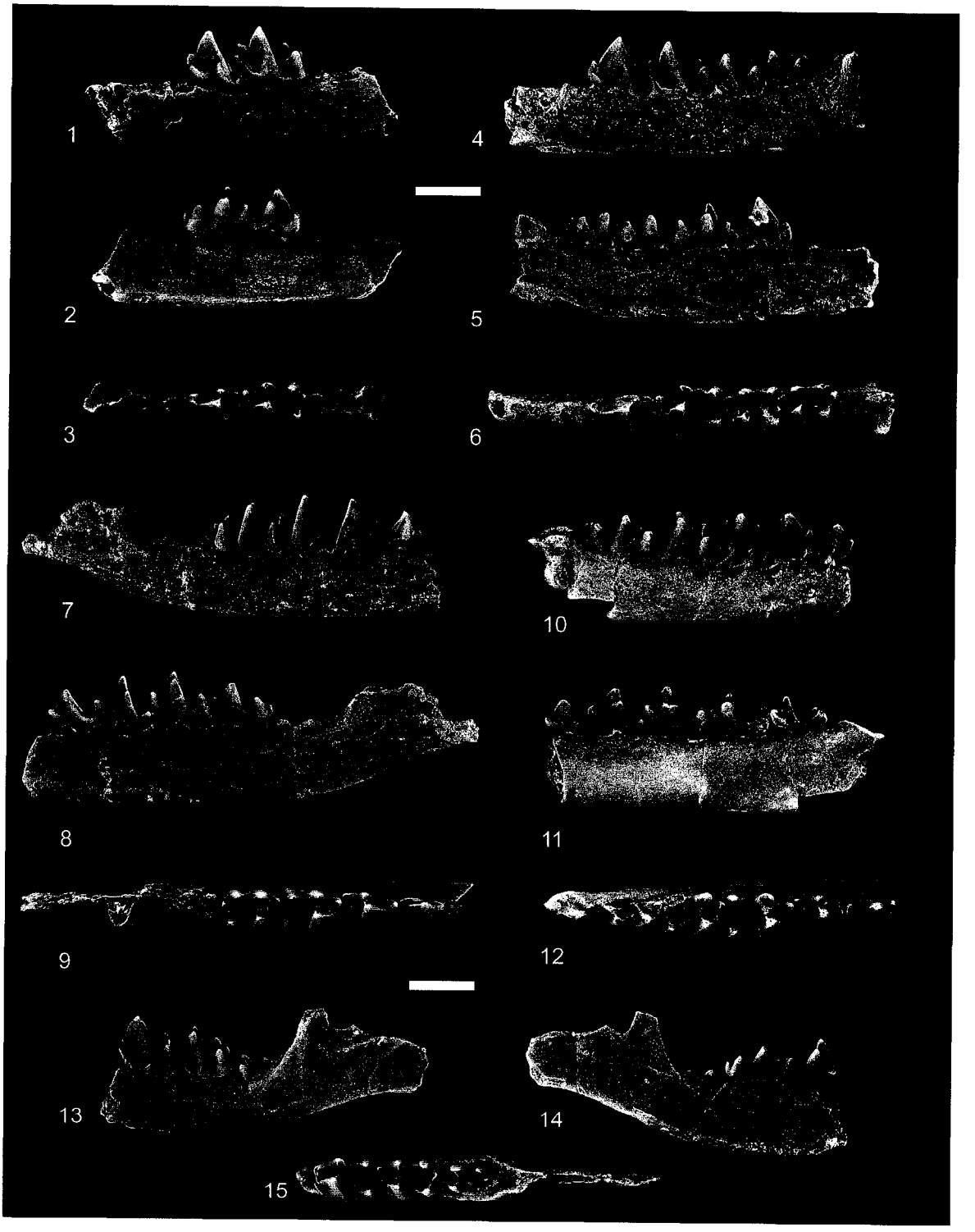
1
4
2
5
3
6
7
10
8
11
9
12
13
14
15

Figure 5.5.—1-12. Litolestes avitodelphus new species from the early middle Tiffanian (Ti3) DW-2 (DW2) and Joffre Bridge Roadcut lower level (JBLL) localities, Paskapoo Formation, Alberta. 1-3, UALVP 40523 (JBLL), incomplete left dentary with i1 (root only), c (crown broken), p3-4, and alveoli for i2-3, p1-2 in 1, labial, 2, lingual, and 3, occlusal views; 4-6, 47276 (DW2), incomplete right dentary with p3-4, m1-2 in 4, labial, 5, lingual, and 6, occlusal views; 7-9, UALVP 47275 (DW2), incomplete left dentary with p3-4, m1-2 in 7, labial, 8, lingual, and 9, occlusal views; 10-12, UALVP 40528 (holotype, DW2), incomplete left dentary with p4, m1-3, and alveoli for p3 in 10, labial, 11, lingual, and 12, occlusal views. Scale bars = 2 mm.

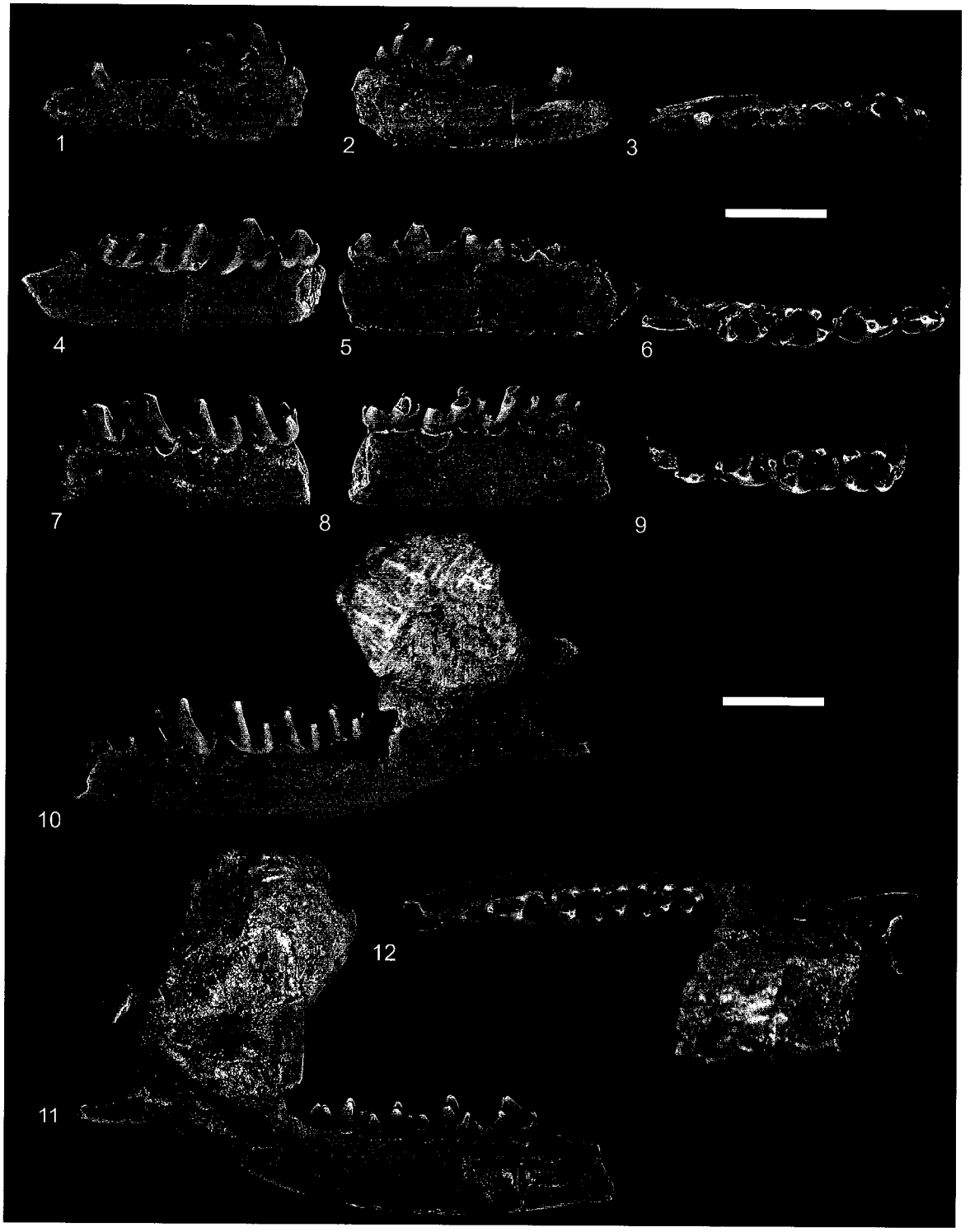
1
2
3
4
5
6
7
8
9
10
11
12

Figure 5.6.—1-6. Litocherus notissimus (Simpson) from the early middle Tiffanian (Ti3) DW-2 and Joffre Bridge Roadcut lower level (JBLL) localities, Paskapoo Formation, Alberta. 1-3, UALVP 47273 (?♂, DW2), incomplete right maxilla with upper canine, P2-4 (labial half of P4 only), M1 (paracone missing), and P1 roots in 1, labial, 2, oblique lingual, and 3, occlusal views; 4-6, UALVP 47248 (?♀, JBLL), incomplete right maxilla with upper canine, P1-4 (P3 and P4 broken), and M1 (broken) in 4, labial, 5, oblique lingual, and 6, occlusal views. Scale bars = 2 mm.

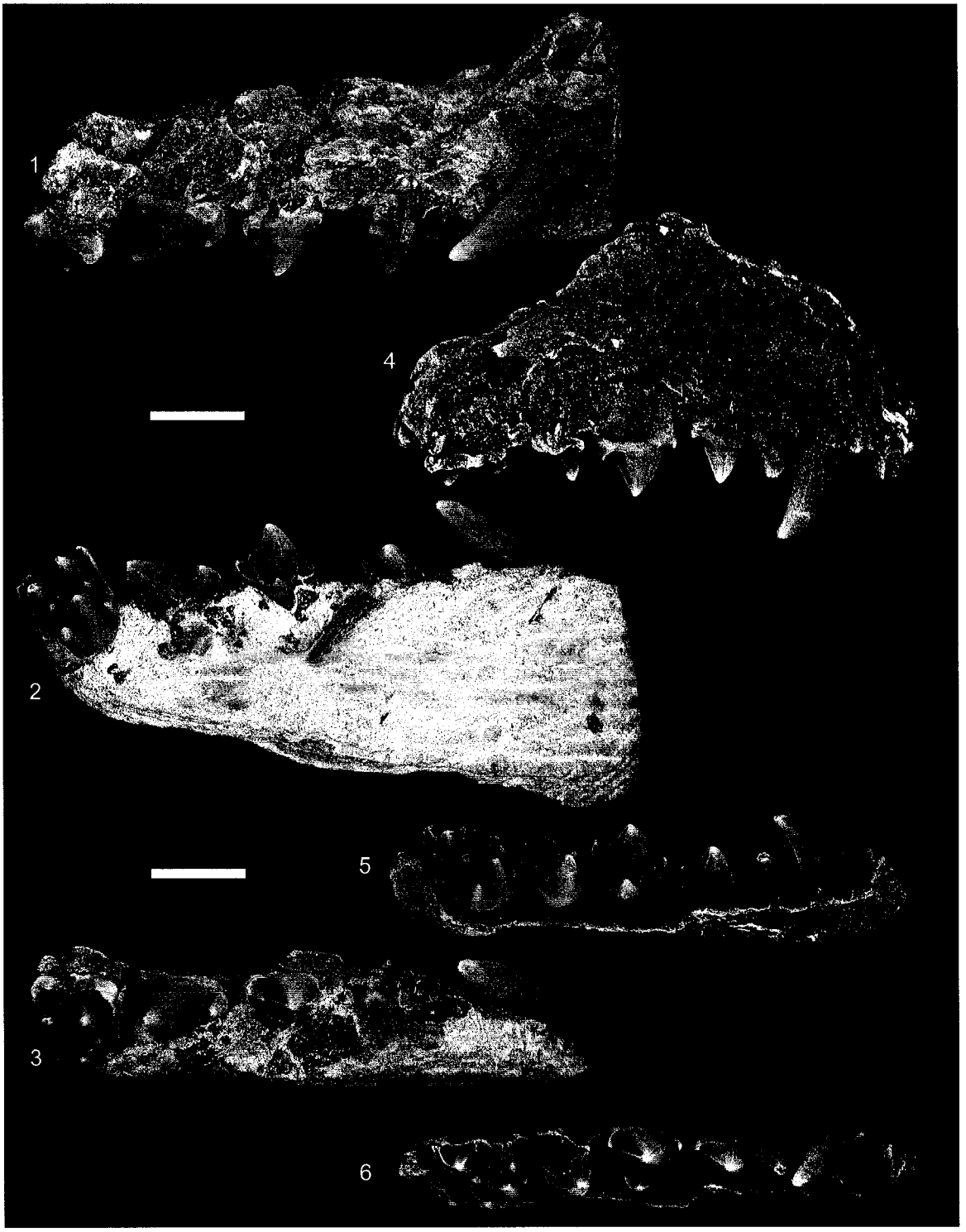
1
4
2
5
3
6

Figure 5.7.—1-9. Litocherus notissimus (Simpson) from the early middle Tiffanian (Ti3) DW-2 locality, Paskapoo Formation, Alberta. 1-3, UALVP 33864 (DW2), incomplete left maxilla with P2-4, M1-3, and alveoli for upper canine and P1 in 1, labial, 2, oblique lingual, and 3, occlusal views; 4-9, UALVP 47272 (DW2), incomplete left and right maxillae with left P2-4, M1, right P3-4, M1-3, and alveoli for P2 [associated incomplete right dentary with p2, p4 (trigonid only), and alveoli for p1, p3 not figured] in 4, 7, labial, 5, 8, oblique lingual, and 6, 9, occlusal views. Scale bars = 2 mm.

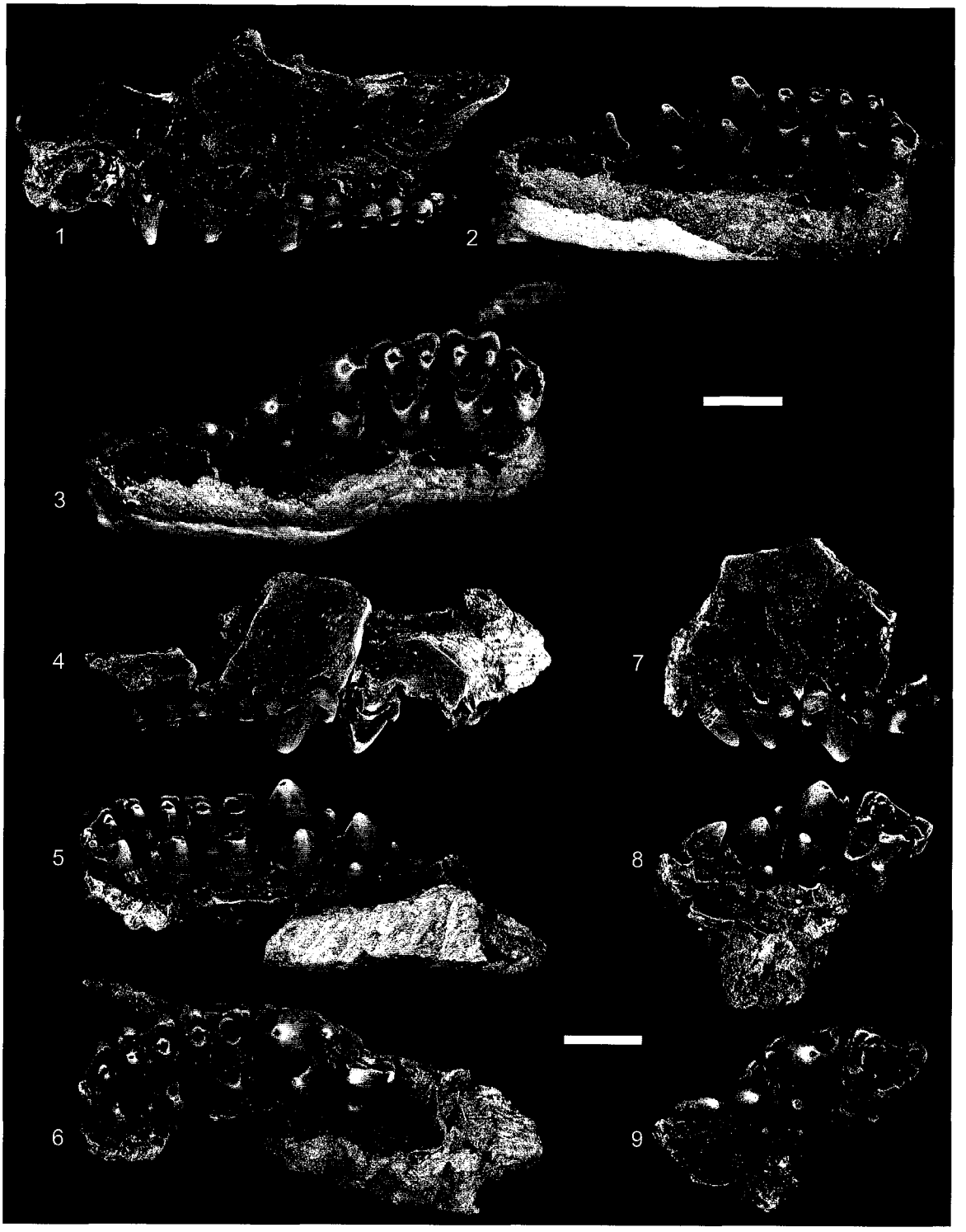
1
2
3
4
5
6
7
8
9

Figure 5.8.—1-12. Litocherus notissimus (Simpson) from the early middle Tiffanian (Ti3) DW-2 (DW2) and Joffre Bridge Roadcut lower level (JBLL), localities, Paskapoo Formation, Alberta. 1-3, UALVP 40510, incomplete left dentary with posterior root of p2, p3-4, m1 in 1, labial, 2, lingual, and 3, occlusal views; 4-6, UALVP 40515 (?♂, JBLL), incomplete left dentary with c, p3-4, m1-2, and alveoli for p1-2, m3 in 4, labial, 5, lingual, and 6, occlusal views; 7-9, UALVP 40668 (?♀, JBLL), incomplete left dentary with c, p2 (talonid only), p3-4, m1-2, and alveoli for i2-3, p1, m3 in 7, labial, 8, lingual, and 9, occlusal views; 10-12, UALVP 47314 (?♂, DW2), incomplete left dentary with c, p1-4, m1-2 in 10, labial, 11, lingual, and 12, occlusal views. Scale bars = 2 mm.

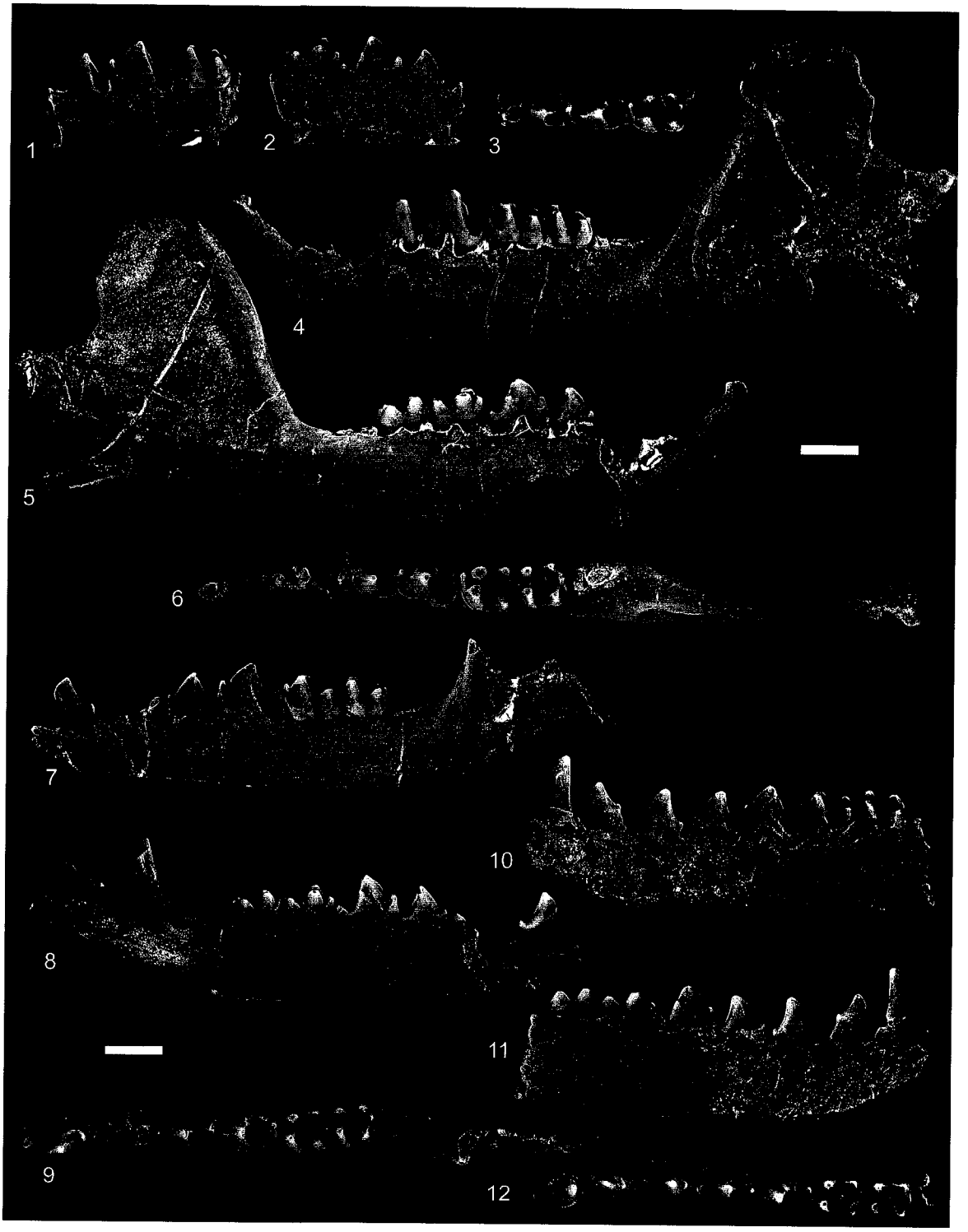
1
2
3
4
5
6
7
8
9
10
11
12

Figure 5.9.—1-9. Litocherus notissimus (Simpson) from the early middle Tiffanian (Ti3) DW-2 (DW2) locality, Paskapoo Formation, Alberta. 1-4, UALVP 40527 (JBM1), incomplete right dentary with p2-4, m1-3, and alveoli for c, p1 in 1, labial, 2, lingual, and 3, occlusal views; 4-6, UALVP 47325 (DW2), incomplete right dentary with erupting p4, m1-3, and alveoli for p2-3 in 4, labial, 5, lingual, and 6, occlusal views; 7-9, UALVP 47324, incomplete right dentary with erupting p3-4, m2-3, and alveoli for p1-2, m1 in 7, labial, 8, lingual, and 9, occlusal views. 10-15. Litocherus notissimus (Simpson) from the early Tiffanian (Ti2) Scarritt Quarry, Fort Union Formation, Montana. 10-12, UM 89802 (?♂), incomplete left dentary with lower canine, p3-4, m1-3, and alveoli for i1-3, p1-2 in 10, labial, 11, lingual, and 12, occlusal views; 13-15, UM 89801 (?♀), incomplete right dentary with lower canine, p2-4, m1, and alveolus for p1 in 13, labial, 14, lingual, and 15, occlusal views. Scale bars = 2 mm.

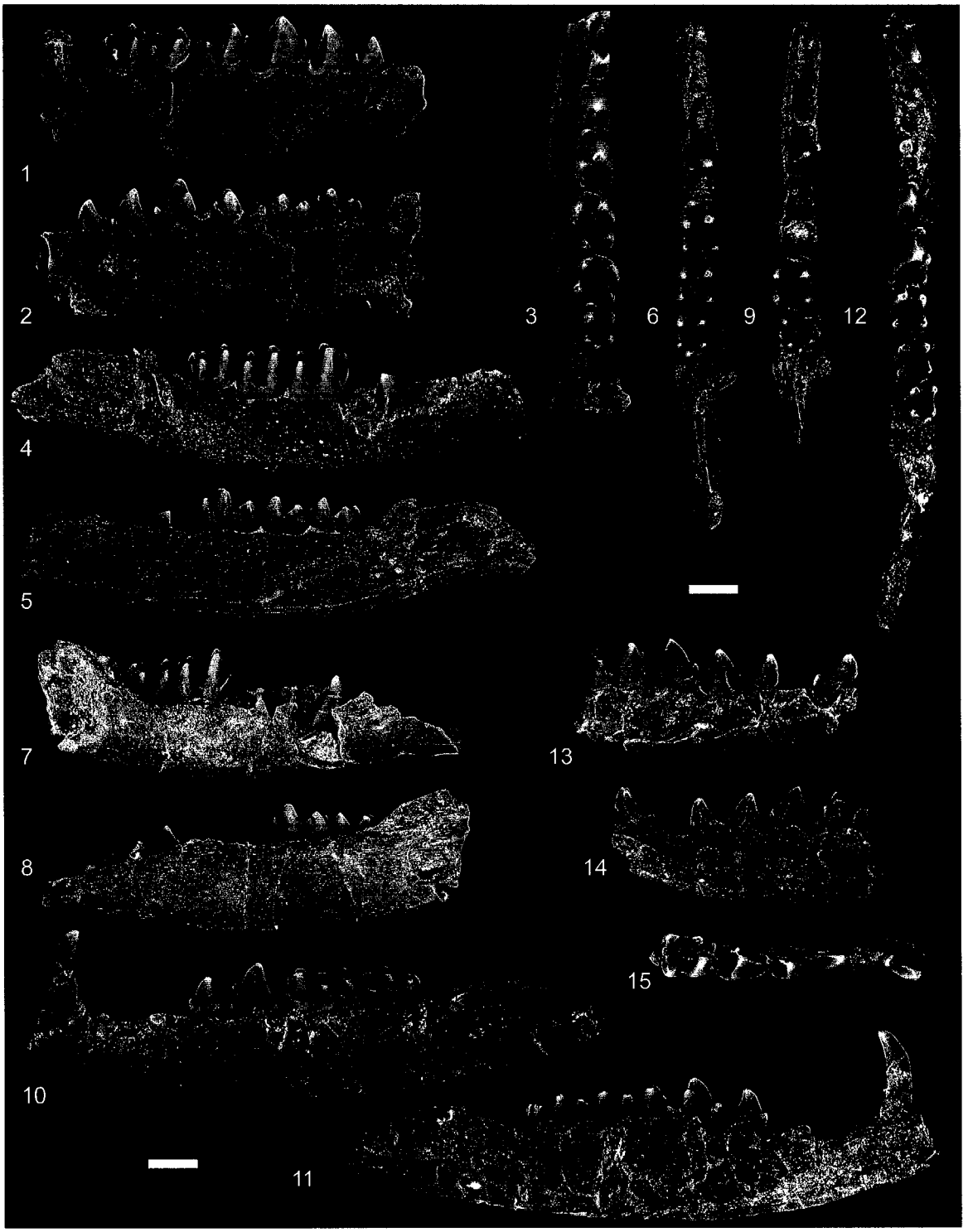
1
2
3
4
5
6
7
8
9
10
11
12
13
14
15

Figure 5.10.—1-4. Litocherus notissimus (Simpson) from the early middle Tiffanian (Ti3) DW-2 locality, Paskapoo Formation, Alberta. 1-4,UALVP 46379, incomplete left dentary with p2-4, m1-3, and alveoli for c, p1, and associated left and right petromastoids, basisphenoid, right innominate (ischium, complete acetabulum, partial iliac blade), left innominate (ischium and partial acetabulum), left femoral diaphysis and distal epiphysis, left calcaneum, left cuboid, left entocuneiform, left metatarsal V, left proximal and intermediate phalanges. 1, block with associated cranial and postcranial remains, right dentary removed; 2-4, incomplete right dentary in 2, labial, 3, lingual, and 4, occlusal views. Scale bars = 2 mm.

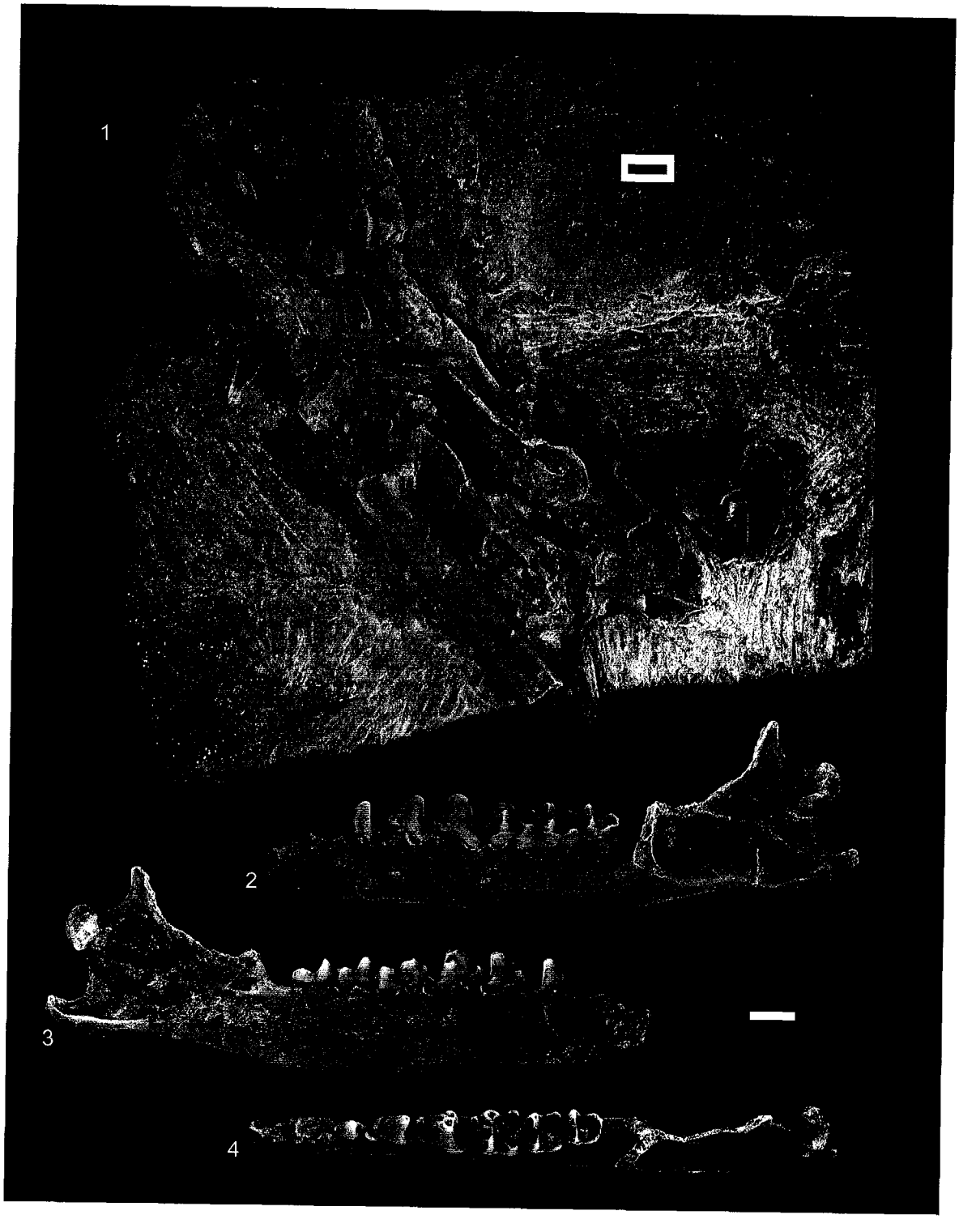
1
2
3
4

Figure 5.11.—1-8. Litocherus notissimus (Simpson) from the early middle Tiffanian (Ti3) DW-2 locality, Paskapoo Formation, Alberta. 1-8, UALVP 46379, associated left and right petromastoids from block in Figure 9. 1-4, left petromastoid in 1, medial, 2, lateral, 3, dorsal, and 4, ventral views; 5-8, left petromastoid in 5, medial, 6, lateral, 7, dorsal, and 8, ventral views. Scale bars = 2 mm.

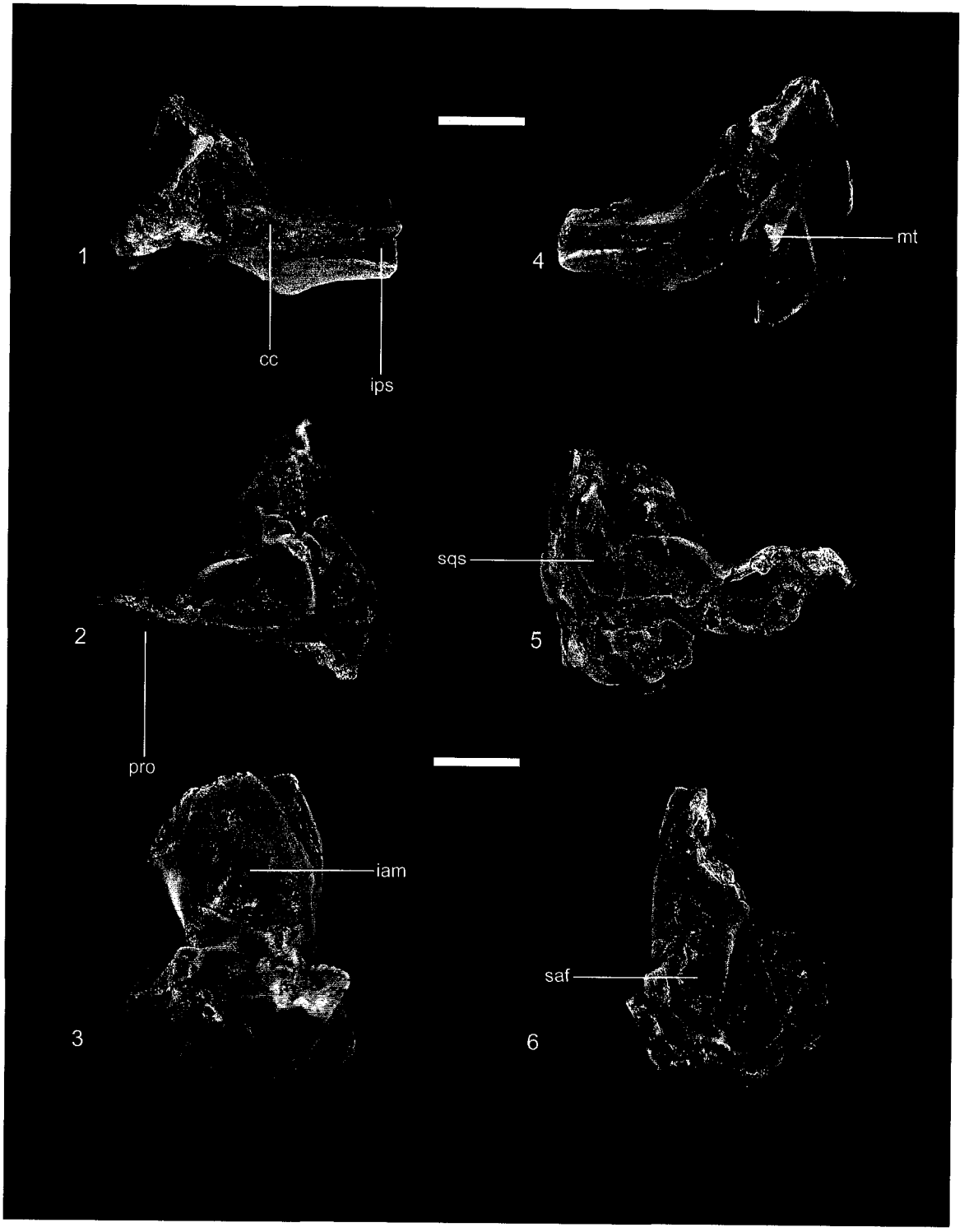
1
cc
ips
4
mt
2
pro
sqs
5
3
iam
saf
6

Figure 5.12.—1, 2. Litocherus notissimus (Simpson) from the early middle Tiffanian (Ti3) DW-2 locality, Paskapoo Formation, Alberta. UALVP 46379, associated left and right petromastoids from block in Figure 9. Left petromastoid in 1, ventral view; right petromastoid in 2, ventral view. Scale bar = 1 mm.

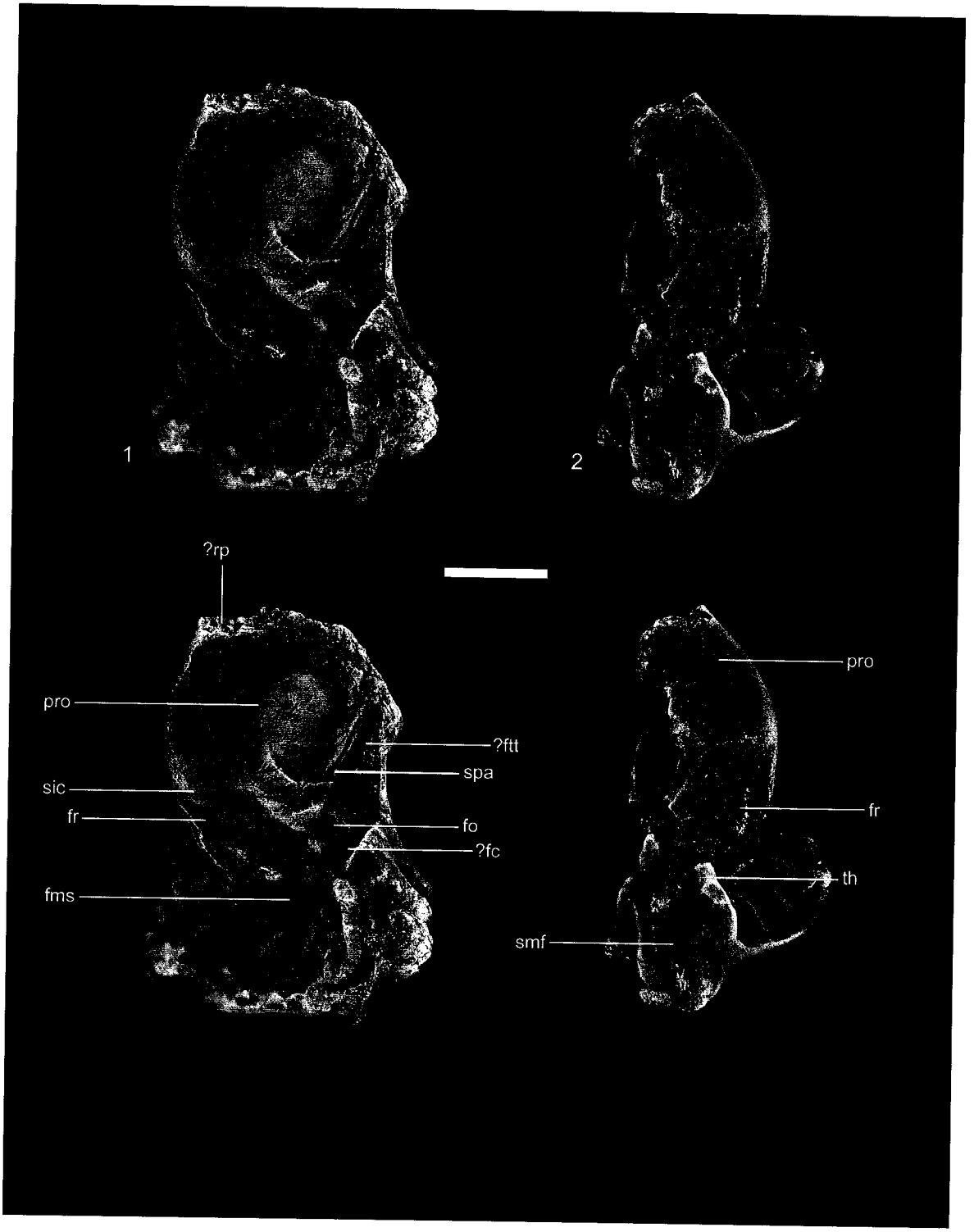
1
2
?rp
pro
?ftt
spa
sic
fr
fo
?fc
fms
pro
fr
th
smf

Figure 5.13.—1-11. Litocherus notissimus (Simpson) from the early middle Tiffanian (Ti3) DW-2 locality, Paskapoo Formation, Alberta. UALVP 46379, associated incomplete left and right innominates and incomplete left femur from block in Figure 9. 1-3, incomplete left innominate in 1, lateral, 2, medial, and 3, dorsal views; 4-6, incomplete right innominate in 4, lateral, 5, medial, and 6, dorsal views; 7-11, incomplete left femoral diaphysis and distal epiphysis in 7, anterior, 8, posterior, 9, lateral, 10, medial, and 11, distal views. Scale bars = 2 mm.

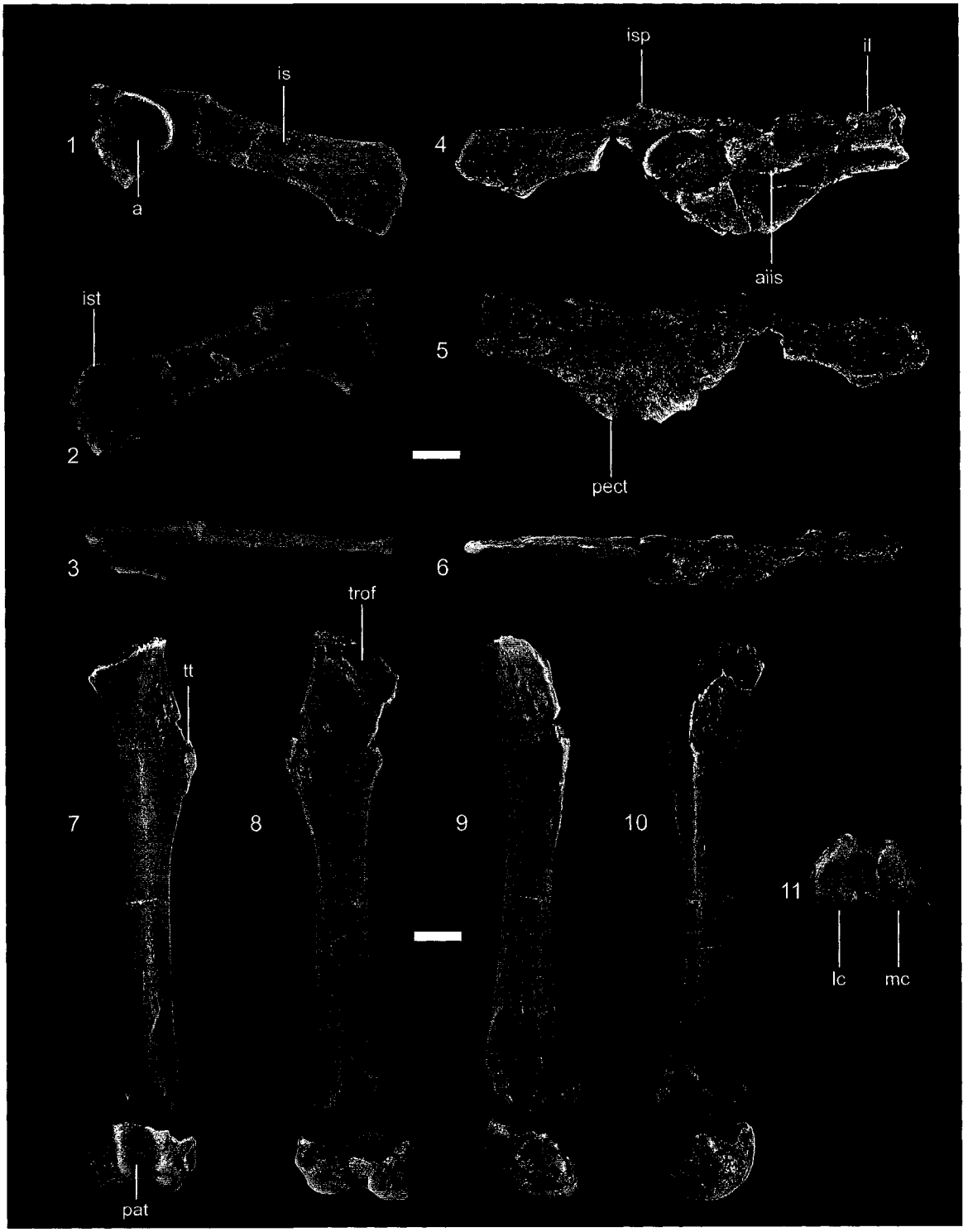
1
is
a
4
isp
il
aiis
2
ist
5
pect
3
6
7
tt
pat
8
trof
9
10
11
lc
mc

Figure 5.14.—1-12. Litocherus notissimus (Simpson) from the early middle Tiffanian (Ti3) DW-2 locality, Paskapoo Formation, Alberta. 1-6, UALVP 46378, right astragalus (incomplete right maxilla with P2-3, associated incomplete left dentary with p3-4 and alveoli for p1-2, m1-3, and associated left and right innominates not figured) in 1, dorsal, 2, ventral, 3, lateral, 4, medial, 5, proximal, and 6, distal views; 7-12, UALVP 46379, left calcaneum from block in Figure 9 in 7, dorsal, 8, ventral, 9, lateral, 10, medial, 11 proximal, and 12, distal views. Scale bars = 1 mm.

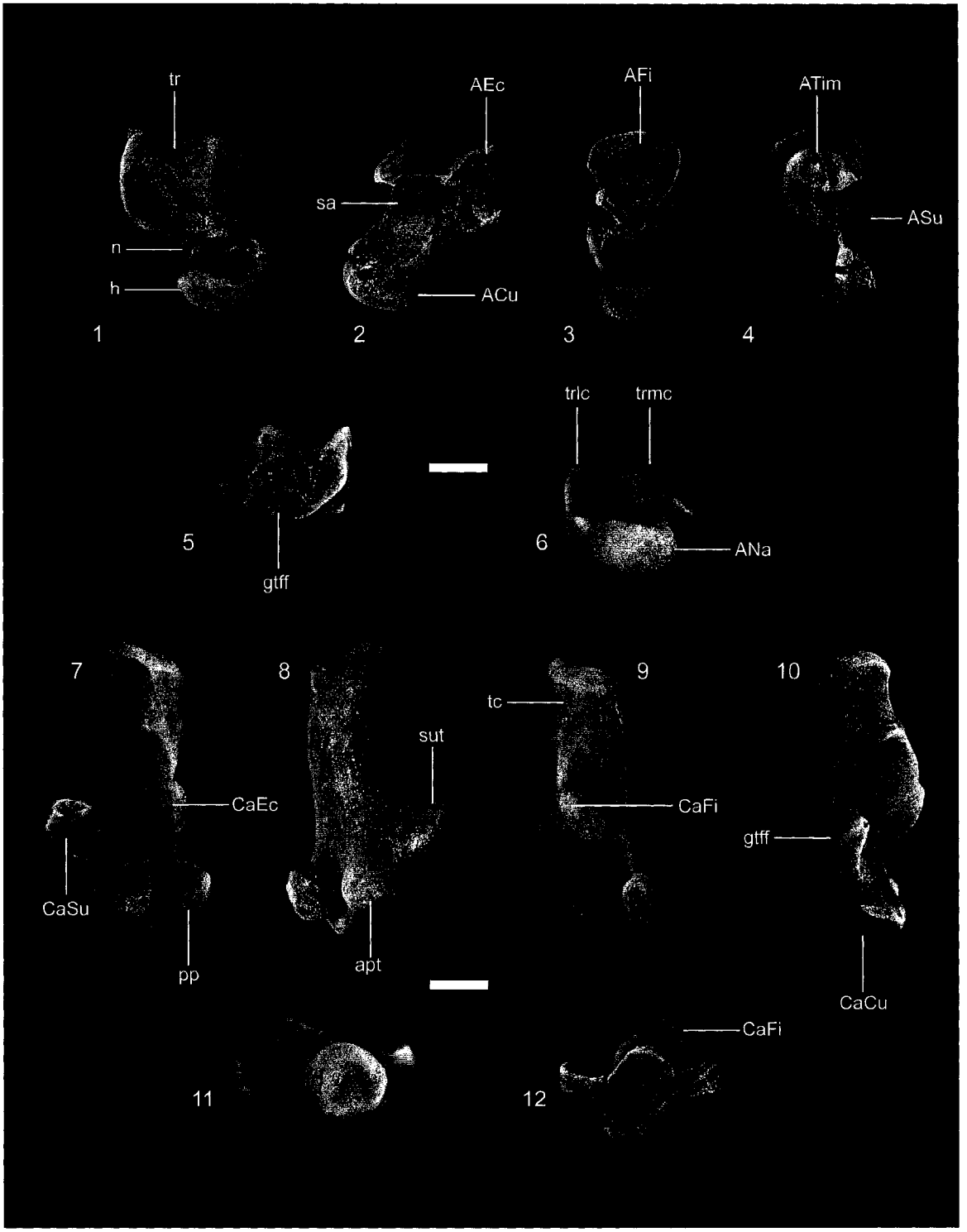
tr
n
h
1
AEc
sa
ACu
2
AFi
3
ATim
ASu
4
gtff
5
trlc
trmc
ANa
6
7
CaEc
CaSu
pp
8
sut
apt
9
tc
CaFi
10
gtff
CaCu
11
CaFi
12

Figure 5.15.—1-23. Litocherus notissimus (Simpson) from the early middle Tiffanian (Ti3) DW-2 locality, Paskapoo Formation, Alberta. 1-6, UALVP 46379, left cuboid from the block in Figure 9 in 1, dorsal, 2, ventral, 3, lateral, 4, medial, 5, proximal, and 6, distal views; 7-11, left entocuneiform from block in Figure 9 in 7, dorsal, 8, ventral, 9, lateral, 10, medial, and 11 proximal views; 12-15, left metatarsal V from block in Figure 9 in 12, dorsal, 13, ventral, 14, lateral, and 15, medial views; 16-20, left proximal phalanx from block in Figure 9 in 16, dorsal, 17, ventral, 18, lateral, 19, medial, and 20, proximal views; 21-23, incomplete left intermediate phalanx from block in Figure 9 in 21, dorsal, 22, ventral, and 23, proximal views. Scale bars = 2 mm.

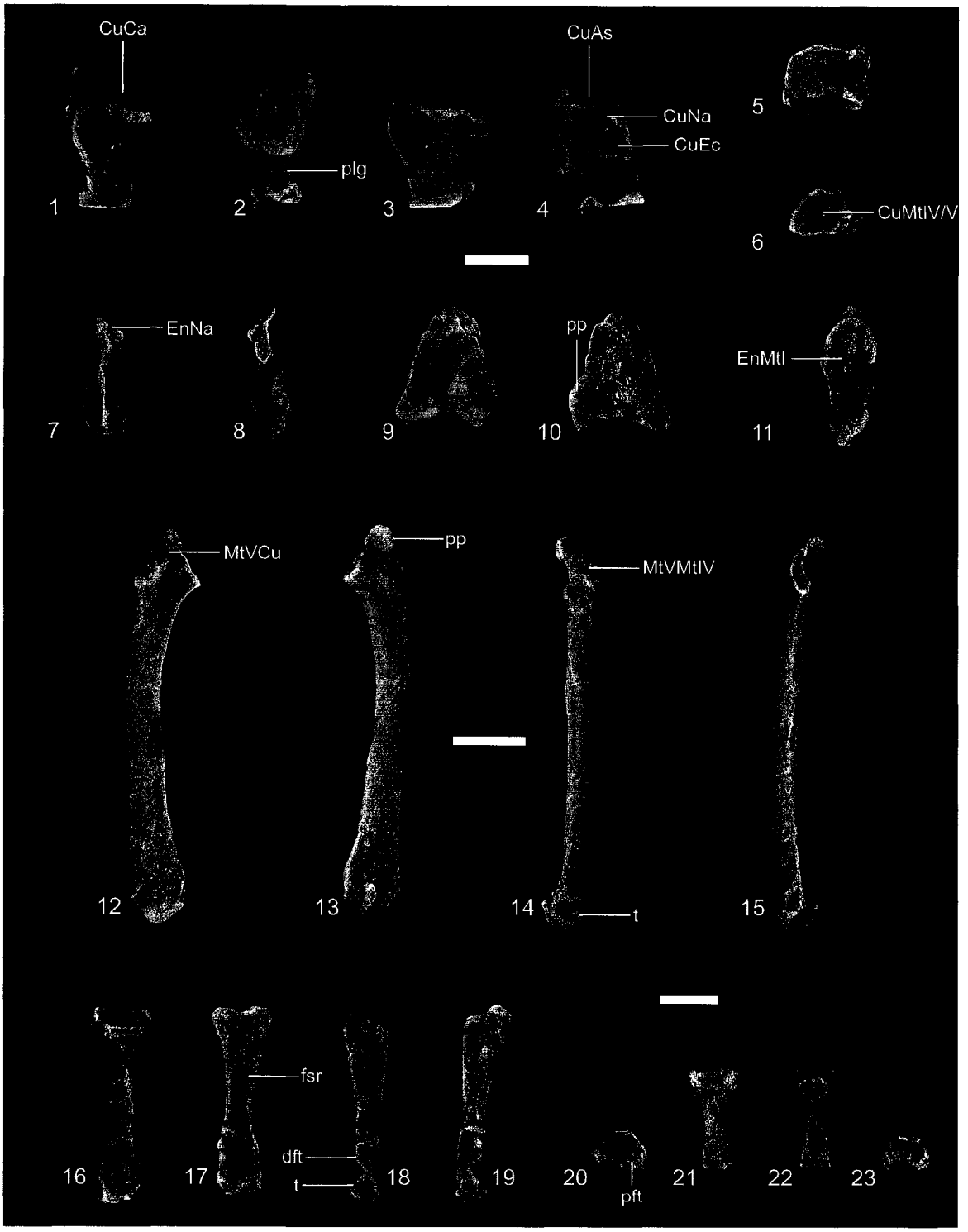
CuCa
CuAs
CuNa
CuEc
plg
CuMtIV/V
EnNa
pp
EnMtI
MtVCu
pp
MtVMtIV
t
fsr
dft
t
pft
1
2
3
4
5
6
7
8
9
10
11
12
13
14
15
16
17
18
19
20
21
22
23

Figure 5.16.—1-12. Litocherus sp., cf. L. zygeus from the early middle Tiffanian (Ti3) DW-2 (DW2) and Birchwood (BW) localities, Paskapoo Formation, Alberta. 1-3, UALVP 39287 (BW), right P4 in 1, labial, 2, oblique lingual, and 3, occlusal views; 4-6, UALVP 47814 (DW2), left P4 in 4, labial, 5, oblique lingual, and 6, occlusal views; 7, 8, UALVP 47248, right M2 in 7, oblique lingual and 8, occlusal views; 9-11, UALVP 47250 (DW2), incomplete right dentary with p2-4, m1-3, and alveolus for p1 in 9, labial, 10, lingual, and 11 occlusal views; 12-14, UALVP 47251 (DW2), incomplete right dentary with p4, m1-2, and alveoli for p3, m3 in 12, labial, 13, lingual, and 14, occlusal views. Scale bars = 2 mm.

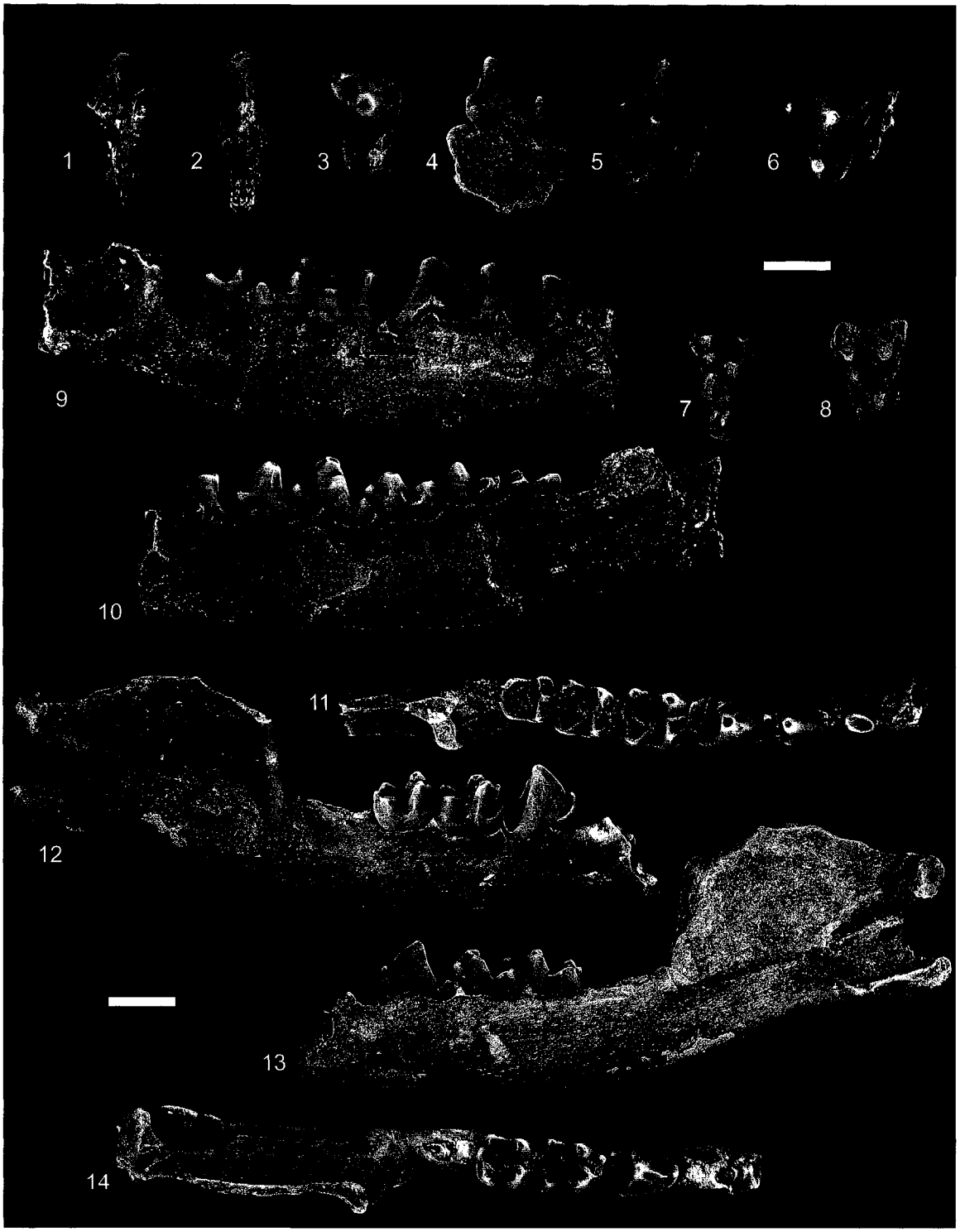
1
2
3
4
5
6
9
7
8
10
11
12
13
14

Figure 5.17.—1-12. Litocherus sp., cf. L. zygeus from the early middle Tiffanian (Ti3) DW-2 (DW2), Birchwood (BW), and Hand Hills West upper level (HHW) localities, Paskapoo Formation, Alberta. 1-3, UALVP 47249 (DW2), incomplete right dentary with p4, m1-2, and alveoli for p3, m3 in 1, labial, 2, lingual, and 3, occlusal views; 4-6, UALVP 39477 (BW), incomplete right dentary with p4, m1-2, and alveoli for p2-3, m3 in 4, labial, 5, lingual, and 6, occlusal views; 7-9, UALVP 47254, incomplete right dentary with p4, m1-2, and alveoli for p1-3, m3 in 7, labial, 8, lingual, and 9, occlusal views; 10-12, UALVP 35114 (HHW), incomplete left dentary with p4, m1-2 in 10, labial, 11, lingual, and 12, occlusal views. Scale bars = 2 mm.

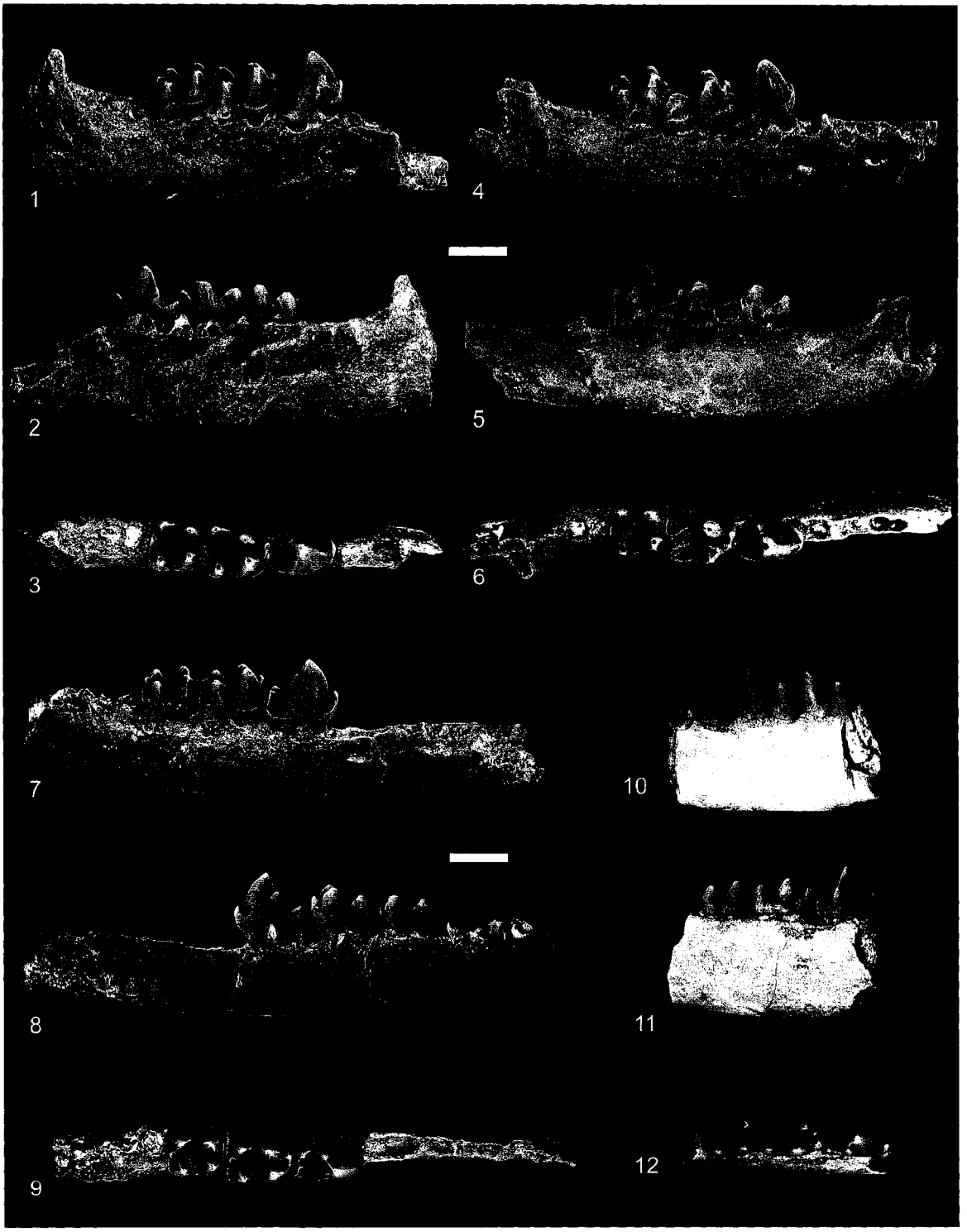
1
4
2
5
3
6
7
10
8
11
9
12

Figure 5.18.—1-18. Nayloria albertensis new genus and species from the early middle Tiffanian (Ti3) DW-2 (DW2) and Joffre Bridge Mammal Sit No. 1 (JBMS) localities, Paskapoo Formation, Alberta. 1-3, UALVP 47258, incomplete left maxilla with P3-4 (P4 broken), M1-2, and alveoli for M3 in 1, labial, 2, oblique lingual, and 3, occlusal views; 4-6, UALVP 40525 (holotype, DW2), incomplete left dentary with i1-2, c, p1, p4, m1-3, and alveoli for i3, p2-3 in 4, labial, 5, lingual, and 6, occlusal views; 7-9, UALVP 40528 (DW2), incomplete left dentary with m1-3 in 7, labial, 8, lingual, and 9, occlusal views; 10-12, UALVP 47273 (JBMS), incomplete right dentary with p2-4, m1-3, and alveoli for c, p1 in 10, labial, 11, lingual, and 12, occlusal views; 13-15, UALVP 47262, incomplete right dentary with p3-4 and alveoli for c, p1-2 in 13, labial, 14, lingual, and 15, occlusal views; 16-18, UALVP 47266, incomplete left dentary with p2-4 and alveolus for p1 in 16, labial, 17, lingual, and 18, occlusal views. Scale bars = 2 mm.

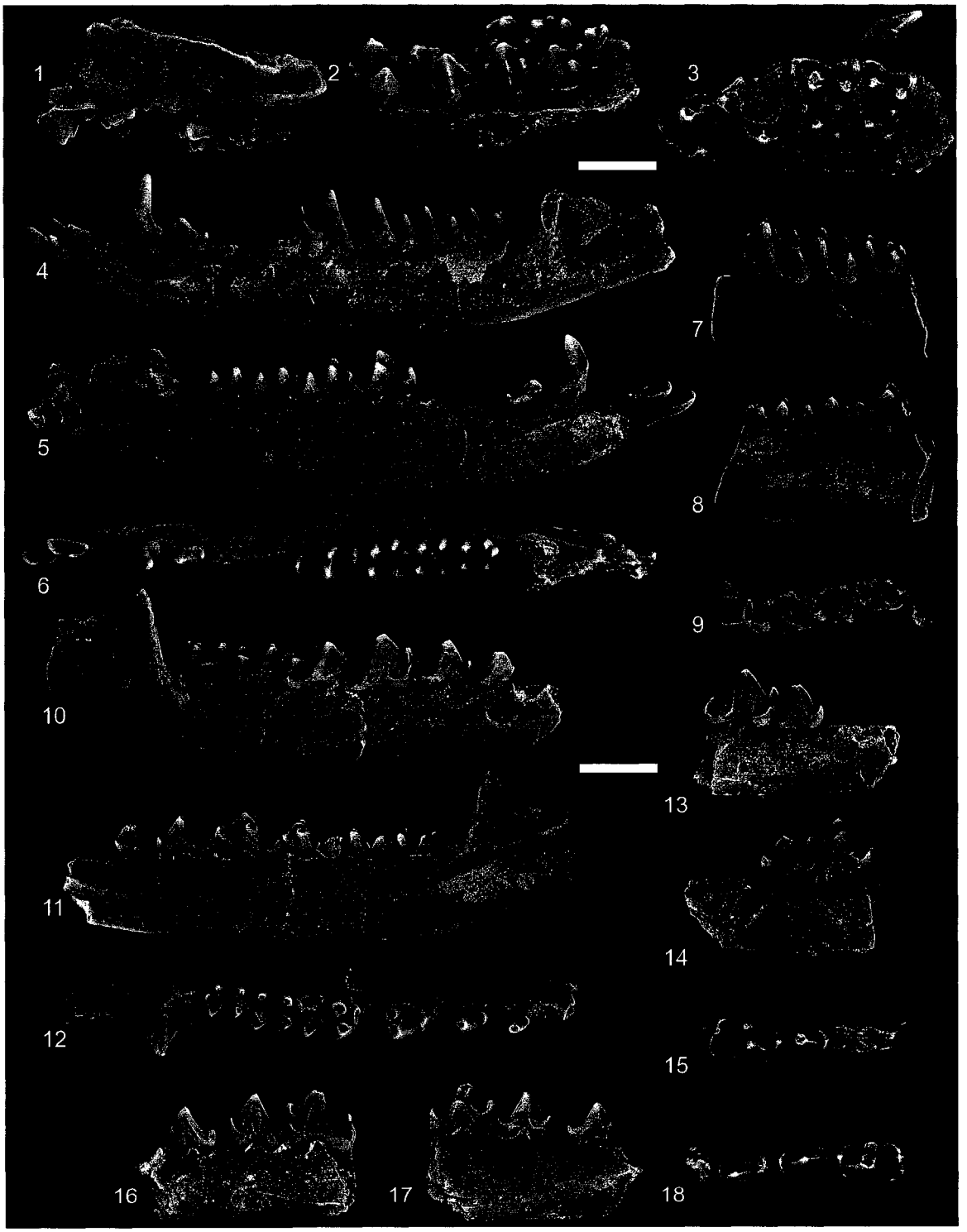
1
2
3
4
5
6
7
8
9
10
11
12
13
14
15
16
17
18

Figure 5.19.—1-9. Adeloxenus adapisoricoides new genus and species from the early middle Tiffanian (Ti3) DW-2 locality, Paskapoo Formation, Alberta. 1-3, UALVP 46997 (holotype), incomplete right dentary with p2-4, m1-3 in 1, labial, 2, lingual, and 3, occlusal views; 4-6, UALVP 46998, incomplete right dentary with m1 and alveoli for i1-3, c, p1-4, m2-3 in 4, labial, 5, lingual, and 6, occlusal views; 7-9, UALVP 46999, right m1 in 7, labial, 8, lingual, and 9, occlusal views.

10-15. "Adapisorella" sp. from the early middle Tiffanian (Ti3) DW-1 (DW1) and Hand Hills West upper level (HHW) localities, Paskapoo Formation, Alberta. 10-12, UALVP 35098 (HHW), left m2 in 10, labial, 11, lingual, and 12, occlusal views; 13-15, UALVP 46996 (DW1), right m2 in 13, labial, 14, lingual, and 15, occlusal views.

Scale bars = 2 mm.

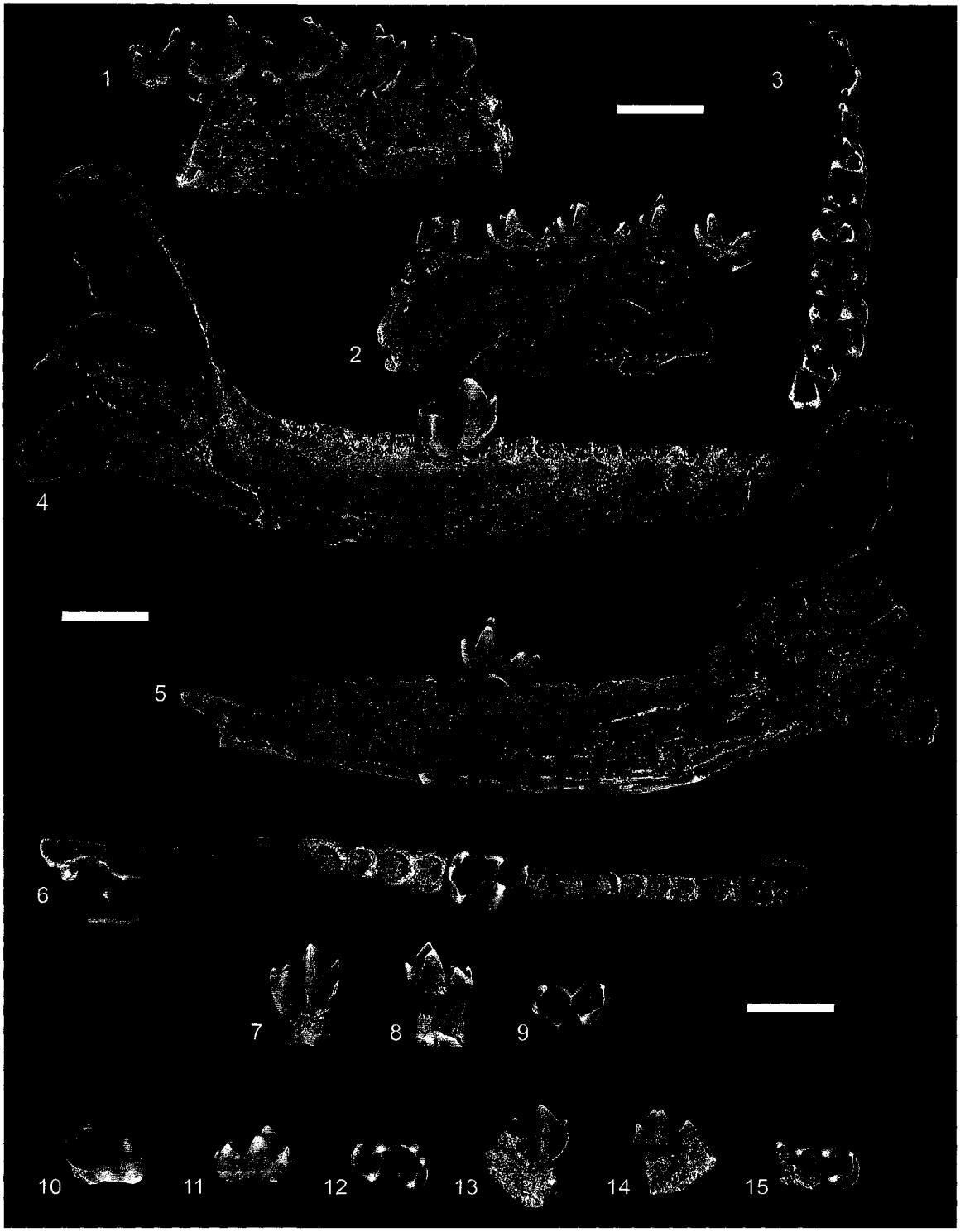
1
2
3
4
5
6
7
8
9
10
11
12
13
14
15

Figure 5.20.—1-18. Diacocherus sp., cf. D. meizon from the early middle Tiffanian (Ti3) DW-2 (DW2) and Hand Hills West upper level (HHW) localities, Paskapoo Formation, Alberta. 1-3, UALVP 47357 (HHW), right P4 in 1, labial, 2, oblique lingual, and 3, occlusal views; 4-6, UALVP 47351 (DW2), right M1 in 4, labial, 5, oblique lingual, and 6, occlusal views; 7-9, UALVP 47356 (DW2), right m1 in 7, labial, 8, lingual, and 9, occlusal views; 10-12, UALVP 47353 (DW2), incomplete right dentary with dp4, m1, and alveoli for p3 in 10, labial, 11, lingual, and 12, occlusal views; 13-15, UALVP 47354 (DW2), incomplete right dentary with m1-2 in 13, labial, 14, lingual, and 15, occlusal views; 16-18, UALVP 35117 (HHW), left m2 in 16, labial, 17, lingual, and 18, occlusal views. Scale bars = 2 mm.

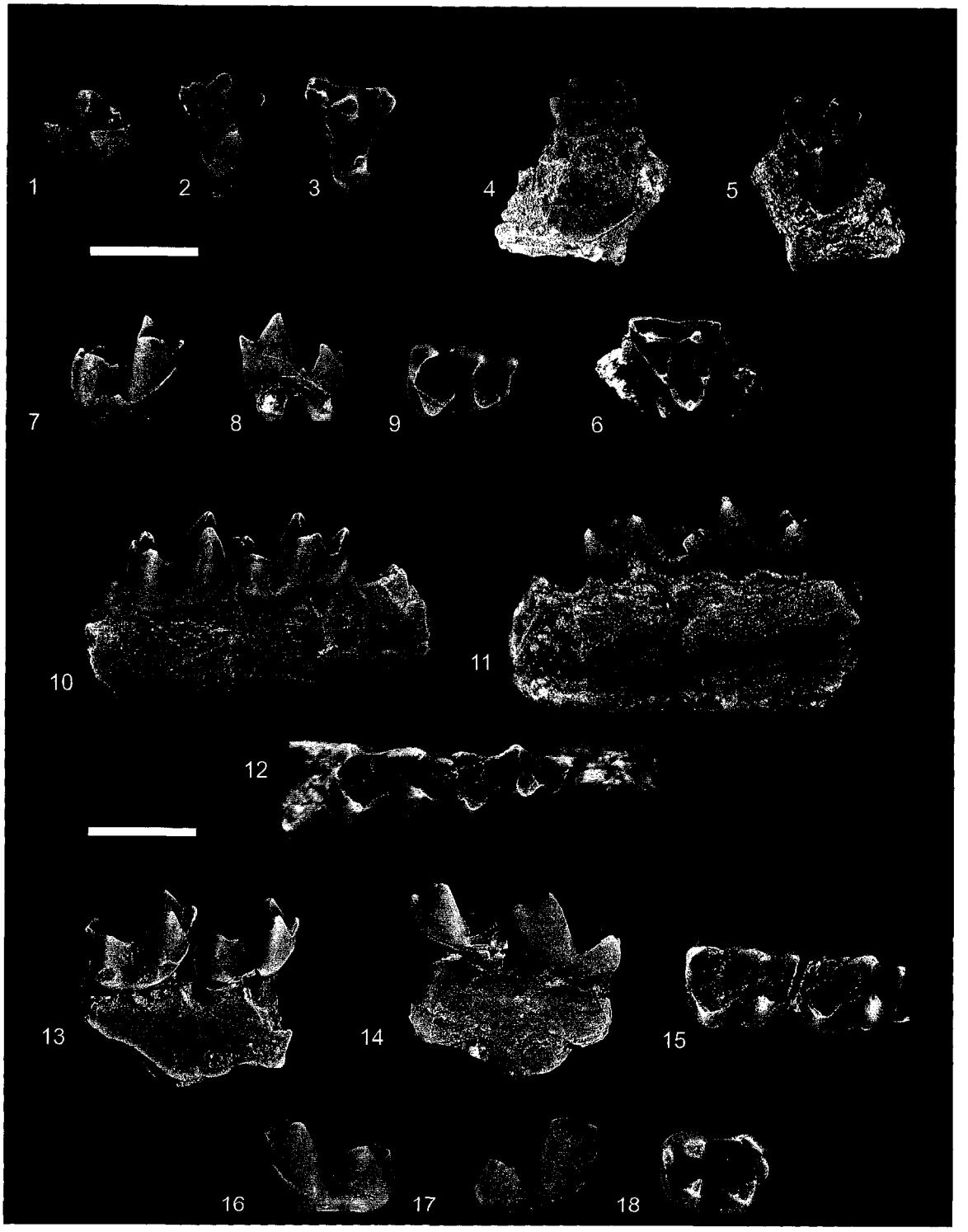
1
2
3
4
5
7
8
9
6
10
11
12
13
14
15
16
17
18

Figure 5.21.—1-18. "Leptacodon" munusculum from the early middle Tiffanian (Ti3) DW-2 (DW2) and Joffre Bridge Roadcut lower level (JBLL) localities, Paskapoo Formation, Alberta. 1-3, UALVP 33862 (DW2), incomplete right maxilla with P3-4, M1-3, and alveoli for P2 in 1, labial, 2, oblique lingual, and 3, occlusal views; 4-6, UALVP 47289 (JBLL), left M1 in 4, labial, 5, lingual, and 6, occlusal views; 7-9, UALVP 47291 (DW2), associated right M2 and M3 in 7, 10, labial, 8, 11, lingual, and 9, 12, occlusal views; 13-15, UALVP 47295 (DW2), incomplete left dentary with p1-4, m1 (talonid only), m2-3, and alveolus for c in 13, labial, 14, lingual, and 15, occlusal views; 16-18, UALVP 47298 (DW2), incomplete left dentary with p3-4, m1-3, and alveoli for p2 in 16, labial, 17, lingual, and 18, occlusal views. Scale bars = 2 mm.

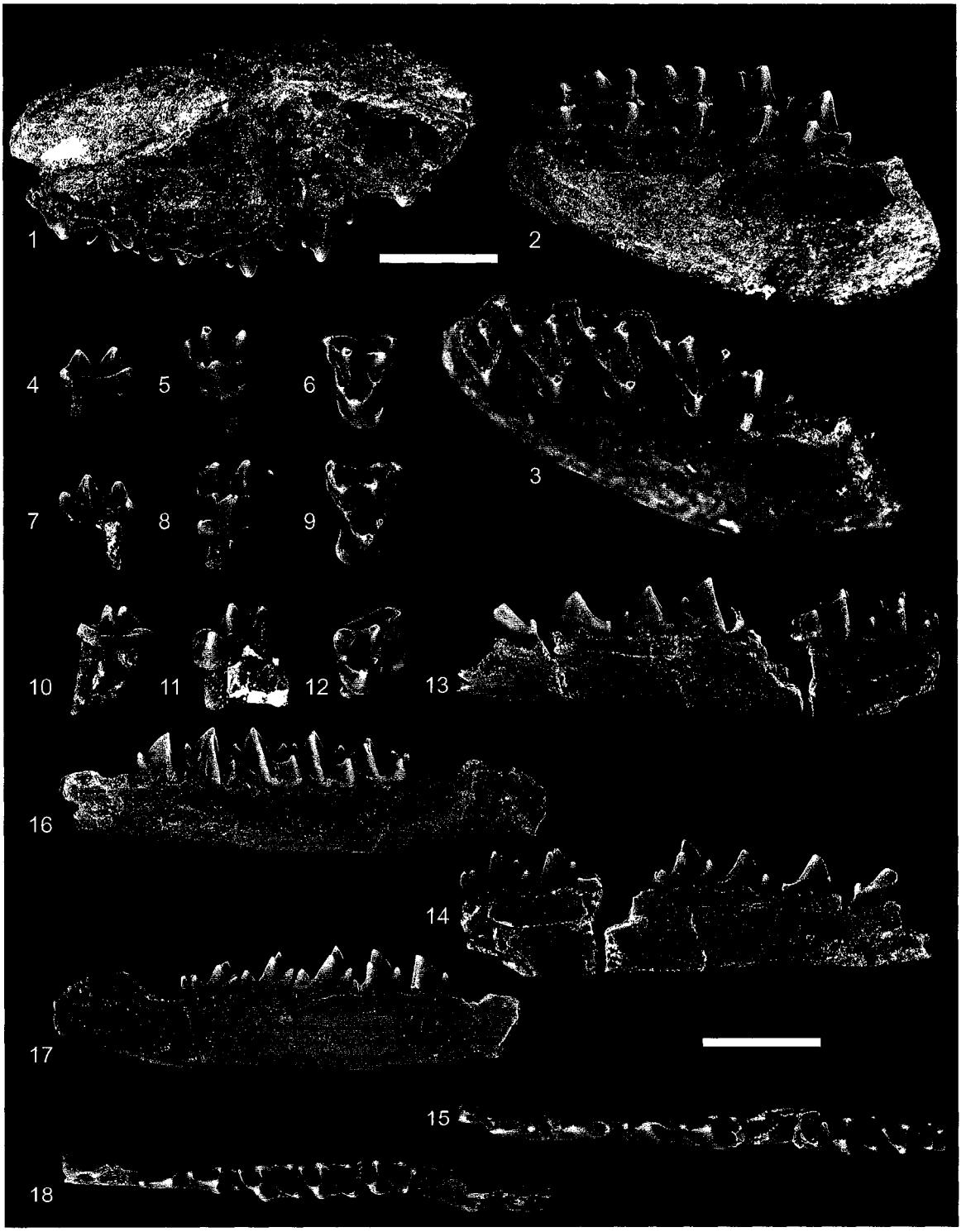
1
2
3
4
5
6
7
8
9
10
11
12
13
14
15
16
17
18

Figure 5.22.—1-12. "Leptacodon" munusculum from the early middle Tiffanian (Ti3) DW-2 locality, Paskapoo Formation, Alberta. 1-3, UALVP 47297 (DW2), incomplete right dentary with p2-4, m1-3 in 1, labial, 2, lingual, and 3, occlusal views; 4-6, UALVP 47307 (DW2), incomplete right dentary with canine root, p2, p4, and alveoli for p1, p3 in 4, labial, 5, lingual, and 6, occlusal views; 7-9, UALVP 47296, incomplete left dentary with p2-4, m1-3, and alveoli for c, p1 in 7, labial, 8, lingual, and 9, occlusal views; 10-12, UALVP 47313, incomplete left dentary with m2-3 in 10, labial, 11, lingual, and 12, occlusal views. Scale bars = 2 mm.

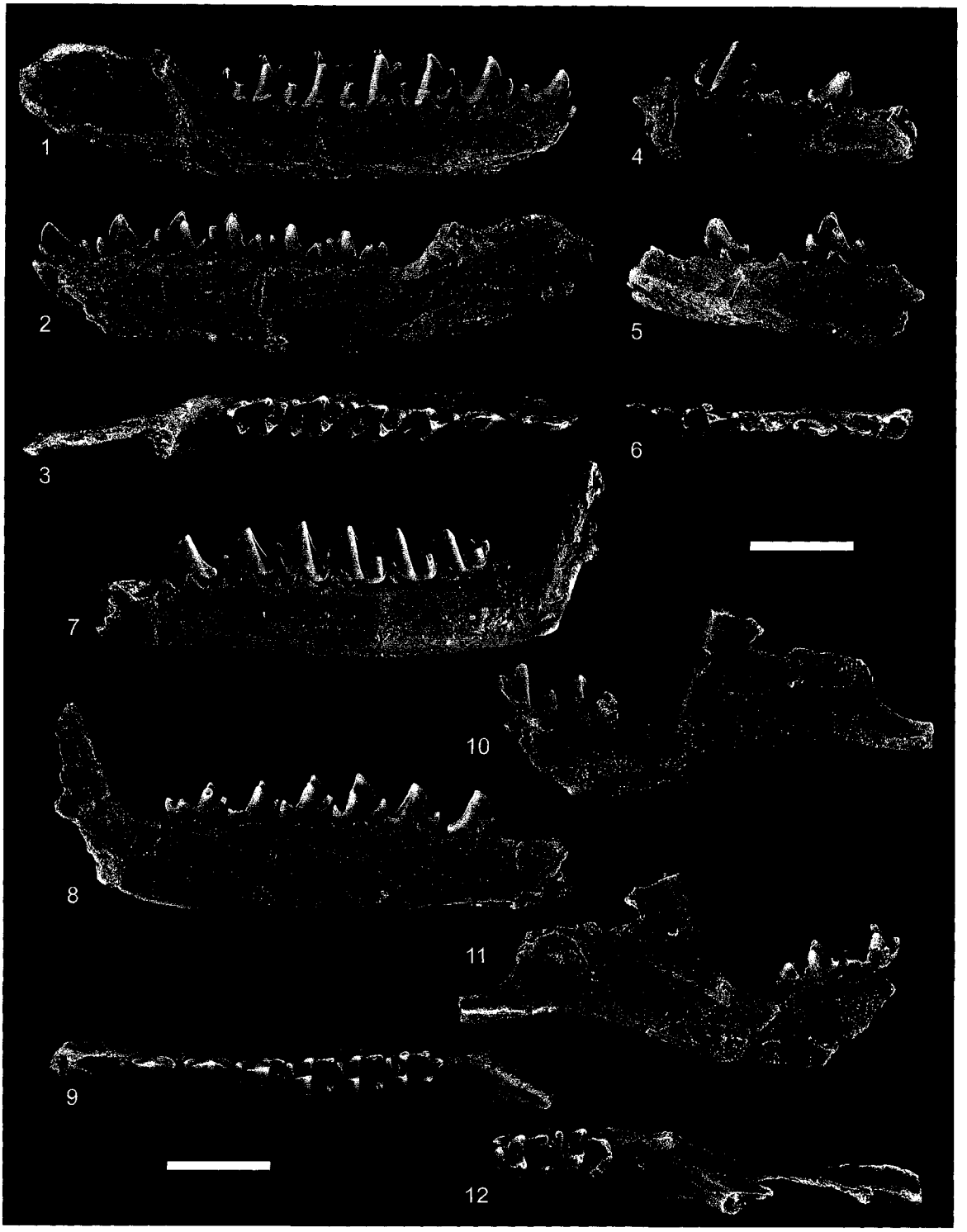
1
4
2
5
3
6
7
10
8
11
9
12

Figure 5.23.—1-19. Psydronyctia smithorum new genus and species from the early middle Tiffanian (Ti3) DW-1 (DW1) and DW-2 (DW2) localities, Paskapoo Formation, Alberta. 1-3, UALVP 47327 (DW2), incomplete right maxilla with P4, M1-2 in 1, labial, 2, oblique lingual, and 3, occlusal views; 4, UALVP 47326 (DW2), incomplete right maxilla with RP3-4 (broken), M1-3 in occlusal view; 5-10, UALVP 47328 (DW2), associated M1 and M2 in 5, 8, labial, 6, 9, oblique lingual, and 7, 10, occlusal views; 11-13, UALVP 47337 (DW2), incomplete right dentary with p1-3 and alveoli for ?i2-3, c in 11, labial, 12, lingual, and 13, occlusal views; 14-16, UALVP 43100 (holotype, DW2), incomplete right dentary with p3-4, m1-3, and alveoli for ?i2-3, c, p1-2 in 14, labial, 15, lingual, and 16, occlusal views; 17-19, UALVP 40508 (DW1), incomplete right dentary with p3-4, m1-3, and alveoli for c, p1-2 in 17, labial, 18, lingual, and 19, occlusal views. Scale bars = 2 mm.

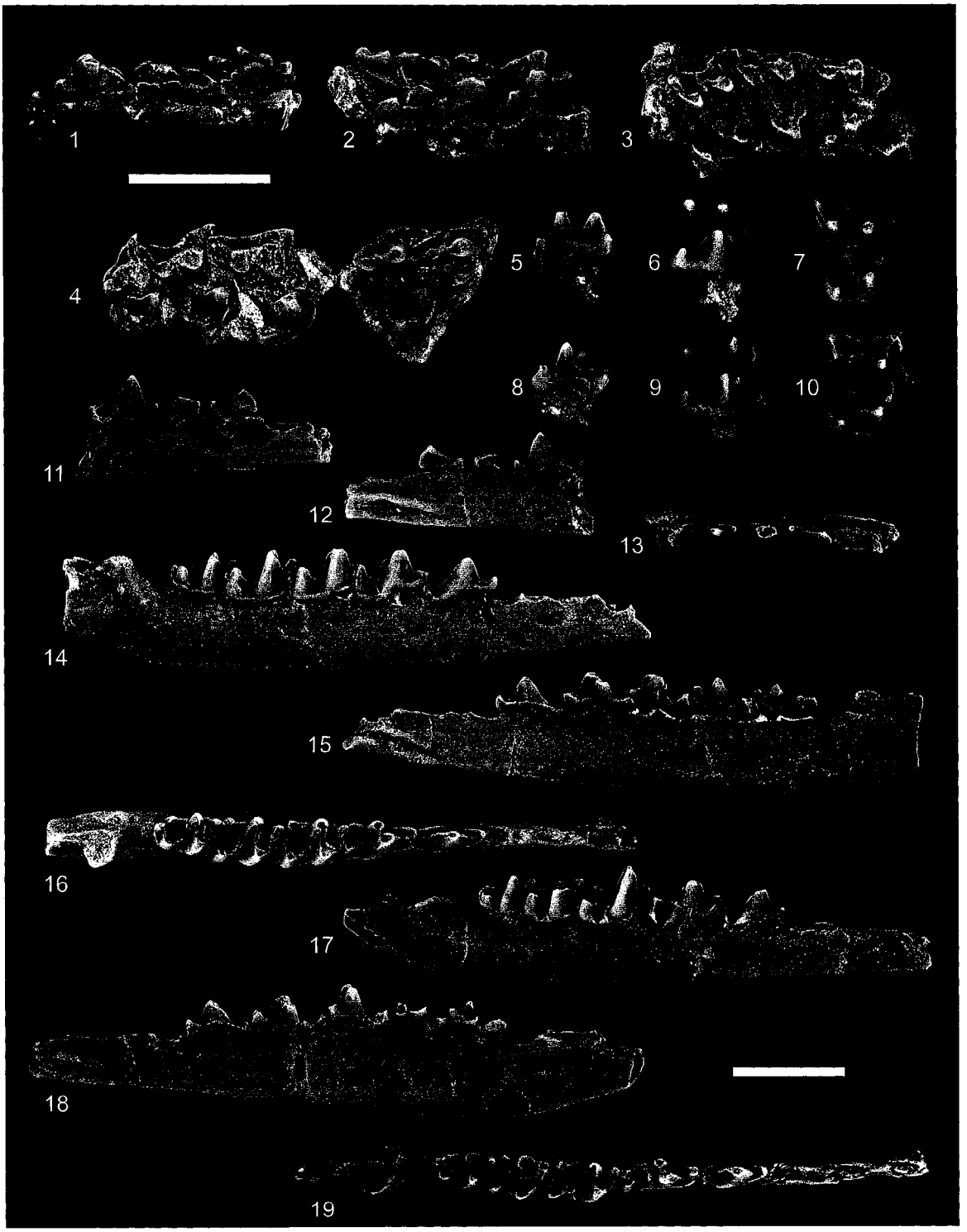
1
2
3
4
5
6
7
8
9
10
11
12
13
14
15
16
17
18
19

Figure 5.24.—1-18. Psydronyctia smithorum new genus and species from the early middle Tiffanian (Ti3) DW-2 (DW2) and Joffre Bridge Roadcut lower level (JBLL) localities, Paskapoo Formation, Alberta. 1-3, UALVP 47333 (DW2), incomplete left dentary with p3-4, m2-3, and alveoli for c, p1-2, and m1 in 1, labial, 2, lingual, and 3, occlusal views; 4-6, 40501 (JBLL), incomplete left dentary with p4, m1-2 (m2 trigonid only) in 4, labial, 5, lingual, and 6, occlusal views; 7-9, UALVP 47332 (DW2), incomplete right dentary with p2, p4, m1-3, and alveoli for p1 and p3 in 7, labial, 8, lingual, and 9, occlusal views; 10-12, UALVP 47349 (DW2), incomplete right dentary with m2 in 10, labial, 11, lingual, and 12, occlusal views; 13-15, 47340 (DW2), incomplete right dentary with p4, m1-2, and alveoli for m3 in 13, labial, 14, lingual, and 15, occlusal views; 16-18, UALVP 47348 (DW2), incomplete left dentary with m2 and alveoli for m3 in 16, labial, 17, lingual, and 18, occlusal views. Scale bars = 2 mm.

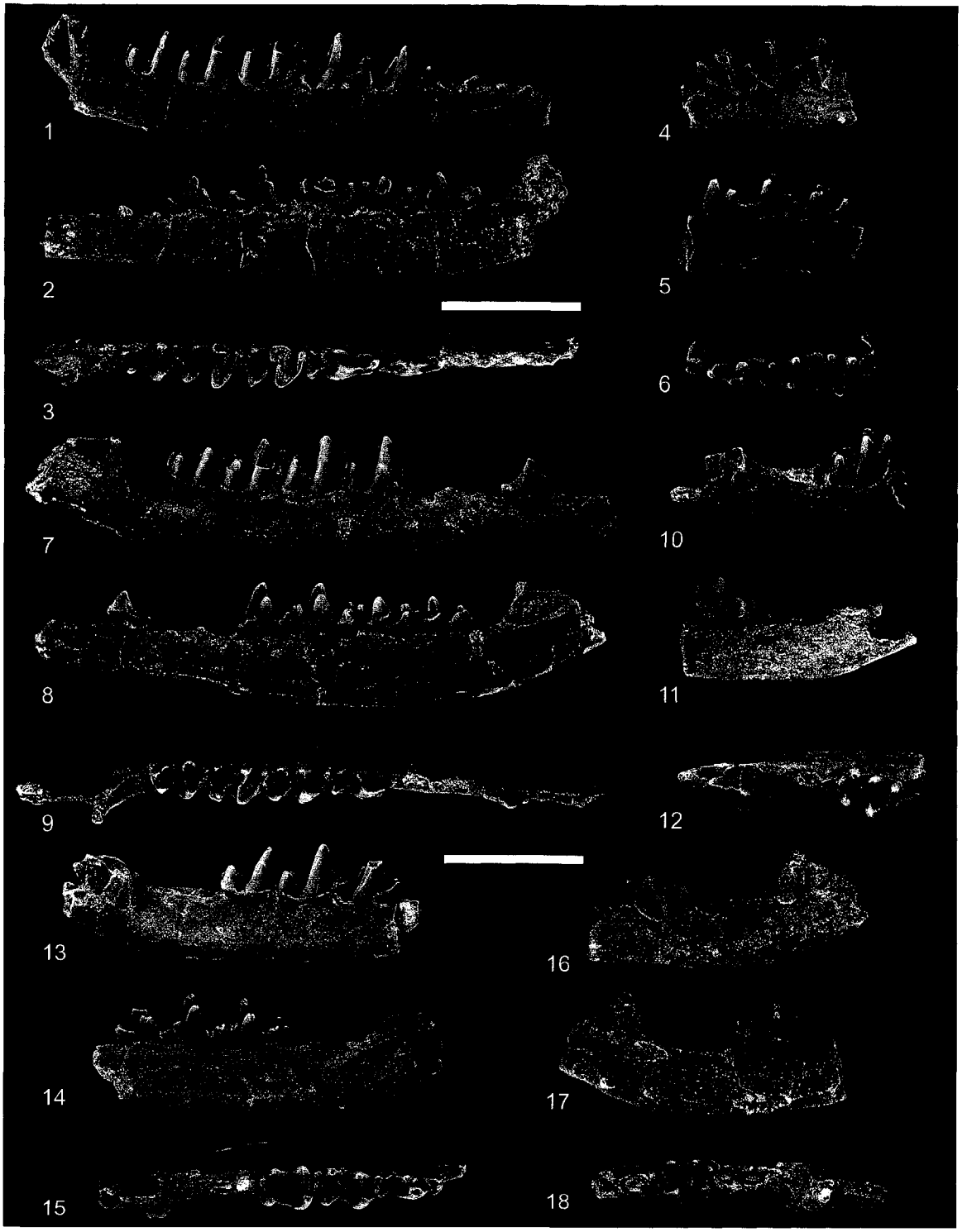
1
2
3
4
5
6
7
8
9
10
11
12
13
14
15
16
17
18

Figure 5.25.—1-18. Lipotyphla, genus and species indeterminate from the early middle Tiffanian (Ti3) DW-2 (DW2) and Birchwood (BW) localities, Paskapoo Formation, Alberta. 1-3, UALVP 47323 (DW2), incomplete right maxilla with P3-4, M1, and alveoli for P2 in 1, labial, 2, oblique lingual, and 3, occlusal views; 4-6, UALVP 47324 (DW2), incomplete left maxilla with M1 and alveoli for M2-3 in 4, labial, 5, oblique lingual, and 6, occlusal views; 7-21, UALVP 47322 (DW2), associated right P4, M1-3, and incomplete left maxilla with M2-3 (fragmentary left P3-4 not figured); right P4 in 7, labial, 8, oblique lingual, and 9, occlusal views; right M1 in 10, labial, 11, oblique lingual, and 12, occlusal views; right M2 in 13, labial, 14, oblique lingual, and 15, occlusal views; right M3 in 16, labial, 17, oblique lingual, and 18, occlusal views; incomplete left maxilla with M2-3 in 19, labial, 20, oblique lingual, and 21, occlusal views; 22-28, UALVP 47321 (DW2), incomplete left maxilla with M1-2 and associated incomplete left dentary with m1-3; incomplete left maxilla with M2-3 in 22, labial, 23, oblique lingual, 24, occlusal (M1), and 25, occlusal (M2) views; incomplete left dentary with m1-3 in 26, labial, 27, lingual, and 28, occlusal views; 29-31, UALVP 47325, incomplete right dentary with p1, p4, m1-3, and alveoli for c, p2-3 in 29, labial, 30, lingual, and 31, occlusal views. Scale bars = 2 mm.

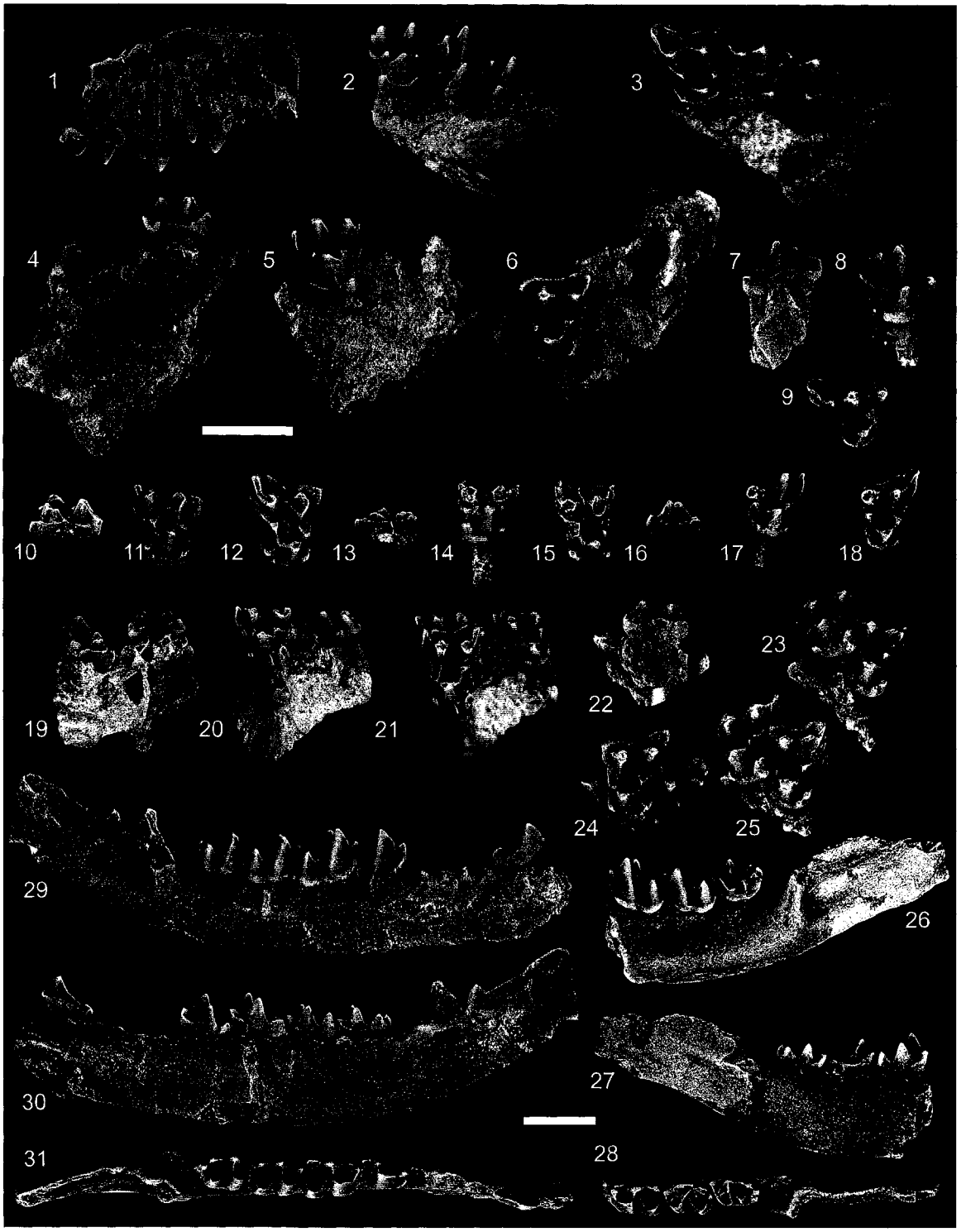
1
2
3
4
5
6
7
8
9
10
11
12
13
14
15
16
17
18
19
20
21
22
23
24
25
26
27
28
29
30
31

Figure 5.26.—1-23. Bessoecetor thomsoni Simpson from the early middle Tiffanian (Ti3) DW-2 (DW2) locality, Paskapoo Formation, Alberta. 1-3, UALVP 47368, incomplete right maxilla with P3-4 in 1, labial, 2, oblique lingual, and 3, occlusal views; 4-6, UALVP 47365, incomplete right maxilla with M1-2 in 4, labial, 5, oblique lingual, and 6, occlusal views; 7-9, UALVP 47362, incomplete left maxilla with P4, M1-3, (associated incomplete left dentary with p2-4, m1-2 not figured) in 7, labial, 8, oblique lingual, and 9, occlusal views; 10, 11, UALVP 47363, incomplete left maxilla with P4, M1-3, and alveoli for P2-3 in 10, labial, and 11, occlusal views; 12-14, UALVP 47372, right M1 in 12, labial, 13, oblique lingual, and 14, occlusal views; 15-17, UALVP 47378, right M2 in 15, labial, 16, oblique lingual, and 17, occlusal views; 18-20, UALVP 47382, incomplete right dentary with p2-4, m1-3, and alveoli for c, p1 in 18, labial, 19, lingual, and 20, occlusal views; 21-23, UALVP 47384, incomplete right dentary with c, p4, m1-3, and alveoli for p1-3 in 21, labial, 22, lingual, and 23, occlusal views. Scale bars = 2 mm.

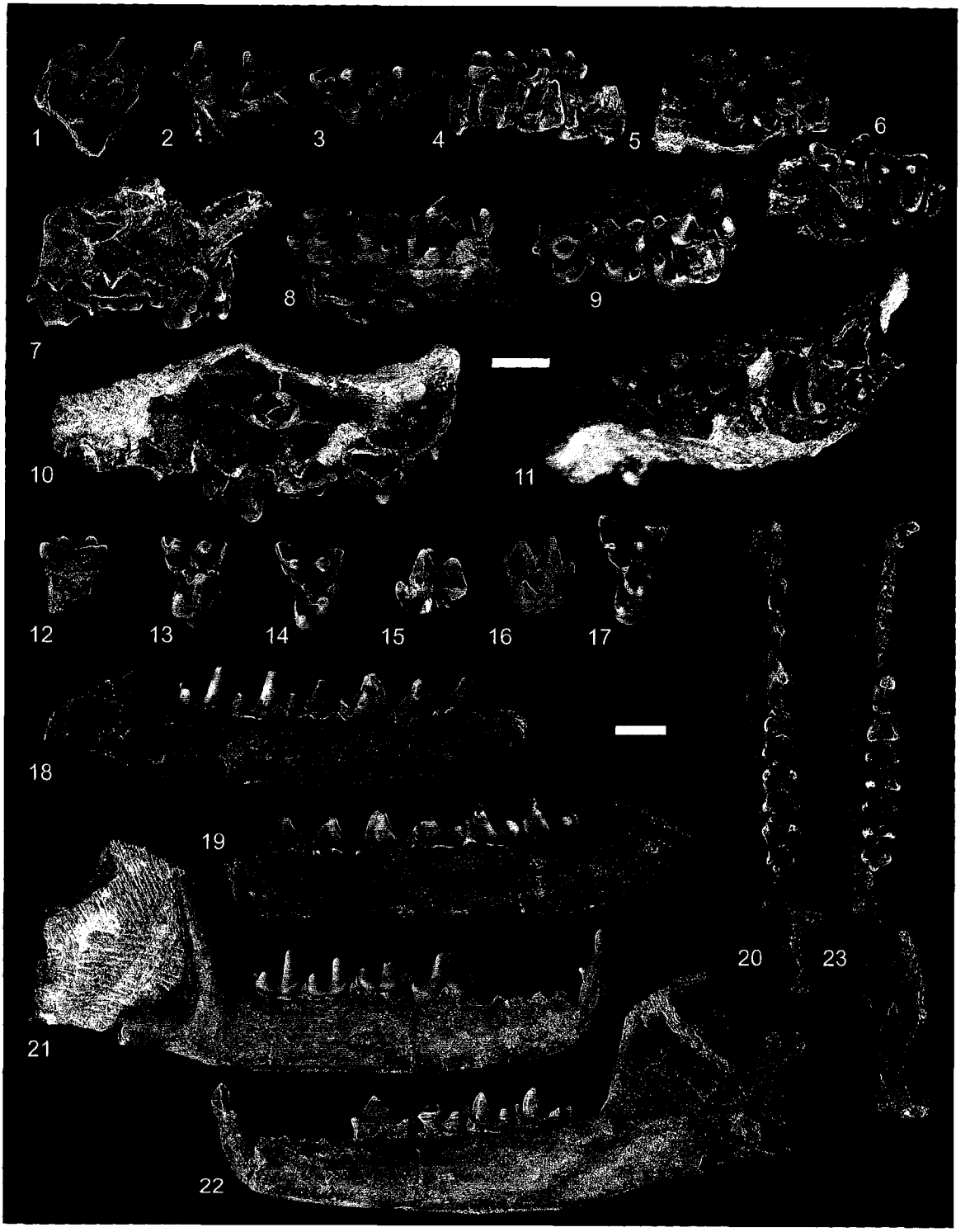
1
2
3
4
5
6
7
8
9
10
11
12
13
14
15
16
17
18
19
20
21
22
23

Figure 5.27.—1-18. Bessoecetor thomsoni Simpson from the early middle Tiffanian (Ti3) DW-2 (DW2) locality, Paskapoo Formation, Alberta. 1-3, UALVP 47386, incomplete right dentary with p4, m1-3 in 1, labial, 2, lingual, and 3, occlusal views; 4-6, UALVP 47390, incomplete left dentary with p2 (talonid only), p3-4, m2-3, and alveoli for c, p1, m1 in 4, labial, 5, lingual, and 6, occlusal views; 7-9, UALVP 47383, incomplete right dentary with p2-3, m1-3, and alveoli for c, p1, p4 in 7, labial, 8, lingual, and 9, occlusal views; 10-12, UALVP 47386, incomplete left dentary with p4, m1-3 in 10, labial, 11, lingual, and 12, occlusal views; 13-15, UALVP 47392, incomplete left dentary with m1-3 in 12, labial, 13, lingual, and 14, occlusal views; 16-18, UALVP 47408, incomplete right dentary with dp4, erupting p2-3, erupting m3, and alveoli for p1, m1-2 in 21, labial, 22, lingual, and 23, occlusal views. Scale bars = 2 mm.

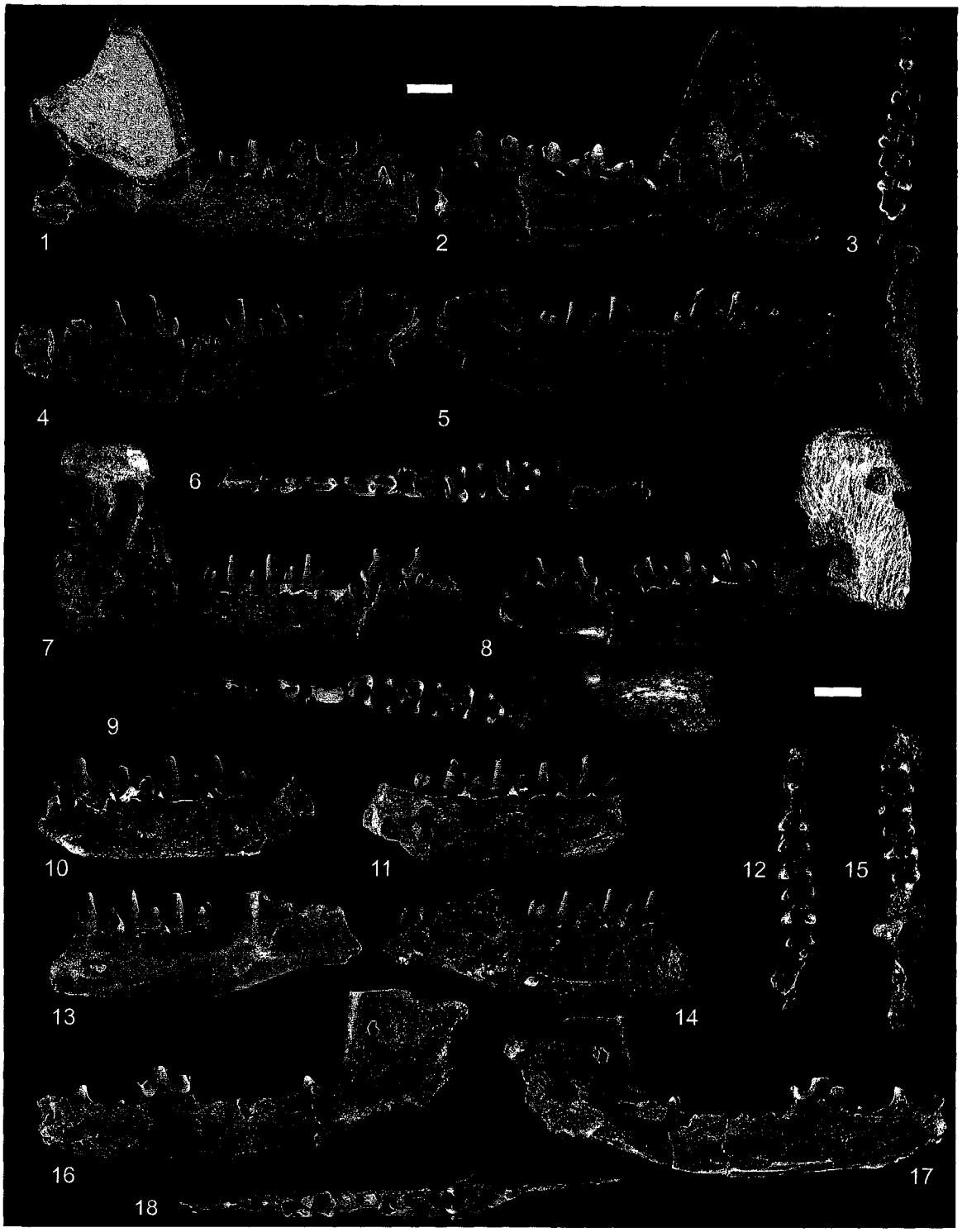
1
2
3
4
5
6
7
8
9
10
11
12
15
13
14
16
17
18

Figure 5.28.—1-26. Bessoecetor septentrionalis (Russell) from the early middle Tiffanian (Ti3) DW-2 locality, Paskapoo Formation, Alberta. 1-3, UALVP 47815 (DW2), incomplete right maxilla with P3-4, M1-2 in 1, labial, 2, oblique lingual, and 3, occlusal views; 4-8, UALVP 47420 (DW2), incomplete right maxilla with P4, M1-3 in 4, labial, 5, lingual, 6, occlusal, 7, medial, and 8, dorsal views; 9-11, UALVP 47427, right M1 in 9, labial, 10, lingual, and 11, occlusal views; 12-14, UALVP 47432 in 12, labial, 13, lingual, and 14, occlusal views; 15-17, UALVP 47816, incomplete right dentary with ?i2, p2 (talonid only), and alveoli for i3, c, p1, and anterior root of p2 in 15, labial, 16, lingual, and 17, occlusal views; 18-20, UALVP 47444, incomplete left dentary with p3-4 and alveoli for c, p1-2 in 18, labial, 19, lingual, and 20, occlusal views; 21-23, UALVP 47443, incomplete right dentary with p3-4 and alveoli for c, p1-2 in 21, labial, 22, lingual, and 23, occlusal views; 24-26, UALVP 47441, incomplete right dentary with p3-4, m1, and alveoli for c, p1-2 in 24, labial, 25, lingual, and 26, occlusal views. Scale bars = 2 mm.

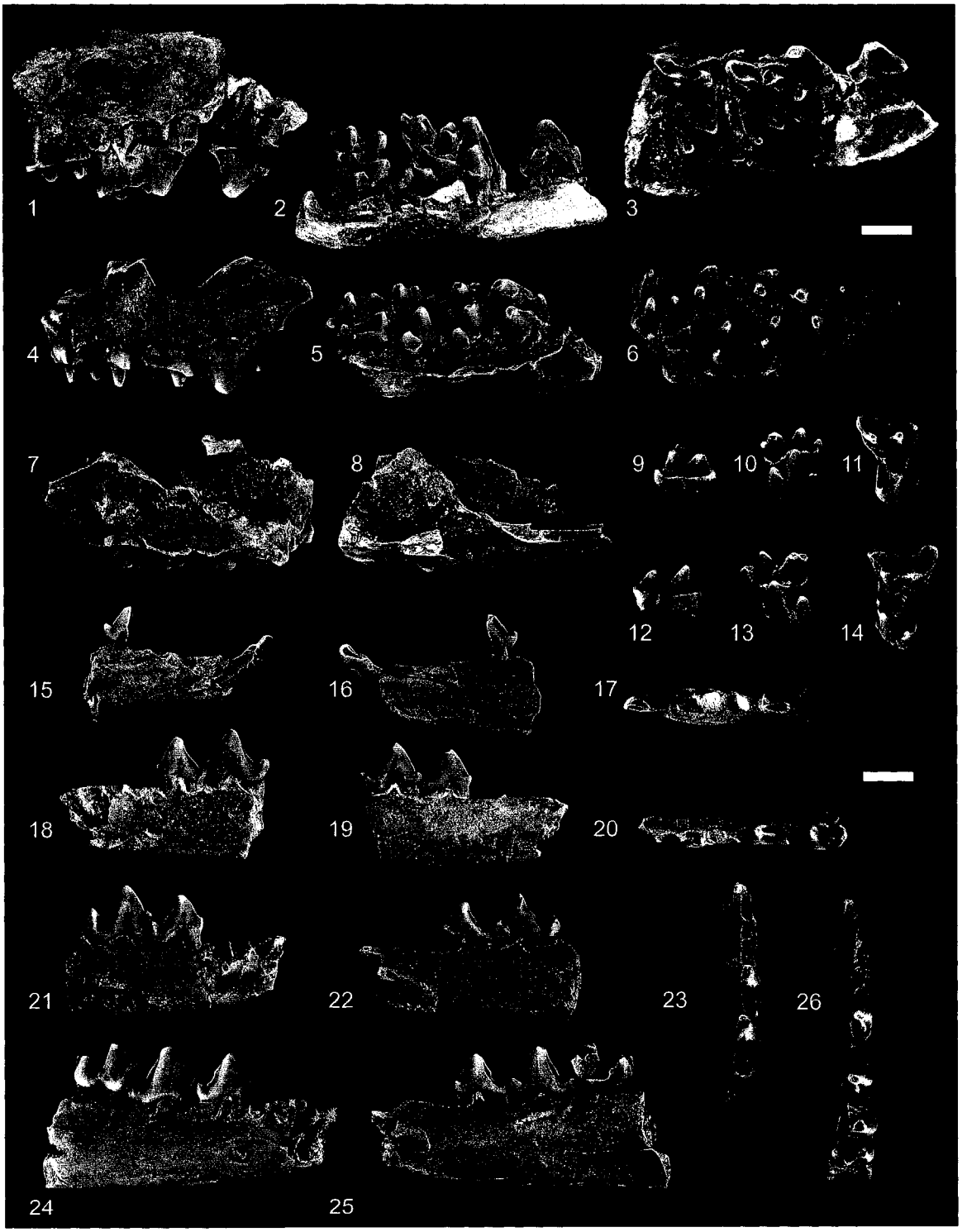
1
2
3
4
5
6
7
8
9
10
11
12
13
14
15
16
17
18
19
20
21
22
23
26
24
25

Figure 5.29.—1-18. Bessoecetor septentrionalis (Russell) from the early middle Tiffanian (Ti3) DW-2 locality, Paskapoo Formation, Alberta. 1-3, UALVP 47438, incomplete left dentary with p4, m1-3 in 1, labial, 2, lingual, and 3, occlusal views; 4-6, UALVP 47436, incomplete right dentary with p2-4, m1-3, and alveoli for c, p1 (associated incomplete left dentary with p3, m2-3, and alveoli for p2, p4, m1, not figured) in 4, labial, 5, lingual, and 6, occlusal views; 7-12, UALVP 47437, incomplete right dentary with p3 (talonid only), p4, m1-3, and alveoli for p2 and associated incomplete left dentary with m1-3 in 7, 10, labial, 8, 11, lingual, and 9, 12, occlusal views; 13-15, UALVP 47449, incomplete right dentary with m2-3 in 12, labial, 13, lingual, and 14, occlusal views.

?Bessoecetor sp. 16-18, UALVP 47817, right m1 in 16, labial, 17, lingual, and 18, occlusal views.

Scale bars = 2 mm.

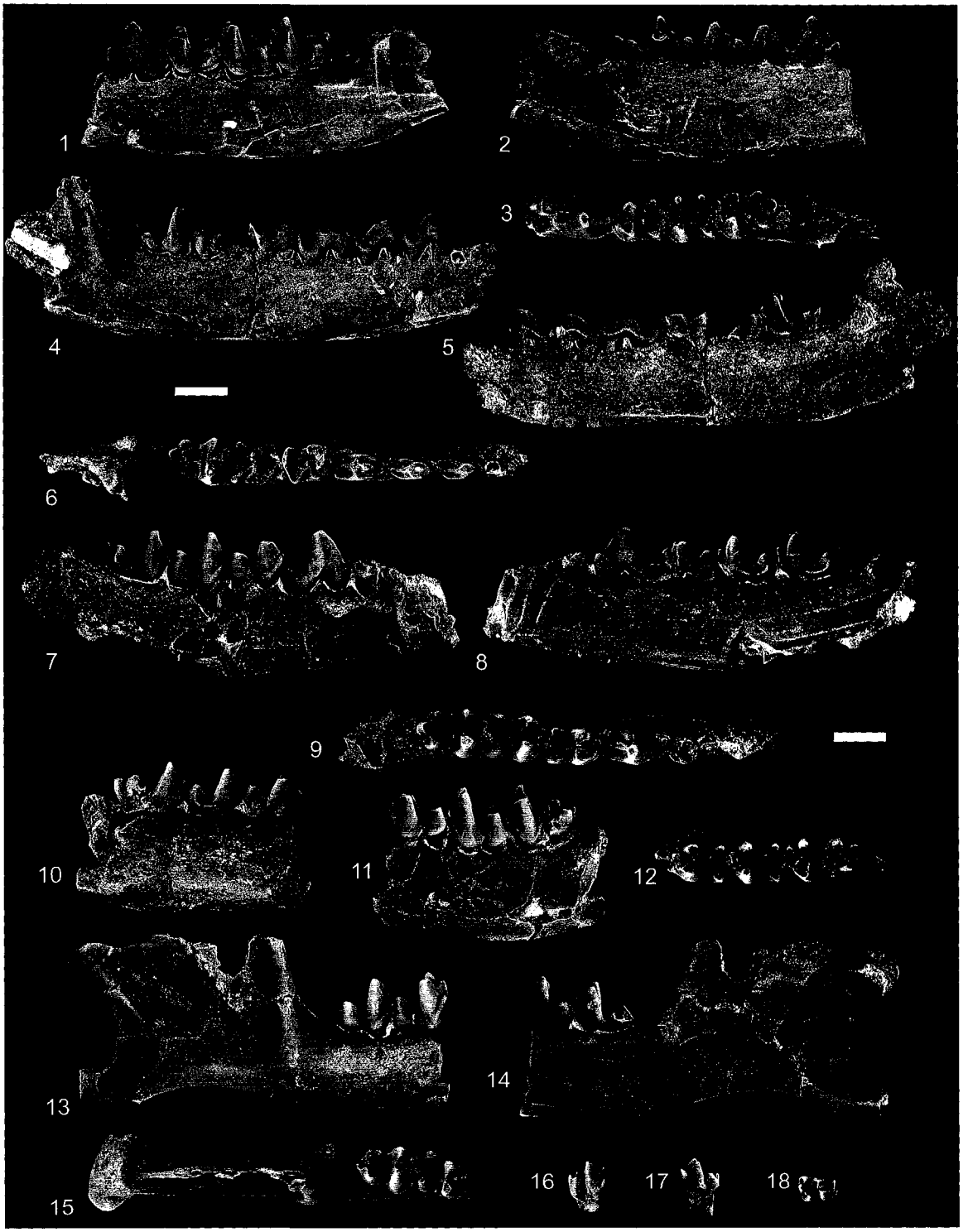
1
2
3
4
5
6
7
8
9
10
11
12
13
14
15
16
17
18

Figure 5.30.—Bisonalveus toxidens new species from the early middle Tiffanian (Ti3) DW-2 locality, Paskapoo Formation, Alberta. 1, UALVP 43114 (holotype), incomplete skull and lower jaws (anterior to right); left upper dentition shown in lingual view. Scale bar = 5 mm.


mx
pmx
C
?I3

Figure 5.31.—1-26. Bisonalveus toxidens new species from the early middle Tiffanian (Ti3) DW-2 (DW2) and Birchwood (BW) localities, Paskapoo Formation, Alberta. 1, 2, UALVP 47820 (DW2), right I3 in 1, anterior and 2, posterior views; 3, 4, UALVP 47677 (BW), right upper canine in 3, anterior and 4, posterior views; 5, 6, UALVP 47472 (DW2), right upper canine in 5, anterior and 6, posterior views; 7, 8, UALVP 43115 (DW2), left upper canine in 7, anterior and 8, posterior views; 9-11, UALVP 47462 (DW2), incomplete right maxilla with P3-4, M1-3, and alveoli for C, P1-2 in 9, labial, 10, oblique lingual, and 11, occlusal views; 12-14, UALVP 47463 (DW2), incomplete left maxilla with P3-4, M1-3 in 12, labial, 13, oblique lingual, and 14, occlusal views; 15-17, UALVP 47467 (DW2), incomplete left maxilla with M1-3 in 15, labial, 16, oblique lingual, and 17, occlusal views; 18-20, UALVP 47461, incomplete left maxilla with P4, M1-3 (associated incomplete right dentary with p3-4, m1, and alveoli for c, p1-2 not figured) in 18, labial, 19, oblique lingual, and 20, occlusal views; 21-23, UALVP 47479 (DW2), left M1 in 21, labial, 22, oblique lingual, and 23, occlusal views; 24-26, UALVP 47484 (DW2), left M2 in 24, labial, 25, oblique lingual, and 26, occlusal views. Scale bars = 2 mm.

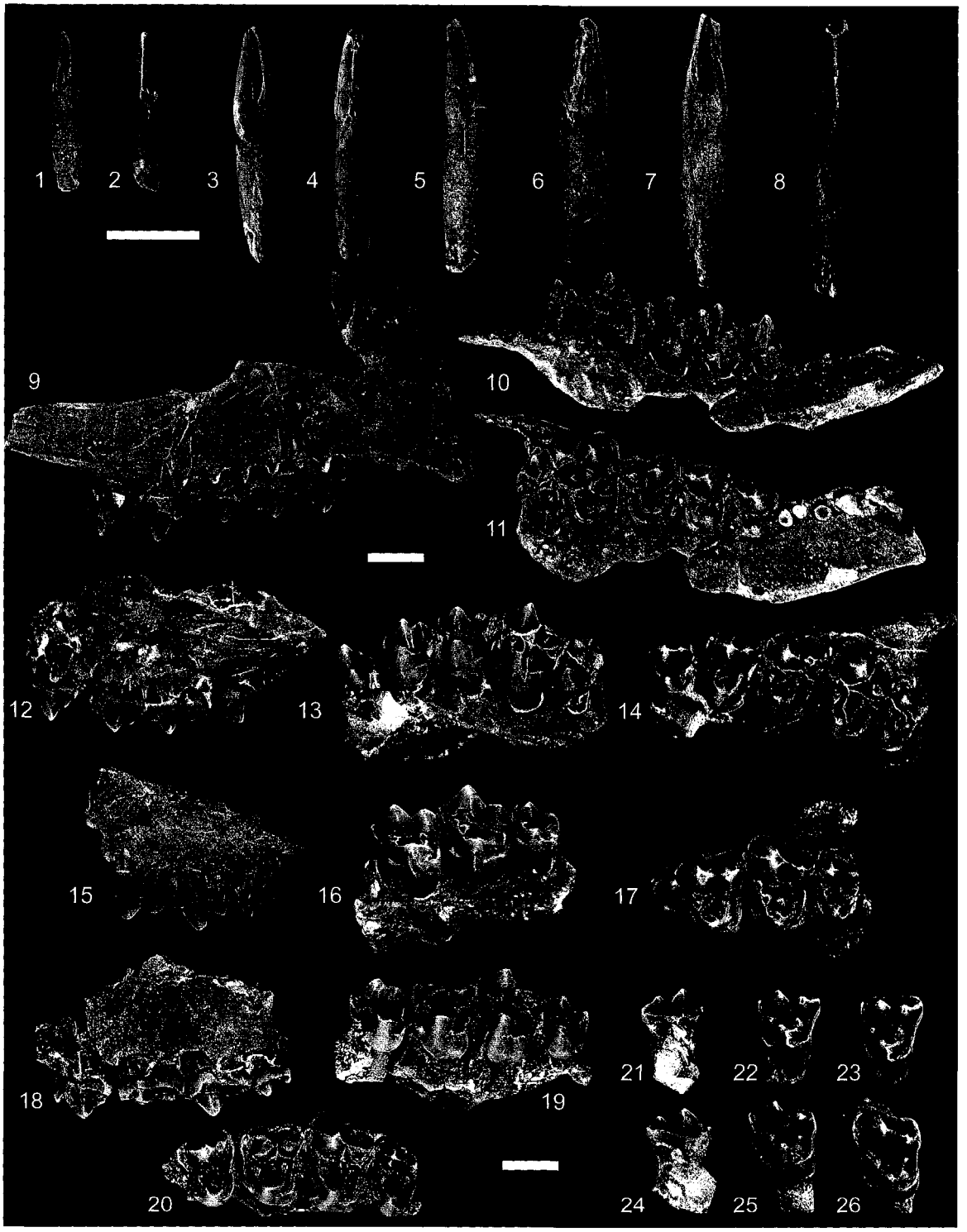
1
2
3
4
5
6
7
8
9
10
11
12
13
14
15
16
17
18
19
20
21
22
23
24
25
26

Figure 5.32.—1-19. Bisonalveus toxidens new species from the early middle Tiffanian (Ti3) DW-2 locality, Paskapoo Formation, Alberta. 1-4, UALVP 47502, incomplete right dentary with c, p1-4, m1-3, and alveoli for i1-3 in 1, anterior, 2, labial, 3, lingual, and 4, occlusal views; 5-7, UALVP 47503, incomplete right dentary with c, p1-4, m1-3, and alveoli for i1-3 in 5, labial, 6, lingual, and 7, occlusal views; 8-10, UALVP 47521, incomplete left dentary with p2-4, and alveoli for i1-3, p1 in 8, labial, 9, lingual, and 10, occlusal views; 11-13, UALVP 40560, incomplete left dentary with p3-4, m1-3, and alveoli for c, p1-2 in 11, labial, 12, lingual, and 13, occlusal views; 14-16, UALVP 47506, incomplete left dentary with p3-4, m1-3, and alveoli for p1-2 in 14, labial, 15, lingual, and 16, occlusal views; 17-19, UALVP 47510, incomplete left dentary with p3-4, m1, and alveoli for c, p1-2 in 17, labial, 18, lingual, and 19, occlusal views. Scale bars = 2 mm.

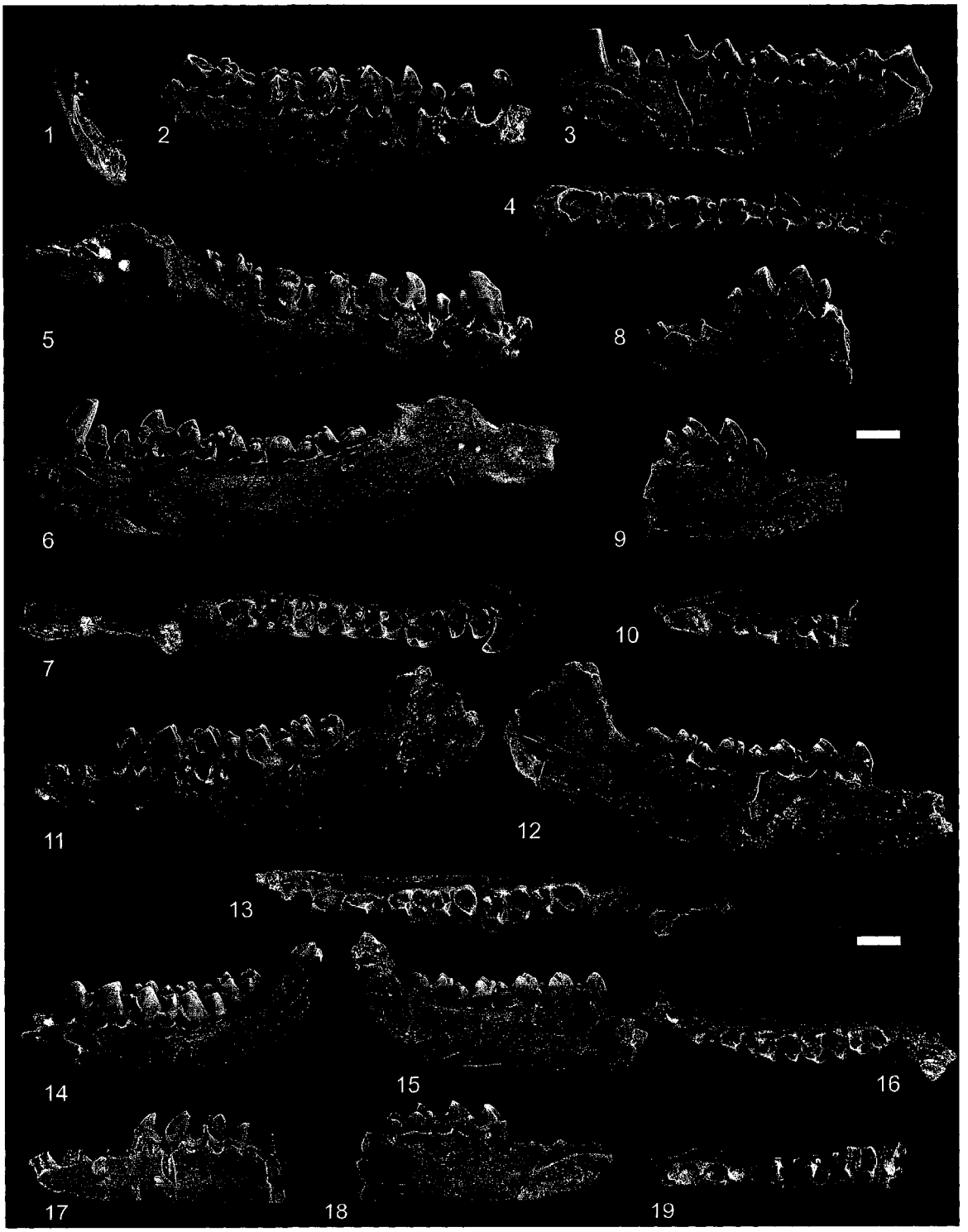
1
2
3
4
5
8
6
9
7
10
11
12
13
14
15
16
17
18
19

Figure 5.33.—1-15. Bisonalveus toxidens new species from the early middle Tiffanian (Ti3) DW-2 locality, Paskapoo Formation, Alberta. 1-3, UALVP 47514, incomplete right dentary with p4, m1-3 in 1, labial, 2, lingual, and 3, occlusal views; 4-6, UALVP 47536, incomplete right dentary with m2-3 in 4, labial, 5, lingual, and 6, occlusal views; 7-9, UALVP 47511, incomplete left dentary with p4, m1-3, and alveoli for p1-3 in 7, labial, 8, lingual, and 9, occlusal views; 10-12, UALVP 47538, incomplete right dentary with m2-3 in 10, labial, 11, lingual, and 12, occlusal views. Scale bars = 2 mm.

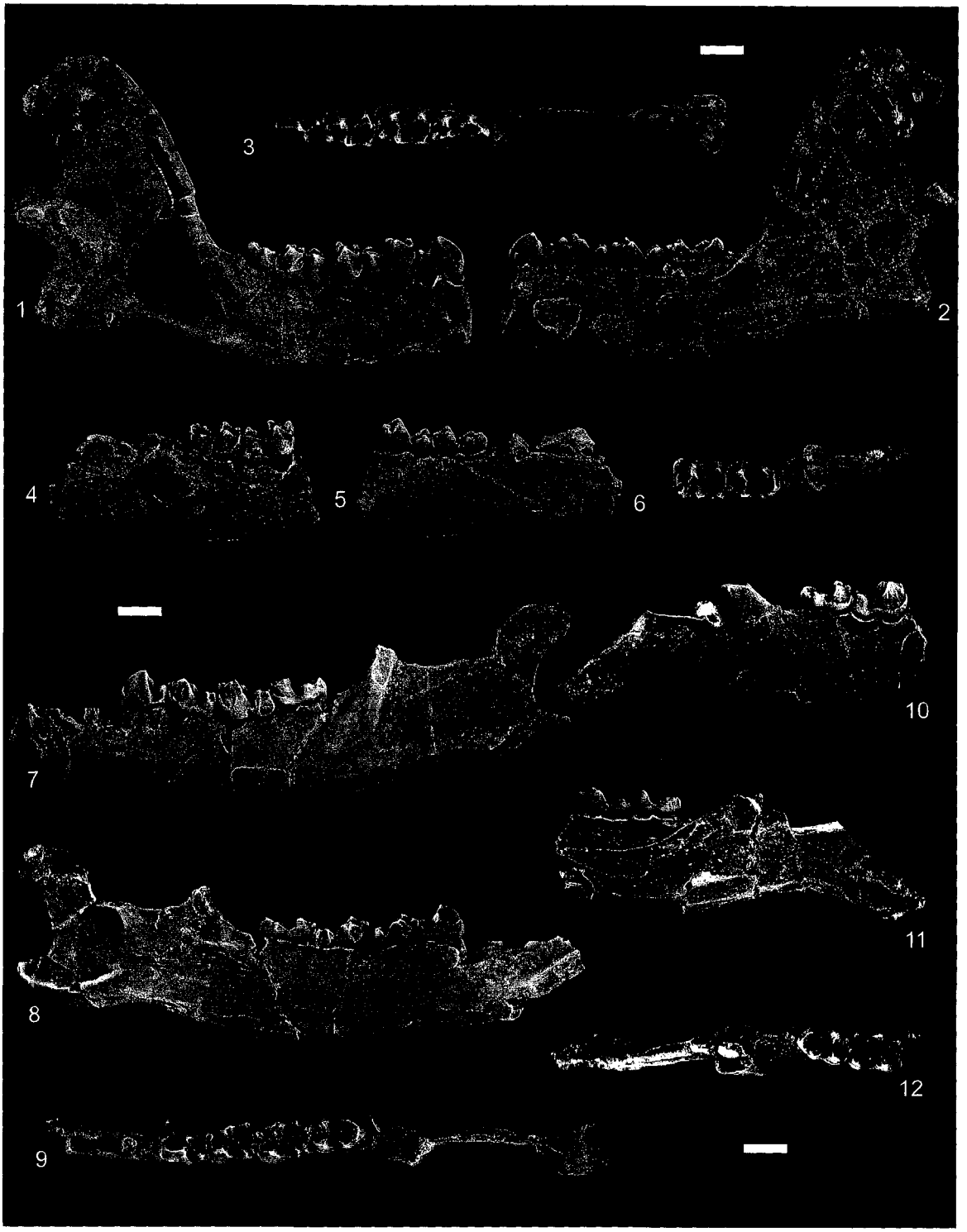
1
2
3
4
5
6
7
8
9
10
11
12

Figure 5.34.—1-6. Bisonalveus toxidens new species from the early middle Tiffanian (Ti3) DW-2 locality, Paskapoo Formation, Alberta. 1-3, UALVP 40535, incomplete left dentary with dp3-4, m1-2, erupting m3, and alveoli for c, p1-2 in 1, labial, 2, lingual, and 3, occlusal views; 4-6, UALVP 47525, incomplete left dentary with dp3, erupting p4, m1, and alveoli for c, p1-2, m2-3 in 4, labial, 5, lingual, and 6, occlusal views.

7-12. Paleotomus senior (Simpson) from the early middle Tiffanian (Ti3) DW-2 locality, Paskapoo Formation, Alberta. 7-9, UALVP 47692, left P4 in 7, labial, 8, oblique lingual, and 9, occlusal views; 10-12, UALVP 47693, left m2 in 10, labial, 11, lingual, and 12, occlusal views.

13-21. Paleotomus junior Scott, Fox, and Youzwyshyn from the early middle Tiffanian (Ti3) DW-2 locality, Paskapoo Formation, Alberta. 13-15, UALVP 47694, left P4 in 13, labial, 14, oblique lingual, and 15, occlusal views; 16-18, UALVP 47695, incomplete right dentary with p3-4, m1-2, and alveoli for ?i3, c, p1-2, m3 in 16, labial, 17, lingual, and 18, occlusal views; 19-21, UALVP 47696, incomplete right dentary with p2-4 and alveoli for c, p1 in 19, labial, 20, lingual, and 21, occlusal views.

Scale bars = 2 mm.

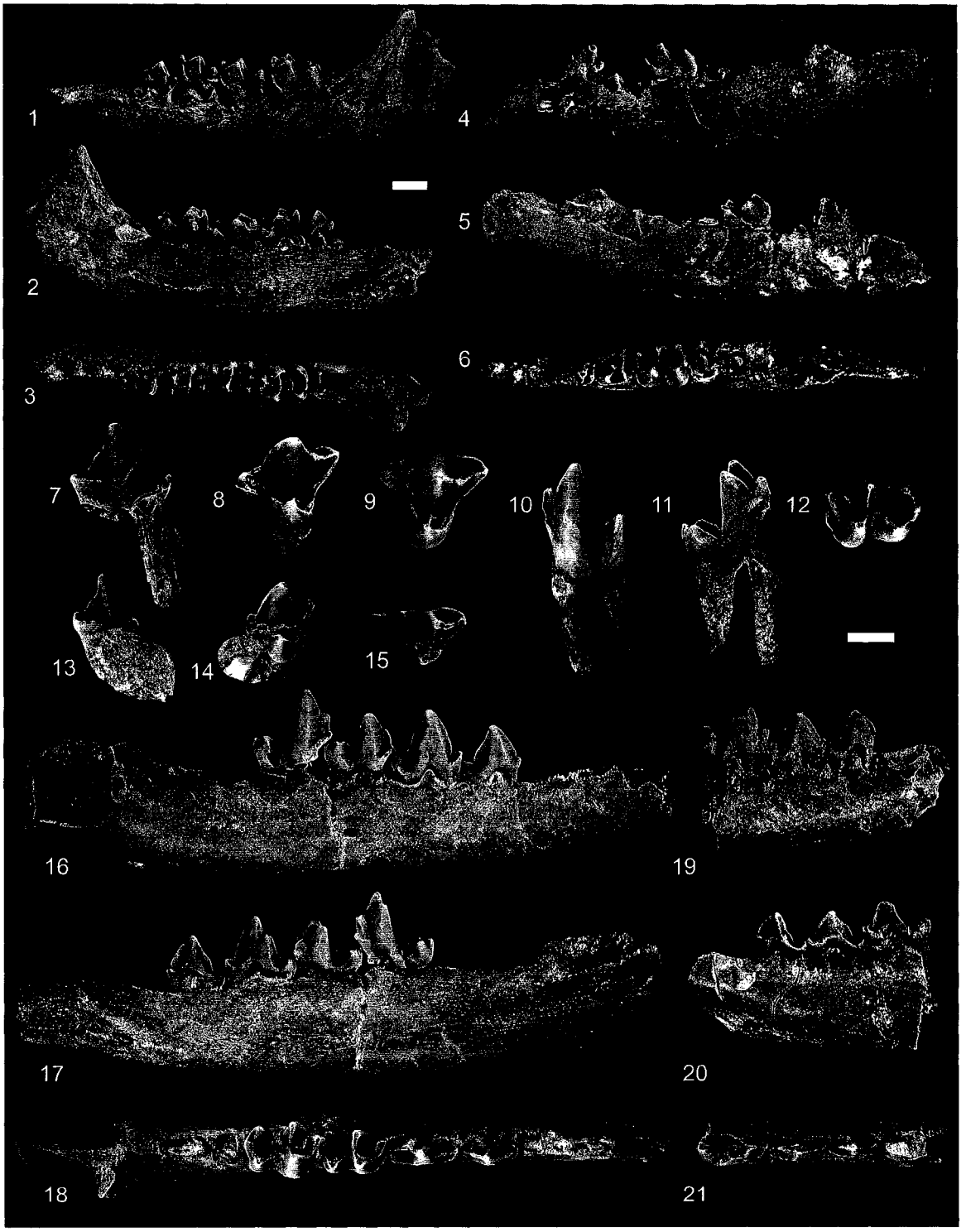
1
4
2
5
3
6
7
8
9
10
11
12
13
14
15
16
19
17
20
18
21

Figure 5.35.—1-25. Unuchinia dysmathes Holtzman from the early middle Tiffanian (Ti3) DW-2 (DW2) and Joffre Bridge Roadcut lower level (JBLL) localities. 1-5, UALVP 47818, incomplete right premaxilla with I1 and alveolus for I2, associated incomplete right maxilla with P3-4, M1-3, and alveoli for P2, and associated incomplete left maxilla with P2-3; incomplete right premaxilla and maxilla in 1, labial and 2, occlusal views; incomplete left maxilla in 3, labial, 4, lingual, and 5, occlusal views; 6, 7, UALVP 47706, left I1 in 6, lateral and 7, medial views; 8, 9, UALVP 47707, left I1 in 8, lateral and 9, medial views; 10-12, UALVP 47712, left I2 in 10, lateral, 11, medial, and 12, occlusal views; 13-15, UALVP 47713, left I2 in 13, lateral, 14, medial, and 15, occlusal views; 16-18, UALVP 47716, right P2 in 16, labial, 17, lingual, and 18, occlusal views; 19-21, UALVP 47718, right M1 in 19, labial, 20, lingual, and 21, occlusal views; 22-24, UALVP 47699 (JBLL), left M2 in 22, labial, 23, lingual, and 24, occlusal views. Scale bars = 2 mm.

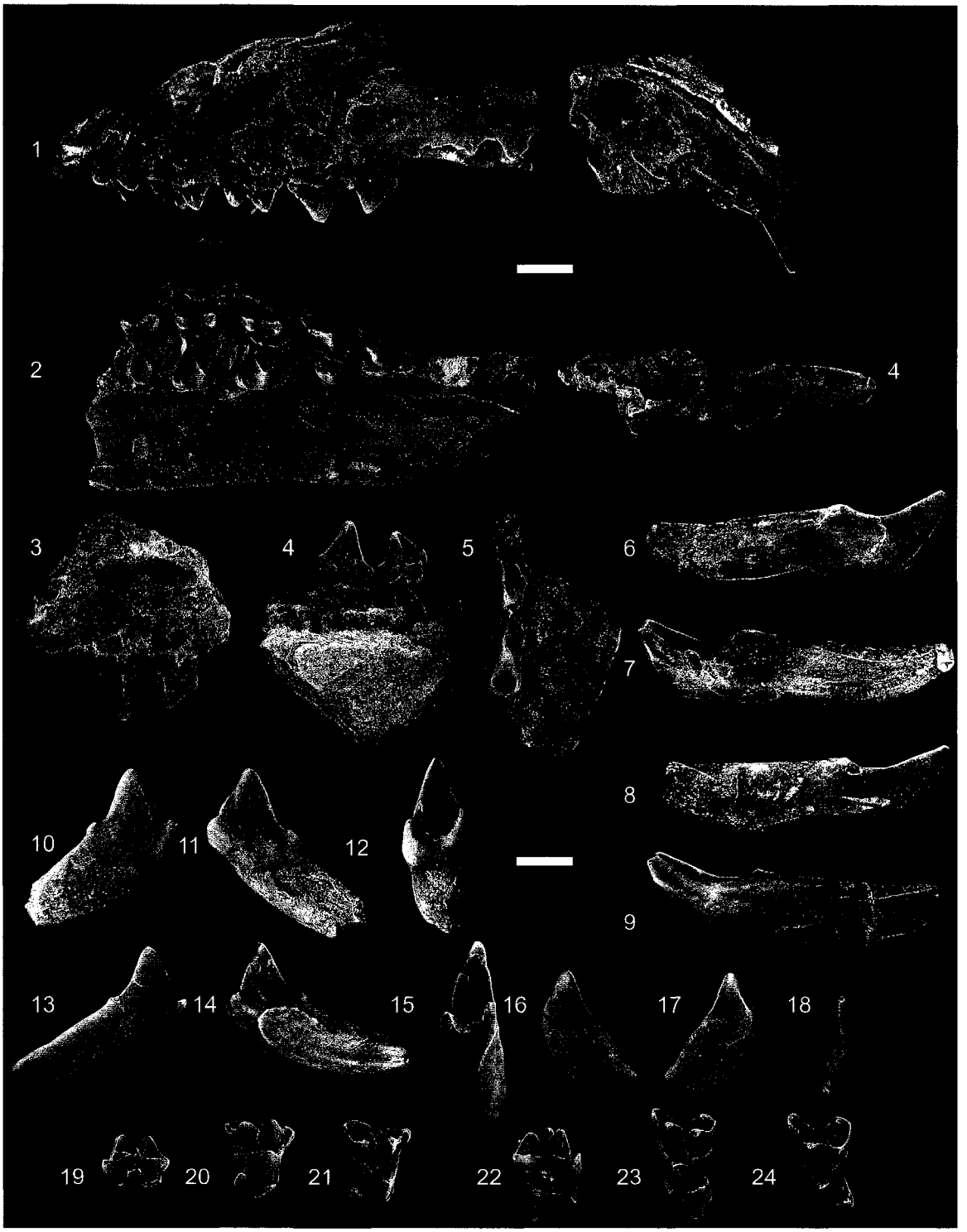
1
2
4
3
4
5
6
7
10
11
12
8
9
13
14
15
16
17
18
19
20
21
22
23
24

Figure 5.36.—1-21. Unuchinia dysmathes Holtzman from the early middle Tiffanian (Ti3) DW-1 (DW1), DW-2 (DW2), and Birchwood (BW) localities, Paskapoo Formation, Alberta. 1-3, UALVP 47722 (DW2), incomplete left dentary with i1-2 in 1, lateral, 2, medial, and 3, occlusal views; 4-6, UALVP 47702 (DW1), right i1 in 4, lateral, 5, medial, and 6, occlusal views; 7-9, UALVP 47726 (DW2), right i2 in 7, lateral, 8, medial, and 9, occlusal views; 10-12, UALVP 47727 (DW2), right p2 in 10, labial, 11, lingual, and 12, occlusal views; 13-15, UALVP 47727 (DW2), right p2 in 13, labial, 14, lingual, and 15, occlusal views; 16-18, UALVP 39495 (BW), right p2 in 16, labial, 17, lingual, and 18, occlusal views; 19-21, UALVP 47721, incomplete right dentary with p4, m1-2, and associated i1-2, m3 in 19, labial, 20, lingual, and 21, occlusal views. Scale bars = 2 mm.

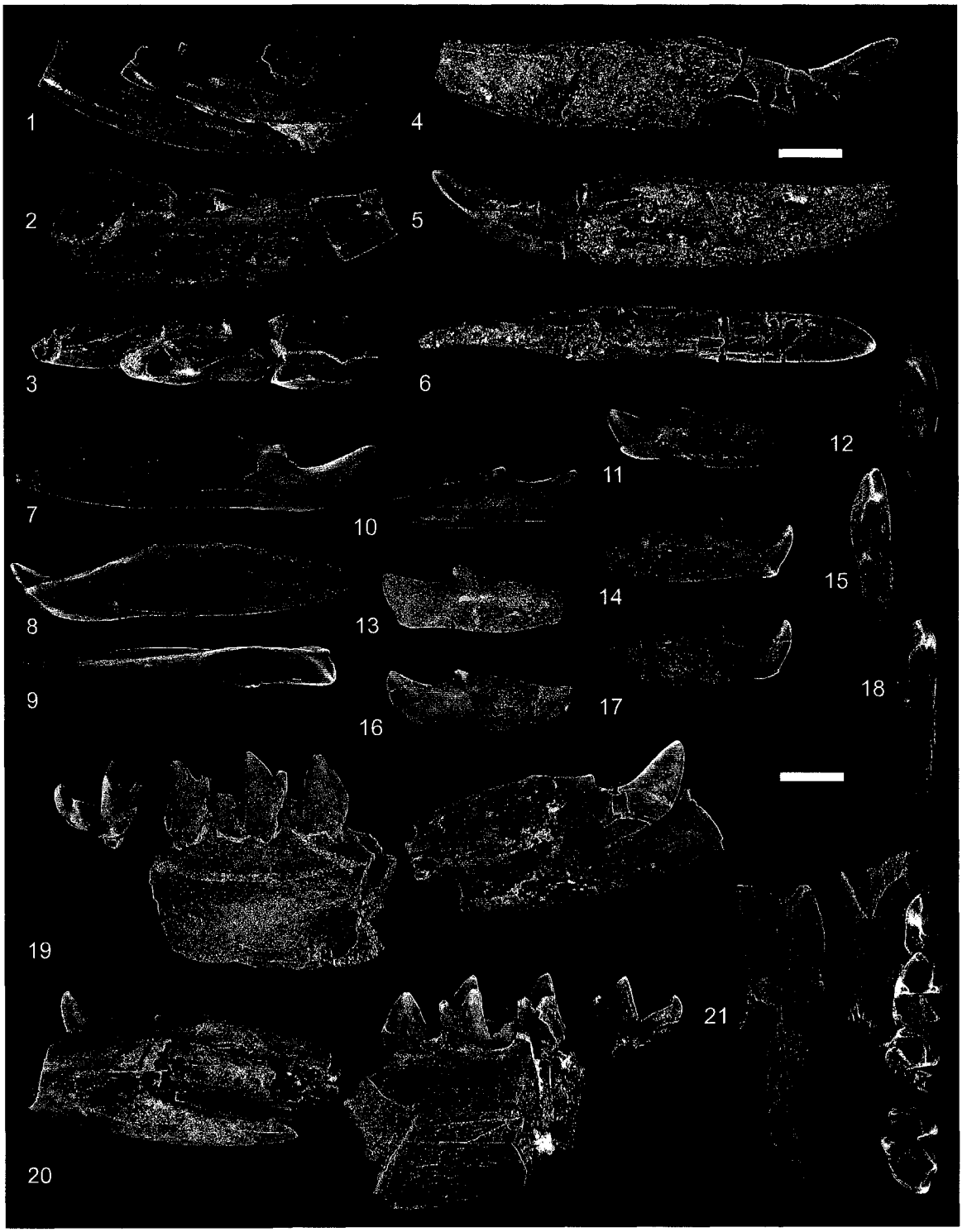
1
2
3
4
5
6
7
8
9
10
11
12
13
14
15
16
17
18
19
20
21

Figure 5.37.—1-12. Unuchinia dysmathes Holtzman from the early middle Tiffanian (Ti3) DW-2 locality, Paskapoo Formation, Alberta. 1-3, UALVP 47720, incomplete right dentary with p4 (talonid only), m1-3, and alveoli for p2-3 in 1, labial, 2, lingual, and 3, occlusal views; 4-6, UALVP 47819, incomplete left dentary with p2, p4, m1, and alveoli for i1-2, p3, m2-3 in 4, labial, 5, lingual, and 6, occlusal views; 7-9, UALVP 47729, left m1 in 7, labial, 8, lingual, and 9, occlusal views; 10-12, UALVP 47732, left m2 in 10, labial, 11, lingual, and 12, occlusal views. Scale bars = 2 mm.


1
2
3
4
5
6
7
8
9
10
11
12

Figure 5.38.—1-3. ?Gelastops sp. from the early middle Tiffanian (Ti3) DW-2 locality, Paskapoo Formation, Alberta. 1-3, UALVP 47800, left M1 in 1, labial, 2, lingual, and 3, occlusal views.

4-8. Pararyctes pattersoni Van Valen from the early middle Tiffanian (Ti3) DW-2 locality, Paskapoo Formation, Alberta. 4-8, UALVP 40952, incomplete skull having right lateral incisor, right upper canine, right P1-4, M1-3, left P1, P3-4, M1-3, and alveoli for left medial and lateral incisors, C, P2, and associated incomplete right dentary with medial incisor root, lateral incisor (base of crown), c, p1-4, m1-3 (associated postcranial bones not figured); skull in 4, dorsal view; skull and right dentary in 5, right lateral view; skull and right dentary in 6, left lateral view (skull), medial view (dentary); skull and right dentary in 7, palatal (skull) and occlusal (dentary) views; right dentary in 8, posterior view. Scale bars = 2 mm.

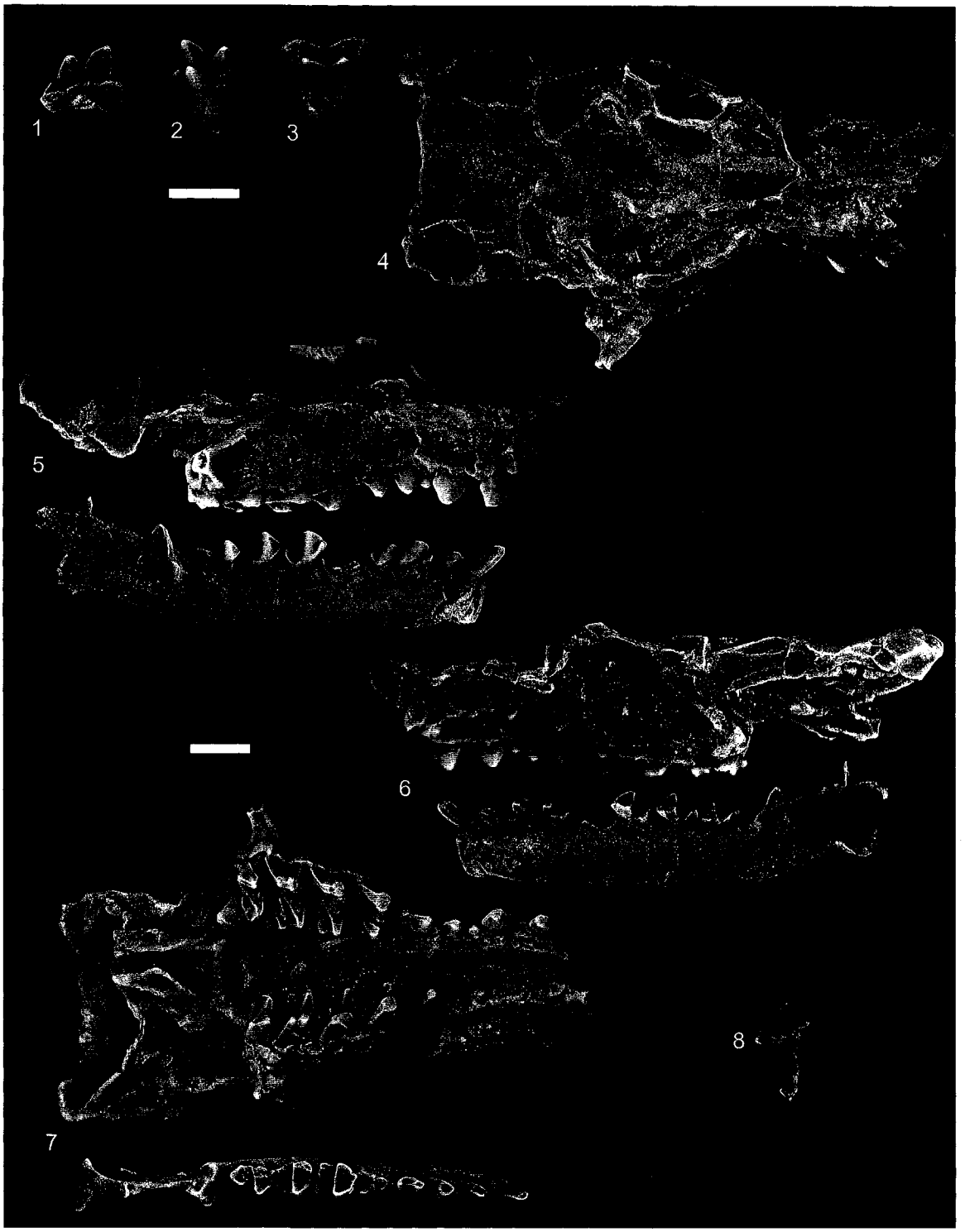
1
2
3
4
5
6
7
8

Figure 5.39.—1-14. Pararyctes pattersoni Van Valen from the early middle Tiffanian (Ti3) DW-2 locality, Paskapoo Formation, Alberta. 1-4, UALVP 47741, incomplete left maxilla with posterior root of upper canine, P1, P3-4, M1-3, and alveoli for anterior root of upper canine, P2 in 1, labial, 2, lingual, 3, occlusal, and 4, medial views (arrow points to the groove for the lacrimal duct); 5-8, UALVP 40564, incomplete right maxilla with P3-4, M1-2 (M2 damaged) in 5, medial, 6, lingual, 7, occlusal views, and 8, medial views; 9-11, UALVP 47755, incomplete left dentary with medial and lateral incisors (roots), c, p1-4, m1-3 in 9, labial, 10, lingual, and 11, occlusal views; 12-14, UALVP 47763, incomplete left dentary with p4, m1-3, and alveoli for c, p1-3 in 12, labial, 13, lingual, and 14, occlusal views. Scale bars = 2 mm.

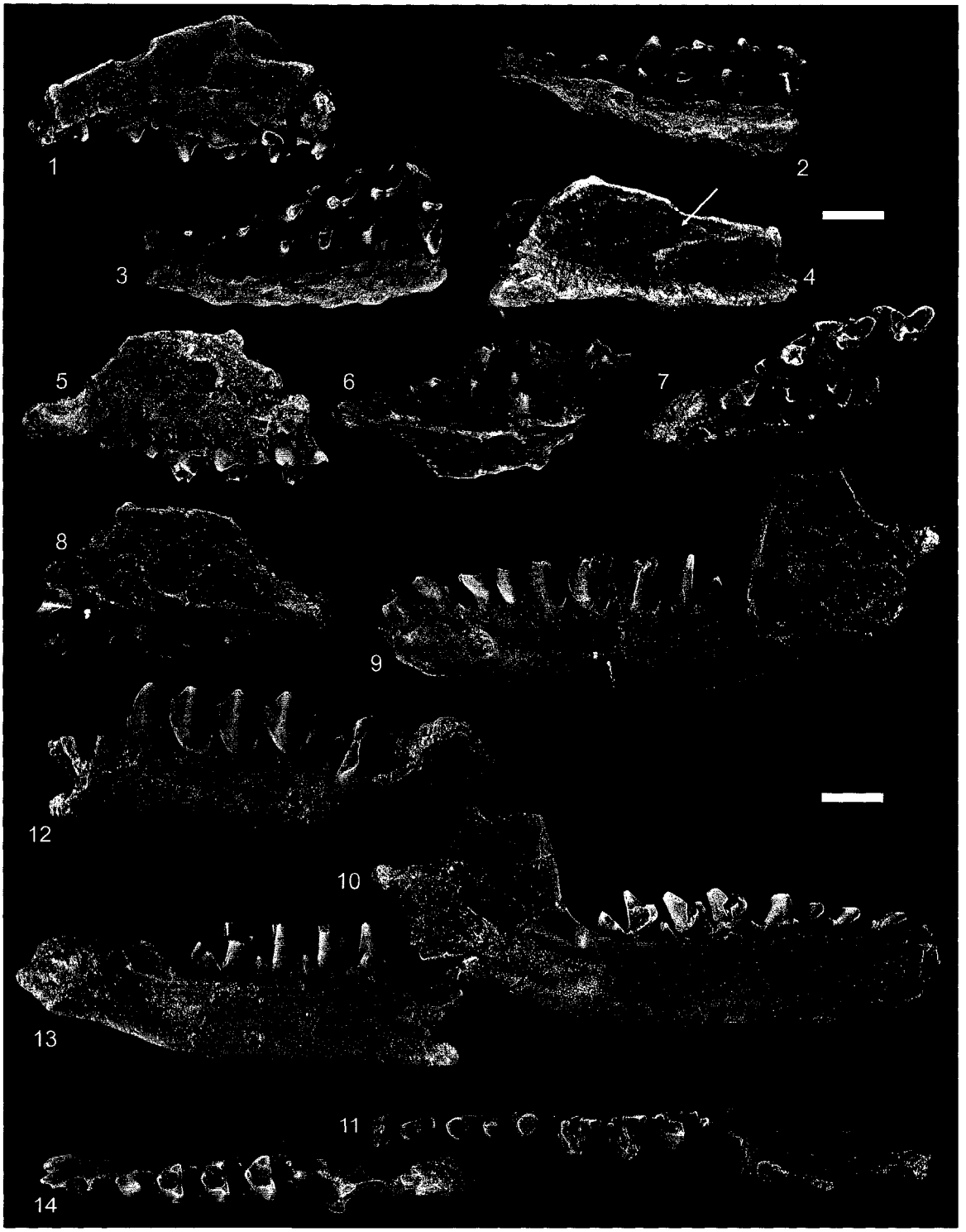
1
2
3
4
5
6
7
8
9
12
10
13
11
14

Figure 5.40.—1-13. Pararyctes pattersoni Van Valen from the early middle Tiffanian (Ti3) DW-2 locality, Paskapoo Formation, Alberta. 1-3, UALVP 47760, incomplete right dentary with c, p4, m1-3, and alveoli for medial and lateral incisors, p1-3 in 1, labial, 2, lingual, and 3, occlusal views; 4-9, UALVP 47756, incomplete right dentary with lower lateral incisor, c, p1-4, m1 (talonid only), m2-3, and associated lower medial incisor; incomplete dentary in 4, labial, 5, lingual, and 6, occlusal views; associated lower medial incisor in 7, lateral, 8, medial, and 9, occlusal views; 10-13, UALVP 47759, incomplete right dentary with lower lateral incisor, c, p4, m1-3, and alveoli for lower medial incisor, p1-3 in 10, labial, 11, lingual, 12, occlusal, and 13, posterior views. Scale bars = 2 mm.

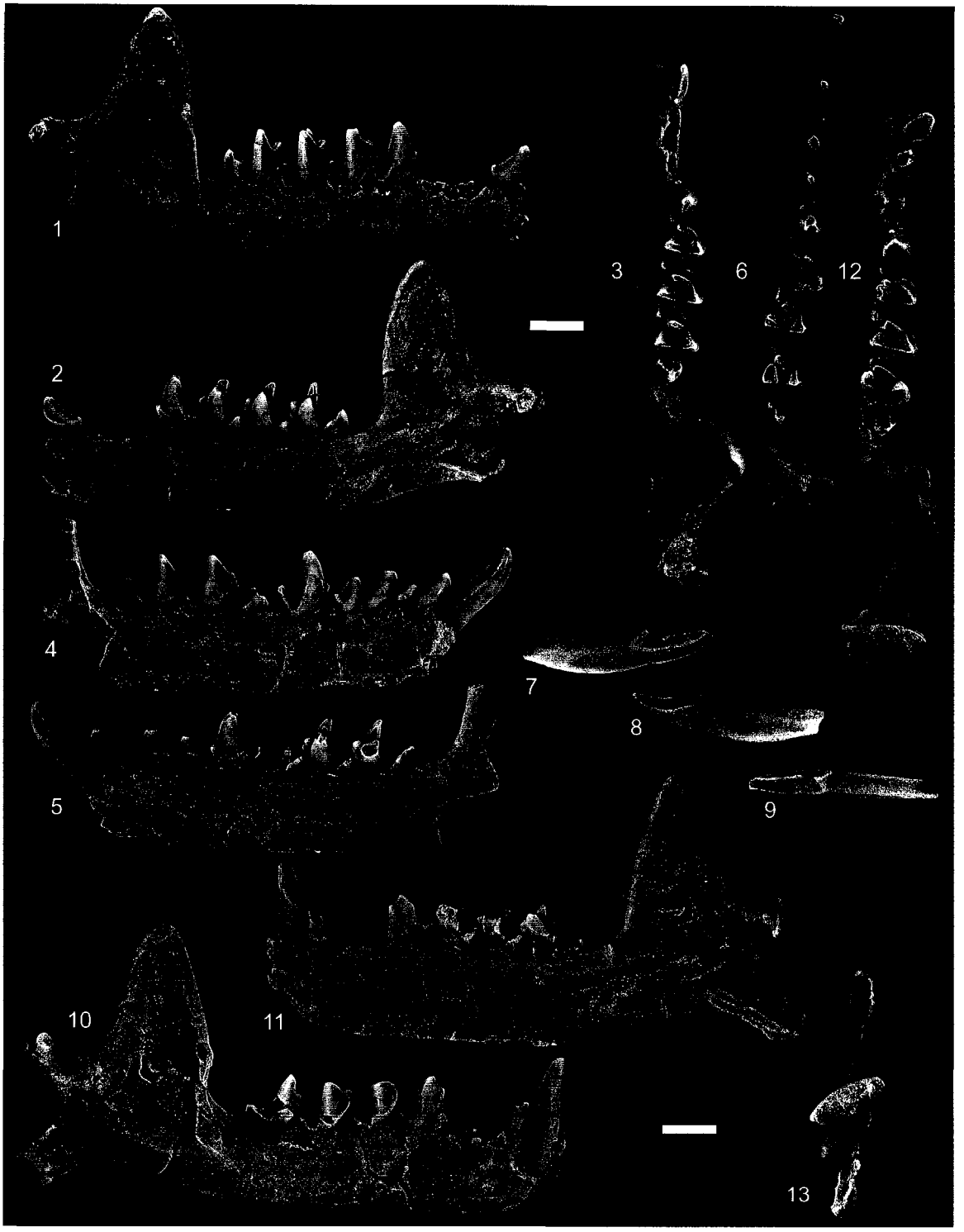
1
2
3
4
5
6
7
8
9
10
11
12
13

Figure 5.41.—1-6. Pararyctes pattersoni Van Valen from the early middle Tiffanian (Ti3) DW-2 locality, Paskapoo Formation, Alberta. 1-3, UALVP 47755, incomplete right dentary with lower medial and lateral incisors (roots), c, p1-4, m1-3 in 1, labial, 2, lingual, and 3, occlusal views; 4-6, UALVP 47769, incomplete right dentary with dp3-4, m1, and alveoli for m2-3 in 4, labial, 5, lingual, and 6, occlusal views.

7-9. Pararyctes colossa new species from the early middle Tiffanian (Ti3) DW-2 locality, Paskapoo Formation, Alberta. 7-9, UALVP 47800 (holotype), incomplete right dentary with m1-3 in 7, labial, 8, lingual, and 9, occlusal views.

Scale bars = 2 mm.

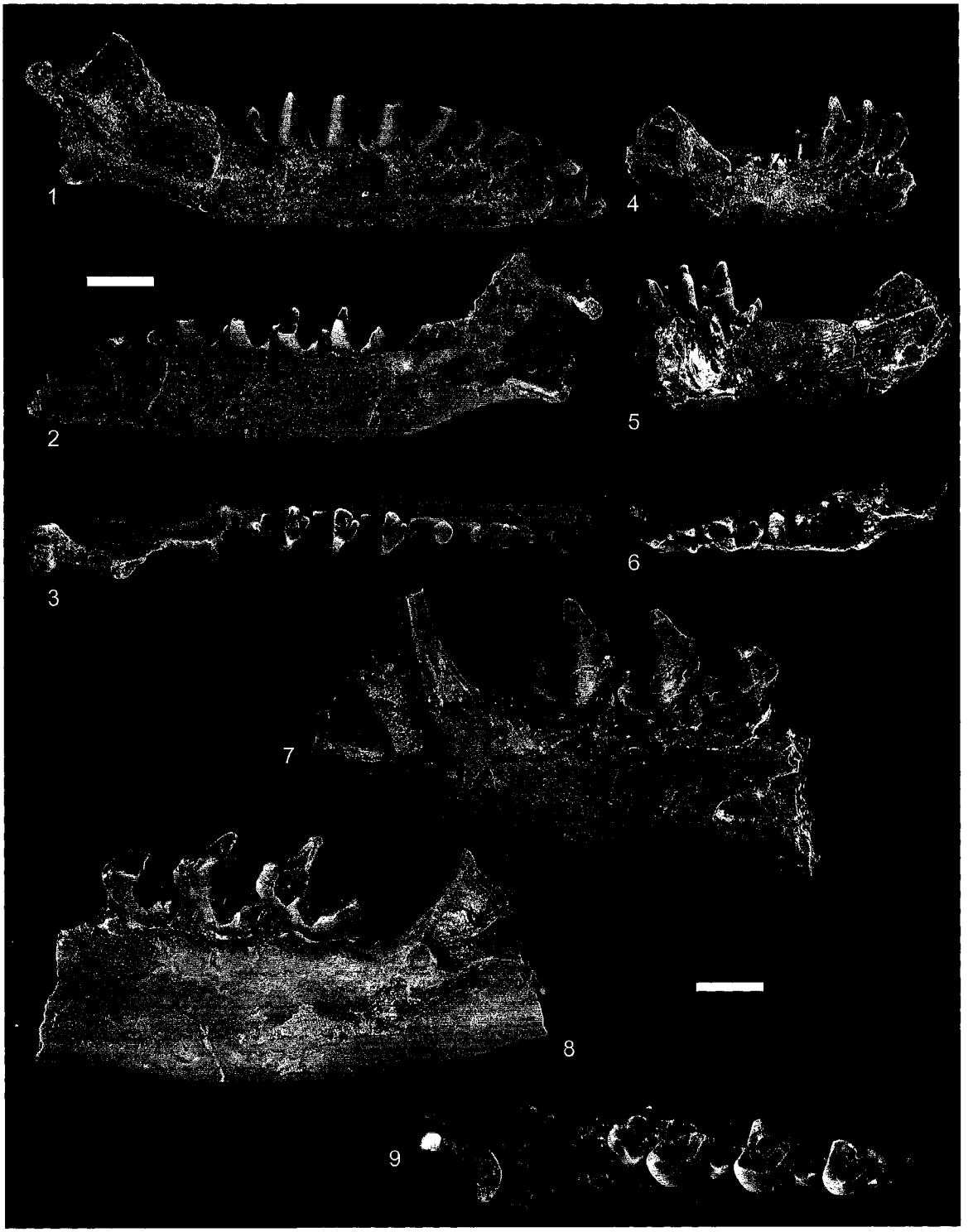
1
2
3
4
5
6
7
8
9

Figure 5.42.—1-3. Camera lucida outline drawings of occlusal views of P4 of various lipotyphlans as illustrative of the states of character 10. 1, uncatalogued UALVP specimen, right P4 of Prodiacodon furor Novacek from the earliest Tiffanian (Ti1), Paskapoo Formation, Alberta (state 0). 2, PU 21193, left P4 (reversed from original) of Litolestes ignotus Jepsen from the late Tiffanian (Ti5), Fort Union Formation, Wyoming (state 1). 3, uncatalogued IRScNB specimen, right P4 of Amphidozotherium cayluxi Filhol from the late Eocene, Belgium (state 2). Outline drawings have been scaled to approximately the same dimensions of P4 of Prodiacodon. Scale bar = 2 mm.

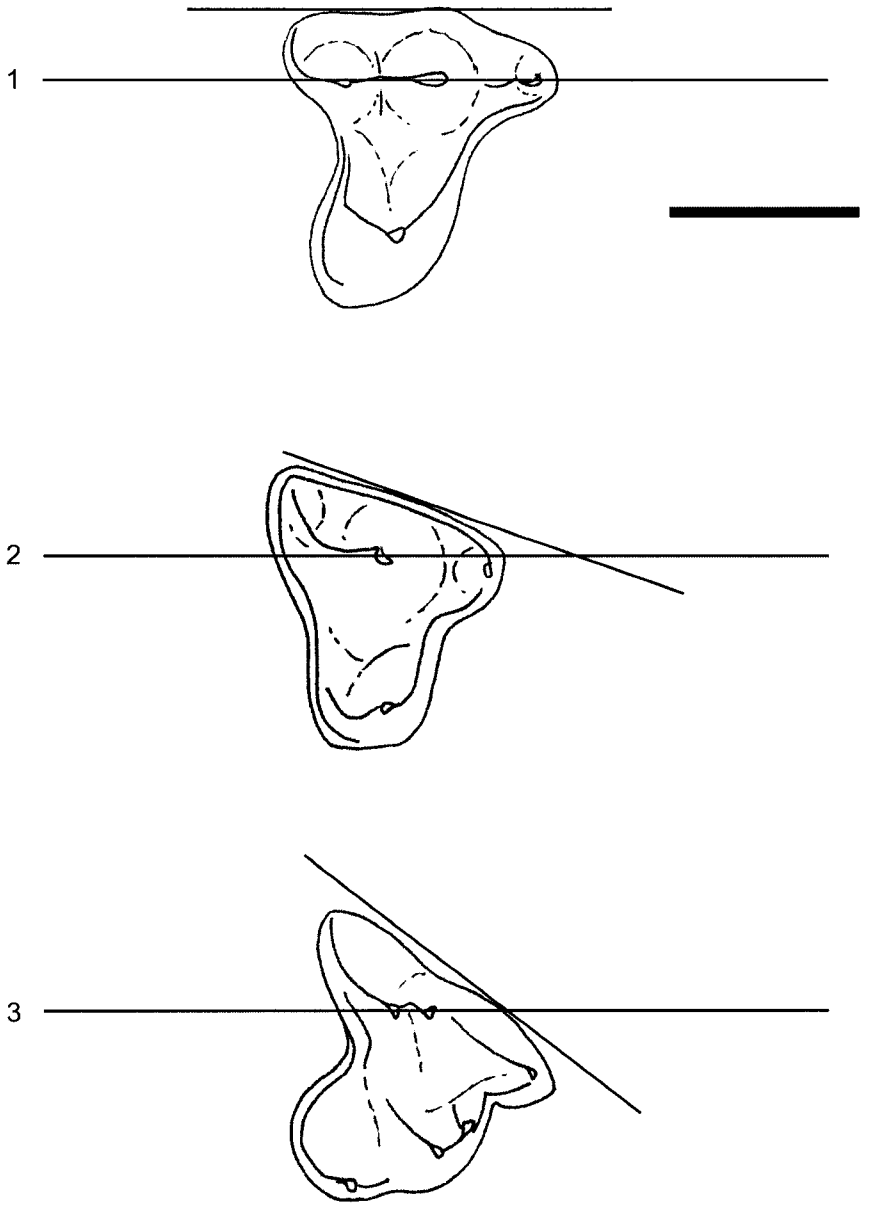
1
2
3

Figure 5.43.—1-4. Camera lucida outline drawings of occlusal views of P4 of various lipotyphlans as illustrative of the states of character 12. 1, PU 21193, left P4 (reversed from original) of Litolestes ignotus Jepsen from the late Tiffanian (Ti5), Fort Union Formation, Wyoming (state 0). 2, UALVP 40514, left P4 (reversed from original) of Xynolestes denommei new genus and species from the early middle Tiffanian (Ti3), Paskapoo Formation, Alberta (state 1). 3, UALVP 33862, right P4 of "Leptacodon" munusculum Simpson from the early middle Tiffanian (Ti3), Paskapoo Formation, Alberta (state 2). 4, uncatalogued UALVP specimen, right P4 of Prodiacodon furor Novacek from the earliest Tiffanian (Ti1), Paskapoo Formation, Alberta (state 3). Outline drawings have been scaled to approximately the same dimensions of P4 of Prodiacodon. Scale bar = 2 mm.

1

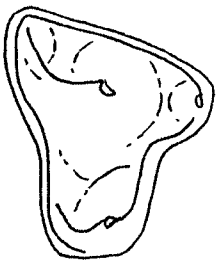

2

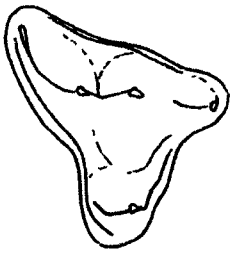

3

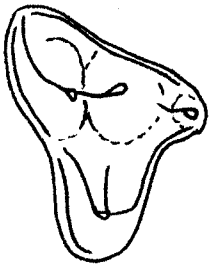

4

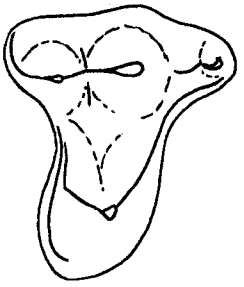

Figure 5.44.—1-3. Camera lucida outline drawings of occlusal views of P4 of various lipotyphlans as illustrative of the states of character 13. 1, uncatalogued UALVP specimen, right P4 (reversed from original) of "Adapisorella" from the late middle Tiffanian (Ti4), Paskapoo Formation, Alberta (state 0). 2, IRScNB M1918, left P4 of Euronyctia "belgica" from the upper Landenian (Paleocene-Eocene), Tirlemont Formation, Dormaal, Belgium (state 1). 3, UALVP 22333, left P4 of Diacocherus sp., cf. D. meizon from the late middle Tiffanian (Ti4), Paskapoo Formation, Alberta (state 2). Outline drawings have been scaled to approximately the same dimensions of P4 of Diacocherus. Scale bar = 1 mm.

1

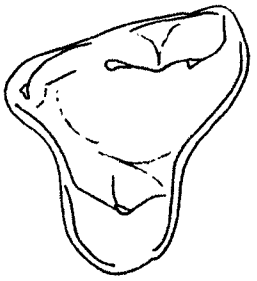

2

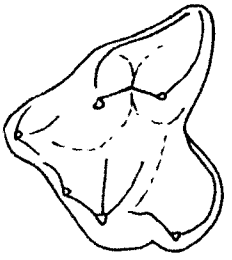

3

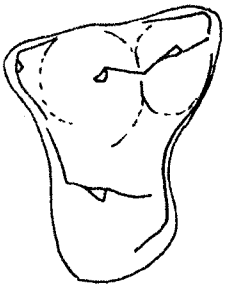

Figure 5.45.—1-4. Camera lucida outline drawings of occlusal views of P4 of various lipotyphlans as illustrative of the states of character 15. 1, UALVP 3256, right P4 (parastylar area reconstructed from UALVP 2645)of Cimolestes cerberoides Lillegraven from the Late Cretaceous (Lancian), Scollard Formation, Alberta (state 0). 2, UALVP 33862, right P4 of "Leptacodon" munusculum Simpson from the early middle Tiffanian (Ti3), Paskapoo Formation, Alberta (state 1). 3, uncatalogued IRScNB specimen, right P4 of Amphidozotherium cayluxi Filhol from the late Eocene, Belgium (state 2); 4, IRScNB M1804, right P4 of Macrocranion vandebroeki Weitzel, 1949 upper Landenian (Paleocene-Eocene), Tirlemont Formation, Dormaal, Belgium (state 3). Outline drawings have been scaled to approximately the same dimensions of P4 of Cimolestes. Scale bar = 1 mm.

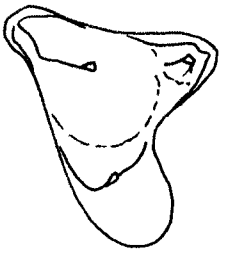

1

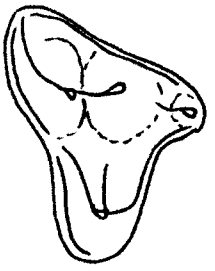

2

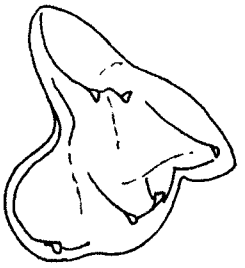

3

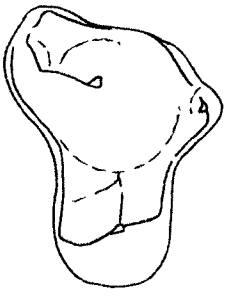

4

Figure 5.46.—1-4. Camera lucida outline drawings of occlusal views of M1 of various lipotyphlans as illustrative of the states of character 22. 1, UALVP 33862, right P4 of "Leptacodon" munusculum Simpson from the early middle Tiffanian (Ti3), Paskapoo Formation, Alberta (state 0). 2, UALVP 47298, right M1 of Litocherus notissimus Simpson from the early middle Tiffanian (Ti3), Paskapoo Formation, Alberta (state 1). 3, IRScNB M1919, right M1 of Euronyctia "belgica" from the upper Landenian (Paleocene-Eocene), Tirlemont Formation, Dormaal, Belgium (state 2); 4, uncatalogued UALVP specimen, right M1 of Adapisorex sp. from the late middle Tiffanian (Ti4), Paskapoo Formation, Alberta (state 3). Outline drawings have been scaled to approximately the same dimensions of P4 of Adapisorex. Scale bar = 2 mm.

1

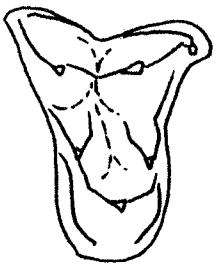

2

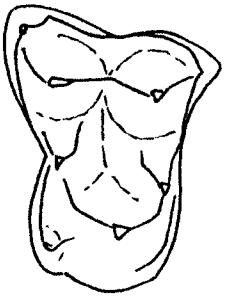

3

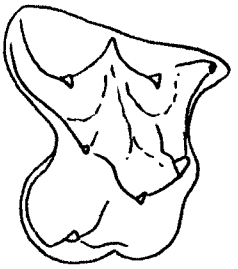

4

Figure 5.47.—1-4. Camera lucida outline drawings of occlusal views of M1-2 of various lipotyphlans as illustrative of the states of character 24. 1, uncatalogued UALVP specimens, right M1-2 of Diacocherus meizon Gingerich from the late middle Tiffanian (Ti4), Ravenscrag Formation, Saskatchewan (state 0). 2, UALVP 47258, left M1 -2 (reversed from original) of Nayloria albertensis new genus and species from the early middle Tiffanian (Ti3), Paskapoo Formation, Alberta (state 1). 3, UALVP 33862, right M1-2 of "Leptacodon" munusculum Simpson from the early middle Tiffanian (Ti3), Paskapoo Formation, Alberta (state 2); 4, IRScNB M1919, M1920, right M1-2 of Euronyctia "belgica" from the upper Landenian (Paleocene-Eocene), Tirlemont Formation, Dormaal, Belgium (state 3). Outline drawings have been scaled to approximately the same dimensions of M1 of Nayloria. Scale bar = 1 mm.

1

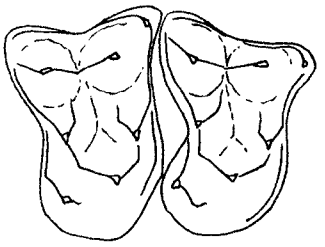

2

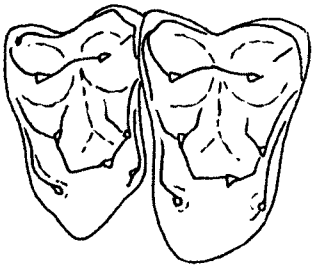

3

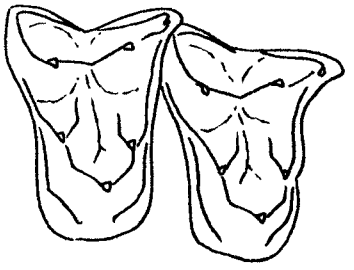

4

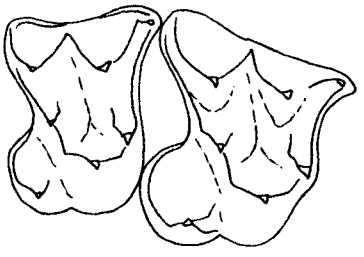

Figure 5.48.—1-3. Camera lucida outline drawings of occlusal views of upper molars of various lipotyphlans as illustrative of the states of character 25. 1, uncatalogued UALVP specimens, right M1 of Adapisorex sp. from the late middle Tiffanian (Ti4), Paskapoo Formation, Alberta (state 0). 2, UALVP 47329, right M1 of Psydronyctia smithorum new genus and species from the early middle Tiffanian (Ti3), Paskapoo Formation, Alberta (state 1). 3, IRScNB M1813, right M2 of Wyonycteris richardi from the upper Landenian (Paleocene-Eocene), Tirlemont Formation, Dormaal, Belgium (state 3). Outline drawings have been scaled to approximately the same dimensions of M1 of Adapisorex. Scale bar = 1 mm.

1

2

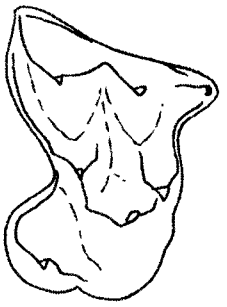

3

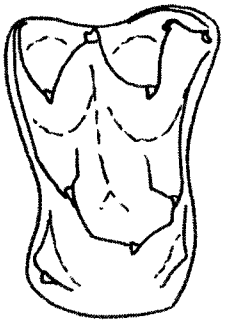

Figure 5.49.—1-4. Camera lucida outline drawings of occlusal views of upper molars of various lipotyphlans as illustrative of the states of character 34. 1, UALVP 3132, right P4 (reversed from original) of Cimolestes cerberoides Lillegraven from the Late Cretaceous (Lancian), Scollard Formation, Alberta (state 0). 2, UALVP 33862, right M1 of "Leptacodon" munusculum Simpson from the early middle Tiffanian (Ti3), Paskapoo Formation, Alberta (state 1). 3, UALVP 47298, right M1 of Litocherus notissimus Simpson from the early middle Tiffanian (Ti3), Paskapoo Formation, Alberta (state 2); 4, IRScNB M1919, right M1 of Euronyctia "belgica" from the upper Landenian (Paleocene-Eocene), Tirlemont Formation, Dormaal, Belgium (state 2). Outline drawings have been scaled to approximately the same dimensions of M1 of Cimolestes. Scale bar = 3 mm.

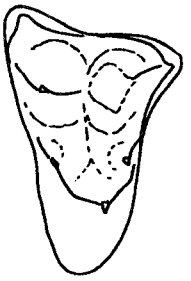

1

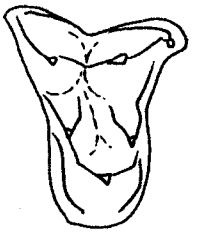

2

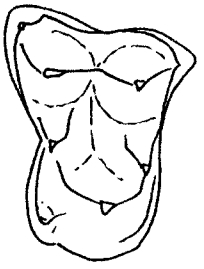

3

4

Figure 5.50.—1, 2. Camera lucida outline drawings of labial views of p2-3 of various lipotyphlans as illustrative of the states of character 49. 1, UALVP 47295, left p2-3 of "Leptacodon" munusculum Simpson from the early middle Tiffanian (Ti3), Paskapoo Formation, Alberta (state 0). 2, UALVP 46886 (holotype), left p2-3 (reversed from original) of Xynolestes denommei new genus and species from the early middle Tiffanian (Ti3), Paskapoo Formation, Alberta (state 1). Scale bar = 1 mm.

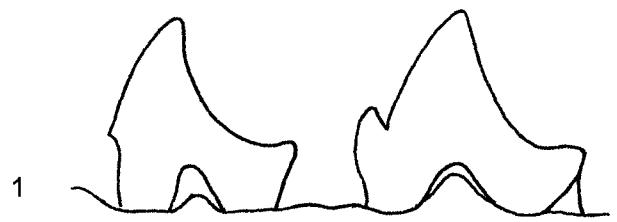
1

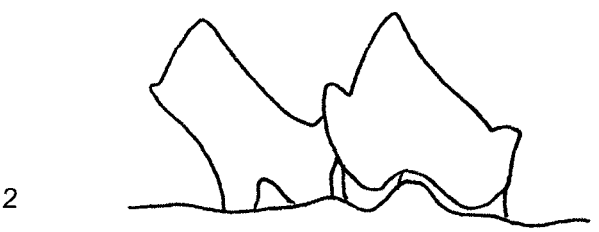
2

Figure 5.51.—1, 2. Camera lucida outline drawings of lingual views of p4 of various lipotyphlans as illustrative of the states of character 55. 1, UALVP 47301, right p4 (reversed from original) of "Leptacodon" munusculum Simpson from the early middle Tiffanian (Ti3), Paskapoo Formation, Alberta (state 0). 2, UALVP 40528 (holotype), left p4 of Litolestes avitodelphus new species from the early middle Tiffanian (Ti3), Paskapoo Formation, Alberta (state 1). Outline drawings have been scaled to approximately the same dimensions of p4 of Litolestes. Scale bar = 1 mm.

1

2

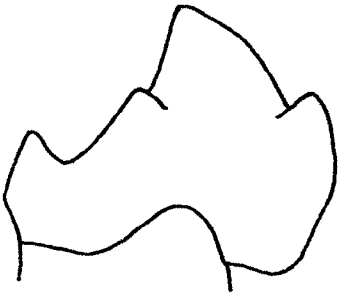

Figure 5.52.—1-4. Camera lucida outline drawings of occlusal views of p4 of various lipotyphlans as illustrative of the states of character 57. 1, UALVP 43100 (holotype), right p4 of Psydronyctia smithorum new genus and species from the early middle Tiffanian (Ti3), Paskapoo Formation, Alberta (state 0). 2, UALVP 40668, left p4 (reversed from original) of Litocherus notissimus Simpson from the early middle Tiffanian (Ti3), Paskapoo Formation, Alberta (state 1); 3, UM 71650 (holotype), left p4 (reversed from original) of Leptacodon rosei Gingerich from the middle Clarkforkian (Cf2), lower Willwood Formation, Wyoming (state 2); 4, YPM 148, right p4 of Echinosorex gymnura Raffles from the Recent of Borneo (state 3). Outline drawings have been scaled to approximately the same dimensions of p4 of Litocherus. Scale bar = 2 mm.

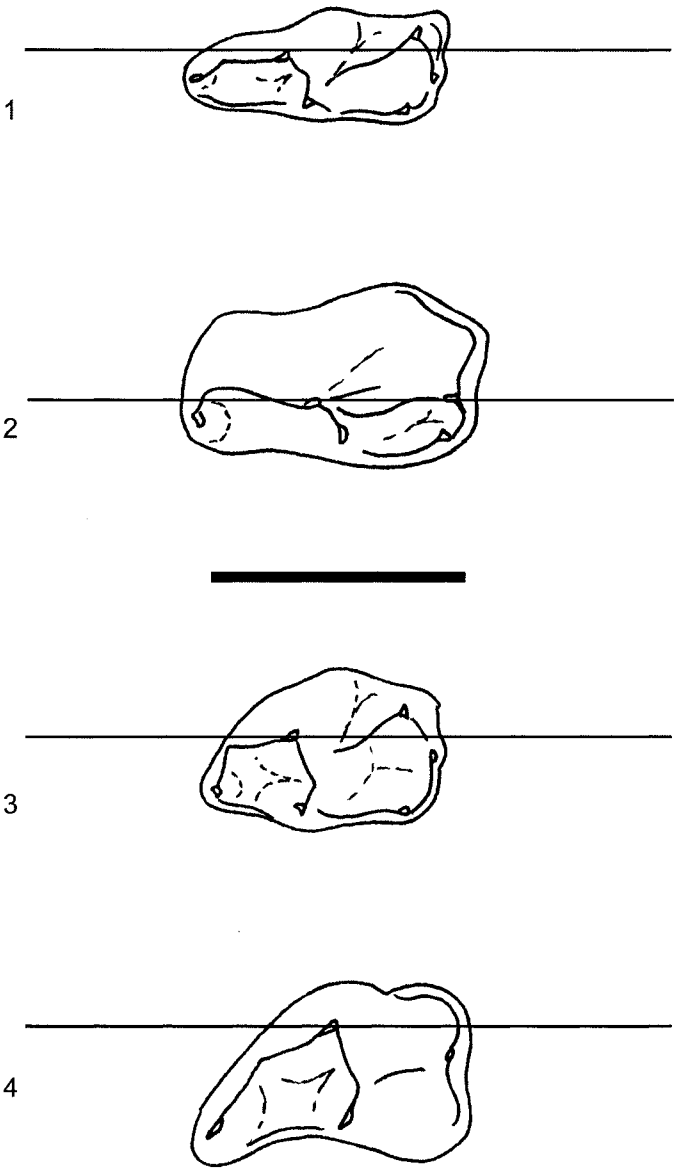
1
2
3
4

Figure 5.53.—1-4. Camera lucida outline drawings of oblique anterolingual views of p4 of various lipotyphlans as illustrative of the states of character 58. 1, UALVP 6411, right p4 of Cimolestes cerberoides Lillegraven from the Late Cretaceous (Lancian), Scollard Formation, Alberta (state 0). 2, UALVP 47329, right p4 of Litocherus notissimus Simpson from the early middle Tiffanian (Ti3), Paskapoo Formation, Alberta (state 1); 3, UALVP 47813 (holotype), right p4 of Limaconyssus subnuba new species from the late middle Tiffanian (Ti4), Paskapoo Formation, Alberta (state 2); 4, uncatalogued UALVP specimen, right p4 of Prodiacodon furor Novacek from the earliest Tiffanian (Ti1), Paskapoo Formation, Alberta (state 3). Outline drawings have been scaled to approximately the same dimensions of p4 of Cimolestes. Scale bar = 2 mm.

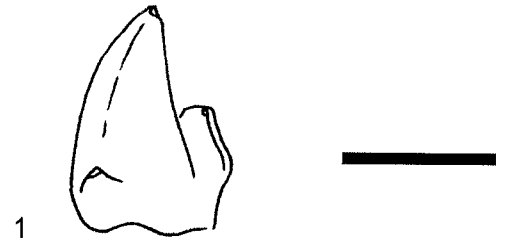

1

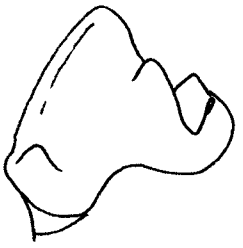

2

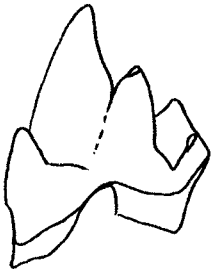

3

4

Figure 5.54.—1-3. Camera lucida outline drawings of lingual views of m1 of various lipotyphlans as illustrative of the states of characters 67 and 68. 1, UALVP 3372, right m1 (reversed from original) of Cimolestes cerberoides Lillegraven from the Late Cretaceous (Lancian), Scollard Formation, Alberta (state 0). 2, UALVP 47301, left m1 of "Leptacodon" munusculum Simpson from the early middle Tiffanian (Ti3), Paskapoo Formation, Alberta (state 1); 3, uncatalogued UALVP specimen, left m1 of Adapisorex sp. from the late middle Tiffanian (Ti4), Paskapoo Formation, Alberta (state 2). Outline drawings have been scaled to approximately the same dimensions of m1 of Adapisorex. Scale bar = 2 mm.

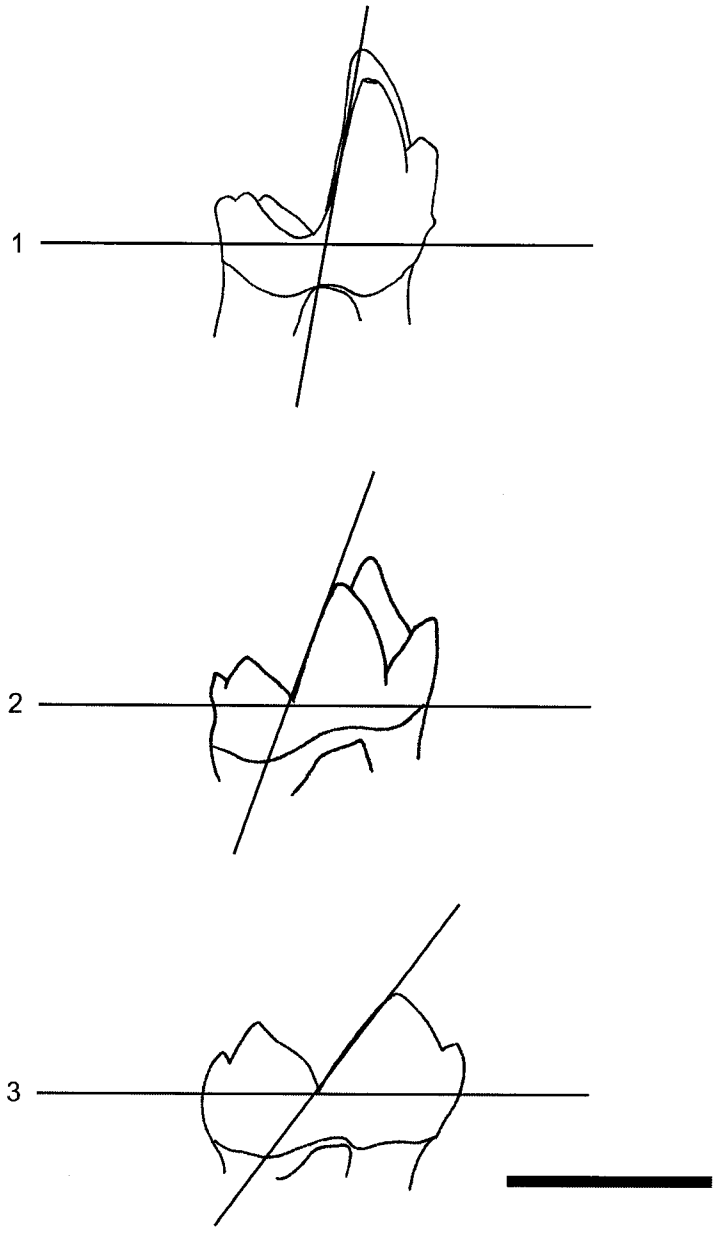
1
2
3

Figure 5.55.—1, 2. Camera lucida outline drawings of lingual views of m1-2 of various lipotyphlans as illustrative of the states of character 72. 1, UALVP 47301, right m1-2 of "Leptacodon" munusculum Simpson from the early middle Tiffanian (Ti3), Paskapoo Formation, Alberta (state 0). 2, uncatalogued UALVP specimen, right m1-2 of Diacocherus meizon Gingerich from the late middle Tiffanian (Ti4), Paskapoo Formation, Alberta (state 1). Outline drawing of UALVP 47301 scaled to approximately the same dimensions of m1-2 of Diacocherus. Scale bar = 1 mm.

1

2

Figure 5.56.—1-3. Camera lucida outline drawings of occlusal views of lower molars of various lipotyphlans as illustrative of the states of character 74. 1, UALVP 47813 (holotype), right m1-2 (reversed from original) of Limaconyssus subnuba new species from the late middle Tiffanian (Ti4), Paskapoo Formation, Alberta (state 0). 2, uncatalogued UALVP specimen, left m1-2 of Adapisorex sp. from the late middle Tiffanian (Ti4), Paskapoo Formation, Alberta (state 1); 3, AMNH 11485 (cast of holotype), left m2 of Entomolestes grangeri from the middle Eocene, upper Bridger Formation, Wyoming (state 2). Outline drawings have been scaled to approximately the same dimensions of m1-2 of Adapisorex. Scale bar = 2 mm.

1

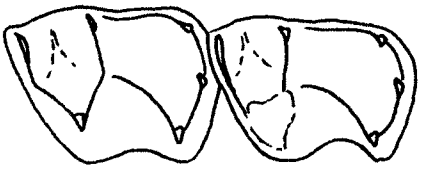

2

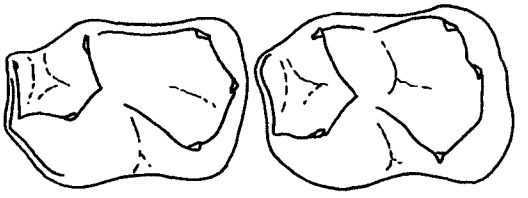

3

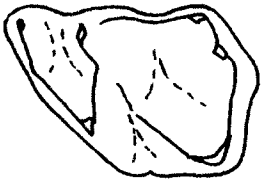

Figure 5.57.—1-3. Camera lucida outline drawings of occlusal views of m3 of various lipotyphlans as illustrative of the states of character 98. 1, uncatalogued UALVP specimen, right m3 of Diacocherus meizon Gingerich from the late middle Tiffanian (Ti4), Paskapoo Formation, Alberta (state 0). 2, UALVP 40668, left m3 (reversed from original) of Litocherus notissimus Simpson from the early middle Tiffanian (Ti3), Paskapoo Formation, Alberta (state 1); 3, uncatalogued UALVP specimen, left m3 of Adapisorex sp. from the late middle Tiffanian (Ti4), Paskapoo Formation, Alberta (state 2). Outline drawings have been scaled to approximately the same dimensions of m3 of Adapisorex. Scale bar = 2 mm.

1

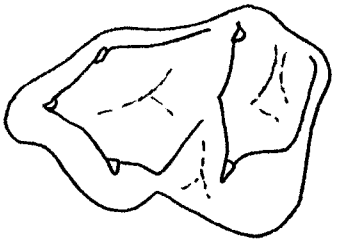

2

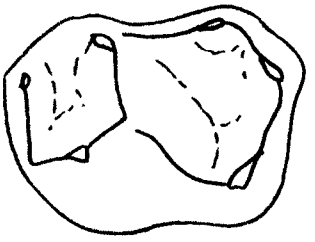

3

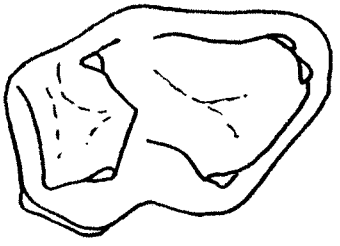

Figure 5.58.—Strict consensus of 20 optimal trees of 785 steps (CI=0.456; RI=0.528; RC=0.241) derived from analysis of the dataset in Appendix 2.

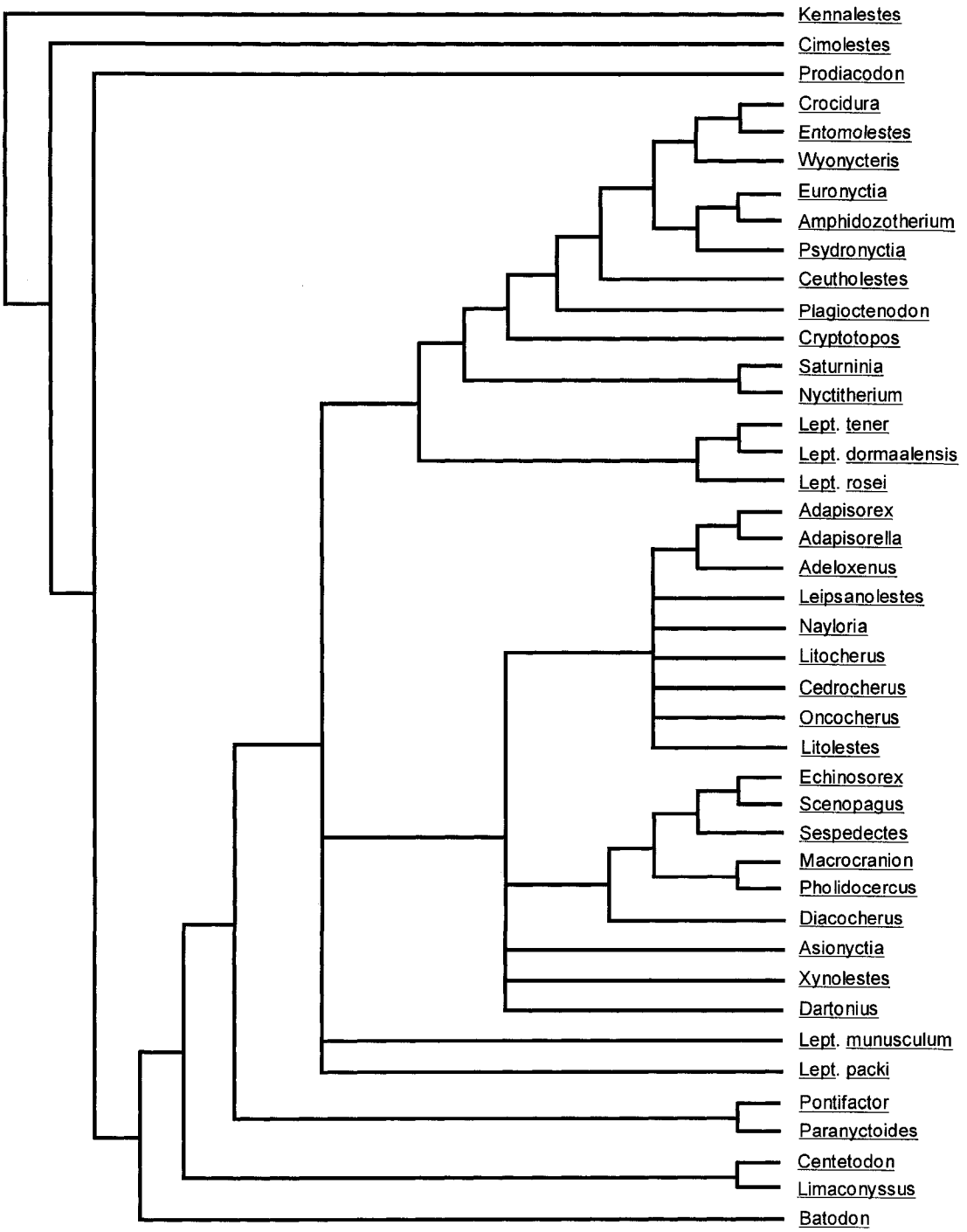
Kennalestes
Cimolestes
Prodiacodon
Crocidura
Entomolestes
Wyonycteris
Euronyctia
Amphidozotherium
Psydronyctia
Ceutholestes
Plagioctenodon
Cryptotopos
Saturninia
Nyctitherium
Lept. tener
Lept. dormaalensis
Lept. rosei
Adapisorex
Adapisorella
Adeloxenus
Leipsanolestes
Nayloria
Litocherus
Cedrocherus
Oncocherus
Litolestes
Echinosorex
Scenopagus
Sespedectes
Macrocranion
Pholidocercus
Diacocherus
Asionyctia
Xynolestes
Dartonius
Lept. munusculum
Lept. packi
Pontifactor
Paranyctoides
Centetodon
Limaconyssus
Batodon

Figure 5.59.—50% majority rule consensus of 20 optimal trees of 785 steps (CI=0.456; RI=0.528; RC=0.241) derived from analysis of the dataset in Appendix 2. Numbers adjacent to nodes above branch indicate decay index. Numbers below branch indicate the percentage of optimal trees in which the clade was recovered; if a number does not appear below the branch, then the clade was recovered in all 20 optimal trees.

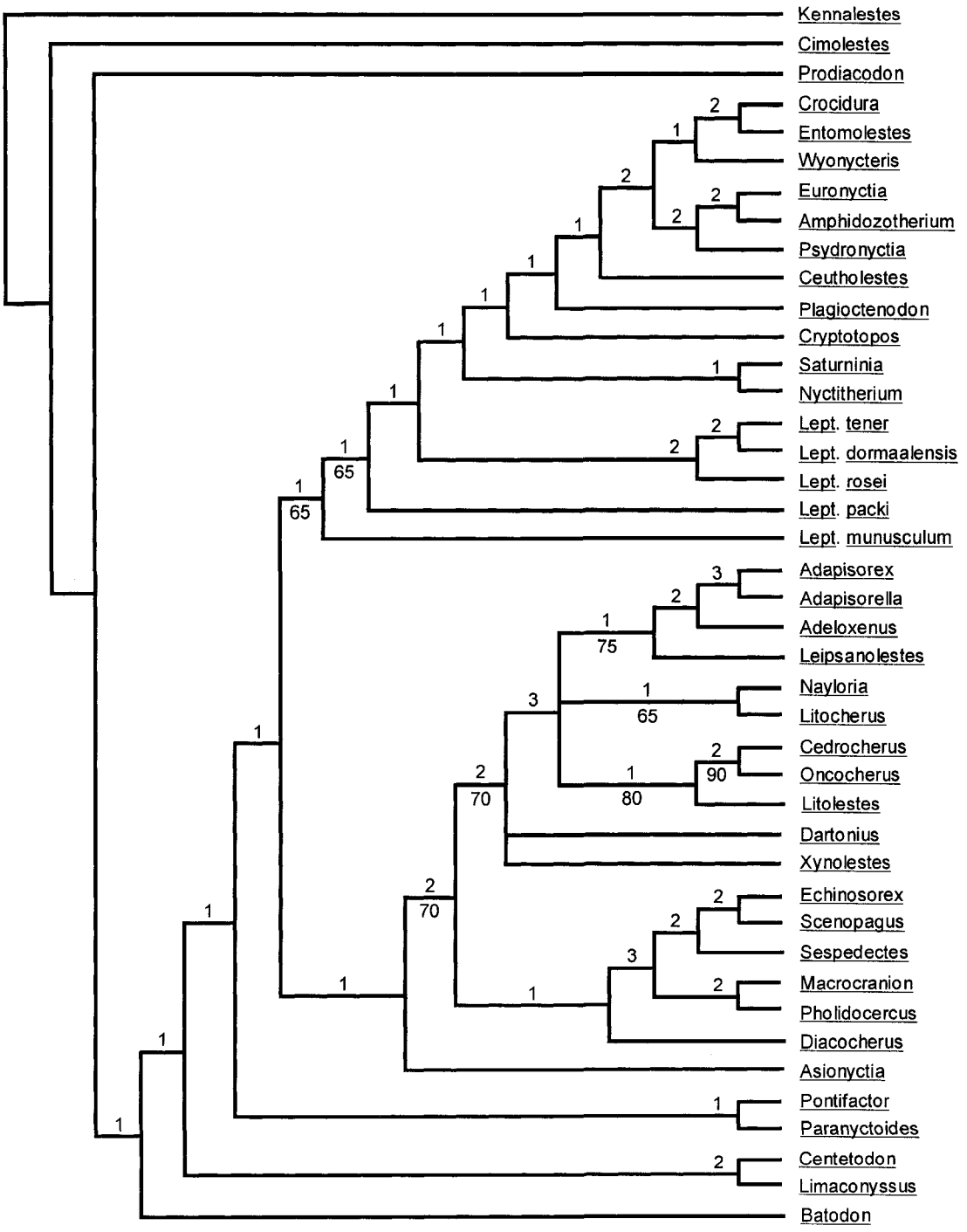
Kennalestes
Cimolestes
Prodiacodon
Crocidura
Entomolestes
Wyonycteris
Euronyctia
Amphidozotherium
Psydronyctia
Ceutholestes
Plagioctenodon
Cryptotopos
Saturninia
Nyctitherium
Lept. tener
Lept. dormaalensis
Lept. rosei
Lept. packi
Lept. munusculum
Adapisorex
Adapisorella
Adeloxenus
Leipsanolestes
Nayloria
Litocherus
Cedrocherus
Oncocherus
Litolestes
Dartonius
Xynolestes
Echinosorex
Scenopagus
Sespedectes
Macrocranion
Pholidocercus
Diacocherus
Asionyctia
Pontifactor
Paranyctoides
Centetodon
Limaconyssus
Batodon

Figure 5.60.—One of the 20 optimal trees (tree 10) of 785 steps (CI=0.456; RI=0.528; RC=0.241) derived from analysis of the dataset in Appendix 2 selected for discussion in the text; all nodes are labeled. The preferred tree differs from the 50% majority rule consensus tree in having resolved the position of Xynolestes and Dartonius, and that of the clade of (Litocherus+Nayloria). Some of the major nodes are discussed in the text, and character support at each node is listed in Appendix 3.

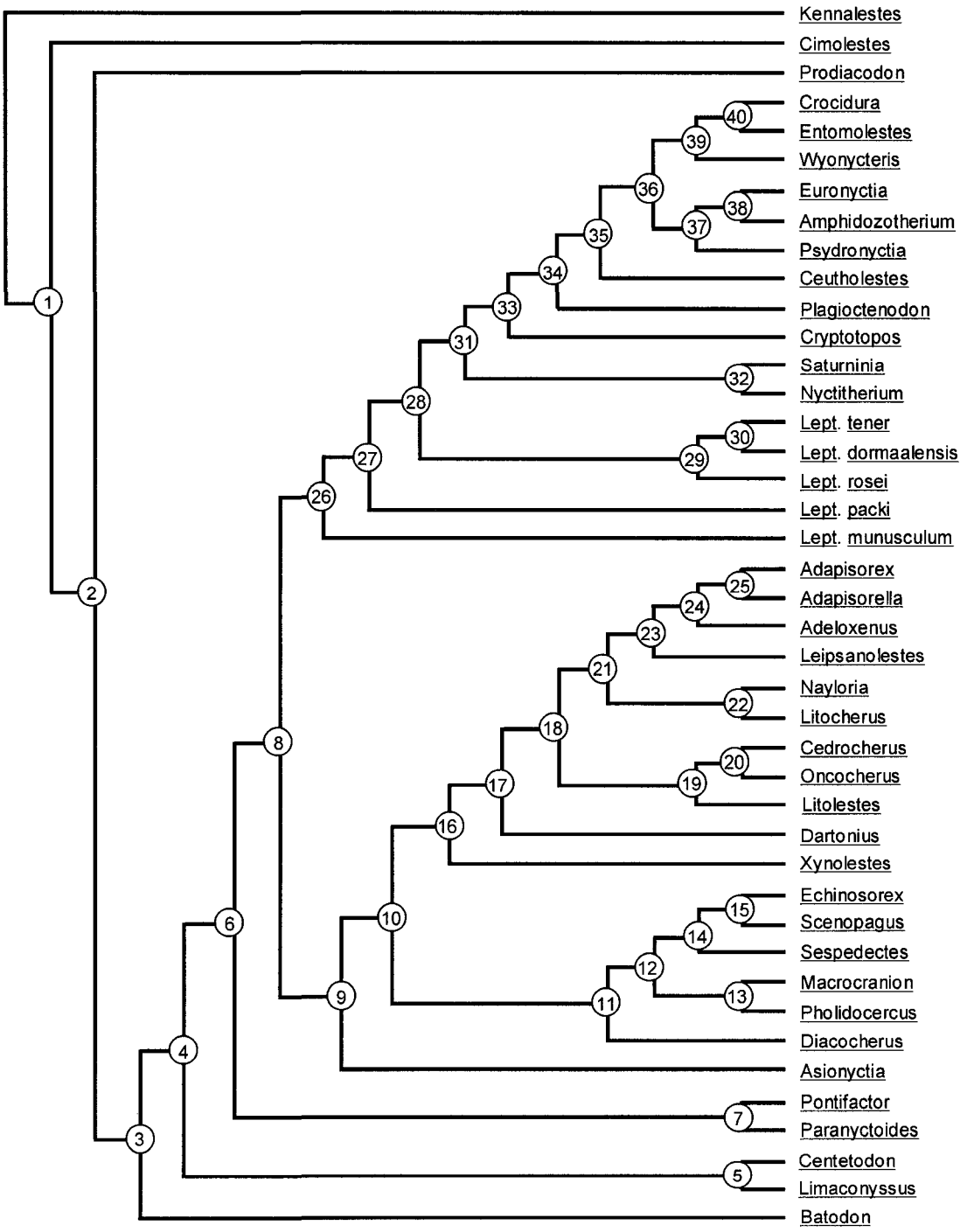
Kennalestes
Cimolestes
Prodiacodon
Crocidura
Entomolestes
Wyonycteris
Euronyctia
Amphidozotherium
Psydronyctia
Ceutholestes
Plagioctenodon
Cryptotopos
Saturninia
Nyctitherium
Lept. tener
Lept. dormaalensis
Lept. rosei
Lept. packi
Lept. munusculum
Adapisorex
Adapisorella
Adeloxenus
Leipsanolestes
Nayloria
Litocherus
Cedrocherus
Oncocherus
Litolestes
Dartonius
Xynolestes
Echinosorex
Scenopagus
Sespedectes
Macrocranion
Pholidocercus
Diacocherus
Asionyctia
Pontifactor
Paranyctoides
Centetodon
Limaconyssus
Batodon
1
2
3
4
5
6
7
8
9
10
11
12
13
14
15
16
17
18
19
20
21
22
23
24
25
26
27
28
29
30
31
32
33
34
35
36
37
38
39
40

5.7 Appendix 2.—Taxa Selected for Analysis and Source Data († = Extinct)

5.7.1 Outgroup Taxa

†Kennalestes Kielan-Jaworowska, 1969

Species: †Kennalestes gobiensis Kielan-Jaworowska, 1969 (Bayan Dzak, Mongolia, ?early Campanian)

References: Kielan-Jaworowska, 1969; Crompton and Kielan-Jaworowska, 1978; Kielan-Jaworowska et al., 1979; Kielan-Jaworowska, 1981; McKenna et al., 2000; Luo et al., 1999; Kielan-Jaworowska et al, 2004; Archibald and Averianov, 2006

†Cimolestes Marsh, 1889

Species: †Cimolestes cerberoides Lillegraven, 1969 [UALVP 2973 (lectotype), 66841, 6728, 66102, 3733, 2190, 6720, 6411, 66163, 66120 (KUA-1 locality, Alberta, Lancian)]

References: Lillegraven, 1969; Clemens, 1973; Fox and Youzwyshyn, 1994; Fox, 1994

†Prodiacodon Matthew, 1929

Species: †Prodiacodon puercensis (Matthew, in Matthew and Granger, 1918) [AMNH 16011 (holotype), 16748, 16598 (Torrejon Arroyo, New Mexico, To2)]

†Prodiacodon sp., cf. P. puercensis [UALVP 25234-25240, 25242-24250, 25252, (Cochrane 2, Alberta, Ti1)]

†Prodiacodon furor Novacek, 1977 [UALVP 429, 25324-25328, 25330-25332, 25334-25337, 25341, 25345, (Cochrane 2, Alberta, Ti1)]

†Prodiacodon tauricinerei (Jepsen, 1930) [YPM-PU 13104 (holotype), 13267 (paratype) (Omorhamphus Site, Wyoming, Wasatchian)]

References: Matthew and Granger, 1918; Matthew, 1929; Jepsen, 1930; Novacek, 1977, 1986; Youzwyshyn, 1988

5.7.2 Ingroup Taxa

†"Adapisorella"

Species: †"Adapisorella" sp. [UALVP 46996 (DW-2, Alberta, Ti3); UALVP 35098 (Hand Hills West upper level, Alberta, Ti3); uncatalogued UALVP specimens (Gao Mine locality, Alberta, Ti4)]

†Adapisorex Lemoine, 1883

Species: †Adapisorex sp. [uncatalogued UALVP specimens (Gao Mine locality, Alberta, Ti4)]

†Adapisorex abundans Russell 1964 [MNHN C-4444, C-4455, C-1171, C-4354, composite upper dentition (C) (Walbeck, Germany, ?Ti3)]

References: Russell, 1964

†Amphidozotherium Filhol, 1877

Species: †Amphidozotherium cayluxi Filhol, 1877 [IRScNB 310, 324, 347, 383, 396, 409, 413, 426, 554, 563, 619, 672 (C) (Hoogenbutsel, Belgium, Eocene)]

References: Sigé, 1974, 1976; Rose and Gingerich, 1987; Hooker and Weidmann, 2000

†Asionyctia Missiaen and Smith, 2005

Species: † Asionyctia guoi Missiaen and Smith, 2005 (Subeng locality, Inner Mongolia, China, late Paleocene)

References: Missiaen and Smith, 2005

†Batodon Marsh, 1892

Species: †Batodon tenius Marsh, 1892 [UALVP 4081, 3082, 3714, 3721, 3688, 4047, 3688 (KUA-1 locality, Alberta, Lancian)]

References: Marsh, 1892; Lillegraven, 1969; Clemens, 1973; Lillegraven et al., 1981; Bloch et al., 1998; Wood and Clemens, 2001

†Cedrocherus Gingerich, 1983

Species: †Cedrocherus ryani Gingerich, 1983 [UM 82028 (C) (Cedar Point Quarry, Wyoming, Ti3)]

†Cedrocherus aceratus Gunnell, 1994 (Chappo Type locality, Wyoming, Ti3)

References: Gingerich, 1983; Novacek et al., 1985; Gunnell, 1994

†"Adeloxenus" new genus

Species: †"Adeloxenus" sp. [UALVP 46997, 46998, 46999, 47247 (DW-2, Alberta, Ti3); YPM-PU 20811, 18466, 19957 (Cedar Point Quarry, Wyoming, Ti3)]

References: Secord, 2004

†Centetodon Marsh, 1872

Species: †Centetodon bembicophagus Lillegraven, McKenna, and Krishtalka, 1981 [AMNH 55656.001-.002, 55657.001-.002, 89729, 91856, 91857, 91858, 91859 (various localities, Wyoming, Bridgerian)]

†Centetodon pulcher Marsh, 1872 [AMNH 12063, 91876, 91873, 91871, 91875, 91874, 91870, 91869, 91878 (various localities, Wyoming, Bridgerian)]

†Centetodon marginalis (Cope, 1873) [AMNH 1799.001-.003, 749534, various localities, Wyoming, Orellan)

References: Krishtalka and West, 1979; Lillegraven et al., 1981; Asher et al., 2005.

†Ceutholestes Rose and Gingerich, 1987

Species: †Ceutholestes dolosus Rose and Gingerich 1987 [UM 82503 (holotype) (C) (SC-62 locality, Wyoming, Cf2)]

References: Rose and Gingerich, 1987

Crocidura Wagler

Species: Crocidura hirta Peters [TMP 99.58.2 (Tanganyika, Africa)]

References: Butler et al., 1989; Grenyer and Purvis, 2003; Hutterer, 2005

†Cryptotopos Crochet, 1974

Species: †Cryptotopos beatus Crochet, 1974 (Quercy Phosphorites, France, middle Eocene)

References: Sigé, 1976; Hooker and Weidmann, 2000

†Dartonius Novacek, Bown, and Schankler, 1985

Species: †Dartonius jepseni (Novacek, Bown, and Schankler, 1985) [UCMP 45949 (holotype) (C), Four Mile Creek area, Colorado, Wasatchian)

References: McKenna, 1960; Bown and Schankler, 1982; Novacek et al., 1985; Novacek, 1985

†Diacocherus Gingerich, 1983

Species: †Diacocherus meizon Gingerich, 1983 [UALVP 47351, 47352, 47353, UALVP 47354, 47355, 47356 (DW-2, Alberta, Ti3); UALVP 47357, 35119, 35117, 35120, 35134, 47358 (Hand Hills West upper level, Alberta, Ti3); uncatalogued UALVP specimens (Gao Mine locality, Alberta, Ti4); UM 82023 (C), YPM-PU 14988, 19959, 19999, 20012, 20022, 20023, 20053, 20057, 20072, 20646, 20847, 20874, 20887, 21288, 21388, 21396, 21429, 21435, 21853 (Cedar Point Quarry, Wyoming, Ti3)]

References: Gingerich, 1983; Secord, 2004

Echinosorex Blainville, 1838

Species: Echinosorex gymnura (Raffles) [YPM 148 (Borneo)]

References: Frost et al., 1991; Gould, 1995, 2001

†Entomolestes Matthew, 1909

Species: † Entomolestes grangeri Matthew 1909 [AMNH 91837, East Hill locality, Wyoming, Eocene; AMNH 91834, 91832, 91819, 91831, Hutch Quarry, Wyoming, Eocene; AMNH 91828, 91829, Sage Creek North, Wyoming, Eocene; AMNH 91816, Bill's Peak, Wyoming, Eocene; AMNH 91815, Wyoming, Eocene]

References: Robinson, 1966a; Krishtalka, 1976a; Krishtalka and West, 1977; Novacek et al., 1985

†Euronyctia Sigé, 1997

Species: †Euronyctia "belgica" [IRScNB M1920, M1916, M1921, M1919, M1918, M1917, and uncatalogued specimens, Tirlemont Formation, Dormaal, Belgium, Paleocene-Eocene]

†Euronyctia montana Sigé, 1997 (Sossis localities, Lleida, Spain, late Eocene)

†Euronyctia grisollensis (Sigé, 1976) (Grisolles, France, late Eocene)

References: Sigé, 1976, 1997; Hooker and Weidmann, 2000

†Leipsanolestes Simpson 1928

Species: †Leipsanolestes siegfriedti Simpson 1928 [AMNH 22179, 22193, 22178, 22192, 22177, 22158, 22236, 22194, 22174 (C) (Bear Creek, Montana, Cf1); UM 71660 (C) (SC-188, Wyoming, Cf1)]

References: Simpson, 1928; Bown, 1979; Rose, 1981a; Bown and Schankler, 1982; Novacek et al., 1985

†Leptacodon Matthew and Granger, 1921

Species: †Leptacodon dormaalensis (Quinet, 1964) [IRScNB M1239, M1238, uncatalogued specimens (C) (Dormaal, Belgium, Paleocene-Eocene)]

References: Quinet, 1964; Smith, 1996.

†"Leptacodon" munusculum Simpson, 1935a [UALVP specimens (see earlier in the text); uncatalogued UALVP specimens (Gao Mine locality, Alberta, Ti4); AMNH 35941, 35940, 35942, 35951, 35943 (Gidley Quarry, Montana, To2); YPM-PU 14593 (Douglass Quarry, Montana, Ti1)]

References: Simpson, 1935a-b, 1937a; Krishtalka, 1976b; Krause and Gingerich, 1983; Youzwyshyn, 1988; Scott, 2003

†Leptacodon packi Jepsen, 1930 [YPM-PU 14166, 14111, 13296 (holotype) (Princeton Quarry, Wyoming, Ti5); YPM-PU 19486 (Schaff Quarry, Wyoming, Ti5)]

References: Jepsen, 1930; Krishtalka, 1976b; Secord, 2004

†Leptacodon rosei Gingerich, 1987 [UM 71650, 71661, 71662 (C), various SC localities, Wyoming, Cf1]

References: Rose, 1981a; Gingerich, 1987; Bloch, 2001

†Leptacodon tener Matthew and Granger, 1921 [AMNH 17395 (Mason Pocket, Colorado, Ti4)]
References: Simpson, 1935b, 1937a-b; McKenna, 1968; Krishtalka, 1976b; Smith, 1996

†Limaconyssus Gingerich, 1987
Species: †Limaconyssus habrus Gingerich, 1987 [UM 86724 (C) (SC-29, Wyoming, Cf2)]
†Limaconyssus subnuba new species [UALVP specimens (see earlier in the text)]
†Limaconyssus incomperta new species [UALVP specimens (see earlier in the text); uncatalogued UALVP specimens (Gao Mine, Alberta, Ti4)]
References: Gingerich, 1987; Youzwyshyn, 1988

†Litocherus Gingerich, 1983
Species: †Litocherus notissimus Gingerich, 1983 [UALVP specimens (see earlier in the text);
UM 89739-89759, 89761-89768, 89770-89794, 89801-89848, 89850-89853, 89856-89881, UM 89884-89891, 85002 (Scarritt Quarry, Montana, Ti2)
References: Simpson, 1936; Krishtalka, 1976a; Gingerich, 1983; Novacek et al., 1985

†Litolestes Jepsen, 1930
Species: †Litolestes avitodelphus new species [UALVP specimens (see earlier in the text)]
†Litolestes ignotus Jepsen, 1930 [YPM-PU 13352 (holotype), 14164, 21193, 14064, 14168, 14127, 14039, 14037, 13348 (paratype), 14114, 13974, 17679 Princeton Quarry, Wyoming, Ti5); YPM-PU 19362, 19361, 19377, 21182, 19376, 19380, 19378, 19364, 19416 (Schaff Quarry, Wyoming, Ti5)]
References: Jepsen, 1930; Krishtalka, 1976a; Schwartz and Krishtalka, 1976; Novacek et al., 1985; Secord, 2004

†Macrocranion Weitzel, 1949

Species: †Macrocranion vandebroeki (Quinet, 1964) [IRScNB M1808, M1807, M1803, M1805, M1799, M1806, M1802, M1801, M1800, M1804, uncatalogued specimens (C) (Dormaal, Belgium, Paleocene-Eocene)]
†Macrocranion nitens (Matthew, 1918) [YPM-PU 30655, 24380, 23077, 23087, 27941, 30443, 30553, 30597, 30622, 30657, 30654 (various Gray Bull Beds localities, Wyoming, Wasatchian)]
References: Weitzel, 1949; Krishtalka, 1976a; Bown and Schankler, 1982; Novacek et al., 1985; Storch, 1993; Smith and Smith, 1995; Smith, 1996; Storch, 1996; Smith et al., 2002

†Nayloria new genus
Species: †Nayloria albertensis [UALVP 47272, 47273 (Joffre Bridge Road Cut lower level, Alberta, Ti3); UALVP 40525 (holotype), 47258, 47259, 47260, 40502, 47261, 40528, 47262, 47263, 47264, 47265 (DW-2, Alberta, Ti3); UALVP 47266, 47267, 39499 (Birchwood, Alberta, Ti3); UALVP 47268, UALVP 47269-47271 (Hand Hills West upper level, Alberta, Ti3)]

†Nyctitherium Marsh, 1872
Species: †Nyctitherium serotinum (Marsh, 1872) [AMNH 128571, 128630 (C) (Absoroka Range locality, Wyoming, Eocene); YPM-PU 13517 (Grizzly Buttes locality, Wyoming, Eocene)]
†Nyctitherium velox Marsh, 1872 [AMNH 128965 (C), 12377, 128970 (C of YPM-PU 16058), YPM-PU 15257, 15258, 15259, 16056, 15251, 13509, 14936, 13510 (holotype), 14946 (various localities, Wyoming, Eocene)]
References: Matthew, 1909, 1918; McKenna, 1960; Robinson, 1968; Krishtalka, 1976b

†Oncocherus Scott, 2006
Species: †Oncocherus krishtalkai Scott, 2006 [UALVP 43134 (holotype), 43135-43137 (Crestomere School locality, Alberta, Ti4); UALVP 22222, 22223, 22225, 22226, 22228, 22229, 22231-22246, 22329, 22342, 22344, 22347-22349, 22441, 22448, 22449, 22454, 22463, 22469, 22471, 22474, 22480, 22482, 22487, 22493, 22495, 22497, 22500, 22509,

22689-22695, 22703-22705, 22710, 23867, 23869-23880, 23882-23886, 23898, 24251, 24256, 39730, 39744-39747, 39749, 39750 (Swan Hills locality, Alberta, Ti4); UALVP 10858, 43138-43143, 9319, UALVP 9317, 9660 (Roche Percée locality, Saskatchewan, Ti4)]

References: Stonley, 1988; Scott, 2006

†Paranyctoides Fox 1979

Species: †Paranyctoides sternbergi Fox 1979 [UALVP 14822 (holotype), 14823, 2042, 6998, 4271, 6771, 14825 (Irvine locality, Alberta, Judithian)]

†Paranyctoides maleficus Fox 1984 [5573 (holotype), 5520, 5571, 5572, 16174-16173, 16178-16181 (Verdigris Coulee, Alberta, Aquilan)]

References: Fox, 1979, 1984

†Pholidocercus Koenigswald and Storch, 1983

Species: †Pholidocercus hassiacus Koenigswald and Storch, 1983 (Grube Messel, Germany, middle Eocene)

References: Koenigswald and Storch, 1983; MacPhee et al., 1988

†Plagioctenodon Bown 1979

Species: †Plagioctenodon krausae Bown 1979 [UW 9592, 9682 (holotype), 7047 (C) (No Water localities, Wyoming, Wasatchian)]

References: Bown, 1979; Bown and Schankler, 1982; Smith, 1996

†Pontifactor West, 1974

Species: †Pontifactor bestiola West, 1974 [AMNH 15103, 102100 (composite P4-M2), 91792, (various localities, Wyoming, Wasatchian); USGS 10449, 10456 (C) (various localities, Wyoming, Wasatchian); YPM-PU 17671 (C) (unknown locality, Wyoming, Eocene)]

References: West, 1974; Krishtalka, 1976b; Bown and Schankler, 1982

†Psydronyctia new genus

Species: †Psydronyctia smithorum new species [UALVP specimens (see earlier in the text)]

†Saturninia Stehlin, 1940

Species: †Saturninia gracilis Stehlin, 1940 [AMNH 100040 (C) (La Debruge locality Db 592, France, late Eocene)]

References: Stehlin, 1940; Sigé, 1976, 1997; Hooker and Weidmann, 2000; Sigé and Storch, 2001

†Scenopagus McKenna and Simpson, 1959

Species: †Scenopagus curtidens (Matthew, 1909) [AMNH 48183 (Qu88, New Mexico, Eocene); AMNH 113785, (cast of USGS 2026), 113784 (cast of USGS 2002), 12058, 12619, 113787 (cast of USGS 2041), 113786 (cast of USGS 2033) (various localities, Wyoming, Bridgerian); YPM 13610-1A, 1B, 2, 16912, 15255, 16913, 16914 (various localities, Wyoming, Bridgerian)]

†Scenopagus edenensis (McGrew, 1959) [AMNH 55685, Morrow Creek locality, Wyoming, Bridgerian; AMNH 56035 (UCMP locality V-5628, Tabernacle Butte, Wyoming, Eocene)]

References: Matthew, 1909; McKenna and Simpson, 1959; McGrew, 1959; Robinson, 1966b; Krishtalka, 1976a

†Sespedectes Stock, 1935

Species: †Sespedectes sp., cf. S. singularis [AMNH 129001 (cast of UCMP 85681), 129004 (cast of UCMP 99048), 129002 (cast of UCMP 96144), 129005 (cast of UCMP 99357), 128922 (cast of LACM 5200), 128921 (cast of LACM 5197) (various localities, California, Eocene)]

References: Novacek, 1985; Walsh, 1998

†Wyonycteris Gingerich, 1987

Species: †Wyonycteris chalix Gingerich, 1987 [UM 76910 (holotype), 76917 (SC-29, Wyoming, Cf3)]

†Wyonycteris richardi Smith, 1995 [IRScNB M1809 (holotype), M35, M1809-M1813, uncatalogued specimens (Dormaal, Belgium, Paleocene-Eocene)]
References: Gingerich, 1987; Smith, 1995; Bloch, 2001

Xynolestes new genus
Species: Xynolestes denommei new species [UALVP specimens (see earlier in the text)]

5.8 Appendix 3.—Data Matrix

A=0,1; B=0,2; C=0,3; D=0,1,2; E=1,2; F=1,3; G=2,3. Character numbers correspond to those described in the text. Figures at the end of each scoring sequence are number of scored states (excluding question marks or hyphens) and completeness (=number of scored states/98).

Kennalestes	0000100100 0100100020 0001000000 01010-0001 1?00?00002 02002--0-3 1000000000 0100000000 A000000000 00000000; 92, 94%
Cimolestes	0??0000100 0A00002E20 1011000000 00000-0101 ?????00000 12AA0000-G 0000A40000 0000000000 0000100101 00000100; 89, 91%
Prodiacodon	0100000001 030011012A 00A1000010 0102100101 0111110000 10A0020300 1F01A10000 0100000000 0000000100 00000000; 98, 100%
Crocidura	0110012292 0011202221 2F132A0211 1003103900 114???1??? ????2299093 9020201000 0022002102 A0A1110012 20012129; 89, 91%
Adapisorex	0??10?0A0A 220A102212 1F11001012 1AA230A011 ?????10100 10E2101110 1G01212220 1101211022 0001020000 1000E012; 90, 92%
"Adapisorella"	0001???10E 02001A2212 1111001011 1112210111 1????00002 10121EA210 1301212220 1101201022 0001020000 10001012; 91, 93%
Echinosorex	0111101102 20122022A2 3313000012 1102312210 0110100102 0202003103 00B0A12110 0122110012 1011021009 30122029; 98, 100%
Leptacodon tener	???0010111 0210112221 1012000011 12A21A0001 10????000? 0000020200 1100111110 0001001101 B001020001 00011000; 90, 92%
Leptacodon munusculum	00?0??0002 0E10102221 1012000011 110110000E ??20110000 0010020111 0110121100 0000000000 2101A10001 000000A0; 93, 95%

Leptacodon dormaalensis	???0?????1 0210102221 1012000011 1102100000 ?????0000? ???0010200 1100111100 0001001000 0001010001 00001000; 81, 83%
Leptacodon rosei	???0?????2 0210102221 1012000011 110210000A ??31110000 2010012200 111A111100 0001001000 000101000A 00000000; 88, 90%
Leptacodon packi	?0?0??0??2 0110102221 1012000011 1101A00001 ??????0000 00000A02A0 0110E11100 000A000001 0001010001 00000001; 86, 88%
Asionyctia	???0?????2 0010102201 1012000011 1102100001 ?????1001? 12001100-2 0000131100 0100000100 0001000001 00000000; 83, 85%
Batodon	???0?????1 0A10002221 1002000001 11010-0001 ?????00000 1000000202 1000200000 0100000000 0?00000?0 00000000; 82, 84%
Centetodon	2010110101 0010102221 A003000011 110E100B0E 112010A000 00000A0202 1A00220000 0000000000 A101000110 00001000; 98, 100%
Limaconyssus	???0?????? ?????????? ?????????? ?????????? ?????01000 11100202A2 1C00210000 0000B00000 0101000110 00101100; 54, 55%
Cryptotopos	11?0???10E 0211201E21 2213000011 1113101000 ????11000A A0000AB200 11101F1100 0000000000 310101A000 00000001; 90, 92%
Saturninia	01?0???10E 0211212221 1012000001 110G10C100 113111000A E00B0AB200 1C00E11100 0000000000 000100B11A 00100A01; 94, 96%
Euronyctia	???0?????2 02112012B1 22A3EA0112 1003101000 ??3?01000A 0002002210 1E11131100 0000201101 3101010012 00102111; 87, 89%
Psydronyctia	11?0??0002 0211201221 2213100112 1003101001 ?????11002 0110020210 1101211100 0000200000 3101010112 00001011; 90, 92%

Nyctitherium	00?0??0?01 0201212221 00A2AA0A11 120310000A ????200000 1?00010200 1100231100 0000000000 B1A1100001 00100001; 88, 90%
Amphidozotherium	?1?0??0??2 0111201221 2203100A02 1003101100 1132010110 3200000100 10002G1100 0000200000 2101000110 00102111; 92, 94%
Litocherus	00010A0A0A 10001A2211 1111000011 111E200001 11?11A0A00 1BA10DAA1E 1EA0E12120 11010A1000 0001020001 10A11001; 97, 99%
Nayloria	0001???001 0??0112211 1111000011 1112200?1 ??2010010B 1111021E12 0GA0232120 1101200100 2001030001 10011001; 90, 92%
Diacocherus	1001010000 AE20102212 FA10000011 1EA2E00002 1011110010 01A00E0210 1200110100 1100010000 0000011001 00000000; 98, 100%
Scenopagus	?0?0???101 0012302211 101A000011 1102310001 ?????10112 2B02101112 0000111101 0010010102 1000121000 10001000; 88, 90%
Xynolestes	00?0??0001 0110102211 1011000011 1212200002 ??20110010 EA1002A112 0110231100 0000000110 G101120001 00011001; 93, 95%
Wyonycteris	???0?????? ??????????1 22A3210111 01A2100000 ??????000? 2202000112 A1011F1100 0000000001 G10111001E 00011011; 73, 75%
Sespedectes	20?2111100 1010302212 1111000011 1002302G01 ?????10112 0200102113 0020A02220 1100010000 1000121000 11001010; 92, 94%
Pontifactor	?0?0??0102 0010302211 3102210012 011121000? ?????????? ?????????? ?????????? ?????????? ?????????? ????????; 35, 36%
Pholidocercus	0002011110 1020302212 3310010010 1102300G12 2111210110 20000??112 0000112220 1011010001 0001021000 10000000; 96, 98%

Paranyctoides ???0?????? ??????????0 0002010011 01010-00?? ??????????
???20000-E 1000011000 0000B0000A 0001010000 00100000;
63, 64%

Oncocherus 0??1???002 1100102211 1111000011 1112200001 ?????00100
1BA01A111G 0C00112120 0101201110 0001020001
10022001; 88, 90%

Macrocranion 0001000100 1000302212 101A000011 1002310001
??10110110 G200001112 0B00E12221 0011010101
0001AG100A 11000000; 96, 98%

Litolestes 0??1??0101 00A0102211 1111000011 1E12200001
1131110100 1BA11D1E12 0B00222120 0001A01010
00A102A001 10022001; 94, 96%

Leipsanolestes ???1?????? ?????????? ?????????? ?????????? ??????0???
???011011A 1200212120 0001010111 1001021000 10011001;
47, 48%

Entomolestes ???0?????? ?????????? ?????????? ?????????? ??????0110
121201021D 00201A2210 0002102111 1001131002 00011011;
55, 56%

Dartonius ???0?????? ?????????? ?????????? ?????????? ??????011?
1002122101 0000111100 0100000010 0001021001 1011????;
48, 49%

Ceutholestes ???0?????? ?????????? ?????????? ?????????1 ??31110000
1020022304 1111010101 0110010100 0002010012 00101011;
58, 59%

Adeloxenus ???1?????? ?????????? ?????????? ?????????? ???1000100
1010112201 1E01112110 0101001000 0001010000 10001012;
56, 57%

Cedrocherus ???1?????? ?????????? ?????????? ?????????? ??????010?
1210110102 0111112020 0101211010 0001131001 10022001;
52, 53%

Plagioctenodon ???0?????? ?????????? ?????????? ?????????? ??????0011
E110122200 111121110? 0100000000 0101021011 00000001;
52, 53%

5.9 Appendix 4.—Apomorphy Lists

The list of apomorphies applies to each of the numbered nodes on the preferred cladogram as illustrated in Figure 5.60. The character number is followed by a brief character description in parentheses, and then the transformation from one state to another. A solid arrow (➡) represents an unequivocal transformation, occurring in both ACCTRAN and DELTRAN optimizations. An outline arrow (⇨) represents an equivocal transformation that occurs in either ACCTRAN (A) or DELTRAN (D) optimizations, but not in both.

Kennalestes → node 1

5 (upper canine roots) 1➡0
12 (P4 metacone) 1⇨0 (A)
17 (P4 paraconule) 0⇨2 (A)
18 (P4 metaconule size) 0➡1
21 (ectoflexus on M1-2) 0⇨1 (A)
38 (conular cristae) 0⇨1 (A)
43 (i1 crown) 0⇨1 (A)
50 (size of p2) 2➡0
51 (size of p3) 0➡1
55 (origin of p4 paraconid) 2➡0
60 (width of p4 talonid basin) 3⇨2 (A)
65 (posterior exodaenodonty on p4) 0⇨1 (A)
66 (contact of p4 cristid obliqua and postvallid wall) 0⇨1 (A)
88 (molar hypoconid height) 0➡1

node 1 → Cimolestes

15 (P4 posterior cingulum) 1➡0
17 (P4 paraconule) 0⇨2 (D)
21 (ectoflexus on M1-2) 0⇨1 (D)
23 (molar stylocone) 0➡1
32 (molar anterior cingulum) 1➡0
34 (posterior cingulum on M1-2) 1➡0
38 (conular cristae) 0⇨1 (D)
61 (length of p4 talonid basin) 1➡0
66 (contact of p4 cristid obliqua and postvallid wall) 1⇨4 (A)
72 (molar paraconid origin) 1➡0
85 (molar postcristid) 0➡1
91 (hypoconulid position on m1-2) 0➡1
96 (width of m3 talonid) 0➡1

node 1 → node 2

10 (P4 labial margin) 0➡1
20 (anterior stylar shelf on M1-2) 0⇨1 (A)
29 (separateness of molar paracone and metacone) 0⇨1 (A)
35 (hypocone on M1-2) 0⇨1 (A)
52 (paraconid on p3) 2➡0
58 (metaconid on p4) 0➡2

node 2 → Prodiacodon

2 (position of the infraorbital foramen) 0➡1
8 (P3 metacone) 1➡0
12 (P4 metacone), 0⇨3 (A) 1⇨3 (D)
16 (P4 anterior cingulum) 0➡1
17 (P4 paraconule) 2⇨0 (A)
21 (ectoflexus on M1-2) 1⇨0 (A)
29 (separateness of molar paracone and metacone) 0⇨1 (D)
34 (posterior cingulum on M1-2) 1➡2
35 (hypocone on M1-2) 0⇨1 (D)
38 (conular cristae) 0⇨1 (D)
41 (angular process size and shape) 1➡0
43 (i1 crown) 0⇨1 (D)
44 (size of i2) 0➡1
46 (lower canine) 0➡1
56 (development of p4 paraconid) 0➡2
58 (metaconid on p4) 2➡3
60 (width of p4 talonid basin) 2⇨0 (A), 3⇨0 (D)
62 (position of p4 entoconid) 0➡(1&3)
64 (size of p4 hypoconulid) 0➡1
66 (contact of p4 cristid obliqua and postvallid wall) 0⇨1 (D)

node 2 → node 3

6 (upper canine morphology) 0⇨1 (A)
13 (P4 postcrista) 0➡1
17 (P4 paraconule) 0⇨2 (D)
18 (P4 metaconule) 1➡2
20 (anterior stylar shelf on M1-2) 0⇨1 (D)
24 (postmetacrista on M1-2) 1➡2
30 (position of molar protocone) 0➡1
31 (size of molar protocone) 0➡1
38 (conular cristae) 1⇨0 (A)
43 (i1 crown) 1⇨2 (A)
60 (width of p4 talonid basin) 3⇨2 (D)

65 (posterior exodaenodonty on p4) 1⇨2 (A), 0⇨1 (D)

node 3 → Batodon

15 (P4 posterior cingulum) 1➡0
21 (ectoflexus on M1-2) 0⇨1 (D)
29 (separateness of molar paracone and metacone) 1⇨0 (A)
35 (hypocone on M1-2) 1⇨0 (A)
66 (contact of p4 cristid obliqua and postvallid wall) 1⇨0 (A)

node 3 → node 4

6 (upper canine morphology) 0⇨1 (D)
12 (P4 metacone) 1⇨0 (D)
29 (separateness of molar paracone and metacone) 0⇨1 (D)
35 (hypocone on M1-2) 0⇨1 (D)
43 (crown of i1) 0⇨2 (D)
66 (contact of p4 cristid obliqua and postvallid wall) 0⇨1 (D)
72 (molar paraconid origin) 1➡0
84 (molar entocristid notch) 0➡1

node 4 → node 5

1 (anterior root of zygomatic arch) 0⇨2 (A)
3 (extent of jugal on maxilla) 0⇨1 (A)
5 (upper canine roots) 0⇨1 (A)
24 (postmetacrista on M1-2) 2⇨3 (A)
47 (premolar lingual cingulids) 0⇨1 (A)
65 (posterior exodaenodonty on p4) 1⇨2 (D)
82 (molar cristid obliqua shape) 0➡1
89 (anteroposterior compression of molar hypoconid and protoconid) 0➡1
95 (size of m3) 0➡1

node 5 → Centetodon

1 (anterior root of zygomatic arch) 0⇨2 (D)
3 (extent of jugal on maxilla) 0⇨1 (D)
5 (upper canine roots) 0⇨1 (D)
24 (postmetacrista on M1-2) 2⇨3 (D)
51 (size of p3) 1➡0
66 (contact of p4 cristid obliqua and postvallid wall) 1➡2

node 5 → Limaconyssus

47 (premolar lingual cingulids) 0⇨1 (D)
52 (paraconid on p3) 0➡1

53 (talonid on p3) 0➡1
56 (development of p4 paraconid) 0➡2
93 (posterior cingulid) 0➡1
96 (width of m3 talonid) 0➡1

node 4 → node 6

10 (P4 labial margin) 1➡2
19 (P4 postprotocrista) 2⇨1 (A)
46 (lower canine) 0⇨1 (A)
58 (metaconid on p4), 2➡1
59 (position of p4 metaconid), 0⇨1 (A)
65 (posterior exodaenodonty on p4) 2⇨1 (A)
67 (height of molar trigonid) 0➡1
86 (molar entoconid height) 0⇨1 (A)
88 (molar hypoconid height) 1➡0

node 6 → node 7

15 (P4 posterior cingulum) 1⇨3 (A)
21 (ectoflexus on M1-2) 1⇨0 (A)
26 (molar mesostyle) 0➡1
31 (size of molar protocone) 1➡0
36 (molar hypocone crest) 0⇨1 (A)
54 (size of p4) 0⇨2 (A)
58 (metaconid on p4) 1⇨0 (A)
65 (posterior exodaenodonty on p4) 1⇨0 (A)
93 (posterior cingulid) 0⇨1 (A)

node 7 → Pontifactor

15 (P4 posterior cingulum) 1⇨3 (D)
19 (P4 postprotocrista) 2⇨1 (D)
21 (ectoflexus on M1-2) 0➡2
22 (parastylar lobe on M1) 0➡1
25 (molar centrocrista) 0➡2
30 (position of molar protocone) 1➡2
33 (molar pericone) 0➡1
35 (hypocone on M1-2) 1➡2
36 (molar hypocone crest) 0⇨1 (D)

node 7 → Paranyctoides

20 (anterior stylar shelf on M1-2) 1➡0
35 (hypocone on M1-2) 1➡0
54 (size of p4) 0⇨2 (D)

58 (metaconid on p4) 1⇨0 (D)
65 (posterior exodaenodonty on p4) 1⇨0 (D)
86 (molar entoconid height) 0⇨1 (D)
93 (posterior cingulid) 0⇨1 (D)

node 6 → node 8

8 (P3 metacone) 1⇨0 (A)
21 (ectoflexus on M1-2) 0⇨1 (D)
23 (molar stylocone) 0➡1
46 (lower canine) 0⇨1 (D)
56 (development of p4 paraconid) 0➡1
61 (length of p4 talonid basin) 1➡0 (A)
68 (inclination of molar trigonid) 0➡1
91 (hypoconulid position on m1-2) 0➡1

node 8 → node 9

34 (posterior cingulum on M1-2) 1➡2
49 (p2-3 crowns) 0➡1
52 (paraconid on p3) 0⇨2 (A)
72 (molar paraconid origin) 0➡1
86 (molar entoconid height) 1⇨0 (A)

node 9 → Asionyctia

19 (P4 postprotocrista) 1⇨0 (A), 2⇨0 (D)
52 (paraconid on p3) 0⇨2 (D)
55 (origin of p4 paraconid) 0➡1
58 (metaconid on p4) 1➡0
66 (contact of p4 cristid obliqua and postvallid wall) 1➡3
78 (talonid dimensions on m1-2) 0➡1

node 9 → node 10

10 (P4 labial margin) 2➡1
19 (P4 postprotocrista) 2⇨1 (D)
24 (postmetacrista on M1-2) 2⇨0 (A)
35 (hypocone on M1-2) 1➡2
56 (development of p4 paraconid) 1⇨2 (A)
57 (position of p4 paraconid) 0⇨1 (A)
59 (position of p4 metaconid) 0⇨1 (D)
86 (molar entoconid height) 0➡2

node 10 → node 11

4 (principal cusps) 0➡1
10 (P4 labial margin) 1➡0
11 (P4 parastylar lobe) 0⇨1 (A)
13 (P4 postcrista) 1⇨2 (A)
20 (anterior stylar shelf on M1-2) 1➡2
24 (postmetacrista on M1-2) 2⇨0 (D)
43 (crown of i1) 2➡1
51 (size of p3) 1➡0
71 (molar metaconid size) 0⇨1 (A)
76 (form of the m2-3 paraconid/paracristid) 0➡1
84 (molar entocristid notch) 1⇨0 (A)
87 (entoconid position on m1 and m2) 0➡1

node 11 → Diacocherus

1 (anterior root of zygomatic arch) 0➡1
8 (P3 metacone) 1⇨0 (D)
12 (P4 metacone) 0➡1&2
13 (P4 postcrista) 1⇨2 (D)
40 (number of mental foramina) 1➡2
42 (condyle shape) 1➡0
44 (size of i2) 0➡1
52 (paraconid on p3) 2⇨1 (A), 0⇨1 (D)
57 (position of p4 paraconid) 1⇨0 (A)
58 (metaconid on p4) 1➡2
60 (width of p4 talonid basin) 2➡0
61 (length of p4 talonid basin) 0➡1
62 (position of p4 entoconid) 0➡2
67 (height of molar trigonid) 1➡0
71 (molar metaconid size) 0⇨1 (D)
84 (molar entocristid notch) 2⇨1 (D)
86 (molar entoconid height) 2➡1

node 11 → node 12

7 (P2 roots) 0⇨1 (A)
8 (P3 metacone) 0⇨1 (A)
15 (P4 posterior cingulum) 1➡3
35 (hypocone on M1-2) 2➡3
38 (conular cristae) 0⇨2 (A)
41 (angular process size and shape) 1⇨0 (A)
48 (dimensions of p1-3) 0➡1
56 (development of p4 paraconid) 2➡0
57 (position of p4 paraconid) 0⇨1 (D)
67 (height of molar trigonid) 1➡2
68 (inclination of molar trigonid) 1⇨2 (A)

69 (valley facing sides of trigonid cusps) 0⇨2 (A)
73 (form of the m1 paraconid/paracristid) 0⇨1 (A)
90 (hypoconulid size and height on m1-2) 0➡1
91 (hypoconulid position on m1-2) 1➡0

node 12 → node 13

11 (P4 parastylar lobe) 0⇨1 (D)
41 (angular process size and shape) 0⇨2 (A)
51 (size of p3) 0➡2
68 (inclination of molar trigonid) 1⇨2 (D)
69 (valley facing sides of trigonid cusps) 0⇨2 (D)
72 (molar paraconid origin) 1➡0
73 (form of the m1 paraconid/paracristid) 0⇨1 (D)
74 (shape of m1 paracristid) 0➡1
80 (talonid width on m1-2) 0➡1
84 (molar entocristid notch) 0⇨1 (A)

node 13 → Macrocranion

6 (upper canine morphology) 1➡0
7 (P2 roots) 1⇨0 (A)
13 (P4 postcrista) 2⇨0 (A), 1⇨0 (D)
32 (molar anterior cingulum) 1➡0
36 (molar hypocone crest) 0➡1
38 (conular cristae) 2⇨0 (A)
52 (paraconid on p3) 0⇨2 (D)
70 (molar metaconid height) 0➡1
71 (molar metaconid size) 1⇨0 (A)
78 (molar talonid basin) 0➡1
92 (anterior cingulid) 0➡1

node 13 → Pholidocercus

4 (principal cusps) 1➡2
7 (P2 roots) 0⇨1 (D)
9 (P3 protocone) 0➡1
13 (P4 postcrista) 1⇨2 (D)
21 (ectoflexus on M1-2) 1➡3
22 (parastylar lobe on M1) 0➡3
26 (molar mesostyle) 0➡1
30 (position of molar protocone) 1➡0
38 (conular cristae) 0⇨23 (D)
39 (parastylar lobe on M3) 0➡1
40 (number of mental foramina) 1➡2
41 (angular process size and shape) 1⇨2 (D)

44 (size of i2) 0➡1
45 (size of i3) 1➡2
52 (paraconid on p3) 2⇨0 (A)
71 (molar metaconid size) 0⇨1 (D)

node 12 → node 14

3 (extent of jugal on maxilla) 0⇨1 (A)
5 (upper canine roots) 0➡1
7 (P2 roots) 0⇨1 (D)
13 (P4 postcrista) 2⇨1 (A)
24 (postmetacrista on M1-2) 0⇨1 (A)
37 (conules on M1-2) 0⇨2 (A)
50 (size of p2) 0➡2
52 (paraconid on p3) 0⇨2 (D)
55 (origin of p4 paraconid) 0⇨1 (A)
60 (width of p4 talonid basin) 2⇨3 (A)
81 (cristid obliqua position) 0➡1
85 (molar postcristid) 0⇨1 (A)
95 (size of m3) 0➡1

node 14 → Sespedectes

1 (anterior root of zygomatic arch) 0➡2
4 (principal cusps) 1➡2
11 (P4 parastylar lobe) 0⇨1 (D)
22 (parastylar lobe on M1) 0➡1
24 (postmetacrista on M1-2) 0⇨1 (D)
32 (molar anterior cingulum) 1➡0
37 (conules on M1-2) 0⇨2 (D)
38 (conular cristae) 0⇨23 (D)
55 (origin of p4 paraconid) 0⇨1 (D)
57 (position of p4 paraconid) 1➡2
60 (width of p4 talonid basin) 2⇨3 (D)
63 (size of p4 hypoconid) 0➡2
66 (contact of p4 cristid obliqua and postvallid wall) 1➡0
68 (inclination of molar trigonid) 1⇨2 (D)
69 (valley facing sides of trigonid cusps) 0⇨2 (D)
71 (molar metaconid size) 0⇨1 (D)
73 (form of the m1 paraconid/paracristid) 1⇨0 (A)
84 (molar entocristid notch) 1⇨0 (D)
85 (molar postcristid) 0⇨1 (D)
92 (molar anterior cingulid) 0➡1
97 (position of m3 hypoconulid) 0➡1

node 14 → node 15

6 (upper canine morphology) 1⇨0 (A)
10 (P4 labial margin) 0➡1
11 (P4 parastylar lobe) 1⇨0 (A)
14 (P4 hypocone) 0➡2
36 (molar hypocone crest) 0➡1
68 (inclination of molar trigonid) 2⇨1 (A)
69 (valley facing sides of trigonid cusps) 2⇨0 (A)
71 (molar metaconid size) 1⇨0 (A)
80 (talonid width on m1-2) 0➡2

node 15 → Scenopagus

20 (anterior stylar shelf on M1-2) 2➡1
37 (conules on M1-2) 2⇨0 (A)
38 (conular cristae) 2⇨0 (A)
51 (size of p3) 0➡2
54 (size of p4) 0➡2
55 (origin of p4 paraconid) 0⇨1 (D)
60 (width of p4 talonid basin) 3⇨2 (A)
67 (height of molar trigonid) 2➡1
70 (molar metaconid height) 0➡1
72 (molar paraconid origin) 1➡0
73 (form of the m1 paraconid/paracristid) 0⇨1 (D)
78 (talonid dimensions on m1-2) 0➡1
84 (molar entocristid notch) 1⇨0 (D)
85 (molar postcristid) 0⇨1 (D)

node 15 → Echinosorex

2 (position of the infraorbital foramen) 0➡1
3 (extent of jugal on maxilla) 0⇨1 (D)
6 (upper canine morphology) 1⇨0 (D)
10 (P4 labial margin) 1➡2
11 (P4 parastylar lobe) 0➡2
15 (P4 posterior cingulum) 3➡2
21 (ectoflexus on M1-2) 1➡3
22 (parastylar lobe on M1) 0➡3
24 (postmetacrista on M1-2) 1➡3
30 (position of molar protocone) 1➡2
37 (conules on M1-2) 0⇨2 (D)
38 (conular cristae) 0⇨2 (D)
39 (parastylar lobe on M3) 0➡1
40 (number of mental foramina) 1➡0
41 (angular process size and shape) 1⇨0d
46 (lower canine) 1➡0

49 (p2-3 crowns) 1➡0
55 (origin of p4 paraconid) 1⇨0 (A)
57 (position of p4 paraconid) 1➡3
59 (position of p4 metaconid) 1➡0
60 (width of p4 talonid basin) 2⇨3 (D)
69 (valley facing sides of trigonid cusps) 0⇨1 (A)
73 (form of the m1 paraconid/paracristid) 1⇨2 (A)
74 (shape of m1 paracristid) 0➡2
75 (position of m1 metaconid) 0➡1
79 (molar talonid basin) 0➡1
83 (molar ectocingulid) 0➡1
84 (molar entocristid notch) 0⇨1 (A)
85 (molar postcristid) 1⇨0 (A)
90 (hypoconulid size and height on m1-2) 1➡0
93 (molar posterior cingulid) 0➡1
94 (size of m2) 0➡2
95 (size of m3) 1➡2
97 (position of m3 hypoconulid) 0➡2

node 10 → node 16

24 (postmetacrista on M1-2) 0⇨1 (A), 2⇨1 (D)
33 (molar pericone) 0➡1
52 (paraconid on p3) 2⇨0 (A)
53 (talonid on p3) 0⇨1 (A)
65 (posterior exodaenodonty on p4) 1⇨2 (A)
79 (molar talonid basin) 0➡1
94 (size of m2) 0➡1
95 (size of m3) 0➡1
98 (size and form of m3 hypoconulid) 0➡1

node 16 → Xynolestes

8 (P3 metacone) 1⇨0 (D)
12 (P4 metacone) 0➡1
32 (molar anterior cingulum) 1➡2
40 (number of mental foramina) 1➡2
53 (talonid on p3) 0⇨1 (D)
56 (development of p4 paraconid) 1⇨2 (D)
62 (position of p4 entoconid) 0➡1
63 (size of p4 hypoconid) 0➡1
65 (posterior exodaenodonty on p4) 1⇨2 (D)
66 (contact of p4 cristid obliqua and postvallid wall) 1➡3
72 (molar paraconid origin) 1➡0
78 (talonid dimensions on m1-2) 0➡1

81 (cristid obliqua position) 0➡2&3
82 (molar cristid obliqua shape) 0➡1
85 (molar postcristid) 0➡1

node 16 → node 17

13 (P4 postcrista) 1⇨0 (A)
22 (parastylar lobe on M1) 0⇨1 (A)
44 (size of i2) 0⇨1 (A)
46 (lower canine) 1⇨0 (A)
48 (dimensions of p1-3) 0➡1
55 (origin of p4 paraconid) 0➡1
90 (hypoconulid size and height on m1-2) 0➡1

node 17 → Dartonius

53 (talonid on p3) 1⇨0 (A)
54 (size of p4) 0➡2
56 (development of p4 paraconid) 1⇨2 (D)
57 (position of p4 paraconid) 1⇨2 (A), 0⇨2 (D)
59 (position of p4 metaconid) 1➡0
60 (width of p4 talonid basin) 2➡1
65 (posterior exodaenodonty on p4) 2⇨1 (A)
87 (molar entoconid position on m1 and m2) 0➡1
93 (molar posterior cingulid) 0➡1

node 17 → node 18

4 (principal cusps) 0➡1
13 (P4 postcrista) 1⇨0 (D)
22 (parastylar lobe on M1) 0⇨1 (D)
44 (size of i2) 0⇨1 (D)
49 (p2-3 crowns) 1➡0
53 (talonid on p3) 0⇨1 (D)
56 (development of p4 paraconid) 2⇨1 (A)
67 (height of molar trigonid) 1➡2
69 (valley facing sides of trigonid cusps) 0➡2
74 (shape of m1 paracristid) 0➡1
77 (m2-3 paracristid/paraconid shape) 0⇨1 (A)

node 18 → node 19

43 (crown of i1) 2⇨3 (A)
52 (paraconid on p3) 0⇨2 (A)
77 (m2-3 paracristid/paraconid shape) 0⇨1 (D)
94 (size of m2) 1➡2

95 (size of m3) 1➡2

node 19 → Litolestes

8 (P3 metacone) 0⇨1 (A)
43 (crown of i1) 2⇨3 (D)
46 (lower canine) 0⇨1 (A)
54 (size of p4) 0➡1
57 (position of p4 paraconid) 0⇨1 (D)
65 (posterior exodaenodonty on p4) 1⇨2 (D)
66 (contact of p4 cristid obliqua and postvallid wall) 1➡2
72 (molar paraconid origin) 1➡0

node 19 → node 20

10 (P4 labial margin) 1⇨2 (A)
11 (P4 parastylar lobe) 0⇨1 (A)
12 (P4 metacone) 0⇨1 (A)
65 (posterior exodaenodonty on p4) 2⇨1 (A)
75 (position of m1 metaconid) 0➡2

node 20 → Oncocherus

8 (P3 metacone) 1⇨0 (D)
10 (P4 labial margin) 1⇨2 (D)
11 (P4 parastylar lobe) 0⇨1 (D)
12 (P4 metacone) 0⇨1 (D)
46 (lower canine) 1⇨0 (D)
57 (position of p4 paraconid) 0⇨1 (D)
78 (talonid dimensions on m1-2) 0➡1

node 20 → Cedrocherus

52 (paraconid on p3) 0⇨2 (D)
57 (position of p4 paraconid) 1⇨0 (A)
59 (position of p4 metaconid) 1➡0
62 (position of p4 entoconid) 0➡1
63 (size of p4 hypoconid) 0➡1
64 (size of p4 hypoconulid) 0➡1
68 (inclination of molar trigonid) 1➡0
76 (form of the m2-3 paraconid/paracristid) 0➡1
85 (molar postcristid) 0➡1
86 (molar entoconid height) 2➡3
87 (molar entoconid position on m1 and m2) 0➡1

node 18 → node 21

46 (lower canine) 1⇨0 (D)
61 (length of p4 talonid basin) 0⇨1 (A)
62 (position of p4 entoconid) 0➡2
65 (posterior exodaenodonty on p4) 1⇨2 (D)
79 (molar talonid basin) 0⇨1 (A)

node 21 → node 22

16 (P4 anterior cingulum) 0⇨1 (A)
54 (size of p4) 0➡1
55 (origin of p4 paraconid) 1➡0
56 (development of p4 paraconid) 1⇨2 (A)
71 (molar metaconid size) 0➡1
79 (molar talonid basin) 1⇨0 (D)

node 22 → Nayloria

8 (P3 metacone) 1⇨0 (D)
16 (P4 anterior cingulum) 0⇨1 (D)
44 (size of i2) 1➡0
52 (paraconid on p3) 0➡1
56 (development of p4 paraconid) 1⇨2 (D)
61 (length of p4 talonid basin) 1⇨0 (A)
66 (contact of p4 cristid obliqua and postvallid wall) 1➡3
75 (position of m1 metaconid) 0➡2
77 (m2-3 paracristid/paraconid shape) 1⇨0 (A)
78 (talonid dimensions on m1-2) 0➡1
81 (cristid obliqua position) 0➡2
86 (molar entoconid height) 2➡3

node 22 → Litocherus

11 (P4 parastylar lobe) 0➡1
61 (length of p4 talonid basin) 0⇨1 (D)
77 (m2-3 paracristid/paraconid shape) 0⇨1 (D)

node 21 → node 23

8 (P3 metacone) 0⇨1 (A)
12 (P4 metacone) 0⇨2 (A)
20 (anterior stylar shelf on M1-2) 1⇨2 (A)
27 (size of paracone on M1-2) 0⇨1 (A)
39 (parastylar lobe on M3) 0⇨1 (A)
45 (size of i3) 1⇨0 (A)
60 (width of p4 talonid basin) 2➡0
61 (length of p4 talonid basin) 0⇨1 (D)

91 (hypoconulid position on m1-2) 1➡0

node 23 → Leipsanolestes

57 (position of p4 paraconid) 1⇨0 (A)
72 (molar paraconid origin) 1➡0
76 (form of the m2-3 paraconid/paracristid) 0➡1
77 (m2-3 paracristid/paraconid shape) 1⇨0 (A)
78 (talonid dimensions on m1-2) 0➡1
79 (molar talonid basin) 0⇨1 (A)
80 (talonid width on m1-2) 0➡1
81 (cristid obliqua position) 0➡1
87 (entoconid position on m1 and m2) 0➡1

node 23 → node 24

58 (metaconid on p4) 1⇨2 (A)
64 (size of p4 hypoconulid) 0➡1
68 (inclination of molar trigonid) 1➡2
77 (m2-3 paracristid/paraconid shape) 0⇨1 (D)
94 (size of m2) 1➡0
97 (position of m3 hypoconulid) 0➡1
98 (size and form of m3 hypoconulid) 1➡2

node 24 → Adeloxenus

45 (size of i3) 10 (D)
57 (position of p4 paraconid) 12 (A)
58 (metaconid on p4) 1⇨2 (D)
59 (position of p4 metaconid) 1➡0
60 (width of p4 talonid basin) 0➡1
65 (posterior exodaenodonty on p4) 2➡1
69 (valley facing sides of trigonid cusps) 2➡1
79 (molar talonid basin) 1⇨0 (D)
86 (molar entoconid height) 2➡1

node 24 → node 25

12 (P4 metacone) 0⇨2 (D)
20 (anterior stylar shelf on M1-2) 1⇨2 (D)
27 (size of paracone on M1-2) 0⇨1 (D)
39 (parastylar lobe on M3) 0⇨1 (D)
54 (size of p4) 0➡2
62 (position of p4 entoconid) 2⇨3 (A)
68 (inclination of molar trigonid) 1⇨2 (D)
71 (molar metaconid size) 0➡1

75 (position of m1 metaconid) 0➡2
79 (molar talonid basin) 0⇨2 (A), 1⇨2 (D)
80 (talonid width on m1-2) 0➡2

node 25 → "Adapisorella"

36 (molar hypocone crest) 0➡1
38 (conular cristae) 0➡1
48 (dimensions of p1-3) 1➡0
50 (size of p2) 0➡2
58 (metaconid on p4) 1⇨2 (D)
62 (position of p4 entoconid) 2⇨3 (D)

node 25 → Adapisorex

11 (P4 parastylar lobe) 0➡2
30 (position of molar protocone) 1➡2
35 (hypocone on M1-2) 2➡3
46 (lower canine) 0➡1
56 (development of p4 paraconid) 1➡0
57 (position of p4 paraconid) 0⇨1 (D)
58 (metaconid on p4) 2⇨1 (A)
76 (form of the m2-3 paraconid/paracristid) 0➡1

node 8 → node 26

12 (P4 metacone) 0➡1
19 (P4 postprotocrista) 1⇨2 (A)
51 (size of p3) 1➡0
60 (width of p4 talonid basin) 2⇨0 (A)
62 (position of p4 entoconid) 0➡1
63 (size of p4 hypoconid) 0➡1
86 (molar entoconid height) 0⇨1 (D)

node 26 → Leptacodon munusculum

8 (P3 metacone) 1⇨0 (D)
53 (talonid on p3) 0➡1
56 (development of p4 paraconid) 1➡2
59 (position of p4 metaconid) 0⇨1 (D)
60 (width of p4 talonid basin) 0⇨1 (A), 2⇨1 (D)
66 (contact of p4 cristid obliqua and postvallid wall) 1➡2
81 (cristid obliqua position) 0➡2
82 (molar cristid obliqua shape) 0➡1

node 26 → node 27

8 (P3 metacone) 0⇨1 (A)
43 (crown of i1) 2⇨3 (A)
44 (size of i2) 0⇨1 (A)
58 (metaconid on p4) 1➡2
59 (position of p4 metaconid) 1⇨0 (A)
60 (width of p4 talonid basin) 2⇨0 (D)
98 (size and form of m3 hypoconulid) 0⇨1 (A)

node 27 → Leptacodon packi

80 (talonid width on m1-2) 0➡1
98 (size and form of m3 hypoconulid) 0⇨1 (D)

node 27 → node 28

2 (position of the infraorbital foramen) 0⇨1 (A)
12 (P4 metacone) 1➡2
34 (posterior cingulum on M1-2) 1➡2
40 (number of mental foramina) 1⇨0 (A)
43 (crown of i1) 2⇨3 (D)
44 (size of i2) 0⇨1 (D)
61 (length of p4 talonid basin) 0➡1

node 28 → node 29

9 (P3 protocone) 0⇨1 (A)
42 (condyle shape) 1⇨0 (A)
74 (shape of m1 paracristid) 0➡1
77 (m2-3 paracristid/paraconid shape) 0➡1
98 (size and form of m3 hypoconulid) 1⇨0 (A)

node 29 → Leptacodon rosei

51 (size of p3) 0➡2
53 (talonid on p3) 0➡1
57 (position of p4 paraconid) 0➡2

node 29 → node 30

10 (P4 labial margin) 2➡1
46 (lower canine) 1⇨0 (A)
63 (size of p4 hypoconid) 1➡0
95 (size of m3) 0➡1

node 30 → Leptacodon dormaalensis

40 (number of mental foramina) 1⇨0 (D)
46 (lower canine) 1⇨0 (D)

node 30 → Leptacodon tener

9 (P3 protocone) 0⇨1 (D)
16 (P4 anterior cingulum) 0➡1
32 (molar anterior cingulum) 1➡2
40 (number of mental foramina) 0⇨1 (A)
42 (condyle shape) 1⇨0 (D)
56 (development of p4 paraconid) 1➡2
69 (valley facing sides of trigonid cusps) 0➡1
78 (talonid dimensions on m1-2) 0➡1
80 (talonid width on m1-2) 0➡1
86 (molar entoconid height) 1➡2
94 (size of m2) 0➡1

node 28 → node 31

14 (P4 hypocone) 0➡1
15 (P4 posterior cingulum) 1➡2
34 (posterior cingulum on M1-2) 2➡3
40 (number of mental foramina) 1⇨0 (D)
51 (size of p3) 0➡1
82 (molar cristid obliqua shape) 0⇨1 (A)
98 (size and form of m3 hypoconulid) 0⇨1 (D)

node 31 → node 32

10 (P4 labial margin) 2⇨1 (A)
16 (P4 anterior cingulum) 0➡1
63 (size of p4 hypoconid) 1➡0
65 (posterior exodaenodonty on p4) 1⇨2 (A)
86 (molar entoconid height) 1➡0
93 (posterior cingulid) 0➡1

node 32 → Nyctitherium

2 (position of the infraorbital foramen) 1⇨0 (A)
10 (P4 labial margin) 2⇨1 (D)
13 (P4 postcrista) 1➡0
21 (ectoflexus on M1-2) 1➡0
32 (molar anterior cingulum) 1➡2
46 (lower canine) 1➡0
65 (posterior exodaenodonty on p4) 1⇨2 (D)

66 (contact of p4 cristid obliqua and postvallid wall) 1➡3
82 (molar cristid obliqua shape) 0⇨1 (D)
85 (molar postcristid) 0➡1

node 32 → Saturninia

2 (position of the infraorbital foramen) 0⇨1 (D)
29 (separateness of molar paracone and metacone) 1➡0
38 (conular cristae) 0➡1
62 (position of p4 entoconid) 1➡0&3
82 (molar cristid obliqua shape) 1⇨0 (A)
88 (molar hypoconid height) 0➡1
89 (anteroposterior compression of molar hypoconid and protoconid) 0➡1

node 31 → node 33

1 (anterior root of zygomatic arch) 0⇨1 (A)
2 (position of the infraorbital foramen) 0⇨1 (D)
17 (P4 paraconule) 2⇨1 (A)
21 (ectoflexus on M1-2) 1➡2
22 (parastylar lobe on M1) 0➡2
24 (postmetacrista on M1-2) 2➡3
37 (conules on M1-2) 0⇨1 (A)
57 (position of p4 paraconid) 0⇨2 (A)
82 (molar cristid obliqua shape) 0⇨1 (D)

node 33 → Cryptotopos

1 (anterior root of zygomatic arch) 0⇨1 (D)
17 (P4 paraconule) 2⇨1 (D)
33 (molar pericone) 0➡1
37 (conules on M1-2) 0⇨1 (D)
81 (cristid obliqua position) 0➡3
91 (hypoconulid position on m1-2) 1➡0

node 33 → node 34

8 (P3 metacone) 1⇨0 (A)
25 (molar centrocrista) 0⇨1 (A)
28 (shape of molar paracone and metacone) 0⇨1 (A)
32 (molar anterior cingulum) 1⇨0 (A)
53 (talonid on p3) 1⇨0 (A)
56 (development of p4 paraconid) 1➡2
64 (size of p4 hypoconulid) 0➡1
72 (molar paraconid origin) 0⇨1 (A)
89 (anteroposterior compression of molar hypoconid and protoconid) 0➡1

node 34 → Plagioctenodon

49 (p2-3 crowns) 0➡1
50 (size of p2) 0➡1
52 (paraconid on p3) 0➡1
53 (talonid on p3) 0⇨1 (D)
55 (origin of p4 paraconid) 0➡1
57 (position of p4 paraconid) 0⇨2 (D)
65 (posterior exodaenodonty on p4) 1➡2
72 (molar paraconid origin) 0⇨1 (D)
86 (molar entoconid height) 1➡2
87 (entoconid position on m1 and m2) 0➡1

node 34 → node 35

90 (Hypoconulid size and height on m1-2) 1➡2
95 (Size of m3) 0➡1
97 (Position of m3 hypoconulid) 0➡1

node 35 → Ceutholestes

40 (number of mental foramina) 0➡1
53 (talonid on p3) 1➡2
57 (position of p4 paraconid) 0⇨2 (D)
58 (metaconid on p4) 2➡3
60 (width of p4 talonid basin) 0➡4
65 (posterior exodaenodonty on p4) 1➡0
67 (height of molar trigonid) 1➡0
70 (molar metaconid height) 0➡1
72 (molar paraconid origin) 0⇨1 (D)
73 (form of the m1 paraconid/paracristid) 0➡1
76 (form of the m2-3 paraconid/paracristid) 0➡1
78 (talonid dimensions on m1-2) 0➡1
82 (molar cristid obliqua shape) 1➡0
84 (molar entocristid notch) 1➡2
93 (posterior cingulid) 0➡1

node 35 → node 36

25 (molar centrocrista) 0⇨1 (D)
28 (shape of molar paracone and metacone) 0⇨1 (D)
44 (size of i2) 1⇨2 (A)
45 (size of i3) 1⇨0 (A)
52 (paraconid on p3) 0⇨2 (A)
56 (development of p4 paraconid) 2⇨0 (A)

57 (position of p4 paraconid) 2⇨0 (A)
59 (position of p4 metaconid) 0➡1
63 (size of p4 hypoconid) 1➡0
72 (molar paraconid origin) 1⇨0 (A)
81 (cristid obliqua position) 0➡3

node 36 → node 37

17 (P4 paraconule) 2⇨1 (D)
30 (position of molar protocone) 1➡2
32 (molar anterior cingulum) 1⇨0 (D)
37 (conules on M1-2) 0⇨1 (D)
51 (size of p3) 1➡0
65 (posterior exodaenodonty on p4) 1⇨2 (A)
75 (position of m1 metaconid) 0➡2
88 (molar hypoconid height) 0⇨1 (A)

node 37 → Psydronyctia

1 (anterior root of zygomatic arch) 0⇨1 (D)
8 (P3 metacone) 1⇨0 (D)
40 (number of mental foramina) 0➡1
47 (premolar lingual cingulids) 0➡1
50 (size of p2) 0➡2
52 (paraconid on p3) 2➡1
53 (talonid on p3) 0⇨1 (D)
56 (development of p4 paraconid) 0⇨2 (A)
65 (posterior exodaenodonty on p4) 1⇨2 (D)
88 (molar hypoconid height) 0⇨1 (D)

node 37 → node 38

23 (molar stylocone) 1⇨0 (A)
45 (size of i3) 1⇨0 (D)
53 (talonid on p3) 1⇨0 (A)
56 (development of p4 paraconid) 2⇨0 (D)
66 (contact of p4 cristid obliqua and postvallid wall) 1➡3
93 (posterior cingulid) 0➡1
95 (size of m3) 1➡2
96 (width of m3 talonid) 0➡1

node 38 → Amphidozotherium

12 (P4 metacone) 2➡1
23 (molar stylocone) 1⇨0 (D)
29 (separateness of molar paracone and metacone) 1➡0

38 (conular cristae) 0➡1
44 (size of i2) 1⇨2 (D)
48 (dimensions of p1-3) 0➡1
49 (p2-3 crowns) 0➡1
51 (size of p3) 0➡3
52 (paraconid on p3) 0⇨2 (D)
58 (metaconid on p4) 2➡1
59 (position of p4 metaconid) 1➡0
62 (position of p4 entoconid) 1➡0
64 (size of p4 hypoconulid) 1➡0
65 (posterior exodaenodonty on p4) 1⇨2 (D)
81 (molar cristid obliqua position) 3➡2
86 (molar entoconid height) 1➡0
88 (molar hypoconid height) 0⇨1 (D)
91 (hypoconulid position on m1-2) 2➡0

node 38 → Euronyctia

52 (paraconid on p3) 2⇨0 (A)
54 (size of p4) 0➡2
57 (position of p4 paraconid) 0➡2
63 (size of p4 hypoconid) 0➡1
65 (posterior exodaenodonty on p4) 2⇨1 (A)
77 (m2-3 paracristid/paraconid shape) 0➡1
78 (talonid dimensions on m1-2) 0➡1
80 (talonid width on m1-2) 0➡1
88 (molar hypoconid height) 1⇨0 (A)

node 36 → node 39

1 (anterior root of zygomatic arch) 1⇨0 (A)
7 (P2 roots) 0⇨2 (A)
8 (P3 metacone) 0⇨2 (A)
12 (P4 metacone) 2⇨0 (A)
17 (P4 paraconule) 1⇨2 (A)
25 (molar centrocrista) 1➡2
26 (molar mesostyle) 0⇨1 (A)
37 (conules on M1-2) 1⇨0 (A)
43 (crown of i1) 3⇨4 (A)
52 (paraconid on p3) 0⇨2 (D)
54 (size of p4) 0➡2
58 (metaconid on p4) 2⇨1 (A)
60 (width of p4 talonid basin) 0⇨2 (A)
61 (length of p4 talonid basin) 1⇨0 (A)
80 (talonid width on m1-2) 0➡1
85 (molar postcristid) 0➡1

94 (size of m2) 0➡1

node 39 → Wyonycteris

26 (molar mesostyle) 0⇨1 (D)
31 (size of molar protocone) 1➡0
32 (molar anterior cingulum) 0⇨1 (A)
34 (posterior cingulum on M1-2) 3➡2
51 (size of p3) 1➡2
53 (talonid on p3) 1⇨0 (A)
56 (development of p4 paraconid) 2⇨0 (D)
58 (metaconid on p4) 2⇨1 (D)
60 (width of p4 talonid basin) 0⇨2 (D)

node 39 → node 40

22 (parastylar lobe on M1) 2⇨1 (A)
28 (shape of molar paracone and metacone) 1⇨2 (A)
37 (conules on M1-2) 0⇨3 (A)
48 (dimensions of p1-3) 0⇨1 (A)
49 (p2-3 crowns) 0⇨1 (A)
56 (development of p4 paraconid) 0⇨1 (A)
62 (position of p4 entoconid) 1➡0
63 (size of p4 hypoconid) 0➡2
64 (size of p4 hypoconulid) 1➡0
66 (contact of p4 cristid obliqua and postvallid wall) 1⇨0 (A)
74 (shape of m1 paracristid) 0➡2
77 (m2-3 paracristid/paraconid shape) 0➡2
78 (talonid dimensions on m1-2) 0➡1
81 (cristid obliqua position) 3➡1
82 (molar cristid obliqua shape) 1➡0

node 40 → Entomolestes

48 (dimensions of p1-3) 0⇨1 (D)
49 (p2-3 crowns) 0⇨1 (D)
53 (talonid on p3) 0⇨1 (D)
56 (development of p4 paraconid) 2⇨1 (D)
58 (metaconid on p4) 1⇨2 (A)
61 (length of p4 talonid basin) 1⇨0 (D)
67 (height of molar trigonid) 1➡2
68 (inclination of molar trigonid) 1➡2
69 (valley facing sides of trigonid cusps) 0➡1
75 (position of m1 metaconid) 0➡1
79 (molar talonid basin) 0➡1
86 (molar entoconid height) 1➡3

87 (entoconid position on m1 and m2) 0➡1
89 (anteroposterior compression of molar hypoconid and protoconid) 1➡0

node 40 → Crocidura

7 (P2 roots) 0⇨2 (D)
8 (P3 metacone) 1⇨2 (D)
12 (P4 metacone) 2⇨0 (D)
22 (parastylar lobe on M1) 2⇨1&3 (D)
28 (shape of molar paracone and metacone) 1⇨2 (D)
32 (molar anterior cingulum) 1⇨0 (D)
37 (conules on M1-2) 0⇨3 (D)
43 (crown of i1) 3⇨4 (D)
47 (premolar lingual cingulids) 0➡1
55 (origin of p4 paraconid) 0➡2
58 (metaconid on p4) 1➡0
60 (width of p4 talonid basin) 2➡3
65 (posterior exodaenodonty on p4) 1➡2
66 (contact of p4 cristid obliqua and postvallid wall) 1⇨0 (D)
68 (inclination of molar trigonid) 1➡0
73 (form of the m1 paraconid/paracristid) 0➡2
80 (talonid width on m1-2) 1➡2
90 (hypoconulid size and height on m1-2) 0➡2
95 (size of m3) 1➡2
96 (width of m3 talonid) 0➡1
97 (position of m3 hypoconulid) 1➡2

6 New Viverravids (Mammalia, Carnivora) from the Late Paleocene of Alberta, Canada

6.1 Introduction

CARNIVORA ARE a taxonomically and ecologically diverse order of primarily flesh-eating eutherians that today comprise 92 genera in 7 families (Nowak, 1999). The earliest carnivorans are known with certainty from the early Paleocene of North America and Asia (e.g., Cope, 1882; Simpson, 1935; Matthew, 1937; Qiu and Li, 1977; Gingerich and Winkler, 1985; Fox and Youzwyshyn, 1994; Flynn, 1998); slightly younger carnivorans have been reported from the late Paleocene or earliest Eocene of Morocco (Cappetta et al., 1978; Gheerbrant et al., 1993; Gheerbrant, 1995; Gheerbrant et al., 1998), but these have yet to be described in detail. The oldest carnivorans are classified in two families: the Viverravidae, comprising the stratigraphically earliest taxa, have lost the upper and lower third molars (Gingerich and Winkler, 1985), while a second family, the Miacidae, are more primitive than viverravids in their retention of the upper and lower third molars, but are unknown prior to the latest Paleocene (Clarkforkian North American Land Mammal Age, see Rose, 1981; Gingerich, 1983; Flynn, 1998). A number of authors have suggested that the viverravids may be ancestral, or at least closely related, to the Feliformia, or "cat-like" carnivorans, while the miacids are possibly related to the Caniformia, or "dog-like" carnivorans (e.g., Flynn and Galiano, 1982; Bryant, 1991; Hunt and Tedford, 1993; Flynn, 1998); the evidence for these groupings, however, is not persuasive, and the opinions of Gingerich and Winkler (1985), Fox and Youzwyshyn (1994), and, more recently, Wesley-Hunt and Flynn (2005) that Viverravidae and Miacidae represent archaic radiations of Carnivora that acquired feliform and caniform characteristics independently of later carnivorans, are followed here [the conclusion of Wesley-Hunt and Flynn (2005) to exclude Viverravidae and Miacidae from Carnivora is not followed, see later in the text]. Although both archaic carnivoran families are obviously of central importance in understanding the early evolutionary history of the order, the Viverravidae have received comparatively less attention (Gingerich and Winkler, 1985 and Fox and Youzwyshyn, 1994 are notable

exceptions), a fact that may be owing to the quality and amount of material available. While many of the earliest miacids are represented by well-preserved specimens that include significant parts of the cranial and postcranial anatomy (e.g., Oödectes Wortman, 1901, Vulpavus Marsh, 1871, Quercygale Kretzoi, 1945; see Wesley-Hunt and Flynn, 2005; Wesley-Hunt and Werdelin, 2005), fossils of the earliest viverravids are generally more poorly preserved and are represented almost exclusively by dental and gnathic remains. Viverravids are never particularly common in collections of Paleocene age, an unfortunate situation that has seriously hindered a better understanding of their anatomy and phylogeny; nonetheless, the scant material now available hints at a poorly understood taxonomic diversity: eleven genera are currently recognized (Viverravus Marsh, 1872; Didymictis Cope, 1875; Ictidopappus Simpson, 1935; Protictis Matthew, 1937; Simpsonictis MacIntyre, 1962; Bryanictis MacIntyre, 1966; Pappictidops Qui and Li, 1977; Intyrictis Gingerich and Winkler, 1985; Raphictis Gingerich and Winkler, 1985; Pristinictis Fox and Youzwyshyn, 1994; Ravenictis Fox and Youzwyshyn, 1994), and of these, Pristinictis, Ravenictis, Intyrictis, and Ictidopappus are monotypic.

Viverravids are first known from middle Puercan (Pu2) sediments in the Ravenscrag Formation of Saskatchewan, where a single species, Ravenictis krausei Fox and Youzwyshyn, 1994 has been documented (a second viverravid, represented by a deciduous P3, may be present in the Rav W-1 fauna); by the middle Torrejonian (To2) and earliest Tiffanian (Ti1), at least four genera are known (Protictis, Simpsonictis, Bryanictis, Pristinictis; Youzwyshyn, 1988; Fox, 1990; Fox and Youzwyshyn, 1994; Scott, 2003). Stratigraphically younger viverravids from western Canada have yet to be examined in detail, but specimens from the late middle Tiffanian (Ti4) Gao Mine locality of south central Alberta, and from the Roche Percée localities of southeastern Saskatchewan (Fox, 1990), suggest that viverravid diversity may have been even greater during this time than during the earlier parts of the late Paleocene. This chapter describes new dental and gnathic material of late Paleocene (early middle Tiffanian, Ti3) age viverravids from south central Alberta, including a new species of the previously monotypic genus Raphictis, and an enigmatic new genus and species with teeth that most closely resemble those of the primitive viverravids Simpsonictis and Protictis paralus Holtzman, 1978. Cusp terminology for the carnivoran p4 follows Flynn and Galiano

(1982) in recognizing a first posterior accessory cusp and second posterior accessory cusp; the "anterior accessory cusp" is considered a paraconid here. Measurements follow Gingerich and Winkler (1985).

6.2 Systematic Paleontology

Class MAMMALIA Linnaeus, 1758

Subclass THERIA Parker and Haswell, 1897

Infraclass EUTHERIA Gill, 1872

Order CARNIVORA Bowdich, 1821

Family VIVERRAVIDAE Wortman and Matthew, 1899

Comments on carnivoran classification.—Wyss and Flynn (1993) were among the first authors to suggest that a distinction should be made between carnivorans of archaic aspect (the Viverravidae and Miacidae) and living carnivorans (the so-called crown clade); under this paradigm, the nomen Carnivora is restricted to the last common ancestor of living carnivorans and all descendants thereof, while the more inclusive clade "Carnivoramorpha" encompasses the crown clade plus Viverravidae and Miacidae. Despite cogent arguments against such a classification (e.g., Fox and Youzwyshyn, 1994), recent comprehensive studies of the relationships between extant carnivorans and those of archaic aspect (e.g., Bryant, 1996; Flynn and Wesley-Hunt, 2005; Polly et al., 2006) continue to recognize "Carnivoramorpha", with a paraphyletic Miacidae and monophyletic Viverravidae as successive outgroups to the crown clade Carnivora. While a distinction between carnivorans of archaic aspect and those of modern aspect based on synapomorphy is unproblematic, the decision to restrict the nomen Carnivora to the crown clade and exclude the viverravids and miacids [both families have long been regarded as carnivorans (e.g., Wortman and Matthew, 1899; Teilhard de Chardin, 1915; Matthew, 1937; Simpson, 1945)] seems contrary to effective communication, one of the central purposes of any classification. As Fox and Youzwyshyn (1994) indicated, the P4/m1/M1 shearing complex of carnivorans is uniquely derived, and unambiguously circumscribes a clade of eutherians that have traditionally been referred to as carnivorans;

as such, a stem-based concept that retains the Viverravidae and Miacidae in Carnivora is favoured here.

Genus DIDYMICTIS Cope, 1875

Limnocyon MARSH, 1872, pp. 126-127 (in part).
Didymictis COPE, 1875, p. 5.

Type species.—Limnocyon protenus Cope, 1874.

Other included species.—Didymictis leptomylus Cope, 1880; D. altidens Cope, 1880; D. proteus Simpson, 1937; D. dellensis Dorr, 1952; D. vancleveae Robinson, 1966.

DIDYMICTIS DELLENSIS Dorr, 1952

Figures 6.1.1-6.1.5

Didymictis dellensis DORR, 1952, p. 85.
Protictis dellensis GINGERICH and WINKLER, 1985, p. 117.
Didymictis proteus SIMPSON, 1937: POLLY, 1997, p. 34 (in part).

Holotype.—UM 27232, incomplete right dentary with c, p1, p3-4, m1-2, and alveoli for p2 (Dorr, 1952, p.85). Dell Creek Quarry, Hoback Formation of Wyoming, late Paleocene (late Tiffanian, Ti5, Plesiadapis simonsi/P. gingerichi Lineage Zone of Lofgren et al., 2004).

Material examined.—From DW-2: UALVP 47801, lower canine; UALVP 47802, incomplete left dentary having m2.

Age and occurrence.—Early middle Tiffanian (Plesiadapis rex/P. churchilli Lineage Zone, Ti3, late Paleocene) to latest Tiffanian (Plesiadapis gingerichi/P. cookei Lineage Zone, Ti6, late Paleocene) of the Western Interior of North America.

Description.—Lower canine: An isolated lower canine from the DW-2 locality closely resembles that of Didymictis dellensis from the late Tiffanian (Ti5) Princeton locality (Gingerich and Winkler, 1985) and is referred here to that species. The crown is

strongly recurved and bears a sharp apex. The posterior surface of the crown bears a sharp keel that extends from apex to base, and a conspicuous crest is developed medially, extending from the base of the crown dorsally, but fades away as it nears the apex. Numerous faint longitudinal grooves invest the enamel.

m2 (L=5.6; TrW=3.0; TaW=2.8; N=1): The trigonid of m2 is equilaterally triangular in occlusal outline, with low, slightly inflated cusps: the protoconid is the largest trigonid cusp, followed by the slightly smaller metaconid and paraconid. Small but distinct carnassial notches (i.e., notches that resemble inverted keyholes) are developed in the deepest parts of the paracristid and protocristid. The talonid is long and as wide as the trigonid, with a large hypoconid, a subequally large and finger-like hypoconulid, and smaller, more poorly differentiated entoconid. The talonid basin on m2 slopes posterolabially-anterolingually. The labial cingulid is robust, extending posteriorly past the hypoflexid and hypoconid to the labial wall of the hypoconulid, where it then terminates; the cingulid is heavily cuspidate, with large cuspules developed below the paracristid notch and at the level of the hypoflexid.

Discussion.—Didymictis dellensis was originally based on specimens from the late Tiffanian (Ti5) Dell Creek Quarry of western Wyoming (Dorr, 1952); it was later transferred to Protictis by Gingerich and Winkler (1985), who cited differences in the relative height of the m1 trigonid and narrowness of the m2 talonid as important features that would justify the removal of D. dellensis from Didymictis. The results of a stratocladistic analysis of Paleocene and Eocene viverravids from Wyoming prompted Polly (1997) to synonymize P. dellensis with D. proteus Simpson, 1937, with "P." dellensis representing the earliest occurrence of D. proteus. "Protictis" dellensis clearly differs from other species of Protictis [e.g., P. haydenianus (Cope, 1882), P. agastor Gingerich and Winkler, 1985]: the p4 is longer relative to its height, and the paraconid is lower and more poorly developed, and is clearly separated from the protoconid by a wide notch (in contrast, p4 of Protictis has a well-developed paraconid that is closely appressed to the protoconid, and is separated from it by a narrow, slit-like carnassial notch). The m2 of "P." dellensis is significantly larger relative to m1 than that of any species of Protictis (excluding the enigmatic P. paralus, in which m2 is significantly enlarged relative to m1), with a higher and better developed trigonid and, importantly, a

considerably longer and wider talonid and a complete labial cingulid (in contrast, the m2 of Protictis is small relative to m1, with a reduced talonid and incomplete labial cingulid). While agreeing with Polly's (1997) returning of "P." dellensis to Didymictis, the evidence that D. dellensis is conspecific with D. proteus is not persuasive: the p4 of D. proteus bears a considerably better-developed paraconid and more robust first posterior accessory cusp, and the molar crowns are much lower, and bear massive, bunodont cusps that are well-suited for crushing, rather than the more sectorial crowns in D. dellensis.

The teeth from DW-2 closely resemble those of Didymictis dellensis in the holotype (UM 27232), differing primarily in its smaller size and minor details of the crown anatomy (e.g., the m2 talonid in UALVP 47802 bears a relatively better developed entoconid than does UM 27232, and the trigonid cusps in UALVP 47802 are sharper and more sectorial than are those in UM 27232). Gingerich and Winkler (1985) interpreted the difference in size between the holotype of D. dellensis and specimens collected from Princeton Quarry and Fossil Hollow as owing to sexual dimorphism, but suggested in light of the scant material available that the smaller morphs might represent a second viverravid species. The single referred m2 from Alberta obviously cannot satisfactorily resolve this problem, and Gingerich and Winkler's (1985) interpretation of a single, sexually dimorphic species is provisionally followed here. The occurrence of D. dellensis at DW-2 represents the earliest record of the species, and the first such occurrence in Alberta.

?DIDYMICTIS sp.

Figures 6.1.6-6.1.11

Material examined.—From DW-2: UALVP 47803, 47804, incomplete p4.

Description.—p4 (L=6.5, N=1; mean W=2.85, SD=0.07, CV=2.48, N=2): The crown is dominated by a trenchant protoconid and well-developed posterior accessory cusps. The paraconid is low but robust, subconical, and is closely appressed to the base of the protoconid. A weak crest extends posterolabially from the apex of the paraconid, but whether or not it continued to the apex of the protoconid cannot be determined. Unlike the p4 of Protictis and Bryanictis, a carnassial notch is not developed between the

protoconid and paraconid, and in this regard the referred teeth more closely resemble the p4 of Didymictis dellensis (see Dorr, 1952; Gingerich and Winkler, 1985). The massive and conical first posterior accessory cusp is developed high on the posterolabial shoulder of the protoconid, while the second posterior accessory cusp is somewhat labiolingually compressed and bladelike, and is positioned posterior to, and slightly more lingual than the first posterior accessory cusp. The protoconid and posterior accessory cusps are connected by robust crests that are heavily worn, and deep carnassial notches are developed between the protoconid and first posterior accessory cusp, and between the posterior accessory cusps. The crown is moderately expanded posterolingually, and a faint cingulid is present lingual to the second posterior accessory cusp, but a distinct basin is not developed. The anterior and posterior cingulids are robust, but their continuity across the labial side of the crown cannot be determined on either of the specimens at hand. The enamel is weakly wrinkled.

Discussion.—The referred specimens resemble the p4 of Protictis in having a robust first posterior accessory cusp, and an enlarged and somewhat blade-like second posterior accessory cusp (MacIntyre, 1966; Flynn and Galiano, 1982; Flynn, 1998); the teeth differ from p4 of Protictis, however, in that the paraconid is small, and a carnassial notch is not developed between it and the protoconid, and in this regard more closely resemble p4 in Didymictis. The referred p4s are smaller than that of any species of Didymictis (including D. dellensis), however, and the second posterior accessory cusp is more pronounced and blade-like than it is in most p4s of Didymictis [the second posterior accessory cusp on p4 of D. dellensis and some p4s of D. proteus and D. leptomylus Cope, 1880 can be blade-like (see Polly, 1997), but not to the same degree as that in UALVP 47803 or 47804]. The meaning of these contradictory features must await the discovery of better preserved specimens. The greatly reduced paraconid is atypical of p4 of Protictis, while a blade-like second posterior accessory cusp is unusual, but not unknown, in Didymictis; as such, the two teeth from DW-2 are referred with question to Didymictis.

Genus RAPHICTIS Gingerich and Winkler, 1985.

Raphictis GINGERICH and WINKLER, 1985, p. 122.

Type species.—Raphictis gausion Gingerich and Winkler, 1985.

Other included species.—Raphictis iota, new species.

Revised diagnosis.—Differs from all other viverravids in having tall, sharp cusps, and a molar talonid that is skewed labially and is oblique to the anteroposterior axis of the trigonid. Differs further from all other viverravids in having P4 with weaker developed parastyle and protocone.

RAPHICTIS IOTA new species

Figures 6.2, 6.5.9, 6.5.10; Table 6.1

Raphictis sp., cf. R. gausion: FOX, 1990, pp. 60-61

Diagnosis.—Smallest species of Raphictis (length m1 approximately 10 percent shorter than m1, R. gausion). Differs further from R. gausion in having a relatively larger paraconid and first posterior accessory cusp on p4, and in having a more posteriorly positioned paraconid and shorter talonid on m1.

Description.—Upper dentition (Figs. 6.2.1-6.2.6): P4: The crown of P4 resembles that in other viverravids in being triangular in occlusal outline, with a strong embayment between the parastyle and protocone. The paracone is tall and slightly compressed labiolingually, and leans posteriorly. A sharp parastyle is developed directly anterior to the paracone: the cusp is well set off from the base of the paracone, and its apex projects slightly anteriorly. A well-developed preparacrista extends from the paraconal apex anteriorly and faintly lingually, but it is neither notched nor continuous with an opposing crest from the parastyle. The postparacrista curves sharply posterolingually from the paraconal apex to a deep, slit-like notch. The metastylar blade is oriented oblique to the paracone, and is high and sharp; the labial face of the blade presents two swellings suggestive of a metacone and metastyle, although distinct cusps are not differentiated. The conical protocone is slightly larger and taller than the parastylar cusp, and is well set

off from the base of the paracone, with a broad V-shaped notch separating the two cusps. The protocone is anterolingual to the paracone, but posterior to the level of the parastylar cusp, and the embayment between the two cusps is wide and deep. A robust posterior cingulum runs uninterrupted from low on the protocone to the metastylar blade; the ectocingulum is strong anteriorly, but weakens considerably posteriorly.

M1: Although the M1 crown of Raphictis iota resembles that of other viverravids in being asymmetrically triangular in outline, it is considerably more transverse relative to its length. The hook-like parastylar lobe is elongate and projects strongly labially, with the parastyle only slightly anterior to the level of the paracone; as a result, the anterior edge of the crown is longer, and the ectoflexus is proportionately deeper than in most other viverravids. The parastyle has been erased by wear, but the dimensions of its base suggest that the cusp was low; a stylocone is not developed. The paracone and metacone are stout, arising from a common base, with steep and moderately convex lingual sides. The paracone is twice the height of the metacone, swollen at its base, and leans anteriorly and labially; the metacone is greatly reduced and leans slightly lingually. The preparacrista extends labially from the paraconal apex to the ectocingulum; it is low and weakly blade-like, but a carnassial notch is not developed. The centrocrista is broadly V-shaped in labial view and is incised with a tiny notch at its deepest point. The postmetacrista is low and poorly developed, extending uninterrupted to the posterolabial corner of the crown; a carnassial notch is not developed in the postmetacrista. The paraconule is larger and more labial than the metaconule, and the preparaconular and postmetaconular cristae are low, and continue labially as a narrow para- and metacingulum; the metacingulum extends to the metastylar lobe where it joins the ectocingulum, while the paracingulum fades away slightly labial of the level of the paracone. The internal conular cristae are undeveloped. The protocone is sharp and slightly lower than the paracone; it is strongly compressed anteroposteriorly and leans anteriorly to nearly the same degree as the paracone. The protoconal cristae are low and blunt; a narrow, slit-like notch is developed in the preprotocrista, separating the paraconule and protocone. The protoconal cingula are low and narrow, incomplete lingually, and extend only a short distance labially.

Dentary and lower dentition (Figs. 6.2.10-6.2.15): Although the dentary is badly damaged in UALVP 47805, it preserves the posteriormost parts of the horizontal ramus, a portion of the coronoid process, the condyle, and proximal parts of the angular process. The ramus is shallow but robust, and is nearly elliptical in cross section. The anterior margin of the coronoid process ascends steeply from the mandibular ramus, and the masseteric fossa is deeply excavated. The cylindrical condyle is developed at the terminus of a stout condylar process, and although its medialmost parts are missing, the condyle was obviously large, transverse, medially sloping, and positioned at the level of the tooth row. The angular process is broken distally, but the dimensions of the proximal parts suggest it was relatively short, and was in all likelihood hooked distally. A low shelf is developed medially, increasing the area of distal attachment of the internal pterygoid musculature, and a large mandibular foramen occurs just dorsal to the base of the angular process.

p4: The p4 of Raphictis iota is elongate and narrow, with a sharp paraconid, protoconid, and sectorial posterior accessory cusp dominating the crown. The conical paraconid is robust, low, and somewhat set off anteriorly from the base of the protoconid, similar to p4 in R. gausion and Simpsonictis; a moderately developed paracristid connects the apex of the protoconid to the paraconid. A weak crest extends from the apex of the protoconid to the first posterior accessory cusp, and a shallow notch separates the two cusps. The first posterior accessory cusp is developed low on the posterolabial shoulder of the protoconid, and is laterally compressed and blade-like, with the labial side convex and the lingual side flat. The second posterior accessory cusp is positioned slightly posterolingual to the first posterior accessory cusp, and its apex is little elevated above the base of the crown. Poorly developed cingulids are developed posterolabially and posterolingually.

m1: The m1 of Raphictis iota closely resembles that of R. gausion: the crown consists of a tall trigonid bearing tall sharp cusps, and a low trigonid that is skewed labially. The paraconid is lower than the metaconid and projects slightly anteriorly, giving the trigonid an "open" appearance lingually; the metaconid and protoconid are faintly recurved. Small carnassial notches are developed in the paracristid and protocristid. The talonid is shorter and narrower than those of other viverravids. The

hypoconid and hypoconulid are well developed, while the entoconid and entocristid are greatly reduced; the basin is shallow, and slopes steeply posterolabially-anterolingually. Weak anterior and posterior cingulids are present, but are discontinuous along the labial side of the crown.

m2: The trigonid of m2 projects slightly above the talonid of m1, and the talonid is long and narrow. The trigonid is equilaterally triangular in occlusal outline, with tall, sharp cusps. The protoconid is the largest trigonid cusp, followed by the slightly smaller metaconid and paraconid; as with m1, the protoconid and metaconid on m2 are slightly recurved. The paracristid and protocristid are broadly notched, with no evidence of carnassial notches at their deepest points. The talonid is faintly skewed labially: the hypoconulid is long and finger-like, while the hypoconid is smaller and lower; the entoconid and entocristid are only weakly developed, and the talonid is virtually open lingually. The anterior cingulid is robust and short; a posterior cingulid is not developed.

Etymology.—Iota, Greek, small, in reference to the small size of R. iota relative to the larger R. gausion.

Holotype.—UALVP 47806, incomplete left dentary with p4 and alveoli for m1 (Figs. 2.7-2.9). Gao Mine locality, Paskapoo Formation of Alberta, late Paleocene [late middle Tiffanian, Ti4 (Fox, 1988), Plesiadapis churchilli/P. simonsi Lineage Zone of Lofgren et al., 2004].

Other material examined.—From DW-2: UALVP 47807, M1; UALVP 47808, m1; UALVP 47805, incomplete right dentary with m1 talonid and m2.

From Birchwood: UALVP 39418, m1; UALVP 39419, incomplete m1.

From Gao Mine: UALVP 47809, P4.

Occurrence.—Early middle Tiffanian (Plesiadapis rex/P. churchilli Lineage Zone, Ti3, late Paleocene) to late middle Tiffanian (Plesiadapis churchilli/P. simonsi Lineage Zone, Ti4, late Paleocene) of the Western Interior of North America.

Discussion.—The referred specimens most closely resemble homologous teeth of Raphictis gausion from the early middle Tiffanian (Ti3) Cedar Point Quarry of Wyoming (Gingerich and Winkler, 1985), differing principally in their smaller size (e.g., mean length m1, R. iota=3.35 versus mean length m1, R gausion=3.70), but in a number of other ways as well. For example, the p4 in UALVP 47806 is smaller relative to m1 than

is p4 in R. gausion (the p4 in R. gausion is, on average, longer than m1, whereas p4 in R. iota is shorter than m1), and the paraconid is stronger and more dorsally projecting. Additionally, the m1 trigonid in R. iota is relatively lower than that in R. gausion, and the m2 talonid is slightly wider. Taken together, these differences indicate that the specimens from Alberta represent a species distinct from R. gausion and are here referred to a new species of Raphictis, R. iota.

The specimens from Alberta document for the first time parts of the upper dentition of Raphictis. The P4 resembles that of other viverravids generally in occlusal outline and in the major features of the crown, but differs in a number of ways. The cusps on P4 and M1 of Raphictis are relatively taller and more sharp than are those of other viverravids, in keeping with tall, sharp cusps of the lower dentition, and the P4 is small relative to M1, also in keeping with similar proportions in the lower dentition. The P4 parastyle and protocone are very weak in Raphictis, differing from the larger and more inflated parastyle and protocone that characterize the P4 of Pristinictis, Protictis, and Bryanictis (see MacIntyre, 1966; Meehan and Wilson, 2002); furthermore, the protocone is only slightly anterior of the level of the paracone in Raphictis, similar to that on P4 of Pristinictis, Protictis, and primitive viverravids generally (Fox and Youzwyshyn, 1994). The P4 is more derived than that of Pristinictis in having a longer and less transversely oriented metastylar blade, and in this respect the P4 of Raphictis more closely resembles that of Viverravus. The M1 of Raphictis is transverse relative to its length, proportions that are similar to those on M1 of Ravenictis Fox and Youzwyshyn, 1994, with the protocone being anteroposteriorly compressed and the protoconal cingula only weakly developed. The parastylar shelf labial of the paracone is wide, but the preparacrista is not developed into a high blade as it is in many viverravids, nor is a carnassial notch developed in its deepest parts; similarly, the postmetacrista is virtually undeveloped, and a carnassial notch is not present. The relative closeness of the paracone and metacone on M1 of Raphictis may be of important phylogenetic interest: the two cusps are strongly connate basally, similar to, but even more connate than the paracone and metacone in Pristinictis, and approaches the condition on M1 of Protictis agastor. The unusual combination of P4 and M1 characters suggests that the dentition of Raphictis may have been adapted to slicing and piercing, with the P4 being of central importance

during the slicing phase (elongated metastylar blade, reduced parastyle and protocone); in contrast, M1 shear is greatly reduced in Raphictis (weak preparacrista blade, carnassial notches weak or undeveloped) and was instead replaced by adaptations for piercing (tall, nearly vertical sharp cusps, greatly reduced protoconal cingula).

The dentition of Raphictis presents a curious mosaic of primitive and derived characters, and its phylogenetic position is uncertain. Gingerich and Winkler (1985) indicated that Raphictis could most realistically be derived from a species of Protictis, and McKenna and Bell (1997) apparently concurred, referring Raphictis to the Didymictinae, along with Didymictis and Protictis. While a close phylogenetic relationship between Protictis and Didymictis is possible (see Flynn and Galiano, 1982; Polly, 1997), the suggestion of a close relationship of these taxa with Raphictis seems to have been founded on symplesiomorphies. For example, the relatively "closed" m1 trigonid (resulting from a more anteroposteriorly compressed trigonid) of Raphictis, while resembling that of Protictis and Didymictis, is likely primitive for carnivorans generally, being present on m1 of the primitive viverravids Pristinictis and Protictis haydenianus (MacIntyre, 1966; Flynn and Galiano, 1982; Fox and Youzwyshyn, 1994); similarly, the P4 of Raphictis bears a protocone that is only slightly anterior of the level of the paracone, similar to the P4 of Pristinictis, Protictis, and Didymictis, this character is also likely primitive for viverravids and carnivorans generally (Fox and Youzwyshyn, 1994). Many of the features of the dentition of Raphictis do not suggest a close relationship with Protictis or Didymictis at all: for example, the paraconid on p4 of Raphictis is relatively small and clearly separate from the protoconid, with no carnassial notch intervening between the two cusps; this contrasts with p4 of Protictis and, to a lesser degree, Didymictis, in which the paraconid is robust and more closely appressed to the protoconid, and a well-developed carnassial notch is developed in the paracristid in Protictis (see Flynn and Galiano, 1982). Additionally, the parastyle and protocone on P4 of Raphictis are both small and uninflated and differ significantly from the larger and more bulbous cusps on P4 of Protictis. The connate paracone and metacone on M1 of Raphictis may be of some importance, but the distribution of this character state has not been investigated extensively; it is present in Pristinictis and Protictis agastor (see Fox and Youzwyshyn, 1994), but also in some specimens of Didymictis proteus (see Polly,

1997), and even in specimens that have been referred to Simpsonictis (see Fox and Youzwyshyn, 1994); clearly the phylogenetic importance of this feature must await a more thorough analysis of early carnivorans than is attempted here. For the present, Raphictis is best referred only to the Viverravidae, and a more precise estimate of its phylogenetic relationships must await the discovery of better preserved specimens and a more comprehensive review of Viverravidae.

RAPHICTIS sp.

Figures 6.3.1-6.3.3

Material examined.—From DW-2: UALVP 47810, incomplete right maxilla with P4 and alveoli for P2-3.

Description and discussion.—The P4 in UALVP 47810 closely resembles that of Raphictis iota, differing principally in its larger size, in having a relatively larger protocone, and in the metastylar blade being less oblique to the anteroposterior axis of the crown. UALVP 47810 may represent a new species of Raphictis that is larger than either R. gausion or R. iota, but its formal naming and diagnosis are deferred until a larger sample is obtained.

Genus CERVICTIS new genus

Protictis MATTHEW, 1937: FOX, 1990, p. 61 (in part).

Type and only known species.—Cervictis thula.

Diagnosis.—As for the type and only known species.

Etymology.—Cervus, Greek, deer, in reference to the City of Red Deer; ictis, Greek, weasel, a common suffix for viverravid genus nomina.

CERVICTIS THULA new species

Figures 6.3.4-6.3.8, 6.4, 6.5.7-6.5.8; Table 6.2

Protictis paralus HOLTZMAN, 1978: FOX, 1990, p. 61.

Diagnosis.—Differs from all other viverravids in having P4 with protocone nearly directly lingual of the parastyle, and in p4 paraconid being small, low, and well separated from the protoconid on a prominent, anteroventrally jutting lobe. Differs from all other viverravids except Simpsonictis and Protictis paralus in having m2 large relative to m1. Differs from Simpsonictis in being larger, with p4 being relatively longer and lower crowned, and in m1 being lower crowned; differs further from Simpsonictis in having p4 with paraconid well separated from the protoconid, in having a larger and better differentiated first posterior accessory cusp and a higher and more sectorial posterior accessory cusp, in having weaker exodaenodonty at the posterior root, and in having a more anteriorly leaning m1 paraconid. Differs from Protictis paralus in having a relatively larger m2, a more anteriorly positioned p4 paraconid, and a lower and less labially extending m1 paraconid.

Description.—Upper dentition (Fig. 6.3): P3: The P3 of Cervictis is two-rooted, with the posterior root compressed and more transverse than the anterior root. The crown is labiolingually compressed and dominated by a tall paracone and a smaller metastylar cusp. A weak crest extends anteriorly from the paraconal apex, fading away as it approaches the poorly developed parastylar lobe; a parastylar cusp is not present. A stronger crest runs posteriorly from the paraconal apex to a low but conspicuous metastylar cusp, but a carnassial notch is not developed in the crest. A weak bulge is present lingual to the paracone, but a distinct protocone is not developed. Faint cingula occur in the shallow embayment between the parastylar lobe and protoconal bulge, and between the protoconal bulge and the metastylar cusp.

P4: The occlusal outline of P4 of Cervictis is Y-shaped, with the parastyle and protocone forming the arms of the Y and a deep anterior embayment developed between the two cusps. The paracone is the largest and tallest cusp: it is slightly compressed labiolingually, with flat lingual and faintly convex labial sides, and leans posteriorly. A sharp preparacrista extends anterolingually from the paraconal apex to near the base of the bulbous, conical parastyle; the preparacrista does not meet an opposing crest from the parastyle, nor is a carnassial notch developed. The postparacrista curves posteriorly and

slightly lingually from the paraconal apex, forming a deep notch at its union with the metastylar blade; the notch is narrow and slit-like, but an inverted keyhole-like excavation is not developed in its deepest parts, contrasting with P4 of Protictis (e.g., P. agastor and P. haydenianus) and Bryanictis (see MacIntyre, 1966). The metastylar blade is high and sharp, and is nearly in line with (UALVP 47811, Fig. 3.6), or slightly oblique to (UALVP 47812, Fig. 3.8) the paracone. The conical protocone is subequal in size and height to the parastylar cusp; it is well anterolingual to the level of the paracone, directly lingual from the parastylar cusp, and the embayment between the two cusps is narrow and deep. A short cingulum is developed along the anterior margin of the crown in the embayment between the parastylar cusp and protocone, connecting the two cusps; a more robust posterior cingulum runs uninterrupted from low on the protocone to the metastylar blade. Labially, a weak ectocingulum can be developed opposite the valley between the parastylar cusp and paracone, and opposite the metastylar blade.

M1: The M1 of Cervictis resembles that of other viverravids: the crown is asymmetrically triangular in outline, with an enlarged, hook-like parastylar lobe and a reduced metastylar lobe, and with the sectorial trigon cusps enclosing a moderately deep, posteriorly sloping basin. The parastyle is low, three-sided, and is set off on an anteriorly projecting, hook-like lobe; a weak swelling in the position of a stylocone is developed at the juncture of the preparacrista and ectocingulum, but a discrete cusp is not present. The paracone and metacone are stout, with steep and convex lingual sides; the paracone is tall and leans anteriorly, while the metacone is lower and leans slightly lingually, and both cusps are separated for nearly their entire height [i.e., the cusps do not arise from a common base as on M1 of Pristinictis (see Fox and Youzwyshyn, 1994) or Raphictis]. The preparacrista extends almost directly labially from the paraconal apex to the ectocingulum: the crest is low and is neither blade-like nor incised by a carnassial notch. The centrocrista is broadly V-shaped in labial view, straight (i.e., is not deflected labially), and is incised by a weak notch at its lowest point. The postmetacrista extends labially from the metaconal apex to the base of the cusp, where a small notch is developed, and then continues as an elevated, heavy blade to the posterolabial corner of the crown. Both conules are well developed: the paraconule is large and leans anteriorly, while the metaconule is smaller and more nearly vertical, more lingual in position, and on

a lower occlusal plane (owing to the posteriorly sloping trigon basin). The preparaconular and postmetaconular cristae are well developed and extend labially as the paracingulum and metacingulum to the parastylar and metastylar lobes, respectively. The internal conular wings are more variably developed than are the external conular wings: when present, they are weaker than the external conular cristae, but in some specimens (e.g., UALVP 47816) they are wholly undeveloped. The protocone is slightly lower than the paracone and is anteroposteriorly compressed, with an acute apex; the protocone leans anteriorly to nearly the same degree as the paracone. The protoconal cristae are short and sharp, and terminate at the conules; a slit-like carnassial notch separates the paraconule from the preprotoconal crista. The protoconal cingula are well developed, especially the posterior cingulum, which is wide and shelf-like; both cingula can bear irregularly sized cuspules, and a tiny hypocone is present in two specimens (UALVP 47811, 47816).

M2: UALVP 47812 preserves the only M2 of Cervictis in the present sample. The M2 is smaller than M1, but the crown is relatively longer compared to its width; the M2 is positioned directly posterior to M1, rather than being inset lingually. The crown of M2 resembles that of M1 in being asymmetrically triangular in outline, with enlarged parastylar and greatly reduced metastylar lobes. The parastylar lobe is not drawn out as a hook-like process as it is on M1, but rather is bluntly rounded, abutting the metastylar corner of M1, and an ectoflexus is not developed. The paracone and metacone are both large and stout, and although the metacone is smaller than the paracone, it is not reduced in size to the same degree as on M2 of other viverravids (e.g., P. haydenianus, see MacIntyre, 1966); as on M1, the paracone on M2 leans slightly anteriorly. The stylar shelf is wide anteriorly, in keeping with the enlarged parastylar lobe, and a conspicuous, low ectocingulum rims the labial margin of the crown; there is no evidence of a stylocone or parastylar cusp, although these structures may have been present originally but subsequently erased by wear. The short preparacrista is heavily worn, but it does not appear to have formed a raised blade, nor was it deeply notched. As with M1, the paracone and metacone on M2 are separate at their bases, and the centrocrista is widely V-shaped. Both conules are well developed and closely appressed to the bases of the paracone and metacone: the paraconule is larger and more lingually positioned than the

metaconule, and both conules bear conspicuous conular cristae; the preparaconular and postmetaconular cristae continue labially as a strong paracingulum and weaker metacingulum, respectively. The anteriorly projecting protocone is about the same height as the metacone, is slightly compressed anteroposteriorly, and bears an acute apex. A small notch is developed in the preprotoconal crista just lingual of the paraconule. The wide anterior cingulum extends to the level of the paraconule, while the posterior cingulum is shorter and faintly cuspidate.

Dentary and lower dentition (Fig. 6.4): The referred dentaries most closely resemble that described by Holtzman (1978) for Protictis paralus, but differ in being deeper, and in having two, rather than four, mental foramina (one opens below the anterior root of p1, while the other opens below the anterior root of p3). The horizontal ramus of UALVP 47817 (Figs. 6.4.6-6.4.8) is notably deeper and wider than that of the other dentaries (e.g., UALVP 47817 mandibular depth=5.9 versus UALVP 47813 mandibular depth=5.0), but the dentition is otherwise identical. While the difference in mandible depth is suggestive of sexual dimorphism, such a phenomenon is poorly documented in viverravids [Gingerich and Winkler (1985) and Polly (1997) reported weak dimorphism in the dentition of a number of Paleocene viverravids from the Bighorn Basin of Wyoming], and the small size of the present sample prohibits more conclusive statements in these regards (e.g., the differences in mandibular depth could also be owing to differences in age); clearly a better understanding of sexual dimorphism in Paleocene viverravids must await the accumulation of much larger samples than are presently available.

Lower canine: Two isolated lower canines are referred here to Cervictis. The crown is much smaller than UALVP 47801 (referred to Didymictis dellensis; see earlier in the text), and the dimensions of the root are nearly identical to those of the canine alveolus in UALVP 47817 and 47818 (incomplete dentaries that are referable to Cervictis). The crown resembles that in UALVP 47801 in being strongly recurved, in the posterior surface supporting a sharp keel that extends from apex to base, and in having numerous longitudinal grooves in the enamel. As in D. dellensis, the crown of the lower canine of Cervictis supports a prominent crest on its medial side, but unlike that in D. dellensis, a deep, gutter-like groove developed just above the crest.

p1: The p1 of Cervictis is known only from its alveolus: the alveolar rim is somewhat elongate and bean-shaped in dorsal outline, with a slight constriction at the midpoint of the labial margin, suggesting that p1 was two-rooted, with fully separate or weakly fused roots [a two-rooted p1 occupying a single alveolus is known in other viverravids, e.g., Didymictis protenus (Cope, 1880) and Viverravus acutus Matthew, 1915; see Polly, 1997]. A long diastema separates the p1 alveolus from that of the lower canine, and shorter diastemata separate p1 from p2, and p2 from p3.

p2: The p2 crown is elongate and blade-like and supports a tall and slightly recurved protoconid and a lower talonid cusp. The talonid of p2 is expanded somewhat labiolingually, and bears a sharp cusp that is connected to the apex of the protoconid by a weak crest; a weak swelling is developed on this crest in UALVP 47817, suggestive of an incipient first posterior accessory cusp. The crown is weakly exodaenodont at the posterior root.

p3: The p3 crown resembles that of p2: it is elongate, blade-like, and supports a tall protoconid that is slightly recurved; the protoconid is about the same height as that on p2. The talonid of p3 is expanded labiolingually as on p2, but the talonid cusp (second posterior accessory cusp) on p3 is much better developed, being both taller and more strongly blade-like. A sharp crest extends anteriorly and slightly labially from the apex of the talonid cusp, meeting a longer but otherwise similar crest extending posteriorly from the apex of the protoconid; a deep carnassial notch is formed at their juncture. A first posterior accessory cusp is present on both p3s at hand: it is incipiently developed in UALVP 47813 (Figs. 6.4.3-6.4.5), but it is much stronger in UALVP 47817 (Figs. 6.4.6-6.4.8) and is set off from the protoconid and second posterior accessory cusp by carnassial notches. A faint crest extends anterolingually from the talonid cusp, partially enclosing a shallow basin.

p4: The p4 is elongate and labiolingually compressed, with only a slight labiolingual expansion posteriorly; the crown consists primarily of a trenchant protoconid and a tall, blade-like heel. Unlike p4 of most other viverravids, the p4 crown of Cervictis is low relative to its length. A weak paracristid extends anterolingually from the apex of the protoconid to a small, conical paraconid. The p4 paraconid of Cervictis is unusual: it set off from the protoconid on an anteroventrally jutting prominence, and a carnassial

notch is not developed between the paraconid and protoconid; the paraconid is inflated at its base, and its apex is directed somewhat posterodorsally and lingually. The anterior margin of the protoconid is long and steep, and the protoconid is nearly vertical, rather than recurved. A large, conical first posterior accessory cusp is developed on the posterolabial shoulder of the protoconid, and the apices of the paraconid, protoconid, and first posterior accessory cusp are in line and are oriented obliquely anterolingually-posterolabially along the crown. The second posterior accessory cusp, while nearly as high as the first posterior accessory cusp, is more labiolingually compressed and blade-like, and is positioned slightly posterolingual to the first posterior accessory cusp. A deep, slit-like notch separates the first posterior accessory cusp from the protoconid, while a much wider notch separates the two posterior accessory cusps. Sharp crests extend anterolabially and anterolingually from the apex of the second posterior accessory cusp: the anterolabial crest runs to the notch between the two posterior accessory cusps, while the anterolingual crest extends to the level of the first posterior accessory cusp, enclosing a shallow talonid basin. A discrete entoconid is not present on any p4 at hand, but an ill-defined hypoconid can occur immediately adjacent to the apex of the second posterior accessory cusp. Labial cingulids are weakly developed or absent.

m1: As with other viverravids, the m1 of Cervictis bears a tall trigonid and a much lower talonid. The protoconid is the largest and tallest trigonid cusp: it is subtriangular in coronal section, with a somewhat inflated lingual side. The metaconid occurs high on the posterolingual shoulder of the protoconid; it is smaller and lower than the protoconid, and is connected to it by a sharp protocristid that bears a weak, keyhole-shaped carnassial notch in its deepest part. The metaconid apex is directed dorsally and lingually. The paraconid is approximately one half to two thirds the height of the metaconid, slightly higher than that in Simpsonictis, and is somewhat anteroposteriorly compressed and blade-like; it is positioned near the longitudinal midline of the crown, rather than farther lingually. The m1 paraconid of Cervictis differs from that of many other viverravids, including that of Pristinictis and Protictis, in leaning strongly anteriorly, rather than being more nearly vertical; the inclination of the paraconid in Cervictis further enhances the difference in height between it and the metaconid. A sharp paracristid connects the protoconid and paraconid: the protoconid arm is long and is

raised as a distinct blade, whereas the paraconid arm is much shorter; a keyhole-shaped carnassial notch is developed at the juncture of the protoconid and paraconid arms of the paracristid. The talonid is low and deeply basined, and supports three well-developed cusps. The hypoconid is the largest and tallest talonid cusp, occupying nearly half the width of the talonid, while the entoconid is much lower; on some specimens the entoconid is developed as a discrete cusp (e.g., UALVP 47813, Figs. 6.4.3-6.4.5), while in other specimens it is more fully incorporated into the entocristid (e.g., UALVP 47822). The hypoconulid is smaller and lower than the hypoconid and entoconid, and is connected to the hypoconid by a sharply notched hypocristid; its finger-like apex is directed nearly dorsally. The entocristid is sharp but low, leaving the talonid basin nearly open lingually; a weak entoconulid can occur on the entocristid. The cristid obliqua is directed anterolingually from the apex of the hypoconid, and a sharp notch is developed at its union with the postvallid wall. The anterior cingulid is invariably weakly developed on each of the m1s at hand, but the posterior cingulid is more variable: in UALVP 47817 (Fig. 6.4.6), it is poorly developed, forming no more than a low ridge at the hypoconid; in UALVP 47813 (Fig. 6.4.3), however, the posterior cingulid is prominent, extending labially from the apex of the hypoconulid, and then continuing anteriorly along the labial side of the hypoconid to the hypoflexid.

m2: The m2 of Cervictis differs from that of all other viverravids except Simpsonictis and Protictis paralus in being very large relative to m1, with the trigonid projecting well above the level of the m1 talonid. The trigonid cusps are tall and sectorial, rather than lower and more bulbous, and the protoconid and metaconid are subequal in height. The protoconid is somewhat swollen lingually, and is connected to the slightly lower and blade-like paraconid by a widely notched paracristid; as on m1, the paraconid on m2 leans anteriorly. The metaconid projects dorsally and lingually, and is connected to the protoconid by a widely notched protocristid. The talonid is only slightly longer than the trigonid, contrasting with m2 of Viverravus in which the talonid is much longer than the trigonid; the flat, basin-facing walls of the entoconid and hypoconid unite to form a shallow, V-shaped talonid basin that slopes anterolingually. The hypoconid and hypoconulid are nearly equal in size and height and are connected by a sharply notched hypocristid; the hypoconulid is finger-like and projects dorsally and slightly

anteriorly. The entoconid is small but discrete, and a sharp entocristid connects it to the postvallid wall. The cristid obliqua is long and arcuate, and joins the postvallid wall below the level of the protocristid notch. The anterior cingulid is relatively stronger than that on m1, but the posterior cingulid is virtually undeveloped and is restricted to the area below the hypocristid notch.

Etymology.—Thule, Greek, northern, in reference to the northern distribution of the species.

Holotype.—UALVP 47813, incomplete left dentary with p2-4, m1-2, and alveoli for c, p1. DW-2 locality, Paskapoo Formation of Alberta, late Paleocene [early middle Tiffanian, Ti3 (Fox, 1990), Plesiadapis rex/P. churchilli Lineage Zone of Lofgren et al., 2004].

Other material examined.—From DW-2: UALVP 47811, incomplete left maxilla with P3-4, M1; UALVP 47812, incomplete right maxilla with P4, M1-2; UALVP 47814, incomplete right dentary with P4, M1-2; UALVP 47815, 47816, M1; UALVP 47817, incomplete right dentary with p2-4, m1-2, and alveoli for c, p1; UALVP 47818, incomplete right dentary with p4, m1-2, and alveoli for c, p1-3; UALVP 47819, incomplete left dentary with m1 talonid and m2; UALVP 47820, 47821, lower canine; UALVP 47822, 47823, m1.

From Birchwood: UALVP 47852, associated P4, M1; UALVP 39414, P4; UALVP 47853, incomplete right dentary with m1-2 and alveoli for p3-4; UALVP 39415, p4; UALVP 39416, incomplete m1; UALVP 39417, incomplete m2.

From Hand Hills West upper level: UALVP 47854, incomplete left dentary with m2.

Age and occurrence.—Early middle Tiffanian (Plesiadapis rex/P. churchilli Lineage Zone, Ti3, late Paleocene) of the Western Interior of North America.

6.3 Conclusions

The Relationships of Cervictis

Although the dentition of Cervictis resembles those of other viverravids generally, the unusual combination of character states outlined in the diagnosis occurs in no other viverravid taxon; the differences are similar in scope to those separating other viverravid genera, and the specimens from Alberta are recognized here as representing a new genus. Perhaps the most striking features that distinguish Cervictis from other viverravids pertain to p4 (Fig. 6.5). For example, the anterior slope of the p4 crown in Cervictis is somewhat sinusoidal in labial view, being slightly concave ventrally but becoming more convex towards the protoconid apex, and the protoconid is nearly vertical, rather than recurved. The paraconid is very small, slightly recurved, and is set off from the protoconid on a prominent lobe in Cervictis; the paraconid on p4 of a few viverravids is somewhat separate from the protoconid [see, e.g., p4 of Simpsonictis (Figs. 6.5.1, 6.5.2) and Raphictis (Figs. 6.5.9, 6.5.10)], but in no other viverravid is it as far anterior of the protoconid, nor is it reduced to the same degree as that in Cervictis. Among previously known viverravids, Cervictis most closely resembles Simpsonictis and Protictis paralus in comparable parts of the dentition: each has a p4 with a strongly developed, blade-like second posterior accessory cusp, an m1 paraconid that is not strongly appressed to the protoconid, and an m2 that is significantly enlarged relative to m1; of these similarities, only the position of the m1 paraconid seems derived among viverravids, with the remaining similarities likely being primitive for carnivorans generally (Flynn and Galiano, 1982; Fox and Youzwyshyn, 1994). The teeth of Cervictis resemble more closely those of P. paralus than those of Simpsonictis, but nonetheless differ from the teeth of both of these taxa in a number of important ways:

1) The teeth of Cervictis are more robust, with more swollen cusps and blunter crests;

2) The metacone on M1 of Cervictis is larger and higher than it is in P. paralus, and the protocone is significantly more compressed anteroposteriorly; additionally, the protoconal cingula are more prominent and shelf-like in Cervictis, and a low hypocone is occasionally developed;

3) The p4 of Cervictis is longer and lower than that of Simpsonictis and P. paralus;

4) The first posterior accessory cusp on p4 of Cervictis, although better developed than that in Simpsonictis, is smaller and more poorly differentiated than that in P. paralus;

5) The p4 paraconid is much smaller in Cervictis, and it is set off from the protoconid on a distinct, anteroventrally projecting lobe; consequently, the anterior slope of the p4 is longer in Cervictis, and the protoconid is more nearly vertical, rather than recurved;
6) The p4 paracristid is weak or undeveloped in Cervictis, whereas that in P. paralus is stronger and drawn out anteriorly as a blade; a weak paracristid is seen on p4 of Simpsonictis and may be primitive for Carnivora generally;
7) The trigonid on m1 and m2 is relatively higher in Cervictis than it is in P. paralus, but relatively lower than in Simpsonictis;
8) The m1 paraconid is lower, less transverse and bladelike, and more anteriorly leaning in Cervictis than it is in Simpsonictis and P. paralus; consequently, the m1 trigonid appears more "open" in Cervictis, and is similar in this regard to the m1 of Viverravus (see, e.g., Flynn and Galiano, 1982);
9) The m1 metaconid in Cervictis arises from a higher position on the posterior shoulder of the protoconid than it does in P. paralus;
10) The m2 of Cervictis is larger than that of P. paralus, both with respect to absolute size and relative to m1, the trigonid projects further above the talonid of m1, and the m2 trigonid is relatively wider [it is noted here that the measurements presented by Gingerich and Winkler (1985) for the holotype m2 of P. paralus disagree with Holtzman's (1978) measurements (e.g., length m2=3.9, Holtzman, 1978, versus length m2=4.4, Gingerich and Winkler, 1985), and are further contradicted by the scale in Gingerich and Winkler (1985, figure 8); measurements taken for m2 from a cast of SMM P77.6.64 for this study confirm Holtzman's (1978) original measurements];
11) Diastemata are developed between c and p1, and usually between p1 and p2 in Cervictis.

The similarities in the dentitions of Cervictis and Simpsonictis are fewer than are those of P. paralus, and pertain mostly to the size of m2. In both genera the m2 is large, with the trigonid projecting well above the level of the m1 talonid; this is particularly evident in S. tenuis (Simpson, 1935), the oldest and presumably most primitive species of Simpsonictis (Gingerich and Winkler, 1985), where the m2 is approximately half the size of m1. Although the m2 of Cervictis is also enlarged relative to m1, it is proportionately smaller than in S. tenuis, and approaches the condition in S. pegus Gingerich and

Winkler, 1985. Beyond the similarity in relative m2 size, the dentitions of Cervictis and Simpsonictis differ significantly: for example, the p4 crown of Simpsonictis is high relative to its length, and bears a stronger paraconid that is more closely appressed to the protoconid, and a weaker first posterior accessory cusp; additionally, the posterior parts of p4 are more greatly expanded labiolingually in Simpsonictis, giving the crown a triangular shape in occlusal outline. The trigonid cusps on m1 and m2 are relatively taller and more gracile in Simpsonictis, and the paraconid is more nearly vertical, rather than anteriorly leaning.

Although many of the similarities between Cervictis and other viverravids seem to be plesiomorphic (e.g., M1 paracone and metacone nearly fully separate, weak M1 preparacrista blade, long M2, large, blade-like p4 second posterior accessory cusp, low m1 paraconid, large m2), with these character states being present in more basal viverravids, including Simpsonictis and Pristinictis (MacIntyre, 1962; Flynn and Galiano, 1982; Gingerich and Winkler, 1985; Fox and Youzwyshyn, 1994), a few characters may be derived among Viverravidae:

1) The P4 protocone being positioned far anteriorly, and the metastylar blade being elongate and not as transverse across the crown;

2) The p4 paraconid being reduced in size and positioned far anterior of the protoconid;

3) The molar paraconid being more anteriorly positioned.

In their review of early carnivoran relationships, Flynn and Galiano (1982) cited a more open m1 trigonid and anteriorly positioned p4 paraconid as potential synapomorphies that might unite Simpsonictis and Viverravus to the exclusion of other viverravids; although Cervictis shares these character states with Simpsonictis and Viverravus, other characters contradict such a relationship (e.g., strong conules on M1 and M2, basined talonid on p4, relatively higher metaconid on m1), or are more widely distributed among viverravids and are uninformative (e.g., high p4 second posterior accessory cusp, relatively elongate m2 talonid); given the poor understanding of the distribution of primitive and derived character states among viverravids, a better understanding of the phylogenetic position of Cervictis must await a more comprehensive analysis of Viverravidae than is attempted here.

6.4 Literature Cited

BOWDICH, T. E. 1821. An analysis of the natural classifications of Mammalia for the use of students and travelers. J. Smith, Paris, 115 pp.

BRYANT, H. N. 1991. Phylogenetic relationships and systematics of the Nimravidae (Carnivora). Journal of Mammalogy, 72:56-78.

BRYANT, H. N. 1996. Explicitness, stability, and universality in the phylogenetic definition and usage of taxon names: a case study of the phylogenetic taxonomy of the Carnivora (Mammalia). Systematic Biology, 45:174-189.

CAPPETTA, H., J.-J. JAEGER, M. SABATIER, J. SUDRE, and M. VIANEY-LIAUD. 1978. Découverte dans le Paléocène du Maroc des plus anciens mammifères eutheriens d'Afrique. Géobios, 11:257-263.

COPE, E. D. 1874. Report on the vertebrate fossils discovered in New Mexico, with descriptions of new species. Annual Report, Chief of Engineers, 1874, Appendix FF, Washington (Government Printing Office) 1874:3-18.

COPE, E. D. 1875. Systematic catalogue of Vertebrata of the Eocene of New Mexico, collected in 1874. Report to the Engineer Department, United States Army Geographical Survey West of the 100 Meridian:1-37.

COPE, E. D. 1880. On the genera of the Creodonta. Proceedings of the Academy of Natural Sciences of Philadelphia, 1875:444-448.

COPE, E. D. 1882. Synopsis of the vertebrata of the Puerco Eocene epoch. Proceedings of the American Philosophical Society, 20:461-471.

DORR, J. A. 1952. Early Cenozoic stratigraphy and vertebrate paleontology of the Hoback Basin, Wyoming. Bulletin of the Geological Society of America, 63:59-94.

FLYNN, J. J. 1998. Early Cenozoic Carnivora ("Miacoidea"), pp. 110-123. In C. M. JANIS, K. M. SCOTT, and L. L. JACOBS (eds.), Evolution of Tertiary mammals of North America. Volume 1: Terrestrial carnivores, ungulates, and ungulatelike mammals. Cambridge University Press, Cambridge.

FLYNN, J. J., and H. GALIANO. 1982. Phylogeny of early Tertiary Carnivora, with a description of a new species of Protictis from the middle Eocene of northwestern Wyoming. American Museum Novitates, 2725:1-64.

FLYNN, J. J., and G. D. WESLEY-HUNT. 2005. Phylogeny and early diversification of the Carnivora, pp. 175-198. In J. D. ARCHIBALD and K. D. ROSE (eds.), The Rise of Placental Mammals: Origins and Relationships of the Major Extant Clades. Johns Hopkins University Press, Baltimore.

FOX, R. C. 1988. Late Cretaceous and Paleocene mammal localities of southern Alberta. Occasional Paper of the Tyrrell Museum of Palaeontology, 6:1-38.

FOX, R. C. 1990. The succession of Paleocene mammals in western Canada, pp. 51-70. In T. M. BOWN and K. D. ROSE (eds.), Dawn of the Age of Mammals in the Northern Part of the Rocky Mountain Interior. Geological Society of America Special Paper, 243.

FOX, R. C., and G. P. YOUZWYSHYN. 1994. New primitive carnivorans (Mammalia) from the Paleocene of western Canada, and their bearing on relationships of the order. Journal of Vertebrate Paleontology, 14:382-404.

GHEERBRANT, E. 1995. Les mammifères paléocènes du bassin d'Ouarzazate (Maroc). III. Adapisoriculidae et autres mammifères (Carnivora, ?Creodonta, Condylarthra, ?Ungulata et incertae sedis). Palaeontographica Abteilung A, 237:39-132.

GHEERBRANT, E., H. CAPPETTA, M. FEIST, J.-J. JAEGER, J. SUDRE, M. VIANEY-LIAUD, and B. SIGÉ. 1993. La succession des faunes de vertébrés d'âge paléocène supérieur et éocène inférieur dans le bassin d'Ouarzazate, Maroc. Contexte géologique, portée biostratigraphique et paléogéographique. Newsletters on Stratigraphy, 28:33-58.

GHEERBRANT, E., J. SUDRE, S. SEN, C. ABRIAL, C. MARANDAT, B. SIGÉ, and M. VIANEY-LIAUD. 1998. Nouvelles données sur les mammifères du Thanetien et de l'Ypresien du bassin d'Ouarzazate (Maroc) et leur contexte stratigraphique. Palaeovertebrata, 27:155-202.

GILL, T. 1872. Arrangement of the families of mammals with analytical tables. Smithsonian Miscellaneous Collections, 11:1-98.

GINGERICH, P. D. 1983. Systematics of early Eocene Miacidae (Mammalia, Carnivora) in the Clark's Fork Basin, Wyoming. Contributions from the Museum of Paleontology, The University of Michigan, 26:197-225.

GINGERICH, P. D., and D. A. WINKLER. 1985. Systematics of Paleocene Viverravidae (Mammalia, Carnivora) in the Bighorn Basin and Clark's Fork Basin, Wyoming. Contributions from the Museum of Paleontology, The University of Michigan, 27:87-128.

HOLTZMAN, R. C. 1978. Late Paleocene mammals of the Tongue River Formation, western North Dakota. Report of Investigation, North Dakota Geological Survey, 65:1-88.

HUNT, R. M., and R. H. TEDFORD. 1993. Phylogenetic relationships within the aeluroid Carnivora and implications of their temporal and geographic distribution, pp. 53-73. In F. S. SZALAY, M. J. NOVACEK, and M. C. MCKENNA (eds.), Mammal Phylogeny: Placentals. Springer-Verlag, New York.

KRETZOI, M. 1945. Bemerkungen über das Raubtiersystem. Annales Historico-Naturale, Museum Nationale Hungaricum, 38: 59-83.

LINNAEUS, C. 1758. Systema naturae per regna tria naturae, secundum classes, ordines, genera, species cum characteribus, differentiis, synonymis, locis. Tomus I: Regnum animale. Editio decima, reformata. Laurentii Salvii, Stockholm [Facsimile reprinted in 1956 by the British Museum of Natural History].

LOFGREN, D. L., J. A. LILLEGRAVEN, W. A. CLEMENS, P. D. GINGERICH, and T. E. WILLIAMSON. 2004. Paleocene biochronology: The Puercan through Clarkforkian Land Mammal Ages, pp. 43-105. In M. O. WOODBURNE (ed.), Late Cretaceous and Cenozoic Mammals of North America: Biostratigraphy and Geochronology. Columbia University Press, New York.

MACINTYRE, G. T. 1962. Simpsonictis, a new genus of viverravine miacid (Mammalia, Carnivora). American Museum Novitates, 2118:1-4.

MACINTYRE, G. T. 1966. The Miacidae (Mammalia, Carnivora). Part I. The systematics of Ictidopappus and Protictis. Bulletin of the American Museum of Natural History, 131:115-210.

MARSH, O. C. 1871. Notice of some new fossil mammals and birds from the Tertiary formations of the West. American Journal of Science, Series 3, 2:120-127.

MARSH, O. C. 1872. Preliminary description of new Tertiary mammals. Part I. American Journal of Science, 4:122-128.

MATTHEW, W. D. 1915. Part I: Order Ferae (Carnivora). Suborder Creodonta, pp. 4-103. In W. D. MATTHEW and W. GRANGER (auths.), A revision of the lower Eocene Wasatch and Wind River faunas, Bulletin of the American Museum of Natural History, 34.

MATTHEW, W. D. 1937. Paleocene faunas of the San Juan Basin, New Mexico. Transactions of the American Philosophical Society, New Series, 30:1-510.

MCKENNA, M. C. and S. K. BELL. 1997. Classification of Mammals above the Species Level. Columbia University Press, New York.

MEEHAN, T. J., and R. W. WILSON. 2002. New viverravids from the Torrejonian (middle Paleocene) of Kutz Canyon, New Mexico and the oldest skull of the Order Carnivora. Journal of Paleontology, 76:1091-1101.

NOWAK, R. M. 1999. Walker's Mammals of the World. The Johns Hopkins University Press, Baltimore.

PARKER, T. J., and W. A. HASWELL. 1897. A Text-book of Zoology. Vol. 2. Macmillan Press, London, 301 pp.

POLLY, P. D. 1997. Ancestry and species definition in paleontology: a stratocladistic analysis of Viverravidae (Carnivora, Mammalia) from Wyoming. Contributions from the Museum of Paleontology, The University of Michigan, 30:1-53.

POLLY, P. D., G. WESLEY-HUNT, R. E. HEINRICH, G. DAVIS, and P. HOUDE. 2006. Earliest known carnivoran auditory bulla and support for a recent origin of crown-group Carnivora (Eutheria, Mammalia). Palaeontology, 49:1019-1027.

QUI Z., and LI C. 1977. Miscellaneous mammalian fossils from the Paleocene of Qianshan Basin, Anhui. Vertebrata PalAsiatica, 15:94-102. [in Chinese]

ROBINSON, P. 1966. Fossil Mammalia of the Huerfano Formation, Eocene, of Colorado. Bulletin of the Peabody Museum of Natural History, 21:1-95.

ROSE, K. D. 1981. The Clarkforkian Land Mammal Age and mammalian faunal composition across the Paleocene-Eocene boundary. The University of Michigan Papers on Paleontology, 26:1-197.

SCOTT, C. S. 2003. Late Torrejonian (middle Paleocene) mammals from south central Alberta, Canada. Journal of Paleontology, 77:745-768.

SIMPSON, G. G. 1935. New Paleocene mammals from the Fort Union of Montana. Proceedings of the United States National Museum, 83:221-244.

SIMPSON, G. G. 1937. Notes on the Clark Fork, upper Paleocene, fauna. American Museum Novitates, 954:13-24.

SIMPSON, G. G. 1945. The principles of classification and a classification of mammals. Bulletin of the American Museum of Natural History, 85:14-350.

TEILHARD DE CHARDIN, P. 1915. Les carnassiers des Phosphorites de Quercy. Annales de Paleontologie, Paris, 9:103-192.

WESLEY-HUNT, G. D., and J. J. FLYNN. 2005. Phylogeny of the Carnivora: basal relationships among the carnivoramorphans, and assessment of the position of "Miacoidea" relative to Carnivora. Journal of Systematic Palaeontology, 3:1-28.

WESLEY-HUNT, G. D., and L. WERDELIN. 2005. Basicranial morphology and phylogenetic position of the upper Eocene carnivoramorphan Quercygale. Acta Palaeontologica Polonica, 50:837-846.

WORTMAN, J. L. 1901. Studies of Eocene Mammalia in the Marsh Collection, Peabody Museum. Part I. Carnivora. American Journal of Science, 11:1-145.

WORTMAN, J. L., and W. D. MATTHEW. 1899. The ancestry of certain members of the Canidae, the Viverridae, and Procyonidae. Bulletin of the American Museum of Natural History, 12:109-139.

WYSS, A. R., and J. J. FLYNN. 1993. A phylogenetic analysis and definition of the Carnivora, pp. 32-52. In F. S. SZALAY, M. J. NOVACEK, and M. C. MCKENNA (eds.), Mammal Phylogeny: Placentals. Springer-Verlag, New York.

YOUZWYSHYN, G. P. 1988. Paleocene mammals from near Cochrane, Alberta. Unpublished M. Sc. thesis, University of Alberta, Edmonton, 484 pp.

Table 6.1.—Combined measurements and descriptive statistics for the dentition of Raphictis iota new species from the early middle Tiffanian (Ti3) DW-2 and Birchwood localities, and the late middle Tiffanian (Ti4) Gao Mine locality, Paskapoo Formation, Alberta.

Element	P	N	OR	M	SD	CV
P4	L	1	3.3	—	—	—
	W	1	2.3	—	—	—
M1	L	1	2.5	—	—	—
	W	1	3.8	—	—	—
p4	L	1	3.0	—	—	—
	W	1	1.1	—	—	—
m1	L	2	3.2-3.5	3.35	0.21	6.33
	TrW	2	1.9-2.1	2.00	0.14	7.07
	TaW	3	1.5-1.7	1.60	0.10	6.25
	TrH	2	3.8	3.80	0	0
m2	L	1	2.5	—	—	—
	TrW	1	1.3	—	—	—
	TaW	1	1.1	—	—	—
	TrH	1	1.6	—	—	—

Table 6.2.—Combined measurements and descriptive statistics for the dentition of Cervictis thula new genus and species from the early middle Tiffanian (Ti3) DW-2, Birchwood, and Hand Hills West upper level localities, Paskapoo Formation, Alberta.

Element	P	N	OR	M	SD	CV
P3	L	1	2.9	—	—	—
	W	1	1.5	—	—	—
P4	L	4	5.3-5.4	5.35	0.06	1.08
	W	4	3.1-3.3	3.23	0.10	2.97
M1	L	5	4.0-4.2	4.06	0.09	2.20
	W	5	5.3-5.5	5.40	0.07	1.31
M2	L	1	2.7	—	—	—
	W	1	3.9	—	—	—
p2	L	2	2.9-3.0	2.95	0.07	2.40
	W	2	1.1	1.10	0	0
p3	L	2	3.0-3.1	3.05	0.07	2.32
	W	2	1.3	1.30	0	0
p4	L	4	4.1-4.3	4.18	0.10	2.29
	W	4	1.8-1.9	1.85	0.06	3.12
m1	L	5	4.2-4.3	4.24	0.05	1.29
	TrW	5	2.9-3.0	2.94	0.05	1.86
	TaW	6	2.0-2.2	2.13	0.08	3.83
m2	L	6	4.0-4.2	4.10	0.09	2.18
	TrW	6	2.1-2.3	2.20	0.08	2.87
	TaW	6	1.7-1.9	1.77	0.08	4.62

Figure 6.1.—1-5. Didymictis dellensis Dorr from the early middle Tiffanian (Ti3) DW-2 locality, Paskapoo Formation, Alberta. 1, 2, UALVP 47801, right lower canine in 1, lateral and 2, medial view; 3-5, UALVP 47802, incomplete left dentary with m1 roots and m2 in 3, lateral (m2 in labial view), 4, medial (m2 in oblique anterolingual view), and 5, dorsal (m2 in anterior view).

6-11, ?Didymictis sp. 6-8, UALVP 47803, incomplete left p4 in 6, labial, 7, lingual, and 8, occlusal view; 9-11, UALVP 47804, right p4 in 9, labial, 10, lingual, and 11, occlusal view.

Scale bars = 2 mm.

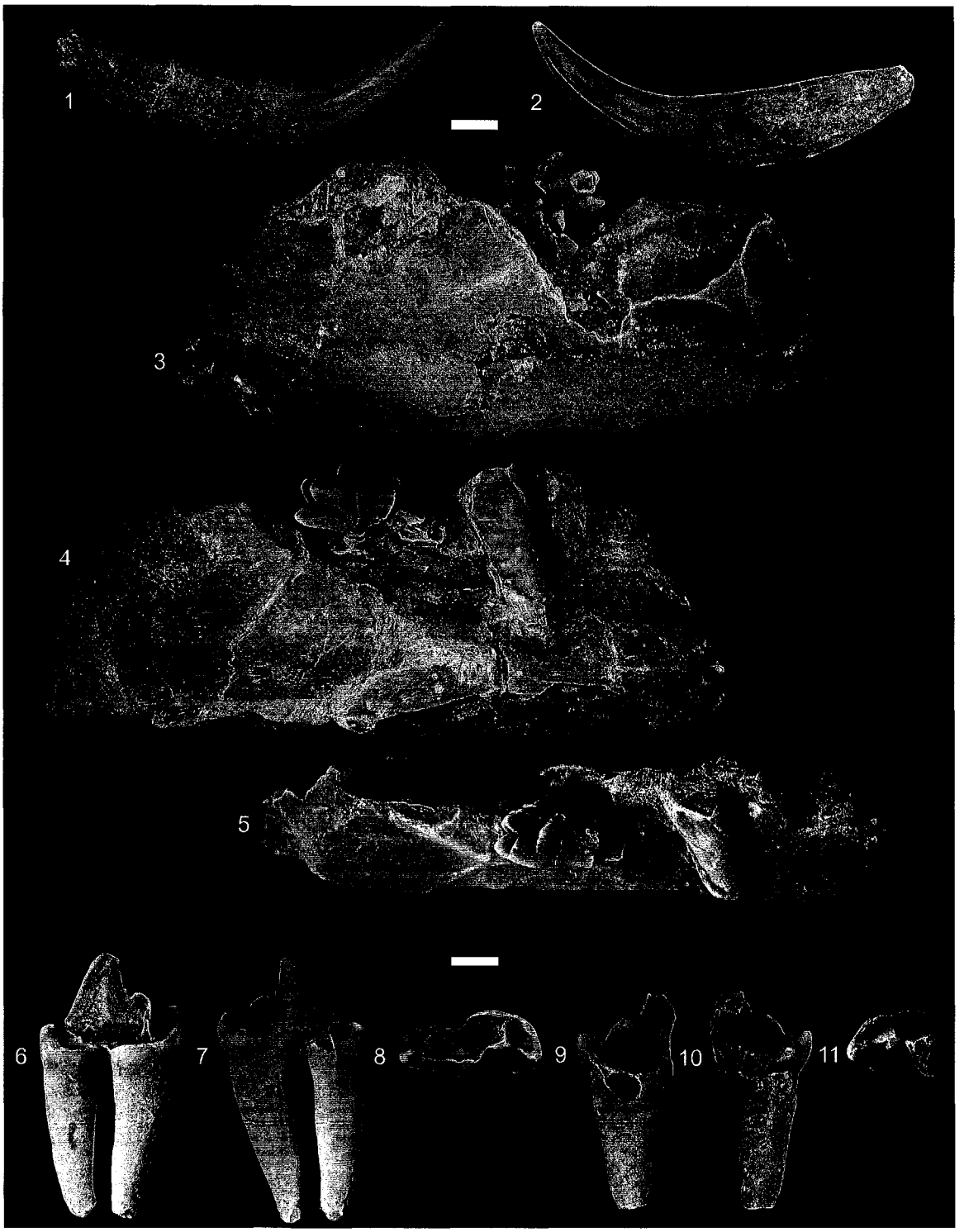
1
2
3
4
5
6
7
8
9
10
11

Figure 6.2.—1-15. Raphictis iota new species from the early middle Tiffanian (Ti3) DW-2 (DW2) locality, and the late middle Tiffanian (Ti4) Gao Mine (GM) locality, Paskapoo Formation, Alberta. 1-3, UALVP 47809 (GM), left P4 in 1, labial, 2, oblique lingual, and 3, occlusal view; 4-6, UALVP 47807 (DW2), left M1 in 4, occlusal, 5, labial, and 6, oblique lingual view; 7-9, UALVP 47806 (holotype, GM), incomplete left dentary with p4 and alveoli for m1 in 7, labial, 8, lingual, and 9, occlusal view; 10-12, UALVP 47808 (DW2), right m1 in 10, labial, 11, lingual, and 12, occlusal view; 13-15, UALVP 47805 (DW2), incomplete right dentary with m1 talonid and m2 in 13, labial, 14, lingual, and 15, occlusal view. Scale bars = 2 mm.

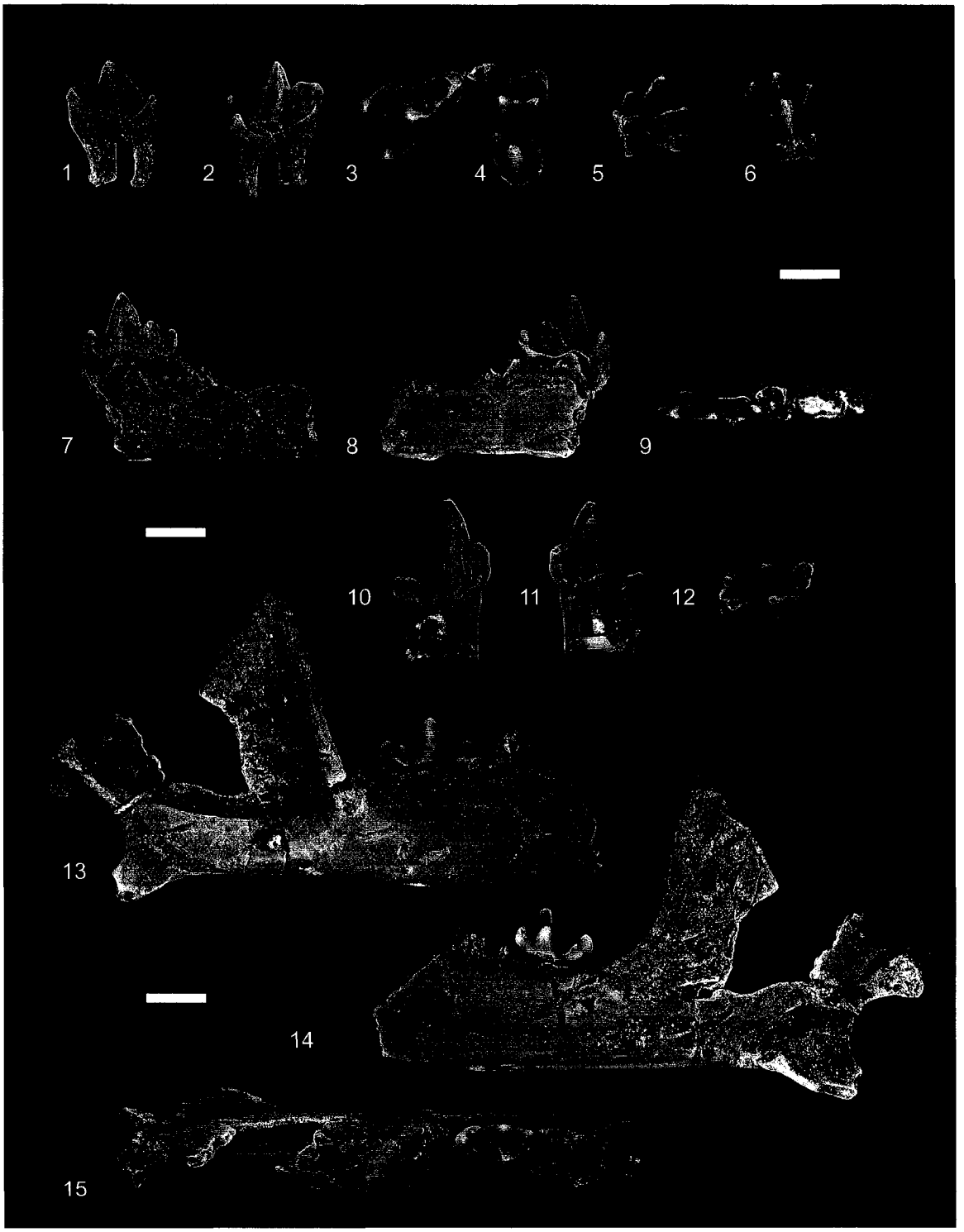
1
2
3
4
5
6
7
8
9
10
11
12
13
14
15

Figure 6.3.—1-3. Raphictis sp. from the early middle Tiffanian (Ti3) DW-2 locality, Paskapoo Formation, Alberta. 1-3, UALVP 47810, incomplete right maxilla with P4 in 1, labial, 2, oblique lingual, and 3, occlusal view.

4-8. Cervictis thula new genus and species from the early middle Tiffanian (Ti3) DW-2 locality, Paskapoo Formation, Alberta. 4-6, UALVP 47811, incomplete left maxilla with P3-4, M1 in 4, labial, 5, oblique lingual, and 6, occlusal view; 7, 8, UALVP 47812, incomplete right maxilla with P4, M1-2 in 7, labial and 8, occlusal view.

Scale bars = 2 mm.

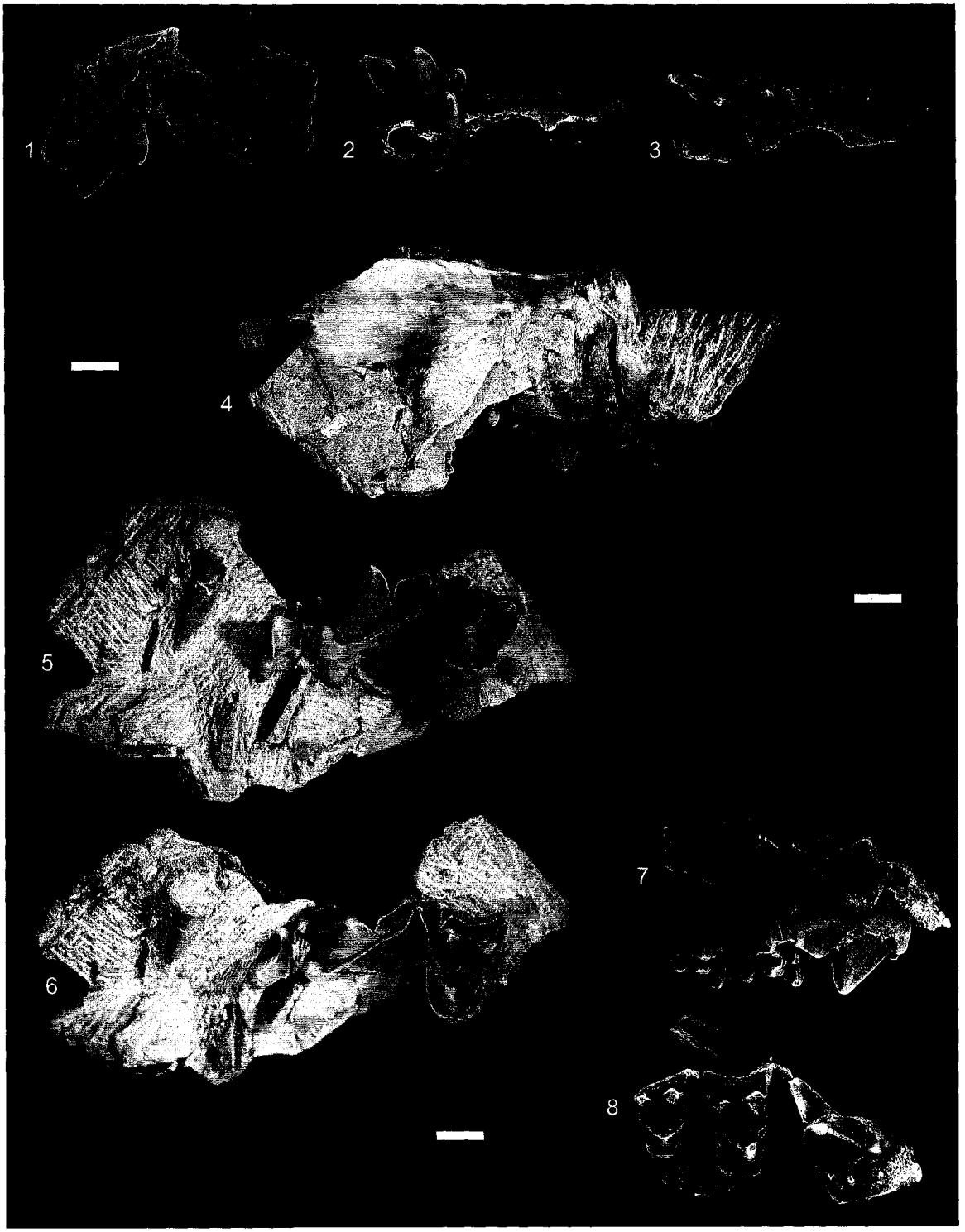
1
2
3
4
5
6
7
8

Figure 6.4.—1-8. Cervictis thula new genus and species from the early middle Tiffanian (Ti3) DW-2 locality, Paskapoo Formation, Alberta. 1, 2, UALVP 47820, lower right canine in 1, lateral and 2, medial view; 3-5, UALVP 47813 (holotype), incomplete left dentary with p2-4, m1-2, and alveoli for c, p1 in 3, labial, 4, lingual, and 5, occlusal view; 6-8, UALVP 47817, incomplete right dentary with p2-4, m1-2, and alveoli for c, p1 in 6, labial, 7, lingual, and 8, occlusal view. Scale bars = 2 mm.

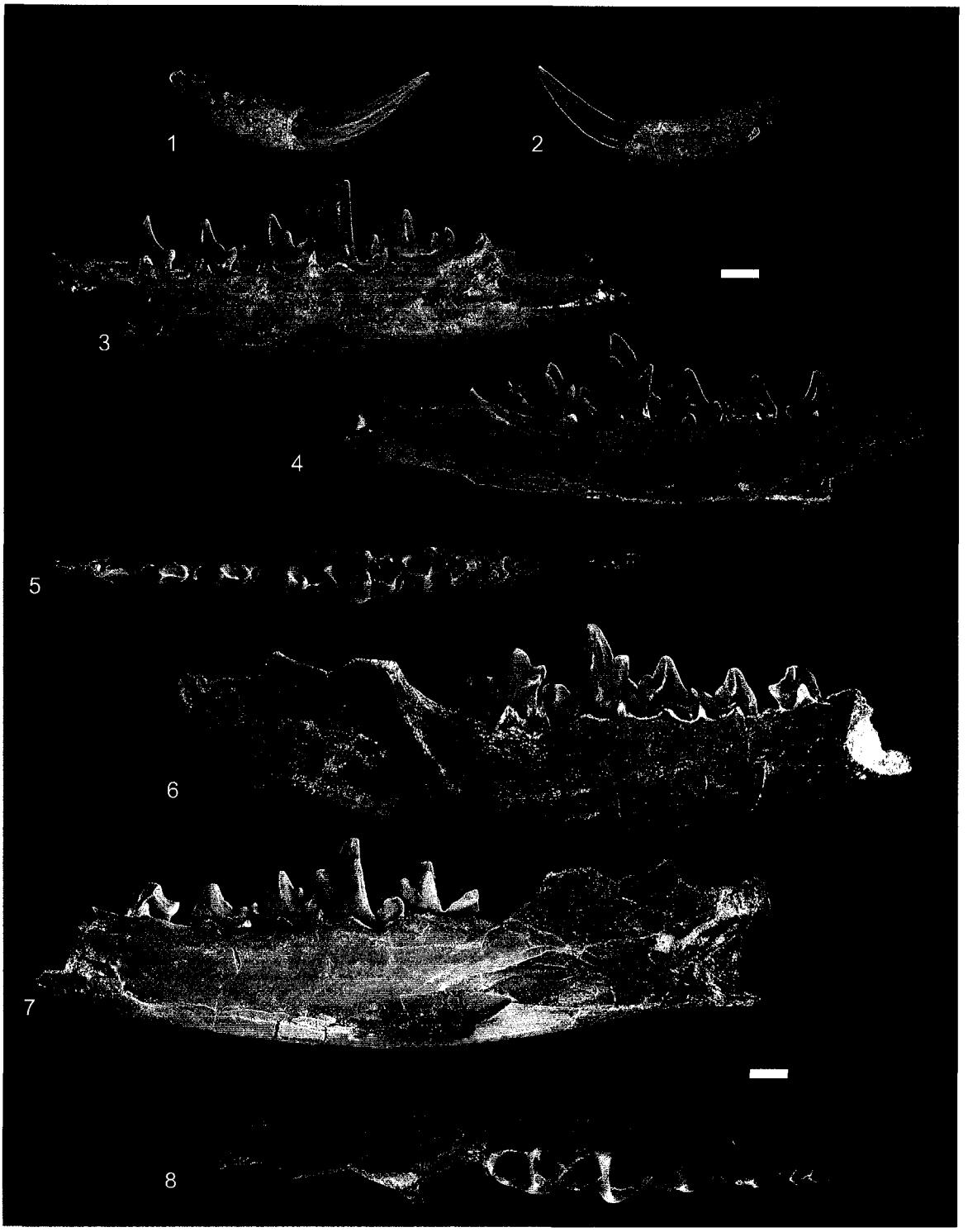
1
2
3
4
5
6
7
8

Figure 6.5.—1-12. Outline drawings of p4 of various viverravids in labial and occlusal views. 1, 2, Simpsonictis tenuis (Simpson) from the middle Torrejonian (To2) Gidley Quarry, Fort Union Formation of Montana; AMNH 35350 (reversed from original) in 1, labial, and 2, occlusal views.

3, 4, Protictis paralus Holtzman from the late middle Tiffanian (Ti4) Judson locality, Fort Union Formation of North Dakota; SMM P77.6.64 (holotype, reversed from original) in 3, labial, and 4, occlusal views.

5, 6, Viverravus schaffi (Gingerich and Winkler) from the late Tiffanian (Ti5) Schaff Quarry, Fort Union Formation of Wyoming; YPM-PU 19365 (holotype) in 5, labial, and 6, occlusal views.

7, 8, Cervictis thula new genus and species from the early middle Tiffanian (Ti3) DW-2 locality, Paskapoo Formation of Alberta; UALVP 47813 (holotype) in 7, labial, and 8, occlusal views.

9, 10, Raphictis iota new species from the early middle Tiffanian (Ti3) DW-2 locality, Paskapoo Formation of Alberta; UALVP 47806 (holotype) in 9, labial, and 10, occlusal views.

11, 12, Protictis minor Meehan and Wilson from KUVP New Mexico locality 13, Nacimiento Formation of New Mexico; KUVP 7081 (holotype, reversed from original) in 11, labial, and 12, occlusal views.

Outline drawings of p4 of Simpsonictis, Protictis paralus, Cervictis, Raphictis, and Protictis minor have been scaled to approximately the same dimensions of p4 of Viverravus schaffi. Scale bars = 2 mm.

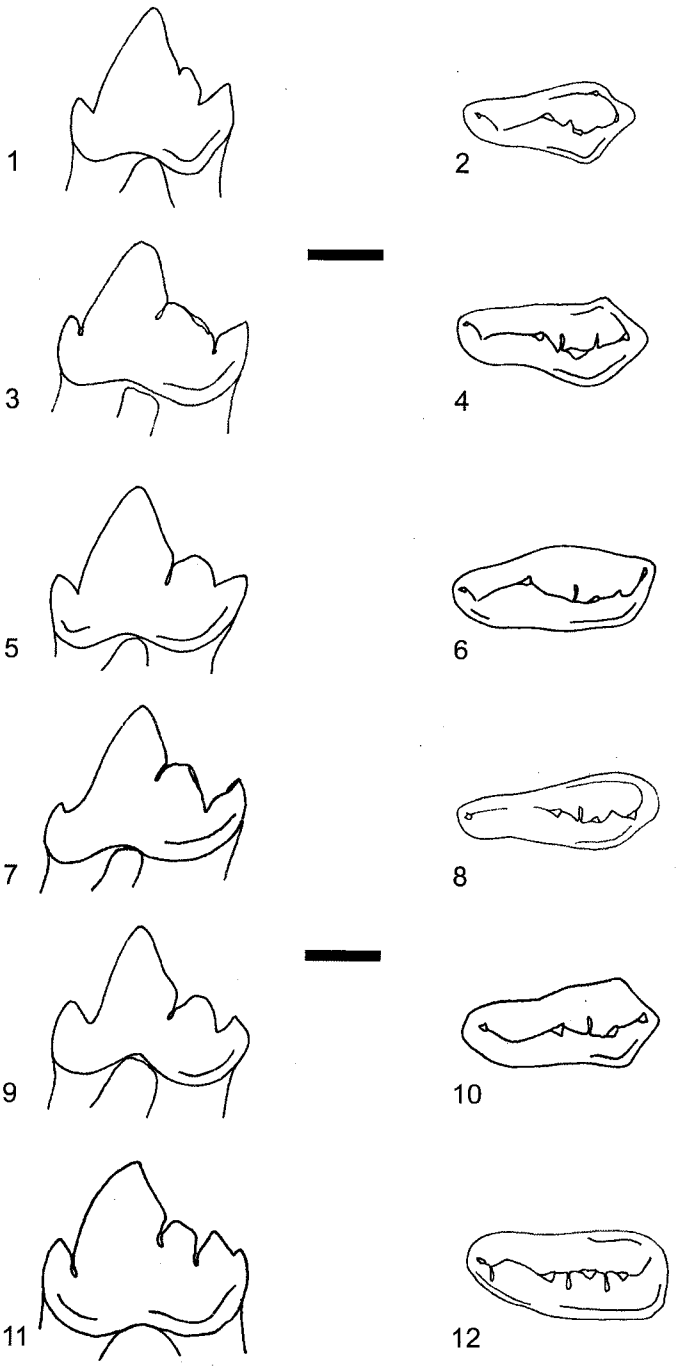
1
2
3
4
5
6
7
8
9
10
11
12

7 Paleocene Plesiadapiforms (Mammalia, Primates) from Alberta, Canada, and the Relationships of Picrodontidae Simpson[3]

7.1 Introduction

FEW GROUPS of early Tertiary placental mammals are as well known, more intensively studied, or whose systematic relationships are more controversial than the Plesiadapiformes. These distinctions have been gained in part because of the historic and largely prevailing view that the group may have shared a recent common ancestor with, or perhaps even represents the ancestral stock from which Euprimates (primates of modern aspect, or crown primates) ultimately arose (Matthew and Granger, 1921; Gidley, 1923; Gingerich, 1976; Szalay and Delson, 1979; but see, e.g., Gunnell, 1989; Beard, 1990; Kay et al., 1992 for opposing views), and in part because plesiadapiforms are thought to have played a central role in the origin and evolution of Archonta (or Euarchonta of Waddell et al., 1999 and Silcox et al., 2005), a more inclusive group containing primates, scandentians (tree shrews) and dermopterans (flying lemurs) (and see Beard, 1990; Kay et al., 1990, 1992; Beard, 1993a-b; Sargis, 2002a-b; Bloch et al., 2002). Although their dentitions are extremely diverse (compare, e.g., the teeth of Carpolestidae and Paromomyidae), plesiadapiforms are united in having (where known) an enlarged pair of upper and lower medial incisors (with the upper incisors being further elaborated in some advanced forms by having the apex divided into two or more distinct cusps), and in having low-crowned lower molars with anteriorly leaning trigonids and broad talonids, and an enlarged, often lobate m3 hypoconulid; many have P4 and the upper molars bearing a well-developed postprotocone fold (Simpson, 1935; Szalay and Delson, 1979; Gunnell, 1989; Silcox, 2001; Silcox and Gunnell, in press). The suborder comprises 11 or 12 families that are known principally from the Paleocene and Eocene of North America and Europe, although more recently described material from Asia and Africa suggests the group may have occupied a much wider geographical range than was previously believed (Beard and Wang, 1995; Hooker et al., 1999; Fu et al., 2002; Smith et al., 2004).

[3] Parts of this chapter have been published. Scott and Fox, 2005. Journal of Paleontology, 79:635-657.

The status of Plesiadapiformes, or a subset of Plesiadapiformes, as the sister group of Euprimates has received some support in recent computer-assisted cladistic analyses (e.g., Silcox, 2001; Bloch and Boyer, 2002; Silcox et al., 2005; Bloch et al., 2007), but the subject continues to be intensively debated (e.g., Bloch and Boyer, 2002; Kirk et al., 2003; Bloch and Boyer, 2003); in fact, while most recent analyses have suggested that plesiadapiforms are primates (Van Valen, 1994; Silcox, 2001; Bloch and Boyer, 2002; Silcox, 2003; Bloch et al., 2007), a consensus on even this most fundamental issue has yet to be reached (see, e.g., the contrasting opinions of Martin, 1968; Cartmill, 1972, 1974; Gingerich, 1976; Krishtalka and Schwartz, 1978; MacPhee et al., 1983; Wible and Covert, 1987; Andrews, 1988; Beard, 1989; Gingerich, 1990; Beard, 1990; Martin, 1990a-b; Gingerich et al., 1991; Kay et al., 1990, 1992; Beard, 1993a-b; Rose et al., 1993; Rose, 1995; McKenna and Bell, 1997; Kirk et al., 2003). Furthermore, it has been suggested recently that Plesiadapiformes are paraphyletic with respect to Euprimates (i.e., some plesiadapiforms may be more closely related to Euprimates than to other plesiadapiforms) and that the nomen be abandoned in favour of new taxonomic names that recognize only monophyletic groups (see, e.g., Silcox, 2001; Bloch et al., 2007). Plesiadapiformes here follows the usage of Clemens (2004) and provisionally includes all primates that fall outside the taxon Euprimates (sensu Hoffstetter, 1977). Additionally, the new nomina proposed by Bloch et al. (2007) are not used here: the hypothesized sister group relationships of either Carpolestidae and Euprimates (Bloch and Boyer, 2002) or Plesiadapoidea and Euprimates (=Euprimateformes, see Bloch et al., 2007) are not without controversy (e.g., Kirk et al., 2003), and rest, at least in part, on what are here considered biologically implausible character reversals (e.g., the enlarged I1 of plesiadapiforms reversing to a size and coronal morphology that is more similar to that of I2 in the earliest euprimates; the re-acquisition of p1; see Bloch et al., 2007, fig. 4, node 5; and see Gunnell, 1989 for similar sentiments). Although the larger issue of plesiadapiform-euprimate relationships is admittedly sidestepped here, the fact that Plesiadapiformes have yet to be unequivocally shown to be non-monophyletic suggests that its traditional usage (i.e., designating a potentially monophyletic group of primates of archaic aspect) is appropriate for the present purposes.

Plesiadapiforms are among the best-studied Paleocene mammals from western Canada. They are first known from the ?middle Puercan (Pu2) Rav W-1 locality of Saskatchewan (Johnston, 1980; Johnston and Fox, 1984; Fox, 1997), represented by rare specimens of an as yet unidentified species of the purgatoriid Purgatorius Van Valen and Sloan, 1965. By middle Torrejonian (To2) time in Alberta, however, at least six genera in four families are known (Scott, 2003), and by the late Paleocene (Ti1-4) of both Alberta and Saskatchewan, plesiadapiforms are among the most taxonomically diverse and numerically abundant placental mammals in many local faunas (Krause, 1978; Fox, 1984a-c; Youzwyshyn, 1988; Fox, 1990a, 1991a, 1994, 2002; Scott, 2004). The principal aim of this chapter is to document previously undescribed plesiadapiforms from the Paleocene of Alberta, particularly those from the early middle Tiffanian (Ti3, late Paleocene) Blindman River and Birchwood localities, and focusing especially on the taxonomy and phylogenetic relationships of Picrodontidae, an unusual and poorly known plesiadapiform family. Since 1908, the peculiar North American primate Picrodus Douglass has been thought to contain only a single species, P. silberlingi Douglass; new collections from the Paskapoo Formation of Alberta, however, reveal that a rich complex of Picrodus species lived during the Paleocene, and three of these, Picrodus calgariensis, P. canpacius, and P. lepidus, are described herein as new. The new picrodontid specimens are known from several localities in Alberta that span the middle Torrejonian to the early middle Tiffanian parts of the Paleocene, and represent the first significant addition to knowledge of picrodontids in nearly 20 years.

7.2 Systematic Paleontology

Class MAMMALIA Linnaeus, 1758

Subclass THERIA Parker and Haswell, 1897

Infraclass EUTHERIA Gill, 1872

Grandorder ARCHONTA Gregory, 1910

Order PRIMATES Linnaeus, 1758

Suborder PLESIADAPIFORMES Simons, 1972

Family MICROMOMYIDAE Szalay, 1974

Genus MICROMOMYS Szalay, 1973

Micromomys SZALAY, 1973, p. 76.

Type species.—Micromomys silvercouleei Szalay, 1973.

Other included species.—Micromomys vossae Krause, 1978; M. willwoodensis Rose and Bown, 1982; M. fremdi Fox, 1984a.

MICROMOMYS FREMDI Fox, 1984a

Figure 7.1; Tables 7.1, 7.2

Micromomys fremdi FOX, 1984a, p. 1262.

Holotype.—UALVP 21010, incomplete left dentary with ?c, p2-4, m1-3, and alveolus for i1 (Fox, 1984, p. 1262). DW-2 locality, Paskapoo Formation of Alberta, late Paleocene [early middle Tiffanian, Ti3 (Fox, 1990b), Plesiadapis rex/P. churchilli Lineage Zone of Lofgren et al., 2004].

Material examined.—From DW-2: UALVP 46678, incomplete left maxilla with upper canine, P2-4, and associated and incomplete right dentary with p4, m1-3, and alveoli for c, p2-3; UALVP 21015, incomplete left maxilla with P2 (damaged), P3-4, M1-3; UALVP 21014, incomplete left maxilla with damaged P4, M1-3; UALVP 21012, incomplete left dentary with p4, m2-3, and alveoli for p3, m1; UALVP 21011, incomplete right dentary with c, p3-4, m1-3, and alveoli for p2; UALVP 21013, incomplete right dentary with p3-4, m2-3, and alveoli for ?i1, c, p2, m1; UALVP 40655, incomplete left dentary with p3-4, m1-3; UALVP 40653, incomplete right dentary with p3-4, m1-3; UALVP 40652, incomplete left dentary with m3; UALVP 46679, incomplete left dentary with p4, m1-3, and alveoli for p3; UALVP 46680, incomplete left dentary with p4, m1-3, and alveoli for c, p2-3; UALVP 46681, incomplete left dentary with p3-4, m1.

Age and occurrence.—Type locality only.

Description.—The dentition of Micromomys fremdi was described in detail by Fox (1984a) and need not be repeated in detail here. Recently prepared specimens referable to M. fremdi provide additional information on the anterior dentition, including the first discovered upper canine for the species.

Upper dentition (Figs. 7.1.1-7.1.3, 7.1.7-7.1.9): UALVP 46678 preserves four teeth in partial articulation with a fragmentary maxilla (i.e., the teeth are partially extruded from their alveoli and the bone is crushed, but the teeth are clearly from a single individual). The more fully molariform of these teeth are identified as P3-4, owing to their close resemblance with similar teeth of Micromomys fremdi in UALVP 21015 (Fox, 1984a, and Figs. 7.1.7-7.1.9). The two remaining teeth are premolariform and are identified here as the upper canine (the larger of the two), and P2, in keeping with a similar pattern seen in the lower dentition (Fox, 1984a). It may be argued that the smaller of the two premolariform teeth is in fact P1, with P2 having been lost prior to burial and subsequent collection of UALVP 46678, but this possibility is rejected here for the following reasons: 1) although many plesiadapiforms do show an incongruous loss of teeth between the upper and lower series [such that reduced, non-occluding upper teeth may be retained while their lower counterparts have been lost, e.g., Pronothodectes gaoi Fox, 1990a (Boyer, Scott, and Fox, in prep), Picrodus calgariensis (see later in this chapter), Tinimomys graybulliensis (Rose et al., 1993)], these non-occluding teeth are usually always small, and are in most cases single-rooted, whereas the tooth identified as P2 in M. fremdi is two-rooted and large; 2) the length of P2 in UALVP 46678 is virtually the same as that occupied the P2 alveoli in UALVP 21015; and 3) manual occlusion of UALVP 46678 with UALVP 21010 or UALVP 21011 (incomplete dentaries with teeth) indicates that the upper canine and the tooth identified here as P2 are together too large to have been accommodated by the diastema between the lower canine and p2, as would be necessary if the questionable tooth was in fact P1. It is likely, then, that the anteriormost teeth in UALVP 46678 represent a two-rooted upper canine and P2, and that these teeth occluded with their lower counterparts. Although the present evidence does not indicate the presence of P1, the interpretation favoured here does not discount the possibility that a small P1 may have been retained in M. fremdi. An incomplete maxilla of an undescribed species of Micromomys from the late Tiffanian Y2K Quarry of Wyoming

apparently retains a two-rooted upper canine (known only from its alveoli in UM 110140), and the P2 described by Secord (2004) closely matches that of the P2 of M. fremdi.

Upper canine: The upper canine is two-rooted, similar to that reported for Tinimomys Szalay, 1974, Dryomomys Bloch, Silcox, Boyer, and Sargis, 2007, and primitive microsyopids (Gunnell, 1989; Silcox, 2001; Silcox and Gunnell, in press). Unlike that in Dryomomys, the upper canine in Micromomys fremdi is enlarged relative to P2 and P3. The crown consists primarily of an enlarged, mediolaterally compressed and slightly recurved paracone; a sharp crest extends from the paraconal apex towards the base of the crown, and joins a very small posterior cuspule.

Upper premolars: P2: The crown of P2 closely resembles that of the upper canine, but is slightly smaller and less compressed labiolingually.

P3-4: The P3 and P4 in UALVP 46678 resemble those on UALVP 21010 described by Fox (1984a), differing mainly in both teeth being slightly larger and more transverse, and in P3 having a well-developed metacone connected to the paracone by a deeply notched centrocrista.

Lower dentition (Figs. 7.1.4-7.1.6, 7.1.10-7.1.18): The lower dentition of Micromomys fremdi was described in detail by Fox (1984). Three new specimens (UALVP 46678, 46679, 46680) preserve parts of the lower dentition, but do not add significantly to what is already known.

Discussion.—Other than the newly discovered upper canine, the additional specimens of Micromomys fremdi reported here add little to Fox's (1984a) original description. Although the Micromomyidae have become much better known in the years since M. fremdi was first described, with additional species of Micromomys having been discovered in late Paleocene and Eocene horizons in Wyoming (e.g., Bloch, 2001; Secord, 2004), M. fremdi is still known only from the type locality. The taxonomic position of Micromomyidae historically has been unstable, with the family being variously allied with paromomyids (e.g., Szalay, 1974; Szalay and Delson, 1979), microsyopids (e.g., Rose and Bown, 1982; Fox, 1984a; Gunnell, 1989), or as a divergent family of uncertain affinity (e.g., Silcox, 2001). The results of analyses of recently discovered micromomyid crania and postcrania suggest that Micromomyidae are among

the most primitive primates (Bloch et al., 2007), an opinion that is consistent with Fox's (1984a) suggestions that were made over twenty years earlier.

Superfamily PLESIADAPOIDEA Trouessart, 1897

Family PLESIADAPIDAE Trouessart, 1897

Genus PRONOTHODECTES Gidley, 1923

Pronothodectes GIDLEY, 1923, p. 12.

*

Type species.—Pronothodectes matthewi Gidley, 1923.

Other included species.—Pronothodectes jepi Gingerich, 1975; P. gaoi Fox, 1990a.

PRONOTHODECTES GAOI Fox, 1990a

Figures 7.2-7.7; Tables 7.3, 7.4

Pronothodectes gaoi FOX, 1990a, p. 639.

Holotype.—UALVP 31238, incomplete left dentary with p3-4, m1-2, and alveoli for i1-2, c, p2 (Fox, 1990a, p. 639). DW-2 locality; Paskapoo Formation of Alberta, late Paleocene [early middle Tiffanian, Ti3 (Fox, 1990b), Plesiadapis rex/P. churchilli Lineage Zone of Lofgren et al., 2004].

Material examined.—From Erickson's Landing: AMNH 15543D, E, M2; AMNH 15543H, m1; AMNH 15543G, m2; AMNH 15543F, ?m3.

From DW-1: UALVP 31396, incomplete right maxilla with P3-4, M1; UALVP 46682, I1; UALVP 46683, M3; UALVP 46684, m3.

From DW-2: UALVP 46685, incomplete skull with left and right I1-2, C, P2-4, M1-3; UALVP 46686, incomplete right maxilla with P2-3, M1-3, alveoli for upper canine and P4, and associated incomplete right dentary with p3-4, m1-2; UALVP 46687, incomplete skull with right I1, P2 (roots), P3-4, M1-3, alveolus for upper canine, and

associated petrosal; UALVP 46688, incomplete left maxilla with C, P2-4, M1-2, and associated I1 root; UALVP 46689, incomplete left maxilla with P2-4, M1-2; UALVP 46690, incomplete right maxilla with M1-3; UALVP 46691, incomplete right maxilla with P3-4, M1; UALVP 46692, incomplete left maxilla with M1-2; UALVP 46693, M1 and associated p4, m2; UALVP 46694-46714 (total: 21), I1; UALVP 46715-46718 (total: 4), DP4; UALVP 46719-46723 (total: 5), P4; UALVP 40597, 46724-46730, M1 (total: 7); UALVP 46731-46741, M2 (total: 11); UALVP 40658, 46742-46750, M3 (total: 9); UALVP 46751-46755, M1 or M2 (total: 5); UALVP 31238 (holotype), incomplete left dentary with p3-4, m1-2, and alveoli for i1-2, c, p2; UALVP 31240, incomplete left dentary with p3-4, m1-2, and alveoli for i1-2, c, p2, m3; UALVP 31536, incomplete right dentary with i1-2, c, p2-3; UALVP 34125, incomplete left dentary with p4, m1-3; UALVP 31538, incomplete left dentary with p4, m1-3, and alveoli for i1, c, p2-3; UALVP 31239, incomplete left dentary with p3-4, m1, and alveoli for i1-2, c, p2; UALVP 31537, incomplete left dentary with p3, and alveoli for i1, c, p2, p4; UALVP 46756, incomplete left dentary with m2-3 and associated p4; UALVP 46757, incomplete left dentary with i1, p4, m2-3, and alveoli for m1; UALVP 46758, incomplete left dentary with p3-4, m1-3, and associated i1; UALVP 46759, incomplete right dentary with p4, m1-3; UALVP 46760, incomplete left dentary with m1-2, and alveoli for m3; UALVP 46761, incomplete right dentary with p4, m1-2, and associated i1; UALVP 46762, incomplete left dentary with m1-2, and alveoli for i1-2, c, p3-4, m3; UALVP 46763, incomplete left dentary with m2 and alveoli for m1, m3; UALVP 46764-46775, i1 (total: 12); UALVP 46776-46778, p3 (total: 3); UALVP 46779-46783, p4 (total: 5); UALVP 46784-46787, m1 (total: 4); UALVP 46788-46791, m2 (total: 4); UALVP 46792-46798, m3 (total: 7).

From Mel's Place: UALVP 46799, P4.

From Birchwood: UALVP 39359, incomplete right maxilla with P3-4, M1-3; UALVP 46800, incomplete left maxilla with M1-3; UALVP 39366, incomplete right maxilla with M2-3; UALVP 39326-28, 39331, 39333-34, 46801-46815, I1 (total: 21); UALVP 46816, P3; UALVP 39341-43, P4; UALVP 39361-62, 39364, 46817, M1 (total: 4); UALVP 39301, 39360, 39363, 39365, 39376, M2 (total: 5); UALVP 39367-70, 46818-46823, M3 (total: 6); UALVP 39313, incomplete left dentary with i1, p4, m1-3,

and alveoli for i2, c, p2-3; UALVP 39373, incomplete left dentary with m2 and alveoli for i1-2, c, p2-4, m1; UALVP 39372, incomplete left dentary with i1, p3, and alveoli for i2, c, p2, p4, m1-2; UALVP 39371, incomplete right dentary with p4, m1-3, and alveoli for i1-2, c, p2-3; UALVP 46824, incomplete right dentary with p4, m1-3; UALVP 46825, incomplete left dentary with p4, m1-3, and alveoli for i1-2, c, p2-3; UALVP 46826, incomplete left dentary with p4, m1-3; UALVP 39346, incomplete left dentary with p3-4, m1-2, and alveoli for i1-2, c, p2, m3; UALVP 46827, incomplete right dentary with i1, p4 (talonid), m1-3, and alveoli for i2, c, p2-3; UALVP 39345, incomplete right dentary with p4, m1-3; UALVP 39344, incomplete left dentary with m1-2; UALVP 39347, incomplete right dentary with m1-2; UALVP 39315-17, 39319, 39321, 39323-24, 46828-46838, i1 (total: 11); UALVP 39335, p3; UALVP 39336-40, p4 (total: 5); UALVP 39348, 39351, 39358, 39381-83, m1 (total: 6); UALVP 39349-50, 39352-55, 39374, 39384-5, 46839, m2 (total: 10); UALVP 39356-57, 39375, m3.

Age and occurrence.—Early middle Tiffanian (Plesiadapis rex/P. churchilli Lineage Zone, Ti3, late Paleocene) of Alberta (Fox, 1990a-b).

Description.—Upper dentition (Figs. 7.2-7.5): I1: Twenty two upper central incisors of Pronothodectes gaoi have been recovered from the Blindman River and Birchwood localities. The I1 closely resembles that of other plesiadapids in being elongate and faintly curved, with a broadly concave occlusal surface. The robust crown bears two prominent apical cusps, the anterocone and laterocone, and a slightly smaller basal cusp, the posterocone. A small mediocone is developed dorsal and slightly posterior to the level of the anterocone. The anterocone is the largest of the apical cusps, being taller and wider at its base than the laterocone, and with its apex directed slightly laterally. Two well-developed crests originate at the apex of the anterocone: the first extends posterolaterally, forming a deep notch between the anterocone and laterocone, while the second is shorter and curves posteromedially to the mediocone. A raised ridge of enamel on the medial side of the anterocone marks a point of articulation of the opposing I1, and this surface usually bears a flattened, subovoid wear facet (e.g., UALVP 46695). The apex of the laterocone is directed more posteriorly than that of the anterocone, and a long crest extends from its apex posteriorly and dorsally, defining the lateral margin of the occlusal surface of the crown. A centroconule is not developed on

any of the specimens; instead, the enamel between and slightly dorsal to the anterocone and laterocone is smooth. The mediocone is poorly developed on each of the I1s at hand, appearing most often as a small nipple-like protuberance (e.g., UALVP 46695, Fig. 7.3.9); a weak crest extends a short distance posterodorsally from the mediocone, defining part of the medial margin of the occlusal surface before fading away. The posterocone is conical, and its sharp apex is directed nearly ventrally; although the posterocrista is conspicuous on UALVP 39332, it is otherwise undeveloped on each of the other specimens at hand.

I2: The I2 of Pronothodectes gaoi is preserved in articulation with a crushed but otherwise nearly complete skull [UALVP 31396; this specimen is currently under study and will be described elsewhere (Boyer, Scott, and Fox)], and is the first discovered I2 for the genus. The crown is considerably smaller than that of the enlarged I1, but is larger than that of the upper canine. The tooth is single-rooted and the crown supports a large, somewhat swollen paracone; a short crest runs posteriorly from the paraconal apex to near the base of the crown, where it then swings medially and forms a short, weak cingulum.

Upper canine: The upper canine of Pronothodectes was previously unknown. The tooth is single-rooted, and the crown closely resembles that of I2. The paracone is faintly compressed mediolaterally, and a short crest runs posteriorly from its apex, forming a weak posterolingual cingulum.

Upper premolars: P2: The P2 crown of Pronothodectes gaoi is preserved in two specimens, and by its roots in a third specimen; a short diastema separates the canine from P2 in each of these specimens. The P2 is two-rooted, with the posterior root larger and more nearly vertical. The crown is triangular in outline, and consists primarily of an inflated paracone. A weak preparacrista runs anteriorly from the apex of the paracone where it joins a similarly weak anterior cingulum; the postparacrista is more sharply defined, and extends posteriorly to join the posterior cingulum at the posterolabial corner of the crown. An ectocingulum is not developed. Although a distinct protocone is not developed, the crown bulges posterolingually, and the anterior and posterior cingula approach, but do not unite with one another at the lingual margin of the crown. Neither the metacone nor the conules are developed.

P3: The P3 of Pronothodectes gaoi bears three roots, the anterior and lingual of which are subequal in diameter, and the posterior root being smaller. The paracone is large and swollen at its base, but becomes somewhat labiolingually compressed apically. The metacone is only weakly differentiated from the paracone: the two cusps are connate for nearly their entire height, and their apices are connected to one another by a short, widely notched centrocrista. A weak preparacrista extends anteriorly from the paracone to a low but prominent parastylar cusp developed at the union of the ectocingulum and anterior cingulum; an acute notch is present at the deepest part of the preparacrista. The postmetacrista runs posteriorly to join the ectocingulum and posterior cingulum; a metastyle is not developed. The ectocingulum is usually strong anteriorly, but weakens considerably posteriorly, and continues to the metastylar corner of the crown in only one specimen (UALVP 46689). A well-developed paraconule intervenes between the paracone and protocone: it is somewhat labiolingually compressed and ridge-like in most specimens, and is oriented slightly oblique, rather than perpendicular, to the transverse axis of the crown. Conular cristae are not developed. The protocone is lower than the paracone and metacone, conical, and has its apex directed slightly anteriorly. A short preprotocrista curves labially towards the paraconule, and can bear a small swelling just prior to its union with the paraconule; the postprotocrista is undeveloped. The anterior cingulum is weak or absent on all specimens at hand; on one (UALVP 31396), it joins the preprotocrista before continuing to the parastylar corner of the crown. The posterior cingulum extends uninterrupted along the posterior margin of the crown, fading out as it nears the lingual extent of the protocone; the posterior cingulum does not ascend the protocone as a postprotocone fold.

DP4: Four plesiadapid DP4s have been recovered from DW-2 and are tentatively referred to Pronothodectes gaoi. The crown is subrectangular in outline, with a slightly longer labial than lingual margin; a well-developed paracone, metacone, protocone, and conules enclose a deep trigon basin. The paracone is the largest cusp on the crown, followed by the lower and less massive metacone; a sharp, deeply notched centrocrista connects the apices of the paracone and metacone. The stylar shelf is narrow, and a small mesostyle is developed on the ectocingulum at the level of the centrocrista notch, although the centrocrista itself is not deflected labially and does not contact the

mesostyle; a small metastylar cusp can be developed on the postmetacrista. The conules are robust, subequal, and circular in cross section. The paraconule is positioned slightly anterior to the level of the paracone, and a conspicuous preparaconular crista connects its apex to the anterior cingulum; the postparaconular crista and metaconular cristae are undeveloped. The protocone is massive, its base occupying nearly half the width of the crown, and its apex is approximately the same height as that of the paracone and metacone; the lingual wall of the protocone is long and sloping, whereas its basin-facing side is steep and nearly flat. The protoconal cingula are wide and robust. The posterior cingulum extends to the apex of the protocone as a prominent postprotocone fold; a faint swelling on the posterior cingulum hints at an incipient hypocone, but a discrete cusp is not present on any of the specimens at hand.

P4: The crown of P4 is larger and more transverse than that of P3, but is otherwise similar: the paracone and metacone are connate for most of their height, the centrocrista is short and shallowly notched, the paraconule is compressed, ridge-like, and obliquely oriented relative to the transverse axis of the crown, the preprotocrista bears a swelling just lingual to its union with the paraconule, and the protocone is conical, with an acute, anterodorsally directed apex. The crown of P4 differs from that of P3 in the following ways: 1) the ectocingulum is considerably stronger and is labially continuous; 2) the parastylar cusp is larger and more robust; 3) the preprotocrista is more sharply defined, and continues to the parastyle; 4) the anterior cingulum, although short, is stronger; and 5) the posterior cingulum forms a well-defined postprotocone fold, extending from the apex of the protocone posteriorly and labially (this in turn imparts a more nearly rectangular occlusal outline to the crown compared to that of P3). A short ridge immediately lingual to the paraconule is developed on two specimens (UALVP 46719, 46720), with one of these ridges (UALVP 46719) bearing a series of small cuspules.

Upper molars: The M1 and M2 of Pronothodectes gaoi closely resemble one another, differing mainly in the crown of M1 having a more anteriorly projecting parastylar corner, and in M2 being slightly longer and wider. The crown of M3 is nearly equidimensional to that of M2, but as in M3 of other eutherians generally, the metastylar corner is undeveloped and the metacone is somewhat lingual relative to the level of the

paracone. The crown of M1 and M2 is subquadrate in outline, while that of M3 is subovate; each of the molars is transverse relative to its length, and bears well-developed cusps and conules. The stylar shelf is reduced, although not to the same degree as in some species of Plesiadapis (e.g., Ples. rex, see Gingerich, 1976, pl. 4H), and the bases of the paracone and metacone are swollen and extend close to the labial margin of the crown. While the ectocingulum is robust, its continuity across the labial side of the crown on M1 and M2 is variable: on most specimens it is interrupted by a notch near the level of the deepest part of the centrocrista, essentially dividing the cingulum into more or less equal anterior and posterior parts; on other specimens the notch is undeveloped, and the cingulum is continuous. The ectocingulum on M3 is continuous to the level of the metacone, at which point it weakens and eventually fades away. Small cuspules can occur on the ectocingulum on each of the molars, but a discrete mesostyle like that on upper molars of many species of Plesiadapis is not developed on M1 or M2 (e.g., Ples. rex, see Gingerich, 1976, pl. 4H); a small mesostyle is present on M3 (Figs. 7.5.13, 7.5.14). The paracone and metacone narrow apically and are connected to one another by a wide and deeply notched centrocrista; the paracone is subequal to or slightly larger than the metacone on M1-2, and its base extends farther lingually; the metacone is reduced on M3. A sharp preparacrista connects the paraconal apex to the heavy ectocingulum and paracingulum; a low and somewhat anteriorly projecting parastylar spur is developed at the union of these three crests on M1. The postmetacrista curves posterolabially to join the ectocingulum and posterior cingulum on M1-2, but is undeveloped on M3. Both paraconule and metaconule are swollen and closely appressed to the base of their respective labial cusp on M1-2, while on M3 the metaconule is absent and the postprotocrista instead extends to the base of the metacone. Of the conular cristae, only the preparaconular crista is consistently well developed, joining the anterior cingulum and continuing as the paracingulum to the parastylar corner of the crown; the postparaconular crista is weak or absent, and the metaconular cristae are undeveloped. The trigon basin is broad and the protocone massive, especially on M3 where it occupies nearly two-thirds the width of the crown; the protoconal apex leans anteriorly on each of the upper molars, with the posterior wall becoming less steep from M1 to M3. The lingual side of the protocone is long and sloping; in some specimens (e.g., UALVP

39301) the lingual wall is especially long, and the enamel terminates as one or two distinct lingual lobes at the crown-root junction. The protoconal cingula are prominent, especially the wide posterior cingulum; the cingula extend to the labial corners of the crown, but fail to meet lingually. The postprotocone fold is sharply defined on each of the molars, forming a conspicuous posterior shelf as it turns abruptly labially to join the posterior cingulum; the posterior shelf is particularly prominent on M3.

Lower dentition (Figs. 7.5.18-7.5.20, 7.6, 7.7): The lower anterior dentition of Pronothodectes gaoi was described in detail by Fox (1990a). Since that publication, a number of additional specimens referable to Pro. gaoi have been recovered from the Blindman River localities, as well as from the early middle Tiffanian Birchwood locality of central Alberta. Evidence for the number and disposition of the anterior teeth of Pro. gaoi can now be evaluated for twelve specimens, all of which preserve alveoli for an enlarged, procumbent medial incisor (i1), a lower lateral incisor (i2), canine, and second lower premolar, although only UALVP 31536 preserves the crowns of i2 and the lower canine (see Fox, 1990a, fig. 5).

i1: The lower first incisor of Pronothodectes gaoi is enlarged and mediolaterally compressed, with the narrow tip directed anterodorsally and slightly medially. A margoconid is present on all specimens at hand, and the margocristid is sharply defined, extending anteriorly to the apex of the crown; a second crest defining the medial margin of the occlusal surface of the crown runs posteromedially from the tip, but fades away before reaching the margoconid. Although the i1 varies in length and width, the crown is both shorter and shallower than i1 of Ples. anceps and Ples. rex (see Gingerich, 1976, pls. 3B, 3C), and in these regards more closely approaches the proportions of i1 of Pro. matthewi.

i2: The discovery of 12 additional mandibles of Pronothodectes gaoi preserving the anterior alveoli from the Blindman River and Birchwood localities sheds some light on the variation in development of i2. Although none of the new specimens preserve i2, its alveolus is invariably present, clearly indicating that i2 is in fact a feature that characterizes Pro. gaoi, rather than being variably present [as is apparently the case, e.g., for p2 in Plesiadapis churchilli (see Gingerich, 1976), or the lower canine in Ples. anceps (see Watters and Krause, 1986)]. The i2 alveolus is best seen in UALVP 39372

(Birchwood locality), where it is preserved in its entirety: the aperture is circular and closely appressed to the alveolar rim of i1, and is somewhat displaced towards the lateral margin of the dentary. In UALVP 39372, the aperture is slightly larger than that for the lower canine, but it appears to have been slightly smaller in UALVP 46827 and 46762, while in UALVP 39313 it is very small. The contours of the i2 alveolus are best seen on UALVP 31238 (holotype), 31240, and 46762, where the anteriormost parts of the jaw have been broken away, essentially sectioning the i2 alveolus in the transverse plane. The alveolus is narrow throughout its depth, in keeping with the thin i2 root as described by Fox (1990a), and extends ventrally and slightly posteriorly along the labial side of the jaw. Although i2 is not preserved in articulation with the jaw in any of the new specimens at hand, the orientation of its alveolus suggests that it was slightly procumbent, similar to i2 in other species of Pronothodectes (Gingerich, 1976). The crown of i2 is small and peg-like, somewhat elongate, with a low, flattened apex.

Lower canine: The lower canine of Pronothodectes gaoi is as yet known only from UALVP 31536, although its alveolus is present on 14 specimens preserving the anteriormost parts of the jaw. The alveolar aperture is subequal in diameter to that of p2 in UALVP 31536, but smaller in UALVP 46827 and 39372. Parts of the alveolar walls of the lower canine are exposed in UALVP 39373, and their contours indicate that the canine was shallowly rooted, narrow, and nearly vertically implanted in the jaw. A short diastema intervenes between the canine alveolus and p2, an observation made by Fox (1990a) for the hypodigm specimens; the diastema varies slightly in length, and a small foramen is sometimes present on the alveolar surface of the diastema, occupying the position of the undeveloped p1. The crown of the lower canine in Pro. gaoi is slightly larger but otherwise resembles that of i2 in being small and peg-like, with a low, blunt apex.

Lower premolars: p2: The single-rooted p2 is preserved only in UALVP 31536. The crown is premolariform, with a low, somewhat bulbous protoconid, and a weakly developed heel.

p3-4: The lower posterior premolars of Pronothodectes gaoi closely resemble one another and those of other plesiadapids generally, and differ mainly in p4 being slightly taller and considerably wider. The crowns of p3-4 are premolariform and are dominated

by a tall, inflated, and slightly anteriorly leaning protoconid. The crown is faintly sinusoidal in anterior view, with the apex of the protoconid skewed lingually, and the labial side of the crown bulging labially. A short but well-defined paracristid extends anteriorly from the protoconid apex, while a longer but comparatively weaker protocristid runs posteriorly; neither a paraconid nor a metaconid is developed. The talonid on p3 consists only of a transversely oriented ridge that rises to an apex at the longitudinal midline of the crown, where a small cuspule can be developed at its summit; the talonid ridge curls anteriad at its lingual extremity, forming a weak shelf. The talonid on p4 resembles that on p3, but the ridge extends farther lingually, and the low lingual shelf is more prominent. The hypoflexid is anteroposteriorly short and relatively shallow on both p3 and p4.

Lower molars: m1-2: The m1-2 in Pronothodectes gaoi differ from one another primarily in m2 being wider than m1, and in having a more closely appressed paraconid and metaconid. The crowns of m1 and m2 resemble those of other plesiadapids generally: they are low crowned, with small, bunodont cusps, anteriorly leaning trigonids, and broad, shallowly basined talonids. The m1 trigonid bears a well-developed and inflated protoconid and metaconid, and a slightly smaller paraconid that together enclose a shallow basin; the low paracristid sweeps anteriorly and lingually from the protoconid apex to the paraconid, forming a weak anterior shelf. The metaconid is positioned slightly posterior to the level of the protoconid, and the two cusps are connected by a shallowly notched protocristid. The m2 trigonid is wider than that on m1, forming a more nearly isosceles triangle in occlusal outline. In contrast with m1, the paraconid is large and swollen, higher, and more closely appressed to the metaconid, which is itself reduced in size. The inflated paracristid is low and forms a prominent anterior shelf. The talonid on m1 and m2 is wider than the trigonid when measured from the lingual margin of the crown to the swollen labial base, although the basin itself can be narrower. The talonid bears a massive hypoconid and slightly smaller entoconid. The hypoconulid is variably developed on both m1 and m2: it can be a single, anteroposteriorly compressed cusp (e.g., UALVP 46762, m1), whereas on other specimens (e.g., UALVP 46788, m2) it is bifid, being transected by a narrow cleft; on still other specimens (e.g., UALVP 46789, m2), it is fully incorporated into the postcristid, with barely any swelling indicating its

vestigial presence. The basin-facing wall of the hypoconid slopes gently anterolingually towards the deepest part of the talonid basin, whereas those of the entoconid and hypoconulid are steeper. The entoconid is well-developed, conical, and the posterolingual margin of the crown is squared off. A mesoconid swelling is present on the cristid obliqua, although a distinct cusp is never developed; the cristid obliqua continues to the metaconid apex on m1 (a "stepped" postvallid of Silcox, 2001), but joins the postvallid wall low and labial to the level of the protocristid notch on m2. The anterior and posterior cingulids are strongly developed on m1 and m2, although they do not meet labially; the anterior cingulid is especially prominent, and on some specimens (e.g., UALVP 46790, m2) one or two small cuspules can be developed on the cingulid at the hypoflexid.

m3: The morphology of m3 has figured importantly in plesiadapid systematics (see, e.g., Gingerich, 1976), particularly the development of the hypoconulid lobe. Fox (1990a) briefly described the m3 in UALVP 31538, the only m3 referable to Pronothodectes gaoi at that time, whereas the current sample includes 22 m3s. The crown consists of an anteroposteriorly short trigonid and posteriorly expanded talonid bearing a lobate hypoconulid. The protoconid and paraconid are subequal in size and height, and are transversely opposed from one another. The metaconid is variably developed: in most specimens (e.g., UALVP 39313) it is smaller than the paraconid and closely appressed to it, with the two cusps being connate for almost their entire height, while in other specimens (e.g., UALVP 39356), it is subequal to the paraconid and separated from it by a narrow notch. As on m1 and m2, the paracristid on m3 is low and sweeps anterolingually from the protoconid to form an anterior shelf. The protocristid is long and concave dorsally, rather than being distinctly notched. The talonid is elongate, with a broad and shallow basin bounded by a tall, massively developed hypoconid, a poorly differentiated entoconid, and an enlarged and lobate hypoconulid. Although a few specimens have a more angular hypoconulid lobe (i.e., the posterior margin of the crown is labiolingually expanded and appears "squared off" in occlusal view, e.g., UALVP 46826), the majority of specimens have a more smoothly rounded lobe (e.g., UALVP 39313, 39356), similar to that in other species of Pronothodectes and stratigraphically earlier species of Nannodectes (Gingerich, 1976). Incipient fissures can sometimes be

developed on the hypoconulid lobe of some of the m3s at hand, superficially partitioning the lobe into multiple parts (e.g., UALVP 39313), but deep posterior and posterolingual clefts are never developed, nor do the fissures extend into the talonid basin as they do in many species of Plesiadapis, including Ples. rex. The cristid obliqua contacts the postvallid wall low and labial, and occasionally can bear a mesoconid swelling close to its contact with the trigonid. The anterior cingulid is robust, extending posteriorly past the hypoflexid to the hypoconid; the posterior cingulid is represented only by a short shelf-like structure below the embrasure between the hypoconid and the hypoconulid lobe.

Discussion.—A major revision of Pronothodectes gaoi is currently in preparation (Boyer, Scott, and Fox, in prep.), and will include descriptions of the skull and postcranium. Fox (1990a) discussed in detail the pertinent dental features that distinguish Pro. gaoi from congeners and other plesiadapids, and these need not be repeated here. A result of the current study has been recognition that the overlap in the ranges of dental measurements for each tooth locus in Pro. gaoi with those of Ples. rex is less than was initially understood from the hypodigm alone, with measurements at some loci (e.g., those of P3/p3 and P4/p4) falling completely outside the ranges reported by Gingerich (1976) for Ples. rex, and in some cases (e.g., P4, M1) overlapping the upper ranges of similar loci in Pro. jepi and Nannodectes. Gingerich (1991) challenged the validity of Pro. gaoi on the basis of the overlapping ranges of dental measurements with those of Ples. anceps (but see Fox, 1991b); despite the fact that the coronal dimensions of Pro. gaoi more closely approximate those of Ples. anceps than they do Ples. rex, the important coronal features that distinguish Pro. gaoi from congeners and from species of Plesiadapis hold true for the larger samples from Birchwood and the Blindman River localities, leaving no doubt of the validity of Pro. gaoi. Each of the dentaries in the present sample preserving the anteriormost parts of the lower jaw possesses alveoli for the lateral incisor and canine, loci that are together diagnostic of Pronothodectes among plesiadapids. Gingerich's (1991) claim that a fissured heel on m3 is a derived feature known only in species of Plesiadapis (and, by extension, that Pro. gaoi should be considered a species of Plesiadapis) was rebutted by Fox (1991b); it can be added that incipiently fissured m3 heels are also known in specimens of Pro. matthewi from the late

Torrejonian Who Nose? locality (Scott, 2003), further suggesting that fissuring of the m3 talonid was independently acquired in multiple plesiadapid lineages. In light of the much larger sample of Pro. gaoi, both from the Blindman River and Birchwood localities, there is no evidence that would indicate the presence of Ples. rex or of any other plesiadapid taxon at these localities; as such, both samples are referred here to Pro. gaoi. Specimens collected from Erickson's Landing (Simpson, 1927) that were subsequently referred to Plesiadapis rex (see Gingerich, 1976) are provisionally referred here to Pro. gaoi.

As discussed by Fox (1990b), a direct consequence of the discovery of Pronothodectes gaoi is the disruption of Gingerich's (1976) plesiadapid biozonation of the Paleocene of the Bighorn Basin of Wyoming (a biozonation that was ultimately extrapolated to include other sedimentary basins in the Western Interior of North America). The recognition that Pronothodectes gaoi represents the only plesiadapid at the Blindman River, Joffre Bridge, and Birchwood localities is problematic in that Plesiadapis rex, the standard index taxon for the early middle Tiffanian (Ti3; see Gingerich, 1976; Lofgren et al., 2004), is no longer demonstrably present, and the relative age of these localities is now uncertain. These problems will be addressed in Chapter 12.

Family SAXONELLIDAE Russell, 1964

Genus SAXONELLA Russell, 1964

Saxonella RUSSELL, 1964, p. 128.

Type species.—Saxonella crepaturae Russell, 1964.
Other included species.—Saxonella naylori Fox, 1991a.

SAXONELLA NAYLORI Fox, 1991a

Figure 7.8; Table 7.5

Saxonella naylori FOX, 1991a, p. 335.

Holotype.—UALVP 16201, incomplete left dentary with i1, p3-4, m1 (Fox, 1991a, p. 335). DW-2 locality; Paskapoo Formation of Alberta, late Paleocene [early middle Tiffanian, Ti3 (Fox, 1990b), Plesiadapis rex/P. churchilli Lineage Zone of Lofgren et al., 2004].

Material examined.—From DW-2: UALVP 31608, incomplete right maxilla with P2-4, M1-3; UALVP 29356, incomplete right maxilla with P3-4, M1-3; UALVP 31493, incomplete left maxilla with 46841 (broken), P4, M1-2; UALVP 40461, incomplete left maxilla with P4, M1-2; UALVP 46840, incomplete right maxilla with P3, M1-2, and alveoli for P4; UALVP 46842, incomplete right maxilla with M1-3 (M3 broken); UALVP 46843, incomplete left maxilla with M1; UALVP 31494, 31495, P3; UALVP 46844, 46845, M2; UALVP 29355, incomplete left dentary with p3-4, m1; UALVP 29357, incomplete right dentary with p3-4, m1-2; UALVP 46846, incomplete right dentary with p3 (broken), p4, m1-2, and anterior alveolus for m3; UALVP 40640, i1; UALVP 40636, p4.

From Birchwood: UALVP 39498, m2.

Age and occurrence.—Early middle Tiffanian (Plesiadapis rex/P. churchilli Lineage Zone, Ti3, late Paleocene) of Alberta (Fox, 1990a).

Description and discussion.—Saxonella was originally based on an incomplete lower jaw and several isolated teeth from Paleocene age fissure deposits of the Walbeck localities in Germany (Russell, 1964). The unexpected discovery of a new species of Saxonella from the Paleocene of western Canada, announced nearly twenty years later (Fox, 1984c), provided further evidence of Euramerican dispersals of Paleocene age mammals, as well as additional evidence for a middle Tiffanian age for the Walbeck localities. Saxonella was first described as a member of the Carpolestidae, a family of plesiadapiforms with upper and lower premolars that superficially resemble those of saxonellids (Russell, 1964; McKenna, 1967); as many authors subsequently pointed out (e.g., Van Valen, 1969; Rose, 1975; Fox, 1991a), the plagiaulacoid lower premolars are developed at different loci in carpolestids and saxonellids, and the function of the shearing lower premolars differed significantly in the two families. Although most authors have subsequently followed Rose (1975) in classifying Saxonella in a monotypic family, the Saxonellidae, a consensus on the position of Saxonellidae as a member of the

Plesiadapoidea, a more inclusive taxon that also contains the Plesiadapidae and Carpolestidae, is yet to be reached (see, e.g., Gingerich, 1976; Fox, 1991a). Clearly a resolution to these problems can only come with a better knowledge of the more primitive members of each of the plesiadapoid families.

Since Fox's (1991a) treatment of Saxonella naylori, only a few additional specimens have been recovered from DW-2 and Birchwood, and these are virtually identical to those described by Fox (1984c, 1991a, and see Webb, 1996). Fossils of S. naylori are as yet unknown from localities outside of Alberta, despite more than 20 years of collecting in the Western Interior of North America since the species was first discovered.

Family CARPOLESTIDAE Simpson, 1935

Comments on carpolestid classification.—McKenna and Bell's (1997) recent classification places the Carpolestidae within the Tarsiiformes, a parvorder of Euprimates (i.e., primates of modern aspect), but the justification for such an unorthodox view is not apparent in that publication. Gidley (1923) and Simpson (1928) considered carpolestids to be "tarsiids," although "Tarsiidae" as recognized by these authors differs considerably from that of Tarsiiformes as recognized today. Gingerich's (1975, 1976) was among the first to include plesiadapiforms, including the carpolestids, with the tarsiiforms in his Plesiotarsiiformes. While some recent studies has favoured a close relationship between derived carpolestids and euprimates (see, e.g., Bloch and Boyer, 2001), none has advocated the inclusion of the Carpolestidae in Euprimates. Carpolestidae is recognized here as a highly specialized plesiadapiform family, following the opinions of Rose (1975), Fox (1994), Bloch et al. (2001), and Bloch et al. (2007).

Genus ELPHIDOTARSIUS Gidley, 1923

Elphidotarsius GIDLEY, 1923, p. 10.

Type species.—Elphidotarsius florencae Gidley, 1923.

Other included species.—Elphidotarsius shotgunensis Gazin, 1971; E. russelli Krause, 1978; E. wightoni Fox, 1984b.

ELPHIDOTARSIUS WIGHTONI Fox, 1984

Figures 7.9-7.11; Tables 7.6, 7.7

Elphidotarsius wightoni FOX, 1984b, p. 1268.

Holotype.—UALVP 21001, incomplete left dentary with i1, c, p4, m1-3, and alveoli for i2 and p3 (Fox, 1984b, p. 1268). DW-2 locality, Paskapoo Formation of Alberta, late Paleocene [early middle Tiffanian, Ti3 (Fox, 1990b), Plesiadapis rex/P. churchilli Lineage Zone of Lofgren et al., 2004].

Material examined.—From DW-1: UALVP 21002, incomplete left maxilla with P1-4, M1-3, and alveolus for C; UALVP 46847, incomplete right maxilla with P3 (broken), P4, M1-2, and alveoli for P1-2; UALVP 21009, incomplete left dentary with p4, m1-3, and alveoli for c, p3.

From DW-2: UALVP 33859, associated incomplete maxillaries with left P3-4, M1-3, and alveoli for P1-2, and right P3-4, M1-3, and alveoli for C, P1-2; UALVP 46848, incomplete left maxilla with P1-4, M1-2; UALVP 40608, incomplete right maxilla with P2-4, M1-3; UALVP 21007, incomplete right maxilla with P3-4, M1-3, and alveoli for P1-2; UALVP 40609, incomplete left maxilla with P3-4, M1-3, and alveoli for P1-2; UALVP 40651, incomplete right maxilla with P3-4, M1-2; UALVP 46849, incomplete left maxilla with P3-4, M3, and alveoli for P1-2, M1-2; UALVP 40607, incomplete right maxilla with P2-3; UALVP 46850, P3; UALVP 40600, incomplete left dentary with p4, m1-2, and alveoli for i1-2, c, p3, m3, and associated incomplete right dentary with p4 and alveoli for i2, c, p3; UALVP 46851, incomplete left dentary with i2, c, p4, m1-3 (m2-3 broken), and alveoli for i1, p3; UALVP 40601, incomplete left dentary with i2, c, p4, m1-3, and alveolus for p3; UALVP 21006, incomplete left dentary with p4, m1-3, and associated ?i2, ?c; UALVP 46852, incomplete right dentary with c, p4, m1-3, and alveoli for i1-2, p3; UALVP 40603, incomplete right dentary with i2, p4, m1-3, and alveoli for c, p3; UALVP 21004, incomplete right dentary with c, p4, m1-3; UALVP

40599, incomplete right dentary with p4, m1-3; UALVP 40610, UALVP 46853, incomplete right dentary with p4, m1-2, and associated i1; UALVP 46854, incomplete left dentary with p4, m1-3 (m3 broken); UALVP 46855, 46856, incomplete right dentary with p4, m1-3, and alveoli for i1-2, c, p3; UALVP 21008, incomplete right dentary with p4, m1-2, and alveoli for i1-2, c, p3, m3; UALVP 40606, incomplete right dentary with p4, m1-3, and alveoli for c, p3; UALVP 21005, incomplete right dentary with p4, m1-2, and alveoli for p3, m3; UALVP 46857, incomplete left dentary with p4, and alveoli for i1-2, c, p3; UALVP 46858, associated p4, m1; UALVP 46860, i1.

From Birchwood: UALVP 39303, incomplete right dentary with p4, m1-2, and alveoli for c, p3, m3; UALVP 46859, incomplete left dentary with p4, m1-2, and alveoli for p3, m3; UALVP 39304, incomplete right dentary with p4, m2, and alveoli for p3, m1, m3; UALVP 39305, p4.

Age and occurrence.—Early middle Tiffanian (Plesiadapis rex/P. churchilli Lineage Zone, Ti3, late Paleocene) of Alberta (Fox, 1990a).

Description.—Fox's (1984b) thorough treatment of the upper and lower dentition of Elphidotarsius wightoni precludes the need for detailed descriptions here. Newly prepared specimens of E. wightoni from DW-2 and Birchwood document for the first time the crown of the lower lateral incisor, and documents some of the variation at other loci.

Upper dentition (Figs. 7.9, 7.11): Unfortunately none of the newly prepared specimens of E. wightoni preserves teeth or alveoli anterior to P1; as such, the number and anatomy of the upper incisors, and the coronal anatomy of the upper canine remain unknown.

Upper premolars: UALVP 46848 (Figs. 7.9.1-7.9.3) preserves P2 in articulation with the maxilla, and a second, more anterior tooth that has been rotated dorsally such that the paraconal apex now faces anteriorly. This anterior tooth is identified as P1 on the basis of its similarity to that in UALVP 21002, and by its root, which is stout (even more so than that for P2), and clearly could not be accommodated by the small canine alveolus preserved on UALVP 33859 (see Fox, 1994; the upper canine alveolus in E. wightoni is smaller than that for P1 or P2). The crown of P1 in UALVP 46848 is better preserved than in UALVP 21002: it closely resembles that of P2, consisting primarily of a large,

labiolingually compressed and anteriorly leaning paracone, and a low posterior cuspule. Weak crests extend anteriorly and posteriorly from the paraconal apex, and a well-developed cingulum is developed lingually.

P3: Two maxillae were included in the hypodigm of Elphidotarsius wightoni (Fox, 1984b), and P3 and P4 were known only from these specimens; the current sample includes nine P3s and seven P4s. The crown of P3 is subtrapezoidal in occlusal outline, with the labial side longer than lingual side (see Fig. 7.7.11). The labial row bears a prominent parastyle, paracone, and metacone. A fourth labial cusp, the metastyle, is incipiently developed on one specimen (UALVP 46850): the metastyle on this specimen is closely appressed to the metacone, and although the apices of both cusps have been worn flat, there is a clear swelling on the postmetacrista, with faint, vertical indentations on the labial and lingual sides of the crown intervening between the two cusps. The parastylar lobe is not developed as a prominent anteroexternal spur (as it is in some species of Carpodaptes, Carpolestes, and Carpomegadon, see Bloch et al., 2001; Fox, 2002). The posterior cingulum is sinusoidal (i.e., convex posterior to the protocone, but becomes concave as it continues labially) on each P3 at hand, forming a deep indentation characteristic of P3 of post-Elphidotarsius florencae carpolestids (Silcox, 2001; Silcox et al., 2001); a small cusp is developed on the posterior cingulum just lingual to the intermediate ridge.

P4: The occlusal outline of P4 is slightly more variable than that of P3 (see Fig. 7.7.11): it is subtriangular in some specimens (e.g., UALVP 46848), with the lingual half of the crown notably "pinched" anteroposteriorly, while in other specimens (e.g., UALVP 40651) it is subquadrate, with the postprotocone fold+posterior cingulum more posteriorly extending. Four robust cusps are present in the labial row of P4, differing from P3 by the addition of a preparaconal cusp; one specimen, UALVP 40651, bears a small metastylar cusp on the shoulder of the metacone. The preparaconal cusp, paracone, and metacone are all nearly equal in size, but the metacone is usually slightly taller than the paracone (subequal in UALVP 40608), and is significantly taller than the preparaconal cusp. The intermediate row consists of an enlarged central cusp that is positioned immediately lingual to the paracone, and a pair of ridges, one anterior, the other posterior, extending from the apex of the central cusp; additional cusps are not

developed on the intermediate ridge, in contrast with P4 of Carpodaptes and other stratigraphically younger carpolestids (Silcox, 2001; Bloch et al., 2001; Fox, 2002), although tiny cuspules may have been present originally but have been erased by wear. The protocone is tall, anteroposteriorly compressed, and located immediately lingual to the central cusp in the intermediate row; its apex is sharp, and is nearly as tall as the paracone and central cusp. A strong preprotoconal crista is developed in all but one specimen, running obliquely anterolabially across the crown towards the intermediate ridge. A large swelling is developed on the preprotoconal crista in a number of specimens (best seen in UALVP 40651 and 46848): this swelling probably represents the paraconule, and a short, anterolabially directed preparaconular crista connects the paraconule to the intermediate ridge. If these identifications are correct, the paraconule and preparaconular crista, at least on P4, are not incorporated into the intermediate ridge. Although a preprotoconal crista is not developed on UALVP 40608, a paraconule is clearly present, in addition to the preparaconal crista. Faint swellings of enamel are sometimes present on the protoconal cingula, but neither a hypocone nor a pericone is developed.

Lower dentition (Figs. 7.10, 7.11): i1: The lower medial incisor of Elphidotarsius wightoni was previously known only in UALVP 21001, the holotype; a second specimen, UALVP 46860, preserves this tooth in association with a fragmentary jaw containing p4, m1-2. The crown of i1 resembles that in the holotype in being relatively short and deep, procumbent, and in bearing a margoconid developed posteriorly at the union of a pair of conspicuous crests that circumscribe a broad occlusal surface.

i2: The i2 of Elphidotarsius wightoni was known previously only by its root (Fox, 1984b); the lateral incisor is now known in its entirety from three specimens, UALVP 46851, 40601, and 40603. The i2 is small and anteriorly leaning, likely abutting the base of the enlarged medial incisor in life. The crown bears a low, squat principal cusp and a tiny, variably developed heel [=margoconid?]. Two crests arise from the apex of the principal cusp: the first runs posteriorly and slightly medially; the second crest extends ventromedially and posteriorly, forming a prominent medial cingulid. The two crests meet at the posterior margin of the crown, and a small, conical heel can be developed at

their union. The crests circumscribe a broad, dorsomedially directed occlusal surface, much like that in the medial incisor.

Lower premolars: p4: The newly prepared p4s of Elphidotarsius wightoni closely resemble those described by Fox (1984b), with the height and strength of the anterior accessory cusp, development of the exodaenodont lobes, and robustness of the heel exhibiting the greatest variation. The crown is low relative to its length (see Fig. 7.7.11), and invariably bears three robust and well-differentiated apical cusps, a small anterior apical cusp, and a heel. The apical cusps are aligned anteroposteriorly, as in p4 of other carpolestids, although not in such a straight line as those of E. russelli (se Krause, 1978; Silcox et al., 2001). A small apical cusp is invariably developed anteriorly, and although it varies slightly in both its height and size, it is always smaller and lower than the second apical cusp, and is usually slightly offset lingually relative to the second apical cusp. The third apical cusp is occasionally subequal, but most often lower in height than the second apical cusp, and is slightly offset labially. The low heel is offset posteriorly from the apical cusps and is most often represented by a transverse ridge that rises to a peak near its midpoint; on some specimens the lingual part of the ridge is expanded into a low basin, and on one specimen (UALVP 40601) the lingual ridge continues anteriorly as a conspicuous cingulid. Exodaenodonty is developed anteriorly and posteriorly: both of the lobes are inflated and bulge labially, with the posterior lobe often the larger and more ventrally extending. A shallow notch is usually developed between the two lobes ventrally, and the crown is faintly hourglass-shaped in occlusal outline.

Molars: The newly prepared upper and lower molars differ little from those described by Fox (1984b) for the hypodigm, and their descriptions are not repeated here.

Discussion.—The newly referred specimens of Elphidotarsius wightoni closely resemble those described by Fox (1984b) and document some of the variability in coronal anatomy, but otherwise add little in the way of new information. Nothing of the p3 in E. wightoni is yet known, including the number of roots: prior to discovery of E. wightoni, Rose (1975) differentiated Elphidotarsius from other carpolestids in part by its possession of a small, two-rooted p3 that occupies a single alveolus. The walls of the p3 alveolus in specimens of E. wightoni do not bear vertical bony crests labially and lingually, as is often the case for dentaries in other taxa where two roots occupy the same alveolus (e.g.,

the erinaceomorph Entomolestes grangeri Matthew, see Novacek et al., 1985), suggesting that p3 may have in fact been single-rooted, as it is in other post-Elphidotarsius carpolestid species that retain this tooth [despite the lack of evidence regarding the coronal anatomy and number of roots on p3 in E. wightoni, two recent analyses of carpolestid relationships (Bloch et al., 2001; Silcox et al., 2001) incorrectly code root number in E. wightoni as "partially or wholly fused roots occupying one alveolus" (Bloch et al., 2001, p.131) or "two roots" (Silcox et al., 2001, p.150); inexplicably, Bloch et al. (2001) further score E. wightoni as having a single rooted p2, which is incorrect: p2 is not present in E. wightoni].

Despite having a reduced antemolar dentition similar to that in species of Carpodaptes and Carpolestes (Rose, 1975; Beard and Wang, 1995; Beard, 2000; Bloch et al., 2001; Fox, 2002), the lower and comparatively less elaborate crown of p4 in E. wightoni suggests it may be more distantly related to Carpodaptes than are other, post-Elphidotarsius florencae species of Elphidotarsius, a conclusion arrived at in recent analyses of carpolestid phylogeny (Bloch et al., 2001; Silcox et al., 2001). Newly prepared specimens from the earliest Tiffanian (Ti1) Aaron's locality of south central Alberta (Fox, 1990b), however, suggest that the phylogeny of Elphidotarsius species is even more complex than previously understood: the new specimens document a new, but as yet unnamed, species of Elphidotarsius with a p4 that is similar in coronal anatomy to that in E. russelli, but possessing alveoli for a nearly complete antemolar dentition (i.e., i1-3, c, p2-3, a condition definitively known only in E. shotgunensis). These new specimens will be described elsewhere (Scott and Fox, in prep.)

Elphidotarsius wightoni is restricted to the early middle Tiffanian (Ti3) of Alberta, and is known from the Hand Hills West upper level locality (MacDonald, 1996) in addition to the occurrences documented here.

Genus CARPODAPTES Matthew and Granger, 1921

Carpodaptes MATTHEW and GRANGER, 1921, p. 6.

Type species.—Carpodaptes aulacodon Matthew and Granger, 1921.

Other included species.—Carpodaptes hazelae Simpson, 1936; C. hobackensis Dorr, 1952; C. cygneus (Russell, 1967); C. stonleyi Fox, 2002.

CARPODAPTES HAZELAE Simpson, 1936

Figures 7.12, 7.14.1-7.14.6, 7.15; Tables 7.8, 7.9

Carpodaptes hazelae SIMPSON, 1936, p. 21.

Holotype.—AMNH 33854, incomplete right dentary with p4, m1-3 (Simpson, 1936, p. 21). Scarritt Quarry, Fort Union Formation of Montana, late Paleocene (early Tiffanian, Ti2, Plesiadapis anceps/P. rex Lineage Zone of Lofgren et al., 2004).

Material examined.—From Joffre Bridge Roadcut lower level: UALVP 46861, incomplete right maxilla with P3-4 and alveoli for M1; UALVP 46862, incomplete left maxilla with P3 and alveoli for P2, M1-2; UALVP 40624, incomplete left maxilla with M2-3 and alveoli for M1; UALVP 40611, incomplete right dentary with c, p4, m1, and alveoli for i1-2, p3; UALVP 40617, incomplete right dentary with p4, m1-2; UALVP 46863, m1.

From DW-1: UALVP 40616, incomplete right dentary with m1-2 and alveoli for m3.

From DW-2: UALVP 40626, incomplete left premaxilla with I1-2 and alveolus for I3; UALVP 33930, incomplete right premaxilla with I1-2 and alveolus for I3; UALVP 21003, incomplete left premaxilla with I1 and alveoli for I2-3; UALVP 33857, incomplete right premaxilla with I1 and roots for I2-3; UALVP 33858, 40612-13, I1 (total: 3); UALVP 46864, incomplete right maxilla with P1-4, M1-3; UALVP 33860, incomplete left maxilla with P2-4, M1-3, and alveolus for P1; UALVP 40605, incomplete left maxilla with P3-4, M1-3, and alveoli for P1-2; UALVP 40636, incomplete right maxilla with P3-4, M1-3; UALVP 40623, incomplete left maxilla with P3-4, M2-3, and alveoli for P1-2, M1; UALVP 40625, incomplete right maxilla with P3-4; UALVP 46865, incomplete right maxilla with M1-3; UALVP 40629, incomplete left maxilla with P4, M1-2; UALVP 40638, incomplete left maxilla with M2-3; UALVP 46866, incomplete right maxilla with P4, M1 (broken); UALVP 40622, associated P4, M1, M3;

UALVP 46867, incomplete left maxilla with P3-4 (both broken); UALVP 40602, 40633, P3; UALVP 40632, P4; UALVP 40634, incomplete right dentary with i1-2, p3-4, and alveolus for c; UALVP 40676, incomplete right dentary with p4, m1-3, and alveoli for i1-2, c, p3; UALVP 46868, incomplete right dentary with p4, m1-3, and alveoli for c, p3; UALVP 40630, incomplete right dentary with p4, m1-3; UALVP 46869, 40635, incomplete left dentary with p4, m1-3; UALVP 40618, incomplete left dentary with p4, m1-2 (broken), and alveoli for c, p3; UALVP 46870, incomplete left dentary with p4, m1-2, and alveoli for c, p3; UALVP 46871, incomplete left dentary with p4, m1-2, and alveoli for i2, c, p3, and m3; UALVP 46872, incomplete right dentary with p4, m1-2; UALVP 40619, incomplete left dentary with m1-2 and alveoli for m3; UALVP 40615, 40631, incomplete left dentary with m1-3; UALVP 40657, incomplete left dentary with m2-3 and alveoli for m1; UALVP 40635, i1; UALVP 40627, 46873, 46874, p4 (total: 3); UALVP 46875, 46876, 46877, m1 (total: 3); UALVP 40621, m2; UALVP 46878, 46879, 46880, 46881, 46882, m3 (total: 5).

From DW-3: UALVP 40637, incomplete right maxilla with P3-4 (both broken).

From Mel's Place: UALVP 40598, M2;

From Burbank: UALVP 40628, incomplete left dentary with p4, m1-2.

From Birchwood: UALVP 39306, incomplete left maxilla with P3-4 (both broken), M1-2, and alveoli for P1-2, M3; UALVP 46883, incomplete left dentary with p4, m1-3, and alveoli for i1-2, c, p3; UALVP 39307, incomplete left dentary with p4, m1-3, and alveoli for c, p3; UALVP 39308, incomplete left dentary with p4, m1; UALVP 38309, incomplete right dentary with p4 and alveoli for c, p3;

Age and occurrence.—Early Tiffanian (Plesiadapis anceps/P. rex Lineage Zone, Ti2, late Paleocene) to early middle Tiffanian (Plesiadapis rex/P. churchilli Lineage Zone, Ti3, late Paleocene) of the Western Interior of North America (Lofgren et al., 2004).

Description.—Fox (1984b, 1994) described the premaxilla and I1 of Carpodaptes hazelae from the DW-2 locality, and discussed the maxillary dental formula based on a brief description of UALVP 33860. C. hazelae is the best represented species in the family, with large samples known from the type locality (Scarritt Quarry, early Tiffanian, Ti2) and Cedar Point Quarry (early middle Tiffanian, Ti3) (Simpson, 1936, 1937; Rose,

1975, 1981; Krause and Maas, 1990; Silcox, 2001; Silcox et al., 2001). The following descriptions focus on previously unknown or poorly known teeth for C. hazelae, as well as the P3-4 and p4 and m1, teeth considered diagnostic for carpolestids generally (Rose, 1975).

Upper dentition (Figs. 7.12, 7.13.1-7.13.11, 7.15): Upper incisors: Fox (1984b, 1994) demonstrated that the premaxillary of C. hazelae contains alveoli for three upper incisors, and described I1 and I2. A second specimen, UALVP 40626, also preserves I2 in articulation with the premaxilla, as well as the alveolus for I3. The crown is both smaller and lower than that of I1, and bears a tall, sharp central cusp and a low, shelf-like posterior cingulum that supports a small, conical cuspule. The posterior cingulum extends along the medial side of the crown anteriorly past the level of the central cusp, then wraps around to the lateral side of the crown before fading away. A lateral cingulum is not developed. The I3 of C. hazelae remains unknown.

Upper premolars: P1-2: UALVP 46864 preserves P1 and P2 in articulation with the maxilla; Fox (1994) suggested that the upper canine was not present in Carpodaptes hazelae, and this is corroborated by UALVP 46864: although the P1 and P2 are slightly displaced from their alveoli, there is no indication of a smaller alveolus anterior to that for P1 (as there is in E. wightoni, see Fox, 1994 and earlier in this chapter). The crown of P1 consists of a large, sharply pointed paracone and a smaller, lower posterior cuspule. A cingulum is developed along the lingual side of the paracone, becoming heavier and more conspicuous posteriorly as it approaches, and eventually joins with, the posterior cuspule. Although the cingulum bulges posterolingually, a protocone is not developed, and the P1 bears but a single, stout root. The P2 closely resembles P1, but is smaller, the crown is more nearly circular in occlusal view, and a posterior cuspule is not developed. The P1 and P2 are crowded together anterior to P3, with no diastemata intervening between any of the teeth.

P3: The P3 of Carpodaptes hazelae is subtrapezoidal in occlusal outline (see Fig. 7.15), with its labial margin longer than its lingual margin, and the anterior and posterior margins converging lingually. As in P3 of other carpolestids, the biting surface is dominated by three subparallel rows of cusps, one labial, one intermediate, and one lingual. The parastylar lobe is broadly rounded and projects only slightly anteriorly, and

in no specimen is it spur-like and strongly anteriorly projecting like that in Carpolestes and Carpomegadon (see Bloch et al., 2001). The labial row invariably bears four well-developed cusps. The conical parastyle is slightly lower and anteriorly offset from the paracone. Four crests are usually associated with the parastyle, all extending from its apex: one crest runs posteriorly to the notch separating the parastyle and paracone, while a second crest extends labially a short distance towards the ectocingulum. A third crest, the preparaconular crista (Silcox et al., 2001), sweeps posterolingually to the paraconule, the major cusp of the intermediate row; the preparaconular crista can be high and continuous, or can bear a deep notch at its midpoint. A fourth crest extends anteriorly to the anterior cingulum, and a small cuspule can be developed at their union. The remaining three labial cusps are closely approximated, connate throughout most of their height, and decrease in size and height posteriorly. The paracone is the largest of the labial cusps, followed by the slightly lower metacone, and even lower metastyle. A well-developed crest connects the apices of the labial cusps, and a number of weaker and variably developed crests can extend labially and lingually from the apices of each cusp. The ectocingulum is most often weakly continuous, although in some specimens it is conspicuous only anteriorly and posteriorly, and on some specimens it is wholly undeveloped. Weak exodaenodonty is developed at both labial roots. The intermediate row supports a large paraconule that is slightly lingual to the level of the embrasure between the parastyle and paracone, and a high ridge extending posterolabially from the paraconular apex to the postmetastylar crest; the ridge probably incorporates the postparaconular crista, and can be weakly cuspidate. A deep sulcus separates the intermediate ridge from the cusps of the labial row. A large protocone and slightly smaller and lower hypocone constitute the lingual cusp row. The protocone is anteriorly positioned, lingually opposite the parastyle and slightly anterior to the level of the paraconule, and its apex is directed somewhat anteriorly; the base of the protocone does not bulge lingually as in other species of Carpodaptes (e.g., C. cygneus, C. stonleyi, see Fox, 2002). A robust crest extends anterolabially from the protoconal apex, curving towards the anterolabial corner of the crown where it joins the preparaconal cusp+ectocingulum; this crest likely represents the confluent preprotoconal crista and anterior cingulum. As on P3 of C. cygneus (see Fox, 2002), a second, weaker crest

representing the remnants of the postprotoconal crista extends a short distance labially from the protoconal apex before fading away. The hypocone is smaller and lower than the protocone, and its apex is positioned more lingual than that of the protocone. The postprotocone fold is shallowly notched in unworn specimens, and the posterior cingulum can be moderately to strongly sinusoidal in occlusal view, being convex posteriorly then convex anteriorly as it curves from the hypoconal apex to the posteriormost part of the intermediate cusp row.

P4: The P4 of Carpodaptes hazelae is subtrapezoidal to subrectangular in occlusal outline, and is wider relative to its length compared to P3 (see Fig. 7.15). The labial side is considerably longer than the lingual side, and the crown narrows at the level of the intermediate cusp row, giving the crown a somewhat "pinched" appearance in occlusal outline. As with that of P3, the crown of P4 consists of three subparallel rows of cusps. Although as many as six cusps in the labial row have been reported for P4 of C. hazelae (Rose, 1975; Silcox et al., 2001), each P4 in the present sample invariably has five, with the two anteriormost cusps (parastyle and preparaconal cusp) being lower and set off anteriorly from the remaining three cusps by a notch. The parastyle and preparaconal cusp are vertical, whereas the remaining three cusps lean slightly posteriorly. The paracone is the largest and tallest cusp in the labial row: it is conical, sharp, and convex both labially and lingually. The metacone is slightly lower than the paracone and closely appressed to it, with the two cusps connate for most of their height, and a small metastyle is developed on the posterior shoulder of the metacone. A sharp crest joins the apices of the labial cusps, and continues posterolabially from the metastylar apex to join the ectocingulum. Weak exodaenodonty is developed at both labial roots, and a low but conspicuous ectocingulum extends across the labial margin of the crown. A deep sulcus separates the cusps of the labial row from the intermediate row. The intermediate row is convex lingually and contains a large, centrally positioned cusp that is connected to the parastylar and metastylar corners of the crown by a high crest; irregularly sized cuspules can be developed on these crests. The lingual row consists of a tall, spirelike protocone, and lower hypocone and pericone. The protocone is positioned just lingual to the central cusp of the intermediate row, with both of these cusps transversely in line with the paracone. Protoconal cristae are developed on two specimens (e.g., UALVP 40633): the

weak postprotocrista extends labially from the protoconal apex, while the stronger preprotocrista runs anteriorly to the anterior cingulum. Although the pericone and hypocone are closely appressed to the protocone, they can be lingual in position, squeezing the protocone labially (e.g., UALVP 40632), or slightly more lingual, with the protocone wedged between the two (e.g., UALVP 46864). Irrespective of the positions of the pericone and hypocone, a short crest invariably connects the apex of the protocone to that of the pericone, and a similarly short postprotocone fold connects the protocone to the hypocone. The protoconal cingula are high and sharp: the anterior cingulum extends a short distance anteriorly from the apex of the pericone, and then bends abruptly labially and continues on towards the parastylar corner; the cingulum bulges posteriorly at the level of the sulcus between the intermediate row and the protocone, forming a spur-like indentation. The posterior cingulum mirrors the path of the anterior cingulum, and forms a similar spur-like indentation opposite that on the anterior side of the crown. Both protoconal cingula terminate at the level of the intermediate row.

Lower dentition (Figs. 7.13.13-7.13.24, 7.14.1-7.14.6, 7.15): i1: The lower medial incisor is preserved in two specimens, UALVP 40635 (an isolated tooth that was reported in Silcox et al., 2001) and in articulation with the mandible in UALVP 40634. The i1 of Carpodaptes hazelae is procumbent and shallowly concave dorsally, similar to the i1 of other plesiadapoids. The crown resembles the i1 of Elphidotarsius more so than that of other species of Carpodaptes or Carpolestes: the crown is short and deep, rather than elongate and pincer-like, and the occlusal surface is flat to slightly convex [compare Figs. 7.13.13-7.13.15 (i1, C. hazelae) with Figs. 7.14.7-7.14.9 (i1, C. stonleyi)]. Two robust crests extend posteriorly from the apex of the crown, circumscribing a broad and slightly dorsomedially oriented occlusal surface. The crests converge at the posterodorsal margin of the crown as a heavy basal cingulid, but a margoconid is not developed.

i2: Although the i2 crown is much smaller than that of i1 (it is nearly the same size as p3), the overall coronal anatomy more closely resembles that of the medial incisor. The protoconid is somewhat dorsoventrally compressed and projects anteriorly, overlapping the posterodorsal surface of i1. A pair of robust crests circumscribe the occlusal surface of i2, which, like that on i1, is oriented somewhat dorsomedially. A small cuspule constitutes the heel of i2. The i2 is somewhat displaced labially on all

specimens preserving the tooth or its alveolus. Although Rose (1975) and Biknevicius (1986) did not address the function of i2 in their analyses of the carpolestid masticatory cycle, the coronal anatomy and orientation of i2 in the present sample suggests that the masticatory function of i1 may have continued onto the crown of i2.

Lower canine: The lower canine of Carpodaptes hazelae is preserved in UALVP 40611, although its crown is severely damaged and most of the protoconid is missing. Judging by the parts that remain, the crown appears to have been smaller but otherwise similar to that for i2 in having a large protoconid that was probably procumbent, and a small, unicuspid heel. The posteriormost parts of the occlusal surface of the lower canine are preserved in UALVP 40611, and these are bounded by robust crests, similar to those on i1 and i2. The parts of the lower canine preserved in UALVP 40611 are consistent with those in UM 89937 [from the early Tiffanian (Ti2) Scarritt Quarry of Montana], the only other lower canine reported for C. hazelae (Silcox et al., 2001).

Lower premolars: p3: The p3 of Carpodaptes hazelae is closely appressed to the much larger p4, and in this way superficially resembles the small, peg-like p3 of many ptilodontoid multituberculates. Although the crown resembles that of i2 and the lower canine, it differs in being larger and more "squat", with the crown dorsoventrally compressed and labiolingually wide. The crown bears but one low, bunodont cusp, the protoconid, and a low, transverse crest posteriorly. The crest continues labially and lingually as a stout cingulid, and a small exodaenodont lobe is developed.

p4: The p4 of Carpodaptes hazelae is well known, and has been extensively described (e.g., Simpson, 1936, 1937; Rose, 1975; Silcox et al., 2001). The present sample includes 19 p4s, allowing a detailed account of variation and a comparison with p4 of C. hazelae from other well-sampled localities in the Western Interior of North America. As in other carpolestids, the p4 of C. hazelae is modified as a large plagiaulacoid blade that bears numerous apical cuspules that together form a serrated apical crest, and a lower talonid cusp. The crown is high relative to its length (Fig. 7.15), and is similarly proportioned to p4 of C. aulacodon and Carpomegadon jepseni (compare Fig. 7.15 with outlines in Rose, 1975, figs. 11, 20, and Bloch et al., 2001, fig. 6), but differs from the much lower p4 of Elphidotarsius, C. cygneus, and C. stonleyi (see Fox, 2002, fig. 4). The p4 varies considerably in size (Fig. 7.15 and Table 7.9), and a weak

bimodality was detected in the lateral profile (see Fig. 7.15 and discussed further later in this chapter). The crown is weakly hourglass-shaped in occlusal outline, with slight indentations labially and lingually at the transverse midline. The dorsal margin of the serrated crest can be smoothly rounded (e.g., UALVP 40676) or more peaked (e.g., UALVP 40630), but it invariably supports five well-differentiated apical cusps; a much smaller sixth apical cusp is developed low on the anterior side of the crown in two specimens (e.g., UALVP 40676). On unworn specimens, the fourth cusp (fifth cusp of six-cusped specimens) is usually the largest and highest (e.g., UALVP 40630), although on some specimens (e.g., UALVP 40634) the apogee occurs at the third and fourth cusps together; the first cusp (on five-cusped specimens) is much smaller than any of the other apical cusps, whereas cusps two, three, and five are more nearly equal in size. The ultimate apical cusp is sometimes displaced posteriorly from the penultimate cusp. Labial and lingual ridges descend from the cusps of the serrated crest: those on the labial side are weakly developed, whereas those on the lingual side are more prominent. The talonid is lower than that on p4 of many other species of Carpodaptes and Carpolestes (compare, e.g., Fig. 7.15 with Rose, 1975, fig. 11), and consists of but a single cusp developed at the summit of a transversely aligned, anteroposteriorly compressed crest; the cusp is somewhat lingually displaced on each p4 at hand. A sharp crest extends ventrolabially from the first cusp towards the anterior exodaenodont lobe, forming a weak anterior cingulid. Similar crests run ventrolabially and ventrolingually from the talonid cusp: the labial crest is longer than the lingual crest, extending to the posterior exodaenodont lobe and forming a short cingulid; the lingual crest continues a short distance anteriorly as a lingual cingulid, ventral to the weakly excavated posterolingual depression (Rose, 1975; Krause, 1978; Fox, 2002). The crown is strongly exodaenodont: the posterior lobe is usually the larger and deeper (e.g., UALVP 40634), although the two lobes are subequal on some specimens (e.g., UALVP 46883). Lobes are also developed lingually, with a deep cleft intervening between the two ventrally; although they are better defined lingually, the lobes are much shallower than those on the labial side of the crown.

Lower molars: m1: The m1 of Carpodaptes hazelae has been described previously (Simpson, 1936; Rose, 1975). The crown is strongly exodaenodont, with both lobes

jutting ventrolabially. The trigonid of m1 abuts the talonid of p4, forming part of the p4/m1 wedging system that is characteristic of carpolestids generally (Biknevicius, 1986), with the apex of the paraconid elevated well above that of the level of talonid cusp on p4. The trigonid is anteroposteriorly elongate, whereas the talonid is anteroposteriorly compressed. The paraconid is subconical and arises from a point high on the anterolingual face of the protoconid, and projects slightly anteriorly. A weak paracristid runs anteriorly from the protoconid apex before abruptly curling lingually to join the paraconid; a shallow notch is usually developed in the paracristid. The protoconid is larger and taller than either the paraconid or metaconid, and its lingual wall is considerably swollen. As on m1 of other carpolestids, the metaconid on m1 in C. hazelae is displaced posterolingually, leaving the trigonid broadly open lingually; the trigonid angle (i.e., the angle formed at the intersection of imaginary lines drawn between the paraconid and protoconid, and between the metaconid and protoconid) is roughly 130-135 degrees. The metaconid is subequal to the paraconid in size, but arises from a relatively lower position on the protoconid. The long protoconid arm of the protocristid meets the much shorter and weaker metaconid arm, and a deep notch is formed at their union; the metaconid arm of the protocristid becomes confluent with the cristid obliqua near the metaconid apex. The talonid is wider than long and bears a deep, nearly V-shaped basin. A conspicuous sulcus is formed as the postvallid wall meets the flattened basin-facing wall of the entoconid and postcristid deep in the basin; the sulcus is oriented labiolingually and continues to the open lingual margin of the talonid. The hypoconid is low and inflated, and connected to the metaconid by a robust and arcuate cristid obliqua; although the hypoflexid is shallow, it is vertically extensive and often bears long, parallel wear facets. The entoconid is small and conical, subequal in height to the hypoconid, and positioned posterolingually. The hypoconulid is virtually undeveloped and is nearly incorporated into the postcristid; on some specimens it is represented only by a slight elevation on the postcristid. The anterior and posterior cingulids are weakly developed.

Discussion.—Although Carpodaptes hazelae is one of the best known carpolestids, having been thoroughly described by Simpson (1936) and Rose (1975), the monophyly of this species has been questioned. Rose (1975) noted considerable variation in the samples of C. hazelae from the type locality and the slightly younger

(Ti3) Cedar Point Quarry, but cautiously attributed these differences to intraspecific variation owing to age, provenance, or both. Fox (2002) suggested that C. hazelae may be a composite species, arguing that upper dentitions referred by Krishtalka (1973) and Youzwyshyn (1988) to Carpodaptes sp., cf. C. hazelae from the Police Point (Ti4) and Cochrane 2 (Ti1) localities of Alberta, as well as those referred by Holtzman (1978) to C. cygneus from the early middle Tiffanian (Ti3) Brisbane locality of North Dakota, while C. hazelae-like in their coronal anatomy, differed from C. hazelae (sensu Rose, 1975 for samples from Scarritt Quarry and Cedar Point Quarry) in their smaller size and more gracile construction [similar differences were noted by Rose (1975) between the topotypic and Cedar Point Quarry samples]. The combined samples from the Blindman River and Birchwood localities exhibit a significant degree of variation, especially in the labial profile of p4, where a weak bimodality is present (Fig. 7.15): the smaller p4 variants are lower crowned relative to their length, the prepenultimate apical cusp tends to be more inflated than the other cusps, and the talonid is relatively lower than that in the larger morph [it is noted here that the variation in the lateral profile of p4 may be enhanced by the development of the posterior exodaenodont lobe: the base of the posterior lobe serves as a landmark for orienting the outlines, and its depth varies considerably; the lobe can be relatively deep, making the crown appear tall relative to length, whereas in others it is weak, making the crown appear more nearly round in lateral view. Other mammals with plagiaulacoid teeth (e.g., multituberculates) often show a similar, wide range of variation in the development of the exodaenodont lobe; see, e.g., Chapter 3]. Variation is less pronounced in the upper dentition, although both P4 morphs identified by Rose (1975) in the Scarritt Quarry and Cedar Point Quarry samples occur in the combined Blindman River and Birchwood samples (i.e., the P4 protocone can occur at the lingual margin of the crown, see Fig. 7.12.8, or be essentially squeezed labially by the enlarged hypocone and pericone, see Fig. 7.13.11). The meaning of these variations is unclear, particularly given the comparatively small samples from Alberta and the fact that similar ranges of variation have been discovered in coeval but geographically disparate populations of C. hazelae (those from Scarritt Quarry and Cedar Point Quarry, and those from the Blindman River and Birchwood localities, i.e., the different variants are not patterned geographically, but instead occur together at single

localities). The weak bimodality in the lateral profile of p4 in the present sample gives some support to Fox's (2002) opinions as to the composite nature of C. hazelae, but a satisfactory resolution to the problem awaits an analysis of all of the relevant specimens (i.e., topotypic specimens of C. hazelae, as well as specimens of C. cf. hazelae from Cochrane 2, Police Point, and Brisbane).

Superfamily PAROMOMYOIDEA Simpson, 1940
Family PAROMOMYIDAE Simpson, 1940

Genus IGNACIUS Matthew and Granger, 1921

Ignacius MATTHEW and GRANGER, 1921, p. 5.

Type species.—Ignacius frugivorus Matthew and Granger, 1921.

Other included species.—Ignacius fremontensis (Gazin, 1971); I. graybullianus Bown and Rose, 1976; ?Ignacius mcgrewi (Bown and Rose, 1976); I. clarkforkensis Bloch, Silcox, Boyer, and Sargis, 2007.

IGNACIUS FRUGIVORUS Matthew and Granger, 1921
Figures 7.14.10-7.14.17; Table 7.10

Ignacius frugivorus MATTHEW and GRANGER, 1921, p. 5.
Phenacolemur frugivorus SIMPSON, 1935, p. 19.

Holotype.—AMNH 17368, incomplete left maxilla with P2, P4, M1-2 (Matthew and Granger, 1921, p. 5). Mason Pocket locality, Animas Formation of Colorado, late Paleocene (late middle Tiffanian, Ti4, Plesiadapis churchilli/P. simonsi Lineage Zone of Lofgren et al., 2004).

Material examined.—From Joffre Bridge Roadcut lower level: UALVP 46884, incomplete left maxilla with P4, M1.

From DW-2: UALVP 40662, incomplete maxilla with P4, M1; UALVP 40664, 40665, M1; UALVP 40660, M2; UALVP 46885, associated p4 (broken), m1-2; UALVP 40661, p4; UALVP 46886, m1; UALVP 40659, m3.

From Birchwood: UALVP 39302, incomplete left maxilla with M1-3; UALVP 46887, incomplete right dentary with i1, p4, and alveoli for m1-2.

Age and occurrence.—Earliest Tiffanian (Plesiadapis praecursor/P. anceps Lineage Zone, Ti1, late Paleocene) to latest Tiffanian (Plesiadapis gingerichi/Rodentia Interval Zone, Ti6, late Paleocene) of the Western Interior of North America (Lofgren et al., 2004).

Discussion.—The dentition of Ignacius frugivorus has been described by Matthew and Granger (1921), Simpson (1935), and Bown and Rose (1976); the holotype was figured by Szalay and Delson (1979, fig. 19A). The specimens from DW-2 and Birchwood resemble those described and figured by Krause (1978) from the late middle Tiffanian (Ti4) Roche Percée locality of Saskatchewan, and those from the type locality (Simpson, 1935), but differ from these in the following ways:

1) P4 is smaller relative to M1, and the crown is more transverse relative to its length (i.e. it is more nearly rectangular in outline, rather than being square), and the talon is better developed and more posteriorly extending. The paracone is less inflated at its base, and the parastylar lobe does not protrude labially. Additionally, the preprotocrista extends directly to the parastylar corner of the crown, rather than terminating at the anterolingual base of the paracone (noted by Krause, 1978 for the Roche Percée sample); in this respect, the Blindman River and Birchwood specimens more closely resemble the topotypic P4s (Simpson, 1935).

2) The upper molars are more transverse relative to their length, and have talons that bulge lingually such that the protocone and talon appear somewhat lobe-like in lingual view. The talon of M3 in particular is broader, longer anteroposteriorly, and is smoothly rounded posterolingually.

3) The molar paracone and metacone are more closely appressed to one another, and the stylar shelf is better developed labial of the metacone.

4) The M3 is larger relative to the other upper molars.

5) The m1 trigonid is more triangular in occlusal view, with the paracristid extending more directly transversely from the protoconid to the paraconid. This differs from m1s from Roche Percée in particular, in which the trigonid is more nearly square, with the paracristid extending anteriorly before bending sharply lingually towards the paraconid, and forming an anterior "pocket" (and in this regard more closely resembles m1 of Phenacolemur).

UALVP 40661, an isolated p4, is considerably smaller than that on UALVP 46887 from the Birchwood locality, and is smaller than p4s of I. frugivorus reported from the early middle Tiffanian (Ti3) Cedar Point Quarry and late Paleocene (Ti4) Divide Quarry of Wyoming (Secord, 2004). Additionally, the talonid on UALVP 40661 is only slightly wider than the protoconid, imparting a subovate occlusal outline to the crown, rather than wedge-shaped occlusal outline that is more characteristic of I. frugivorus. Although the dimensions of UALVP 40661 are smaller than those for p4 of I. frugivorus in other samples, they are nonetheless nearly identical to those recorded by Simpson (1935) for a topotypic p4 from Mason Pocket.

Family PICRODONTIDAE Simpson, 1937

Systematic history.—Picrodontidae comprise an enigmatic family of small, peculiarly specialized plesiadapiform primates known from only the Paleocene of North America. Although occurring at numerous Torrejonian and Tiffanian localities in the Western Interior, picrodontids are poorly documented, being mostly represented by isolated teeth and fragments of jaws with teeth. This limited evidence and a lack of intermediates between picrodontids and other mammals has made difficult a satisfactory determination of their relationships.

Douglass (1908) described the first known picrodontids, which were also the first plesiadapiforms discovered in North America. He named Picrodus silberlingi, based on an incomplete dentary having p4-m1, and Megopterna minuta, from a dentary fragment containing an m1 talonid and m2; both holotypes are from the Silberling Quarry, Lebo Formation, Montana. Douglas thought that P. silberlingi was possibly a caenolestid

marsupial and M. minuta, since shown to be a junior synonym of P. silberlingi (Simpson, 1937), an insectivoran.

The next picrodontid to be described was Zanycteris paleocenus Matthew, 1917, based on a crushed skull containing much of the upper dentition from the Mason Pocket locality, Animas Formation of Colorado (Lofgren et al., 2004). Matthew (1917) proposed that Zanycteris was a phyllostomatid bat, comprising the earliest, and only Paleocene, record of Chiroptera; he made no reference to the two species that Douglass (1908) had named, evidently failing to realize that they were related to Zanycteris. Recognition that Picrodus, Megopterna, and Zanycteris are a natural group came only with Simpson's (1937) monograph on Paleocene mammals from the Crazy Mountain Field, Montana. In this work, he synonymized Douglass's Megopterna minuta with Picrodus silberlingi and classified Picrodus and Zanycteris in a new family, Picrodontidae. He demonstrated that the bat-like features of the picrodontid dentition were only adaptive and did not warrant Matthew's "extraordinary conclusion that the Chiroptera had already in the Middle Paleocene achieved this peculiar and aberrant molar pattern and at the same time had lost, or not yet acquired, characters otherwise universal among chiropterans" (p. 135; and see Simpson, 1935). Anticipating that future discoveries would better reveal their relationships, Simpson (1937) classified picrodontids noncommittally, as incertae sedis in "?Insectivora."

McGrew and Patterson (1962) extended the picrodontid record to the late Paleocene Fort Union Formation of Wyoming (Saddle and Shotgun local faunas), describing a small collection of fragmentary jaws and teeth, which they referred to Picrodus cf. P. silberlingi. Included were two incomplete maxillae, one containing M1-2, the other M1; the teeth differed in several features from M1-2 of Zanycteris and were identified as the first known parts of the Picrodus upper dentition. McGrew and Patterson (1962) also compared picrodontid and phyllostomatid teeth, concluding with Simpson (1937) that the resemblances to bats were only superficial, mostly limited to the wrinkled enamel that covers the broad, low occlusal surfaces of the molars. McGrew and Patterson (1962), like Simpson (1937), tentatively classified picrodontids in Insectivora.

Szalay (1968) reviewed the Picrodontidae, presenting the first detailed descriptions of the jaws and teeth of Picrodus and determined that picrodontids were

early primates within a monotypic superfamily Picrodontoidea; he believed that picrodontids were descended from a paromomyid ancestor, as represented, for example, by Palaechthon (see Szalay, 1968, p.49). Szalay (1968) synonymized McGrew and Patterson's (1962) Picrodus cf. P. silberlingi with P. silberlingi, and redescribed Z. paleocenus, still known from only the holotype. Szalay (1968) also undertook a functional analysis of the Picrodus dentition, focussing on the best known and most highly specialized teeth, M1/m1, and concluded, as had Matthew (1917) and McGrew and Patterson (1962), that picrodontids were probably frugivores. Szalay and Delson (1979) still classified the Picrodontidae as primates, but within the superfamily Paromomyoidea, suborder Plesiadapiformes.

In 1982, Tomida described a third picrodontid, Draconodus apertus, based on isolated M1 and M2 from the early Torrejonian North Horn Formation, Dragon Canyon, Utah, the earliest discovered occurrence of the family (Tomida, 1982; Lofgren et al., 2004). Tomida (1982) recognized that Draconodus is more primitive than Picrodus or Zanycteris in crucial aspects of M1 morphology, and reaffirmed the homology of M1 of picrodontids with that of other primates, not with "P5" as had been advocated by Schwartz and Krishtalka (1977).

In the years since Szalay and Delson (1979), picrodontids have been widely accepted as plesiadapiforms (e.g., Gunnell, 1989; Silcox and Gunnell, in press). In that context, Williams (1985) described Picrodus teeth that had not been part of Szalay's (1968) review, focusing on molar variation in what he considered P. silberlingi. He synonymized Draconodus with Picrodus, recognizing P. apertus (Tomida, 1982) as a second species of the genus and emphasized the resemblances between the molars of picrodontids and glossophagine phyllostomatid bats, suggesting that picrodontids, like glossophagines, ate mostly pollen and nectar, not fleshy fruits. Van Valen (1994) revalidated Draconodus in his review of plesiadapiform relationships.

Type genus.—Picrodus Douglass, 1908.

Other genera.—Zanycteris Matthew, 1917; Draconodus Tomida, 1982.

Revised diagnosis.—Differing from other plesiadapiforms in the following combination of characters: molars decrease in size from M1/m1 to M3/m3; upper molar crowns low and broad and cusps reduced in height; M1 stylar shelf reduced or lost

anteriorly but metastylar area expanded posterolabially; M1 postprotocone fold+postcingulum robustly constructed; M2 parastylar lobe finger-like and projecting labially.

Age and occurrence.—Early Torrejonian (Periptychus carinidens/Protoselene opisthacus Interval Zone, To1, early Paleocene) to early middle Tiffanian (Plesiadapis rex/P. churchilli Lineage Zone, Ti3, late Paleocene) of the Western Interior of North America (Lofgren et al., 2004).

Genus PICRODUS Douglass, 1908

Picrodus DOUGLASS, 1908, p. 17.
Megopterna DOUGLASS, 1908, p. 18.

Type species.—Picrodus silberlingi Douglass, 1908.

Other included species.—Picrodus calgariensis new species; P. canpacius new species; P. lepidus new species.

Revised diagnosis.—Differs from Draconodus in having larger and anteroposteriorly longer upper molars relative to width, with reduced, less distinct paracone and metacone, wider stylar shelf; continuous, more elongate centrocrista; longer and wider trigon basin, and reduced or absent conules. Differs from Zanycteris in having a reduced upper canine, retention of P1, and M1 with reduced paracone and parastylar lobe, anteriorly narrower stylar shelf, a more expanded metastylar lobe, and in the postprotocone fold+posterior cingulum being more expanded posteriorly.

Age and occurrence.—Middle Torrejonian (Protoselene opisthacus/Mixodectes pungens Interval Zone, To2, early Paleocene) to early middle Tiffanian (Plesiadapis rex/P. churchilli Lineage Zone, Ti3, late Paleocene) of the Western Interior of North America.

Remarks.—An outcome of the present chapter is that the name Picrodus silberlingi as used by workers after Douglass (1908) is of uncertain status as to its contents. A revision of Picrodontidae currently in preparation (Scott and Fox, in prep.) will address the taxonomic status of P. silberlingi. For the present chapter, the name P.

silberlingi refers only to the type specimen [CMNH 1675, incomplete right dentary with p4, m1, from Silberling Quarry, upper Lebo Formation of Montana (Simpson, 1937, pl. 1)] and specimens from the late Torrejonian (To3) Medicine Rocks and Mehling Site of Montana (examined here firsthand and as reported in Szalay, 1968 and Williams, 1985).

PICRODUS CALGARIENSIS new species

Figures 7.16.1-7.16.12, 7.19.1-7.19.3; Table 7.11

Picrodus silberlingi SCOTT, 2003, p. 756.

Diagnosis.—Differs from other known species of Picrodus as follows: P4 subquadrate, with well-developed protocone; M1 with taller paracone and metacone, well-defined notch between postparacrista and premetacrista; M2 transversely wider, with taller paracone and metacone; p4 with robust paracristid and low, unicuspid, unbasined talonid; m1 paraconid in anterior position, low on trigonid, paracristid elongate; m2 cristid obliqua meeting postvallid wall lingually, beneath apex of protoconid; m2 talonid squarish posteriorly, retaining distinct hypoconulid; molar enamel mostly smooth.

Description.—Skull and upper dentition (Figs. 7.16.1-7.16.6): Maxilla: Two incomplete maxillae have been recovered from the Who Nose? locality; together, they preserve the facial process and nearly the entire post-incisor dentition, as well as the maxillary root of the zygomatic arch and part of the nasal cavity and palate. In UALVP 45655, the better-preserved specimen, the snout is narrow anteriorly but flares laterally beginning at P3, as in Zanycteris paleocenus (cast of holotype, AMNH 17180). The facial process of the maxilla is high and in UALVP 45656 retains the infraorbital foramen, dorsal to P4 at the anterior end of the infraorbital canal; it is large and circular, and faces anterolaterally and slightly ventrally. The maxillary foramen, at the posterior end of the canal, is not preserved, but was probably above the posterior parts of M1.

In UALVP 45656, the anterior root of the zygomatic arch is robust, arising from the maxilla above M2. Its lateral surface is incised by a shallow but wide, irregular depression that extends on to the facial process of the maxilla above M1; this depression

is bordered ventrally by a narrow discontinuous ridge. The depression is the scar marking the overlap of the jugal process of the zygomatic arch on to the maxilla, as in therian mammals generally. From the dimensions of the scar, this part of the jugal was dorsoventrally deep, indicating that the arch was stout. Anteroventrally, the scar divides, implying that the jugal was forked anteriorly into a more elongate dorsal process and a shorter, blunt, ventral process. The ridge below the scar was closely adjacent to the edge of the jugal ventrally. Anterior to the scar for the jugal in UALVP 45656, the dorsal edge of the maxilla becomes thicker where it formed parts of the anteroventral rim of the orbit. More posteriorly, within the scar, the maxilla thins to a feather edge dorsally and was probably overlapped above by the jugal and, hence, excluded from the orbital rim. If this interpretation is correct, and the maxilla constituted the anteroventral rim of the orbit, the lacrimal and jugal could not have met within the rim, a derived condition among tribosphenic therians, even for plesiadapiforms (e.g., Plesiadapis tricuspidens, see Russell, 1964, fig. 13), suggesting that the lacrimal in Picrodus was reduced.

In UALVP 45655 the facial process of the maxilla is medially exposed. Dorsally, this surface displays the anterior part of a depression above P3-4 and a smaller depression above P2. These depressions possibly were associated with the turbinal conchae—the posterior cavity marking the position of one of the ectoturbinals, the anterior cavity associated with the maxilloturbinal (Novacek, 1986). A faint groove passing obliquely below these depressions may mark the course of the nasolacrimal duct. This groove is paralleled ventrally by a wider channel that divides anteriorly, sending a branch ventromedially towards the dorsal surface of the palate and a deep depression there; the function of this channel and depression is unknown.

Parts of the palatal process of the maxilla are preserved in both specimens, medially to the midline suture in both and anteriorly to the level of the canine alveolus in UALVP 45655. Neither specimen shows evidence of an incisive foramen or other vacuity in the parts of the palatal process that are preserved. More posteriorly, UALVP 45656 retains a fragment of the palatine bone, displaced slightly from the maxilla and extending to the same level as the anterior side of M1. A large vascular foramen, probably the posterior palatal foramen, opens opposite M2 and is posteriorly adjacent to the suture with the maxilla. A thickened edge of the palate medial to the posteriormost

parts of M3 appears to be part of the rim of the choana formed by the palatine; laterally adjacent to this rim, the sutural articulation between the maxilla and palatine is clearly visible.

Upper canine: None of the upper dentition anterior to M1 in Picrodus has been described previously. The anteriormost tooth preserved in UALVP 45655 is the first of three premolariform teeth in place anterior to P4; this tooth is interpreted to be P1 as discussed below. Anteriorly adjacent to P1 is a small alveolus that housed a small, single-rooted canine. The reasons for this conclusion are as follows: on UALVP 45655, the bone of the snout and palate is preserved a short distance further anteriorly from this alveolus, ending at a broken edge, but the bone up to this edge shows no sign of an additional alveolus. Hence, a diastema intervened between the empty alveolus and any teeth anterior to it [it is assumed that the premaxilla of Picrodus calgariensis housed teeth at least at two incisor loci, as in other plesiadapiforms for which appropriately preserved specimens are available (Silcox, 2001)]. A diastema between the posteriormost incisor and the upper canine would not be unique to P. calgariensis, but is commonly seen in tribosphenic therians, even in other plesiadapiforms in which the upper canine is reduced and the lower canine absent (e.g., Ignacius graybullensis as illustrated by Szalay and Delson, 1979, fig. 21). If, however, the empty alveolus housed the posteriormost incisor and not the canine, with the canine either having been lost or represented by the tooth that we have identified as P1, a diastema would have occurred within the incisor row but none more posteriorly, a pattern not otherwise occurring in any known eutherian and rejected on that account.

If this interpretation is correct, no evidence is preserved as to the number or configuration of the upper incisors in UALVP 45655 and hence, in P. calgariensis or picrodontids more generally. Although the canine alveolus has been identified in UALVP 45655, a suture between the premaxilla and maxilla cannot be discerned. The bone of the side of the snout and the remnant of the palate in this specimen is split apart at the level of P1, but from the contour of the exposed surfaces, this break appears to be only an artifact, not separation of two bones along a suture. As a result of the break, P1 has been displaced anteriorly from P2, creating a substantial gap between the two teeth.

Upper premolars: P1: In UALVP 45655, P1 has been partly extruded from its alveolus. It has a simple, premolariform crown, longer than wide, and a thick root that is grooved along its lingual side, suggesting its incipient division; the end of the root is housed in the alveolus, however, and cannot be observed. The paracone is stout, somewhat recurved, and slightly swollen lingually. A tiny cuspule is seen on its anterior side, near its base; two short crests extend from this cuspule, one posterolingually along the side of the paracone and the other towards its apex. A weak metastylar area, bearing a short, rounded crest and incipient cusp, arises posteriorly.

P2: P2 is two-rooted; the posterior root is somewhat wider transversely than the anterior root, which is broken. The tooth is closely similar to P1 but the paracone is slightly lower and the metastylar area projects more strongly posteriorly; overall, the crown is longer than wide. A faint swelling is in the position of the anterior basal cuspule on P1 and the base of the crown is somewhat swollen lingually; there is no protocone. A posterior crest runs from the apex of the paracone to the metastylar area, ending at a cuspule posteriorly. This cuspule resembles the posterolabial cuspule on P1, but is stronger.

P3: The crown is small, premolariform, subequal in size but slightly lower than that of P2, and longer than wide; a short space intervenes between P2 and P3. The paracone is stouter than on P2; the parastylar lobe projects as a weak anterior cingulum from the base of the paracone. The metastylar area is more expanded than in P2, forming a broad surface that slopes posteriorly and is bordered posterolingually by an elevated ridge. This ridge is homologous with the postcingulum on P4 and arises from the posterolingual face of the paracone near its base. Posterolabially, the posterior cingulum ends at a small metastylar cuspule, smaller than on P2 but obviously homologous with it. The protocone and conules are undeveloped. P3 is two-rooted; the posterior root is considerably larger in diameter than the anterior root, in keeping with the expanded posterior surface that it supports.

P4: P4 is almost certainly three-rooted (see later in this chapter), although the crown fits tightly to the maxilla in both UALVP 45655 and 45656, making it impossible to determine directly if there are separate posterolabial and lingual roots. P4 is subrectangular, slightly longer labially than lingually and roughly intermediate in size

between P3 and M1. There is no stylar shelf: the base of the paracone is at the labial edge of the tooth and only a weak ectocingulum is present posterior to the paracone. A small parastylar lobe arises as a cingulum at the base of the paracone, but no parastylar cusp is developed. The paracone is large and conical, and a short, steep postparacrista extends from it to the posterolabial corner of the crown; paraconule, metacone, and metaconule are absent. The protocone is a small but well-defined subconical cusp close to the paracone. A short preprotocrista runs from the apex of the protocone to the base of the paracone; another crest arises posterolingually on the protocone and continues around the edge of the shallow basin that makes up most of the occlusal surface of the tooth. This crest probably represents the postprotocone fold+posterior cingulum, but no hypocone is evident to indicate the division between the two: the junction may be at the base of the protocone, where the crest is lowest and swings posterolabially. On M1, the postprotocrista is labial to the postprotocone fold+posterior cingulum, but there is no evidence of a postprotocrista on P4 in either UALVP 45655 or 45656. A metastylar cusp is undeveloped, and this part of the crown is overlapped by M1 in each specimen. Most of the biting surface of P4 lies posterior to the axis between the paracone and protocone; this surface slopes gently posteriorly overall and displays only a few faint, irregular ridges. The roots (only the anterolabial and lingual roots can be seen) are perpendicular to the base of the crown.

In the context of the other new species of Picrodus from Alberta (see later in this chapter), P4 of P. calgariensis most resembles P4 in P. canpacius (from Cochrane 2, see later in this chapter) but is more primitive as determined through comparison with homologous teeth in Purgatorius unio Van Valen and Sloan, 1965, a purgatoriid here considered among the most dentally primitive plesiadapiforms (see, e.g., Gunnell, 1989; Silcox and Gunnell, in press), as follows: It is slightly larger and more rectangular in outline; the paracone and protocone are taller and more nearly vertical relative to the occlusal surface posterior to these cusps; the protocone is larger relative to the paracone; the postparacrista and postprotocone fold+posterior cingulum are higher; the small parastylar lobe contrasts with the absence of the lobe in P. canpacius; and the posterior slope of the crown in P. calgariensis is less steep (discussed more fully later in the chapter). P4 of P. canpacius is three-rooted, making it virtually certain that P4 in P.

calgariensis is three-rooted as well, with a lingual root supporting its more robust protocone.

Upper molars: M1: In its major aspects, M1 of P. calgariensis resembles M1 of P. silberlingi (Szalay, 1968; Szalay and Delson, 1979; Williams, 1985) and P. cf. P. silberlingi (McGrew and Patterson, 1962), sharing large size, irregularly triangular outline, low crown, broad and low occlusal surfaces, and low cusps and crests. In respect to the other new species of Picrodus from Alberta, M1 of P. calgariensis most resembles M1 in P. canpacius, but is more primitive as follows: The stylar shelf is narrower, especially anteriorly; the ectocingulum is subequal in length but lower and less robust overall; the mesostyle is weaker; the paracone and metacone are taller and not so completely incorporated into the centrocrista; the preparacrista is absent (in UALVP 45655) or short and limited to the anterior side of the paracone (in UALVP 45656) (it is weak to absent in P. canpacius); the centrocrista is more deeply notched, forming a short postparacrista and a long premetacrista; the parastylar lobe is better developed; a remnant of the paraconule is present; the preparaconular crista and postparaconular crista ("hypoparacrista" of Szalay and Delson, 1979, fig. 6b) are more robust; the postmetaconular crista is continuous with the metacingulum, but neither metaconule nor premetaconular crista is developed; the protocone and preprotocrista are subequal in height with those of P. canpacius, but the base of the protocone extends less lingually and the lingual face of the protocone is steeper in P. calgariensis; and the anterior cingulum is narrower, not extending as far labially nor approaching the preprotoconal crista, preparaconular crista, or paracingulum.

In P. calgariensis, the trigon and talon basins of M1 are clearly distinct from one another, occupying different occlusal planes and separated by the postprotocrista; this crest extends from the apex of the protocone to the metacone (and includes the "hypometacrista" of Szalay and Delson, 1979, fig. 6b). By contrast, in P. canpacius, two crests are in the position of the postprotocrista: One extends from the protocone apex and fades posteriorly; the other, posterolabial to the first, has its origin at the base of the protocone and extends to the metacone. This pattern is like that in M1 of P. silberlingi as illustrated by Szalay and Delson (1979, fig. 6b), but these authors identified the crest coming from the protocone apex as the postprotocone fold and the more labial crest as

the postprotocrista. M1 of P. calgariensis demonstrates, however, that both of these crests are in fact parts of the postprotocrista, which is subdivided in more advanced species of Picrodus. Hence, the entirety of the subdivided crest on M1 of advanced Picrodus, including P. silberlingi, is homologous with the single crest in more primitive picrodontids (and plesiadapiforms more generally) in which a continuous postprotocrista runs posterolabially from the protocone to the region of the metacone [see M1 of Draconodus apertus (e.g., Tomida, 1982, fig. 1) and Zanycteris paleocenus (e.g., Schwartz and Krishtalka, 1977, fig. 2)]. Moreover, Williams (1985, p. 52) noted that on some M1s that he referred to P. silberlingi, the postprotocrista is a single crest, continuous from the apex of the protocone to the metacone, in agreement with the homologies of the crest as interpreted here.

The postprotocone fold on M1 of P. calgariensis arises from the protocone apex lingual to the postprotocrista and separate from it, and extends posteriorly to a small hypocone (better developed on UALVP 45655). Past the hypocone, it continues posterolabially as the posterior cingulum, ending at the side of the crown below the base of the metacone. In contrast to P. silberlingi, P. canpacius, and P. lepidus (new species from DW-2, see later in the text), the posterior cingulum in P. calgariensis does not approach or join with the postprotocrista or with the metacingulum, but is vertically displaced from them. Hence, the relationship between the postprotocone fold+posterior cingulum in P. calgariensis is just as in other plesiadapiforms, with the major difference being that the fold is long and the posterior cingulum short in Picrodus. If the interpretation of these structures is correct, that of Szalay (1968), in which the entire lingualmost crest in P. silberlingi was termed the posterior cingulum, or Szalay and Delson (1979, fig. 6b), in which the crest anterolingual to the hypocone in P. silberlingi was unidentified and the crest posterolabial to the hypocone was termed the "posthypocone crista" (a neomorphic structure), needs to be revised.

In P. calgariensis, the enamel of the trigon and talon basins of M1 is nearly entirely smooth, with only a few weak ridges near the postprotocrista. This texture differs from that in M1 of the other species of Picrodus and Z. paleocenus, in which the M1 enamel is crenulated; comparison with the enamel on M1 of Purgatorius indicates that the smooth enamel on M1 of P. calgariensis is the more primitive pattern, with

increasing crenulation of the enamel characterizing M1 of the stratigraphically younger species of Picrodus and Zanycteris (see later in this chapter).

M2: M2 of P. calgariensis is present in UALVP 45655 and 45656, maxillae that also contain P4 and M1. M2 of Picrodus had been previously known in P. silberlingi (Szalay, 1968; Williams, 1985) and P. cf. P. silberlingi (McGrew and Patterson, 1962) and is also documented by M2 of P. canpacius. M2 of P. calgariensis and P. canpacius are closely similar, but differ in key features (with M2 of P. calgariensis being the more primitive) as follows: M2 in P. calgariensis is larger relative to M1 and more transverse relative to its length; the stylar shelf is wider, especially opposite the metacone; the mesostyle is larger; the parastylar lobe is more robust; the paracone and metacone are taller and are distinct cusps, not merely the raised ends of the centrocrista; the paracone is taller relative to the metacone; the centrocrista is interrupted by a broad V-shaped notch just posterior to its mid-length; the preparacrista is higher and extends across the parastylar lobe to its anterolabial border; the postmetacrista, although short and weak, is stronger; the paraconule is small but better defined; the preparaconular crista+paracingulum is longer, extending labially past the base of the paracone and joining the preparacrista; a short, faint postparaconular crista (the "hypoparacrista" of Szalay and Delson, 1979) is present but worn, leaving its original dimensions unknown; the metaconule is absent (as on M2 of P. canpacius); lingual to the metacone are several short, irregular ridges, but none that can be confidently identified as conular cristae; the protocone is taller and its lingual face more nearly vertical; the preprotocrista is longer and higher; the anterior cingulum is weaker; the postprotocrista is well developed and separates the trigon basin from the talon basin (this crest is absent and the basins confluent on M2 of P. canpacius); there is no evidence of a hypocone (which may be owing to wear on the available specimens); and the enamel covering the biting surfaces of the crown is smoother, with ridges limited to the area lingual to the metacone.

M3: Exclusive of AMNH 17180, the holotype of Zanycteris paleocenus, UALVP 45656 is the only picrodontid specimen now known in which M3 is preserved within a maxilla that also contains more anterior teeth. Earlier, Youzwyshyn (1988) referred two isolated M3s from Cochrane 2 to P. silberlingi, the first discovered for Picrodus. As shown by UALVP 45656, M3 in P. calgariensis is anteroposteriorly shorter and

transversely narrower than M2 and subtrapezoidal in occlusal outline, with nearly parallel anterior and posterior sides; the labial and lingual sides converge towards one another posteriorly and the posterolingual corner of the crown forms a smoothly curved arc, as in M2, but is more expanded posteriorly. The stylar shelf is wider anteriorly than posteriorly and the parastylar lobe projects strongly labially, but less so than in M2. A small mesostyle on the ectocingulum is slightly anterior to the metacone and posterior to its position on M2. The paracone is a small subconical cusp; the metacone is scarcely developed, consisting of only a slight elevation at the posterior end of the centrocrista. The centrocrista is low and gradually descends posteriorly from the apex of the paracone; there is no V-shaped notch along its length. A small, ill-defined paraconule is present at the base of the paracone. The preparaconular crista extends labially from the paraconule to become the paracingulum anterior to the paracone and then further labially joins with the low preparacrista; this latter crest continues out onto the parastylar lobe, along its anterior edge. The postparaconular crista, metaconule, and metaconular cristae appear undeveloped, although these surfaces are somewhat worn in this specimen. The protocone is low but robust and positioned lingual to the paracone; a narrow anterior cingulum is present near the base of its anterior side. The preprotocrista is weak and the postprotocrista absent; the trigon and talon basins are fully confluent. The posterolingual margin of the crown is furnished by the postprotocone fold+posterior cingulum; there is no hypocone. The enamel of the biting surfaces is smooth.

In comparison to the picrodontid M3s from Cochrane 2 (Youzwyshyn, 1988; see later in this chapter), M3 in UALVP 45656 is subequal in size, but has a wider stylar shelf and stronger parastylar lobe; larger mesostyle; taller, more conical paracone; stronger paraconule and preparaconular crista+paracingulum+preparacrista; taller, more robust protocone; and higher postprotocone fold+posterior cingulum. Moreover, the occlusal basin is relatively small, unlike the broadly expanded basin in M3 of P. canpacius; the posterolingual corner of the crown in the latter is squarish, in contrast to the curved corner in P. calgariensis. Finally, the occlusal enamel is smooth, versus the densely crenulated enamel in P. canpacius. In each of these differences, M3 of P. calgariensis is clearly the more primitive.

Dentary and lower dentition (Figs. 7.16.7-7.16.12): UALVP 43294 is an incomplete left dentary containing an enlarged incisor, p4, and m1-2, the only dentary and articulated lower dentition of P. calgariensis now known. The dentary closely resembles that of P. silberlingi as described by Szalay (1968), but is virtually complete anteriorly, missing only a small chip from the alveolar rim of the enlarged incisor. No teeth were developed more anteriorly. The mandibular body of UALVP 43294 is short and deep; it is broken behind m3, with the coronoid, condylar, and angular processes missing. Anteriorly, the symphyseal surface is raised above the adjacent bone and is divided into an upper and lower arm (superior and inferior torus), which meet anteriorly and diverge posteriorly. The upper arm is deeper, whereas the lower arm is longer, extending to below the anterior root of p4: the bone in the depression between them is penetrated by several nutritive foramina. The symphyseal surfaces are smooth, implying that the dentaries were only loosely attached in life. A large mental foramen opens laterally under the anterior root of p3 and a small nutritive foramen opens medially below the anterior root of m3. The dentary contains three alveoli between the anterior incisor and p4.

i1: The enlarged anteriormost tooth in P. silberlingi has been identified as i1 by Szalay (1968) and Szalay and Delson (1979) [it is now known that the assumptions that Schwartz and Krishtalka (1977) invoked to support their interpretation of the picrodontid dental formula (e.g., loss of M3/m3, with the enlarged anteriormost lower tooth in P. silberlingi (s. l.) being the canine) are invalid (e.g., Tomida, 1982; Luckett, 1993), and this alternative is not considered any further here]. Simpson (1937) described an isolated i1 from Gidley Quarry, Montana, "associated with" USNM 9866, a dentary fragment containing m1 referred to P. silberlingi, but this incisor (having "a series of eight or nine ridges or angulations") belongs to some other, non-picrodontid taxon.

The crown of i1 in UALVP 43294 is pristine, without damage or evidence of wear: it is elongate, mediolaterally compressed, procumbent but curving somewhat dorsally, widest near its base and then tapering gradually towards its tip. Its occlusal surface is narrow, facing mostly medially and only slightly dorsally. A dorsolateral and a ventromedial crest, both of which fade towards the base of the crown, border the sides of the occlusal surface; the ventromedial crest is the more robust. Between the crests, the

crown is moderately inflated, forming an elongate, low, rounded ridge that is narrower and higher apically but never forms a sharp edge. There is no margoconid. The root is stout, deeper than wide, and enters the dentary at about a 45-degree angle.

Lower teeth between i1 and p4: Between i1 and p4 in UALVP 43294 is a row of three small alveoli, the first of which is directly behind and closely adjacent to i1; no diastemata occur between these alveoli or between the third alveolus and p4. The most anterior alveolus is the smallest, but the exact size of the second and third cannot be determined owing to breakage of their walls; nonetheless, both appear to have been slightly larger than the first. These alveoli are interpreted as having housed small, single-rooted i2, p2, and p3, identifications compatible with the interpretation of the upper antemolar dentition of P. calgariensis and with the pattern of loss of antemolar teeth in plesiadapiforms generally [Silcox (2001) showed that the loci of antemolar teeth in plesiadapiforms need not correspond between upper and lower jaws]. However, Szalay's (1968) identification of the teeth at these positions as i2, c, p3 in P. silberlingi seems no less realistic. In fact, the evidence now available is incapable of resolving the identification of these loci in P. calgariensis or other known picrodontids. Indeed, reduction from the antemolar count of i1-3, c, p1-4 in the ancestral plesiadapiform (Silcox, 2001) could have led to equally plausible alternatives in Picrodus than specified by Szalay's (1968) or in this study—for example, perhaps these teeth are i1, c, p1-4 as in Palenochtha weissae (see Gunnell, 1989). Szalay (1968), Gunnell (1989), and Silcox (2001) considered the realistic alternatives, and no new, decisive information can be added here as to which is to be preferred.

p4: The p4 in UALVP 42394 is much smaller than m1, as in all other picrodontid specimens in which these teeth are known. The tooth is two-rooted, with each root housed in its own alveolus; the anterior root, which is partly exposed at a break on the medial side of the dentary, slants obliquely anteriorly. The crown of p4 is simple, consisting of a tall protoconid having a pointed apex and an anteriorly sloping posterior wall, and a small, low talonid; the crown is exodaenodont, with a single lobe of enamel labially. A short, but robust paracristid, the first record of this structure on a picrodontid p4, arises from high on the anterior face of the protoconid and curves on to the medial side of the cusp; no paraconid is developed. Posterolabially, a crest descends from the

apex of the protoconid to its base but does not continue on to the talonid; a postvallid crest has not previously been observed on p4 of Picrodus (e.g., Silcox, 2001). The metaconid is absent. The talonid supports a small, rounded posterior cusp, the hypoconulid, closely adjacent to the base of the protoconid. The hypoflexid is very shallow, but distinct, with the external wall of the talonid meeting the protoconid in a labial position; there is no cristid obliqua.

In comparison to p4 in UALVP 45659, a specimen of P. canpacius from Cochrane 2, p4 of UALVP 42394 is taller and larger overall, the protoconid is more compressed labiolingually, and the heel is lower; p4 of UALVP 45659 lacks a paracristid but displays a moderately developed postvallid crest, comparable to that in UALVP 42394.

Lower molars: m1: The m1 of P. calgariensis is known from two isolated teeth, UALVP 43295 and 45657, as well as from the dentary, UALVP 43294. Collectively, these teeth display the coronal features of m1 that have long been known in P. silberlingi (Szalay, 1968) and accepted as characteristic of picrodontids: The trigonid is relatively small and leans anteriorly, projecting over the talonid of p4; the trigonid cusps are tiny and poorly defined; the talonid is greatly expanded and especially elongated posteriorly; the crown is exodaenodont and the hypoflexid shallow; and the enamel of the talonid basin is marked by closely spaced, short crenulations (on the m1 of P. calgariensis, however, these ridges tend to be elongated and more or less transverse to the length of the talonid basin). In P. calgariensis, m1 displays a labial cingulid along the base of the trigonid anterior to the hypoflexid; this cingulid can be smooth or cuspidate (UALVP 43295) and additional cuspules can be developed labially along the base of the talonid (e.g., UALVP 45657), but no cingulid is present there.

The m1 of P. calgariensis closely resembles that of P. canpacius in size and proportions but differs as follows: The paraconid is lower on the trigonid; the trigonid angle is more obtuse, with the paraconid in a more anterior position; the paracristid is longer and is anteriorly directed through most of its length before turning lingually to meet the paraconid; the labial wall of the trigonid is straight or shallowly concave in anterior or posterior view, not inflated; the protoconid is taller relative to the metaconid (UALVP 45660); the cristid obliqua swings further labially along the widest parts of the talonid; the entoconid (Szalay and Delson, 1979, fig. 6f) is subconical in contrast to the

more elongate, ridge-like structure in P. canpacius; and the occlusal surface of the talonid is more strongly twisted, especially posteriorly, where it plunges more steeply posterolingually. Some m1s of P. calgariensis (e.g., UALVP 43294) show only a few crenulations on the occlusal surface of the talonid, while in others (e.g., UALVP 43295), these are numerous and broadly distributed, as in P. canpacius (although somewhat coarser and more elongate than in that species).

m2: The m2 of P. calgariensis is known from only UALVP 43294, the incomplete dentary from the Who Nose? locality. No picrodontid m2s are available from Cochrane 2 for comparison, so the m2s of P. silberlingi at hand and in the literature (McGrew and Patterson, 1962; Szalay, 1968; Williams, 1985) are used instead. In P. calgariensis, as in other species of Picrodus, m2 is smaller than m1 and less specialized; it differs from m2 of P. silberlingi as follows: The trigonid is longer relative to its width and narrower anteriorly; the paracristid is longer and descends more steeply; the paraconid arises from a more ventral position; the protoconid is taller relative to the paraconid and metaconid; the metaconid is reduced; the talonid is shorter and not as wide; the talonid basin is deeper; the hypoflexid is deeper and the cristid obliqua more lingually positioned; the labial cingulid is weaker; the posterolingual and posterolabial corner of the talonid each approximates a right angle in contrast to the more rounded talonid rim in P. silberlingi; and the enamel of the talonid basin is smooth except for a few wrinkles at the base of the hypoconulid, unlike the denser and more extensive crenulations in P. silberlingi. In sum, m2 of P. calgariensis is more gracile and less adapted for a crushing function than is m2 in P. silberlingi.

The homologies of the talonid cusps in Picrodus have long been uncertain. On m2 of P. silberlingi and the other species of Picrodus, there are two prominent cusps on the lingual rim of the talonid: Szalay (1968) equated these with the entoconid (more anterior) and hypoconulid, while Schwartz and Krishtalka (1977) and Williams (1985) identified them as a "twinned" entoconid. Silcox (2001) considered the homologies of the talonid cusps in picrodontids to be "questionable"; while this sentiment may hold true with respect to m1 (the most specialized of the picrodontids lower molars), UALVP 43284 permits a choice among these alternatives for m2 and m3. On m2 of this specimen, the posterior rim of the talonid is elevated about midway along its length and

displays a small, circular wear facet that penetrates the enamel; the wall of the talonid directly under this facet bulges posteriorly. This clearly is the remnant of the hypoconulid, reduced further and lost in m2 of more advanced species of Picrodus. Both of the lingual cusps are present on this tooth; they are subconical, robust, and the more posterior is somewhat the taller. The entoconid must be one of the two, with the other neomorphic. The hypoconid is anterolabial to the hypoconulid, separated from it by a shallow notch: it is worn, but was probably little elevated originally.

m3: The third lower molar of Picrodus calgariensis is unknown. From the size and spacing of its alveoli in UALVP 43294, m3 was located directly posterior to m2 and was smaller than m2, as in other species of Picrodus.

Etymology.—Calgariensis, after the City of Calgary, Alberta, the site of the type locality.

Holotype.—UALVP 45655, incomplete left maxilla with P1-4, M1-2. Who Nose? locality, Paskapoo Formation of Alberta, early Paleocene [middle Torrejonian, To2 (Scott, 2003), Protoselene opisthacus/Mixodectes pungens Interval Zone of Lofgren et al., 2004].

Other material examined.—UALVP 45656, incomplete maxilla with P4, M1-3; UALVP 43294, incomplete dentary with i1, p4, m1-2; UALVP 43295, 45657, m1.

Age and occurrence.—Middle Torrejonian (Protoselene opisthacus/Mixodectes pungens Interval Zone, To2, early Paleocene) of North America (Lofgren et al., 2004).

Discussion.—UW 17806, an isolated left M2 from UW locality V-82004, closely resembles that of P. calgariensis from Who Nose? and is referred here to that species. Like M2 of P. calgariensis from Who Nose?, UW 17806 is subrectangular in occlusal outline, has a prominent parastylar lobe, wide stylar shelf and robust mesostyle, broad notch between the paracone and metacone, strong postprotocrista separating the trigon and talon basins, and no crenulations of the enamel. This specimen had been previously identified by Hartman (1986, p. 38) as pertaining to P. silberlingi.

Although closely related to Picrodus canpacius and P. silberlingi, P. calgariensis is more primitive in virtually every dental character in which alternative states occur (as assessed by comparison with teeth of Purgatorius), a conclusion in agreement with the earlier age of the Who Nose? locality (To2) relative to Cochrane 2 (Ti1) (Youzwyshyn,

1988; Fox, 1990; Scott, 2003). P. calgariensis is coeval with P. silberlingi (middle Torrejonian), but the latter taxon has yet to be discovered in Canada.

PICRODUS CANPACIUS new species

Figures 7.16.13-7.16.23, 7.19.13-7.19.15; Table 7.12

Diagnosis.—Differs from P. calgariensis in having subovate P4 with smaller paracone and protocone that lean anteriorly relative to base of crown; differs from P. calgariensis and P. silberlingi in nearly confluent trigon and talon basins of M1-3, postprotocrista reduced or absent; differs from P. silberlingi in m3 having a more anteroposteriorly compressed trigonid and a U-shaped notch between the protoconid and metaconid; enamel crenulation dense and covering most of occlusal surfaces of the molars.

Description.—Upper dentition (Figs. 7.16.13-7.16.15): Upper premolars: P4: Among the teeth referred to P. canpacius is UALVP 11753, a P4 from Cochrane 2 identified as a right M3 of P. silberlingi by Krause (1978) in his pioneering work on plesiadapiforms from western Canada (and see Gingerich et al., 1983). Youzwyshyn's (1988) collection and description of UALVP 24918, a maxilla with P4-M1 referred by him to P. silberlingi showed that UALVP 11753 is a P4, a tooth that in species of Picrodus is easily distinguished from M3 once articulated dentitions are available. UALVP 11753 is from the left side not the right, and to identify its features correctly, needs to be rotated 90 degrees counterclockwise from Krause's (1978, fig. 9k) orientation of the tooth: his "anterior" side is labial, his "posterior" side is lingual, and his "metacone" is the protocone (Youzwyshyn, 1988). Upper teeth anterior to P4 in P. canpacius are unknown.

P4 of P. canpacius from Cochrane 2 is subovate, with its length and width nearly equal, resembling P4 of P. calgariensis in this regard but with a less "squarish" coronal outline than the tooth in the earlier species. Posteriorly, the crown expands into a broad surface that is shallowly concave and covered with irregularly crenulated enamel. A low postparacrista, lower than in P. calgariensis, borders this surface labially. In addition to the differences cited in the description of P. calgariensis above, P4 of P. canpacius has a

more robust ectocingulum, a lower paracone and protocone, which lean anteriorly, and a short preprotocrista, weaker than in P. calgariensis. Like P4 of P. silberlingi, P4 of P. canpacius is three-rooted: an anterolabial root is beneath the paracone, a posterolabial root is beneath the trigon basin, and a lingual root supports the lingual apex of the crown, posterior to the protocone. The spacing of the alveoli in YPM-PU 22860 suggests that P4 in P. silberlingi is larger and anteroposteriorly longer relative to its width than in P. canpacius. If P4 of P. canpacius is held manually with its posterior occlusal surface horizontal, a further difference from P4 of P. calgariensis is apparent: the strongly leaning paracone and protocone are paralleled by the orientation of the roots, which slant obliquely posteriorly; by contrast, paracone, protocone, and roots are vertical in P. calgariensis. But when P4 of P. canpacius is articulated in the maxilla (as in UALVP 24918), the paracone, protocone, and roots are vertically oriented, and the posterior biting surface slopes steeply posteriorly; in P. calgariensis (UALVP 45655, 45656), this surface is nearly horizontal. Hence, P4s of P. calgariensis and P. canpacius differ not only in size, shape, and cusp and crest development, but also in orientation in the jaw. The steeply sloping P4 in UALVP 24918 is not an artifact nor is it pathological, unique to this specimen: the angle at which the cusps and roots meet the body of the crown matches the angle of the cusps and roots in the isolated P4s from Cochrane 2 (UALVP 11753, 45663) and hence is an original feature in P. canpacius.

Upper molars: M1: Krause (1978) referred UALVP 11740, an M1 from Cochrane 2 (his "Cochrane Site 11"), to P. silberlingi, and Youzwyshyn (1988) added UALVP 24917 (M1) and 24918 (M1-2). Two more M1s, UALVP 45664 and 45667, collected from Cochrane 2 after Youzwyshyn's work was completed, are virtually identical to Krause's and Youzwyshyn's specimens and are here referred to P. canpacius. Together, these M1s most resemble M1 of P. silberlingi, but differ as follows: The enamel covering the trigon and talon basins is densely crenulated, lending a superficially beaded appearance to these surfaces (enamel crenulation is weaker in P. silberlingi); the trigon and talon basins occupy nearly the same plane (in P. silberlingi, the basins are usually more vertically displaced from one another); the postprotocrista is divided into two crests, one arising from the protocone apex but fading posterolingually, the other—labial

to the first—arising from the side of the protocone and extending to the metacone; and the talon basin is either wider, extends further labially, or both.

M2: M2 of P. canpacius from Cochrane 2 is documented by UALVP 45662 and 45665, collected after Youzwyshyn's (1988) study. Although the structure of these teeth most resembles M2 of P. silberlingi among the species of Picrodus recognized here, it differs in a number of important features: It is significantly smaller; only a trace of the postprotocrista remains so that the trigon and talon basins are fully confluent; and the enamel crenulations are finer and more densely developed.

M3: Youzwyshyn (1988) referred two M3s (UALVP 24916, 24922) to P. silberlingi, the first of the genus to be recognized [as noted above, UALVP 11753, identified as M3 of P. silberlingi by Krause (1978) is a P4 (Youzwyshyn, 1988)]. UALVP 22922 is damaged posterolingually, but UALVP 24916 is unbroken though somewhat worn. M3 is smaller than M2, subquadrate, slightly longer lingually than labially, with nearly parallel anterior and posterior sides, and wider anteriorly than posteriorly. Its labial side slants more steeply posterolingually than in M2 and its posterolingual corner forms a right angle. The parastylar lobe is weak, the stylar shelf narrow and absent altogether posteriorly, and the ectocingulum is low; the mesostyle is a faint swelling midway along the ectocingulum. The paracone and metacone are but the raised ends of the centrocrista; the paracone is taller than the metacone. A short, weak preparacrista runs anterolabially from the paracone to the edge of the crown. The centrocrista forms a shallow arc between the paracone and metacone: there is no V-shaped notch along its length. The preparaconular crista extends anterolabially to meet the paracingulum, which runs labially to the preparacrista. Paraconule, metaconule, and metaconular crests are absent. The protocone is low and lingual to the paracone; on UALVP 24922, a small cuspule represents the anterior cingulum, absent on UALVP 24916. The trigon and talon basins form a broad, shallow depression, bordered posterolingually by the postprotocone fold+posterior cingulum and covered by crenulated enamel; no postprotocrista or hypocone is evident.

M3 of Picrodus is otherwise known only in P. calgariensis (UALVP 45656). M3 of P. canpacius differs in its smaller size, weaker parastylar lobe and stylar shelf, reduced

paracone, confluent and broader trigon and talon basins, and stronger crenulation of the enamel.

Lower dentition (Figs. 7.16.16-7.16.23): i1-p3: Lower teeth anterior to p4 of P. canpacius are unknown from Cochrane 2, but UALVP 45659, a dentary fragment with p4-m1, retains the alveoli for i2, p2, and p3. Each of these teeth was single-rooted, as in P. calgariensis and P. silberlingi. The alveoli are not well preserved, but suggest that i2 was procumbent and that p2 may have been slightly smaller than i2 or p3. The alveoli are in a straight row and are evenly spaced.

Lower premolars: p4: The p4 of Picrodus canpacius is known only from UALVP 45659; it is simple and premolariform, with a tall protoconid, small talonid, and two roots. A faint paracristid is present; paraconid and metaconid are absent. A postvallid crest runs from near the protoconid apex to the talonid; a low hypoconulid arises about midway along the posterior edge of the talonid. A short cristid obliqua is present labially. In comparison to p4 in P. silberlingi, p4 of UALVP 45659 is smaller relative to m1, the protoconid is lower and more conical, the paracristid weaker, and the talonid shorter anteroposteriorly.

Lower molars: m1: Youzwyshyn (1988) had only an incomplete m1 of Picrodus from Cochrane 2 (UALVP 24921) available for study, referring it to P. silberlingi, but four additional specimens (UALVP 45658-45661) were collected after Youzwyshyn's work was completed. These show that m1 of P. canpacius most resembles that of P. silberlingi but differs as follows: The trigonid is more slender; the crown, especially the talonid, is lower; and the enamel crenulations are more dense and anteriorly more extensive, rising on to the base of the postvallid wall.

m2: The m2 of P. canpacius has yet to be discovered.

m3: The m3 of P. canpacius is known from a single, well-preserved tooth from Cochrane 2, UALVP 24919. It differs from m3 of P. silberlingi (YPM-PU 16577, the only m3 of this species at hand), as follows: The crown is shorter and narrower; the trigonid is anteroposteriorly shorter; the paracristid arises as a vertical ridge from the anterior face of the protoconid, turns lingually across the trigonid to the anterolabial side of the metaconid, not forming a near-horizontal shelf anterior to the protoconid and metaconid; there is no protocristid; the notch between the protoconid and metaconid is

broadly U-shaped, not V-shaped, and the trigonid and talonid basins are confluent; the talonid is subovate in occlusal outline; there is no hypoflexid; and the enamel covering the floor of the talonid basin is coarsely crenulated over its posterior two-thirds and smooth more anteriorly. As on m3 of P. silberlingi, the protoconid and metaconid are subconical cusps, with the metaconid the larger, but both are reduced in size in comparison to their counterparts in YPM-PU 16577. In both species, there is no paraconid, the twinned entoconid cusps are well developed, the hypoconid is at the posterolabial corner of the talonid, and there is no evidence of a hypoconulid.

Etymology.—Canpacius, from "Canadian Pacific," referring to the setting of the type locality, overlooking the main line of the Canadian Pacific Railroad near Cochrane, Alberta.

Holotype.—UALVP 24918, incomplete right maxilla with P4, M1. Cochrane 2 locality, Paskapoo Formation of Alberta, late Paleocene [earliest Tiffanian, Ti1 (Youzwyshyn, 1988; Fox, 1990; Scott et al., 2002), Plesiadapis praecursor/P. anceps Lineage Zone of Lofgren et al., 2004].

Other material examined.—From Cochrane 2: UALVP 11753, 45663, 45666, P4; UALVP 11740, 24917, 45664, 45667, M1; UALVP 45662, 45665, M2; UALVP 24916, 24922, M3; UALVP 45659, incomplete dentary with p4, m1; UALVP 45658, incomplete dentary with m1; UALVP 24921, 45660, 45661, m1; UALVP 24919, m3.

From Aaron's Locality: UALVP 45913, incomplete right dentary with p4, m1.

Age and occurrence.—Earliest Tiffanian (Plesiadapis praecursor/P. anceps Lineage Zone, Ti1, late Paleocene) to early Tiffanian (Plesiadapis anceps/P. rex Lineage Zone, Ti2, late Paleocene) of the Western Interior of North America.

Discussion.—Krause (1978) first documented a P. silberlingi-like species at Cochrane 2, based mostly on M1 (UALVP 11740), the most diagnostic upper tooth of the genus. UALVP collections made after Krause's study enabled Youzwyshyn (1988) to elaborate on the Cochrane species, especially in regards to P4, the first recognized tooth at this locus since discovery of picrodontids 80 years earlier (Douglass, 1908). The Cochrane 2 specimens of P. canpacius include those that Youzwyshyn (1988) and Fox (1990b) referred to P. silberlingi.

McGrew and Patterson (1962) referred UW 1780 (incomplete maxilla with M1-2, from the Saddle locality) and MCZ 8363 (incomplete maxilla with M1, from the Shotgun local fauna) to Picrodus cf. P. silberlingi; Szalay (1968) included them in his P. silberlingi. The teeth in both specimens are virtually identical to M1-2 of P. canpacius from Cochrane 2 and are here refered to this species; the teeth differ from comparable teeth of P. silberlingi in, for example, the less expanded metastylar area of M1, less separation of the trigon and talon basins, loss of the M2 postprotocrista, and better-developed enamel crenulations. Additional specimens of P. canpacius from the United States include USNM 309870, a right P4 from the Bangtail Locality (Ti1), Fort Union Formation, Montana, identified as an M3 of P. silberlingi by Gingerich et al. (1983) following Krause (1978): this tooth shows no significant differences from P4 of P. canpacius from Cochrane 2. USNM 309875, an incomplete left dentary containing i1-2, p3-4, m1-3 (Gingerich et al., 1983, p. 966, fig. 6), also from Bangtail, is referred to P. canpacius as well: it most resembles the Cochrane 2 specimens UALVP 45659 and 24919 in morphology of m1 and m3, respectively. However, the p4 on this specimen differs from that on UALVP 45659 in having a more robust talonid with two cusps.

Picrodus canpacius closely resembles P. silberlingi in comparable parts of the dentition, but is somewhat more advanced in modification of P4/p4 and in the greater specialization of the molars.

PICRODUS LEPIDUS new species

Figures 17.1-17.9, 19.7-19.9, 19.16-19.18, 20; Table 7.13

Diagnosis.—Differs from other species of Picrodus as follows: P4 teardrop-shaped in occlusal outline, longer than wide, two-rooted, protocone absent or a tiny cuspule; lower antemolar dentition crowded, p3 reduced, p4 having an inflated crown and single root; enamel crenulation tending to be finer and more extensive on the molars.

Description.—Upper dentition (Figs. 7.17.1-7.17.3): Upper premolars: P2 and P3: P2 and P3 of P. lepidus are unknown, but UALVP 40646 and 40650 (holotype), incomplete maxillae with P4, M1-2, preserve two alveoli anterior to P4 (no evidence is available concerning upper teeth anterior to these in P. lepidus). In UALVP 40646, each

alveolus holds a broken root, with the diameter of the anterior root being somewhat the larger; the relative sizes of the alveoli are the same in UALVP 40650. These alveoli probably housed a single-rooted P2 and P3, respectively: they are as distant from each other as the posterior alveolus is from the anterior alveolus of P4, and the roots in UALVP 40646 do not converge at the palatal surface as if in support of a common crown. If so, P3 in P. lepidus was reduced relative to P2 and P4, as is p3 relative to p2 and p4 (see later in this chapter). In P. calgariensis, the only other picrodontid in which upper teeth anterior to P4 are known, P3 is two-rooted, the posterior root is larger than the anterior root, especially transversely, and the gaps between roots of adjacent premolars are longer than those between roots of single teeth—a pattern that cannot be reconciled with that in UALVP 40646 or 40650.

P4: P4 of P. lepidus is preserved in UALVP 40646 and 40650. Its coronal anatomy is significantly different from the subrectangular P4 of P. calgariensis or subovate P4 of P. canpacius: in P. lepidus the crown is teardrop-shaped in occlusal view, narrow anteriorly and wide posteriorly, and longer than wide overall; it is larger relative to M1 than in the earlier species. Its labial side is nearly straight, while its posterolingual side forms a smooth, semicircular arc. The parastylar and metastylar lobes and stylar shelf are undeveloped; a short, weak ectocingulum is present labially. Anteriorly on UALVP 40646, a weak cingulum arises at the base of the paracone and joins with the ectocingulum anterolabially and the preprotocrista anterolingually. On UALVP 40650, this cingulum is faint and is limited to the lingual side of the paracone, not extending further anteriorly nor joining to the ectocingulum. The paracone is the only major cusp; it is anterolabially positioned, and is conical and erect, in contrast to P. canpacius, in which the P4 paracone leans anteriorly. The anterior side of the paracone is somewhat convex anteriorly, while its posterior side slopes gradually posteriorly into the posterolingual basin. There are no preparacrista, paraconule, or paraconular crests. The postparacrista is elongate, limits the occlusal basin labially, is faintly crenulated along its length, and extends to the posterolabial corner of the crown; no metacone, metaconule, or metaconular crests are developed. The occlusal basin is shallow, longer than wide, with smooth enamel, except posterolabially where the floor of the basin is weakly swollen and the enamel marked by one or two faint ridges. The protocone is undeveloped on UALVP

40650 but on UALVP 40646 is represented by a tiny cuspule, close to the base of the paracone; on UALVP 40650 there is only a slight elevation of the lingual ridge in this position. On UALVP 40646, a short, low preprotocrista extends labially from this lingual cuspule to the base of the paracone. There is no hypocone. The base of P4 fits tightly against the maxilla in both specimens, but breakage of the bone in UALVP 40646 reveals that P4 is two-rooted, with the posterior root expanded beneath the entire posterior edge of the crown; both roots are perpendicular to the plane of the crown, not slanting posteriorly as in P. canpacius.

P4 of P. calgariensis, P. silberlingi (e.g., YPM-PU 22860, alveoli), and P. canpacius is three-rooted, with the protocone in P. canpacius and P. calgariensis better developed than in P. lepidus. Alveoli indicate that P4 of Zanycteris paleocenus is two-rooted (e.g., Szalay and Delson, 1979, fig. 30), but the tooth itself is unknown.

Upper molars: M1: M1 of P. lepidus is known from UALVP 40643, 40646, and 40650, maxillae also containing M2. M1 of P. lepidus most resembles that of P. canpacius in size and occlusal anatomy, although differing in several details: As in P. canpacius, M1 of P. lepidus is substantially larger than P4, is low and broad, and varies somewhat in occlusal outline, from subrectangular (UALVP 40643) to subtriangular (UALVP 40650); the ectocingulum tends to be longer, lower, and weaker than in P. canpacius, and not as elevated anteriorly, with little development of a mesostyle, and can be irregularly crenulated (UALVP 40646) or smooth (UALVP 40650); the parastylar lobe, although small, is more anteriorly projecting than in P. canpacius, and the anterior cingulum is more robust; the metastylar lobe is shorter in P. lepidus, more rounded distally, and not as posteriorly oblique; anteriorly, M1 is shallowly notched to receive the posterior side of P4; this notch tends to be deeper than in P. canpacius. The protocone is the largest cusp on M1 and is positioned lingually opposite the paracone; consequently, most of the biting surface of the crown is posterior to a transverse line between the paracone and protocone, as in P. calgariensis, P. silberlingi, and P. canpacius. In P. lepidus, the talon basin of M1 seems slightly larger and less well separated from the trigon basin than in P. canpacius among the specimens at hand, but the differences here are small and might be only a function of the few specimens available for comparison. As in P. canpacius, the postprotocone fold turns horizontally and grades into the posterior

cingulum; the junction between the two is marked by the hypocone, a small cuspule in this species (e.g., UALVP 40650). As in P. canpacius, the posterior cingulum is short, extending only from the hypocone to the posterior side of the crown at the base of the metacone, where it joins with or comes near to the labial extremity of the postprotocrista. Anteriorly, the trigon basin of M1 is limited by the preprotocrista, which is straight and fades away lingual to the paracone. More lingually, near the apex of the protocone, this crest forms a cuspule subequal in size to the protocone apex and closely adjacent to it labially. This variant also occurs in P. calgariensis, P. silberlingi, and P. canpacius, but not at other molar loci nor in other picrodontids. In P. lepidus, the crenulated enamel on M1 is more extensive than in P. canpacius, extending from the centrocrista over the entire trigon and talon basins and even over the occlusal surfaces of the parastylar lobe and precingulum.

M2: M2 of P. lepidus is known from three maxillae that also contain M1, UALVP 40643, 40646, and 40650. It closely resembles M2 of P. canpacius, being nearly equal in size, but M2 of P. lepidus is longer anteroposteriorly relative to its width. In P. lepidus, the parastylar lobe is weaker, the stylar shelf narrower, the centrocrista longer, and the occlusal basin more expanded posteriorly; the postprotocrista is undeveloped, leaving the trigon and talon basins confluent with each other, as in P. canpacius. Crenulation of the enamel is similar in the two species and greater than on M2 of either P. silberlingi or P. calgariensis.

M3: M3 of P. lepidus is unknown, but its alveoli are preserved in UALVP 40650. The tooth was three-rooted and from the spacing of its roots was probably smaller than M2, as in other species of Picrodus. The diameter of the lingual alveolus is greater than those of the labial alveoli, indicating that the lingual root was relatively large. The lingual root of M3 in P. canpacius is enlarged and supports much of the lingual part of the occlusal basin, which is expanded posterolingually; perhaps similar proportions characterize M3 in P. lepidus.

Dentary and lower dentition (Figs. 7.17.4-7.17.12): Dentary: The dentary of P. lepidus is known from four specimens (UALVP 40647, 40648, 40649, 45914); in none is it complete. The i1 is not preserved, but parts of its alveolus remain in UALVP 40647 and 40649. Three premolars are retained in UALVP 40647, while m1-3 are present in

UALVP 40647 and 40649, and m1 in UALVP 45914. Most of the dentary posterior to the tooth row is preserved in UALVP 40647 and 40649, including the condylar and angular processes. The horizontal ramus in P. lepidus and P. calgariensis is closely similar in parts that can be compared, although UALVP 40647 displays two and 40649, three, mental foramina below p2-m1; in UALVP 43294 (P. calgariensis), there is but one mental foramen. The dentary anterior to m1 in UALVP 40647 and 40649 is shorter than in P. calgariensis and, as described below, the teeth between i1 and m1 are small and crowded together, a pattern not known in other species of Picrodus. The dentary is well preserved posteriorly in UALVP 40647 and 40649; only the dorsalmost parts of the coronoid process are missing. This process is vertically deep and anteroposteriorly long, with broad surfaces for insertion of the mandibular adductors. The masseteric fossa occupies the height of the coronoid process to the ventral border of the dentary and on to the horizontal ramus under m3. The fossa is limited anteriorly by a raised ridge that strengthens ventrally. Medially, the temporalis fossa is nearly as deep as the masseteric fossa: a rounded crest defines it anteriorly and a broad, low ridge along the base of the coronoid process limits it ventrally. A large mandibular foramen opens beneath this ridge directly above the base of the angular process. In UALVP 40648, a deep channel for the inferior alveolar nerve and vessels as they passed to the mandibular foramen extends posterodorsally to the broken edge of the bone. The condylar process is robust in UALVP 40647 and 40649, and as in P. silberlingi (Szalay, 1968), is well above the tooth row. The process tapers posteriorly: its dorsal border is horizontal, while its ventral border ascends posterodorsally. As in P. silberlingi (Szalay, 1968), the condyle is small, subovate in outline, wider medially than laterally, and only slightly wider than long; its articulating surface is gently convex anteroposteriorly and transversely, and faces posterodorsally. The slender angular process extends posteroventrally at an angle of about 150-degrees from the long axis of the dentary. In UALVP 40649, the process probably retains its "in-life" proportions, bending weakly mediad along its length, but it is not inflected. A strong ridge divides the medial side of the process into upper and lower surfaces for the insertion of the internal pterygoid muscle above the ridge and external masseter below. The end of the angular process is somewhat hooked dorsally, as in P. silberlingi (Szalay, 1968).

i1: The antemolar alveoli preserved in UALVP 40647 and 40649 imply that P. lepidus retained i1-2, p2-4, as in P. calgariensis. As noted above, i1 is not preserved in these specimens, but from its alveolus was undoubtedly enlarged and procumbent as in P. calgariensis. In UALVP 45914, an incomplete dentary containing m1, the lateral side of the dentary has been broken away, exposing the alveolus for i1 along much of its length: it is inclined obliquely anteriorly and terminates posteriorly beneath the anterior root of m1.

i2: The i2 was lost before burial in both UALVP 40647 and 40649, but was housed in a small alveolus closely adjacent to the alveolus for i1. The i2 alveolus is positioned posterolabial to i1, not directly posterior to it as in P. calgariensis; i2 in USNM 309875 (referred above to P. canpacius) displays the same posterolabial position in respect to i1.

Lower premolars: p2: In UALVP 40649, a short diastema intervenes between the alveoli for i2 and p2. In UALVP 40647, p2 is in place and has a single stout root that, owing to damage to the lateral side of the dentary, is exposed through much of its length. In UALVP 45914, the alveolus for p2 is exposed laterally: it is short and curves posteriorly as it nears the alveolus of i1 below. The crown of p2 (in UALVP 40647) is small and premolariform. The protoconid juts strongly anteriorly: its anterior face is smoothly rounded and its apex blunt; there is no paraconid, paracristid, or metaconid. A small talonid extends posteriorly, meeting the anteroventral face of p3. A posterior crest arises posteriorly from the protoconid apex, curves gently labially near the base of the cusp, and continues on to the talonid, along the junction between its dorsal and labial surfaces. There are no talonid cusps.

p3: In UALVP 40647, p3 is much smaller than p2, "squeezed" between p2 and the still larger p4. It has one root and a simple, premolariform crown, with a blunt protoconid and small talonid; the protoconid overlaps the talonid of p2. Paracristid, paraconid, and metaconid are absent. A posterior crest, like that on p2, runs from the tip of the protoconid to the talonid, ending in a small cuspule. The crown of p3 is obliquely rotated, from anterolabial to posterolingual, apparently an "in-life" orientation. In UALVP 45914, the alveolus for p3, which is exposed laterally, is narrow, straight, and

short, about half the length of the alveolus for p4, and the alveolus for p2 curves posteriorly beneath it.

p4: The p4 in UALVP 40647 has been damaged during burial, but its major features are retained. Unlike p4 of P. calgariensis, P. silberlingi, and P. canpacius, p4 of P. lepidus is single-rooted: the root is comparatively large and faintly grooved on its labial side, as if fused from the two roots of more primitive species of Picrodus. The antemolar alveoli in UALVP 40649 are incomplete, but show the same relative sizes as in UALVP 40659 and that p4 had a single large root. In UALVP 45914, the inner wall of the large p4 alveolus is exposed and is subdivided by a low dorsoventral ridge; this ridge probably fitted into a shallow groove on the lingual side of the root. In this specimen, the p4 alveolus ends ventrally just above the posterior limit of the alveolus for i1. In UALVP 40647, the crown of p4 has been somewhat crushed and its parts displaced from their original position, but it appears to have been premolariform, with a blunt, somewhat procumbent protoconid and well-developed talonid; the walls of both parts of the tooth are swollen. There is no paracristid, talonid basin, or talonid cusps. The protoconid overhangs p3 posterolabially and the talonid abutted against the base of the m1 trigonid. Although p4 in P. lepidus is larger than p2 or, especially, p3, it is significantly smaller with a simpler crown than p4 of P. calgariensis, P. silberlingi, or P. canpacius.

Lower molars: m1: The m1 of P. lepidus is known from UALVP 40647 and 40649; in UALVP 40647, the crown is deeply worn. The m1 of P. lepidus is closely similar to that of P. canpacius but differs in being slightly smaller and more gracile, the paraconid is in a more posterior position such that the trigonid cusps form a more nearly equilateral triangle, and the enamel crenulations are finer, denser, and extend further dorsally on the postvallid wall.

m2: The m2 is known from four specimens, UALVP 40645, 40647, 40648, and 40649. The crown is subovate in occlusal outline, with the trigonid substantially narrower than the talonid. When unworn, the enamel covering the talonid basin is densely crenulated. As wear continued, this texture was erased from anterior to posterior, and in deeply worn teeth (e.g., UALVP 40647), it has been removed altogether, leaving the floor of the basin smooth. In comparison to m2 of P. silberlingi (m2 of P. canpacius from Cochrane 2 has yet to be discovered), m2 of P. lepidus is lower crowned, subequal

in length but with a narrower and slightly more procumbent trigonid; the paraconid is more posterior and the trigonid angle less open; the talonid is shorter, wider relative to its length, and its rim more rounded posteriorly; the coronal walls are less swollen, especially on the trigonid; the cristid obliqua is more labial in position; the hypoflexid is shallower; the labial cingulid is weaker or absent; and the enamel crenulations within the talonid basin are finer, denser, and extend further anteriorly.

m3: The m3 of P. lepidus is present in UALVP 40647 (in which it is deeply worn) and UALVP 40649. The tooth is subrectangular, with a compressed trigonid and an elongate talonid. The paraconid is absent; a low transverse crest curves anteriorly between the protoconid and metaconid, which are low and subequal in height. The protoconid-metaconid notch is broadly open, forming a shallow U-shaped valley, and there is no raised protocristid; the enamel of the valley surface is moderately ridged and grooved. The talonid is slightly wider than the trigonid and has nearly parallel sides. The cristid obliqua extends far anteriorly, to the apex of the protoconid; there is no hypoflexid. The enamel of the talonid basin forms closely spaced, short ridges and grooves. The m3 of P. lepidus most resembles m3 of P. canpacius, except that in P. lepidus the trigonid is wider and more procumbent, the protoconid and metaconid are lower and less well defined, the notch between these cusps is broader and shallower, and the talonid is slightly longer. The m3 of P. silberlingi (YPM-PU 16577) differs from that of P. lepidus in retaining a small paraconid; taller, more erect, and less compressed trigonid; taller and more robust protoconid and metaconid; low protocristid; more lingual cristid obliqua in meeting the postvallid; squarish corners of the talonid; and nearly smooth enamel in the talonid basin.

Etymology.—Lepidus, Latin, pleasant, agreeable, the reaction on realizing that the specimens described here document a new species of Picrodus.

Holotype.—UALVP 40650, incomplete maxilla with P4, M1-2. DW-2 locality; Paskapoo Formation of Alberta, late Paleocene [early middle Tiffanian, Ti3 (Fox, 1990), Plesiadapis rex/P. churchilli Lineage Zone of Lofgren et al., 2004].

Other material examined.—From DW-2: UALVP 40646, incomplete maxilla with P4, M1-2; UALVP 40643, incomplete maxilla with M1-2; UALVP 40642, M1; UALVP 40647, incomplete right dentary with p2-4, m1-3, and alveoli for i1-2; UALVP 40649,

incomplete right dentary with m1-3 and alveoli for i1-2, p2-4; UALVP 45914, incomplete dentary with m1 and alveoli for i1, p2-4; UALVP 40648, incomplete dentary with m2; UALVP 40645, m2.

Age and occurrence.—Type locality only.

Discussion.—Citation of a picrodontid occurring at DW-2 was given by Fox (1990b) as "Zanycteris paleocena" while Silcox (2001) identified UALVP 40650 and 40647 from DW-2 as P. silberlingi. The specimens concerned pertain to P. lepidus, as described above. P. lepidus is the most derived of the new species from Alberta, showing reduction in the premolar dentition, shorter jaws, and further specialization of the molars for a grinding or "pulping" function. It could have descended from a P. canpacius-like ancestor.

PICRODUS sp.

Figures 7.17.10-7.17.12

Material examined.—From Joffre Bridge Roadcut lower level: UALVP 40644, incomplete right dentary with m1 and alveoli for m2-3.

Discussion.—UALVP 40644 is an incomplete right dentary, with m1 and alveoli for m2-3; the coronoid and condylar processes are missing, but the angular process is complete. The locality is of early middle Tiffanian (Ti3) age (Fox, 1990b), correlative with DW-2. Although UALVP 40644 differs significantly from comparable specimens of Picrodus lepidus at DW-2, implying that it is from a different species, its formal naming is deferred pending the discovery of more and better-preserved specimens from both localities.

The m1 (L=2.1, TaW=1.0) on UALVP 40644 differs importantly from m1 of P. lepidus in the anterior position of the paraconid and straightness of the paracristid, resembling m1 of P. silberlingi (in P. lepidus the paraconid is more posterior, the paracristid short, and the trigonid cusps form an equilateral triangle). UALVP 40644 seems not to pertain to P. silberlingi, however: as in P. lepidus, the enamel ridges in the talonid basin are finer, denser, and extend over the entire floor of the basin and onto the postvallid wall, a more advanced pattern than in P. silberlingi. Other differences are seen

between UALVP 40644 and the lower jaw/dentition of P lepidus. As noted above, a unique feature of P. lepidus is p4 supported by a single large root. UALVP 40644 is broken anterior to m1, but the posterior wall of the alveolus that housed a root of p4 is exposed down this broken edge. Its dimensions suggest that the diameter of the alveolus when complete was substantially less than for the single root of p4 in P. lepidus, as in species having a two-rooted p4; hence, p4 in UALVP 40644 may have been two-rooted. Additionally, the dentary of UALVP 40644 is shallower, the tooth row from m1 to m3 longer, and the angular process more slender than in P. lepidus. This process displays the prominent medial crest separating the pterygoid fossa from a more ventral surface, for insertion of the external masseter.

7.3 Conclusions

Dental Evolution in Picrodus

The demonstration that Picrodus displays a modest species diversity permits reconstruction of dental trends within the genus. The species that document these trends, P. calgariensis, P. silberlingi, P. canpacius, and P. lepidus, appear to have been the products of successive origins in North America during the first half of the Paleocene.

Although P. calgariensis is the most primitive known species of Picrodus, it already displays the diagnostic pattern of the Picrodus dentition. No intermediates in regards this pattern are known between P. calgariensis and other genera, whether Zanycteris, Draconodus, or something else. Plainly, the adaptive shift from dentally less specialized ancestors that is manifest in the peculiar morphologies of M1 and m1, especially in the expansion of their occlusal surfaces to low, broad crushing or "pulping" platforms, had already taken place by the advent of P. calgariensis. Only later do enamel crenulations extend across these surfaces (as in P. canpacius and P. lepidus), but as a refinement of M1/m1 morphology, not as an initial part of it.

Picrodus calgariensis also provides unique insight into evolution of the anterior upper dentition of Picrodus, as shown by UALVP 45655, the holotype. If the homologies proposed here are correct, the upper canine is greatly reduced yet P1 is retained in a

species that had already evolved the highly specialized M1 and m1 that are diagnostic of the genus. By contrast Zanycteris has an enlarged tooth in the upper canine position (the more primitive state), but lacks P1, its place taken by a diastema between the canine and P2; there is no diastema between the upper canine and P4 in P. calgariensis. P1 was lost in most plesiadapiforms known from adequately preserved specimens, being retained other than in picrodontids only in the primitive plesiadapoid Chronolestes Beard and Wang, 1995 (and see Silcox, 2001) and primitive carpolestids (Fox, 1994). The fate of the upper canine and P1 in Picrodus more derived than P. calgariensis is presently uncertain, owing to lack of specimens in which the anterior upper dentition is preserved.

In P. calgariensis, P2 and P3 are small, two-rooted premolariform teeth. The history of these teeth in Picrodus thereafter is mostly unknown, but it is concluded here that P2-3 were retained in P. lepidus, the most advanced of the well-known species of the genus. Two specimens from DW-2, UALVP 40646 and 40650, preserve alveoli anterior to P4, and from their size and spacing, these housed single-rooted P2 and P3. This suggests a reduction in the length of the upper jaw during evolution leading to P. lepidus, corresponding to the reduction in the length of the dentary and the lower antemolar tooth row.

This study shows that evolution of the upper dentition in Picrodus followed a peculiar pattern, with M1 remaining relatively stable in size and morphology while greater change affected P4 and M2-3. P4 evolved from a subrectangular three-rooted tooth in P. calgariensis to a subovate (in P. canpacius) and then tear drop-shaped tooth (in P. lepidus), longer than wide, with reduction and loss of the protocone and loss of the lingual root. M1 of P. calgariensis already has the distinctive features of the tooth present in all known species of Picrodus: the coronal outline is asymmetrically triangular and the metastylar area expanded, the parastylar area suppressed, the stylar shelf shortened anteriorly, the ectocingulum elevated and swollen, the paracone and metacone reduced, the centrocrista elongated, with a short postparacrista and long premetacrista, and the conules are reduced or lost. During evolution of Picrodus thereafter, the paracone and metacone become lower still, the centrocrista is longer, lower, but more nearly equal in height along its length (losing the notch between the postparacrista and premetacrista), the precingulum is longer and wider, the occlusal surfaces of the trigon and talon basin

increase in area, occupy the same level, and become confluent; and a weak postprotocrista divides to form two discontinuous ridges. M2 and M3 are narrower relative to their lengths, the parastylar lobe and stylar shelf are reduced, the centrocrista more continuous, the postprotocrista suppressed, and the trigon and talonid basins become confluent and expand posterolingually. Perhaps change in molar structure reflects subtle changes in food habits to softer, more easily masticated foods, but with no significant shift in other niche requirements as might be reflected in changing tooth and hence body size.

The lower dentition of Picrodus is somewhat better known than the upper, especially anteriorly: the enlarged lower incisor, i1, has been identified in one specimen of P. calgariensis, UALVP 43294. In subsequent species of Picrodus, this tooth increases in size, becomes straighter, with longer and higher dorsal and ventromedial crests (e.g., YPM-PU 17630, P. silberlingi), and a basal margoconid (e.g., MCZ 20409, Picrodus sp.), convergent on the margoconid on i1 of other plesiadapiforms. Unexpectedly, the occlusal surface of i1 in P. calgariensis has a strong medial orientation, a microsyopid feature (Silcox, 2001).

In UALVP 43294, the dentary of P. calgariensis, three alveoli open between i1 and p4; these housed single-rooted i2, p2, and p3 followed by a two-rooted p4, the primitive pattern of the antemolar lower dentition in Picrodus. However, these loci appear to have been retained during evolution to even P. lepidus, but in that species p4 is single-rooted, p3 very tiny, "squeezed" between p2 and p4, and the dentary anterior to m1 somewhat shortened accordingly.

In the evolution of Picrodus, m1, like M1, remained relatively stable, with differences expressed mostly in minor proportions (e.g., inflation of the trigonid walls), position of the paraconid, and in increased crenulation of the enamel. Greater change affected m2 and m3, with lowering, greater anteroposterior compression, and stronger procumbency of the trigonid, reduction and loss of the paraconid, expansion of the talonid, and expanded crenulation of the enamel lining the talonid basin. Overall, molar evolution within Picrodus saw a loss of puncturing and vertical slicing capacity and greater adaptation for crushing or "pulping" of food items in teeth showing little change in coronal size.

The Relationships of Picrodontidae

The relationships of picrodontids were long a matter of uncertainty, with early workers allying these peculiar mammals with marsupials (Douglass, 1908), bats (Matthew, 1917), insectivorans (Simpson, 1937; McGrew and Patterson, 1962), or dermopterans (Romer, 1966). Szalay's (1968) study, the first comprehensive review of picrodontid anatomy and relationships, concluded that picrodontids are primates, within what are now dubbed plesiadapiforms (Simons, 1972); the postprotocone fold on the upper molars, seen even in Draconodus (Tomida, 1982) appears to be decisive evidence in this regard.

By contrast, the position of picrodontids within plesiadapiforms has not been easily resolved and at present no consensus concerning this important issue has emerged. Whereas Szalay (1968, p. 50 fn.) considered picrodontids to be descendants from primitive paromomyids, Schwartz and Krishtalka (1977, fig. 8) identified the dentally specialized Phenacolemur Matthew, 1915 as the picrodontid sister-group. Both Tomida (1994) and Van Valen (1994, fig. 1) suggested direct descent of picrodontids from Purgatorius, but because of their strongly developed postprotocone fold, Silcox (2001) proposed her paraphyletic "Palaechthonidae" as containing the picrodontid ancestor (although as discussed by Silcox, 2001, the probable paraphyly of "Palaechthonidae" presents difficulties when attempting to assess the meaning of this statement). The presence and development of the postprotocone fold has figured prominently in assessing both plesiadapiform/euprimate relationships (e.g., Szalay et al., 1987; Beard, 1993a) and plesiadapiform interrelationships (e.g., Silcox, 2001). A poorly developed postprotocone fold, one in which the connection between the protocone and the posterior cingulum is discontinuous or weak, occurs on M1 and M2 in basal plesiadapiforms such as Purgatorius and Pandemonium Van Valen, 1994; a stronger developed postprotocone fold, one in which the crest connecting the protocone and posterior cingulum is complete and generally well developed, is present on M1-2 in paromomyoids (sensu Silcox, 2001 and including "palaechthonids", paromomyids, and picrodontids) and plesiadapoids, although the strength of the fold increases during the evolution of each of these groups.

While the upper molars of picrodontids have a well-developed postprotocone fold, the purported special resemblance in this feature to "palaechthonids" (see Silcox, 2001) is only with advanced species of the latter [e.g., Palaechthon alticuspis (see Szalay and Delson, 1979, fig. 14)], and a significant morphological "gap" between the unusually divergent picrodontid dentition and that of all paromomyoids remains. As such, the resemblance between picrodontids and "palaechthonids" vis-à-vis a strong postprotocone fold can have little significance unless accompanied by more distinctive picrodontid-like features—but these features have not been found in "palaechthonids" nor in any other primitive plesiadapiform that is presently known: None show a tendency to reduce P4/p4 to become significantly smaller than M1/m1; none show a tendency to enlarge M1/m1 while decreasing M2/m2 and M3/m3 (instead, M2/m2 are the largest molars in all of the candidate groups); none show suppression of the hypoconulid on m3 (instead, this cusp is characteristically enlarged in plesiadapiforms, with m3 usually the longest of the lower molars); and none show decrease in coronal height of the molars or modification of the molar cusps and crests towards picrodontid-like patterns. Moreover, a strong postprotocone fold is also present on upper molars of plesiadapoids (including plesiadapids, carpolestids, and saxonellids), proportions believed to have evolved independently of those in paromomyoids, and further suggesting that the evolutionary lability of the postprotocone fold and its development may be great. Classifications (and hence implied relationships to one another) of the candidate ancestral groups differ widely (compare, e.g., classifications of plesiadapiforms by Gunnell, 1989, Van Valen, 1994, and Silcox, 2001), a further indication that the fossil evidence necessary to illuminate picrodontid relationships is not dense enough to resolve the questions that it raises, no matter the methodology of systematic analysis employed.

When picrodontids first appear, some of their unusual dental specializations are already evident: for example, the record of Draconodus, although sparse, is good enough to show that M2 is substantially smaller than M1, implying that the picrodontid gradient of decreasing molar size from M1/m1 to M3/m3 was already established by early Torrejonian time. This gradient is not found in other plesiadapiforms and for it to have evolved prior to Draconodus implies that picrodontids had a significant earlier history, extending deep into the Puercan (Szalay, 1968 had a similar opinion, before the discovery

of Draconodus). The Puercan ancestors of picrodontids were probably plesiadapiforms of generalized "purgatoriid" dental grade (whether or not they were phyletically "purgatoriids"), with molars that differed little in size from M1/m1 to M3/m3 but that displayed a postprotocone fold. The interpretation of the upper post-incisor dental formula of Picrodus calgariensis presented here, with retention of the canine and four premolars, is independent of, yet agrees with, this conclusion. By contrast, it is difficult to envisage a picrodontid ancestry from plesiadapiforms that had already evolved m3 with an enlarged or lobate hypoconulid (as in the paromomyids and "palaechthonids" of Silcox, 2001), which was then reduced and lost prior to the origin of Draconodus. Anatomical and temporal constraints seem to require that picrodontids were among the first plesiadapiforms to arise during the Puercan from an ancestral stock that had an m3 of generalized proportions and that had retained the upper canine and P1.

7.4 Literature Cited

ANDREWS, P. 1988. A phylogenetic analysis of the primates, pp. 143-175. In M J. BENTON (ed.), The Phylogeny and Classification of the Tetrapods, Vol. 2: Mammals. Systematics Association Special Volume 35B, Clarendon Press, Oxford.

BEARD, K. C. 1989. Postcranial Anatomy, Locomotor Adaptations, and Paleoecology of Early Cenozoic Plesiadapidae, Paromomyidae, and Micromomyidae (Eutheria, Dermoptera). Unpublished Ph. D. Dissertation, The Johns Hopkins University, 677 pp.

BEARD, K. C. 1990. Gliding behavior and paleoecology of the alleged primate family Paromomyidae (Mammalia, Dermoptera). Nature, 345: 340-341.

BEARD, K. C. 1993a. Phylogenetic systematics of the Primatomorpha, with special reference to Dermoptera, pp. 129-150. In F. S. SZALAY, M. J. NOVACEK, and M. C. MCKENNA (eds.), Mammal Phylogeny: placentals. Springer-Verlag, New York.

BEARD, K. C. 1993b. Origin and evolution of gliding in Early Cenozoic Dermoptera (Mammalia, Primatomorpha), pp. 63-90. In R. D. E. MACPHEE (ed.), Primates and their Relatives in Phylogenetic Perspective. New York: Plenum Press.

BEARD, K. C., and J. WANG. 1995. The first Asian plesiadapoids (Mammalia: Primatomorpha). Annals of Carnegie Museum, 64:1-33.

BLOCH, J. I. 2001. Mammalian paleontology of freshwater limestones from the Paleocene-Eocene of the Clarks Fork Basin, Wyoming. Unpublished Ph. D. dissertation, The University of Michigan, Ann Arbor, 358 pp.

BLOCH, J. I., and D. M. BOYER. 2002. Grasping primate origins. Science, 298:1606-1610.

BLOCH, J. I., M. T. SILCOX, and E. J. SARGIS. 2002. Origin and relationships of Archonta (Mammalia, Eutheria); re-evaluation of Eudermoptera and Primatomorpha. Journal of Vertebrate Paleontology, 22, supplement to no. 3:37A.

BLOCH, J. I., and D. M. BOYER. 2003. Response to comment on grasping primate origins. Science, 300: 741c.

BLOCH, J. I., D. C. FISHER, K. D. ROSE, and P. D. GINGERICH. 2001. Stratocladistic analysis of Paleocene Carpolestidae (Mammalia, Plesiadapiformes) with description of a new late Tiffanian genus. Journal of Vertebrate Paleontology, 21:119-131.

BLOCH, J. I., M. T. SILCOX, D. M. BOYER, and E. J. SARGIS. 2007. New Paleocene skeletons and the relationship of plesiadapiforms to crown-clade primates. Proceedings of the National Academy of Sciences, 104:1159-1164.

BOWN, T. M., and K. D. ROSE. 1976. New early Tertiary primates and a reappraisal of some Plesiadapiformes. Folia Primatologica, 26:109-138.

CARTMILL, M. 1972. Arboreal adaptations and the origin of the order primates, pp. 97-122. In R. H. TUTTLE (ed.), The Functional and Evolutionary Biology of Primates. Aldine Press, Chicago.

CARTMILL, M. 1974. Rethinking primate origins. Science, 184:436-443.

CLEMENS, W.A. 2004. Purgatorius (Plesiadapiforms, Primates?, Mammalia), a Paleocene immigrant into northeastern Montana: stratigraphic occurrences and incisor proportions, pp. 3-13. In M. R. DAWSON and J. A. LILLEGRAVEN (eds.), Fanfare

for an Uncommon Paleontologist: papers in honor of Malcolm C. McKenna. Bulletin of the Carnegie Museum of Natural History, 36.

DORR, J. A. 1952. Early Cenozoic stratigraphy and vertebrate paleontology of the Hoback Basin, Wyoming. Bulletin of the Geological Society of America 63, 59-94.

DOUGLASS, E. 1908. Vertebrate fossils from the Fort Union beds. Annals of Carnegie Museum, 5:11-26.

FOX, R. C. 1984a. The dentition and relationships of the Paleocene primate Micromomys Szalay, with a description of a new species. Canadian Journal of Earth Sciences, 21:1262-1267.

FOX, R. C. 1984b. A new species of the Paleocene primate Elphidotarsius Gidley: its stratigraphic position and evolution. Canadian Journal of Earth Sciences, 21:1268-1277.

FOX, R. C. 1984c. First North American record of the Paleocene primate Saxonella. Journal of Paleontology, 58:892-895.

FOX, R. C. 1990a. Pronothodectes gaoi n. sp., from the late Paleocene of Alberta, Canada, and the early evolution of the Plesiadapidae (Mammalia, Primates). Journal of Paleontology, 64:637-647.

FOX, R. C. 1990b. The succession of Paleocene mammals in western Canada, pp. 51-70. In T. M. BOWN and K. D. ROSE (eds.), Dawn of the Age of Mammals in the Northern Part of the Rocky Mountain Interior, North America. Geological Society of America Special Paper, 243.

FOX, R. C. 1991a. Saxonella (Plesiadapiformes: ?Primates) in North America: S. naylori, sp. nov., from the late Paleocene of Alberta, Canada. Journal of Vertebrate Paleontology, 11:334-349.

FOX, R. C. 1991b. Systematic Position of Pronothodectes gaoi Fox from the Paleocene of Alberta: Reply. Journal of Paleontology, 65:700-701.

FOX, R. C. 1994. The primitive dental formula of the Carpolestidae (Plesiadapiformes, Mammalia) and its phylogenetic implications. Journal of Vertebrate Paleontology, 13 (for 1993):516-524.

FOX, R. C. 1997. Late Cretaceous and Paleocene mammals, Cypress Hills region, Saskatchewan, and mammalian evolution across the Cretaceous-Tertiary boundary, pp. 70-85. In L. MCKENZIE-MCANALLY (ed.), Upper Cretaceous and Tertiary stratigraphy and paleontology of southern Saskatchewan. Canadian Paleontology Conference Field Trip Guidebook, 6.

FOX, R. C. 2002. The dentition and relationships of Carpodaptes cygneus (Russell) (Carpolestidae, Plesiadapiformes, Mammalia), from the late Paleocene of Alberta, Canada. Journal of Paleontology, 76:864-881.

FU, J.-F., J.-W. WANG, and Y.-S. TONG. 2002. The new discovery of the Plesiadapiformes from the early Eocene of Wutu Basin, Shandong Province. Vertebrata PalAsiatica, 40: 219-227.

GAZIN, C. L. 1971. Paleocene primates from the Shotgun Member of the Fort Union Formation in the Wind River Basin, Wyoming. Proceedings of the Biological Society of Washington, 84:13-38.

GIDLEY, J. W. 1923. Paleocene primates of the Fort Union, with discussion of relationships of Eocene primates. Proceedings of the U. S. National Museum, 63:1-38.

GILL, T. 1872. Arrangement of the families of mammals with analytical tables. Smithsonian Miscellaneous Collections, 11:1-98.

GINGERICH, P. D. 1975. New North American Plesiadapidae (Mammalia, Primates) and a biostratigraphic zonation of the middle and upper Paleocene. Contributions from the Museum of Paleontology, The University of Michigan, 24:135–148.

GINGERICH, P. D. 1976. Cranial anatomy and evolution of early Tertiary Plesiadapidae (Mammalia, Primates). Museum of Paleontology, The University of Michigan, Papers on Paleontology, 15:1-140.

GINGERICH, P. D. 1990. Mammalian order Proprimates—response to Beard. Journal of Human Evolution, 19:821-822.

GINGERICH, P. D. 1991. Systematic Position of Pronothodectes gaoi Fox from the Paleocene of Alberta. Journal of Paleontology, 65:699.

GINGERICH, P. D., P. HOUDE, and D. W. KRAUSE. 1983. A new earliest Tiffanian (late Paleocene) mammalian fauna from the Bangtail Plateau, western Crazy Mountain Basin, Montana. Journal of Paleontology, 57:957-970.

GINGERICH, P. D., D. DASHZEVEG, and D. E. RUSSELL. 1991. Dentition and systematic relationships of Altanius orlovi (Mammalia, Primates) from the early Eocene of Mongolia. Geobios, 24:637-646.

GREGORY, W. K. 1910. The orders of mammals. Bulletin of the American Museum of Natural History, 27:1-254.

GUNNELL, G. F. 1989. Evolutionary history of Microsyopoidea (Mammalia, ?Primates) and the relationship between Plesiadapiformes and Primates. University of Michigan Papers on Paleontology, 27:1-157.

HARTMAN, J. E. 1986. Paleontology and biostratigraphy of lower part of Polecat Bench Formation, southern Bighorn Basin, Wyoming. Contributions to Geology, University of Wyoming, 24:11-63.

HOFFSTETTER, R. 1977. Phylogénie des primates. Bulletins et Mémoires de la Société d'Anthropologie de Paris, t. 4, serie XIII:327-346.

HOLTZMAN, R. C. 1978. Late Paleocene mammals of the Tongue River Formation, western North Dakota. Report of Investigation of the North Dakota Geological Survey, 65: 1-88.

HOOKER, J. J., D. E. RUSSELL, and A. PHELIZON. 1999. A new family of Plesiadapiformes (Mammalia) from the Old World lower Paleogene. Palaeontology, 42: 377-407.

JOHNSTON, P. A. 1980. First record of Mesozoic mammals from Saskatchewan. Canadian Journal of Earth Sciences, 17:512-519.

JOHNSTON, P. A., and R. C. FOX. 1984. Paleocene and Late Cretaceous mammals from Saskatchewan, Canada. Palaeontographica Abteilung A, 186:163-222.

KAY, R. F., R. W. THORINGTON, and P. HOUDE. 1990. Eocene plesiadapiform shows affinities with flying lemurs not primates. Nature, 345: 342-344.

KAY, R. F., J. G. M. THEWISSEN, and A. D. YODER. 1992. Cranial anatomy of Ignacius graybullianus and the affinities of the Plesiadapiformes. American Journal of Physical Anthropology, 89: 477-498.

KIRK, E. C., M. CARTMILL, R. F. KAY, and P. LEMELIN. 2003. Comment on "Grasping Primate Origins. Science, 300:741.

KRAUSE, D. W. 1978. Paleocene primates from western Canada. Canadian Journal of Earth Sciences, 15:1250-1271.

KRAUSE, D. W., and M. C. MAAS. 1990. The biogeographic origins of late Paleocene–early Eocene mammalian immigrants to the Western Interior of North America, pp. 71-105. In T. M. BOWN and K. D. ROSE (eds.), Dawn of the Age of Mammals in the Northern Part of the Rocky Mountain Interior. Geological Society of America, Special Paper, 243.

KRISHTALKA, L. 1973. Late Paleocene mammals from the Cypress Hills, Alberta. Special Publications of the Museum, Texas Tech University, 2:1–77.

KRISHTALKA, L., and J. H. SCHWARTZ. 1978. Phylogenetic relationships of plesiadapiform-tarsiiform primates. Annals of Carnegie Museum, 47:515-540.

LINNAEUS, C. 1758. Systema naturae per regna tria naturae, secundum classes, ordines, genera, species cum characteribus, differentiis, synonymis, locis. Tomus I: Tegnum animale. Editio decima, reformata. Laurentii Salvii, Stockholm, 824 pp.

LOFGREN, D. L., J. A. LILLEGRAVEN, W. A. CLEMENS, P. D. GINGERICH, and T. E. WILLIAMSON. 2004. Paleocene biochronology: The Puercan through Clarkforkian Land Mammal Ages, pp. 43-105. In M. O. WOODBURNE (ed.), Late Cretaceous and Cenozoic Mammals of North America: Biostratigraphy and Geochronology. Columbia University Press, New York.

LUCKETT, W. P. 1993. An ontogenetic assessment of dental homologies in therian mammals, pp. 182-204. In F. S. SZALAY, M. J. NOVACEK, AND M. C. MCKENNA (eds.), Mammal Phylogeny: Mesozoic Differentiation, Multituberculates, Monotremes, Early Therians, and Marsupials. Springer-Verlag, New York.

MACDONALD, T. E. 1996. Late Paleocene (Tiffanian) mammal-bearing localities in superposition, from near Drumheller, Alberta. Unpublished M. Sc. thesis, University of Alberta, Edmonton, 248 pp.

MACPHEE R. D. E., M. CARTMILL, and P. D. GINGERICH. 1983. New Paleogene primate basicrania and the definition of the order Primates. Nature, 301:509-511

MARTIN, R. D. 1968. Toward a new definition of Primates. Man, 3: 377-401.

MARTIN, R. D. 1990a. Primate origins and evolution: a phylogenetic approach. Princeton University Press, Princeton, 804 pp.

MARTIN, R. D. 1990b. Some relatives take a dive. Nature, 345:291-292.

MATTHEW, W. D. 1915. Part IV.—Entelonychia, Primates, Insectivora (part), pp. 429-483. In W. D. MATTHEW and W. GRANGER (eds.), A revision of the lower Eocene Wasatch and Wind River faunas. Bulletin of the American Museum of Natural History, 34.

MATTHEW, W. D. 1917. A Paleocene bat. Bulletin of the American Museum of Natural History, 37:569-571.

MATTHEW, W. D. and W. GRANGER. 1921. New genera of Paleocene mammals. American Museum Novitates, 13:1-13.

MCGREW, P. O., and B. PATTERSON. 1962. A picrodontid insectivore(?) from the Paleocene of Wyoming. Breviora, 175:1-9.

MCKENNA, M. C. 1967. Classification, range, and deployment of the prosimian primates. Problems Actuels de Paleontologie, 163:603-609.

MCKENNA, M. C. 1980. Late Cretaceous and Early Tertiary vertebrate paleontological reconnaissance, Togwotee Pass area, northwestern Wyoming, pp. 321-343. In L. L. JACOBS (ed.), Aspects of Vertebrate History. Museum of Northern Arizona Press, Flagstaff.

MCKENNA, M. C., and S. K. BELL. 1997. Classification of Mammals Above the Species Level. Columbia University Press, New York.

NOVACEK, M. J. 1986. The skull of leptictid insectivorans and the higher-level classification of eutherian mammals. Bulletin of the American Museum of Natural History, 183:1-111.

NOVACEK, M. J., T. M. BOWN, and D. SCHANKLER. 1985. On the classification of the early Tertiary Erinaceomorpha (Insectivora, Mammalia). American Museum Novitates, 2822:1-22.

PARKER, T. J., and W. A. HASWELL. 1897. A Text-book of Zoology. Vol. 2. Macmillan Press, London, 301 pp.

ROMER, A. S. 1966. Vertebrate Paleontology (third edition). University of Chicago Press, Chicago, 468 pp.

ROSE, K. D. 1975. The Carpolestidae, early Tertiary primates from North America. Bulletin of the Museum of Comparative Zoology, 147:1-74.

ROSE, K. D. 1981. The Clarkforkian Land Mammal Age and mammalian faunal composition across the Paleocene-Eocene boundary. University of Michigan Papers on Paleontology, 26:1-197.

ROSE, K. D. 1995. The earliest primates. Evolutionary Anthropology, 3:159-173.

ROSE, K. D., and T. M. BOWN. 1982. New plesiadapiform primates from the Eocene of Wyoming and Montana. Journal of Vertebrate Paleontology, 2:63-69.

ROSE, K. D., K. C. BEARD, and P. HOUDE. 1993. Exceptional new dentitions of the diminutive plesiadapiforms Tinimomys and Niptomomys (Mammalia), with comments on the upper incisors of Plesiadapiformes. Annals of Carnegie Museum, 62: 351-361.

RUSSELL, D. E. 1964. Les mammifères Paléocène d'Europe. Mémoires du Muséum National d'Histoire Naturelle, Nouvelle Série, Série C, 13:1-324.

RUSSELL, L. S. 1967. Paleontology of the Swan Hills area, north-central Alberta. Contributions in Life Sciences from the Royal Ontario Museum, 71: 1-31.

SARGIS, E. J. 2002a. A multivariate analysis of the postcranium of tree shrews (Scandentia, Tupaiidae) and its taxonomic implications. Mammalia, 66: 579-598.

SARGIS, E. J. 2002b. The postcranial morphology of Ptilocercus lowii (Scandentia, Tupaiidae): an analysis of primatomorphan and volitantian characters. Journal of Mammalian Evolution, 9: 137-160.

SCHWARTZ, J. H., and L. KRISHTALKA. 1977. Revision of Picrodontidae (Primates, Plesiadapiformes): dental homologies and relationships. Annals of Carnegie Museum, 46:55-70.

SCOTT, C. S. 2003. Late Torrejonian (middle Paleocene) mammals from south central Alberta. Journal of Paleontology, 77:745-768.

SCOTT, C. S. 2004. Taxonomically diverse late Paleocene mammal localities from south central Alberta, Canada. Journal of Vertebrate Paleontology, 24, supplement to no. 3:111A.

SCOTT, C. S., R. C. FOX, and G. P. YOUZWYSHYN. 2002. New earliest Tiffanian (late Paleocene) mammals from Cochrane 2, southwestern Alberta, Canada. Acta Palaeontologica Polonica, 47:691-704.

SECORD, R. 2004. Late Paleocene biostratigraphy, isotope stratigraphy, and mammalian systematics of the northern Bighorn Basin, Wyoming. Unpublished Ph. D. dissertation, The University of Michigan, Ann Arbor, 532 pp.

SILCOX, M. T. 2001. A phylogenetic analysis of Plesiadapiformes and their relationship to Euprimates and other archontans. Unpublished Ph. D. dissertation, The Johns Hopkins University, Baltimore, Maryland, 728 pp.

SILCOX, M. T. 2003. New discoveries on the middle ear anatomy of Ignacius graybullianus (Paromomyidae, Primates) from ultra high resolution X-ray computed tomography. Journal of Human Evolution, 44:73-86.

SILCOX, M. T., and G. F. GUNNELL. In press. Plesiadapiformes, pp. XX-XX. In C. M. JANIS, G. F. GUNNELL, AND M D. UHEN (eds.), Evolution of Tertiary Mammals of North America Vol. 2: Marine Mammals and Smaller Terrestrial Mammals. Cambridge University Press.

SILCOX, M. T., D. W. KRAUSE, M. C. MAAS, and R. C. FOX. 2001. New specimens of Elphidotarsius russelli (Mammalia, ?Primates, Carpolestidae) and a revision of plesiadapoid relationships. Journal of Vertebrate Paleontology, 21:132-152.

SILCOX, M. T., J. I. BLOCH, E. J. SARGIS, and D. M. BOYER. 2005. Euarchonta, pp. 127-144. In K. D. ROSE and J. D. ARCHIBALD (eds.), The Rise of Placental Mammals. The Johns Hopkins University Press, Baltimore.

SIMONS, E. L. 1972. Primate Evolution: An Introduction to Man's Place in Nature. The Macmillan Company, New York.

SIMPSON, G. G. 1927. Mammalian fauna and correlation of the Paskapoo Formation of Alberta. American Museum Novitates, 268:1-10.

SIMPSON, G. G. 1928. A new mammalian fauna from the Fort Union of southern Montana. American Museum Novitates, 297:1-15.

SIMPSON, G. G. 1935. The Tiffany fauna, upper Paleocene. I.—Multituberculata, Marsupialia, Insectivora, and ?Chiroptera. American Museum Novitates, 795:1-19.

SIMPSON, G. G. 1936. A new fauna from the Fort Union of Montana. American Museum Novitates, 873: 1-27.

SIMPSON, G. G. 1937. The Fort Union of the Crazy Mountain Field, Montana, and its mammalian faunas. Bulletin of the United States National Museum, 169:1-287.

SIMPSON, G. G. 1940. Studies on the earliest primates. Bulletin of the American Museum of Natural History, 77:185-212.

SMITH T., J. VAN ITTERBEECK, and P. MISSIAEN. 2004. Oldest plesiadapiform (Mammalia, Proprimates) from Asia and its palaeobiogeographical implications for faunal interchange with North America. Comptes Rendus Palévol, 3:43–52.

SZALAY, F. S. 1968. The Picrodontidae, a family of early primates. American Museum Novitates, 2329:1-55.

SZALAY, F. S. 1973. New Paleocene primates and a diagnosis of the new suborder Paromomyiformes. Folia Primatologica, 19:73-87.

SZALAY, F. S. 1974. A new species and genus of early Eocene primate from North America. Folia Primatologica, 22:243-250.

SZALAY, F. S., and E. DELSON. 1979. Evolutionary History of the Primates. Academic Press, New York.

SZALAY, F. S., A. L. ROSENBERGER, and M. DAGOSTO. 1987. Diagnosis and differentiation of the order Primates. Yearbook of Physical Anthropology, 30:75-105.

TOMIDA, Y. 1982. A new genus of picrodontid primate from the Paleocene of Utah. Folia Primatologica, 37:37-43.

TOMIDA, Y. 1994. Phylogenetic reconstruction of mammals based on cheek tooth morphology. Honyuri Kagaku, 34:19-29.

TROUESSART, E.-L. 1897. Catalogus Mammalium tam viventium quam fossilium, 1. R. Friedlander & Sohn, Berlin, 664 pp.

VAN VALEN, L. 1969. A classification of the primates. American Journal of Physical Anthropology, 30:295-296.

VAN VALEN, L. 1994. The origin of the plesiadapid primates and the nature of Purgatorius. Evolutionary Monographs, 15:1-79.

VAN VALEN, L. and R. E. SLOAN. 1965. The earliest primates. Science, 150:743-745.

WADDELL, P. J., N. OKADA, AND M. HASEGAWA. 1999. Towards resolving the interordinal relationships of placental mammals. Systematic Biology, 48:1-5.

WATTERS, J. P., and D. W. KRAUSE. 1986. Plesiadapid primates and biostratigraphy of the North American late Paleocene. American Journal of Physical Anthropology, 69:277.

WEBB, M. W. 1996. Late Paleocene mammals from near Drayton Valley, Alberta. Unpublished M. Sc. thesis, University of Alberta, Edmonton, 258 pp.

WIBLE J. R., and H. H. COVERT. 1987. Primates: cladistic diagnosis and relationships. Journal of Human Evolution, 16:1-22.

WILLIAMS, J. A. 1985. Morphology and variation in the posterior dentition of Picrodus silberlingi (Picrodontidae). Folia Primatologica, 45:48-58.

YOUZWYSHYN, G. P. 1988. Paleocene mammals from near Cochrane, Alberta. Unpublished M. Sc. thesis, University of Alberta, Edmonton, 484 pp.

Table 7.1.—Measurements and descriptive statistics for the upper dentition of Micromomys fremdi Fox from the early middle Tiffanian (Ti3) DW-2 locality, Paskapoo Formation, Alberta.

Element	P	N	OR	M	SD	CV
C	L	1	1.1	—	—	—
	W	1	0.5	—	—	—
P2	L	1	0.8	—	—	—
	W	1	0.6	—	—	—
P3	L	2	0.8-1.0	0.90	0.14	15.71
	W	2	0.7	0.70	0	0
P4	L	2	1.4-1.5	1.45	0.07	4.88
	W	2	0.9-1.0	0.95	0.07	7.44
M1	L	2	1.1-1.2	1.15	0.07	6.15
	W	2	1.6	1.60	0	0
M2	L	2	1.1-1.2	1.15	0.07	6.14
	W	2	1.8-2.0	1.90	0.14	7.44
M3	L	2	0.9	0.90	0	0
	W	2	1.6-1.7	1.65	0.07	7.44

Table 7.2.—Measurements and descriptive statistics for the lower dentition of Micromomys fremdi Fox from the early middle Tiffanian (Ti3) DW-2 locality, Paskapoo Formation, Alberta.

Element	P	N	OR	M	SD	CV
c	L	1	0.8	—	—	—
	W	1	0.5	—	—	—
p2	L	1	0.9	—	—	—
p3	L	5	0.8-1.0	0.90	0.07	7.86
	W	4	0.4-0.5	0.45	0.06	12.83
p4	L	9	1.4-1.8	1.52	0.13	8.55
	W	8	0.9-1.2	1.01	0.10	9.79
m1	L	7	1.0-1.3	1.20	0.10	8.33
	TrW	7	0.8-1.0	0.93	0.07	8.14
	TaW	7	0.8-1.0	0.85	0.07	9.18
m2	L	8	1.1-1.3	1.16	0.07	6.40
	TrW	8	0.8-1.0	0.90	0.07	8.40
	TaW	8	0.8-1.0	0.89	0.08	9.40
m3	L	9	1.3-1.6	1.44	0.11	7.83
	TrW	9	0.7-0.9	0.77	0.06	8.57
	TaW	9	0.7-0.9	0.79	0.06	7.62

Table 7.3.—Combined measurements and descriptive statistics for the upper dentition of Pronothodectes gaoi Fox from the early middle Tiffanian (Ti3) DW-2 and Birchwood localities, Paskapoo Formation, Alberta.

Element	P	N	OR	M	SD	CV
C	L	2	1.2	—	0	0
	W	2	1.0	—	0	0
P2	L	2	1.4	—	0	0
	W	2	1.2	—	0	0
P3	L	6	1.6-1.9	1.78	0.12	6.56
	W	6	2.2-2.8	2.38	0.23	9.72
P4	L	14	1.8-2.3	2.10	0.15	7.23
	W	14	3.0-3.5	3.23	0.17	5.22
M1	L	17	2.2-2.8	2.62	0.16	6.08
	W	17	3.2-4.3	3.82	0.27	6.94
M2	L	25	2.5-3.1	2.80	0.17	6.06
	W	25	3.6-4.6	4.25	0.24	5.73
M3	L	18	2.5-3.1	2.75	0.18	6.39
	W	17	3.5-4.5	4.05	0.22	5.39

Table 7.4.—Combined measurements and descriptive statistics for the lower dentition of Pronothodectes gaoi Fox from the early middle Tiffanian (Ti3) DW-2 and Birchwood localities, Paskapoo Formation, Alberta.

Element	P	N	OR	M	SD	CV
i1	D	28	3.0-4.3	3.72	0.30	8.19
p2	L	1	1.1	—	—	—
	W	1	0.8	—	—	—
p3	L	14	1.8-2.2	1.96	0.11	5.57
	W	14	1.5-1.9	1.69	0.14	8.34
p4	L	24	2.0-2.4	2.14	0.12	5.83
	W	24	1.8-2.2	2.03	0.11	5.36
m1	L	26	2.5-3.0	2.72	0.13	4.77
	TrW	24	1.9-2.5	2.30	0.18	7.65
	TaW	25	2.1-3.1	2.48	0.22	8.85
m2	L	30	2.6-3.2	2.95	0.15	5.10
	TrW	30	2.5-3.3	2.77	0.20	7.27
	TaW	30	2.6-3.3	2.94	0.18	6.16
m3	L	21	4.0.-5.1	4.45	0.26	5.89
	TaW	21	2.4-3.2	2.82	0.19	6.60

Table 7.5.—Combined measurements and descriptive statistics for the dentition of Saxonella naylori Fox from the early middle Tiffanian (Ti3) DW-2 and Birchwood localities, Paskapoo Formation, Alberta.

Element	P	N	OR	M	SD	CV
P2	L	1	0.8	—	—	—
	W	1	0.6	—	—	—
P3	L	6	2.0-2.2	2.12	0.08	3.56
	W	5	2.1-2.5	2.28	0.15	6.51
P4	L	3	1.4-1.5	1.47	0.06	3.94
	W	3	2.3-2.4	2.33	0.06	2.47
M1	L	6	1.5-1.8	1.63	0.12	7.41
	W	6	2.3-2.4	2.32	0.04	1.76
M2	L	7	1.5-1.7	1.60	0.06	3.61
	W	7	2.3-2.5	2.39	0.07	2.89
M3	L	1	1.7	—	—	—
	W	2	2.0	0	0	0
p3	L	3	1.7-1.8	1.73	0.06	3.33
	W	3	1.2-1.4	1.30	0.10	7.69
p4	L	5	1.4-1.6	1.48	0.08	5.65
	W	4	1.4-1.5	1.43	0.05	3.51
m1	L	4	1.7	1.70	0	0
	TrW	4	1.3-1.4	1.35	0.06	4.28
	TaW	4	1.4	1.40	0	0
m2	L	2	1.6-1.7	1.65	0.07	4.29
	TrW	2	1.3	1.30	0	0
	TaW	2	1.4-1.5	1.45	0.07	4.88

Table 7.6.—Combined measurements and descriptive statistics for the upper dentition of Elphidotarsius wightoni Fox from the early middle Tiffanian (Ti3) DW-1, DW-2, and Birchwood localities, Paskapoo Formation, Alberta.

Element	P	N	OR	M	SD	CV
P1	L	2	0.7	0.70	0	0
	W	2	0.5-0.6	0.55	0.07	12.86
P2	L	4	0.6-0.7	0.68	0.05	7.41
	W	4	0.5-0.6	0.53	0.05	9.52
P3	L	11	1.5-1.7	1.58	0.08	4.75
	W	11	1.6-1.8	1.74	0.08	4.66
P4	L	10	1.5-1.7	1.61	0.07	4.58
	W	10	1.8-2.1	1.95	0.08	4.36
M1	L	9	1.1-1.3	1.19	0.06	5.05
	W	9	1.9-2.0	1.96	0.05	2.70
M2	L	9	1.1-1.3	1.19	0.08	6.58
	W	9	1.8-2.0	1.93	0.07	3.66
M3	L	7	1.1-1.2	1.14	0.06	4.68
	W	7	1.5-1.8	1.67	0.13	7.50

Table 7.7.—Combined measurements and descriptive statistics for the lower dentition of Elphidotarsius wightoni Fox from the early middle Tiffanian (Ti3) DW-1, DW-2, and Birchwood localities, Paskapoo Formation, Alberta.

Element	P	N	OR	M	SD	CV
c	L	7	0.5-0.7	0.59	0.07	11.78
	W	7	0.4-0.5	0.49	0.04	7.78
p4	L	22	1.7-2.1	1.91	0.12	6.10
	W	22	1.0-1.3	1.19	0.09	7.93
m1	L	19	1.2-1.4	1.32	0.08	6.34
	TrW	19	0.9-1.2	1.03	0.07	7.26
	TaW	18	0.8-1.2	1.04	0.10	9.76
m2	L	18	1.0-1.3	1.20	0.09	7.56
	TrW	18	0.9-1.1	1.03	0.08	7.42
	TaW	17	0.9-1.3	1.03	0.10	9.39
m3	L	12	1.6-1.9	1.71	0.09	5.27
	TrW	12	0.9-1.2	1.07	0.09	8.32
	TaW	12	0.9-1.2	1.08	0.10	9.51

Table 7.8.—Combined measurements and descriptive statistics for the upper dentition of Carpodaptes hazelae Simpson from the early middle Tiffanian (Ti3) Joffre Bridge Roadcut lower level, DW-2, Mel's Place, and Birchwood localities, Paskapoo Formation, Alberta.

Element	P	N	OR	M	SD	CV
P1	L	1	1.0	—	—	—
	W	1	0.5	—	—	—
P2	L	2	0.9-1.0	0.95	0.07	7.44
	W	2	0.7	0	0	0
P3	L	9	1.8-2.1	1.94	0.11	5.81
	W	9	2.0-2.4	2.23	0.14	6.33
P4	L	11	1.8-2.2	1.95	0.12	6.21
	W	11	2.1-2.7	2.40	0.19	7.91
M1	L	9	1.1-1.3	1.24	0.07	5.84
	W	9	1.8-2.2	2.03	0.15	7.38
M2	L	11	1.1-1.4	1.30	0.10	7.69
	W	11	1.8-2.3	2.05	0.16	7.96
M3	L	10	1.0-1.2	1.11	0.09	7.89
	W	10	1.7-2.0	1.90	0.11	5.55

Table 7.9.—Combined measurements and descriptive statistics for the lower dentition of Carpodaptes hazelae Simpson from the early middle Tiffanian (Ti3) Joffre Bridge Roadcut lower level, DW-1, DW-2, Burbank, and Birchwood localities, Paskapoo Formation, Alberta.

Element	P	N	OR	M	SD	CV
i2	L	1	1.0	—	—	—
	W	1	0.5	—	—	—
p3	L	1	1.1	—	—	—
	W	1	0.7	—	—	—
p4	L	19	2.2-2.7	2.44	0.16	6.45
	W	19	1.3-1.8	1.48	0.13	8.61
m1	L	22	1.3-1.7	1.47	0.13	9.01
	TrW	22	1.1-1.4	1.24	0.08	6.39
	TaW	22	1.1-1.3	1.24	0.07	5.88
m2	L	18	1.2-1.5	1.31	0.09	6.87
	TrW	17	1.1-1.3	1.20	0.09	7.80
	TaW	17	1.1-1.5	1.33	0.10	7.87
m3	L	12	1.8-2.1	1.93	0.10	5.01
	TrW	12	1.1-1.4	1.28	0.11	8.28
	TaW	12	1.1-1.3	1.23	0.07	5.28

Table 7.10.—Combined measurements and descriptive statistics for the dentition of Ignacius frugivorus Matthew and Granger from the early middle Tiffanian (Ti3) Joffre Bridge Roadcut lower level, DW-2, and Birchwood localities, Paskapoo Formation, Alberta.

Element	P	N	OR	M	SD	CV
P4	L	2	1.7	1.70	0	0
	W	2	2.4	2.4	0	0
M1	L	4	1.8-1.9	1.83	0.05	2.74
	W	4	2.7-3.0	2.83	0.13	4.45
M2	L	2	1.8	1.80	0	0
	W	2	2.9	2.90	0	0
M3	L	1	1.6	—	—	—
	W	1	2.5	—	—	—
p4	L	2	1.6-1.9	1.75	0.21	12.12
	W	2	1.0-1.3	1.15	0.21	18.45
m1	L	3	1.9-2.1	1.97	0.12	5.87
	TrW	3	1.5-1.6	1.57	0.06	3.69
	TaW	3	1.7-1.8	1.73	0.06	3.33
m2	L	1	2.1	—	—	—
	TrW	1	1.7	—	—	—
	TaW	1	1.9	—	—	
m3	L	1	3.0	—	—	—
	TrW	1	1.6	—	—	—
	TaW	1	1.6	—	—	—

Table 7.11.—Measurements and descriptive statistics for the dentition of Picrodus calgariensis new species from the middle Torrejonian (To2) Who Nose? locality, Paskapoo Formation, Alberta.

Element	P	N	OR	M	SD	CV
P1	L	1	0.6	—	—	—
	W	1	0.4	—	—	—
P2	L	1	0.7	—	—	—
	W	1	0.4	—	—	—
P3	L	1	0.7	—	—	—
	W	1	0.5	—	—	—
P4	L	2	1.2	1.20	0	0
	W	2	1.0-1.1	1.05	0.07	6.73
M1	L	2	2.5-2.6	2.55	0.07	2.77
	W	2	2.6	2.60	0	0
M2	L	2	1.2-1.3	1.25	0.07	5.66
	W	2	1.9	1.90	0	0
M3	L	1	1.1	1.10	—	—
	W	1	1.5	1.50	—	—
p4	L	1	0.8	—	—	—
	W	1	0.6	—	—	—
m1	L	3	2.3-2.5	2.40	0.10	4.17
	TaW	3	1.1	1.10	0	0
m2	L	1	1.7	—	—	—
	TaW	1	1.1	—	—	—

Table 7.12.—Combined measurements and descriptive statistics for the dentition of Picrodus canpacius new species from the earliest Tiffanian (Ti1) Cochrane 2 and Aaron's localities, Paskapoo Formation, Alberta.

Element	P	N	OR	M	SD	CV
P4	L	4	1.0-1.1	1.08	0.05	4.65
	W	4	0.9-1.0	0.95	0.06	6.08
M1	L	4	2.3-2.4	2.35	0.05	2.46
	W	4	2.5-2.7	2.63	0.09	3.64
M2	L	2	1.2	1.20	0	0
	W	2	1.5-1.6	1.55	0.07	4.56
M3	L	2	1.10	1.10	0	0
	W	2	1.30	1.30	0	0
p4	L	2	0.8-0.9	0.85	0.07	8.32
	TrW	2	0.5-0.6	0.55	0.07	12.86
m1	L	3	2.4-2.5	2.47	0.06	2.34
	TaW	3	1.0-1.1	1.03	0.06	5.59
m3	L	1	1.3	—	—	—
	TaW	1	1.0	—	—	—

Table 7.13.—Measurements and descriptive statistics for the dentition of Picrodus lepidus new species from the early middle Tiffanian (Ti3) DW-2 locality, Paskapoo Formation, Alberta.

Element	P	N	OR	M	SD	CV
P4	L	2	1.3-1.4	1.35	0.07	5.23
	W	2	0.9	0.90	0	0
M1	L	3	2.2-2.3	2.27	0.06	2.54
	W	3	2.4-2.5	2.43	0.06	2.37
M2	L	3	1.3-1.4	1.33	0.05	4.33
	W	3	1.5	1.50	0	0
p4	L	1	0.9	—	—	—
	W	1	0.6	—	—	—
m1	L	2	2.20	2.20	0	0
	TaW	2	0.9-1.0	0.95	0.07	7.44
m2	L	4	1.5-1.6	1.57	0.05	3.17
	TaW	4	0.8-1.0	0.90	0.08	9.07
m3	L	2	1.40	1.40	0	0
	TaW	2	0.9	0.90	0	0

Figure 7.1.—1-18. Micromomys fremdi Fox from the early middle Tiffanian (Ti3) DW-2 locality, Paskapoo Formation, Alberta. 1-6, UALVP 46678, incomplete left maxilla with upper canine, P2-4, and associated and incomplete right dentary with p4, m1-3, and alveoli for c, p2-3 with incomplete left maxilla with upper canine in 1, lingual, 2, occlusal, and P4 in 3, occlusal view, and incomplete right dentary in 4, labial, 5, lingual, and 6, occlusal view; 7-9, UALVP 21015, incomplete left maxilla with P2 (damaged), P3-4, M1-3 in 7, labial, 8, oblique lingual, and 9, occlusal view; 10-12, UALVP 46680, incomplete left dentary with p4, m1-3, and alveoli for c, p2-3 in 10, labial, 11, lingual, and 12, occlusal view; 13-15, UALVP 46679, incomplete left dentary with p4, m1-3, and alveoli for p3 in 13, labial, 14, lingual, and 15, occlusal view; 16-18, UALVP 21011, incomplete right dentary with c, p3-4, m1-3, and alveoli for p2 in 16, labial, 17, lingual, and 18, occlusal view. Scale bars = 2 mm.

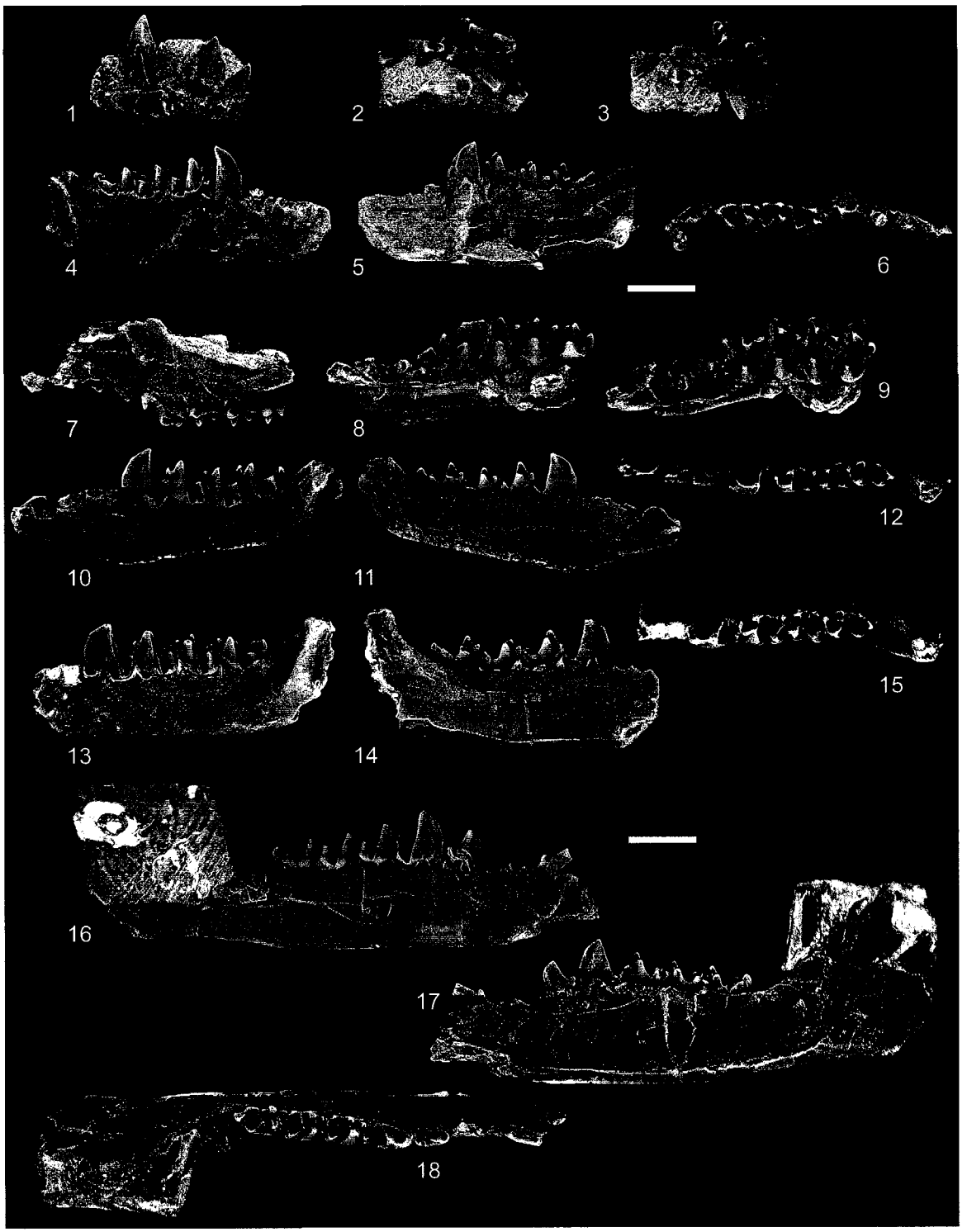
1
2
3
4
5
6
7
8
9
10
11
12
13
14
15
16
17
18

Figure 7.2.—1-3. Pronothodectes gaoi Fox from the early middle Tiffanian (Ti3) DW-2 (DW2) locality, Paskapoo Formation, Alberta. 1-3, UALVP 31396, incomplete skull in 1, dorsal (anterior to left), 2, palatal (anterior to left, arrow pointing to I2), and 3, right lateral (anterior to right, arrow pointing to I2) view. Scale bar = 2 mm.

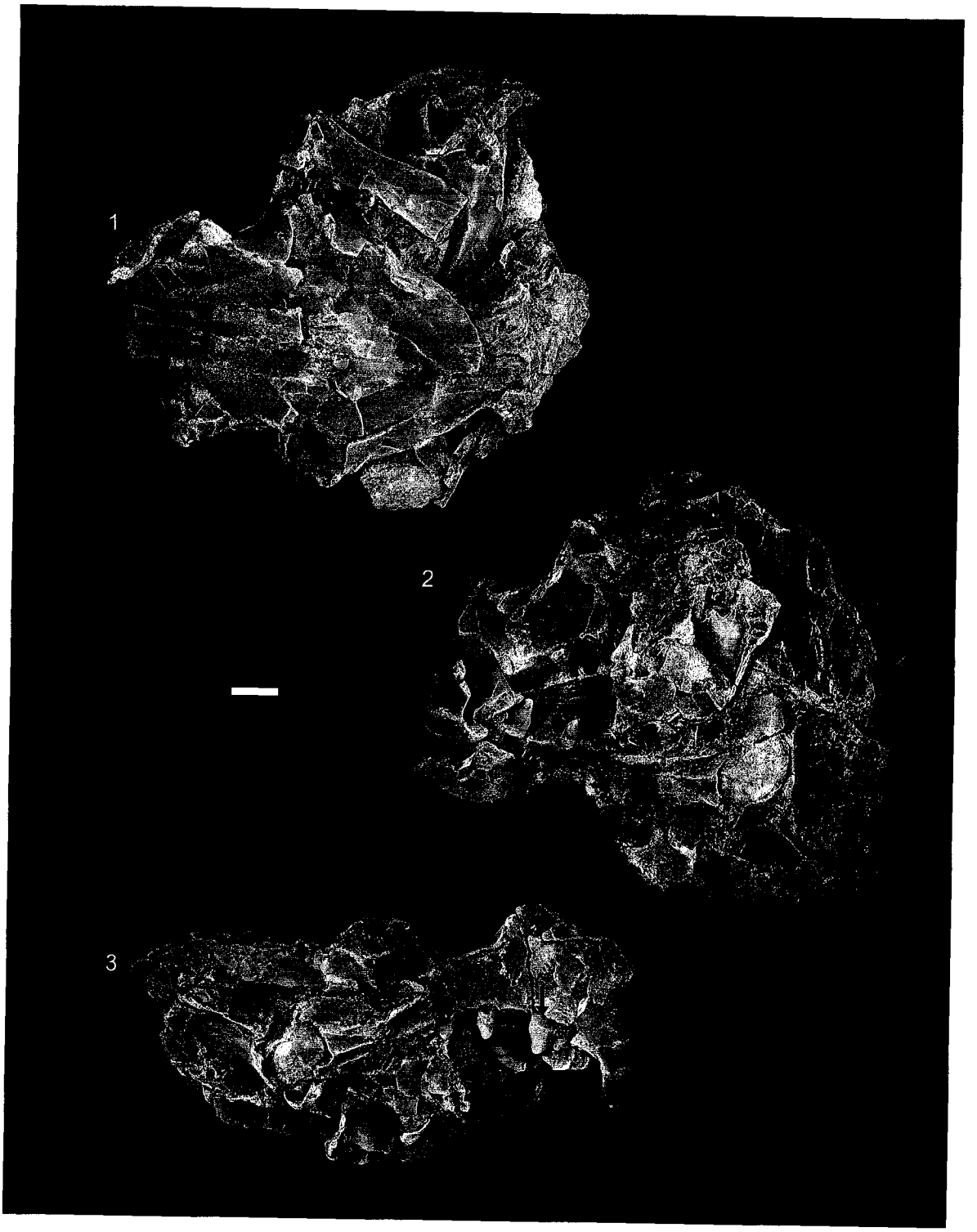
1
2
3

Figure 7.3.—1-13. Pronothodectes gaoi Fox from the early middle Tiffanian (Ti3) DW-2 (DW2) and Birchwood (BW) localities, Paskapoo Formation, Alberta. 1-3, UALVP 46801 (BW), right I1 in 1, lateral, 2, medial, and 3, occlusal view; 4-6, UALVP 46694 (DW2), left I1 in 4, lateral, 5, medial, and 6, occlusal view; 7-9, UALVP 46695 (DW2), right I1 in 7, lateral, 8, medial, and 9, occlusal view; 10-12, UALVP 46696 (DW2), left I1 in 10, lateral, 11, medial, and 12, occlusal view; 13, 14, UALVP 46687 (DW2), incomplete skull with right I1 (displaced), P2 (roots), P3-4, M1-3, and alveolus for upper canine (associated petrosal not figured); cheek teeth in 13, labial and 14, occlusal (P3) and semi-occlusal (molars) view. Scale bars = 2 mm.


1
2
3
4
5
6
7
8
9
10
11
12
13
14

Figure 7.4.—1-20. Pronothodectes gaoi Fox from the early middle Tiffanian (Ti3) DW-1 (DW1), DW-2 (DW2), and Birchwood (BW) localities, Paskapoo Formation, Alberta. 1-3, UALVP 46688 (DW2), incomplete left maxilla with C, P2-4, M1-2, and associated I1 root in 1, labial, 2, oblique lingual, and 3, labial view; 4-6, UALVP 31396 (DW1), incomplete right maxilla with P3-4, M1 in 4, labial, 5, oblique lingual, and 6, occlusal view; 7-9, UALVP 39359 (BW), incomplete right maxilla with P3-4, M1-3in 7, labial, 8, oblique lingual, and 9, occlusal view; 10-12, UALVP 46715 (DW2), left DP4 in 10, labial, 11, oblique lingual, and 12, occlusal view; 13, 14, UALVP 46816 (BW), left P3 in 13, oblique lingual and 14, occlusal view; 15, 16, UALVP 39342 (BW), right P4 in 15, oblique lingual and 16, occlusal view; 17, 18, UALVP 46719 (DW2), left P4 in 17, oblique lingual and 18, occlusal view; 19, 20, UALVP 46720 (DW2), right P4 in 19, oblique lingual and 20, occlusal view. Scale bars = 2 mm.

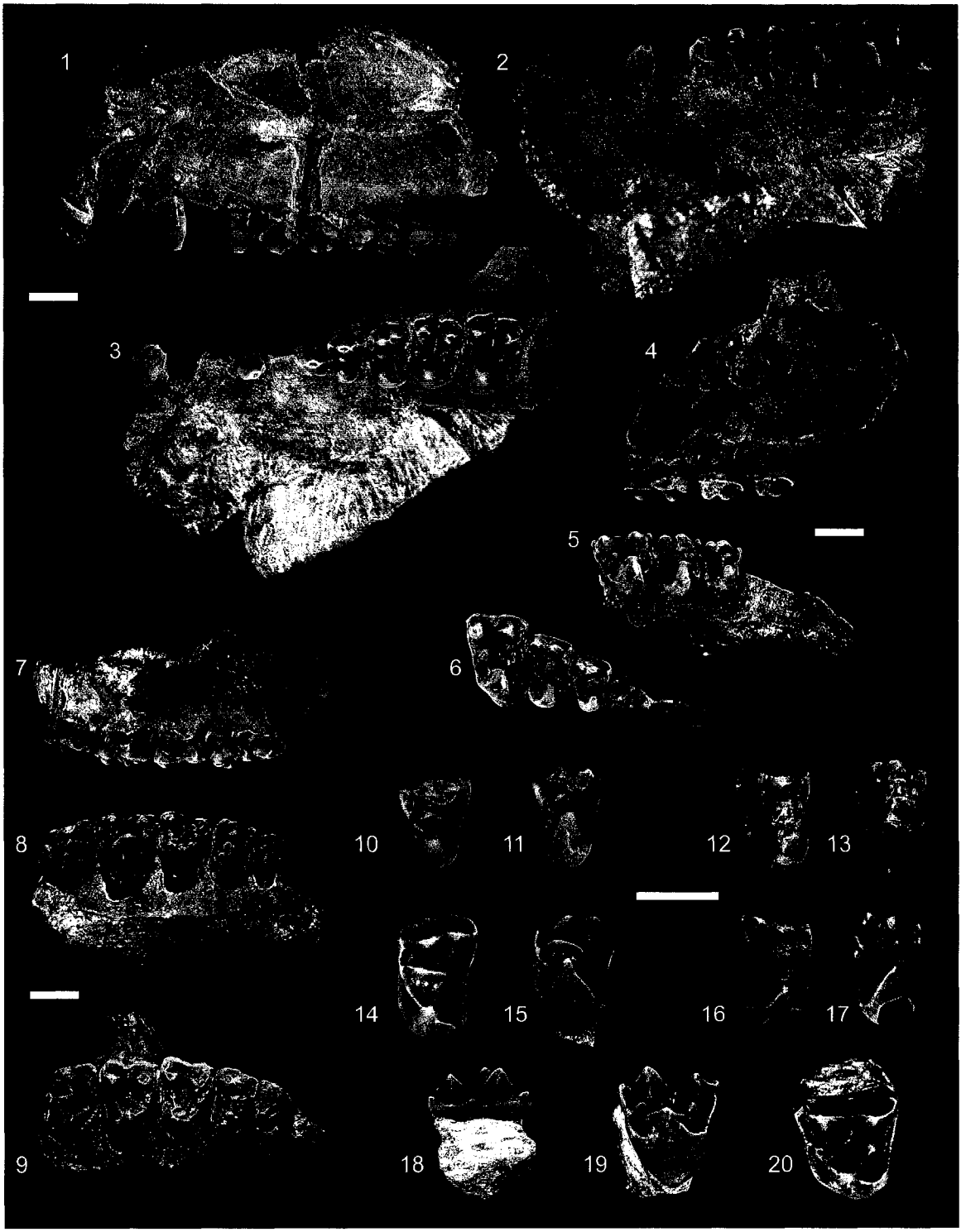
1
2
3
4
5
6
7
8
9
10
11
12
13
14
15
16
17
18
19
20

Figure 7.5.—1-20. Pronothodectes gaoi Fox from the early middle Tiffanian (Ti3) DW-2 (DW2) and Birchwood (BW) localities, Paskapoo Formation, Alberta. 1, 2, UALVP 46724 (DW2), left M1 in 1, oblique lingual and 2, occlusal view; 3, 4, UALVP 46725 (DW2), left M1 in 3, oblique lingual and 4, occlusal view; 5, 6, UALVP 46726 (DW2), left M1 in 5, oblique lingual and 6, occlusal view; 7, 8, UALVP 39301 (BW), right M2 in 7, oblique lingual and 8, occlusal view; 9, 10, UALVP 46731 (DW2), left M2 in 9, oblique lingual and 10, occlusal view; 11-12, UALVP 46732 (DW2), left M2 in 11, oblique lingual and 12, occlusal view; 13, 14, UALVP 46818 (BW), left M3 in 13, oblique lingual and 14, occlusal view; 15-20, UALVP 46686 (DW2), incomplete right maxilla with P2-3, M1-3, alveoli for upper canine and P4, and associated incomplete right dentary with p3-4, m1-2; maxilla in 15, labial, 16, oblique lingual, and 17, occlusal view; dentary in 18, labial, 19, lingual, and 20, occlusal view. Scale bar = 2 mm.

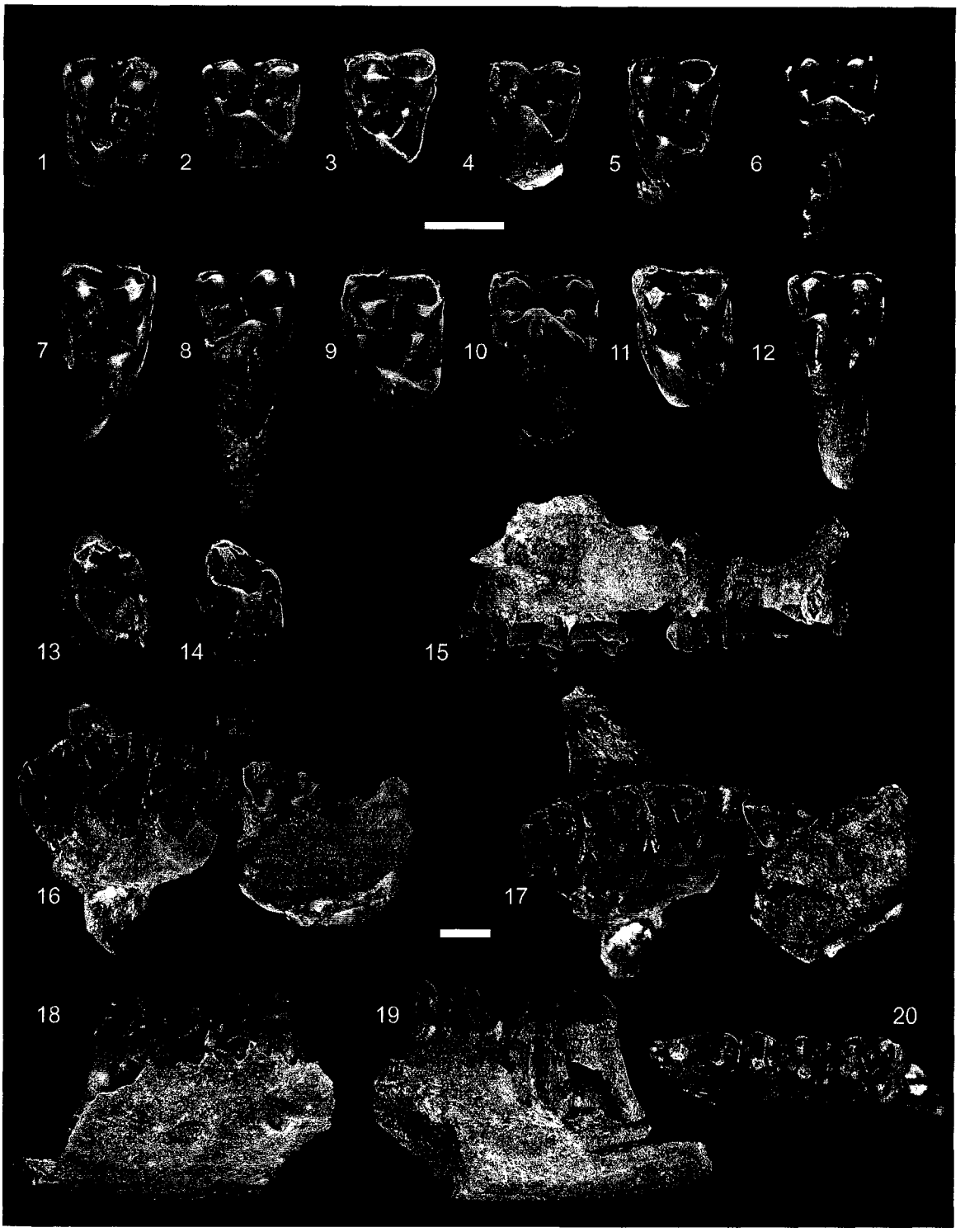
1
2
3
4
5
6
7
8
9
10
11
12
13
14
15
16
17
18
19
20

Figure 7.6.—1-12. Pronothodectes gaoi Fox from the early middle Tiffanian (Ti3) DW-2 (DW2) and Birchwood (BW) localities, Paskapoo Formation, Alberta. 1-3, UALVP 46764 (DW2), left i1 in 1, lateral, 2, medial, and 3, occlusal view; 4-6, UALVP 46765 (DW2), right i1 in 4, lateral, 5, medial, and 6, occlusal view; 7-9, UALVP 39313 (BW), incomplete left dentary with i1, p4, m1-3, and alveoli for i2, c, p2-3 in 7, labial, 8, lingual, and 9, occlusal view; 10-12, UALVP 46762 (DW2), incomplete left dentary with m1-2, and alveoli for i1-2, c, p3-4, m3 in 10, labial, 11, lingual, and 12, occlusal view; box (12A) shows UALVP 46762 in oblique labial view at higher magnification; note the alveoli for i1-2, c, and p2. Scale bars = 2 mm.

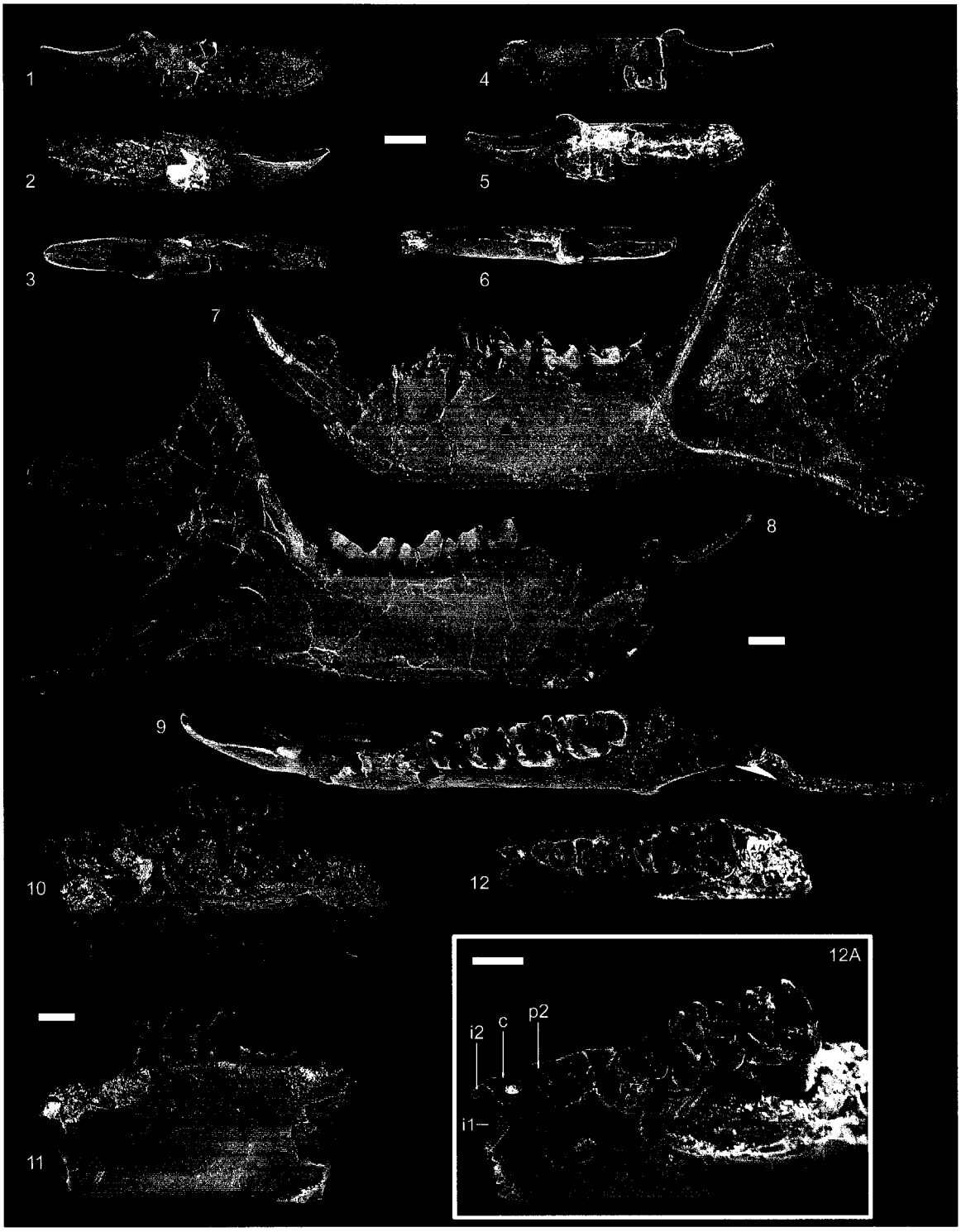
1
2
3
4
5
6
7
8
9
10
11
12
12A
i2
c
p2
i1

Figure 7.7.—1-21. Pronothodectes gaoi Fox from the early middle Tiffanian (Ti3) DW-2 (DW2) and Birchwood (BW) localities, Paskapoo Formation, Alberta. 1-3, UALVP 46827 (BW), incomplete right dentary with i1, p4 (talonid), m1-3, and alveoli for i2, c, p2-3 in 1, labial, 2, lingual, and 3, occlusal view; box (3A) shows UALVP 46827 in oblique labial view at higher magnification; note the alveoli for i2, c, and p2; 4-6, UALVP 46826 (BW), incomplete left dentary with p4, m1-3 in 4, labial, 5, lingual, and 6, occlusal view; 7-9, UALVP 39335 (BW), left p3 in 7, labial, 8, lingual, and 9, occlusal view; 10-12, UALVP 46776 (DW2), left p3 in 10, labial, 11, lingual, and 12, occlusal view; 13-15, UALVP 39336 (BW), left p4 in 13, labial, 14, lingual, and 15, occlusal view; 16-18, UALVP 46779 (DW2), left p4 in 16, labial, 17, lingual, and 18, occlusal view; 19-21, UALVP 39356 (BW), left m3 in 19, labial, 20, lingual, and 21, occlusal view. Scale bars = 2 mm.

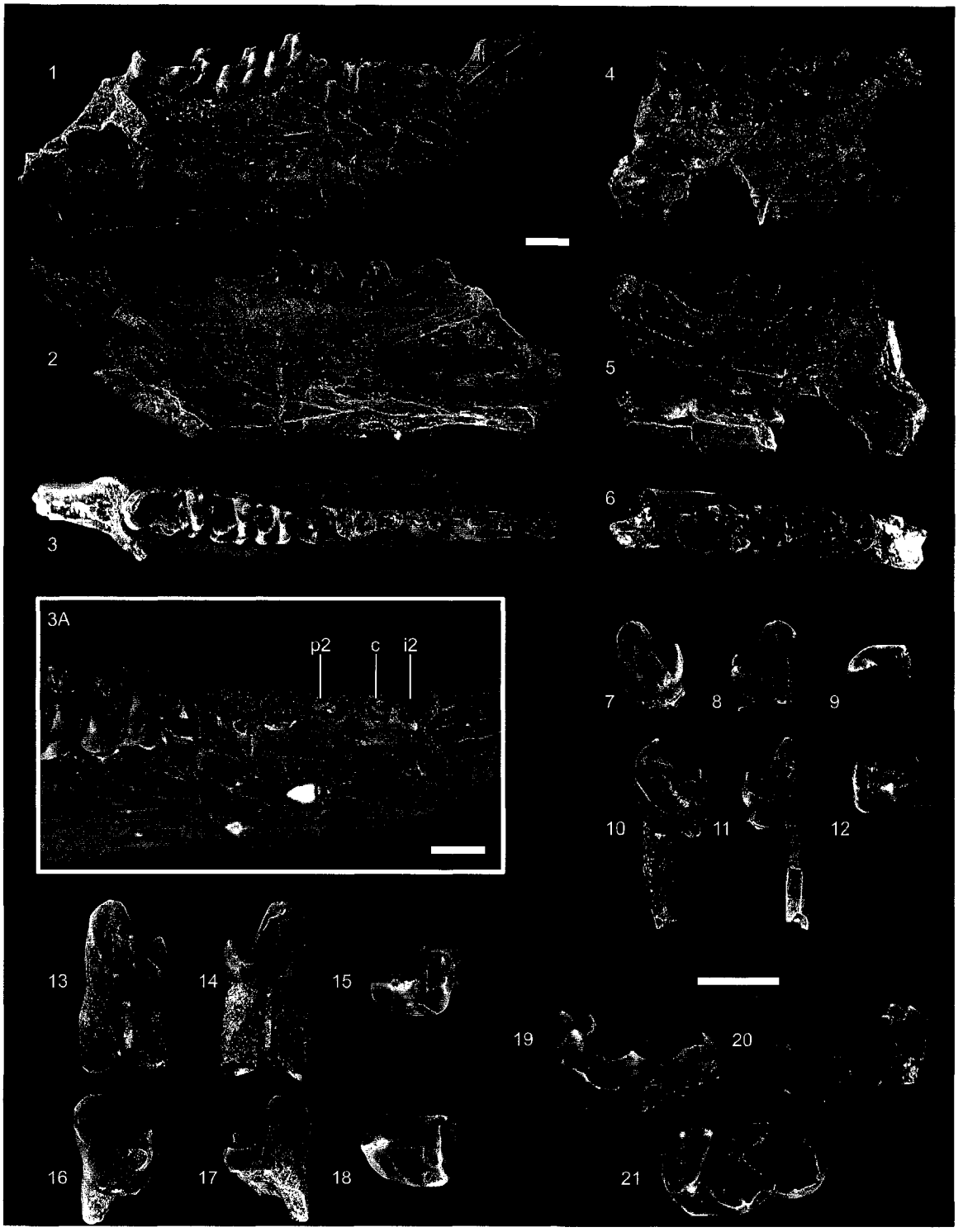
1
2
3
4
5
6
3A
p2
c
i2
7
8
9
10
11
12
13
14
15
16
17
18
19
20
21

Figure 7.8.—1-12. Saxonella naylori Fox from the early middle Tiffanian (Ti3) DW-2 locality, Paskapoo Formation, Alberta. 1-3, UALVP 31608, incomplete right maxilla with P2-4, M1-3 in 1, labial, 2, oblique lingual, and 3, occlusal view; 4-6, UALVP 46840, incomplete right maxilla with P3, M1-2, and alveoli for P4 in 4, labial, 5, oblique lingual, and 6, occlusal view; 7-9, UALVP 39355, incomplete left dentary with p3-4, m1 in 7, labial, 8, lingual, and 9, occlusal view; 10-12, UALVP 46846, incomplete right dentary with p3 (broken), p4, m1-2, and anterior alveolus for m3 in 10, labial, 11, lingual, and 12, occlusal view. Scale bars = 2 mm.

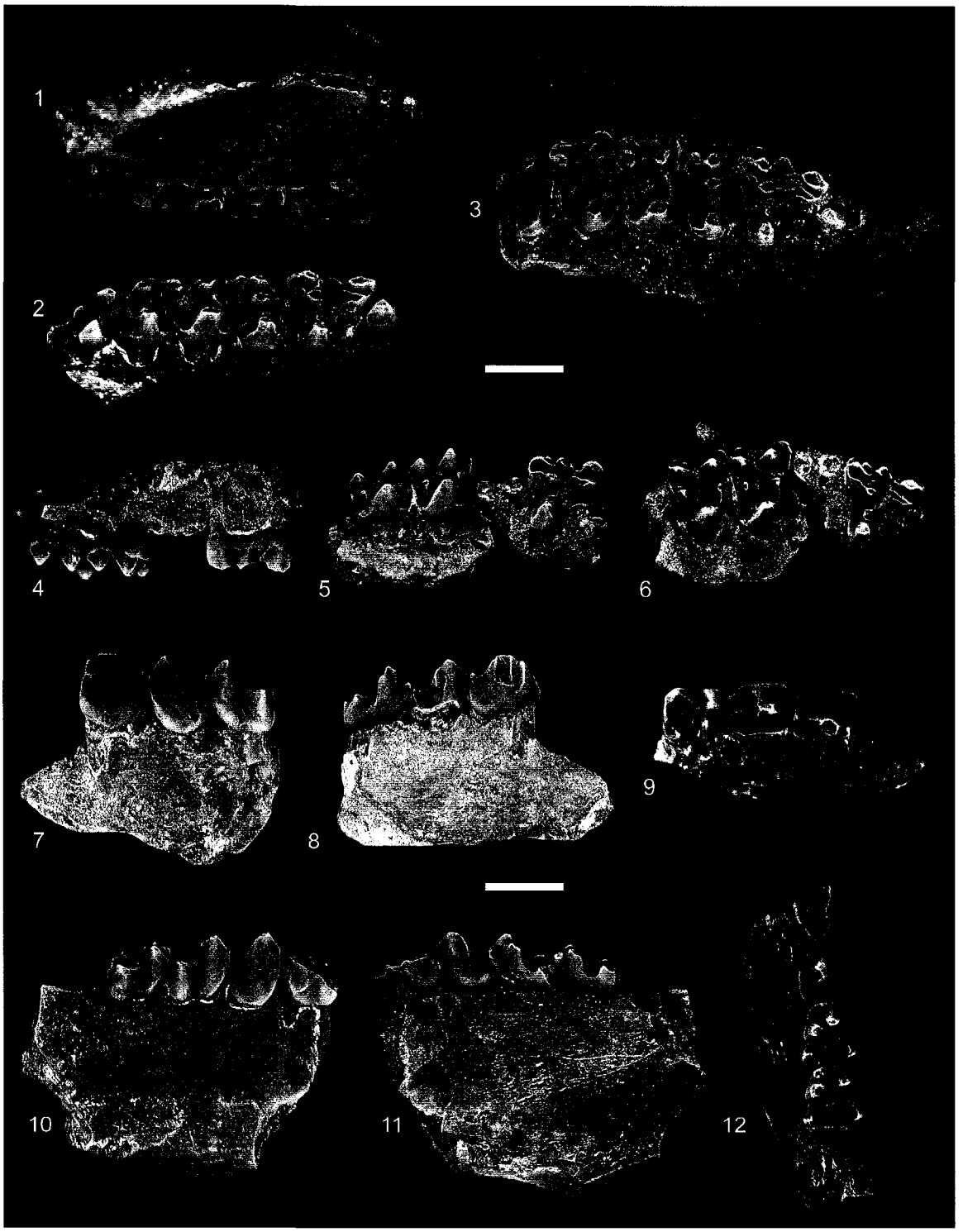
1
2
3
4
5
6
7
8
9
10
11
12

Figure 7.9.—1-15. Elphidotarsius wightoni Fox from the early middle Tiffanian (Ti3) DW-1 (DW1) and DW-2 (DW2) localities, Paskapoo Formation, Alberta. 1-3, UALVP 46848 (DW2), incomplete left maxilla with P1-4, M1-2 in 1, labial, 2, oblique lingual, and 3, occlusal view; 4-6, UALVP 21007 (DW2) , incomplete right maxilla with P3-4, M1-3, and alveoli for P1-2 in 4, labial, 5, oblique lingual, and 6, occlusal view; 7-9, UALVP 21002 (DW1), incomplete left maxilla with P1-4, M1-3, and alveolus for C in 7, labial, 8, oblique lingual, and 9, occlusal view; 10-12, UALVP 40651 (DW2), incomplete right maxilla with P3-4, M1-2 in 10, labial, 11, oblique lingual, and 12, occlusal view; 13-15, UALVP 40608 (DW2), incomplete right maxilla with P2-4, M1-3 in 13, labial, 14, oblique lingual, and 15, occlusal view. Scale bars = 2 mm.

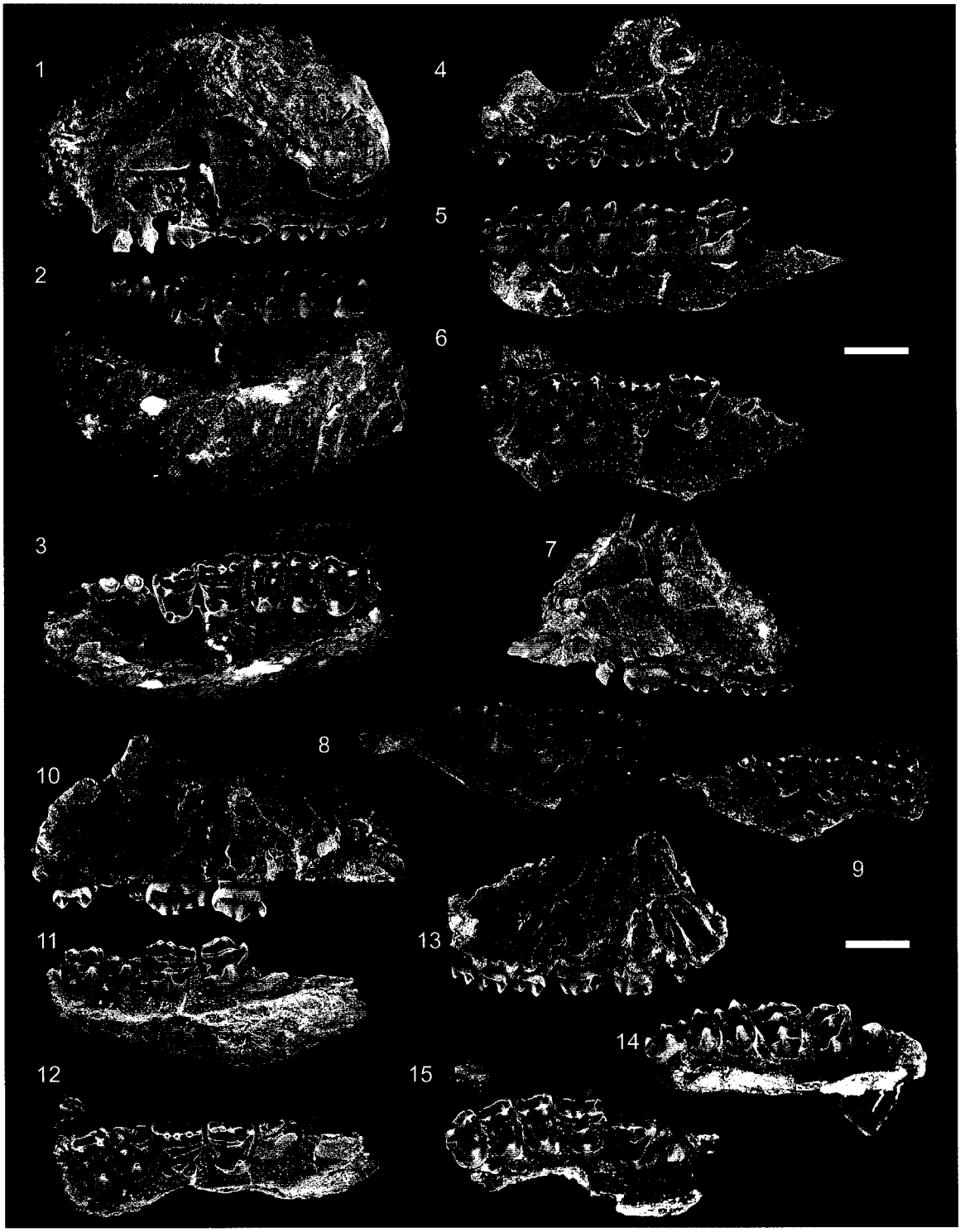
1
2
3
4
5
6
7
8
9
10
11
12
13
14
15

Figure 7.10.—1-15. Elphidotarsius wightoni Fox from the early middle Tiffanian (Ti3) DW-2 locality, Paskapoo Formation, Alberta. 1-3, UALVP 21001 (holotype), incomplete left dentary with i1, c, p4, m1-3, and alveoli for i2 and p3 in 1, labial, 2, lingual, and 3, occlusal view; 4-6, UALVP 40601, incomplete left dentary with i2, c, p4, m1-3, and alveolus for p3 in 4, labial, 5, lingual, and 6, occlusal view; 7-9, UALVP 40603, incomplete right dentary with i2, p4, m1-3, and alveoli for c, p3 in 7, labial, 8, lingual, and 9, occlusal view; 10-12, UALVP 46851, incomplete left dentary with i2, c, p4, m1-3 (m2-3 broken), and alveoli for i1, p3 in 10, labial, 11, lingual, and 12, occlusal view; 13-15, UALVP 46860, right i1 (associated incomplete right dentary with p4, m1-2 not figured) in 13, lateral, 14, medial, and 15, occlusal view. Scale bars = 2 mm.

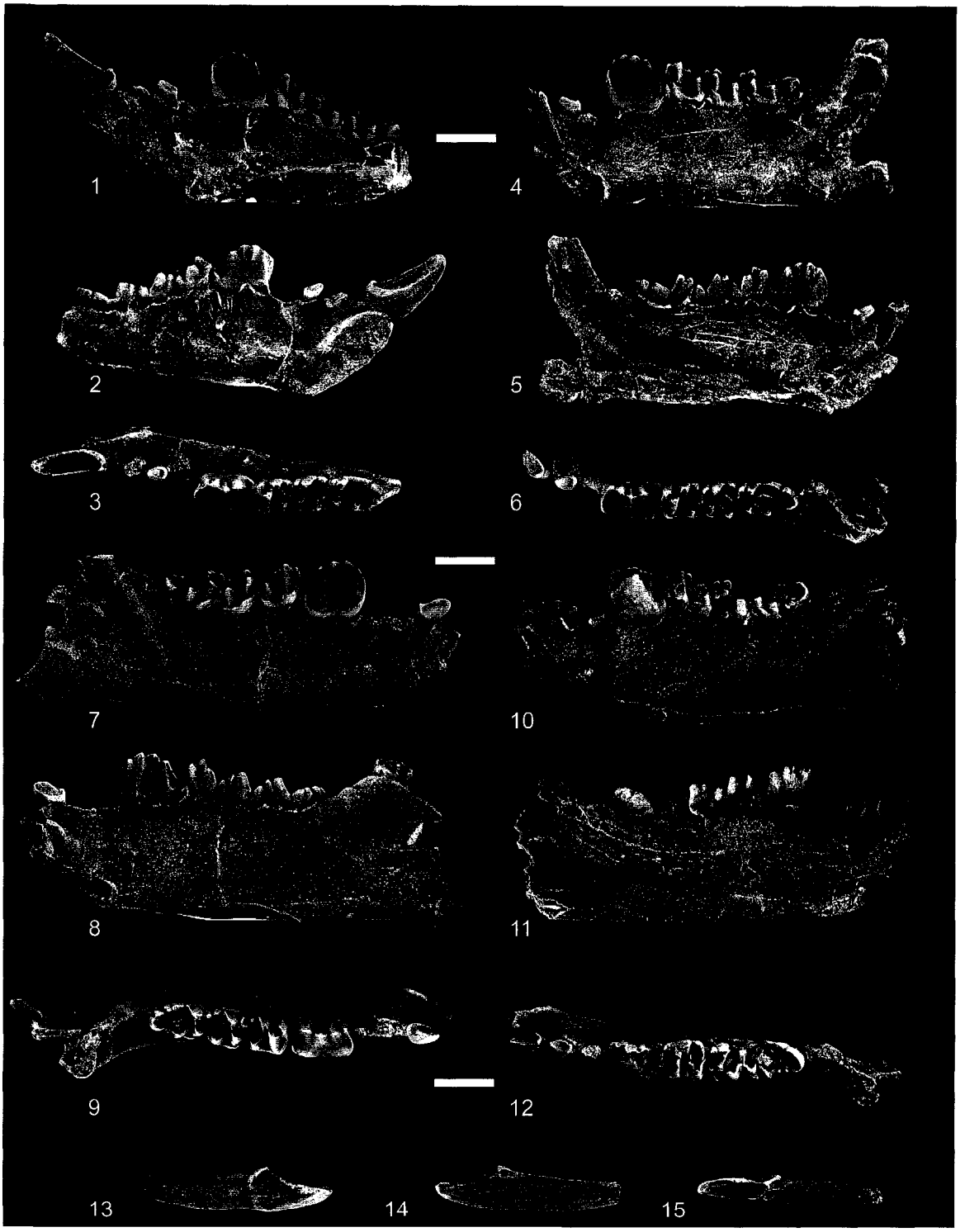
1
4
2
5
3
6
7
10
8
11
9
12
13
14
15

Figure 7.11.—1-3. Elphidotarsius wightoni Fox from the early middle Tiffanian (Ti3) DW-2 and Birchwood localities, Paskapoo Formation, Alberta. Camera lucida outline drawings of occlusal profiles of 1, P3 (N=8) and 2, P4 (N=7), and labial profiles of 3, p4 (N=10). Shaded areas indicate total range of variation. P3s were oriented about a line passing through the first cusp in the labial row and the protocone, and a perpendicular line passing through the last cusp in the labial row. P4s were oriented about a line passing through the first cusp in the labial row and the last cusp in the lingual row, and a perpendicular line passing through the last cusp in the labial row (Krause, 1978). The p4s were oriented about a vertical line passing through the penultimate apical cusp and the ventral notch, and a perpendicular horizontal line that touches the base of the posterior lobe (Krause, 1978). Scale bar = 2 mm.

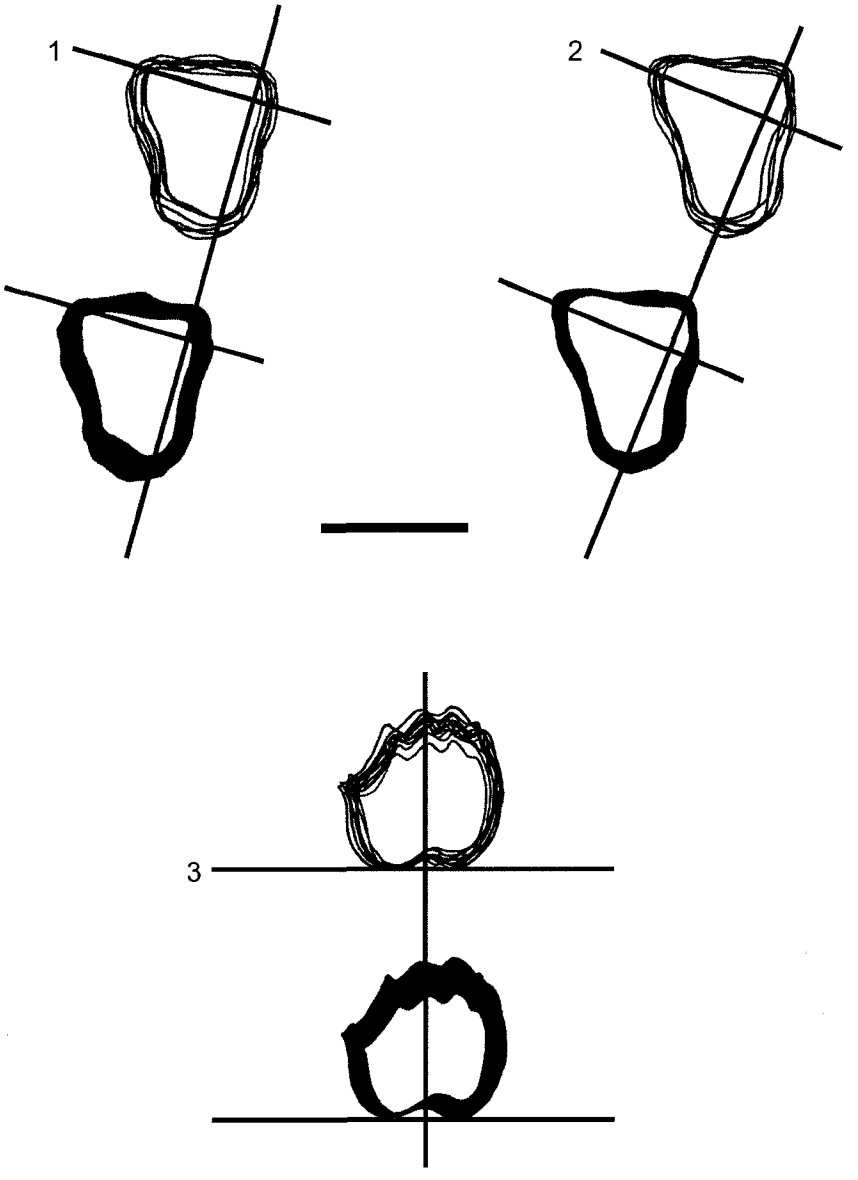
1
2
3

Figure 7.12.—1-15. Carpodaptes hazelae Simpson from the early middle Tiffanian (Ti3) DW-2 locality, Paskapoo Formation, Alberta. 1-3, UALVP 21003, incomplete left premaxilla with I1 and alveoli for I2-3 (arrow points to I3 alveolus) in 1, lateral, 2, medial, and 3, occlusal view; 4-6, UALVP 40626, incomplete left premaxilla with I1-2 and alveolus for I3 (arrow points to I3 alveolus) in 4, lateral, 5, medial, and 6, occlusal view; 7-9, UALVP 46864, incomplete right maxilla with P1-4, M1-3 in 7, labial, 8, oblique lingual, and 9, occlusal view; 10-12, UALVP 40605, incomplete left maxilla with P3-4, M1-3, and alveoli for P1-2 in 10, labial, 11, oblique lingual, and 12, occlusal view; 13-15, UALVP 33860, incomplete left maxilla with P2-4, M1-3, and alveolus for P1 in 13, labial, 14, oblique lingual, and 15, occlusal view. Scale bars = 2 mm.

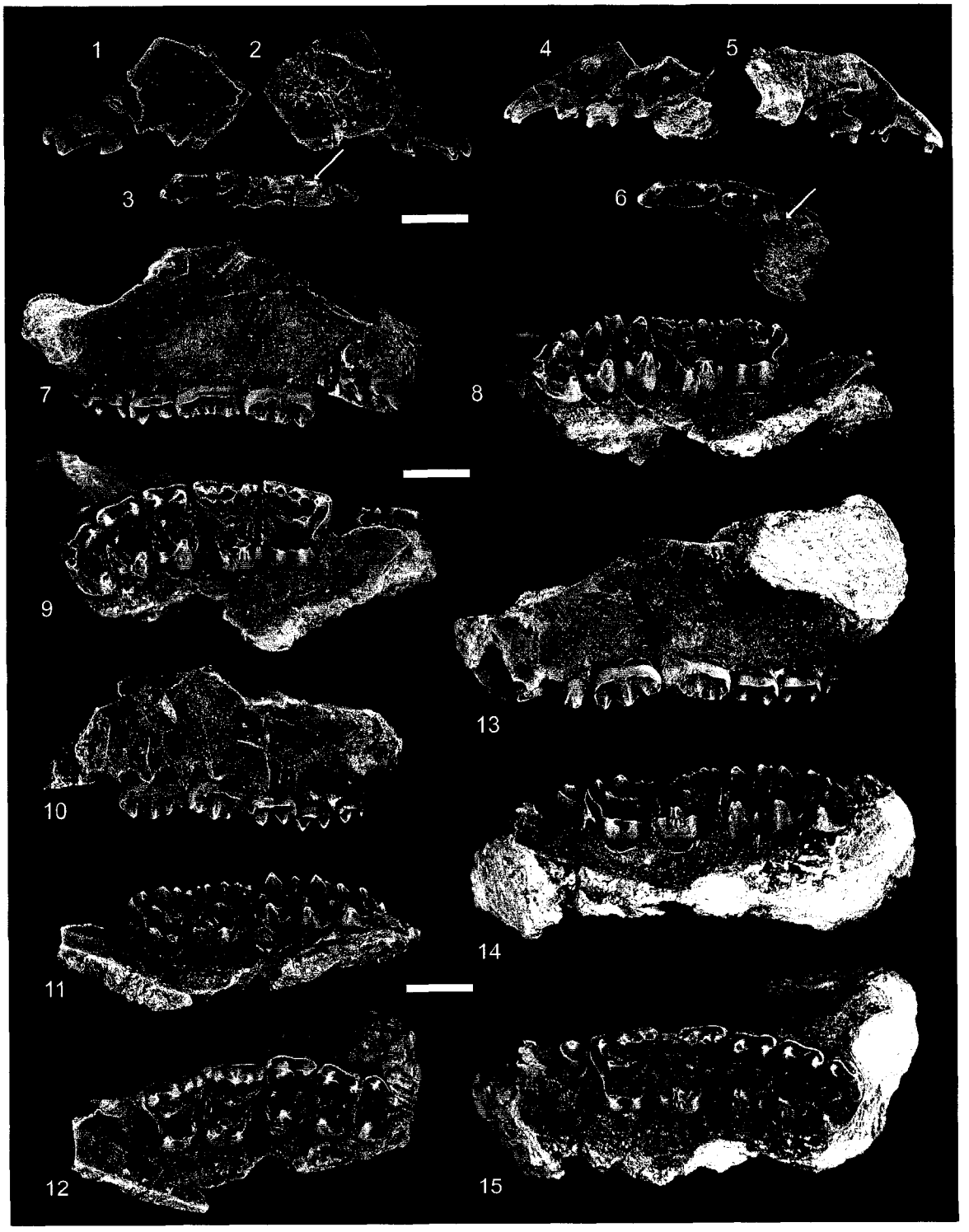
1
2
3
4
5
6
7
8
9
10
11
12
13
14
15

Figure 7.13.—1-24. Carpodaptes hazelae Simpson from the early middle Tiffanian (Ti3) Joffre Bridge Roadcut lower level (JBLL) and DW-2 (DW2) localities, Paskapoo Formation, Alberta. 1-3, UALVP 46862 (JBLL), incomplete left maxilla with P3 and alveoli for P2, M1-2 in 1, labial, 2, oblique lingual, and 3, occlusal view; 4-6, UALVP 40629 (DW2), incomplete left maxilla with P4, M1-2 in 4, labial, 5, oblique lingual, and 6, occlusal view; 7-9, UALVP 40633 (DW2), left P3 in 7, labial, 8, oblique lingual, and 9, occlusal view; 10-12, UALVP 40632 (DW2), right P4 in 10, labial, 11, oblique lingual, and 12, occlusal view; 13-15, UALVP 40635 (DW2), right i1 in 13, lateral, 14, medial, and 15, occlusal view; 16-18, UALVP 40634 (DW2), incomplete right dentary with i1-2, p3-4, and alveolus for c in 16, labial, 17, lingual, and 18, occlusal view; 19-21, UALVP 40630 (DW2), incomplete right dentary with p4, m1-3 in 19, labial, 20, lingual, and 21, occlusal view; 22-24, UALVP 40676 (DW2), incomplete right dentary with p4, m1-3, and alveoli for i1-2, c, p3 in 22, labial, 23, lingual, and 24, occlusal view. Scale bars = 2 mm.

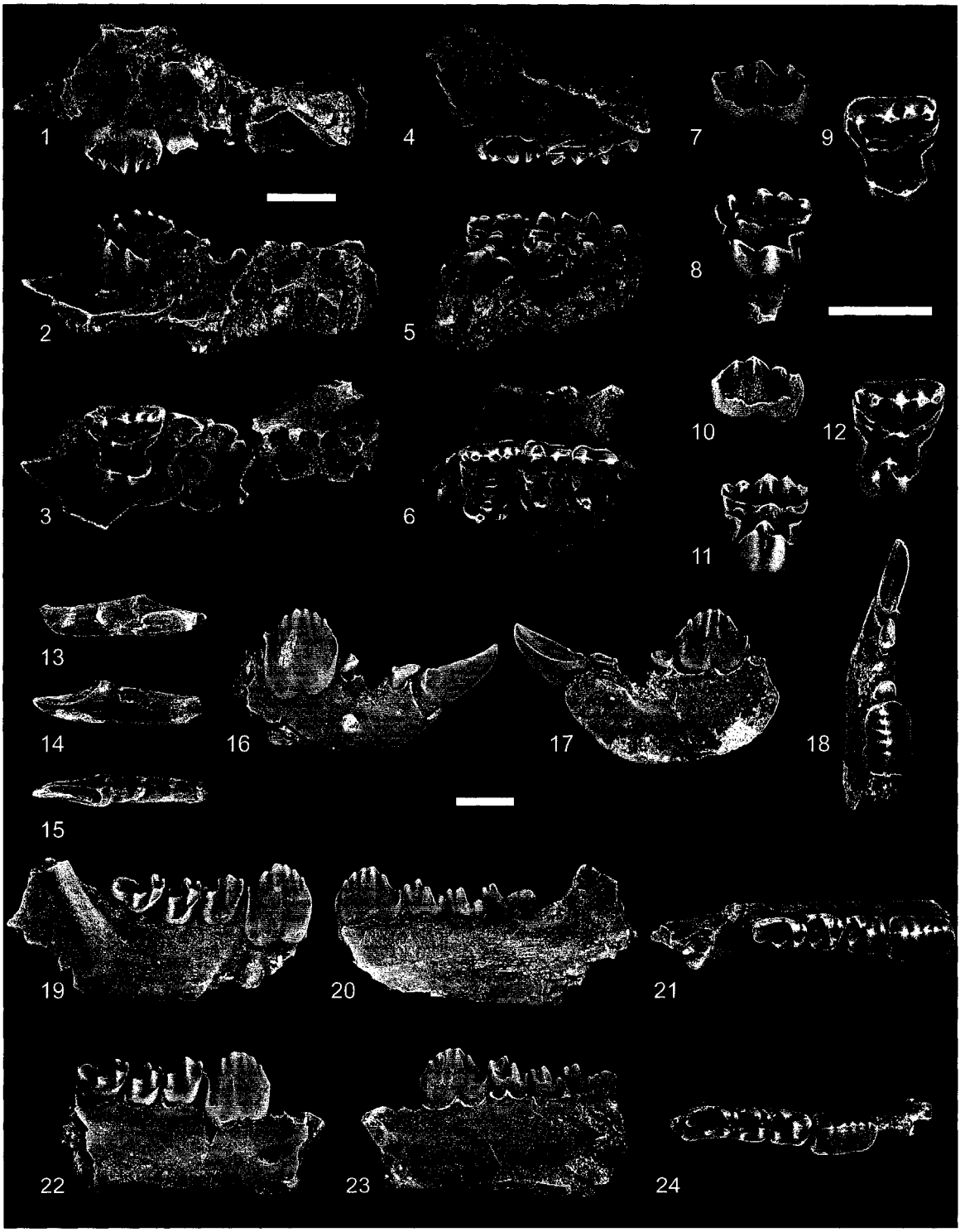
1
4
7
9
2
5
8
3
6
10
12
11
13
14
16
17
18
15
19
20
21
22
23
24

Figure 7.14.—1-6. Carpodaptes hazelae Simpson from the early middle Tiffanian (Ti3) DW-2 (DW2) and Birchwood (BW) localities, Paskapoo Formation, Alberta. 1-3, UALVP 46869 (DW2), incomplete left dentary with p4, m1-3 in 1, labial, 2, lingual, and 3, occlusal view; 4-6, UALVP 46883 (BW), incomplete left dentary with p4, m1-3, and alveoli for i1-2, c, p3 in 4, labial, 5, lingual, and 6, occlusal view.

7-9. Carpodaptes stonleyi Fox from the late middle Tiffanian (Ti4) Roche Percée locality, Ravenscrag Formation, Saskatchewan. UALVP 46882, right i1 in 7, lateral, 8, medial, and 9, occlusal view.

10-17. Ignacius frugivorus Matthew and Granger from the early middle Tiffanian (Ti3) Joffre Bridge Roadcut lower level (JBLL) and Birchwood (BW) localities, Paskapoo Formation, Alberta. 10, 11, UALVP 39302 (BW), incomplete left maxilla with M1-3 in 10, oblique lingual and 11, occlusal view; 12-14, UALVP 46884 (JBLL), incomplete left maxilla with P4, M1 in 12, labial, 13, lingual, and 14, occlusal view; 15-17, UALVP 46887 (BW), incomplete right dentary with i1, p4, and alveoli for m1-2 in 15, labial, 16, lingual, and 17, occlusal view.

Scale bars = 2 mm.

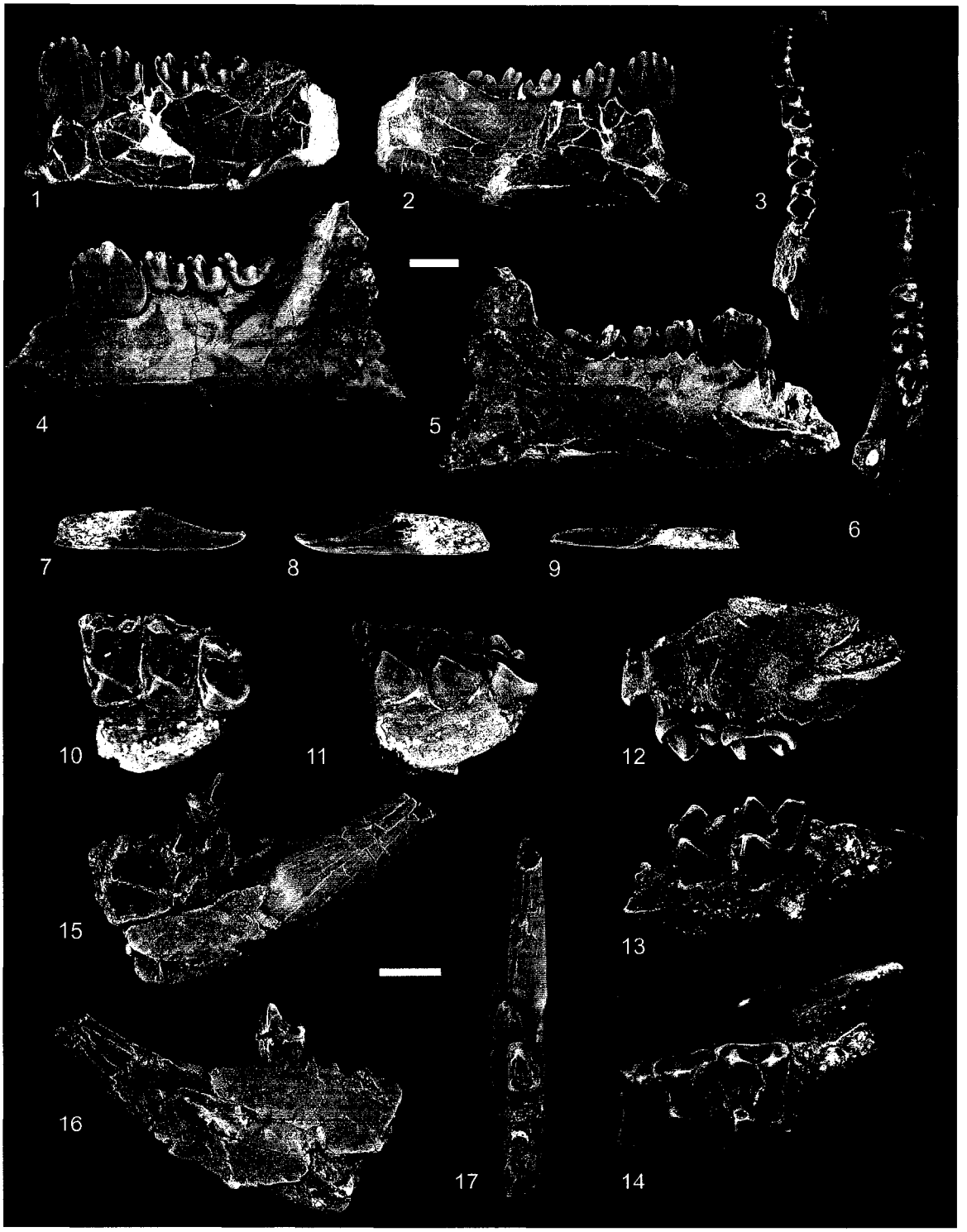
1
2
3
4
5
6
7
8
9
10
11
12
13
14
15
16
17

Figure 7.15.—1-3. Carpodaptes hazelae Simpson from the early middle Tiffanian (Ti3) Joffre Bridge Roadcut lower level, DW-2, Burbank, and Birchwood localities, Paskapoo Formation, Alberta. Camera lucida outline drawings of occlusal profiles of 1, P3 (N=7) and 2, P4 (N=5), and labial profiles of 3, p4 (N=14). Shaded areas indicate total range of variation. P3s and P4s were oriented about a line passing through the first cusp in the labial row and the last cusp in the lingual row, and a perpendicular line passing through the last cusp in the labial row (Krause, 1978). The p4s were oriented about a vertical line passing through the penultimate apical cusp and the ventral notch, and a perpendicular horizontal line that touches the base of the posterior lobe (Krause, 1978). Scale bar = 2 mm.

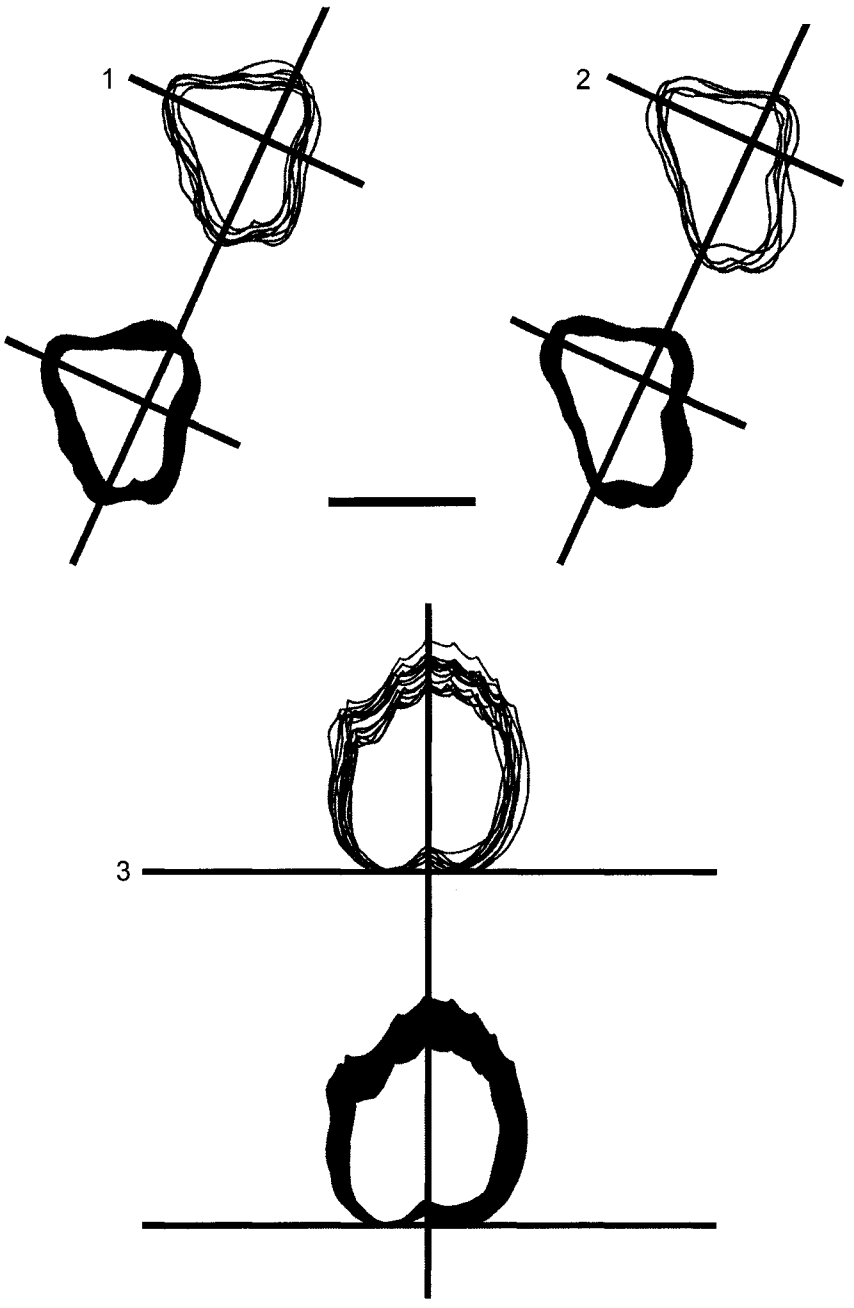
1
2
3

Figure 7.16.—1-12, Picrodus calgariensis new species from the middle Torrejonian (To2) Who Nose? locality, Paskapoo Formation, Alberta. 1-3, UALVP 45656, incomplete right maxilla with P4, M1-3 in 1, labial, 2, oblique lingual, and 3, occlusal view; 4-6, UALVP 45655 (holotype), incomplete left maxilla with P1-4, M1-2 in 4, oblique lingual (arrow points to groove for lacrimal duct), 5, occlusal, and 6, labial view; 7-9, UALVP 43294, incomplete left dentary with i1, p4, m1-2, and alveoli for i2, p2-3, and m3 in 7, labial, 8, lingual, and 9, occlusal view; 10-12, UALVP 45657, right m1 in 10, labial, 11, lingual, and 12, occlusal view.

13-23, Picrodus canpacius new species from the earliest Tiffanian (Ti1) Cochrane 2 locality, Paskapoo Formation, Alberta. 13, 14, UALVP 24918 (holotype), incomplete right maxilla having P4, M1 in 13, labial and 14, lingual view; 15, composite upper dentition with P4, M1-3 in occlusal view [composite includes UALVP 24918 (holotype), UALVP 45662, left M2 (reversed from original), UALVP 24916, left M3 (reversed from original)]; 16, 17, UALVP 45659, incomplete left dentary with p4, m1 in 16, labial and 17, occlusal view; 18-20, UALVP 45660, right m1 in 18, labial, 19, lingual, and 20 occlusal view; 21-23, UALVP 24919, left m3 in 21, labial, 22, lingual, and 23, occlusal view.

Scale bars =2 mm.


1
4
5
2
6
3
7
9
10
11
8
12
16
17
13
14
18
19
20
15
21
22
23

Figure 7.17.—1-9, Picrodus lepidus new species from the early middle Tiffanian (Ti3) DW-2 locality, Paskapoo Formation, Alberta. 1-3, UALVP 40650 (holotype), incomplete left maxilla with P4, M1-2, and alveoli for P3 in 1, labial, 2, oblique lingual, and 3, occlusal view; 4-6, UALVP 40647, incomplete right dentary with p2-4, m1-3, and alveoli for i1-2 in 4, labial, 5, lingual, and 6, occlusal view; 7-9, UALVP 40649, incomplete right dentary with m1-3 and alveoli for i1-2, p2-4 in 7, labial, 8, lingual, and 9, occlusal view.

10-12, Picrodus sp. from the early middle Tiffanian (Ti3) Joffre Bridge Roadcut lower level locality, Paskapoo Formation, Alberta. UALVP 40644, incomplete right dentary with m1 and alveoli for m2-3 in 10, labial, 11, lingual, and 12, occlusal view.

Scale bar = 2 mm.

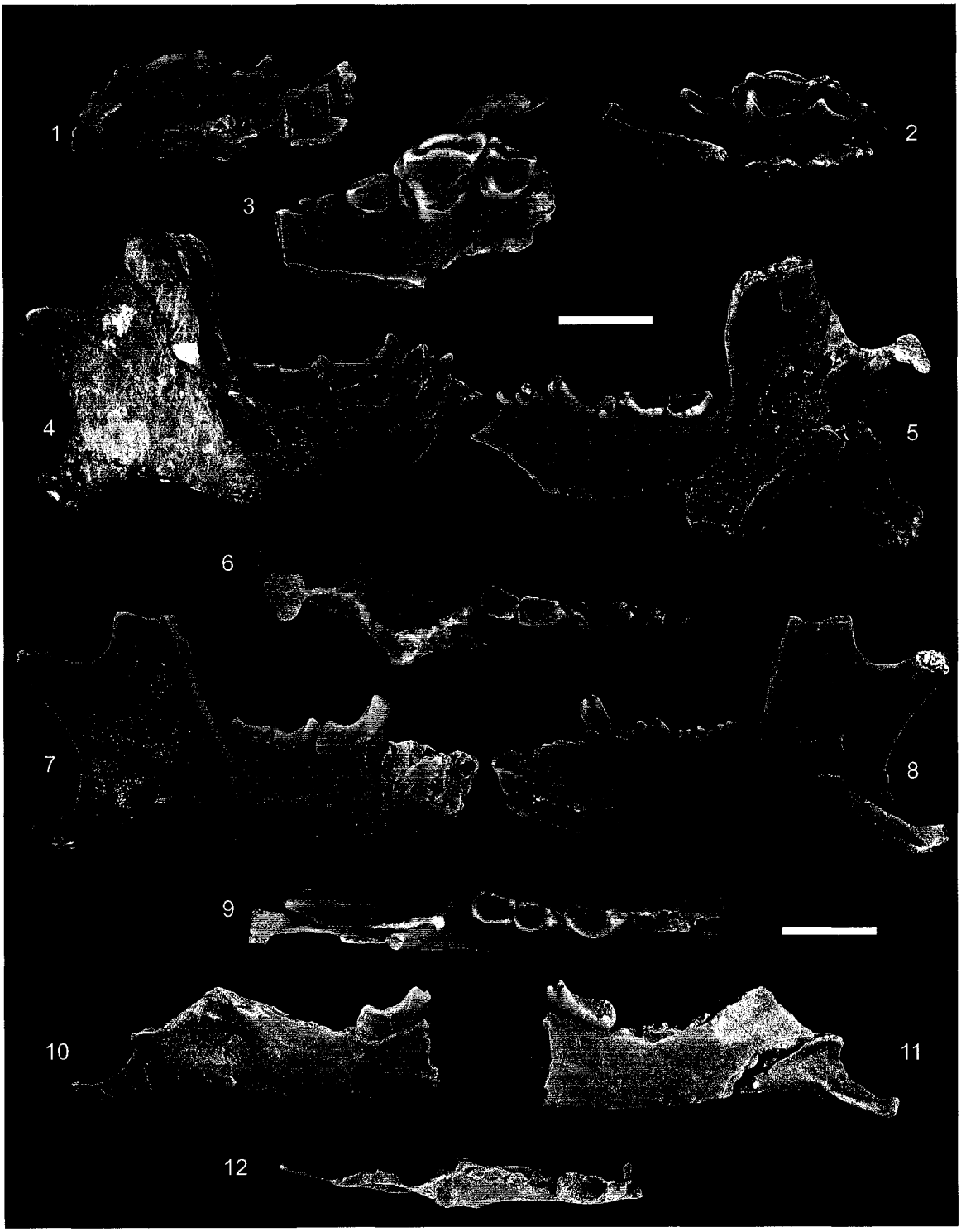
1
2
3
4
5
6
7
8
9
10
11
12

Figure 7.18.—1-4, Camera lucida outline drawings comparing incomplete upper dentitions of species of Picrodus Douglass. 1, P. calgariensis, Who Nose? locality, middle Torrejonian (To2), Paskapoo Formation, Alberta, UALVP 45656, incomplete right maxilla with P4, M1-3; 2, P. silberlingi Douglass, Medicine Rocks (Mehling Site), late Torrejonian (To3), Tongue River Formation, Montana, YPM-PU 19768, incomplete left maxilla with M1-2 (reversed from original); 3, P. canpacius, Cochrane 2 locality, earliest Tiffanian (Ti1), Paskapoo Formation, Alberta, composite of UALVP 24918 (holotype), incomplete right maxilla with P4-M1, and UALVP 45662, left M2 (reversed from original); 4, P. lepidus, DW-2 locality, early middle Tiffanian (Ti3), Paskapoo Formation, Alberta, UALVP 40650, incomplete left maxilla with P4, M1-2 (holotype, reversed from original). Scale bar = 2 mm.

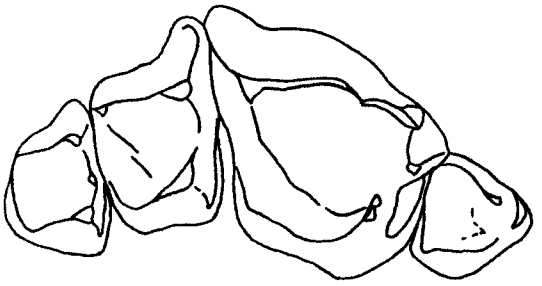

1

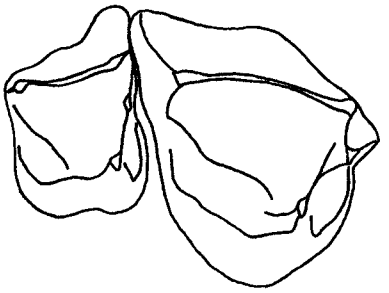

2

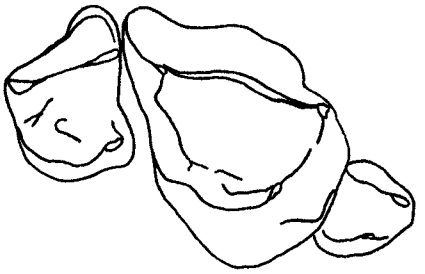

3

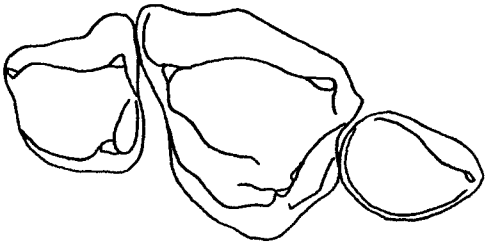

4

Figure 7.19.—Camera lucida outline drawings comparing m2s and m3s of species of Picrodus Douglass. 1-3, P. calgariensis, Who Nose? locality, middle Torrejonian (To2), Paskapoo Formation, Alberta, UALVP 43294, left m2 in 1, labial, 2, lingual, and 3, occlusal view; 4-6, P. silberlingi, Medicine Rocks (Mehling Site), late Torrejonian (To3), Tongue River Formation, Montana, YPM-PU 19746, left m2 in 4, labial, 5, lingual, and 6, occlusal view; 7-9, P. lepidus, DW-2 locality, early middle Tiffanian (Ti3), Paskapoo Formation, Alberta, UALVP 40645, left m2 in 7, labial, 8, lingual, and 9 occlusal view; 10-12, P. silberlingi, Site 1,Torrejonian (To3), Tongue River Formation, Montana, YPM-PU 16577, left m3 in 10, labial, 11, lingual, and 12, occlusal view; 13-15, P. canpacius, Cochrane 2 locality, earliest Tiffanian (Ti1), Paskapoo Formation, Alberta, UALVP 24919, left m3 in 13, labial, 14, lingual, and 15, occlusal view; 16-18, P. lepidus, DW-2 locality, early middle Tiffanian (Ti3), Paskapoo Formation, Alberta, UALVP 40647, right m3 (reversed from original) in 7, labial, 8, lingual, and 9, occlusal view. Scale bar = 2 mm.

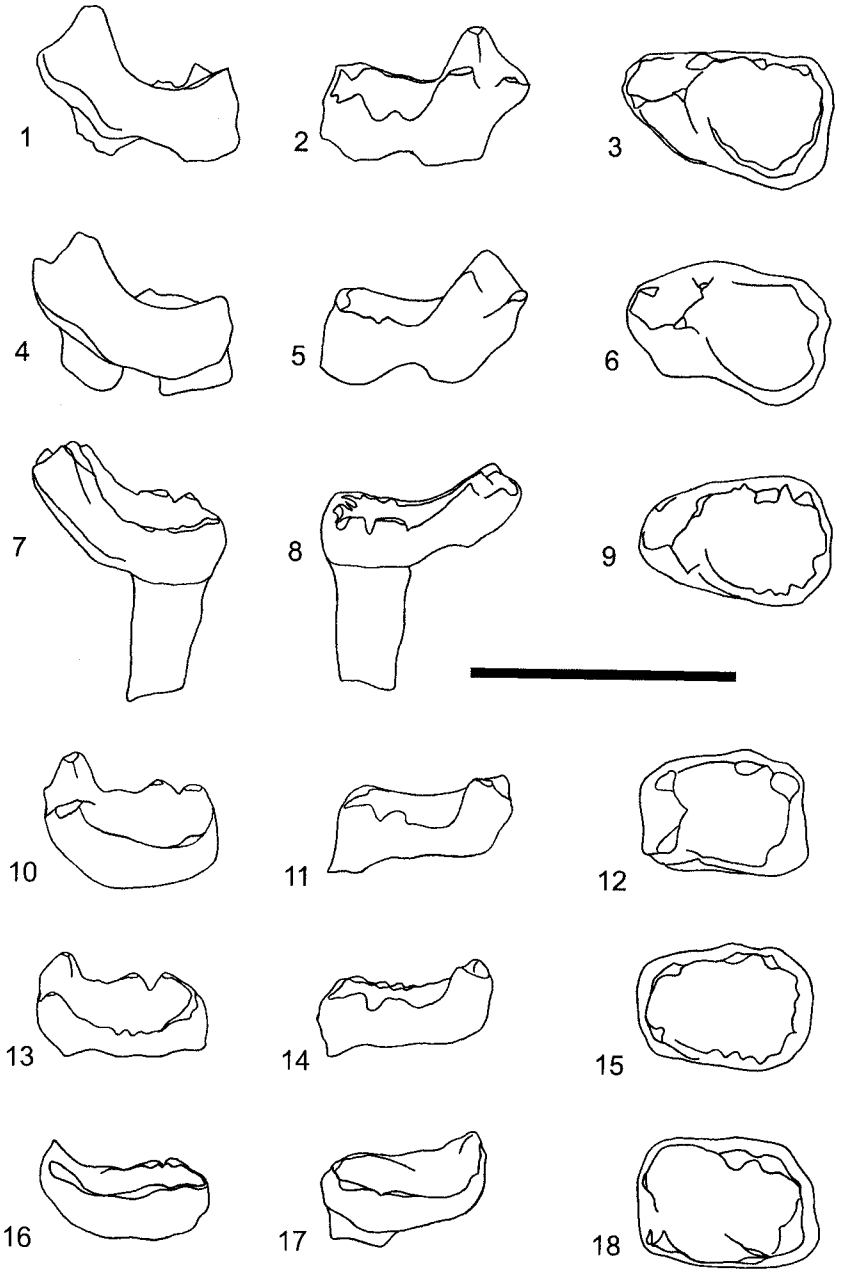
1
2
3
4
5
6
7
8
9
10
11
12
13
14
15
16
17
18

Figure 7.20.—Picrodus lepidus. Camera lucida drawing of UALVP 45914, incomplete left dentary with m1 and exposed alveoli for i1, p2-4 (the alveolus for i2 is not preserved); from the early middle Tiffanian (Ti3) DW-2 locality, Paskapoo Formation, Alberta. Scale bar = 2 mm.

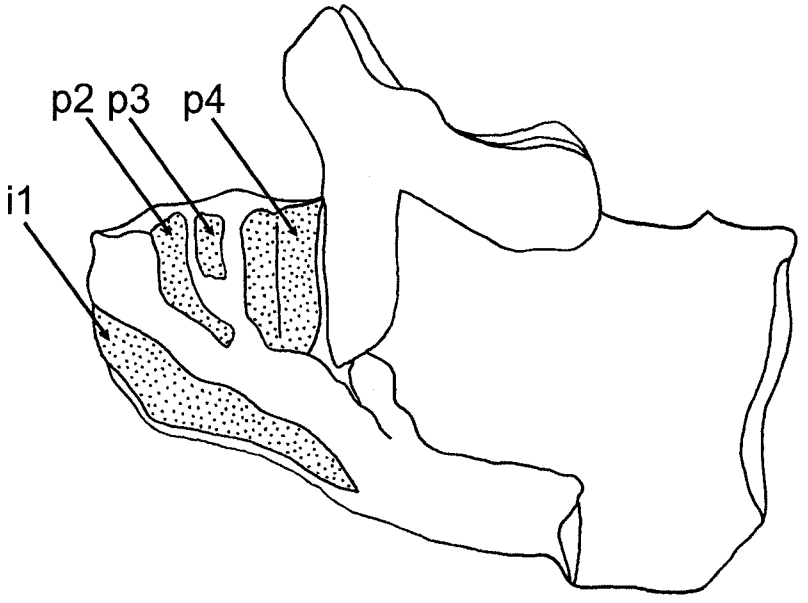
p2 p3 p4
i1

8 New Species of Elpidophorus Simpson and Eudaemonema Simpson (Mammalia, Archonta) from the Late Paleocene of Alberta, Canada, and the Systematic Position of Elpidophorus

8.1 Introduction

ELPIDOPHORUS AND EUDAEMONEMA are enigmatic eutherians of uncertain phylogenetic affinity. Compared to many other North American mammals of Paleocene age, Elpidophorus and Eudaemonema were relatively shorter-lived geologically [both genera are first known from the middle Torrejonian (To2) and apparently went extinct by the late middle Tiffanian (Ti4)], limited in their geographic distribution (both are known only from the more northern parts of the Western Interior of North America), and are never particularly abundant at any one locality (Simpson, 1927, 1935, 1936, 1937; Szalay, 1969a; Rose, 1975, 2006, in press; Scott, 2003). Nonetheless, Elpidophorus and Eudaemonema have figured importantly in recent discussions of Archonta, a clade of primate and primate-like eutherians (see, e.g., Silcox, 2001; Silcox et al., 2005; Bloch et al., 2007; Rose, in press). The peculiar suite of dental characters seen in Elpidophorus and Eudaemonema are reminiscent of those in Dermoptera, a group of nocturnal glissant eutherians that are today restricted to southeast Asia. Dermoptera here refers to a stem-based clade consisting of the last common ancestor of the living dermopterans Galeopterus and Cynocephalus, and fossil taxa more closely related to these genera than to other eutherians. Although recent classifications consider a number of extinct archontan taxa close to, or even within Dermoptera (including the Paromomyidae and Plagiomenidae, see e.g., Beard, 1990, 1993a-b; McKenna, 1990; McKenna and Bell, 1997), the evidence and rationale for these groupings have been vigorously challenged (see, e.g., MacPhee et al., 1989; Krause, 1991; Silcox, 2001; Silcox et al., 2007). As a consequence of these resemblances, Elpidophorus and Eudaemonema are often placed within the Dermoptera as stem taxa representing the earliest divergence of the clade (see, e.g., Rose, 1975; Rose and Simons, 1977; Szalay and Lucas, 1996; Stafford and Szalay, 2000), and although a consensus on this has yet to be reached (see, e.g., Simpson, 1945; Szalay, 1969a; Scott, 2005), the archontan affinities of the two genera are generally

agreed upon. Interestingly, the shifting opinions regarding whether Elpidophorus and Eudaemonema are more closely related to dermopterans, plagiomenids, mixodectids, or some other archontan group are, for the most part, founded upon virtually the same evidence that was available to Simpson when he first described Elpidophorus in 1927; with minor exceptions, few additional specimens have been brought to bear on the problem.

The present chapter centers on exceptionally well-preserved fossils of Elpidophorus and Eudaemonema collected from localities of middle and late Tiffanian (late Paleocene) age from central and south central Alberta, Canada. Among the most anatomically informative of these specimens are near-complete lower jaws of Elpidophorus, documenting for the first time the lower replacement dentition almost in its entirety, and providing the first direct evidence of the number and morphology of the lower incisors, information that is crucial to understanding the phylogenetic position of Elpidophorus within Archonta. Specimens of Elpidophorus collected at the Blindman River localities of south central Alberta (see Fox, 1990a; Scott, 2004) document the presence of two species, the genotype E. elegans Simpson, 1927, as well as a new species, while recently collected specimens from the Swan Hills Site 1 locality of northern Alberta record a new and unusual species of Elpidophorus (Stonley, 1988). Although specimens of Eudaemonema are rare in Alberta, evidence from the Blindman River and Gao Mine localities indicate the presence of a new, highly derived species, doubling the taxonomic diversity of the genus and extending its stratigraphic range into the late middle Tiffanian.

While these new collections contribute significantly to a better understanding of the craniodental and gnathic anatomy, taxonomic diversity, and stratigraphic and geographic occurrences of these two enigmatic genera, they also provide important information bearing on the phylogenetic relationships of Elpidophorus and Eudaemonema, both to one another, as well as to other archontan groups. With the greatly increased knowledge of the anatomy and diversity gleaned from these newly collected specimens, the previously proposed affinities of Elpidophorus and Eudaemonema can be more critically evaluated.

Taxonomic History

The genotype Elpidophorus elegans was based on specimens collected in 1910 by Barnum Brown and field parties from the American Museum of Natural History during a reconnaissance for dinosaur fossils along the Red Deer River of south central Alberta, Canada (Simpson, 1927; Fox, 1990a). The hypodigm was recovered from a sandstone block discovered in talus along the banks of the river near Erickson's Landing [although the Erickson's Landing locality, and hence the source of the sandstone block, has never been rediscovered, Simpson (1927) indicated the source was located in a bluff some 150 feet above river level. Further references to Brown's expedition and discovery of the fossiliferous block in Allan and Sanderson (1945) suggest Erickson's Landing is near the Brookseley Bridge, the remains of which are located adjacent to the present Joffre Bridge, suggesting the source of the slump block was probably at or near the UALVP Joffre Bridge mammal sites (and see Stonley, 1988)]. Simpson (1927) noted the unusual structure of the molars, and indicated that the genus did not compare favourably with any known mammalian taxon; he referred E. elegans with uncertainty to the Oxyclaenidae, a family that was then thought to be closely related to creodonts, but is now considered to be among the most basal condylarths (see McKenna and Bell, 1997). In his review of the Eocene Wasatchian faunas of the United States, Matthew (1918) made reference to the then undescribed specimens of E. elegans as part of a larger discussion on the possible dermopteran or talpid affinities of a new family of peculiar eutherians, the Plagiomenidae. Matthew (1918) was the first to suggest a possible phylogenetic link between Elpidophorus, plagiomenids, and dermopterans, although he conservatively refrained from referring Elpidophorus and Plagiomenidae to Dermoptera, preferring instead to place them in his admittedly artificial Insectivora.

Eudaemonema cuspidata Simpson, 1935, the type and only species of Eudaemonema, was described by Simpson (1935) and referred with question to the Mixodectidae, a family of primate-like or insectivoran-like eutherians that was named by Cope (1883) to include taxa that are now recognized as mixodectids (sensu stricto), microsyopids, tarsiiform primates, and an oxyclaenid condylarth. Although Simpson expressed reservations about the mixodectid affinities of Eudaemonema, he cited

similarities in the morphology of p4 between Eudaemonema and Cynodontomys Cope, 1882, and noted that the molar morphology of Eudaemonema closely resembled that of Mixodectes Cope, 1883. A year later, Simpson (1936) reported on a new species of Elpidophorus from the early Tiffanian Scarritt Quarry of Montana; the new species, E. patratus Simpson, 1936 added significant new information regarding the dental and gnathic anatomy of Elpidophorus, and prompted Simpson to remove Elpidophorus from the Oxyclaenidae and place it within the Mixodectidae. Simpson (1936) was particularly impressed with the similarities between P3 of E. patratus and P4 of the microsyopid Cynodontomys angustidens (Matthew, 1915), and believing that Matthew (1915) had misidentified the P4 of Cynodontomys (Simpson thought the specimen, AMNH 16875, represented P3-4, rather than P4-M1, but see Gunnell, 1989), Simpson (1936) suggested that Elpidophorus and Cynodontomys were closely related, and retained both in the Mixodectidae as part of the Insectivora. Simpson (1936) addressed the possibility that mixodectids and plagiomenids were closely related, positing that mixodectids (including Elpidophorus) and plagiomenids may have shared a recent common ancestor.

Although Elpidophorus was named in 1927, the first specimen that would later be recognized as belonging to that genus was collected by A. C. Silberling in the winter of 1903 from the Fort Union beds of Montana, at what would subsequently be named Silberling Quarry (Simpson, 1937). The specimen (PU 14201), which remained undescribed until Simpson's (1937) monographic study of the Crazy Mountain Field and its fossil mammal faunas, constituted the type and only specimen of a new species of Elpidophorus, E. minor Simpson, 1937. Simpson (1937) considered the positions of Elpidophorus and Eudaemonema in greater detail, outlining characters that apparently linked Eudaemonema, Elpidophorus, Mixodectes, and the microsyopid Cynodontomys, but suggested that although he believed the genera may be closely related, each was clearly "...on different lines of phyletic descent." (p. 129). Simpson also indicated that even though a number of seemingly derived characters linked mixodectids and plagiomenids [e.g., premolar molarization, weak hypocones, broad talonids, similar to what Matthew (1918) had indicated years earlier], a number of conflicting characters (e.g., differences in the structure of the mesostyle, central molar hypoconulids in plagiomenids) strongly suggested that the relationship could not be particularly close.

Simpson (1937) acknowledged Matthew's (1918) views on the dermopteran affinities of Plagiomenidae, but dismissed the possibility of a mixodectid-dermopteran relationship. Simpson (1945) further formalized these views in his classification of the Mammalia, reviving the monotypic superfamily Mixodectoidea of Cope (1883) and referring to it the Mixodectidae [which included Elpidophorus, Eudaemonema, and a number of mixodectids (s. s.) and microsyopids], all within the Insectivora; in contrast with his previous position, Simpson (1945) followed Matthew (1918) in considering plagiomenids basal dermopterans.

McKenna (1960) revisited the proposed phylogenetic positions of Elpidophorus and Eudaemonema in his review of the Eocene Four Mile mammal fauna of Colorado, and on the basis of newly discovered specimens of Cynodontomys, noted that mixodectids (s. l.) fell into at least three distinct groups: Mixodectes and Dracontolestes Gazin, 1941, the microsyopids Cynodontomys, Microsyops Leidy, 1872, and Craseops Stock, 1934, and Elpidophorus and Eudaemonema. McKenna reasoned that the comparisons made by Simpson (1936) were between Elpidophorus, Eudaemonema, and derived, rather than primitive microsyopids, and that the similarities in the molarized posterior premolars and molar mesostyles were likely the result of convergence, rather than indicative of a close relationship, and that Eudaemonema and Elpidophorus did not bridge the structural gap between mixodectids and primitive microsyopids as proposed by Simpson (1936). Consequently, McKenna removed Eudaemonema from the Mixodectidae and allied it tentatively with extant tupaiids, while referring Elpidophorus to the Plesiadapidae, a group of archaic primates.

Van Valen (1967) was the first to explicitly include Mixodectidae (including Elpidophorus and Eudaemonema) within the Dermoptera, although he considered dermopterans more closely related to macroscelidians than to microsyopids, plesiadapids, or any other archontan group. Van Valen (1967) concurred with Simpson's (1945) opinion of Mixodectoidea, but transferred the plagiomenids to the Galeopithecoidea, along with the extant colugos, a view followed by Sloan (1969) but not by D. Russell (1964, 1967) or L. Russell (1967). Although authors quibbled as regards the higher level affinities of Elpidophorus and Eudaemonema, there was general agreement that both

genera were closely related to each other, and were part of a higher level taxonomic grouping that included the mixodectids (s. s.).

In 1969, Szalay published a comprehensive review of Mixodectidae and Microsyopidae, describing and evaluating all of the mixodectid genera known at the time. Szalay (1969a) separated Mixodectidae from Microsyopidae, synonymized Simpson's E. patratus with the genotype E. elegans, and considered Elpidophorus and Eudaemonema mixodectid insectivorans, together with Mixodectes, Dracontolestes, and Remiculus Russell, 1964 from the Paleocene of France. Szalay (1969a) believed Remiculus and Eudaemonema most closely approximated the primitive condition in Mixodectidae, and that Mixodectes, despite its earlier stratigraphic occurrence, was probably among the most derived; although Elpidophorus was placed in Mixodectidae, Szalay noted "outstanding differences" (p. 236) that separated it from more typical mixodectids, including Eudaemonema. Furthermore, Szalay (1969a) compared the mixodectid dentition with those of various plagiomenids, including new specimens of Plagiomene Matthew, 1918, Planetetherium Simpson, 1928, and Thylacaelurus Russell, 1954, with the resulting declaration that mixodectids generally, and Elpidophorus particularly, bear no close relationship to plagiomenids or dermopterans, agreeing instead with Simpson's (1937) assessment of the groups. Szalay (1969a) continued to regard Mixodectidae as insectivorans.

Although authors subsequent to Szalay (1969a) supported Van Valen's (1967) and Sloan's (1969) views of plagiomenids as dermopterans (e.g., Rose, 1973; Russell et al., 1973; Krishtalka, 1976; Schwartz and Krishtalka, 1976; Novacek, 1980), a shift in opinion regarding the affinities of Elpidophorus arrived with the publication of Rose (1975). On reconsideration of the available evidence, and in contrast with the opinions of most other authors, Rose (1975) contended that of the differences in dental features between Elpidophorus and plagiomenids that were first noted by Simpson (1937), only one, the structure of the molar mesostyle, clearly separated the two. Furthermore, Rose (1975) discussed a number of dental resemblances that might suggest a special relationship between Elpidophorus and Plagiomene, an opinion further elaborated by Rose and Simons (1977). Rather than now being considered near-ancestral to

Plagiomenidae (as, e.g., Sloan, 1969 had suggested), Rose (1975) placed Elpidophorus in Plagiomenidae as a stem member, and considered it the earliest member of Dermoptera.

Rose's (1975) hypotheses were subsequently evaluated by Gunnell (1989) in his comprehensive review of Microsyopidae. Gunnell (1989) included all of the relevant mixodectid and plagiomenid taxa in the first computer-assisted cladistic analysis of both groups; not only did his results support Rose's (1975) inclusion of Elpidophorus in Dermoptera, but also suggested the inclusion of Eudaemonema as a basal taxon, and Remiculus as a comparatively derived dermopteran (but see Russell, 1964 for a different opinion). Although not explicitly discussed in Gunnell (1989), his proposed phylogeny suggests that Elpidophorus is paraphyletic, with E. elegans being more closely related to a clade composed of Remiculus+Plagiomenidae than it is to E. minor, and Plagiomenidae are rendered polyphyletic. Gunnell's (1989) results were partly corroborated in an analysis by McKenna (1990), with Elpidophorus and Eudaemonema occurring as successive outgroups to the subfamilies Plagiomeninae and Ekgmowechashalinae, all within Plagiomenidae, and these results were incorporated into the most recent classification of Mammalia by McKenna and Bell (1997). Interestingly, Plagiomenidae (including Elpidophorus and Eudaemonema) were not included in Beard's (1993a) review of "Primatomorpha" (including Dermoptera), despite there being craniodental evidence available for Plagiomene and Ellesmene Dawson, Hickey, Johnson, Morrow, 1986 (see MacPhee et al., 1989). Szalay and Lucas (1996) published the first descriptions of postcranial material referable to a mixodectid, noting a number of similarities with the postcranium of the scandentian Ptilocercus Gray. Importantly, Szalay and Lucas (1996) were the first to explicitly refer Mixodectidae to the Archonta, and this opinion has since been followed (e.g., McKenna and Bell, 1997; Silcox, 2001; Silcox et al., 2005; Bloch et al., 2007).

The most comprehensive review to date of archaic archontan taxa is an as yet unpublished doctoral dissertation by Silcox (2001). Although Silcox's study focused primarily on the interrelationships of Plesiadapiformes, she included mixodectid and plagiomenid taxa in her large dataset in order to understand better the relationships of plesiadapiforms to other archontan groups; importantly, her analysis included extant dermopterans, taxa that were not included in previous cladistic analyses that also

included Elpidophorus and Eudaemonema (e.g., Gunnell, 1989; McKenna, 1990). Silcox (2001) found some support for a monophyletic Volitantia (Chiroptera+Dermoptera, including Plagiomenidae and Elpidophorus), and included Elpidophorus in Plagiomenidae in her resulting classification; the position of Mixodectidae (s. s.) within Archonta was unresolved. Similar results were documented in Silcox et al. (2005), although these authors were more noncommittal on the dermopteran status of Elpidophorus and Plagiomenidae; Bloch et al.'s (2007) recent analysis of Archonta place Plagiomenidae (including Elpidophorus) as the sister group of Dermoptera.

It can be appreciated from the preceding review that the phylogenetic positions of Elpidophorus and Eudaemonema are still a matter of some debate, although a consensus on their probable archontan affinities seems to have been reached (and see Rose, in press). It bears repeating, however, that the shifting opinions on the affinities of Elpidophorus and Eudaemonema, whether based on the results of traditional systematics or computer-assisted cladistics, rests on reinterpretation of basically the same information that was available to Simpson in the early part of the twentieth century. In contrast to the vastly improved fossil record of many archontan groups (e.g., plesiadapiforms, plagiomenids), the published record of Elpidophorus and Eudaemonema has not improved since Szalay's (1969a) review, and as a result, many of the important characters that could potentially bear on the phylogenetic positions of these taxa have remained unknown.

8.2 Systematic Paleontology

Class MAMMALIA Linnaeus, 1758

Subclass THERIA Parker and Haswell, 1897

Infraclass EUTHERIA Gill, 1872

Grandorder ARCHONTA Gregory, 1910

Order uncertain

Family MIXODECTIDAE Cope, 1883

Subfamily MIXODECTINAE (Matthew, 1915)

Genus EUDAEMONEMA Simpson, 1935

Eudaemonema SIMPSON, 1935, p. 231.

Type species.—Eudaemonema cuspidata Simpson, 1935.

Other included species.—Eudaemonema thlastes new species.

EUDAEMONEMA THLASTES new species

Figure 8.1; Table 8.1

Diagnosis.—Differs from Eudaemonema cuspidata in being approximately 25 percent larger, with upper molars more nearly square in occlusal outline, and in having larger molar conules, protocones, and hypocones. Differs further from E. cuspidata in having a more fully molarized p3, and in having lower molar trigonids with broad, low anterior shelves formed by the anteriorly extended paracristids.

Description.—Upper dentition (Figs. 8.1.1-8.1.12): M1: The crown of M1 is subrectangular in outline, with straight anterior and concave posterior margins, and with the principal cusps enclosing a wide, deep basin. The stylar shelf is relatively narrow opposite the paracone, but widens posteriorly, and a shallow ectoflexus divides the labial margin of the crown into near-symmetrical para- and metastylar lobes. The paracone and metacone are large and subconical, with the metacone extending slightly farther lingually at its base. As in other mixodectids, the M1 centrocrista in Eudaemonema is deflected towards the labial margin of the crown where it faintly bulges into the ectoflexus. The centrocrista is tightly U-shaped in occlusal view, similar to that in Mixodectes, and the more labial parts of the postparacrista and premetacrista sometimes coalesce near the labial margin of the crown, forming a conspicuous mesostyle. Weak cuspules can be developed on the preparacrista, postmetacrista, and low ectocingulum. The paraconule and metaconule are subequal in size and height, and stoutly constructed. The external conular cristae are robust, and extend to the parastylar and metastylar lobes as the paracingulum and metacingulum, respectively; the internal conular cristae run labially and join the paracone and metacone. The large, anteriorly leaning protocone is

positioned slightly anterior to the transverse midline of the crown. A massive, conical hypocone is developed on the expanded posterior cingulum; its dimensions are similar to those on M1 of Mixodectes, but its base is less turgid and does not jut posterolingually. The anterior cingulum is heavy, and can extend across the lingual margin of the protocone and join with the hypocone+posterior cingulum. The enamel is weakly wrinkled.

M2: The crown of M2 closely resembles that of M1, differing mainly in its larger size, greater width (and more nearly rectangular occlusal outline), and significantly larger hypocone. The M2 centrocrista bulges farther labially than that on M1, and the mesostyle is more conspicuous.

M3: Despite its reduced metastylar area, the M3 of Eudaemonema thlastes is slightly longer than and nearly as wide as M2. The prominent, finger-like parastylar lobe projects anterolabially. The large paracone and smaller metacone are widely separated, with the metacone projecting somewhat posteriorly; the centrocrista closely resembles that on M1 and M2, forming a prominent bulge at the labial margin of the crown. Small cuspules can be developed on the low but heavy ectocingulum. Unlike those on M1 and M2, the conules and conular cristae on M3 are poorly developed: a small paraconule and weak preparaconular crista occur just lingual to the base of the paracone, while the metaconule is represented only by a vague bulge of the enamel of the postprotocrista; metaconular cristae are not developed. The protocone is massive, subconical, and leans slightly anteriorly. The protoconal cingula are well developed, particularly the posterolingually expanded posterior cingulum, but they are discontinuous around the lingual side of the protocone; a hypocone is not present. The enamel is weakly wrinkled.

Lower dentition (Figs. 8.1.13-8.1.21): p3: The p3 crown in Eudaemonema thlastes consists of a tall protoconid, low metaconid, rudimentary paraconid, and a bicuspid talonid. The protoconid is labiolingually compressed and bladelike, and is connected to the tiny, anteriorly positioned paraconid by a robust paracristid. The metaconid is swollen and subconical, and is developed off the posterolingual shoulder of the protoconid; the two cusps are connected by a short protocristid. The p3 talonid is well developed in E. thlastes, consisting of two large cusps and a lingually sloping basin. The entoconid is the larger talonid cusp and is connected to the taller hypoconid by a sharp

postcristid; an entocristid is not developed and the talonid basin is open lingually. The heavy cristid obliqua ascends the postvallid wall, terminating just below the protocristid notch. A short, weak metastylid crest occurs on the posterior side of the metaconid. Neither anterior nor posterior cingulid is developed.

p4: The p4 of Eudaemonema thlastes resembles p3 but is more fully molariform, with a better-developed paraconid/paracristid, metaconid and entoconid. The protoconid is somewhat inflated, conical, and less labiolingually compressed than it is on p3. A robust paracristid extends a short distance anteriorly from the protoconid apex before bending abruptly lingually, and the paraconid is entirely incorporated into the paracristid. The paraconid/paracristid complex and p3 talonid together form a broad, lingually slanting platform that furnished an extensive surface for the protocone and posterior cingulum of P4 during centric occlusion; heavy wear on the paracristid of p4 suggests that the P4 of E. thlastes had a well-developed posterior cingulum, or perhaps even a hypocone. The metaconid is considerably larger than that on p3, and is subequal in size and height to the protoconid; it is positioned slightly more anterior compared to that on p3 (although it is still posterior to the level of the protoconid), and is connected to the protoconid by a short, sharp protocristid. The talonid on p4 consists of a tall, spirelike entoconid and a lower but more massive hypoconid; the two cusps are connected by a sharp postcristid. The talonid basin is deep and open lingually. The cristid obliqua ascends the postvallid wall to just below the protocristid notch, and a thick metastylid crest runs from the metaconid to the talonid notch. As with p3, an ectocingulid is not developed.

m1: The lower molars of Eudaemonema thlastes closely resemble those of E. cuspidata in most respects: the lower molars increase in size and height from m1 to m3; the crowns lean slightly anteriorly and labially (raising the lingual parts of the crown above the labial parts); the protocristid notch becomes increasingly wider from m1 to m3; and the metaconid and entoconid become taller and more massive posteriorly (Gunnell, 1989 reported the molar entoconid of Eudaemonema as being weakly developed, but this is not true for either E. cuspidata or E. thlastes). The trigonid of m1 supports a tall and bulbous protoconid and metaconid, and a low, lingually slanting anterior paraconid/paracristid shelf. Although the metaconid is larger than that on p4, and the

protocristid is heavier, the paracristid similarly sweeps anteriorly before turning abruptly lingually, fully incorporating the paraconid and forming a low, lingually slanting shelf. The talonid of m1 is significantly wider than that on p4, with a deeper basin and better-developed cusps. Both entoconid and hypoconid are tall and sharp. A poorly developed hypoconulid occurs lingual to the long axis of the crown, and is connected to the entoconid by a short postcristid, and to the hypoconid by a low hypocristid. The talonid basin slopes lingually towards the open and U-shaped talonid notch, while the cristid obliqua crosses the midline of the crown and ascends the postvallid wall towards the apex of the metaconid. A prominent metastylid crest runs from the metaconid apex to the talonid notch. A narrow cingulid occurs posterior to hypoconulid, but the ectocingulid is otherwise undeveloped.

m2: The m2 of Eudaemonema thlastes resembles m1, differing mainly in its larger size, better-developed cusps, and broader talonid and paraconid/paracristid shelf. The metaconid on m2 is larger and taller than on m1, the protocristid is wider and more widely notched, the entoconid and hypoconid are taller and more nearly conical, and the hypoconulid is slightly better developed. As on m1, a thick metastylid crest runs from the metaconid apex to the talonid notch, but accessory crests also can be developed, running anterolabially from the metaconid towards trigonid basin. The cristid obliqua ascends the postvallid wall towards the summit of the metaconid. An ill-defined anterior cingulid is present, in addition to the weak posterior cingulid, but the two remain discontinuous labially.

m3: The m3 is longer, wider, and taller than m2, and the crown is slightly flexed at its midpoint, elevating the talonid cusps to nearer the plane of the trigonid cusps. The trigonid is dominated by a stout, posteriorly leaning metaconid that is connected to the lower protoconid by a widely notched protocristid. The paracristid is long and low, curving gently towards the anterolingual side of the crown; the anterior shelf is much longer and broader on m3 than it is on m1 or m2, furnishing a flat and lingually sloping platform for the large hypocone of M2. The talonid of m3 is slightly narrower than on m2, but is significantly longer: the entoconid and hypoconid are lower compared to those on m1 and m2, but the hypoconulid is much better developed, and projects posteriorly and dorsally. The lingual slope of the talonid basin on m3 is less extreme than either m1

or m2, but the entocristid is similarly undeveloped, and the talonid is fully open lingually. The cristid obliqua joins the postvallid wall below the protocristid notch, the metastylid is robust, and an accessory crest is developed on the anterior side of the metaconid.

Etymology.—Thlastes, Greek noun, crusher, in reference to the enlarged molar hypocones and broad anterior cingulid shelves.

Holotype.—UALVP 46418, incomplete left dentary with p2 (talonid), p3-4, m1-2, m3 (trigonid). Gao Mine locality, Paskapoo Formation of Alberta, late Paleocene [late middle Tiffanian, Ti4 (Fox, 1988), Plesiadapis churchilli/P. simonsi Lineage Zone of Lofgren et al., 2004].

Other material examined.—From DW-2: UALVP 46419, M1; UALVP 46420, M2; UALVP 46421, 46422, M3; UALVP 46423, M1 or M2; UALVP 46424, m2; UALVP 46425, incomplete right dentary with m1 (talonid) and m2.

From Birchwood: UALVP 39409, M1; UALVP 39410, M2; UALVP 39411, M3; UALVP 39462, m2.

From Gao Mine: UALVP 46426, m3.

Age and occurrence.—Late Paleocene (early middle to late middle Tiffanian, Ti3-Ti4) of western Canada.

Discussion.—Eudaemonema was known previously from a single species, E. cuspidata, based on specimens from the middle Torrejonian (To2) Gidley Quarry of Montana (Simpson, 1935, 1937). In the 70 years since Simpson's (1935) report, E. cuspidata has been identified from only a few localities, all of which are restricted to the northern parts of the Western Interior of North America (see, e.g., Simpson, 1937; Szalay, 1969a; Hartman, 1986; Youzwyshyn, 1988; Lofgren et al., 2004; Rose, in press). Fox (1990a) reported the occurrence of a new species of Eudaemonema in a faunal list for the early middle Tiffanian (Ti3) DW-2 locality of Alberta, an identification confirmed by Webb (1996) during his study on the early middle Tiffanian Birchwood local fauna of central Alberta (at which E. thlastes also occurs). The occurrence of Eudaemonema at the Swan Hills Site 1 locality (see Russell, 1967) is erroneous: ROM 05615, identified as a left M3 of Eudaemonema cf. E. cuspidata was identified as an incomplete right deciduous P4 referable to a new species of Elpidophorus (Stonley, 1988, and see later in

this chapter), while a second, uncatalogued specimen is referable to the pantolestid Bessoecetor Simpson, 1936 (see Stonley, 1988).

Simpson (1935, 1937) considered the dentition of Eudaemonema closest to that of the mixodectid Mixodectes and the microsyopid Cynodontomys, referring both to the Mixodectidae. The phylogenetic position of Eudaemonema has since been repeatedly shuffled, at times being allied with either the mixodectids Mixodectes and Remiculus Russell, 1964 (e.g., Szalay, 1969a), or the putative plagiomenid Elpidophorus (e.g., McKenna, 1990; McKenna and Bell, 1997, but see later in this chapter), with the most recent classification placing Eudaemonema together with Elpidophorus as stem plagiomenids within a more inclusive Dermoptera (McKenna and Bell, 1997, but see MacPhee et al., 1989 for an opposing view). Eudaemonema is here considered a mixodectid, with the totality of its dental features closest to those of Mixodectes, as Simpson and Szalay suggested (and see later in this chapter).

Eudaemonema thlastes differs from E. cuspidata primarily in the larger size of its teeth, and in possessing a suite of dental adaptations that increase the potential for crushing at the expense of shear, particularly the enlarged molar protocones and hypocones, and low, shelf-like paraconids+paracristids on the lower molars. The upper molars of E. thlastes differ further from those of E. cuspidata in their more squarish occlusal outlines, in having lower, more bunodont cusps, broader trigon basins, larger and more inflated conules, and a better-developed mesostyle. The p3 of E. thlastes is semimolariform, rather than premolariform, with a well-developed talonid supporting two cusps. The low, shelf-like paraconid+paracristid on p4 and the lower molars of E. thlastes differs markedly from the nearly cuspate paraconid on p4 and m1-3 of E. cuspidata; additionally, the molar hypoconulid is stronger in E. thlastes, the entoconid and hypoconid are taller, and the talonid basin is broader. The distribution of wear facets on the molars of E. thlastes closely resembles that on molars of E. cuspidata, with buccal, or Phase I, facets (see Crompton, 1971; Butler, 1973; Kay and Hiiemäe, 1974) 2a, 3a, and 6 on the uppers, and facets 1 and 5 well-developed on the lowers, suggesting vertical shear remained important in E. thlastes (see Rose and Simons, 1977). In contrast, lingual, or phase II (grinding) wear facets 9 and 10 on the upper and lower molars are much better developed in E. thlastes. Phase 9 facets have been scoured into the labial

side of the enlarged protocone, with corresponding facets on the lingual wall of the hypoconid and cristid obliqua; additionally, an extensive phase 10 facet is developed on the hypocone and posterior cingulum, reducing them to a flat and continuous, labially sloping surface in heavily worn specimens. A corresponding facet is developed on the paraconid+paracristid of the lower molars, with the anterior shelf furnishing a broad platform on which the corresponding molar hypocone acted.

The occurrence of Eudaemonema thlastes extends the geographic range of Eudaemonema to central Alberta from Montana, and the stratigraphic range into the late middle Tiffanian (Ti4); as such, Eudaemonema is the last surviving mixodectid known.

Subfamily ELPIDOPHORINAE new subfamily

Type genus.—Elpidophorus Simpson, 1927

Diagnosis.—Differ from mixodectines in having upper molars with a wider stylar shelf with flaring parastylar and metastylar lobes, a labially (rather than anterolabially) directed preparacrista, a more strongly labially deflected centrocrista, larger conules on P3 and P4, and a poorly developed molar hypocone. Elpidophorines are further distinguished from mixodectines in having three lower incisors (none of which is markedly enlarged) and a p4 that bears a metaconid that is better-differentiated from the protoconid.

Genus ELPIDOPHORUS Simpson, 1927

Elpidophorus SIMPSON, 1927, p. 5.

Type species.—Elpidophorus elegans Simpson, 1927.

Other included species.—Elpidophorus minor Simpson, 1937; E. simpsoni new species; E. clivus new species.

ELPIDOPHORUS SIMPSONI new species

Figures 8.2, 8.3, 8.10.1, 8.10.4, 8.10.7, 8.10.10, 8.11.1, 8.11.5, 8.11.9, 8.11.13; Tables 8.2, 8.3

Diagnosis.—Differs from E. minor in being approximately 30 percent larger, in having better developed p4 and molar metaconids, and in having a stronger m3 hypoconulid. Differs from E. elegans in retaining P1/p1, and in having cheek teeth less transverse relative to length; differs further from E. elegans in having a prominent p3 paraconid, in having P3-P4 paracone and metacone more fully connate, and in M3 being smaller and shorter. Differs from E. clivus new species in P4 centrocrista being undeflected labially, and in P4 lacking a hypocone and having weaker conules. Differs further from E. clivus in having a less fully molariform p4, and in having higher, more anteriorly projecting molar paraconids.

Description.—Maxilla (Figs. 8.2.1-8.2.3): The maxilla of Elpidophorus simpsoni is known from two specimens, with UALVP 40590 the more nearly complete and more informative. The facial process projects dorsally, well above the level of the infraorbital foramen, indicating that the snout of E. simpsoni was deep. The anterior root of the zygomatic arch takes origin above the second and third molars, and the zygomatic process flares posterolaterally. A well-defined jugal facet is developed along the dorsal parts of the zygomatic process of the maxilla, suggesting that the jugal was well exposed on the side of the face, and together with the maxilla probably formed the anterior and ventralmost parts of the orbital rim. The small, subcircular infraorbital foramen opens above the level of the posterior root of P3; its aperture is undivided internally, and opens anteriorly and faintly laterally.

Upper dentition (Figs. 8.2.1-8.2.12): Upper canine: The upper canine of Elpidophorus, known only from its alveolus previously, is preserved in articulation with the maxilla in UALVP 40590. The tooth is single-rooted and premolariform, with a moderately tall and faintly recurved paracone dominating the crown. A short crest extends anteriorly from the paraconal apex, meeting a small cuspule low on the anterior side of the paracone; weak cingula extend a short distance labially and lingually from the cuspule. A second crest, longer and thicker than the first, extends posteriorly from the paraconal apex to a second small cuspule located low on the posterior side of the

paracone. The base of the paracone is slightly inflated, and the enamel is faintly wrinkled.

Upper premolars: P1: The first premolar of Elpidophorus simpsoni is known only from its alveolus in UALVP 40590. The tooth has but a single root, and judging by the diameter of the alveolus, P1 was smaller than either the canine or P2. A diastema is not present, either between C and P1, or between P1 and P2.

P2: The P2 of Elpidophorus simpsoni has two roots occupying separate alveoli, the posterior of which is larger and wider than the anterior. The crown is premolariform and significantly lower than both the canine and P3, and is dominated by a swollen paracone that is both shorter and more erect (i.e. not recurved) than that of the canine. Weak anterior and posterior cuspules are developed, similar to those on the canine, but these are better developed on P2, and the crests connecting them to the paraconal apex are more conspicuous. Cingula extend from the anterior and posterior cuspules, encircling the crown: the cingulum is prominent lingually, where it forms a slight bulge posterior to the level of the paraconal apex, but narrows considerably labially. The enamel is slightly wrinkled.

P3: The crown of P3 supports a well-developed paracone, weaker metacone, and small protocone supported by a lingual root; the cusps together form a near-equilateral triangle in occlusal outline. When viewed from labial aspect, the crown leans posteriorly, and a deep exodaenodont lobe is developed at the anterior root. The paracone is tall and conical, and is connected to a robust anterior cuspule by a sharp preparacrista; a short, sharp notch is developed in the preparacrista close to the anterior cuspule. The metacone occurs on the posterior shoulder of the paracone, and although faint labial and lingual indentations suggest its incipient separation from the paracone, the two cusps are connate throughout most of their height, with only the apices clearly differentiated and connected to one another by a short centrocrista. The postmetacrista extends a short distance to the posterolabial margin of the crown where a small metastylar cusp can be present. Neither paraconule nor metaconule is present. The protocone is variably developed: it is robust on UALVP 40590, approximately half the height of the paracone, whereas on UALVP 40584 it is smaller and lower, and on UALVP 40572, it is merely a nipple-like protuberance on the lingual cingulum; regardless of its development, the protocone is

supported by a separate root, the proportions of which reflect the development of the protocone. Thick anterior and posterior cingula extend from the para- and metastylar corners of the crown to the protocone, but do not meet lingually; a narrow ectocingulum runs along the labial margin of the crown, and can bear numerous tiny cuspules. As with P2, the enamel of P3 is wrinkled.

P4: The P4 of E. simpsoni differs from P3 in having a more prominent metacone and protocone. When viewed from the labial aspect, the crown can be seen to lean posteriorly, and a deep exodaenodont lobe is developed over the anterior root; the ectocingulum is thick posteriorly, but narrows appreciably towards the deepest part of the exodaenodont lobe, where it can then continue to the anterolabial part of the crown, or disappear completely. As on P3, the paracone on P4 is the largest and tallest cusp; the metacone is taller and considerably better developed than on P3, and although it is connate with the paracone for nearly half its height, the two cusps become better separated towards their summits, with the apices connected by a longer and more deeply notched centrocrista. A robust parastylar cusp is developed at the anterolabial corner of the crown, and a deeply notched preparacrista connects this cusp to the paracone; a strong wear facet from occlusion with the p4 protoconid is often scoured into the notch and along the preparacrista on heavily worn specimens (e.g. UALVP 46428). The short postmetacrista curves to the posterolabial corner of the crown where a small cuspule can be developed. Unlike that of P3, the P4 crown of E. simpsoni bears large, well-developed conules: the paraconule is slightly more lingual than the metaconule, abutting the base of the protocone, while the metaconule is most often subequal in size and height to the paraconule (e.g., UALVP 40590), but can be smaller (e.g., UALVP 40587) or wholly undeveloped (e.g., UALVP 40596). The preparaconular and postmetaconular cristae are generally well developed, joining the anterior and posterior cingula near the bases of the paracone and metacone, and then extending as the paracingulum and metacingulum to the parastylar and metastylar corners of the crown, respectively; the internal conular cristae are only weakly developed. The protocone is tall and anteriorly leaning, with its apex at about the same level as that of the metacone; short cristae extend from the protoconal apex to the conules. The anterior and posterior cingula are prominent but discontinuous lingually; there is no trace of a hypocone.

Upper molars: The upper molars of Elpidophorus are much better known than the more anterior parts of the dentition (e.g., Szalay, 1969a). The crowns are subrectangular in outline (subtriangular in M3), with a conical paracone, metacone, massive protocone, and bulbous conules. The most characteristic feature of the molars, however, is the development of dilambdodonty, a condition in which the centrocrista is deflected labially and, with the elongate preparacrista and postmetacrista, forms a W-shaped ectoloph.

M1: The paracone and metacone on M1 of E. simpsoni are subequal in size and height, although the metacone extends slightly farther lingually at its base. A shallow ectoflexus divides the labial side of the crown into weakly differentiated parastylar and metastylar lobes: the parastylar lobe is the larger of the two, projecting slightly anteriorly, while the metastylar lobe extends farther labially. The stylar shelf is narrow, particularly opposite the paracone, but widens significantly opposite the metacone. A short preparacrista and longer postmetacrista extend labially, joining the ectocingulum and forming the outside arms of the ectoloph; accessory crests are developed on the labial side of the paracone and metacone, and extend labially across the stylar shelf where they join the ectocingulum. The centrocrista is deflected towards the labial margin of the crown, forming a prominent bulge that invades the ectoflexus and disrupts the continuity of the stout ectocingulum. A cusp (i.e., a mesostyle proper) is not developed at the junction of the centrocrista and ectocingulum, nor do the postparacrista and premetacrista coalesce. Rather, the postparacrista and premetacrista remain separate and form parts of the anterior and posterior walls of a long, obliquely posterolabially-anterolingually oriented trough that extends to the labial wall of the protocone; the labial apex of the centrocrista forms a distinctive loop that closes off the trough at its labial extremity. The paracone and metacone are widely separated by the trough, and the flat opposing walls of the paracone and metacone are marked with parallel wear striae from contact with the hypoconid. The conules are large and inflated, and their associated crests are well developed. The preparaconular and postmetaconular cristae run for a short distance before joining the anterior and posterior cingula, and then extend as the para- and metacingulum to their respective stylar lobes; small, irregular cuspules are often developed on the conular cristae. The internal conular cristae are stronger than those on P4, with their flat basin-facing sides forming part of the walls of the oblique trough. The

massive protocone is both long and broad, and its apex is at the same height as that of the paracone and metacone. When the maxilla is held horizontally, the protoconal apex leans slightly anteriorly, although its base is positioned opposite to the centrocrista "loop". Short but conspicuous cristae extend from the protoconal apex to the conules. The anterior and posterior cingula are heavy, discontinuous lingually, and a small hypocone is developed on the posterior cingulum (e.g., UALVP 40590, Figs. 8.2.1-8.2.3). The enamel is moderately wrinkled.

M2: The M2 of E. simpsoni closely resembles M1, differing mainly in its greater overall width and wider parastylar lobe. The preparacrista, centrocrista, and postmetacrista are longer than those on M1, and the centrocrista "loop" projects farther labially, increasing the labiolingual width of the W-shaped ectoloph. As on M1, an oblique trough runs from the trigon basin to the centrocrista "loop". The swollen conules and their associated crests are similar to those on M1, and the external conular cristae join the anterior and posterior cingula near the lingual base of the paracone and metacone. The protocone is large and leans anteriorly, while the anterior and posterior cingula are heavy and discontinuous lingually; the hypocone is slightly larger than on M1.

M3: The M3 of E. simpsoni is nearly the same width as M2, but is asymmetrically triangular in outline, with an enlarged parastylar lobe and greatly reduced metastylar lobe. Although the cusps and conules are lower and generally less swollen than on M1 and M2, the M3 is similarly dilambdodont, with the centrocrista deflected labially, forming a prominent "loop"; unlike M1 or M2, however, the metastylar arm of the W-shaped ectoloph is considerably reduced. The oblique trough formed from the basin-facing walls of the paracone, metacone, conules and protocone is well developed, albeit slightly shallower than that on M2. The protocone leans anteriorly, the posterior cingulum is reduced, and a hypocone is not developed.

Dentary (Figs. 8.2.13-8.2.15, 8.3.1-8.3.12): Nine specimens from the Joffre Bridge Mammal Site No. 1 collectively document the anatomy of the dentary of E. simpsoni. None of the specimens is complete, although UALVP 46427 preserves the jaw posteriorly to the level of the ascending ramus of the coronoid process; the condylar process, condyle, and angular process are unknown. The horizontal ramus is boat-shaped in lateral view, with a smoothly convex ventral margin. The ramus is shallow compared

to that of E. elegans (see later in this chapter), with its deepest parts below m2 and m3; the jaw becomes shallower towards p3, then immediately deepens at the symphysis. The symphyseal surface is considerably raised above the level of the surrounding bone, and extends obliquely posteroventrally from the first incisor alveolus, terminating at a large bony boss at the level of the anterior root of p3. The more anterior and dorsal parts of the symphyseal surface are smooth, but the bone becomes increasingly rough posteroventrally, eventually forming an interdigitating network of bony hillocks and crevasses; although there is no evidence of the two dentaries having been co-ossified in life, the interdigitation of the symphyseal surfaces would undoubtedly have provided great stability during mastication. The bony boss at the posterior margin of the symphyseal surface is drawn out posteriorly and ventrally as a stout crest, and may represent the distal attachment of the anterior digastric or mylohyoid musculature. Three mental foramina are usually present laterally: the largest and least variable of the foramina occurs below p2, its circular aperture opening anterolaterally and slightly dorsally; a horizontal septum subdivides this foramen in two specimens into smaller dorsal and larger ventral canals. The remaining foramina are more variable in size and position, although both are always small and most often occur below p4. The anteriormost parts of the coronoid process and masseteric fossa are preserved only in UALVP 46427. The coronoid process arises at a steep angle from behind m3, and a thick crest delimits the anterior margin of the deeply excavated masseteric fossa. From what can be seen of the pterygoideus and temporalis fossae, both were only weakly excavated; a conspicuous tubercle is developed on the medial surface of the dentary, slightly posterior to the m3. The mandibular foramen is not preserved on any of the specimens at hand. The cheek teeth of E. simpsoni are arranged in a shallow arc that is convex labially, and although the teeth are canted lingually, when the mandibular ramus is held such that the symphyseal surface is vertical (presumably the "in life" position), the biting surfaces of the teeth face dorsally, and the coronoid process flares laterally.

Lower dentition (Figs. 8.2.13-8.2.15, 8.3): Lower incisors: The number and anatomy of the lower incisors in Elpidophorus were previously unknown. The most nearly complete specimens indicate Elpidophorus possessed three lower incisors, confirming Szalay's (1969a) prediction, but no single specimen at hand preserves all of

these teeth in their entirety, and i3 is known only from its root and crown base. None of the lower incisors in E. simpsoni is markedly enlarged, a feature that distinguishes Elpidophorus from mixodectines (compare, e.g., with lower incisors of Mixodectes; see Szalay, 1969a, pl. 20, fig. 5); in fact, the lower incisors in Elpidophorus are relatively small compared to those of contemporaneous mammals with similarly procumbent lower incisors (e.g., plesiadapids, apatemyids). The lower incisors are strongly procumbent, entering the dentary at an angle of approximately 30 degrees from horizontal and with the occlusal surfaces facing dorsally and slightly medially. The i1 and i2 are of similar morphology, with i2 larger than i1: the roots are laterally compressed and moderately deep, while the crowns are spatulate, long and narrow, and slightly constricted posteriorly. The medial and lateral margins of the crown are drawn out as weak crests, and the faintly concave occlusal surfaces face dorsally. The tips of i1-2 are chisel-like and usually exhibit heavy apical wear, particularly at the lateral margin where a faint notch is often scoured. The i3 is smaller than i1-2, and its root is more nearly circular in cross section, rather than strongly compressed, suggesting that the coronal anatomy of i3 may differ from that of i1-2, although confirmation of this must obviously await discovery of specimens preserving i3 in its entirety. The i3 is positioned at the extreme lateral margin the jaw, and is essentially wedged between the much larger i2 anteromedially and the swollen canine posterolaterally.

Lower canine: The lower canine of E. simpsoni is preserved in UALVP 40588, the first evidence of this tooth in Elpidophorus. The crown consists principally of a tall protoconid and small heel, and is slightly procumbent, with its anterior parts overlapping the posterior margin of the i3 crown. The protoconid is mediolaterally compressed and bladelike, but becomes considerably swollen towards its base, so much so that the width of the canine is nearly twice that of the succeeding p1. Short anterior and longer posterior crests extend from the apex of the protoconid: the anterior crest (paracristid) runs anterolabially and forms a low shelf, although a paraconid is not developed; the second crest runs posteriorly to the low, single-cusped heel. A stout postcristid extends transversely from the apex of the heel, forming a moderately deep lingual pocket and a shallow hypoflexid. Anterior and posterior cingulids are not developed.

Lower premolars: p1: The single-rooted p1 resembles the lower canine, albeit is significantly smaller, and the crown is less procumbent. The protoconid is low, labiolingually compressed and bladelike, and swollen at its base; the paracristid swings anterolingually, forming a short, low shelf, whereas the posterior crest runs to a low, unicuspid heel. As on the lower canine, the transverse postcristid forms a pocket on the posterolingual side of the swollen protoconid base, and a faint hypoflexid labially. Cingulids are not developed.

p2: The p2 of E. simpsoni is two-rooted and the crown is dominated by a tall, labiolingually compressed protoconid and a low, single-cusped heel. The protoconid is bladelike, as on p1, but is taller, more nearly vertical, and considerably more swollen at its base. A heavy paracristid runs anterolingually from the protoconid apex, forming a low shelf; a small paraconid can be developed at the anterior margin of the crown. A second crest arising from the protoconid apex runs posterolabially to a high, unicuspid heel; a narrow notch is developed in the deepest part of the posterior crest, setting the heel off from the base of the protoconid. As on p1, a thick postcristid extends labially and lingually from the apex of the heel on p2, forming a lingual pocket and a shallow hypoflexid.

p3: The p3 crown of E. simpsoni resembles that of p2, but differs in being larger and more swollen, and with a much better developed paraconid. The protoconid is tall and more nearly conical than on p2, but its base is similarly swollen. A heavy paracristid extends from the protoconid apex anteriorly and faintly labially to a conspicuous paraconid, rather than forming a low shelf. The paraconid is variably developed, ranging from a small and conical, nearly vertical cusp that is appressed to the base of the protoconid (e.g., UALVP 46427, Figs. 8.2.13-8.2.15) to a larger, labiolingually compressed and bladelike cusp that projects anterolingually (e.g., UALVP 40588, Figs. 8.3.1-8.3.3); in any case, a notch in the deepest part of the paracristid separates the paraconid from the base of the protoconid, and weak cingulids are developed anterolingually and anterolabially. The talonid on p3 is considerably better developed than that on p2: it is bicuspid on all specimens at hand, with a large hypoconid and smaller entoconid. The cristid obliqua is sharp and deeply notched, extending from the hypoconid to the summit of the protoconid. A weak postcristid connects the apices of the

hypoconid and entoconid, closing off the shallow talonid basin posteriorly; the entocristid is undeveloped, leaving the basin open lingually. The hypoflexid is relatively deeper than on p2, and a weak cingulid is present posteriorly.

p4: As with other species of Elpidophorus, the p4 of E. simpsoni is molariform, with a well-developed paraconid, metaconid, and protoconid, and well-differentiated talonid cusps. The conical protoconid is the largest and tallest cusp. The metaconid, lower and weaker than the protoconid, arises from low on the lingual side of the protoconid, with its dorsolingually directed apex lingually opposite or slightly posterolingual to that of the protoconid. The protoconid and metaconid are connate for nearly two-thirds of their height, and their apices are joined by a short and sharply notched protocristid. The paraconid is significantly larger than on p3: it is considerably swollen at its base but becomes increasingly compressed and bladelike apically, and its apex projects anteriorly. A sharp and widely V-shaped paracristid connects the paraconid and protoconid, and a slit-like notch can be developed at its deepest part. The talonid is relatively better developed than that of p3, being slightly wider than the trigonid and with the robust hypoconid and entoconid partially enclosing a shallow basin. The hypoconulid can vary from being a small but conspicuous cusp positioned slightly posterolabial to the entoconid and connected to it and the hypoconid by a high postcristid (e.g., UALVP 40588), to being no more than a bulge on the postcristid and separated from the entoconid by a deep notch (e.g., UALVP 46427); on some specimens the hypoconulid is not developed at all (e.g., UALVP 40582). The cristid obliqua is heavy and joins the postvallid wall at or just slightly labial to the protocristid notch, forming a deep hypoflexid. As on p3, the entocristid on p4 is undeveloped, leaving the talonid basin open lingually. With the exception of the short anterior cingulid, an ectocingulid is not developed, and the enamel is faintly wrinkled.

Lower molars: The lower molars of E. simpsoni resemble those of other species of Elpidophorus (see Simpson, 1927, 1936; Szalay, 1969a; Rose, in press): the crowns are skewed such that the lingual parts are higher than the labial parts, and lean somewhat anterolingually (although as noted earlier, the lingual cant of the crowns becomes less apparent when the dentary is held in an "in life" position); the talonids are wider than the trigonids; and well-developed anterior cingulids are present. The prominent paracristid,

protocristid, cristid obliqua, and hypocristid together form a well-defined, W-shaped ectolophid that complements the ectoloph of the upper molars.

m1: The trigonid of m1 is dominated by a tall metaconid and shorter protoconid that are connected by a deeply notched protocristid; the paraconid is poorly defined, being represented only by a slight swelling near the lingual terminus of the long paracristid. The apices of the trigonid cusps define an isosceles triangle in occlusal outline, with the two long arms of the triangle formed by the paracristid and protocristid. The talonid is markedly wider than the trigonid, with the bulbous base of the hypoconid jutting labially and forming a prominent exodaenodont lobe. While the spirelike entoconid is the tallest talonid cusp, the hypoconid is the larger cusp, being much more massive at its base. A small but conspicuous hypoconulid abuts the posterolabial side of the entoconid, and a deep notch separates the two cusps (the so-called nyctalodont condition of Menu and Sigé, 1971); the apex of the hypoconulid projects posterodorsally. A well-defined hypocristid connects the hypoconid with the hypoconulid, while the postcristid, instead of connecting the entoconid with the hypoconulid, extends directly labially into the talonid basin. Although the entocristid is low, it forms a conspicuous raised edge, meeting a metastylid crest extending from the posterior side of the metaconid to the talonid; together these crests form a V-shaped talonid notch and enclose the lingual margin of the talonid basin. An entoconulid is not developed. The cristid obliqua joins the postvallid wall labial to the protocristid notch, and a slit-like notch can be developed at its deepest part; a rudimentary mesoconid swelling is usually developed. The cingulids are heavy anteriorly and posteriorly, but remain discontinuous labially: the anterior cingulid curves across the labial side of the protoconid and forms a prominent ledge below the deep hypoflexid, while the posterior cingulid extends to the hypoconulid, forming a heavy shelf. The enamel is wrinkled, especially on the postvallid wall, where it is thrown into thick folds.

m2: The m2 of E. simpsoni closely resembles m1, differing mainly in the greater width of the trigonid and talonid, the more anteroposteriorly compressed trigonid, and in having a taller and larger metaconid. The paraconid is more labial in position compared to that on m1, and the paracristid and protocristid are more transverse, lengthening the arms of the anterior "V" of the ectolophid. The talonid on m2 is considerably wider than

that on m1, with both the labial and lingual margins bulging outwards; the hypoconulid is well developed, but the mesoconid remains a poorly defined swelling on the cristid obliqua. The enamel of the postvallid wall is deeply furrowed.

m3: Although the m3 is longer than either m1 or m2, it is narrower, and the talonid is subequally wide or slightly narrower than the trigonid. As with m1 and m2, the metaconid is the largest and tallest trigonid cusp, followed by a lower metaconid and paraconid; the paraconid on m3 is fully incorporated into the paracristid, and the paraconid+paracristid is lower and more shelf-like compared to m1 and m2. The entoconid and hypoconid are smaller and lower than on the other molars, but the conical and sharp hypoconulid is considerably larger. As with m1 and m2, the postcristid runs labially from the entoconid into the talonid basin, rather than to the hypoconulid, whereas the hypocristid runs lingually from the hypoconid apex towards the base of the entoconid, nearly bypassing the hypoconulid before turning abruptly posteriorly and ascending the anterior side of the hypoconulid to its apex. The weak mesoconid is similar to that on m1 and m2, and the enamel of the postvallid wall is heavily wrinkled.

Etymology.—Named in honour of George Gaylord Simpson for his early work on Elpidophorus.

Holotype.—UALVP 46427, incomplete right dentary with i1, i3 (i3 crown broken), c, p1-4 (p1 crown broken), m1-3, and alveolus for i2. Joffre Bridge Mammal Site No. 1, Paskapoo Formation of Alberta, late Paleocene [early middle Tiffanian, Ti3 (Fox, 1990a), Plesiadapis anceps/P. rex Lineage Zone of Lofgren et al., 2004].

Other material examined.—From Joffre Bridge Roadcut lower level: UALVP 40584, incomplete right maxilla with P2-3; UALVP 40572, 40595, P3; UALVP 46428, P4; UALVP 46429, M3; UALVP 40574, incomplete left dentary with p2-4, m1-3, and alveoli for 1-3, c, p1; UALVP 46431, incomplete left dentary with p1-4, m1, and alveoli for i2-3; UALVP 40586, incomplete right dentary with m1-2, alveoli for p1-4, m3, and associated i1 or i2; UALVP 40582, incomplete right dentary with p4 and alveoli for p1-3; UALVP 46432, incomplete left dentary with p4, m1-3 (all broken), and alveoli for p1-3; UALVP 46434, isolated m1 (trigonid).

From Joffre Bridge Mammal Site No. 1: UALVP 40590, incomplete left maxilla with C, P2-4, M1-3, and alveolus for P1; UALVP 40588, incomplete left dentary with i1-

3 (i3 broken), c, p1-4; UALVP 46430, incomplete left dentary with m2-3; UALVP 40589, incomplete right dentary with i1, i2-3 (broken), p1-3, p4 (broken), and canine alveolus; UALVP 46433, isolated left i1 or i2.

From DW-2: UALVP 40596, P4; UALVP 46435, M1; UALVP 46436, M3; UALVP 46437, 46438, isolated m2.

From Mel's Place: UALVP 46439, isolated m2.

Age and occurrence.—Early middle Tiffanian (Plesiadapis rex/P. churchilli Lineage Zone, Ti3, late Paleocene) of Alberta.

Discussion.—Although the dentition of Elpidophorus simpsoni resembles that of the better-known E. elegans (see later in this chapter), it differs in a number of important ways. The lower cheek teeth of E. simpsoni are longer relative to their width than are those of E. elegans, especially the lower molars, where the trigonid is less anteroposteriorly compressed and the metaconid is more nearly vertical, rather than lingually leaning. The P3/p3-P4/p4 of E. simpsoni are less fully molariform than those of E. elegans, with the paracone and metacone being weakly differentiated from one another (especially on P3), and the conules are smaller and less inflated. The upper molar centrocrista is deflected labially, but barely protrudes into the ectoflexus, and the protocone is nearly opposite the centrocrista loop, rather than anteriorly shifted. The relationships of E. simpsoni are considered in more detail later in this chapter.

E. simpsoni and E. elegans were sympatric during the late Paleocene in Alberta: in addition to their occurrence at the Blindman River and Joffre Bridge localities, E. simpsoni and E. elegans are also known from the earliest Tiffanian (Ti1) Cochrane 2 and Aaron's localities (Youzwyshyn, 1988; Fox, 1990a; pers. obs.).

ELPIDOPHORUS ELEGANS Simpson, 1927

Figures 8.4-8.6, 8.10.2, 8.10.5, 8.10.8, 8.10.11, 8.11.3, 8.11.7, 8.11.11, 8.11.15; Tables 8.4, 8.5

Elpidophorus elegans SIMPSON, 1927, p. 5.

Elpidophorus patratus SIMPSON, 1936, p. 11.

Revised diagnosis.—Differs from Elpidophorus minor in being 30 percent larger, in p4 having a larger metaconid and wider talonid, and lower molars being more transverse and having stronger cingulids. Differs from E. simpsoni in lacking P1/p1, and in cheek teeth being more transverse relative to length; differs further from E. simpsoni in P3-P4 having a better-separated paracone and metacone and labially deflected centrocrista and larger M3. Differs from E. clivus in being 15 percent larger, in P4 having a more weakly deflected centrocrista, an undeveloped hypocone and relatively weaker conules, and upper molars having weaker hypocones; differs further from E. clivus in p4 and lower molars having higher and more bladelike paraconids, and molar trigonids being less anteroposteriorly compressed.

Material examined.—From Joffre Bridge Roadcut lower level: UALVP 40587, incomplete maxilla with P4, M1-2; UALVP 40569, associated P2-3; UALVP 46440, P3; UALVP 40571, M2; UALVP 40585, incomplete right dentary with p3-4, m1-3, and alveoli for i1-3, c, p2; UALVP 40583, incomplete left dentary with m1, m3, and alveoli for p4, m2; UALVP 40578, incomplete right dentary with m2, and alveoli for p4, m1, and m3; UALVP 40593, incomplete and edentulous left dentary with roots of p3-4, m1-3, alveoli for i1-3, c, p2, and associated m1-2; UALVP 46442, p4

From Erickson's Landing: AMNH 15542, incomplete left dentary with m2-3.

From Joffre Bridge Mammal Site No. 1: UALVP 40570, incomplete right maxilla with P2-4, M1-3, and alveolus for C; UALVP 43097, incomplete left dentary with i1-2, p3-4, m1-3, and alveoli for i3, c, p2; UALVP 46441, incomplete left dentary with p2-4, and alveoli for c.

From DW-1: UALVP 40566, incomplete left maxilla with P3-4, M1-3.

From DW-2: UALVP 46443, incomplete and associated right and left maxillae with RP3-4, M1-3, and alveoli for C, P2, and LP2-4, M1-3, and alveolus for C; UALVP 40568, incomplete right maxilla with P4, M1-3, and associated M2; UALVP 40565, incomplete left maxilla with P4, M1-2; UALVP 40567, incomplete right maxilla with M1-3; UALVP 46444, incomplete right maxilla with M1-2; UALVP 46445, incomplete left maxilla with P3-4; UALVP 46446, incomplete left maxilla with fragmentary M1 and alveoli for P2-4, M2; UALVP 40594, incomplete and edentulous right maxilla with alveoli for C, P2-4, M1-3; UALVP 46447, P4; UALVP 46448, 46449, 46450, 46451,

46452, M2; UALVP 46453, M3; UALVP 46454, incomplete right dentary with p2-4, m1-3, and alveoli for i1-3, c; UALVP 40577, incomplete left dentary with p3-4, m1-2, and alveoli for i1-3, c, p2, and m3; UALVP 34126, incomplete right dentary with p3-4, m1-2; UALVP 46455, incomplete right dentary with p4, m1-3 (m3 trigonid only); UALVP 46456, incomplete right dentary with p4, m1-3, and alveoli for i1-3, c, p2-3; UALVP 40579, incomplete left dentary with p4, m1-3; UALVP 46457, incomplete right dentary with m1-3, and alveoli for i1-3, c, p2-4; UALVP 46458, incomplete left dentary with m1-3, and alveoli for p3-4; UALVP 46459, incomplete left dentary with m1-3, and alveoli for p4; UALVP 40592, incomplete right dentary with m1-3 (m3 trigonid only); UALVP 40576, incomplete right dentary with m2-3; UALVP 40580, incomplete right dentary with ?m2; UALVP 40674, incomplete left dentary with m2; UALVP 40575, incomplete right dentary with m3; UALVP 46460, i1; UALVP 46461, 46462, 46463, i2; UALVP 46464, p3; UALVP 46465, m2; UALVP 40591, 40673, m3.

From Birchwood: UALVP 39392, incomplete left maxilla with P2-4, M1-3; UALVP 39393, P3; UALVP 39394, 39395, P4; UALVP 39396, M2; UALVP 46466, 46467, M3; UALVP 39399, incomplete right dentary with p3-4, m1-2, and alveoli for i1-3, c, p2; UALVP 46468, incomplete right dentary with p3-4, m1-3, and alveoli for p2; UALVP 39398, incomplete left dentary with p4, m1-3, and alveoli for p2-3; UALVP 39397, incomplete left dentary with p4, m1-2, and alveoli for i2-3, c, p2-3, and m3; UALVP 46469, incomplete right dentary with p4, m1; UALVP 39405, incomplete right dentary with m2-3; UALVP 46470, incomplete left dentary with m1, and alveoli for m2-3; UALVP 46471, incomplete left dentary with m3; UALVP 39400, incomplete right dentary with i1-2; UALVP 39401, 39412, 39413, isolated lower incisor; UALVP 39402, lower canine; UALVP 39403, 39404, p3; UALVP 46472, m2; UALVP 46473, 39406, m3.

Age and occurrence.—Earliest Tiffanian (Plesiadapis praecursor/P. anceps Lineage Zone, Ti1, late Paleocene) to early middle Tiffanian (Plesiadapis rex/P. churchilli Lineage Zone, Ti3, late Paleocene) of the Western Interior of North America (Lofgren et al., 2004).

Description.—The dentition of Elpidophorus elegans has been described in detail by Simpson (1927, 1936) and Szalay (1969a). The teeth of E. elegans closely resemble

those of E. simpsoni, and descriptions here will focus primarily on previously unknown parts of the dentition, including the lower incisors, canine, and anterior premolars, and an assessment of the more pertinent differences between the dentitions of E. elegans and E. simpsoni.

Maxilla: Incomplete maxillae of Elpidophorus elegans are known from a number of specimens in the current sample that collectively document the facial process and infraorbital foramen, anterior root of the zygomatic arch, and parts of the bony secondary palate. Examination of the comparable skull elements of E. elegans and E. simpsoni reveals a number of important differences. For example, although the maxillary facial process in E. elegans and E. simpsoni is tall, the infraorbital foramen in E. elegans is much larger, with a taller and more ovate aperture (see UALVP 40570, Figs. 8.4.1, and compare with UALVP 40590, E. simpsoni, Fig. 8.2.1); an enlarged infraorbital foramen has been interpreted as indirect evidence of mobile lips or a highly tactile rhinarium in other fossil mammals (see, e.g., Radinsky and Ting, 1984). Additionally, the zygomatic arch of E. elegans is considerably stouter at its root compared with that of E. simpsoni, and originates slightly more anteriorly (e.g., UALVP 40566). Although the palatal process of the maxilla bears numerous tiny nutritive foramina, there is no evidence of palatal vacuities.

Upper dentition (Fig. 8.4): Upper canine: The present sample includes several incomplete maxillae of E. elegans, and although none contains teeth anterior to P2, three specimens preserve evidence of an alveolus anterior to P2 that apparently housed a single-rooted tooth. None of the specimens at hand clearly preserves the premaxilla-maxilla suture, making the identity of the alveolus uncertain; comparisons with the upper dentition in E. simpsoni (which has a complete post-incisor dentition, with an upper canine and four premolars), however, indicate that the alveolus likely represents the canine locus for the following reasons:

1) The alveolar rim is best seen in the left and right maxillae of UALVP 46443, and especially in UALVP 40570 (Figs. 8.4.2, 8.4.3), with the large, circular aperture being as large as the combined two alveoli for P2; in contrast, the P1 alveolus in Elpidophorus simpsoni (UALVP 40590, Fig. 8.2.3) is small, suggesting that P1 was smaller than the upper canine and P2, as is usually the case in tribosphenic therians

generally, whereas the upper canine is larger and clearly occupied a correspondingly larger alveolus;

2) The alveolus is separated from P2 by a short diastema in UALVP 46443 (Fig. 8.4.10, arrow), a common occurrence in mammals that have lost P1 but retained the upper canine and P2 (e.g., Pronothodectes gaoi Fox, 1990b, see Chapter XX); in UALVP 40590 (E. simpsoni), the P1 alveolus closely abuts the upper canine and P2, with no diastemata developed;

3) As explained later in this chapter, the lower dentition of E. elegans clearly lacks a lower canine, although this admittedly carries less weight given that incongruent losses of upper and lower antemolar teeth have occurred repeatedly in other mammalian groups (e.g., plesiadapiforms, see Silcox, 2001).

4) There is no evidence of an alveolus anterior to the putative canine alveolus, although the bone is largely damaged in this area in each of the specimens at hand that preserves these parts.

A poorly preserved premaxilla and maxilla from the early Tiffanian (Ti2) Scarritt Quarry of Montana, referred to E. elegans by Szalay (1969a), further complicates matters. The specimen, AMNH 35963, preserves P4, M1-3, and alveoli for an indeterminate number of teeth between the enlarged anterior alveolus (presumably for I2, see Szalay, 1969a) and P4. Although the five alveoli immediately anterior of P4 presumably housed a two-rooted P2 and three-rooted P3, the number of alveoli anterior to P2 cannot be unequivocally determined, nor can the position of the premaxilla-maxilla suture. As a consequence, Szalay (1969a) cautiously suggested that two alveoli, representing C and P1, occurred between the enlarged anterior alveolus and the anterior alveolus for P2, but given the poor preservation of the most crucial parts of AMNH 35963, the alternative interpretations seem no less plausible. Although AMNH 35963 was not examined directly for this study, the closely appressed P3 paracone and metacone, as well as the relatively smaller proportions of M3 (when compared with M3 in E. elegans) are characteristic of the upper dentition of E. simpsoni (see earlier in this chapter), suggesting AMNH 35963 may be better referred to that taxon; as such, the alveoli may well represent those for C and P1, as Szalay (1969a) originally suggested.

Upper premolars: P2: The upper premolars of E. elegans closely resemble those of E. simpsoni, but are larger, with better-developed cusps, conules, and crests. The two-rooted P2 of E. elegans is only slightly longer and wider than P2 of E. simpsoni, but has a significantly more swollen base, better-developed metastylar cusp, and a weaker anterior crest. A faint posterolingual swelling is developed over the lingual half of the posterior root.

P3: The P3 of E. elegans supports a fully differentiated paracone, metacone, and a generally well-developed protocone. As in E. simpsoni, the posteriorly leaning crown of P3 is triangular in occlusal outline, and a strong exodaenodont lobe occurs at the anterior root. The paracone and metacone are both well developed, with the metacone slightly smaller and shorter; the cusps are better differentiated and further separated from one another than in E. simpsoni, and their apices are connected by a thick and deeply V-shaped centrocrista, the deepest part of which contains a narrow, slit-like notch. A low but robust cusp is developed anterior of the paracone. The postmetacrista in E. elegans is much more conspicuous than in E. simpsoni, sweeping posterolabially to the metastylar corner of the crown where it joins one, or sometimes two small metastylar cusps. The conules are variably developed: on some specimens (e.g., UALVP 46443) only a prominent metaconule is present, while on others (e.g., UALVP 40570) a small paraconule and metaconule can occur, and on still other specimens (e.g., UALVP 40566) both conules can be wholly undeveloped. The protocone is consistently larger and more inflated than that on P3 of E. simpsoni.

P4: The P4 of E. elegans resembles that of E. simpsoni, but differs in a number of important ways. The paracone and metacone are better differentiated from one another in E. elegans, with the bases more clearly separate and the apices connected by a widely notched, and in some specimens a weakly (e.g., UALVP 39395, Fig. 8.4.16) or moderately (UALVP 39394, Fig. 8.4.13) labially deflected centrocrista. The parastylar and, especially, metastylar cusp are more robust, and the preparacrista and postmetacrista are longer. The shelf-like conules are larger and more inflated than those in E. simpsoni, and each is separated from the base of the protocone by a narrow notch; the conular cristae are prominent. The protocone of E. elegans is much taller and more massive than in E. simpsoni, and labial exodaenodonty is better developed.

Upper molars: The upper molars of E. elegans resemble those of E. simpsoni, but are more robust, with more swollen cusps and crests; they further differ as follows:

1) The molars of E. elegans are larger and more transverse than those of E. simpsoni, particularly M3, which is notably more transverse and longer;

2) The preparacrista and especially the postmetacrista (the outer arms of the W-shaped ectoloph) are longer in E. elegans, and the stylar shelf is correspondingly wider;

3) The oblique trough in E. elegans is longer and wider;

4) The conules are larger and more inflated in E. elegans, and are separated from the protocone by deep notches in the protoconal cristae;

5) The conular cristae are stronger in E. elegans, and in some specimens the preparaconular and postmetaconular cristae remain separate from the anterior and posterior cingulum, respectively (the external conular cristae fuse with the protoconal cingula in E. simpsoni);

6) The protocone is more anterior (its apex is more nearly in-line with that of the paracone), and the crowns are somewhat oblique, rather than nearly perpendicular, to the long axis of the skull;

7) The hypocone is better differentiated from the posterior cingulum; on some specimens (e.g., UALVP 46443, Fig. 8.4.10) it is somewhat swollen at its base, forming a distinct hypoconal lobe.

Dentary (Figs. 8.5.1-8.5.6, 8.6): The dentary of E. elegans is resembles that in E. simpsoni: for example, the horizontal ramus is boat-shaped in lateral view, the dentary becomes shallower towards p3, then deepens at the symphysis, and the symphyseal surface is raised above the level of the surrounding bone, forming an interdigitating network of bony hillocks and crevasses; additionally, a thick crest delimits the anterior margin of the deeply excavated masseteric fossa, and three mental foramina are usually developed). Despite these similarities, the dentary of E. elegans differs from that of E. simpsoni in a number of important ways. The horizontal ramus is deeper and more robust, particularly anteriorly where the lower incisors are implanted more nearly vertically (see later in this chapter), and the symphyseal surface is raised higher from the surrounding bone and is considerably more rugose, suggesting a tighter suturing of the two dentaries in life. Although the coronoid process is poorly preserved in the specimens

at hand, its anterior parts indicate that it was deep and more steeply inclined from the horizontal ramus than that in E. simpsoni (see especially UALVP 46468, Figs. 8.6.7-8.6.9). The robust angular process extends posteroventrally at an angle of about 160-degrees from the long axis of the dentary. A strong ridge divides the medial side of the process into upper and lower surfaces for the insertion of the internal pterygoid above and external masseter below. The distal parts of the angular process are not preserved in any of the specimens at hand.

Lower dentition (Figs. 8.5, 8.6): Lower incisors: The i1-2 of E. elegans are known from isolated (e.g., UALVP 46461, 46462, Figs. 8.5.7-8.5.12) and articulated (e.g., UALVP 43097, Figs. 8.5.1-8.5.3) specimens; the i3 is known only from its alveolus. The i1-2 of E. elegans are larger and more robust than those of E. simpsoni, and are implanted in the dentary more nearly vertically, at an angle of approximately 45 degrees from horizontal; the roots are oriented more nearly dorsoventrally, and the crowns project well above the level of the alveolar surface of the jaw. While the crown of i1 is closely similar in both taxa, the i2 is more complex in E. elegans: the i2 crown is faintly expanded apically, swollen basally, and appears somewhat S-shaped in occlusal view. The crown is shallowly notched anteromedially, forming a large, anterolaterally projecting apical cusp, and a smaller medial cuspule that abuts the lateral side of i1 (see UALVP 39400, Figs. 8.5.13-8.5.15). Wear is concentrated at the apex of i2, but also laterally, with a deep facet often having been scoured into the crown between the apical cusp and the base. The i3 is unknown, but the dimensions and position of its alveolus indicates the tooth was relatively smaller than in E. simpsoni, and "squeezed" farther towards the lateral margin of the dentary.

The lower jaw of E. elegans preserves alveoli for only two teeth between the i3 alveolus and p3, and these are interpreted as having housed a single-rooted lower canine and a one, or sometimes two-rooted p2. A short diastema usually intervenes between the lower canine and p2 (e.g., UALVP 40585, 43097, AMNH 33856), but in some specimens (e.g. UALVP 46457) the canine alveolus is more closely appressed to that for p2.

Lower canine: A single lower canine, UALVP 39402, is referred here to E. elegans: it closely resembles that of E. simpsoni in being premolariform, with a procumbent crown, and well-developed posterior basal cuspule; it is larger and slightly

more swollen than in E. simpsoni, but is relatively smaller when compared to the other cheek teeth.

Lower premolars: p2: Although the p2 of E. elegans closely resembles that in E. simpsoni, it differs in its smaller size relative to the other cheek teeth (similar to the canine), in being more swollen, and in having a much more poorly developed anterior cuspule and anterior crest. The p2 can be single-rooted (e.g. UALVP 43097) or double-rooted (e.g. UALVP 46457), but in either case the root or roots occupy a single alveolus.

p3: The p3 of E. elegans differs from that of E. simpsoni in being slightly larger, but considerably more swollen, in having a more poorly developed anterior cuspule, and in having better-developed talonid cusps.

p4: Although the p4 of E. elegans, like that of E. simpsoni, is a large, molariform tooth, it differs from that of E. simpsoni in a number of important ways. The crown is larger and more transverse, with better-developed cusps, especially the lingually leaning metaconid, which becomes the dominant trigonid cusp. The protocristid is notably longer, particularly the metaconid arm. The paraconid is taller and more robust, and can project anteriorly or be positioned more lingually; the paracristid notch is wider. The talonid of E. elegans is significantly wider than that of E. simpsoni, in most cases jutting labially past the level of the trigonid, and the hypoconid is much more prominent. When present, the hypoconulid in E. elegans is similar to that in E. simpsoni, ranging from a weakly developed cusp that can abut the entoconid (UALVP 40585, Figs. 8.6.4-8.6.6), to an ill-defined swelling or series of cuspules on the postcristid, to being wholly undeveloped (UALVP 46454, Figs. 8.6.1-8.6.3).

Lower molars: As with the upper molars, the lower molars of E. elegans resemble those of E. simpsoni, but differ in the following ways:

1) The crowns of E. elegans are larger, swollen, and more transverse, especially m3;

2) The crowns of E. elegans lean further lingually than do those of E. simpsoni, particularly the metaconid and entoconid, significantly lengthening the protocristid and postcristid;

3) The paraconid/paracristid of E. elegans extends farther lingually, lengthening the paracristid (anterior arm of the ectolophid);

4) The metaconid is considerably taller and more inflated on the molars of E. elegans, and the disparity in size between the metaconid and protoconid is much greater than it is in E. simpsoni;

5) The hypoconulid is relatively more poorly developed and more lingual on m1-2 in E. elegans, effectively forming a longer and more nearly continuous hypocristid between the hypoconid and the entoconid;

6) The entoconid is taller, the hypoconid is more robust, and the mesoconid is stronger in E. elegans.

Discussion.—The sample from Alberta is among the largest known for E. elegans, and documents parts of the dental and gnathic anatomy that were poorly known or previously unknown. Perhaps the most unexpected discovery is that the snout and lower jaws of E. elegans appear to be foreshortened compared to those in E. simpsoni: E. elegans apparently lacked P1/p1 [although loss of P1/p1 is a relatively common trend in archontans and other groups of mammals (e.g., plesiadapiform primates, scandentians), it was previously unknown for any species of Elpidophorus]; the p2-3 in E. elegans are smaller relative to p4 when compared to those in E. simpsoni, and are notably wide relative to their length, appearing somewhat "squat" is labial view; and the anterior post-incisor dentition in E. elegans is crowded towards the anterior part of the dentary. Furthermore, the dentary in E. elegans is more robust and deeper than that in E. simpsoni, and the coronoid process is more nearly vertical. Taken together, the shorter and deeper jaws, reduced anterior dentition, wider, more bulbous lower premolars, enhanced dilambdodonty, and generally more robust teeth suggest that E. elegans may have been better-suited for processing food items that were more resistant than was E. simpsoni. The phylogenetic relationships of E. elegans are discussed later in this chapter.

ELPIDOPHORUS CLIVUS new species

Figures 8.7, 8.8, 8.10.3, 8.10.6, 8.10.9, 8.10.12, 8.11.4, 8.11.8, 8.11.12, 8.11.16; Tables 8.6, 8.7

Diagnosis.—Differs from all other species of Elpidophorus in having a more fully molariform P4/p4, lower molars with anteroposteriorly compressed trigonids and

significantly wider talonids, and in having a well-differentiated hypocone on M1-2. Differs further from E. simpsoni and E. elegans in being approximately 15 percent smaller, in having a strongly labially deflected P4 centrocrista, in having a reduced molar hypoconulid, and in having a much taller metaconid relative to protoconid, with a greatly elongate metaconid arm of the protocristid. Differs further from E. minor in being approximately 15 percent larger, with more fully molariform p3-4, and in having a much wider molar trigonid and talonid.

Description.—Upper dentition (Fig. 8.7): Upper canine or P1: UALVP 22625 closely resembles the upper canine of E. simpsoni, differing primarily in its smaller size. The crown is premolariform, and consists of a tall paracone and swollen base; a weak paracristid extends anteriorly from the paraconal apex to a faintly developed basal cuspule, while a second crest runs posterolingually, weakening as it nears the base of the crown. The crown of UALVP 22625 differs from the upper canine of E. simpsoni in having a proportionately more swollen base, weaker anterior cuspule, and in lacking a posterobasal cusp. Although UALVP 22625 resembles the upper canine in E. simpsoni, it may well represent P1 instead. Maxillae preserving the anteriormost parts of the post-incisor dentition of E. clivus are not yet known, and P1 is unknown for any species of Elpidophorus (although its coronal anatomy likely differs little from that of the upper canine or P2); a choice between these alternatives must obviously await discovery of better preserved specimens than are presently available.

Upper premolars: P2: The crown of P2 more closely resembles that of E. elegans than that of E. simpsoni in having a weak posterolingual swelling at the posterior root; the crown is significantly less swollen than in E. elegans, however, with a deeper exodaenodont lobe at the anterior root, and the metastylar cuspule is weaker.

P3: The crown of P3 is subtriangular in outline, with well-developed principal cusps. The paracone and metacone are well separated from each other, with a deeply notched centrocrista connecting the apices of the two cusps; the premetacrista in UALVP 40584 is weakly deflected labially. A robust cusp is developed at the parastylar corner of the crown, its apex joining with the heavy ectocingulum and anterior cingulum. The metacone is proportionately taller than that on P3 of E. simpsoni and E. elegans, and the postmetacrista is longer and can bear one or two small metastylar cuspules. The

ectocingulum is variably developed, being heavier and more nearly complete across the labial margin of the crown (e.g. UALVP 22264, Fig. 8.7.7) or narrower and more diffuse (e.g. UALVP 22263, Fig. 8.7.10); as on P2, the exodaenodont lobe on P3 is better developed than that in E. simpsoni or E. elegans. The protocone is tall, subconical, and well separated from the base of the paracone and metacone. Conspicuous protoconal cristae extend labially from the apex, joining the anterior and posterior cingula; a weak crest that extends labially from the protoconal apex into the trigon basin is developed on one specimen (UALVP 22262). A small paraconule, and on one specimen (UALVP 22262) a prominent metaconule, is present, although the conular cristae are poorly developed in each of the P3s at hand. The anterior and posterior cingula are discontinuous lingually.

P4: As with other species of Elpidophorus, the P4 of E. clivus is fully molariform. The crown is as wide, or wider, than that of M1, and bears well-developed principal cusps and conules. The metacone is considerably stronger than that on P4 of E. elegans: the cusp is as tall, and in some specimens taller, than the paracone, and the two cusps are fully separate from base to apex. Unlike P4 in E. simpsoni and E. elegans, the P4 centrocrista in E. clivus is fully deflected labially, forming a notable labial protuberance; the centrocrista is looped at its labial margin, similar to that on the upper molars, and closes off the labial extremity of a trough that extends obliquely anterolingually-posterolabially from the labial side of the protocone. The basin-facing sides of the paracone, metacone, and conules are flat, forming parts of the labial walls of the oblique trough. A salient parastylar cusp is developed anterior and slightly lingual to the paracone, and is separated from the latter by a deep notch in the preparacrista; the postmetacrista is long, sweeping to the posterolabial corner of the crown. The conules are robust and shelf-like, with flattened labial sides; the metaconule is larger, taller, and more labially positioned than the paraconule. The external conular cristae are better developed than the internal cristae, and the preparaconular crista extends anteriorly to the anterior cingulum, abutting the crest and not continuing to the parastylar cusp as the paracingulum (in contrast to some specimens of E. elegans in which the preparaconular crista can extend to the parastylar cusp dorsal of the anterior cingulum). The protocone is anteriorly positioned, similar to that in E. elegans, and low protoconal cristae connect the

protocone to the conules. The protoconal cingula are robust, particularly the posterior cingulum where a small hypocone can be developed (e.g., UALVP 22362, Figs. 8.7.22-8.7.24).

Upper molars: The upper molars of E. clivus resemble those of E. elegans, differing primarily in their smaller size and, more importantly, in the development of a larger, more prominent hypocone. The M1 hypocone in E. clivus is somewhat crest-like apically, but becomes greatly swollen towards its base, bulging posteriorly and forming a distinct lobe that is separated from the protocone by a wide cleft. The hypoconal lobe effectively squares off the posterior margin of the crown, and M1 is hence more nearly rectangular in occlusal view than is that in E. simpsoni or E. elegans. The M2 hypocone is larger and more cuspate than that on M1, with the hypoconal lobe separated from the protocone by a wider cleft. The upper molars of E. clivus generally resemble those of E. elegans and E. simpsoni, but differ in the following ways:

1) The protocone in E. clivus is positioned farther anterior than that in E. simpsoni, at about the same level as that in E. elegans;

3) The M3 of E. clivus is proportionately smaller relative to M2 than in other species of Elpidophorus;

4) The cusps and conules of E. clivus are more bulbous and swollen than those of E. simpsoni and, to a lesser extent, those of E. elegans.

Lower dentition: Lower incisors: The lower first incisor is represented by UALVP 22379, a badly damaged specimen with only the apical half of the crown intact. The tooth is robust and proportionately much larger than i1 of E. simpsoni and E. elegans. The apex is chisel-like, similar to that in E. simpsoni and E. elegans, with the crown faintly notched at its apicolateral margin, forming a small but distinct lateral cuspule.

The i2 of E. clivus closely resembles that of E. elegans: the crown is faintly expanded apically, and the lateral margin is slightly concave between apex and base; it differs from that in E. elegans in the medial margin of the crown being significantly more concave in occlusal view. The apex of the crown is shallowly notched towards its apicomedial margin, forming a small but distinct anteromedial cuspule that likely would have abutted the lateral cuspule of i1 in life. The lateral margin of the crown is heavily worn, similar to that in E. elegans.

Lower canine or p1: UALVP 39760 and 39765 closely resemble the lower canine and p1 in E. simpsoni: the teeth are slightly procumbent and premolariform, with a large, swollen protoconid dominating the crown; a short crest extends from the protoconid apex anteriorly to a low, shelf-like cuspule, while a second crest runs posteriorly to a small but conspicuous heel.

Lower premolars: p2: The p2 of E. clivus is two-rooted, although it cannot be determined from the evidence at hand whether or not the tooth occupied one or two alveoli. The crown closely resembles that of E. simpsoni and E. elegans: the protoconid is more nearly vertical than that on the canine or p1, and it is the largest and best-developed cusp on the crown. The crown differs from that in E. simpsoni or E. elegans in lacking an anterior cuspule (the paracristid curves anterolingually from the protoconal apex, but a distinct cusp is not formed), and the hypoconid is more labially positioned, and the postcristid is transversely longer.

p3: The crown of p3 consists of a tall, vertical, and basally swollen protoconid and a short but well-developed talonid. A thick crest curves anterolingually from the protoconid apex to a small basal cuspule; on one specimen (UALVP 22346, Figs. 8.8.16-8.8.18) a larger, more anteriorly projecting paraconid is developed. A long cristid obliqua extends posteriorly to the talonid, connecting the protoconid apex with that of the tall hypoconid; the cristid obliqua can be sharply notched at its deepest part. The talonid cusps are variably developed: for example, in UALVP 22330 (Figs. 8.8.13-8.8.15), a small hypoconulid and entoconid can be discerned as swellings on the lingually sloping postcristid, while on UALVP 22346 (Figs. 8.8.16-8.8.18) two cusps are present, and on UALVP 22258, only the hypoconid is developed. The talonid basin is short and shallow, but is notably wider transversely than on p3 of E. simpsoni and E. elegans, with the hypoconid positioned farther labially. A weak posterior cingulid can be present, and often bears a small cuspule.

p4: The p4 trigonid in E. clivus is equilaterally triangular in occlusal view, with trigonid cusps that are somewhat less swollen than in other species of Elpidophorus. The metaconid is the largest and tallest trigonid cusp; it is relatively better developed, farther anterior, and less lingually leaning than in other species of Elpidophorus. A deeply notched protocristid, formed by an elongate metaconid arm and much shorter protoconid

arm, connects the metaconid to the lower protoconid. The paraconid is unusual compared to that in other species of Elpidophorus: it is considerably less swollen and more lingually positioned, and leans anteriorly to form a broad, flat platform. Heavy wear is usually developed on the paracristid, and the platform-like paraconid probably furnished a broad surface for grinding as the paraconid apex became lowered through extended wear. The talonid is significantly wider than that in E. simpsoni and E. elegans, with taller and more spirelike cusps. The hypoconid is lower but more massive than the entoconid, and is positioned labial of the level of the protoconid, significantly lengthening the cristid obliqua; a hypoconulid is not developed, and the hypoconid and entoconid are connected to one another by a long postcristid. The entocristid is raised and bladelike, and a heavy accessory crest extends from the entoconid into the talonid basin. The ectocingulid is generally better developed than in other species of Elpidophorus, particularly below the hypoflexid where it forms a conspicuous shelf.

Lower molars: The lower molars of E. clivus differ from those of E. simpsoni and E. elegans as follows:

1) The anteroposterior compression of the trigonids is greater in E. clivus, and the trigonids are more transverse;

2) The cusps are less inflated, proportionately taller, and more nearly spirelike;

3) The trigonids of E. clivus lean anteriorly, similar to those of E. elegans, but differing from those of E. simpsoni in which they are more nearly vertical;

4) Paraconid/paracristid are lower and more anteriorly projecting in E. clivus, forming a low shelf, and differing from the higher and more crest-like paracristid in other species of Elpidophorus;

5) The talonids of E. clivus are relatively more transverse, and cusps are higher and more spirelike than are those of E. simpsoni and E. elegans, and the mesoconid is poorly developed;

6) The hypoconulid is considerably weaker in E. clivus, especially on m2;

7) The m3 of E. clivus is smaller than in other species of Elpidophorus, and the talonid is wider than the trigonid.

Discussion.—E. clivus was described by Stonley (1988) as part of his thesis research on late middle Tiffanian (Ti4) mammals from the Swan Hills locality of north central Alberta. The relationships of E. clivus are discussed in detail later in this chapter.

Etymology.—Clivus, Latin, hill, in reference to the Swan Hills of north central Alberta.

Holotype.—UALVP 22317, incomplete right dentary with p4, m1-3. Swan Hills Site 1 locality, Paskapoo Formation of Alberta, late Paleocene [late middle Tiffanian, Ti4 (Stonley, 1988; Fox, 1990a), Plesiadapis rex/P. churchilli Lineage Zone of Lofgren et al., 2004].

Other material examined.—UALVP 22377, incomplete maxilla with P4, M1; UALVP 22625, 23842, ?upper canine or P1; UALVP 22409, 22711, 39759, P2; UALVP 22263, 22264, 22556, P3; ROM 05610, UALVP 22259, 22260, 22261, 22262, 22361, 22362, 22488, 22557, 22558, 22559, 22560, 22561, 22563, 22564, 22565, 22713, 22720, P4; UALVP 5783, 22265, 22266, 22267, 22268, 22363, 22364, 22365, 22366, 22367, 22368, 22369, 22370, 22371, 22488, 22489, 22514, 22566, 22567, 22568, 22569, 22570, 22571, 22572, 22573, 22721, 23841, M1; ROM 05609, UALVP 22269, 22270, 22271, 22272, 22273, 22372, 22518, 22574, 22575, 22576, 22577, 22578, 22579, 22580, 22581, 22722, 23838, 23840, M2; ROM 05611, UALVP 22274, 22278, 22374, 22582, 22583, 22584, 22585, 22586, 22587, M3; UALVP 22318, incomplete dentary with m1-2; ROM 05612, incomplete dentary with m2-3; UALVP 22378, 22379, 23839, lower incisors; UALVP 22712, 22717,?lower canine or p1; UALVP 22258, p2; UALVP 22330, 22345, 22346, p3; ROM 05621, 05627, UALVP 22280, 22284, 22285, 22286, 22287, 22288, 22289, 22316, p4; UALVP 22282, 22283, 22375, 22376, 22588, 22716, 22718, m1; UALVP 22279, 22281, 22589, 22590, m2; ROM 05613, UALVP 22275, 22276, 22277, 22373, 22591, 22592, 22715, 22719, m3.

Age and occurrence.—Type locality only.

ELPIDOPHORUS species indeterminate

Figure 8.9

Material examined.—From Joffre Bridge Mammal Site No. 1: UALVP 40581, 46474, upper incisors.

From DW-1: UALVP 46475, upper incisor.

From DW-2: UALVP 46476, 46477, upper incisors.

From Birchwood: UALVP 39391, upper incisor.

From Swan Hills Site 1: UALVP 22472, 22527, upper incisors.

Description.—Articulated upper incisors of Elpidophorus remain unknown, despite nearly 80 years of collecting since Simpson (1927) first described E. elegans. Associated upper incisors were discovered with the holotypes of E. elegans (described briefly by Simpson in 1927) and E. "patratus" (described briefly by Simpson in 1936). Szalay (1969a) provided a more thorough description of the incisor associated with the holotype of E. "patratus" (AMNH 33857), suggesting it probably represented the medial upper incisor of E. elegans. Included in the UALVP collections are a number of isolated upper incisors from the Blindman River, Joffre Bridge, Birchwood, and Swan Hills localities that closely resemble the teeth described by Simpson and Szalay, and are tentatively referred here to Elpidophorus. Because two species of Elpidophorus have been identified at the Blindman River and Joffre Bridge localities (E. simpsoni, E. elegans), and because the number of upper incisors in Elpidophorus remains unknown, referral of one or both incisor morphs to one species or the other is not possible at the present time; as such, they will be described as morphs. The isolated incisors from Swan Hills almost certainly pertain to E. clivus.

Upper incisor type A: Type A upper incisors have been recovered at DW-2 and Joffre Bridge. The crown closely resembles that in AMNH 33857, an isolated, presumably medial upper incisor associated with the type specimen of E. "patratus" (=E. elegans, see Szalay, 1969a); the tooth was originally described by Simpson (1936) and redescribed and figured by Szalay (1969a). The crown is anteroposteriorly compressed and multicuspate. The term "lobate" has sometimes been used when describing the crown of the upper and lower incisors of Elpidophorus (see e.g., Rose, 1975), presumably to emphasize perceived similarities with the lobed or digitate incisors of plagiomenids and extant dermopterans. This terminology is not adopted here: the crown of the referred upper incisors of Elpidophorus is mitten-like and bears a number of discrete and sharply

differentiated cusps that are connected to one another by raised crests, as opposed to being subdivided into a number of lobes or tines by deep valleys; in these respects the upper incisor crown of Elpidophorus is no more "lobate" than are the upper central incisors of, e.g., plesiadapids. The root is long and stout, and tapers gently towards the base. The crown is anteroposteriorly compressed and mitten-like, with convex anterior and shallowly excavated posterior sides; it is arcuate in lateral view, and bends medially towards the opposing incisor. Three conspicuous cusps are arranged sequentially on the crown in a shallow mediolateral arc: the central cusp is the largest and tallest on the crown: it is subovate in cross section, with a swollen base, and an apex that projects anteriorly, laterally, and ventrally. A short, sharp, V-shaped crest connects the central cusp to the smaller, lower medial cusp. The swollen medial cusp is more nearly conical than the central cusp, and its apex projects anteriorly and ventrally; an interdental facet is developed along its medial side. A deep sulcus occurs just dorsal of the apex of the medial cusp on its posterior side, and extends dorsally towards the base of the crown where it abruptly ends; the medial wall of the sulcus is raised as a conspicuous crest that is heavily worn. A long sharp crest running posterolaterally connects the central cusp to a much smaller and lower posterolateral cusp; a similar, but much shorter crest runs posteriorly from the posterolateral cusp to an incipient cuspule, and then towards the base of the crown where it fades away. The base of the crown is slightly swollen and is superficially divided by a shallow, dorsoventrally directed sulcus. Strong apical wear is developed on each of the three main cusps, and two large, circular facets have been scoured into the posterior surface of the crown: the larger of these facets is developed below the central and medial cusps, while the smaller occurs on the swollen base adjacent to the posterolateral cusp.

Upper incisor type B: The crown of incisor type B closely resembles that of type A, but is slightly larger and the cusps are more robust. The central cusp of type B is relatively larger than that on type A, more strongly compressed and bladelike, and the crests extending from its apex to the medial and posterolateral cusps are sharper. The most conspicuous differences in coronal anatomy between types A and B incisors pertain to the accessory cusps and the basal parts of the crown. The medial cusp on incisor type B is about the same size as that on type A, but is more compressed and bladelike, and

separated from the apical cusp by a sharper and more widely notched crest; the interdental facet on the medial surface of the medial cusp is prominent, and the deep sulcus seen on type A incisors is instead replaced by a weak flange on type B incisors. In contrast to the single, poorly developed posterolateral cusp on type A incisors, two, or sometimes three well-developed posterolateral cusps occur on type B incisors: these cusps decrease in size and height posterolaterally, and are closely appressed to one another, with narrow, slit-like notches developed between each. The base of the crown is divided into distinct posteromedial and posterolateral lobes, similar to that in type A incisors, but the lobes in type B incisors are considerably more swollen, and the sulcus separating them is much better defined.

Swan Hills incisors: Two fragmentary upper incisors (UALVP 22472 and 22527) have been recovered from the Swan Hills locality, and although the two teeth are damaged, the parts that remain closely resemble comparable structures on incisor types A and B. UALVP 22472 and 22527 are incomplete apically, but judging from the dimensions of the parts that are preserved, the median incisor of E. clivus was smaller than either type A or type B incisors, but was similarly enlarged relative to the cheek teeth, anteroposteriorly compressed, and polycuspate. The most striking difference between the upper medial incisor of E. clivus and type A and B incisors is the development of the posterolateral lobe: it is proportionately much larger in UALVP 22472 and 22527 than on either type A or type B incisor, and it bears a large, conical cusp; in one specimen (UALVP 22527), the cusp is connected posteriorly to a small, incipiently developed cuspule by a low crest, and in both specimens the posterolateral lobe cusp is connected to the penultimate accessory cusp by a sharp crest.

Discussion.—Despite more than 80 years of subsequent collecting, AMNH 33857 remains the only specimen known in which an upper incisor has been discovered in association with other parts of the dentition that can be confidently referred to Elpidophorus; the unusual, mitten-like upper incisors in the present sample are provisionally referred to Elpidophorus based on this association. The number of upper incisors in Elpidophorus is unknown, although AMNH 35963 (incomplete premaxilla and maxilla of E. elegans, Scarritt Quarry, Montana) documents the presence of at least two enlarged teeth, both of which were probably contained in the premaxilla (Szalay, 1969a).

Szalay (1969a) interpreted AMNH 35963 as having alveoli for two enlarged incisors, followed by a smaller canine; the premaxilla-maxilla suture apparently cannot be discerned in this specimen, and Szalay acknowledged the possibility that the smaller alveolus could have held a reduced I3, with a tiny canine and larger P1 (the area in question is damaged on AMNH 35963 such that the presence of one or two alveoli cannot be determined). The present sample cannot resolve these uncertainties. While incisor types A and B almost certainly represent different morphs of the medial incisor (both have well-developed interdental facets medially, suggesting the opposing I1s abutted one another in life; interdental facets are not developed laterally), the presence of two species of Elpidophorus from the Blindman River and Joffre Bridge localities makes unequivocal referral of the incisor morphs to one species or the other impossible.

8.3 Conclusions

Interrelationships of Species of Elpidophorus

The evidence now available indicates that four species of Elpidophorus were present in the Western Interior of North America during the Paleocene: E. minor, E. simpsoni, E. elegans, and E. clivus. E. minor is known only from the middle to late Torrejonian (To2-To3, early Paleocene) (Simpson, 1937; Gunnell, 1989; Scott, 2003; Rose, in press), whereas E. simpsoni and E. elegans are known from the earliest Tiffanian through the early middle Tiffanian (Ti1-Ti3, late Paleocene; Simpson, 1927, 1936; Szalay, 1969a; Rose, 1981; Krause and Gingerich, 1983; Fox, 1990a; Krause and Maas, 1990; Rose, in press). E. clivus is known only from the late middle Tiffanian (Ti4) Swan Hills locality, and is the youngest species of Elpidophorus. The four nominal species represent distinct stages of dental evolution in the history of Elpidophorus, progressing from primitive (E. minor) to derived (E. clivus), a conclusion that is partly, and independently, supported by their relative stratigraphic positions (i.e., the earlier occurring and more primitive E. minor is known from older sediments, while the most derived species, E. clivus, is known from the youngest sediments; E. simpsoni and E. elegans are contemporaneous from the earliest through early middle Tiffanian). The

assessment of the interrelationships of Elpidophorus species is based on a morphocline of increasing molarization of the upper posterior premolars, particularly P4, and in the relative development of dilambdodonty on the premolars and molars, with weaker dilambdodonty characterizing E. minor, and increased upper premolar molarization and stronger dilambdodonty characterizing successively younger species. An alternative hypothesis, one that would have E. clivus as the most basal species of Elpidophorus, with subsequent premolarization of the upper posterior premolars and weaker dilambdodonty, is dismissed here as biologically unlikely: although premolar premolarization is thought to have occurred in some eutherian groups (e.g., erinaceomorph lipotyphlans, mesonychians, some pentacodontids; see Van Valen, 1969; Szalay, 1969b; Novacek, 1982; Novacek et al., 1985; Zhou, 1995), a trend towards weaker dilambdodonty from an ancestral condition in which it was already very well developed is wholly unknown. Rather, dilambdodonty is achieved independently in many eutherian groups, and is enhanced, rather than de-emphasized, during their evolutionary histories (e.g., pantodonts, soricids, scandentians, amphidozotheriine nyctitheriids; see Simons, 1960; Repenning, 1967; Sigé, 1976; Butler, 1980). The totality of evidence suggests that Elpidophorus conforms to this general trend, with younger species having developed more fully molariform premolars and stronger dilambdodonty.

In E. minor, the p3 consists of a large protoconid and unicuspid talonid, and while the p4 is clearly molariform, it has a relatively weak paraconid and unicuspid talonid (Fig. 8.11.1). In contrast, the p3 talonid of E. simpsoni bears a significantly wider, basined talonid, with a correspondingly longer cristid obliqua; the paraconid on p4 is stronger in E. simpsoni, and the talonid is wider, with a long cristid obliqua and hypocristid that together form the posterior arms of the W-shaped ectolophid (Fig. 8.11.2). The p3 in E. elegans and E. clivus closely resembles that in E. simpsoni (but is shorter relative to its length, see later in this chapter), but the p4 talonid becomes progressively wider in the former two species, with a markedly more elongate cristid obliqua and hypocristid (Figs. 8.11.3, 8.11.4). In E. clivus, the p4 metaconid is taller than the protoconid, and leans somewhat lingually, further increasing the length of the protocristid (one of the anterior arms of the ectolophid). The evolution of the upper premolars parallels the trends seen in the lower premolars, an expectation of separate

parts of an integrated functional complex. The protocone on P3 is weak in E. simpsoni (the upper dentition of E. minor is not known), but becomes better developed in E. elegans and E. clivus, and the paracone and metacone become better differentiated (Figs. 8.10.1-8.10.3). The paracone and metacone on P4 are connate for most of their height in E. simpsoni, and the centrocrista is short and weakly notched; in contrast, the two cusps become better differentiated and their apices are farther apart in E. elegans and E. clivus, and the centrocrista becomes significantly longer, particularly in E. clivus, where it is deflected to the labial margin of the crown (i.e., fully dilambdodont) (Figs. 8.10.4-8.10.6). Dilambdodonty is further enhanced in E. elegans and E. clivus by development of an elongate, sweeping postmetacrista.

The evolution of the molars in Elpidophorus closely paralleled that of the premolars. The lower molars of E. minor possess a relatively short (i.e., weakly transverse) paracristid, a deep and narrowly notched protocristid, a narrow talonid, and a well-developed and lingual hypoconulid. During evolution of Elpidophorus thereafter, the molar paraconid became more fully incorporated into the paracristid, and the paraconid/paracristid complex extended farther lingually; the metaconid became the dominant trigonid cusp (being larger overall and taller), and in E. elegans and E. clivus it leans lingually; the protocristid became significantly longer, especially the metaconid arm (in E. elegans and E. clivus the metaconid arm is almost twice the length of the protoconid arm); the talonid widened considerably, with a corresponding elongation of the cristid obliqua and hypocristid; and the hypoconulid became weaker and farther lingual, abutting the entoconid, or can be wholly absent in some specimens of E. elegans and E. clivus (Figs. 8.11.5-8.11.6). Evolution of the upper molars of Elpidophorus affected the labial parts of the crown more so than the lingual parts: the ectoloph on M1 and M2 of E. simpsoni is well-developed, but the centrocrista does not protrude far into the ectoflexus, and the preparacrista is only weakly developed, especially on M1; by contrast, the centrocrista is longer and bulges farther into the ectoflexus on M1 and M2 of E. elegans and E. clivus, the preparacrista is longer and directed more labially, rather than anterolabially, and the stylar shelf labial to the paracone is wider (Figs. 8.10.7-8.10.12). Interestingly, the hypocone, previously considered a vestigial structure in Elpidophorus (e.g., Rose, 1975) became larger in E. elegans and, especially, in E. clivus, suggesting the

trend in Elpidophorus was towards an increasingly quadritubercular upper molar condition (Stonley, 1988).

The Systematic Position of Elpidophorus

The higher level classification of Elpidophorus and Eudaemonema is still a matter of debate. While a consensus on the probable archontan affinities of the two taxa seems to have been reached (Rose, in press), the issue of whether they represent stem dermopterans (as McKenna and Bell, 1997, e.g., suggest) or near-dermopterans (as Bloch et al., 2007, e.g., suggest) remains unresolved, and will likely remain so until the fossil record of undoubted dermopterans becomes better known, and possibly until basicranial and postcranial data are known for the earliest putative dermopterans. In contrast, the lower level classification of Elpidophorus and Eudaemonema has been comparatively uncontroversial: Eudaemonema has been almost unanimously classified as a mixodectid (although McKenna and Bell, 1997 curiously consider it a plagiomenid), and since the publication of Rose (1975) and Rose and Simons (1977), Elpidophorus has most often been interpreted as representing the earliest plagiomenid (Plagiomenidae are a family of North American dermopteran-like eutherians known almost exclusively from dentitions; Matthew, 1918; Rose, 1975; Gunnell, 1989; Silcox et al., 2005; Rose, in press). Although Rose's (1975) hypothesis is predicated on a suite of putative apomorphies shared by Elpidophorus and plagiomenids to the exclusion of mixodectids and other archontans, the comparisons made in that paper were between E. elegans and plagiomenids; the results of this study, however, suggest that E. elegans is a derived species of Elpidophorus, and that the more meaningful comparisons would be with the more basal, but more poorly known E. minor and E. simpsoni. In light of the wealth of new information provided by the specimens from the Blindman River localities and elsewhere in Alberta, the putative synapomorphies outlined by Rose (1975) as uniting Elpidophorus and plagiomenids are re-evaluated.

Lower incisors.—In his discussion of the affinities of Mixodectidae, Simpson (1937) suggested that the lower incisors of mixodectids (including Elpidophorus) differed from those of plagiomenids in being markedly enlarged (at least i1) and in having lost i3.

Prior to this study, no information on the number or coronal anatomy of the lower incisors was conclusively known for Elpidophorus, but the evidence now available indicates that Elpidophorus retains i3, and that neither i1 or i2 is markedly enlarged (at least not to the same degree as i1-2 in Mixodectes and Eudaemonema; Szalay, 1969a). Although the lower incisors of Elpidophorus resemble those of some plagiomenids (e.g., Plagiomene) with respect to size and orientation, these similarities are likely primitive for archontans (e.g., three relatively unenlarged, procumbent lower incisors characterize the most basal primates, including Purgatorius Van Valen and Sloan, 1965, Palaechthon Gidley, 1923, dermopterans, and scandentians; Butler, 1980; Stafford and Szalay, 2000; Silcox, 2001; Clemens, 2004) or eutherians generally (e.g., Kennalestes Kielan-Jaworowska, 1969, Bulaklestes Nessov, 1985; and see Kielan-Jaworowska et al., 1979; Kielan-Jaworowska, 1981; Archibald and Averianov, 2006). More recent analyses (e.g., Silcox, 2001; Silcox et al., 2005; Bloch et al., 2007) have linked Elpidophorus to plagiomenids on the basis of a perceived similarity in the structure of the i1-2 crowns, with the condition in Elpidophorus being equated with the bilobate lower incisors of plagiomenids and, even more remarkably, with the pectinate lower incisors of extant dermopterans (the "incipiently lobate" condition in Elpidophorus, the lobate condition in plagiomenids, and the tined lower incisors in Dermoptera are viewed by these authors as forming a morphocline). As discussed earlier in this chapter, the i1 and i2 crowns in E. simpsoni (the most primitive species of Elpidophorus for which information on the lower incisors is available) are elongate and subspatulate, with chisel-like apices; in more advanced species of Elpidophorus (e.g., E. elegans), the medial incisor becomes faintly notched apically, forming a small lateral cuspule, while the i2 forms a similar cuspule, but on its medial margin; the crown of i3 is unknown, but the tooth was smaller than i1-2 and the crown may even have been premolariform. The crowns of the lower incisors of the best-known plagiomenid, Plagiomene, differ substantially from those of Elpidophorus: they are apically broad and deeply bilobate, with subequal medial and lateral lobes; their occlusal surfaces face more medially (the occlusal surfaces of the lower incisors face nearly dorsally in E. simpsoni); and the incisors decrease in size dramatically from i1-3. While the coronal anatomy of the lower incisors in Elpidophorus may simply be primitive for Plagiomenidae, the elongate, subspatulate crowns more

closely resemble those in the scandentians Ptilocercus and Dendrogale Gray (see Butler, 1980), and to a lesser degree those of the mixodectines Mixodectes and Eudaemonema than those of any plagiomenid or dermopteran, and this coronal anatomy may be primitive for archontans generally. In any case, lobate incisors cannot be used as a synapomorphy uniting Elpidophorus and plagiomenids: even if the weakly cuspate i1-2 crowns of E. elegans and E. clivus are considered "incipiently lobate" (see Silcox, 2001), the condition does not characterize the most primitive species (i.e., E. simpsoni), but rather arose within the Elpidophorus lineage and would be convergent on that account.

Hypoconulid position.—Simpson (1937) noted that the position of the molar hypoconulid differs between Elpidophorus and Plagiomenidae, with that in the former being displaced towards the entoconid, but in a more median position in the latter. Rose (1975) suggested that the molar hypoconulid in E. minor is only slightly closer to the entoconid than to the hypoconid, but the molar hypoconulid in PU 14241 (type of E. minor; Simpson, 1937; Szalay, 1969a) and in UALVP 44149 (referred to E. sp., cf. E. minor; Scott, 2003) is clearly much closer to the entoconid than it is in any plagiomenid; the lingually displaced hypoconulid may be a synapomorphy of Elpidophorus+mixodectids, as Szalay (1969a) suggested. Interestingly, the hypoconulid in dermopterans is positioned well lingual of the anteroposterior midline, similar to that in advanced species of Elpidophorus, but not in Plagiomenidae (Stafford and Szalay, 2000).

Structure of the mesostyle.—Simpson (1936, 1937) and Szalay (1969a) have discussed the differences in the structure of the "mesostyle" of Elpidophorus (and mixodectids) and that of Plagiomene (and other plagiomenids). Within Archonta, a number of probably non-homologous structures have been considered "mesostyles", and all of these structures have been considered equivalent in the most recent cladistic analyses of archontan relationships (Silcox, 2001; Bloch et al., 2007). These purported "mesostyles" include:

1) A thickening of the ectocingulum into a discrete cusp that can occur independently of a deflected centrocrista (Figs. 8.12.1-8.12.4). This kind of mesostyle is best seen on the upper molars of various primates, including derived species of Plesiadapis (e.g., P. churchilli Gingerich), some paromomyids, and picrodontids (e.g., P. calgariensis, see

Chapter 7). On the upper molars of derived species of Plesiadapis (e.g., P. churchilli), the centrocrista can be deflected labially, and its apex can coalesce with the mesostyle, such that the two appear continuous, but the ectocingulum is uninterrupted along the labial margin of the crown. The same pattern seems to occur in microsyopids (see Gunnell, 1989).

2) The "mesostyle" of mixodectids consists of a labially deflected centrocrista that bulges well past the labial margin of the crown (Figs. 8.12.5, 8.12.6). The apex of the centrocrista loops around, creating a labially convex lip that closes off the oblique trough of the molars; importantly, the rounded apex of the centrocrista disrupts the continuity of the ectocingulum. In some specimens of Eudaemonema and Mixodectes, the labial apex of the centrocrista is tightly looped, and a cuspule can form at its apex, but this cusp is clearly not homologous with that in plesiadapiforms and microsyopids (i.e., it forms on the centrocrista rather than the ectocingulum). The basic pattern of a looped centrocrista is seen in Mixodectes, Eudaemonema, and Remiculus, and is also seen in many bats (e.g., Myotis Kaup; Fig. 8.12.8), dermopterans (Fig. 8.12.7), and scandentians (e.g., Urogale Mearns), with a few derived scandentians (e.g., Dendrogale) having the centrocrista bearing a single cusp, or divided and bearing two cusps (see Butler, 1980); unlike the mesostyles in plesiadapiforms, however, the cusps are borne on the centrocrista, rather than on the ectocingulum.

3) The "mesostyle" of plagiomenids is more difficult to evaluate. Plagiomenids retain a complete and continuous ectocingulum, with no intrusion into the ectoflexus by the centrocrista (see, e.g., Matthew, 1918, fig. 29; Szalay, 1969a, pl. 29, figs. 3-5; MacPhee et al., 1989, fig. 9A; Fig. 8.12.9); the oblique trough in plagiomenids is closed labially by the ectocingulum rather than the centrocrista. Large cusps are developed on the stylar shelf even in the most primitive plagiomenids (e.g., Planetetherium, Plagiomene), and these cusps are connected to the paracone and metacone by multiple crests. While the anteriormost and posteriormost of these crests are probably homologous with the preparacrista and postmetacrista, respectively, the homologies of the central crests are less clear. Although some authors (e.g., Silcox, 2001; Bloch et al., 2007) have interpreted these crests as representing the centrocrista (in which case the large stylar cusps are possibly homologous with parts of the centrocrista in mixodectids, or the

"mesostyles" in scandentians), the evidence for such a determination is ambiguous, particularly given the proliferation of crests surrounding the paracone and metacone in plagiomenids. For example, poorly developed crests in the position of an undeflected centrocrista can be discerned on some specimens (e.g., PU 13732, AMNH 15208, Plagiomene; AMNH 95713, Tarka McKenna, 1990, and see Rose and Simons, 1977, fig. 4), in addition to those running labially to the stylar cusps (this is true also of the posterior upper premolars where the centrocrista is even better developed), suggesting the possibility that the crests supporting the stylar cusps may be neomorphic. If this is the case, then the "mesostyle" of plagiomenids represents only a proliferation of stylar cusps, and is clearly different from the two previously described "mesostyles".

Hershkovitch (1971) defined a mesostyle (=ectostyle of Hershkovitz, 1971) as a cusp that is developed from a swelling of the ectocingulum, and in this sense the term "mesostyle" corresponds most closely with that structure on the molars of some plesiadapiforms and microsyopids; the fact that a mesostyle can occur with no deflection of the centrocrista suggests that these two characters are not developmentally interrelated, and that clearly a labially deflected centrocrista is not equivalent to an ectocingular cusp (=mesostyle s. s.). What has been called the "mesostyle" in Elpidophorus is closest to that seen in mixodectids: it is formed by a labially deflected centrocrista that disrupts the ectocingulum and bulges into the ectoflexus (moderately developed in E. simpsoni, prominent in E. elegans and E. clivus), whereas the "mesostyle" of plagiomenids is formed by well-developed stylar cusps (borne on the stylar shelf and not on the ectocingulum), with the centrocrista possibly being weakly developed and not deflected labially; neither of these "mesostyles" is equivalent to that of plesiadapiforms.

Proliferation of accessory cusps.—Rose (1975) suggested a proliferation of accessory cusps in the upper and lower dentition of Elpidophorus links it to plagiomenids. As described earlier, the stylar shelf (i.e., that part of the crown between the labial bases of the paracone and metacone and the ectocingulum) of Elpidophorus does not support distinct cusps, although the ectocingulum can bear tiny, ill-defined cuspules, and an occasional cuspule is developed on the postmetacrista in E. elegans. In the lower dentition, additional cuspules can be developed in E. elegans, particularly a strong mesoconid, as well as a doubled hypoconulid and occasional incipient metastylid.

Accessory cusps are more poorly developed in E. simpsoni, but a mesoconid is always present; an entoconulid, doubled hypoconulid, and metastylid are not developed in any species of Elpidophorus. Interestingly, the one accessory cusp on the lower molars that is most often developed in Elpidophorus, the mesoconid, is not present in plagiomenids, while the entoconulid, a cusp that is very well developed in plagiomenids, is absent in Elpidophorus and other mixodectids.

Anterolingually procumbent lower cheek teeth.—The lower molars of plagiomenids are unusual in that the lingual cusps are elevated well above the labial cusps such that the trigonid and talonid basins slope linguolabially, and the metaconid and entoconid are anteriorly displaced relative to the protoconid and hypoconid; these unusual features have been cited as important apomorphies shared by Elpidophorus, plagiomenids, and dermopterans to the exclusion of other archontans (Rose, 1975; McKenna, 1990; Silcox, 2001). Simpson (1937) and Szalay (1969a), however, demonstrated that anterolingually procumbent lower cheek teeth also characterize mixodectids (the procumbency is weaker than in Elpidophorus and plagiomenids). Interestingly, the lower molars of extant dermopterans do not have the lingual parts of the crown elevated above the labial parts to nearly the same degree as in plagiomenids or mixodectids (MacPhee et al., 1989; Stafford and Szalay, 2000).

Low, shelf-like paraconid.—Rose (1975) suggested that a low and shelf-like paraconid characterizes plagiomenid lower molars, but this is not true of Plagiomene or Worlandia, in which it remains high and bladelike. A low and shelf-like molar paraconid is characteristic of Elpidophorus and mixodectids, and it is clearly not a synapomorphy of Plagiomenidae, whether Elpidophorus is included or not.

Talonid of m3 narrower than trigonid.—A transversely narrow m3 talonid is present in plagiomenids, but the trigonid and talonid in Elpidophorus can be subequal in width, slightly narrower, and a few specimens of E. elegans have a talonid that is wider than the trigonid.

Transverse median valley (oblique trough) in upper molars.—The oblique trough is present in plagiomenids and Elpidophorus, but also in Eudaemonema, Mixodectes, and Remiculus (Simpson, 1937; Russell, 1964; Szalay, 1969a), as well as the omomyid Ekgmowechashala MacDonald, 1963 (considered a plagiomenid by McKenna, 1990 but

not by Stafford and Szalay, 2000 or Rose, in press). Although the trough is particularly well developed in E. elegans, it is much less so in E. simpsoni and in this regard more closely approximates the condition in Mixodectes. An oblique trough is also developed in desmanine talpids (see MacPhee et al., 1989), cyriacotheriid pantodonts (Rose and Krause, 1982, and see Chapter 10), microchiropteran bats (e.g., Myotis), soricids (e.g., Sorex Linnaeus) and a number of other mammals.

Conules prominent and bulbous.—Rose (1975) suggested that the large conules on the upper molars of Elpidophorus and plagiomenids clearly differentiate these taxa from mixodectids, but this is true only with respect to Mixodectes (the conules in Mixodectes are small and uninflated, see Szalay, 1969a). The conules in Eudaemonema, and to a lesser degree Remiculus, are similar in relative size and inflation to those in E. simpsoni.

Protocone position and structure.—An anteriorly displaced molar protocone, such as that in plagiomenids, is one in which the base is shifted anteriorly, such that a line drawn labiolingually along the transverse midline of the crown would pass almost completely posterior to the protocone, and the protoconal apex is in line with, or even anterior to, the apices of the paracone and paraconule. The upper molars of many mammals (e.g., plesiadapiform primates such as Purgatorius, the pantolestid Bessoecetor Simpson, 1936, the nyctitheriid Leptacodon Matthew and Granger, 1921) have a protocone that leans anteriorly (either from simply leaning anteriorly, or having the lingual half of the tooth "twisted" anteriorly), such that the apex is anterior to a labiolingual line bisecting the crown; in these cases, however, the base of the protocone remains at or near the midline. The protocone in E. simpsoni is virtually on the transverse midline of the crown, well posterior to the level of the paracone and paraconule, and its apex leans slightly anteriorly. In contrast, the protocone in plagiomenids is displaced far anteriorly such that the paracone, paraconule, and protocone are all in-line near the anterior margin of the crown. The protocone is much more anteriorly positioned in E. elegans and, especially, in E. clivus, but this clearly evolved within the history of Elpidophorus. Furthermore, there are differences in the structure of the protocone: in Elpidophorus (and mixodectids), the protocone is large (occupying about half the width of the crown) and turgid, especially at its base, and the

lower molar talonid is longer than broad and shallowly concave; in contrast, the protocone of plagiomenids is smaller (occupying only about one-fourth to one-third the width of the crown), anteroposteriorly compressed, flat anteriorly and posteriorly, and bears a sharply pointed apex, while the occluding lower molar talonid basin is much broader than long, and the basin-facing walls of the entoconid, hypoconulid, and hypoconid slope anteriorly, forming a deep, V-shaped basin with the postvallid wall.

Prominent cingulids on p4, m1-3: While the lower molars of Elpidophorus bear a well-developed anterior cingulid, it is weakly developed on p4 in E. simpsoni and E. minor, and in no species of Elpidophorus is an ectocingulum developed (i.e., a cingulum that is complete labially). McKenna (1990, fig. 12, character 3) suggested that lower molars bearing a strong anterolabial cingulum is a character that unites plagiomenids+Elpidophorus+Eudaemonema+mixodectids, but clearly this cannot be the case as Eudaemonema cuspidata lacks cingulids of any kind (Szalay, 1969a); in any event, a well-developed anterior cingulid is present in Nyctitheriidae [the outgroup used in McKenna's (1990) analysis] and is probably primitive for eutherians (Archibald and Averianov, 2006).

Small hypocone: The hypocone in E. simpsoni is small but conspicuous, similar to that in Remiculus, whereas a hypocone is wholly undeveloped in plagiomenids; the protoconal cingula are well developed in plagiomenids and Elpidophorus, but also in Mixodectes, Eudaemonema, Remiculus, scandentians, plesiadapiforms, and most other archontans. The putatively derived loss of a hypocone in Elpidophorus+plagiomenids as hypothesized by Rose (1975) and McKenna (1990) is true only if it is assumed that the two share a recent common ancestor that resembled Mixodectes (in which the upper molar hypocone is well developed), but there is no evidence to suggest that was the case; in any event, a weak or undeveloped hypocone is probably primitive for Archonta (see, e.g., upper molars of Purgatorius, Ptilocercus).

Molariform posterior premolars: Rose (1975) considered the molarization of the posterior premolars to be an important feature uniting Elpidophorus and plagiomenids. The posterior premolars of plagiomenids are nearly as large as the first molar: the crowns of the upper premolars are molariform, with the P3-4 bearing a large protocone, clearly differentiated and separate paracone and metacone, strong conules, and a proliferation of

stylar cusps; the p3-4 bear a well-developed metaconid, high, bladelike paraconid, and a talonid that supports three cusps and a deep basin that is as wide or wider than the trigonid (Rose, 1973). In contrast, the P3 in E. simpsoni is considerably smaller than P4, and the crown is much less molariform than the plagiomenid P3, with a poorly developed protocone, a weakly separated paracone and metacone, and undeveloped conules. The P4 in Elpidophorus is molariform, but the crown is smaller than that of M1, and the paracone and metacone are incompletely separate. Rose (1975) characterized the p3 of E. elegans as "submolariform", but as described earlier in this chapter, the p3 in E. elegans, like that in E. minor and E. simpsoni, is only weakly molarized (and see Simpson, 1936, fig. 5; Szalay, 1969a, pl. 24, figs. 3-6), and neither p3 nor p4 is molarized to nearly the same degree as that in Plagiomene and other plagiomenids. In any case, a molarized p4 characterizes not only plagiomenids and Elpidophorus, but also Remiculus and Eudaemonema (the main differences in this regard between plagiomenids and Elpidophorus on the one hand, and Remiculus and Eudaemonema on the other, are the former two taxa having a better-developed paraconid and slightly stronger metaconid).

Other differences between Elpidophorus and Plagiomenidae that were not pointed out by Rose (1975) include:

Molar cristid obliqua-trigonid contact: The cristid obliqua in Elpidophorus contacts the postvallid wall below the protocristid notch and continues a short distance dorsally, similar to that in mixodectids. In contrast, the low cristid obliqua in plagiomenids contacts the postvallid wall far labially, similar to that in Galeopterus, whereas the cristid obliqua in Cynocephalus joins the postvallid slightly more lingually (Stafford and Szalay, 2000).

Molar size: The molars of plagiomenids significantly decrease in size from m1 to m3 (Rose, 1973; Bown and Rose, 1979; Rose, in press), whereas those of Elpidophorus are subequal.

Molar entoconid: The molar entoconid in plagiomenids is the tallest talonid cusp (even taking into account the fact that the lingual parts of the crown are elevated above the labial parts), being over half the height of the metaconid. In contrast, the entoconid in Elpidophorus is subequal with the hypoconid in height.

There is unquestionably a superficial resemblance in the teeth of Elpidophorus and plagiomenids, an observation made by Matthew (1918) when Plagiomene was first described; closer inspection, however, reveals a number of important differences that suggest that the dentitions of the two taxa are specialized in different ways. While the upper and lower molars of Elpidophorus clearly resemble those of other dilambdodont mammals, such is not the case in plagiomenids. For example, the upper molars of plagiomenids lack an elongated preparacrista and postmetacrista, and the centrocrista has not been convincingly demonstrated to be labially deflected; in other words, the characteristic W-shaped ectoloph, seen clearly in Elpidophorus and mixodectids, is undeveloped in plagiomenids. Similarly, in the lower molars of plagiomenids the metaconid and protoconid are nearly vertical (as opposed to the metaconid being significantly taller and lingually leaning), the protocristid is short, the cristid obliqua is low and poorly developed and joins the postvallid at the labial extremity (i.e., the cristid obliqua arm of the ectolophid is very short), the hypoconulid is central, rather than far lingual, and the hypocristid is virtually undeveloped. In contrast, Elpidophorus resembles mixodectids and other dilambdodont mammals in the upper and lower molars bearing strongly developed ectolophs, with salient parastylar and metastylar lobes, well-defined ectolophids, low shelf-like molar paraconids, and deeply concave talonid basins. Additionally, the lower incisor and molar proportions differ significantly between the two taxa, with those in plagiomenids decreasing in size from i1 to i3, and from m1 to m3, whereas the i2 and m2 in Elpidophorus are the largest in each series.

The results of this study indicate that the majority of characters cited by Rose (1975) as potentially uniting Elpidophorus and plagiomenids to the exclusion of mixodectids are less meaningful when comparisons with E. simpsoni and E. minor, rather than E. elegans, are made. In fact, with the exception of robust lower molar cingulids, the characters outlined by Rose (1975) distinguish Elpidophorus from the Plagiomenidae, and do not indicate that the two taxa are more closely related to one another to the exclusion of other archontans. Furthermore, the differences in the dental anatomy of Elpidophorus and Plagiomenidae suggest that the phylogenetic position of Elpidophorus is closest to Mixodectidae, as Simpson (1936, 1937) and Szalay (1969a) earlier proposed; as such, Elpidophorus is here returned to the Mixodectidae. Elpidophorus and other

mixodectids can be united to the exclusion of other archontans (including plagiomenids) by their possessing a combination of a pre- or semimolariform p3 (increasingly molarized in advanced species of Eudaemonema and Elpidophorus), anterolingually procumbent lower molars (emphasized in Elpidophorus) that bear a low shelf-like paraconid, a shallowly concave talonid basin, a lingually positioned hypoconulid, and a mesoconid; they are further united in having upper molars that bear a strongly labially deflected centrocrista, strong anterior and posterior cingula, and a moderately elongated preparacrista and postmetacrista. This characterization of the family is essentially the same as that proposed by Szalay (1969a) and more recently by Rose (in press). Two distinct groups can be recognized within Mixodectidae, the first consisting of Mixodectes, Dracontolestes Gazin, 1941 (possibly synonymous with Mixodectes; see Gunnell, 1989), and Eudaemonema, and the second consisting of Elpidophorus and possibly Remiculus; the differences between these two groups are appropriately expressed at the subfamilial level, with Elpidophorus, and possibly Remiculus, comprising a new subfamily, the Elpidophorinae, while the remaining mixodectids are referred to a second subfamily, the Mixodectinae [originally proposed by Matthew (1915)]. Mixodectines have weakly developed conules on P4, upper molars that bear an anterolabially directed preparacrista and an enlarged, bulbous hypocone, and two enlarged, procumbent lower incisors; they also possess lower molars that are weakly anterolingually procumbent, and have a very weak or undeveloped entocristid (leaving the talonid open lingually). Although a number of the characters used here to define Mixodectinae are possibly primitive for Mixodectidae or Archonta generally (e.g., weak conules on P4, procumbent lower incisors), as Gunnell (1989) noted in his study of Mixodectidae, the combination of characters is diagnostic of no other archontan clade; furthermore, some of the characters are almost certainly derived (e.g., two greatly enlarged lower incisors, large and inflated hypocone), particularly when compared to, e.g., the dentition of the scandentian Ptilocercus, a taxon that is frequently regarded as representing an approximation of the ancestral archontan morphotype (Sargis, 2002a-c; Bloch et al., 2003; Olson et al., 2004; Bloch et al., 2007), or to that of Purgatorius, putatively the earliest archontan (Silcox, 2001; Clemens, 2004; Silcox et al., 2005). Elpidophorus is notably divergent from mixodectines in having upper molars with a

wider stylar shelf and flaring parastylar and metastylar lobes, a labially (rather than anterolabially) directed preparacrista, a more strongly labially deflected centrocrista, larger conules, and a poorly developed hypocone; it is further distinguished from the mixodectines in having three lower incisors (none of which is markedly enlarged) and a p4 that bears a metaconid that is better-differentiated from the protoconid. The phylogenetic position of Remiculus is less certain: Russell (1964) and Szalay (1969a) considered it closer to Eudaemonema than to Elpidophorus, but Gunnell (1989) suggested a closer relationship with Elpidophorus or Plagiomenidae; the genus has more recently been considered a nyctitheriid lipotyphlan (McKenna and Bell, 1997), although the evidence for this is not persuasive. The record of Remiculus is sparse, consisting only of isolated teeth (see Russell, 1964; Szalay, 1969a; Smith, 1997); although the genus shares some characters with Elpidophorus [e.g., wide stylar shelf with a labially directed preparacrista, a strongly labially deflected centrocrista, enlarged, shelf-like conules, and a weak hypocone (formed on the posterior cingulum in both taxa, contra Gunnell, 1989)], it differs in a number of significant ways (e.g., smaller and lower p4 paraconid, more cuspate molar paraconids, weaker mesoconids). Until the record of Remiculus becomes better known, the genus is probably best referred to the Mixodectidae, subfamily incertae sedis.

The phylogenetic position of Mixodectidae and Plagiomenidae relative to Dermoptera remains uncertain, and resolution of this problem is well beyond the scope of the current study. Clearly there are resemblances in the dentitions of all three groups, but the meaning of these resemblances is complicated by the poor fossil record of dermopterans [the earliest record of the order is from the Eocene of Thailand (Ducrocq et al., 1992), but see Szalay and Stafford, 2000], and the occurrence of one or more of these characters in other archontan or eutherian groups (MacPhee et al., 1989). McKenna and Bell (1997), presumably following the work of Beard (1993a), classified mixodectids, plagiomenids, and a number of other eutherian groups (e.g., paromomyids) in a taxonomically broad Dermoptera, but the results of recent analyses of archontan and dermopteran relationships (e.g., Szalay and Lucas, 1996; Szalay and Stafford, 2000; Silcox, 2001; Rose, in press) cast considerable doubt on these referrals; the conclusions of MacPhee et al.'s (1989) study of the basicranium of Plagiomene are particularly

damning to a plagiomenid-dermopteran relationship. Given the limited evidence now available, a satisfactory resolution to the interrelationships of mixodectids, plagiomenids, and dermopterans seems unlikely until the fossil record of each group becomes better known; in this light Matthew's (1918) and Simpson's (1937) conservative interpretations of the interrelationships of these groups seem as appropriate now as they did in the early parts of the twentieth century.

8.4 Literature Cited

ALLAN, J. A., and J. O. G. SANDERSON. 1945. Geology of Red Deer and Rosebud Sheets, Alberta. Alberta Research Council Report, 13:1-116.

ARCHIBALD, J. D., and A. O. AVERIANOV. 2006. Late Cretaceous asioryctitherian eutherian mammals from Uzbekistan and phylogenetic analysis of Asioryctitheria. Acta Palaeontologica Polonica, 51:351-376.

BEARD, K. C. 1990. Gliding behavior and paleoecology of the alleged primate family Paromomyidae (Mammalia, Dermoptera). Nature, 345: 340-341.

BEARD, K. C. 1993a. Phylogenetic systematics of the Primatomorpha, with special reference to Dermoptera, pp. 129-150. In F. S. SZALAY, M. J. NOVACEK, and M. C. MCKENNA (eds.), Mammal Phylogeny: Placentals. Springer-Verlag, New York.

BEARD, K. C. 1993b. Origin and evolution of gliding in Early Cenozoic Dermoptera (Mammalia, Primatomorpha), pp. 63-90. In R. D. E. MACPHEE (ed.), Primates and their Relatives in Phylogenetic Perspective. New York: Plenum Press.

BLOCH, J. I., D. M. BOYER, and P. HOUDE. 2003. New skeletons of Paleocene-Eocene micromomyids (Mammalia, Primates): functional morphology and implications for euarchontan relationships. Journal of Vertebrate Paleontology 23, supplement to no. 3:35A.

BLOCH, J. I., M. T. SILCOX, D. M. BOYER, and E. J. SARGIS. 2007. New Paleocene skeletons and the relationship of plesiadapiforms to crown-clade primates. Proceedings of the National Academy of Sciences, 104:1159-1164.

BOWN, T. M., and K. D. ROSE. 1979. Mimoperadectes, a new marsupial, and Worlandia, a new dermopteran, from the lower part of the Willwood Formation (early Eocene), Bighorn Basin, Wyoming. Contributions from the Museum of Paleontology, The University of Michigan, 25:89-104.

BUTLER, P. M. 1973. Molar wear facets of early Tertiary North American primates. Symposium of the IVth International Congress on Primatology, 3:1-27.

BUTLER, P. M. 1980. The tupaiid dentition, pp. 171-204. In W. P. LUCKETT (ed.), Comparative Biology and Evolutionary Relationships of Tree Shrews. Plenum Press, New York.

CLEMENS, W.A. 2004. Purgatorius (Plesiadapiforms, Primates?, Mammalia), a Paleocene immigrant into northeastern Montana: stratigraphic occurrences and incisor proportions, pp. 3-13. In M. R. DAWSON and J. A. LILLEGRAVEN (eds.), Fanfare for an Uncommon Paleontologist: Papers in Honor of Malcolm C. McKenna. Bulletin of the Carnegie Museum of Natural History, 36.

COPE, E. D. 1882. Contributions to the history of the Vertebrata of the lower Eocene of Wyoming and New Mexico, made during 1881. I. The fauna of the Wasatch beds of the basin of the Big Horn River. II. The fauna of the Catathlaeus beds, or lowest Eocene, New Mexico. Proceedings of the American Philosophical Society, 10:139-197.

COPE, E. D. 1883. On the mutual relationships of the bunotherian Mammalia. Proceedings of the Academy of Natural Sciences Philadelphia, 35:77-83.

CROMPTON, A. W. 1971. The origin of the tribosphenic molar, pp. 65-87. In D. M KERMACK and K. A. KERMACK (eds.), Early Mammals. Zoological Journal of the Linnean Society, 50, supplement to no. 1.

DAWSON, M. R., L. J. HICKEY, K. JOHNSON, and C. J. MORROW, Jr. 1986. Discovery of a dermopteran skull from the Paleogene of Arctic Canada. National Geographic Research, 2:112-115.

DUCROCQ, S, E. BUFFETAUT, H. BUFFETAUT-TONG, J. J. JAEGER, Y. JONGKANJANASOONTORN, and V. SUTEETHORN. 1992. First fossil flying lemur; a dermopteran from the late Eocene of Thailand. Palaeontology, 35: 373-380.

FOX, R. C. 1988. Late Cretaceous and Paleocene mammal localities of southern Alberta. Occasional Paper of the Tyrrell Museum of Palaeontology, 6:1-38.

FOX, R. C. 1990a. The succession of Paleocene mammals in western Canada, pp. 51-70. In T. M. BOWN and K. D. ROSE (eds.), Dawn of the Age of Mammals in the Northern Part of the Rocky Mountain Interior. Geological Society of America Special Paper, 243.

FOX, R. C. 1990b. Pronothodectes gaoi n. sp., from the late Paleocene of Alberta, Canada, and the early evolution of the Plesiadapidae (Mammalia, Primates). Journal of Paleontology, 64:637-647.

GAZIN, C. L. 1941. The mammalian faunas of the Paleocene of central Utah, with notes on geology. Proceedings of the United States National Museum, 91:1-53.

GIDLEY, J. W. 1923. Paleocene primates of the Fort Union, with discussion of relationships of Eocene primates. Proceedings of the United States National Museum, 63:1-38.

GILL, T. 1872. Arrangement of the families of mammals with analytical tables. Smithsonian Miscellaneous Collections, 11:1-98.

GREGORY, W. K. 1910. The orders of mammals. Bulletin of the American Museum of Natural History, 27:1-254.

GUNNELL, G. F. 1989. Evolutionary history of Microsyopoidea (Mammalia, ?Primates) and the relationship between Plesiadapiformes and Primates. University of Michigan Papers on Paleontology, 27:1-157.

HARTMAN, J. E. 1986. Paleontology and biostratigraphy of lower part of Polecat Bench Formation, southern Bighorn Basin, Wyoming. Rocky Mountain Geology, 24:11-63.

HERSHKOVITZ, P. 1971. Basic crown patterns and cusp homologies of mammalian teeth, pp. 95-150. In A. A. DAHLBERG (ed.), Dental Morphology and Evolution. University of Chicago Press, Chicago.

KAY, R. F., and K. M. HIIEMÄE. 1974. Jaw movement and tooth use in Recent and fossil primates. American Journal of Physical Anthropology, 40:227-256.

KIELAN-JAWOROWSKA, Z. 1969. Preliminary data on the Upper Cretaceous eutherian mammals from Bayn Dzak, Gobi Desert, pp. 171-191. In Z. KIELAN-

JAWOROWSKA (ed.), Results of the Polish-Mongolian Palaeontological Expeditions, pt. I. Palaeontologia Polonica 19.

KIELAN-JAWOROWSKA, Z. 1981. Evolution of the therian mammals in the Late Cretaceous of Asia. Part IV. Skull structure in Kennalestes and Asioryctes. Palaeontologia Polonica, 42:25-78.

KIELAN-JAWOROWSKA, Z., T. BOWN, and J. A. LILLEGRAVEN. 1979. Eutheria, pp. 182-191. In J. A. LILLEGRAVEN, Z. KIELAN-JAWOROWSKA, and W. A. CLEMENS (eds.), Mesozoic Mammals. The First Two-thirds of Mammalian History. University of California Press, Berkeley.

KRAUSE, D. W. 1991. Were paromomyids gliders? Maybe, maybe not. Journal of Human Evolution, 21:177-188.

KRAUSE, D. W., and P. D. GINGERICH. 1983. Mammalian fauna from Douglass Quarry, earliest Tiffanian (late Paleocene) of the eastern Crazy Mountain Basin, Montana. Contributions from the Museum of Paleontology, The University of Michigan, 26:157-196.

KRAUSE, D. W., and M. C. MAAS. 1990. The biogeographic origins of late Paleocene–early Eocene mammalian immigrants to the Western Interior of North America, pp. 71-105. In T. M. BOWN and K. D. ROSE (eds.), Dawn of the Age of Mammals in the Northern Part of the Rocky Mountain Interior. Geological Society of America, Special Paper, 243.

KRISHTALKA, L. 1976. North American Nyctitheriidae (Mammalia, Insectivora). Annals of Carnegie Museum, 52:1-28.

LEIDY, J. 1872. On the fossil vertebrates in the early Tertiary formations of Wyoming, pp. 353-377. In F. V. Hayden's Report of the U. S. Geological Survey of the Territories, 5.

LINNAEUS, C. 1758. Systema naturae per regna tria naturae, secundum classes, ordines, genera, species cum characteribus, differentiis, synonymis, locis. Volume I: Regnum Animale. Editio decima, reformata. Laurenti Salvii, Stockholm. [Facsimile reprinted in 1956 by the British Museum (Natural History)]

LOFGREN, D. L., J. A. LILLEGRAVEN, W. A. CLEMENS, P. D. GINGERICH, and T. E. WILLIAMSON. 2004. Paleocene biochronology: The Puercan through Clarkforkian

Land Mammal Ages, pp. 43-105. In M. O. WOODBURNE (ed.), Late Cretaceous and Cenozoic mammals of North America: Geochronology and Biostratigraphy. Columbia University Press, New York.

MACDONALD, J. R. 1963. The Miocene faunas from the Wounded Knee area of western South Dakota. Bulletin of the American Museum of Natural History, 125:139-238.

MACPHEE, R. D. E., M. CARTMILL, AND K. D. ROSE. 1989. Craniodental morphology and relationships of the supposed Eocene dermopteran Plagiomene (Mammalia). Journal of Vertebrate Paleontology, 9:329-349.

MATTHEW, W. D. 1915. Part IV. Entelonychia, Primates, Insectivora (part), pp. 429-483. In W. D. MATTHEW and W. GRANGER, A revision of the lower Eocene Wasatch and Wind River faunas. Bulletin of the American Museum of Natural History, 34.

MATTHEW, W. D. 1918. Part V. Insectivora (continued), Glires, Edentata, pp. 565-657. In W. D. MATTHEW and W. GRANGER, A revision of the lower Eocene Wasatch and Wind River faunas. Bulletin of the American Museum of Natural History, 38.

MATTHEW, W. D., and W. GRANGER. 1921. New genera of Paleocene mammals. American Museum Novitates, 13:1-7.

MCKENNA, M. C. 1960. Fossil Mammalia from the early Wasatchian Four Mile fauna, Eocene of northwest Colorado. University of California Publications in Geological Sciences, 37:1-130.

MCKENNA, M. C. 1990. Plagiomenids (Mammalia: ?Dermoptera) from the Oligocene of Oregon, Montana, and South Dakota, and middle Eocene of northwestern Wyoming, pp. 211-234. In T. M. BOWN and K. D. ROSE (eds.), Dawn of the Age of Mammals in the Northern Part of the Rocky Mountain Interior. Geological Society of America Special Paper, 243.

MCKENNA, M. C., and S. K. BELL. 1997. Classification of Mammals Above the Species Level. Columbia University Press, New York.

MENU, H., and B. SIGÉ. 1971. Nyctalodontie et myotodontie, importants charactères de grades évolutifs chez les chiroptères entomophages. Comptes Rendus Hebdomadaires de l'Académie des Sciences, Paris, Série D, 272:1735-1738.

NESSOV, L.A. [NESOV, L.A.] 1985. New mammals from the Cretaceous of Kyzylkum [in Russian]. Vestnik Leningradskogo Universiteta, Seriâ 7, 17: 8-18.

NOVACEK, M. J. 1980. Cranioskeletal features in tupaiids and selected Eutheria as phylogenetic evidence, pp. 35-93. In W. P. LUCKETT (ed.), Comparative Biology and Evolutionary Relationships of Tree Shrews, Plenum Press, New York.

NOVACEK, M. J. 1982. Diacodon alticuspis, an erinaceomorph insectivore from the early Eocene of northern New Mexico. Contributions to Geology, 20:135-149.

NOVACEK, M. J., T. M. BOWN, and D. SCHANKLER. 1985. On the classification of the early Tertiary Erinaceomorpha (Insectivora, Mammalia). American Museum Novitates, 2813:1-22.

OLSON, L. E., E. J. SARGIS, and R. D. MARTIN. 2004. Phylogenetic relationships among treeshrews (Scandentia): a review and critique of the morphological evidence. Journal of Mammalian Evolution, 11:49-71.

PARKER, T. J., and W. A. HASWELL. 1897. A Text-book of Zoology. Vol. 2. Macmillan Press, London, 301 pp.

RADINSKY, L., and S.-Y. TING. 1984. The skull of Ernanodon, an unusual fossil mammal. Journal of Mammalogy, 65:155-158.

REPENNING, C. A. 1967. Subfamilies and genera of the Soricidae. Geological Survey Professional Paper, 565:1-74.ROSE, K. D. 1973. The mandibular dentition of Plagiomene (Dermoptera, Plagiomenidae). Breviora, 411:1-17.

ROSE, K. D. 1973. The mandibular dentition of Plagiomene (Dermoptera, Plagiomenidae). Breviora, 411:1-17.

ROSE, K. D. 1975. Elpidophorus, the earliest dermopteran (Dermoptera, Plagiomenidae). Journal of Mammalogy, 56:676-679.

ROSE, K. D. 1981. The Clarkforkian Land Mammal Age and mammalian faunal composition across the Paleocene-Eocene boundary. University of Michigan Papers on Paleontology, 26:1-197.

ROSE, K. D. 2006. The Beginning of the Age of Mammals. The Johns Hopkins University Press, Baltimore.

ROSE, K. D. In press. Plagiomenidae and Mixodectidae, pp. XX-XX. In C. M. JANIS, K. M. SCOTT, and L. L. JACOBS (eds.), Evolution of Tertiary Mammals of North America, volume 2: Cambridge University Press, Cambridge.

ROSE, K. D., and E. L. SIMONS. 1977. Dental function in the Plagiomenidae: origin and relationships of the mammalian order Dermoptera. Contributions from the Museum of Paleontology, The University of Michigan, 24:221-236.

ROSE, K. D., and D. W. KRAUSE. 1982. Cyriacotheriidae, a new family of early Tertiary pantodonts from western North America. Proceedings of the American Philosophical Society, 126:26-50.

RUSSELL, D. E. 1964. Les Mammifères paléocènes d'Europe. Mémoirs du Museum National d'Histoire Naturelle (France), Nouvelle Série, Série C, 13:1-321.

RUSSELL, D. E. 1967. La Paléocène continental d'Amerique du Nord. Mémoirs du Museum National d'Histoire Naturelle (France), Nouvelle Série, Série C, 16:1-99.

RUSSELL, D. E., P. LOUIS, and D. E. SAVAGE. 1973. Chiroptera and Dermoptera of the French early Eocene. University of California Publications in Geological Sciences, 95:1-57.

RUSSELL, L. S. 1954. Mammalian fauna of the Kishenehn Formation, southeastern British Columbia. Annual Report of the National Museum of Canada for 1952-53, Bulletin, 132:92-111.

RUSSELL, L. S. 1967. Paleontology of the Swan Hills area, north-central Alberta. Contributions in Life Sciences from the Royal Ontario Museum, 71:1-31.

SARGIS, E. J. 2002a. Functional morphology of the hindlimb of tupaiids (Mammalia, Scandentia) and its phylogenetic implications. Journal of Morphology, 254: 149-185.

SARGIS, E. J. 2002b. Functional morphology of the forelimb of tupaiids (Mammalia, Scandentia) and its phylogenetic implications. Journal of Morphology, 253: 10-42.

SARGIS, E. J. 2002c. The postcranial morphology of Ptilocercus lowii (Scandentia, Tupaiidae): an analysis of primatomorphan and volitantian characters. Journal of Mammalian Evolution, 9: 137-160.

SCHWARTZ, J. H., and L. KRISHTALKA. 1976. The lower antemolar teeth of Litolestes ignotus, a late Paleocene erinaceid (Mammalia, Insectivora). Annals of Carnegie Museum, 46:1-6.

SCOTT, C. S. 2003. Late Torrejonian (middle Paleocene) mammals from south central Alberta, Canada. Journal of Paleontology, 77:745-768.

SCOTT, C. S. 2004. Taxonomically diverse late Paleocene mammal localities from south central Alberta, Canada. Journal of Vertebrate Paleontology 24, supplement to no. 3:111A.

SCOTT, C. S. 2005. New material of Elpidophorus Simpson (Mammalia, Eutheria) from Alberta, Canada, and an assessment of the taxonomic position of the genus. Proceedings of the 10th North American Paleontological Conference.

SIGÉ. B. 1976. Insectivores primitifs de l'Éocène supérieur et Oligocène inférieur d'Europe occidentale. Nyctithériidés. Mémoires du Muséum National d'Histoire Naturelle, Série C, 34:1-140.

SILCOX, M. T. 2001. A phylogenetic analysis of Plesiadapiformes and their relationship to Euprimates and other archontans. Unpublished Ph. D. dissertation, The Johns Hopkins University, Baltimore, Maryland, 728 pp.

SILCOX, M. T., J. I. BLOCH, E. J. SARGIS, and D. M. BOYER. 2005. Euarchonta (Dermoptera, Scandentia, Primates), pp. 127-144. In K. D. ROSE and J. D. ARCHIBALD (eds.), The Rise of Placental Mammals, The Johns Hopkins University Press, Baltimore.

SIMONS, E. L. 1960. The Paleocene Pantodonta. Transactions of the American Philosophical Society, new series, 50:1-99.

SIMPSON, G. G. 1927. Mammalian fauna and correlation of the Paskapoo Formation of Alberta. American Museum Novitates, 268:1-10.

SIMPSON, G. G. 1928. A new mammalian fauna from the Fort Union of southern Montana. American Museum Novitates, 297:1-15.

SIMPSON, G. G. 1935. New Paleocene mammals from the Fort Union of Montana. Proceedings of the United States National Museum, 83:221–244.

SIMPSON, G. G. 1936. A new fauna from the Fort Union of Montana. American Museum Novitates, 873:1-27.

SIMPSON, G. G. 1937. The Fort Union of the Crazy Mountain Field, Montana and its mammalian faunas. Bulletin of the United States Museum, 169:1-287.

SIMPSON, G. G. 1945. The principles of classification and a classification of mammals. Bulletin of the American Museum of Natural History, 85:1-350.

SLOAN, R. E. 1969. Cretaceous and Paleocene terrestrial communities of western North America. Proceedings of the North American Paleontology Convention, 1969:427-453.

SMITH, T. 1997. Les insectivores s. s. (Mammalia, Lipotyphla) de la transition Paléocène-Éocène de Dormaal (MP 7, Belgique): implications biochronologiques et paléogéographiques, pp. 687-696. In J. P. AGUILAR, S. LEGENDRE, and J. MICHAUX (eds.), Actes du Congrès Biochrom '97, Mémoires et Travaux de l'Institut de Montpellier de l'École Pratique des Hautes Études, Montpellier, 21.

STOCK, C. 1934. Microsyopsinae and Hyopsodontidae in the Sespe upper Eocene, California. Proceedings of the National Academy of Science, 20:349-354.

STONLEY, G. J. 1988. Late Paleocene Mammals of the Swan Hills Local Fauna (Paskapoo Formation), Alberta. Unpublished M. Sc. thesis, University of Alberta, Edmonton, 265 pp.

STAFFORD, B. J., and F. S. SZALAY. 2000. Craniodental functional morphology and taxonomy of dermopterans. Journal of Mammalogy, 81:360-385.

SZALAY, F. S. 1969a. Mixodectidae, Microsyopidae, and the insectivore-primate transition. Bulletin of the American Museum of Natural History, 140:193-330.

SZALAY, F. S. 1969b. Origin and evolution of function of the mesonychid condylarth feeding mechanism. Evolution, 23:703-720.

SZALAY, F. S., and S. G. LUCAS. 1996. The postcranial morphology of Paleocene Chriacus and Mixodectes and the phylogenetic relationships of archontan mammals. New Mexico Museum of Natural History and Science Bulletin, 7:1-47.

VAN VALEN, L. 1967. New Paleocene insectivores and insectivore classification. Bulletin of the American Museum of Natural History, 135:217-284.

VAN VALEN, L. 1969. The multiple origins of the placental carnivores. Evolution, 23:118-130.

VAN VALEN, L., and R. E. SLOAN. 1965. The earliest primates. Science, 150:743-745.

WEBB, M. W. 1996. Late Paleocene mammals from near Drayton Valley, Alberta. Unpublished M. Sc. thesis, University of Alberta, Edmonton, 258 pp.

YOUZWYSHYN, G. P. 1988. Paleocene mammals from near Cochrane, Alberta. Unpublished M. Sc. thesis, University of Alberta, Edmonton, 484 pp.

ZHOU, Y. 1995. Evolution of Paleocene-Eocene Mesonychidae (Mammalia, Mesonychia). Unpublished Ph. D. dissertation, The University of Michigan, Ann Arbor, 402 pp.

Table 8.1.—Combined measurements and descriptive statistics for the dentition of Eudaemonema thlastes new species from the early middle Tiffanian (Ti3) DW-2 and Birchwood localities, Paskapoo Formation, Alberta.

Element	P	N	OR	M	SD	CV
M1	L	2	4.0-4.1	4.05	0.07	1.75
	W	2	4.8-5.0	4.90	0.14	2.89
M2	L	2	4.2-4.4	4.30	0.14	3.29
	W	2	5.2-5.4	5.30	0.14	2.67
M3	L	3	3.9-4.2	4.03	0.15	3.79
	W	3	5.5-5.8	5.60	0.17	3.09
p3	L	1	2.6	—	—	—
	W	1	1.7	—	—	—
p4	L	1	3.5	—	—	—
	W	1	2.4	—	—	—
m1	L	1	4.2	—	—	—
	TrW	1	2.6	—	—	—
	TaW	2	3.0-3.1	3.05	0.07	2.32
m2	L	4	4.4-4.7	4.58	0.15	3.28
	TrW	4	2.6-2.7	2.65	0.06	2.18
	TaW	4	3.2-3.3	3.25	0.06	1.78
m3	L	1	5.2	—	—	—
	TrW	2	2.5-2.7	2.60	0.14	5.44
	TaW	1	2.7	—	—	—

Table 8.2.—Combined measurements and descriptive statistics for the upper dentition of Elpidophorus simpsoni new species from the early middle Tiffanian (Ti3) DW-2, Joffre Bridge Roadcut lower level, and Joffre Bridge Mammal Site No. 1 localities, Paskapoo Formation, Alberta.

Element	P	N	OR	M	SD	CV
C	L	1	2.0	—	—	—
	W	1	1.6	—	—	—
P2	L	2	2.1	2.10	0	0
	W	2	1.5-1.7	1.60	0.14	8.84
P3	L	4	3.3-3.5	3.40	0.08	2.40
	W	4	3.5-3.6	3.53	0.05	1.42
P4	L	2	3.5	3.50	0	0
	W	2	4.2-4.4	4.30	0.14	3.29
M1	L	2	3.7-3.8	3.75	0.07	1.89
	W	2	5.0-5.2	5.10	0.14	2.77
M2	L	1	3.8	—	—	—
	W	1	5.5	—	—	—
M3	L	2	3.0-3.1	3.05	0.07	2.32
	W	2	5.0-5.1	5.05	0.07	1.40

Table 8.3.—Combined measurements and descriptive statistics for the lower dentition of Elpidophorus simpsoni new species from the early middle Tiffanian (Ti3) DW-2, Mel's Place, Joffre Bridge Roadcut lower level, and Joffre Bridge Mammal Site No. 1 localities, Paskapoo Formation, Alberta.

Element	P	N	OR	M	SD	CV
c	L	1	2.2	—	—	—
	W	1	1.5	—	—	—
p1	L	3	2.0-2.1	2.03	0.06	2.84
	W	3	1.4-1.7	1.50	0.17	11.55
p2	L	5	2.0-2.3	2.16	0.13	6.21
	W	5	1.3-1.5	1.40	0.07	5.05
p3	L	5	2.4-2.6	2.52	0.08	3.32
	W	5	2.0-2.3	2.16	0.13	6.21
p4	L	6	3.6-3.9	3.75	0.10	2.80
	W	6	2.6-2.9	2.77	0.10	3.73
m1	L	4	3.8-3.9	3.83	0.05	1.31
	TrW	5	2.7-2.9	2.80	0.07	2.53
	TaW	4	3.0-3.3	3.18	0.13	3.96
m2	L	6	3.7-4.1	3.93	0.14	3.47
	TrW	6	2.8-3.1	2.98	0.12	3.92
	TaW	6	3.1-3.4	3.23	0.12	3.75
m3	L	3	4.8-5.0	4.90	0.10	2.04
	TrW	3	2.8-3.0	2.90	0.10	3.45
	TaW	3	2.7-3.0	2.87	0.15	5.33

Table 8.4.—Combined measurements and descriptive statistics for the upper dentition of Elpidophorus elegans Simpson from the early middle Tiffanian (Ti3) DW-1, DW-2, Joffre Bridge Roadcut lower level, Joffre Bridge Mammal Site No. 1, and Birchwood localities, Paskapoo Formation, Alberta.

Element	P	N	OR	M	SD	CV
P2	L	4	2.2-2.4	2.30	0.08	3.55
	W	4	1.7-1.9	1.80	0.08	4.54
P3	L	8	3.4-3.9	3.55	0.16	4.52
	W	8	3.6-3.8	3.69	0.06	1.74
P4	L	11	3.6-4.1	3.85	0.16	4.24
	W	11	4.4-5.0	4.68	0.19	4.14
M1	L	10	3.8-4.1	3.96	0.13	3.19
	W	10	5.0-5.4	5.16	0.13	2.45
M2	L	18	3.7-4.1	3.92	0.14	3.56
	W	18	5.4-6.1	5.69	0.20	3.51
M3	L	9	3.3-3.5	3.38	0.08	2.47
	W	9	5.0-5.4	5.17	0.11	2.16

Table 8.5.—Combined measurements and descriptive statistics for the lower dentition of Elpidophorus elegans Simpson from the early middle Tiffanian (Ti3) DW-2, Joffre Bridge Roadcut lower level, Joffre Bridge Mammal Site No. 1, and Birchwood localities, Paskapoo Formation, Alberta.

Element	P	N	OR	M	SD	CV
p2	L	2	2.0-2.3	2.15	0.21	9.87
	W	2	1.7	1.70	0	0
p3	L	12	2.5-3.0	2.73	0.18	6.66
	W	12	2.2-2.7	2.40	0.14	5.89
p4	L	16	3.7-4.3	3.92	0.19	4.95
	W	16	2.7-3.3	2.99	0.16	5.45
m1	L	20	3.6-4.1	3.90	0.16	3.99
	TrW	20	3.0-3.2	3.11	0.09	2.74
	TaW	20	3.2-3.7	3.39	0.16	4.62
m2	L	22	4.0-4.4	4.15	0.14	3.30
	TrW	22	3.1-3.6	3.25	0.15	4.62
	TaW	22	3.2-3.9	3.58	0.21	5.97
m3	L	18	4.7-5.3	5.03	0.19	3.72
	TrW	20	2.9-3.3	3.07	0.13	4.11
	TaW	18	2.8-3.3	3.06	0.17	5.41

Table 8.6.—Measurements and descriptive statistics for the upper dentition of Elpidophorus clivus new species from the late middle Tiffanian (Ti4) Swan Hills locality, Paskapoo Formation, Alberta.

Element	P	N	OR	M	SD	CV
C/P1	L	2	1.8-1.9	1.85	0.07	3.80
	W	2	1.3-1.4	1.35	0.07	5.20
P2	L	2	1.9	1.90	0	0
	W	2	1.3-1.4	1.35	0.07	5.20
P3	L	3	3.1-3.2	3.13	0.06	1.80
	W	2	2.9-3.1	3.00	0.14	4.70
P4	L	5	3.4-3.5	3.44	0.06	1.60
	W	3	4.0-4.3	4.13	0.15	3.70
M1	L	9	3.1-3.4	3.28	0.11	3.3
	W	8	4.0-4.6	4.41	0.20	4.40
M2	L	7	3.1-3.4	3.27	0.10	2.90
	W	7	4.8-4.9	4.83	0.05	1.00
M3	L	3	2.7-2.8	2.77	0.06	2.10
	W	3	4.1-4.4	4.23	0.15	3.60

Table 8.7.—Measurements and descriptive statistics for the lower dentition of Elpidophorus clivus new species from the late middle Tiffanian (Ti4) Swan Hills locality, Paskapoo Formation, Alberta.

Element	P	N	OR	M	SD	CV
c/p1	L	2	1.5-1.7	1.60	0.14	8.80
	W	2	1.2-1.3	1.25	0.07	5.70
p2	L	1	2.1	—	—	—
	W	1	1.6	—	—	—
p3	L	3	2.2-2.5	2.25	0.07	3.1
	W	4	1.7-1.8	1.73	0.06	3.3
p4	L	4	3.2-3.4	3.30	0.12	3.50
	W	8	2.2-2.7	2.45	0.19	7.90
m1	L	3	3.1-3.2	3.17	0.06	1.80
	TrW	4	2.5-2.6	2.55	0.06	2.30
	TaW	3	2.6-2.7	2.63	0.06	2.20
m2	L	5	3.0-3.5	3.26	0.23	7.10
	TrW	6	2.3-2.7	2.48	0.13	5.40
	TaW	6	2.6-2.9	2.77	0.10	3.70
m3	L	3	3.9-4.1	4.00	0.10	2.50
	TrW	4	2.3-2.7	2.48	0.17	6.90
	TaW	6	2.2-2.5	2.33	0.10	4.40

Figure 8.1.—1-21. Eudaemonema thlastes new species from the early middle Tiffanian (Ti3) DW-2 locality (DW2) and late middle Tiffanian (Ti4) Gao Mine locality (GM), Paskapoo Formation, Alberta. 1-3, UALVP 46419 (DW2), left M1 in 1, labial, 2, oblique lingual, and 3, occlusal view; 4-6, UALVP 46420 (DW2), left M2 in 4, labial, 5, oblique lingual, and 6, occlusal view; 7-9, UALVP 46421 (DW2), right M3 in 7, labial, 8, oblique lingual, and 9, occlusal view; 10-12, UALVP 46422 (DW2), right M3 in 10, labial, 11, oblique lingual, and 12, occlusal view; 13-15, UALVP 46418 (GM, holotype), incomplete left dentary with p2 (talonid), p3-4, m1-2, m3 (trigonid) in 13, labial, 14, lingual, and 15, occlusal view; 16-18, UALVP 46425 (DW2), incomplete right dentary with m1 (talonid) and m2 in 16, labial, 17, lingual, and 18, occlusal view; 19-21, UALVP 46426 (GM), right m3 in 19, labial, 20, lingual, and 21, occlusal view. Scale bars = 2 mm.

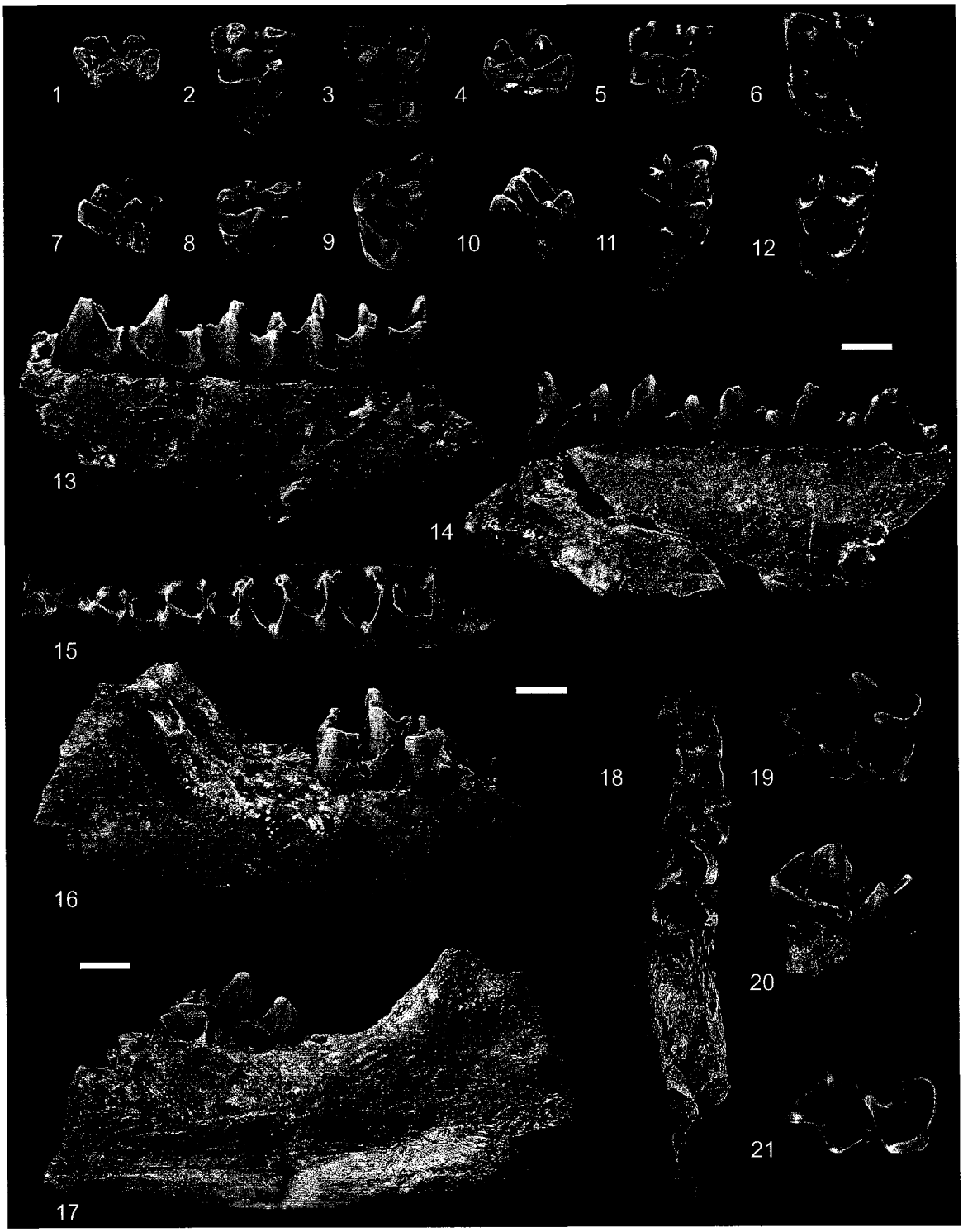
1
2
3
4
5
6
7
8
9
10
11
12
13
14
15
16
17
18
19
20
21

Figure 8.2.—1-15. Elpidophorus simpsoni new species from the early middle Tiffanian (Ti3) Joffre Bridge Roadcut lower level (JBLL) and Joffre Bridge Mammal Site No. 1 localities, Paskapoo Formation, Alberta. 1-3, UALVP 40590 (JBMS), incomplete left maxilla with C, P2-4, M1-3, and alveolus for P1 in 1, labial, 2, oblique lingual, and 3, occlusal view; 4-6, UALVP 40584 (JBLL), incomplete right maxilla with P2-3 in 4, labial, 5, oblique lingual, and 6, occlusal view; 7-9, UALVP 40572 (JBLL), left P3 in 7, labial, 8, oblique lingual, and 9, occlusal view; 10-12, UALVP 46428 (JBLL), left P4 in 10, labial, 11, oblique lingual, and 12, occlusal view; 13-15, UALVP 46427 (holotype, JBMS)), incomplete right dentary with i1, i3 (i3 crown broken), c, p1-4 (p1 crown broken), m1-3, and alveolus for i2 in 13, labial, 14, lingual, and 15, occlusal view. Scale bars = 2 mm.

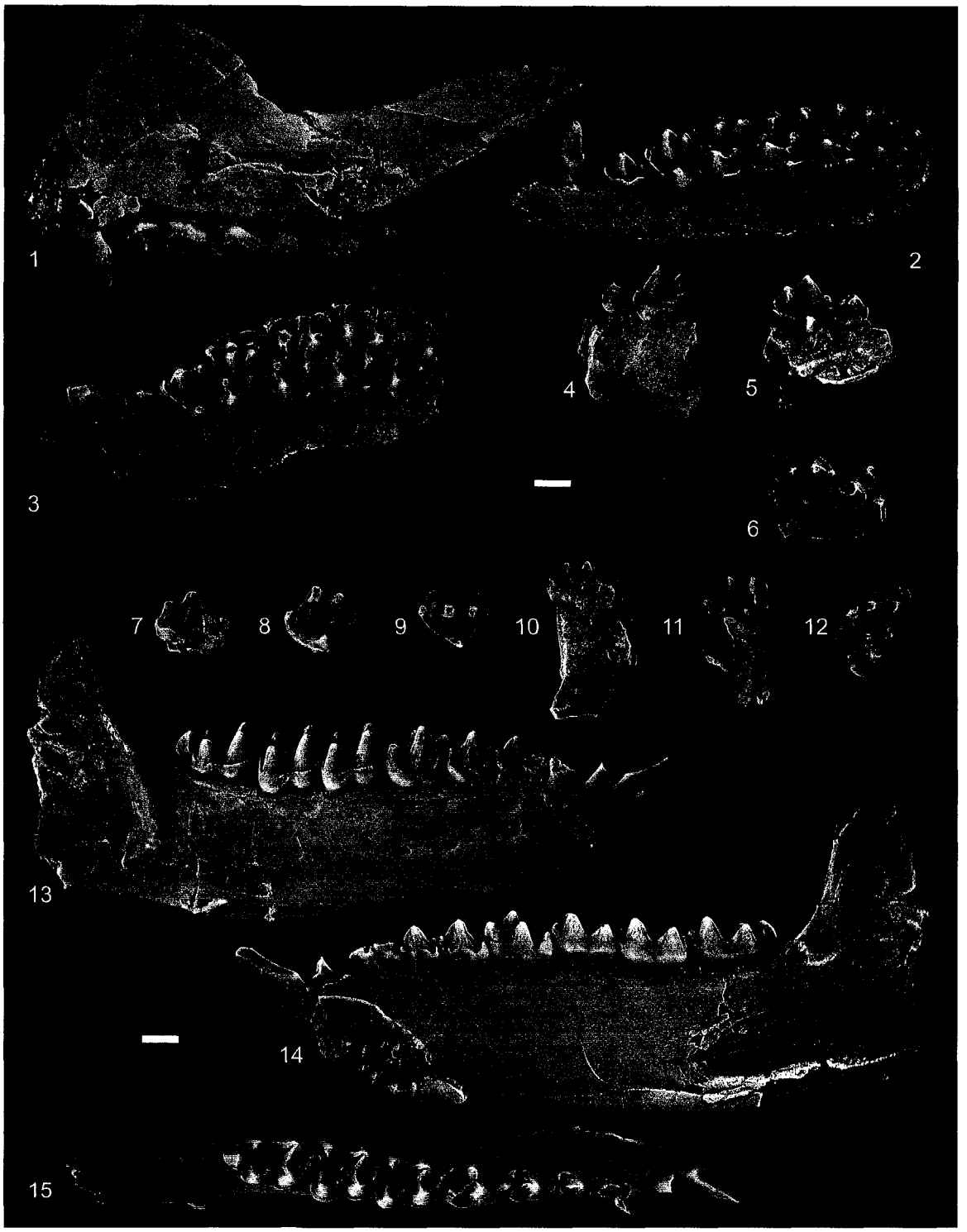
1
2
3
4
5
6
7
8
9
10
11
12
13
14
15

Figure 8.3.—1-15. Elpidophorus simpsoni new species from the early middle Tiffanian (Ti3) Joffre Bridge Roadcut lower level (JBLL) and Joffre Bridge Mammal Site No. 1 (JBMS) localities, Paskapoo Formation, Alberta. 1-3, UALVP 40588 (JBMS), incomplete left dentary with i1-3 (i3 broken), c, p1-4 in 1, labial, 2, lingual, and 3, occlusal view; 4-6, UALVP 40589 (JBMS), incomplete right dentary with i1, i2-3 (broken), p1-3, p4 (broken), and canine alveolus in 4, labial, 5, lingual, and 6, occlusal view; 7-9, UALVP 40582 (JBLL), incomplete right dentary with p4 and alveoli for p1-3 in 7, labial, 8, lingual, and 9, occlusal view; 10-12, UALVP 46431 (JBLL), incomplete left dentary with p1-4, m1, and alveoli for i2-3 in 10, labial, 11, oblique lingual, and 12, occlusal view; 13-15, UALVP 46433 (JBMS), isolated left i1 or i2 in 13, medial, 14, lateral, and 15, occlusal view. Scale bars = 2 mm.

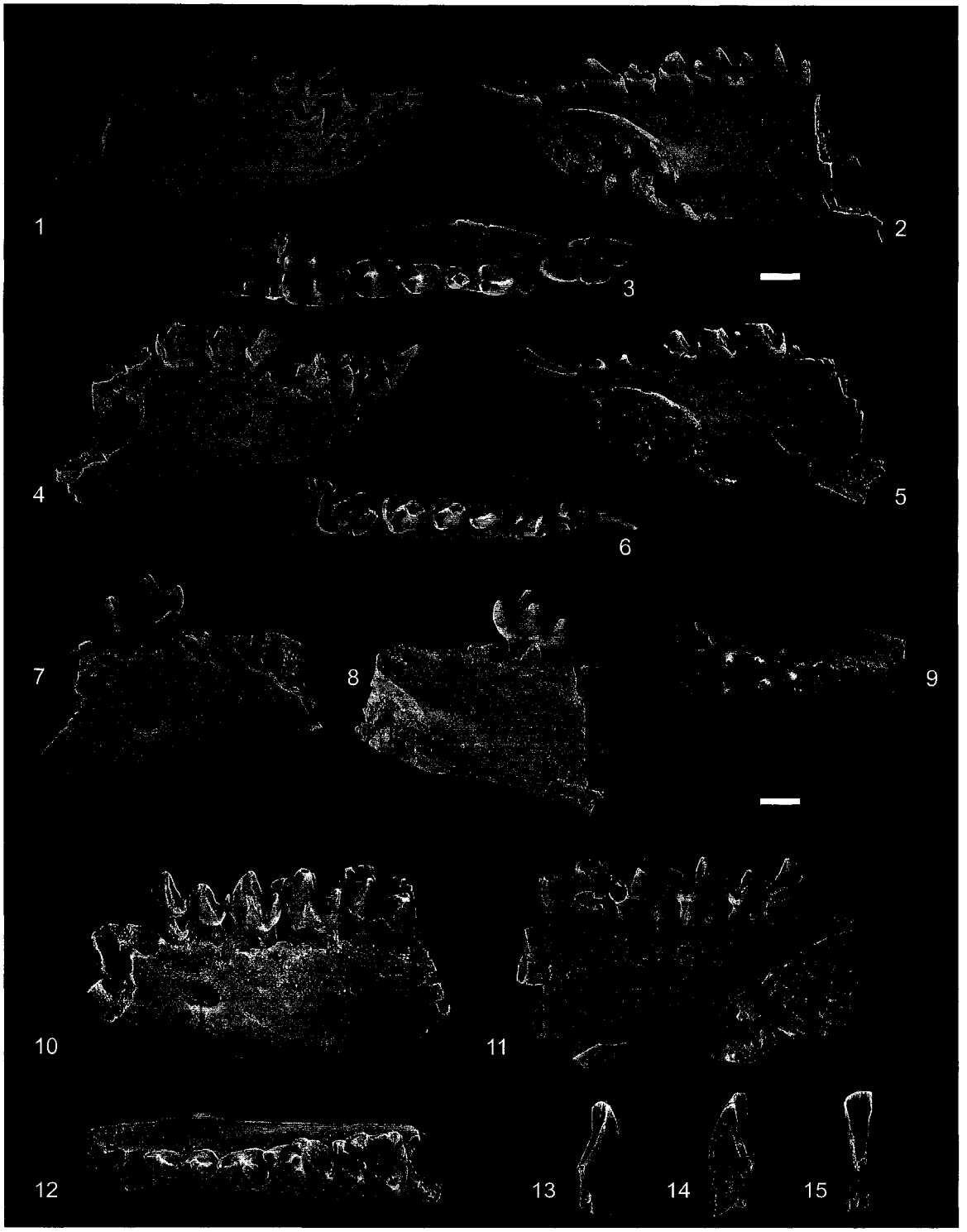
1
2
3
4
5
6
7
8
9
10
11
12
13
14
15

Figure 8.4.—1-16. Elpidophorus elegans Simpson from the early middle Tiffanian (Ti3) DW-1 (DW1), DW-2 (DW2), Joffre Bridge Mammal Site No. 1 (JBMS), and Birchwood (BW) localities, Paskapoo Formation, Alberta. 1-3, UALVP 40570 (JBMS), incomplete right maxilla with P2-4, M1-3, and alveolus for C in 1, labial, 2, oblique lingual, and 3, occlusal view; 4-6, UALVP 40566 (DW1), incomplete left maxilla with P3-4, M1-3 in 4, labial, 5, oblique lingual, and 6, occlusal view; 7-9, UALVP 40568 (DW2), incomplete right maxilla with P4, M1-3 (associated M2 not shown) in 7, labial, 8, oblique lingual, and 9, occlusal view; UALVP 46443 (DW2), incomplete and associated right and left maxillae with RP3-4, M1-3, and alveoli for C, P2, and LP2-4, M1-3, and alveolus for C in 10, occlusal view (arrow points to diastema between the upper canine and P2 alveolus); 11-13, UALVP 39392 (BW), right P4 in 11, labial, 12, oblique lingual, and 13, occlusal view; 14-16, UALVP 39395 (BW), left P4 in 14, medial, 15, lateral, and 16, occlusal view. Scale bars = 2 mm.

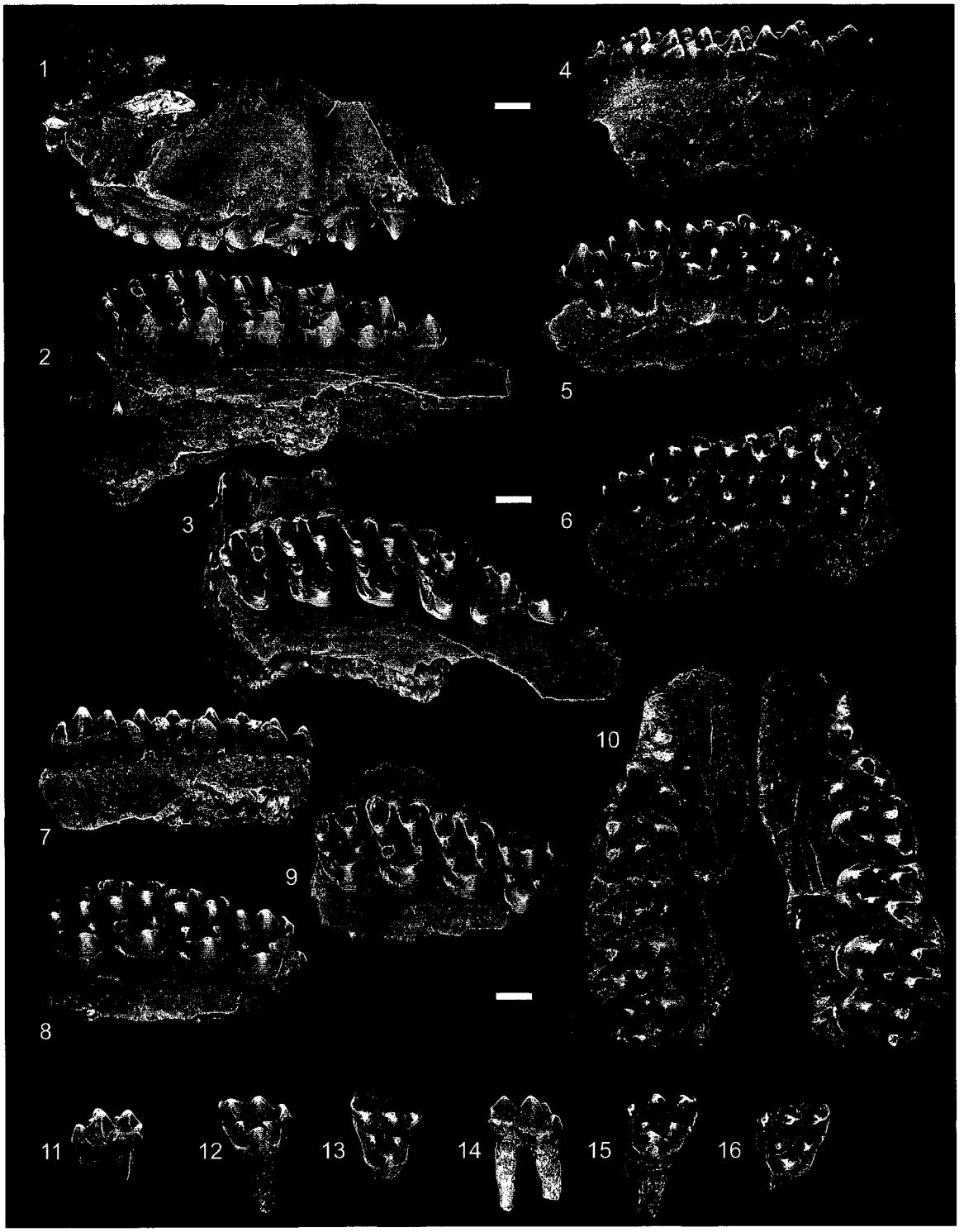
1
2
3
4
5
6
7
8
9
10
11
12
13
14
15
16

Figure 8.5.—1-15. Elpidophorus elegans Simpson from the early middle Tiffanian (Ti3) DW-2 (DW2), Joffre Bridge Mammal Site No. 1 (JBMS), and Birchwood (BW) localities, Paskapoo Formation, Alberta. 1-3, UALVP 43097 (JBMS), incomplete left dentary with i1-2, p3-4, m1-3, and alveoli for i3, c, p2 in 1, labial, 2, lingual, and 3, occlusal view; box (3A) shows anterior parts of UALVP 43097 in occlusal view at higher magnification; note the alveoli for c and p2, and that p1 is undeveloped; 4-6, UALVP 46457 (DW2), incomplete right dentary with m1-3, and alveoli for i1-3, c, p2-4 in 4, labial, 5, lingual, and 6, occlusal view; box (4A) shows anterior parts of UALVP 46457 in labial view at higher magnification; note the alveoli for c and p2, and that p1 is undeveloped; 7-9, UALVP 46461 (DW2), right i2 in 7, lateral, 8, medial, and 9, occlusal view; 10-12, UALVP 46462 (DW2), left i2 in 10, lateral, 11, medial, 12, occlusal view; 13-15, UALVP 39400 (BW), incomplete dentary with i1-2 in 14, lateral, 15, medial, and 16, occlusal view. Scale bars = 2 mm.

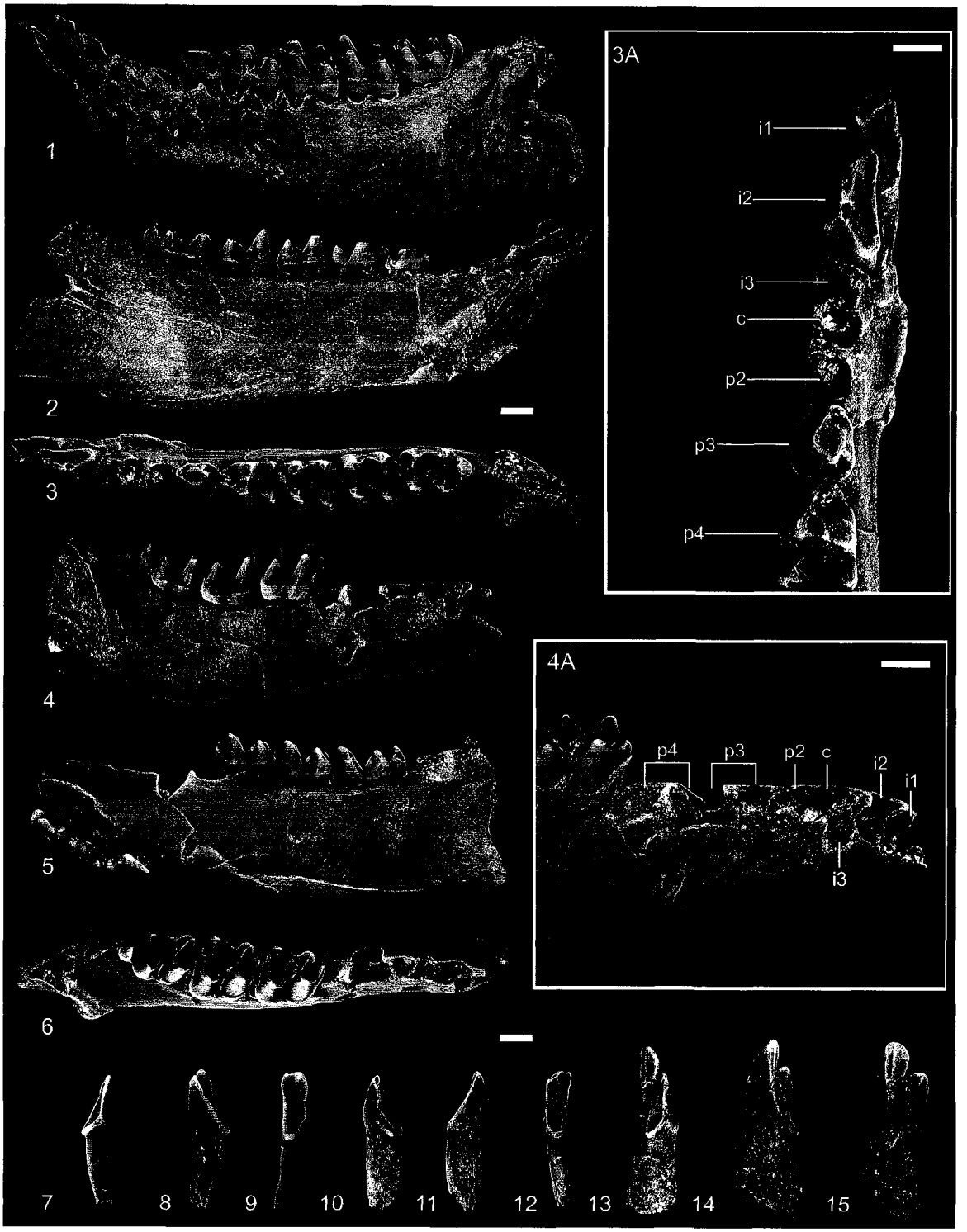
1
2
3
4
5
6
3A
i1
i2
i3
c
p2
p3
p4
4A
p4
p3
p2
c
i2
i1
i3
7
8
9
10
11
12
13
14
15

Figure 8.6.—1-15. Elpidophorus elegans Simpson from the early middle Tiffanian (Ti3) DW-2 (DW2), Joffre Bridge Roadcut lower level (JBLL), and Birchwood (BW) localities, Paskapoo Formation, Alberta. 1-3, UALVP 46454 (DW2), incomplete right dentary with p2-4, m1-3, and alveoli for i1-3, c in 1, labial, 2, lingual, and 3, occlusal view; 4-6, UALVP 40585 (JBLL), incomplete right dentary with p3-4, m1-3, and alveoli for i1-3, c, p2 in 4, labial, 5, lingual, and 6, occlusal view; 7-9, UALVP 46468 (BW), incomplete right dentary with p3-4, m1-3, and alveoli for p2 in 7, labial, 8, lingual, and 9, occlusal view. Scale bars = 2 mm.

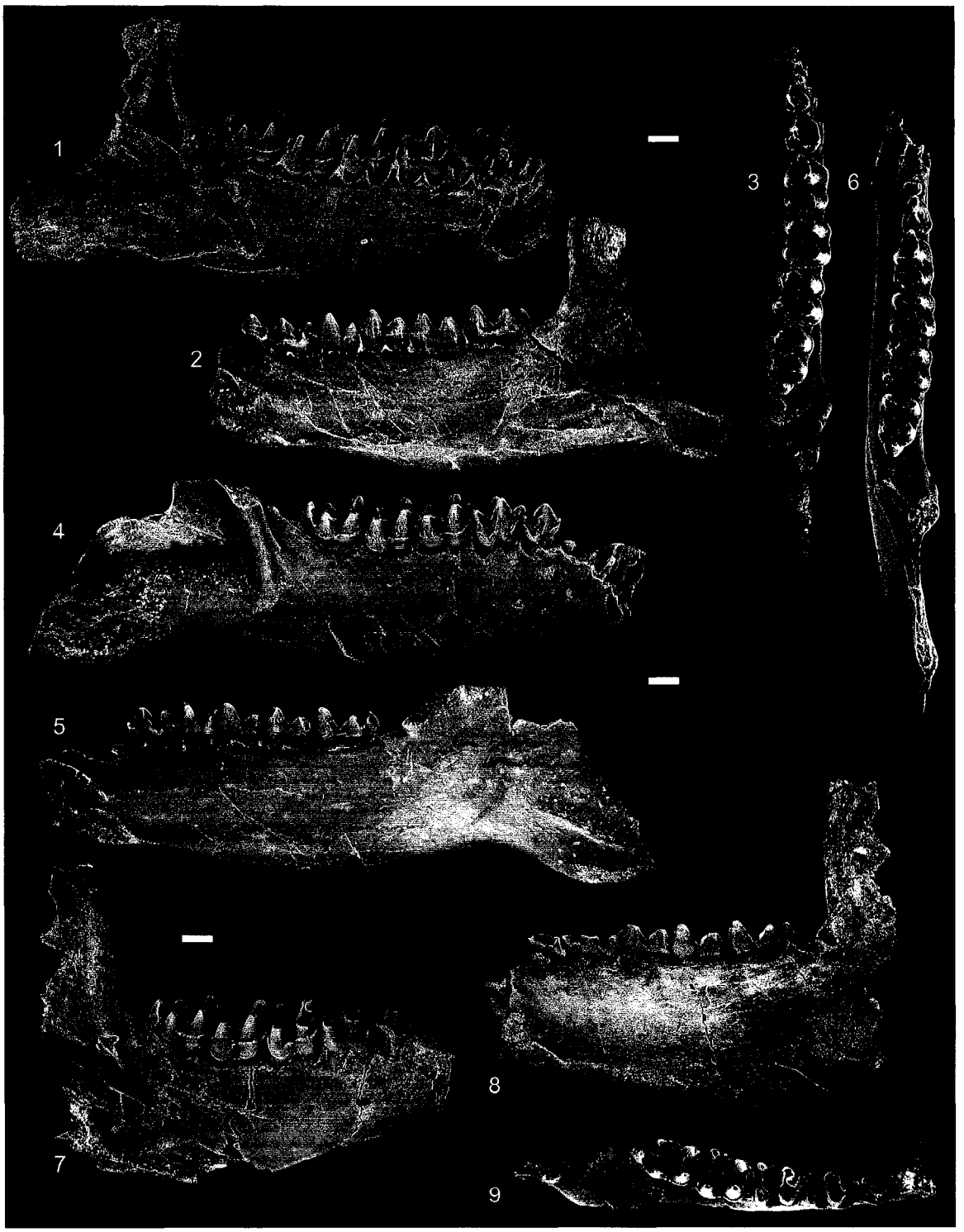
1
2
3
6
4
5
7
8
9

Figure 8.7.—1-37. Elpidophorus clivus new species from the late middle Tiffanian (Ti4) Swan Hills locality, Paskapoo Formation, Alberta. 1-3, UALVP 22625, left upper canine or P1 in 1, labial, 2, lingual, and 3, occlusal view; 4-6, UALVP 39759, right P2 in 4, labial, 5, lingual, and 6, occlusal view; 7-9, UALVP 22264, left P3 in 7, labial, 8, oblique lingual, and 9, occlusal view; 10-12, UALVP 22263, left P3 in 10, labial, 11, oblique lingual, and 12, occlusal view; 13-15, UALVP 22361, right P4 in 13, labial, 14, oblique lingual, and 15, occlusal view; 16-18, UALVP 22362, left P4 in 16, labial, 17, oblique lingual, and 18, occlusal view; 19-21, UALVP 22363, right M1 in 19, labial, 20, oblique lingual, and 21, occlusal view; 22-24, UALVP 22364, right M1 in 22, labial, 23, oblique lingual, and 24, occlusal view; 25-27, UALVP 22269, right M2 in 25, labial, 26, oblique lingual, and 27, occlusal view; 28-30, UALVP 23838, left M2 in 28, labial, 29, oblique lingual, and 30, occlusal view; 31-33, UALVP 22274, right M3 in 31, labial, 32, oblique lingual, and 33, occlusal view; 34-36, UALVP 22584, right M3 in 34, labial, 35, lingual, and 36, occlusal view; 37, composite left upper dentition [UALVP 39759 (reversed), UALVP 22264, UALVP 22362, UALVP 22363 (reversed), UALVP 22269 (reversed), UALVP 22274 (reversed)] in occlusal view. Scale bars = 2 mm.

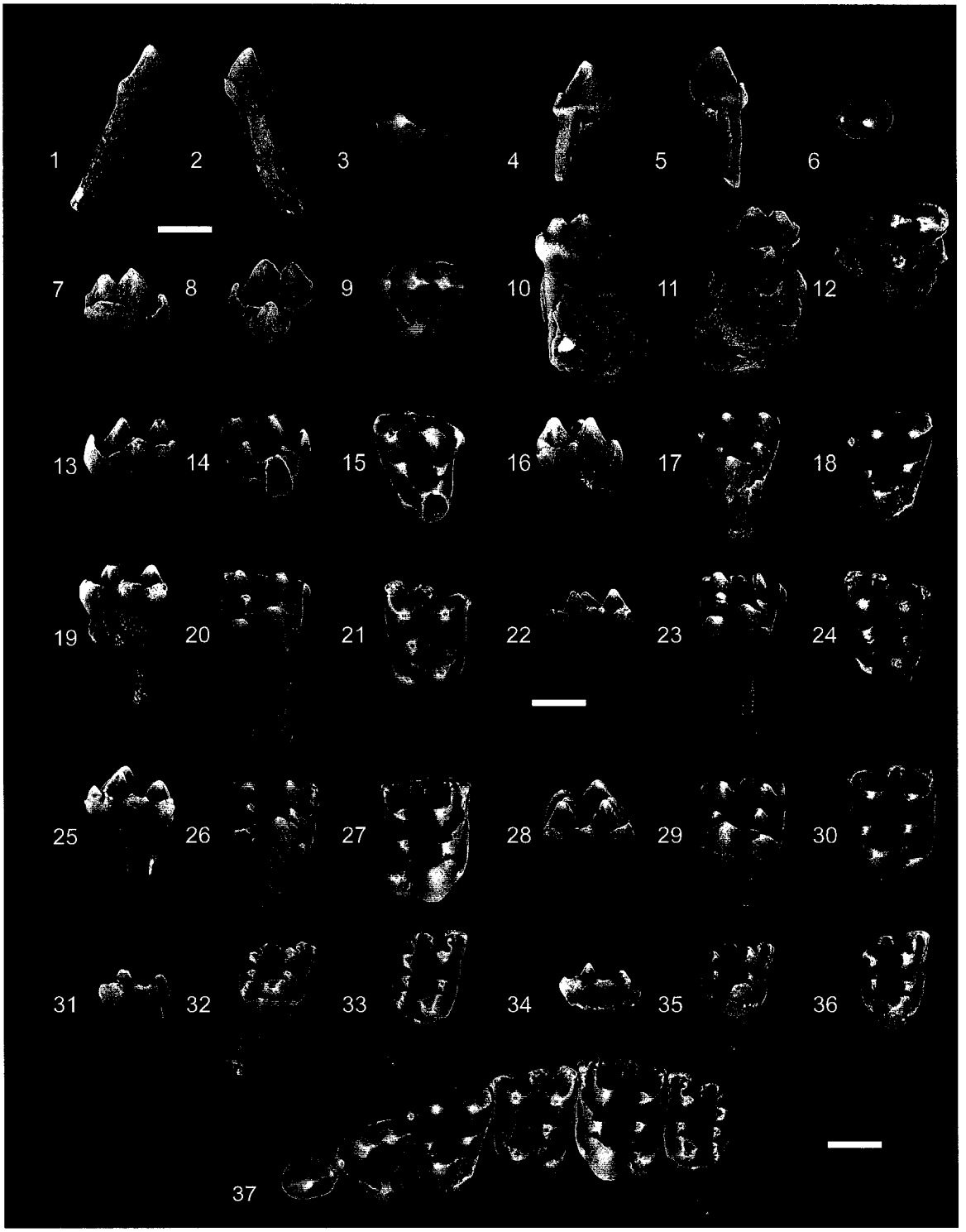
1
2
3
4
5
6
7
8
9
10
11
12
13
14
15
16
17
18
19
20
21
22
23
24
25
26
27
28
29
30
31
32
33
34
35
36
37

Figure 8.8.—1-36. Elpidophorus clivus new species from the late middle Tiffanian (Ti4) Swan Hills locality, Paskapoo Formation, Alberta. 1-3, UALVP 22379, left i1 in 1, lateral, 2, medial, and 3, occlusal view; 4-6, UALVP 23839, left i2 in 4, lateral, 5, medial, and 6, occlusal view; 7-9, UALVP 22712, right lower canine or p1 in 7, labial, 8, lingual, and 9, occlusal view; 10-12, UALVP 22258, right p2 in 10, labial, 11, lingual, and 12, occlusal view; 13-15, UALVP 22230, right p3 in 13, labial, 14, lingual, and 15, occlusal view; 16-18, UALVP 22346, left p3 in 16, labial, 17, oblique lingual, and 18, occlusal view; 19-21, UALVP 22317 (holotype), incomplete right dentary with p4, m1-3 in 19, labial, 20, lingual, and 21, occlusal view; 22-24, UALVP 22285, left p4 in 22, labial, 23, lingual, and 24, occlusal view; 25-27, UALVP 22286, incomplete left dentary with p4 and alveoli for p3 in 25, labial, 26, lingual, and 27, occlusal view; 28-30, UALVP 22283, left m1 in 28, labial, 29, oblique lingual, and 30, occlusal view; 31-33, UALVP 22281, right m2 in 31, labial, 32, lingual, and 33, occlusal view; 34-36, UALVP 22318, incomplete left dentary with m1-2 in 34, labial, 35, lingual, and 36, occlusal view. Scale bars = 2 mm.

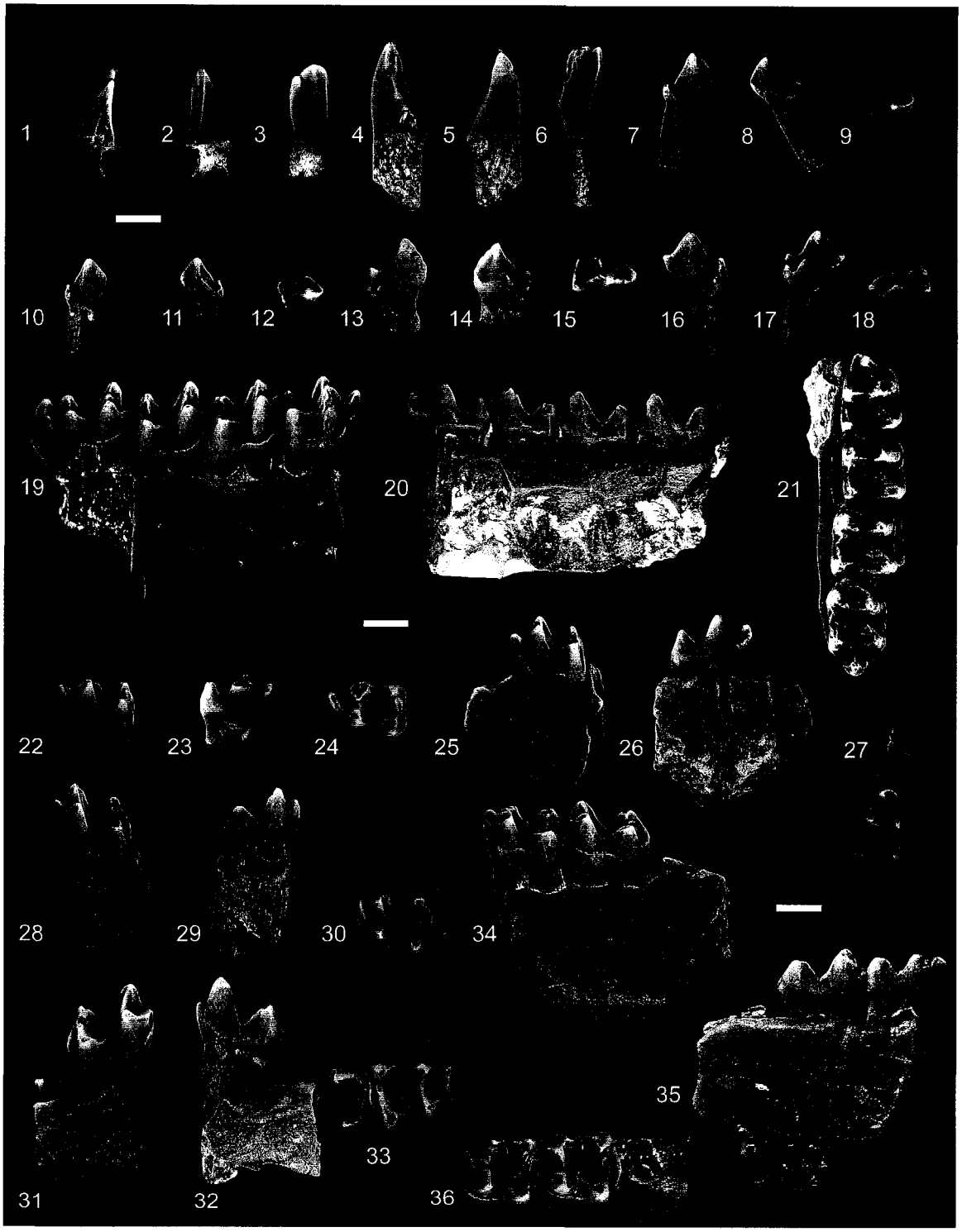
1
2
3
4
5
6
7
8
9
10
11
12
13
14
15
16
17
18
19
20
21
22
23
24
25
26
27
28
29
30
34
31
32
33
36
35

Figure 8.9.—1-14. Elpidophorus species indeterminate from the early middle Tiffanian (Ti3) DW-2 (DW2), Joffre Bridge Mammal Site No. 1 (JBMS), and Birchwood (BW) localities, and the late middle Tiffanian (Ti4) Swan Hills (SH) locality, Paskapoo Formation, Alberta. 1-4, UALVP 40581 (JBMS), upper right medial incisor in 1, anterior, 2, postero-occlusal, 3, medial, and 4, oblique lateral view; 5-8, UALVP 46476 (DW2), upper right medial incisor in 5, anterior, 6, postero-occlusal, 7, medial, and 8, oblique lateral view; 9-12, UALVP 39391 (BW), upper left medial incisor in 9, anterior, 10, postero-occlusal, 11, medial, and 12, oblique lateral view; 13, UALVP 22527 (SW), incomplete upper right medial incisor in oblique lateral view; 14, UALVP 22472 (SW), incomplete upper right medial incisor in oblique lateral view. Scale bars = 2 mm.

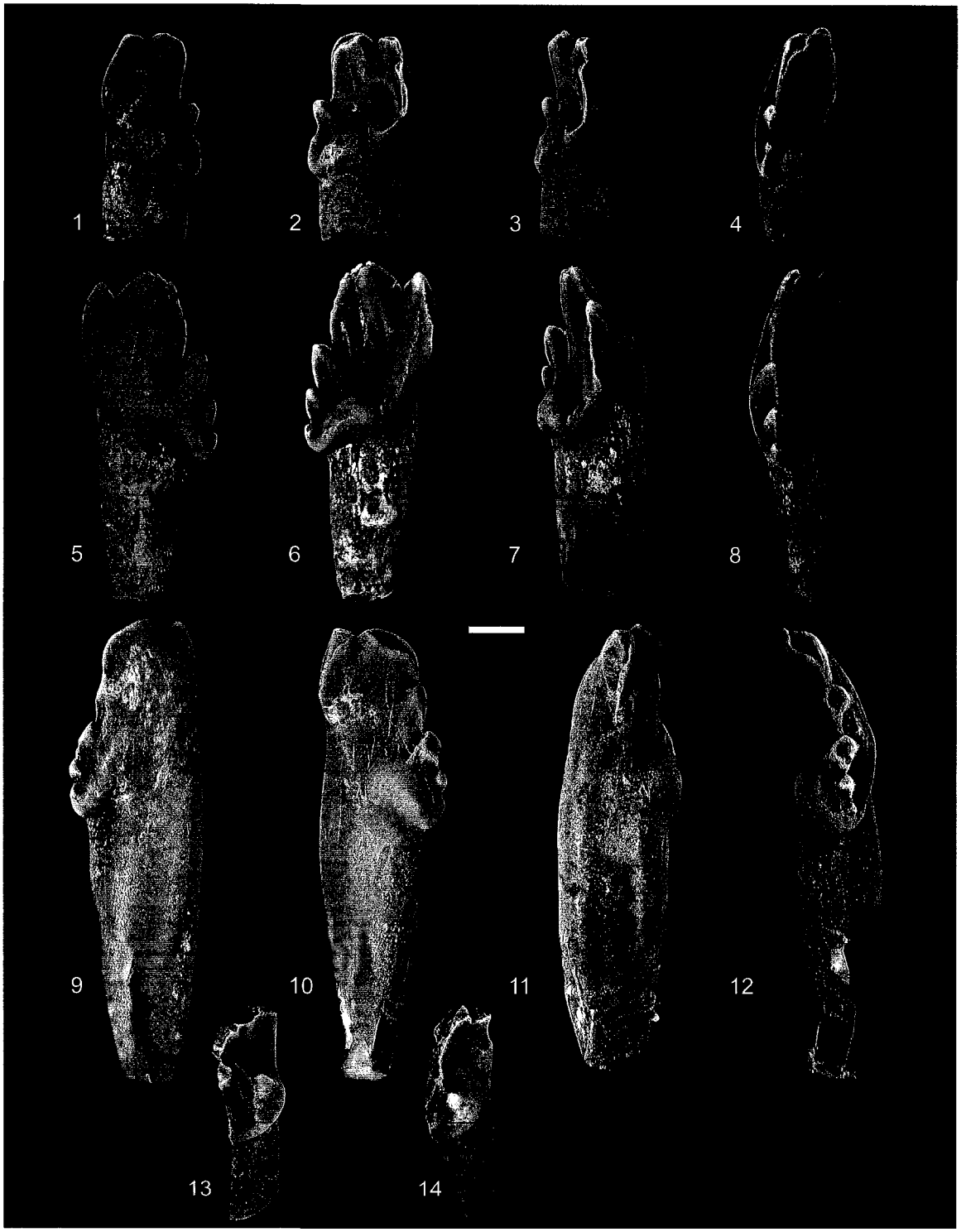
1
2
3
4
5
6
7
8
9
10
11
12
13
14

Figure 8.10.—1-14. Camera lucida outline drawings of P3-4, M1-2 in occlusal view. 1, 4, 7, 10, Elpidophorus simpsoni new species from the early middle Tiffanian (Ti3) DW-2 (DW2), Joffre Bridge Roadcut lower level (JBLL), and Joffre Bridge Mammal Site No. 1 (JBMS) localities, Paskapoo Formation, Alberta. 1, UALVP 40584 (JBLL), P3; 4, UALVP 40596 (DW2), P4; 7, UALVP 40590 (JBMS), M1 (reversed from original); 10, UALVP 40590 (JBMS), M2 (reversed from original).

2, 5, 8, 11, Elpidophorus elegans Simpson from the early middle Tiffanian (Ti3) DW-2 (DW2) and Joffre Bridge Mammal Site No. 1 (JBMS) localities, Paskapoo Formation, Alberta. 2, UALVP 46443 (DW2), P3; 5, UALVP 46443 (DW2), P4; 8, UALVP 40570 (JBMS), M1; 11, UALVP 46443 (DW2), M2.

3, 6, 9, 12, Elpidophorus clivus new species from the late middle Tiffanian (Ti4) Swan Hills locality, Paskapoo Formation, Alberta. 3, UALVP 22264 (reversed from original), P3; 6, UALVP 22362 (reversed from original), P4; 9, UALVP 22364, M1; 12, UALVP 22269, M2.

Outline drawings of the dentitions of Elpidophorus elegans and Elpidophorus clivus have been scaled to approximately the same dimensions of comparable teeth of Elpidophorus simpsoni. Scale bars = 2 mm.

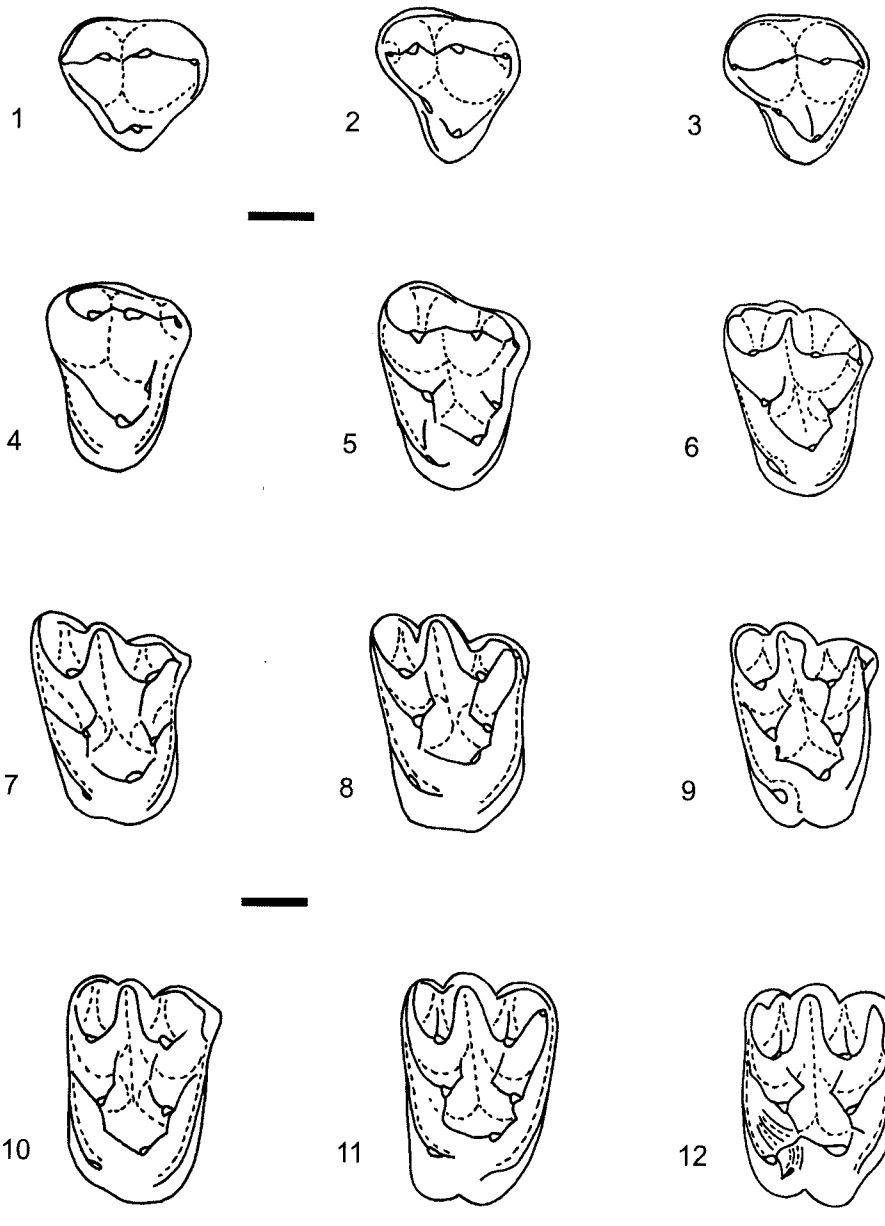
1
2
3
4
5
6
7
8
9
10
11
12

Figure 8.11.—1-14. Camera lucida outline drawings of p3-4, m1-2 in occlusal view. 1, 5, 9, 13, Elpidophorus minor Simpson from the middle Torrejonian (To2) Silberling Quarry, Fort Union Formation, Montana. 1, PU 14201, p3; 5, PU 14201, p4; 9, PU 14201, m1; 13, PU 14201, m2.

2, 6, 10, 14, Elpidophorus simpsoni new species from the early middle Tiffanian (Ti3) Joffre Bridge Mammal Site No. 1 (JBMS) locality, Paskapoo Formation, Alberta. UALVP 46427 (reversed from original), p3; 6, UALVP 40588, p4; 10, UALVP 46427 (reversed from original), m1; 14, UALVP 46427 (reversed from original), m2.

3, 7, 11, 15, Elpidophorus elegans Simpson from the early middle Tiffanian (Ti3) DW-2 (DW2) locality, Paskapoo Formation, Alberta. 3, UALVP 46454, p3; 7, UALVP 46454, p4; 11, UALVP 46457, m1; 15, UALVP 46457, m2.

4, 8, 12, 16, Elpidophorus clivus new species from the late middle Tiffanian (Ti4) Swan Hills locality, Paskapoo Formation, Alberta. 4, UALVP 22230, p3; 8, UALVP 22286 (reversed from original), p4; 12, UALVP 22317, m1; 16, UALVP 22317, m2.

Outline drawings of the dentitions of Elpidophorus minor, Elpidophorus elegans, and Elpidophorus clivus have been scaled to approximately the same dimensions of comparable teeth of Elpidophorus simpsoni. Scale bars = 2 mm.

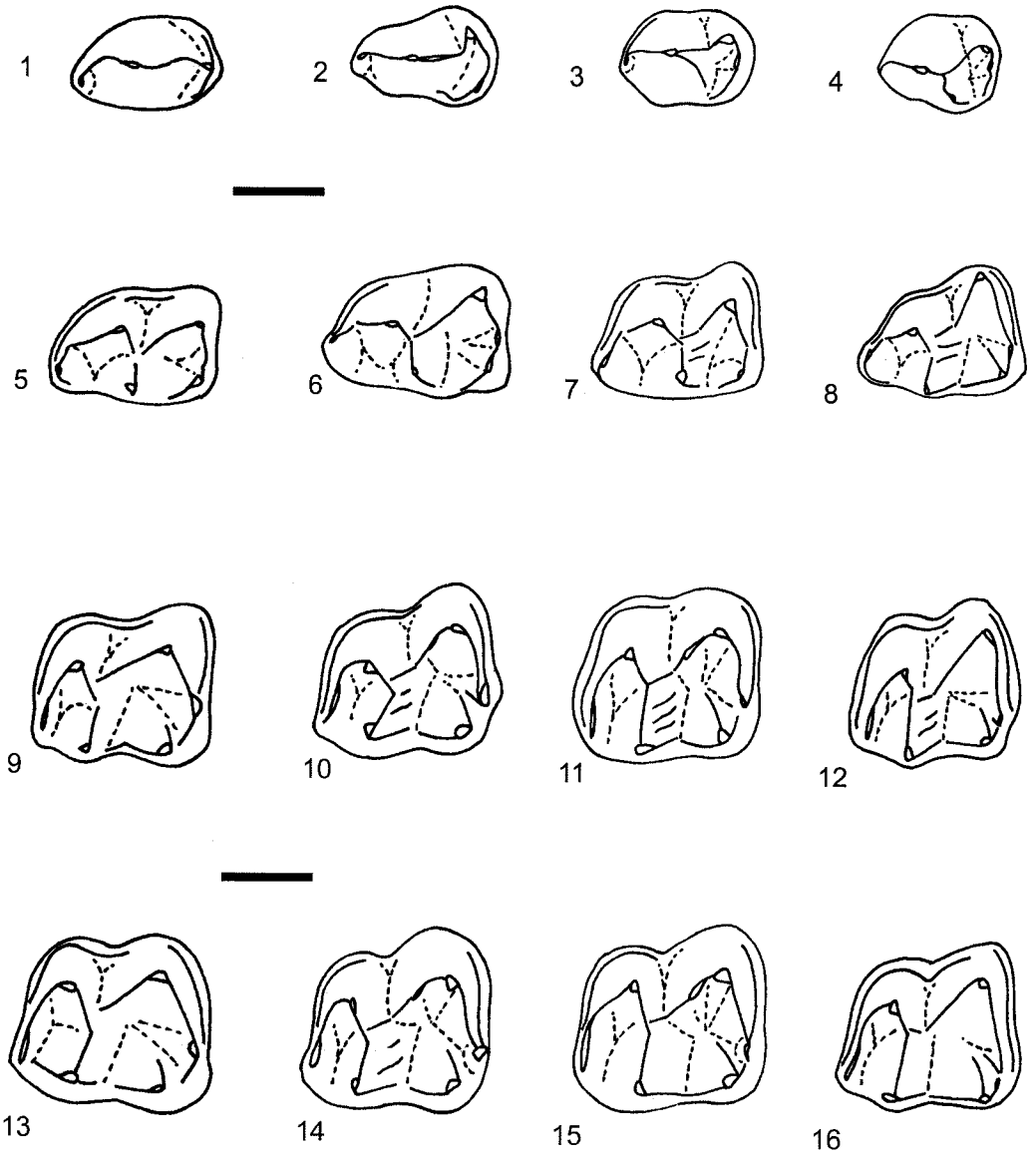
1
2
3
4
5
6
7
8
9
10
11
12
13
14
15
16

Figure 8.12.—1-8. Camera lucida outline drawings of upper molars in occlusal view illustrating the various structures that have been considered "mesostyles" (arrows). 1-3, Plesiadapis churchilli Gingerich from the late middle Tiffanian (Ti4) Roche Percée locality, Ravenscrag Formation, Saskatchewan. 1, UALVP 46883, RM1; 2, UALVP 46884, RM2; 3, UALVP 46885, RM2.

4, Picrodus sp., cf. P. canpacius from the Tiffanian Rock Wren locality, Hanna Formation, Wyoming. UW 28614, incomplete left maxilla with P4-M1 (only M1 figured).

5, Eudaemonema thlastes new species from the early middle Tiffanian (Ti3) DW-2 locality, Paskapoo Formation, Alberta. UALVP 46420, LM2.

6, Elpidophorus simpsoni new species from the early middle Tiffanian (Ti3) Joffre Bridge Mammal Site No. 1, Paskapoo Formation, Alberta. UALVP 40590, LM1.

7, Cynocephalus volans Boddaert, from the Recent of southeast Asia. Uncatalogued UAMZ specimen, RM2.

8, Myotis lucifugus Le Conte, from the Recent of southern Alberta. Uncatalogued UAMZ specimen, LM2.

9, Plagiomene multicuspis Matthew from the early Wasatchian (Wa1) Gray Bull Beds, lower Willwood Formation, Wyoming. PU 13272, RM1.

Outline drawings of the dentitions of Plesiadapis, Picrodus, Eudaemonema, Cynocephalus, Myotis, and Plagiomene have been scaled to approximately the same dimensions of comparable teeth of Elpidophorus simpsoni. Scale bars = 2 mm.

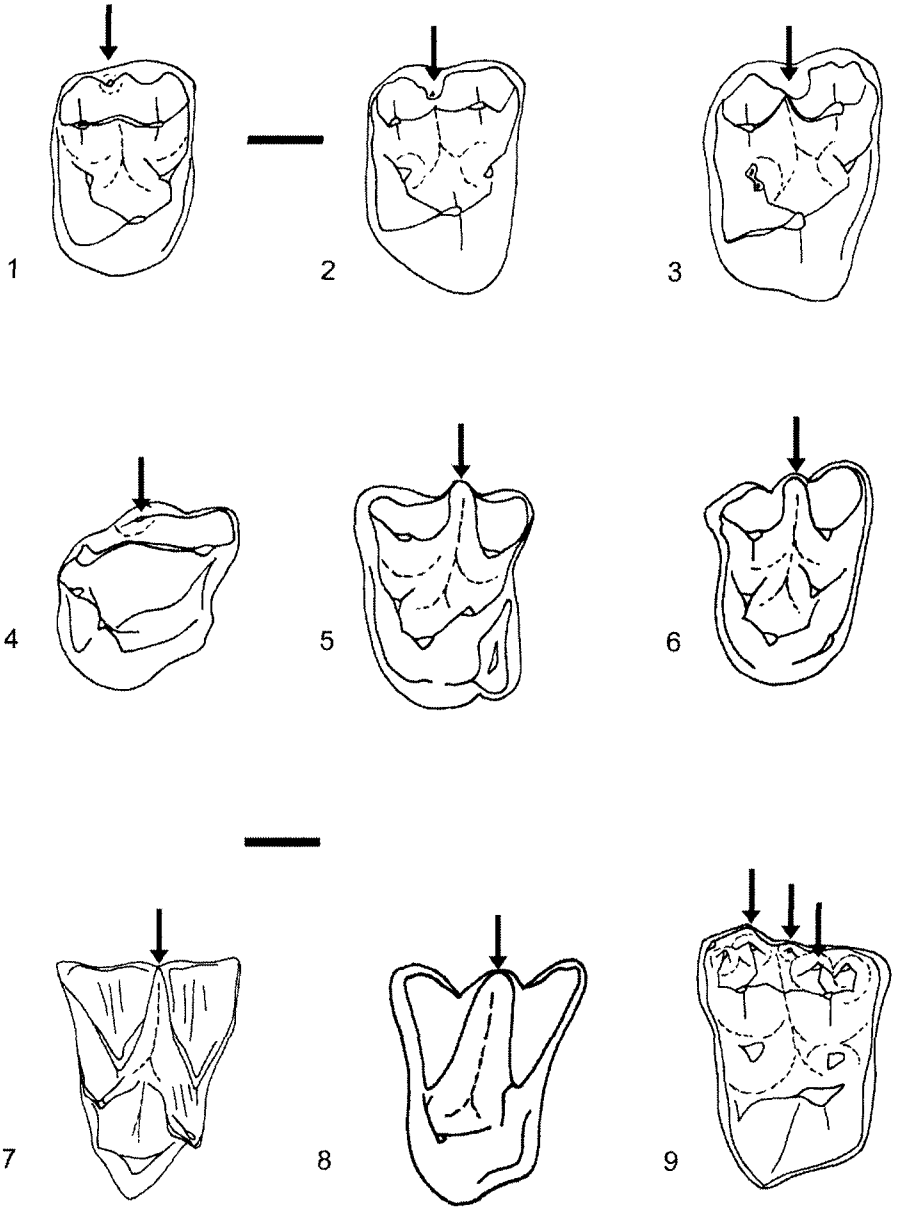
1
2
3
4
5
6
7
8
9

9 Paleocene Condylarths and Mesonychians (Mammalia, Archaic Ungulata) from Alberta, Canada, with Descriptions of Two New Arctocyonids

9.1 Introduction

CONDYLARTHS ARE among the most taxonomically diverse eutherians in the early Tertiary of North America, and often constitute the majority of specimens from localities of early Paleocene age (e.g., Matthew, 1937; Johnston and Fox, 1984; Robison, 1986; Williamson, 1996; Eberle and Lillegraven, 1998; Eberle, 2003; Middleton and Dewar, 2004). Condylarthra here refers to a higher-level grouping of eutherian mammals generally regarded as archaic ungulates (Cifelli, 1983; Archibald, 1998), although more recent work has suggested at least some hyopsodontid condylarths may be more closely related to macroscelideans (Zack, Penkrot, Bloch ,and Rose, 2005). Cope's (1881a) original concept of Condylarthra included what are now recognized as members of the families Phenacodontidae, Periptychidae, and Hyopsodontidae; since that time, the taxonomic content of Condylarthra has changed significantly, but there is general agreement that the taxon likely represents an adaptive grade of broadly similar, omnivorous to carnivorous ungulate-like mammals united primarily on the basis of primitive features of the dentition (Prothero et al., 1988; Archibald, 1998; Muizon and Cifelli, 2000). Attempts have been made at rectifying the problem, from distributing various condylarth taxa among more derived groups, to the abandonment of Condylarthra altogether as a formal taxon (e.g., Archibald, 1998; and see Muizon and Cifelli, 2000 for discussion). Condylarthra here follows the usage and rationale of Muizon and Cifelli (2000), and is, in essence, the same usage of Simpson (1945) as modified by Van Valen (1978).

The early evolution of condylarths is important for a number of reasons: after their initial appearance in the latest Cretaceous (Johnston, 1980; Johnston and Fox, 1984; Fox, 1989, 1990), the subsequent diversification of condylarths during the Puercan Land Mammal Age was explosive, with adaptive radiations into a variety of ecological niches (see discussions in Hunter, 1997, 1999); the large numbers of condylarth specimens from Paleocene localities provide unique opportunities to study of aspects of early Tertiary

mammalian community structure (e.g., Van Valen, 1978, 1988) and faunal turnover (e.g., Rose, 1981; Eberle and Lillegraven, 1998), biostratigraphy (e.g., Williamson, 1996), and detailed microevolutionary studies (e.g., Libed, 2001, 2003); and perhaps most importantly, Condylarthra are believed to contain the ancestors of extinct and extant ungulate groups, most notably the artiodactyls and perissodactyls, two of the most diverse and ecologically dominant orders of mammals.

Condylarths from western Canada are first known from the Late Cretaceous and early Paleocene of Saskatchewan, and are represented primarily by isolated teeth and rare jaw fragments (e.g., Johnston, 1980; Johnston and Fox, 1984; Fox, 1989, 1990, 1997; Spivak, 1997). Although the larger collections from the early and middle parts of the Tiffanian of Alberta document a greater diversity of condylarths than do those from Saskatchewan (e.g., Russell, 1932, 1958; Youzwyshyn, 1988; Fox, 1990; Webb, 1996), with more numerous and better-preserved specimens, these collections have remained undescribed. The objectives of this chapter are twofold: first, to document and describe condylarths from the Paleocene of Alberta, focusing primarily on the early middle Tiffanian (Ti3) Blindman River and Birchwood localities; and second, to discuss briefly changes in condylarth taxonomic composition during the early and middle Tiffanian of western Canada, and compare these differences with those recorded during the equivalent period of time in the northern part of the Western Interior of the United States.

9.2 Systematic Paleontology

Class MAMMALIA Linnaeus, 1758

Subclass THERIA Parker and Haswell, 1897

Infraclass EUTHERIA Gill, 1872

Grandorder UNGULATA Linnaeus, 1766

Order CONDYLARTHRA Cope, 1881a

Family OXYCLAENIDAE Scott, 1892

Genus CHRIACUS Cope, 1883a

Lipodectes COPE, 1881b, p. 1019 (in part).

Deltatherium COPE, 1881b: COPE, 1882a, p. 463 (in part).

Chriacus COPE, 1883a, p. 80 (in part).

Tricentes COPE, 1884a, p. 314 (in part).

Pelycodus COPE, 1875: COPE, 1884b, p. 255 (in part).

Epichriacus SCOTT, 1892, p. 296.

Metachriacus SIMPSON, 1935a, p. 235.

?Spanoxyodon SIMPSON, 1935a, p. 236.

Type species.—Lipodectes pelvidens (Cope, 1881b).

Other included species.—Chriacus baldwini (Cope, 1882a); C. gallinae Matthew, 1915; C. calenancus Van Valen, 1978; C. katrinae Van Valen, 1978; C. metacometi Van Valen, 1978; C. oconostotae Van Valen, 1978; C. badgleyi Gingerich, 1989.

CHRIACUS sp., cf. C. BALDWINI

Figures 9.1.1-9.1.4

Material examined.—From DW-2: UALVP 46478, associated M1 and M2.

Description.—Upper molars: M1 (L=6.1; W=6.8): The M1 of C. sp., cf. C. baldwini is subquadrate in occlusal outline, with straight anterior and posterior sides and a squared to slightly rounded lingual margin. The paracone and metacone are deeply worn, but the dimensions of their bases suggest they were probably subequal in size and height, and slightly taller than the protocone. A shallow ectoflexus divides the labial side of the crown into weakly differentiated lobes: the parastylar lobe is drawn out anteriorly as a hook-like process, while the metastylar lobe is more smoothly rounded. The stylar shelf is greatly reduced, with only the low but prominent ectocingulum remaining; the ectocingulum is continuous, and joins the anterior and posterior cingula. The paracone and metacone are subconical, with the base of the paracone extending farther lingually. The conules are enlarged, with flat basin-facing sides, and are separated from the bases of the paracone and metacone by narrow, slit-like notches. The external conular cristae terminate near the lingual bases of the paracone and metacone, and do not continue

labially as the para- and metacingulum; the postparaconular and premetaconular cristae extend up the lingual sides of the paracone and metacone to their apices. The apex of the inflated protocone is slightly anterior to the transverse midline of the crown. The protoconal cingula meet lingually, and the posterolingually expanded posterior cingulum bears a large hypocone.

M2 (L=6.2; W=8.6): When compared to M1, the M2 of Chriacus sp., cf. C. baldwini is wider and more nearly rectangular in occlusal outline, and the parastylar lobe is notably reduced. The conical paracone and metacone are subequal in size, with the paracone being slightly taller and more labial; these cusps, together with the protocone, enclose a moderately deep trigon basin. The preparacrista, centrocrista, and postmetacrista are all weakly developed, whereas the ectocingulum is robust. The conules are closely appressed to the paracone and metacone, but are separated from them by deep, narrow notches. The conules are inflated, with the metaconule being the larger and slightly more lingual. As on M1, the external conular cristae on M2 terminate near the lingual bases of the paracone and metacone, and the heavy postparaconular and premetaconular cristae ascend the lingual sides of the paracone and metacone towards their apices. The protoconal cingula meet lingually, and the posterior cingulum bears a large, conical hypocone; a small pericone is developed anterolingually. The enamel is wrinkled, especially on the floor of the trigon basin.

Discussion.—The teeth of Chriacus baldwini differ from those of C. pelvidens in their smaller size, in M1 having a more prominent, hook-like parastylar lobe, and in the lingual cingulum being more robust, and while the specimens from DW-2 resemble the teeth of C. baldwini in these regards, they differ in a number of ways. For example, the teeth of C. sp., cf. C. baldwini are larger than those of C. baldwini, with the crowns more nearly square, rather than rectangular in outline (i.e., the length/width ratio is lower), and in having better-developed cingula and hypocones. The significance of these differences is uncertain, especially in light of the broad range of variation for C. baldwini accepted by Van Valen (1978) in his revision of the species (Van Valen considered Tricentes crassicollidens Cope, 1884a, Chriacus truncatus Cope, 1884a, C. schlosserianus Cope, 1888, Metachriacus provocator Simpson, 1935a, and Spanoxyodon latrunculus Simpson, 1935a subjective junior synonyms of C. baldwini). The coronal anatomy of M1 and M2

in UALVP 46478 falls within the range of variation given in the diagnosis by Van Valen (1978) for C. baldwini, but the teeth of other species of Chriacus (e.g., C. pelvidens) and even those of other oxyclaenid genera (e.g., Mimotricentes Simpson, 1937) could reasonably be referred to C. baldwini given the permitted range of variation. Pending a revision of Chriacus and the discovery of better preserved specimens from Alberta, the teeth from DW-2, although most closely resembling those of C. baldwini, are referred here only to C. sp., cf. C. baldwini.

C. baldwini is long-ranging, both stratigraphically (early Torrejonian to late Tiffanian) and geographically (Texas to central Alberta) (e.g., Schiebout, 1974; Williamson and Lucas, 1993; Williamson, 1996). Should their referral to C. baldwini be confirmed, the specimens from Alberta would represent the youngest occurrence of the taxon in Canada, and the northernmost record yet known.

CHRIACUS OCONOSTOTAE Van Valen, 1978

Figures 9.1.5-9.1.12

Chriacus oconostotae VAN VALEN, 1978, p. 54.

Holotype.—YPM-PU 20782, incomplete left dentary with p4, m1-2 (Van Valen, 1978, p. 54). Cedar Point Quarry, Fort Union Formation of Wyoming, late Paleocene (early middle Tiffanian, Ti3, Plesiadapis rex/P. churchilli Lineage Zone of Lofgren et al., 2004).

Material examined.—From DW-2: UALVP 46479, m2; UALVP 46480, incomplete m2; UALVP 46481, m3.

From Birchwood: UALVP 39222, M1.

Age and occurrence.—Early middle Tiffanian (Plesiadapis rex/P. churchilli Lineage Zone, Ti3, late Paleocene) of the Western Interior of North America (Lofgren et al., 2004).

Description.—M1 (L=8.6; W=9.2): The coronal outline of M1 is subtrapezoidal, with the labial side longer than the lingual side. Although the paracone and metacone are appreciably worn, the shape and dimensions of their bases suggest that both cusps were

tall and subconical, that the paracone was the larger of the two, and that both were slightly taller than the protocone. The well-developed parastylar lobe projects anteriorly, but is not hooked as on M1 of Chriacus baldwini; the metastylar lobe is smoothly rounded and extends much farther labially than does the parastylar lobe. A weak ectoflexus occurs approximately midway along the well-developed ectocingulum. The paraconule and metaconule are robust, and the conular cristae are high and sharp; the postparaconular and premetaconular cristae are deeply notched near their union with the bases of the paracone and metacone, respectively. The protocone is massive, occupying nearly half the width of the crown, and short pre- and postprotocristae extend labially from the protoconal apex to the conules. The protoconal cingula are discontinuous lingually, and the posterior cingulum is expanded posterolingually, forming a shallow talon basin; the hypocone, although appreciably worn, appears to have been low. The enamel is weakly wrinkled.

Lower molars: m2 (L=9.3; TrW=6.2; TaW=5.9): The crown of m2 is rectangular in occlusal view, and while the trigonid and talonid are equally wide, the former is much taller than the latter. The protoconid and metaconid are swollen and nearly equal in size and height, and both are larger and taller than the paraconid. The paraconid is lingual in position, well separated from the metaconid, and is nearly vertical; the paracristid is low, widely notched, and a large accessory cusp is developed at its deepest point. The protoconid and metaconid are transversely opposed, and the two cusps are connected by a broad, V-shaped protocristid. A crest originating near the apex of the metaconid extends anterolingually into the trigonid basin, but quickly weakens and does not form the conspicuous transverse crest that characterizes arctocyonine lower molars (Cifelli, 1983); faint protostylid and metastylid crests extend from the postvallid wall to the anterolabial and anterolingual margins of the deeply basined talonid. Although its apex is missing, the hypoconid was clearly the largest talonid cusp, occupying nearly half the width of the talonid; the smaller entoconid is transversely opposed to the hypoconid, and its basin-facing wall is flat and slopes anterolabially. The hypoconulid is low and occurs at the peak of a robust posterior cingulid. The low, sharp hypocristid and postcristid are nearly confluent, and partially exclude the hypoconulid from the rim of the talonid basin; the cristid obliqua joins the postvallid wall below the protocristid notch, and the hypoflexid is

deep. Although the anterior and posterior cingulids are well developed, they are discontinuous labially.

m3 (L=9.9; TrW=5.8; TaW=5.0): The trigonid of m3 is shorter and lower than that of m2, and the cusps are less swollen. The protoconid and metaconid were probably the same height (the protoconid is damaged on this specimen), and the paraconid is smaller and more labial than on m2. The paracristid is low and broadly notched, and a small, medially positioned accessory cusp occurs at the deepest part of the crest; as on m2, the protocristid on m3 is low and widely notched. While the metastylid crest is only weakly developed, the protostylid crest is stout and extends to the hypoflexid. The talonid is longer and narrower than that of m2, and the cusps are tall and spirelike, with the hypoconid the largest, followed by the entoconid and the slightly smaller hypoconulid. The entoconid is appressed to the hypoconulid, with the postcristid having been reduced to a deep notch between the two cusps; the hypocristid is longer and widely V-shaped, extending lingually to the entoconid and fully excluding the hypoconulid from the talonid rim. The finger-like hypoconulid occurs at the apex of the posterior cingulid and projects anterodorsally. The anterior and posterior cingulids are strongly developed, but as on m2, are discontinuous labially.

Discussion.—The tall trigonids and small paraconids of the lower molars most closely resemble those in Chriacus oconostotae from the early middle Tiffanian Cedar Point and Chappo Type localities of Wyoming (Van Valen, 1978; Gunnell, 1994), with the teeth from Alberta differing only in their slightly larger size and more lingual paraconid on m2. The conspicuous accessory cusps on the paracristid of the molar trigonids on UALVP 46479 and 46481 are characteristic of molars of Metachriacus Simpson, 1935a (see Simpson, 1937), a taxon previously synonymized with Chriacus (Van Valen, 1978), but recently revalidated (McKenna and Bell, 1997). In spite of this Metachriacus-like feature, the totality of coronal features on UALVP 46479 and 46481 more closely resembles that of Chriacus: the trigonids are tall relative to the talonids; the paraconids are conspicuous and lingual, rather than weak and slightly more labial; the hypocone is better developed; and the protoconal cingula are weaker. The M1 of C. oconostotae has not been described previously: UALVP 39222 resembles M1 of Chriacus pelvidens and Chriacus katrinae, but differs from these in its larger size, better-developed

metastylar lobe, more posterolingually projecting hypocone, and in the protoconal cingula being discontinuous lingually.

The specimens of C. oconostotae from DW-2 and Birchwood document the first occurrence of the taxon outside of Wyoming.

Genus THRYPTACODON Matthew, 1915

Thryptacodon MATTHEW, 1915, p. 7.

Type species.—Thryptacodon antiquus Matthew, 1915.

Other included species.—Thryptacodon pseudarctos Simpson, 1928; T. orthogonius (Russell, 1929); T. australis Simpson, 1935b; T. barae Gingerich, 1989.

THRYPTACODON AUSTRALIS Simpson, 1935b

Figures 9.1.13-9.1.26, 9.2; Table 9.1

Thryptacodon australis SIMPSON, 1935b, p. 20.

Holotype.—AMNH 17384, incomplete left dentary with c, p1,3-4, m1-3, and associated right dentary having c, p1-4, m1-3, possibly associated LM2 and postcranial remains (Simpson, 1935b, p. 20). Mason Pocket locality, Animas Formation of Colorado, late Paleocene (late middle Tiffanian, Ti4, Plesiadapis churchilli/P. simonsi Lineage Zone of Lofgren et al., 2004).

Material examined.—From DW-2: UALVP 46482, incomplete left dentary with c, p1-4, m1-2; UALVP 46483, m1; UALVP 46484, m2.

From Birchwood: UALVP 46485, M2; UALVP 39230, incomplete right dentary with m1-2; UALVP 39231, incomplete m2; UALVP 39232, 46486, m3s.

Age and occurrence.—Early Tiffanian (Plesiadapis anceps/P. rex Lineage Zone, Ti2, late Paleocene) to late Clarkforkian (Phenacodus/Ectocion Acme-Zone, Cf3, latest Paleocene) of the Western Interior of North America (Lofgren et al., 2004).

Description.—M2: The crown of M2 is rectangular in outline, and bears low, swollen cusps and conules. The paracone and protocone are subequal in height, and both are slightly taller than the metacone; the principal cusps enclose a deep but narrow trigon basin. The parastylar and metastylar lobes are virtually undeveloped, with their margins smoothly rounded, and the prominent ectocingulum low and continuous labially. The paracone and metacone are inflated, especially at their bases, and the apices of both cusps are smoothly rounded; the preparacrista, postmetacrista, and centrocrista are weakly developed. The conules are low and blunt, and the paraconule is smaller and more labial than the metaconule. The external conular cristae join the protoconal cingula and continue as the para- and metacingulum to the labial corners of the crown; the postparaconular crista ascends the lingual face of the paracone, fading away as it nears the apex, whereas the premetaconular crista is shorter and weakens towards the base of the metacone. The protocone is massive and swollen, with its apex positioned slightly anterior to the transverse midline of the crown. The protoconal cingula are continuous lingually, and the posterior cingulum supports a low, bulbous hypocone that is connected to the base of the protocone by a short, weak crest. The enamel on M2 is faintly wrinkled.

Dentary and lower dentition (Figs. 9.1.15-9.1.26, 9.2): UALVP 46482 is badly damaged: the horizontal ramus is nearly complete to the level of m3, but the condylar, angular, and coronoid processes are missing. The ramus posterior to p2 is dorsoventrally shallow, mediolaterally narrow, and faintly convex ventrally (and see descriptions in Simpson, 1935b; Holtzman, 1978). The dentary widens anterior to p2, coincidental with the posteriormost parts of the symphysis, and the bone becomes significantly thicker. A small, teardrop-shaped mental foramen is developed below the anterior root of p3, while a larger, subcircular foramen opens anterolaterally below p1 (Fig. 9.1.15, arrows). The articular surface of the symphysis is deep anteriorly, but quickly pinches out below p2; laminae of heavily rugose bone delimit the dorsal and ventral extents of the articular surface, and the bone between the laminae is faintly concave, rugose, and perforated by a large foramen (Fig. 9.1.16, arrow). Although the rugosities on the articular surface are suggestive of the mandibular rami having been tightly sutured in life, there is no evidence of the two having been co-ossified.

Lower incisors: While none of the lower incisor crowns are preserved in UALVP 46482, three small alveoli, two of which contain parts of the incisor roots, document their number and position (Fig. 9.2). Two alveoli, probably those for i1 and i2, are developed medially, adjacent to the symphyseal surface: the smaller alveolus, probably for i1, is immediately ventral to the canine alveolus and is separated from it by a thin wall of bone; it is subcircular and contains a small part of the i1 root. The second alveolus is ventral to that for i1: it is larger than the i1 alveolus, subcircular, and contains part of the i2 root. The alveolus for i3 is lateral and slightly dorsal to the i2 alveolus, and the bone separating the two alveoli is perforated longitudinally by a number of small neurovascular canals. The i3 alveolus is about the same size as that for i1, mediolaterally compressed, and is directed anteriorly and dorsally. The arrangement of the incisor alveoli on UALVP 46482 is nearly identical to that on UALVP 9689, an undescribed dentary of Arctocyon sp., cf. A. acrogenius from the late middle Tiffanian (Ti4) Roche Percée locality of Saskatchewan (pers. obs.): as on UALVP 46482, the incisor alveoli on UALVP 9689 are crowded, with i1 dorsal to i2, and i3 developed at the lateral margin of the dentary. The unusual arrangement of the lower incisors in UALVP 46482 differs significantly from that of T. antiquus (see Gingerich and Rose, 1979), in which i1-3 are arranged mediolaterally across the anterior margin of the jaw and may have functioned as a tooth comb, similar to those in lemuriform primates. Although the incisors are not preserved in UALVP 46482, the size and orientation of their alveoli suggest the teeth were small and crowded together, closely appressed to the canine, and probably directed more anterodorsally, rather than being strongly procumbent. While the function of the lower incisors in T. antiquus as a tooth comb used in grooming behaviour is debatable, the size and disposition of the comparable teeth in T. australis differ significantly from those in T. antiquus, and imply a different function; furthermore, as UALVP 46482 demonstrates, the arrangement of the lower incisors in T. antiquus is not representative of Thryptacodon generally, and may be only a peculiarity of T. antiquus itself Although morphological differences of this sort often warrant separation at the generic level, such action is not taken here pending recovery of better-preserved specimens from Alberta, particularly mandibles preserving articulated lower incisors.

Lower canine: The canine is tall, mediolaterally compressed, and splays slightly laterally. A deep wear facet is developed on the posterolabial side of the crown, creating a sharp, bladelike posterior edge similar to that reported for T. antiquus (Gingerich and Rose, 1979).

Lower premolars: Parts of the crowns of four premolars are preserved in UALVP 46482. Most of p1 has been broken away, leaving only the base of the crown and root; the tooth was small and single-rooted, slightly procumbent (as evidenced by the anterodorsal-posteroventral orientation of the root and alveolus), and separated from the canine and p2 by short diastemata. The p2 and p3 in T. australis are subequal in size and height, two-rooted, and crown of each supports a tall and trenchant, faintly recurved protoconid and a unicuspid heel. Neither a paraconid nor metaconid is developed, and a heavy crest runs posteriorly from the protoconid apex to the heel. The p2 is separated from p3 by a short diastema. The crown of p4 is broken posteriorly, leaving only the tall and faintly recurved protoconid. A short cingulid is developed anteriorly along the base of the protoconid; the paraconid is not present, but a faint swelling on the lingual shoulder of the protoconid is suggestive of an incipiently developed metaconid. A robust crest extends from the apex of the protoconid posteriorly, and undoubtedly joined with the heel (see, e.g., Simpson, 1935b, fig.8); a weaker crest extends anteriorly from the protoconid apex to the anterior cingulid. The posterior crests on p3 and p4 are not serrated.

Lower molars: m1: The m1 of T. australis is somewhat pyriform in occlusal outline, with the talonid being significantly wider than the trigonid. The trigonid is elevated well above the level of the talonid and leans slightly anteriorly; its cusps are low and swollen. The apices of the protoconid and slightly lower metaconid are smoothly rounded, and the two cusps are connected by a short and deeply notched protocristid; the anteriorly projecting paraconid is compressed and partially incorporated into the bladelike paracristid. The low, massive hypoconid is the largest cusp on the crown, and its flattened basin-facing wall, together with that of the smaller entoconid, forms a deep V-shaped talonid basin. The hypoconulid is short, blunt, and appressed to the entoconid, and a small entoconulid and weaker mesoconid are developed on the entocristid and

cristid obliqua, respectively. The anterior and posterior cingulids are well developed, but are discontinuous labially.

m2: The crown of m2 resembles that of m1 in being pyriform in outline, but the talonid is even wider relative to the trigonid, and the trigonid is lower, with the apices of the principal cusps barely above the level of the m1 talonid. The cusps on m2 are more massive than those on m1, especially the hypoconid, which occupies more than half the width of the talonid. The paraconid is small and conical, slightly labial to the lingual margin of the crown, and closely appressed to the metaconid, while the protoconid and metaconid are low and nearly equal in height. The talonid is broader and longer than on m1, but the basin is similarly deep and V-shaped. The anterior and posterior cingulids are better developed on m2 than on m1, but remain discontinuous (the posterior cingulid continues across the labial side of the hypoconid, terminating at the hypoflexid, whereas the anterior cingulid does not continue labially).

m3: The m3 of T. australis is teardrop-shaped in outline, with the crown narrowing posteriorly and the finger-like hypoconulid forming the apex of the "teardrop". The crown is shorter and slightly narrower than on m2, and the trigonid is lower and more anteroposteriorly compressed. The transversely opposed protoconid and metaconid are both swollen, with smoothly rounded apices that are connected to one another by a broad and shallowly notched protocristid. The paraconid is almost fully incorporated into the anteriorly convex paracristid, but it is occasionally represented by an ill-defined anteromedial swelling on the paracristid. The talonid basin is both narrower and shallower than on m1 or m2, but is similarly V-shaped, with the basin-facing walls of the entoconid and hypoconid flattened. The massive hypoconid is nearly twice the size of either the entoconid or hypoconulid, and is connected to the hypoconulid by a heavy hypocristid. The entoconid and hypoconulid are closely appressed and connected to one another by a short, shallowly notched postcristid. The entoconulid is poorly developed. The weak anterior and posterior cingulids are discontinuous labially.

Discussion.—The hypodigm of Thryptacodon australis is from the late middle Tiffanian (Ti4) Mason Pocket locality of Colorado, and although the taxon is known from other localities of late middle Tiffanian age (Simpson, 1935b; Rose, 1981; Fox, 1990; Gunnell, 1994), it is rare outside of the northern parts of the Western Interior of the

United States (e.g., Holtzman, 1978; Fox, 1990; Krause and Maas, 1990; Gunnell, 1994). The sample of T. australis from western Canada is particularly poor, having been discovered only at the late middle Tiffanian (Ti4) Roche Percée locality (Fox, 1990) in addition to the occurrences documented here. Specimens of T. australis from the Birchwood and Blindman River localities are virtually identical, and closely resemble teeth from the late middle Tiffanian (Ti4) Judson locality of North Dakota (Holtzman, 1978; Kihm and Hartman, 2004), differing only in their slightly smaller size and shorter m3. The Blindman River and Birchwood specimens differ from comparable teeth in the Roche Percée sample primarily in their smaller size, less swollen cusps, and weaker hypocone on M2.

The teeth of T. australis resemble those of T. orthogonius (Russell, 1929), an observation made by Holtzman (1978) in his study of middle Tiffanian (Ti3-4) mammals from the Judson and Brisbane localities of North Dakota [Holtzman compared the Judson and Brisbane samples of T. australis with specimens of "Thryptacodon demari" Gazin, 1941 and "Thryptacodon belli" Gazin, 1941, both from the early Tiffanian (Ti2) Ledge locality of Wyoming; T. "demari" and T. "belli" were recently considered subjective synonyms of T. orthogonius, see Scott et al. (2002)]. Comparisons of teeth of T. australis in the present sample with those of T. orthogonius from the earliest Tiffanian Cochrane 2 locality (Youzwyshyn, 1988; Fox, 1990; Scott et al., 2002) have revealed the following differences, in addition to those observed by Holtzman (1978) and Scott et al. (2002): 1) the molar cusps of T. australis are bunodont, being more swollen than those of T. orthogonius, and with blunter apices; 2) the molar cingula/cingulids of T. australis are weaker; 3) the trigon cusps of T. australis are more closely appressed to one another, conical, and their bases more inflated than those of T. orthogonius; 4) the trigonids of T. australis are less anteroposteriorly compressed; 5) a well-developed entoconulid occurs on m1-2 of T. australis; 6) the m3 entocristid of T. australis is relatively longer than in T. orthogonius; and 7) the teeth of T. australis are slightly larger than those of T. orthogonius.

T. australis from the Birchwood locality is the northernmost record of the genus, and together with the Blindman River localities document the first occurrence of the species in Alberta.

Family ARCTOCYONIDAE Giebel, 1855

Subfamily ARCTOCYONINAE Giebel, 1855

Genus ARCTOCYON Blainville, 1841

Arctocyon BLAINVILLE, 1841, p. 73.

Paleocyon BLAINVILLE, 1841, p. 73.

Heteroborus COPE, 1880, p. 79.

Hyodectes COPE, 1880, p. 79.

Mioclaenus COPE, 1881c: COPE, 1883b, p. 547.

Claenodon SCOTT, 1892, p. 298.

Arctotherium LEMOINE, 1896, p. 342.

Neoclaenodon GIDLEY, 1919, p. 547 (in part)

Arctocyonides LEMOINE, 1891: VAN VALEN, 1978, p. 55 (in part).

Mentoclaenodon WEIGELT, 1960: VAN VALEN, 1978, p. 55 (in part).

Type species.—Arctocyon primaevus Blainville, 1841.

Other included species.—A. ferox (Cope, 1883b); A. corrugatus (Cope, 1883b); A. matthesi Russell, 1964; A. acrogenius (Gazin, 1956).

ARCTOCYON FEROX (Cope, 1883b)

Figures 9.3.1-9.3.24; Table 9.2

Mioclaenus ferox COPE, 1883b, p. 547.

Claenodon ferox SCOTT, 1892, p. 298.

Arctocyon ferox RUSSELL, 1964, p. 137.

Arctocyonides ferox VAN VALEN, 1978, p. 55.

Holotype.—AMNH 3268, teeth and fragmentary postcranium. Type locality unknown; specified by Matthew (1937) and Taylor (1984) as being in the Nacimiento

Formation, San Juan Basin, New Mexico, and probably of early Paleocene (middle Torrejonian, To2, Protoselene opisthacus/Mixodectes pungens Interval Zone of Lofgren et al., 2004) age.

Material examined.—From DW-2: UALVP 46487, M1; UALVP 46488, 46489, M2; UALVP 43104, incomplete dentary with p4, m1-3; UALVP 46490, associated c, p1, p4; UALVP 46491, p3; UALVP 46492, m1; UALVP 46493, incomplete m1; UALVP 46494, m2; UALVP 46495, incomplete m2; UALVP 46496, m3.

From Birchwood: UALVP 46497, incomplete M1 or M2; UALVP 46498, c; UALVP 46499, p1; UALVP 46500, p4; UALVP 46501, m1; UALVP 46502, 39224, m2; UALVP 46503, incomplete m2; UALVP 46504, 46505, m3.

Age and occurrence.—?Middle Torrejonian (Protoselene opisthacus/Mixodectes pungens Interval Zone, To2, early Paleocene) to early middle Tiffanian (Plesiadapis rex/P. churchilli Lineage Zone, Ti3, late middle Paleocene) of the Western Interior of North America (Lofgren et al., 2004).

Description.—Upper dentition (Figs. 9.3.1-9.3.4): Upper molars: M1: The referred M1's closely resemble that of A. ferox from the Nacimiento and Fort Union formations of the Western Interior of the United States (e.g., Matthew, 1937; Simpson, 1937; Kondrashov and Lucas, 2004). The crown is nearly square in outline, with massive and subequal paracone, metacone, and protocone enclosing a shallow trigon basin, and a smaller and lower hypocone. The enamel is heavily wrinkled, on both the basin-facing and exterior sides of the principal cusps, where it is convoluted into thick ridges and deep grooves. The stylar shelf is weak, with only the robust ectocingulum developed labial to the paracone and metacone. The paracone is slightly smaller and more labial than the metacone, and leans labially; both cusps are low and massive, with flat lingual and convex labial sides. The preparacrista, centrocrista, and postmetacrista are short and heavy, and bear numerous, irregularly sized cuspules. The paraconule is about half the height of the paracone, whereas the metaconule is considerably more swollen and farther lingual than the paraconule. The conular cristae are heavy and bear irregular cuspules, and the preparaconular and postmetaconular cristae join the protoconal cingula and continue on to the parastylar and metastylar corners of the crown as the paracingulum and metacingulum, respectively. The protocone is nearly twice the size of the paracone and

metacone, with steep lingual and shallow labial sides, and the protoconal cristae are inflated and heavily cuspate. The robust protoconal cingula meet lingually and run uninterrupted to the parastylar and metastylar corners of the crown. The low, bulbous hypocone occurs immediately posterior to the protocone on the posterior cingulum.

M2: The M2 of A. ferox is wider than M1, and subrectangular, rather than square in outline. Most of the coronal features of M2 resemble those of M1: the enamel is heavily wrinkled; the principal cusps are massive and low, swollen, and enclose a broad, shallow basin; the conules are swollen; the cristae are heavily cuspate; and the hypocone is low, with a rounded apex. The M2 crown differs from that of M1 in having a slightly deeper ectoflexus that divides the labial margin of the crown into symmetrical lobes; the preparaconular and postmetaconular cristae are better developed; and the hypocone is larger and more closely appressed to the protocone. As with M1, the protoconal cingula are cuspate and continuous lingually.

Lower dentition (Figs. 9.3.5-9.3.24): Lower canine: Two lower canines are referred to A. ferox, one of which (UALVP 46490) was found in association with p1 and p4. A broad wear facet on the posterolabial surface of the crown identifies UALVP 46490 as a lower, rather than an upper canine; although UALVP 46498 exhibits little wear on the crown (it is nearly pristine and likely from an immature individual), it is otherwise morphologically identical to UALVP 46490. The lower canine of A. ferox is considerably enlarged relative to the cheek teeth. The crown is mediolaterally compressed, weakly sinusoidal in posterior view, and becomes deeper towards the base of the enamel. The anterior and posterior margins of the crown are drawn out as sharp, serrated crests, the posterior of which terminates at a small cuspule at the base of the enamel. Although the enamel covers only slightly less than half the length of the crown anteriorly, it is much more extensive posteriorly.

Lower premolars: p1: The single-rooted p1 is virtually identical to that of A. ferox and A. corrugatus from the Torrejonian Nacimiento Formation of New Mexico (Matthew, 1937, pl. I, figs. 3a-b, pl. II, figs. 1a-b). The crown consists primarily of a faintly recurved protoconid that is strongly convex labially and faintly concave lingually; well-developed serrated crests are developed anteriorly and posteriorly, and the posterior

crest terminates at a small cuspule. A low and heavy cingulid bearing a small cuspule is developed lingually.

p3: A tall protoconid and a robust, bicuspid heel dominate the crown of p3. The protoconid is vertical rather than recurved, and the enamel on the anterior surface extends far ventrally; an interdental facet is not developed anteriorly, and a diastema was likely present between p2 and p3, consistent with previously described lower jaws of A. ferox (Gidley, 1919; Matthew, 1937). Neither a paraconid nor metaconid is developed. A thick crest originating at the protoconid apex extends posteriorly to the heel, and while serrations were probably present originally (as they are in, e.g., AMNH 2459, see Matthew, 1937), the crest on UALVP 46491 is heavily worn and the serrations are erased. The talonid consists of a large hypoconid, with a smaller cuspule developed on the cingulid posterolingually. The weak anterior cingulid wraps around the anterior side of the protoconid before fading away labially and lingually, while the better-developed posterior cingulid forms a narrow shelf posterolabially and posterolingually. The enamel on p3 is weakly wrinkled.

p4: The p4 of A. ferox is substantially taller and wider than p3. A massive protoconid dominates the crown, and a strong anterior crest connects the protoconal apex to the ledge-like anterior cingulid, on which a small, medially positioned cuspule can be developed. Neither a paraconid nor metaconid is present. The talonid on p4 is better developed than on p3, and consists of a swollen hypoconid that is slightly lingual to the anteroposterior midline of the crown; a robust and serrated crest connects the hypoconid to the apex of the protoconid. Small labial cuspules can be developed adjacent to the hypoconid, and a well-developed cusp (?entoconid) is present on the lingual cingulid of one specimen (UALVP 43104). The prominent anterior and posterior cingulids are high and continuous labially, and bear a number of small cuspules. The enamel is more heavily wrinkled than on p3.

Lower molars: m1: The m1 of A. ferox is considerably lower than p4, with the trigonid and talonid nearly equal in height, and both barely above the level of the p4 talonid. The enamel on m1 is much more strongly wrinkled than on the premolars, particularly the floor of the talonid basin and on the postvallid wall, where it is thrown into heavy folds; the crests and cingulids are irregularly cuspate. A constriction occurs

between the trigonid and talonid, imparting a pyriform outline to the crown, with the talonid being longer and wider than the trigonid. The bulbous protoconid and metaconid are low and subequal in size; the paraconid is poorly developed, being almost completely incorporated into the low, cuspate paracristid. Although the protocristid is weakly developed, it bears a battery of small cuspules. Crests originating at the apices of the protoconid and metaconid extend into the shallow trigonid basin, uniting mid-sagittally and forming a strong notch anterior to the much broader protocristid notch. The talonid is virtually unbasined, and is essentially a broad, flat platform, and the major cusps are swollen; well-developed protostylid and metastylid crests occur on the postvallid wall, and extend posteriorly to the hypoflexid and entocristid, respectively. The hypoconid is the largest cusp on the crown, the width of its base occupying over half the area of the talonid; its apex is low and its basin-facing wall is shallow and flat, and although the entoconid is subequal in height to the hypoconid, it is only about half as large. The small hypoconulid is wedged between the much larger hypoconid and entoconid. The talonid crests are low and bear numerous tiny cuspules. The ectocingulid is robust and positioned high on the crown.

m2: The crown of m2 is both longer and wider than that of m1, and the trigonid and talonid are more nearly equal in width; as on m1, a constriction occurs between the trigonid and talonid on m2, but the outline is dumbbell-shaped, rather than pyriform. Although the crown is approximately the same height as that of m1, the ectocingulid on m2 is much higher and the cusps are relatively lower. As in m1, the trigonid and talonid of m2 are nearly equal in height, and the cusps are low and swollen. The metaconid is the largest trigonid cusp, followed by a slightly smaller and transversely opposed protoconid; the paraconid can be vestigial and appressed to the metaconid, or fully incorporated into the paracristid. The low and cuspate paracristid does not extend anterolingually from the protoconid apex as on m1, but instead runs lingually to meet the metaconid; as a result, the trigonid of m2 is relatively, although not absolutely, anteroposteriorly shorter than on m1. The transverse crests extending into the trigonid basin from the protoconid and metaconid are better developed than those on m1, and the protocristid is similarly low and broadly notched. Protostylid and metastylid crests are present on the postvallid wall and extend posteriorly to the hypoflexid and entocristid,

respectively. The talonid is slightly longer than the trigonid and the basin is even shallower than on m1, forming a nearly horizontal platform. The hypoconid is the largest talonid cusp, followed by a smaller and lower entoconid; the hypoconulid is almost completely incorporated into the postcristid. The enamel is heavily wrinkled, especially in the talonid basin and on the postvallid wall.

m3: The m3 of A. ferox is significantly smaller than m2, with a shorter and narrower trigonid and talonid, and relatively lower cusps. The trigonid bears a swollen protoconid and metaconid; a paraconid is not present on any of the specimens at hand, having been fully incorporated into the low, cuspate paracristid. The transverse trigonid crests, as well as the protostylid and metastylid crests, are weakly developed. The talonid basin is shallow and its floor is elevated to nearly the same level as the trigonid basin; the protocristid is only faintly developed, and the trigonid and talonid basins form a virtually continuous occlusal surface. Unlike that of m1 and m2, the talonid of m3 is narrower than the trigonid, and the cusps are smaller. The hypoconid is the largest, tallest, and best differentiated of the talonid cusps, while the entoconid is smaller and less conspicuous, having been partially incorporated into the long, arcuate entocristid. The hypoconulid projects posteriorly and can be narrow and finger-like (e.g., UALVP 43104, Fig. 9.3.15), or broader and lobe-like (e.g., UALVP 46496, Fig. 9.3.24). The ectocingulid is lower than on m1 or m2, but is similarly robust and labially continuous. As on m1 and m2, the enamel on m3 is heavily wrinkled, especially in the trigonid and talonid basins.

Discussion.—The referred teeth closely resemble those of Arctocyon ferox from the Nacimiento and Fort Union formations of New Mexico and Montana (e.g., Matthew, 1897, 1901, 1937; Gidley, 1919; Simpson, 1937; Kondrashov and Lucas, 2004), differing primarily in their smaller size [e.g., mean length, m2=11.8, combined samples from Birchwood and DW-2, Alberta, versus mean length, m2=12.7, combined samples from localities in the Western Interior of the United States (Kondrashov and Lucas, 2004)], and in the upper molars being less transverse [e.g., width M2=13.8, DW-2, Alberta, versus mean width M2=14.3, combined samples from localities in the Western Interior of the United States (Kondrashov and Lucas, 2004)]. They differ from teeth of the middle-late Tiffanian A. acrogenius in being smaller and in the upper molars being relatively more transverse (i.e., more nearly rectangular, rather than square). Of potential

taxonomic interest are the serrations on the lower canine and premolars: the teeth from the Birchwood and Blindman River localities are serrated anteriorly and posteriorly, in contrast to homologous teeth of other arctocyonines, in which only the posterior crests are serrated. Although the specimens from Alberta are exceptional in their preservation, it seems unlikely that such a feature would have been overlooked in the much larger samples from the San Juan or Crazy Mountains basins; nonetheless, the significance of this character must await further sampling from the Alberta localities.

Arctocyon ferox is stratigraphically long-ranging (middle Torrejonian, To2 to early middle Tiffanian, Ti3) and geographically widespread (New Mexico to Alberta); it is known from the earliest Tiffanian (Ti1) Cochrane 2 and Aaron's localities of Alberta (Youzwyshyn, 1988; Fox, 1990; pers. obs.), and its occurrence at Birchwood and DW-2 represents the youngest and northernmost record for the species.

ARCTOCYON CORRUGATUS (Cope, 1883b)

Figures 9.3.25, 9.3.26; Table 9.3

Claenodon corrugatus COPE, 1883b, p. 556.
Neoclaenodon montanensis GIDLEY, 1919, p. 547.
?Neoclaenodon latidens GIDLEY, 1919, p. 554.
Claenodon latidens: SIMPSON, 1937, p. 187.
?Claenodon vecordensis SIMPSON, 1935a, p. 232.
Claenodon montanensis: SIMPSON, 1937, p. 181.
Arctocyonides montanensis VAN VALEN, 1978, p. 55.

Holotype.—AMNH 3258, incomplete right maxilla with P4, M1-3. Type locality unknown, but described by Matthew (1937, p. 36) as "Middle Paleocene, Torrejon Formation, San Juan Basin, New Mexico", possibly (but not certainly) the early Paleocene (middle Torrejonian, To2, Protoselene opisthacus/Mixodectes pungens Interval Zone, or late Torrejonian, To3, Mixodectes pungens/Plesiadapis praecursor Interval Zone of Lofgren et al., 2004).

Material examined.—From DW-2: UALVP 46506, M1.

From Birchwood: UALVP 39234, 46507, 46508, M1; UALVP 46509, M2; UALVP 46510, 46511, M3.

Age and occurrence.—Late Torrejonian (Mixodectes pungens/Plesiadapis praecursor Interval Zone, To3, early Paleocene) to early middle Tiffanian (Plesiadapis rex/P. churchilli Lineage Zone, Ti3, late Paleocene) of the Western Interior of North America (Lofgren et al., 2004).

Description.—Upper dentition (Figs. 9.3.25, 9.3.26): Upper molars: M1: The crown of M1 is subquadrate in outline, with straight anterior and weakly convex posterior margins. The principal cusps are massive, low, and subequal in size and height; the parastylar lobe, metastylar lobe, and stylar shelf are undeveloped. The heavy ectocingulum is continuous, and a faint ectoflexus occurs midway along the length of the crown, dividing the labial margin into weak para- and metastylar lobes. The paracone and metacone are swollen, closely approximated, and connected by a short, acutely notched centrocrista; the preparacrista, postmetacrista, and centrocrista are low, blunt, and bear numerous cuspules. Although both conules are well developed, the metaconule is nearly twice the size of the paraconule, and is situated more lingually; the conular cristae are short, low, and poorly developed, particularly the postparaconular and premetaconular cristae. The protocone is considerably swollen, and its apex is positioned anterior to the midline, directly lingual to the paracone; the short protoconal cristae terminate near the lingual base of the paraconule and metaconule. The bulbous hypocone is smaller and more labial than in M1 of A. ferox, and the anterior and posterior cingula are higher. The enamel is weakly wrinkled, in contrast with the more heavily wrinkled enamel on M1 of A. ferox.

M2: M2 of A. corrugatus resembles that in A. ferox: the crown is more transverse than M1, subrectangular in outline with smoothly rounded labial and lingual margins, and bears low and massive principal cusps that enclose a shallow basin. The conules are inflated, with the metaconule the larger and more lingual of the two. The M2 differs from M1 in having a deeper ectoflexus and more smoothly rounded metastylar lobe, a smaller hypocone, and in having heavier anterior and posterior cingula.

M3: The subovate outline of M3 contrasts with the more nearly quadrate outlines of M1 and M2, and the metastylar area is weakly developed. The paracone is larger,

taller, and farther labial than the metacone, and the ectocingulum, although prominent anteriorly, weakens posteriorly and all but disappears as it nears the metacone. A conspicuous ridge extending a short distance lingually from the midpoint of the ectocingulum intervenes between the paracone and metacone. The conules and conular cristae are weakly developed, and often cannot be differentiated from the wrinkled and cuspate enamel of trigon basin. The protocone on M3 is relatively lower than that on M1 and M2, and is nearly the same height as the paracone. The short protoconal cristae bear numerous cuspules. The hypocone cannot be distinguished from the cuspate enamel of the posterior cingulum. The protoconal cingula are lingually continuous and the enamel is moderately wrinkled.

Discussion.—Kondrashov and Lucas (2004) recently revised the taxonomy of North American species of Arctocyon and consider "Neoclaenodon montanensis" a subjective junior synonym of A. corrugatus, and this opinion is followed here. The teeth referred here to A. corrugatus differ from those of A. ferox primarily in their smaller size, in being transverse relative to their length, in having a more poorly developed hypocone, in the trigonid of m2 being wider than the talonid, and in having weaker wrinkling of the enamel.

A. corrugatus and A. ferox are contemporaneous in Alberta during the Tiffanian; the occurrence of A. corrugatus at Birchwood and DW-2 represents the youngest and northernmost record for the taxon.

Genus BOREOCYON new genus

Colpoclaenus PATTERSON and MCGREW, 1962 (in part).

Type species.—Boreocyon gigas new species.

Other included species.—Boreocyon alpinus new species; B. augur new species.

Diagnosis.—Differs from other arctocyonines in having upper molars that are relatively more transverse, with taller protocones, poorly developed conules, a weak or undeveloped M2 hypocone, and in having an enlarged M3. Differs further in p4 being smaller relative to m1, in lower molars increasing in size from m1-m3, with cusps that

are less swollen and more fully incorporated into the paracristid and protocristid, deeper talonid basins, and m3 having a longer, broader talonid with large, lobate hypoconulid. Differs from Insidioclaenus new genus (see later in this chapter) in upper molars being more transverse, having weaker conules, lingually continuous protoconal cingula, and in the m3 talonid being much longer and broader. Differs further from Mentoclaenodon, Arctocyonides, and Arctocyon in having relatively wider upper molars, p4 with a well-developed metaconid, and in having less swollen molar cusps and crests.

Etymology.—Boreas, Greek, north wind or northern, in reference to the northern distribution for the genus; kyon, Greek, dog, a common suffix in arctocyonine condylarth taxon nomina.

BOREOCYON GIGAS new species

Figures 9.4.1-9.4.18; Tables 9.4, 9.5

Colpoclaenus keeferi PATTERSON AND MCGREW, 1962: FOX, 1990 (in part).

Diagnosis.—Differs from B. alpinus new species and B. augur new species in being larger (M1, B. gigas approximately 18 percent longer than M1, B. alpinus; m3, B. gigas approximately 45 percent longer than m3, B. augur) Differs further from B. alpinus in upper molars having weaker conules and in lower molars with more labially positioned paraconids. Differs further from B. augur in having a weaker and more labial m3 paraconid.

Description.—The teeth of UALVP 46512 were found associated in the same block; parts of the skull, mandible, and postcranium were also discovered, but most of the bone has been severely eroded, and none of the teeth were found in articulation with the skull or dentary. Nonetheless, UALVP 46512 is likely from a single individual: the upper and lower dentition is from the left and right sides, and is represented by a single tooth per locus (i.e., there is no indication that UALVP 46512 may preserve a second individual as evidenced by, e.g., two LP4s); none of the teeth described below can be referred to another arctocyonine taxon known from DW-2; and the isolated upper and lower teeth fit tightly when manually occluded.

Upper dentition (Figs. 9.4.1-9.4.6): Upper incisors: Three upper incisors are preserved in UALVP 46512, two from the right side of the jaw and one from the left. The exact number of upper incisors cannot be determined from the evidence at hand, but it is probable that there were three, the same as in other arctocyonines (e.g., Arctocyon and Arctocyonides, see Russell, 1964), resulting in a dental formula of 3/3, 1/1, 4/4, 3/3. Referral of the incisors to their correct loci has proven impossible, as the teeth are virtually identical in size and anatomy. The crowns are anteroposteriorly compressed, with convex anterior and flat posterior sides; the apices are acute and the bases are swollen. The lateral edge of the crown is long and oblique to the dorsoventral axis, whereas the medial edge is more nearly vertical; wear is strongly developed posteromedially.

Upper canine: The upper canine is similar to that in other arctocyonines in being large, curved, and mediolaterally compressed. The crown is subovate in cross section, with the anterior surface strongly convex; the posterior margin is drawn out as a heavy, serrated crest, and a large wear facet is present anteromedially. The enamel on the anterior surface extends further dorsally than on the posterior surface.

Upper premolars: P1: P1 of Boreocyon gigas is two-rooted, with the posterior root the larger of the two. The crown is labiolingually compressed, slightly posteriorly leaning, and consists of a tall, trenchant paracone and a weakly differentiated posterior cuspule. The base of the crown is somewhat swollen, suggestive of an incipient protocone, but a distinct cusp is not present. A well-developed serrated crest originating at the paraconal apex extends posteriorly to the posterobasal cuspule. Cingula are not developed.

P2: The roots of P2 are oriented anterodorsally-posteroventrally, and the crown leans posteriorly. The tooth is two-rooted, the posterior root being nearly twice the size of the anterior root. The crown is subtriangular in outline and consists primarily of a massive, subconical paracone. The metacone is undeveloped, and although the crown is swollen posterolingually, suggesting the incipient development of a protocone, neither a lingual root nor a distinct cusp is present. The anterior surface of the paracone is convex, with no development of a preparacrista, whereas the posterior surface is more nearly vertical and bears a serrated postparacrista; the postparacrista joins the

ectocingulum+posterior cingulum posteriorly, and a small posterobasal cuspule can be developed at their junction. The anterior and posterior cingula are continuous lingually, as well as with the weakly developed ectocingulum, and the irregularly cuspate posterior cingulum is especially robust. The enamel is weakly wrinkled.

P3: The crown of P3 is larger than that of P2, and is more nearly equilaterally triangular in outline; as with P2, the two roots and the crown lean posteriorly. The crown of P3 consists primarily of a large, subconical paracone, and while an incipient cuspule can be developed directly lingual to the paracone on the lingually bulging cingulum (e.g., UALVP 46512), a protocone supported by a separate lingual root is not developed. The anterior side of the paracone is long and sloping, and a weakly developed preparacrista extends anteriorly to a small parastylar cusp. A small, bladelike metacone is developed on the posterior shoulder of the paracone, with a sharply notched, serrated centrocrista connecting the two cusps; a sharp postmetacrista runs posteriorly from the metacone to the posterior cingulum. The anterior and posterior cingula are well developed and irregularly cuspate, and are continuous lingually as well as with the weak ectocingulum. The enamel is moderately wrinkled.

P4: The P4 of Boreocyon gigas is three-rooted; the lingual root is nearly twice the size of either of the two labial roots. The posteriorly leaning crown is subtriangular in outline, and consists of a massive paracone and smaller protocone; a metacone is not developed. As in the other upper premolars, the anterior side of the P4 paracone is long and posteriorly sloping, and a heavy preparacrista connects the apex of the paracone to a well-developed parastylar cusp. The postparacrista is swollen and serrated, and extends posteriorly to join the metacingulum and ectocingulum. The lingual part of the crown is much better developed than it is on P2 or P3, with a large, conical protocone occupying the anterolingual corner of the crown; protoconal cristae are present, but weak. The conules are best characterized as incipient: the small paraconule is appressed to the protocone while the larger metaconule occurs at the junction of the postprotocrista and posterior cingulum. The protoconal cingula join one another lingually, and extend to the parastylar and metastylar corners of the crown, where they join the ectocingulum. Numerous cuspules are developed on the cingula, and the enamel is wrinkled.

Upper molars: M1: The upper molars of B. gigas are transverse relative to their length, with broad shallow basins, robust and continuous protoconal cingula, and wrinkled enamel; as with those of other arctocyonines, the molar crests of Boreocyon bear numerous, irregularly sized cuspules. The crown of M1 is rectangular in outline, and although the trigon cusps are low, their apices are sharp, contrasting with the more massive, swollen, and bunodont cusps of most other arctocyonines; the cusps together enclose a shallow trigon basin. The paracone and metacone are subequal in size and height, with the paracone positioned slightly labial to the level of the metacone. The parastylar corner of the crown juts anteriorly, while the metastylar corner is smoothly rounded. The ectocingulum is continuous, becoming more prominent posteriorly, and bears numerous cuspules. The preparacrista, centrocrista, and postmetacrista are short and sharp, and a short crest originating near the deepest part of the centrocrista runs labially to join the ectocingulum. The paraconule can be weak or absent, whereas the metaconule is larger and better differentiated, although both conules are poorly developed compared to those of other arctocyonines. The preparaconular and postmetaconular cristae join the anterior and posterior cingulum, and continue labially as the para- and metacingulum, respectively; the internal conular wings are conspicuous, and ascend the lingual side of the paracone and metacone to their apices. The protocone is nearly the same height as the paracone and metacone, but is considerably more massive, and while the protoconal cingula are lower than those of other arctocyonines (e.g., compare with M1 of Arctocyon ferox, see earlier in the text), they are prominent and lingually continuous. The hypocone is robust, but is notably lower and less inflated than on M1 of other arctocyonines.

M2: The M2 of B. gigas is larger than M1, and is significantly more transverse. The crown is subrectangular in outline and bears low but sharp principal cusps that enclose a basin that is both broader and shallower than on M1. The heavy ectocingulum resembles that on M1 in being low and continuous, and the ectoflexus is shallow. As on M1, the paracone on M2 is labial to the level of the metacone, and the two cusps are connected by a broadly notched, V-shaped centrocrista; the preparacrista and postmetacrista are short and extend to the paracingulum and metacingulum, respectively. The conules are poorly differentiated and appear only as faint swellings at the union of

the weak conular cristae; as on M1, the metaconule on M2 is slightly larger than the paraconule, and the postparaconular and premetaconular cristae ascend the lingual faces of the paracone and metacone to their respective apices. The protocone is enlarged, although not to nearly the same degree as that on M2 of other arctocyonines, and its apex is sharp, rather than being inflated and smoothly rounded. Long protoconal cristae connect the apex of the protocone to the conules. The low protoconal cingula are lingually continuous, and while the posterior cingulum is prominent posterior to the protocone, a hypocone is not developed.

M3: The M3 of Boreocyon differs from that of other arctocyonines in being enlarged relative to M1. The crown is subovate in outline, with a weakly convex anterior margin and reduced metastylar area. The protocone is the largest of the principal cusps, followed by the slightly smaller paracone and metacone; the trigon cusps enclose a basin that is nearly as broad as that in M2. The ectocingulum is prominent anteriorly but weakens posteriorly, terminating at the level of the metacone. As on M1 and M2, the paracone on M3 is more labial than the metacone, and the two cusps are connected by a widely notched centrocrista. The metaconule on M3 is considerably more robust and swollen than on M1 or M2, and can be twinned in some specimens (e.g., UALVP 39225), whereas the paraconule is only weakly developed. The postparaconular crista, although less conspicuous than on M1 or M2, similarly extends to the apex of the paracone, whereas the premetaconular crista is absent. The protoconal cingula run labially, eventually joining the external conular cristae and continue as the para- and metacingulum to the anterolabial and posterolabial corners of the crown; the protoconal cingula are lingually continuous, and a hypocone is not developed.

Lower dentition (Figs. 9.4.7-9.4.18): Lower incisors: The two lower incisors preserved in UALVP 46512 are from opposite sides of the mandible. The teeth are small, with spatulate, anteroposteriorly compressed crowns that have blunt apices. The anterior side is virtually flat, whereas the posterior surface is somewhat concave, and the crown is bordered by weak medial and lateral crests; a swollen, dorsoventrally oriented crest bisects the posterior side of the crown into roughly equal halves.

Lower canine: The enlarged lower canine of B. gigas is sharp, recurved, and mediolaterally compressed, with the lateral surface convex and the medial surface

virtually flat. When viewed from posterior aspect, the tooth appears sinusoidal, bending laterally near the crown-root junction before twisting medially towards the tip; when the root is oriented parasagittally, the crown splays labially. A robust, serrated crest is developed along the posterior side of the crown, extending posteroventrally from the apex to the crown-root junction; unlike lower canines of Arctocyon ferox (see earlier in this chapter), those of B. gigas are not serrated anteriorly. Occlusion with the opposing upper canine has produced a strong wear facet posterolaterally.

Lower premolars: p1: The p1 of B. gigas is small and single-rooted. The crown is labiolingually compressed and consists of a large protoconid; weakly developed anterior and posterior crests extend from the protoconid apex towards the base of the crown.

p2: The p2 of B. gigas is substantially larger than p1. The tooth is two-rooted, with the posterior root the larger of the two. The crown consists of a short but trenchant protoconid and a small, unicuspid talonid. Weak crests extend from the protoconid apex anteriorly to near the base of the crown and posteriorly to the talonid cusp.

p3: The crown of p3 is slightly longer and wider than that of p2, the protoconid is similarly tall and trenchant, and the heel is more strongly developed and bicuspid. A weak crest runs anteriorly from the protoconid apex to the anterior cingulid, and a tiny cuspule can be developed at their junction. A small metaconid can be present low on the posterolingual shoulder of the protoconid, with a weak protocristid connecting the two cusps; the paraconid is not developed on any p3 at hand. A serrated cristid obliqua extends posteriorly from the protoconid apex towards the hypoconid, and a narrow, slit-like notch is formed at its deepest part. A smaller and lower entoconid is connected to the hypoconid by a short postcristid; the two talonid cusps and their associated crests delimit a shallow basin that is open lingually. The anterior and posterior cingulids are robust, but discontinuous labially. The enamel is moderately wrinkled.

p4: The p4 of B. gigas resembles p3: the crown consists of a tall protoconid, a weakly developed metaconid, and a bicuspid heel, and although the crown is longer and wider than that of p3, the crowns of both are nearly equal in height. The crown of p4 differs from that of p3 in the following ways: the anterior crest is stronger and is serrated; the metaconid is better differentiated and higher on the posterolingual side of the protoconid; the protocristid is thicker and more heavily cuspate; a metastylid crest is

developed; the cristid obliqua is heavier and more coarsely serrated; the hypoconid is relatively lower, and a notch between the protoconid and hypoconid is not developed; the entoconid is larger; the talonid basin is wider; and the ectocingulid is higher and complete labially. The enamel of p4 is wrinkled much in the same manner as on p3.

Lower molars: m1: The lower molars of B. gigas are relatively high crowned compared to those of most other arctocyonines, and increase in size posteriorly to m3. The trigonid cusps are considerably less swollen than those of other arctocyonines, but are nonetheless low, being little elevated above the trigonid basin, and their apices are poorly differentiated from the strongly wrinkled and cuspate enamel. The talonid basins are deep, rather than shallow and platform-like (compare with, e.g., lower molars of Arctocyon). The crown of m1 is weakly pyriform in outline, with the talonid wider than the trigonid. The trigonid is dominated by a large protoconid and metaconid that are connected by a low and shallowly notched protocristid. A heavily cuspate paracristid extends anteriorly from the protoconid apex before bending abruptly lingually, imparting a subquadrate occlusal outline to the trigonid; the paraconid is poorly differentiated from the paracristid. As on molars of other arctocyonines, well-developed crests extend from the apices of the protoconid and metaconid into the trigonid basin; the crests are cuspate, but are sharper, higher, and less swollen than those in other arctocyonines, and a notch is formed at their junction in the deepest part of the basin. A low protocristid is developed posterior to the transverse crest, and poorly developed metastylid and protostylid crests extend posteroventrally to the entocristid and hypoflexid, respectively. In contrast with that of most other arctocyonines, the talonid basin on m1 in Boreocyon is deep and cuplike, rather than shallow and platform-like. The hypoconid and entoconid are nearly equal in size and height, and their apices are poorly differentiated, and are instead incorporated into the high, cuspate talonid crests; the hypoconulid is greatly reduced in size and is poorly differentiated from the cuspate postcristid. The cristid obliqua is low and joins the postvallid surface near its labial extremity. Although the ectocingulid is well developed and continuous, it is notably lower than on m1 of Arctocyon.

m2: Compared to m1, the crown of m2 is longer and wider, the trigonid and talonid are more nearly equal in width, and although the trigonid is wider than on m1, it is more anteroposteriorly compressed. The trigonid cusps resemble those on m1 in that

their apices are poorly differentiated from the wrinkled enamel and cuspate crests: the metaconid on m2 is slightly larger and farther posterior to the level of the protoconid than on m1, while the paraconid is closely appressed to the protoconid and poorly differentiated from the low, cuspate paracristid. The transverse crests and protocristid are similar to those on m1, differing only in their being more widely notched. The talonid basin on m2 is deep and cuplike, and its borders are formed by a well-developed hypoconid and cuspate talonid crests; like those on m1, the entoconid and hypoconulid are virtually undifferentiated, and the hypocristid and postcristid form a continuous, cuspate crest that closes off the posterior parts of the talonid basin. The ectocingulid is robust and continuous.

m3: Unlike the m3 of most other arctocyonines, that of B. gigas is enlarged, being significantly longer than m2 and nearly as wide. The coronal anatomy of m3 is superficially plesiadapid-like in having a long talonid that bears a wide, lobe-like hypoconulid; in these respects the m3 of Boreocyon broadly resembles that of Insidioclaenus (see later in this chapter). The crown of m3 is flexed such that it appears concave dorsally in lateral view, bringing the hypoconulid lobe to nearly the same height as the apex of the metaconid, and with the long posterior root extending posteroventrally. The trigonid is nearly the same width as that on m2, but the protoconid is smaller; the paraconid is poorly differentiated from the paracristid and slightly more labial than on m2. The transverse trigonid crests are high and cuspate, and the protocristid is better developed than it is on either m1 or m2. The hypoconulid lobe is the highest talonid cusp by virtue of the strong flexure of the crown, but it is approximately the same size and height as the hypoconid when both are viewed in the same plane; the entoconid is better differentiated than on m1 or m2, and the talonid crests are similarly cuspate. The cristid obliqua joins the postvallid surface at its labial extremity.

Etymology.—Gigas, Latin, giant, in reference to the large size of the teeth of B. gigas.

Holotype.—UALVP 46512, associated right IX-X, C, P1-4, M1-3, left IX, P4, M1-3, right ix, c, p1, incomplete p2-4, m1-3, left ix, c, incomplete m1 (Fig. 9.4). DW-2 locality, Paskapoo Formation of Alberta, late Paleocene [early middle Tiffanian, Ti3 (Fox, 1990), Plesiadapis rex/P. churchilli Lineage Zone of Lofgren et al., 2004)].

Other material examined.—From DW-2: UALVP 46513, incomplete maxilla with P3-4, M1; UALVP 46514, 46515, 46516, C (total: 3); UALVP 46517, 46518, P2; UALVP 46519, P3; UALVP 46520, P4; UALVP 46521, M2; UALVP 46522, p2; UALVP 46523, p4; UALVP 46524, incomplete dentary with m1; UALVP 46525, 46526, 46527, m1 (total: 3); UALVP 46528, incomplete dentary with m2-3.

From Birchwood: UALVP 46529, M1; UALVP 39237, 46601, M2; UALVP 39225, 39226, M3; UALVP 46530, 46531, p3; UALVP 46532, 46533, p4; UALVP 39202, incomplete dentary with m2-3; UALVP 39203, incomplete dentary with m1-2; UALVP 39204, 39213, m1; UALVP 39211, 39211, incomplete m2; UALVP 46534, m3; UALVP 39214, incomplete m3.

Age and occurrence.—Early middle Tiffanian (Plesiadapis rex/P. churchilli Lineage Zone, Ti3, late Paleocene) of Alberta (Fox, 1990; Webb, 1996).

BOREOCYON ALPINUS new species

Figure 9.5.1-9.5.10; Table 9.6

Colpoclaenus sp.: FOX, 1990.

Colpoclaenus cf. C. keeferi: FOX, 1990 (in part).

Diagnosis.—Differs from Boreocyon gigas in being smaller (M1, B. alpinus approximately 18 percent shorter than M1, B. gigas) and in having relatively better developed conules and conular cristae, sharper cusps, and a more anteroposteriorly compressed upper molar protocone.

Description.—Upper dentition (Figs. 9.5.1-9.5.4): Upper molars: M1: M1 of Boreocyon alpinus resembles that in B. gigas (e.g., the crown is subrectangular in outline, the principal cusps are uninflated with acute apices, and the stylar shelf is greatly reduced), but differs in a few notable features: 1) the protocone is more anteroposteriorly compressed; 2) the cusps are relatively higher and more acute, and enclose a basin that is both deeper and narrower; 3) the paracone and metacone are more nearly in line (contrast with M1 in B. gigas in which the paracone is labial to the level of the metacone); 4) the conules and their associated crests are better developed (although both conules are weak

compared to those of other arctocyonines); 5) the posterior cingulum is lower; and 6) the crown is smaller (approximately 18 percent shorter). The enamel is wrinkled much as in M1 of B. gigas.

M2: The referred M2 from Cochrane 2 is badly damaged, with enough of the crown remaining only to allow its identification and referral to B. alpinus. Other than the crown being smaller and the ectocingulum weaker, UALVP 46538 closely resembles M2 of B. gigas.

Lower dentition (Figs. 9.5.5-9.5.10): Lower molars: m1: The m1 of B. alpinus closely resembles that in B. gigas, differing mainly in its smaller size, relatively wider talonid, and in having slightly better differentiated cusps. The paraconid is more distinct from the paracristid compared to that on m1 of B. gigas, and it is more lingual in position and better separated from the metaconid. As on m1 of B. gigas, the transverse trigonid crests on m1 of B. alpinus are sharp and the protocristid is broadly V-shaped. The hypoconid and entoconid are subequal in size and height, the talonid crests are sharp and cuspate, and although the hypoconulid is better differentiated than on m1, B. gigas, it is nonetheless weak and almost entirely incorporated into the postcristid/hypocristid; the talonid basin is deep and cuplike. The robust ectocingulid is low and labially continuous, and the enamel is wrinkled.

m2: Other than its smaller size, very little distinguishes m2 of B. alpinus from that of B. gigas. The m2 of B. gigas is more robust than that of B. alpinus, and the paraconid is slightly more labial in position.

Etymology.—Alpinus, Latin, mountain, in reference to discovery of B. alpinus at localities near the Foothills of Alberta.

Holotype.—UALVP 46535, isolated right M1 (Figs. 9.5.3, 9.5.4). Diss locality, Paskapoo Formation of Alberta; age uncertain, although the co-occurrence of B. alpinus and the multituberculate Parectypodus corystes at Cochrane 2 and Aaron's locality argues for a late Paleocene [earliest Tiffanian, Ti1 (Youzwyshyn, 1988; Fox, 1990; Scott et al., 2002), Plesiadapis praecursor/P. anceps Interval Zone of Lofgren et al., 2004] age for Diss.

Other material examined.—From Cochrane 2: UALVP 46536, 25018, m1; UALVP 46537, m2; UALVP 46538, incomplete M2.

From Aaron's locality: UALVP 46539, incomplete m2 or m3.

From Dankeshane: UALVP 46540, M1.

Age and occurrence.—Earliest Tiffanian (Plesiadapis praecursor/P. anceps Interval Zone, Ti1, late Paleocene) of Alberta (Youzwyshyn, 1988; Fox, 1990; Scott et al., 2002).

BOREOCYON AUGUR new species

Figure 9.5.11-9.5.13

Colpoclaenus sp., cf. C. procyonoides: SCOTT, 2003.

Diagnosis.—Differs from Boreocyon gigas and B. alpinus in being significantly smaller (m3, B. augur approximately 45 percent shorter than m3, B. gigas). Differs further from B. gigas in having a more distinct and lingually positioned m3 paraconid and a weaker hypoconulid lobe.

Description.—The type and only specimen from Who Nose? (m3) was described in detail by Scott (2003) (UALVP 44173 was identified in that paper as pertaining to Colpoclaenus sp., cf. C. procyonoides).

Etymology.—Augur, Latin, diviner, augury, foreseer, in reference to the earlier occurrence of B. augur relative to B. alpinus and B. gigas.

Holotype.—UALVP 44173, isolated left m3 (Figs. 9.5.11-9.5.13). Who Nose? locality, Paskapoo Formation of Alberta, early Paleocene [middle Torrejonian, To2 (Scott, 2003), Protoselene opisthacus/Mixodectes pungens Interval Zone of Lofgren et al., 2004].

Other material examined.—UALVP 46541, fragmentary M1.

Age and occurrence.—Type locality only.

Discussion.—Recognition of Boreocyon as an arctocyonine is based on the wrinkled enamel, serrated canines and posterior premolars, robust cingula, and well-developed transverse trigonid crests, characters that have been considered synapomorphies of Arctocyoninae (Cifelli, 1983; Prothero et al., 1988; Archibald, 1998); the phylogenetic position of Boreocyon relative to other arctocyonines is, however, less

clear. Unlike most arctocyonines (e.g., Arctocyon, Arctocyonides, Mentoclaenodon), the teeth of Boreocyon are higher crowned, with less swollen cusps, lower cingula/cingulids, weaker conules and hypocones, and deeper talonid basins; furthermore, the upper molars of Boreocyon are considerably more transverse relative to their length, and the lower molars increase in size through m3. Boreocyon is unique among arctocyonines in having weak carnassial function between P3 and p3, evidenced by the development of slit-like notches between the P3 paracone and metacone, and in the cristid obliqua on p3. In many of these respects, the dentition of Boreocyon broadly resembles that of many loxolophine condylarths, particularly that of Baioconodon Gazin, 1941, and to a lesser degree Lambertocyon Gingerich, 1979 (considered a loxolophine by Cifelli, 1983, but see Gingerich, 1979 and McKenna and Bell, 1997 for different opinions), yet the teeth of Boreocyon lack putative loxolophine apomorphies (e.g., twinned molar entoconid and hypoconulid, m3 paraconid medially positioned, M3 with postcingular cusp; Cifelli, 1983; Archibald, 1998), and many of these features (e.g., transverse molars, weaker hypocone, less bunodont cusps) are likely plesiomorphic for archaic ungulates generally (compare with the dentitions of, e.g., Protungulatum Sloan and Van Valen, 1965 and Oxyclaenus Cope, 1884a, and see Johnston and Fox, 1984; Lofgren, 1995; Eberle and Lillegraven, 1998).

The dentition of Boreocyon presents a curious mosaic of arctocyonine (e.g., serrations on the canines and posterior premolars, strongly wrinkled enamel) and loxolophine (e.g., transverse molars, unreduced M3/m3, more acute cusps) features, in addition to a number of autapomorphies (e.g., highly cuspate molar crests, reduced conules, greatly enlarged m3 hypoconulid lobe, molars increase in size through m3), making it difficult to reconcile its phylogenetic position among arctocyonines. As currently conceived, Arctocyoninae comprise a relatively unified group of genera characterized by low-crowned molars having bunodont cusps, enlarged and sabre-like serrated canines, subquadrate to subrectangular upper molars with anteriorly positioned protocones, well-developed transverse trigonid crests, and strongly wrinkled enamel; although the teeth of Boreocyon clearly share some of these apomorphies, they differ in a number of features (e.g., higher crowned molars, acute cusps, tall protocone), and the genus cannot be presently allied with any known arctocyonine taxon.

The record of Boreocyon in western Canada extends from the middle Torrejonian (B. augur, Who Nose? locality, To2) to early middle Tiffanian (B. gigas, Blindman River and Birchwood localities, Ti3); a third species, B. alpinus, is known from the earliest Tiffanian (Cochrane 2, Aaron's locality, Dankeshane, Ti1). The holotype of B. alpinus is from the Diss locality of the western Alberta Foothills: the age of Diss is uncertain, but has been considered Torrejonian based in part on the co-occurrence of the "palaechthonid" Palaechthon Gidley, 1923 and the multituberculate Parectypodus corystes Scott, 2003, a taxon initially thought also to occur at the early Puercan Rav W-1 locality of Saskatchewan (Johnston and Fox, 1984; Fox, 1990). P. corystes has since been discovered at the Who Nose? and Cochrane 2 localities, and its affinity with the Rav W-1 species of Parectypodus has been questioned (Scott, 2003). The occurrence of P. corystes and B. alpinus (taxa otherwise known from the middle Torrejonian and earliest Tiffanian) at Diss suggests the local fauna could be even younger than previously believed (Jerzykiewicz and Sweet, 1986; Demchuk, 1987; Fox, 1990).

Boreocyon is uncommon in the middle Torrejonian and earliest Tiffanian of Alberta, where it is represented by a total of nine specimens, but by early middle Tiffanian time it is among the best represented of the archaic ungulates.

Genus INSIDIOCLAENUS new genus

Tetraclaenodon SCOTT, 1892: SIMPSON, 1936, p. 26 (in part); FOX, 1990 (in part).
Desmatoclaenus GAZIN, 1956: VAN VALEN, 1978, p. 57 (in part).

Type species.—Desmatoclaenus mearae Van Valen, 1978.

Other included species.—Insidioclaenus praeceps new species.

Diagnosis.—Differs from all other arctocyonines except Colpoclaenus and Landenodon Quinet, 1968 in having principal trigon cusps high and closely spaced, protocone with long lingual slope, and protoconal cingula discontinuous lingually. Differs further from all other arctocyonines except Colpoclaenus and Landenodon in p1 being two-rooted, in p4 having a tricuspid talonid with deep basin, and in having molars with high talonid cusps and deep basins. Differs further from Colpoclaenus in upper

molars being less transverse relative to length with better-developed para- and metacingulum, weak or absent preparacrista and postmetacrista, and in having weaker molar paraconids. Differs further from Landenodon in cheek teeth being higher crowned, in having a shorter and wider p3-4, and in having a larger m3 bearing a longer and more lobate talonid.

Etymology.—Insidiosus, Latin, cunningly deceitful, in reference to the confusing taxonomic history of the type species Desmatoclaenus mearae.

INSIDIOCLAENUS MEARAE (Van Valen, 1978) new combination

Figures 9.5.14-9.5.20; Tables 9.7, 9.8

Desmatoclaenus mearae VAN VALEN, 1978, p. 57.

cf. Tetraclaenodon sp.: FOX, 1990, p. 57.

Colpoclaenus sp.: FOX, 1990, p. 65.

Revised diagnosis.—Differs from Insidioclaenus praeceps new species (see later in this chapter) in being 7 percent smaller (mean length m1, I. mearae=7.1 versus mean length m1, I. praeceps=7.6), with upper molars relatively more transverse, and in having weaker conules and cingula. Differs further in molar ectocingulum being weak or undeveloped labial to the paracone, in p4 lacking a metaconid, and in having weaker molar ectocingulids.

Holotype.—UCMP 114308, incomplete right maxilla having M1-2 (Van Valen, 1978, p. 57). Saddle locality, Fort Union Formation of Wyoming, late Paleocene [early Tiffanian, Ti2 (Gazin, 1956), Plesiadapis anceps/P. rex Lineage Zone of Lofgren et al., 2004].

Material examined.—From Aaron's locality: UALVP 46542, incomplete right maxilla having M2-3; UALVP 46543, 46544, M1; UALVP 46545, M2; UALVP 46546, 46547, M3; UALVP 46548, incomplete right dentary having p4, m1-3; UALVP 46549, incomplete right dentary having p2-4, m1-3; UALVP 46550, p4; UALVP 46551, m1.

From Calgary 2E/7E: UALVP 122, m2.

From Joffre Pipeline: TMP 86.223.1, m3.

Age and occurrence.—Late Torrejonian (Mixodectes pungens/Plesiadapis praecursor Interval Zone, To3, early Paleocene) to early middle Tiffanian (Plesiadapis rex/P. churchilli Lineage Zone, Ti3, late Paleocene) of the Western Interior of North America (Lofgren et al., 2004).

Description.—Upper dentition (Figs. 9.5.14-9.5.17): Upper molars: M1: The M1 of I. mearae is subquadrate in outline, with the crown being nearly as long as it is wide. The swollen principal cusps are subequal in height and closely approximated, together enclosing a deep trigon basin. A small cusp is present on the anteriorly projecting parastylar lobe, but the stylar shelf is otherwise undeveloped. The ectocingulum is conspicuous labial to the metacone and continues anteriorly to the level of the centrocrista notch, where it bends lingually and forms a short ridge; the ectocingulum is very weak or undeveloped labial to the paracone. The paracone is slightly smaller and more labial than the metacone; the preparacrista is undeveloped, the postmetacrista is weak, and the centrocrista is inflated and irregularly cuspate. While both conules are robust and swollen, the metaconule is larger and more lingually extending than the paraconule. The postparaconular and premetaconular cristae extend labially towards the base of the paracone and metacone where they are shallowly notched, and can continue a short distance up the lingual side of the paracone and metacone; the preparaconular and postmetaconular cristae are short and extend towards the anterior and posterior cingula, but terminate near the lingual base of the paracone and metacone. The apex of the protocone is anterior of an imaginary line drawn lingually from the centrocrista notch. The lingual side of the protocone is long and sloping, and the protoconal cristae are short and markedly inflated. The hypocone is approximately the same size and height as the metaconule, and closely appressed to the protocone. The wide protoconal cingula extend to the anterolabial and posterolabial corners of the crown, but are discontinuous lingually. The enamel is weakly wrinkled.

M2: The M2 of I. mearae is shorter but more transverse than M1, and the principal cusps are more tightly grouped. The parastylar corner of the crown does not project anteriorly as on M1, and the ectocingulum is more nearly complete along the labial side of the paracone. The cusps are swollen, particularly the protocone, and the metaconule and hypocone are relatively weaker than those on M1. As on M1, the

protoconal cingula on M2 extend uninterrupted to the para- and metastylar corners of the crown, but are discontinuous lingually. The enamel is wrinkled, especially on the floor of the trigon basin, and the crests are all weakly cuspate.

M3: The M3 of I. mearae differs from M1 and M2 primarily in its smaller size and in having a greatly reduced metacone and metastylar area. The ectocingulum is discontinuous along the labial side of the paracone, and the principal cusps are large and swollen; the metaconule is larger than the paraconule, and is slightly more lingual than that on M2. The protoconal cingula are heavy, continuous to the para- and metastylar corners of the crown, and discontinuous lingually. The enamel is wrinkled as on M1 and M2.

Dentary (Figs. 9.5.18-9.5.20): UALVP 46549 from Aaron's locality preserves an incomplete horizontal ramus with p2-4, m1-3: the ramus is moderately convex ventrally, and is faintly curved in occlusal view, with the teeth oriented along an arc that is concave lingually. The anteriormost part of a shallow masseteric fossa is preserved posterolabially, and a small mental foramen is developed below the level of p3. Nothing can be said of the incisors of I. mearae, as the anteriormost parts of the dentary are missing; the posterior wall of the canine alveolus remains, however, and its size and orientation indicates the canine was large and directed anterodorsally and slightly labially.

Lower dentition (Figs. 9.5.18-9.5.20): Lower premolars: p1: Alveoli for a two-rooted p1 occur between the canine and p2: part of the small anterior root for p1 is still in its alveolus, immediately posterior to the canine alveolus; only the lingual wall of the posterior alveolus of p1 is preserved, but its size indicates the posterior root was larger than the anterior root. A short diastema separates p1 and p2.

p2: The premolar crowns of I. mearae consist of tall, vertical (i.e., not recurved) protoconids, and variably developed talonids. A long crest connects the protoconid apex to a weak anterolingual swelling on p2; a more prominent, serrated crest runs posteriorly from the protoconid apex to the unicuspid talonid. Short crests bearing minute cuspules extend for a short distance labially and lingually from the talonid cusp.

p3: The crown of p3 resembles that of p2, but is larger, with more pronounced crests, the anterior of which unites with a short but conspicuous anterobasal crest that

wraps around the lingual side of the protoconid to form a short lingual cingulid. The serrated cristid obliqua runs from the protoconid apex to the talonid: the talonid on p3 is wide, and differs from that on p2 in having two cusps, a small hypoconid and larger entoconid; a robust crest runs from the hypoconid labially, forming a short posterior cingulid.

p4: The p4 of I. mearae is subequal in size with m1, but is only slightly taller; it is similar in these regards to p4 in Boreocyon, and differing from other arctocyonines in which the p4 is usually greatly enlarged. The crown resembles that of p3 in having a tall protoconid with robust anterior and serrated posterior crests, but differs in the following ways: the crown is larger overall; the anterobasal cingulid is higher, and a small cuspule is developed at its apex; a weak ectocingulid is present; the paracristid and cristid obliqua are heavier, and both are more conspicuously serrated; an additional crest is developed on the lingual side of the postvallid wall, running posteriorly to join with a low entocristid; the talonid is basined, with a distinct entoconid, hypoconid, weak hypoconulid, and cristid obliqua. A distinct metaconid is not present on any of the premolars, although a vague swelling on the posterolingual shoulder of the p4 protoconid suggests its incipient development.

Lower molars: m1: The lower molars of I. mearae resemble those of most other arctocyonines in having inflated, bunodont cusps, weak paraconids, and well-developed transverse trigonid crests. The crown of m1 is roughly pyriform in outline, with a constriction between the trigonid and wider talonid. The trigonid is higher relative to the talonid when compared with those of other arctocyonines, and in this respect resembles the m1 of Boreocyon. The protoconid and metaconid are nearly equal in size and height, inflated, and transversely opposed from one another; the paraconid is high and appressed to the metaconid, but poorly differentiated from the thick paracristid. As in molars of other arctocyonines, inflated crests originating at the apices of the protoconid and metaconid of m1 extend inwards, uniting in the trigonid basin and forming a deep cleft anterior to the weak protocristid notch. The talonid basin is deeper than those of other arctocyonines (deeper even than that in Boreocyon, see earlier in this chapter), and the cusps are considerably swollen; weak protostylid and metastylid crests extend to the hypoflexid and entocristid, respectively. The hypoconid is the largest talonid cusp,

followed by a smaller entoconid, and while the hypoconulid is small, it is fully differentiated from the postcristid, occurring slightly posterolabial to the entoconid. The cuspate cristid obliqua and entocristid are short and low and both crests form notches just prior to their union with the postvallid wall. A continuous ectocingulid is not developed on m1 of I. mearae, differing from those in other arctocyonines. The enamel is wrinkled, especially on the floor of the talonid basin and on the postvallid wall.

m2: The m2 of I. mearae closely resembles m1, differing mainly in its larger size and greater anteroposterior compression of the trigonid. The paraconid is weaker than that on m1, being almost completely incorporated into the paracristid and anterior side of the metaconid. The protostylid and metastylid crests are stronger than on m1. The talonid basin is deep and the talonid cusps are high, and although the hypoconid and entoconid are subequal in height as on m1, the hypoconulid is better developed. The anterior and posterior cingulids are conspicuous, but the two do not meet labially as an ectocingulid.

m3: The m3 of I. mearae differs from m1 and m2 in being longer and narrower, and in having an enlarged, lobate hypoconulid. The paraconid is small and poorly differentiated from the metaconid, and the paracristid is heavier and more cuspate than on m2. The talonid is similar to that on m3 of Boreocyon in being superficially plesiadapiform-like: the talonid is long with a broad, lobe-like hypoconulid, a distinct hypoconid, and a crest-like entoconid. Each of the talonid cusps is coarsely wrinkled and deeply furrowed on the basin-facing wall, and the floor of the talonid bears numerous irregular cuspules and enamel folds. As on m1 and m2, the anterior and posterior cingulids on m3 are robust, but remain discontinuous.

INSIDIOCLAENUS PRAECEPS new species

Figures 9.5.21-9.5.32, 9.6.1-9.6.6; Table 9.9

Tetraclaenodon sp.: SIMPSON, 1936, p. 26.

cf. Tetraclaenodon sp.: FOX, 1990, p. 57.

Colpoclaenus, cf. C. keeferi: FOX, 1990, p. 59.

Desmatoclaenus sp.: FOX, 1990, p. 59.

Colpoclaenus keeferi: Fox, 1990, pp. 61-62, 65.

Diagnosis.—Differs from I. mearae in being 7 percent larger (mean length m1, I. praeceps=7.6 versus mean length m1, I. mearae=7.1), with upper molars more nearly square in outline, and in having better-developed conules and cingula. Differs further from I. mearae in molar ectocingulum being complete labial to the paracone, in p4 having an incipient metaconid, and in having better-developed molar ectocingulids.

Description.—Upper dentition (Figs. 9.5.21-9.5.26): Upper premolars: Only P3 and P4 of I. praeceps have been discovered, with one specimen (UALVP 46563) preserving these teeth in association with upper molars (Figs. 9.5.21, 9.5.22). P3 of I. praeceps is three-rooted and the crown is triangular in outline, consisting primarily of a large paracone, a small but conspicuous parastylar cusp anterior to the paracone, and a prominent protocone. The ectocingulum is weakly developed. The paracone is faintly compressed labiolingually and leans posteriorly, and a metacone is not present. The preparacrista can be weak or absent, whereas the postparacrista is conspicuous, cuspate, and joins the metacingulum near the posterolabial corner of the crown. The protocone is slightly lower and more nearly vertical than the paracone (i.e., its apex does not lean posteriorly to the same degree), and is connected to the conules by short protoconal cristae: the preprotoconal crista extends labially to a weak paraconule, while the postprotoconal crista is more robust, cuspate, and joins the large metaconule before continuing on to the posterolabial corner of the crown as a stout metacingulum. The protoconal cingula are well developed but discontinuous with one another lingually.

P4: P4 of I. praeceps resembles P3, but the crown is larger, the preparacrista is better developed, and a small metacone is present on the posterior shoulder of the paracone. P4 further differs from P3 in having stronger protoconal cristae, a larger metaconule, and in the protoconal cingula being continuous lingually. The enamel on P3 and P4 is coarsely wrinkled.

Upper molars: The upper molars of I. praeceps differ from those of I. mearae primarily in their larger size, greater length relative to width (i.e., the molars are more nearly square in occlusal outline), in M2 being longer than M1, and in having more swollen cusps. The cusps and conules of I. praeceps are lower and more rounded than

those of I. mearae, and are more widely spaced from each other, resulting in a more open trigon basin. The ectocingulum on M1 and M2 of I. praeceps is heavier and more cuspate than on I. mearae, and is complete labially. The parastylar lobe on M1 does not project anteriorly as in I. mearae, and the protoconal cingula are more robust, especially the posterior cingulum+metacingulum.

Lower dentition (Figs. 9.5.27-9.5.32, 9.6.1-9.6.6): Lower premolars: Only the p4 is known for I. praeceps, and it closely resembles that of I. mearae: the crown is dominated by a tall and trenchant protoconid, the talonid is tricuspid and basined, and the paracristid and cristid obliqua are weakly serrated. The p4 of I. praeceps differs from that of I. mearae in being both smaller and shorter relative to the molars, in having an incipient metaconid developed on the posterolingual shoulder of the protoconid, and in having a stronger, more nearly continuous ectocingulid.

Lower molars: The lower molars of I. praeceps closely resemble those of I. mearae in having inflated cusps, weak paraconids, and well-developed transverse trigonid crests, but differ in their larger size and greater degree of cusp inflation. The lower molars of I. praeceps differ further from those of I. mearae in the following ways: the m1 of I. praeceps is larger relative to m2 (i.e., the ratio of m1 length to m2 length is larger), and the talonid is considerably wider; the paraconid is further reduced in I. praeceps, and is essentially incorporated into the paracristid+metaconid on m2; the talonid cusps are more inflated, especially the hypoconid and hypoconulid; and the ectocingulid is stronger and more nearly continuous.

Etymology.—Praeceps, Latin, steep; in reference to the long and steep lingual slope of the upper molar protocones.

Holotype.—UALVP 46552, associated right M1-3 (Fig. 9.5.25, 9.5.26). DW-2 locality, Paskapoo Formation of Alberta, late Paleocene [early middle Tiffanian, Ti3 (Fox, 1990), Plesiadapis rex/P. churchilli Lineage Zone of Lofgren et al., 2004].

Other material examined.—From Cochrane 2: UALVP 46553, P4; UALVP 46554, 46555, 46556, M1; UALVP 46557, 46558, 46559, M2; UALVP 25019, incomplete M2; UALVP 46560, M3; UALVP 25079, 46561, m1; UALVP 46562, incomplete m2.

From Burbank: UALVP 46563, associated LP3, M2-3 and RP4.

From DW-2: UALVP 46564, P3; UALVP 46565, P4; UALVP 46566, 46567, M1; UALVP 46568, M2; UALVP 34127, incomplete left dentary with p4, m1; UALVP 46569, m1; UALVP 46570, 46571, m2.

From Birchwood: UALVP 39235, P3; UALVP 46572, M1; UALVP 39223, 39229, M2; UALVP 39215, M3; UALVP 39218, p4; UALVP 39215, 46573, m1; UALVP 39216, incomplete m1; UALVP 39218, 46574, m2; UALVP 39217, 39219, 46575, incomplete m2.

Occurrence.—Earliest Tiffanian (Plesiadapis praecursor/P. anceps Lineage Zone, Ti1, late Paleocene) to early middle Tiffanian (Plesiadapis rex/P. churchilli Lineage Zone, Ti3, late Paleocene) of the Western Interior of North America.

Discussion.—Van Valen (1978) named "Desmatoclaenus" mearae based on UCMP 114308, a fragmentary maxilla with M1 and M2 (see Figs. 9.5.14, 9.5.15) from the early Tiffanian (Ti2) Bison Basin of south central Wyoming, but provided neither a description of the specimen, nor justification for the referral, stating only that the two teeth were "Smaller than [those of] D. hermaeus and with larger hypocone" (Van Valen, 1978, p. 57). Among the specimens from the earliest Tiffanian (Ti1) Aaron's locality of Alberta are teeth that are virtually identical to M1 and M2 of "D." mearae, as well as most of the lower dentition (the upper and lower dentitions were associated on the basis of size and a tight fit when manually occluded). Comparisons between the teeth of "D." mearae (cast of UCMP 114308 plus the specimens from Aaron's locality) and topotypic specimens of D. hermaeus Gazin, 1941 and D. paracreodus Gazin, 1941, both from the Puercan and Torrejonian (early Paleocene) of Utah (Gazin, 1941; Robinson, 1986; Williamson, 1996; see Figs. 9.6.7-9.6.16), indicate UCMP 114308 is not referable to Desmatoclaenus, but rather to a new genus, Insidioclaenus. The teeth of Desmatoclaenus differ from those of Insidioclaenus as follows:

1) The upper molars of Desmatoclaenus are transverse relative to their length, with the principal cusps lower and farther apart (i.e., enclosing a shallower, broader trigon basin), and the lingual slope of the protocone is less steep, while those in Insidioclaenus are more nearly square in outline, with closely spaced principal cusps, and steep lingual slopes;

2) The preparacrista and postmetacrista are well developed on the upper molars of Desmatoclaenus, but these are poorly developed or absent in Insidioclaenus;

3) The molar preparaconular and postmetaconular cristae are well developed in Desmatoclaenus, and continue as the para- and metacingulum to the labial and lingual corners of the crown; in contrast, the preparaconular and postmetaconular cristae are weaker and shorter in Insidioclaenus, and do not continue labially as the para- and metacingulum, terminating instead near the lingual bases of the paracone and metacone.

4) Although the molar conules are inflated in both taxa, those of Desmatoclaenus are much more prominent, particularly the metaconule;

5) The molar paraconids in Desmatoclaenus are well developed and lingual in position, and they are distinct from the metaconids, while those in Insidioclaenus are poorly differentiated from the paracristids and are closely appressed to the metaconids;

6) Transverse trigonid crests are not developed on the molars of Desmatoclaenus, but these are conspicuous and inflated in Insidioclaenus;

7) The molar talonid basins in Desmatoclaenus are shallow and platform-like, forming a broad crushing surface to receive the enlarged protocone on the upper molars; the molar talonids in Insidioclaenus are deep and narrow, consistent with the higher and more acute protocones;

8) The molar cristids obliquae in Desmatoclaenus are prominent and extend dorsally to near the protocristid notches, whereas in Insidioclaenus they are low and join the postvallid wall near the labial margin;

9) The hypoconulid on m3 in Desmatoclaenus is a well-developed, conical cusp, while in Insidioclaenus it is broader, lower, and lobe-like;

10) The metaconid on p4 is well developed in Desmatoclaenus (Gazin, 1941, fig. 19), but is weak or absent in Insidioclaenus, especially on p4 of I. mearae, the earlier and putatively more primitive of the two species.

The removal of "D." mearae from Desmatoclaenus leaves four nominal species of the genus, all from the early Paleocene (Puercan and Torrejonian) of the United States: D. hermaeus, D. paracreodus (but possibly synonymous with D. hermaeus, see West, 1976 and Cifelli et al., 1995, but see Robison, 1986 for a different opinion), D. protogonioides (Cope, 1882b), and D. dianae Van Valen, 1978. An isolated upper molar from the early

Tiffanian (Ti2) Scarritt Quarry of Montana (AMNH 33898), questionably referred to Tetraclaenodon by Simpson (1936), closely resembles M1 of Insidioclaenus (these similarities were noted by Van Valen, 1978 and Thewissen, 1990 in comparison with "Desmatoclaenus"), and is here referred to I. praeceps.

Although the taxonomic position of Desmatoclaenus (s. s.) has historically been unclear (see, e.g., Gazin, 1941; West, 1976; Cifelli, 1983; Robison, 1986; Cifelli et al., 1995; McKenna and Bell, 1997; Archibald, 1998), that of Insidioclaenus seems somewhat more certain. The wrinkled enamel, serrated posterior lower premolars, and transverse trigonid crests are considered arctocyonine synapomorphies (e.g., Cifelli, 1983; Archibald, 1998), with the teeth of Insidioclaenus most closely resembling those of Landenodon and especially Colpoclaenus. The inflated cusps and conules, and reduced paraconids on teeth of Insidioclaenus also bear superficial resemblance to those of basal phenacodontids, particularly those of Tetraclaenodon (see, e.g., the opinions of Simpson, 1936; Gazin, 1941; Robison, 1986; Van Valen, 1978, 1988; but see also Cifelli, 1983 and Thewissen, 1990 for different opinions). The dentition of Insidioclaenus differs from that in Tetraclaenodon and other phenacodontids, however, in having a less fully molarized P4/p4 (e.g., the metacone on P4 of Insidioclaenus is poorly differentiated, the metaconid on p4 is rudimentary or absent, and a paraconid is not developed); the cusps are smaller and less swollen; the paraconids are small; the trigonids bear well developed transverse crests; the talonid basins are deeper; and the talonid of m3 is much different, with the hypoconulid and hypoconid lobe-like, rather than as distinct cusps. Despite the superficially phenacodontid-like inflation of the cusps, the totality of dental characters in Insidioclaenus more closely resembles that of arctocyonines; as such, Insidioclaenus is referred here to the Arctocyoninae.

The teeth of Insidioclaenus most closely resemble those of Colpoclaenus, and to a lesser degree those of Boreocyon among arctocyonine taxa: all three share lower molars that are relatively high-crowned compared to those of other arctocyonines, deep talonid basins, and lobate m3 hypoconulids. Patterson and McGrew (1962) named Colpoclaenus based on specimens that were collected from the earliest Tiffanian (Ti1) Shotgun local fauna, Wyoming, with the hypodigm consisting of 10 isolated teeth. Comparisons between these teeth and those of Insidioclaenus reveal many similarities: for example, the

upper molars of Colpoclaenus (e.g., UW 1933, identified as M1 but here identified as M2, and UW 1934, M3) resemble those of Insidioclaenus in having tightly grouped cusps enclosing a deep trigon basin, inflated conules, and a long lingual slope, but differ in being more transverse and in having better-developed preparaconular and postmetaconular cristae. The lower molars of Insidioclaenus broadly resemble those of Colpoclaenus, but differ in having weaker paraconids, deeper talonid basins, and in lacking the unusual "infolding" of the trigonid enamel (Patterson and McGrew, 1962). The relationship between Insidioclaenus and Boreocyon appears to be remote: although both taxa possess lower molars that are higher crowned compared to those of other arctocyonines, a p4 that is small relative to the molars, and a lobate m3 hypoconulid, the remainder of the dentitions differs significantly. For example, the upper molars of Boreocyon are transverse and subrectangular in outline, while those of Insidioclaenus are more nearly square; the molar cusps in Boreocyon are uninflated, widely spaced from one another, and bear sharp apices, while those in Insidioclaenus are swollen, bunodont, and tightly grouped; and the cingula and cingulids in Boreocyon are lower but heavier than those in Insidioclaenus. The present evidence argues for a closer relationship between Insidioclaenus and Colpoclaenus, with the two taxa sharing a number of characters (e.g., closely spaced upper molar cusps, inflated conules, long lingual slope, lobate m3 hypoconulid); although the teeth of Boreocyon approach those Insidioclaenus and Colpoclaenus in a few characters, these are contradicted by a majority of others, suggesting the similarities, including a lobate m3 hypoconulid, likely arose independently.

Insidioclaenus is known from the late Torrejonian (To3) to the early middle Tiffanian (Ti3) of Alberta, Montana, and Wyoming; although I. mearae and I. praeceps overlap temporally, they have yet to be documented together at any one locality.

Family PHENACODONTIDAE Cope, 1881a

Subfamily MENISCOTHERIINAE Cope, 1882c

Genus ECTOCION Cope, 1882d

Oligotomus COPE, 1873: COPE, 1882e, p. 182 (in part).

Ectocion COPE, 1882d, p. 522.

Gidleyina SIMPSON, 1935a, p. 240.

Prosthecion PATTERSON and WEST, 1973, p. 2.

Type species.—Oligotomus osbornianus Cope, 1882e

Other included species.—Ectocion parvus Granger, 1915; E. superstes Granger, 1915; E. collinus Russell, 1929; E. major (Patterson and West, 1973); E. mediotuber Thewissen, 1990; E. cedrus Thewissen, 1990; E. ignotum Novacek, Ferrusquia-Villafranca, Flynn, Wyss, and Norell, 1991.

ECTOCION sp., cf. E. CEDRUS

Figures 9.6.17-9.6.32, 9.7.1-9.7.18; Tables 9.10, 9.11

Material examined.—From DW-2: UALVP 46576, DP4; UALVP 46577, 46578, 46579, 46580, 46581, M1 or M2 (total: 5); UALVP 46582, M3; UALVP 46583, m1; UALVP 46584, m2; UALVP 46881, m3.

From Birchwood: UALVP 39253, 39254, ?DP3; UALVP 39250, 39251, 39252, 46585, P3 (total: 4); UALVP 39256, 39257, DP4; UALVP 39259-61, P4 (total: 3); UALVP 39240, incomplete maxilla with M1-2; UALVP 39241-44, 46586, M1 or M2 (total: 5); UALVP 39246-48, M3 (total: 3); UALVP 39274-79, p3 (total: 6); UALVP 39280, 39281, 46587, 46588, dp4 (total: 4); UALVP 39282-84, p4 (total: 3); UALVP 39262, incomplete dentary with p4, m1-2; UALVP 39268, incomplete dentary with m2; UALVP 39264, incomplete dentary with m2-3; UALVP 39263, incomplete dentary with m2-3; UALVP 39265, 46589, m1; UALVP 39266, 39269, 39270, m2 (total: 3); UALVP 39271, m3; UALVP 39267, 39273, incomplete m2; UALVP 39272, incomplete m3.

Description.—Upper dentition (Figs. 9.6.17-9.6.32): Upper premolars: DP3: Two teeth from the Birchwood locality are identified as DP3 of Ectocion sp., cf. E. cedrus. DP3 is three-rooted and the crown is subtriangular in outline, with a closely approximated paracone and metacone and a shorter but more massive protocone. The elongate parastylar lobe projects anterolabially and is connected to the paracone by a long

preparacrista; neither a stylar shelf nor metastylar lobe is developed, and although the cuspate ectocingulum is robust anteriorly, it quickly fades away towards the level of the centrocrista. The conical paracone and metacone are nearly connate, and a short, deeply cleft centrocrista joins their apices; a small cuspule is present posterior to the metacone on the short postmetacrista. The conules and conular cristae are poorly developed. The posterior cingulum is prominent, extending posterolabially to the small metastylar cusp; the anterior cingulum is undeveloped. Additional crests extend transversely across the trigon basin and connect the protocone to the lingual sides of the paracone and metacone. A hypocone is not developed.

P3: The P3 of Ectocion sp., cf. E. cedrus is three-rooted, and the crown forms a nearly equilateral triangle in occlusal outline. A low and weak ectocingulum is present. The paracone and metacone are slightly compressed labiolingually, and are connate throughout most of their height, with only their apices separate; the paracone is the taller and larger of the two cusps, and is connected to the metacone by a short, shallowly notched centrocrista. A conspicuous parastylar cusp and weaker metastylar cusp are present, similar to the P3 in E. cedrus; a small paraconule can be present, whereas the metaconule is undeveloped. The conical protocone is shorter than either the paracone or metacone and bears low, weakly developed cristae.

DP4: The crown of DP4 is nearly square in outline. The principal cusps are well developed, and the addition of a robust hypocone gives the crown a strongly quadritubercular appearance. The parastylar lobe juts anteriorly and supports a stout parastylar cusp; neither a stylar shelf nor metastylar lobe is developed. The paracone and metacone are of equal size and height, and are connected to one another by a short centrocrista; a robust mesostyle is developed slightly labial to the centrocrista notch, forming a slight bulge along the labial margin of the crown that interrupts the low ectocingulum. Both the paraconule and the metaconule are swollen and appressed to the bases of the paracone and metacone, respectively, and the conular cristae are weak. The protocone and hypocone are well developed (both appreciably worn in UALVP 39256, Fig. 9.6.21), with the hypocone shorter, more bulbous, and slightly posterolingual to the protocone. The protoconal cingula meet lingually.

P4: P4 in E. sp., cf. E. cedrus is slightly smaller than that in E. cedrus from the early middle Tiffanian (Ti3) Cedar Point Quarry, Wyoming, and the crown is subtriangular in outline, rather than rectangular (Thewissen, 1990, fig. 9). The crown consists of a subequal paracone and protocone, and a smaller metacone, all enclosing a shallow trigon basin. As with P3, a well-developed parastylar cusp is developed directly anterior to the paracone; the paracone and metacone are connate for nearly their entire height, in contrast with P4 in E. cedrus in which the two cusps are better separated (Thewissen, 1990). The ectocingulum is weakly developed and irregularly cuspate, and joins the para- and metacingulum anteriorly and posteriorly. The paraconule is swollen and closely appressed to the base of the paracone, and a stout preparaconular crista joins the anterior cingulum, and then continues to the parastyle; the metaconule is considerably smaller than the paraconule and nearer to the swollen protocone. The short postprotoconal crista can extend posterolabially to the metaconule, or directly posteriorly to join with the posterior cingulum. A hypocone is not developed, and the enamel is wrinkled, especially on the floor of the trigon basin.

Upper molars: Other than M2 being slightly larger than M1, the anatomy of these teeth is nearly identical. The crown is subrectangular in outline and quadritubercular, with the principal cusps and hypocone being nearly equal in size and height. The paracone is labial to the level of the metacone, and the bluntly rounded parastylar lobe projects anterolabially, making the labial margin of the crown oblique to the anteroposterior axis of the tooth. The paracone and metacone are conical with sharp apices. The centrocrista is deflected labially, narrowing to a point (rather than being smoothly rounded as it is in, e.g., Elpidophorus Simpson, 1927b) and a prominent, conical mesostyle is developed at its labial most point. Both the paraconule and the metaconule are enlarged, the former being more swollen and more labial than the latter; the preparaconular crista is low but conspicuous, whereas the remaining conular cristae are poorly developed or absent. The lingual half of the crown is dominated by the large, swollen protocone and hypocone. The widely expanded posterior cingulum supports the bulbous hypocone, and is discontinuous with the anterior cingulum. The enamel is weakly wrinkled. The M3 in E. sp., cf. E. cedrus differs from M1 and M2 primarily in

being smaller, with a more poorly developed metastylar area, in having a weaker mesostyle and conules, and in lacking a hypocone.

Lower dentition (Figs. 9.7.1-9.7.18): Lower premolars: p3: The p3 crown consists primarily of a large, inflated protoconid and a low, stout hypoconid. The paraconid is low and poorly developed, and is connected to the apex of the protoconid by a robust, sweeping paracristid; the metaconid is not present, although a vague swelling of enamel can occur low on the posterolingual shoulder of the protoconid, suggesting its incipient development The hypoconid is labiolingually compressed and bladelike, and is connected to the postvallid wall by a heavy cristid obliqua; a metastylid crest is sometimes present, and a weak protostylid crest occurs on one specimen (UALVP 39276). The anterior and posterior cingulids are conspicuous, although labially discontinuous.

dp4: The trigonid on dp4 in E. sp., cf. E. cedrus is triangular in occlusal outline, with the cusps enclosing a shallow basin. The lingually positioned paraconid is anterior to, and well separated from, the metaconid, and its apex is connected to that of the protoconid by a long, widely notched paracristid; an additional cusp can be developed on the paracristid, giving the paraconid a "twinned" appearance. The metaconid is taller and slightly more posterior than the protoconid, and the apices of both cusps are connected by a deeply notched protocristid; robust protostylid and metastylid crests extend posteriorly and ventrally from the postvallid wall, and a tiny protostylid is present on one specimen (UALVP 39284). The talonid is wider than the trigonid, and the large and swollen cusps enclose a deep basin; the hypoconid and entoconid are larger than the hypoconulid, and all three cusps are larger than the entoconulid and mesoconid. The stout cristid obliqua contacts the postvallid wall ventral to the protocristid notch; the entocristid is low and poorly developed, and the talonid is open lingually. The enamel is weakly wrinkled.

p4: The p4 in E. sp., cf. E. cedrus is larger than p3, with a better-developed trigonid and talonid. The paraconid is higher and better differentiated than on p3, the paracristid is shorter, and a large metaconid occurs posterior to the level of the protoconid. The metaconid and protoconid are connate for nearly their entire height, with their apices connected only by a weak protocristid. Small accessory cuspules can be developed on the paracristid anterolingually near the base of the paraconid and

metaconid, and on the inflated protostylid and metastylid crests. The shallow talonid basin is bounded labially by a large hypoconid and posteriorly by a subequal and closely appressed entoconid and hypoconulid; a weaker entoconulid and mesoconid can be developed. The cristid obliqua is stout and joins the postvallid wall ventrolingual to the protocristid notch; the entocristid is low as on p3, and the talonid is correspondingly open lingually. The enamel is weakly wrinkled.

Lower molars: The m1 and m2 in E. sp., cf. E. cedrus are subrectangular in outline, with weak constrictions between the trigonids and talonids. The crowns are low, with anteriorly leaning trigonids that are only slightly taller than the talonids. The metaconid is the largest trigonid cusp, followed by a smaller protoconid; the paraconid is low and closely appressed to the metaconid, and is connected to the protoconid by a long, sweeping paracristid. The talonid basins are broad and deep, and their cusps and crests are well differentiated: the hypoconid is the largest and tallest cusp, followed by a subequal and closely spaced entoconid and hypoconulid; a weak entoconulid can be developed. The cristid obliqua is robust, extending dorsally on the postvallid wall to just below the protocristid notch, and a thick protostylid crest and cusp occur at the labial extremity of the postvallid wall. The entocristid is low and weakly developed, and the talonid is virtually open lingually. The m3 in E. sp., cf. E. cedrus is longer but narrower than either m1 or m2. The trigonid is lower than on m1 or m2, the protoconid is smaller, and the hypoconulid is more prominent and leans slightly posteriorly. As with that on the premolars, the lower molar enamel is weakly wrinkled.

Discussion.—The teeth of E. sp., cf. E. cedrus most closely resemble those in E. cedrus from the early middle Tiffanian Cedar Point Quarry, Wyoming (Thewissen, 1990), but differ in a number of ways. For example, the posterior cingulum on P4 is weaker in E. sp., cf. E. cedrus, giving the crown a triangular, rather than subquadrate outline; the molar mesostyles in E. sp., cf. E. cedrus are stronger, and the centrocrista is deflected farther labially than those in E. cedrus; the molar trigonids are narrower and less anteroposteriorly compressed than those in E. cedrus, and the crowns are subquadrate, rather than triangular in outline; and the paraconid on p4 of E. sp., cf. E. cedrus is more lingual, and the metaconid more posterior than on p4 of E. cedrus. Additionally, the paracone and metacone are closely appressed on P4 of E. sp., cf. E.

cedrus, and the metaconid on p3 is undeveloped, in contrast to E. cedrus in which the P4 paracone and metacone are better separated, and the p3 metaconid is well developed.

The majority of the differences between E. cedrus and E. sp., cf. E. cedrus are characters of the posterior premolars, teeth that are considered taxonomically useful in distinguishing species of Ectocion (Thewissen, 1990); in particular, the P4 and p3 of E. sp., cf. E. cedrus more closely resemble comparable teeth in E. collinus Russell, 1929 than they do E. cedrus, suggesting that the specimens from DW-2 and Birchwood may represent a new, more primitive species of Ectocion that was coeval with the more derived E. cedrus. The naming of a new species is deferred until a larger sample of E. sp., cf. E. cedrus is accumulated, and variation can be better assessed. Two specimens that were collected from Erickson's Landing (AMNH 15543J, 15543K; Simpson, 1927b) are probably referable to E. sp., cf. E. cedrus.

Order MESONYCHIA Van Valen, 1969

Family MESONYCHIDAE Cope, 1875

Genus DISSACUS Cope, 1881b

Hyoenodictis LEMOINE, 1880, p. 5.
Mesonyx COPE, 1872: COPE, 1881a, p. 484 (in part).
Dissacus COPE, 1881b, p. 1018.
Hyaenodictis LEMOINE, 1891, p. 272.
Plesidissacus LEMOINE, 1894, p. 362.
Plagiocristodon CHOW and QI, 1978, p. 80.

Type species.—Mesonyx navajovius Cope, 1881a.

Other included species.—D. europaeus (Lemoine, 1891); D. praenuntius Matthew, 1915; D. rotundus Wang, 1975; D. indigenus Dashzeveg, 1976; D. magushanensis Yan and Tang, 1976; D. serratus (Chow and Qi, 1978); D. argentus O'Leary and Rose, 1995; D. serior O'Leary and Rose, 1995; D. willwoodensis O'Leary

and Rose, 1995; D. zengi Ting, Wang, Schiebout, Koch, Clyde, Bowen, and Wang, 2004; D. zanabazari Geisler and McKenna, 2007.

DISSACUS sp., cf. D. NAVAJOVIUS (Cope, 1881a)

Figures 9.7.19-9.7.28

Material examined.—From DW-2: UALVP 46590, ?M2; UALVP 46591, c.

From Birchwood: UALVP 39221, p4; UALVP 39220, m1 or m2.

Description.—?M2 (L=13.5; W=12.6): The posterior premolars and molars of mesonychids are nearly homodont, making identification of isolated teeth difficult (see, e.g., O'Leary and Rose, 1995; Zhou, 1995). The strongly developed protocone on UALVP 46590 is well separated from the bases of the paracone and metacone, and the overall morphology is most consistent with M2s of Dissacus (see Matthew, 1937 and O'Leary and Rose, 1995). The crown of UALVP 46590 is triangular in outline, and bears large, robust cusps: the paracone is the largest cusp, followed by the smaller protocone and metacone. A well-developed parastylar cusp occurs immediately anterior to the paracone, and a sharp preparacrista extends posteriorly from its apex, connecting it to the paracone. The paracone and metacone are conical, and are joined for nearly half their height; the centrocrista is short and sharply notched, and the metacone leans posteriorly. Although the ectocingulum is low and relatively inconspicuous, it is continuous, joining the anterior and posterior cingula. The protocone is tall and subconical; well-developed protoconal cristae run labially from the protoconal apex towards the bases of the paracone and metacone, and the labial side of the protocone between the cristae is virtually flat. Neither paraconule nor metaconule is developed, and the protoconal cingula are lingually discontinuous.

Lower canine (W=10.4; D=14.4): UALVP 46591 closely resembles lower canines of other mesonychids: the crown is robust, conical, and slightly recurved, and the root is stout and slightly compressed bilaterally. A deep, near-vertical wear facet has been incised into the posterolateral surface of the crown from occlusion with the opposing upper canine.

p4 (L=14.0; W=5.5): The p4 in D. sp., cf. D. navajovius is similar to those of other species of Dissacus in being labiolingually compressed, and in having a small anterobasal paraconid, a tall and posterior-leaning protoconid, and bladelike hypoconid that are joined to each other by a sharp longitudinal ridge (O'Leary and Rose, 1995). The paraconid on UALVP 39221 is offset anterolingually from the base of the protoconid; the protoconid is only weakly posterior leaning, similar to p4 of D. navajovius and differing from other species of Dissacus in which the protoconid leans more strongly posteriorly. The talonid consists of a tall, bladelike hypoconid connected to the protoconid by a long, centrally positioned cristid obliqua; a deep, slit-like notch occurs at the junction of the cristid obliqua and postvallid wall. A weak postcristid extends lingually from the summit of the hypoconid, and continues a short distance anteriorly as a low lingual cingulid; a short but prominent posterior cingulid flanks the labial side of the hypoconid.

m1 or m2 (L=18.6; TrW=6.7; TaW=5.9): UALVP 39220 closely resembles p4 in coronal morphology, differing mainly in its larger size, more nearly vertical protoconid, and in the development of a rudimentary metaconid immediately lingual to the protoconid apex. UALVP 39220 differs further from p4 in having a larger paraconid and a distinct, slit-like notch between the paraconid and protoconid.

Discussion.—The specimens from DW-2 and Birchwood resemble homologous teeth of D. navajovius (Figs. 9.7.19-9.7.28 and compare with O'Leary and Rose, 1995, fig. 3), differing mainly in their larger size (e.g., length p4, D. sp., cf. D. navajovius = 14.0 versus length p4, D. navajovius = 9.4-12.8; see Zhou, 1995 for dental measurements of D. navajovius from the Western Interior of North America). The significance of these differences in size must await the advent of a larger sample from Alberta.

9.3 Conclusions

Condylarth Diversity during the Late Paleocene in Western Canada, and the Decline of the Hyopsodontidae

Although a diversity of eutherians has been documented at Lancian age faunas in the Western Interior of North America (e.g., Marsh, 1889; Simpson, 1927a, 1929; L. S.

Russell, 1952, 1964; Sloan and Van Valen, 1965; Lillegraven, 1969; Clemens, 1973; Johnston, 1980; Archibald, 1982; Johnston and Fox, 1984; Fox, 1989; Storer, 1991; Lofgren, 1995; Clemens, 1995; Hunter and Pearson, 1996; Hunter et al., 1997; Lillegraven and Eberle, 1999; Webb, 2001), condylarths were among the first to exploit successfully many of the newly vacated ecological niches made available after the catastrophic K/T extinction event (Van Valen, 1978; Hunter, 1997; Archibald, 1982, 1998; Hunter, 1999). Condylarths quickly radiated following the extinction of the dinosaurs, reaching their highest taxonomic diversity during the late Torrejonian and earliest Tiffanian, and although they declined thereafter through to the late Eocene, condylarth taxonomic diversity and abundance (as estimated by minimum individuals) often remained locally high (Archibald, 1998). A comparison of absolute numbers of condylarth taxa at the earliest Tiffanian (Ti1) Cochrane 2 locality (with a total sample size of 260 identifiable condylarth specimens) with that from the early middle Tiffanian (Ti3) DW-2 locality (with a sample size of 74 identifiable condylarth specimens) appears to support these assertions: ten genera in five condylarth families are known from the Cochrane 2 locality, whereas only six genera in three families are recorded at DW-2, with one family, Hyopsodontidae, being entirely absent. In contrast, taxonomic diversity at coeval localities in Montana and Wyoming does not show as pronounced a decline: for example, condylarth diversity at the earliest Tiffanian (Ti1) Douglass Quarry of Montana is high, with nine genera in four families (with a total sample size of 487 identifiable condylarth specimens; Krause and Maas, 1990; Zack et al., 2005), whereas the early middle Tiffanian Cedar Point Quarry is only slightly lower in taxonomic diversity, with eight genera in four families (with a total sample size of 471 identifiable condylarth specimens; Rose, 1981; Secord, 2004), with hyopsodontids remaining taxonomically diverse and numerically abundant.

Localities of earliest Tiffanian age (Ti1) from Alberta (e.g., Cochrane 2, Aaron's locality; Youzwyshyn, 1988; Fox, 1990) are dominated by the phenacodontid Ectocion and the oxyclaenid Thryptacodon, similar to coeval localities in Montana (e.g., Douglass Quarry; Krause and Gingerich, 1983; Krause and Maas, 1990) and Wyoming (e.g., Shotgun locality; Gunnell, 1989). Hyopsodontids are taxonomically diverse in the earliest Tiffanian of Alberta, particularly at Cochrane 2 where at least three, and possibly

four taxa are present [Litomylus dissentaneus Simpson, 1935a, Litomylus grandaletes Scott, Fox, and Youzwyshyn, 2002, Gingerichia hystrix Zack, Penkrot, Krause, and Maas, 2005, and a second apheliscine (pers. obs.)]. By early middle Tiffanian time (Ti3), however, local faunas from Alberta have a higher taxonomic diversity of oxyclaenids and arctocyonids compared to other condylarths, with phenacodontid abundance remaining relatively high, and hyopsodontids being wholly absent (e.g., the oxyclaenids Chriacus oconostotae, C. sp., cf. C. baldwini, and Thryptacodon australis, and the arctocyonids Arctocyon ferox, A. corrugatus, Boreocyon gigas, Insidioclaenus praeceps occur at DW-2 and Birchwood). In contrast, Thryptacodon, phenacodontids, and hyopsodontids were more abundant in Montana and Wyoming during the early middle Tiffanian compared to western Canada (e.g., Thryptacodon australis and the phenacodontids Phenacodus grangeri Simpson, 1935b and Ectocion cedrus at Cedar Point Quarry, and the hyopsodontid Dorraletes diminutivus (Dorr, 1952) at the Chappo Type locality constitute nearly twice the minimum numbers of individuals compared to the next most abundant condylarth taxon; Rose, 1981; Gingerich, 1983; Gunnell, 1994; Secord, 2004), while other oxyclaenids, and especially arctocyonids decrease both in taxonomic diversity and abundance.

The marked decrease in hyopsodontid diversity and numbers in the Western Interior of North America during the Tiffanian is of particular interest. Hyopsodontids are first known from the Lancian of southwestern Saskatchewan (Johnston and Fox, 1984; Fox, 1989) and are well represented at Cochrane 2 and Aaron's locality, but are not documented at any post-earliest Tiffanian (Ti1) locality in western Canada, including the well-sampled Gao Mine locality (late middle Tiffanian, Ti4; pers. obs.) of south central Alberta, and the Roche Percée locality (late middle Tiffanian, Ti4) of southeastern Saskatchewan (Fox, 1990). Hyopsodontids are known from the late Eocene Swift Current Creek beds of southwestern Saskatchewan, but even here the usually abundant taxon Hyopsodus is rare (Russell and Wickenden, 1933; Storer, 1984) (it should be noted however that Clarkforkian and early Eocene localities are unknown in western Canada, and hyopsodontids may have reappeared much earlier; however, no hyopsodontids are known from any of the well-sampled early middle and late middle Tiffanian (Ti3-Ti4) localities in Alberta or Saskatchewan). Hyopsodontid diversity and numbers also decline

in the Bighorn Basin of Wyoming, but to a much less degree (Rose, 1981; Gingerich, 1983): five hyopsodontid genera are known to have survived at least until the late middle Tiffanian (Ti4) in Wyoming (Haplaletes, Dorreletes, Aletodon, Phenacodaptes, and Utemylus), and three (Aletodon, Apheliscus, and Phenacodaptes) survived into the earliest Clarkforkian (Cf1) (Fig. 9.8). Given that hyopsodontids were taxonomically diverse in the northern parts of the Western Interior during the earliest Tiffanian, and remained diverse into the Eocene in the northwestern parts of the United States, their complete absence in western Canadian local faunas (representing a geographical range extending from the Swan Hills of north central Alberta to southeastern Saskatchewan, and two depocentres, the Alberta Syncline and Williston Basin) during the early middle and late middle Tiffanian is unusual. While preservational biases, weathering, collecting bias, and aspects of taphonomy all can affect the taxonomic composition of fossil assemblages (Rose, 1981; Badgley, 1986; Behrensmeyer, 1988; Wilson, 1996), none of the western Canadian localities examined in this study appears significantly biased in these ways. Although size-sorting has likely occurred to some degree (e.g., DW-2, where large-bodied taxa like pantodonts are poorly represented), the evidence for it having been a major contributing factor to the absence of hyopsodontids in western Canada is not persuasive: the teeth of most middle Tiffanian (Ti3-4) hyopsodontids (e.g., Haplaletes, Dorraletes, Aletodon) are smaller than those of contemporary pantodonts and larger arctocyonids, and were closer in size to those of many of the eutherians that are well-represented from the middle Tiffanian of western Canada [e.g., Bessoecetor septentrionalis (Russell, 1929), Carpodaptes hazelae Simpson, 1936]. All other factors being equal, it seems implausible that size sorting could strongly influence the representation of one group (e.g., Hyopsodontidae) in the fossil record, while another group with individuals of presumably similar body size (as inferred from similar dental measurements; e.g., litocherine erinaceomorphs) are comparatively unaffected and well-represented in the record. Gingerich (1983) suggested the decline in hyopsodontid diversity during the late Paleocene in the Bighorn Basin of Wyoming coincided with adaptive radiations of other groups of placental mammals, most notably plesiadapid primates, a group that is well represented in the Tiffanian of western Canada. In addition to plesiadapids, two other eutherian taxa, the pentacodontid Bisonalveus Gazin, 1956,

and the erinaceomorph Litocherus Gingerich, 1983, are among the most abundantly represented taxa in local faunas during the Tiffanian in western Canada (Youzwyshyn, 1988; Fox, 1990; Webb, 1996; MacDonald, 1996; Scott, 2004; Chapter 5). Bisonalveus and Litocherus have hyopsodontid-like dentitions (Litocherus was originally classified in the Hyopsodontidae, see Simpson, 1935; Gingerich, 1983), and may have filled similar adaptive roles [postcranial data suggest that at least some hyopsodontids may have been ambulatory or even arboreal (Penkrot and Zack, 2003; Zack et al., 2005), while Litocherus may have been ambulatory or scansorial (see Chapter 5); postcranial remains are unknown for contemporary pentacodontids]. The co-occurrences of Litocherus and hyopsodontids are particularly revealing (Fig. 9.8): Litocherus is poorly represented at Cochrane 2 and Aaron's locality, whereas hyopsodontids are diverse and well represented; by early middle Tiffanian time, however, Litocherus is significantly better represented (it is the second most abundant taxon at DW-2), whereas hyopsodontids are absent. A similar situation occurs at localities in the Crazy Mountains Basin of Montana: Litocherus has yet to be recorded at the earliest Tiffanian Douglass Quarry, where hyopsodontids are common (Krause and Maas, 1990); in contrast, Litocherus is the second most abundant taxon at the early Tiffanian (Ti2) Scarritt Quarry, where hyopsodontids have not been documented (Krause and Maas, 1990). Although Litocherus is known from a few localities in Wyoming along with hyopsodontids (e.g., Chappo Type locality), it is never well represented, constituting only a very minor component of the local fauna (i.e. few individuals), whereas sympatric hyopsodontids were much more abundant (e.g., Dorraletes at the Chappo Type locality, see Gingerich, 1983; Gunnell, 1994).

While it is tempting to attribute the decline of Hyopsodontidae during the Paleocene in western Canada to competitive exclusion by pentacodontids or erinaceomorphs, such cause and effect scenarios are rarely so straightforward (as Gingerich, 1983 noted for the decline in hyopsodontids in the Paleocene of Wyoming). Although Bisonalveus and Litocherus increase in taxonomic diversity and abundance during the early and middle parts of the Tiffanian, a number of other mammalian taxa from the Tiffanian of western Canada diversify during this time (e.g., the neoplagiaulacid multituberculate Neoplagiaulax Lemoine, 1882, the insectivoran Pararyctes Van Valen,

1966, and the archontan Elpidophorus Simpson, 1927b), while others sharply decline (e.g., the peradectine marsupial Peradectes Matthew and Granger, 1921, the paromomyid primate Ignacius Matthew and Granger, 1921, and the phenacodontid Ectocion), suggesting at the very least a more complex interplay between mammalian communities and extrinsic environmental conditions. Nonetheless, given the evidence from local faunas in both western Canada and Montana and Wyoming, the pattern of declining diversity in Hyopsodontidae, and Condylarthra generally, in the Western Interior of North America during the Paleocene is likely real, rather than only apparent, and could well represent the beginnings of the well-documented faunal and floral reorganizations that culminated at the Paleocene-Eocene Thermal Maximum (Rose, 1981; Krause and Maas, 1990; Maas et al., 1995; Gunnell, 1998; Gingerich and Ting, 2004; Wing, 2004).

9.4 Literature Cited

ARCHIBALD, J. D. 1982. A study of Mammalia and geology across the Cretaceous-Tertiary boundary in Garfield County, Montana. University of California Publications in Geological Sciences, 122:1-286.

ARCHIBALD, J. D. 1998. Archaic ungulates ("Condylarthra"), pp. 292-331. In C. M. JANIS, K. M. SCOTT, and L. L. JACOBS (eds.), Evolution of Tertiary Mammals of North America Volume 1: Terrestrial Carnivores, Ungulates, and Ungulatelike Mammals. Cambridge University Press, Cambridge, Massachusetts.

BADGLEY, C. 1986. Taphonomy of mammalian fossil remains from Siwalik rocks of Pakistan. Paleobiology, 12:119-142.

BEHRENSMEYER, A. K. 1988. Vertebrate preservation in fluvial channels. Palaeogeography, Palaeoclimatology, Palaeoecology, 63:183-199.

BLAINVILLE, de, H. M. D. 1841. Ostéographie, et description iconographique des Mammifères récents et fossiles (Carnivores), vols. I et II. Paris.

CHOW, M., and T. QI. 1978. Paleocene mammalian fossils from Nomogen Formation of Inner Mongolia. Vertebrata PalAsiatica, 16:77-85.

CIFELLI, R. L. 1983. The origin and affinities of the South American Condylarthra and early Tertiary Litopterna (Mammalia). American Museum Novitates, 2772:1-49.

CIFELLI, R. L., N. J. CZAPLEWSKI, and K. D. ROSE. 1995. Additions to the knowledge of Paleocene mammals from the North Horn Formation, central Utah. Great Basin Naturalist, 55:304-314.

CLEMENS, W. A. 1973. Fossil mammals of the type Lance Formation, Wyoming. Part II. Marsupialia. University of California Publications in Geological Sciences, 62:1-122.

CLEMENS, W. A. 1995. A latest Cretaceous, high paleolatitude mammalian fauna from the north slope of Alaska, pp. 15-16. In Z. KIELAN-JAWOROWSKA, N. HEINTZ, and H. A. NAKREM (eds.), Fifth Symposium on Mesozoic Terrestrial Ecosystems and Biota. Contributions from the Paleontological Museum, 364, University of Oslo.

COPE, E. D. 1872. Descriptions of some new Vertebrata from the Bridger group of the Eocene. Paleontological Bulletin, 6:1-6.

COPE, E. D. 1873. On the extinct Vertebrata of the Eocene of Wyoming observed by the expedition of 1872 with notes on the geology. U. S. Geological Survey of Montana, Idaho, Wyoming, and Utah. Sixth Annual Report of the U. S. Geological Survey of the Territories by F. V. Hayden:546-649.

COPE, E. D. 1875. Systematic catalogue of Vertebrata of the Eocene of New Mexico by parties of the expedition of 1874, Chapter 12: Fossils of the Eocene period. Geographical Surveys west of the 100th Meridian, G. M. Wheeler, Corps of Engineers, U. S. Army, Washington, 4:37-282.

COPE, E. D. 1880. On the genera of the Creodonta. Proceedings of the American Philosophical Society, 19:76-82.

COPE, E. D. 1881a. On some Mammalia of the lowest Eocene beds of New Mexico. Proceedings of the American Philosophical Society, 19:484-495.

COPE, E. D. 1881b. Notes on Creodonta. American Naturalist, 15:1018-1020.

COPE, E. D. 1881c. Mammalia of the lower Eocene. American Naturalist, 15:829-831.

COPE, E. D. 1882a. Synopsis of the Vertebrata of the Puerco Eocene epoch. Proceedings of the American Philosophical Society, 20:461-471.

COPE, E. D. 1882b. Some new forms from the Puerco Eocene. American Naturalist, 16:833-834.

COPE, E. D. 1882c. New characters of the Perissodactyla Condylarthra. American Naturalist, 16:334.

COPE, E. D. 1882d. Notes on Eocene Mammalia. American Naturalist, 16:522.

COPE, E. D. 1882e. Contributions to the history of the Vertebrata of the lower Eocene of Wyoming and New Mexico, made during 1881. Proceedings of the American Philosophical Society, 20:139-197.

COPE, E. D. 1883a. On the mutual relationships of the bunotherian Mammalia. Proceedings of the Academy of Natural Sciences Philadelphia, 35:77-83.

COPE, E. D. 1883b. First addition to the fauna of the Puerco Eocene. Proceedings of the American Philosophical Society, 20:545-563.

COPE, E. D. 1884a. Second addition to the knowledge of the fauna of the Puerco Epoch. Proceedings of the American Philosophical Society, 21:309-324.

COPE, E. D. 1884b. The Creodonta. American Naturalist, 18:255-267.

COPE, E. D. 1888. Synopsis of the vertebrate fauna of the Puerco Series. Transactions of the American Philosophical Society, 15, new series:298-361.

DASHZEVEG, D. 1976. New mesonychids (Condylarthra, Mesonychidae) from the Paleogene of Mongolia. Sovmestnaâ Soviet-Mongolian Paleontologičeskaâ Ekspediciâ (Trudy), 3:14-31. [in Russian]

DEMCHUK, T. D. 1987. Palynostratigraphy of Paleocene strata of the central Alberta plains. Unpublished M. Sc. thesis, University of Alberta, Edmonton, 151 pp.

DEMCHUK, T. D. 1990. Palynostratigraphic zonation of Paleocene strata in the central and south-central Alberta Plains. Canadian Journal of Earth Sciences, 27:1263-1269.

DORR, J. A., JR. 1952. Early Cenozoic stratigraphy and vertebrate paleontology of the Hoback Basin, Wyoming. Geological Society of America Bulletin, 69:1217-1244.

DORR, J. A., JR. 1958. Early Cenozoic vertebrate paleontology, sedimentation, and orogeny in central western Wyoming. Geological Society of America Bulletin, 63:59-94.

DORR, J. A., JR., and P. D. GINGERICH. 1980. Early Cenozoic mammalian paleontology, geologic structure, and tectonic history in the overthrust belt near LaBarge, western. Contributions to Geology, University of Wyoming, 18:101-115.

EBERLE, J. J. 2003. Puercan mammalian systematics and biostratigraphy in the Denver Formation, Denver Basin, Colorado. Rocky Mountain Geology, 38:143-169.

EBERLE, J. J., and J. A. LILLEGRAVEN. 1998. A new important record of earliest Cenozoic mammalian history: Eutheria and paleogeographic/biostratigraphic summaries. Rocky Mountain Geology, 33:49-117.

FOX, R. C. 1989. The Wounded Knee local fauna and mammalian evolution near the Cretaceous-Tertiary boundary, Saskatchewan, Canada. Palaeontographica Abteilung A, 208:11-59.

FOX, R. C. 1990. The succession of Paleocene mammals in western Canada, pp. 51-70. In T. M. BOWN and K. D. ROSE (eds.), Dawn of the Age of Mammals in the Northern Part of the Rocky Mountain Interior. Geological Society of America Special Paper, 243.

FOX, R. C. 1997. Late Cretaceous and Paleocene mammals, Cypress Hills region, Saskatchewan, and mammalian evolution across the Cretaceous-Tertiary boundary, pp. 70-85. In L. MCKENZIE-MCANALLY (ed.), Upper Cretaceous and Tertiary stratigraphy and paleontology of southern Saskatchewan. St. John's, Newfoundland, Canadian Paleontology Conference, Field Trip Guidebook No. 6, Geological Association of Canada (Paleontology Division).

GAZIN, C. L. 1941. The mammalian faunas of the Paleocene of central Utah, with notes on geology. Proceedings of the United States National Museum, 91:1-53.

GAZIN, C. L. 1956. Paleocene mammalian faunas of the Bison Basin in south-central Wyoming. Smithsonian Miscellaneous Collections, 131:1-57.

GEISLER, J. H., and M. C. MCKENNA. 2007. A new species of mesonychian mammal from the lower Eocene of Mongolia and its phylogenetic relationships. Acta Palaeontologica Polonica, 52: 189-212.

GIDLEY, J. W. 1919. New species of claenodonts from the Fort Union (basal Eocene) of Montana. Bulletin of the American Museum of Natural History, 41:541-556.

GIDLEY, J. W. 1923. Paleocene primates of the Fort Union, with discussion of the relationships of the Eocene primates. Proceedings of the U. S. National Museum, 63:1-38.

GIEBEL, C. G. 1855. Die Säugetiere in zoologischer, anatomischer und palaeontologischer Beziehung umfassend dargestellt. 1108 pp. Abel, Leipzig.

GILL, T. 1872. Arrangement of the families of mammals with analytical tables. Smithsonian Miscellaneous Collections, 11:1-98.

GINGERICH, P. D. 1979. Lambertocyon eximius, a new arctocyonid (Mammalia, Condylarthra) from the late Paleocene of western North America. Journal of Paleontology, 53:524-529.

GINGERICH, P. D. 1983. New Adapisoricidae, Pentacodontidae, and Hyopsodontidae (Mammalia, Insectivora and Condylarthra) from the late Paleocene of Wyoming and Colorado. Contributions from the Museum of Paleontology, The University of Michigan, 26: 227-255.

GINGERICH, P. D. 1989. New earliest Wasatchian mammalian fauna from the Eocene of northwestern Wyoming: composition and diversity in a rarely sampled high-floodplain assemblage. University of Michigan Papers on Paleontology, 28:1-97.

GINGERICH, P. D., and K. D. ROSE. 1979. Anterior dentition of the Eocene condylarth Thryptacodon: convergence with the tooth comb of lemurs. Journal of Mammalogy, 60:16-22.

GINGERICH, P. D., and S. TING. 2004. Paleocene-Eocene boundary and faunal change in relation to climate. Journal of Vertebrate Paleontology, 24, supplement to no. 3:64A.

GRANGER, W. 1915. Part III.-Order Condylarthra. Families Phenacodontidae and Meniscotheriidae, pp. 329-361. In W. D. MATTHEW and W. GRANGER (eds.), A revision of the lower Eocene Wasatch and Wind River faunas. Bulletin of the American Museum of Natural History, 39.

GUNNELL, G. F. 1989. Evolutionary history of Microsyopoidea (Mammalia, ?Primates) and the relationship between Plesiadapiformes and Primates. University of Michigan Papers on Paleontology, 27:1-157.

GUNNELL, G. F. 1994. Paleocene mammals and faunal analysis of the Chappo Type Locality (Tiffanian), Green River Basin, Wyoming. Journal of Vertebrate Paleontology, 14:81-104.

GUNNELL, G. F. 1998. Mammalian faunal composition and the Paleocene/Eocene epoch/series boundary: evidence from the northern Bighorn Basin, Wyoming, pp. 409-427. In M.-P. AUBRY, S. LUCAS, and W. A. BERGGREN (eds.), Late Paleocene-Early Eocene Climatic and Biotic Events in the Marine and Terrestrial Records. Columbia University Press, New York.

HARTMAN, J. E. 1986. Paleontology and biostratigraphy of lower part of Polecat Bench Formation, southern Bighorn Basin, Wyoming. Contributions to Geology, University of Wyoming, 24:11-63.

HOLTZMAN, R. C. 1978. Late Paleocene mammals of the Tongue River Formation, western North Dakota. Report of Investigation, North Dakota Geological Survey, 65:1-88.

HUNTER, J. P. 1997. Adaptive radiation of early Paleocene condylarths. Journal of Vertebrate Paleontology, 17, supplement to no. 3:54A.

HUNTER, J. P. 1999. The radiation of Paleocene mammals with the demise of the dinosaurs: evidence from southwestern North Dakota. Proceedings of the North Dakota Academy of Science, 53:141-144.

HUNTER, J. P., and D. A. PEARSON. 1996. First record of Lancian (Late Cretaceous) mammals from the Hell Creek Formation of southwestern North Dakota. Cretaceous Research, 17:633-643.

HUNTER, J. P., J. H. HARTMAN, and D. W. KRAUSE. 1997. Mammals and molluscs across the Cretaceous-Tertiary boundary from Makoshika State Park and vicinity (Williston Basin), Montana. Contributions to Geology, University of Wyoming, 32:61-114.

JEPSEN, G. L. 1930. New vertebrate fossils from the Lower Eocene of the Bighorn Basin, Wyoming. Proceedings of the American Philosophical Society, 69:117–131.

JERZYKIEWICZ, T., and A. R. SWEET. 1986. The Cretaceous-Tertiary boundary in the central Alberta Foothills; 1, Stratigraphy. Canadian Journal of Earth Sciences, 23:1356-1374.

JOHNSTON, P. A. 1980. First record of Mesozoic mammals from Saskatchewan. Canadian Journal of Earth Sciences, 17:512-519.

JOHNSTON, P. A., and R. C. FOX. 1984. Paleocene and Late Cretaceous mammals from Saskatchewan, Canada. Palaeontographica Abteilung A, 186:163-222.

KIHM, A. J., and J. H. HARTMAN. 2004. A reevaluation of the Brisbane and Judson local faunas (late Paleocene) of North Dakota, pp. 97-108. In M. R. DAWSON and J. A. LILLEGRAVEN (eds.), Fanfare for an uncommon paleontologist: papers in honor of Malcolm C. McKenna. Bulletin of Carnegie Museum of Natural History, 34.

KONDRASHOV, P. E., and S. G. LUCAS. 2004. Arctocyon (Mammalia, Arctocyonidae) from the Paleocene of North America, pp. 11-20. In S. G. LUCAS, K. E. ZEIGLER, and P. E. KONDRASHOV (eds.), Paleogene Mammals. Bulletin of the New Mexico Museum of Natural History and Science, 26.

KRAUSE, D. W., and P. D. GINGERICH. 1983. Mammalian fauna from Douglass Quarry, earliest Tiffanian (late Paleocene) of the eastern Crazy Mountain Basin, Montana. Contributions from the Museum of Paleontology, The University of Michigan, 26:157-196.

KRAUSE, D. W. and M. C. MAAS 1990. The biogeographic origins of late Paleocene-early Eocene mammalian immigrants to the Western Interior of North America, pp. 71-105. In T. M. BOWN and K. D. ROSE (eds.), Dawn of the Age of Mammals in the Northern Part of the Rocky Mountain Interior, North America. Geological Society of America Special Paper, 243.

KRISHTALKA, L., C. C. BLACK, and D. W. RIEDEL. 1975. Paleontology and geology of the Badwater Creek area, central Wyoming. Part 10. A late Paleocene mammal fauna from the Shotgun Member of the Fort Union Formation. Annals Carnegie Museum, 45:179-212.

LEMOINE, V. 1880. Sur les ossements fossiles des terrains tertiares inférieursdes environs de Reims. Association française pour l'Avancement des Sciences, Paris, 8:585-594.

LEMOINE, V. 1882. Sur deux Plagiaulax tertiaires, recueillis aux environs de Reims. Comptes rendus de l'Academie des sciences, Paris, 95:1009-1011.

LEMOINE, V. 1891. Étude d'ensemble sur les dents des mammifères fossiles des environs Reims. Bulletin de la Société Géologique de France, 3e série, 19:263-290.

LEMOINE, V. 1894. Etude sur les os du pied des mammifères de la faune cernaysienne et sur quelques pieces osseusses nouvelles de cet horizon paleontology. Bulletin de la Société Géologique de France, 3e série, 21:353-368.

LEMOINE, V. 1896. Étude sur les couches de l'Éocène inférieur remois qui continental la faune Cernaysienne, et sur deux types nouveux de cette faune. Bulletin de la Société Géologique de France, 3:333-344.

LIBED, S. A. 2001. Anagenetic evolution of Tetraclaenodon, a Paleocene "condylarth" from the San Juan Basin of New Mexico and phenacodontid phylogeny. Journal of Vertebrate Paleontology, 23, supplement to no. 3:71A.

LIBED, S. A. 2003. A new late Paleocene "condylarth" (Mammalia) from the San Juan Basin, New Mexico. Journal of Vertebrate Paleontology, 21, supplement to no. 3:73A.

LILLEGRAVEN, J. A. 1969. Latest Cretaceous mammals of upper part of Edmonton Formation of Alberta, Canada, and review of marsupial-placental dichotomy in mammalian evolution. University of Kansas Paleontological Contributions, 50 (Vertebrata 12):1-122.

LILLEGRAVEN, J. A., and J. J. EBERLE. 1999. Vertebrate faunal changes through Lancian and Puercan time in southern Wyoming. Journal of Paleontology, 73:691-710.

LINNAEUS, C. 1758. Systema naturae per regna tria naturae, secundum classes, ordines, genera, species cum characteribus, differentiis, synonymis, locis. Volume I: Regnum Animale. Editio decima, reformata. Laurenti Salvii, Stockholm. [Facsimile reprinted in 1956 by the British Museum (Natural History)]

LINNAEUS, C. 1766. Systema naturae per regna tria naturae, secundum classes, ordines, genera, species cum characteribus, differentiis, synonymis, locis. Volume I: Regnum Animale. Editio decima, reformata. Laurenti Salvii, Stockholm. [12th edition of Linnaeus 1735]

LOFGREN, D. L. 1995. The Bug Creek problem and the Cretaceous-Tertiary transition at McGuire Creek, Montana. University of California Publications in Geological Sciences, 140:1-185.

LOFGREN, D. L., J. A. LILLEGRAVEN, W. A. CLEMENS, P. D. GINGERICH, and T. E. WILLIAMSON. 2004. Paleocene biochronology: The Puercan through Clarkforkian

Land Mammal Ages, pp. 43-105. In M. O. WOODBURNE (ed.), Cenozoic mammals of North America: geochronology and biostratigraphy. Columbia University Press, New York.

MAAS, M. C., M. R. L. ANTHONY, P. D. GINGERICH, G. F. GUNNELL, and D. W. KRAUSE. 1995. Mammalian generic diversity and turnover in the late Paleocene and early Eocene of the Bighorn and Crazy Mountains basins, Wyoming and Montana (USA). Palaeogeography, Palaeoclimatology, and Palaeoecology, 115:181-207.

MACDONALD, T. E. 1996. Late Paleocene (Tiffanian) mammal-bearing localities in superposition, from near Drumheller, Alberta. Unpublished M. Sc. thesis, University of Alberta, Edmonton, 248 pp.

MARSH, O. C. 1889. Discovery of Cretaceous Mammalia. American Journal of Science, 38:81-92.

MATTHEW, W. D. 1897. A revision of the Puerco fauna. Bulletin of the American Museum of Natural History, 9:259-323.

MATTHEW, W. D. 1901. Additional observations on the creodonts. Bulletin of the American Museum of Natural History, 14:1-38.

MATTHEW, W. D. 1915. A revision of the lower Eocene Wasatch and Wind River faunas, Part I: Order Ferae (Carnivora). Suborder Creodonta. Bulletin of the American Museum of Natural History, 34:4-103.

MATTHEW, W. D. 1937. Paleocene faunas of the San Juan Basin, New Mexico. Transactions of the American Philosophical Society, New Series, 30:1-510.

MATTHEW, W. D., and W. GRANGER. 1921. New genera of Paleocene mammals. American Museum Novitates, 13:1-7.

MCKENNA, M. C. and S. K. BELL. 1997. Classification of Mammals Above the Species Level. Columbia University Press, New York.

MIDDLETON, M. D., and E. W. DEWAR. 2004. New mammals from the early Paleocene Littleton fauna (Denver Formation, Colorado), pp. 59-80. In S. G. LUCAS, K. E. ZEIGLER, and P. E. KONDRASHOV (eds.), Paleogene Mammals. Bulletin of the New Mexico Museum of Natural History and Science, 26.

MUIZON, C. de, and R. L. CIFELLI. 2000. The "condylarths" (archaic Ungulata, Mammalia) from the early Palaeocene of Tiupampa (Bolivia): implications on the origin of the South American ungulates. Geodiversitas, 22:47-150.

NOVACEK, M. J., I. FERRUSQUIA-VILLAFRANCA, J. J. FLYNN, A. R. WYSS, and M. A. NORELL. 1991. Wasatchian (early Eocene) mammals and other vertebrates from Baja California, Mexico: the Lomas Las Tetas de Cabra fauna. Bulletin of the American Museum of Natural History, 208:1-88.

O'LEARY, M. A., and K. D. ROSE. 1995. New mesonychian dentitions from the Paleocene and Eocene of the Bighorn Basin, Wyoming. Annals of Carnegie Museum, 64:147-172.

PARKER, T. J., and W. A. HASWELL. 1897. A Text-book of Zoology. Vol. 2. Macmillan Press, London, 301 p.

PATTERSON, B., and P. MCGREW. 1962. A new arctocyonid from the Paleocene of Wyoming. Breviora, 174:1-10.

PATTERSON, B., and R. M. WEST. 1973. A new late Paleocene phenacodont (Mammalia, Condylarthra) from western Colorado. Breviora, 403:1-7.

PENKROT, T. A., S. P. ZACK, K .D. ROSE, and J. I. BLOCH. 2003. Postcrania of early Eocene Apheliscus and Haplomylus (Mammalia: "Condylarthra"). Journal of Vertebrate Paleontology, 23, supplement to no. 3:86A.

PROTHERO, D. R., E. M. MANNING, and M. FISCHER. 1988. The phylogeny of the ungulates, pp. 201-234. In M. J. BENTON (ed.), The Phylogeny and Classification of the Tetrapods, Volume 2: Mammals. Systematics Association Special Volume, 35B.

QUINET, G. E. 1968. Les Mammifères du Landénien continental belge: étude de la morphologie dentaire comparée des "carnivores" de Dormaal. Mémoires de l'Institute Royal des Sciences Naturelles de Belgique, 158:1-64.

RIGBY, J. K., JR. 1980. Swain Quarry of the Fort Union Formation, middle Paleocene (Torrejonian), Carbon County, Wyoming: geologic setting and mammalian fauna. Evolutionary Monographs, 3:1-179.

ROBISON, S. F. 1986. Paleocene (Puercan-Torrejonian) mammalian faunas of the North Horn Formation, central Utah. Brigham Young University Geology Studies, 33:87-133.

ROSE, K. D. 1981. The Clarkforkian Land Mammal Age and mammalian faunal composition across the Paleocene-Eocene boundary. The University of Michigan Papers on Paleontology, 26:1-197.

RUSSELL, D. E. 1964. Les Mammifères paléocènes d'Europe. Mémoirs du Museum National d'Histoire Naturelle (France), Nouvelle Série, Série C, 13:1-321.

RUSSELL, L. S. 1929. Paleocene vertebrates from Alberta. American Journal of Science, 17:162-178.

RUSSELL, L. S. 1932. New data on the Paleocene mammals of Alberta, Canada. Journal of Mammalogy, 13:38-54.

RUSSELL, L. S. 1952. Cretaceous mammals of Alberta. Bulletin of the National Museum of Canada, 126:110-119.

RUSSELL, L. S. 1958. Paleocene mammal teeth from Alberta. National Museum of Canada Bulletin, 147:96-103.

RUSSELL, L. S. 1964. Cretaceous non-marine faunas of western North America. Royal Ontario Museum, University of Toronto, Life Sciences Contribution, 61:1-24.

RUSSELL, L. S., and T. D. WICKENDEN. 1933. An Upper Eocene vertebrate fauna from Saskatchewan. Transactions of the Royal Society of Canada Third Series, Section IV, 27:53-67.

SCHIEBOUT, J. A. 1974. Vertebrate paleontology and paleoecology of Paleocene Black Hills Formation, Big Bend National Park, Texas. Bulletin of the Texas Memorial Museum, 24:1-88.

SCOTT, C. S. 2003. Late Torrejonian (middle Paleocene) mammals from south central Alberta, Canada. Journal of Paleontology, 77:745-768.

SCOTT, C. S. 2004. Taxonomically diverse late Paleocene mammal localities from south central Alberta, Canada. Journal of Vertebrate Paleontology, 24, supplement to no. 3:111A.

SCOTT, C. S., R. C. FOX, and G. P. YOUZWYSHYN. 2002. New earliest Tiffanian (late Paleocene) mammals from Cochrane 2, southwestern Alberta, Canada. Acta Palaeontologica Polonica, 47:691-704.

SCOTT, W. B. 1892. A revision of the North American Creodonta, with notes on some genera which have been referred to that group. Proceedings of the Academy of Natural Sciences Philadelphia, 44:291-323.

SECORD, R. 1998. Paleocene mammalian biostratigraphy of the Carbon Basin, southeastern Wyoming, and age constraints on local phases of tectonism. Rocky Mountain Geology, 33:119-154.

SECORD, R. 2004. Late Paleocene biostratigraphy, isotope stratigraphy, and mammalian systematics of the northern Bighorn Basin, Wyoming. Unpublished Ph. D. dissertation, The University of Michigan, Ann Arbor, 532 pp.

SIMPSON, G. G. 1927a. Mammalian fauna of the Hell Creek Formation of Montana. American Museum Novitates, 267:1-7.

SIMPSON, G. G. 1927b. Mammalian fauna and correlation of the Paskapoo Formation of Alberta. American Museum Novitates, 268:1-10.

SIMPSON, G. G. 1928. A new mammalian fauna from the Fort Union of southern Montana. American Museum Novitates, 297: 1-15.

SIMPSON, G. G. 1929. American Mesozoic Mammalia. Memoirs of the Peabody Museum of Yale University, 3:1-235.

SIMPSON, G. G. 1935a. New Paleocene mammals from the Fort Union of Montana. Proceedings of the United States National Museum, 83:221-244.

SIMPSON, G. G. 1935b. The Tiffany fauna, upper Paleocene. III. Primates, Carnivora, Condylarthra, and Amblypoda. American Museum Novitates, 817:1-28.

SIMPSON, G. G. 1936. A new fauna from the Fort Union of Montana. American Museum Novitates, 873:1-27.

SIMPSON, G. G. 1937. The Fort Union of the Crazy Mountain Field, Montana and its mammalian faunas. Bulletin of the United States Museum, 169:1-287.

SIMPSON, G. G. 1945. The principles of classification and a classification of mammals. Bulletin of the American Museum of Natural History, 85: 14-350.

SLOAN, R. E., and L. VAN VALEN. 1965. Cretaceous mammals from Montana. Science, 148:220-227.

SPIVAK, D. N. 1997. Early Paleocene (Puercan) mammals from the Ravenscrag Formation, Saskatchewan, Canada. Journal of Vertebrate Paleontology, 17, supplement to no. 3:78A.

STORER, J. E. 1984. Mammals of the Swift Current Creek local fauna (Eocene: Uintan), Saskatchewan. Natural History Contributions from the Regina Museum of Natural History, 7:1-158.

STORER, J. E. 1991. The mammals of the Gryde local fauna, Frenchman Formation (Maastrichtian: Lancian), Saskatchewan. Journal of Vertebrate Paleontology, 11:350-369.

TAYLOR, L. H. 1984. Review of Torrejonian mammals from the San Juan Basin, New Mexico. Unpublished Ph. D. dissertation, The University of Arizona, 553 pp.

THEWISSEN, J. G. M. 1990. Evolution of Paleocene and Eocene Phenacodontidae (Mammalia, Condylarthra). University of Michigan Papers on Paleontology, 29:1-107.

TING, S., Y. WANG, J. A. SCHIEBOUT, P. L. KOCH, W. C. CLYDE, G. J. BOWEN, and Y. WANG. 2004. New early Eocene mammalian fossils from the Hengyang Basin, Hunan China, pp. 291-301. In M. R. DAWSON and J. A. LILLEGRAVEN (eds.), Fanfare for an uncommon paleontologist: papers in honor of Malcolm C. McKenna. Bulletin of Carnegie Museum of Natural History, 34.

VAN VALEN, L. 1966. Deltatheridia, a new order of mammals. Bulletin of the American Museum of Natural History, 132:1-126.

VAN VALEN, L. 1969. The multiple origins of placental carnivores. Evolution, 23:118-130.

VAN VALEN, L. 1978. The beginning of the Age of Mammals. Evolutionary Theory, 4:45-80.

VAN VALEN, L. 1988. Paleocene dinosaurs or Cretaceous ungulates in South America? Evolutionary Monographs, 10:1-79.

WANG, B. Y. 1975. Paleocene mammals of Chaling Basin, Hunana. Vertebrata PalAsiatica, 13:154-164. [in Chinese]

WEBB, M. W. 1996. Late Paleocene mammals from near Drayton Valley, Alberta. Unpublished M. Sc. thesis, University of Alberta, Edmonton, 258 pp.

WEBB, M. W. 2001. Fluvial architecture and Late Cretaceous mammals of the Lance Formation, southwestern Bighorn Basin, Wyoming. Unpublished Ph. D. dissertation, University of Wyoming, Laramie, 172 pp.

WEST, R. M. 1976. The North American Phenacodontidae (Mammalia, Condylarthra). Milwaukee Public Museum Contributions in Biology and Geology, 6:1-78.

WEIGELT, J. 1960. Die Arctocyoniden von Walbeck. Freiberger Forschungshefte, 77: 1-241.

WILLIAMSON, T. E. 1996. The beginning of the age of mammals in the San Juan Basin, New Mexico: biostratigraphy and evolution of Paleocene mammals of the Nacimiento Formation. Bulletin of the New Mexico Museum of Natural History, 8:1-141.

WILLIAMSON, T. E. and S. G. LUCAS. 1993. Paleocene vertebrate paleontology of the San Juan Basin, New Mexico. Bulletin of the New Mexico Museum of Natural History and Science, 2:105-135.

WILSON, M. V. H. 1996. Taphonomy of a mass-death layer of fishes in the Paleocene Paskapoo Formation at Joffre Bridge, Alberta, Canada. Canadian Journal of Earth Sciences, 33:1487-1498.

WING, S. 2004. Implications of Paleocene-Eocene floral change for mammals. Journal of Vertebrate Paleontology, 24, supplement to no. 3:131A.

WINTERFELD, G. F. 1982. Mammalian paleontology of the Fort Union Formation (Paleocene), eastern Rock Springs Uplift, Sweetwater County, Wyoming. University of Wyoming Contributions to Geology, 21:73-112.

YAN, D. F., and Y. J. TANG. 1976. Mesonychids from the Paleocene of Anhui. Vertebrata PalAsiatica, 14:252-258. [in Chinese]

YOUZWYSHYN, G. P. 1988. Paleocene mammals from near Cochrane, Alberta. Unpublished M. Sc. thesis, University of Alberta, Edmonton, 484 pp.

ZACK, S. P., T. A. PENKROT, J. I. BLOCH, and K. D. ROSE. 2005. Affinities of "hyopsodontids" to elephant shrews and a Holarctic origin of Afrotheria. Nature, 434: 497-501.

ZACK, S. P., T. A. PENKROT, D. W. KRAUSE, and M. C. MAAS. 2005. A new apheliscine "condylarth" from the late Paleocene of Montana and Alberta and the phylogeny of "hyopsodontids". Acta Palaeontologica Polonica, 50:809-830.

ZHOU, Y. 1995. Evolution of Paleocene-Eocene Mesonychidae (Mammalia, Mesonychia). Unpublished Ph. D. dissertation, The University of Michigan, Ann Arbor, 402 pp.

Table 9.1.—Combined measurements and descriptive statistics for the dentition of Thryptacodon australis Simpson from the early middle Tiffanian (Ti3) DW-2 and Birchwood localities, Paskapoo Formation, Alberta.

Element	P	N	OR	M	SD	CV
M2	L	1	5.9	—	—	—
	W	1	7.4	—	—	—
p2	L	1	3.2	—	—	—
	W	1	1.6	—	—	—
p3	L	3	1.1-1.2	1.13	0.06	5.09
	W	3	0.5-0.6	0.53	0.06	10.83
m1	L	2	6.0-6.2	6.10	0.14	2.32
	TrW	2	3.4	3.40	0	0
	TaW	2	4.2	4.20	0	0
m2	L	3	6.3-7.4	6.77	0.57	8.40
	TrW	3	4.5-5.1	4.87	0.32	6.61
	TaW	4	5.4-5.6	5.48	0.10	1.75
m3	L	2	6.2-6.9	6.55	0.49	7.56
	TrW	2	4.6-4.8	4.70	0.14	3.01
	TaW	2	3.8-4.0	3.90	0.14	3.63

Table 9.2.—Combined measurements and descriptive statistics for the dentition of Arctocyon ferox (Cope) from the early middle Tiffanian (Ti3) DW-2 and Birchwood localities, Paskapoo Formation, Alberta.

Element	P	N	OR	M	SD	CV
M1	L	1	10.2	11.70	—	—
	W	1	10.9	12.90	—	—
M2	L	2	10.4	10.40	0	0
	W	2	13.8-14.2	14.00	0.30	2.02
c	W	2	5.0-5.6	5.30	0.42	8.00
	D	2	9.1	9.10	0	0
p1	L	2	2.9-3.8	3.35	0.64	19.00
	W	2	2.9-3.4	3.15	0.35	11.22
p3	L	2	7.7-9.0	8.35	0.92	11.01
	W	2	4.3-4.8	4.55	0.35	7.77
p4	L	3	11.5-12.2	11.70	0.40	3.44
	W	3	6.0-6.1	6.10	0.06	0.01
m1	L	3	10.2-10.7	10.40	0.25	2.41
	TrW	3	6.6-6.7	6.67	0.06	0.87
	TaW	4	8.0-8.3	8.28	0.38	4.56
m2	L	5	11.2-12.5	11.82	0.53	4.45
	TrW	6	8.9-10.5	9.32	0.59	6.38
	TaW	4	8.6-10.6	9.38	0.45	4.80
m3	L	4	9.6-12.0	10.78	0.99	9.17
	TrW	4	7.2-8.0	7.58	0.35	4.62
	TaW	4	5.8-6.6	6.15	0.41	6.70

Table 9.3.—Combined measurements and descriptive statistics for the dentition of Arctocyon corrugatus (Cope) from the early middle Tiffanian (Ti3) DW-2 and Birchwood localities, Paskapoo Formation, Alberta.

Element	P	N	OR	M	SD	CV
M1	L	3	8.7-9.1	8.87	0.21	2.35
	W	3	9.9-10.4	10.07	0.29	2.87
M2	L	2	8.3-9.0	8.65	0.49	5.72
	W	2	12.3	12.30	0	0
M3	L	2	6.4-6.8	6.60	0.28	4.29
	W	2	9.6-10.2	10.15	0.07	0.70

Table 9.4.—Combined measurements and descriptive statistics for the upper dentition of Boreocyon gigas new genus and species from the early middle Tiffanian (Ti3) DW-2 and Birchwood localities, Paskapoo Formation, Alberta.

Element	P	N	OR	M	SD	CV
C	W	2	5.0-7.0	6.00	1.41	23.57
	D	2	8.0-9.1	8.55	0.78	9.10
P1	L	1	5.1	—	—	—
	W	1	2.7	—	—	—
P2	L	2	6.4-7.0	6.70	0.42	6.33
	W	2	4.8-5.0	4.90	0.14	2.89
P3	L	3	6.4-7.7	7.07	0.65	9.21
	W	3	5.4-5.9	5.57	0.29	5.19
P4	L	3	6.7-8.5	7.73	0.93	12.01
	W	3	7.8-9.2	8.67	0.76	8.74
M1	L	3	8.2-9.6	8.87	0.70	7.92
	W	4	10.1-12	11.15	0.90	8.10
M2	L	2	9.9-10.4	10.15	0.35	3.48
	W	2	13-14.9	13.95	1.34	9.63
M3	L	4	8.0-9.0	8.70	0.47	5.39
	W	4	11.7-13.6	12.78	0.93	7.27

Table 9.5.—Combined measurements and descriptive statistics for the lower dentition of Boreocyon gigas new genus and species from the early middle Tiffanian (Ti3) DW-2 and Birchwood localities, Paskapoo Formation, Alberta.

Element	P	N	OR	M	SD	CV
c	W	2	4.8-5.0	4.90	0.14	2.89
	D	2	8.0-8.3	8.15	0.21	2.60
p1	L	1	3.2	—	—	—
	W	1	1.6	—	—	—
p2	L	2	5.2-5.9	5.55	0.49	8.92
	W	2	2.6-2.9	2.75	0.21	7.71
p3	L	3	6.7-6.8	6.73	0.06	0.86
	W	3	3.4-4.0	3.73	0.31	8.18
dp4	L	1	8.0	—	—	—
	TrW	1	4.0	—	—	—
	TaW	1	4.6	—	—	—
p4	L	4	7.5-8.2	7.88	0.30	3.79
	W	4	4.2-5.0	4.53	0.36	7.94
m1	L	7	8.2-9.1	8.64	0.39	4.47
	TrW	8	5.6-6.6	6.21	0.29	4.72
	TaW	7	6.2-7.0	6.73	0.28	4.18
m2	L	4	9.0-10.7	9.65	0.82	8.48
	TrW	4	7.6-8.2	7.80	0.27	3.47
	TaW	4	7.7-8.6	8.08	0.41	5.09
m3	L	4	11.7-13.3	12.33	0.64	5.21
	TrW	4	7.2-8.0	7.68	0.34	4.45
	TaW	3	7.2-7.4	7.33	0.12	1.57

Table 9.6.—Combined measurements and descriptive statistics for the dentition of Boreocyon alpinus new species from the ?late Torrejonian (To3) Diss locality, and the earliest Tiffanian (Ti1) Cochrane 2, Aaron's, and Dankeshane localities, Paskapoo Formation, Alberta.

Element	P	N	OR	M	SD	CV
M1	L	2	7.5-7.6	7.55	0.07	0.94
	W	2	9.4-9.6	9.50	0.14	1.49
m1	L	2	7.8-8.0	7.90	0.14	1.79
	TrW	2	5.1-5.3	5.20	0.14	2.72
	TaW	2	5.6-5.9	5.75	0.21	3.69
m2	L	1	9.0	—	—	—
	TrW	1	7.2	—	—	—
	TaW	1	7.2	—	—	—

Table 9.7.—Combined measurements and descriptive statistics for the upper dentition of Insidioclaenus mearae new combination from the ?late Torrejonian (To3) Calgary 2E/7E locality, the earliest Tiffanian (Ti1) Aaron's locality, and the ?early middle Tiffanian (Ti3) Joffre Pipeline locality, Paskapoo Formation, Alberta.

Element	P	N	OR	M	SD	CV
P4	L	1	5.8	—	—	—
	W	1	6.2	—	—	—
M1	L	2	6.6-6.9	6.75	0.21	3.14
	W	2	7.4-7.7	7.55	0.21	2.81
M2	L	1	6.4	—	—	—
	W	1	8.4	—	—	—
M3	L	1	5.8	—	—	—
	W	1	8.4	—	—	—

Table 9.8.—Combined measurements and descriptive statistics for the lower dentition of Insidioclaenus mearae new combination from the ?late Torrejonian (To3) Calgary 2E/7E locality, the earliest Tiffanian (Ti1) Aaron's locality, and the ?early middle Tiffanian (Ti3) Joffre Pipeline locality, Paskapoo Formation, Alberta.

Element	P	N	OR	M	SD	CV
p2	L	1	5.0	—	—	—
	W	1	2.9	—	—	—
p3	L	1	6.4	—	—	—
	W	1	3.8	—	—	—
p4	L	3	7.5-7.8	7.67	0.15	1.99
	W	3	4.0-4.6	4.23	0.32	7.59
m1	L	2	7.0-7.2	7.10	0.14	1.99
	TrW	2	5.3-5.4	5.35	0.07	1.32
	TaW	2	5.6-6.0	5.80	0.28	4.88
m2	L	2	7.5-7.8	7.65	0.21	2.77
	TrW	2	6.2-6.7	6.45	0.35	5.48
	TaW	2	6.3-6.5	6.40	0.14	2.21
m3	L	3	8.8-9.0	8.93	0.12	1.29
	TrW	3	5.4-5.6	5.47	0.12	2.11
	TaW	3	5.2-5.3	5.27	0.06	1.10

Table 9.9.—Combined measurements and descriptive statistics for the dentition of Insidioclaenus praeceps new species from the earliest Tiffanian (Ti1) Cochrane 2 locality, and the early middle Tiffanian (Ti3) DW-2, Burbank, and Birchwood localities, Paskapoo Formation, Alberta.

Element	P	N	OR	M	SD	CV
P3	L	3	6.2-6.7	6.53	0.29	4.42
	W	3	6.9-7.5	7.20	0.30	4.17
P4	L	1	7.0	—	—	—
	W	1	7.9	—	—	—
M1	L	5	7.0-8.2	7.46	0.46	6.11
	W	6	8.8-9.8	9.33	0.34	3.69
M2	L	5	8.1-8.3	8.22	0.08	1.02
	W	5	10.3-11.2	10.68	0.37	3.47
M3	L	4	6.4-7.0	6.68	0.32	4.80
	W	4	8.4-9.3	8.83	0.44	5.01
p4	L	2	7.8-7.9	7.85	0.07	0.90
	W	2	4.3-4.5	4.40	0.14	3.21
m1	L	8	7.2-8.0	7.58	0.25	3.37
	TrW	8	5.3-6.0	5.58	0.23	4.15
	TaW	7	5.6-6.7	6.20	0.39	6.31
m2	L	4	8.5-10.0	9.10	0.73	8.08
	TrW	5	6.7-7.8	7.36	0.43	5.81
	TaW	5	6.9-7.7	7.46	0.33	4.41

Table 9.10.—Measurements and descriptive statistics for the upper dentition of Ectocion sp., cf. E. cedrus from the early middle Tiffanian (Ti3) DW-2 and Birchwood localities, Paskapoo Formation, Alberta.

Element	P	N	OR	M	SD	CV
DP3	L	2	6.0-6.2	6.10	0.14	2.32
	W	2	4.0	4.00	0	0
P3	L	4	5.8-6.6	6.10	0.35	5.68
	W	4	5.0-5.8	5.33	0.34	6.39
DP4	L	2	5.5-6.1	5.80	0.42	7.31
	W	2	5.9-6.3	6.10	0.28	4.64
P4	L	3	5.5-5.7	5.57	0.12	2.07
	W	3	6.2-6.8	6.53	0.31	4.68
M1	L	4	6.2-7.1	6.58	0.39	5.87
	W	4	7.2-8.8	8.00	0.67	8.42
M2	L	3	6.7-7.1	6.90	0.20	2.90
	W	2	8.8-9.5	9.15	0.49	5.41
M3	L	3	5.1-5.8	5.53	0.38	6.84
	W	2	6.3-7.8	7.05	1.06	15.04

Table 9.11.—Measurements and descriptive statistics for the lower dentition of Ectocion sp., cf. E. cedrus from the early middle Tiffanian (Ti3) DW-2 and Birchwood localities, Paskapoo Formation, Alberta.

Element	P	N	OR	M	SD	CV
p3	L	4	4.5-5.2	4.85	0.26	5.95
	W	5	2.5-3.2	2.78	0.38	11.20
dp4	L	4	6.0-7.1	6.60	0.45	6.89
	TrW	4	3.4-3.5	3.43	0.05	1.46
	TaW	4	3.7-4.3	4.00	0.24	6.12
p4	L	3	6.2-6.6	6.37	0.21	3.27
	W	3	3.8-4.3	4.03	0.25	6.24
m1	L	5	5.5-6.5	5.96	0.43	7.27
	TrW	5	4.0-5.1	4.60	0.49	10.65
	TaW	5	4.3-5.4	4.88	0.44	9.10
m2	L	8	6.0-7.7	6.58	0.58	8.75
	TrW	7	4.5-5.2	4.69	0.27	5.70
	TaW	8	4.0-5.2	4.68	0.34	7.30
m3	L	3	6.5-6.9	6.73	0.21	3.09
	TrW	3	4.3-4.6	4.43	0.15	3.45
	TaW	3	3.8-4.2	3.93	0.23	5.87

Figure 9.1.—1-4. Chriacus sp., cf. C. baldwini (Cope) from the early middle Tiffanian (Ti3) DW-2 locality, Paskapoo Formation, Alberta. 1-4, UALVP 46478, associated left M1 (1, 2) and M2 (3, 4) in 1, 3, occlusal and 2, 4, oblique lingual view.

5-12. Chriacus oconostotae Van Valen from the early middle Tiffanian (Ti3) DW-2 (DW2) and Birchwood (BW) localities, Paskapoo Formation, Alberta. 5, 6, UALVP 39222 (BW), left M1 in 5, occlusal and 6, lingual view; 7-9, UALVP 46479 (DW2), left m2 in 7, labial, 8, lingual, and 9, occlusal view; 10-12, UALVP 46481 (DW2), left m3 in 10, labial, 11, lingual, and 12, occlusal view.

13-26. Thryptacodon australis Simpson from the early middle Tiffanian (Ti3) DW-2 (DW2) and Birchwood (BW) localities, Paskapoo Formation, Alberta. 13, 14, UALVP 46485 (BW), right M2 in 13, occlusal and 14, oblique lingual view; 15-17, UALVP 46482 (DW2), incomplete left dentary with c, p1-4, m1-2 in 15, labial, 16, lingual, and 17, occlusal view (arrows point to the mental foramina); 18-20, UALVP 39320 (BW), incomplete right dentary with m1-2 in 18, oblique labial, 19, lingual, and 20, occlusal view; 21-23, UALVP 46484 (DW2), right m2 in 21, oblique labial, 22, lingual, and 23, occlusal view; 24-26, UALVP 46486 (DW2), right m3 in 24, labial, 25, lingual, and 26, occlusal view.

Scale bars = 5 mm.

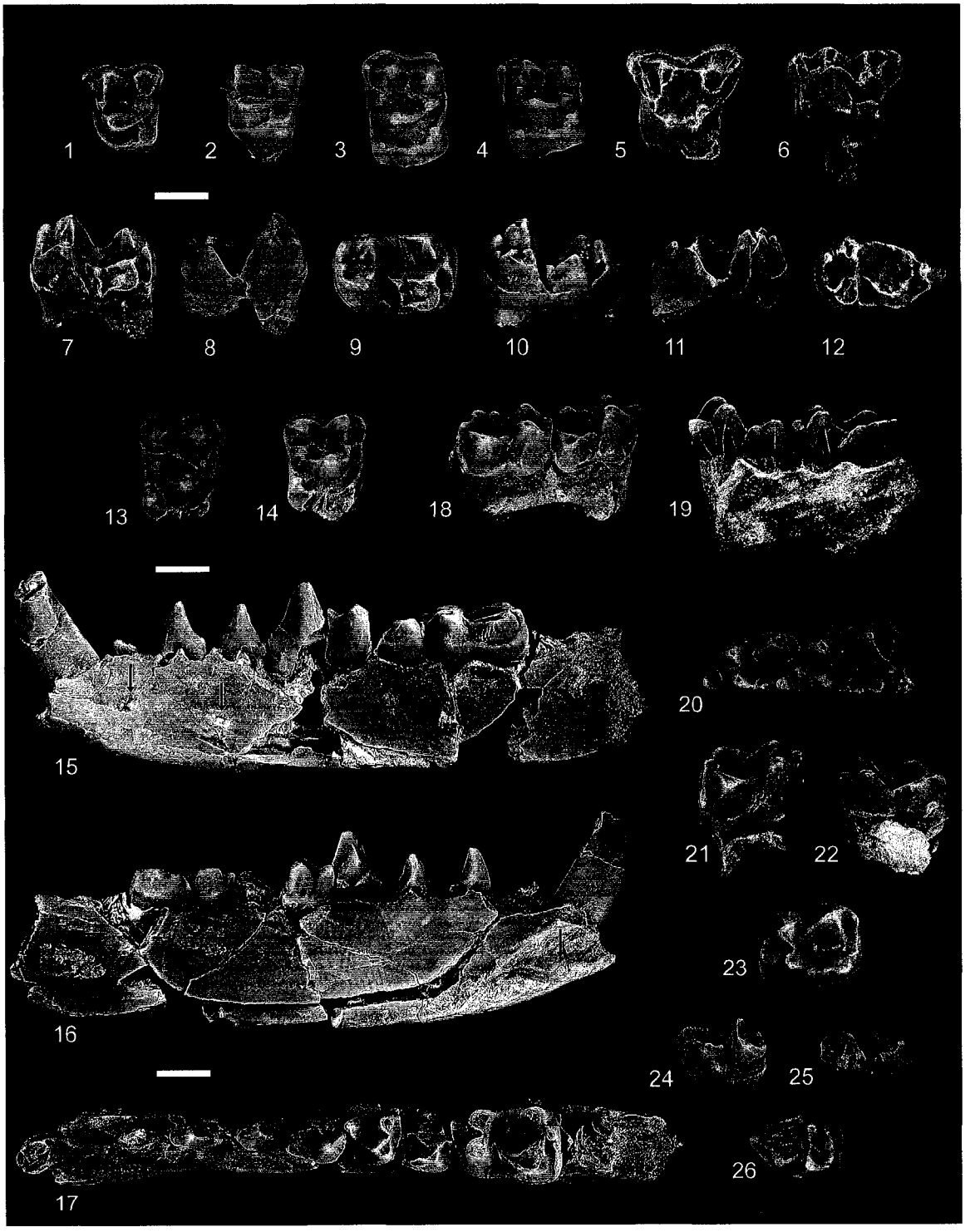
1
2
3
4
5
6
7
8
9
10
11
12
13
14
18
19
15
20
21
22
16
23
24
25
17
26

Figure 9.2.—Thryptacodon australis Simpson from the early middle Tiffanian (Ti3) DW-2 locality, Paskapoo Formation, Alberta. Outline drawing of UALVP 46482, incomplete left dentary with c, p1-4, m1-2 in anterior view showing lower canine and alveoli for i1-3. Medial to left, lateral to right. i1=alveolus for i1; i2=alveolus for i2; i3=alveolus for i3; nv. c.=neurovascular canal. Scale bar = 2mm.

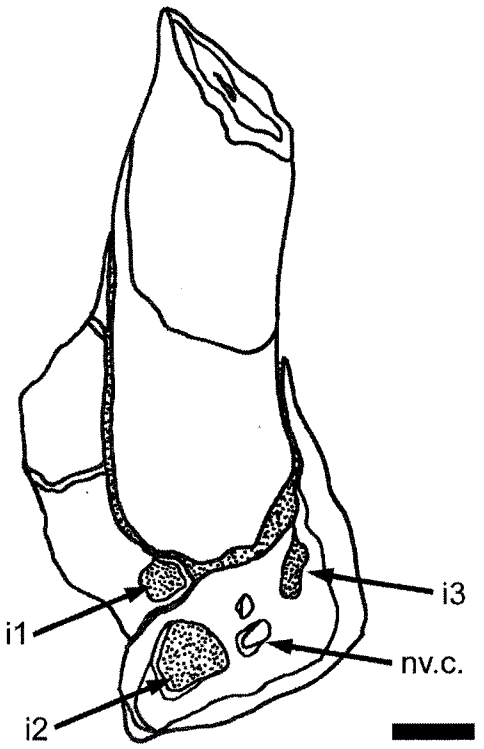
i1
i2
i3
nv.c.

Figure 9.3.—1-24. Arctocyon ferox (Cope) from the early middle Tiffanian (Ti3) DW-2 (DW2) and Birchwood (BW) localities, Paskapoo Formation, Alberta. 1, 2, UALVP 46487 (DW2), left M1 in 1, occlusal and 2, lingual view; 3, 4, UALVP 46488 (DW2), right M2 in 3, occlusal and 4, lingual view; 5, 6, UALVP 46498 (BW), right lower canine in 5, lateral and 6, posterior view; 7-9, UALVP 46490 (DW2), left p1 in 7, labial, 8, lingual, and 9, occlusal view; 10-12, UALVP 46491 (DW2), right p3 in 6, labial, 7, lingual, and 8, occlusal view; 13-15, UALVP 43104 (DW2), associated left p4, m1-3 in 13, labial, 14, lingual, and 15, occlusal view; 16-18, UALVP 46500 (BW), left p4 in 16, labial, 17, lingual, and 18, occlusal view; 19-21, UALVP 46502 (BW), right m2 in 19, labial, 20, lingual, and 21, occlusal view; 22-24, UALVP 46496 (DW2), right m3 in 22, labial, 23, lingual, and 24, occlusal view.

25, 26. Arctocyon corrugatus (Cope) from the early middle Tiffanian (Ti3) DW-2 (DW2) and Birchwood (BW) localities, Paskapoo Formation, Alberta. 25, 26, composite left upper molars including UALVP 46506 (DW2), left M1, UALVP 46509 (BW), left M2, and UALVP 46511 (BW), right M3 (reversed from original) in 25, occlusal and 26, oblique lingual view.

Scale bars = 5mm.

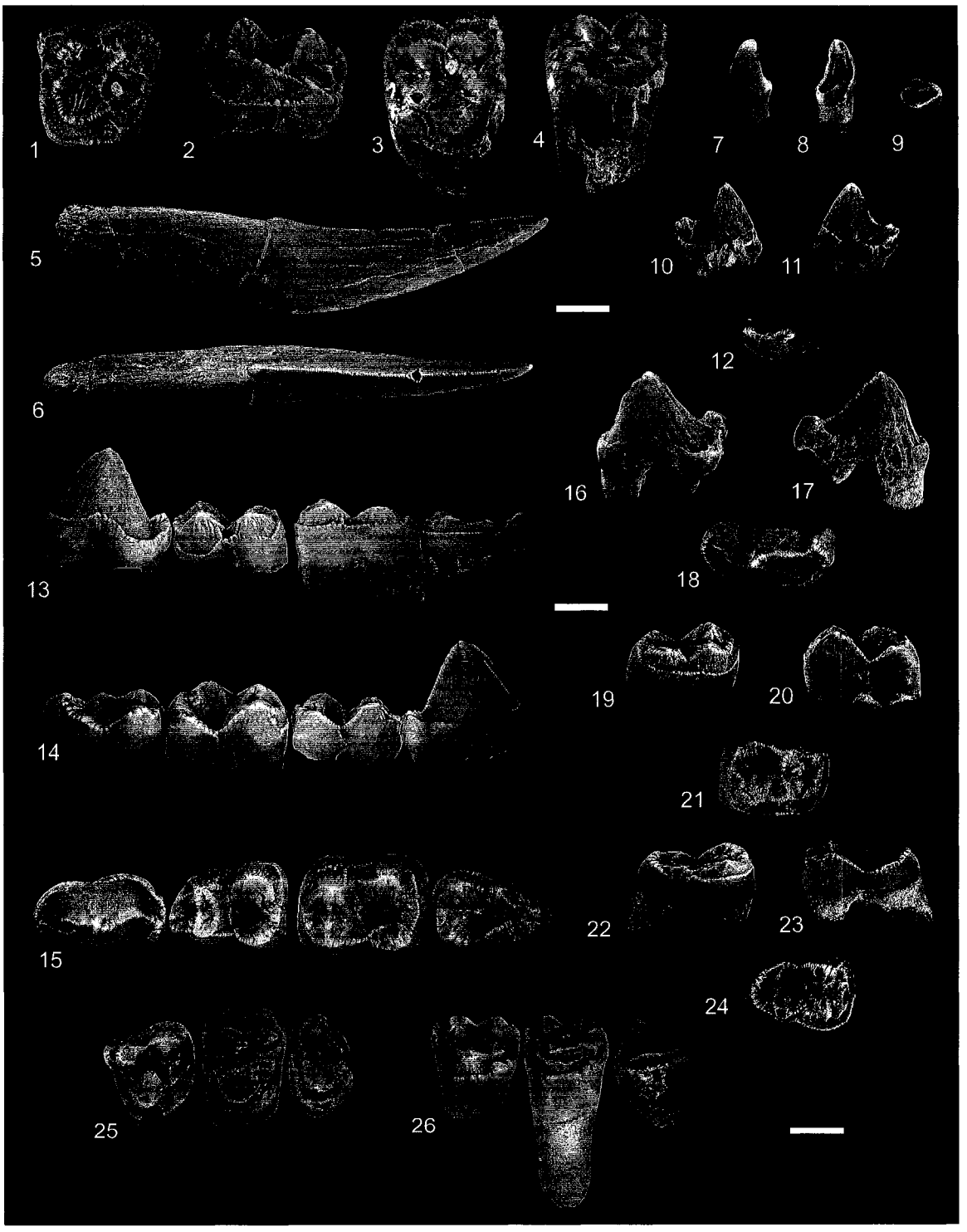
1
2
3
4
7
8
9
5
10
11
6
12
16
17
13
18
14
19
20
21
15
22
23
24
25
26

Figure 9.4.—1-18. Boreocyon gigas new genus and species from the early middle Tiffanian (Ti3) DW-2 (DW2) and Birchwood (BW) localities, Paskapoo Formation, Alberta. 1, 2, composite right upper dentition including UALVP 46512 [holotype, DW2, associated left I1 (reversed from original), right I1-3, right C, right P1-3, left P4 (reversed from original), left M1 (reversed from original), right M3], and UALVP 46602 (BW), right M2 in 1, occlusal and 2, oblique lingual view; 3, 4, UALVP 46529 (BW), left M1 in 3, occlusal and 4, oblique lingual view; 5, 6, UALVP 39225 (BW), left M3 in 5, occlusal and 6, oblique lingual view; 7-9, composite right lower dentition including UALVP 46512 [holotype, DW-2, associated right ?i2, left ?i3 (reversed from original), right lower canine, right p1, right m1-3], UALVP 46522 (DW2), left p2 (reversed from original), UALVP 46530 (BW), left p3 (reversed from original), UALVP 46523 (DW2), left p4 (reversed from original) in 7, labial, 8, lingual, and 9, occlusal view; 10-12, UALVP 46532 (BW), right p4 in 10, labial, 11, lingual, and 12, occlusal view; 13-15, UALVP 46525 (DW2), left m1 in 13, labial, 14, lingual, and 15, occlusal view; 16-18, UALVP 46534 (BW), left m3 in 16, oblique labial, 17, lingual, and 18, occlusal view. Scale bars = 5mm.

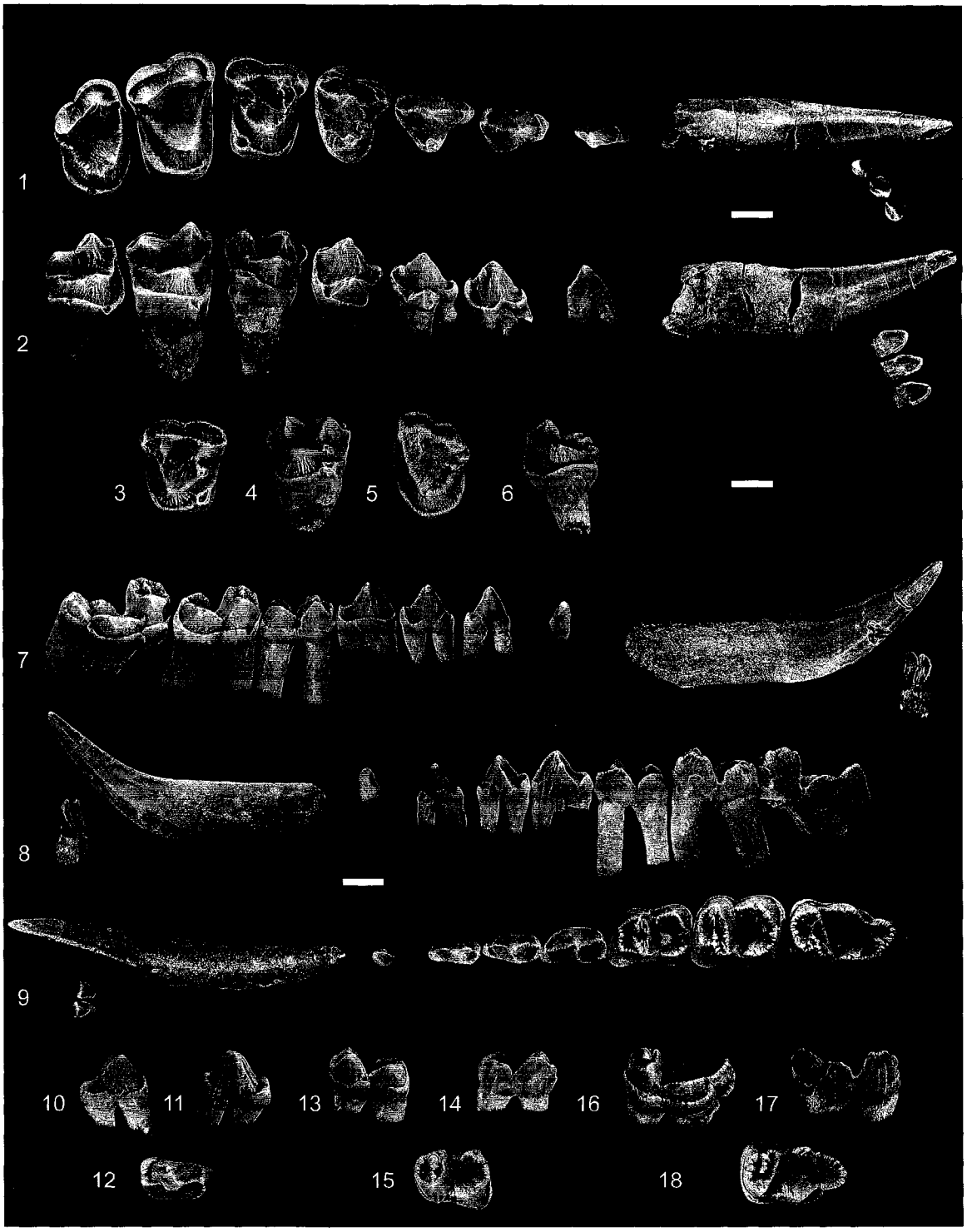
1
2
3
4
5
6
7
8
9
10
11
13
14
16
17
12
15
18

Figure 9.5.—1-10. Boreocyon alpinus new species from the ?late Torrejonian (To3) Diss locality (DS), and the earliest Tiffanian (Ti1) Cochrane 2 (C2), and Dankeshane (DK) localities, Paskapoo Formation, Alberta. 1, 2, UALVP 46540 (DK), left M1 in 1, occlusal and 2, oblique lingual view; 3, 4, UALVP 46535 (holotype, DS), right M1 in 3, occlusal and 4, oblique lingual view; 5-7, UALVP 46536 (C2), left m1 in 5, labial, 6, lingual, and 7, occlusal view; 8-10, UALVP 46537 (C2), right m2 in 8, labial, 9, lingual, and 10, occlusal view.

11-13. Boreocyon augur new species from the middle Torrejonian (To2) Who Nose? locality, Paskapoo Formation, Alberta. UALVP 46173 (holotype), left m3 in 11, labial, 12, lingual, and 13, occlusal view.

14-20. Insidioclaenus mearae new combination from the earliest Tiffanian (Ti1) Aaron's locality (AL), Paskapoo Formation, Alberta, and the early Tiffanian (Ti2) Saddle locality (SL), Fort Union Formation, Wyoming. 14, 15, UCMP 114308 (cast of holotype, SL), incomplete right maxilla with M1-2 in 14, occlusal and 15, oblique lingual view; 16, 17, composite left upper dentition including UALVP 46543 (AL), left M1, UALVP 46545 (AL), left M2, UALVP 46546 (AL), right M3 (reversed from original) in 16, occlusal and 17, oblique lingual view; 18-20, UALVP 46549 (AL), incomplete right dentary with p2-4, m1-3 in 18, labial, 19, lingual, and 20, occlusal view.

21-32. Insidioclaenus praeceps new species from the earliest Tiffanian (Ti1) Cochrane 2 (C2) locality, and the early middle Tiffanian (Ti3) Burbank (BB), DW-2 (DW2), and Birchwood (BW) localities, Paskapoo Formation, Alberta. 21, 22, composite left upper dentition including UALVP 46563 (BB), left P3, M2-3, and associated right P4 (reversed from original) in 21, occlusal and 22, oblique lingual view; 23-24, composite right upper dentition including UALVP 46566 (DW2), left M1 (reversed from original), UALVP 46557 (C2), right M2, UALVP 46560 (C2), right M3 in 23, occlusal and 24, oblique lingual view; 25, 26, UALVP 46552 (holotype, DW2), associated right M1-3 in 25, occlusal and 26, oblique lingual view; 27-29, UALVP 34127 (DW2), incomplete left dentary with p4, m1 in 27, labial, 28, lingual, and 29, occlusal view; 30-32, UALVP 39218 (BW), left p4 in 30, labial, 31, lingual, and 32, occlusal view.

Scale bars = 5mm.

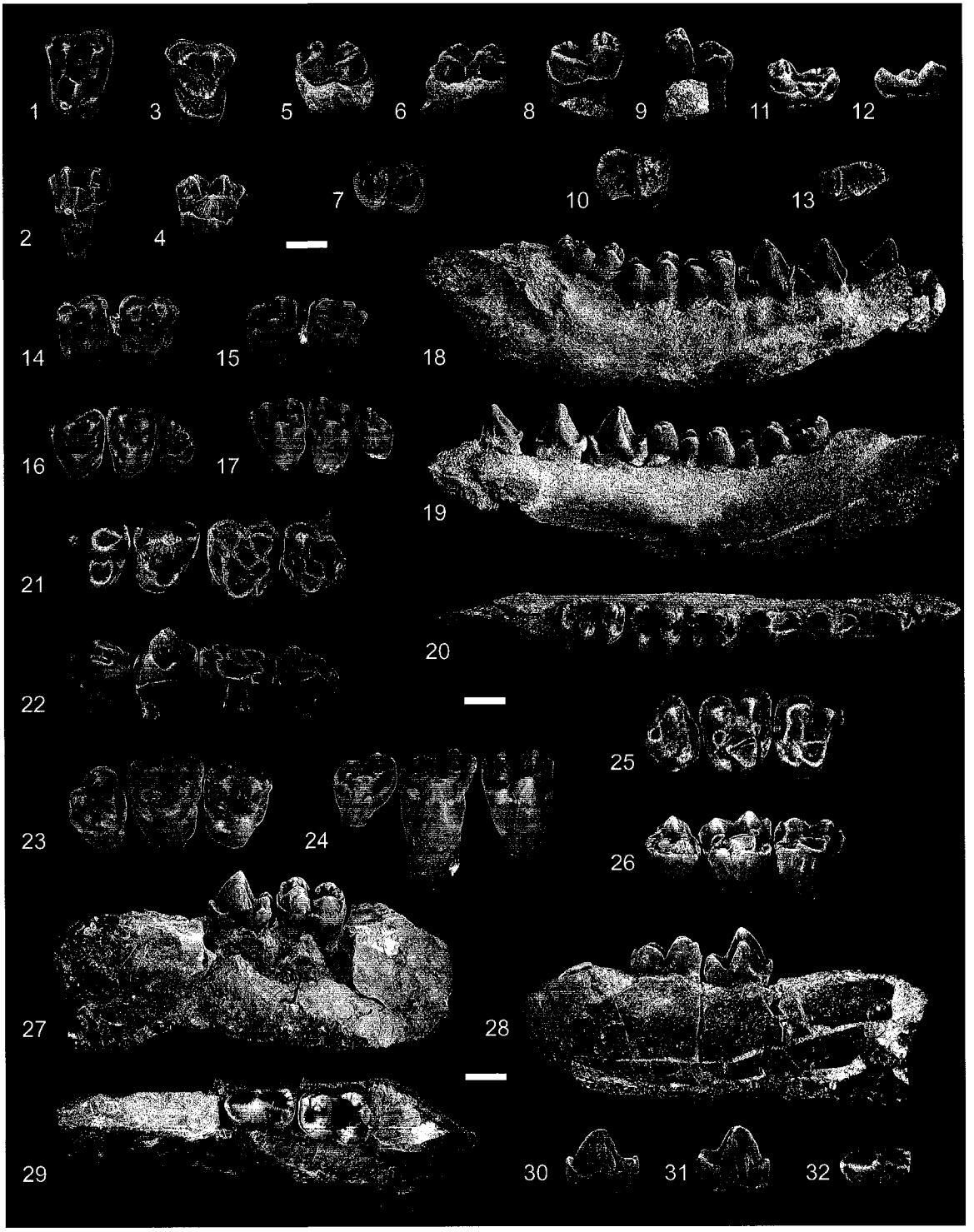
1
3
5
6
8
9
11
12
2
4
7
10
13
14
15
18
16
17
19
21
20
22
25
23
24
26
27
28
29
30
31
32

Figure 9.6.—1-6. Insidioclaenus praeceps new species from the earliest Tiffanian (Ti1) Cochrane 2 (C2) locality, and the early middle Tiffanian (Ti3) DW-2 (DW2) locality, Paskapoo Formation, Alberta. 1-3, UALVP 46561 (C2), right m1 in 1, labial, 2, lingual, and 3, occlusal view; 4-6, UALVP 46570 (DW2), left m2 in 4, labial, 5, lingual, and 6, occlusal view.

7, 8. Desmatoclaenus hermaeus Gazin from the late Puercan (Pu3) Wagonroad locality, North Horn Formation, Utah. 7, 8, USNM 16202 (holotype, in part), left P3-4, M2-3 in 7, occlusal and 8, oblique lingual view.

9-16. Desmatoclaenus paracreodus Gazin from the late Puercan (Pu3) Wagonroad locality, North Horn Formation, Utah. 9, 10, USNM 16177 (paratype), incomplete right maxilla with M2-3 in 9, occlusal and 10, oblique lingual view; 11-13, USNM 16194 (paratype), incomplete left dentary with m2 in 11, labial, 12, lingual, and 13, occlusal view; 14-16, USNM 16196 (paratype), left m2 in 14, labial, 15, lingual, and 16, occlusal view.

17-32. Ectocion sp., cf. E. cedrus from the early middle Tiffanian (Ti3) DW-2 (DW2) and Birchwood (BW) localities, Paskapoo Formation, Alberta. 17, 18, UALVP 39253 (BW), right DP3 in 17, occlusal and 18, oblique lingual view; 19, 20, UALVP 46585 (BW), left P3 in 19, occlusal and 20, oblique lingual view; 21, 22, UALVP 39256 (BW), left DP4 in 21, occlusal and 22, oblique lingual view; 23, 24, UALVP 39260 (BW), left P4 in 23, occlusal and 24, oblique lingual view; 25, 26, UALVP 39242 (BW), left M1 in 25, occlusal and 26, oblique lingual view; 27, 28, UALVP 46577 (DW2), right ?M2 in 27, occlusal and 28, oblique lingual view; 29-30, UALVP 39240 (BW), incomplete right maxilla with M1-2 in 29, occlusal and 30, oblique lingual view; 31, 32, UALVP 39247 (BW), right M3 in 31, occlusal and 32, oblique lingual view.

Scale bars = 5mm.

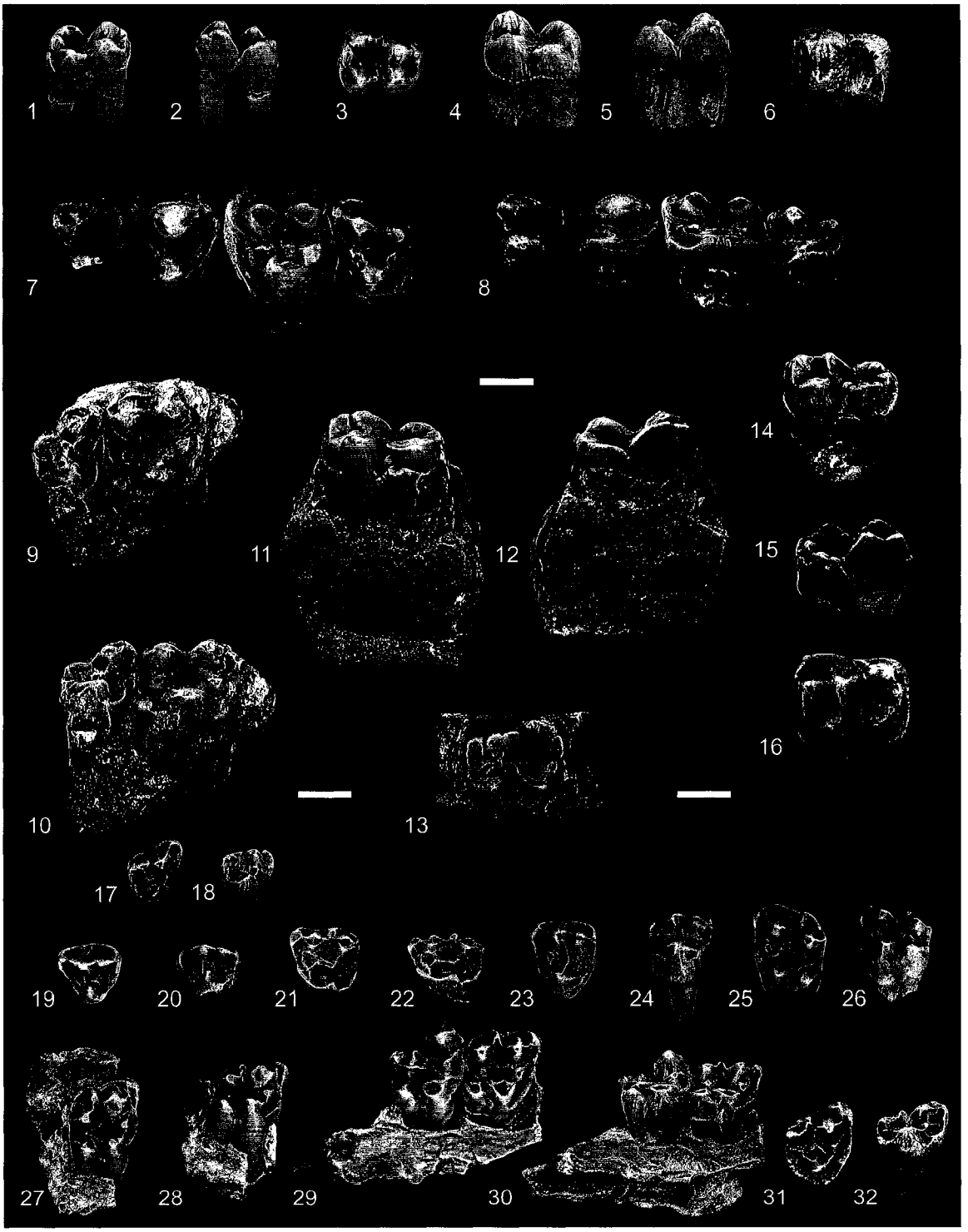
1
2
3
4
5
6
7
8
9
11
12
14
15
10
13
16
17
18
19
20
21
22
23
24
25
26
27
28
29
30
31
32

Figure 9.7.—1-18. Ectocion sp., cf. E. cedrus from the early middle Tiffanian (Ti3) DW-2 (DW2) and Birchwood (BW) localities, Paskapoo Formation, Alberta. 1-3, UALVP 39279 (BW), right p3 in 1, labial, 2, lingual, and 3, occlusal view; 4-6, UALVP 46588 (BW), left dp4 in 4, labial, 5, lingual, and 6, occlusal view; 7-9, UALVP 39284 (BW), right p4 in 7, labial, 8, lingual, and 9, occlusal view; 10-12, UALVP 39262 (BW), incomplete left dentary with dp4, m1-2 in 10, labial, 11, lingual, and 12, occlusal view; 13-15, UALVP 39264 (BW), incomplete right dentary with m2-3 in 13, labial, 14, lingual, and 15, occlusal view; 16-18, UALVP 46881 (DW2), right m3 in 16, labial, 17, lingual, and 18, occlusal view.

19-28. Dissacus sp., cf. D. navajovius (Cope) from the early middle Tiffanian (Ti3) DW-2 (DW2) and Birchwood (BW) localities, Paskapoo Formation, Alberta. 19, 20, UALVP 46590 (DW2), left ?M2 in 19, occlusal and 20, oblique lingual view; 21, 22, UALVP 46591 (DW2), right lower canine in 21, labial and 22, lingual view; 23-25, UALVP 39221 (BW), left p4 in 23, labial, 24, lingual, and 25, occlusal view; 26-28, UALVP 39220 (BW), left m1 or m2 in 26, labial, 27, lingual, and 28, occlusal view.

Scale bars = 5mm.

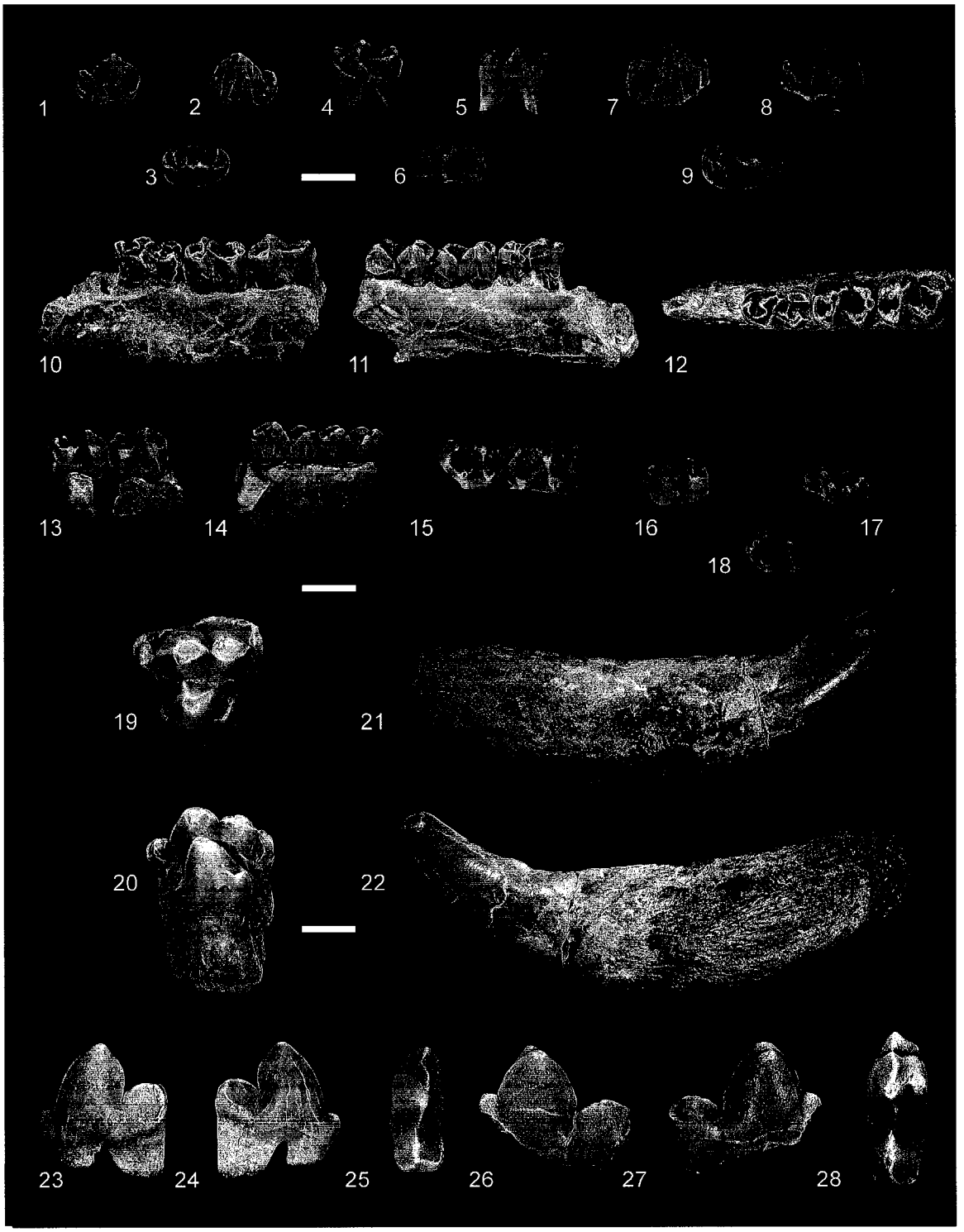
1
2
4
5
7
8
3
6
9
10
11
12
13
14
15
16
17
18
19
21
20
22
23
24
25
26
27
28

Figure 9.8.—Stratigraphic ranges of select hyopsodontid condylarths and Litocherus from western Canada (solid bar) and Montana and Wyoming (hatched bar). Taxa are depicted as ranging from the onset of the earliest zone to the close of the youngest zone in which they have been discovered, but their real extents within these zones are unknown. A thin bar connecting two successive stratigraphic occurrences represents an interval in which taxa have not yet been discovered. Note particularly the absence of hyopsodontid condylarths in western Canada after the earliest Tiffanian (Ti1). Source data in Appendix A.

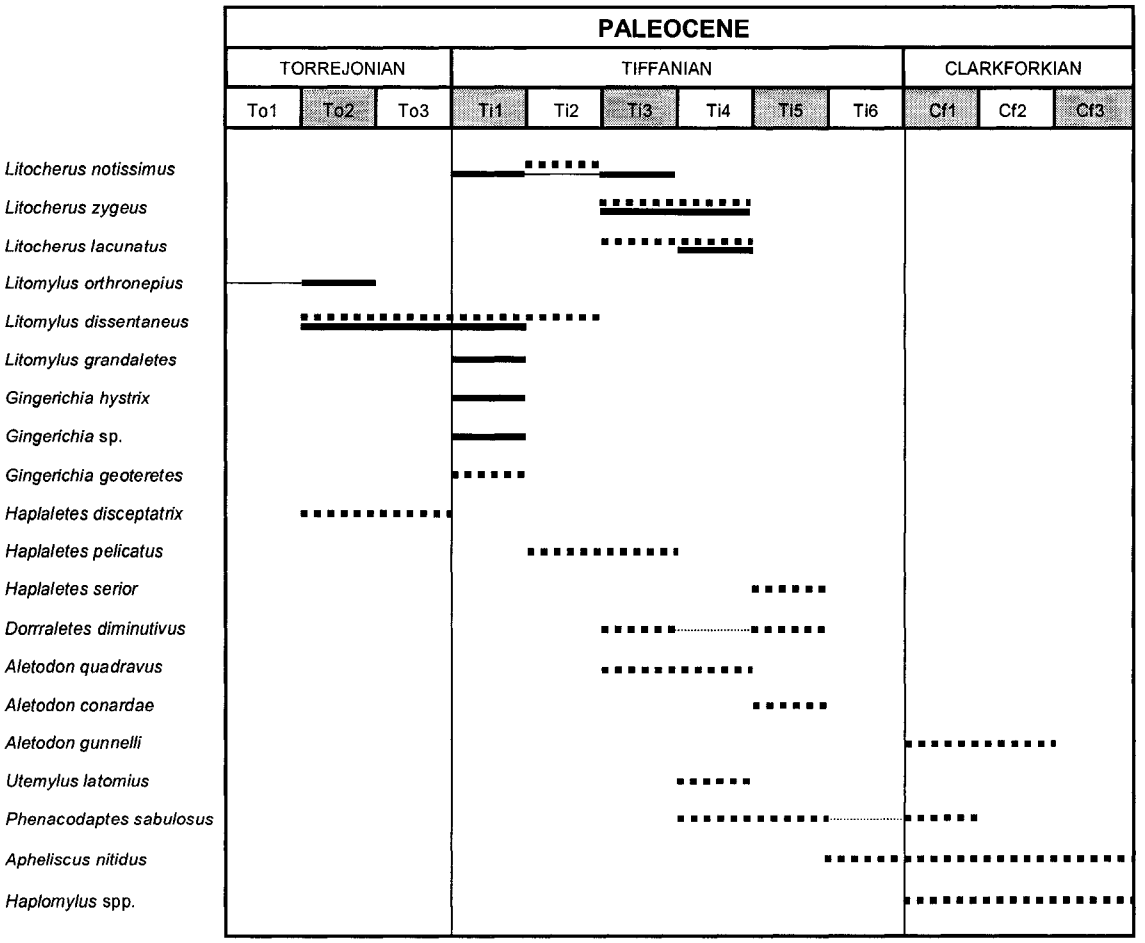
PALEOCENE
TORREJONIAN
TIFFANIAN
CLARKFORKIAN
To1
To2
To3
Ti1
Ti2
Ti3
Ti4
Ti5
Ti6
Cf1
Cf2
Cf3
Litocherus notissimus
Litocherus zygeus
Litocherus lacunatus
Litomylus orthronepius
Litomylus dissentaneus
Litomylus grandaletes
Gingerichia hystrix
Gingerichia sp.
Gingerichia geoteretes
Haplaletes disceptatrix
Haplaletes pelicatus
Haplaletes serior
Dorraletes diminutivus
Aletodon quadravus
Aletodon conardae
Aletodon gunnelli
Utemylus latomius
Phenacodaptes sabulosus
Apheliscus nitidus
Haplomylus spp.

9.5 Appendix 5.—Source data for stratigraphic ranges in Figure 9.8.8. Localities in square brackets represent western Canadian occurrences that are unpublished.

Litocherus notissimus (Simpson)

Ti1: Cochrane 2, [Aaron's locality]

Ti2: Scarritt Quarry

Ti3: Joffre Bridge NE, Joffre Bridge Roadcut lower level, DW-1, DW-2, Mel's Place, Birchwood

References: Simpson, 1936; Gingerich, 1983; Youzwyshyn, 1988; Fox, 1990; Chapter 5

Litocherus zygeus Gingerich (including L. sp., cf. L. zygeus)

Ti3: Joffre Bridge Roadcut lower level, DW-2, Birchwood, Hand Hills West upper level, Judson, Cedar Point Quarry

Ti4: [Swan Hills], [Roche Percée], Brisbane

References: Holtzman, 1978; Rose, 1981; Gingerich, 1983; Fox, 1990; Secord, 2004; Chapter 5

Litocherus lacunatus (Gazin)

Ti3: Chappo Type locality, Circle locality, Battle Mountain

Ti4: [Roche Percée], Titanoides locality, Rock Springs Uplift

References: Gazin, 1956; Dorr, 1958; Winterfeld, 1982; Gingerich, 1983; Fox, 1990

Litomylus orthronepius Johnston and Fox (including L. sp., cf. L. orthronepius)

Pu3: Rav W-1

To2: Who Nose?

References: Johnston and Fox, 1984; Scott, 2003 (identified as Litomylus sp.)

Litomylus dissentaneus Simpson

To2: [Who Nose?], Gidley Quarry

To3: [Nordic Ski Quarry], Rock Bench Quarry, Cedar Mountain localities, Swain Quarry

Ti1: Cochrane 2, [Aaron's locality], Douglass Quarry

Ti2: Ledge locality, Saddle locality

References: Simpson, 1937; Gazin, 1956; Rigby, 1980; Rose, 1981; Krause and Gingerich, 1983; Hartman, 1986; Youzwyshyn, 1988; Fox, 1990

Litomylus grandaletes Scott, Fox, and Youzwyshyn

Ti1: Cochrane 2, [Aaron's locality]

References: Youzwyshyn, 1988; Scott et al., 2002

Gingerichia hystrix Zack, Penkrot, Maas, and Krause

Ti1: Cochrane 2

References: Youzwyshyn, 1988; Zack, Penkrot, Krause, and Maas, 2005

Gingerichia sp.

Ti1: [Cochrane 2]

Gingerichia geoteretes Zack, Penkrot, Krause, and Maas

Ti1: Douglass Quarry

Reference: Zack, Penkrot, Krause, and Maas, 2005

Haplaletes disceptatrix Simpson

To2: Gidley Quarry

To3: Rock Bench Quarry, Halfway Hill, Swain Quarry, Cedar Mountain localities

References: Simpson, 1937; Rigby, 1980; Rose, 1981; Hartman, 1986; Secord, 1998

Haplaletes pelicatus Gazin

Ti2: Saddle locality

Ti3: Twin Creek locality

References: Gazin, 1956

Haplaletes serior Gazin

Ti5: Titanoides locality

References: Gazin, 1956

Dorraletes diminutivus (Dorr)

Ti3: Chappo Type locality, Judson

Ti4: Brisbane, Olive locality

References: Dorr, 1952; Holtzman, 1978; Dorr and Gingerich, 1980; Gingerich, 1983; Gunnell, 1994

Aletodon quadravus Gingerich

Ti3: Battle Mountain, Chappo Type locality, Cedar Point Quarry

Ti4: Brisbane

References: Holtzman, 1978; Rose, 1981; Gingerich, 1983; Gunnell, 1994

Aletodon conardae Winterfeld

Ti5: Rainy Day Resurrection

References: Winterfeld, 1982; Gingerich, 1983

Aletodon gunnelli Gingerich

Clarkforkian: Specimens of A. gunnelli are known from numerous localities in the Clarkforkian (Cf1-Cf3) of Wyoming, summarized in Rose, 1981, and Secord, 2004

Utemylus latomius Gingerich

Ti4: Mason Pocket

References: Gingerich, 1983

Phenacodaptes sabulosus Jepsen

Ti4: Malcolm's locality

Ti5: Princeton Quarry, Schaff Quarry

Clarkforkian: Specimens of P. sabulosus are known from numerous localities in the Clarkforkian (Cf1-Cf3) of Wyoming, summarized in Rose, 1981, and Secord, 2004.

References: Jepsen, 1930; Krishtalka, Black, and Riedel, 1975.

Apheliscus nitidus Simpson

Ti6: UM locality SC191

Clarkforkian: Specimens of A. nitidus are known from numerous localities in the Clarkforkian (Cf1-Cf3) of Wyoming, summarized in Secord, 2004.

Haplomylus spp.

Clarkforkian: Specimens of Haplomylus are known from numerous localities in the Clarkforkian (Cf1-Cf3) of Wyoming, summarized in Rose, 1981 and Secord, 2004.

10 Late Paleocene Pantodonts (Mammalia, Eutheria) from Alberta, Canada, and the Relationships of Cyriacotheriidae Rose and Krause

10.1 Introduction

PANTODONTA ARE a clade of generally large-bodied, heavily built herbivorous or omnivorous eutherians known principally from Laurasian localities of Paleocene and Eocene age. Although the geologically earliest members were probably no larger than the size of a modern opossum (Didelphis Kerr), members of the primarily Eocene family Coryphodontidae may have exceeded 500 kg in weight, approaching the size of living Cape buffalo (Syncerus Hodgson) (see Lucas, 1986; Gingerich, 1989; but see Gingerich, 1990 for contrasting predictions of body mass based on limb bone dimensions). Pantodonts are characterized by having brachydont dentitions, with prominent, V-shaped ectolophs on the upper third and fourth premolars, and dilambdodont molars (i.e., the upper molars bear a W-shaped ectoloph formed by the elongate preparacrista, centrocrista, and postmetacrista, while the lower molars bear a W-shaped ectolophid formed by the paracristid, protocristid, cristid obliqua, and hypocristid; Simons, 1960; Lucas, 1982, 1993) with small conules and weak or undeveloped hypocones. The pantodont skull is low and massive, although small compared to body size, and the postcranium of larger-bodied taxa exhibits graviportal adaptations, with massive, pillar-like limbs, and pentadactyl, hoofed fore- and hindlimbs. While pantodonts rank among the largest mammals that existed during the Paleocene in North America and elsewhere, their fossils are never particularly abundant, and consist more often than not of incomplete teeth and isolated postcranial bones, a fact that has seriously hampered a broader understanding of their early evolution and biogeography.

What little is known about the early evolution of North American Pantodonta is based primarily on a few well-preserved specimens from the Paleocene of New Mexico, Wyoming, Colorado, and North Dakota (e.g., Cope, 1873; Matthew, 1937; Patterson, 1933, 1939; Simons, 1960; Holtzman, 1978; Gingerich and Childress, 1983). Although the pantodont record from western Canada is equally depauperate (see, e.g., reports in Russell, 1948; Fox, 1990; Scott, 2005), two relatively recently discovered specimens

from the early middle Tiffanian (Ti3) Joffre Bridge locality document cranial and postcranial remains of a new genus and species of large titanoideid, and well-preserved specimens of a new genus and species of small cyriacotheriid have been recovered from the Blindman River and Birchwood localities. This chapter describes these, as well as other pantodonts from the late Paleocene of Alberta, Canada. The specimens provide new information on the craniodental and postcranial anatomy of Paleocene titanoideids, including aspects of sexual dimorphism, and provide important new evidence that bears on the relationships of cyriacotheriids, a group of otherwise poorly represented and equally poorly understood small-bodied pantodonts known only from the Western Interior of North America.

10.2 Systematic Paleontology

Class MAMMALIA Linnaeus, 1758
Subclass THERIA Parker and Haswell, 1897
Infraclass EUTHERIA Gill, 1872
Order PANTODONTA Cope, 1873
Superfamily PANTOLAMBDOIDEA (Cope, 1883)
Family TITANOIDEIDAE Patterson, 1934

Comments on pantodont classification.—The ungulate-like features of pantodonts have long been a source of considerable confusion with respect to the taxonomic position of the group, with earlier classifications allying pantodonts with other primitive ungulate or ungulate-like groups (see, e.g., Cope, 1873; Osborn, 1898; Gregory, 1910; Matthew, 1937; Simpson, 1937, 1945; Patterson, 1939; Simons, 1960; Van Valen, 1988). Until relatively recently, most authors have regarded pantodonts either as an order within the Paenungulata (consisting of pantodonts, dinoceratans, proboscideans, hyracoids, sirenians, and pyrotheres) following Simpson (1945), or a suborder within the Amblypoda (consisting of pantodonts, dinoceratans, xenungulatans, and pyrotheres) following Cope (1875). A radical departure from this classification scheme came with McKenna's (1975) cladistic-based classification of Mammalia, in which pantodonts were

placed in the Ferae, closely related to the palaeoryctoid Didelphodus Cope, 1882b (and see Lucas, 1982, 1993, 1998); this hypothesis has been reiterated by McKenna and Bell (1997), with pantodonts, tillodonts (including the enigmatic Deltatherium Cope, 1881), taeniodonts, palaeoryctids, and a number of other seemingly disparate (anatomically and phylogenetically) groups comprising the order Cimolesta (some of these groups were treated in Chapter 5 as members of the Insectivora). As pointed out by Rose (2006), however, evidence for the monophyly of this group is weak, as is evidence for monophyly of Cimolestes Marsh, 1889 itself, the genus central to the concept of Cimolesta (e.g., Fox and Youzwyshyn, 1994). Lucas (1982, 1993, 1998) has repeatedly endorsed a close relationship between pantodonts and didelphodontines (=Cimolestidae of McKenna and Bell, 1997), indicating that characters of the carpus and tarsus that have been traditionally cited as uniting pantodonts with amblypods or paenungulates are primitive [although it is noted here that Szalay (1977) has indicated that the tarsus of putative basal pantodonts like Bemalambda Chow, Chang, Wang, and Ting, 1973 lack the specializations seen in the ankle of other cimolestans; see Rose, 2006). According to Lucas (1993:186), the "...Didelphodontine-pantodont relatedness is predicated on striking dental similarities between the most primitive pantodonts [e.g., bemalambdids] and didelphodontines...", yet acknowledged that dental synapomorphies that would unite pantodonts and didelphodontines are few. While a close relationship between pantodonts and cimolestans cannot be unequivocally rejected, the available evidence in support of this relationship is not persuasive. Clearly if plesiomorphic postcranial features are as uninformative in identifying monophyletic taxa as Lucas (1982, 1993, 1998) maintains, then so too are plesiomorphic dental characters (which are the only characters of "striking similarity" between cimolestans and basal pantodonts). Viewed in this light, pantodonts seem to represent yet another group of early Tertiary mammals having a suite of unusual dental autapomorphies superposed onto an otherwise primitive dentition [e.g., the well-developed ectoloph (derived character) on the transverse upper premolars (primitive) of bemalambdids], and their phylogenetic position seems as uncertain now as it did when Simpson (1945) referred the order to the Paenungulata; as such, Pantodonta are here considered an eutherian order of uncertain higher level affinities.

Genus JOFFRELAMBDA new genus

Type and only known species.—Joffrelambda spivaki new species.

Diagnosis.—As for the type and only species.

Etymology.—Joffre, in reference to the hamlet of Joffre, Alberta; lambda, Greek, in reference to the W-shaped ectolophs of the upper molars, and a common suffix in pantodont generic names.

JOFFRELAMBDA SPIVAKI new species

Figures 10.1-10.8; Tables 10.1, 10.2

cf. Titanoides sp.; FOX, 1990, p. 63.

Diagnosis.—Large titanoideid pantodont (M1 approximately 30% longer than M1 in T. primaevus and T. looki, p3 approximately 20% shorter than in T. major) differing from Titanoides in upper premolars and molars being longer relative to width, and in having smaller, more nearly conical upper and lower canines, with the lower canine lacking a strongly developed posterior blade. Differs further from Titanoides in having upper premolars and molars with a shallower ectoflexus, and upper molars with a weaker (i.e., less labially projecting) centrocrista, a more labially positioned paracone and metacone, and in lacking a strongly flaring metastylar lobe on M1-2. Differs further from Titanoides in lower premolars having better developed talonids, and lower molars that are lower crowned, with better differentiated hypoconulids.

Description.—Upper dentition (Figs. 10.1, 10.3): The upper dentition is best seen in the holotype (UALVP 46592), where all of the teeth but the upper incisors are represented.

Upper canine (♂): Two upper canine coronal anatomies are known for Joffrelambda, and are tentatively interpreted as representing sexual dimorphs. The upper canine crown of the male morph, preserved only in the holotype skull, is large and somewhat elongate anteroposteriorly, but rather than being nearly triangular in cross section (with the medial side virtually flat) as in T. primaevus, the cross section of the

upper canine in T. spivaki is subovate, and in this regard most closely resembles the upper canine in Pantolambda among North American pantodonts. Although the crown is caniniform, with a faintly recurved apex, it is not nearly as elongate or sabre-like as those in species of Titanoides in which this tooth is known. A strong wear facet is developed anteromedially from occlusion with the lower canine.

Upper canine (♀): UALVP 39492, an isolated, partially damaged upper canine from the Birchwood locality (see Webb, 1996) is referred to Joffrelambda, and is tentatively interpreted as representing the upper canine of the female morph. The crown of UALVP 39492 is reduced in size and height, and, like that of the male morph, is not sabre-like. The tooth consists of a single massive cusp and a long, stout root. The crown is slightly compressed laterally, subovate in cross section, and faintly recurved; two prominent crests extend anterodorsally and posterodorsally from the apex, dividing the crown into strongly convex labial and weakly convex lingual sides. A weakly defined lingual cingulum is developed along the base of the crown, but quickly fades away posteriorly. Occlusion with the corresponding lower canine has produced a broad, shallow facet on the anterior side of the crown.

Upper premolars: P1: A diastema is not developed between the upper canine and P1. As in Titanoides, the P1 of Joffrelambda is double rooted, with the roots being anteroposteriorly compressed and stout. The crown is triangular in occlusal outline, and the labial side is indented by a shallow ectoflexus. Most of the topology of the crown has been erased by wear, but the broad V-shaped wear facet suggests the crown bore a well-developed ectoloph, and in this regard probably differed little from the P1 of other pantolambdoid pantodonts. A conspicuous ectocingulum is developed posterolabially but fades away anteriorly; the ectocingulum continues around the posterolabial side of the crown, and extends anterolingually as a low posterior cingulum. A protocone is not developed.

P2-4: The remaining upper premolars closely resemble one another in most aspects of their coronal anatomy, and are most economically described together. The crowns are somewhat triangular in outline, although the deeply emarginated labial margin provides a distinctly Y-shaped outline to the crowns. The crowns are slightly longer labially than lingually, and are wider than long. The angle between the parastylar and

metastylar lobes is narrow on P2 but becomes somewhat wider on P3-4; the ectocingulum is robust on P2-4, low, and continuous labially. Each of the crowns of P2-4 consists of a well-developed, V-shaped ectoloph formed by the tall paracone and sharply defined paraconal cristae, and a low, conical protocone. The ectoloph is better developed on the posterior premolars, with the preparacrista and postparacrista becoming longer and higher from P2 to P4, and the apex of the paracone is tall and sharp. The protocone on each of P2-4 is lower than the paracone, swollen basally, nearly vertical, and the apex is positioned anterior to a line drawn transversely through the deepest part of the ectoflexus. The preprotoconal crista is short, extending labially to a weakly developed paraconule, then continuing as the paracingulum to the parastylar lobe where it joins the ectocingulum; the preprotoconal crista becomes longer and better developed from P2 to P4, being nearly undeveloped on P2, but much more robust on P4. The postprotoconal crista is undeveloped on P2, but a faint crest is developed on P3, and a stronger one on P4. The paraconule is weak but present on P2-4, appearing most often as a small swelling on the preprotoconal crista that is closely appressed to the base of the paracone; the metaconule is undeveloped. The anterior cingulum is low and narrow, extending on P2-3 from the lingual side of the protocone uninterrupted to the parastylar corner of the crown where it unites with the ectocingulum and preparacrista; the anterior cingulum on P4 continues around the lingual side of the protocone where it unites with the posterior cingulum. The posterior cingulum is developed to different degrees on each of P2-4: on P2, it is robust, extending posteriorly from the protoconal apex and forming a low but conspicuous shelf; on P3, the posterior cingulum, while still robust, projects less posteriorly, and the shelf is relatively narrower than that on P2, but still continues to the protoconal apex; and on P4, the posterior cingulum is only slightly better developed than the anterior cingulum, but instead of extending to the protoconal apex as in P2-3, it continues around to the lingual side of the protocone where it unites with the anterior cingulum. The trigon basins on P2-4 are open posteriorly, and slope anteroposteriorly. The enamel on the premolars is weakly wrinkled.

Upper molars: The upper molars of Joffrelambda are similar to those of Titanoides (see, e.g., Simons, 1960; Holtzman, 1978; Gingerich and Childress, 1983), particularly in their increasing size from M1 to M3, in being somewhat anteroposteriorly

elongate relative to their width, and bearing a well-developed W-shaped ectoloph and a labially projecting parastylar lobe.

M1: The crown of M1 is subtriangular in outline, and is only slightly broader than long. A moderately deep ectoflexus divides the labial side of the crown into unequal lobes: the parastylar lobe is anteroposteriorly short and its apex is smoothly rounded, while the metastylar lobe is longer and drawn out posterolabially. The stylar lobes on M1 do not flare anteriorly and posteriorly as they do in Titanoides (compare, e.g., with Simons, 1960, fig. 10; Gingerich and Childress, 1983, fig. 6), and the coronal outline is much closer to that of an isosceles, rather than equilateral triangle. The ectoloph is well developed: the preparacrista and postmetacrista are high, weakly cuspidate (e.g., UALVP 43111, Figs. 10.3.7-10.3.9), and extend to the respective parastylar and metastylar corners of the crown where they join the ectocingulum. The rounded apex of the centrocrista is deflected to the labial margin of the crown, where it forms a faint bulge in the ectocingulum; a cuspidate mesostyle is not developed. The paracone is slightly larger and taller, and more lingually extending than the metacone; both cusps are concave labially. Although the protocone is lower than the paracone, it is considerably more massive, occupying nearly half the width of the crown. The preprotoconal crista is short, extending labially to a weak paraconule, and then continuing as the paracingulum to the anterolabial corner of the crown where it joins the ectocingulum; the postprotoconal crista is longer than the preprotoconal crista, and sweeps posterolabially to the metastylar corner of the crown where it joins the ectocingulum. A metaconule is not developed. The protoconal cingula are heavy and continuous lingually.

M2: The M2 closely resembles M1, differing principally in its larger size and relatively greater width.

M3: M3 differs from M2 in its being of slightly larger size [and in this regard more closely resembles M3 in T. primaevus than in T. gidleyi (compare with Simons, 1960, fig. 10; Gingerich and Childress, 1983, fig. 6)]. The parastylar lobe on M3 is much more pronounced relative to that on M2, and the metacone and metastylar lobe are greatly reduced; the centrocrista is deflected even farther labially, forming a more conspicuous bulge at the labial margin of the crown. As on M1 and M2, a weak

paraconule is developed on M3, and the protoconal cingula are similarly robust and continuous lingually. The upper molar enamel is heavily wrinkled.

Lower dentition (Figs. 10.1, 10.4): The lower dentition of a putative male morph is preserved in its entirety in UALVP 46592 (holotype), although the lower incisors have been worn down to their bases. Two associated incomplete dentaries of a putative female morph are known from DW-2, and although the mandibular rami are badly damaged such that only the teeth could be salvaged, each of the lower dental loci is represented by at least one tooth from the left or right side.

Lower incisors: The holotype mandible preserves three lower incisors on the left and right sides, and although the crowns have been worn flat, the dimensions of their bases indicate that they increase in size from i1 through i3, consistent with the lower incisors of Titanoides and pantolambdoid pantodonts generally (Matthew, 1937; Patterson, 1939; Simons, 1960). Relatively unworn lower incisors are preserved in the female morph (UALVP 46593): the crowns of i1-3 (Li1=7.5, Wi1=5.5; Li2=9.5, Wi2=6.0; Li3=10.7, Wi3=6.5) each support a single anteroposteriorly compressed cusp, with convex anterior and flat posterior sides. A prominent crest extends medially from the apex of the main cusp to a low and poorly differentiated cuspule, while a longer crest extends laterally to the base of the crown; together these crests flank the main cusp and form short medial and longer lateral wings. The medial and lateral crests can continue a short distance along the posterior surface of the crown, forming a low but discontinuous cingulid, and a weak anterior cingulid is present on i1. The enamel on each of i1-3 is slightly wrinkled.

Lower canine (♂): As with the upper canine, two lower canine anatomies are known for Joffrelambda. The lower canine in the holotype mandible (male morph) is large and caniniform, with a tall and posteriorly recurved crown. The lower canine of Joffrelambda differs significantly from that of Titanoides: the crown is subovate in cross section in Joffrelambda, rather than being strongly triangular or D-shaped, and the bladelike anterior and posterior wings that are characteristic of the lower canine of Titanoides are undeveloped in Joffrelambda.

Lower canine (♀): The lower canine of the female morph differs from that of the male morph in size and coronal anatomy. The crown is little enlarged relative to the

postcanine teeth, and approaches the dimensions of the lower canine of females of T. nanus (see Gingerich, 1996). The root is long and stout, subovate in cross section, and curves gently posteroventrally. A shallow, posteroventrally directed groove occurs on the medial side of the root. The crown is low relative to its length, and supports a large, somewhat anteriorly leaning principal cusp and smaller, weakly differentiated anterior and posterior cuspules. Two prominent crests extend anteriorly and posteriorly from the apex of the principal cusp, dividing the crown into strongly convex labial and weakly convex lingual sides. The anterior of these crests extends anterolingually to a low, bladelike basal cuspule, while the posterior crest runs posterolingually to a tiny cuspule near the base of the crown. A cingulid is developed anterolabially and continues around the anterior side of the crown, and then a short distance lingually as a weakly cuspidate cingulid. The enamel of the lower canine is wrinkled.

Lower premolars: The four lower premolars of Joffrelambda increase in size and height from p1 to p4, and each has coarsely wrinkled enamel.

p1: The p1 is two-rooted [a condition in pantodonts known only in titanoideids, some cyriacotheriids (see later in this chapter), and some coryphodontids], with the anterior root nearly vertical and the posterior root curving posteroventrally. The crown of p1 is D-shaped in outline, convex labially and flat lingually, and consists of a large trigonid and a small, single-cusped talonid. The protoconid is the largest and tallest cusp, and is connected to the slightly lower, bladelike paraconid by a short, deeply notched paracristid. The metaconid is developed posterolingual to the protoconid, and is both smaller and shorter than the paraconid. The talonid consists of a low hypoconid that is connected to the metaconid by a short cristid obliqua. Anterior and posterior cingulids are developed, and are continuous labially as a low, weak ectocingulid.

p2: The p2 of Joffrelambda differs from p1 primarily in its larger size and better-developed cusps. The paraconid and metaconid are larger and extend farther lingually than those on p1, particularly the paraconid, which is conspicuously farther lingual than is the metaconid; the paraconid and metaconid are subequal in size, and are anteroposteriorly compressed, forming high blades. The protocristid is widely notched, and a weak metastylid is developed in some specimens. The talonid consists of but a single cusp, the hypoconid, which is better developed than that on p1; a low postcristid

extends from the apex of the hypoconid anterolingually, partially enclosing a shallow talonid basin. The stout cristid obliqua joins the postvallid wall high on the metaconid. The anterior and posterior cingulids are robust and cuspidate, and are continuous labially as a faintly developed ectocingulid; the anterior cingulid wraps around the anterolingual side of the paraconid, jutting lingually as a conspicuous shelf, and a short cuspule can be developed at its lingual extremity.

p3: The p3 of Joffrelambda is larger and the crown slightly higher than that of p2, and whereas the paraconid and metaconid on p2 are subequal in size, the metaconid on p3 is much the larger and more swollen, and is only slightly lower than the protoconid. The paracristid and protocristid are well developed, and together form an acute V-shape in occlusal view. A weak metastylid crest can be present on the postvallid wall. The talonid is longer and wider than on p2, and although the hypoconid is large and distinct, the hypoconulid and entoconid remain undifferentiated from the low and weakly cuspidate postcristid. The cingulids are heavier than those on p2: the anterior cingulid similarly wraps around the anterolingual side of the paraconid, but juts farther lingually than on p2, and the anterolingual cingulid is more prominent; the posterior cingulid is more cuspidate and wider, forming a conspicuous shelf labial of the talonid.

The p4 crown is significantly larger and higher than that of p3, and the cusps are more massive. The metaconid is the dominant trigonid cusp: it is relatively larger than on p3, more swollen and less bladelike, and bears a robust metastylid crest along its posterolingual side. The paracristid and protocristid are heavily worn on all p4s at hand, but these crests were clearly longer and higher than those on p3. The talonid is longer and wider than on p3, and the hypoconid is better differentiated and more labial; a weak entoconid can be developed, but the hypoconulid remains undifferentiated from the postcristid. As on p3, the postcristid (or entocristid, should the entoconid be present) on p4 is low and only weakly developed, leaving the talonid open lingually. The cristid obliqua resembles that on p2 and p3, but joins the talonid in a relatively more labial position. The anterior and posterior cingulids are robust and bear numerous tiny cuspules, and the ectocingulid is stronger than on p3.

Lower molars: The lower molars of Joffrelambda resemble those of Titanoides in being dilambdodont and increasing in size from m1 to m3.

m1: The crown of m1 is both lower and narrower than that of p4, and the trigonid is only slightly elevated above the talonid. The paraconid and metaconid are subequal in size and height, and are connected to one another by a shallowly notched protocristid; although the low paraconid is somewhat anteroposteriorly compressed, it remains distinct from the paracristid, and is situated lingually, with its apex connected to the protoconid by a long, weakly notched paracristid. A thick metastylid crest extends from the posterolingual side of the metaconid to the talonid notch, although the metastylid itself is not developed. The talonid is slightly narrower than the trigonid, and of approximately equal length. A massive hypoconid dominates the talonid, with the hypoconulid small and situated near the posterolingual margin of the crown; neither an entoconid nor an entocristid is developed, and the talonid is open lingually. The cristid obliqua is long and heavy, joining the postvallid wall near the posterolingual extremity of the metaconid, and a slightly shorter hypocristid extends from the hypoconid apex to the hypoconulid. The cristid obliqua and hypocristid form an acute, V-shaped crest in occlusal view that along with the paracristid and protocristid define a well-developed dilambdodont ectolophid. The anterior and posterior cingulids are strongly developed, cuspidate, and unite labially as a faint ectocingulid.

m2: The m2 closely resembles m1, differing mainly in its greater size. The trigonid is similarly low, barely higher than the talonid, and the ectolophid is strongly developed. As on m1, the hypoconulid on m2 is lingually positioned, the entoconid and entocristid are undeveloped, and the talonid is open lingually.

m3: The m3 is the largest of the lower molars, being nearly twice the length of m1. As on m1 and m2, the protoconid and metaconid are subequal in size and height, while the paraconid is low and anteroposteriorly compressed. The talonid is only slightly narrower than the trigonid, and bears large and well-differentiated hypoconid, entoconid, and hypoconulid that together enclose a shallow basin. The hypoconulid differs from that on m3 of Titanoides in being cuspate rather than crest-like (Simons, 1960), and is only slightly lingual of the mid-longitudinal axis of the crown. A tiny entoconulid can occur in the deepest part of the talonid notch, although the entocristid itself is not developed. The cristid obliqua joins the postvallid wall well lingual of the protocristid notch, forming a deep hypoflexid. The ectocingulid on m3 is better developed than on m1 or m2, and

extends posteriorly to the hypoconulid. The enamel on each of the molars is coarsely wrinkled.

Axial skeleton: Skull (Figs. 10.1, 10.2): The anatomy of the skull and postcranium of North American pantodonts is among the best known for any group of Paleocene mammals, despite the comparatively small sample sizes. Among the titanoideids, nearly complete skulls of T. primaevus and T. looki are known from the Tiffanian of Colorado and North Dakota (Patterson, 1939; Holtzman, 1978), and incomplete skulls of T. zeuxis have been reported from the Tiffanian of Texas (Schiebout, 1974). Two incomplete skulls of Joffrelambda are known [UALVP 46592 (holotype) and TMP 2001.25.03], both having been collected from the upper level of the Joffre Bridge Roadcut; of these, UALVP 46592 is the more nearly complete, with the snout of TMP 2001.25.03 having been damaged prior to excavation. Only a brief description of the major features of the skull is provided here; the cranial anatomy of Joffrelambda will be described in greater detail elsewhere (Scott and Fox, in prep.)

Both specimens preserve the skull and mandible. UALVP 46592 is the more informative specimen in that the jaws are abducted, exposing the palate and occlusal surfaces of the upper and lower teeth, whereas the jaws in TMP 2001.25.03 are adducted and the teeth are in tight occlusion. The skull is bilaterally compressed in both specimens, a result of significant post-mortem deformation; the right side of the cranium in both specimens has been shifted slightly anteriorly, distorting the original proportions of the skull and fracturing most of the dermal roofing bones. The basicranium, although likely present, is obscured by the mandible in both specimens. Despite the postmortem deformation, the cranium of Joffrelambda is clearly higher and more vaulted than that of Titanoides (compare with Simons, 1960, fig. 1), and in this regard is more similar to the skull of Pantolambda (see, e.g., Matthew, 1937). The skull bears thick zygomatic arches, well-developed sagittal and occipital crests, and great postorbital length. The narial opening is large and deep, similar to that in T. primaevus and barylambdids; it has been suggested that the size and shape of the narial opening in Titanoides might be indicative of having had a large flexible snout in life (Simons, 1960), and this may have been true of Joffrelambda as well.

The dermal roofing bones are badly damaged in both specimens, and many of the sutures have been obliterated by extensive cracking or co-ossification. The premaxilla is poorly preserved in UALVP 46592, but it is obviously much smaller than the maxilla, and lacks the strong facial process seen in Pantolambda and other pantolambdoideans (Simons, 1960). The maxilla is dorsoventrally deep and anteroposteriorly long, and contributes to the anteroventral rim of the orbit. The depth of the facial process of the maxilla is similar to that in Titanoides and some barylambdids, and is relatively deeper than in Pantolambda (see Matthew, 1937; Patterson, 1935; Simons, 1960). The infraorbital foramen, marking the exit of the infraorbital vessels and infraorbital ramus of the fifth cranial nerve from the infraorbital canal, occurs dorsal to P4, slightly anterodorsal to the anterior root of the zygomatic arch; the foramen is large, subovate, and opens anterolaterally. The position of the infraorbital foramen is similar to that in Titanoides, but farther posterior than in barylambdids and Pantolambda. Bilateral compression of the cranium has distorted the shape and position of the orbit, and although it appears small on both specimens, its exact dimensions cannot be determined. The orbit is delimited dorsally by the anterior parts of the temporal ridge of the frontal, and ventrally by the zygomatic process of the maxilla and the jugal; a postorbital process is not developed, and the extent of the maxillary contribution to the medial wall of the orbit is unknown. A facial exposure of the lacrimal cannot be discerned on either specimen, although the structure has been observed on skulls of Titanoides (see Simons, 1960) and the barylambdid Barylambda faberi (Patterson, 1933, 1935).

The zygomatic arch of Joffrelambda is massive and deep, proportions that have almost certainly been exaggerated by postmortem compression; nonetheless, the arch is much more robust than it is in Titanoides, and it approaches the proportions of the arch on skulls of Barylambda. The anterior root of the zygomatic arch is formed from the stout zygomatic process of the maxilla that originates dorsal to M1 and projects laterally from its base. The jugal is deep, forming the bulk of the middle part of the zygomatic arch; the bone tapers at both ends, anterodorsally towards its contact with the maxilla and posteroventrally to its contact with the zygomatic process of the squamosal. The jugal is overlapped posterolaterally by the deep zygomatic process of the squamosal, but continues below the squamosal to a point just anterior to the glenoid fossa. The

ventrolateral surface of the jugal is rugose and crested for the proximal attachment of the superficial masseter. The anterior parts of the jugal are heavily damaged or otherwise distorted in both specimens.

The nasal extends posteriorly along the dorsal rim of the maxilla, and a conspicuous posterior expansion indents the frontal. The frontal bears a robust temporal ridge anterodorsally, but both specimens are too distorted to trace its progression anteriorly, and the contribution of the frontal to the orbital wall cannot be determined. The temporal ridges extend posteromedially and meet mid-sagittally, forming a robust sagittal crest. The frontoparietal suture is slightly posterior to the union of the temporal ridges, and the majority of the sagittal crest is formed by the parietals. As in Titanoides, the posterodorsal extremities of the frontals of Joffrelambda form a narrow, V-shaped process at their union that is wedged between the anterior parts of the parietals (Simons, 1960).

The parietals and squamosals form the bulk of the posterior skull roof in Joffrelambda. Fusion and extensive cracking have obliterated the parietosquamosal sutures, making it impossible to determine the relative contribution of the parietal and squamosal to the skull roof; in any case, the parietal and squamosal together are extensive, providing a large area of proximal attachment for the temporalis musculature, and the surface of both bones is perforated by large nutritive foramina. The sagittal crest is well developed, especially posteriorly, and a small interparietal separates the parietals posteriorly. The squamosal bears a well-developed zygomatic process that is underlain by the glenoid fossa and robust postglenoid process; the zygomatic process deepens just anterior to the glenoid fossa before tapering anterodorsally along its contact with the jugal. The zygomatic process of the squamosal is deeper than that in Titanoides, with proportions approaching those on skulls of barylambdids (see, e.g., Patterson, 1935). The glenoid fossa is transversely broad and deeply concave, and is directed anteroventrally. Although the medial extent of the glenoid fossa cannot be observed in either specimen, its lateral parts suggest its transverse axis is oriented more nearly perpendicular to the anteroposterior axis of the skull; the orientation of the fossa is similar to that reported by Schiebout (1974) for T. zeuxis, and differs from that in T. primaevus and other pantolambdoideans in which the fossa is oriented more obliquely to the anteroposterior

axis (Simons, 1960). The meatal surface of the squamosal posterior to the postglenoid process is smooth and concave ventrally, forming the dorsal margin of the auditory canal. The mastoid is drawn out as a weak tubercle posterior to the canal, and a discrete stylomastoid foramen cannot be seen on either specimen. A large, subovate condylar foramen is developed slightly anterior to the base of the massive, subspherical occipital condyle.

Although the occiput in both specimens is considerably distorted, obscuring the sutures and damaging the foramen magnum, it is generally similar to that in Titanoides in being low in occipital aspect, semicircular in outline, and was likely directed posterodorsally-anteroventrally such that the posterodorsal tip projected posteriorly past the level of the condyles (Patterson, 1939; Simons, 1960 and contrast with the more nearly vertical occiput in barylambdids). A prominent vertical median crest is developed posteroventral to the interparietal; small pits, ridges, and depressions for insertion of the neck musculature are developed on the occipital surface adjacent to the crest. The occipital crest, formed from at the junction of the occipital and parietal, is high and narrow; the occipital surface of the crest bears heavy rugosities for muscle attachment. The foramen magnum is large, but its exact shape and orientation cannot be determined, and the dorsal atlantal facet is weakly rounded. The occipital condyles are massive and project posteriorly, and their articular surfaces are strongly convex.

Dentary (Figs. 10.1, 10.2, 10.4.13): The dentary of Joffrelambda is best observed in the holotype. The two mandibular rami are clearly co-ossified, and the anterolateral parts bear flanges; these flanges are weaker than those in Titanoides, presumably in correlation with the smaller lower canine root in Joffrelambda. The horizontal ramus is robust and deep, with a slight dorsoventral constriction at the level of the third premolar; a tiny mental foramen opens below p4, slightly posterior to that in T. primaevus (Simons, 1960). The masseteric fossa is shallow, with its anterodorsal extent marked by a thick crest that fades away ventrally, similar to that in Pantolambda (see Matthew, 1937). The coronoid process is steeply inclined from the horizontal ramus, and is taller than that in Titanoides, and more closely resembles the coronoid process on the dentary of Pantolambda cavarictus and barylambdids; the canines in Joffrelambda, Pantolambda, and barylambdids are much smaller than those in Titanoides, and the tall coronoid

process in each of these taxa may have allowed a much narrower gape compared to Titanoides (Simons, 1960). The apex of the coronoid process in Joffrelambda is drawn out as a short, posteriorly directed hook, while its anterior border bears a thick coronoid crest, and the temporalis fossa is moderately excavated. The posterior margin of the coronoid process is deeply excavated, forming a C-shaped emargination that extends from the apex to the high condyle. The condylar process is stout and juts laterally as a conspicuous protuberance that supports the lateral part of the condyle; the medial parts of the condylar process and condyle cannot be directly observed on either specimen, but the exposed articular surface of the condyle is somewhat flattened and slopes dorsomedially-ventrolaterally. The condyle is positioned well above the level of the tooth row. The angular process is drawn out posteroventrally as a rounded process, closely resembling the angular process in Pantolambda cavarictus and barylambdids, and converging on those of many other archaic mammals (e.g., Tillodonta, some phenacodontid condylarths) and modern ungulates (e.g., Tragelaphus de Blainville, equids; see Radinsky, 1985). The expanded angular process possibly correlates with better developed masseter and internal pterygoid musculature, and may also be correlated with the reduced canines and narrower gape of Joffrelambda (Simons, 1960).

Postcranium: TMP 2001.25.03 and UALVP 46592 preserve significant parts of the postcranium, including the scapulae, parts of the fore- and hindlimb, carpus, manus, tarsus, pes, pelvis, and a number of vertebrae. As with the skull, only parts of the postcranium are described here, with the remainder to be described elsewhere (Scott and Fox, in prep.).

Axial skeleton: Cervical vertebrae: Atlas (Fig. 10.2): The atlas of Joffrelambda is preserved in partial articulation with the skull in TMP 2001.25.03: the vertebra has been rotated 180 degrees in the transverse plane and inverted such that the posterior surface is exposed on the left posterolateral side of the skull and the neural arch is in a ventral position. The neural canal is large and O-shaped, and the neural arch is low; a distinct spinous process is not developed. Only the proximal part of the left transverse process is preserved, but its dimensions indicate it was stout but short. The posterior articular facets for the axis are weakly concave and teardrop-shaped in posterior view, with the apices directed ventromedially. The transverse foramen is preserved only on the left side: its

posterior opening is subcircular, while the anterior aperture is crushed. A small part of the anterior articular facet is visible on the left lateral mass, its articular surface being deeply excavated for reception of the massive occipital condyle.

?C4 (Fig. 10.5): A second cervical vertebra, possibly C4, is preserved in TMP 2001.25.03. The vertebra is damaged, with part of the left and entire right transverse process having been removed prior to burial; additionally, a small bone, possibly a carpal, and a large part of a rib adhere to the right side of the neural arch (Fig. 10.6). The centrum has suffered postmortem deformation and is anteroposteriorly compressed and dorsoventrally skewed such that the anterior face is higher than the posterior face. As preserved, the centrum is subovate in anterior view and is anteroposteriorly compressed, more so than are the cervical vertebrae in Titanoides; the anterior articular surface is slightly concave, while the posterior articular surface is deeper and more cuplike. The neural canal is large and the arch is robust, with thick laminae; a weak, low spinous process is present. The prezygapophyses and postzygapophyses are well developed and are supported by stout pedicles: the prezygapophyseal articular surfaces are faintly convex dorsally and slope ventromedially, while those of the postzygapophyses are broader, concave dorsally, and are directed ventrally and slightly laterally. Only the base of the left transverse process is preserved in TMP 2001.25.03: it is anteroposteriorly short and shallow, directed ventrolaterally and slightly posteriorly, and is perforated by the large transverse foramen.

Appendicular skeleton: Ulna (Figs. 10.6.1-10.6.3): TMP 2001.25.03 preserves the right ulna from slightly proximal to the coronoid process to the distal epiphysis. As with other pantodont ulnae, the diaphysis of TMP 2001.25.03 is flattened mediolaterally, and widens, both anteroposteriorly and mediolaterally, towards the distal epiphysis. The olecranon and anconeal processes, and the proximal half of the trochlear notch are missing, but judging from the breadth of the coronoid process, the trochlear notch was wide and well excavated for reception of the large humeral trochlea. The coronoid process is well developed and projects anteromedially from the diaphysis, and the radial notch is shallowly concave for articulation with the expanded radial head (see later in this chapter); heavy vertical ridges are developed along the lateral side of the diaphysis above and below the radial notch, and one of these, the supinator crest, continues along the

anterior edge of the diaphysis distal to the radial notch as a prominent interosseous crest. A shallow brachialis fossa is developed anteromedially, just distal to the coronoid process. The distal epiphysis is well preserved in TMP 2001.25.03: the bone is thick and rugose, convex distally, and bears two conspicuous protuberances, the ulnar head and the styloid process. The ulnar head is developed on the anterodistal margin of the distal epiphysis, just distal to the epiphyseal suture, and faces anterodistally and slightly laterally; the articular surface of the head is ovate in outline and weakly convex for articulation with the sigmoid cavity of the radius. The styloid process is larger and more posterodistal than the ulnar head, and is weakly set off from the distal epiphysis by a faint constriction. The strongly convex articular surface is rotated medially, and is faintly divided into a larger anterior and smaller posterior lobe, presumably for contact with the cuneiform and pisiform, respectively.

Radius (Figs. 10.6.4-10.6.8): The proximal third of the radius is preserved in TMP 2001.25.03; from the head to just distal to the bicipital tuberosity; the radius in UALVP 46592 is preserved in its entirety, and although it is badly eroded, its proximodistal length seems undistorted. The radial head is broad and subovate in proximal outline, and weakly concave on its articular surface, forming a shallow cup for articulation with the humeral capitulum; a weak capitular eminence is present on its anterior surface. A strap-like articular facet is developed posteromedially for articulation with the ulnar radial notch, and the neck is not strongly constricted distal to the head. The bicipital tuberosity is weakly developed. The diaphysis is slender in TMP 2001.25.03, but slightly more robust in UALVP 46592. As with other pantodonts, the radial diaphysis is faintly bowed laterally and widens considerably distally; although the distal epiphysis is preserved in UALVP 46592, it has suffered severe postmortem erosion, with only the shallowly concave lunar facet being well-preserved.

Carpus and manus: Parts of the right manus are preserved in TMP 2001.25.03, including all of the ungual phalanges; a single carpal element, the left unciform, was also recovered. UALVP 46592 preserves the left lunate and metacarpals I-V, and a number of proximal and intermediate phalanges. Fragmentary carpals are preserved in both specimens, but these are severely damaged and are not described here. An isolated magnum (UALVP 46559) from DW-2 is also referred to Joffrelambda.

Lunate (Figs. 10.7.1-10.7.3): The lunate is preserved in UALVP 46592 and closely resembles that described by Simons (1960) for Titanoides primaevus. The radial facet is shallowly convex and extensive, covering much of the proximal surface of the bone. The anterior surface is notably rugose, and the bone is densely pitted with tiny nutritive foramina. There are no discernable facets for articulation with the scaphoid medially or the cuneiform laterally, although a vaguely flattened surface is developed distomedially and possibly represents an area of articulation with the centralar portion of the scaphoid (or with the os centrale should this have been retained as a separate element). The distal surface bears two distinct facets: a long, gutter-like facet for articulation with the magnum is developed medially, and extends to the posterior margin of the bone where it becomes mediolaterally wider and deeper; the second facet is shallowly concave and faces laterally and distally, and represents the area of articulation for the unciform. The posterior surface of the lunate is drawn out posterolaterally as a hook-like process that wraps around the posterior side of the dorsal tubercle of the unciform.

Magnum (Figs. 10.7.4-10.7.6): The magnum of Joffrelambda closely resembles that in Titanoides (Simons, 1960). The distal surface consists principally of an elongate, concave facet for articulation with McIII; the facet is wide posteriorly but narrows anteriorly, and its distolateral extremity bears a small, raised area of smooth bone that probably represents an area of articulation for McIV. A narrow, strip-like facet for McII is developed medially, paralleling a similar but wider facet for McIII; this is in contrast to Titanoides in which the facet for McII is restricted to the distomedial extremity of the magnum (Simons, 1960). The proximal surface of the magnum is drawn out posteriorly as a conspicuous and strongly convex knob for articulation with the lunate; the smooth articular surface of the knob extends anteriorly as a narrow strip. The facet for the unciform extends proximally from the apex of the knob to the distal margin of the bone, but is restricted posterolaterally by a large pit that probably housed a ligament that extended between the magnum and the unciform. The facets for the scaphoid and trapezoid on the medial face of the magnum are only weakly developed. The areal extent of the anterior surface of the magnum is considerably smaller compared to that in Titanoides, and is more nearly rectangular, rather than triangular, in outline.

Unciform (Figs. 10.7.7-10.7.9): The unciform of Joffrelambda is preserved in TMP 2001.25.03 and differs little from that described by Simons (1960) for other pantolambdoideans: the bone is large and wedge-shaped in anterior view, and narrows posteriorly and laterally; the body is drawn out posterodistally as a distinct tubercle. The articular facet for the cuneiform is shallowly concave and faces posterodorsally, while the articular facet for the lunate is slightly convex, similar to that in barylambdids, and is set off from the body of the unciform as a conspicuous knob or tubercle; the lunate facet is much more areally extensive than that in T. looki (see Patterson, 1939). The facet for the magnum extends proximodistally along most of the medial side of the body of the unciform, and a thin, strap-like facet is developed on the distomedial extremity for articulation with McIII. The distal facets are shallowly concave for reception of the proximal articular surfaces of McIV and McV.

Sesamoids (Figs. 10.7.10, 10.7.11): Sesamoid bones have not been documented previously for any species of Titanoides, but nine such bones were recovered with UALVP 46592, as well as numerous isolated sesamoids in the UALVP collections. The sesamoids are somewhat bean-shaped, with a roughened and strongly convex plantar surface, and a smoothly concave articular surface. It is likely the sesamoids are associated with the manus given their occurrence with the carpals, metacarpals, and phalanges in UALVP 46592, and were probably developed at the interphalangeal joints.

Metacarpals (Fig. 10.8): Metacarpals are preserved in both TMP 2001.25.03 and UALVP 46592, although these bones are on the whole poorly preserved, showing significant postmortem distortion; as a result, little more than general descriptions and broad comparisons can be made. TMP 2001.25.03 preserves McI from the left manus and McII from the right manus, while UALVP 46592 preserves McI-V from the left manus. The metacarpals generally are proximodistally short and stout relative to those in Pantolambda, and their proximal and distal extremities are not as mediolaterally broad as those in barylambdids. The proximal epiphysis of McII is more deeply concave than that on McI, and relatively longer; the small facet for articulation with the trapezium (proximolaterally), and larger facet for articulation with McIII (proximomedially) are both slightly concave and subovate in outline. The proximal epiphysis of McIV and McV lacks the deep concavity seen on McII, and bears a flat or slightly convex articular

surface; the proximal articular surface of McV is somewhat expanded mediolaterally, and bears a weak tubercle for the tendon of the extensor carpi ulnaris muscle. A facet for articulation with the cuneiform is not developed on McV. McIII and McIV are subequal in length, suggesting the axis of weight on the manus of Joffrelambda may have been paraxonic, similar to that in Titanoides (see Coombs, 1983).

Phalanges (Fig. 10.8): The proximal phalanges of Joffrelambda are known from both specimens: they are foreshortened but are longer than broad, and slightly longer than comparable phalanges in T. primaevus and T. looki. The proximal articular surface is a shallow, evenly concave fossa that is oriented proximodorsally (as opposed to the more proximally oriented facets of T. primaevus; see Coombs, 1983). The distal trochlea bears stout and convex condyles for articulation with the intermediate phalanx, and the articular surface extends well onto the plantar surface of the phalanx, suggesting that significant plantarflexion at the proximal interphalangeal joint was possible. The proximodorsal surface bears a raised crest that may have functioned in preventing hyperextension at the metacarpophalangeal joint (Coombs, 1983). Weak flexor sheath tubercles are developed distoplantarly.

The intermediate phalanges are shorter than the proximal phalanges, are nearly as broad as long, and are relatively deep at the epiphyses. The proximal articular facet is bisected dorsoplantarly by a weak keel; the shallowly concave facet is deeper dorsoplantarly than it is mediolaterally wide, and is oriented more proximally, rather than proximodorsally. The large condyles of the distal trochlea are separated from one another by a deep notch; the condyles define a semicircle in lateral and medial view, and their articular surfaces extend far onto the dorsal and plantar surfaces of the phalanx, suggesting that a wide range of dorsi- and plantarflexion of the ungual phalanx was possible. A raised crest is developed proximodorsally, similar to that on the proximal phalanx, but this crest is much more prominent on the intermediate phalanges. Robust flexor tubercles are developed plantarly.

The manual ungual phalanges of Joffrelambda, like those in Titanoides, are unique among pantodonts in being massive and claw-like, dorsoplantarly deep and mediolaterally narrow. The dorsal surface is strongly convex in lateral profile, and bears a heavy keel that extends to the plantar surface where it then bifurcates and continues

posteriorly as paired, rugose ridges. The plantar surface is flat, with the exception of a strongly developed ungual tubercle, and the proximal articular facet is deeply excavated for articulation with the trochlea of the intermediate phalanx. Central fissuring is not developed. The dorsal surface of each ungual is rugose and perforated by numerous tiny foramina, suggesting each may have bore a keratinous sheath in life.

Etymology.—Named in honour of Dan Spivak, Royal Tyrrell Museum of Palaeontology, for his contributions to the UALVP collections, and for his role in the discovery and excavation of TMP 2001.03.25.

Holotype.—UALVP 46592, incomplete skull and left and right dentaries, cervical and lumbar vertebrae, left and right scapulae, left radius, left lunate and unciform, left metacarpals I-V, manual sesamoids, pelvis, astragalus, unidentified fragmentary carpals, ribs. Joffre Bridge Roadcut upper level, Paskapoo Formation of Alberta, late Paleocene [early middle Tiffanian, Ti3 (Fox, 1990), Plesiadapis anceps/P. rex Lineage Zone of Lofgren et al., 2004].

Other material examined.—From Joffre Bridge Roadcut upper level: TMP 2001.03.25, incomplete skull and left and right dentaries, with associated atlas, cervical vertebrae, right distal ulna, right proximal radius, left unciform.

From DW-2: UALVP 46593, incomplete associated right and left dentaries with right i1-3, c, p1-4, m1-2, and left c, p2-4, m1-3 (m2 talonid only); UALVP 46888, right proximal radius; UALVP 46559, right magnum.

From Birchwood: UALVP 39492, associated upper left canine, incomplete LP3, incomplete RP4, incomplete left M1 or M2, left and right M3; UALVP 43111, M1; UALVP 39487-88, M3; UALVP 46594, i3; UALVP 46595, 46596, 46597, p4; UALVP 46598, m2 (talonid only).

Age and occurrence.—Early middle Tiffanian (Plesiadapis rex/P. churchilli Lineage Zone, Ti3, late Paleocene) of Alberta.

Discussion.—The taxonomy of titanoideid pantodonts is sorely in need of revision: as few as two, to as many as six species of Titanoides are currently recognized (e.g., Simons, 1960; Gingerich, 1996; and comments by Lucas, 1982), with many of the nominal species based on single specimens (e.g., T. major Simons, 1960). In addition to small sample sizes, sexual dimorphism has been suggested for many pantodont taxa (e.g.,

Simons, 1960, Gingerich and Childress, 1983 for dimorphism in the barylambdid Barylambda churchilli Gingerich and Childress, 1983, and Gingerich, 1996, for dimorphism in T. nanus, and for a brief discussion on dimorphism in Titanoides), further complicating identifications. For the purposes of discussing Joffrelambda, all nominal species of Titanoides, with the exception of T. simpsoni Simons, 1960 (see Gingerich and Childress, 1983), are provisionally recognized here. The teeth of Joffrelambda are closest in size to those of T. major, T. primaevus, and T. looki, but differ from these, as well as from teeth of other species of Titanoides, in a number of important ways, the most obvious of which pertain to the upper and lower canines.

The upper canines of T. looki and T. primaevus are greatly enlarged, elongate, and sabre-like, with the medial surface flat, the posteromedial surface raised as a sharp crest, and the crown being nearly triangular in cross-section. Additionally, the upper canine in these taxa is set off from the body of the maxilla on a laterally projecting flange, possibly to accommodate the enlarged root, and the crown is oriented anterolaterally-posteromedially. In contrast, the upper canine in Joffrelambda is unmodified, being only slightly bilaterally compressed and subovate in cross section, and it is not set off from the body of the maxilla, being more nearly in line with the cheek teeth. As with the upper canines, the lower canines of Joffrelambda and Titanoides show a number of significant differences [the lower canine in T. gidleyi is perhaps the least derived among species of Titanoides where this tooth is known (e.g., YPM 16453, see Secord, 2004), and is the more useful for comparison on that account]. The lower canine crown in T. gidleyi is turgid, with a strongly convex lateral surface and flattened anterior and medial sides; the crown and root are strongly D-shaped in cross section, with the convex side facing externally. The crown is erect and the posterior parts are drawn out as an elongate blade; a second blade is developed anteriorly and medially, and a poorly defined third crest descends from the apex of the principal cusp posteromedially. The crown is somewhat exodaenodont anteriorly, with distinct lobes being developed on the medial and lateral surfaces. In contrast, the lower canine in Joffrelambda possesses none of these features: the crown and root are subconical and not elongate, and neither an anterior nor a posterior blade is developed, and in these regards the tooth more closely resembles the lower canine in Pantolambda. Although the size of the lower canine of

Joffrelambda is more comparable to that in T. nanus among species of Titanoides, it nonetheless differs in its shorter length and in not having a posterior blade.

Although the premolars of Joffrelambda resemble those of Titanoides, they differ in interesting ways. P1 and p1 in Joffrelambda are two-rooted, P2-3 have a well-developed posterior cingulum that is shelf-like and extends to the apex of the protocone, and the protocone is displaced somewhat anterior of the transverse midline of the crown, similar to that in T. primaevus. The upper premolars differ, however, in that the postprotocrista, wholly undeveloped in species of Titanoides, is present on P3 and P4 of Joffrelambda: it is weakly developed on P3, but relatively conspicuous on P4, with the posterior cingulum remaining low and continuing around the lingual side of the protocone, rather than ascending to the protoconal apex. The lower premolars in Joffrelambda are low crowned, with uncompressed trigonids, bladelike paraconids, and strongly developed talonids, contrasting with those in Titanoides in which the trigonids are anteroposteriorly compressed, the paraconids are weaker and less lingually projecting, and the talonids are both shorter and narrower, with more poorly developed basins.

The upper molars of Joffrelambda differ from those of Titanoides in being subquadrate rather than triangular in coronal outline, with weakly flaring para- and metastylar lobes, with the preparacrista and postmetacrista more nearly equal in length, and in having a small but conspicuous paraconule on M1-3; in these regards, the upper molars of Joffrelambda more closely approximate the proportions and coronal anatomy of upper molars in Pantolambda. The lower molars of Joffrelambda resemble those of Titanoides, but are relatively lower crowned and more robust, with uncompressed trigonids, and the m3 bears a conspicuous, cuspate hypoconulid.

Although Joffrelambda is referable to the Titanoideidae, having acquired many of the diagnostic characters of the dentition and skeleton (including, e.g., a two-rooted P1/p1, in having a shelf-like posterior cingulum on at least P2-3, and in having a clawed manus), it is more primitive than Titanoides in most dental characters (as assessed by comparison with teeth of Pantolambda, the most basal North American pantolambdoid pantodont; Matthew, 1937; Simons, 1960), including T. zeuxis and T major, species that are coeval with Joffrelambda, but have yet to be discovered in Canada. Lucas (1998) characterized Titanoides as 1) lacking a postprotocrista on P3-4; 2) in having the

paraconal and metaconal arms of the centrocrista united at a mesostylar cusp; 3) in having greatly enlarged upper and lower canines; 4) an unfused symphysis; 5) a rounded snout; and 6) large body size. Many of Lucas' (1998) characterizations were based on specimens of T. primaevus and T. looki, the two best known species of Titanoides. It is worth noting here that the figures in Lucas (1998) are misleading in that none of the line drawings in fact pertain to Titanoides: figs. 18.3A and C pertain to Pantolambda bathmodon (18.3A from Osborn, 1898 as corrected in Simons, 1960, fig. 2; 18.3C from Matthew, 1937, fig. 38, reversed in Lucas, 1998), while figure 18.3B pertains to Pantolambda cavarictus (18.3B from Matthew, 1937, fig. 43, reversed in Lucas, 1998); additionally, figs. 18.3B-C are originally from Matthew, 1937, not Simons, 1960 as indicated by Lucas (1998). The craniodental evidence in Joffrelambda, however, indicates that many of these features are likely derived or otherwise peculiar to individual species of Titanoides, rather than characterizing the genus or the family as a whole. For example, the teeth of Joffrelambda resemble those of Pantolambda, and by inference are more primitive than those of Titanoides, in having a well-developed postprotocrista on P3-4, a weak molar paraconule, more nearly rectangular upper molar occlusal outlines, and unmodified upper and lower canines; furthermore, the proportions of the zygomatic arch and angular process are more consistent with those structures in Pantolambda than with those of the more derived species of Titanoides. Although Lucas (1982, 1993, 1998) suggests that the presence of a mesostyle (i.e., a discrete cusp) is characteristic of titanoideid upper molars, such a structure has not been described for any species of Titanoides (see, e.g., descriptions of upper molars in Patterson, 1939; Simons, 1960; Holtzman, 1978; Gingerich, 1996); the upper molar centrocrista of Joffrelambda does not bear a mesostyle, but given the lability of this feature in other groups of mammals and the generally poor sample sizes for most of the various species of Titanoides, the presence or absence of this structure is not considered here to be of taxonomic importance.

The discovery of Joffrelambda complicates recent opinions on the systematic position of titanoideids. Lucas' (1982, 1993, 1998) phylogeny unites titanoideids with a clade of Asian pantodonts, the Pantolamdodontidae (including Harpyodus Wang, 1979, Archaeolambda Flerov, 1952, Altilambda Chow and Wang, 1978, Pastoralodon Chow and Qi, 1978, and Pantolambdodon Granger and Gregory, 1934), citing features such as

narrow upper molar trigon basins, the M1 metastylar lobe being longer (i.e., extending further labially) than the parastylar lobe, and in having a clawed manus. Although Joffrelambda possesses clawed unguals and a relatively deep rostrum (the rostrum is known only in Pantolambdodon among pantolambdodontids, see Ding et al., 1987), very few synapomorphies seem to unite titanoideids with pantolambdodontids. For example, the metastylar lobe is not appreciably longer than the parastylar lobe on M1 of Joffrelambda (the metastylar lobe is somewhat more elongate in derived species of Titanoides, but not overly so, see Simons, 1960), and it clearly is not of the proportions seen on M1 of, e.g., Pantolambdodon or Archaeolambda (see Flerov, 1952; Ding et al., 1987; Ting et al., 1996), nor are these molar proportions achieved in any species of Titanoides. Furthermore, the canines and premolars of pantolambdodontids are small, the crowns of the cheek teeth are very high (especially in Altilambda and Archaeolambda, see Flerov, 1952; Chow and Wang, 1978), the premolar and molar paraconids are high and bladelike, and the structure of the molar ectoloph is completely different between the two groups (the centrocrista is deflected labially and is smoothly rounded in titanoideids, forming a loop-like structure that forms a bulge in the ectocingulum, whereas the centrocrista in pantolambdodontids forms an acute angle labially that does not form a bulge, and usually bears a tall, spirelike mesostyle at its labial extremity). These differences, combined with the radical difference in body size between titanoideids and most pantolambdodontids, suggests that a relationship between the two groups is distant at best, and that the closest relatives of titanoideids may be better sought among North American pantolambdoideans.

TITANOIDEIDAE, genus and species indeterminate

Figures 10.9, 10.10

Material examined.—From Joffre Bridge Mammal Site No. 1: UALVP 34124, incomplete right dentary having p3, m2-3, talonid of m1, and alveoli for i3, c, p1-p2.

From DW-2: UALVP 46600, associated incomplete left proximal ulna, left carpus and manus including scaphoid, lunate, trapezium, magnum, unciform, McII, McIII or IV,

proximal part of McV, three proximal phalanges, one intermediate phalanx, sesamoids, plus fragmentary carpals and metacarpals.

Description.—Dentary: The dentary of UALVP 34124 is broken into two main pieces: the more anterior of these pieces preserves a premolar that is identified as p3, while the posterior part contains m2-3. The horizontal ramus is heavy and robust at the symphysis, and a bony flange is developed on the ventrolateral surface adjacent to the alveoli for the lower canine and p1; the flange becomes more prominent posteriorly towards the alveoli for p2. The external flange is less conspicuous than that on the dentary of Pantolambda bathmodon (e.g., Matthew, 1937; Simons, 1960), and more closely resembles that of Joffrelambda (see above). The articulating surface is long and inclined anteriorly at an angle of approximately 45 degrees from horizontal, considerably shallower than in dentaries of T. primaevus (see Simons, 1960). The bone of the symphyseal surface is rugose and bears numerous tuberosities, implying that the articulating surfaces of the two dentaries interdigitated and may have been co-ossified in life, a condition known conclusively only in Joffrelambda and some adult individuals of Titanoides among titanoideids. The horizontal ramus narrows posterior to the symphysis and becomes much more gracile, so much so that the labial walls of the p1 and p2 alveoli form conspicuous bulges on the lateral surface of the dentary; the ramus is narrowest ventral to the alveoli for p1 in the parts preserved, widening again below the posterior root of p2. A faint vertical trough is developed on the lateral surface of the dentary between the canine alveolus and the anterior alveolus of p1; this trough may have accommodated the medial surface of the upper canine while the jaws were in occlusion. A tiny mental foramen is developed anteroventral to the alveolus for i3.

Lower dentition (Figs. 10.9.1-10.9.3): Only the p3, m2-3, and the talonid of m1 are preserved in UALVP 34124, in addition to alveoli for i3, c, and p1-2. The dentary is missing between the preserved premolar and the talonid of m1, resulting in some ambiguity as to the identity of the lone premolar. The tooth is interpreted as p3, rather than p4, for the following reasons:

1) The coronal anatomy most closely resembles that of p3 among titanoideids, especially that of T. zeuxis (e.g., lower and more poorly developed metaconid relative to paraconid, weaker talonid);

2) The anterior and posterior parts of the jaw cannot be joined at matching surfaces, suggesting parts of the dentary between the posterior premolar and m1 talonid are missing;

3) As there are only two sets of alveoli anterior to the premolar, interpreting this tooth as p4, rather than p3, necessitates either loss of p1 or the presence of single-rooted p1 and p2, both unknown among species of Joffrelambda, Titanoides, and pantodonts generally (Simons, 1960, but see Muizon and Marshall, 1992 for descriptions of single-rooted p1 and p2 in the early Paleocene pantodont Alcidedorbignya inopinata Muizon and Marshall, 1992 from the early Paleocene of Bolivia).

Lower incisors: The alveolus for i3 is immediately anterior to that for the lower canine, with the two separated by a thin wall of bone. The alveolus is damaged medially, but the shape and dimensions of the parts of the alveolar wall that remain indicate i3 was a small, shallowly rooted tooth; the orientation of the alveolar wall and disposition of the incomplete aperture suggest i3 stood nearly vertically in its alveolus.

Lower canine: The aperture of the canine alveolus is large and subovate in outline, and the dimensions of the alveolus (L=13.0, W=7.5) approach those of lower canines of the female morph of Joffrelambda, although it seems unlikely the canines in both taxa resembled one another: the canine root in the female morph of Joffrelambda is weakly convex on its medial surface, whereas that in UALVP 34124 is strongly convex (a part of the canine root is preserved in UALVP 34124, confirming its shape, see Fig. 10.9.3); and the lower canine in the female morph of Joffrelambda is directed anteriorly, with a posteroventrally curving root and anteriorly leaning crown; although the crown of the canine is not preserved in UALVP 34124, the alveolar walls suggest the tooth was more nearly vertical and the crown relatively more elongate.

Short diastemata separate the canine, p1, and p2, similar to TMM 41217-1, an incomplete dentary of T. zeuxis from the Black Peaks Formation of Texas (Schiebout, 1974). There are two subcircular alveoli for p1, with the posterior alveolus being the larger of the two.

Lower premolars: p2: The p2 in UALVP 34124 is represented only by its anterior root and posterior alveolus. The anterior root is strongly compressed anteroposteriorly, oriented slightly anterolingually-posterolabially, and is wider than the posterior alveolus.

The posterior alveolus is subovate in outline and is separated from the anterior root of p3 by a thin alveolar wall.

p3: The crown of p3 (L=15.0, W=12.0) is dominated by a large protoconid, a lower metaconid, and a small paraconid. Although the apex of the paraconid has been erased by wear, the shape and position of the facet indicate that it was small and cuspidate, not anteroposteriorly compressed and bladelike as in p3 of Joffrelambda, and its base is more swollen. The talonid consists only of a small labial hypoconid; weaker cuspules are developed lingually, but neither an entoconid nor a hypoconulid are distinct, and the cristid obliqua is poorly developed. Anterior and posterior cingulids are present but are weaker than those in Joffrelambda. The p3 most closely resembles that in T. zeuxis, differing from p3 in other titanoideids in the paraconid being small relative to the metaconid, and in having a weak talonid and poorly developed posterior cingulid.

p4: Only the anterior root and part of the posterior alveolus of p4 are preserved in UALVP 34124. The root is strongly compressed anteroposteriorly, and is oriented more nearly transversely, rather than anterolingually-posterolabially as in p2. The posterior alveolus is short, indicating the posterior root was compressed anteroposteriorly.

Lower molars: The m1 talonid is badly damaged, and little can be said of its anatomy. The talonid is comparable to that on m1 of Joffrelambda in size (m1 of Joffrelambda is reduced relative to m2 and m3, see earlier in this chapter), and the posterior cingulid is weakly developed.

m2: The crown of m2 (L=19.0, TrW=*13.0, TaW=11.5) is subrectangular in outline. The trigonid is badly damaged, with only part of the protoconid remaining. The talonid is relatively shorter than on m2 of Joffrelambda, and the angle of the posterior V of the ectolophid is narrower. The hypoconulid on m2 in UALVP 34124 is crest-like, with numerous cuspules, while the entoconid and entocristid are undeveloped.

m3: The trigonid and talonid of m3 are subequal in length and width, and the crown is subrectangular in outline (L=23.0; TrW=12.5, TaW=11.5). The ectolophid is robust, with the paracristid, protocristid, cristid obliqua, and hypocristid all well developed. Despite the trigonid cusps and crests having been deeply worn, the metaconid was clearly the largest and tallest cusp, followed by the lower protoconid and paraconid; together, the trigonid cusps define a near-equilateral triangle in occlusal outline. The

paraconid apex in UALVP 34124 is significantly lower than that of the metaconid, and is unusual in that it projects strongly anteriorly, as if the entire cusp had been tilted forward at its base. The anterior cingulid is robust and continues around the paraconid as a lingual cingulid. The talonid is relatively shorter than on m3 of Joffrelambda, and the hypoflexid is both shorter and deeper. The hypoconulid is crest-like, rather than cuspidate, and is connected to a conspicuous entoconid by a cuspidate postcristid. An entocristid is not developed, although a small cuspule is developed at the deepest part of the talonid notch. The posterior cingulid is strongly developed, and meets the anterior cingulid along the labial side of the crown as a robust ectocingulid.

An associated left proximal ulna, carpus, and manus recovered from the DW-2 locality are provisionally referred here to Titanoideidae, genus and species indeterminate.

Ulna (Figs. 10.9.4-10.9.6): UALVP 46600 preserves the proximal third of the left ulna, including most of the olecranon process and trochlear notch, as well as the coronoid process, radial notch, and part of the diaphysis. The olecranon process is incomplete proximally, and its original dimensions cannot be accurately inferred from the parts that remain; its posterior surface is heavily rugose at the site of attachment for the triceps musculature. The anconeal process has been broken off, but the dimensions of the parts that remain indicate it likely was not as pronounced as the coronoid process, and the trochlear notch was probably more broadly open proximally than that in Pantolambda (Matthew, 1937). A well-developed, proximodistally oriented brachialis fossa occurs distal to the coronoid process. The radial notch is virtually flat, and a conspicuous supinator crest descends anteroventrally along the lateral side of the shaft to near the anterior margin where it continues distally as a prominent interosseous crest.

Carpus and manus: Lunate (Figs. 10.10.1-10.10.3): The lunate closely resembles that in Joffrelambda, differing only in its smaller size, and in the facet for the magnum being more poorly differentiated from the facet for the centralar portion of the scaphoid (or os centrale).

Magnum (Figs. 10.10.4-10.10.6): The magnum in UALVP 46600 closely resembles that in Joffrelambda, differing mainly in being deeper proximodistally, and in having an anterior surface that is more nearly triangular, rather than rectangular, in outline.

Unciform (Figs. 10.10.7-10.10.9): The unciform in UALVP 46600 is relatively deeper proximodistally than that of Joffrelambda, and the lunate facet is more clearly set off from the body of the unciform. These exceptions notwithstanding, the unciform is closely similar in both taxa.

Metacarpals (Figs. 10.10.12-10.10.23): McII, McIV, and the proximal half of McV are preserved in UALVP 46600, and their anatomies are virtually identical to those in Joffrelambda, differing only in their smaller size and in McV having a more mediolaterally elongate epiphysis and a more strongly developed external tubercle for the extensor carpi ulnaris tendon.

Phalanges (Figs. 10.10.24-10.10.33): Three proximal and two intermediate phalanges are preserved in UALVP 46600. As with the metacarpals, the phalanges in UALVP 46600 are virtually identical to comparable elements in Joffrelambda, and differ only in their smaller size and in the proximal phalanges having better developed flexor sheath tubercles.

Discussion.—The two-rooted p1 suggests that UALVP 34124 is best referred to the Titanoideidae, but the scant material precludes a more precise identification. The referred specimens are closest in size to comparable elements of Titanoides zeuxis among titanoideids, but the possibility that they represent an unusually small female morph of Joffrelambda cannot be unequivocally ruled out. T. zeuxis is known definitively only from the type locality in the Melville Formation of Montana, approximately 1000 ft. (300 m) above Scarritt Quarry and probably correlative with Simpson's Crazy Mountain Locality 13 (Simpson, 1937; Simons, 1960; Gingerich, 1996). Simpson's Locality 13 is the type locality for the plesiadapid primate Plesiadapis rex (see Gingerich, 1996), and would thus be of early middle Tiffanian (Ti3) age (Lofgren et al., 2004). Additional specimens have been referred to T. zeuxis from the DeBeque Formation of Colorado (Simons, 1960), and from the Black Peaks Formation of Texas (Schiebout, 1974). The teeth in UALVP 34124 differ from those of T. zeuxis in having a smaller and differently shaped lower canine (inferred from the dimensions and shape of the alveolus in UALVP 34124), a weaker p3 paraconid and talonid, and in having a strongly anteriorly projecting m3 paraconid, as opposed to the much more nearly vertical m3 paraconid in T. zeuxis. A

more precise referral of these specimens must await recovery of better preserved material than is presently available.

Family PANTOLAMBDIDAE Cope, 1883

Genus CAENOLAMBDA Gazin, 1956

Caenolambda GAZIN, 1956, p. 48.

?CAENOLAMBDA sp.

Figures 10.11.1, 10.11.2

Material examined.—From Burbank: UALVP 46602, isolated right M1 or M2 (L=*11.0; W=*18.2).

Description.—The crown of UALVP 46602 is damaged and is missing the metastylar lobe. The crown is anteroposteriorly short and transversely wide, with the paracone and metacone of subequal size and height, and a shorter but considerably more massive protocone. The parastylar lobe projects strongly labially; the preparacrista is high and sharp, slightly cuspidate, and extends to the labial margin of the crown where it bifurcates, sending a short branch anteriorly to join the paracingulum+ectocingulum, and a second branch an indeterminate distance posteriorly. Although the centrocrista and postmetacrista are damaged, their orientation indicates that the crown of UALVP 46602 was dilambdodont, with a well-developed, W-shaped ectoloph. The protocone is large and subconical. The protoconal cristae are low but well developed: the preprotoconal crista is short, extending only a short distance anterolabially before joining the robust, conical paraconule; the postprotoconal crista is longer, running posterolabially to a poorly differentiated metaconule. The preparaconular crista continues as a robust paracingulum to the anterolabial corner of the crown. The protoconal cingula are well developed, particularly posteriorly: the posterior cingulum is heavy and projects posterolingually as a conspicuous ledge; the anterior cingulum is narrower, and the two cingula unite across the lingual side of the protocone. The enamel is weakly wrinkled.

Discussion.—Although nearly half the size, UALVP 46602 most closely resembles NMC 8870, an incomplete left upper molar from the Paskapoo Formation of western Alberta (Russell, 1948). Russell provisionally referred NMC 8870 to Pantolambda, but noted differences in the shape of the protocone and coronal outline; in his systematic review of the Paleocene Pantodonta, Simons (1960) referred NMC 8870 to Caenolambda based on comparisons with the upper dentition of the then recently described Caenolambda pattersoni (see Jepsen, 1930). UALVP 46602 more closely resembles M1 and M2 of Caenolambda than those of Titanoides in the anterior margin of the crown being straighter and not projecting anteriorly; in having a much better developed paraconule; and in the postprotoconal cingulum being much better developed, extending posterolingually as a ledge.

PANTOLAMBDOIDEA, genus and species indeterminate

Figures 10.11.3-10.11.8

Material examined.—From DW-2: UALVP 46603, P1 (W=7.5); UALVP 46604 (L=14.8; W=11.0), 46605 (W=10.8), P2.

Description.—Three anterior premolars from DW-2 are referred here to an indeterminate pantolambdoid taxon. The P1 (UALVP 46603) is two-rooted, with both roots being anteroposteriorly compressed. The crown of UALVP 46603 is premolariform and bears a large, central paracone; a weak swelling occurs posterolingually, but a distinct protocone is not developed. A high and well-developed preparacrista and postmetacrista extend from the paraconal apex to the anterolabial and posterolabial corners of the crown, and together form a prominent, V-shaped ectoloph; the postmetacrista divides posterolabially, sending one branch posteriorly to join with the posterior cingulum+ectocingulum, and another branch a short distance labially. A deep ectoflexus divides the labial margin of the crown into symmetrical lobes, and the ectocingulum is cuspidate and continuous labially. The anterior and posterior cingula are robust. P2 resembles P1 in having a similarly developed ectoloph, but differs in being larger overall, in having a large protocone supported by a separate lingual root, a deeper ectoflexus, and a heavier ectocingulum.

Discussion.—The referred specimens are much smaller than P1-2 in Joffrelambda spivaki, and are larger than homologous teeth in cyriacotheriids (see later in this chapter). Although P1 is two-rooted, its coronal anatomy differs from that on P1 of titanoideids. The referred P2s are closest to those of Pantolambda, particularly in the weakly developed protocone. A more precise referral of these specimens must obviously await discovery of better preserved material than is presently available.

Family CYRIACOTHERIIDAE Rose and Krause, 1982

Genus PRESBYTERIA new genus

Cyriacotherium; SCOTT, 1997, p. 74A.
Cyriacotherium; FOX, 1990, pp. 61, 67.
Cyriacotherium; SCOTT, 2003, p. 759.
Cyriacotherium; SCOTT, 2005, p. 112A.

Type and only known species.—Presbyteria rhodoptyx new species

Diagnosis.—As for the type and only species.

Etymology.—Persbyteros, Greek, elder, in reference to the earlier occurrence of Presbyteria relative to Cyriacotherium.

PRESBYTERIA RHODOPTYX new species

Figures 10.11.9-10.11.33, 10.12, 10.13; Tables 10.3, 10.4

Cyriacotherium, cf. C. argyreum; FOX, 1990, p.61.
Cyriacotherium sp.; FOX, 1990, p.67.

Diagnosis.—Differs from Cyriacotherium in having incipiently dilambdodont upper posterior premolars and semimolariform lower posterior premolars. Differs further from Cyriacotherium in having weaker molar conules, an undeveloped metastylar lobe on

M3, a well-developed lower molar entoconid, and a more labially positioned lower molar hypoconulid.

Description.—Upper dentition (Figs. 10.11, 10.13): Upper premolars: P1: P1 of Presbyteria is semimolariform, two-rooted, and longer than wide. The crown is expanded lingually and is asymmetrically triangular in outline, with its lingual apex slightly posterior to the transverse midline of the crown. The anterior root is circular in cross section, while the posterior root is anteroposteriorly compressed, wider than the anterior root, and arises from the entire labiolingual width of the crown. The stylar shelf, ectoflexus, and ectocingulum are undeveloped, although a series of irregular cuspules extends across the labial side of the crown. A tall, sharp paracone dominates the biting surface of the crown, its labial side flat and its lingual side swollen; an incipient metacone is developed posterior to the paraconal apex, and its lingual wall is slightly swollen. The paracone and metacone are connate for nearly their entire height, and although the apex of the metacone is worn, it originally was clearly lower than that of the paracone. The parastylar and metastylar crests are high and sharp: the preparacrista divides near the anterolabial corner of the crown, with one branch extending anteriorly to the weak anterior cingulum, and the second crest curving posterolabially and fading away towards the labial margin of the crown. The postmetacrista extends posterolabially to a low but conspicuous metastylar cusp, and then continues to the posterolabial corner of the crown. A distinct protocone is not present, and a short, coarsely cuspidate lingual cingulum is developed on the posterolingual part of the crown.

P2: P2 is three-rooted and the crown is more fully molariform than on P1, with a well-developed paracone, incipient metacone, and low, ill-defined protocone. The posterior root is appressed to, yet separate from the lingual root, and both are stouter than the anterior root. A deep ectoflexus divides the labial side of the crown into well-defined parastylar and metastylar lobes; the protocone is posteriorly positioned and the crown is Y-shaped in occlusal outline. A low ectocingulum supporting irregular cuspules is continuous labially, and with the anterior and posterior cingulum. The paracone and metacone are similar to those on P1: the labial side of both cusps is flat while the lingual side is swollen; the paraconal apex is high and sharp; and the weakly differentiated metacone is developed on the posterior shoulder of the paracone. The preparacrista is

higher, longer, and more robust than on P1, and bears a number of irregularly-sized cuspules; it curves anterolabially and divides, sending one branch posterolabially to join the ectocingulum, and the other branch anteriorly to a low, well-developed parastylar cusp. The postmetacrista runs posterolabially from the metaconal apex to a large metastylar cusp, and then continues on to the posterolabial corner of the crown where it joins the ectocingulum+posterior cingulum; a deep notch separates the metacone and metastylar cusp. Neither paraconule nor metaconule is present. A discrete protocone is not developed, and the lingual side of the crown consists only of a heavy cingulum that supports a series of coarse cuspules. The enamel is weakly wrinkled.

P3: The P3 of Presbyteria is larger and wider than P2, and the crown is Y-shaped in occlusal outline. The tooth is three-rooted as on P2, but the crown is more fully molariform, with the metacone better differentiated and the protocone larger and more cusp-like. The lingual root on P3 is stouter than that on P2, and is further separated from the posterior root. The stylar shelf is wide and the ectoflexus deep, dividing the labial side of the crown into well-defined lobes that are swollen on their labial sides; as on P2, the labial margin of the crown supports a low, cuspidate ectocingulum that is continuous with the paracingulum and metacingulum. The paracone and metacone are connate for most of their height, but their apices are further separated than those on P2, and the two cusps are connected by a shallowly notched centrocrista; the labial side of the paracone and metacone is flat, while the lingual side is more swollen. The preparacrista is high and irregularly cuspidate, and extends to the anterolabial corner of the crown where it divides: the labial branch curves posterolabially and joins the ectocingulum, while the anterior branch is deeply notched, separating the paracone from the conspicuous parastylar cusp. The postmetacrista is variably developed: it is longer and more cuspidate than on P2, and can extend posterolabially, forming a deep notch before climbing to the apex of the large metastylar cusp, and then bifurcating near the posterolabial corner of the crown; alternatively, the metastylar cusp can be weakly developed, and the postmetacrista can extend directly to the posterolabial corner of the crown where it joins with the ectocingulum+metacingulum. The protocone is large and swollen at its base, and a distinct apex is present, rather than a series of cuspules as on P2. The protoconal cristae are well developed and continue labially to the weak conules, then further labially

as the paracingulum and metacingulum. A small but distinct paraconule is developed on the preprotoconal crista slightly anterolabial to the apex of the protocone. The metaconule is variably developed: it is small on UALVP 43107, whereas on UALVP 46608 it is the strongest in a series of small cusps on the postprotoconal crista. Protoconal cingula are not developed, and the enamel is wrinkled.

P4: P4 is considerably wider than long and subtriangular in outline, with the lingual apex directly lingual to the deepest part of the ectoflexus (i.e., the apex is not skewed posteriorly as on P1-2). The crown is almost fully molariform, with the paracone, metacone, and protocone all better differentiated than those on P3. The ectoflexus is deeper and narrower than on P3, with the parastylar and metastylar lobes closely appressed. The stylar shelf is broad, and the low, robust ectocingulum is continuous with the paracingulum and metacingulum. Although the paracone and metacone arise from a common base and are connate for most of their height, their apices are better separated and their lingual sides more swollen than on P3. A short, sharply notched centrocrista joins the apices of the paracone and metacone; the centrocrista is faintly deflected labially at its midpoint, but does not form a W-shaped ectoloph with the preparacrista and postmetacrista as on P4 of Cyriacotherium (i.e., P4 dilambdodonty is only incipiently developed in Presbyteria). The preparacrista and postmetacrista are high and extend far labially; the preparacrista divides as it nears the anterolabial corner of the crown, while the postmetacrista joins with the ectocingulum+metacingulum at the posterolabial corner. The protocone is taller and more nearly conical than on P3, and the protoconal cristae are short, steep, and can develop slit-like notches near their union with the conules. The paraconule is large and inflated, whereas the metaconule can be weakly (e.g., UALVP 43108) or strongly (e.g., UALVP 46609) developed; the internal conular wings are not developed. The protoconal cingula are low and poorly developed, but are continuous lingually.

DP4: UALVP 47053 is identified as a deciduous P4 of Presbyteria on the basis of its small size and similarity to the upper molars in that genus (i.e., the crown is fully molariform and dilambdodont); it differs from the upper molars in that the crown is nearly as long as it is wide, proportions that are similar to those of deciduous P4s of pantolambdoideans generally (Simons, 1960). The crown is subequal in size with P3,

subtriangular in occlusal outline, and is fully molariform, with a well-developed paracone, metacone, protocone, and robust conules. Unlike the permanent P4, the DP4 is fully dilambdodont, with a conspicuous W-shaped ectoloph. The paracone and metacone are crescentic in cross section, with strongly concave labial and convex lingual sides. The preparacrista and postmetacrista are high and bladelike, faintly cuspidate, and sweep towards the anterolabial and posterolabial corners of the crown, respectively. The centrocrista is fully deflected to the labial margin of the crown, forming a weak bulge in the ectocingulum; the centrocrista arms of the W-shaped ectoloph are slightly asymmetrical, with the postparaconal arm being slightly longer than the premetaconal arm. Both conules are strongly developed, subequal in size, and bear robust external wings that continue as the para- and metacingulum to the labial margin of the crown; the internal conular cristae are undeveloped. The protocone is slightly lower than the paracone and metacone, but is more massive, occupying nearly half the width of the crown. As on the molars (see later in this chapter), the protoconal apex of P4 is situated lingual to the level of the centrocrista notch. The protoconal cristae are low, and the protoconal cingula are weak and discontinuous lingually. The enamel on UALVP 47053 is notably thinner than it is on P4 and the upper molars.

Upper molars: M1 or M2: UALVP 46670, an isolated tooth, is the most nearly complete M1 or M2 referable to Presbyteria, and although it resembles M1-2 in Cyriacotherium argyreum, its identity as an M1 or an M2 cannot be determined (size was the major criterion in differentiating M1 from M2 in C. argyreum, see Rose and Krause, 1982). The crown of UALVP 46670 is subtriangular in outline, and the ectoflexus is relatively deep despite the weak bulge formed by the apex of the labially deflected centrocrista. The crown is strongly dilambdodont: the ectoloph formed by the preparacrista, centrocrista, and postmetacrista is high and sharp, and the centrocrista extends labially, disrupting the continuity of the low ectocingulum; the apex of the centrocrista is faintly notched in UALVP 46670. Small, irregularly spaced cuspules are developed on the preparacrista and postmetacrista. The paracone and metacone are widely separated, their lingual sides swollen, and their labial sides concave; the protocone is larger and more inflated than on P4, and the protoconal cristae are short and steep. The conules are considerably larger and more swollen than on P4, and their internal wings are

undeveloped; together, the cusps and conules enclose a deep trigon basin that extends obliquely labially as a narrow trough, similar to upper molars of mixodectids (e.g., Elpidophorus) and plagiomenids (and see Chapter 8). The paracingulum and metacingulum are well developed and join the ectocingulum at the anterolabial and posterolabial corners of the crown. The protoconal cingula are stronger than on P4, but are discontinuous around the lingual side of the protocone. A hypocone is not developed.

M3: The crown of M3 is subtriangular in outline, with well-developed parastylar and greatly reduced metastylar lobes. The ectoloph is strong anteriorly, with the preparacrista projecting as far labially as that on M1-2, and the centrocrista deflected labially and forming a distinct bulge on the labial margin of the crown; the postmetacrista is poorly developed, in keeping with the reduced metastylar lobe. As on the M1 or M2, the centrocrista on M3 is notched at its apex. A low but robust ectocingulum extends along the labial side of the crown, joining the paracingulum and metacingulum. The trigon cusps resemble those on M1 and M2: the paracone and metacone are widely separated, tall, and their apices are acute; the basin-facing sides of the paracone, metacone, and protocone are somewhat swollen; and the protoconal cristae are short and steep, and form V-shaped notches near the bases of the conules. Although both conules are prominent, the paraconule is the larger and more swollen, and the preparaconular crista and postmetaconular crista are continuous with the paracingulum and metacingulum, respectively; a small cuspule is present on the metacingulum posterolabial to the metaconule. The protoconal cingula are low, robust, and discontinuous lingually, and a hypocone is not present. A broad, posteriorly sloping wear facet occurs on the posterior side of the protocone from occlusion with the talonid of the opposing m3.

Dentary: The anterior parts of the dentary of Presbyteria are preserved in UALVP 47049. The horizontal ramus is deep and robust, with the bone becoming significantly thicker at the symphysis. The symphyseal surface is preserved almost in its entirety: it is anteroposteriorly short, extending posteriorly to the level of p1, and is relatively shallow (although there is damage to the dorsalmost parts of the symphysis, the articular surface appears not to have extended much higher than approximately one third the depth of the horizontal ramus). The symphyseal surface is raised above the level of the surrounding bone, and heavy crests delimit its dorsal and ventral margins; the bone is rugose,

suggesting that the opposing horizontal rami interdigitated and were at least tightly sutured, or may have been co-ossified like those in species of Cyriacotherium (Rose and Krause, 1982). Two mental foramina are present: the larger and more anterior foramen is ventral to the p1 alveolus, its circular aperture is deeply set in the horizontal ramus and opens anteriorly, laterally, and slightly dorsally. The more posterior foramen is bisected by a vertical crack that extends between p3 and p4; it is smaller than the more anterior foramen, and its circular aperture opens laterally.

Lower dentition (Figs. 10.12, 10.13): Lower incisors: Three incisor alveoli are preserved in UALVP 47049. Each of the three alveoli is subcircular in outline and opens dorsally, indicating that the incisors were nearly vertically implanted in the jaw, consistent with those described by Rose and Krause (1982) for C. argyreum and C. psamminum. The i1 alveolus is small and shallow, and is positioned near the anterior margin of the ramus, while the i2 alveolus is considerably larger, deeper, and inset slightly medially from the lateral margin of the ramus. The i3 alveolus is smaller than that for i2, and is positioned directly anterior to the lower canine. The dimensions and positions of the incisor alveoli in Presbyteria differ from those in Cyriacotherium: in both species of Cyriacotherium, the lower incisors are nearly in-line anteroposteriorly and increase in size from i1 through i3; in contrast, the lower incisors of Presbyteria retain what is believed to be the primitive arrangement in pantodonts in which i2 is larger than either i1 or i3 (as it is in, e.g., bemalambdids, see Chow et al., 1977).

Lower canine: The lower canine of Presbyteria is represented by two specimens, one of which is in a fragmentary dentary with p2-4. The crown of the lower canine is slightly longer than wide, premolariform, and dominated by a large and swollen protoconid. Two bladelike crests originate at the protoconid apex: one curves anterolingually, becoming more conspicuous as it nears the base of the protoconid, while the second extends posteriorly towards the base of the crown. The paraconid, metaconid, and talonid are undeveloped. A faintly cuspidate anterior cingulid is present, fading away as it rounds the anterior side of the protoconid, and a weak posterolingual cingulid can be developed.

Lower premolars: p1: The p1 of Presbyteria is known only from its alveolus in UALVP 47049. It is single rooted, and judging by the dimensions of the alveolus in UALVP 47049, the p1 was smaller than the lower canine.

p2: The crowns of the lower premolars become increasingly molariform from p2-4. The p2 is two-rooted and premolariform, with a large protoconid, a small, short paraconid, and a weak talonid cusp. The protoconid is swollen labially and nearly flat lingually, and the crown is D-shaped in cross section. A long, prominent paracristid extends anteriorly from the protoconid apex before turning sharply lingually to join the paraconid; the paraconid is low, swollen lingually, and connected to a tiny anterobasal cuspule by a short but robust crest. A metaconid is not developed. The talonid consists of but a single low cusp (?hypoconid) connected to the apex of the protoconid by a long, sharp crest (?cristid obliqua). A thick, cuspidate anterior cingulid is present, but does not continue as an ectocingulid around the labial side of the crown. The enamel is swollen along the ventrolingual margin of the crown, and a low, weakly cuspidate cingulid is developed lingual of the talonid cusp. The enamel is wrinkled.

p3: The p3 is larger and taller than p2, and the crown is more fully molariform, with a large paraconid, a weak metaconid, and a well-developed talonid. As on p2, the protoconid is the largest cusp on the crown, with flat lingual and swollen labial sides. The paraconid is slightly larger, more swollen, and more lingual than it is on p2; a short crest connects the paraconid to a low anterobasal cusp, and a sweeping, bladelike paracristid connects the paraconid to the protoconid apex. The metaconid is poorly differentiated from the posterior shoulder of the protoconid, appearing only as a bulge of enamel at the end of a short protocristid (UALVP 47049). The talonid is short and narrow, weakly basined and open lingually, and bears a large median hypoconid and a smaller posterolingual hypoconulid; a narrow notch separates the two cusps. The cristid obliqua joins the postvallid wall towards the lingual margin of the crown, and can ascend the posterior wall of the metaconid. The anterior cingulid resembles that on p2, but is more robust and coarsely cuspidate.

p4: The p4 of Presbyteria differs from p3 in its larger size, especially its width, and in being more fully molariform, with better-developed trigonid and talonid cusps. The metaconid is the largest and tallest cusp on p4, followed by the slightly lower

protoconid and paraconid. The lingually positioned paraconid is faintly compressed anteroposteriorly, and is connected to the protoconid by a bladelike paracristid that often bears one, or sometimes two, large accessory cusps. A crest running posterolingually from the apex of the paraconid can be developed, forming a short and weak anterolingual cingulid. Both the paracristid and protocristid are higher and longer than those on p3, and the protocristid notch is much deeper. A robust, cuspidate metastylid crest extends from near the apex of the metaconid to the talonid notch. The talonid is considerably better developed than on p3: the hypoconid and hypoconulid are larger and better differentiated; a small entoconid is developed, and can be fully separate from, and lingual to, the hypoconulid, or more poorly differentiated and appressed to the hypoconulid; the hypoconid is further labial, the hypoconulid more medial, and a hypocristid is present; and although the talonid is similarly open lingually, the basin is much deeper. The cristid obliqua joins the postvallid surface lingual to the protocristid notch, and continues far up the posterior wall of the metaconid. A prominent anterior cingulid and weaker posterior cingulid are developed, and the hypoflexid shelf is wide. The enamel is weakly wrinkled.

Lower molars: The m1 and m2 of Presbyteria are known from articulated specimens and isolated teeth; m3 is not yet known. The m2 is slightly longer than m1, but is similar in width. The teeth are relatively high crowned when compared to those of most other North American pantodonts, with tall cusps and robust crests; the paracristid, protocristid, cristid obliqua, and hypocristid are tall and sharp, weakly cuspidate, and together form a prominent, W-shaped ectolophid. The metaconid is the largest and tallest cusp, followed by a slightly lower protoconid and smaller and still lower paraconid; together the trigonid cusps enclose a shallow basin that is open lingually. The protocristid notch is deeply V-shaped, a metastylid is developed on the posterior shoulder of the metaconid, and a thick metastylid crest extends posteriorly to the talonid notch. The talonid cusps are high with acute apices, have swollen basin-facing walls, and together enclose a transversely broad, shallow basin. The hypoconid is the largest talonid cusp, and is connected to the postvallid wall by a sharp cristid obliqua; the cristid obliqua supports a clearly defined mesoconid, and joins the postvallid wall well lingual to the protocristid notch. The hypoconulid is slightly lingual to the mid-longitudinal axis of the crown, and its apex is connected to that of the hypoconid by a long hypocristid; a large

entoconid is developed anterolingual to the hypoconulid, and the two cusps are connected by a sharp postcristid. The entocristid is undeveloped and the talonid is open lingually. Although the anterior and posterior cingulids are strongly developed, they remain discontinuous labially, and the hypoflexid short and deep. The enamel is coarsely wrinkled.

Etymology.—Rhodon, Greek, rose; ptyx, Greek, fold. Named for Dr. Kenneth Rose, Center for Functional Anatomy and Evolution, The Johns Hopkins University School of Medicine, Baltimore, and Dr. David Krause, Department of Anatomical Sciences, Stony Brook University, Stony Brook, in recognition of their contributions to knowledge of cyriacotheriids and mammalian paleontology generally.

Holotype.—UALVP 46606, associated incomplete left and right dentaries, each with p4, m1-2 (Figs. 10.12.8-10.12.13). DW-2 locality, Paskapoo Formation of Alberta, late Paleocene [early middle Tiffanian, Ti3 (Fox, 1990), Plesiadapis anceps/P. rex Lineage Zone of Lofgren et al., 2004].

Other material examined.—From DW-1: UALVP 46607, ?lower canine.

From DW-2: UALVP 43105, P1; UALVP 43106, P2; UALVP 43107, 46608, P3; UALVP 46609, P4; UALVP 47053, DP4; UALVP 46670, M1; UALVP 34128, M3; UALVP 47049, incomplete left dentary with c, p2-4, and alveoli for i1-3, p1, and associated fragmentary lower molars; UALVP 46673, lower canine; UALVP 46671, 46672, m1 or m2.

From Dickson Dam: UALVP 46674, ?p4.

From Birchwood: UALVP 43108, P4; UALVP 39485, M1 or M2; UALVP 46675, 46676, 46677, p4.

Age and occurrence.—Early middle Tiffanian (Plesiadapis rex/P. churchilli Lineage Zone, Ti3, late Paleocene) of Alberta.

10.3 Conclusions

The Systematic Position of Presbyteria

The teeth of Presbyteria resemble those of Cyriacotherium argyreum and C. psamminum, the two nominal species of Cyriacotherium: the dentitions in each species show varying degrees of molarization of the posterior premolars, strong molar dilambdodonty, conspicuous conules, and undeveloped hypocones, features considered diagnostic of cyriacotheriids (Rose and Krause, 1982), and leaving little doubt as to the familial affinity of Presbyteria. The teeth of Presbyteria differ from those of Cyriacotherium in a number of important features, however, with these differences indicating that the former occupies a basal position within Cyriacotheriidae.

Some of the most striking differences between the dentitions of Presbyteria and Cyriacotherium are manifest in the coronal anatomy of the premolars. For example, the parastylar and metastylar lobes on the upper premolars of Presbyteria are large and well differentiated, with a relatively deep ectoflexus developed on each of P2-4, features similar to those in primitive pantodonts (e.g., P1-4 of Pantolambda bathmodon Cope, 1882a, P3-4 of Bemalambda nanhsiungensis Chow, Chang, Wang, and Ting, 1973, and to a lesser extent P3-4 of Alcidedorbignya inopinata Muizon and Marshall, 1992) and to those of Late Cretaceous eutherians generally. The anterior upper premolars of Presbyteria are not molariform, with weakly developed protocones (the protocone is undeveloped on P1 and P2, although a swelling of the lingual cingulum accompanied by a lingual root occurs on P2); in contrast, the upper anterior premolars of Cyriacotherium are more fully molariform, with a better-developed protocone supported by a separate lingual root, including one specimen (PU 18823) in which a separate lingual root is developed on P1. A rudimentary metacone is present on P1-2 of Presbyteria, and although it is more conspicuous on P3-4, it remains connate with the paracone and poorly differentiated; in contrast, the metacone is larger and better separated from the paracone on the upper premolars of C. argyreum and C. psamminum. The protocone on P2-3 of Presbyteria is more posterior (i.e., the lingual apex of the crown is posterior to the mid-transverse axis of the crown), whereas those of C. argyreum and, especially, C. psamminum are more anterior. Differences are also seen in the lower premolars. For example, the p1 of Presbyteria is single-rooted, whereas in Cyriacotherium it is double-rooted (the tooth is variably present in C. argyreum); additionally, the p1 in Presbyteria is slightly smaller than the canine, proportions opposite to those in Cyriacotherium in which

the canine is small and nearer the size of i3. The metaconid and protocristid are undeveloped on p2 and p3 of Presbyteria, but these structures are robust on p2-3 of Cyriacotherium, and the metaconid is lingual of the protoconid, increasing the length of the protocristid. The talonid on p2-3 of Presbyteria supports but a single enlarged cusp, the hypoconid, although a poorly developed hypoconulid is present on p3, and a weak hypoconulid and entoconid can be present on p4; in contrast, the talonids on p2-4 of C. argyreum and C. psamminum are broad and more deeply basined, with multiple talonid cusps developed (especially on p3 and p4, where a conspicuous hypoconulid, entoconid, and sometimes mesoconid are usually present).

Perhaps the most significant differences between the premolars of Presbyteria and other Cyriacotherium relate to dilambdodonty, with this specialization being only incipiently developed in Presbyteria. The centrocrista on P3-P4 of Presbyteria is short and not strongly deflected labially; in contrast, the posterior premolar centrocrista in Cyriacotherium is deflected labially (strongly on P4, and particularly so in C. psamminum, where the centrocrista is nearly identical to that on M1 in bulging into the ectoflexus), and the preparacrista and postmetacrista are longer and higher than in Presbyteria. As a result, the ectoloph on P3-4 of C. argyreum, and especially C. psamminum, is exaggerated relative to that in Presbyteria. The paraconid and paracristid on p3-4 of Presbyteria are low, and the paraconid does not extend to the lingual margin of the crown; in contrast, the paraconid and paracristid are higher in Cyriacotherium, and the paraconid is farther lingual, increasing the length of the paracristid (the anterior arm of the ectolophid). The talonid on p3 and p4 of Presbyteria is narrower than the trigonid, and with the exception of the hypoconid, the talonid cusps are weakly developed; in contrast, the width of the talonid on p3-4 in Cyriacotherium is subequal to that of the trigonid, and the talonid cusps are better developed and well separated from one another. Finally, the cristid obliqua on p3 of Presbyteria is short, extending posteriorly or slightly posterolabially to the weak talonid, the hypocristid is poorly developed or absent, and the p4 hypoconulid is positioned on the mid-longitudinal axis of the crown. Conversely, the cristid obliqua on p3 and p4 of Cyriacotherium is much better developed, extending posterolabially from the postvallid wall to the labially positioned hypoconid, the

hypocristid is higher, and the hypoconulid is lingually positioned, further lengthening the hypocristid.

Differences in the structure of the molars of Presbyteria and Cyriacotherium are also apparent, although they are not as pronounced as those of the premolars. The upper molars of Presbyteria are transverse relative to their length, with a deep ectoflexus that divides the labial side of the crown into distinct lobes; these features are similar to those on M1-2 of basal eutherians (e.g., molars of Cimolestes magnus Clemens and Russell, 1965 and Asioryctes Kielan-Jaworowska, 1975) and primitive pantodonts (e.g., molars of Bemalambda), and differ from the upper molars of Cyriacotherium in which the ectoflexus is shallow and the crowns are long relative to their width. The stylar shelves are narrow on the upper molars of Presbyteria, decreasing the length of the preparacrista and postmetacrista; in contrast, the stylar shelves in Cyriacotherium are wider, and the preparacrista and postmetacrista are much longer; this is especially apparent on M3, where the postmetacrista is very long and extends to the labial margin of the crown. In the lower molars, the paraconid in Cyriacotherium is lingual, and usually projects well past the lingual margin of the metaconid, increasing the length of the paracristid, whereas in Presbyteria the paracristid is more labial and correspondingly shorter. The entoconid is well developed in Presbyteria and the hypoconulid is only slightly lingual of the mid-longitudinal axis of the crown; in contrast, the entoconid is absent or greatly reduced in Cyriacotherium, and the hypoconulid is positioned far lingually, similar to that in molars of other pantolambdoid pantodonts (e.g., molars of Pantolambda bathmodon and Titanoides primaevus), greatly increasing the length of the hypocristid.

Other minor features of the dentition of Presbyteria differ from those in Cyriacotherium. The lower incisors of Presbyteria (known only from their alveoli) differ from those of Cyriacotherium in their relative size: in Presbyteria, i2 is the largest of the lower incisors, while those in C. argyreum and C. psamminum increase in size from i1 through i3. The large size of i2 relative to i1 and i3 in Presbyteria may be primitive for Pantodonta, as similar incisor proportions have been documented in the bemalambdids Bemalambda (see Chow et al., 1977) and Hypsilolambda (see Wang, 1975), both considered to be among the most basal pantodonts (Chow et al., 1977; Rose and Krause,

1982; McKenna and Bell, 1997). The lower canine is considerably larger than i3 in Presbyteria, whereas in C. argyreum it is subequal, and smaller than i3 in C. psamminum.

The dentition of Presbyteria displays the plesiomorphic condition of virtually every character examined, a conclusion in agreement with the earlier age of the Blindman River and Birchwood localities (Ti3) relative to the type localities of C. argyreum (late middle to late Tiffanian, Ti4-5) and C. psamminum (latest Tiffanian/early Clarkforkian, Ti6-Cf1).

The Phylogenetic Relationships of Cyriacotheriidae

In the time since their discovery in sediments of the Fort Union Formation of the northern Bighorn Basin of Wyoming, the systematic position of the Cyriacotheriidae continues to be controversial. Although the pantodont affinities of cyriacotheriids were long suspected (McKenna, 1972), it was not until Rose and Krause's (1982) description of Cyriacotherium that these were formalized; agreement on cyriacotheriids as pantodonts has been far from unanimous, however, with other authors suggesting that the phylogenetic affinities of the "Sunday beast" are more likely to be with dermopterans (e.g., Lucas, 1982, 1998; Secord, 2004). The discovery of Presbyteria and the recognition that Cyriacotherium represents a highly derived cyriacotheriid bears on this debate, and offers insight into the relationships of the family to other pantodonts.

Comparisons using either of the two living genera of dermopterans (Galeopithecus Pallas and Cynocephalus Boddaert) are complicated by their highly autapomorphic dentition (Stafford and Szalay, 2000). The fossil record of Dermoptera (sensu stricto) is restricted to Dermotherium major Ducrocq, Buffetaut, Buffetaut-Tong, Jaeger, Jongkanjanasoontorn, and Suteethorn, 1992 from the Eocene of Thailand, and offers little in the way of information beyond that already known for extant dermopterans. The Plagiomenidae, a group of Paleocene-Eocene, dermopteran-like eutherians have been frequently classified with Dermoptera (see, e.g., Matthew, 1918; Rose, 1975; Rose and Simons, 1977; McKenna and Bell, 1997) and have been allied previously with Cyriacotherium (e.g., Lucas, 1998; Secord, 2004); plagiomenids differ significantly from cyriacotheriids and dermopterans (contra Lucas, 1998), however (e.g.,

plagiomenid teeth are characterized by having hypertrophied stylar cusps, non- or weakly dilambdodont upper molars, bilobed lower incisors that decrease in size from i1 to i3, anteriorly skewed lingual cusps on the upper and lower molars, weak, centrally positioned hypoconulids; furthermore, the basicrania of plagiomenids and dermopterans are not similar; see MacPhee et al., 1989) and they are not considered further here. Rose and Krause (1982) pointed out the most salient differences between Cyriacotherium and living dermopterans, including important differences in the structure of the incisors and position of the cristid obliqua on the molar postvallid wall. In his critique of Rose and Krause's (1982) conclusions regarding the systematic position of Cyriacotheriidae, Lucas (1982, 1998) posited a number of characters that he believed distinguished dermopterans, including Cyriacotherium, from pantodonts; the dentition of Presbyteria, however, displays none of these characters, and suggests that the similarities advanced by Lucas (1982, 1998) as indicative of a special relationship between cyriacotheriids and dermopterans are probably convergent. For example, Lucas (1982, 1998) emphasized that unlike the premolars of pantodonts, but like those of dermopterans, the premolars of cyriacotheriids are molariform, and that the upper premolars lacked a V-shaped ectoloph (a V-shaped ectoloph on the upper premolars is considered a synapomorphy of Pantodonta, fide Lucas, 1982, 1993, 1998); while these observations are true of Cyriacotherium, only the P4 and p4 of Presbyteria are molariform (and even then only weakly so, with the P4 metacone connate with and weakly separated from the paracone, and the p4 talonid considerably narrower than the trigonid), whereas the anterior premolars are non-molariform, and the upper premolars support either a V-shaped ectoloph (P1-2) or an incipiently dilambdodont ectoloph (P3-4). Lucas (1982) pointed out that the upper molars of Cyriacotherium resemble those of dermopterans in that each of the arms of the W-shaped ectoloph projects far labially; the ectoloph on the upper molars of Presbyteria, however, projects much less labially, and the centrocrista arms of the ectoloph (the postparacrista and premetacrista) are slightly shorter than the preparacrista and postmetacrista. In contrast to Cyriacotherium and dermopterans, the metastylar lobe on M3 of Presbyteria is virtually undeveloped, as in other pantodonts, and the conules are significantly smaller. In total, the dental anatomy of Presbyteria (a primitive rather than derived cyriacotheriid) strongly indicates that the dermopteran-like

features in Cyriacotherium were developed within the evolutionary history of the family, and are not indicative of a special relationship with dermopterans.

The strong dilambdodonty and molarization of the posterior premolars prompted Rose and Krause (1982) to consider a number of divergent eutherian groups as potential near-cyriacotheriid relatives. As Rose and Krause (1982) have indicated previously, dilambdodonty and molariform premolars have arisen independently in many mammalian groups (e.g., meniscotheriine phenacodontids, hyracoids, nyctitheriid soricomorphs), and that the teeth of pantolambdoid pantodonts bear closest similarity to the cyriacotheriid dentition. Rose and Krause (1982) argued for derivation of Cyriacotherium from a Pantolambda-like ancestor, citing important similarities in the structure of the ectoloph, the absence of molar hypocones, strongly dilambdodont lower molars having a lingual hypoconulid and greatly reduced or absent entoconid, and molarization of the posterior lower premolars. Consequently, Cyriacotherium was classified as a pantolambdoid pantodont in a separate family, Cyriacotheriidae, an opinion that has since been followed by most authors (e.g., McKenna and Bell, 1997). Although the dentition of Presbyteria supports inclusion of the Cyriacotheriidae in Pantodonta, the relationships of the family to other pantodonts are more complicated, particularly since both C. argyreum and C. psamminum can now be viewed as derived members of the family. A comparison of the teeth of Presbyteria with those of Pantolambda (the most basal North American pantolambdoid) reveals the following:

1) The anterior lower premolars of Presbyteria are even less molariform than those of Pantolambda: the metaconid is undeveloped on p2, and is only rudimentary on p3; the talonid consists of but one cusp on p2, and the talonid on p3 is relatively smaller and less molarized than in Pantolambda. Clearly, if the acquisition of a metaconid (and protocristid) on p2 and p3 occurred independently in cyriacotheriids and Pantolambda, then Cyriacotheriidae must have an ancestry that precedes Pantolambda (i.e., if cyriacotheriids were to have been derived from a post-Pantolambda pantolambdoid, the metaconid on p1-3 would have to have been suppressed in Presbyteria, then reacquired in later species of Cyriacotherium);

2) The upper premolars of Presbyteria are incipiently dilambdodont, with the paracone and metacone connate and only slightly separate at their apices; the

preparacrista and postmetacrista are otherwise well developed, and closely resemble the ectoloph on upper premolars of Pantolambda. It seems, then, that the dilambdodont condition of the cyriacotheriid upper premolars may have been derived from a condition in which the upper premolars bore an ectoloph (as in Pantolambda and other pantodonts), with an incipient metacone first appearing on P1-4 of Presbyteria and becoming increasingly better developed in C. argyreum and C. psamminum. The well-developed protoconal cristae that are characteristic of most pantolambdoid pantodonts are already present in Presbyteria.

3) The lower molar entoconid in Presbyteria is large, being subequal to or marginally smaller than the hypoconulid, and the hypoconulid is only slightly lingual of the mid-longitudinal axis of the crown; this differs from the condition in Pantolambda in which the hypoconulid is at the lingual margin of the talonid and reduced in size, while the entoconid is vestigial (Pantolambda bathmodon) or wholly absent (Pantolambda cavarictus) (see Matthew, 1937; Simons, 1960). The size and position of the molar hypoconulid and entoconid in Pantolambda are already derived relative to those structures in more primitive pantodonts (compare, e.g., with the molar hypoconulid and entoconid in Alcidedorbignya and Hypsilolambda), suggesting that should Presbyteria have been derived from a Pantolambda-like ancestor, a suite of reversals would have to have occurred between Pantolambda (entoconid reduced or absent, hypoconulid lingual), Presbyteria (entoconid greatly increased in size and height, hypoconulid shifted to a more labial position), and more derived species of Cyriacotherium (entoconid again having been greatly reduced, hypoconulid again having been shifted to the lingual margin of the talonid).

The preceding comparisons suggest that rather than having been derived from a Pantolambda-like ancestor, cyriacotheriids were more likely derived from a generalized pantolambdoidean in which the premolars were only weakly molariform (i.e., the lower premolar paraconids and talonids were less well-developed than those in Pantolambda, and the upper premolars probably bore a well-developed, V-shaped ectoloph), and that dilambdodonty in the lower molars was incomplete posteriorly, with the hypoconulid in a more labial position (and with the hypocristid correspondingly shorter) and the entoconid fully developed. Although it is noteworthy that Presbyteria shares a number of these

dental characters with the Asian pastorolambdid Altilambda tenuis (e.g., well-developed molar entoconid, hypoconulid more labially positioned, see Wang, 1993; Wang et al., 1992), these features are very likely plesiomorphic for Pantodonta, and are outnumbered by contradictory characters (e.g., the postcanine teeth in Altilambda are hypsodont, the upper molars are very long relative to their width, and the lower postcanine teeth lack anterior and posterior cingulids).

The preceding comparisons further suggest that much of the early evolutionary history of Cyriacotheriidae has yet to be discovered. Although the earliest definitive record of Presbyteria is early middle Tiffanian, isolated teeth from the earliest Tiffanian (Ti1) Aaron's locality (Fox, 1990; Scott, 2005) and the middle Torrejonian (To2) Who Nose? Locality (Scott, 1997, 2003, 2005), both from south central Alberta, indicate that Presbyteria or a Presbyteria-like cyriacotheriid was already present in the earlier parts of the Paleocene of North America. Pantodont fossils have yet to be discovered in sediments older than middle Torrejonian in North America, and the ages of the South American and East Asian pantodont-bearing localities are contentious, with estimates ranging anywhere from Puercan through early Tiffanian (see Lofgren et al., 2004 and references therein). The age of the pantodont-bearing sequence in South America, the Santa Lucia Formation, is controversial (see the contrasting opinions of Van Valen, 1988; Muizon and Marshall, 1992; Sempere et al., 1997; Marshall et al., 1997; Lucas, 1998), as are the ages of the Shanguan and Nongshanian Asian Land Mammal Ages, although some of the pantodont-bearing sediments are believed to occur in magnetic polarity chron C27r, approximately correlative with To2 sediments in North America (Xue et al., 1994; Xue et al., 1996; Wang et al., 1998). A number of authors (e.g., Chow and Wang, 1979; Krause and Maas, 1990; Muizon and Marshall, 1992; Lucas, 1993; Williamson and Lucas, 1993; Beard, 1998; Lucas, 1998) have suggested East Asia as a center of origin for pantodonts, as well as a number of other eutherian groups, while others (e.g., Muizon and Cifelli, 2000; Hunter and Janis, 2006) suggest a North American center of origin. The fossil records of Presbyteria and Cyriacotherium add little to resolving the uncertainty of pantodont origins: the earliest occurrence of the family (from the middle Torrejonian Who Nose? locality) is coeval with that of Pantolambda, suggesting only that a significant part of the evolutionary history of North American pantolambdoidean

pantodonts is unknown; whether this history occurred in North America or elsewhere is as yet unknown, but given the poor stratigraphic control and uncertainty with respect to age of many of the pantodont-bearing deposits from outside North America, a North American origin for the order is not unreasonable.

10.4 Literature Cited

BEARD, K. C. 1998. East of Eden: Asia as an important center of taxonomic origination in mammalian evolution, pp. 5-39. In K. C. BEARD and M. R. DAWSON (eds.), Dawn of the Age of Mammals in Asia, Bulletin of Carnegie Museum of Natural History, 34.

CHOW M., and QI T. 1978. Paleocene mammalian fossils from Nomogen Formation of Inner Mongolia. Vertebrata PalAsiatica, 16:77-85. [in Chinese with English summary]

CHOW M., and WANG B. 1978. A new pantodont genus from the Paleocene of S. China. Vertebrata PalAsiatica, 16:86-90. [in Chinese with English abstract]

CHOW M., and WANG B. 1979. Relationship between the pantodonts and tillodonts and a classification of the order Pantodonta. Vertebrata PalAsiatica, 17:37-48. [in Chinese with English abstract]

CHOW M., CHANG Y., WANG B., and TING S. 1973. New mammalian genera and species from the Paleocene of Nanhsiung, N. Kwangtung. Vertebrata PalAsiatica, 9:286-291. [in Chinese with English summary]

CHOW M., CHANG Y., WANG B., and TING S. 1977. Paleocene mammalian fauna from the Nanxiong Basin, Guangdong. Paleontologica Sinica, New Series C, 20:1-100. [in Chinese with English summary]

CLEMENS, W. A., and L. S. RUSSELL. 1965. Mammalian fossils from the Upper Edmonton Formation. University of Alberta Bulletin (Geology Series), 2:32-40.

COOMBS, M. C. 1983. Large mammalian clawed herbivores: a comparative study. Transactions of the American Philosophical Society, 73:1-96.

COPE, E. D. 1873. On the short-footed Ungulata of the Eocene of Wyoming. Proceedings of the American Philosophical Society, 13:38-74.

COPE, E. D. 1875. Systematic catalogue of Vertebrata of the Eocene of New Mexico by parties of the expedition of 1874, Chapter 12: Fossils of the Eocene period. Geographical Surveys west of the 100th Meridian, G. M. Wheeler, Corps of Engineers, U. S. Army, Washington, 4:37-282.

COPE, E. D. 1881. Mammalia of the Lower Eocene beds. American Naturalist, 15:337-338.

COPE, E. D. 1882a. Two new genera of the Puerco Eocene. American Naturalist, 16:417-418.

COPE, E. D. 1882b. Notes on Eocene Mammalia. American Naturalist, 16:522.

COPE, E. D. 1883. The ancestor of Coryphodon. American Naturalist, 17:406-407.

DING (TING) S., J. A. SCHIEBOUT, and ZHOU M. 1987. A skull of Pantolambdodon (Mammalia, Pantodonta) from Ningxia, North China. Journal of Vertebrate Paleontology, 7:155-161.

DUCROCQ, S., E. BUFFETAUT, H. BUFFETAUT-TONG, J. J. JAEGER, Y. JONGKANJANASOONTORN, and V. SUTEETHORN. 1992. First fossil flying lemur; a dermopteran from the late Eocene of Thailand. Palaeontology, 35: 373-380.

FLEROV, K. K. 1952. Pantodonty (Pantodonta), sobrànnye Mongol'skoĭ paleontologicheskoĭ ekspeditsieĭ Akademii Nauk SSSR. Paleontologicheskiĭ Institut, Trudy, 41:43-50.

FOX, R. C. 1990. The succession of Paleocene mammals in western Canada, pp. 51-70. In T. M. BOWN and K. D. ROSE (eds.), Dawn of the Age of Mammals in the Northern Part of the Rocky Mountain Interior. Geological Society of America, Special Paper, 243.

FOX, R. C., and G. P. YOUZWYSHYN. 1994. New primitive carnivorans (Mammalia) from the Paleocene of western Canada, and their bearing on relationships of the order. Journal of Vertebrate Paleontology, 14:382-404.

GAZIN, C. L. 1956. Paleocene mammalian faunas of the Bison Basin in south-central Wyoming. Smithsonian Miscellaneous Collections, 131:1-57.

GILL, T. 1872. Arrangement of the families of mammals with analytical tables. Smithsonian Miscellaneous Collections, 11:1-98.

GINGERICH, P. D. 1989. Body size of Paleocene-Eocene Coryphodon and other large land mammals in relation to global temperature change. Geological Society of America Abstracts with Programs, 21:113-114.

GINGERICH, P. D. 1990. Prediction of body mass in mammalian species from long bone lengths and diameters. Contributions from the Museum of Paleontology, The University of Michigan, 28:79-92.

GINGERICH, P. D. 1996. New species of Titanoides (Mammalia, Pantodonta) from the middle Clarkforkian (late Paleocene) of northwestern Wyoming. Contributions from the Museum of Paleontology, The University of Michigan, 29:403-412.

GINGERICH, P. D. and C. G. CHILDRESS, JR. 1983. Barylambda churchilli, a new species of Pantolambdidae (Mammalia, Pantodonta) from the late Paleocene of western North America. Contributions from the Museum of Paleontology, The University of Michigan, 26:141-155.

GRANGER, W., and W. K. GREGORY. 1934. An apparently new family of amblypod mammals from Mongolia. American Museum Novitates, 720:1-8.

GREGORY, W. K. 1910. The orders of mammals. Bulletin of the American Museum of Natural History, 27:1-254.

HOLTZMAN, R. C. 1978. Late Paleocene mammals of the Tongue River Formation, western North Dakota. Report of Investigation, North Dakota Geological Survey, 65:1-88.

HUNTER, J. P., and C. M. JANIS. 2006. Spiny Norman in the Garden of Eden? Dispersal and early biogeography of Placentalia. Journal of Mammalian Evolution, 13:89-123.

JEPSEN, G. L. 1930. Stratigraphy and paleontology of the Paleocene of northeastern Park County, Wyoming. Proceedings of the American Philosophical Society, 69:463-528.

KIELAN-JAWOROWSKA, Z. 1975. Preliminary description of two new eutherian genera from the Late Cretaceous of Mongolia, pp. 5-16. In Z. KIELAN-JAWOROWSKA (ed.), Results of the Polish-Mongolian Palaeontological Expeditions, Part VI. Palaeontologica Polonica 33.

KRAUSE, D. W., and M. C. MAAS. 1990. The biogeographic origins of late Paleocene-early Eocene mammalian immigrants to the Western Interior of North America, pp. 71-105. In T. M. BOWN and K. D. ROSE (eds.), Dawn of the Age of Mammals in the Northern Part of the Rocky Mountain Interior, North America. Geological Society of America Special Paper, 243.

LINNAEUS, C. 1758. Systema naturae per regna tria naturae, secundum classes, ordines, genera, species cum characteribus, differentiis, synonymis, locis. Editio decima, reformata. Laurenti Salvii, Stockholm.

LOFGREN, D. L., J. A. LILLEGRAVEN, W. A. CLEMENS, P. D. GINGERICH, and T. E. WILLIAMSON. 2004. Paleocene biochronology: The Puercan through Clarkforkian Land Mammal Ages, pp. 43-105. In M. O. WOODBURNE (ed.), Late Cretaceous and Cenozoic mammals of North America: Geochronology and Biostratigraphy. Columbia University Press, New York.

LUCAS, S. G. 1982. The phylogeny and composition of the order Pantodonta (Mammalia, Eutheria). Proceedings of the Third North American Paleontological Convention, 2:337-342.

LUCAS, S. G. 1986. Systematics, biostratigraphy and evolution of early Cenozoic Coryphodon (Mammalia, Pantodonta). Unpublished Ph. D. dissertation, Yale University, New Haven, 673 pp.

LUCAS, S. G. 1993. Pantodonts, tillodonts, uintatheres, and pyrotheres are not ungulates, pp. 182-194. In F. S. SZALAY, M. J. NOVACEK, and M. C. MCKENNA (eds.), Mammal Phylogeny: Placentals. Springer-Verlag, New York.

LUCAS, S. G. 1998. Pantodonta, pp. 274-283. In C. M. JANIS, K. M. SCOTT, and L. L. JACOBS (eds.), Evolution of Tertiary Mammals of North America, volume 1: Terrestrial Carnivores, Ungulates, and Ungulatelike Mammals. Cambridge University Press, Cambridge.

MACPHEE, R. D. E., M. CARTMILL, and K. D. ROSE. 1989. Craniodental morphology and relationships of the supposed Eocene dermopteran Plagiomene (Mammalia). Journal of Vertebrate Paleontology, 9:329-349.

MARSH, O. C. 1889. Discovery of Cretaceous Mammalia. American Journal of Science, series 3, 38:81-92.

MARSHALL, L. G., T. SEMPERE, and R. F. BUTLER. 1997. Chronostratigraphy of the mammal-bearing Paleocene of South America. Journal of the South American Earth Sciences, 10:49-70.

MATTHEW, W. D. 1918. A revision of the Lower Eocene Wasatch and Wind River faunas. Part V: Insectivora (continued), Glires, Edentata. Bulletin of the American Museum of Natural History, 38:565-657.

MATTHEW, W. D. 1937. Paleocene faunas of the San Juan Basin, New Mexico. Transactions of the American Philosophical Society, New Series, 30:1-510.

MCKENNA, M. C. 1972. Vertebrate paleontology of the Togwotee Pass area, northwestern Wyoming, pp. 80-101. In R. M. WEST (ed.), Guidebook, Field Conference on Tertiary Biostratigraphy of Southern and Western Wyoming. Privately printed.

MCKENNA, M. C. 1975. Toward a phylogenetic classification of the Mammalia, pp. 21-46. In W. P. LUCKETT and F. S. SZALAY (eds.), Phylogeny of the Primates: A Multidisciplinary Approach. Plenum Press, New York.

MCKENNA, M. C., and S. K. BELL. 1997. Classification of Mammals Above the Species Level. Columbia University Press, New York, xii+631 pp.

MUIZON, C. de, and R. L. CIFELLI. 2000. The "condylarths" (archaic Ungulata, Mammalia) from the early Palaeocene of Tiupampa (Bolivia): implications on the origin of the South American ungulates. Geodiversitas, 22:47-150.

MUIZON, C. de, and L. G. MARSHALL. 1992. Alcidedorbignya opinata (Mammalia: Pantodonta) from the early Paleocene of Bolivia: phylogenetic and paleobiogeographic implications. Journal of Paleontology, 66:499-520.

OSBORN, H. F. 1898. Evolution of the Amblypoda. Part I. Taligrada and Pantodonta. Bulletin of the American Museum of Natural History, 10:269-218.

PARKER, T. J., and W. A. HASWELL. 1897. A Text-book of Zoology. Volume 2. Macmillan Press, London, 301 pp.

PATTERSON, B. 1933. A new species of the amblypod Titanoides from western Colorado. American Journal of Science, 25:415-425.

PATTERSON, B. 1934. A contribution to the osteology of Titanoides and the relationships of the Amblypoda. Proceedings of the American Philosophical Society, 73:71-101.

PATTERSON, B. 1935. Second contribution to the osteology and affinities of the Paleocene amblypod Titanoides. Proceedings of the American Philosophical Society, 75:143-162.

PATTERSON, B. 1939. New Pantodonta and Dinocerata from the upper Paleocene of western Colorado. Geological Series of Field Museum of Natural History, 6:351-384.

RADINSKY, L. 1985. Patterns in the evolution of ungulate jaw shape. American Zoologist, 25:303-314.

ROSE, K. D. 1975. Elpidophorus, the earliest dermopteran (Dermoptera, Plagiomenidae). Journal of Mammalogy, 56:676-679.

ROSE, K. D. 2006. The Beginning of the Age of Mammals. The Johns Hopkins University Press, Baltimore, 448 pp.

ROSE, K. D., and E. L. SIMONS. 1977. Dental function in the Plagiomenidae: Origin and relationships of the mammalian order Dermoptera. Contributions from the Museum of Paleontology, The University of Michigan, 24:221-236.

ROSE, K. D., and D. W. KRAUSE. 1982. Cyriacotheriidae, a new family of early Tertiary pantodonts from western North America. Proceedings of the American Philosophical Society, 126:26-50.

RUSSELL, L. S. 1948. A middle Paleocene mammal tooth from the Foothills of Alberta. American Journal of Science. 246:152–156.

SCHIEBOUT, J. 1974. Vertebrate paleontology and paleoecology of Paleocene Black Hills Formation, Big Bend National Park, Texas. Bulletin of the Texas Memorial Museum, 24:1–88.

SCOTT, C. S. 1997. A new Palaeocene mammal site from Calgary, Alberta. Journal of Vertebrate Paleontology 17, supplement to no. 3:74A.

SCOTT, C. S. 2003. Late Torrejonian (middle Paleocene) mammals from south central Alberta, Canada. Journal of Paleontology, 77:745-768.

SCOTT, C. S. 2005. New species of Cyriacotherium (Mammalia: Pantodonta) from the Paleocene of Alberta, Canada. Journal of Vertebrate Paleontology 25, supplement to no. 3:112A.

SECORD, R. 2004. Late Paleocene biostratigraphy, isotope stratigraphy, and mammalian systematics of the northern Bighorn Basin, Wyoming. Unpublished Ph. D. dissertation, The University of Michigan, Ann Arbor, 532 pp.

SEMPERE, T., R. F. BUTLER, D. R. RICHARDS, L. G. MARSHALL, W. SHARP, and C. C. SWISHER, III. 1997. Stratigraphy and chronology of Upper Cretaceous-lower Paleogene strata in Bolivia and northwest Argentina. Geological Society of America Bulletin, 109:709-727.

SIMONS, E. L. 1960. The Paleocene Pantodonta. Transactions of the American Philosophical Society, new series, 50:1-99.

SIMPSON, G. G. 1937. Additions to the upper Paleocene fauna of the Crazy Mountain field. American Museum Novitates, 940:1-15.

SIMPSON, G. G. 1945. The principles of classification and a classification of mammals. Bulletin of the American Museum of Natural History, 85:1-350.

STAFFORD, B. J., and F. S. SZALAY. 2000. Cranio-dental functional morphology and the taxonomy of flying lemurs (Dermoptera, Cynocephalidae). Journal of Mammalogy, 81:360-385.

SZALAY, F. S. 1977. Phylogenetic relationships and a classification of the eutherian Mammalia, pp. 315-374. In M. K. HECHT, P. C. GOODY, and B. M. HECHT (eds.), Major Patterns in Vertebrate Evolution. Plenum Press, New York.

TING, S., J. A. SCHIEBOUT, and Z. JIAJIANG. 1996. New pantodont records from South China. Paleovertebrata, 25:125-132.

VAN VALEN, L. 1988. Paleocene dinosaurs or Cretaceous ungulates in South America? Evolutionary Monographs, 10:1-79.

WANG B. 1975. Paleocene mammals of Chaling Basin, Hunan. Vertebrata PalAsiatica, 13:154-162. [in Chinese]

WANG B. 1979. A new species of Harpyodus and its systematic position, pp. 366-372. In Mesozoic and Cenozoic Red Beds of South China. Science Press, Beijing, People's Republic of China. [in Chinese]

WANG Y. 1993. The skull morphology and phylogeny of non-coryphodontid Pantodonta (Mammalia). Unpublished Ph. D. dissertation, Institute for Vertebrate

Paleontology and Paleoanthropology, Chinese Academy of Sciences, Beijing, People's Republic of China. [in Chinese with English abstract]

WANG Y., YU B., and LI D. 1992. A skull of Altilambda (Mammalia, Pantodonta) from the Paleocene of Qianshan, Anhui. Vertebrata PalAsiatica, 30:221-228. [in Chinese with English summary]

WANG Y., HU Y., CHOW M., and LI C. 1998. Chinese Paleocene mammal faunas and their correlation, pp. 89-123. In K. C. BEARD and M. R. DAWSON (eds.), Dawn of the Age of Mammals in Asia, Bulletin of Carnegie Museum of Natural History, 34.

WEBB, M. W. 1996. Late Paleocene mammals from near Drayton Valley, Alberta. Unpublished M. Sc. thesis, University of Alberta, Edmonton, 258 pp.

WILLIAMSON, T. E. and S. G. LUCAS. 1993. Paleocene vertebrate paleontology of the San Juan Basin, New Mexico. Bulletin of the New Mexico Museum of Natural History and Science, 2:105-135.

XUE X., YUE L., and ZHANG Y. 1994. Magnetostratigraphical, biostratigraphical and lithostratigraphical correlation of the red beds in Shanyang Basin, Shaanxi Province. Science in China (Series B), 24:413-417. [in Chinese]

XUE X., ZHANG Y., BI Y., YUE L., and CHEN D. 1996. The development and environmental changes of the intermontane basins in the eastern part of Qinling Mountains. Geological Publishing House, Beijing, People's Republic of China.

Table 10.1.—Combined measurements and descriptive statistics for the upper dentition of Joffrelambda spivaki new genus and species from the early middle Tiffanian (Ti3) DW-2 and Joffre Bridge Roadcut lower level localities, Paskapoo Formation, Alberta.

Element	P	N	OR	M	SD	CV
C	L (♂)	2	25.0	25.00	0	0
	W (♂)	1	18.0	—	—	—
	L (♀)	1	12.0	—	—	—
	W (♀)	1	12.0	—	—	—
P1	L	2	15.0-15.5	15.25	0.35	2.32
	W	2	9.0-10.2	9.60	0.85	8.84
P2	L	2	15.0-16.2	15.60	0.85	5.44
	W	2	26.5	26.50	0	0
P3	L	2	15.0-17.5	16.25	1.77	10.88
	W	—	—	—	—	—
P4	L	3	16.0-18.0	17.00	1.00	5.88
	W	1	26.5	—	—	—
M1	L	3	19.5-21.0	20.50	0.87	4.22
	W	3	21.5-25.0	23.57	1.83	7.78
M2	L	2	24.5-25.0	24.75	0.35	1.43
	W	2	30.0	30.0	0	0
M3	L	5	17.0-21.5	19.46	1.87	9.59
	W	5	29.5-31.4	30.22	0.71	2.34

Table 10.2.—Combined measurements and descriptive statistics for the lower dentition of Joffrelambda spivaki new genus and species from the early middle Tiffanian (Ti3) DW-2 and Joffre Bridge Mammal Site No. 1 localities, Paskapoo Formation, Alberta.

Element	P	N	OR	M	SD	CV
c	L (♂)	1	19.0	19.00	—	—
	W (♂)	1	12.0	12.00	—	—
	L (♀)	2	14.0	14.00	0	0
	W (♀)	2	10.0	10.0	0	0
p1	L	3	14.0-14.5	14.17	0.29	2.04
	W	3	7.0-8.0	7.67	0.58	7.53
p2	L	2	16.0-17.0	16.50	0.71	4.29
	W	2	12.5	12.50	0	0
p3	L	4	15.0-17.2	16.43	0.99	6.06
	W	4	14.0-17.5	15.75	1.76	11.15
p4	L	6	18.5-20.5	19.42	0.80	4.11
	W	7	14.5-18.5	16.36	1.41	8.59
m1	L	4	20.0-21.0	20.63	0.48	2.32
	TrW	4	13.6-14.5	14.03	0.37	2.63
	TaW	4	12.5-13.0	12.63	0.25	1.98
m2	L	3	24.0-26.0	25.07	1.01	4.02
	TrW	3	16.0	16.00	0	0
	TaW	4	15.0-15.5	15.25	0.29	1.89
m3	L	3	29.2-31.0	30.07	0.90	3.00
	TrW	3	16.5-18.5	17.73	1.08	6.08
	TaW	3	16.0-17.2	17.10	0.14	0.83

Table 10.3.—Combined measurements and descriptive statistics for the upper dentition of Presbyteria rhodoptyx new genus and species from the early middle Tiffanian (Ti3) DW-2 and Birchwood localities, Paskapoo Formation, Alberta.

Element	P	N	OR	M	SD	CV
P1	L	1	5.6	—	—	—
	W	1	3.8	—	—	—
P2	L	1	6.2	—	—	—
	W	1	5.1	—	—	—
P3	L	1	6.9	—	—	—
	W	2	7.6-7.7	7.65	0.07	1.22
P4	L	1	6.3	—	—	—
	W	2	9.2	9.20	0	0
DP4	L	1	6.3	—	—	—
	W	1	6.6	—	—	—
M2	L	1	7.8	—	—	—
	W	1	9.7	—	—	—
M3	L	1	6.3	—	—	—
	W	1	11.2	—	—	—

Table 10.4.—Combined measurements and descriptive statistics for the lower dentition of Presbyteria rhodoptyx new genus and species from the early middle Tiffanian (Ti3) DW-2 and Birchwood localities, Paskapoo Formation, Alberta.

Element	P	N	OR	M	SD	CV
c	L	3	4.0-4.3	4.17	0.15	4.33
	W	3	2.8-3.0	2.93	0.13	3.96
p2	L	1	5.5	—	—	—
	W	1	3.6	—	—	—
p3	L	2	6.2-6.6	6.40	0.28	4.02
	W	2	4.4-4.8	4.60	0.28	5.99
p4	L	4	6.3-6.9	6.65	0.25	4.25
	TrW	5	4.9-5.5	5.16	0.23	4.22
	TaW	3	3.6-4.1	3.83	0.25	6.95
m1	L	2	8.0-8.1	8.05	0.07	7.14
	TrW	2	5.3-5.5	5.40	0.14	3.33
	TaW	2	5.1-5.3	5.20	0.14	3.27
m2	L	2	8.5-8.7	8.60	0.14	2.14
	TrW	2	5.7	5.70	0	0
	TaW	2	5.6-5.8	5.70	0.14	1.87

Figure 10.1.—Joffrelambda spivaki new genus and species from the early middle Tiffanian (Ti3) Joffre Bridge Roadcut upper level locality, Paskapoo Formation, Alberta. UALVP 46592 (holotype skull), nearly complete skull and left and right dentaries in right lateral view. Scale bar = 40mm.

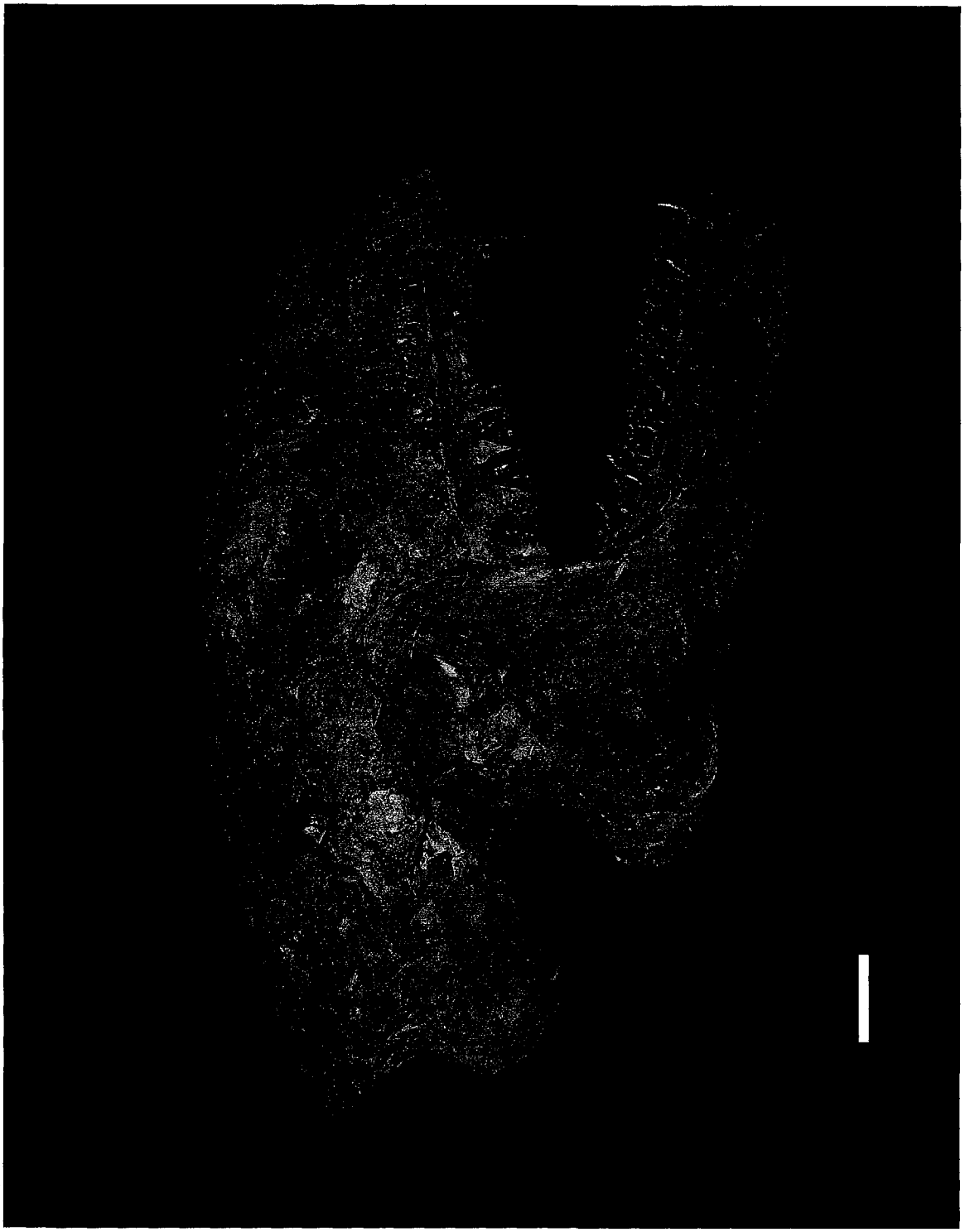

Figure 10.2.—1, 2. Joffrelambda spivaki new genus and species from the early middle Tiffanian (Ti3) Joffre Bridge Roadcut upper level locality, Alberta. 1, 2, TMP 2001.25.03, incomplete skull and left and right dentaries in 1, right lateral and 2, left lateral views. Stippled areas represent parts of the skull and jaws that have been reconstructed in plaster. Scale bar = 40 mm.

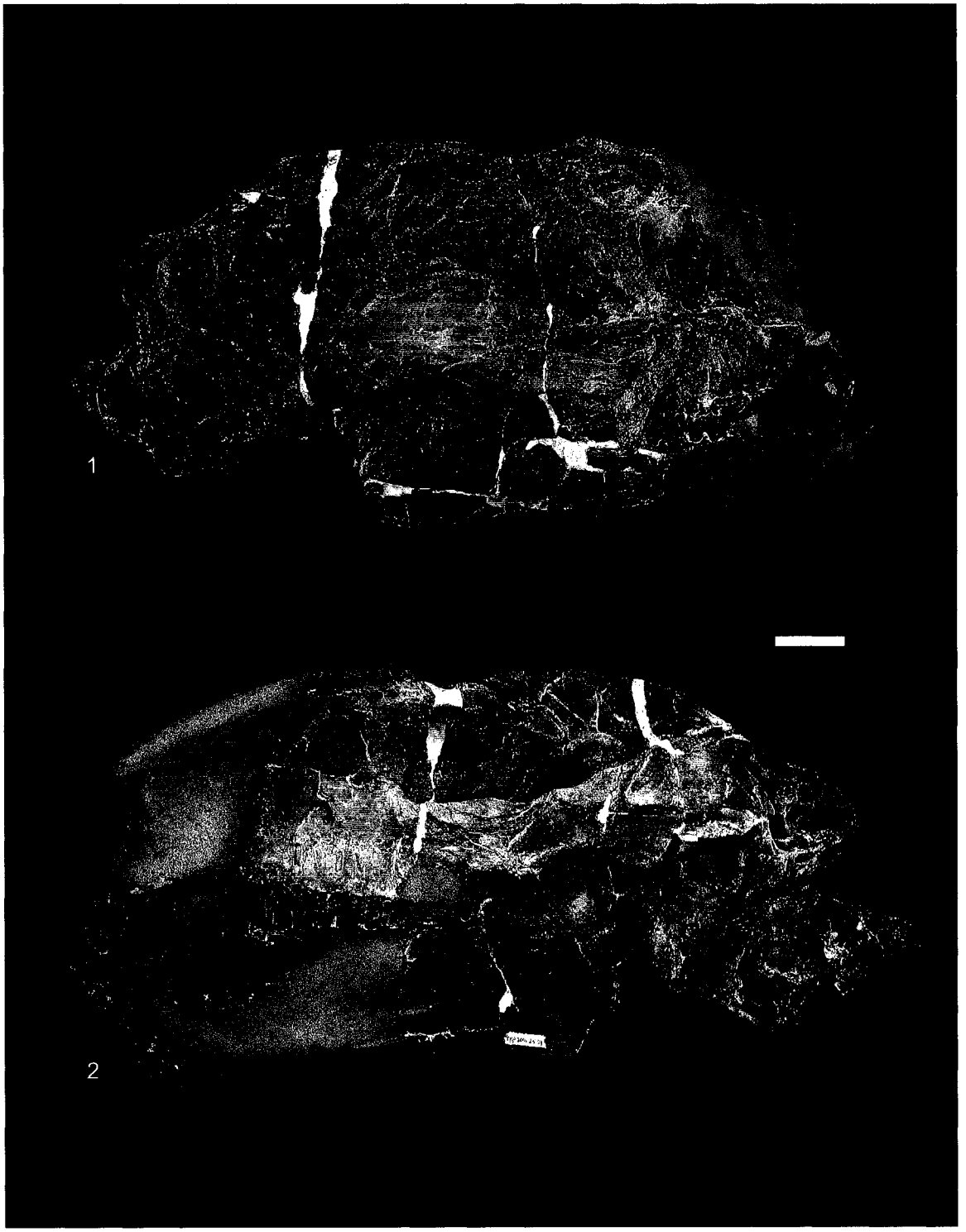
1
2

Figure 10.3.—1-13. Joffrelambda spivaki new genus and species from the early middle Tiffanian (Ti3) Birchwood (BW) and Joffre Bridge Roadcut upper level (JBUL) localities, Paskapoo Formation, Alberta. 1-6, UALVP 39492 (♀, BW), associated incomplete upper left canine and RP4; upper canine in 1, labial, 2, anterior, and 3, occlusal views; RP4 in 4, labial, 5, oblique lingual, and 6, occlusal views; 7-9, UALVP 43111 (BW), left M1 in 7, labial, 8, oblique lingual, and 9, occlusal views; 10-12, UALVP 39488 (BW), left M3 in 10, labial, 11, oblique lingual, and 12, occlusal views; 13, UALVP 46592 (♂, holotype skull, JB), upper dentition [includes left C, P1-2, P4, M1-3 and right C (damaged), P1-4, M1-3] in occlusal view. Scale bars = 40 mm.

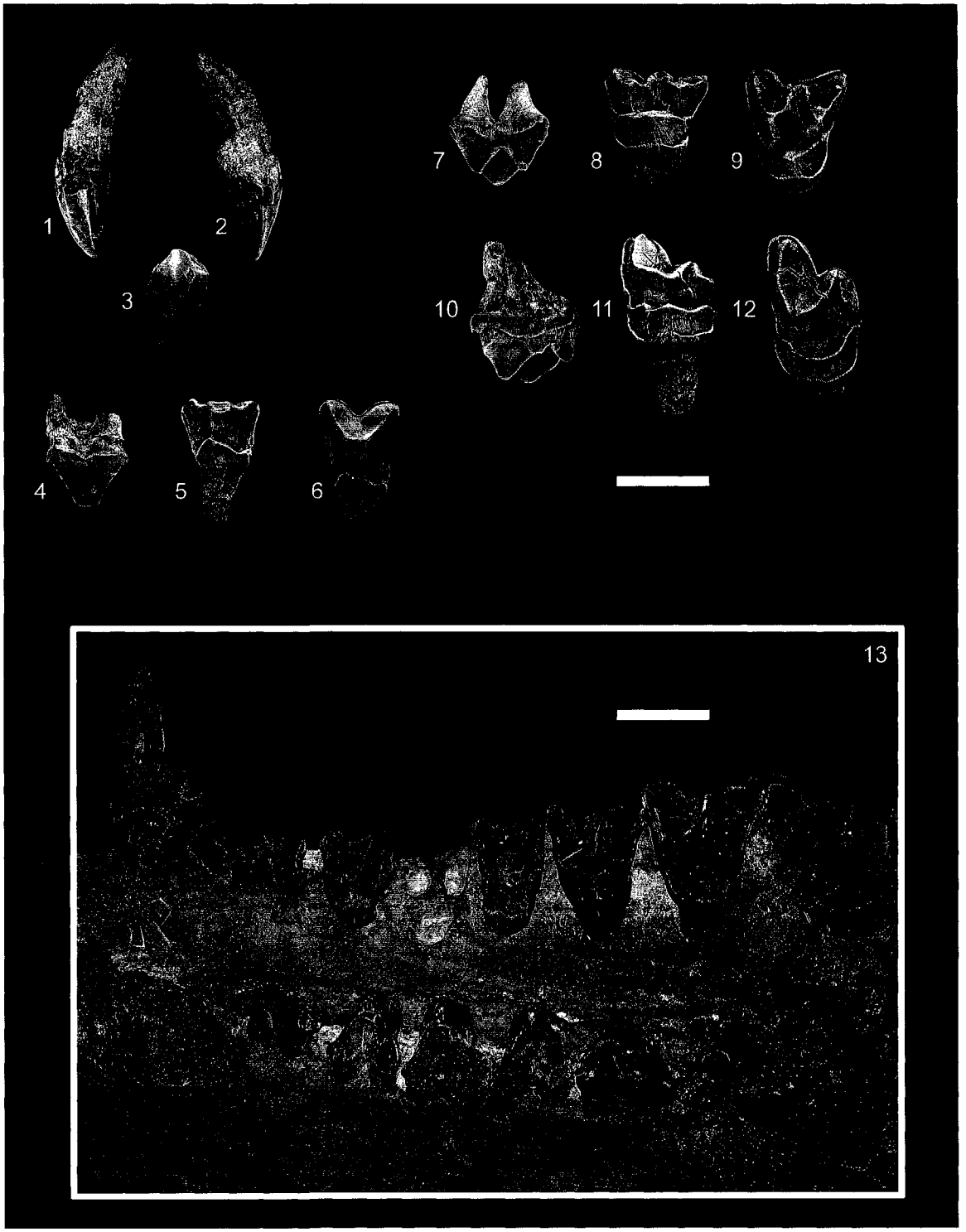
1
2
3
4
5
6
7
8
9
10
11
12
13

Figure 10.4.—1-13. Joffrelambda spivaki new genus and species from the early middle Tiffanian (Ti3) DW-2 (DW2) and Joffre Bridge Roadcut upper level (JBUL) localities, Paskapoo Formation, Alberta. 1-12, UALVP 46593 (♀, DW2), associated left and right lower dentition. 1-3, left i1 in 1, anterior, 2, posterior, and 3, occlusal view; 4-6, left i2 in 4, anterior, 5, posterior, and 6, occlusal view; 7-9, left i3 in 7, anterior, 8, posterior, and 9, occlusal views; 10-12, composite right lower post-incisor dentition including c, p1-4, m1-3 (m1 and m3 from the left side, reversed) in 10, labial, 11, lingual, and 12, occlusal views; 13, UALVP 46592 (♂, holotype mandible, skull digitally removed, JBUL), incomplete left and right dentaries having right i1-3 (roots only), c, p1, p3-4, m1-3, and left i1-3 (roots only), c (root only), p1-4, m1-3 in right lateral view. Scale bars = 40mm.

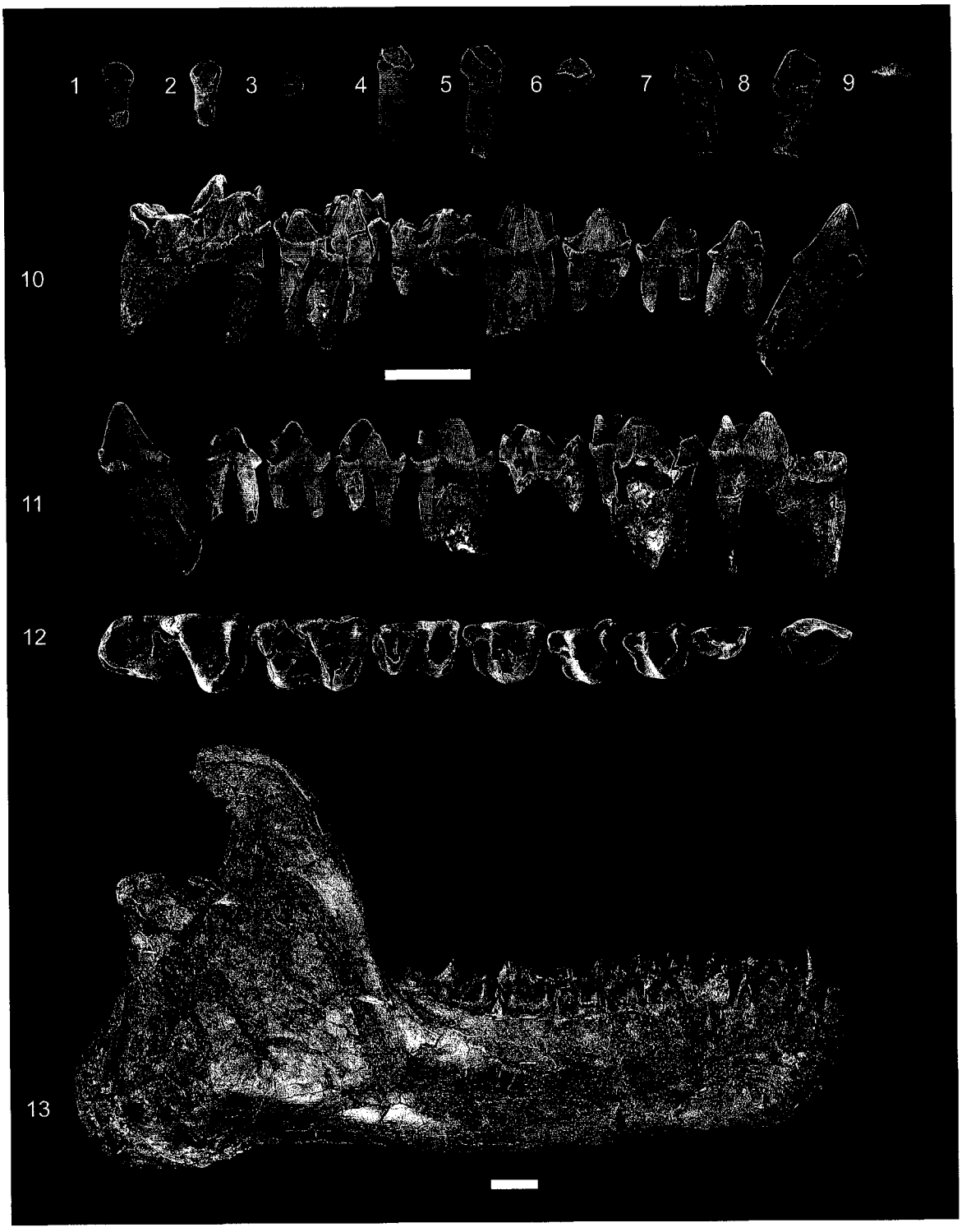
1
2
3
4
5
6
7
8
9
10
11
12
13

Figure 10.5.—1-6. Joffrelambda spivaki new genus and species from the early middle Tiffanian (Ti3) Joffre Bridge Roadcut upper level locality, Paskapoo Formation, Alberta. 1-3, TMP 2001.25.03, incomplete cervical vertebra (?C4) in 1, anterior, 2, posterior, and 3, dorsal views. Scale bar = 40 mm.

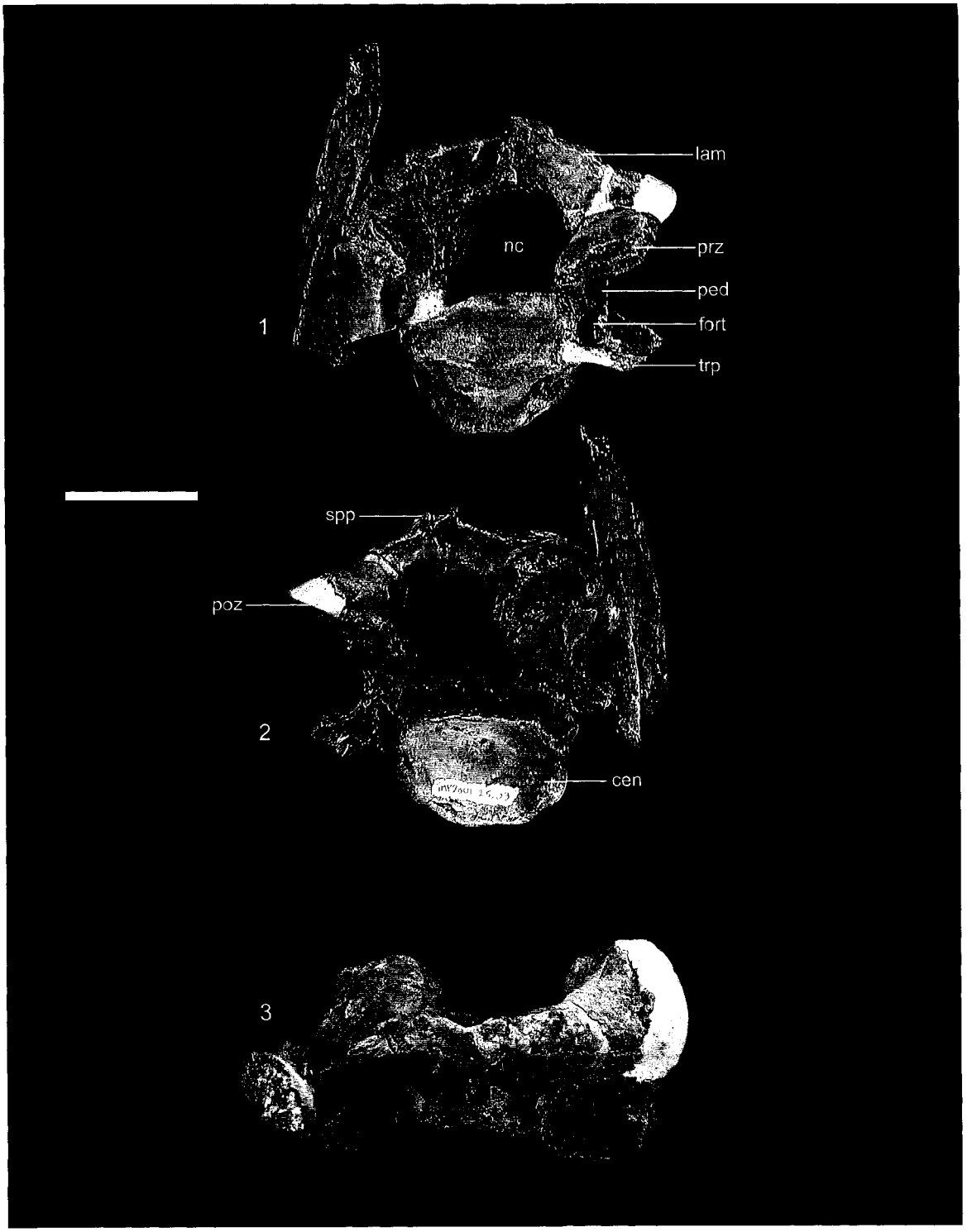
lam
nc
prz
ped
fort
trp
1
spp
poz
2
cen
3

Figure 10.6.—1-8. Joffrelambda spivaki new genus and species from the early middle Tiffanian (Ti3) Joffre Bridge Roadcut upper level locality, Paskapoo Formation, Alberta. 1-3, TMP 2001.25.03, incomplete right ulna in 1, anterior, 2, lateral, and 3, medial views, 4, 5, UALVP 46592 (holotype), left radius in 4, anterior and 5, posterior views; 6-8, TMP 2001.25.03, incomplete right radius in 6, anterior, 7, posterior, and 8, posteromedial views. Scale bars = 40mm.

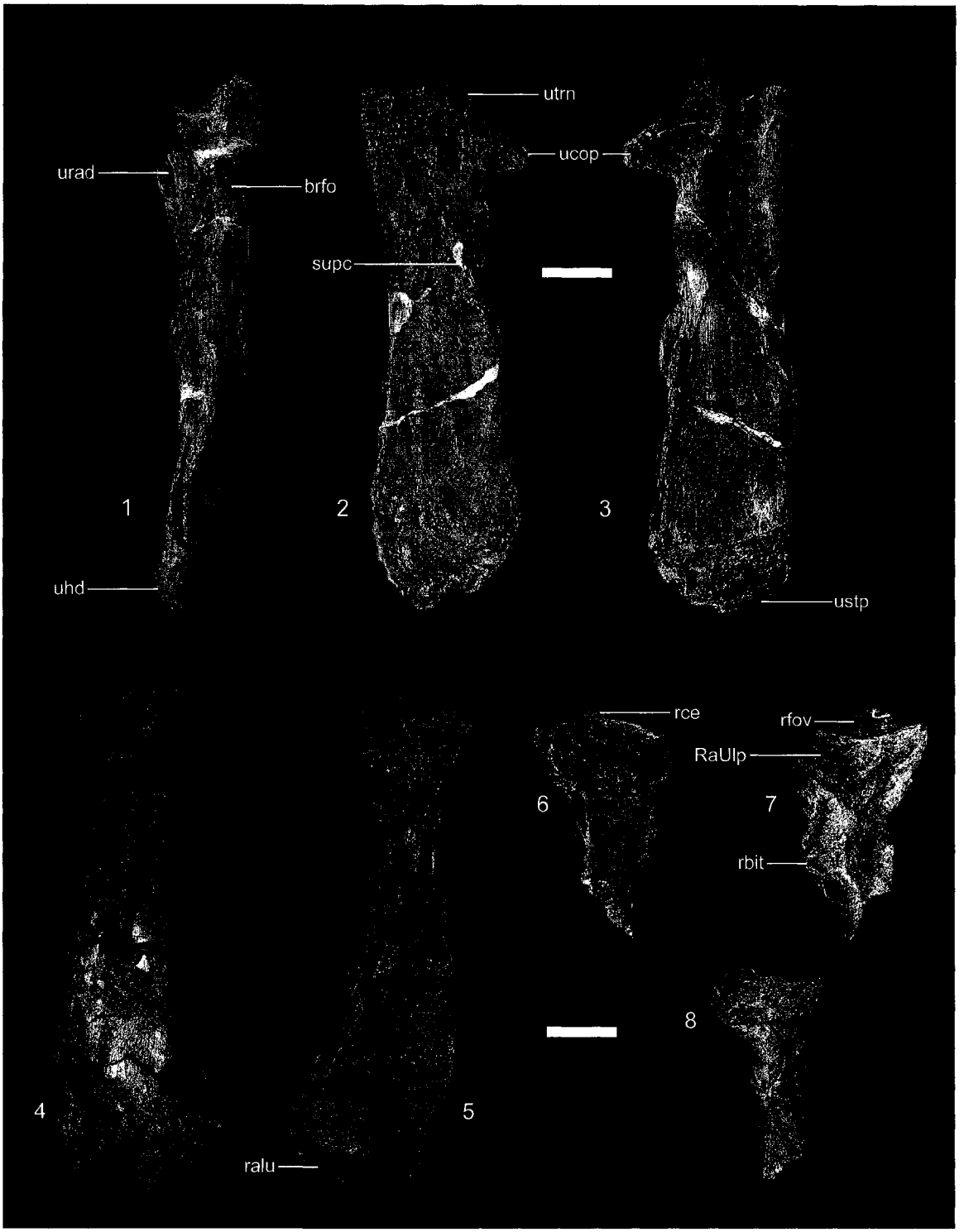
urad
brfo
uhd
1
utrn
ucop
supc
2
3
ustp
rce
rfov
RaUlp
6
7
rbit
8
4
ralu
5

Figure 10.7.—1-11. Joffrelambda spivaki new genus and species from the early middle Tiffanian (Ti3) DW-2 (DW2) and Joffre Bridge Roadcut upper level (JBUL) localities, Paskapoo Formation, Alberta. 1-3, UALVP 46592 (holotype, JBUL), left lunate in 1, proximal, 2, distal, and 3, anterior views; 4-6, UALVP 46559 (DW2), right magnum in 4, proximal, 5, distal, and 6, anterior views; 7-9, TMP 2001.25.03 (JBUL), left unciform in 7, proximal, 8, distal, and 9, anterior views; 10, 11, UALVP 46592 (holotype, JBUL), carpal sesamoids in 10, proximal and 11, plantar views. Scale bars = 40mm.

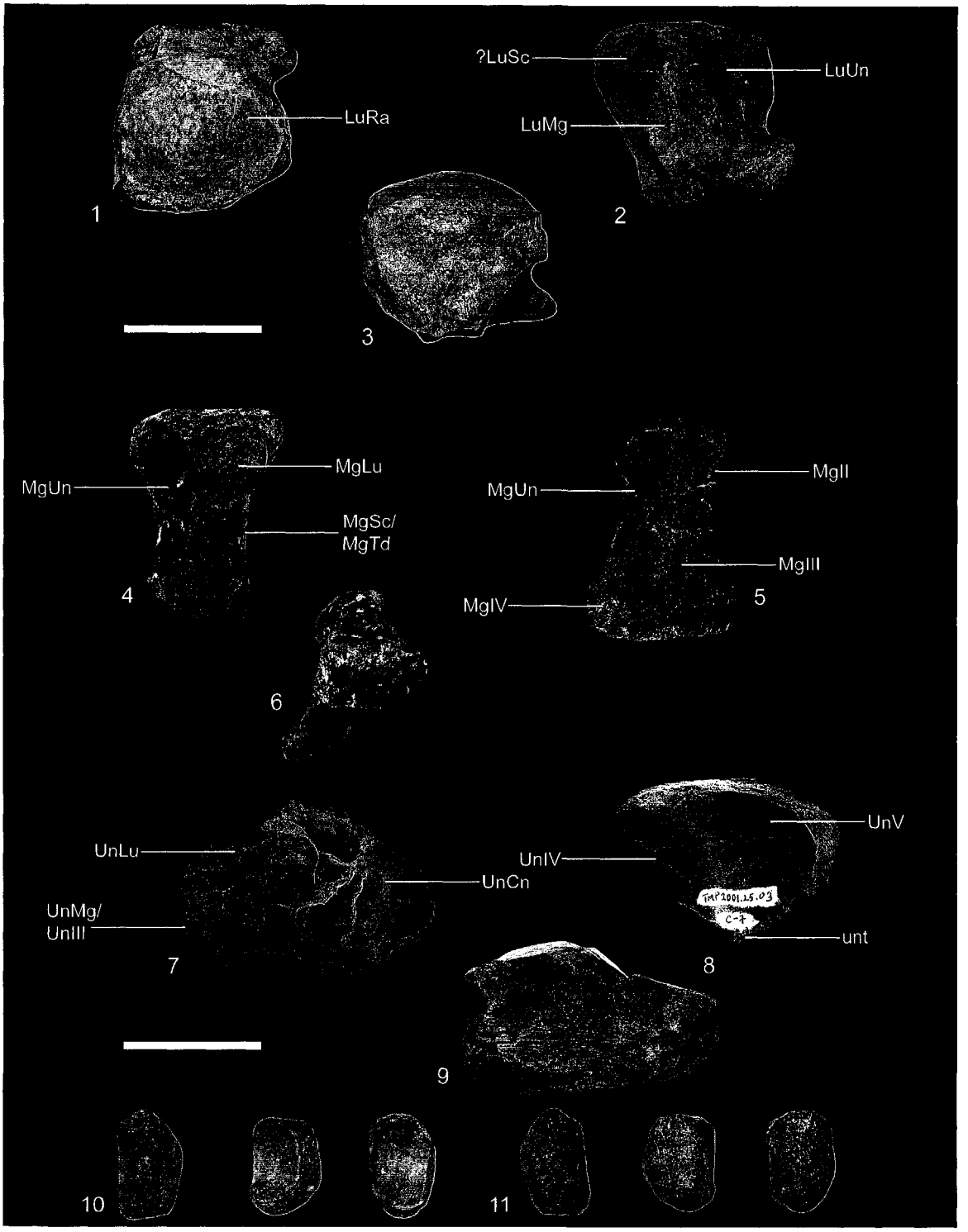
LuRa
1
?LuSc
LuUn
LuMg
2
3
MgLu
MgUn
MgSc/
MgTd
4
MgII
MgUn
MgIII
MgIV
5
6
UnV
UnIV
UnLu
UnCn
UnMg/
UnIII
unt
7
8
9
10
11

Figure 10.8.—1-25. Joffrelambda spivaki new genus and species from the early middle Tiffanian (Ti3) Joffre Bridge Roadcut upper level locality, Paskapoo Formation, Alberta. Composite left manus. 1-5, left pollucal metacarpal and phalanges [(McI and proximal phalanx from UALVP 46592 (holotype), ungual phalanx from TMP 2001.25.03, reversed from original] in 1, dorsal, 2, plantar, 3, medial, and 4, lateral, and 5, proximal (phalanges only) views; 6-10, left McII and phalanges (all from TMP 2001.25.03, reversed from original) in 6, dorsal, 7, plantar, 8, medial, 9, lateral, and 10, proximal (phalanges only) views; 11-15, left McIII and phalanges [(McIII, proximal, and intermediate phalanges from UALVP 46592 (holotype), ungual phalanx from TMP 2001.25.03, reversed from original] in 11, dorsal, 12, plantar, 13, medial, 14, lateral, and 15, proximal (phalanges only) views; 16-20, left McIV and phalanges [(McIV, proximal, and intermediate phalanges from UALVP 46592 (holotype), ungual phalanx from TMP 2001.25.03, reversed from original] in 16, dorsal, 17, plantar, 18, medial, 19, lateral, and 20, proximal (phalanges only) views; 21-25, left McV and phalanges [(McV and proximal phalanx from UALVP 46592 (holotype), intermediate and ungual phalanges from TMP 2001.25.03, reversed from original] in 21, dorsal, 22, plantar, 23, medial, 24, lateral, and 25, proximal (phalanges only) views. Scale bars = 40mm.

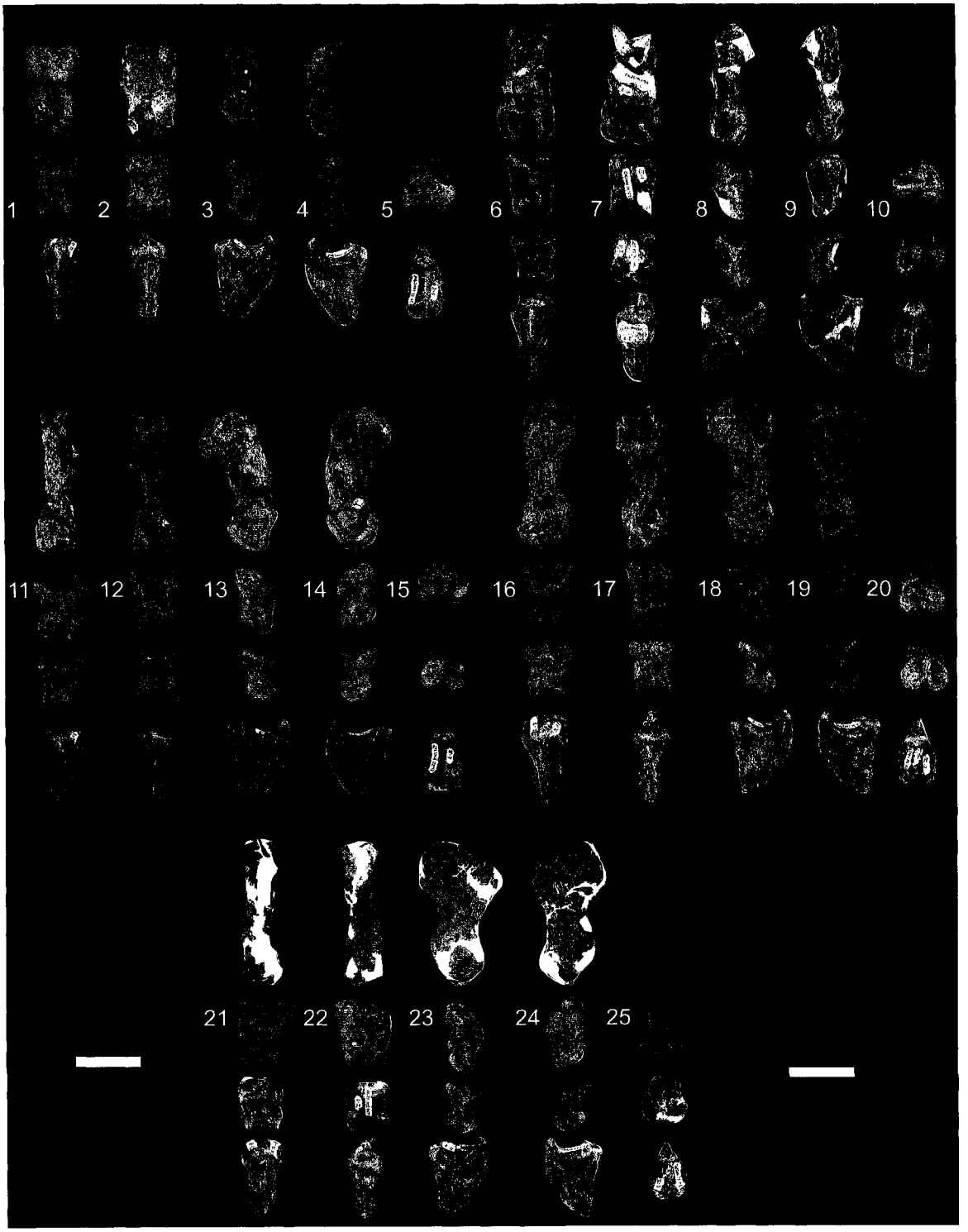
1
2
3
4
5
6
7
8
9
10
11
12
13
14
15
16
17
18
19
20
21
22
23
24
25

Figure 10.9.—1-6. Titanoideidae, genus and species indeterminate from the early middle Tiffanian (Ti3) DW-2 (DW2) and Joffre Bridge Mammal Site No. 1 (JBMS) localities, Paskapoo Formation, Alberta. 1-3, UALVP 34124 (JBMS), incomplete right dentary with p3, talonid of m1, m2-3, and alveoli for the lower canine, p1-2 (anterior root of p2 in alveolus), and p4 (anterior root of p4 in alveolus) in 1, labial, 2, lingual, and 3, occlusal views; UALVP 46600 (DW2), incomplete left ulna (see Fig. 10.1-10.29 for associated left carpus and manus) in 4, anterior, 5, lateral, and 6, medial views. Scale bars = 20mm.

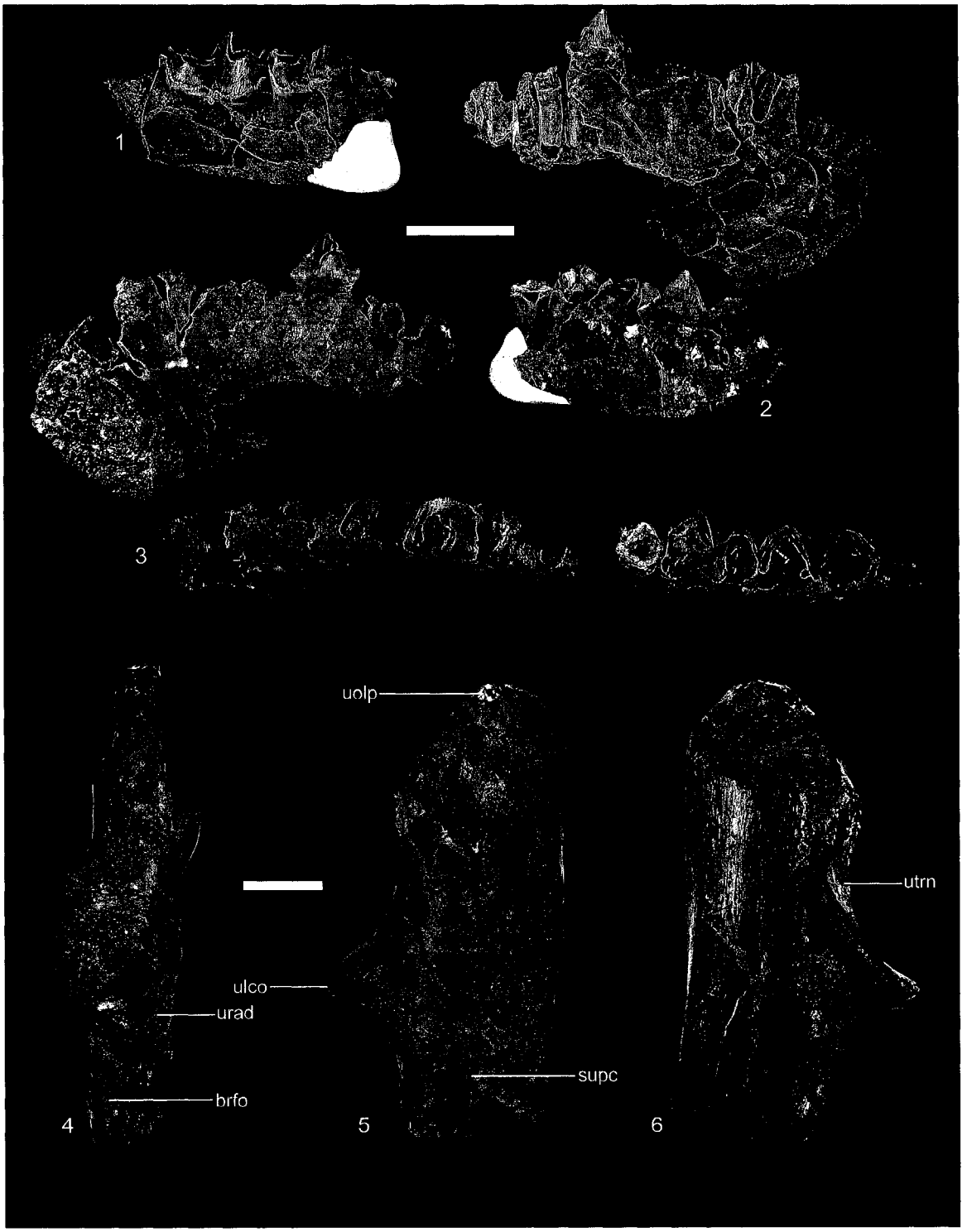
1
2
3
uolp
utrn
ulco
urad
brfo
supc
4
5
6

Figure 10.10.—1-33. Titanoideidae, genus and species indeterminate from the early middle Tiffanian (Ti3) DW-2 locality, Paskapoo Formation, Alberta. 1-27, UALVP 46600, associated left carpus and manus (see Fig. 9.4-9.6 for associated incomplete left ulna). 1-3, left lunate in 1, proximal, 2, distal, and 3, anterior views; 4-6, left magnum in 4, proximal, 5, distal, and 6, anterior views; 7-9, left unciform in 7, proximal, 8, distal, and 9, anterior views; 10, 11, sesamoid in 10, dorsal and 11, plantar views; 12-15, left McII in 12, dorsal, 13, plantar, 14, medial, and 15, lateral views; 16-19, left McIV in 16, lateral, 17, medial, 18, dorsal, and 19, plantar views; 20-23, incomplete left McV in 20, lateral, 21, medial, 22, dorsal, 23, plantar views; 24-28, left proximal phalanx in 24, lateral, 25, medial, 26, dorsal, 27, plantar, and 28, proximal views; 29-33, left intermediate phalanx in 29, lateral, 30, medial, 31, dorsal, 32, plantar, and 33, proximal views. Scale bars = 40mm.

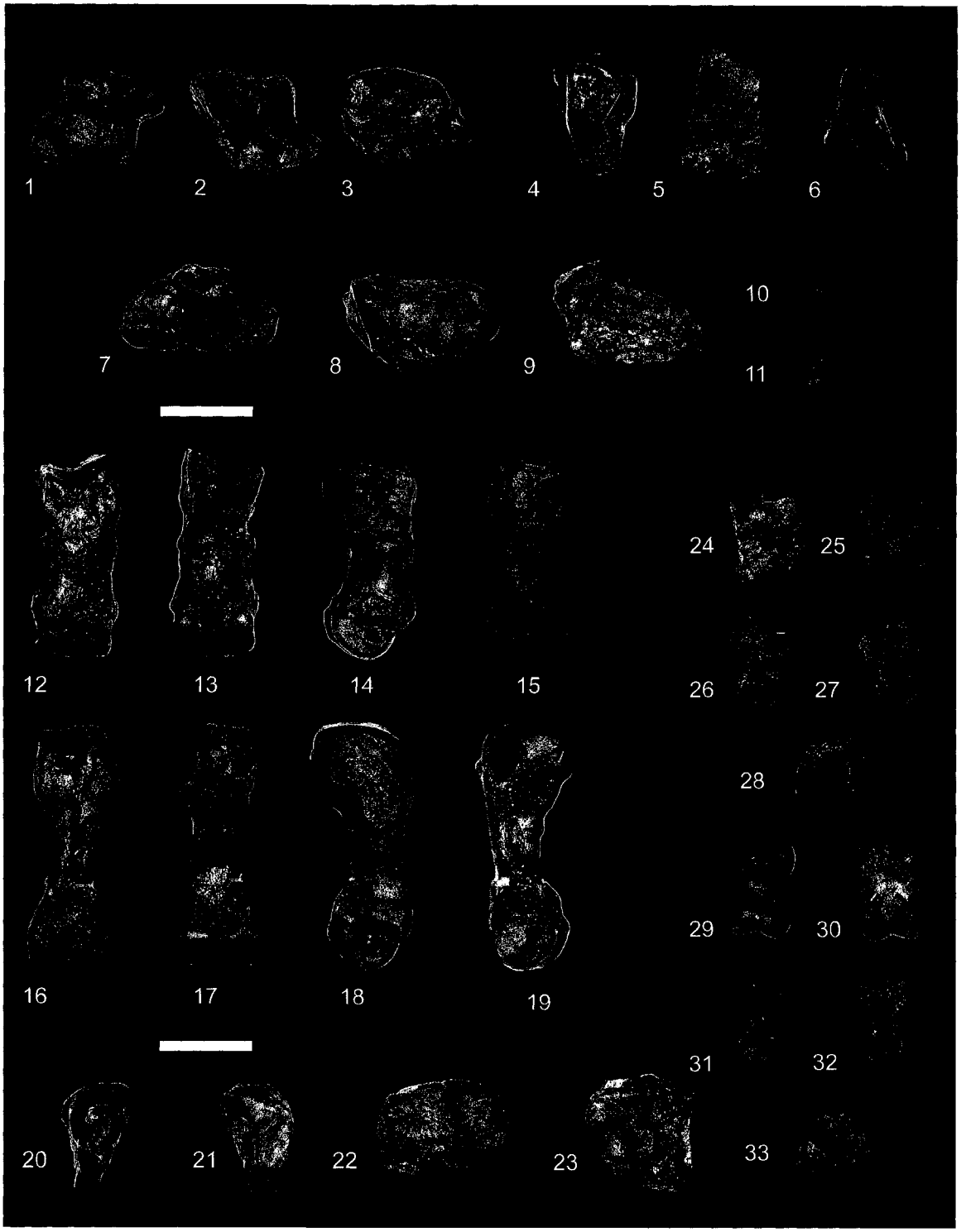
1
2
3
4
5
6
7
8
9
10
11
12
13
14
15
24
25
26
27
16
17
18
19
28
29
30
20
21
22
23
31
32
33

Figure 10.11.—1, 2, ?Caenolambda sp. from the early middle Tiffanian (Ti3) Burbank locality, Paskapoo Formation, Alberta. UALVP 46602, incomplete right M1 or M2 in 1, oblique lingual and 2, occlusal views.

3-8, Pantolambdoidea, genus and species indeterminate from the early middle Tiffanian (Ti3) DW-2 locality, early middle Tiffanian (Ti3), Paskapoo Formation, Alberta. 3-5, UALVP 46603, left P1 in 3, labial, 4, oblique lingual, and 5, occlusal views; 6-8, UALVP 46604, left P2 in 6, labial, 7, oblique lingual, and 8, occlusal views.

9-33. Presbyteria rhodoptyx new genus and species from the early middle Tiffanian (Ti3) Birchwood (BW) and DW-2 (DW2) localities, Paskapoo Formation, Alberta. 9-11, UALVP 43105 (DW2), right P1 in 9, labial, 10, oblique lingual, and 11, occlusal views; 12-14, UALVP 43106 (DW2), left P2 in 12, labial, 13, oblique lingual, and 14, occlusal views; 15-17, UALVP 43107 (DW2), right P3 in 15, labial, 16, oblique lingual, and 17, occlusal views; 18-20, UALVP 43108 (BW), left P4 in 18, labial, 19, oblique lingual, and 20, occlusal views; 21-23, UALVP 46609 (DW2), left P4 in 21, labial, 22, oblique lingual, and 23, occlusal views; 24-26, UALVP 47053 (DW2), left DP4 in 24, labial, 25, oblique lingual, and 26, occlusal views; 27-29, UALVP 46670 (DW2), left M1 or M2 in 27, labial, 28, oblique lingual, and 29, occlusal views; 30-32, UALVP 34128 (DW2), left M3 in 30, labial, 31, oblique lingual, and 32, occlusal views; 33, composite upper left dentition [consisting of UALVP 43105 (P1, reversed from original), UALVP 43106 (P2), UALVP 43107 (P3, reversed from original), UALVP 43108 (P4), UALVP 46670 (?M1), and UALVP 34128 (M3)] in occlusal view.

Scale bars = 5mm.

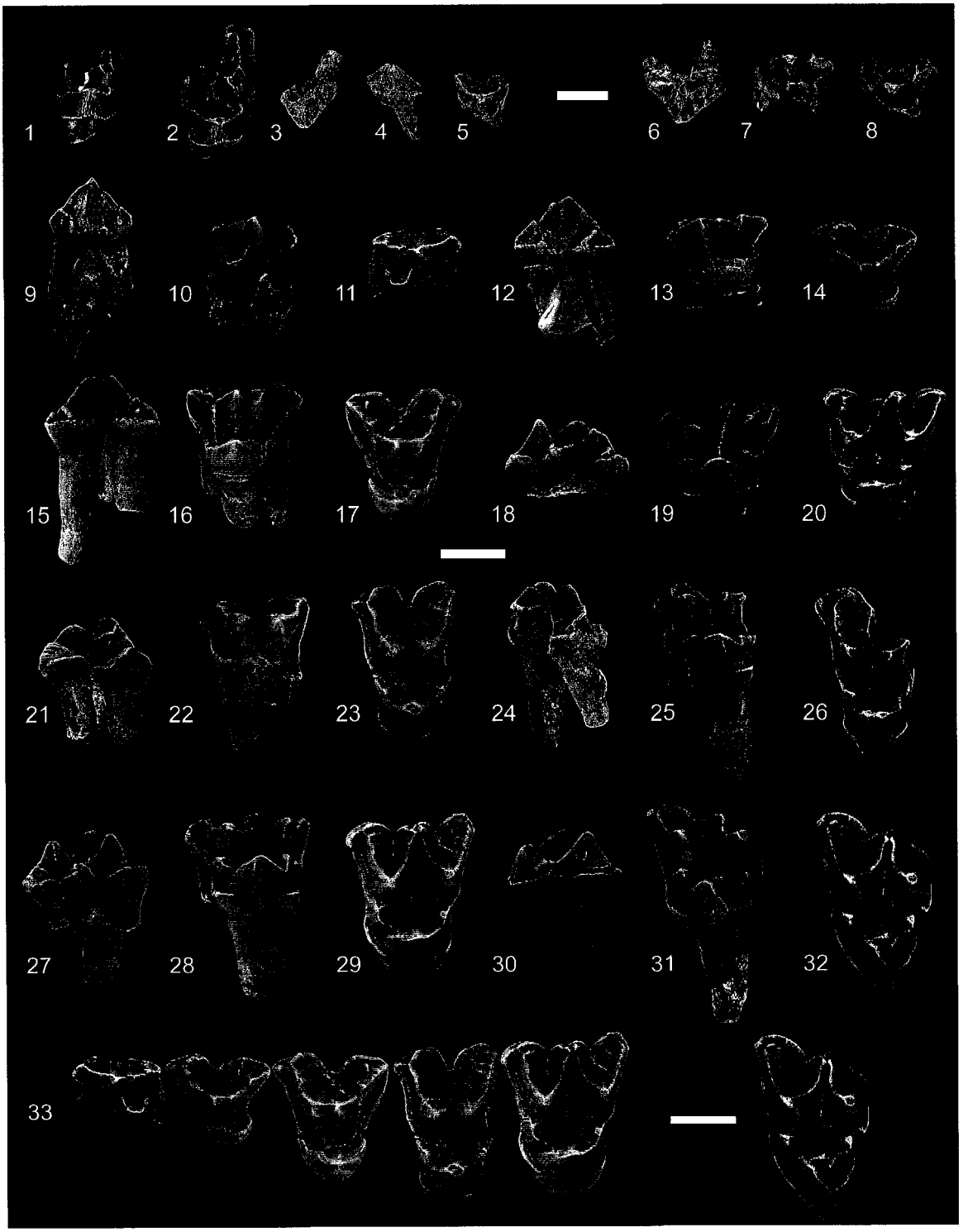
1
2
3
4
5
6
7
8
9
10
11
12
13
14
15
16
17
18
19
20
21
22
23
24
25
26
27
28
29
30
31
32
33

Figure 10.12.—1-13. Presbyteria rhodoptyx new genus and species from the early middle Tiffanian (Ti3) DW-2 locality, Paskapoo Formation, Alberta. 1-4, UALVP 47049, incomplete left dentary with c, p2-4, and alveoli for i1-3, p1 in 1, labial, 2, lingual, 3, occlusal, and 4, anterodorsal views; 5-7, UALVP 46673, lower right canine in 5, labial, 6, lingual, and 7, occlusal views; 8-13, UALVP 46606 (holotype), associated incomplete left and right dentaries with left p4, m1-2 and right p4, m1-2 in 8, 11, labial, 9,12, lingual, and 10, 13, occlusal views. Scale bars = 5 mm.

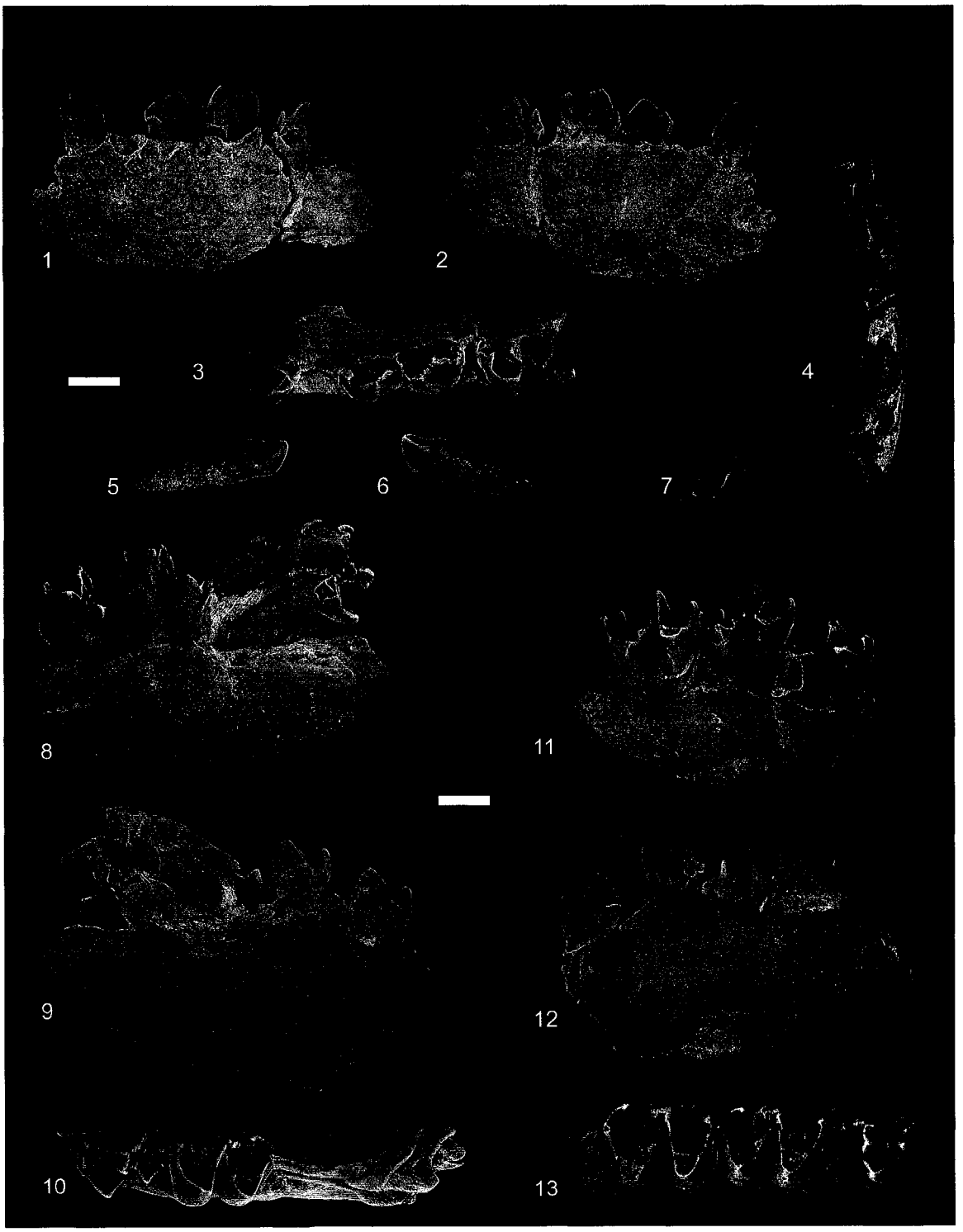
1
2
3
4
5
6
7
8
11
9
12
10
13

Figure 10.13.—1-6. Camera lucida outline drawings of upper and lower dentitions of Cyriacotherium argyreum Rose and Krause, late Tiffanian (?Ti5), Fort Union Formation, Wyoming, Presbyteria rhodoptyx new genus and species, early middle Tiffanian (Ti3), Paskapoo Formation, Alberta, and Pantolambda bathmodon Cope, middle Torrejonian (To2), Nacimiento Formation, New Mexico. 1, 4, Cyriacotherium argyreum. Composite upper right dentition based on PU 18821 (holotype), PU 18822, and PU 18823 in 1, occlusal view (reproduced from Rose and Krause, 1982); composite left lower dentition based on PU 18726, PU 18822, PU 19059, and PU 19060 in 2, occlusal view (reproduced from Rose and Krause, 1982). 2, 5, Presbyteria rhodoptyx. Composite upper right dentition based on UALVP 43105, 43106, 43107, 43108, 46670, and 34128 (all but P1 and P3 reversed from originals) in 2, occlusal view; composite lower left dentition based on UALVP 46673 and UALVP 46606 (holotype) in 4, occlusal view. 3, 6, Pantolambda bathmodon. AMNH 16663, incomplete right maxilla with P1-4, M1-3 in 3, occlusal view (reproduced from Rose and Krause, 1982); composite lower left dentition based on AMNH 16663 and AMNH 16664 in 6, occlusal view (reproduced from Rose and Krause, 1982). Outline drawings of the dentitions of Cyriacotherium and Presbyteria have been scaled such that M1 and m1 are of approximately equal dimensions to homologous teeth of Pantolambda. Scale bars = 5mm.

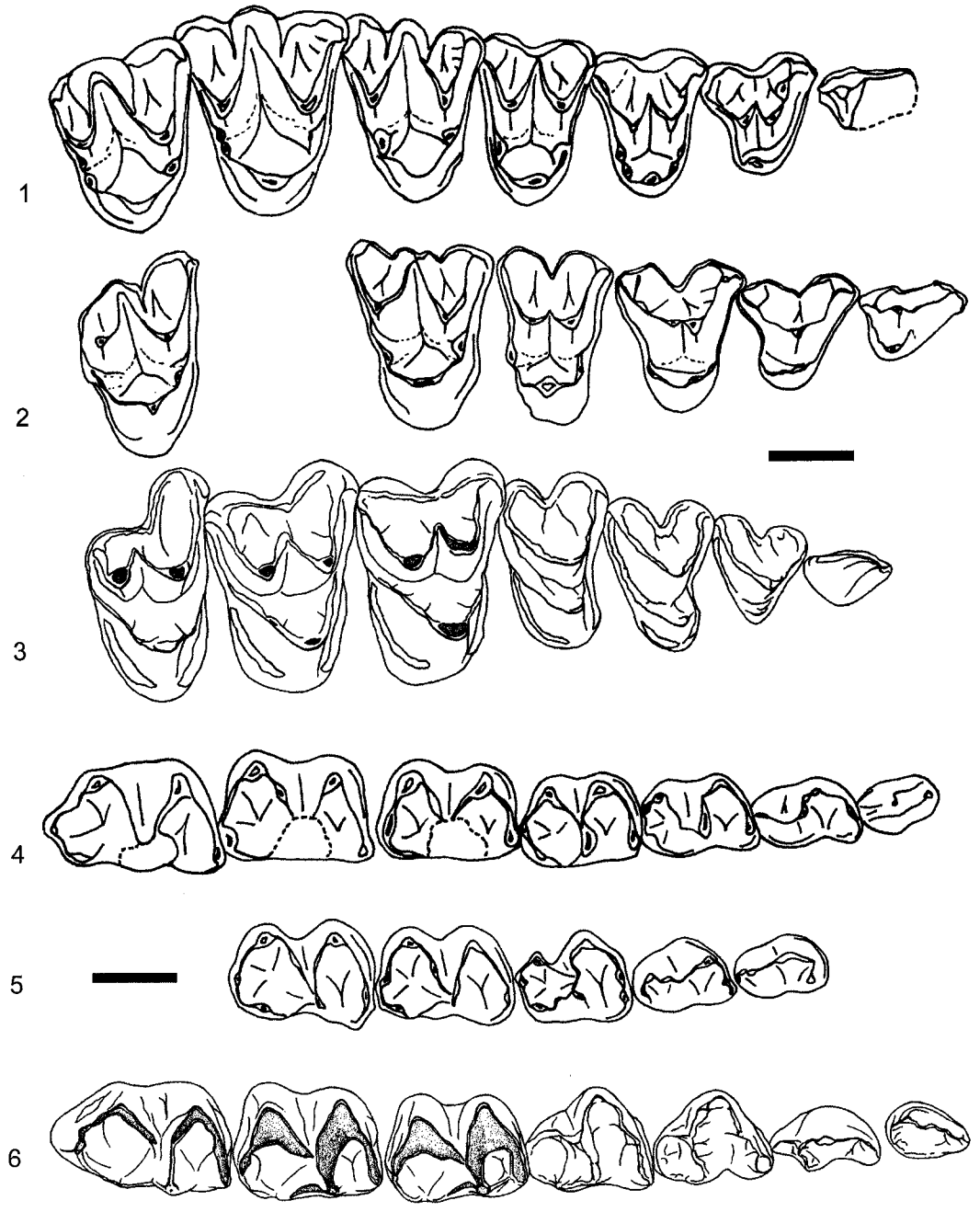
1
2
3
4
5
6

11 Horolodectes sunae, an Enigmatic Mammal from the Late Paleocene of Alberta, Canada

11.1 Introduction

SPECIMENS FROM DW-2 and nearby localities on the Blindman River in south central Alberta are well known for their excellent preservation, and the mammalian faunas documented at these localities often contain taxa that have not been found at well-sampled localities in the more southern parts of the Western Interior (e.g., Fox 1984a-d, 1990a-b; Scott 2003, 2005). In a review of Paleocene mammal localities from western Canada, Fox (1990a) reported on specimens from DW-2 that he believed pertained to three different taxa (reported as "Arctocyonidae, new genus and species 1," "Arctocyonidae, new genus and species 2," and "Aphronorus sp." in the faunal list). After publication of Fox (1990a), the first fossils from the Birchwood locality were discovered, and among these were two nearly complete dentaries and one fragmentary maxilla of an unusual placental mammal with teeth similar to those referred to the three taxa recognized by Fox (1990a) from DW-2. In a faunal study of the Birchwood locality, Webb (1996) and Webb and Fox (1998) demonstrated the association of the specimens from DW-2 and Birchwood, and considered them representative of a new genus and species of oxyclaenid condylarth. Since Webb's (1996) and Webb and Fox's (1998) studies, new specimens of this unusual mammal have been collected from DW-2, Birchwood, and most recently Cochrane 2, sparking a renewed interest in their study and culminating in the current chapter.

11.2 Systematic Paleontology

Class MAMMALIA Linnaeus, 1758

Subclass THERIA Parker and Haswell, 1897

Infraclass EUTHERIA Gill, 1872

Order uncertain

Order uncertain

Genus HOROLODECTES new genus

Type and only known species.—Horolodectes sunae new species.

Diagnosis.—As for the type and only species.

Etymology.—Horologion, Greek noun (feminine), "hourglass"; dektes, Greek noun, "biter". In reference to the peculiar hourglass shaped occlusal outline of the premolars.

HOROLODECTES SUNAE new species

Figures 1-3; Tables 1, 2

Arctocyonidae, new genus and species 1: FOX, 1990a, p. 61.
Arctocyonidae, new genus and species 2: FOX, 1990a, p. 61.
?Aphronorus sp.: FOX, 1990a, p. 61.
Oxyclaenid, new genus and species: WEBB and FOX, 1998, p. 40A.

Diagnosis.—Differs from all other eutherians in having a combination of trenchant premolars with strongly posteriorly leaning crowns, lower premolars premolariform with undeveloped talonids, and lower molars with twinned entoconid and hypoconulid. Differs further in m3 having an enlarged entoconulid, and having entoconulid, entoconid, and hypoconulid closely spaced. Differs further in upper premolars and molars having a well developed, neomorphic anterolabial crest connecting paracone to labial margin of the crown.

Description.—Skull and upper dentition: Maxilla: Seven incomplete maxillae have been recovered from the Birchwood and DW-2 localities, three of which preserve parts of the facial and palatine processes (see Fig. 1.1-1.5, 1.11, 1.12, 1.13-1.17). The facial process of the maxilla is high, especially dorsal to P3; a shallow concavity is developed posterior to the infraorbital foramen, possibly representing the anteriormost part of the antorbital fossa, the site of origin for nasolabial muscles (Butler, 1956;

Turnbull, 1970; Novacek, 1986). The degree of excavation and height of the concavity, in combination with the large diameter of the infraorbital foramen (see below), are indicative of well-developed snout musculature (Novacek, 1986). The anterior root of the zygoma is not evident on any of the specimens at hand (see e.g., Fig. 1.12), suggesting the maxillary process probably originated posterior to M1.

The infraorbital foramen, marking the anterior exit of the infraorbital vessels and nerve from the infraorbital canal, is preserved on three specimens. The large and subovate aperture is dorsal to P3, and opens anteriorly and slightly laterally (Fig. 1.1, 1.11). The infraorbital canal extends posteriorly and medially through the facial process; although the maxillary foramen is not preserved on any of the specimens, parts of the canal walls can be seen on the medial side of UALVP 42073, dorsal to P4, indicating the canal extended to at least the posterior limit of P4, and possibly opened above the posterior parts of M1. The anterior position of the infraorbital foramen implies the canal may have been long relative to that in advanced eutherians, its position more nearly approximating that in Kennalestes Kielan-Jaworowska, 1969, Cimolestes cerberoides Lillegraven, 1969, and primitive eutherians generally (Novacek, 1986). A second, tiny foramen anterior to the infraorbital foramen opens dorsal to P2 on UALVP 42073 (Fig. 1.1); the aperture is subdivided into small, rounded dorsal and smaller, subovate ventral openings.

Little can be said of the palatal process of the maxilla; it is best seen on UALVP 45704, which preserves parts of the process anteriorly to the level of P3, and posteriorly to the lingual alveolus of M2. There is no evidence of palatal vacuities in the parts preserved; a thickened and finished surface medial and anterior to the lingual root of M2, extending anteromedially to about the level of the anterior part of P4, probably represents the surface of articulation of the maxilla with the palatine, although the palatine itself is not preserved. Large nutritive foramina occur adjacent and slightly posterior to the lingual roots of the premolars and molars, and often on the bone between successive teeth.

Upper premolars (Figs. 1.1-1.12, 1.21): UALVP 42073, an incomplete left maxilla with P2-4, and UALVP 45712, an incomplete right maxilla with P2-3, are the only specimens of Horolodectes in the collection that preserve parts of the dentition

anterior to P3. The posterior wall of a small alveolus anterior to P2 on UALVP 42073 housed a small, probably single rooted P1; this interpretation is in keeping with the lower dentition, which includes a reduced p1 and a large canine alveolus.

P2: P2 of Horolodectes is two-rooted, subtriangular in occlusal outline, and slightly lower than P3. The anterior root is stout, nearly circular in cross section, and is oriented anterodorsally; the posterior root is more nearly vertical than the anterior root, wider, and anteroposteriorly compressed. P2 is premolariform and consists of a large, posteriorly leaning paracone. The prevallum surface is long, while the postvallum surface is shorter, flatter, and more nearly vertical, giving the crown an asymmetrically triangular labial profile. A weak bulge of enamel supported by the posterior root arises lingual to the paracone, but a protocone is not developed. A faint preparacrista runs anteriorly to near the base of the crown, while a robust postparacrista extends posteriorly to the base of the paracone. A short, conspicuous crest originating at the paraconal apex extends to the lingual wall of the paracone towards the lingual bulge; a fourth crest, also originating at the paraconal apex, extends a short distance posterolabially before fading into the labial wall of the crown.

P3: A short diastema separates P2 and P3. P3 of Horolodectes is semimolariform, three-rooted, and roughly triangular in occlusal outline. The labial roots are similar to those of P2: the anterior root is stout, circular in cross section, and is oriented anterodorsally, while the posterior root is wider, anteroposteriorly compressed, and more nearly vertical. The enamel at the labial roots is slightly exodaenodont. The lingual root is subequal to or slightly larger than the anterior labial root, circular in cross-section, and is oriented anterodorsally. A large paracone and smaller protocone form the crown of P3, the two separated by a narrow, shallow valley. The paracone is subtriangular in occlusal outline, its labial side nearly flat, while its lingual side is somewhat swollen. A long preparacrista runs to the anterolabial corner of the crown where it joins with a weakly developed precingulum; a short postparacrista extends posteriorly and continues labially as a raised ridge; a small cuspule occurs at the end of this ridge on one specimen (UALVP 39463). A robust crest originating at the apex of the paracone runs labially to near the base of the paracone; the area between this crest and the postparacrista is slightly concave. Neither metacone, paraconule, nor metaconule are developed. The protocone is

smaller and lower than the paracone, subconical, and separated from the base of the paracone by a shallow valley. The preprotocrista is short and directed labially towards the base of the paracone, where it can end or continue along the lingual wall to the paraconal apex; the postprotocrista can be faintly (e.g., UALVP 42073, see Fig. 1.3) or strongly (e.g., UALVP 45717) developed, extending labially from the protoconal apex. A well-developed postcingulum arises from the posterior wall of the protocone and joins the postprotocrista before extending to the posterolabial corner of the crown; in one specimen, it wraps around the lingual side of the protocone (UALVP 42073), but in none of the specimens do the precingulum and postcingulum meet lingually. Posteriorly sloping wear facets on the posterior surfaces of the paracone, protocone, and postcingulum indicate the main shearing surface of P3 is on the postvallum wall, whereas the anterior face of P3 is virtually unworn.

P4: The crown of P4 is hourglass-shaped in occlusal aspect, with a well-developed paracone and protocone. The crown is larger and taller than that of P3, but similarly leans posteriorly, with a long prevallum surface and a shorter, steeper postvallum surface. The lingual root is larger than on P3, in keeping with the enlarged protocone, and the enamel at the anterior root is more exodaenodont. A stylar shelf is not present. The ectocingulum is complete across the labial side of the crown, and although weakly developed anteriorly, it is conspicuous posteriorly, becoming thicker and more robust; a shallow ectoflexus divides the labial side of the crown into nearly symmetrical lobes. The preparacrista, paracone, and postparacrista are similar to those on P3, and the postparacrista, ectocingulum, and postcingulum unite at the posterolabial corner of the crown. As on P3, a stout crest originating at the paraconal apex extends labially towards the ectocingulum, but does not unite with it; the area between this crest and the postparacrista is similarly concave. The protocone is larger and taller than on P3, more closely appressed to the paracone, and is compressed anteroposteriorly. The preprotocrista is shorter than on P3, but is similarly directed toward the base of the paracone where it may end or ascend the lingual wall towards the paraconal apex. A well-developed postprotocrista extends posterolabially from the protoconal apex to join the postcingulum; the trigon basin is shallow, narrow, and slopes posteriorly. The postcingulum is better developed than the precingulum and extends to the posterolabial

corner of the crown; the pre- and postcingulum can unite along the lingual side of the protocone (e.g., UALVP 42073) or can be discontinuous (e.g., UALVP 39465). Wear on the postvallum surface of the crown has produced broad, posteriorly sloping facets on the paracone, postparacrista, protocone, and postprotocrista, in some specimens exposing large areas of dentine. Anterior wear is greater than on P3, with broad but shallow facets on the preparacrista and the anterior side of the paracone and protocone.

Upper molars (Figs. 1.11-1.21): M1 and M2 of Horolodectes are known both from articulated and isolated specimens, including UALVP 45704 in which M1 is in articulation with the maxilla; M3 is known from only a single specimen (UALVP 45719).

M1: M1 is subequal in size to P4; the crown is subtriangular in occlusal view, considerably wider than long, and leans posteriorly as the premolars, although to a lesser degree. The labial roots are smaller than on P4, but are of similar orientation: the anterior root is directed anterodorsally, whereas the posterior is more nearly vertical; the lingual root is larger than either labial root, oval in cross section, and leans anteriorly. A stylar shelf is not developed; a shallow ectoflexus divides the labial side of the crown into weakly differentiated lobes, with the metastylar corner projecting further labially. The ectocingulum is low but conspicuous; a shallow vertical notch can be developed labial to the deepest part of the centrocrista, interrupting the ectocingulum as it progresses along the labial margin of the crown. The preparacrista is short and steep, and joins the well-developed preparaconular crista+paracingulum and ectocingulum at the anterolabial corner of the crown; the postmetacrista is longer than the preparacrista, and curves abruptly labially, joining the postcingulum and ectocingulum. A well-developed crest, similar to that on the upper premolars, extends from the paraconal apex labially to the ectocingulum. The paracone is slightly larger and taller than the metacone, and both are flat labially and swollen on their lingual sides. Both the paraconule and metaconule are prominent and appressed to the bases of the paracone and metacone. The preparaconular and postmetaconular cristae are short; the preparaconular crista runs labially to join the anterior cingulum, while the postmetaconular crista extends a short distance posterolabially, abutting the posterior cingulum. The postparaconular crista meets a short, lingually directed crest arising from near the lingual base of the paracone, and the two crests form a shallow notch at their union; the premetaconular crista is poorly

developed. The protocone is subequal in height to the paracone and metacone, but more massive, with flat labial and convex lingual sides. The protoconal cristae are conspicuous, and form shallow, slit-like notches at their intersection with the lingual side of the paraconule and metaconule. The anterior and posterior cingula are incomplete around the lingual side of the protocone, and although both are robust, the posterior cingulum is nearly twice as wide as the anterior. While a faint swelling can occur on the lingual extremity of the postcingulum, a distinct hypocone is not developed.

M2: M2 of Horolodectes is slightly longer than M1, and the crown is similarly subtriangular in occlusal aspect, but differs in having a rounded rather than acute posterolabial corner that does not project labially (Fig. 1.15). The ectoflexus is shallow, and the ectocingulum is more robust than on M1, and complete labially, with no development of a vertical notch labial to the deepest part of the centrocrista. The paracone is larger than on M1, and the crest connecting the paraconal apex and ectocingulum is longer and more robust. M2 differs further from M1 in having a relatively smaller metacone, a shorter postmetacrista, and a more robust postcingulum. The notches formed between the preprotocrista and paraconule, postprotocrista and metaconule, and between the postparaconular crista and the crest at the base of the paracone, are deeper on M2 than those on M1. A swelling can be developed at the lingual extremity of the postcingulum as on M1, but a hypocone is not present.

M3: Although M3 is known only from an isolated tooth (UALVP 45719), the presence of the unusual crest extending labially from the paraconal apex to the ectocingulum, the large, labially positioned conules, and the slit-like notch between the preprotoconal crista and paraconule (a combination of features seen on M1-2 of Horolodectes, see above) support its referral to Horolodectes. M3 is smaller than M1 or M2, and subtriangular in occlusal view. A stylar shelf is not present; the ectoflexus is shallow as on M1 and M2, dividing the labial side of the crown into acute parastylar and smoothly rounded, reduced metastylar areas. The ectocingulum is robust anteriorly and notched medially as on M1, but fades posteriorly as it approaches the metastylar area; the postmetacrista and metacingulum are not developed. As on M1 and M2, the preparacrista, paracingulum, and preparaconular crista are conspicuous and unite at the anterolabial corner of the crown, and the labial crest running from the paraconal apex to

the ectocingulum is robust. The paracone is larger than the metacone and leans anteriorly; the metacone is low, conical, and joined to the paracone by a widely V-shaped centrocrista. The conules are prominent, although less so than on M1-2, and the postparaconular crista unites with a crest at the lingual base of the paracone, forming a small but well-defined notch. The protocone is large, and a faint, labiolingually oriented ridge bisects its labial side, and the preprotoconal crista forms a deeply incised notch at its union with the paraconule. The protoconal cingula are robust and no hypocone is developed.

Dentary and lower dentition: Eleven incomplete dentaries of Horolodectes have been recovered. The holotype, UALVP 39200, is the most nearly complete, preserving p2-4, m1-3, and the incisor and canine alveoli (see Fig. 2).

Dentary (Figs. 2, 3): The mandibular corpus is long and gently convex ventrally, with its deepest parts occurring posterior to p4, and tapering anteriorly. The medial and lateral surfaces are slightly convex in anterior view, and meet ventrally at a well-defined ridge; this ridge, possibly the area for insertion of the digastric musculature, continues anteriorly to the posterior border of the symphyseal surface and posteriorly to below m1 or m2, where it fades away. Two mental foramina are present labially: the larger and more dorsal occurs ventral to p2, while the second is ventral to the posterior root of p3; both foramina are subovate and open dorsolaterally. The symphyseal surface is long and shallow, and consists of two areas of raised bone forming upper and lower arms: the upper arm is short and deep, while the lower arm is slightly longer posteriorly and shallower; the arms meet anteriorly and the area between the upper and lower arms is slightly concave. The symphyseal bone is smooth and finished, with no evidence of an interdigitating sutural attachment between the dentaries, implying that the symphysis remained unfused in life. The condylar and angular processes are not preserved on any of the specimens, and only parts of the coronoid process remain on one specimen; from the parts preserved, the process was long and its anterior edge was inclined approximately 60 degrees from horizontal. Only the anteriormost part of the masseteric fossa is preserved among the specimens at hand: the fossa is deeply excavated and delimited anteriorly and ventrally by the coronoid and masseteric crest, respectively. The dorsal part of the medial surface of the coronoid process is excavated as a shallow temporalis fossa, with

its ventral extremity marked by a short, longitudinal ridge; the fossa represents the area of insertion for the deep temporalis musculature (see Turnbull, 1970; Wible, 2003). The dentary contains five alveoli anterior to p2; as discussed below, these are interpreted as having housed i1-3, c, and p1.

Lower incisors (Fig. 2.1): The alveoli for three lower incisors are preserved on UALVP 39200; the incisor alveoli, together with the canine and p1 alveoli, are oriented parasagittally and slightly oblique to the rest of the tooth row. The anteriormost alveolus is narrow, subovate, and opens anteriorly; it housed a large, laterally compressed, procumbent medial incisor.

The i2 alveolus is positioned posterior, lateral, and slightly dorsal relative to the i1 alveolus, with no diastema separating the two, implying that i1 and i2 were closely appressed. The i2 alveolus is similar to that for i1: the aperture is large, subovate, and laterally compressed, and the incisor housed in it probably resembled i1.

The alveolus for i3 is much smaller than those for i1-2, and is positioned between the posteroventral margin of the i2 alveolus and the anterolabial rim of the lower canine alveolus, essentially squeezed between the two larger teeth. The i3 alveolus is subcircular and directed anteriorly and laterally, but slightly more dorsal to those of i1-2. There are no diastemata between the i3 alveolus and either that for i2 or the canine, and i3 was probably appressed to i2.

Lower canine (Fig. 2.1): The canine alveolus is the largest of the five alveoli anterior to p2 and is positioned directly behind those for i2 and i3. The aperture is subcircular and oriented anterolabially-posterolingually, slightly oblique to the molar row; the alveolus opens dorsally, anteriorly, and slightly laterally.

Lower premolars (Figs. 2, 3): p1: The p1 of Horolodectes is known only from its alveolus. There is but a single alveolar opening, indicating p1 was single-rooted. The alveolus is subcircular and shallow; like the canine alveolus, it is oriented anterolabially-posterolingually, suggesting the crown of p1 may have splayed labially in much the same manner as that of the modern opossum, Didelphis virginiana Kerr.

p2: The crowns of p2-4 are premolariform and inflated to varying degrees (see e.g., Fig. 2.1, 2.4, 3.1). The p2 of Horolodectes is two-rooted, with a moderately compressed crown that is dominated by a posteriorly leaning protoconid. The anterior

root is stout and circular, and directed anteroventrally, while the posterior root is smaller, anteroposteriorly compressed, and more nearly vertical. The protoconid is tall and inflated, with a pointed apex; in occlusal view, a constriction occurs midway along the length of the crown, dividing the tooth into narrow anterior and wider posterior lobes. The labial side of the protoconid is weakly convex, while the lingual side is flatter; the postvallid surface is shallowly concave. A robust crest originating at the protoconid apex extends to the anterolingual corner of the crown, and neither paraconid nor metaconid is present. The talonid consists only of a raised and thickened crest extending transversely across the posterior side of the protoconid at its base, and on most specimens is elevated at its lingual extremity as an incipient cuspid. Four prominent crests are developed on the postvallid surface, each originating at the protoconid apex: the labial and lingual of these crests extend only a short distance down the postvallid surface before disappearing; the two remaining crests are medial to the labial and lingual crests, are more pronounced, and extend further ventrally on the postvallid surface, nearly reaching the posterior transverse crest. The spaces between the postvallid crests are deep and crevasse-like.

p3: The p3 crown of Horolodectes is larger, taller, and more inflated than that of p2, the roots are larger, and the anterior root is directed similarly anteroventrally. The mid-crown constriction is more pronounced than on p2, and the lobes are relatively and absolutely wider. The crown differs further from that of p2 in a number of features: the protoconid is larger; the crest extending anteriorly from the apex of the protoconid is more prominent; the posterior transverse crest of the talonid is higher, slopes labially, and the incipient lingual cuspid is better developed. A faint lingual cingulid extends posteriorly to meet the transverse crest on some specimens. The postvallid crests are similar to those on p2, but are stronger and sharper, the crevasses between adjacent crests are deeper, and the more lingual of the medial crests extends nearer to the posterolingual base of the crown. The crown is exodaenodont, with well-developed anterior and posterior enamel lobes.

p4: The p4 of Horolodectes is the largest and tallest post-canine tooth, its crown more massive and taller than that of p3; the roots are similar to those on p2-3 but are much stouter. A constriction divides the crown into anterior and posterior lobes as in p2-3, but the constriction is stronger and the lobes are better defined and relatively wider,

especially posteriorly. The protoconid is large and somewhat compressed laterally, and leans posteriorly; its labial and lingual sides are slightly inflated and the enamel is weakly wrinkled. A strongly developed, sharp crest extends from the protoconid apex to the anterolingual corner of the crown, where it joins with a weak lingual cingulid; neither paraconid nor metaconid is present. As with the other premolars, a basined talonid is not developed on p4: the posterior transverse crest is higher and better developed than on p2-3 and bears a stronger lingual cuspule; the transverse crest slopes labially as on p3. The postvallid crests are similar to those on p2 and p3, but are even more prominent and form raised, sharp edges; the crevasses between adjacent crests are deeper and the enamel can be wrinkled. The crown is markedly exodaenodont, with deep enamel lobes over both roots.

Lower molars (Figs. 2, 3): The lower molar crowns of Horolodectes are low, with the trigonids little elevated above the talonids; the cusps are sharp, the talonids are wide and moderately deep, and the crowns lean slightly lingually (see e.g., Fig. 3.1).

m1: The crown of m1 is subrectangular in occlusal outline, with the trigonid slightly narrower than the talonid. The roots are similar to those of p4 but diverge to a lesser degree (i.e., the anterior root projects less anteroventrally). The trigonid is higher than the talonid compared to m2 and m3, and the trigonid cusps are nearly equidistant from each other, forming a near-equilateral triangle in occlusal view; the postvallid surface is oblique, rather than perpendicular, to the long axis of the jaw. The trigonid cusps are subconical with sharp apices and swollen internal walls. The protoconid and metaconid are subequal in both size and height, and their apices lean slightly posteriorly, while the paraconid is smaller and lower, more lingual, and projects anteriorly. The paracristid extends anterolingually from the protoconid apex to that of the paraconid; on unworn specimens, a short, stout crest originating at the paraconid apex descends the posterior side of the paraconid and forms a broad notch near the base of the metaconid. The protocristid is well developed and deeply notched. The talonid of m1 is wider than long and moderately deep; the flat and internally sloping walls of the hypoconid and entoconid form a V-shaped basin. The hypoconid is the largest talonid cusp and is slightly lower than the entoconid; the entoconid is tall, with an acute apex, and is appressed to the lingually positioned hypoconulid. The hypoconulid is slightly lower

than the entoconid and anteroposteriorly compressed; a deep, slit-like notch interrupts the postcristid between the two cusps. Neither an entoconulid nor mesoconid is present. The entocristid is short and high, and the cristid obliqua joins the postvallid surface labial to the protocristid notch. Short, weak anterior and posterior cingulids are developed, but are discontinuous labially; a prominent hypoflexid shelf is present posterior to the protoconid.

m2: The m2 of Horolodectes is of similar size to m1 but the crown is lower, the talonid longer and broader, and the cusps less robust. The trigonid is anteroposteriorly compressed and more transverse than in m1, the postvallid surface is more nearly perpendicular to the long axis of the jaw (rather than obliquely oriented, as in m1), and the trigonid angle is more acute. The protoconid and metaconid are subequal in size, with swollen internal walls; the protoconid is slightly lower than the metaconid, and is smaller and lower relative to that on m1. The paraconid is appressed to the metaconid, is more labial than on m1, and does not project anteriorly. The paracristid is longer, higher, and more transverse than on m1, bending abruptly lingually from the protoconid apex towards the paraconid; the protocristid is shallowly notched. Although the talonid of m2 is longer and broader than that of m1, its overall morphology is similar: the internal walls of the hypoconid and entoconid form a moderately deep, V-shaped basin; the hypoconid is the largest cusp and is slightly lower than the entoconid; the hypoconulid is appressed to the entoconid; and a slit-like notch interrupts the postcristid. Neither an entoconulid nor mesoconid is developed, and the entocristid and cristid obliqua are similar to those on m1. Although the anterior cingulid is more conspicuous than on m1, the ectocingulid remains undeveloped, and the hypoflexid shelf is stronger.

m3: The crown of m3 is lower, longer, and transversely narrower than that of m1 or m2, and the trigonid and talonid are subequal in width and height. The trigonid is anteroposteriorly compressed, even more so than in m2, and the postvallid surface is oriented perpendicular to the long axis of the jaw. Although the trigonid cusps are smaller than on m1 or m2, their morphologies are similar: the paraconid is smaller and less distinct than on m2, being further incorporated into the paracristid, but is similarly high on the trigonid and appressed to the metaconid; the protoconid and metaconid are subequal in size, and their basin-facing walls slightly swollen; and both protoconid and

metaconid are smaller and lower than on m2. The paracristid is longer than on m2 but is otherwise similar in structure, bending sharply lingually from the protoconid and joining the paraconid apex; the protocristid is well developed and the protocristid notch is shallow. The talonid is longer and narrower than in m1 and m2. As in m1 and m2, the internal walls of the hypoconid and entoconid on m3 form a V-shaped basin, and while the hypoconid is the largest talonid cusp, it is lower than the entoconid and hypoconulid. The entoconid and hypoconulid are large, closely appressed and swollen, and the postcristid notch is broader than on m2. A robust entoconulid arises on the entocristid immediately anterior and lingual to the entoconid; the cusp is slightly smaller and lower than either the entoconid or hypoconulid, and is appressed to the entoconid such that the hypoconulid+entoconid+entoconulid forms a comb-like complex along the posterolingual margin of the talonid. A deep, slit-like notch occurs between the entoconid and entoconulid, and the cristid obliqua is low, joining the postvallid surface labial to the protocristid notch. The anterior cingulid is better developed than on m1 and m2, and continues around the protoconid as a short ectocingulid, terminating beneath the hypoflexid; the posterior cingulid is short but conspicuous.

Etymology.—Sunae, in honour of Yongqin Sun, UALVP, for her skilled preparation of even the most delicate of specimens, including many referred to Horolodectes.

Holotype.—UALVP 39200, incomplete right dentary with p2-4, m1-3, and alveoli for i1-3, c, p1 (Figs. 2.1-2.3). Birchwood locality, Paskapoo Formation of Alberta, late Paleocene [early middle Tiffanian, Ti3 (Fox, 1990a), Plesiadapis rex/P. churchilli Lineage Zone of Lofgren et al., 2004)].

Other material examined.—From Cochrane 2: UALVP 46376, 46377, P4; UALVP 46375, M1; UALVP 46374, M2; UALVP 46373, m2; UALVP 46371, 46372, m3.

From the Birchwood locality: UALVP 45704, incomplete right maxilla with P3-4, M1; UALVP 39463, incomplete right maxilla with P3-4; UALVP 45706, incomplete right maxilla with P3-4; UALVP 45720, isolated right P4; UALVP 39464, isolated left P4; UALVP 39465, isolated right P4; UALVP 45705, isolated right M2; UALVP 39201, incomplete right dentary with p2-4, m2-3, and alveoli for c, p1; UALVP 45710,

incomplete right dentary with p3-m1; UALVP 45709, incomplete left dentary with p2-4, m1-2; UALVP 45708, incomplete left dentary with p2-3; UALVP 39290, incomplete left dentary with m2-3; UALVP 39292, isolated right p3; UALVP 39293, isolated left p4; UALVP 45707, isolated left p4; UALVP 39291, isolated right m1; UALVP 39294, isolated left m2.

From the DW-2 locality: UALVP 42073, incomplete left maxilla with P2-4; UALVP 45712, incomplete right maxilla with P2-3; UALVP 45714, incomplete left maxilla with P3-4; UALVP 42074, incomplete right maxilla with M1-2; UALVP 45717, isolated left P3; UALVP 45715, isolated right P4; UALVP 42075, associated (not articulated) left M1 and M2; UALVP 42076, isolated right M1 or M2; UALVP 45718, isolated right M1 or M2; UALVP 45719, isolated right M3; UALVP 45713, incomplete left dentary with p2-4, m1-3; UALVP 45711, incomplete right dentary with p2-4, m1-3; UALVP 45716, incomplete left dentary with p2-4, m1-2; UALVP 46370, incomplete left dentary with p2-3 (erupting), m1-2, and alveoli for m3; UALVP 40667, incomplete left dentary with m1-3.

Age and occurrence.—Earliest Tiffanian (Plesiadapis praecursor/P. anceps Lineage Zone, Ti1) to early middle Tiffanian (Plesiadapis rex/P. churchilli Lineage Zone, Ti3) of Alberta.

11.3 Conclusions

Mandibular Dental Eruption in Horolodectes

UALVP 46370 (Fig. 3.4-3.6) represents an immature individual of Horolodectes sunae, and allows limited inference on the timing of mandibular dental eruption. UALVP 46370 is an incomplete dentary having erupting p2-3, m1-2 in place, and the alveoli for p1, p4, and m3; neither the parts of the dentary anterior to the p1 alveolus, nor the coronoid, condylar, or angular processes are preserved. The corpus of UALVP 46370 is smaller and shallower than that of the holotype (which is from an adult individual, as evidenced by the complete complement of replacement premolars), and none of the deciduous dentition is retained; the replacement p2 is approximately two-thirds erupted,

its crown almost completely above the alveolar rim, while the replacement p3 is just beginning to erupt, the apex of the protoconid being flush with the alveolar rim. Both m1 and m2 are fully erupted, and although both teeth display limited wear, that of m1 is heavier; the m3 is not present.

From the stage of dental eruption on UALVP 46370, it can be inferred that both m1 and m2 erupted before p2 or p3, with m1 probably the earlier as evidenced by heavier wear relative to m2. The p2 preceded p3, both of which were probably preceded by p4, an inference consistent with the wear pattern seen in the upper teeth. Little can be said of the timing of eruption for p1 or m3: although p1 (or dp1, see Luckett, 1993) is not preserved in UALVP 46370, evidence from extant eutherians suggests p1 erupts around the same time or earlier than m1 (Ziegler, 1971; Slaughter et al., 1974; Luckett, 1993); both m1 and m2 have erupted on UALVP 46370, and p1 was probably present at the time of death and lost prior to burial. While the alveoli for m3 indicate the tooth had erupted prior to death, little can be said of its timing relative to the other teeth. Slaughter et al.'s (1974) analysis of dental replacement patterns in eutherian mammals found only a few species in which m3 was the final tooth to erupt; these findings are consistent with studies of dental replacement patterns in extinct eutherians, in which m3 is inferred to have erupted at approximately the same time or prior to p2 (e.g., Gingerich, 1976 for replacement patterns in the plesiadapid primate Plesiadapis Gervais; Bloch et al., 2002 for replacement patterns in the paromomyid primate Acidomomys Bloch, Boyer, Gingerich, and Gunnell, 2002). From the evidence seen on UALVP 46370, the likeliest eruption sequence of the replacement mandibular post-canine dentition of Horolodectes is hypothesized as (?p1/dp1)-m1-m2-p4-p2-p3, with m3 probably erupting at the same time or prior to p2. This replacement sequence is probably derived for eutherians [compare with the eruption sequence in the Late Cretaceous eutherians Asioryctes Kielan-Jaworowska, 1975, and Kennalestes, in which p3 erupts prior to p4, and see discussion in Bloch et al. (1998)] and is also seen in some extant tenrecids (e.g., Tenrec ecaudatus Schreber) and erinaceids (e.g., Echinosorex gymnurus Raffles and Erinaceus Linnaeus) (see Slaughter et al., 1974).

Dental Function in Horolodectes

Coronal structure and distribution of wear facets on mammalian dentitions have long been used to study functional aspects of occlusion and the direction of mandibular movement, and for inferring diet (e.g. Crompton, 1971; Butler, 1973; Fox, 1975; Hiiemae, 1978; Lucas, 1979; Rensberger, 1986; Hunter and Fortelius, 1994; Dewar, 2003). The unusual structure of the premolar crowns in Horolodectes is suggestive of a mode of mastication that emphasized postvallum-prevallid shear, particularly between P4 and m1, and a limited degree of molar shear combined with horizontal grinding.

The trenchant crowns of the upper and lower premolars of Horolodectes are almost certainly adapted for shearing. Shear appears to be primarily between P4 and m1, a condition analogous to that in carnivorans and various lipotyphlans (Butler, 1988; Fox and Youzwyshyn, 1994), with the posterior face of P4, including the postparacrista, postprotocrista, and postcingulum usually heavily worn. A series of successively more heavily worn P4s of Horolodectes demonstrates that wear is initially concentrated along the posteroapical surface of the paracone and protocone, with broad posterodorsally sloping facets developed as wear continues. In some specimens wear is so heavy that extensive areas of dentine are exposed on the posterior parts of the paracone and protocone, and the shearing surface becomes nearly vertical. The corresponding occlusal surface, the prevallid surface and paracristid of m1, shows similarly intense wear: initially, wear is concentrated along the paracristid and anterior side of the protoconid; a broad facet is developed along the anterolabial side of the protoconid during later stages of wear, the paracristid and anterior cingulid become heavily worn, and the paraconid is often planed flat (e.g., UALVP 39200, Fig. 2.1-2.3). The entire prevallid surface is worn virtually flat on the most heavily worn specimens. As P4 becomes further worn, the crowns of P2-3 become more important in shearing function: articulated specimens of P3-P4 showing increasing degrees of wear indicate that in the early stages of wear P4 is the dominant premolar in shearing function; as the crown of P4 becomes more worn (and lower), P3 becomes more involved in shearing, resulting in heavier wear on its crown and greater wear on the prevallid surface of p4. Although postvallum-prevallid shear between P4 and m1 predominates, broad, shallow facets on the anterior part of P4, with complementary facets on the posteroapical part of the p4 protoconid, indicate that

prevallum-postvallid premolar shear became more important after extended wear. The molars of Horolodectes are comparatively primitive, but they too show evidence of limited shearing capability, in addition to their function in grinding: the molar cusps are acute rather than bunodont; the centrocrista, precingulum, paracristid, and protocristid are all sharp; and strong notches are developed between the conules and the paracone and metacone, and on the postcristid between the entoconid and hypoconulid. Although the large molar protocone, broad talonid basin, and wear on the lingual wall of the hypoconid from occlusion with the protocone of the corresponding upper molar are consistent with a grinding component to the masticatory cycle, the weak postcingulum and undeveloped hypocone indicate this function in Horolodectes was not as well developed as in other eutherians (e.g., compare with molars of many condylarths and lipotyphlan insectivorans in which the hypocone is better developed).

The function of the unusual neomorphic, labial paracone crests on the upper premolars and molars is less clear, as they do not directly occlude with any matching surface on the lower teeth. The crests likely functioned initially in the puncture/shear phase of mastication to render more efficiently whatever tissues comprised the diet of Horolodectes.

The Phylogenetic Relationships of Horolodectes

The peculiar dentition of Horolodectes is highly apomorphic and presents a formidable challenge to inferring the likeliest phylogenetic position for the taxon. The combination of highly derived premolars and comparatively primitive molars is a recurring pattern among Late Cretaceous and early Tertiary mammals, well exemplified by pentacodontid pantolestans, stagodontid marsupials, and carpolestid plesiadapiforms to name but a few. Many groups of early Tertiary mammals approach Horolodectes in a few features [e.g., North and South American mioclaenid condylarths (such as Promioclaenus Trouessart, 1904 and Pucanodus Muizon and Marshall, 1991) in having bulbous premolars and appressed paraconids and metaconids, and mixodectids (such as Mixodectes Cope, 1883 and Dracontolestes Gazin, 1941) in having a closely approximated entoconid and hypoconulid], but differ significantly in others (using the

above examples, mioclaenids differ from Horolodectes in having much more bulbous cusps and nearly fused paraconids and metaconids, while mixodectids have well-developed mesostyles and hypocones, as well as well-separated paraconids and metaconids). Of the many groups of Late Cretaceous and early Tertiary eutherians, apheliscine hyopsodontids, pentacodontid pantolestans, "zhelestids", and some oxyclaenid condylarths most resemble Horolodectes dentally: many of the members of these groups possess enlarged or otherwise specialized premolars in combination with comparatively primitive molars. Each of these groups is considered in more detail below.

Apheliscine hyopsodontids.—Apheliscines were originally considered an aberrant group of possible insectivorans (see e.g., Matthew, 1918; Simpson, 1937; Simpson, 1945; Saban, 1954; Gazin, 1959); McKenna (1960) demonstrated the hyopsodontid affinities of apheliscines and referred the group to the Hyopsodontidae (and see McKenna and Bell, 1997). Apheliscinae comprise four nominal genera, Apheliscus Cope, 1875, Phenacodaptes Jepsen, 1930, Epapheliscus Van Valen, 1966, and Gingerichia Zack, Penkrot, Krause, and Maas, 2005. The apheliscine dentition is broadly comparable to that of Horolodectes: P4/p4 are variably enlarged (greater enlargement relative to the molars in Apheliscus), the P4 paracone is bulbous and lobe-like, and the molars are relatively unmodified. The similarities in P4 of Apheliscus and Horolodectes are particularly striking: the crown in both leans posteriorly; the protocone is tall and appressed to the paracone; both paracone and protocone are lobe-like in occlusal view; the anterior and posterior cingula are conspicuous; and the posterodorsally directed wear facets are nearly identical. Despite these similarities, virtually none of the remaining dental features are indicative of close affinity between Horolodectes and apheliscines: the anterior premolars of Horolodectes are modified in much the same manner as P4, with the crowns leaning posteriorly and having a bulbous paracone and strong accessory crests, whereas those in apheliscines are small, with unmodified crowns. The upper molars of Horolodectes have acute cusps, robust conules, weak protoconal cingula, and undeveloped hypocones; in contrast, those of apheliscines have low swollen cusps, weaker conules, stronger cingula (especially the posterior cingulum), and hypocones (conspicuous in Phenacodaptes, weaker in Apheliscus). Additionally, M1 and M2 in Horolodectes are subequal in size and subtriangular in outline, whereas the apheliscine

M2 is larger than M1, and the crowns of M1-2 are either square (Apheliscus) or subrectangular (Phenacodaptes) in outline. Differences in dental structure between Horolodectes and apheliscines are even more apparent in the mandibular dentition: the anterior lower premolars of Horolodectes are all similarly modified, with the crowns consisting of a large and posteriorly leaning protoconid, conspicuous shearing crests on the postvallid surface, and an undeveloped talonid; in contrast, the anterior premolars in apheliscines are lower-crowned, with a weakly developed paraconid and robust talonid cusp. Although p4 in Horolodectes and apheliscines is enlarged, a basined heel is developed on the apheliscine p4 (particularly evident in Apheliscus, weaker in Phenacodaptes, not developed in Horolodectes), and the paraconid is usually present; additionally, exodaenodonty is absent on the apheliscine p4, and the peculiar postvallid shearing crests on p4 of Horolodectes are not present. The lower molar crowns differ significantly: the cusps in Horolodectes are acute, the paraconid is well developed and lingual, the paracristid is sharp, and the talonid basin is broad; in contrast, molars of apheliscines have a weaker and more medially positioned paraconid on m1 (the paraconid is essentially absent on m2-3, being incorporated into the paracristid), the paracristid is blunt and loph-like, and the talonid is narrower. Although there are similarities between Horolodectes and apheliscines in the structure of P4, the majority of dental characters differs markedly and seems to preclude a special relationship between the two.

Pentacodontid pantolestans.—Pentacodontidae was first proposed by Simpson (1937) to include Aphronorus Simpson, 1935 and Pentacodon Scott, 1892, two genera with unusually derived fourth premolars. Following the earlier opinions of Matthew (1909, 1918), Simpson (1937) united pentacodontines (now classified as a subfamily) and pantolestines in the more inclusive Pantolestidae, and considered the group part of a broadly construed Insectivora (and see Simpson, 1945; Chapter 5, this study). McKenna and Bell (1997) have recently revised the classification of pentacodontines, adding to the subfamily the Paleocene Bisonalveus Gazin, 1956, Coriphagus Douglass, 1908, and the Eocene Amaramnis Gazin, 1962. McKenna and Bell (1997) consider pentacodontines (pentacodontids of this study) to be part of a larger Cimolesta, a taxon comprising a number of divergent groups traditionally considered distantly related (e.g., pantodonts, taeniodonts, pholidotans). Enlarged and robust upper and lower fourth premolars in

combination with relatively unmodified molars characterize the dentition of pentacodontids, and in these regards are broadly similar to dentitions of both apheliscines and Horolodectes. Among the pentacodontid genera, the teeth of Aphronorus most closely resemble those of Horolodectes in both premolar and molar morphology: the P4 crowns in both taxa are enlarged and lean posteriorly, with a massive paracone and protocone; the paracone and protocone are lobe-like, giving the crown an hourglass-shaped outline; and the obliquely sloping wear facets on the posterior sides of the paracone and protocone are comparable in both taxa. Additionally, the molar trigonids become increasingly compressed from m1-3 in Horolodectes and Aphronorus, the cusps are acute, the anterior and posterior cingulids are weak, and the ectocingulid is undeveloped (and see e.g., Simpson, 1935, 1937; Gingerich et al., 1983). Despite these similarities, the dentition of Horolodectes differs from that of Aphronorus and other pentacodontids in the following ways:

1) The anterior premolars in Horolodectes are modified in much the same manner as P4, with posteriorly leaning crowns and well-developed shearing crests on the postvallum surfaces, whereas the anterior premolars in pentacodontids are comparatively primitive and unspecialized.
2) In spite of superficial similarities, the coronal structure of P4 in Horolodectes differs significantly from that in Aphronorus and other pentacodontids: the P4 crown in Aphronorus is relatively much larger and more robust than that in Horolodectes; the protocone is less appressed to the paracone, lower, and considerably swollen at its base, rather than compressed; a metacone and often a pericone are developed on the P4 of some pentacodontids (particularly on the molariform P4 of Bisonalveus), whereas neither are present on the P4 of Horolodectes; and the protoconal cingula are strongly developed on the P4 of pentacodontines, especially on P4 of Aphronorus and Pentacodon, in which they form broad, shelf-like platforms. The p4 of pentacodontids is generally larger relative to the molars than in Horolodectes, and the crown usually bears a robust metaconid; additionally, the talonid on pentacodontid p4s is tall (such that trigonid/talonid relief is low) and basined (broadly in Aphronorus and Bisonalveus, less so in Pentacodon and Coriphagus) and bears distinct cusps; in

contrast, p4 of Horolodectes is smaller relative to the molars, with a taller protoconid, and the talonid is undeveloped.

3) The molars of most pentacodontids decrease in size posteriorly, whereas those in Horolodectes remain subequal. The upper molar paracone of Aphronorus and other pentacodontids is usually larger and taller than the metacone, and the protoconal cingula are wide and robust; in contrast, the upper molars of Horolodectes have subequal paracone and metacone and weaker cingula. Although the m2-3 trigonids are somewhat compressed in pentacodontids, they are to a much lesser degree than in Horolodectes, the paraconid is more labial, and the paracristid is both lower and blunter; additionally, the molar talonids in pentacodontids are broad and shallowly basined (especially in Aphronorus and Pentacodon, see e.g., Simpson, 1937; Matthew, 1937), and the hypoconulid is centrally or slightly labially positioned (compare with molars in Horolodectes where the talonid is more deeply basined, the hypoconulid is lingual and appressed to the entoconid, and the entoconulid is greatly hypertrophied and appressed to the entoconid+hypoconulid).

Although the unusual fourth premolars in pentacodontids and Horolodectes superficially resemble one another, significant differences in coronal structure imply these similarities may be the result of convergence, rather than an indication of phylogenetic affinity.

"Zhelestidae".—"Zhelestidae" are an assemblage of primitive ungulate-like mammals known primarily from the Late Cretaceous of Central Asia (Nessov et al., 1998; Archibald, 1998; Muizon and Cifelli, 2000; Archibald et al., 2001; Averianov and Archibald, in press; Archibald and Averianov, in press). The group has been variably allied with ungulatans in a broader "Ungulatomorpha" (see e.g., Archibald, 1996; Nessov et al., 1998), leptictids (see e.g., McKenna and Bell, 1997), and most recently with crown group placentalians in the taxon Laurasiatheria (the taxon "Ungulatomorpha" in this classification scheme has been abandoned, with "Zhelestidae" still considered a paraphyletic assemblage, see Averianov and Archibald, in press). A meaningful comparison between Horolodectes and "Zhelestidae" is complicated by the uncertain status of "zhelestid" monophyly; nonetheless, "zhelestid" dentitions can be characterized by upper molars having narrow stylar shelves, anteroposteriorly expanded protocones,

and conules that are closely appressed to the paracone/metacone, as well as the paraconid of m2-3 being appressed to the metaconid and the molar entoconid and hypoconid being closely approximated (see e.g., molars of Parazhelestes Nessov, 1993 and Eozhelestes Nessov, 1997, and see Archibald et al., 2001, and Archibald and Averianov, in press), and in these regards the dentition of "zhelestids" broadly resembles that of Horolodectes. Much like in the dentitions of apheliscines and pentacodontines, however, the majority of coronal similarities between Horolodectes and "zhelestids" are more widely distributed among Late Cretaceous and early Tertiary eutherians, many of these having been achieved independently in groups that have emphasized grinding at the expense of shear. For example, an enlarged molar protocone (and correlative enlarged talonid basin) is characteristic of "zhelestids" and archaic ungulates generally (see e.g., Nessov et al., 1998; Archibald et al., 2001), but is also seen in the leptictid Gypsonictops Simpson, 1927, the didelphodontine Procerberus Sloan and Van Valen, 1965, and a number of Late Cretaceous and early Tertiary lipotyphlans (e.g., Paranyctoides Fox, 1979, Litocherus Gingerich, 1983). Similarly, lowering of the major molar cusps and crests and inflation of the cusps has occurred many times in eutherians that have shifted from a shearing to a grinding mode of mastication (e.g., Gypsonictops, the basal plesiadapiform Purgatorius Van Valen and Sloan, 1966, and the early Tertiary pantolestine Bessoecetor Simpson, 1936). One of the apparent synapomorphies of "Zhelestidae," a lingually displaced hypoconulid on m1 and m2 (such that the entoconid and hypoconulid are closely approximated, see Archibald et al., 2001), also occurs in Horolodectes, yet even this character has a broader distribution among early eutherians (see e.g., lower molars of the lipotyphlans Paranyctoides and Litolestes Jepsen, 1930), probably correlating with and enlarged protocone (as Archibald et al., 2001 have noted). The dentition of Horolodectes differs further from that of "zhelestids" in the coronal structure of the posterior-leaning lower premolars, in having a single-rooted p1, and in the posterior cingulum continuing to the metastylar corner of the crown dorsal to the postmetacrista. Despite the plesiomorphic similarities between the dentitions of Horolodectes and "zhelestids," a special relationship between the two cannot be demonstrated by synapomorphy, and as such, a close phylogenetic affinity between the two unlikely.

Oxyclaenid condylarths.—Oxyclaenidae was first proposed by Scott (1892) to include a number of dentally plesiomorphic "creodont" genera. Ever since Matthew's (1937) review of the San Juan Basin mammalian faunas, oxyclaenines have been considered a subfamily of the Arctocyonidae, a broadly circumscribed taxon including comparatively plesiomorphic (e.g., Prothryptacodon Simpson, 1935; Oxyclaenus Cope, 1884) and derived (e.g., Anacodon Cope, 1882; Platymastus Van Valen, 1978) forms. McKenna and Bell (1997) have recently raised Oxyclaenidae to family level within a broader Ungulata, and distinct from Arctocyonidae (sensu stricto) (but see Prothero et al., 1988 and Archibald, 1998 for different opinions on ungulatan phylogeny). Despite ambiguities in ungulatan phylogeny, it is generally acknowledged that the most primitive ungulatans are among the oxyclaenid condylarths (sensu Van Valen, 1978; Cifelli, 1983; Muizon and Cifelli, 2000). Horolodectes was initially considered an oxyclaenid (see e.g., Webb, 1996; Webb and Fox, 1998) on the basis of plesiomorphic similarities with teeth of Oxyclaenus [considered to be among the most basal oxyclaenids (Van Valen, 1978; Cifelli, 1983; McKenna and Bell, 1997), but see also Prothero et al. (1988) and Archibald (1998) for different opinions], including primitive molars, large canines, a premolariform p4, and an unreduced number of premolars. Although the upper molars of Horolodectes and Oxyclaenus resemble one another in being wider than long, and having reduced stylar shelves and well-developed conules, they differ in that those of Oxyclaenus and other oxyclaenids have stronger and more lingually complete protoconal cingula, robust hypocones (in some taxa), stronger parastylar lobes and wider stylar shelves, and lower, more bunodont cusps. Additionally, M2 in most oxyclaenids is significantly larger than either M1 or M3 (see e.g., M1-3 of Oxyprimus galadrielae Van Valen, 1978, and M1-3 of Oxyclaenus corax Johnston and Fox, 1984), while the molars in Horolodectes are more nearly equal in size. The lower molars of oxyclaenids, while resembling those in Horolodectes in having broad talonids, differ in being lower, with massive cusps, and in having a more centrally positioned hypoconulid and a robust ectocingulid. Although the m3 hypoconulid of Horolodectes is enlarged (resembling that on m3s of Oxyclaenus and other ungulatans, and a putative synapomorphy of ungulatans, see Prothero et al., 1988; Archibald, 1998), it is posterolingually twinned with an equally large entoconid and slightly smaller entoconulid, and is vertical rather than posteriorly projecting (see

Prothero et al., 1988; Archibald, 1998). Disregarding the unusual structure of the premolars, the basic coronal structure of the dentition of Horolodectes resembles that of basal oxyclaenid "condylarths" (and "zhelestids") only in plesiomorphic characters, many of which occur in other "condylarth" families and in primitive eutherians generally.

The unusual premolar autapomorphies combined with comparatively primitive molars present a number of challenges to inferring the taxonomic position of Horolodectes, even to ordinal level. Among the candidate groups discussed earlier, affinity with either apheliscine hyopsodontids or pentacodontid pantolestans seems unlikely: although members of both of these groups possess upper and lower fourth premolars approaching those of Horolodectes in some superficial aspects, the differences in the structure of the premolars, and even more particularly the molars, suggest that these similarities are best interpreted as owing to convergence, rather than as evidence of a close phylogenetic relationship. Referral of Horolodectes to either of these groups as a highly derived member would require not only reversals in many characters (e.g., a redevelopment and lingual migration of the molar paraconids if referred to Apheliscinae, loss of the P4 metacone and p4 metaconid if referred to Pentacodontidae), but also a significant broadening of the concept of each taxon in order to accommodate the peculiarities of the dentition of Horolodectes; given the evidence at hand we consider either of these alternatives unlikely. The molar dentition of "zhelestids" and basal oxyclaenids more closely resembles that of Horolodectes than does either that of apheliscines or pentacodontines, yet referral of Horolodectes to either of these groups would be based on plesiomorphic characters, many of which occur in other families of "condylarths" or more broadly among other primitive eutherians (e.g., transverse upper molars, broad talonids); we therefore consider this alternative equally unlikely. Because the dentition of Horolodectes is derived in such a unique manner, its placement in any of the above groups seems premature given the available evidence; as such, we refer Horolodectes to Eutheria, order incertae sedis, with the anticipation that future discoveries will provide a better approximation of its phylogenetic affinities.

11.4 Literature Cited

ARCHIBALD, J. D. 1996. Fossil evidence for a Late Cretaceous origin of "hoofed" mammals. Science, 272:1150-1153.

ARCHIBALD, J. D. 1998. Archaic ungulates ("Condylarthra"), pp. 292-331. In C. M. JANIS, K. M. SCOTT, and L. L. JACOBS (eds.), Evolution of Tertiary Mammals of North America Volume 1: Terrestrial Carnivores, Ungulates, and Ungulatelike Mammals. Cambridge University Press, Cambridge, Massachusetts.

ARCHIBALD, J. D., and A. O. AVERIANOV. In press. Mammalian faunal succession in the Cretaceous of the Kyzylkum Desert. Journal of Mammalian Evolution.

ARCHIBALD, J. D., A. O. AVERIANOV, and E. G. EKDALE. 2001. Late Cretaceous relatives of rabbits, rodents, and other extant eutherian mammals. Nature, 414:62-65.

AVERIANOV, A. O., and J. D. ARCHIBALD. In press. Mammals from the mid-Cretaceous Khodzhakul Formation, Kyzylkum Desert, Uzbekistan. Cretaceous Research.

BLOCH, J. I., K. D. ROSE, and P. D. GINGERICH. 1998. New species of Batodonoides (Lipotyphla, Geolabididae) from the early Eocene of Wyoming: smallest mammal known? Journal of Mammalogy, 79:804-827.

BLOCH, J. I., D. M. BOYER, P. D. GINGERICH, and G. F. GUNNELL. 2002. New primitive paromomyid from the Clarkforkian of Wyoming and dental eruption in Plesiadapiformes. Journal of Vertebrate Paleontology, 22:366-379.

BUTLER, P. M. 1956. The skull of Ictops and the classification of the Insectivora. Proceedings of the Zoological Society, London, 126:453-481.

BUTLER, P. M. 1973. Molar wear facets of Tertiary North American primates. Symposium of the Fourth International Congress of Primatology, 3:777-817.

BUTLER, P. M. 1988. Phylogeny of the insectivores, pp. 253-265. In M. J. BENTON (ed.), The Phylogeny and Classification of the Tetrapods, Volume 2: Mammals. Systematics Association Special Volume 35B, Clarendon Press, Oxford.

CIFELLI, R. L. 1983. The origin and affinities of the South American Condylarthra and early Tertiary Litopterna (Mammalia). American Museum Novitates, 2772:1-49.

COPE, E. D. 1875. Systematic catalogue of Vertebrata of the Eocene of New Mexico, collected in 1874. Report to the Engineer Department, U. S. Army, in charge of Lieu. Geo. M. Wheeler. Washington, April 17, 1875, pp. 5-37.

COPE, E. D. 1882. Contributions to the history of the Vertebrata of the lower Eocene of Wyoming and New Mexico, made during 1881. Proceedings of the American Philosophical Society, 20:139-197.

COPE, E. D. 1883. First addition to the fauna of the Puerco Eocene. Proceedings of the American Philosophical Society, 20:545-563.

COPE, E. D. 1884. Second addition to the knowledge of the fauna of Puerco epoch. Proceedings of the American Philosophical Society, 21:309-324.

CROMPTON, A. W. 1971. The origin of the tribosphenic molar; in D. M. KERMACK and K. A. KERMACK (eds.), Early Mammals. Zoological Journal of the Linnean Society (Supplement No. 1), 50:65-87.

DEWAR, E. W. 2003. Functional diversity within the Littleton fauna (early Paleocene), Colorado: evidence from body mass, tooth structure, and tooth wear. PaleoBios, 23:1-19.

DOUGLASS, E. 1908. Vertebrate fossils from the Fort Union beds. Annals of Carnegie Museum, 5:11-26.

FOX, R. C. 1975. Molar structure and function in the Early Cretaceous mammal Pappotherium: evolutionary implications for Mesozoic Theria. Canadian Journal of Earth Sciences, 12:412-442.

FOX, R. C. 1979. Mammals from the Upper Cretaceous Oldman Formation, Alberta. III. Eutheria. Canadian Journal of Earth Sciences, 16:114-125.

FOX, R. C. 1984a. First North American record of the Paleocene primate Saxonella. Journal of Paleontology, 58:892-894.

FOX, R. C. 1984b. The dentition and relationships of the Paleocene primate Micromomys Szalay, with description of a new species. Canadian Journal of Earth Sciences, 21:1262-1267.

FOX, R. C. 1984c. Melaniella timosa n. gen. and sp., an unusual mammal from the Paleocene of Alberta, Canada. Canadian Journal of Earth Sciences, 21:1335-1338.

FOX, R. C. 1984d. A new species of the Paleocene primate Elphidotarsius Gidley: its stratigraphic position and evolution. Canadian Journal of Earth Sciences, 21:1268-1277.

FOX, R. C. 1990a. The succession of Paleocene mammals in western Canada, pp. 51-70. In T. M. BOWN and K. D. ROSE (eds.), Dawn of the Age of Mammals in the Northern Part of the Rocky Mountain Interior. Geological Society of America, Special Paper, 243.

FOX, R. C. 1990b. Pronothodectes gaoi n. sp. from the late Paleocene of Alberta, Canada, and the early evolution of the Plesiadapidae. Journal of Paleontology, 64:637-647.

FOX, R. C. and G. P. YOUZWYSHYN. 1994. New primitive carnivorans (Mammalia) from the Paleocene of western Canada, and their bearing on relationships of the order. Journal of Vertebrate Paleontology, 14:382-404.

GAZIN, C. L. 1941. The mammalian faunas of the Paleocene of central Utah, with notes on geology. Proceedings of the United States National Museum, 91:1-53.

GAZIN, C. L. 1956. Paleocene mammalian faunas of the Bison Basin in south-central Wyoming. Smithsonian Miscellaneous Collections, 131:1-57.

GAZIN, C. L. 1959. Early Tertiary Apheliscus and Phenacodaptes as pantolestid insectivores. Smithsonian Miscellaneous Collections, 139:1-7.

GAZIN, C. L. 1962. A further study of the lower Eocene mammalian faunas of southwestern Wyoming. Smithsonian Miscellaneous Collections, 144:1-98.

GIDLEY, J. W. 1917. Notice of a new Paleocene mammal, a possible relative of the titanotheres. Proceedings of the United States National Museum, 52:431-435.

GILL, T. 1872. Arrangement of the families of mammals with analytical tables. Smithsonian Miscellaneous Collections, 11:1-98.

GINGERICH, P. D. 1976. Cranial anatomy and evolution of early Tertiary Plesiadapidae (Mammalia, Primates). Museum of Paleontology, The University of Michigan, Papers on Paleontology, 15:1-140.

GINGERICH, P. D. 1983. New Adapisoricidae, Pentacodontidae, and Hyopsodontidae (Mammalia, Insectivora and Condylarthra) from the late Paleocene of Wyoming and Colorado. Contributions from the Museum of Paleontology, The University of Michigan, 26:227-255.

GINGERICH, P. D., P. HOUDE, and D. W. KRAUSE. 1983. A new earliest Tiffanian (late Paleocene) mammalian fauna from the Bangtail Plateau, western Crazy Mountain Basin, Montana. Journal of Paleontology, 57:957-970.

HIIEMAE, K. M. 1978. Masticatory movements in primitive mammals, pp. 359-398. In P. M. BUTLER and K. A. JOYSEY (eds.), Development, Function and Evolution of Teeth. Academic Press, London.

HUNTER, J. P. and M. FORTELIUS. 1994. Comparative dental occlusal morphology, facet development, and microwear in two sympatric species of Listriodon (Mammalia: Suidae) from the middle Miocene of Western Anatolia (Turkey). Journal of Vertebrate Paleontology, 14:105-126.

JEPSEN, G. L. 1930. Stratigraphy and paleontology of the Paleocene of northeastern Park County, Wyoming. Proceedings of the American Philosophical Society, 69:463-528.

JOHNSTON, P. A., and R. C. FOX. 1984. Paleocene and Late Cretaceous mammals from Saskatchewan, Canada. Palaeontographica (A), 186:163-222.

KIELAN-JAWOROWSKA, Z. 1969. Preliminary data on the Upper Cretaceous eutherian mammals from Bayn Dzak, Gobi Desert, pp. 171-191. In Z. KIELAN-JAWOROWSKA (ed.), Results of the Polish-Mongolian Palaeontological Expeditions, pt. I. Palaeontologia Polonica 19.

KIELAN-JAWOROWSKA, Z. 1975. Preliminary description of two new eutherian genera from the Late Cretaceous of Mongolia pp. 5-16. In Z. KIELAN-JAWOROWSKA (ed.), Results of the Polish-Mongolian Palaeontological Expeditions, pt. VI. Palaeontologia Polonica 33.

LILLEGRAVEN, J. A. 1969. Latest Cretaceous mammals of upper part of the Edmonton Formation of Alberta, Canada, and review of marsupial-placental dichotomy in mammalian evolution. The University of Kansas Paleontological Contributions, 50 (Vertebrata 12):1–122.

LINNAEUS, C. 1758. Systema naturae per regna tria naturae, secundum classes, ordines, genera, species cum characteribus, differentiis, synonymis, locis. Editio decima, reformata. Laurenti Salvii, Stockholm.

LOFGREN, D. L., J. A. LILLEGRAVEN, W. A. CLEMENS, P. D. GINGERICH, and T. E. WILLIAMSON. 2004. Paleocene biochronology: The Puercan through Clarkforkian Land Mammal Ages, pp. 43-105. In M. O. WOODBURNE (ed.), Late Cretaceous

and Cenozoic mammals of North America: geochronology and biostratigraphy. Columbia University Press, New York.

LUCAS, P. W. 1979. The dental-dietary adaptations of mammals. Neues Jahrbuch für Geologie und Paleontologie, 8:486-512.

LUCKETT, W. P. 1993. An ontogenetic assessment of dental homologies in therian mammals, pp.182-204. In F. S. SZALAY, M. J. NOVACEK, and M. C. MCKENNA (eds.), Mammal Phylogeny: Mesozoic Differentiation, Multituberculates, Monotremes, Early Therians, and Marsupials. Springer-Verlag, New York, New York.

MATTHEW, W. D. 1909. The Carnivora and Insectivora of the Bridger Basin, Middle Eocene. Memoir of the American Museum of Natural History, 9:291-567.

MATTHEW, W. D. 1918. A revision of the Lower Eocene Wasatch and Wind River faunas. Insectivora (cont.), Glires, Edentata. Bulletin of the American Museum of Natural History, 38:565-657.

MATTHEW, W. D. 1937. Paleocene faunas of the San Juan Basin, New Mexico. Transactions of the American Philosophical Society, 30:1-510.

MCKENNA, M. C. 1960. Fossil Mammalia from the early Wasatchian Four Mile fauna Eocene of northwest Colorado. University of California Publications in Geological Sciences, 37:1-130.

MCKENNA, M. C., and S. K. BELL. 1997. Classification of Mammals Above the Species Level. Columbia University Press, New York.

MUIZON, C. de and R. L. CIFELLI. 2000. The "condylarths" (archaic Ungulata, Mammalia) from the early Palaeocene of Tiupampa (Bolivia): implications on the origin of the South American ungulates. Geodiversitas, 22:47-150.

MUIZON, C. de and L. M. MARSHALL. 1991. Nouveaux Condylarthes du Paléocène inférieur de Tiupampa (Bolivie). Bulletin du Muséum national d'Histiore naturelle, 13:201-227.

NESSOV, L. A. 1993. New Mesozoic mammals of middle Asia and Kazakstan and comments about evolution of theriofaunas of Cretaceous coastal plains of Asia. Trud Zoologichyeskogo Instituta, Rossiiskaya Akadyemiya Nauk, 249:105-133. (In Russian with English summary)

NESSOV, L. A. 1997. Cretaceous Nonmarine Vertebrates of Northern Eurasia (Posthumous Edition by L. B. Golovneva and A. O. Averianov). University of Saint Petersburg, Institute of the Earth Crust, Saint Petersburg. (In Russian)

NESSOV, L. A., J. D. ARCHIBALD, and Z. KIELAN-JAWOROWSKA. 1998. Ungulate-like mammals from the Late Cretaceous of Uzbekistan and a phylogenetic analysis of the Ungulatomorpha, pp. 40-88. In K. C. BEARD and M. R. DAWSON (eds.), Dawn of the Age of Mammals in Asia. Bulletin of the Carnegie Museum of Natural History, 34.

NOVACEK, M. J. 1986. The skull of leptictid insectivores and the higher-level classification of the eutherian mammals. Bulletin of the American Museum of Natural History, 183:1-111.

PARKER, T. J., and HASWELL, W. A. 1897. A Text-book of Zoology. Volume 2. Macmillan Press, London, 301 pp.

PROTHERO, D. R., E. M. MANNING, and M. FISCHER. 1988. The phylogeny of the ungulates, pp. 201-234. In M. J. BENTON (ed.), The Phylogeny and Classification of the Tetrapods, Volume 2: Mammals. Systematics Association Special Volume 35B, Clarendon Press, Oxford.

RENSBERGER, J. M. 1986. Early chewing mechanisms in mammalian herbivores. Paleobiology, 12:474-494.

SABAN, R. 1954. Phylogenie des Insectivores. Bulletin du Museum national d'histoire naturelle (France), série 2, 26:419-433.

SCOTT, C. S. 2003. Multituberculate mammals from Western Canada. Proceedings of the 13th Annual Canadian Paleontology Conference, 1:37–38.

SCOTT, C. S. 2005. New neoplagiaulacid multituberculates (Mammalia, Allotheria) from the Palaeocene of Alberta, Canada. Journal of Paleontology, 79:1189-1213.

SCOTT, W. B. 1892. A revision of the North American Creodonta, with notes on some genera which have been referred to that group. Proceedings of the Academy of Natural Sciences of Philadelphia, 44:291-323.

SIMPSON, G. G. 1927. Mammalian fauna and correlation of the Paskapoo Formation of Alberta. American Museum Novitates, 268:1-10.

SIMPSON, G. G. 1935. New Paleocene mammals from the Fort Union of Montana. Proceedings of the United States National Museum, 83:221-224.

SIMPSON, G. G. 1936. A new fauna from the Fort Union of Montana. American Museum Novitates, 873:1-27.

SIMPSON, G. G. 1937. The Fort Union of the Crazy Mountain field, Montana and its mammalian faunas. Bulletin of the United States National Museum, 169:1-287.

SIMPSON, G. G. 1945. The principles of classification and a classification of mammals. Bulletin of the American Museum of Natural History, 85:1-350.

SLAUGHTER, B. H., R. H. PINE, and N. E. PINE. 1974. Eruption of cheek teeth in Insectivora and Carnivora. Journal of Mammalogy, 55:115-125.

SLOAN, R. E., and L. VAN VALEN. 1965. Cretaceous mammals from Montana. Science, 148:220-227.

TROUESSART, E. -L. 1904. Catalogus mammalium tam viventium quam fossilum. Quinquennale supplementum. Berolini, R. Friedlander & Sohn, Berlin. Volume 1 (1904):1-546; Volume 2 (1905):547-929.

TURNBULL, W. D. 1970. Mammalian masticatory apparatus. Fieldiana: Geology, 18:147-356.

VAN VALEN, L. 1966. Deltatheridia, a new order of mammals. Bulletin of the American Museum of Natural History, 132:1-126.

VAN VALEN, L. 1978. The beginning of the Age of Mammals. Evolutionary Theory, 4:45-80.

VAN VALEN, L., and R. E. SLOAN. 1966. The extinction of the multituberculates. Systematic Zoology, 15:261–278.

WEBB, M. W. 1996. Late Paleocene mammals from near Drayton Valley, Alberta. M.Sc. thesis, University of Alberta, Edmonton, 258 pp.

WEBB, M. W., and R. C. FOX. 1998. An unusually specialized oxyclaenid (Mammalia: Condylarthra) from the late Paleocene of central Alberta, Canada. Geological Society of America Abstracts with Programs, 30:40A.

WIBLE, J. R. 2003. On the cranial osteology of the short-tailed opossum Monodelphis brevicaudata (Didelphidae, Marsupialia). Annals of Carnegie Museum, 72:137-202.

ZACK, S. P., T. A. PENKROT, D. W. KRAUSE, and M. C. MAAS. 2005. A new apheliscine "condylarth" from the late Paleocene of Montana and Alberta and the phylogeny of "hyopsodontids". Acta Palaeontologica Polonica, 50:809-830.

ZIEGLER, A. C. 1971. A theory of the evolution of therian dental formulas and replacement patterns. Quarterly Review of Biology, 46:226-249.

Table 11.1.—Combined measurements and descriptive statistics for the upper dentition of Horolodectes sunae new genus and species from the early middle Tiffanian (Ti3) DW-2 and Birchwood localities, Paskapoo Formation, Alberta.

Element	P	N	OR	M	SD	CV
P2	L	2	1.5-1.7	1.60	0.14	9.55
	W	1	1.2	—	—	—
P3	L	7	2.4-2.7	2.54	0.14	5.34
	W	6	2.4-2.5	2.46	0.05	2.01
P4	L	10	2.4-2.7	2.52	0.10	4.44
	W	10	3.1-3.7	3.34	0.22	7.10
M1	L	5	2.4-2.6	2.53	0.07	3.33
	W	5	3.1-3.6	3.43	0.23	7.33
M2	L	4	2.5-2.7	2.60	0.12	4.43
	W	4	3.4-3.6	3.50	0.12	3.01
M3	L	1	2.3	—	—	—
	W	1	3.0	—	—	—

Table 11.2.—Combined measurements and descriptive statistics for the lower dentition of Horolodectes sunae new genus and species from the early middle Tiffanian (Ti3) DW-2 and Birchwood localities, Paskapoo Formation, Alberta.

Element	P	N	OR	M	SD	CV
p2	L	7	1.9-2.4	2.13	0.15	7.66
	W	6	1.1-1.3	1.24	0.11	9.21
p3	L	9	2.1-2.6	2.45	0.15	6.66
	W	8	1.3-1.5	1.46	0.08	6.32
p4	L	9	2.8-3.3	3.01	0.17	5.14
	W	8	1.6-2.1	1.88	0.16	9.09
m1	L	8	2.5-2.9	2.88	0.12	4.11
	TrW	8	1.7-1.9	1.84	0.08	4.12
	TaW	9	1.9-2.3	2.13	0.12	6.55
m2	L	11	2.5-2.9	2.77	0.13	5.15
	TrW	10	1.9-2.1	2.02	0.09	5.05
	TaW	10	2.1-2.9	2.32	0.23	10.12
m3	L	8	2.6-2.9	2.82	0.09	3.33
	TrW	8	1.7-2.2	1.94	0.16	8.02
	TaW	8	1.9-2.3	2.07	0.14	7.02

Figure 11.1.—Horolodectes sunae new genus and species from the early middle Tiffanian (Ti3) DW-2 (DW2) and Birchwood (BW) localities, Paskapoo Formation, Alberta. 1-5, UALVP 42073 (DW2), incomplete left maxilla with P2-4 in 1, labial, 2, oblique lingual, 3, occlusal, 4, oblique anterior, and 5, posterior views; 6-10, UALVP 39465 (BW), right P4 in 6, labial, 7, lingual, 8, occlusal, 9, anterior, and 10, posterior views; 11, 12, UALVP 45704 (DW2), incomplete right maxilla with P3-4, M1 in 11, labial, and 12, occlusal views; 13-17, UALVP 42074 (DW2), incomplete right maxilla with M1-2 in 13, labial, 14, lingual, 15, occlusal, 16, anterior, and 17, posterior views; 18-20, UALVP 45719 (DW2), right M3 in 18, labial, 19, lingual, and 20, occlusal views; 21, composite left upper dentition [UALVP 42073, 42074 (reversed), 45719 (reversed)] in occlusal view. Scale bars = 2mm.

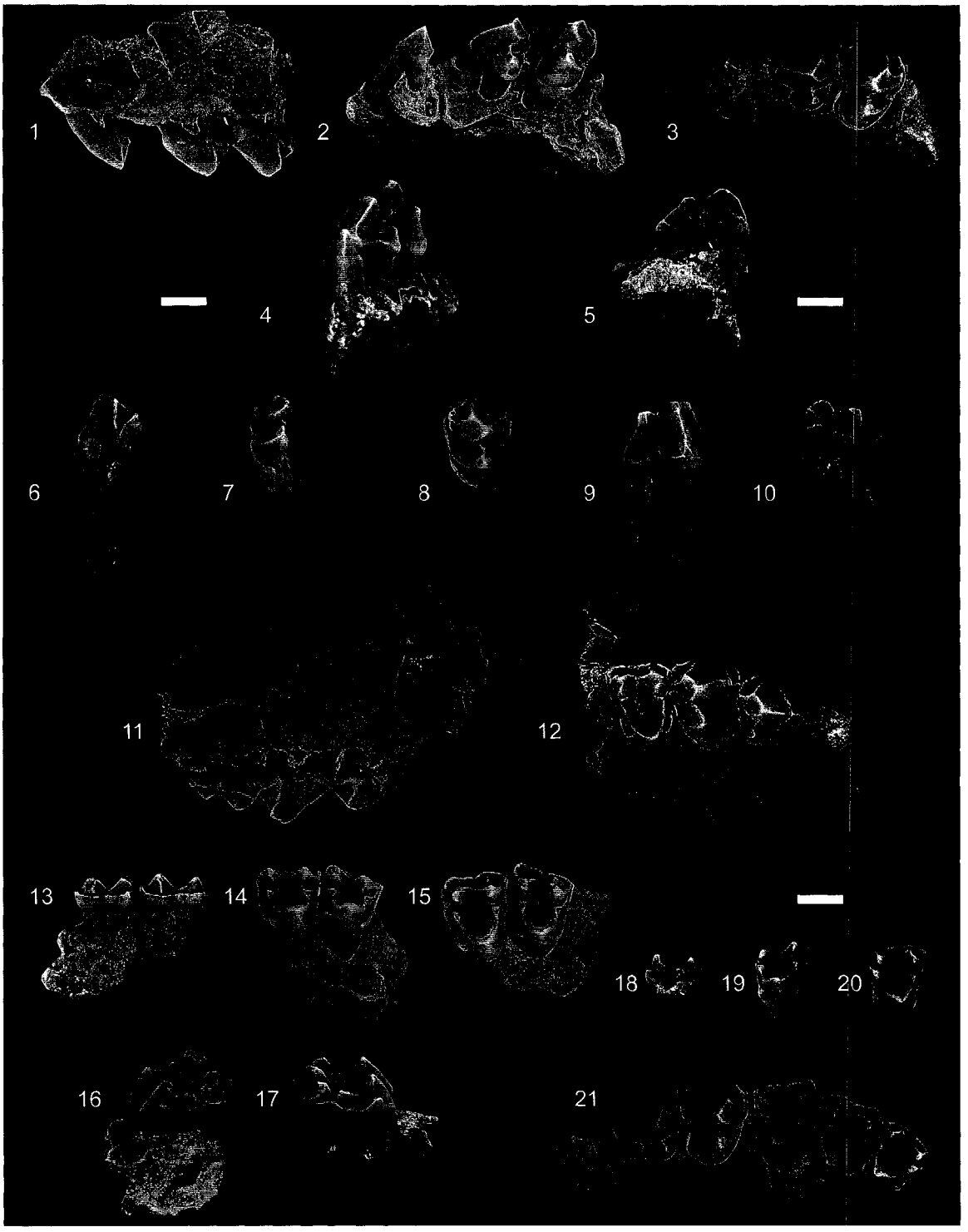
1
2
3
4
5
6
7
8
9
10
11
12
13
14
15
16
17
18
19
20
21

Figure 11.2.—Horolodectes sunae new genus and species from the early middle Tiffanian (Ti3) DW-2 (DW2) and Birchwood (BW) localities, Paskapoo Formation, Alberta. 1-3, UALVP 39200 (BW, holotype), incomplete right dentary with p2-4, m1-3, and alveoli for i1-3, c, p1 in 1, oblique labial, 2, lingual, and 3, occlusal views; inset shows holotype in oblique anterior view with alveoli for i1-3 and c labelled; 4-6, UALVP 45709 (BW), incomplete left dentary with p2-4, m1-2, and alveolus for p1 in 4, labial, 5, lingual, and 6, occlusal views. Scale bars = 2 mm.

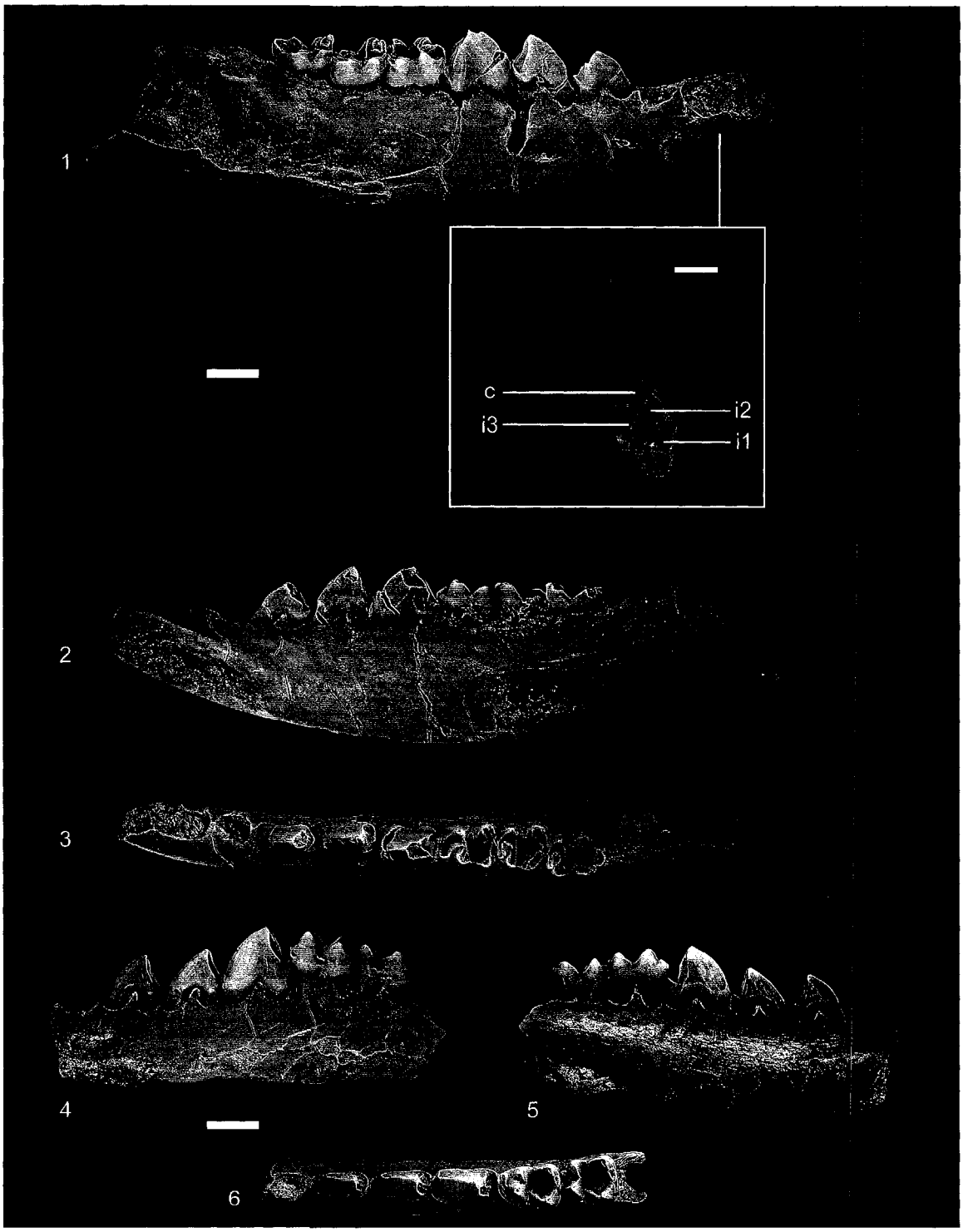
1
c
i3
i2
i1
2
3
4
5
6

Figure 11.3.—Horolodectes sunae new genus and species from the early middle Tiffanian (Ti3) DW-2 (DW2) and Birchwood (BW) localities, Paskapoo Formation, Alberta. 1-3, UALVP 45713, incomplete left dentary with p2-4, m1-3 in 1, oblique labial, 2, lingual, and 3, occlusal views; 4-6, UALVP 46370, incomplete left dentary with p2-3 (erupting), m1-2, and alveoli for m3 in 4, labial, 5, lingual, and 6, occlusal views (white line points to erupting p3); 7, composite left upper dentition [UALVP 42073 and 42074 (reversed)] in labial view, and UALVP 45713, incomplete left dentary with p2-4, m1-3 in oblique labial view. Scale bars = 2mm.

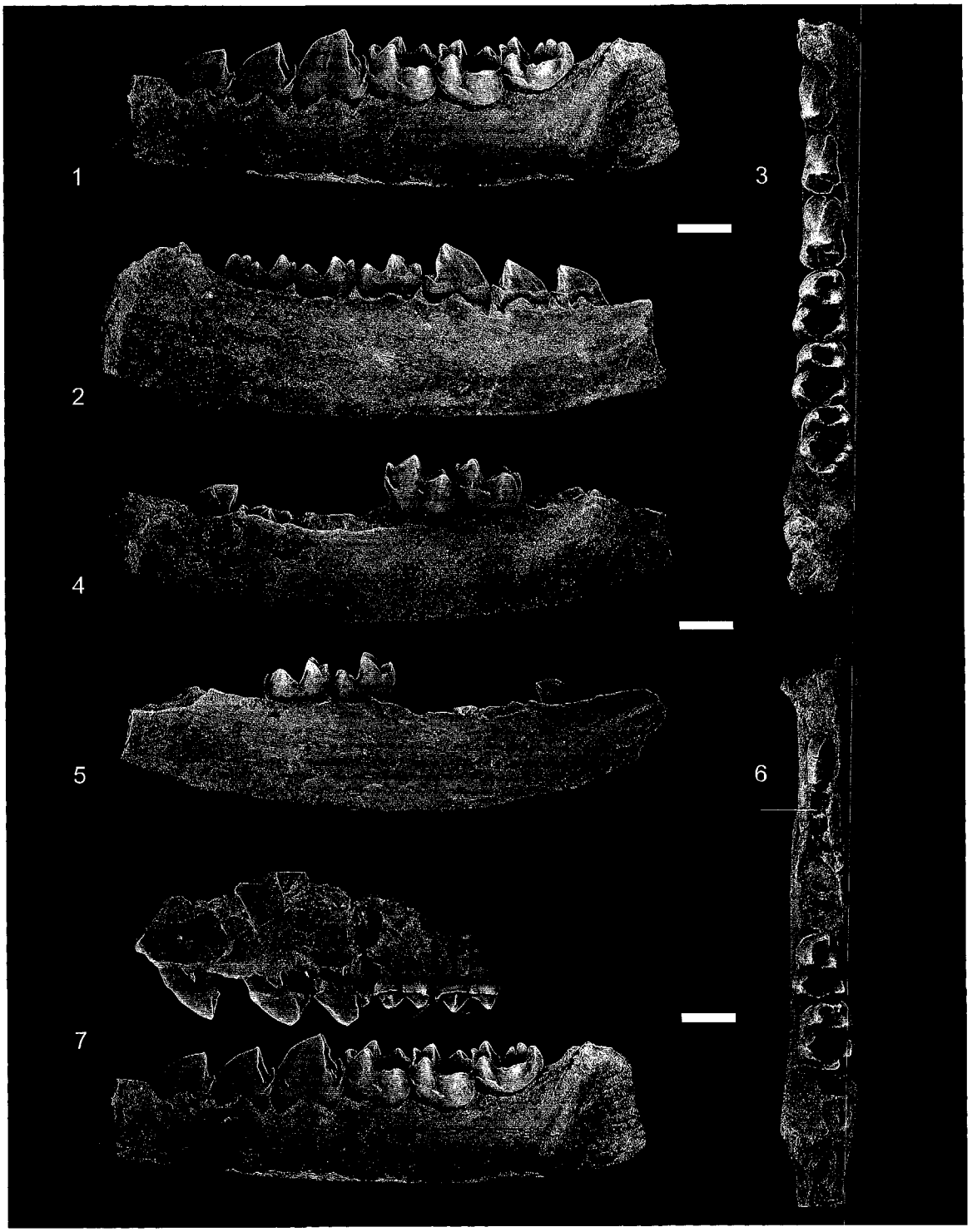
1
2
3
4
5
6
7

12 General Discussion and Conclusions: The Age of the Blindman River and Joffre Bridge Localities, and a Preliminary Analysis of Mammalian Species Diversity during the Early to Late Paleocene in the Alberta Basin

12.1 Introduction

Paleontologists since William Smith **[[[1859?]]]**have employed fossils as a means for correlating physically isolated outcrops, and for placing fossiliferous strata into a relative time frame, with evolution being the causal mechanism of the observed faunal and floral succession preserved in rocks. Previous work on the plesiadapiforms from the Blindman River and Joffre Bridge localities (e.g., Fox, 1984a-c, 1991, 2002) provided the first estimates of relative age for the local fauna (the Blindman River and Joffre Bridge local faunas are pooled for the purposes of this part of the study; they are referred to herein as "the Blindman River/Joffre Bridge local fauna"). Fox (1984b) considered DW-2 to be early middle Tiffanian (Ti3) in age, a conclusion that rested in large part on the presence of the plesiadapid Plesiadapis rex, an index taxon for Ti3 (Gingerich, 1976; Archibald et al., 1987; Lofgren et al., 2004), as well as the presence of Carpodaptes hazelae, a carpolestid plesiadapiform that is considered characteristic of the early middle Paleocene (Archibald et al., 1987; Lofgren et al., 2004); a Ti3 age was assigned to the other Blindman River localities, as well as to the Joffre Bridge Roadcut and Mammal Site No. 1 localities on the basis of stratigraphic position and/or faunal similarity with DW-2 (Fox, 1990a). Although a Ti3 age for the Blindman River/Joffre Bridge localities is consistent with their stratigraphic context in the Alberta Basin and with independent estimators of age (see later in the text), the discovery of Pronothodectes gaoi, a second plesiadapid from DW-2 (Fox, 1990b), seriously complicated the original estimate of age, particularly as it called into question the identification of specimens from the study localities that had been referred previously to Ples. rex.

The preceding nine systematic chapters and the taxonomic identifications therein provide a solid basis for inferring the relative age of the Blindman River and Joffre Bridge localities, and to place these localities into a more refined temporal context than

has been possible previously. The results from the preceding nine chapters also provide an opportunity to examine changes in mammalian faunal diversity during the early and early late parts of the Paleocene in the Alberta Basin, and occasion to revisit Rose's (1981a-b) influential hypotheses of late Paleocene climate change in North America and its effects on mammalian evolution. The large sample from the study localities, combined with those from the earliest Tiffanian (Ti1) Cochrane 2 and the middle Torrejonian (To2) Who Nose? localities of southwestern Alberta, are now sufficiently well-studied so as to allow an adequate test of Rose's (1981a-b) hypotheses using current methods of sample standardization and diversity analysis.

12.2 Age of the Study Localities

Mammals

The continental Cenozoic of North America (approximately 65 mya to present) is temporally subdivided on the basis of fossil mammals, forming a biochronology (i.e., the organization of geologic time according to the process of organic evolution; see Berggren and Van Couvering, 1978), with the irreversibility and unique geologic and temporal duration of evolutionary changes in component fossils providing a sound means for correlation (Woodburne, 1987, 2004). The information gleaned from this biochronology can be extrapolated to, and compared with, similar schemes throughout the world. The first formal biozonation of North American Tertiary continental sediments using fossil mammals was by the Wood Committee in 1941, which refined and expanded on the system of "life zones" that were proposed by Osborn and Matthew (1909) thirty years prior. The "provincial ages" of Wood et al. (1941) were not geochronological ages in the strict sense (see NACSN, 2005) as they were not based on antecedent chronostratigraphic stages tied to measured and described stratigraphic sections (type areas were assigned to each Land Mammal Age, but measured sections were not specified; Secord et al., 2006), and correlating these continental sequences to the marine record (used in defining series and stage boundaries) proved, and continues to prove difficult. Recent advances in magnetostratigraphy and isotope stratigraphy have provided near-synchronous

boundaries that allow a more precise correlation of continental strata to the geomagnetic polarity time scale (GPTS) (Harland et al., 1990; Cande and Kent, 1992, 1995; Agterberg, 2004; Luterbacher et al., 2004; Ogg and Smith, 2004; Woodburne, 2004; Secord et al., 2006), and a number of authors have expressed a desire to reformulate the North American mammalian time scale as a chronostratigraphy with stratotype and reference sections (e.g., Woodburne, 1977, 1987, 1996; Evander, 1986; Alroy, 1994, 1998; Walsh, 1998, 2001). These suggestions have yet to be formalized, however, and the biozonation scheme of the Wood Committee has continued to form the basis for temporally subdividing Tertiary continental deposits in North America (Woodburne, 1987; Woodburne and Swisher, 1995; Lofgren et al., 2004).

The Paleocene of North America is subdivided into four Land Mammal Ages that are recognized on the basis of assemblages of fossil mammals: from oldest to youngest, these are the Puercan, Torrejonian, Tiffanian, and Clarkforkian, with each of the Land Mammal Ages further divided into zones (e.g., the Tiffanian is subdivided into six zones; Gingerich, 1976; Archibald et al., 1987; Lofgren et al., 2004). Fox (1984b, 1990a-b) estimated the age of the Blindman River and Joffre Bridge local faunas as Tiffanian (specifically early middle Tiffanian, or Ti3; see later in the text) based on the presence of both index and characteristic taxa, an age that has since been further supported by independent lines of evidence (e.g., Demchuk, 1990; Lerbekmo et al., 1992; and see later in the text). The Tiffanian Land Mammal Age was initially based on the Tiffany beds of the Animas Formation in the San Juan Basin of southwestern Colorado (Granger, 1917), with the Mason Pocket local fauna as the main reference fauna (Simpson, 1935a-c; Wood et al., 1941; Archibald et al., 1987; Lofgren et al., 2004). The Tiffanian NALMA is currently defined as the temporal interval between the first appearance of the plesiadapiform Plesiadapis and the first appearance of rodents, spanning a temporal interval from approximately 55.0-61.0 mya (Lofgren et al., 2004) or 55.0-61.6 mya (Secord et al., 2006). A recently discovered volcanic ash in the Polecat Bench sequence of the northern Bighorn Basin of Wyoming provides the first radioisotopic calibration point for the late Paleocene (the ash has a weighted mean age of 59.00±0.30 Ma and falls within polarity chron 26r; see Secord et al., 2006). Following the criteria of Lofgren et al. (2004) and Secord et al. (2006), the Blindman River and Joffre Bridge local faunas are

correlative with the Tiffanian NALMA, as indicated at the generic level by the presence of Bisonalveus, Carpodaptes, Litolestes, Raphictis, and Saxonella, taxa that are restricted elsewhere to the Tiffanian NALMA (Lofgren et al., 2004; Secord et al., 2006). Supraspecific taxa, including Didymictis, Ectocion, and Thryptacodon, which make their first appearances during the Tiffanian NALMA, lend support for a Tiffanian age.

Lofgren et al. (2004), following Gingerich (1976) and Archibald et al. (1987), further subdivided the Tiffanian NALMA into six lineage-zones, each of which is based on the successive first and last appearances of non-overlapping species of the plesiadapiform Plesiadapis. Fox (1984b, 1990a) suggested that the age of the Blindman River and Joffre Bridge local faunas as early middle Tiffanian, within the Plesiadapis rex/P. churchilli Lineage Zone (Ti3) of Lofgren et al. (2004); this interpretation was based in part on the presence of the plesiadapid Plesiadapis rex, an index taxon for the early middle Tiffanian (Gingerich, 1976; Archibald et al., 1987; Lofgren et al., 2004). The interpretation of the ages of the study localities became more uncertain with the discovery of Pronothodectes gaoi in the DW-2 local fauna (Fox, 1990b). As discussed in Fox (1990b) and earlier in this study, the dentition of Pro. gaoi closely resembles that of P. rex, both in terms of coronal anatomy and size, and the two taxa are not easily distinguished; furthermore, the results of this study suggest that specimens that were originally thought to pertain to P. rex are better interpreted as belonging to Pro. gaoi, leaving the Blindman River and Joffre Bridge localities without the index plesiadapid for Ti3 (Gingerich, 1976). Despite the absence of P. rex, the local faunas from the study localities are almost certainly early middle Tiffanian in age (Figure 12.1): two additional index taxa, the ?epoicotheriid pholidotan Melaniella and the saxonellid plesiadapiform Saxonella, are identified as Ti3 index taxa by Lofgren et al. (2004), although these taxa are admittedly restricted to localities in the Alberta Basin (Saxonella is also known from the Walbeck localities in Germany; Russell, 1964 and see Chapter 7), but two other taxa identified in this study, the oxyclaenid Chriacus oconostotae and the adapisoricine Adeloxenus, are known only from this interval in Alberta and the Bighorn and Green River basins of Wyoming (Van Valen, 1978; Gunnell, 1994; Secord, 2004). Several taxa from the study localities (e.g., Litolestes, Microcosmodon conus, Mimetodon churchilli, Raphictis, Unuchinia dysmathes) first appear during the early middle Tiffanian in North

America; these so-called "first appearance datums" (or "first appearance events"; see Alroy, 1994) may represent evolutionary first occurrences or immigration events, and are powerful tools for temporal resolution (Woodburne, 1977, 1987, 1996, 2004; Lofgren et al., 2004; but see Alroy, 1998; Walsh, 1998). Furthermore, 23 of the 40 taxa identified by Lofgren et al. (2004) as being characteristic of the early middle Tiffanian (e.g., Carpodaptes, Litocherus, Mimetodon, Paleotomus, Unuchinia) are present in the combined Blindman River/Joffre Bridge local faunas. Several taxa identified in this study are known only from localities of early middle Tiffanian age in the Alberta Basin (e.g., Boreocyon gigas, Cervictis, Joffrelambda, Nayloria, Neoplagiaulax cimolodontoides), and with further collecting at localities outside of the Alberta Basin in the Western Interior of North America these may eventually prove useful in biostratigraphic correlation.

Temporal resolution at the study localities is relatively high, with most of the taxa being consistent with an early middle Tiffanian age (Fig. 12.1). Stratigraphic range extensions are minimal, providing additional evidence for an early middle Tiffanian age and less evidence for significant temporal averaging: of 76 described taxa, only three (Didymictis dellensis, Mimetodon churchilli, Microcosmodon conus) are known to occur previously in strata younger than those of the study localities, and three (Bessoecetor thomsoni, Paleotomus junior, Paleotomus senior) are known to occur previously in older strata.

Pollen

Demchuk's (1987, 1990) palynostratigraphic zonation of strata in the central and south-central Plains represents the only comprehensive analysis of fossil pollen of Paleocene age from the Red Deer River valley. Three palynozones were recognized by Demchuk (1987, 1990) as occurring in the Paskapoo Formation of Alberta: the Aquilapollenites spinulosis zone is represented in the lowermost, or Haynes Member, and part of the overlying Lacombe Member of the Paskapoo Formation (Demchuk, 1990; Demchuk and Hills, 1991), whereas the Caryapollenites wodehousei and Pistillipollenites mcgregorii zones are represented at successive, stratigraphically higher levels of the

Lacombe Member. Demchuk (1987, 1990) suggested that strata cropping out on the Blindman River, as well as those at Joffre Bridge, occur within the Caryapollenites wodehousei palynozone (Fig. 12.2), approximately correlative with palynozone P4 of Nichols and Ott (1978), and indicative of a middle Tiffanian age, but one that is slightly younger than that suggested by fossil mammals (Fox, 1990b).

Magnetostratigraphy

Magnetostratigraphic data for Paleocene age strata in the Red Deer River valley are known from test coreholes and from at least one of the study localities (e.g., Joffre Bridge Roadcut) (Lerbekmo and Coulter, 1985; Lerbekmo et al., 1990; Lerbekmo et al., 1992). These data indicate that Paskapoo strata in the Red Deer River valley encompass magnetochrons 26r through 25r, with all of the study localities falling near the top of magnetochron 26r (Fig. 12.2); these results are consistent with Butler et al.'s (1981) and Butler et al.'s (1987) composite correlations for Paleocene age sections from the San Juan Basin of New Mexico, the Clarks Fork Basin of Wyoming, and the Crazy Mountains Basin of Montana.

12.3 Faunal Comparisons

The Blindman River and Joffre Bridge local faunas are similar in general composition to faunas of middle Tiffanian age from localities in Alberta and other parts of the Western Interior of North America, particularly those from the northern parts of the western United States. Adequately sampled, well-studied middle and early late Tiffanian localities are poorly known from the Western Interior, limiting the number of meaningful comparisons that can be made; nonetheless, comparisons with several near-contemporaneous localities from Alberta, North Dakota, Montana, and Wyoming have resulted a number of interesting discoveries.

The local faunas from the Blindman River and Joffre Bridge bear closest resemblance to near-contemporaneous local faunas from other parts of the Alberta Basin, a discovery that is unsurprising given their close geographic proximity. Among these

localities, the Birchwood locality southwest of Edmonton (Webb, 1996; Scott, 2004 Prochetodon) bears closest resemblance to the Blindman River/Joffre Bridge local fauna, corroborating Webb's (1996) conclusions as regards his study on the mammals from the Birchwood locality. Thirty-two genera and 38 species have been identified as occurring at both localities (Fig. 12.3); in fact, with the exception of a tentatively identified palaechthonid plesiadapiform, all of the taxa known from the Birchwood locality also occur at the Blindman River/Joffre Bridge localities, although the converse is not true (i.e., there are several genera and species that have been documented at the Blindman River/Joffre Bridge localities that have yet to be discovered at Birchwood). Among the 32 genera and 38 species that are common to both local faunas, one genus (Nayloria) and four species (Neoplagiaulax serrator, N. paskapooensis, N. cimolodontoides, and Nayloria albertensis) are shared uniquely. A second early middle Tiffanian local fauna from Alberta, the Hand Hills West upper level locality northeast of Drumheller (Fox, 1990a; MacDonald, 1996), although more poorly sampled than the study localities, nonetheless closely resembles the Birchwood and Blindman River/Joffre Bridge local faunas (and see MacDonald, 1996). Among the near-contemporaneous local faunas known from outside of the Alberta Basin, two in particular, the early middle Tiffanian Cedar Point Quarry (northern part of the Bighorn Basin, Wyoming; Rose, 1981a; Secord, 2004) and Chappo Type locality (northern part of the Green River Basin, Wyoming; Gunnell, 1994) are of particular interest. Both of these localities share a number of taxa with the Blindman River/Joffre Bridge local fauna (24 genera, 18 species at Cedar Point Quarry, 20 genera, 15 species at the Chappo Type locality; Fig. 12.3), and both are more similar to the Alberta localities than are the early middle Tiffanian Judson and Brisbane localities of North Dakota (Holtzman, 1978; Kihm and Hartman, 2004). Fox (1990b) suggested that local fauna from DW-1 and DW-2 most closely resembles that from Cedar Point Quarry among localities from outside of the Alberta Basin, and this suggestion is confirmed by this study. Interestingly, the local fauna from the earliest Tiffanian Cochrane 2 locality of southwestern Alberta (Youzwyshyn, 1988; Fox, 1990a; Scott et al., 2002) bears a strong resemblance to that from the Blindman River and Joffre Bridge: the two local faunas share 33 genera in common, the greatest number among the local faunas included in this comparison, as well as 28 species. Four of the taxa shared

between the two local faunas are unique within the context of this analysis (Limaconyssus incomperta, Limaconyssus subnuba, Paleotomus junior, Chriacus sp., cf. C. baldwini), but these are known from other localities in Alberta or other parts of the Western Interior of North America that were not included here, and most of the other shared taxa are stratigraphically long-ranging (e.g., Mesodma pygmaea, Bessoecetor septentrionalis, Arctocyon). Nonetheless, these stratigraphically long-ranging taxa are clearly present at the study localities, and the Blindman River/Joffre Bridge local faunas contain a mixture of archaic taxa that were previously known only from older horizons in Alberta and elsewhere, as well as taxa that are only known from localities of early middle Tiffanian age or younger.

12.4 Mammalian Diversity During the Late Early and Early Late Paleocene in Alberta: Rose's Hypothesis Revisited

Introduction

Ever since Matthew's (1915) seminal publication on climate change and evolution, the paradigm of climate being a major influence on mammalian evolution has been generally accepted (e.g., Rose, 1981a-b; Webb, 1984; Barnosky, 1989; Vrba, 1992, 1993; Janis, 1993, 1997; Janis and Wilhelm, 1993; Gunnell et al., 1995; Clyde and Gingerich, 1998; Gingerich, 2004, 2006; Secord, 2004), despite a minority of authors having suggested alternative, and perhaps more conservative explanations for the patterns of mammal diversity seen during the early parts of the Tertiary of North America and elsewhere (e.g., Youzwyshyn, 1988; Fox, 1990a; Prothero and Heaton, 1996; Behrensmeyer et al., 1997; Prothero, 1999, 2004; Alroy, 1996, 1998; Alroy et al., 2000; Scott et al., 2002); clearly a consensus on this issue has yet to be achieved. Despite these disagreements, there at least seems to be considerable and convincing evidence for an abrupt change in climate at the Paleocene-Eocene boundary (approximately 55 mya), both in North America specifically and more globally generally, and a number of authors have been able to demonstrate that significant mammalian faunal turnover, either through extinction, immigration, or both, coincided with the so-called Paleocene-Eocene Thermal

Maximum (PETM) (e.g., Gingerich, 1989; Clyde and Gingerich, 1998; Alroy et al., 2000; Gingerich, 2003, 2004, 2006; Smith et al., 2006). While much of the data that bears on paleoclimate at the Paleocene-Eocene boundary, and through the early Tertiary generally, has been accumulated as a result of recent advances in stable isotope analysis (e.g., Koch et al., 1992, 2003; Zachos et al., 1996, 1997, 2001), high-resolution stratigraphy (e.g., Fricke et al., 1998; Meng and McKenna, 1998; Secord, 2004; Chew, 2005; Secord et al., 2006), and refined paleobotanical data (e.g., Wing et al., 1991, 1995; Wilf, 2000), few of these methodologies have been applied to older sequences, particularly those from earlier in the Paleocene [benthic foraminifera of Paleocene age from deep sea cores are known (see Zachos et al., 2001), but these have yet to be studied in detail]. Reconstructions of terrestrial paleoclimate during the early and early late parts of the Paleocene of North America are based on a limited number of paleotemperature proxies, most notably from leaf margin analyses of paleofloras from the Bighorn and Clarks Fork basins of Wyoming (e.g., Wolfe and Hopkins, 1967; Hickey, 1980; Wing et al., 1995; Wilf, 2000), although more recent studies focusing on oxygen isotopes in tooth enamel (e.g., Rose et al., 2007) and marine foraminifera (e.g., Zachos et al., 2001) promise to add significantly to the pool of data that can be brought to bear on inferring paleotemperature during the earlier parts of the Paleocene. Despite the fact that paleoclimate from the earlier parts of the Paleocene is not well understood, there is nonetheless general agreement that the epoch was characterized by warm, subtropical conditions during the Puercan and Torrejonian, followed by cooler, more temperate conditions during the Tiffanian, and then a return to warmer conditions during the latest Tiffanian and Clarkforkian that eventually culminated at the PETM.

Paleocene paleoclimate and its inferred effects on mammalian evolution figured prominently in a pair of classic papers by Rose (1981a-b). Rose (1981a-b) examined the patterns of faunal composition and diversity of sixteen fossil mammal assemblages from the Crazy Mountains, Bighorn, and Clarks Fork basins of Montana and Wyoming, spanning a stratigraphic interval from the middle Torrejonian (To2, early Paleocene) to the early Wasatchian (Wa1, early Eocene), and focused primarily on changes in species richness and heterogeneity as inferred from various indices of diversity (e.g., Simpson, Shannon, Whittaker) and from rank abundance curves of fossil mammal faunas (e.g.,

Rose, 1981a, figs. 77A-C; Rose, 1981b, figs. 4, 5). The results of these analyses suggested that mammalian species richness (i.e., number of species) and evenness (i.e., the relative abundance of any one species in an assemblage) decreased from relatively high levels during the middle and late Torrejonian to significantly lower levels during the Tiffanian, followed by a return to high levels during the latest Tiffanian and on into the Clarkforkian and Wasatchian (Rose, 1981a, figs. 75, 76). Given the then available information as regards paleotemperature, Rose (1981a-b) reasonably hypothesized that the decreases in mammalian species richness and evenness may have been attributable to similar and presumably contemporaneous changes in floral species richness and paleotemperature. The Torrejonian was, as inferred by Rose (1981a-b), characterized by warm, equable conditions that supported rich (i.e., numerous species) and even (i.e., relatively even distribution of individuals among species, and no dominant species present) mammal faunas, whereas the Tiffanian was marked by cooler temperatures and a less equable (i.e., less predictable) environment that supported fewer species, with one or two generalist taxa dominating the fauna. Studies subsequent to those of Rose (1981a-b) have generally supported his opinions. For example, in a study of mammalian evolution and climate during the Paleocene of Montana and Wyoming, Krause and Maas (1990) re-examined Rose's (1981a-b) study localities and, importantly, included large samples from localities that were not used in Rose's (1981a-b) original studies (e.g., Scarritt Quarry and Douglass Quarry). Krause and Maas (1990) confirmed that Rose's (1981a-b) main thesis, that mammalian diversity decreased during the Tiffanian, and then increased during the Clarkforkian and Wasatchian, was essentially correct, but suggested that the pronounced cooling trend did not begin until sometime after the earliest Tiffanian (Ti1), a conclusion based in part on new data obtained from inclusion of the much better sampled earliest Tiffanian Douglass Quarry of Montana. The two most recent analyses of Paleocene mammalian diversity and paleoclimate are studies by Alroy et al. (2000) and Secord (2004), the latter of which is more pertinent to this study. In a comprehensive review of Tiffanian and Clarkforkian mammals from the Bighorn Basin, Secord (2004) re-analyzed Rose's (1981a-b) original samples, including those from the Crazy Mountains Basin and, importantly, updated the taxonomic lists for a number of the study localities in the Bighorn Basin (e.g., Cedar Point Quarry, Princeton Quarry). Secord

(2004) noted that the samples used by Rose (1981a-b) and Krause and Maas (1990) were of disparate sizes, and rationalized that since linear regression statistics indicate that levels of diversity generally are correlated with sample size (Secord, 2004, fig. 4-1, and see Jamniczky et al., 2003), meaningful comparisons using these samples require that they first be standardized. The results of Secord's (2004) analysis, which examined levels of species richness in standardized samples, were consistent with those of Rose (1981a-b) and Krause and Maas (1990), that examined changes in diversity (i.e., richness and evenness). It is emphasized here that the analyses of Krause and Maas (1990) and Secord (2004) basically replicated Rose's (1981a-b) original study, with the addition of newly collected specimens or revised species lists; although Rose (1981a-b) and Secord (2004) were careful to restrict the implications of their results to the Bighorn and Crazy Mountains basins, other studies (e.g., Krause and Maas, 1990) have extrapolated the results of these studies to North America more generally.

While the results of subsequent analyses of the same study localities used in Rose's (1981a-b) original study have continued to support Rose's (1981a-b) initial hypothesis, similar support has not been offered from analyses of coeval localities outside of Montana and Wyoming. In his classic study of earliest Tiffanian (late Paleocene) mammals from the Cochrane 2 locality of southwestern Alberta, Youzwyshyn (1988) demonstrated that species richness in the early parts of the late Paleocene in Alberta exceeded the predicted values necessary to satisfy Rose's (1981a-b) hypothesis: the Cochrane 2 local fauna, represented by more than 2000 identifiable specimens, 65 genera, and 86 species (as known in 1988, but see Appendix 2), far exceeded the predicted species richness levels for the earliest Tiffanian, and exceeded even those for the supposedly more diverse Torrejonian localities in Montana (Gidley Quarry) and Wyoming (Rock Bench Quarry). Youzwyshyn (1988) suggested that sampling error was the likeliest source of the incongruities, with the rigorous screen-washing techniques used at Cochrane 2 able to sample small specimens that would likely be missed in quarrying or surface collecting. Youzwyshyn's (1988) results were emphasized in Fox's (1990a) review of Paleocene mammal evolution in western Canada, and again in Scott et al.'s (2002) report on new mammals from the Cochrane 2 locality, however these data have yet to be incorporated in any meaningful way into larger-scale studies on Paleocene

climate change leading up to the PETM. The large samples from the Blindman River/Joffre Bridge localities, as well as the recently described middle Torrejonian (To2) Who Nose? locality of south central Alberta (Scott, 2003), provide an opportunity to revisit Rose's (1981a-b) hypothesis, and to examine the changes in mammalian diversity during the early parts of the late Paleocene in Alberta.

Methods

General.—While the meaning of "diversity" differs, often significantly, among authors, there seems to be general agreement that the term encompasses two concepts, with the most basic being that of species richness, or a measurement of the absolute number of species in any given fauna; a second concept, species evenness, refers to the relative abundances of species in a given fauna (Peet, 1974; Whittaker, 1977; Rose, 1981a; Krebs, 1989; Magurran, 2003). The combination of species richness and evenness (called heterogeneity or "total" diversity) is believed to represent the best estimate of diversity, and a number of so-called diversity indices have been developed in order to easily compare calculated values from different faunas; as with the meaning of diversity, however, the application of diversity indices, and their interpretation are sometimes difficult, and can differ from author to author. An alternative to diversity indices is the rank abundance curve: such curves provide a visual representation of species richness and species evenness, and can display the relative role that different variables played in its calculation. Rose (1981a-b) assessed changes in mammalian faunal diversity in the Paleocene of Wyoming and Montana by examining the differences in diversity indices and rank abundance curves between successively younger local faunas, while Secord (2004) focused on examining changes in species richness in standardized samples. Given the uncertainties in the use and interpretation of indices, the diversity in Paleocene mammal faunas from Alberta was assessed in this analysis by examining species richness from standardized samples, and species evenness through rank abundance curves.

Sample.—Specimens used in this analysis consist of teeth, jaws with teeth, and, more rarely, incomplete skulls with teeth; isolated postcranial bones were not included.

Total number of specimens and minimum numbers of individuals were compiled for local faunas of middle Torrejonian (Who Nose?, Nordic Ski Quarry, To2), earliest Tiffanian (Cochrane 2, Ti1), and early middle Tiffanian (Blindman River/Joffre Bridge, Ti3) age from the Alberta Basin (see Appendix 2). Locality information can be found in Youzwyshyn (1988), Fox (1990a), Lerbekmo and Sweet (2000), Scott et al. (2002), and Scott (2003). Locality data for the Torrejonian were pooled from Nordic Ski Quarry and from Who Nose?; both of these localities are located in the northwestern part of the City of Calgary, Alberta, and are of a similar age (Scott and Fox, in prep.); the data from the Blindman River/Joffre Bridge localities were similarly pooled. Specimen data were obtained for each taxon in the study localities through firsthand observations, and did not rely on lists. Several taxonomic revisions to the Cochrane 2 and Who Nose? local faunas have been made since the publication of Fox (1990a), Scott et al. (2002), and Scott (2003), and these are reflected in this analysis (the taxonomic listings in Appendix 2 should be viewed as the most current). Estimations of abundance followed the rationale of Secord (2004), who followed the protocol of Clyde and Gingerich (1998) and Behrensmeyer et al. (2000); in short, these studies considered fossil localities as "isotaphonomic groups" on the basis of their inferred taphonomic history and collecting protocols, and abundance was estimated either by total number of specimens or by minimum numbers of individuals. Who Nose?, Nordic Ski, and Cochrane 2 are most consistent with Secord's (2004) "clay gall quarry" group: fossils from these localities are generally preserved in calcareous siltstones at the base of sandstone units, and are often associated with clay galls, fossilized molluscs, and plant debris. Bartels (1987) indicated that similar localities in the Bighorn Basin of Wyoming were probably fluvial in origin, and that vertebrate and plant debris accumulated in lag deposits during channel avulsion, with the fossils bearing evidence of transport. Screen washing and limited quarrying have been the primary means of collecting at these localities. In contrast, the Blindman River/Joffre Bridge localities are generally more consistent with Secord's (2004) "mudstone quarry" group: fossils in this group show little evidence of extended transport, and associated and even articulated remains are sometimes present; "mudstone quarries" often have biases towards small-sized specimens. In contrast to the "clay gall" group, fossils from the "mudstone quarry" group have been collected almost exclusively by

quarrying. Following Clyde and Gingerich (1998) and Secord (2004), abundance for "clay gall" quarries was estimated by total number of specimens, whereas that for "mudstone quarries" was estimated by minimum numbers of individuals. Clearly no single method of estimating numbers of individuals can be regarded as optimal: total number of specimens will likely overestimate the number of individuals, whereas minimum number of individuals will underestimate it (Secord, 2004); for ease of comparison, however, this analysis follows Secord's (2004) protocol.

Sample standardization.—Standardization of samples was achieved using rarefaction, an interpolative technique that estimates the number of species that would be present in a sample that is smaller than the actual sample size [i.e., if a subsample n of a group of N individuals belonging to S species ($n<N$) was examined, how many species s ($s<S$) would be observed?)] (Raup, 1975; Krebs, 1989). Rarefaction generates probability curves that plot number of species as a function of species abundance in the sample (based in this analysis on estimated numbers of individuals), and allows comparisons among samples of different sizes. Tipper (1979) provided a critique of rarefaction and outlined the limitations of this methodology and its use in paleoecology; most of Tipper's (1979) criticisms relate to how adequately the subsamples to be rarefied are representative of the original community from which they were drawn, a problem that is particularly acute for paleontological analyses in which samples may be significantly time-averaged and taphonomically biased (and see similar criticisms in Rose, 1981a; Behrensmeyer, 1991; Gunnell, 1994). Recent studies by Brinkman (1990) and Jamniczky et al. (2003), however, have suggested that many vertebrate microsites meet the majority of Tipper's (1979) criteria, and may be adequate proxies for the parent communities from which they were drawn. For the present purposes, and to facilitate comparisons with Secord's (2004) study, it is assumed here that the samples analyzed in this study are representative of their parent communities, and that the use of rarefaction for sample standardization is appropriate. Rarefaction estimates were made using Rarefaction 1.3 software as developed by Holland (www.uga.edu/strata/software/Software.html).

Rank abundance curves.—An alternative way of comparing diversity is through rank abundance curves. The curve is generated by plotting the relative abundances of

species against their sequence, or rank, from most to least abundant. Species richness is expressed as the number of different species plotted on the graph (i.e., the length of the curve), while species evenness is derived from the slope of the line; a steep slope indicates low evenness as the high ranking species have much higher abundances than the low ranking species, whereas a shallow slope indicates high evenness as the abundances of different species are similar. The construction of rank abundance curves in this analysis follows Rose (1981a-b) in plotting species relative abundance as a percentage on the y-axis, while log species rank is plotted on the x-axis.

Results

The rarefaction curves generated for the localities from Alberta show overlap throughout their extent, with no significant separation of any of the curves from one another (Fig. 12.4). The rarefaction curve generated for the Blindman River/Joffre Bridge localities begins to diverge from that of the Cochrane 2 locality towards the limit of its sample size (470 individuals), but it is fully within the upper error bar (1.96×standard deviation) of the Cochrane 2 curve. The curves indicate that the rarified sample from the Blindman River/Joffre Bridge localities is estimated to contain the greatest number of species (i.e., is richest), followed by the sample from Nordic Ski/Who Nose?, and finally by the sample from Cochrane 2. When these estimates are placed in ascending stratigraphic order, mammalian species richness is estimated to have decreased slightly from the middle Torrejonian (To2) to earliest Tiffanian (Ti1), and then increased on into the early middle Tiffanian (Ti3); given the tight grouping of the three curves and the significant overlap of the error bars, however, the difference in species richness from one locality to the next is probably insignificant. In contrast, the rarefaction curves for coeval localities from Montana and Wyoming show a notably different pattern [these curves are reproduced from Secord's (2004) study in Figure 4B]. The three curves generated from the American data are well separated from one another for most of their respective extents; the three curves are fully separate at the level of approximately 550 individuals, with non-overlapping error bars, suggesting that species richness differs among the three local faunas. As Rose (1981a-b), Krause and Maas (1990), and Secord

(2004) noted previously, species richness among these localities is highest at Gidley Quarry (To2), with Douglass Quarry (Ti1) being at an intermediate level, and finally the Cedar Point Quarry local fauna (Ti3) supporting a relatively low number of species. When non-standardized species richness and rarefied species richness normalized to 300 individuals are plotted against stratigraphic interval (Fig. 12.5), the difference in trends between the American and Albertan data becomes even more apparent. The curves in Figure 5 that were generated from the American data generally agree with Rose's (1981a-b) hypothesis of decreasing species diversity from the Torrejonian to the earliest Tiffanian, although the decrease is much less severe than that reported by Rose (1981a-b) and Secord (2004), undoubtedly a consequence of this study having included more recent data (e.g., Silcox et al., 2001; Scott and Krause, 2006) for the Douglass Quarry locality. Nonetheless, the trend as reported by Rose (1981a-b) is also seen in this study, with species richness decreasing through to the early middle Tiffanian in Montana and Wyoming. In contrast, rarefied species richness for the Alberta data decreases only slightly from Nordic Ski/Who Nose? to Cochrane 2, but increases to the early middle Tiffanian; as noted previously, the difference in the number of species among the three study localities in Alberta is likely not significant.

The rank abundance curves for each of the study faunas are generally similar, and indicate high species richness and evenness (Fig. 12.6). The species abundance distribution for each local fauna defines a relatively shallow curve that corresponds most closely to MacArthur's Type I (broken stick) model (MacArthur, 1957, 1960). MacArthur's broken stick distribution is a standard null model of community structure that predicts the distribution of species' relative abundances when resources are partitioned into niches at random and species evenness is maximized (MacArthur, 1957, 1960; Krebs, 1989); samples in which relative abundance is similar among the included species approximate this theoretical distribution, and the resultant curve usually approaches a straight line. The rank abundance curves for the local faunas from Who Nose?/Nordic Ski Quarry, Cochrane 2 , and the Blindman River/Joffre Bridge localities closely resemble those for the Torrejonian localities from Wyoming (Rock Bench Quarry) and Montana (Gidley Quarry) that were included in Rose's (1981a-b) analyses, as well as that for the late Tiffanian (Ti5) Princeton locality; distributions of this type are

thought to be indicative of high diversity faunas inhabiting relatively predictable environments (May, 1976; Rose, 1981a-b). A notable difference between the results of this study and those of Rose (1981a-b) concerns the rank abundance curves of the early middle Tiffanian (Ti3) localities. In contrast with the high levels of species evenness seen in the Blindman River/Joffre Bridge local faunas, species evenness is decidedly lower in the early Tiffanian (Scarritt Quarry, Crazy Mountains Basin, Montana) and early middle Tiffanian (Cedar Point Quarry, Bighorn Basin, Wyoming) in the United States, with rank abundance curves that more closely approximate the so-called "type IV" distribution (Hutchison, 1961; Goulden, 1969). Faunas having a type IV distribution are generally characterized by low diversity, with one or two dominant species; type IV distributions are thought to be indicative of stressed or otherwise unpredictable environments. When the rank abundance curves from the Alberta samples are placed in ascending stratigraphic order, species evenness remains virtually unchanged from the middle Torrejonian to the early middle Tiffanian in Alberta; a slight drop in evenness is noted between Who Nose?/Nordic Ski and Cochrane 2 (i.e., the Cochrane 2 fauna is slightly less equitable), but this may be owing to the much smaller sample size from the Torrejonian localities relative to the Tiffanian localities. In contrast, coeval samples from the United States show a decrease in species evenness from the middle Torrejonian to the earliest Tiffanian, followed by a sharp decline into the early middle Tiffanian (Rose, 1981a-b).

12.5 Discussion

While a more comprehensive analysis of late Paleocene mammal faunas in Alberta is beyond the scope of the present study, the results of the faunal comparisons and preliminary diversity analysis raise a few interesting points. First, and perhaps most importantly, the results of this analysis suggest that mammalian species diversity in Alberta did not experience a sharp decline during the middle and late parts of the Paleocene as predicted by Rose's (1981a-b) hypothesis, but instead remained high well into the late Paleocene, results that are consistent with conclusions of Youzwyshyn (1988) and Fox (1990a) that were made on the basis of species counts nearly twenty

years earlier. That the results of this analysis corroborate Youzwyshyn (1988) and Fox's (1990a) conclusions are particularly important given that this study relied on similar rationales and methodologies of data standardization as those of more recent studies that have supported Rose's (1981a-b) results (e.g., Secord, 2004); that these differences hold with respect to standardized samples suggests that the disparities in species diversity between the Alberta localities and those from the United States are probably not attributable to differences in sample size alone. Species richness in the samples from Alberta is markedly higher compared to that for samples from localities in other parts of the northern Western Interior of North America, with richness levels at the earliest Tiffanian Cochrane 2 locality far exceeding that of any other Paleocene age mammal locality so far discovered. The results of this study indicate that species richness levels at the early middle Tiffanian Blindman River/Joffre Bridge local fauna, while not as high as those for Cochrane 2, nonetheless exceed those of any coeval local fauna from Alberta or elsewhere. As suggested by the rank abundance curves, the local faunas from Alberta show higher levels of species evenness throughout the late Paleocene compared to coeval localities from the United States. Rose (1981a-b) suggested that the decrease in species evenness through the early late Tiffanian in Wyoming and Montana might be indicative of climatic instability, resulting in the emergence of one or two dominant species in each local fauna (e.g., Plesiadapis rex at Cedar Point Quarry), but the evidence from the Alberta localities supports neither of these assertions.

Taken together, the evidence from the Alberta localities seems to indicate that the level of mammalian diversity remained consistently high during the late Paleocene; indeed, the trends that are suggested by the results of this study indicate that paleoclimate in the more northern parts of the Western Interior of North America either remained virtually unchanged during the middle and late Paleocene, or if significant climatic change did occur, it did not result in a dramatic cause-and-effect response in either mammalian species richness or species evenness as predicted by Rose (1981a-b). While the results of this study differ from those of Rose (1981a-b), Krause and Maas (1990), and Secord (2004), they are consistent with those of Maas et al. (1995) and Alroy et al. (2000), both of which argued for higher levels of mammalian diversity during the middle and late Paleocene than that predicted by the former three studies. The explanation for

these discrepancies is unclear, but it almost certainly includes difficulties in inferring climatic change from paleotemperature proxies, as well as sampling biases that may be difficult, if not impossible to overcome. For example, estimates of mean annual paleotemperature from the paleobotanical and marine foraminifera records during the middle and late Paleocene, although generally mirroring the changes seen in mammal species richness, do not do so unanimously (see, e.g., contrasting estimates of Hickey, 1977, 1980; Wolfe, 1978; Wolfe and Poore, 1982; Shackleton, 1984; Wing et al., 1995; and see Krause and Maas, 1990, fig. 3). Stable isotopes from the marine record often provide a more nearly complete record of putative temperature change, but a strong correspondence between estimates derived from marine isotopes and those from continental temperature proxies (e.g., leaf margins) has yet to be demonstrated; furthermore, recent studies by Alroy et al. (2000), Prothero (2004), and Secord (2004) failed to detect a statistically significant correlation between changes in mammal species richness and changes in paleotemperature as inferred from stable isotopes in the marine record. The availability of well-sampled localities for study clearly affects the analysis and subsequent interpretations of mammal diversity levels. For example, the crucial evidence for a decrease in mammalian species richness during the early parts of the late Paleocene comes primarily from local faunas from the early Tiffanian (Ti2) Scarritt Quarry of Montana and the early middle Tiffanian (Ti3) Cedar Point Quarry of Wyoming, two localities that have unusually low mammalian species diversity (Rose, 1981a-b). While Rose (1981a-b) thought that the Scarritt Quarry sample was probably size-biased, Cedar Point Quarry was considered taphonomically unbiased and an appropriate representation of early middle Tiffanian mammal faunas generally (and see Krause and Maas, 1990; Secord, 2004); doubt has been cast on this assertion, however, by the discovery of several fossil mammal bearing localities of early middle Tiffanian age in the northern parts of the Green River Basin and Hanna Basin, Wyoming, that are significantly more species-rich than Cedar Point Quarry (see, e.g., Gunnell, 1994; Higgins, 2004). Other taphonomic and collecting biases can contribute, in whole or in part, to patterns of species richness and diversity in samples of fossil organisms (e.g., size-sorting, weathering, screen-washing versus surface collecting). Although Rose (1981a-b) discussed a number of these biases, he considered most of them insignificant in

the context of examining long-term patterns of evolution. The results of Youzwyshyn (1988), Fox (1990a), and this study suggest, however, that these biases may be much more significant than previously believed.

A clearer picture of the long term patterns of mammalian evolution during the Paleocene in North America is a desirable goal, but this goal can only be achieved by taking into account all of the available evidence. That climate undoubtedly had an effect on vertebrates and other organisms during the Cenozoic is well established (e.g., Prothero and Berggren, 1992; Prothero et al., 2003), but its effect on terrestrial mammals specifically during the Paleocene is unclear, at least as far as can be determined from conventional means of diversity analysis as employed in this and other analyses. A better understanding of the effects of taphonomic, sedimentological, and sampling biases on the perceived patterns of mammal evolution during the middle and late parts of the Paleocene can only come with the discovery of new fossils, and the continued sampling of previously known, but poorly studied localities.

12.6 Summary of the Dissertation

The major conclusions of this study are as follows:

1) Multituberculates constitute nearly 40 percent of the species so far known from the Blindman River/Joffre Bridge localities, and include neoplagiaulacids, ptilodontids, and microcosmodontids. Neoplagiaulacids are taxonomically diverse, and include a new species of Ectypodus (E. elaphus) and three new species of Neoplagiaulax (N. serrator, N. paskapooensis, N. cimolodontoides). The DW-2 and Joffre Bridge Roadcut upper level localities record the earliest record of Mimetodon churchilli, and records the first sympatric occurrence of two species of Mimetodon (M. silberlingi, M. churchilli), while the DW-2 locality records the earliest record of the microcosmodontid Microcosmodon conus. Ptilodontids are represented by two species of Ptilodus (P. sp. "C" and P. sp. "T"), in addition to a new species of Prochetodon (Pro. speirsae); Pro. speirsae represents the earliest known occurrence of the genus. The new neoplagiaulacids, together with other multituberculates from the Blindman River localities, document unusually high multituberculate diversity in the latter half of the Tiffanian in western Canada. Despite

superficial similarity to some European species of Neoplagiaulax, the new taxa from the Paskapoo Formation apparently show no closer relationship to these than do other North American congeners, suggesting parallel evolution in endemic North America and western European clades.

2) Two marsupial genera have been discovered at the study localities, documenting the first occurrence of three marsupial species at a single locality of early middle Tiffanian age in North America. Peradectes pauli is represented by exceptionally well-preserved specimens, and is here considered a valid taxon; it differs from Peradectes elegans most clearly in the size and coronal anatomy of the lower canines. Typhlodelphys gordi, a new genus and species of didelphimorphian marsupial, is known only from the holotype; it displays a curious mosaic of primitive and derived metatherian character states, and is classified in Didelphimorphia, incertae sedis. Although marsupials are rare in post-Cretaceous-Tertiary boundary sediments, the discovery of Typhlodelphys, as well as three species from a single locality in the late Paleocene, suggests that much of the early Tertiary evolutionary history of the cohort remains unknown.

3) Insectivorans are the best-represented mammalian group at the study localities, constituting approximately 26 percent of the species so far discovered. Lipotyphlans are taxonomically diverse, consisting of erinaceomorphs and soricomorphs; included among the erinaceomorphs are three new genera (Xynolestes, Nayloria, Adeloxenus), while one new soricomorph genus was described (Psydronyctia). Notable among the lipotyphlan specimens is the oldest known erinaceomorph petrosal and postcranium (of Litocherus notissimus), as well as the first record of the upper dentition of the enigmatic soricomorph "Leptacodon" munusculum. Limaconyssus, known previously from only the holotype of the Clarkforkian species L. habrus, is represented by two new species (L. incomperta, L. subnuba) in the study local faunas. The study localities document the first record of sympatric occurrences of the pantolestids Bessoecetor thomsoni and B. septentrionalis, as well as Paleotomus senior and P. junior. A new species of the pentacodontid Bisonalveus was described (B. toxidens); the grooved upper canines of B. toxidens are interpreted as representing the earliest record of a mammalian venom

delivery apparatus. Well-preserved specimens of the rare apatemyid Unuchinia dysmathes were described, including the first known articulated lower incisors and upper dentition; the new specimens confirm previous suggestions that Unuchinia represents the most primitive apatemyid. New specimens of the putative palaeoryctid Pararyctes were described, including a new but poorly represented large-bodied species (P. colossa). A phylogenetic analysis of the earliest lipotyphlans from North America, Western Europe, and East Asia resulted in 20 optimal trees of 785 steps. A soricomorph-erinaceomorph dichotomy was recovered in each of the optimal trees. A close association of Litolestes, Cedrocherus, and Oncocherus with extant erinaceids was not supported, nor was inclusion of "Leptacodon" munusculum or "Leptacodon" packi with other species of Leptacodon. Psydronyctia may represent the earliest and first North American record of Amphidozotheriinae, and Limaconyssus, previously considered an aberrant nyctitheriid, is here considered a geolabidid.

4) Although carnivorans are poorly represented at the study localities, the few specimens are sufficient to document the presence of three genera, one of which (Cervictis) is new. A new species of Raphictis was described (R. iota), and the presence of Didymictis dellensis at the study localities represents the earliest record of the species.

5) Plesiadapiforms are among the most abundantly represented mammals at the study localities. The much larger sample of Pronothodectes gaoi clearly demonstrates the distinctiveness of this taxon relative to Plesiadapis rex, with over 20 lower jaws documenting the presence of a lateral lower incisor and lower canine. New specimens of the carpolestids Elphidotarsius wightoni and Carpodaptes hazelae confirm previous observations regarding the upper dental formula of each, and a weak bimodality in the lateral profile of the p4 of Carpodaptes hazelae is suggestive of there being two species in the sample. The systematics of Picrodontidae are revised: three new species of Picrodus from the Torrejonian (P. calgariensis) and Tiffanian (P. canpacius, P. lepidus) of Alberta are named, each representing a successively younger and dentally more derived member of the genus. The evolution of the picrodontid dentition is marked by several trends, including increase in size of i1, simplification of P4, reduction of molar cusps and crests,

enlargement of the horizontal occlusal surfaces of the molars, and greater crenulation of enamel. From present knowledge, Zanycteris paleocenus is dentally more primitive than Picrodus, Draconodus is a valid genus, and picrodontids probably originated from "purgatoriid-grade" plesiadapiforms in earliest Paleocene time.

6) The systematic positions of Eudaemonema and Elpidophorus were investigated. Eudaemonema is represented by a new species (E. thlastes) that differs from the genotype E. cuspidata in being larger and in having lower crowned teeth that are better adapted to crushing; E. thlastes is also known from the late middle Tiffanian Gao Mine locality of Alberta, and is the youngest mixodectine. Two sympatric species of Elpidophorus are known from the study localities, one of which (E. simpsoni) is new. Eudaemonema and Elpidophorus are here considered mixodectids rather than plagiomenids, and are probably not dermopterans. Eudaemonema and Mixodectes can be united in the Mixodectinae, whereas Elpidophorus and possibly Remiculus are referred to the new mixodectid subfamily Elpidophorinae.

7) A taxonomically diverse but generally poorly represented assemblage of condylarths and mesonychids is known from the study localities. New and previously collected fossils from these localities document the presence of oxyclaenid, arctocyonid, and phenacodontid condylarths, and a single species of the mesonychid Dissacus. This study reports the first occurrence of the oxyclaenid Chriacus oconostotae outside of Wyoming, as well as two new arctocyonid genera, Boreocyon and Insidioclaenus, both of which are known from stratigraphically older horizons in Alberta. Although local faunas from western Canada resemble those at localities of similar age from other parts of the Western Interior in showing a decrease in condylarth taxonomic diversity through the Tiffanian, they differ in taxonomic composition, with arctocyonids remaining taxonomically diverse through the middle Tiffanian. Hyopsodontids are unknown from western Canada after the earliest Tiffanian, and their absence may be related, at least in part, to increased competition from the hyopsodontid-like insectivorans Litocherus and Bisonalveus, both of which are abundantly represented in the early middle Tiffanian of Alberta.

8) A small but taxonomically diverse assemblage of pantodonts is known from the study localities, including a new primitive genus and species of titanoideid (Joffrelambda spivaki) known from two well-preserved specimens that include the skull and significant parts of the postcranium. Two upper and lower canine morphs have been identified for Joffrelambda, suggesting that the genus may be sexually dimorphic. A second unidentified titanoideid, as well as a single tooth possibly pertaining to Caenolambda are known from the study localities. A new genus and species of cyriacotheriid pantodont, Presbyteria rhodoptyx, was described; Presbyteria is more primitive than the genotype Cyriacotherium in having incipiently dilambdodont premolars and a well-developed lower molar entoconid. The new information gained by the discovery of Presbyteria indicates that the Cyriacotheriidae are not dermopterans or plagiomenids, but rather are a long-lived clade of highly derived pantodonts, with a stratigraphic record that extends back into the middle Torrejonian (To2). The ancestry of Cyriacotheriidae, previously believed to with or near the pantolambdoidean Pantolambda, now seems more likely to have been from a generalized pantolambdoidean in which the premolars were only weakly molariform (i.e., the lower premolar paraconids and talonids were less well-developed than those in Pantolambda, and the upper premolars probably bore a well-developed, V-shaped ectoloph), and that dilambdodonty in the lower molars was incomplete posteriorly, with the hypoconulid in a more labial position (and with the hypocristid correspondingly shorter) and the entoconid fully developed.

9) A new eutherian mammal of uncertain taxonomic position was described on the basis of well-preserved dental and gnathic specimens collected primarily from DW-2. Horolodectes sunae is represented by seven incomplete maxillae, eleven incomplete dentaries, and numerous isolated teeth, together preserving nearly all of the post-canine dentition. The unusual dentition of Horolodectes consists of trenchant, posteriorly leaning premolars in combination with comparatively primitive molars, suggestive of a masticatory cycle that consisted primarily of shearing and, to a lesser degree, horizontal grinding. Included among the specimens of Horolodectes is an incomplete dentary of an immature individual, with the teeth having been in various stages of eruption at the time of death. Although the dentition of Horolodectes broadly resembles that of apheliscine

hyopsodontids, pentacodontid pantolestids, and "ungulatomorphs" among eutherian mammals, significant differences in the coronal structure of the teeth prevent unequivocal referral of Horolodectes to any of these groups, or to any known eutherian order.

10) Biostratigraphic evidence from fossil mammals and pollens, in addition to magnetostratigraphic data, indicate that the Blindman River/Joffre Bridge local faunas are early middle Tiffanian (Ti3) in age, a conclusion that is consistent with previous estimates of relative age. Comparisons with near-contemporaneous localities from the Alberta Basin and other parts of the Western Interior of North America indicate that the Blindman River/Joffre Bridge local faunas are taxonomically most similar to other early middle Tiffanian local faunas, especially the Birchwood local fauna from Alberta, and the Cedar Point Quarry local fauna of Wyoming. A preliminary study of faunal diversity, including comparisons of species richness using rarefied samples, indicates that early and early late Paleocene age local faunas from the Alberta Basin (Who Nose? Quarry, Nordic Ski Quarry, Cochrane 2, Blindman River/Joffre Bridge) display high levels of species richness and evenness compared to coeval local faunas from other parts of the Western Interior. These results are incongruent with previous hypotheses that suggest mammalian diversity drops significantly during the late Tiffanian in North America in response to presumably cooler paleotemperatures.

12.7 Literature Cited

AGTERBERG, F. P. 2004. Geomathematics, pp. 106-125. In F. M. GRADSTEIN, J. G. OGG, and A. G. SMITH (eds.), A Geologic Time Scale, Cambridge University Press, Cambridge.

ALROY, J. 1994. Appearance event ordination: a new biochronologic method. Paleobiology, 20:191-207.

ALROY, J. 1996. Constant extinction, constrained diversification, and uncoordinated stasis in North American mammals. Palaeogeography, Palaeoclimatology, Palaeoecology, 127:285-311.

ALROY, J. 1998. Diachrony of mammalian appearance events: implications for biochronology. Geology, 26:23-27.

ALROY, J., P. L. KOCH, and J. C. ZACHOS. 2000. Global climate change and North American mammalian evolution. Paleobiology, 26, supplement to no. 4:259-288.

ARCHIBALD, J. D., P. D. GINGERICH, E. H. LINDSAY, W. A. CLEMENS, D. W. KRAUSE, and K. D. ROSE. 1987. First North American Land Mammal Ages of the Cenozoic era, pp. 24-76. In M. O. WOODBURNE (ed.), Cenozoic Mammals of North America: Geochronology and Biostratigraphy, University of California Press, Berkeley.

BARNOSKY, A. D. 1989. The late Pleistocene event as a paradigm for widespread mammal extinction, pp. 235-254. In S. K. DONOVAN (ed.), Mass Extinctions: Processes and Evidence, Bellhaven Press, London.

BARTELS, W. S. 1987. Fossil reptile assemblages and deposition environments of selected early Tertiary vertebrate bone concentrations, Bighorn Basin, Wyoming. Unpublished Ph. D. dissertation, The University of Michigan, Ann Arbour, 603 pp.

BEHRENSMEYER, A. K. 1991. Terrestrial Vertebrate Accumulations, pp. 291-335. In P. Allison and D.E.G. Briggs (eds.), Taphonomy: Releasing the Data Locked in the Fossil Record. Plenum Press, New York.

BEHRENSMEYER, A. K., N. E. TODD, R. POTTS, and G. E. MCBRINN. 1997. Late Pliocene faunal turnover in the Turkana Basin, Kenya and Ethiopia. Science, 278:1589-1594.

BEHRENSMEYER, A. K, S. M. KIDWELL, and R. A. GASTALDO. 2000. Taphonomy and paleobiology, pp. 103-147. In D. H. ERWIN and S. L. WING (eds.), Deep time: paleobiology's perspective, Paleobiology, 26, supplement to no. 4.

BERGGREN, W. A., and J. A. VAN COUVERING. 1978. Biochronology, pp. 39-55. In G. V. COHEE, M. F. GLAESSNER, and H. D. HEDBERG (eds.), Contributions to the Geologic Time Scale, Volume 6, The American Association of Petroleum Geologists, Tulsa.

BRINKMAN, D. B. 1990. Paleoecology of the Judith River Formation (Campanian) of Dinosaur Provincial Park, Alberta, Canada: evidence from vertebrate microfossil localities. Palaeogeography, Palaeoclimatology, Palaeoecology, 78:37-54.

BUTLER, R. F., P. D. GINGERICH, and E. H. LINDSAY. 1981. Magnetic polarity stratigraphy and biostratigraphy of Paleocene and lower Eocene continental deposits, Clarks Fork Basin, Wyoming: Journal of Geology, 89:299-316.

BUTLER, R. F., D. W. KRAUSE, and P. D. GINGERICH. 1987. Magnetic polarity stratigraphy and biostratigraphy of middle-late Paleocene continental deposits of south-central Montana. Journal of Geology, 95: 647-657.

CANDE, S. C., and D. V. and KENT. 1992. A new geomagnetic polarity timescale for the Late Cretaceous and Cenozoic: Journal of Geophysical Research, 97:13917-13951.

CANDE, S. C., and D. V. and KENT. 1995. Revised calibration of the geomagnetic polarity timescale for the Late Cretaceous and Cenozoic. Journal of Geophysical Research, 100:6093-6095.

CHEW, A. 2005. Biostratigraphy, paleoecology and synchronized evolution in the early Eocene mammalian fauna of the central Bighorn Basin, Wyoming. Unpublished Ph. D. dissertation, The Johns Hopkins University, 661 pp.

CLYDE, W. C., and P. D. GINGERICH. 1998. Mammalian community response to the latest Paleocene thermal maximum: an isotaphonomic study in the northern Bighorn Basin, Wyoming. Geology, 26:1011-1014.

DEMCHUK, T. D. 1987. Palynostratigraphy of Paleocene strata of the central Alberta Plains. Unpublished M. Sc. thesis, University of Alberta, Edmonton, 151 pp.

DEMCHUK, T. D. 1990. Palynostratigraphic zonation of Paleocene strata in the central and south-central Alberta Plains. Canadian Journal of Earth Sciences, 27:1263-1269.

DEMCHUK, T. D., and L. V. HILLS. 1991. A re-examination of the Paskapoo Formation in the central Alberta Plains: the designation of three new members. Bulletin of Canadian Petroleum Geology 39:270-282.

EVANDER, R. L. 1986. Formal redefinition of the Hemingfordian-Barstovian land mammal age boundary. Journal of Vertebrate Paleontology, 6:374-381.

FOX, R. C. 1984a. The dentition and relationships of the Paleocene primate Micromomys Szalay, with a description of a new species. Canadian Journal of Earth Sciences, 21:1262-1267.

FOX, R. C. 1984b. A new species of the Paleocene primate Elphidotarsius Gidley: its stratigraphic position and evolution. Canadian Journal of Earth Sciences, 21:1268-1277.

FOX, R. C. 1984c. First North American record of the Paleocene primate Saxonella. Journal of Paleontology, 58:892-895.

FOX, R. C. 1990a. The succession of Paleocene mammals in western Canada, pp. 51-70. In T. M. BOWN and K. D. ROSE (eds.), Dawn of the Age of Mammals in the Northern Part of the Rocky Mountain Interior, North America, Geological Society of America Special Paper, 243.

FOX, R. C. 1990b. Pronothodectes gaoi n. sp., from the late Paleocene of Alberta, Canada, and the early evolution of the Plesiadapidae (Mammalia, Primates). Journal of Paleontology, 64:637-647.

FOX, R. C. 1991. Saxonella (Plesiadapiformes: ?Primates) in North America: S. naylori, sp. nov., from the late Paleocene of Alberta, Canada. Journal of Vertebrate Paleontology, 11:334-349.

FOX, R. C. 2002. The dentition and relationships of Carpodaptes cygneus (Russell) (Carpolestidae, Plesiadapiformes, Mammalia), from the late Paleocene of Alberta, Canada. Journal of Paleontology, 76:864-881.

FRICKE, H. C., W. C. CLYDE, J. R. O'NEIL, and P. D. GINGERICH. 1998. Evidence for rapid climate change in North America during the latest Paleocene thermal maximum: oxygen isotope compositions of biogenic phosphate from the Bighorn Basin (Wyoming). Earth and Planetary Science Letters, 160:193-208.

GINGERICH, P. D. 1976. Cranial anatomy and evolution of early Tertiary Plesiadapidae (Mammalia, Primates). Museum of Paleontology, The University of Michigan, Papers on Paleontology, 15:1-140.

GINGERICH, P. D. 1989. New earliest Wasatchian mammalian fauna from the Eocene of northwestern Wyoming: composition and diversity in a rarely sampled high-

floodplain assemblage. The University of Michigan Papers on Paleontology, 28:1-97.

GINGERICH, P. D. 2003. Mammalian responses to climate change at the Paleocene-Eocene boundary: Polecat Bench record in northern Bighorn Basin, Wyoming, pp. 463-478. In S. L. WING, P. D. GINGERICH, B. SCHMITZ, and E. THOMAS (eds.), Causes and consequences of globally warm climates in the early Paleogene, Geological Society of America Special Paper, 369.

GINGERICH, P. D. 2004. Paleogene vertebrates and their response to environmental change. Neues Jahrbuch für Geologie und Paläontologie, Abhandlungen, Stuttgart, 234:1-23.

GINGERICH, P. D. 2006. Environment and evolution through the Paleocene-Eocene thermal maximum. Trends in Ecology and Evolution, 21:246-253.

GOULDEN, C. E. 1969. Temporal changes in diversity. Brookhaven Symposia in Biology, 22:96-102.

GRANGER, W. 1917. Notes on Paleocene and lower Eocene mammal horizons of northern New Mexico and southern Colorado. Bulletin of the American Museum of Natural History, 37:821-830.

GUNNELL, G. F. 1994. Paleocene mammals and faunal analysis of the Chappo type locality (Tiffanian), Green River Basin, Wyoming. Journal of Vertebrate Paleontology, 14:81-104.

GUNNELL, G. F., M. E. MORGAN, M. C. MAAS, and P. D. GINGERICH. 1995. Comparative paleoecology of Paleogene and Neogene mammalian faunas: trophic structure and composition. Palaeogeography, Palaeoclimatology, Palaeoecology, 115:2653-286.

HARLAND, B. W., R. L. ARMSTRONG, A. V. COX, L. E. CRAIG, A. G. SMITH, and D. G. SMITH. 1990. A geologic time scale 1989. Cambridge, Cambridge University Press.

HICKEY, L. J. 1977. Stratigraphy and paleobotany of the Golden Valley Formation (early Tertiary) of western North Dakota. Geological Society of America Memoir, 150:1-181.

HICKEY, L. J. 1980. Paleocene stratigraphy and flora of the Clark's Fork Basin, pp. 33-50. In P. D. GINGERICH (ed.), Early Cenozoic paleontology and stratigraphy of the Bighorn Basin, Wyoming, University of Michigan Papers on Paleontology, 24.

HIGGINS, P. 2004. A Wyoming succession of Paleocene mammal-bearing localities bracketing the boundary between the Torrejonian and Tiffanian North American Land Mammal "Ages". Rocky Mountain Geology, 38:247-280.

HOLTZMAN, R. C. 1978. Late Paleocene mammals of the Tongue River Formation, western North Dakota. Report of Investigation of the North Dakota Geological Survey, 65:1-88.

HUTCHISON, G. E. 1961. The paradox of the plankton. American Naturalist, 95:137-145.

JAMNICZKY, H. A., D. B. BRINKMAN, and A. P. RUSSELL. 2003. Vertebrate microsite sampling: how much is enough? Journal of Vertebrate Paleontology, 23:725-734.

JANIS, C. M. 1993. Tertiary mammal evolution in the context of changing climates, vegetation, and tectonic events. Annual Review of Ecology and Systematics, 24:467-500.

JANIS, C. M. 1997. Ungulate teeth, diets, and climatic changes at the Eocene/Oligocene boundary. Zoology: Analysis of Complex Systems, 100:203-220.

JANIS, C. M., and P. B. Wilhelm. 1993. Were there mammalian pursuit predators in the Tertiary? Dances with wolf avatars. Journal of Mammalian Evolution, 1:103-125.

KIHM, A. J., and J. H. HARTMAN. 2004. A reevaluation of the biochronology of the Brisbane and Judson Local Faunas (Late Paleocene) of North Dakota. Bulletin of the Carnegie Museum of Natural History. 36:97-107.

KOCH, P. L., J. C. ZACHOS, and P. D. GINGERICH. 1992. Correlation between isotope records in marine and continental carbon reservoirs near the Paleocene Eocene boundary. Nature, 358:319-322.

KOCH, P. L., J. C. ZACHOS, and D. L. DETTMAN. 1995. Stable isotope stratigraphy and paleoclimatology of the Paleogene Bighorn Basin (Wyoming, USA). Palaeogeography, Palaeoclimatology, Palaeoecology, 115:61-89.

KOCH, P. L., W. C. CLYDE, R. P. HEPPLE, M. L. FOGEL, S. L. WING, and J. C. ZACHOS. 2003. Carbon and oxygen isotope records from the paleosols spanning the Paleocene-Eocene boundary, Bighorn Basin, Wyoming, pp. 49-64. In S. L. WING,

P. D. GINGERICH, B. SCHMITZ, and E. THOMAS (eds.), Causes and Consequences of Globally Warm Climates in the Early Paleogene, Geological Society of America, Special Paper, 369.

KRAUSE, D. W., and P. D. GINGERICH. 1983. Mammalian fauna from Douglass Quarry, earliest Tiffanian (late Paleocene) of the eastern Crazy Mountain Basin, Montana. Contributions from the Museum of Paleontology, The University of Michigan, 26:157-196.

KRAUSE, D. W., and M. C. MAAS. 1990. The biogeographic origins of late Paleocene-early Eocene mammalian immigrants to the Western Interior of North America, pp. 71-105. In: T. M. BOWN and K. D. ROSE (eds.), Dawn of the Age of Mammals in the Northern Part of the Rocky Mountain Interior, Geological Society of America, Special Paper, 243.

KREBS, C. J. 1989. Ecological Methodology. Harper Collins, New York.

LERBEKMO, J. F., and K. C. COULTER. 1985. Late Cretaceous to early Paleocene magnetostratigraphy of a continental sequence: Red Deer Valley, Alberta, Canada. Canadian Journal of Earth Sciences, 22:567-583.

LERBEKMO, J. F., and A. R. SWEET. 2000. Magnetobiostratigraphy of the continental Paleocene in the Calgary area, southwestern Alberta. Bulletin of Canadian Petroleum Geology, 48:285-306.

LERBEKMO, J. F., M. E. EVANS, and G. S. HOYE. 1990. Magnetostratigraphic evidence bearing on the magnitude of the sub-Paskapoo disconformity in the Scollard Canyon-Ardley area of the Red Deer Valley, Alberta. Bulletin of Canadian Petroleum Geology, 38:197-202.

LERBEKMO, J. F., T. D. DEMCHUK, M. E. EVANS, and G. S. HOYE. 1992. Magnetostratigraphy and biostratigraphy of the continental Paleocene of the Red Deer Valley, Alberta, Canada. Bulletin of Canadian Petroleum Geology, 40:24-35.

LOFGREN, D. L., J. A. LILLEGRAVEN, W. A. CLEMENS, P. D. GINGERICH, and T. E. WILLIAMSON. 2004. Paleocene biochronology: The Puercan through Clarkforkian Land Mammal Ages, pp. 43-105. In M. O. WOODBURNE (ed.), Cenozoic

mammals of North America: geochronology and biostratigraphy. Columbia University Press, New York.

LUTERBACHER, H. P., J. R. ALI, H. BRINKHUIS, F. M. GRADSTEIN, J. J. HOOKER, S. MONECHI, J. G. OGG, J. POWELL, U. RÖHL, A. SANFILIPPO, and B. SCHMITZ. 2004. The Paleogene Period, pp. 348-408. In F. M. GRADSTEIN, J. G. OGG, and A. G. SMITH (eds.), A Geologic Time Scale, Cambridge University Press, Cambridge.

MAAS, M. C., M. R. L. ANTHONY, P. D. GINGERICH, G. F. GUNNELL, G. F., and D. W. KRAUSE. 1995. Mammalian generic diversity and turnover in the Late Paleocene and Early Eocene of the Bighorn and Crazy Mountains Basins, Wyoming and Montana (USA). Palaeogeography, Palaeoclimatology, Palaeoecology, 115(special issue):181-207.

MACARTHUR, R. H. 1957. On the relative abundance of bird species. Proceedings of the National Academy of Science, USA, 43:293-295.

MACARTHUR, R. H. 1960. On the relative abundance of species. American Naturalist, 44:25-36.

MACDONALD, T. E. 1996. Late Paleocene (Tiffanian) mammal-bearing localities in superposition, from near Drumheller, Alberta. Unpublished M. Sc. thesis, University of Alberta, Edmonton, 248 pp.

MAGURRAN, A. E. 2003. Measuring Biological Diversity. Blackwell Publishing, Oxford.

MATTHEW, W.D. 1915. Climate and evolution. Annals of the New York Academy of Sciences, 24:171-318.

MAY, R. M. 1976. Patterns in multi-species communities, pp. 142-162. In R. M. MAY (ed.), Theoretical Ecology, Blackwell Publishing, Oxford.

MENG, J., and M. C. MCKENNA. 1998. Faunal turnovers of Palaeogene mammals from the Mongolian Plateau. Nature, 394:364-367.

NASCN. 2005. North American Stratigraphic Code, North American Commission on Stratigraphic Nomenclature. American Association of Petroleum Geologists Bulletin, 89: 1547-1591.

NICHOLS, D. J., and H. L. OTT. 1978. Biostratigraphy and evolution of the Momipites-Caryapollenites lineage in the early Tertiary in the Wind River Basin, Wyoming. Palynology 2:93-112.

OGG, J. G., and A. G. SMITH. 2004. The geomagnetic polarity time scale, pp. 63-86. In F. M. GRADSTEIN, J. G. OGG, and A. G. SMITH (eds.), A Geologic Time Scale, Cambridge University Press, Cambridge.

OSBORN, H. F., and W. D. MATTHEW. 1909. Cenozoic mammal horizons of western North America. U. S. Geological Survey Bulletin, 361:1-138.

PEET, R. K. 1974. The measurement of species diversity. Annual Review of Ecology and Systematics, 5:285-307.

PROTHERO, D. R. 1999. Does climatic change drive mammalian evolution? GSA Today, 9:1-7.

PROTHERO, D. R. 2004. Did impacts, volcanic eruptions, or climate change affect mammalian evolution? Palaeogeography, Palaeoclimatology, Palaeoecology, 214:283-294.

PROTHERO, D. R., and W. A. BERGGREN (eds.). 1992. Eocene-Oligocene Climatic and Biotic Evolution. Princeton University Press, Princeton.

PROTHERO, D. R., and T. H. HEATON. 1996. Faunal stability during the early Oligocene climatic crash. Palaeogeography, Palaeoclimatology, Palaeoecology, 127:257-283.

PROTHERO, D. R., L. C. IVANY, and E. A. NESBITT (eds.). 2003. From Greenhouse to Icehouse: The Marine Eocene-Oligocene Transition. Columbia University Press, New York.

RAUP, D. M. 1975. Taxonomic diversity estimation using rarefaction. Paleobiology, 1:333-342.

ROSE, K. D. 1981a. The Clarkforkian Land Mammal Age and mammalian faunal composition across the Paleocene-Eocene boundary. University of Michigan Papers on Paleontology, 26:1-197.

ROSE, K. D. 1981b. Composition and species diversity in Paleocene and Eocene mammal assemblages: an empirical study. Journal of Vertebrate Paleontology, 3-4:367-388.

ROSE, P. J., D. L. FOX, and G. A. LUDVIGSON. 2007. Mammalian enamel and floodplain carbonate oxygen isotope records of middle Paleocene paleoclimate, Crazy Mountains Basin, Montana. Geological Society of America Abstracts with Programs, 39:76A.

RUSSELL, D. E. 1964. Les Mammifères paléocènes d'Europe. Mémoirs du Museum national d'Histoire naturelle (France), nouvelle série, série C, 13:1-321.

SCOTT, C. S. 2003. Late Torrejonian (middle Paleocene) mammals from south central Alberta, Canada. Journal of Paleontology, 77:745-768.

SCOTT, C. S. 2004. A new species of the ptilodontid multituberculate Prochetodon (Mammalia, Allotheria) from the Paleocene Paskapoo Formation of Alberta, Canada. Canadian Journal of Earth Sciences, 41:237-246.

SCOTT, C. S., and D. W. KRAUSE. 2006. Multituberculates (Mammalia, Allotheria) from the earliest Tiffanian (late Paleocene) Douglass Quarry, eastern Crazy Mountains Basin, Montana. Contributions from the Museum of Paleontology, The University of Michigan, 31: 211-243.

SCOTT, C. S., R. C. FOX, and G. P. YOUZWYSHYN. 2002. New earliest Tiffanian (late Paleocene) mammals from Cochrane 2, southwestern Alberta, Canada. Acta Palaeontologica Polonica, 47:691-704.

SECORD, R. 2004. Late Paleocene biostratigraphy, isotope stratigraphy, and mammalian systematics of the northern Bighorn Basin, Wyoming. Unpublished Ph. D. dissertation, The University of Michigan, Ann Arbor, 532 pp.

SECORD, R., P. D. GINGERICH, M .E. SMITH, W. C. CLYDE, P. WILF, and B. S. SINGER. 2006. Geochronology and mammalian biostratigraphy of middle and upper Paleocene continental strata, Bighorn Basin, Wyoming. American Journal of Science, 306:211-245.

SHACKLETON, N. J. 1984. Oxygen isotope evidence for Cenozoic climatic change, pp. 27-34. In P. BRENCHLEY (ed.), Fossils and Climate, John Wiley and Sons Ltd., Hoboken.

SILCOX, M. T., D. W. KRAUSE, M. C. MAAS, and R. C. FOX. 2001. New specimens of Elphidotarsius russelli (Mammalia, ?Primates, Carpolestidae) and a revision of plesiadapoid relationships. Journal of Vertebrate Paleontology, 21:132-152.

SIMPSON, G. G. 1935a. The Tiffany fauna, upper Paleocene. 1. Multituberculata, Marsupialia, Insectivora, and ?Chiroptera: American Museum Novitates, 795:1-19.

SIMPSON, G. G. 1935b. The Tiffany fauna, upper Paleocene. II. Structure and relationships of Plesiadapis: American Museum Novitates, 816:1-30.

SIMPSON, G. G. 1935c. The Tiffany fauna, upper Paleocene. III. Primates, Carnivora, Condylarthra, and Amblypoda. American Museum Novitates, 817: 1-28.

SMITH, T., K. D. ROSE, and P. D. GINGERICH. 2006. Rapid Asia-Europe-North America dispersal of the earliest Eocene primate Teilhardina. Proceedings of the National Academy of Sciences USA, 103:11223-11227.

TIPPER, J. C. 1979. Rarefaction and rarefiction—the use and abuse of a method in paleoecology. Paleobiology, 5:423-434.

VAN VALEN, L. 1978. The beginning of the Age of Mammals. Evolutionary Theory, 4:45-80.

VRBA, E. S. 1992. Mammals as key to evolutionary theory. Journal of Mammalogy, 1:1-28.

VRBA, E. S. 1993. Turnover pulses, the red queen, and related topics. American Journal of Science, 293:418-452.

WALSH, S. L., 1998. Fossil datum terms, paleobiological event terms, paleontostratigraphy, chronostratigraphy, and the definition of land-mammal "age" boundaries. Journal of Vertebrate Paleontology, 18: 150-179.

WALSH, S. L. 2001. Notes on geochronologic and chronostratigraphic units. Geological Society of America Bulletin, 113:704-713.

WEBB, M. W. 1996. Late Paleocene mammals from near Drayton Valley, Alberta. Unpublished M. Sc. thesis, University of Alberta, Edmonton, 258 pp.

WEBB, S. D. 1984. Ten million years of mammal extinction in North America, pp. 189-210. In P. S. MARTIN and R. G. KLEIN (eds.), Quaternary Extinctions, University of Arizona Press, Tucson.

WHITTAKER, R. H. 1977. Evolution of species diversity in land communities. Evolutionary Biology, 10:1-67.

WILF, P. 2000. Late Paleocene-early Eocene climate changes in southwestern Wyoming: paleobotanical analysis. Geological Society of America Bulletin, 112:292-307.

WING, S. L., T. M. BOWN, and J. D. OBRADOVICH. 1991. Early Eocene biotic and climatic change in interior western North America. Geology, 19:1189-1192.

WING, S. L., J. ALROY, and L. J. HICKEY. 1995. Plant and mammal diversity in the Paleocene to early Eocene of the Bighorn Basin: Palaeogeography, Palaeoclimatology, Palaeoecology, 115: 117-155.

WOLFE, J. A. 1978. A paleobotanical interpretation of Tertiary climates in the northern hemisphere. American Scientist, 66:694-703.

WOLFE, J. A., and D. M. HOPKINS. 1967. Climatic changes recorded by Tertiary land floras in northwestern North America, pp. 67-76. In K. HATAI (ed.), Tertiary correlation and climatic changes in the Pacific Symposium of the Pacific Science Congress, 25.

WOLFE, J. A., and R. Z. POORE. 1982. Tertiary marine and nonmarine climatic trends, pp. 154-158. In Climate in Earth History, Studies in Geophysics, National Academy Press, Washington D. C.

WOOD, C. B., R. W. CHANEY, J. CLARK, E. H. COLBERT, G. L. JEPSEN, J. B. REESIDE, Jr., and C. STOCK. 1941. Nomenclature and correlation of the North American continental Tertiary: Geological Society of America Bulletin, 52:1-48.

WOODBURNE, M. O. 1977. Definition and characterization in mammalian chronostratigraphy: Journal of Paleontology, 51:220-234.

WOODBURNE, M. O. 1987. Cenozoic Mammals of North America: Geochronology and Biostratigraphy. University of California Press, Berkeley, 336 pp.

WOODBURNE, M. O. 1996. Precision and resolution in mammalian chronostratigraphy: principles, practices, examples. Journal Vertebrate Paleontology, 16:531-555.

WOODBURNE, M. O. 2004. Global events and the North American mammalian biochronology, pp. 315–343. In M. O. WOODBURNE (ed.), Cenozoic mammals of North America: geochronology and biostratigraphy. Columbia University Press, New York.

WOODBURNE, M. O., and C. C. SWISHER, III. 1995. Land mammal high-resolution geochronology, intercontinental overland dispersals, sea level, climate, and

vicariance, pp. 335-364. In W. A. BERGGREN, D. V. KENT, M.-P. AUBRY, and J. HARDENBOL (eds.), Geochronology, time scales and global stratigraphic correlation, SEPM Special Publication, 54.

YOUZWYSHYN, G. P. 1988. Paleocene mammals from near Cochrane, Alberta. Unpublished M. Sc. thesis, University of Alberta, Edmonton, 484 pp.

ZACHOS, J. C., T. M. QUINN, and K. A. SALAMY. 1996. High resolution (10^4 years) deep-sea foraminiferal stable isotope records of Eocene-Oligocene climate transition. Paleoceanography, 11:251-266.

ZACHOS, J. C., B. P. FLOWER, and H. PAUL. 1997. Orbitally paced climate oscillations across the Oligocene/Miocene boundary. Nature, 388:567-570.

ZACHOS, J., M. PAGANI, L. SLOAN, E. THOMAS, and K. BILLUPS. 2001. Trends, rhythms, and aberrations in global climate 65 Ma to present. Science, 292:686-693.

Figure 12.1.—Stratigraphic ranges of mammalian taxa known from the Blindman River and Joffre Bridge local faunas. Taxa are depicted as ranging from the onset of the earliest zone to the close of the youngest zone in which they have been discovered, but their real extents within these zones are unknown. A solid line indicates that the species occurs in Alberta and in other parts of the Western Interior of North America; a hatched line indicates that the species is known only from the Alberta Basin; a dotted line indicates that the species is known only from the study localities. An upward pointing arrow indicates a stratigraphic range extension for the species from older strata, whereas a downward pointing arrow indicates a stratigraphic range extension for the species from younger strata. Conferred species are listed at the end of the table and are considered for the purposes of this comparison as representing the compared species. Source data from Lofgren et al. (2004) and from the Paleobiology Database (http://paleodb.org/) and references therein.

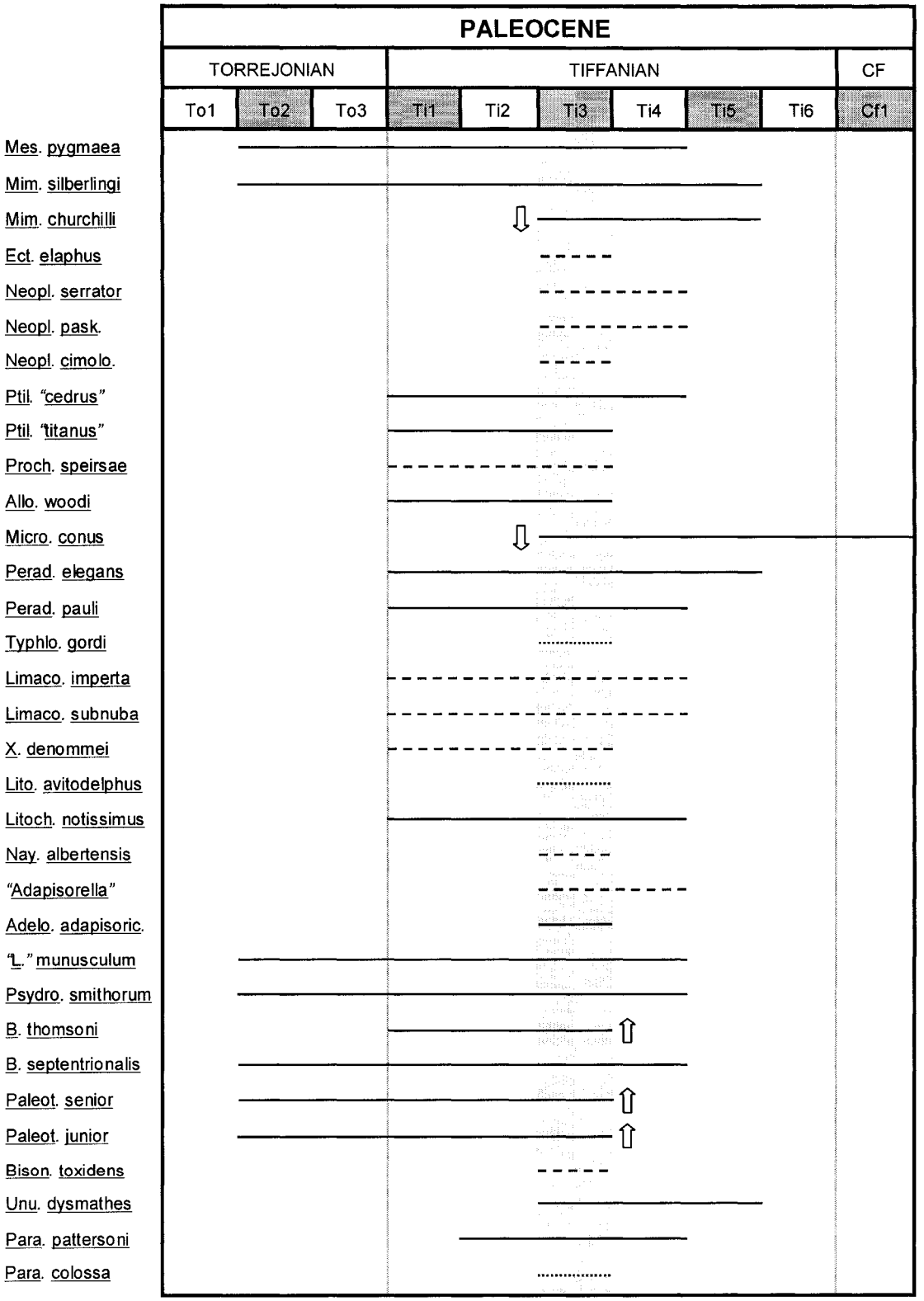
PALEOCENE
TORREJONIAN
TIFFANIAN
CF
To1
To2
To3
Ti1
Ti2
Ti3
Ti4
Ti5
Ti6
Cf1
Mes. pygmaea
Mim. silberlingi
Mim. churchilli
Ect. elaphus
Neopl. serrator
Neopl. pask.
Neopl. cimolo.
Ptil. "cedrus"
Ptil. "titanus"
Proch. speirsae
Allo. woodi
Micro. conus
Perad. elegans
Perad. pauli
Typhlo. gordi
Limaco. imperta
Limaco. subnuba
X. denommei
Lito. avitodelphus
Litoch. notissimus
Nay. albertensis
"Adapisorella"
Adelo. adapisoric.
"L." munusculum
Psydro. smithorum
B. thomsoni
B. septentrionalis
Paleot. senior
Paleot. junior
Bison. toxidens
Unu. dysmathes
Para. pattersoni
Para. colossa

Figure 12.1. (continued)—Stratigraphic ranges of mammalian taxa known from the Blindman River and Joffre Bridge local faunas. Taxa are depicted as ranging from the onset of the earliest zone to the close of the youngest zone in which they have been discovered, but their real extents within these zones are unknown. A solid line indicates that the species occurs in Alberta and in other parts of the Western Interior of North America; a hatched line indicates that the species is known only from the Alberta Basin; a dotted line indicates that the species is known only from the study localities. An upward pointing arrow indicates a stratigraphic range extension for the species from older strata, whereas a downward pointing arrow indicates a stratigraphic range extension for the species from younger strata. Conferred species are listed at the end of the table and are considered for the purposes of this comparison as representing the compared species. Source data from Lofgren et al. (2004) and from the Paleobiology Database (http://paleodb.org/) and references therein.

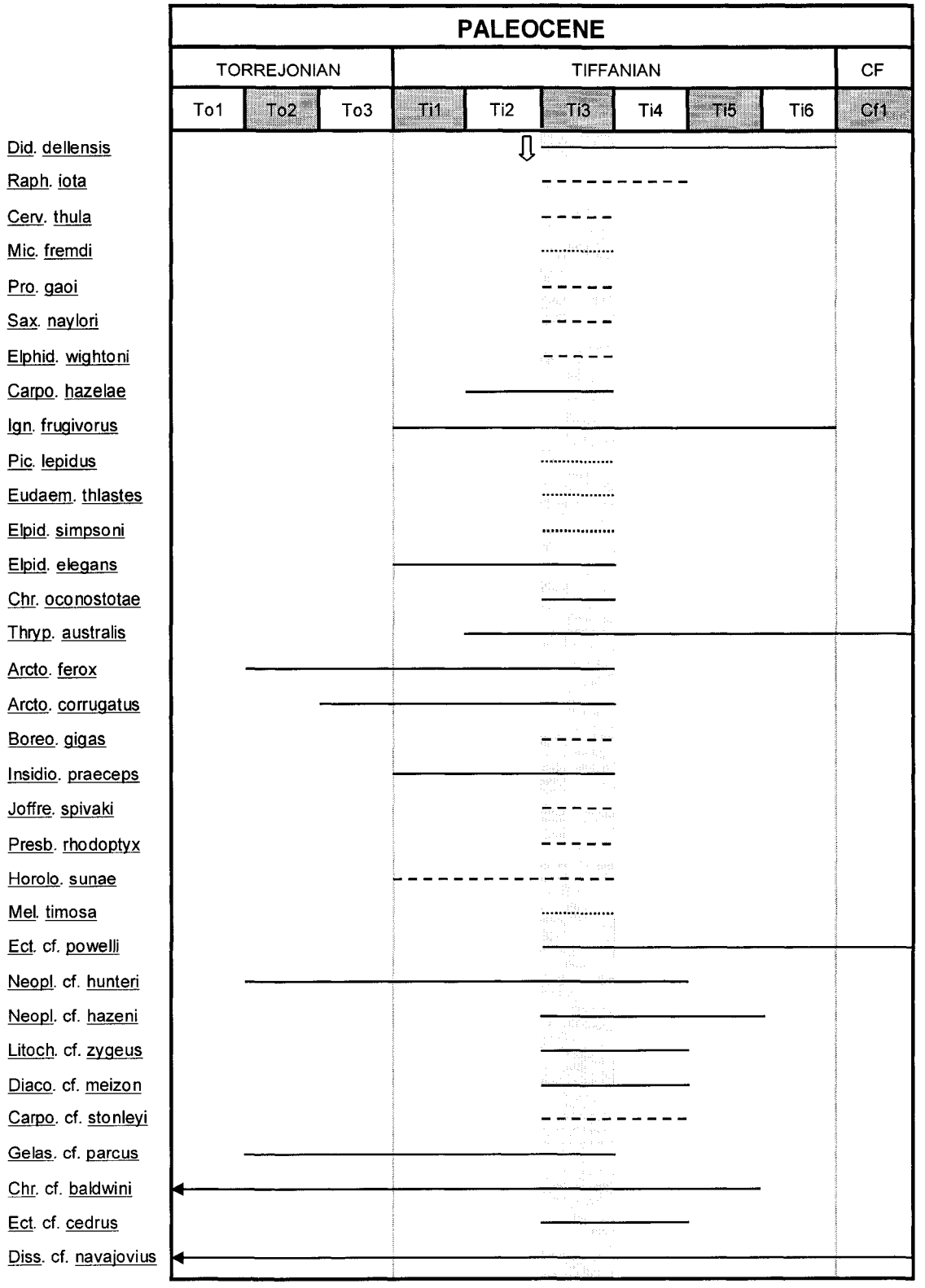
PALEOCENE
TORREJONIAN
TIFFANIAN
CF
To1
To2
To3
Ti1
Ti2
Ti3
Ti4
Ti5
Ti6
Cf1
Did. dellensis
Raph. iota
Cerv. thula
Mic. fremdi
Pro. gaoi
Sax. naylori
Elphid. wightoni
Carpo. hazelae
Ign. frugivorus
Pic. lepidus
Eudaem. thlastes
Elpid. simpsoni
Elpid. elegans
Chr. oconostotae
Thryp. australis
Arcto. ferox
Arcto. corrugatus
Boreo. gigas
Insidio. praeceps
Joffre. spivaki
Presb. rhodoptyx
Horolo. sunae
Mel. timosa
Ect. cf. powelli
Neopl. cf. hunteri
Neopl. cf. hazeni
Litoch. cf. zygeus
Diaco. cf. meizon
Carpo. cf. stonleyi
Gelas. cf. parcus
Chr. cf. baldwini
Ect. cf. cedrus
Diss. cf. navajovius

Figure 12.2.—Diagrammatic stratigraphic section of the Paleocene of the Red Deer River valley area, summarizing the occurrences of fossil mammal localities in the context of palynological zones and magnetozones. Mammal localities are as follows: GAO=Gao Mine locality; JBUL=Joffre Bridge Roadcut upper level; EL=Erickson's Landing; JBLL=Joffre Bridge Roadcut lower level; DW=Blindman River localities (including DW-1, DW-2, DW-3, Mel's Place, and Burbank); JBMS=Joffre Bridge Mammal Site No. 1. Palynozones are as follows: P1=Wodehouseia fimbriata Zone; P2=Momipites wyomingensis Zone; P3=Aquilapollenites spinulosis Zone; P4=Caryapollenites wodehousei Zone; P5=Pistillipollenites mcgregorii Zone. A=Ardley Coal Zone; N=Nevis Coal Zone. Figure adapted from Lerbekmo et al. (1992).

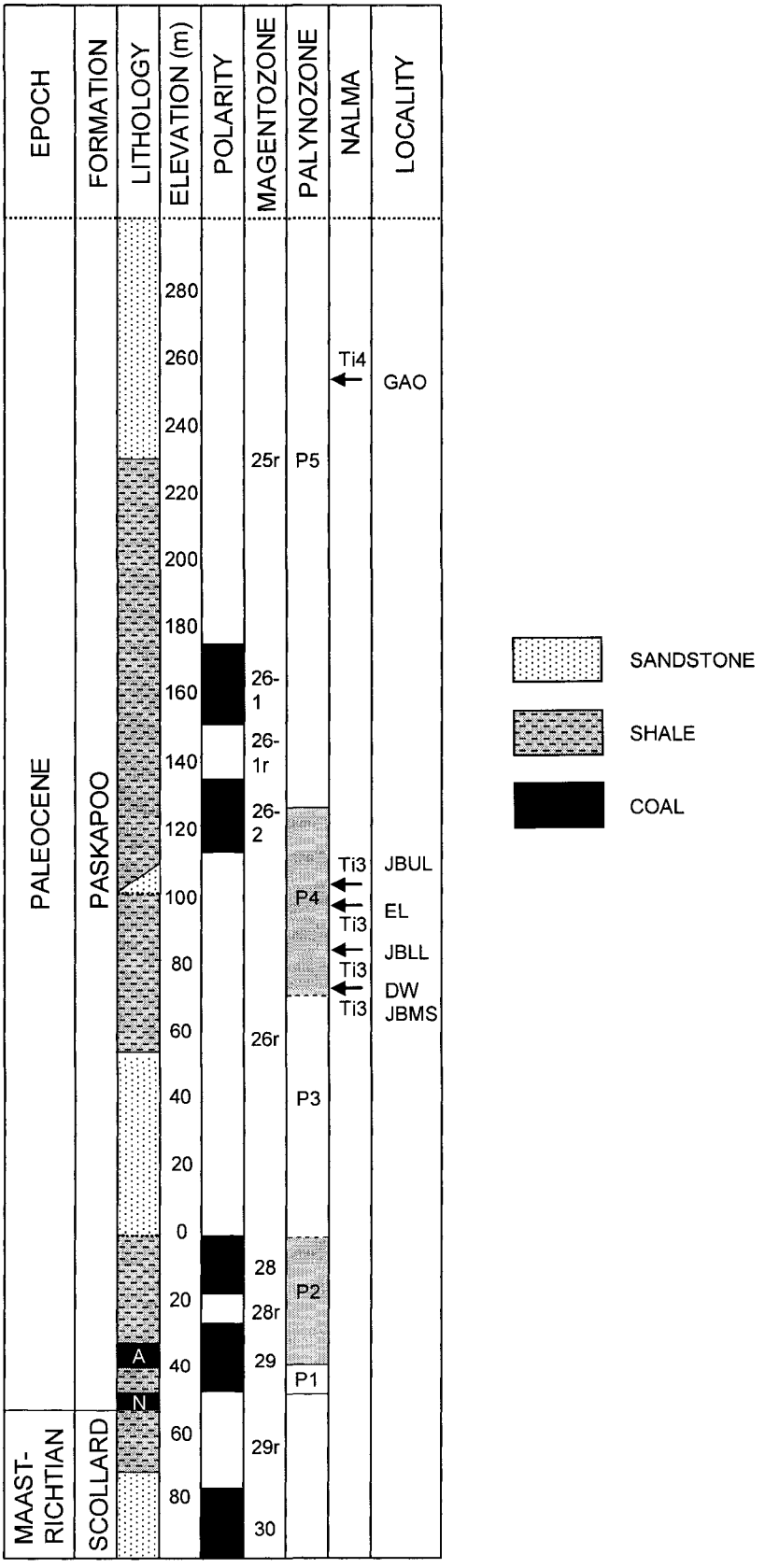
EPOCH
FORMATION
LITHOLOGY
ELEVATION (m)
POLARITY
MAGENTOZONE
PALYNOZONE
NALMA
LOCALITY
PALEOCENE
MAAST-RICHTIAN
PASKAPOO
SCOLLARD
280
260
240
220
200
180
160
140
120
100
80
60
40
20
0
20
40
60
80
A
N
25r
26-1
26-1r
26-2
26r
28
28r
29
29r
30
P5
P4
P3
P2
P1
Ti4
Ti3
Ti3
Ti3
Ti3
GAO
JBUL
EL
JBLL
DW
JBMS
SANDSTONE
SHALE
COAL

Figure 12.3.—Biostratigraphic comparison of mammal species from the Blindman River and Joffre Bridge localities, Paskapoo Formation, Alberta, with occurrences of near-contemporaneous late Paleocene faunas. G=genus level match; GS=genus and species level match; S=species level match. Positive matches in boxes indicate taxa that are shared uniquely. Comparative faunas are as follows: C2=Cochrane 2 locality, earliest Tiffanian (Ti1), Paskapoo Formation, Alberta (Youzwyshyn, 1988; Scott et al., 2002); DQ=Douglass Quarry, earliest Tiffanian (Ti1), Melville Formation, Montana (Krause and Gingerich, 1983; Krause and Maas, 1990; Silcox et al., 2001; Scott and Krause, 2006); SC=Scarritt Quarry, early Tiffanian (Ti2), Fort Union Formation, Montana (Krause and Maas, 1990); BI=Birchwood locality, early middle Tiffanian (Ti3), Paskapoo Formation, Alberta (Webb, 1996); JB=Judson and Brisbane localities, early middle Tiffanian (Ti3, Judson) and late middle Tiffanian (Ti4, Brisbane), Tongue River Formation, North Dakota (Holtzman, 1978; Kihm and Hartman, 2004); CP=Cedar Point Quarry, early middle Tiffanian (Ti3), Fort Union Formation, Wyoming (Rose, 1981a-b; Secord, 2004); CH=Chappo Type locality, early middle Tiffanian (Ti3), Wasatch Formation, Wyoming (Gunnell, 1994); DV=Divide Quarry, late middle Tiffanian (Ti4), Fort Union Formation, Wyoming (Secord, 2004); PR=Princeton Quarry, late Tiffanian (Ti5), Fort Union Formation, Wyoming (Secord, 2004).

	LOCALITIES								
	C2 (Ti1)	DQ (Ti1)	SC (Ti2)	BI (Ti3)	JB (Ti3)	CP (Ti3)	CH (Ti3)	DV (Ti4)	PR (Ti5)
Mes. pygmaea	GS	GS			GS		G		
Mim. silberlingi	GS			GS				GS	
Mim. churchilli									GS
Ect. elaphus		G			G				
Neopl. serrator				GS				G	G
Neopl. pask.				S					
Neopl. cimolo.				S					
Ptil. "cedrus"	GS	GS	GS	GS	GS	GS	GS	G	
Ptil. "titanus"	S		S	S					
Proch. speirsae	GS			GS	G			G	G
Allo. woodi		GS	GS	GS	GS				
Micro. conus									GS
Perad. elegans					GS	GS	GS		GS
Perad. pauli	GS	GS							
Typhlo. gordi									
Limaco. imperta	GS								
Limaco. subnuba	S								
X. denommei	GS			GS					
Lito. avitodelphus								G	G
Litoch. notissimus	GS		GS		G	G	G		
Nay. albertensis				GS					
"Adapisorella"									
Adelo. adapisoric.						GS			
"L." munusculum	GS	GS		GS		GS	GS		
Psydro. smithorum	GS					GS			
B. thomsoni				GS				G	
B. septentrionalis	GS	GS	GS	S	G	G	GS		
Paleot. senior	GS	GS	GS		GS	G	G	G	
Paleot. junior	S								
Bison. toxidens	G	G		GS	G	G			
Unu. dysmathes	G		G	GS	GS	GS	S	G	GS
Para. pattersoni	GS		GS	GS	GS				
Para. colossa									

Figure 12.3. (continued)—Biostratigraphic comparison of mammal species from the Blindman River and Joffre Bridge localities, Paskapoo Formation, Alberta, with occurrences of near-contemporaneous late Paleocene faunas. G=genus level match; GS=genus and species level match; S=species level match. Positive matches in boxes indicate taxa that are shared uniquely. Comparative faunas are as follows: C2=Cochrane 2 locality, earliest Tiffanian (Ti1), Paskapoo Formation, Alberta (Youzwyshyn, 1988; Scott et al., 2002); DQ=Douglass Quarry, earliest Tiffanian (Ti1), Melville Formation, Montana (Krause and Gingerich, 1983; Krause and Maas, 1990; Silcox et al., 2001; Scott and Krause, 2006); SC=Scarritt Quarry, early Tiffanian (Ti2), Fort Union Formation, Montana (Krause and Maas, 1990); BI=Birchwood locality, early middle Tiffanian (Ti3), Paskapoo Formation, Alberta (Webb, 1996); JB=Judson and Brisbane localities, early middle Tiffanian (Ti3, Judson) and late middle Tiffanian (Ti4, Brisbane), Tongue River Formation, North Dakota (Holtzman, 1978; Kihm and Hartman, 2004); CP=Cedar Point Quarry, early middle Tiffanian (Ti3), Fort Union Formation, Wyoming (Rose, 1981a-b; Secord, 2004); CH=Chappo Type locality, early middle Tiffanian (Ti3), Wasatch Formation, Wyoming (Gunnell, 1994); DV=Divide Quarry, late middle Tiffanian (Ti4), Fort Union Formation, Wyoming (Secord, 2004); PR=Princeton Quarry, late Tiffanian (Ti5), Fort Union Formation, Wyoming (Secord, 2004).

	LOCALITIES								
	C2 (Ti1)	DQ (Ti1)	SC (Ti2)	BI (Ti3)	JB (Ti3)	CP (Ti3)	CH (Ti3)	DV (Ti4)	PR (Ti5)
Did. dellensis								GS	GS
Raph. iota	GS			GS		G	G	G	
Cerv. thula	GS			GS					
Mic. fremdi									G
Pro. gaoi	G			GS					
Sax. naylori				GS					
Elphid. wightoni	G		G	GS					
Carpo. hazelae	GS		GS	GS	GS	GS	GS		
Ign. frugivorus	GS	G	GS	GS	GS	GS	GS	GS	
Pic. lepidus	G	G				G	G		
Eudaem. thlastes	G			GS					
Elpid. simpsoni	GS								
Elpid. elegans	S	GS	GS	GS		GS			
Chr. oconostotae	G	G	G	GS		GS	GS		
Thryp. australis	G	G	GS	GS	GS	GS	GS	GS	G
Arcto. ferox	GS			GS	G	G	GS	G	G
Arcto. corrugatus	S	GS	GS	GS			GS		
Boreo. gigas	G			GS					
Insidio. praeceps	GS			GS		GS			
Joffre. spivaki				GS					
Presb. rhodoptyx				GS					
Horolo. sunae	GS			GS					
Mel. timosa									
Ect. cf. powelli			GS			GS	GS		GS
Neopl. cf. hunteri	GS	GS	GS		GS	GS	GS		
Neopl. cf. hazeni				S			S		S
Litoch. cf. zygeus				S	S	S			
Diaco. cf. meizon						GS	GS	G	G
Carpo. cf. cygneus									
Gelas. cf. parcus									
Chr. cf. baldwini	S								
Ect. cf. cedrus	G	G		GS	G	GS	G	GS	G
Diss. cf. navajovius	G	G	G	GS		GS	G	GS	G
TOTALS	33G 28S	18G 10S	18G 15S	32G 38S	18G 12S	24G 18S	20G 15S	16G 6S	15G 7S

Figure 12.4.—Rarefaction curves for localities of middle Torrejonian (Who Nose?/Nordic Ski Quarry), earliest Tiffanian (Cochrane 2, Ti1), and early middle Tiffanian (Blindman River/Joffre Bridge localities, Ti3), Paskapoo Formation, Alberta (A) and coeval localities from Montana (Gidley Quarry, To2, Fort Union Formation; Douglass Quarry, Ti1, Melville Formation) and Wyoming (Cedar Point Quarry, Ti3, Fort Union Formation) (B). Data for the American localities from Rose (1981a-b), Krause and Maas (1990), Silcox et al. (2001), Secord (2004), and Scott and Krause (2006). Number of individuals estimated from number of specimens for Who Nose?/Nordic Ski, Cochrane 2, Gidley Quarry, Douglass Quarry, and Cedar Point Quarry, and from minimum number of individuals for Blindman River/Joffre Bridge. Estimated species for a sample normalized to 300 individuals (hatched line) appears in parentheses following the locality name in the graph (and see discussion in text). Error bars = 1.96×standard deviation.

A

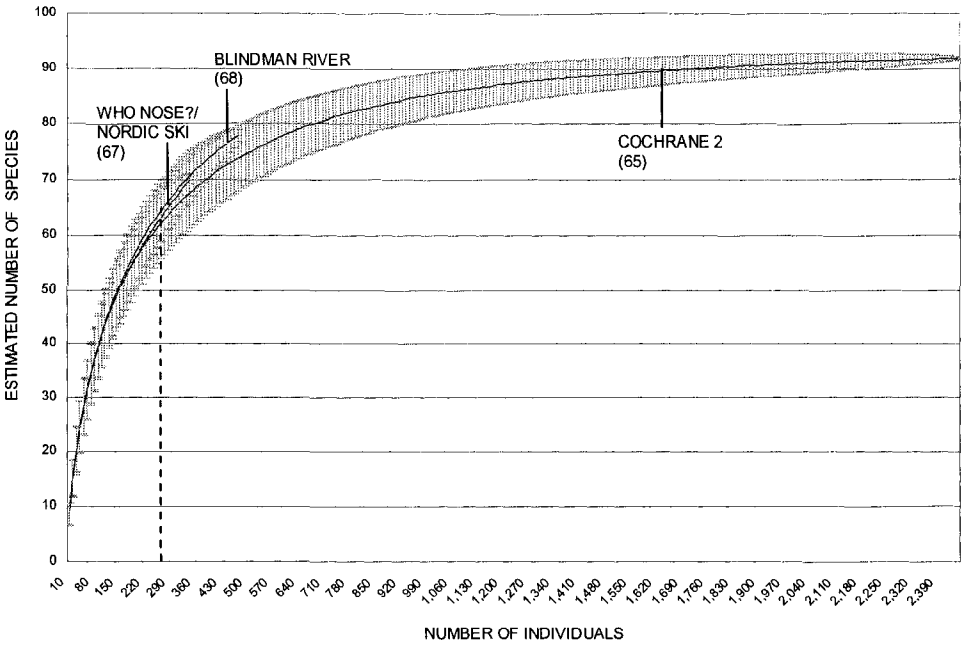
BLINDMAN RIVER
(68)
WHO NOSE?/
NORDIC SKI
(67)
COCHRANE 2
(65)
ESTIMATED NUMBER OF SPECIES
NUMBER OF INDIVIDUALS

B

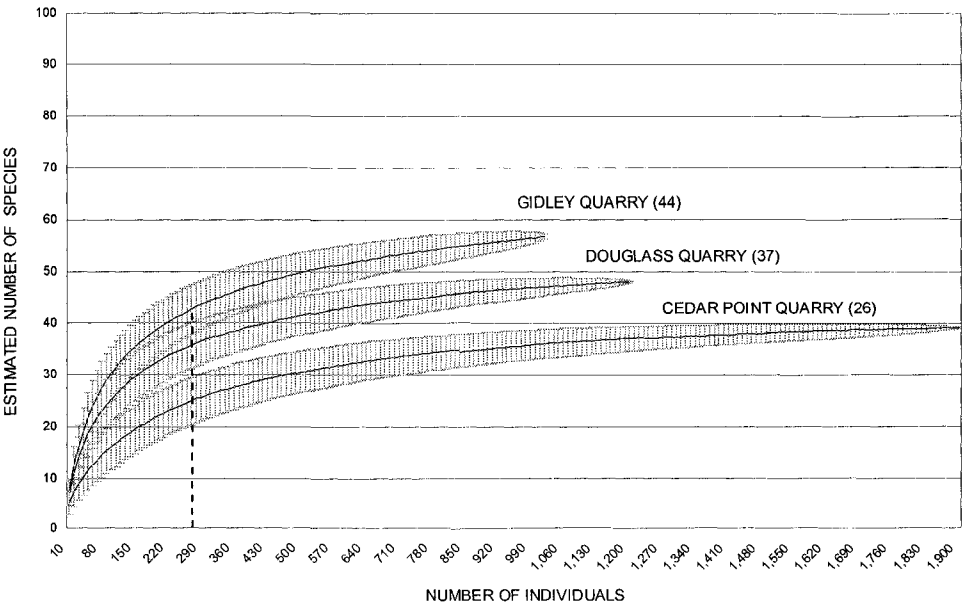
GIDLEY QUARRY (44)
DOUGLASS QUARRY (37)
CEDAR POINT QUARRY (26)
ESTIMATED NUMBER OF SPECIES
NUMBER OF INDIVIDUALS

Figure 12.5.—Curves showing species richness (number of species) in non-standardized (solid line) and standardized (rarefied) (dotted line) samples from the localities in Figure 4, plotted against stratigraphic interval. Rarefied sample normalized to a sample size of 300 individuals. Error bars = 1.96×standard deviation. Lengths of the subdivisions of the Torrejonian and Tiffanian NALMAs are arbitrarily equal in this figure and do not imply equal temporal durations.

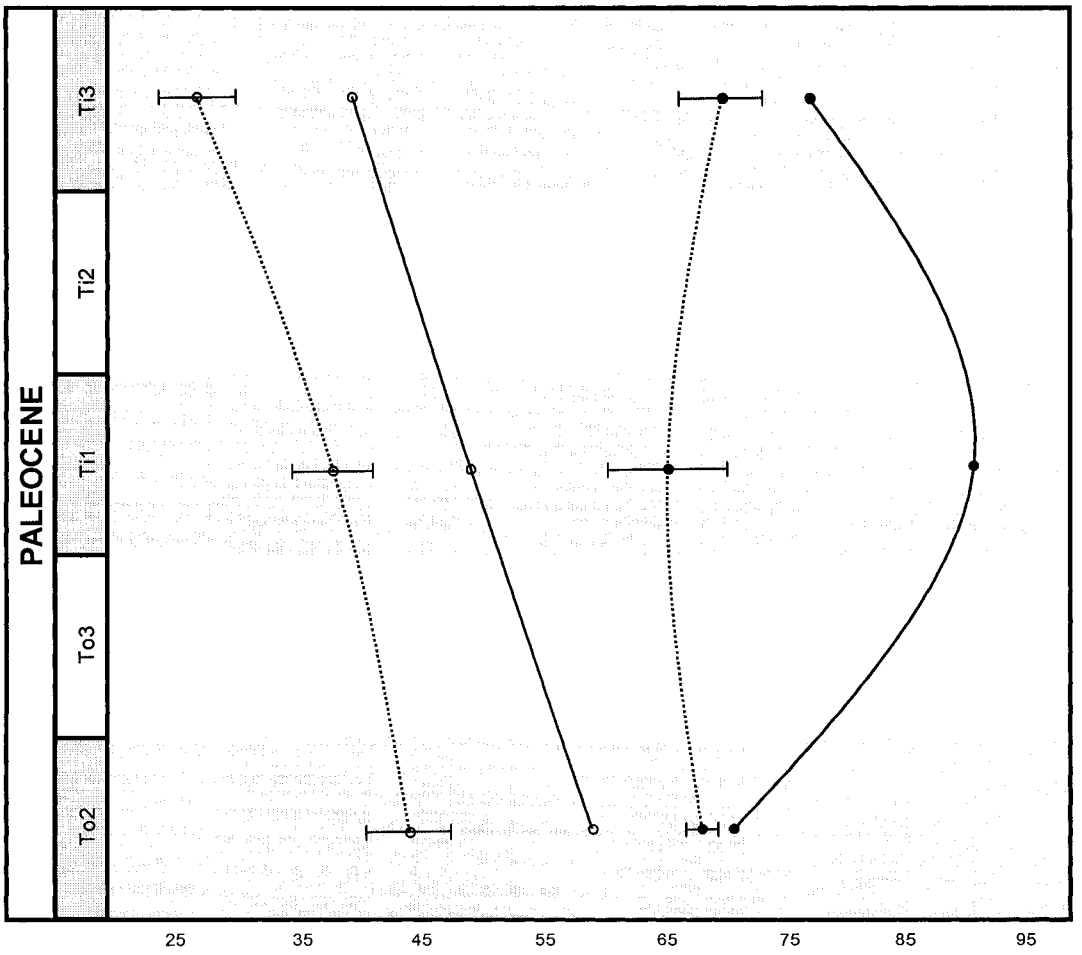

NUMBER OF SPECIES.....

RAREFIED NUMBER OF SPECIES..

AMERICAN DATA.....o

ALBERTA DATA.....•

Figure 12.6.—Rank abundance curves for A, Who Nose?/Nordic Ski Quarry local fauna (To2), B, the Cochrane 2 local fauna (Ti1), and C, the Blindman River/Joffre Bridge local fauna. The log of abundance rank is plotted on the x-axis, while the relative abundance, expressed as a percent, is plotted on the y-axis. The three most common taxa are indicated.

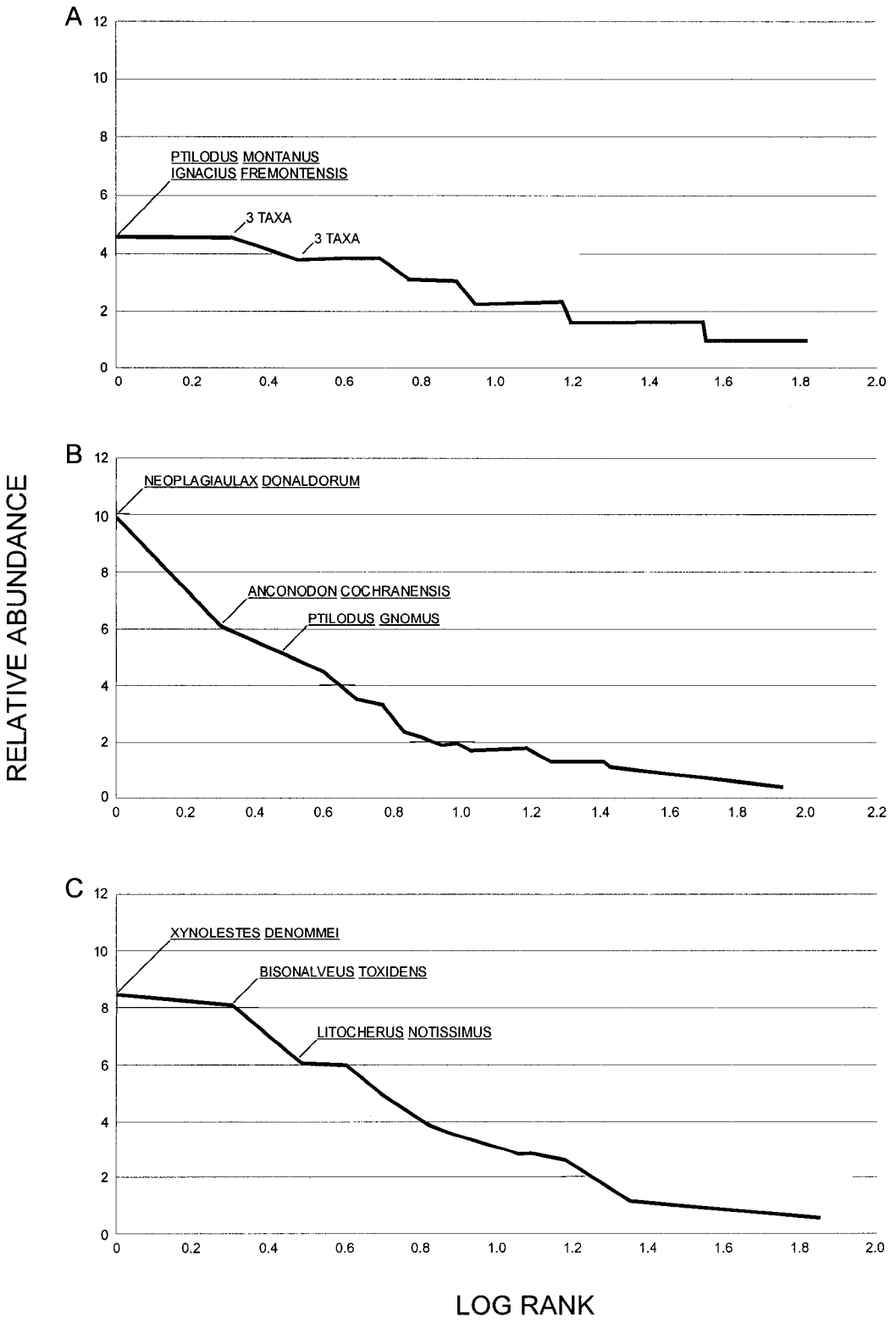
A
B
C
PTILODUS MONTANUS
IGNACIUS FREMONTENSIS
3 TAXA
3 TAXA
NEOPLAGIAULAX DONALDORUM
ANCONODON COCHRANENSIS
PTILODUS GNOMUS
XYNOLESTES DENOMMEI
BISONALVEUS TOXIDENS
LITOCHERUS NOTISSIMUS
RELATIVE ABUNDANCE
LOG RANK

12.8 Appendix 6.—Taxonomic Listing for DW-1, DW-2, DW-3, Mel's Place, Burbank, Joffre Bridge Roadcut (Upper and Lower Levels), Joffre Bridge Mammal Site No. 1, and Erickson's Landing, Paskapoo Formation of South Central Alberta, Canada.

DW-1

Order MULTITUBERCULATA

Suborder PTILODONTOIDEA

Family NEOPLAGIAULACIDAE

?MESODMA sp.

MIMETODON SILBERLINGI (Simpson)

ECTYPODUS ELAPHUS Scott

ECTYPODUS sp., cf. E. POWELLI

Family PTILODONTIDAE

PTILODUS "CEDRUS"

Subclass THERIA

Infraclass METATHERIA

Cohort MARSUPIALIA

Superorder AMERIDELPHIA

Order DIDELPHIMORPHIA

Family PERADECTIDAE

PERADECTES ELEGANS Matthew and Granger

Infraclass EUTHERIA

Superorder INSECTIVORA

Order LIPOTYPHLA

Suborder ERINACEOMORPHA

Family uncertain

XYNOLESTES DENHOMMEI

Family LITOLESTIDAE

Subfamily LITOCHERINAE

LITOCHERUS NOTISSIMUS (Simpson)

Subfamily ADAPISORICINAE

"ADAPISORELLA" sp.

Suborder SORICOMORPHA

Family NYCTITHERIIDAE

Subfamily AMPHIDOZOTHERIINAE

PSYDRONYCTIA SMITHORUM

LIPOTYPHLA, genus and species indeterminate

Order PANTOLESTA

Family PENTACODONTIDAE

BISONALVEUS TOXIDENS

Order APATOTHERIA

Family APATEMYIDAE

Subfamily UNUCHINIINAE

UNUCHINIA DYSMATHES Holtzman

Order uncertain

?PALAEORYCTIDAE

PARARYCTES PATTERSONI Van Valen

Grandorder ARCHONTA

Order PRIMATES

Suborder PLESIADAPIFORMES

Family PLESIADAPIDAE

PRONOTHODECTES GAOI Fox

Family CARPOLESTIDAE

ELPHIDOTARSIUS WIGHTONI Fox

CARPODAPTES HAZELAE Simpson

CARPODAPTES sp., cf. C. CYGNEUS

Order uncertain

Family MIXODECTIDAE

Subfamily ELPIDOPHORINAE

ELPIDOPHORUS ELEGANS Simpson

ELPIDOPHORUS species indeterminate

DW-2

Order MULTITUBERCULATA

Suborder PTILODONTOIDEA

Family NEOPLAGIAULACIDAE

MESODMA PYGMAEA Sloan

?MESODMA sp.

MIMETODON SILBERLINGI (Simpson)

MIMETODON CHURCHILLI Jepsen

ECTYPODUS ELAPHUS Scott

ECTYPODUS sp., cf. E. POWELLI

NEOPLAGIAULAX SERRATOR Scott

NEOPLAGIAULAX PASKAPOOENSIS Scott

NEOPLAGIAULAX CIMOLODONTOIDES Scott

NEOPLAGIAULAX sp., cf. N. HUNTERI

NEOPLAGIAULAX sp., cf. N. HAZENI

NEOPLAGIAULACIDAE genus and species indeterminate

Family PTILODONTIDAE

PTILODUS "CEDRUS"

PTILODUS "TITANUS"

Suborder uncertain

Family MICROCOSMODONTIDAE

ALLOCOSMODON WOODI (Holtzman and Wolberg)

MICROCOSMODON CONUS Jepsen

Subclass THERIA

Infraclass METATHERIA

Cohort MARSUPIALIA

Superorder AMERIDELPHIA

Order DIDELPHIMORPHIA

Family PERADECTIDAE

PERADECTES ELEGANS Matthew and Granger

PERADECTES PAULI Gazin

Family uncertain

TYPHLODELPHYS GORDI

Infraclass EUTHERIA

Superorder INSECTIVORA

Order LIPOTYPHLA

Suborder uncertain

Family GEOLABIDIDAE

LIMACONYSSUS INCOMPERTA

LIMACONYSSUS SUBNUBA

Suborder ERINACEOMORPHA

Family uncertain

XYNOLESTES DENHOMMEI

Family LITOLESTIDAE

Subfamily LITOLESTINAE

LITOLESTES AVITODELPHUS

Subfamily LITOCHERINAE

LITOCHERUS NOTISSIMUS (Simpson)

LITOCHERUS sp, cf. L. ZYGEUS

NAYLORIA ALBERTENSIS

Subfamily ADAPISORICINAE

ADELOXENUS ADAPISORICOIDES

Family uncertain

DIACOCHERUS sp., cf. D. MEIZON

Suborder SORICOMORPHA

Family uncertain

"LEPTACODON" MUNUSCULUM Simpson

Family NYCTITHERIIDAE

Subfamily AMPHIDOZOTHERIINAE

PSYDRONYCTIA SMITHORUM

LIPOTYPHLA, genus and species indeterminate

Order PANTOLESTA

Family PANTOLESTIDAE

BESSOECETOR THOMSONI Simpson

BESSOECETOR SEPTENTRIONALIS (Russell)

? BESSOECETOR sp.

Family PENTACODONTIDAE

BISONALVEUS TOXIDENS

Family uncertain

PALEOTOMUS SENIOR (Simpson)

PALEOTOMUS JUNIOR Scott, Fox, and Youzwyshyn

Order APATOTHERIA

Family APATEMYIDAE

Subfamily UNUCHINIINAE

UNUCHINIA DYSMATHES Holtzman

Order uncertain

Family PALAEORYCTIDAE

Subfamily DIDELPHODONTINAE

GELASTOPS sp., cf. G. PARCUS

?PALAEORYCTIDAE

PARARYCTES PATTERSONI Van Valen

PARARYCTES COLOSSA

Order CARNIVORA

Family VIVERRAVIDAE

DIDYMICTIS DELLENSIS Dorr

?DIDYMICTIS sp.

RAPHICTIS IOTA

RAPHICTIS sp.

CERVICTIS THULA

Order PHOLIDOTA

FAMILY ?EPOICOTHERIIDAE

MELANIELLA TIMOSA Fox

Grandorder ARCHONTA

Order PRIMATES

Suborder PLESIADAPIFORMES

Family MICROMOMYIDAE

MICROMOMYS FREMDI Fox

Family PLESIADAPIDAE

PRONOTHODECTES GAOI Fox

Family SAXONELLIDAE

SAXONELLA NAYLORI Fox

Family CARPOLESTIDAE

ELPHIDOTARSIUS WIGHTONI Fox

CARPODAPTES HAZELAE Simpson

Superfamily PAROMOMYOIDEA

Family PAROMOMYIDAE

IGNACIUS FRUGIVORUS Matthew and Granger

Family PICRODONTIDAE

PICRODUS LEPIDUS Scott and Fox

Order uncertain

Family MIXODECTIDAE

Subfamily MIXODECTINAE

EUDAEMONEMA THLASTES

Subfamily ELPIDOPHORINAE

ELPIDOPHORUS SIMPSONI

ELPIDOPHORUS ELEGANS Simpson

ELPIDOPHORUS species indeterminate

Grandorder UNGULATA

Order CONDYLARTHRA

Family OXYCLAENIDAE

CHRIACUS sp., cf. C. BALDWINI

CHRIACUS OCONOSTOTAE Van Valen

THRYPTACODON AUSTRALIS Simpson

Family ARCTOCYONIDAE

Subfamily ARCTOCYONINAE

ARCTOCYON FEROX (Cope)

ARCTOCYON CORRUGATUS (Cope)

BOREOCYON GIGAS

INSIDIOCLAENUS PRAECEPS

Family PHENACODONTIDAE

Subfamily MENISCOTHERIINAE

ECTOCION sp., cf. E. CEDRUS

Order MESONYCHIA

Family MESONYCHIDAE

DISSACUS sp., cf. D. NAVAJOVIUS

Order PANTODONTA

Superfamily PANTOLAMBDOIDEA

Family TITANOIDEIDAE

JOFFRELAMBDA SPIVAKI

TITANOIDEIDAE, genus and species indeterminate

PANTOLAMBDOIDEA, genus and species indeterminate

Family CYRIACOTHERIIDAE

PRESBYTERIA RHODOPTYX

Order uncertain

Family uncertain

HOROLODECTES SUNAE

DW-3

Order MULTITUBERCULATA

Suborder PTILODONTOIDEA

Family NEOPLAGIAULACIDAE

NEOPLAGIAULAX sp., cf. N. HAZENI

Infraclass EUTHERIA

Superorder INSECTIVORA

Order LIPOTYPHLA

Order PANTOLESTA

Family PENTACODONTIDAE

BISONALVEUS TOXIDENS

Grandorder ARCHONTA

Order PRIMATES

Suborder PLESIADAPIFORMES

Family CARPOLESTIDAE

CARPODAPTES HAZELAE

MEL'S PLACE

Order MULTITUBERCULATA

Suborder PTILODONTOIDEA

Family NEOPLAGIAULACIDAE

NEOPLAGIAULAX CIMOLODONTOIDES Scott

Family PTILODONTIDAE

PTILODUS "CEDRUS"

Infraclass EUTHERIA

Superorder INSECTIVORA

Order LIPOTYPHLA

Suborder ERINACEOMORPHA

Family uncertain

XYNOLESTES DENHOMMEI

Family LITOLESTIDAE

Subfamily LITOCHERINAE

LITOCHERUS NOTISSIMUS (Simpson)

Order uncertain

?PALAEORYCTIDAE

PARARYCTES PATTERSONI Van Valen

Grandorder ARCHONTA

Order PRIMATES

Suborder PLESIADAPIFORMES

Family PLESIADAPIDAE

PRONOTHODECTES GAOI Fox

Family CARPOLESTIDAE

CARPODAPTES HAZELAE Simpson

Order uncertain

Family MIXODECTIDAE

Subfamily ELPIDOPHORINAE

ELPIDOPHORUS SIMPSONI

Order MULTITUBERCULATA

Suborder PTILODONTOIDEA

Family NEOPLAGIAULACIDAE

NEOPLAGIAULAX PASKAPOOENSIS Scott

Infraclass EUTHERIA

Superorder INSECTIVORA

Order PANTOLESTA

Family PANTOLESTIDAE

BESSOECETOR THOMSONI Simpson

BESSOECETOR SEPTENTRIONALIS (Russell)

Grandorder ARCHONTA

Order PRIMATES

Suborder PLESIADAPIFORMES

Family CARPOLESTIDAE

CARPODAPTES HAZELAE

Grandorder UNGULATA

Order CONDYLARTHRA

Family ARCTOCYONIDAE

Subfamily ARCTOCYONINAE

INSIDIOCLAENUS PRAECEPS

Order PANTODONTA

Superfamily PANTOLAMBDOIDEA

Family PANTOLAMBDIDAE

?CAENOLAMBDA sp.

JOFFRE BRIDGE ROADCUT LOWER LEVEL

Order MULTITUBERCULATA

Suborder PTILODONTOIDEA

Family NEOPLAGIAULACIDAE

MESODMA PYGMAEA Sloan

ECTYPODUS ELAPHUS Scott

NEOPLAGIAULAX SERRATOR Scott

Family PTILODONTIDAE

PTILODUS "TITANUS"

Suborder uncertain

Family MICROCOSMODONTIDAE

ALLOCOSMODON WOODI (Holtzman and Wolberg)

Subclass THERIA

Infraclass METATHERIA

Cohort MARSUPIALIA

Superorder AMERIDELPHIA

Order DIDELPHIMORPHIA

Family PERADECTIDAE

PERADECTES PAULI Gazin

Infraclass EUTHERIA

Superorder INSECTIVORA

Order LIPOTYPHLA

Suborder ERINACEOMORPHA

Family uncertain

XYNOLESTES DENHOMMEI

Family LITOLESTIDAE

Subfamily LITOLESTINAE

LITOLESTES AVITODELPHUS

Subfamily LITOCHERINAE

LITOCHERUS NOTISSIMUS (Simpson)

LITOCHERUS sp, cf. L. ZYGEUS

Suborder SORICOMORPHA

Family uncertain

"LEPTACODON" MUNUSCULUM Simpson

Order PANTOLESTA

Family PANTOLESTIDAE

BESSOECETOR THOMSONI Simpson

BESSOECETOR SEPTENTRIONALIS (Russell)

Order APATOTHERIA

Family APATEMYIDAE

Subfamily UNUCHINIINAE

UNUCHINIA DYSMATHES Holtzman

Order uncertain

?PALAEORYCTIDAE

PARARYCTES PATTERSONI Van Valen

Grandorder ARCHONTA

Order PRIMATES

Suborder PLESIADAPIFORMES

Family CARPOLESTIDAE

CARPODAPTES HAZELAE Simpson

Family PICRODONTIDAE

PICRODUS sp., cf. P. LEPIDUS

Superfamily PAROMOMYOIDEA

Family PAROMOMYIDAE

IGNACIUS FRUGIVORUS Matthew and Granger

Order uncertain

Family MIXODECTIDAE

Subfamily ELPIDOPHORINAE

ELPIDOPHORUS SIMPSONI

ELPIDOPHORUS ELEGANS Simpson

JOFFRE BRIDGE ROADCUT UPPER LEVEL

Order MULTITUBERCULATA

Suborder PTILODONTOIDEA

Family NEOPLAGIAULACIDAE

MIMETODON CHURCHILLI Jepsen

Infraclass EUTHERIA

Superorder INSECTIVORA

Order PANTOLESTA

Family PENTACODONTIDAE

BISONALVEUS BROWNI Gazin

Order PANTODONTA

Superfamily PANTOLAMBDOIDEA

Family TITANOIDEIDAE

JOFFRELAMBDA SPIVAKI

JOFFRE BRIDGE MAMMAL SITE NO. 1

Order MULTITUBERCULATA

Suborder PTILODONTOIDEA

Family PTILODONTIDAE

PTILODUS "TITANUS"

PROCHETODON SPEIRSAE Scott

Subclass THERIA

Infraclass METATHERIA

Cohort MARSUPIALIA

Superorder AMERIDELPHIA

Order DIDELPHIMORPHIA

Family PERADECTIDAE

PERADECTES PAULI Gazin

Infraclass EUTHERIA

Superorder INSECTIVORA

Order LIPOTYPHLA

Suborder ERINACEOMORPHA

Family uncertain

XYNOLESTES DENHOMMEI

Family LITOLESTIDAE

Subfamily LITOCHERINAE

LITOCHERUS NOTISSIMUS (Simpson)

NAYLORIA ALBERTENSIS

Grandorder ARCHONTA

Order uncertain

Family MIXODECTIDAE

Subfamily ELPIDOPHORINAE

ELPIDOPHORUS SIMPSONI

ELPIDOPHORUS ELEGANS Simpson

ELPIDOPHORUS species indeterminate

Order PANTODONTA

Superfamily PANTOLAMBDOIDEA

Family TITANOIDEIDAE

TITANOIDEIDAE, genus and species indeterminate

ERICKSON'S LANDING

Subclass THERIA

Infraclass EUTHERIA

Superorder INSECTIVORA

Order PANTOLESTA

Family PANTOLESTIDAE

BESSOECETOR sp.

PANTOLESTIDAE, genus and species indeterminate

Grandorder ARCHONTA

Order PRIMATES

Suborder PLESIADAPIFORMES

Family PLESIADAPIDAE

?PRONOTHODECTES GAOI

Order uncertain

Family MIXODECTIDAE

Subfamily ELPIDOPHORINAE

ELPIDOPHORUS ELEGANS Simpson

Grandorder UNGULATA

Order CONDYLARTHRA

Family PHENACODONTIDAE

Subfamily MENISCOTHERIINAE

cf. ECTOCION CEDRUS

12.9 Appendix 7.—Specimen and Abundance Data for Local Faunas Included in Diversity Analyses.

1. Combined taxon listing including specimen and abundance data for the middle Torrejonian (To2) Who Nose? locality (WN) and late Torrejonian (To3) Nordic Ski Quarry (NS), Paskapoo Formation, Alberta. Numbers and letters in parentheses after each species represent (total number of specimens/minimum number of individuals; relative abundance; locality). Total number of specimens=342; total number of individuals=136; total number of species=70.

Order MULTITUBERCULATA

Suborder PTILODONTOIDEA

Family NEOPLAGIAULACIDAE

MESODMA PYGMAEA Sloan (10/3; 0.0226; WN)

MESODMA new species, cf. M. PYGMAEA (1/1; 0.00752; NS)

XYRONOMYS species indeterminate (4/3; 0.0226; WN)

MIMETODON SILBERLINGI (Simpson) (15/4; 0.03008; WN, NS)

ECTYPODUS SZALAYI Sloan (2/2; 0.01504;WN)

ECTYPODUS species indeterminate (1/1; 0.00752; WN)

PARECTYPODUS SINCLAIRI Simpson (1/1; 0.00752; NS)

PARECTYPODUS SYLVIAE Sloan (5/2; 0.01504; WN)

PARECTYPODUS species indeterminate (1/1; 0.00752; WN)

KRAUSEIA CORYSTES (Scott) (5/2; 0.01504; WN)

NEOPLAGIAULAX HUNTERI (Simpson) (4/2; 0.01504; WN)

NEOPLAGIAULAX sp., cf. N. HUNTERI (1/1; 0.00752; NS)

NEOPLAGIAULAX "NELSONI" Sloan (1/1; 0.00752; WN)

NEOPLAGIAULAX species indeterminate 1 (1/1; 0.00752; WN)

NEOPLAGIAULAX species indeterminate 2 (3/1; 0.00752; WN)

NEOPLAGIAULACIDAE new genus and species (4/2; 0.01504; WN, NS)

NEOPLAGIAULACIDAE genus and species indeterminate (3/2; 0.01504; WN)

Family PTILODONTIDAE

PTILODUS MONTANUS Gidley (40/6; 0.04511; WN)

PTILODUS GNOMUS Scott, Fox, and Youzwyshyn (12/5; 0.03759; WN, NS)

PTILODUS new species, cf. P. MONTANUS (2/2; 0.01504; NS)

BAIOTOMEUS RHOTHONION Scott (9/2; 0.01504; WN)

Family CIMOLODONTIDAE

ANCONODON COCHRANENSIS (Russell) (8/5; 0.03759; WN, NS)

ANCONODON GIDLEYI Simpson (2/1; 0.00752; NS)

Family MICROCOSMODONTIDAE

ACHERONODON species indeterminate (1/1; 0.00752; WN)

Family EUCOSMODONTIDAE

STYGIMYS species indeterminate 1 (4/1; 0.00752; WN)

STYGIMYS species indeterminate 2 (1/1; 0.00752; WN)

Family TAENIOLABIDIDAE

CATOPSALIS new species, cf. C. CALGARIENSIS (3/2; 0.01504; NS)

Subclass THERIA

Infraclass EUTHERIA

Superorder INSECTIVORA

Order LIPOTYPHLA

Family GEOLABIDIDAE

LIMACONYSSUS INCOMPERTA (1/1; 0.00752; WN)

Suborder ERINACEOMORPHA

Family uncertain

cf. MCKENNATHERIUM LADAE (1/1; 0.00752; WN)

Suborder SORICOMORPHA

Family uncertain

"LEPTACODON" MUNUSCULUM Simpson (10/3; 0.02256; WN)

Family NYCTITHERIIDAE

Subfamily AMPHIDOZOTHERIINAE

cf. PSYDRONYCTIA SMITHORUM (1/1; 0.00752; WN)

LIPOTYPHLA genus and species indeterminate (1/1; 0.00752; WN)

Order LEPTICTIDA

Family LEPTICTIDAE

PRODIACODON sp., cf. P. FUROR (3/2; 0.01504; WN, NS)

Order PANTOLESTA

Family PANTOLESTIDAE

BESSOECETOR SEPTENTRIONALIS (26/4; 0.03008; WN)

BESSOECETOR species indeterminate 1 (1/1; 0.00752; WN)

BESSOECETOR species indeterminate 2 (2/2; 0.01504; WN)

Family PENTACODONTIDAE

APHRONORUS sp. indet. (1/1; 0.00752; NS)

cf. APHRONORUS sp. (1/1; 0.00752; WN)

Family uncertain

PALEOTOMUS SENIOR (Simpson) (1/1; 0.00752; WN)

PALEOTOMUS JUNIOR Scott, Fox, and Youzwyshyn (8/1; 0.00752; WN)

Order APATOTHERIA

Family APATEMYIDAE

Subfamily UNUCHINIINAE

UNUCHINIA sp., cf. U. DIAPHANES (4/2; 0.01504; WN)

Order uncertain

Family PALAEORYCTIDAE

Subfamily DIDELPHODONTINAE

GELASTOPS new species, cf. G. PARCUS (9/4; 0.03008; WN, NS)

PROCERBERUS species indeterminate (1/1; 0.00752; WN)

Family uncertain

PARARYCTES sp. (2/1,WN)

PALAEORYCTIDAE genus and species indeterminate (1/2; 0.01504; WN)

Order CARNIVORA

Family VIVERRAVIDAE

PROTICTIS sp., cf. P. HAYDENIANUS (4/2; 0.01504; WN, NS)

SIMPSONICTIS sp., cf. S. JAYNANNEAE (3/1; 0.00752; WN)

VIVERRAVIDAE genus and species indeterminate (1/1; 0.00752; WN)

Grandorder ARCHONTA

Order PRIMATES

Family MICROSYOPIDAE

NAVAJOVIUS sp., cf. N. KOHLHAASAE (1/1; 0.00752; WN)

Suborder PLESIADAPIFORMES

Family PLESIADAPIDAE

PRONOTHODECTES MATTHEWI (Gidley) (19/5; 0.03759; WN)

Superfamily PAROMOMYOIDEA

Family PALAECHTHONIDAE

PLESIOLESTES PROBLEMATICUS (Jepsen) (5/2; 0.01504; WN)

TORREJONIA sp., cf. T. SIROKYI (1/1; 0.00752; WN)

PALENOCHTHA MINOR Simpson (2/2; 0.01504; WN)

Family PAROMOMYIDAE

IGNACIUS FREMONTENSIS (Gazin) (20/6; 0.04511; WN, NS)

PAROMOMYIDAE genus and species indeterminate 1 (3/3; 0.02256; WN)

PAROMOMYIDAE genus and species indeterminate 2 (2/1; 0.00752; WN)

Family PICRODONTIDAE

PICRODUS CALGARIENSIS Scott and Fox (6/2; 0.01504; WN)

Order uncertain

Family MIXODECTIDAE

Subfamily MIXODECTINAE

EUDAEMONEMA CUSPIDATA Simpson (2/2; 0.01504; NS)

Subfamily ELPIDOPHORINAE

ELPIDOPHORUS MINOR Simpson (10/2; 0.01504; WN)

ELPIDOPHORINAE genus and species indeterminate (6/3; 0.02256; WN)

Grandorder UNGULATA

Order CONDYLARTHRA

Family OXYCLAENIDAE

CHRIACUS species indeterminate (1/1; 0.00752; WN)

PROTHRYPTACODON ALBERTENSIS (6/3; 0.02256; WN)

Family ARCTOCYONIDAE

Subfamily ARCTOCYONINAE

BOREOCYON AUGUR (3/1; 0.00752; WN)

ARCTOCYON species indeterminate (1/1; 0.00752; WN)

Family MIOCLAENIDAE

Subfamily Mioclaeninae

cf. Bubogonia saskia (2/1; 0.00752; NS)

Promioclaenus sp., cf. P. acolytus (12/3; 0.02256; WN)

Family Hyopsodontidae

Litomylus new species, cf. L. orthronepius (8/2; 0.01504; WN)

Litomylus dissentaneus Simpson (1/1; 0.00752; NS)

Family Phenacodontidae

Subfamily Phenacodontinae

Tetraclaenodon sp., cf. T. puercensis (1/1; 0.00752; NS)

Eutheria incertae sedis

Order Pantodonta

Family Cyriacotheriidae

Presbyteria new species, cf. P. rhodoptyx (4/2; 0.01504; WN)

2. Taxon listing including specimen and abundance data for the earliest Tiffanian (Ti1) Cochrane 2 locality, Paskapoo Formation, Alberta. Numbers and letters in parentheses after each species represent (total number of specimens/minimum number of individuals; relative abundance). Total number of specimens=2388; total number of individuals=422; total number of species=91.

Order Multituberculata

Suborder Ptilodontoidea

Family Neoplagiaulacidae

Mesodma pygmaea Sloan (71/19; 0.04502)

Mimetodon silberlingi (Simpson) (39/6; 0.01422)

Parectypodus sinclairi Simpson (24/5; 0.01185)

Parectypodus sylviae Sloan (5/3; 0.00711)

Parectypodus new species (14/5; 0.01185)

KRAUSEIA CORYSTES (Scott) (7/4; 0.00948)

NEOPLAGIAULAX HUNTERI (Simpson) (6/2; 0.00474)

NEOPLAGIAULAX DONALDORUM Scott and Krause (257/42; 0.09953)

NEOPLAGIAULACIDAE genus and species indeterminate 1 (2/1; 0.00237)

NEOPLAGIAULACIDAE genus and species indeterminate 2 (2/1; 0.00237)

Family PTILODONTIDAE

PTILODUS GNOMUS Scott, Fox, and Youzwyshyn (169/22; 0.05213)

PTILODUS "CEDRUS" (24/7; 0.01659)

PTILODUS "TITANUS" (14/3; 0.00711)

PROCHETODON SPEIRSAE Scott (10/4; 0.00948)

BAIOTOMEUS RUSSELLI Scott, Fox, and Youzwyshyn (22/9; 0.02132)

Family CIMOLODONTIDAE

ANCONODON COCHRANENSIS (Russell) (110/26; 0.06161)

ANCONODON GIDLEYI Simpson (5/2; 0.00474)

ANCONODON species indeterminate (7/5; 0.01185)

Family MICROCOSMODONTIDAE

ACHERONODON VOSSAE Fox (155/14; 0.03318)

PENTACOSMODON BOWENSIS Fox (19/4; 0.00948)

Family EUCOSMODONTIDAE

EUCOSMODONTIDAE, genus and species indeterminate (7/4; 0.00948)

Subclass THERIA

Infraclass METATHERIA

Cohort MARSUPIALIA

Family PERADECTIDAE

PERADECTES sp., cf. P. PAULI (29/7; 0.01659)

Infraclass EUTHERIA

Order RODENTIA

Family MIMOTONIDAE

MIMOTONIDAE genus and species indeterminate (3/1; 0.00237)

Superorder INSECTIVORA

Order LIPOTYPHLA

Family GEOLABIDIDAE

LIMACONYSSUS INCOMPERTA (7/2; 0.00474)

LIMACONYSSUS SUBNUBA (3/2; 0.00474)

Suborder ERINACEOMORPHA

Family uncertain

XYNOLESTES DENHOMMEI (31/8; 0.01900)

?LITOCHERUS NOTISSIMUS (Simpson) (4/1; 0.00237)

Suborder SORICOMORPHA

Family uncertain

"LEPTACODON" MUNUSCULUM Simpson (10/3; 0.00711)

"LEPTACODON" sp., cf. "L." PACKI (22/5; 0.01185)

Family NYCTITHERIIDAE

Subfamily uncertain

LEPTACODON species indeterminate 1 (20/2; 0.00474)

LEPTACODON species indeterminate 2 (52/8; 0.01900)

Subfamily AMPHIDOZOTHERIINAE

cf. PSYDRONYCTIA SMITHORUM (3/1; 0.00237)

Order LEPTICTIDA

Family LEPTICTIDAE

PRODIACODON CONCORDIARCENSIS Simpson (86/10; 0.02370)

PRODIACODON FUROR Novacek (35/5; 0.01185)

PRODIACODON sp., cf. P. PUERCENSIS (28/3; 0.00711)

MYRMECOBOIDES MONTANENSIS Gidley (10/2; 0.00474)

LEPTICTIDA new genus and species (4/2; 0.00474)

Order PANTOLESTA

Family PANTOLESTIDAE

BESSOECETOR SEPTENTRIONALIS (Russell) (60/7; 0.01659)

Family PENTACODONTIDAE

BISONALVEUS BROWNI Gazin (189/15; 0.03554)

APHRONORUS species indeterminate (15/4; 0.00948)

Family uncertain

PALEOTOMUS SENIOR (Simpson) (6/2; 0.00474)

PALEOTOMUS JUNIOR Scott, Fox, and Youzwyshyn (23/4; 0.00948)

Order APATOTHERIA

Family APATEMYIDAE

Subfamily UNUCHINIINAE

UNUCHINIA sp., cf. U. DIAPHANES (11/2; 0.00474)

Order uncertain

Family PALAEORYCTIDAE

Subfamily PALEORYCTINAE

PALAEORYCTES sp., cf. P. PUNCTATUS (20/2; 0.00474)

Subfamily DIDELPHODONTINAE

DIDELPHODONTINAE genus and species indeterminate 1 (18/4; 0.00948)

DIDELPHODONTINAE genus and species indeterminate 2 (4/2; 0.00474)

DIDELPHODONTINAE genus and species indeterminate 3 (1/1; 0.00237)

DIDELPHODONTINAE genus and species indeterminate 4 (1/1; 0.00237)

Family uncertain

PARARYCTES PATTERSONI Van Valen (64/7; 0.01659)

PARARYCTES RUTHERFORDI Scott, Fox, and Youzwyshyn (5/2; 0.00474)

Order CREODONTA

CREODONTA genus and species indeterminate (1/1; 0.00237)

Order CARNIVORA

Family VIVERRAVIDAE

PRISTINICTIS CONNATA Fox and Youzwyshyn (9/2; 0.00474)

RAPHICTIS IOTA (17/4; 0.00948)

PROTICTIS sp., cf. P. HAYDENIANUS (3/1; 0.00237)

CERVICTIS sp., cf. C. THULA (8/3; 0.00711)

Grandorder ARCHONTA

Order PRIMATES

Family MICROSYOPIDAE

MICROSYOPIDAE genus and species indeterminate (26/5; 0.01185)

Suborder PLESIADAPIFORMES

Superfamily PLESIADAPOIDEA

Family PLESIADAPIDAE

PLESIADAPIS PRAECURSOR Gingerich (15/2; 0.00474)

PLESIADAPIS sp., cf. P. ANCEPS (13/3; 0.00711)

NANNODECTES INTERMEDIUS Gingerich (64/7; 0.01659)

PRONOTHODECTES sp., cf. P. GAOI (1/1; 0.00237)

PLESIADAPIDAE genus and species indeterminate (13/2; 0.00474)

Family CARPOLESTIDAE

CARPODAPTES sp., cf. C. HAZELAE (6/2; 0.00474)

ELPHIDOTARSIUS RUSSELLI Krause (35/4; 0.00948)

ELPHIDOTARSIUS sp., cf. E. SHOTGUNENSIS (3/3; 0.00711)

Superfamily PAROMOMYOIDEA

Family PALAECHTHONIDAE

PLESIOLESTES sp., cf. P. PROBLEMATICUS (8/4; 0.00948)

?TORREJONIA species indeterminate (9/2; 0.00474)

Family PAROMOMYIDAE

IGNACIUS FREMONTENSIS (Gazin) (49/3; 0.00711)

IGNACIUS FRUGIVORUS Matthew and Granger (40/5; 0.01185)

PAROMOMYIDAE genus and species indeterminate (27/5; 0.01185)

Family PICRODONTIDAE

PICRODUS CANPACIUS Scott and Fox (20/4; 0.00948)

Order uncertain

Family MIXODECTIDAE

Subfamily MIXODECTINAE

EUDAEMONEMA sp., cf. E. CUSPIDATA Simpson (5/2; 0.00474)

Subfamily ELPIDOPHORINAE

ELPIDOPHORUS sp., cf. E. SIMPSONI (3/1; 0.00237)

ELPIDOPHORUS ELEGANS Simpson (5/1; 0.00237)

Grandorder UNGULATA

Order CONDYLARTHRA

Family OXYCLAENIDAE

cf. OXYPRIMUS ALBERTENSIS (10/4; 0.00948)

CHRIACUS sp., cf. C. BALDWINI (7/4; 0.00948)

CHRIACUS PELVIDENS Cope (5/1; 0.00237)

THRYPTACODON ORTHOGONIUS (Russell) (36/5; 0.01185)

Family ARCTOCYONIDAE

Subfamily ARCTOCYONINAE

ARCTOCYON FEROX (6/1; 0.00237)

ARCTOCYON CORRUGATUS (5/2; 0.00474)

BOREOCYON ALPINUS (5/2; 0.00474)

INSIDIOCLAENUS PRAECEPS (8/2; 0.00474)

Family HYOPSODONTIDAE

LITOMYLUS DISSENTANEUS Simpson (27/4; 0.00948)

LITOMYLUS GRANDALETES Scott, Fox, and Youzwyshyn (37/7; 0.01659)

GINGERICHIA HYSTRIX Zack, Penkrot, Maas, and Krause (31/4; 0.00948)

GINGERICHIA species indeterminate (7/3; 0.00711)

HYOPSODONTIDAE genus and species indeterminate (6/2; 0.00474)

Family PHENACODONTIDAE

Subfamily PHENACODONTINAE

ECTOCION COLLINUS Russell (69/6; 0.01422)

Family PERIPTYCHIDAE

Subfamily ANISONCHINAE

ANISONCHINAE genus and species indeterminate (1/1; 0.00237)

Order MESONYCHIA

Family MESONYCHIDAE

DISSACUS species indeterminate (4/1; 0.00237)

Order PANTODONTA

Family TITANOIDEIDAE

cf. JOFFRELAMBDA SPIVAKI (2/1; 0.00237)

Order uncertain

Family uncertain

HOROLODECTES SUNAE (9/2; 0.00474)

3. Combined taxon listing including specimen and abundance data for the early middle Tiffanian (Ti3) Blindman River and Joffre Bridge localities, Paskapoo Formation, Alberta. Numbers and letters in parentheses after each species represent (total number of specimens/minimum number of individuals; relative abundance). Total number of specimens=1880; total number of individuals=474; total number of species=76.

Order MULTITUBERCULATA

Suborder PTILODONTOIDEA

Family NEOPLAGIAULACIDAE

MESODMA PYGMAEA (32/6; 0.01266)

?MESODMA species indeterminate (2/2; 0.00422)

MIMETODON SILBERLINGI (8/3; 0.00633)

MIMETODON CHURCHILLI (3/3; 0.00633)

ECTYPODUS ELAPHUS (33/12; 0.02532)

ECTYPODUS sp., cf. E. POWELLI (9/5; 0.01055)

NEOPLAGIAULAX SERRATOR (115/28; 0.05907)

NEOPLAGIAULAX PASKAPOOENSIS (38/9; 0.01899)

NEOPLAGIAULAX CIMOLODONTOIDES (65/18; 0.03797)

NEOPLAGIAULAX sp., cf. N. HUNTERI (2/2; 0.00422)

NEOPLAGIAULAX sp., cf. N. HAZENI (9/2; 0.00422)

NEOPLAGIAULACIDAE genus and species indeterminate (1/1; 0.00211)

Family PTILODONTIDAE

PTILODUS "CEDRUS" (67/14; 0.02954)

PTILODUS "TITANUS" (5/2; 0.00422)

PROCHETODON SPEIRSAE (2/2; 0.00422)

Suborder uncertain

Family MICROCOSMODONTIDAE

ALLOCOSMODON WOODI (83/8; 0.01688)

MICROCOSMODON CONUS (1/1; 0.00211)

Subclass THERIA

Infraclass METATHERIA

Cohort MARSUPIALIA

Family PERADECTIDAE

PERADECTES ELEGANS (15/4; 0.00844)

PERADECTES PAULI (13/3; 0.00633)

Family uncertain

TYPHLODELPHYS GORDI (1/1; 0.00211)

Infraclass EUTHERIA

Superorder INSECTIVORA

Order LIPOTYPHLA

Suborder uncertain

Family GEOLABIDIDAE

LIMACONYSSUS INCOMPERTA (7/4; 0.00844)

LIMACONYSSUS SUBNUBA(1/1; 0.00211)

Suborder ERINACEOMORPHA

Family uncertain

XYNOLESTES DENHOMMEI (101/40; 0.08439)

Family LITOLESTIDAE

Subfamily LITOLESTINAE

LITOLESTES AVITODELPHUS (7/4; 0.00844)

Subfamily LITOCHERINAE

LITOCHERUS NOTISSIMUS (163/29; 0.06118)

LITOCHERUS sp., cf. L. ZYGEUS (11/4; 0.00844)

NAYLORIA ALBERTENSIS (13/5; 0.01055)

Subfamily ADAPISORICINAE

ADELOXENUS ADAPISORICOIDES (6/2; 0.00422)

"ADAPISORELLA" species indeterminate (2/1; 0.00211)

Family uncertain

DIACOCHERUS sp., cf. D. MEIZON (6/3; 0.00633)

Suborder SORICOMORPHA

Family uncertain

"LEPTACODON" MUNUSCULUM (34/16; 0.03376)

Family NYCTITHERIIDAE

Subfamily AMPHIDOZOTHERIINAE

PSYDRONYCTIA SMITHORUM (29/11; 0.02321)

LIPOTYPHLA genus and species indeterminate (7/3; 0.00633)

Order PANTOLESTA

Family PANTOLESTIDAE

BESSOECETOR SEPTENTRIONALIS (44/13; 0.02743)

BESSOECETOR THOMSONI (64/20; 0.04219)

PANTOLESTIDAE genus and species indeterminate (2/1; 0.00211)

Family PENTACODONTIDAE

BISONALVEUS TOXIDENS (171/38; 0.08017)

Family uncertain

PALEOTOMUS JUNIOR (9/3; 0.00633)

PALEOTOMUS SENIOR (2/1; 0.00211)

Order APATOTHERIA

Family APATEMYIDAE

Subfamily UNUCHINIINAE

UNUCHINIA DYSMATHES (50/4; 0.00844)

Order uncertain

Family PALAEORYCTIDAE

Subfamily DIDELPHODONTINAE

GELASTOPS sp., cf. G. PARCUS (1/1; 0.00211)

?PALAEORYCTIDAE

PARARYCTES PATTERSONI (78/23; 0.04852)

PARARYCTES COLOSSA (1/1; 0.00211)

Order CARNIVORA

Family VIVERRAVIDAE

DIDYMICTIS DELLENSIS (4/1; 0.00211)

?DIDYMICTIS species indeterminate (2/2; 0.00422)

RAPHICTIS IOTA (3/1; 0.00211)

RAPHICTIS species indeterminate (1/1; 0.00211)

CERVICTIS THULA (11/2; 0.00422)

Order ?PHOLIDOTA

FAMILY ?EPOICOTHERIIDAE

MELANIELLA TIMOSA (2/2; 0.00422)

Grandorder ARCHONTA

Order PRIMATES

Suborder PLESIADAPIFORMES

Family MICROMOMYIDAE

MICROMOMYS FREMDI (19/7; 0.01477)

Family PLESIADAPIDAE

PRONOTHODECTES GAOI (137/15; 0.03165)

Family CARPOLESTIDAE

ELPHIDOTARSIUS WIGHTONI (30/11; 0.02321)

CARPODAPTES HAZELAE (59/11; 0.02321)

CARPODAPTES sp., cf. C. CYGNEUS (1/1; 0.00211)

Family SAXONELLIDAE

SAXONELLA NAYLORI (17/4; 0.00844)

Superfamily PAROMOMYOIDEA

Family PAROMOMYIDAE

IGNACIUS FRUGIVORUS (10/3; 0.00633)

Family PICRODONTIDAE

PICRODUS LEPIDUS (12/4; 0.00844)

PICRODUS sp., cf. P. LEPIDUS (1/1; 0.00211)

Order uncertain

Family MIXODECTIDAE

Subfamily MIXODECTINAE

EUDAEMONEMA THLASTES (9/2; 0.00422)

Subfamily ELPIDOPHORINAE

ELPIDOPHORUS SIMPSONI (24/6; 0.01266)

ELPIDOPHORUS ELEGANS (59/12; 0.02532)

Grandorder UNGULATA

Order CONDYLARTHRA

Family OXYCLAENIDAE

CHRIACUS sp., cf. C. BALDWINI (4/1; 0.00211)

CHRIACUS OCONOSTOTAE (4/1; 0.00211)

THRYPTACODON AUSTRALIS (6/2; 0.00422)

Family ARCTOCYONIDAE

Subfamily ARCTOCYONINAE

ARCTOCYON FEROX (13/3; 0.00633)

ARCTOCYON CORRUGATUS (2/1; 0.00211)

BOREOCYON GIGAS (17/3; 0.00633)

INSIDIOCLAENUS PRAECEPS (16/4; 0.00844)

Family PHENACODONTIDAE

Subfamily MENISCOTHERIINAE

ECTOCION sp., cf. E. CEDRUS (12/3; 0.00633)

Order MESONYCHIA

Family MESONYCHIDAE

DISSACUS sp., cf. D. NAVAJOVIUS (2/1; 0.00211)

Order PANTODONTA

Superfamily PANTOLAMBDOIDEA

Family TITANOIDEIDAE

JOFFRELAMBDA SPIVAKI (4/3; 0.00633)

TITANOIDEIDAE genus and species indeterminate (3/2; 0.00422)

Family PANTOLAMBDIDAE

?CAENOLAMBDA sp. (1/1; 0.00211)

Family CYRIACOTHERIIDAE

PRESBYTERIA RHODOPTYX (14/3; 0.00633)

PANTOLAMBDOIDEA genus and species indeterminate (3/2; 0.00422)

Order uncertain

Family uncertain

HOROLODECTES SUNAE (20/4; 0.00844)